

**Ongoing Face Recognition
Vendor Test (FRVT)**
Part 1: Verification

Patrick Grother
Mei Ngan
Kayee Hanaoka
Joyce C. Yang
Austin Hom

*Information Access Division
Information Technology Laboratory*

This publication is available free of charge from:
<https://www.nist.gov/programs-projects/face-recognition-vendor-test-frvt-ongoing>

2023/02/09



ACKNOWLEDGMENTS

The authors are grateful for the long-standing support and collaboration of the the Department of Homeland Security's Science & Technology Directorate (S&T) and the Office of Biometric Identity Management (OBIM).

Additionally, the authors are grateful to staff in the NIST Biometrics Research Laboratory for infrastructure supporting rapid evaluation of algorithms.

DISCLAIMER

Specific hardware and software products identified in this report were used in order to perform the evaluations described in this document. In no case does identification of any commercial product, trade name, or vendor, imply recommendation or endorsement by the National Institute of Standards and Technology, nor does it imply that the products and equipment identified are necessarily the best available for the purpose.

INSTITUTIONAL REVIEW BOARD

The National Institute of Standards and Technology's Research Protections Office reviewed the protocol for this project and determined it is not human subjects research as defined in Department of Commerce Regulations, 15 CFR 27, also known as the Common Rule for the Protection of Human Subjects (45 CFR 46, Subpart A).

FRVT STATUS

This report is a draft NIST Interagency Report, and is open for comment. It is the thirty sixth edition of the report since the first was published in June 2017. Prior editions of this report are maintained on the FRVT [website](#), and may contain useful information about older algorithms and datasets no longer used in FRVT.

FRVT remains open: All [four tracks](#) of the FRVT are open to new algorithm submissions. **2023-02-01** changes

since 2022-12-15:

- ▷ We have added results for first algorithms from four developers: CU-Face, Korea ID, Onfido, and TrueID-VNG.
- ▷ We have added results for new algorithms from 21 returning developers: Alchera, Armatura, Cogent-Thales, Dermalog, Didi ChuXing Global Face, Gorilla, Hyperverge, Innovatrics, Intel Research, IntelliVIX, Intema-LGL, Kasikorn Labs, Paravision, Rank One Computing, Sensetime Group, Suprema AI, Tech5, Unissey, U. Coimbra Visteam, Vixvizion (Imagus), and Yuan High-Tech Development.
- ▷ We have retired results for 20 algorithms per our policy to only list results for two algorithms per developer. Results for retired algorithms appear in prior versions of this report in the [archive](#).
- ▷ We have introduced new set of non-frontal portrait to border comparisons. The new images are described in section [2.3](#) and their use in section [3.2](#).

2022-12-15 changes since 2022-11-06:

- ▷ We have added results for first algorithms from four developers: Maxis Biometrics, PT Autentika Digital Indonesia, PT Qlue Performa Indonesia, and STCON.
- ▷ We have added results for new algorithms from 14 returning developers: Adera Global, Aiseemu Technology, Chunghwa Telecom, chtface, FRP, Griaule, Line Corporation, Maxvision Technology, Mukh Technologies, Papilon Savunma, Qnap Security, Realnetworks, Securif AI, SQISoft, and Veridium.
- ▷ We have retired results for 10 algorithms per our policy to only list results for two algorithms per developer. Results for retired algorithms appear in prior versions of this report in the [archive](#).

2022-11-06 changes since 2022-09-26:

- ▷ We have added results for first algorithms from six developers: AFR Engine, CMC Institute of Science and Technology, Saga Densan Center, Turkcell Technology, UXLabs, and Wise AI SDN BHD.
- ▷ We have added results for new algorithms from 14 returning developers: Coretech Knowledge, Cloudwalk - Moontime, Cloudmatrix, Deepglint, Guangzhou Pixel Solutions, Hangzhuo Allu Network Information Technology, NEO Systems, One More Security, Palit Microsystems, Panasonic R+D Center Singapore, Samsung S1, Seventh Sense Artificial Intelligence, Touchless ID, and Veridas Digital Authentication Solutions S.L.
- ▷ We have retired results for 10 algorithms per our policy to only list results for two algorithms per developer. Results for retired algorithms appear in prior versions of this report in the [archive](#).

2022-09-26 changes since 2022-08-30:

- ▷ We have added results for first algorithms from three developers: Codeline, First Credit Bureau Kazakhstan, and InfoCert.
- ▷ We have added results for new algorithms from 14 returning developers: Advancegroup, Armatura LLC, Beijing Hisign Technology, Cybercore, Cyberlink Corp, Herta Security, ICM Airport Technics, InsightFace AI, Metsakuur, NSENSE Corp, Samsung-SDS, Videmo Intelligent Videoanalyse, Vietnam Posts and Telecommunications Group, and Vision Intelligence Center of Meituan.
- ▷ We have retired results for 11 algorithms per our policy to only list results for two algorithms per developer. Results for retired algorithms appear in prior versions of this report in the [archive](#).

2022-08-30 changes since 2022-07-29:

- ▷ We have added results for first algorithms from two developers: Aximetria, Intellibrain Technological Projects
- ▷ We have added results for new algorithms from twelve returning developers: Alchera Inc, Dermalog, Idemia, Incode Technologies Inc, Intellivision, Kasikorn Labs, Megvii/Face++, Techsign, TuringTech.vip, Universidade de Coimbra, Verijelais, Vixvizon
- ▷ We have retired results for six algorithms per our policy to only list results for two algorithms per developer. Results for retired algorithms appear in prior versions of this report in the [archive](#).

2022-07-29 changes since 2022-06-27:

- ▷ We have added results for first algorithms from seven developers: FRP LLC (Hawaii), IMDS Software, Inspur (Beijing) Electronic Information Industry, Intema - LGL Group, PAPAGO, Qaz Biometric Systems, and VIDA-Digital Identity
- ▷ We have added results for new algorithms from nine returning developers: Cyberextruder, Glory, Maxvision Technology, Rank One Computing, Securif AI, Suprema AI, Suprema ID, Toshiba, and Yuan High-Tech Development.
- ▷ We have retired results for nine algorithms per our policy to only list results for two algorithms per developer. Results for retired algorithms appear in prior versions of this report in the [archive](#).

2022-07-29 changes since 2022-06-27:

- ▷ We have added results for first algorithms from seven developers: FRP LLC (Hawaii), IMDS Software, Inspur (Beijing) Electronic Information Industry, Intema - LGL Group, PAPAGO, Qaz Biometric Systems, and VIDA-Digital Identity
- ▷ We have added results for new algorithms from nine returning developers: Cyberextruder, Glory, Maxvision Technology, Rank One Computing, Securif AI, Suprema AI, Suprema ID, Toshiba, and Yuan High-Tech Development.
- ▷ We have retired results for nine algorithms per our policy to only list results for two algorithms per developer. Results for retired algorithms appear in prior versions of this report in the [archive](#).

2022-06-27 changes since 2022-06-03:

- ▷ We have added results for first algorithms from two developers: Krungthai Bank, and Smartbiometrik.

- ▷ We have added results for new algorithms from thirteen returning developers: Aiseemu, Corsight, Digidata, Griaule, Guangzhou Pixel Solutions, Hangzhuo AI Network Information Technology, Neurotechnology, Real Networks, Samsung S1, Sensetime Group, Smart Engines, Verihubs Inteligensia, and VinBigData.
- ▷ We have retired results for eight algorithms per our policy to only list results for two algorithms per developer. Results for retired algorithms appear in prior versions of this report in the [archive](#).

2022-06-03 changes since 2022-05-05:

- ▷ We have added results for first algorithms from seven developers: Jaak IT, Metsakuur, Palit Microsystems, Smarvist Teknoloji, and Touchless ID.
- ▷ We have added results for new algorithms from sixteen returning developers: Cyberlink, FaceOnLive, Kakao Enterprise, Line Corporation (Line Clova), Multi-Modality Intelligence, NEO Systems, and Unissey
- ▷ We have retired results for four algorithms per our policy to only list results for two algorithms per developer. Results for retired algorithms appear in prior versions of this report in the [archive](#).
- ▷ We have moved the results for the twenty human-difficult pairs used in the May 2018 paper *Face recognition accuracy of forensic examiners, superrecognizers, and face recognition algorithms* by Phillips et al. [1]. to the algorithm-specific report cards (example: [PDF](#)).
- ▷ Likewise, we have added figures showing impostor distribution shifts across demographics to the report card.

2022-05-05 changes since 2022-03-18:

- ▷ We have added results for first algorithms from seven developers: Accurascan, DICIO, FacePhi, Pangiam, University of Surrey-CVSSP, and Veridium.
- ▷ We have added results for new algorithms from sixteen returning developers: ACI Software, Canon Inc, Cloudwalk - Moontime Smart Technology, Cybercore,

2022-05-05 changes since 2022-03-18:

- ▷ We have added results for first algorithms from seven developers: Accurascan, DICIO, FacePhi, Pangiam, University of Surrey-CVSSP, and Veridium.
- ▷ We have added results for new algorithms from sixteen returning developers: ACI Software, Canon Inc, Cloudwalk - Moontime Smart Technology, Cybercore, Cyberextruder, Gemalto Cogent, HyperVerge Inc, KuKe3D Technology, Megvii/Face++, Mobbeel Solutions, Panasonic R+D Center Singapore, Qnap Security, Samsung-SDS, Vietnam Posts and Telecommunications Group, Viettel Group, and Vision Intelligence Center of Meituan.
- ▷ We have retired results for 12 algorithms per our policy to only list results for two algorithms per developer. Results for retired algorithms appear in prior versions of this report in the [archive](#).

2022-03-18 changes since 2022-02-23:

- ▷ We have added support for the detection of multiple people in a single image (see Section 1.2). Specifically the API allows an algorithm to extract features from one or more faces it detects in an image. NIST scores such cases as a correct match when any detected face matches the reference photo, and as a false positive when either face matches a non-mated reference photo. The expected effect of doing this will be to improve reported false non-match rates, and to minimally elevate false match rates. This technique was only applied to images of type “border” and “kiosk”.
- ▷ We have added results for first algorithms from four developers: IntelliVIX, Kasikorn Labs, Lebentech Biometrics, and Wicket.
- ▷ We have added results for new algorithms from 10 returning developers: Chunghwa Telecom, Cloudmatrix, Beijing DeepSense Technologies, FarBar Inc, Imagus Technology Pty, Intellivision, Maxvision Technology, NHN Corp, Seventh Sense Artificial Intelligence, and Verigram.
- ▷ We have retired results for 4 algorithms per our policy to only list results for two algorithms per developer. Results for retired algorithms appear in prior versions of this report in the [archive](#).

2022-02-23 changes since 2022-01-24:

- ▷ We have added results for first algorithms from four developers: AFIS and Biometrics Consulting, Digi-data, Graymatics, Hangzhuo Allu Network Information Technology, KnowUTech LLC, Sukshi Technology Innovation, T4iSB, and TuringTech.vip
- ▷ We have added results for new algorithms from 18 returning developers: Cognitec Systems GmbH, GeoVision Inc, Glory, Herta Security, Intel Research Group, InsightFace AI, Kakao Enterprise, N-Tech Lab, Omnidarde Ltd, Papilon Savunma, Paravision, Realnetworks Inc, Reveal Media Ltd, Shenzhen Inst Adv Integrated Tech CAS, Suprema AI Inc, Toshiba, Universidade de Coimbra, and Yuan High-Tech Development
- ▷ We have retired results for 14 algorithms per our policy to only list results for two algorithms per developer. Results for retired algorithms appear in prior versions of this report in the [archive](#).

2022-01-24 changes since 2022-01-20:

- ▷ We have added results for new algorithms from one returning developer: Vocord.

2022-01-20 changes since 2021-12-18:

- ▷ We have added results for first algorithms from four developers: Armatura, Beyne.AI, One More Security, and VinBigData
- ▷ We have added results for new algorithms from 19 returning developers: AuthenMetric, BOE Technology Group, Cybercore, Cyberlink, Dahua Technology, FaceTag Co, Innovatrics, Megvii, Mobbeel Solutions, Neurotechnology, Oz Forensics, Rank One Computing, Regula Forensics, Samsung S1, Securif AI, Sensetime Group, TigerIT Americas, Videmo Intelligente Videoanalyse, and YooniK.
- ▷ We have retired results for 14 algorithms per our policy to only list results for two algorithms per developer. Results for retired algorithms appear in prior versions of this report in the [archive](#).

: 2021-12-16 changes since 2021-11-22:

- ▷ We have added results for first algorithms from five developers: Alfabeta, Cloudmatrix, Euronovate SA, FaceOnLive Inc, and Mobicin Technology.

- ▷ We have added results for new algorithms from ten returning developers: ACI Software, ITMO University, NEO Systems, Guangzhou Pixel Solutions, Panasonic R+D Center Singapore, Qnap Security, Scanovate, Tevian, Unissey, and Vietnam Posts and Telecommunications Group.
- ▷ We have retired results for eight algorithms per our policy to only list results for two algorithms per developer. Results for retired algorithms appear in prior versions of this report in the [archive](#).
- ▷ We have revamped the figure showing performance on 20 pairs of open-source images. It now color-codes false negatives and positives against a default threshold value.

2021-11-22 changes since 2021-10-28:

- ▷ We have added results to the [website](#) for kiosk-collected images where the design and geometry configuration mean that many images have considerable downward pitch angle. In some images, the face is partially cropped. Some images have other background faces.
- ▷ We have stopped using child exploitation images in FRVT, as we lost access to the imagery. All results for that set have been removed from the [website](#), and will be removed from future PDF reports.
- ▷ We have added results for first algorithms from seven new developers: CUDO Communication, Daon, KuKe3D Technology, Mantra Softtech India, Maxvision Technology, Multi-Modality Intelligence, and Samsung-SDS.
- ▷ We have added results for new algorithms from seven returning developers: Acer Incorporated, Cloudwalk-Moontime Smart Technology, Gorilla Technology, ID3 Technology, Incode Technologies, NSENSE Corp., and SQIssoft.
- ▷ We have retired results for six algorithms per our policy to only list results for two algorithms per developer. Results for retired algorithms appear in prior versions of this report in the [archive](#).

2021-10-28 changes since 2021-09-08:

- ▷ We have substantially revised the algorithm-specific report cards that are linked from the [FRVT results page](#). (Example: [HTML](#)).
- ▷ We have added results for first algorithms from eight new developers: Beijing Mendaxia Technology, Beijing Hisign Technology, Biocube Matrics, Clearview AI, Reveal Media, Toppan ID Gate, Verigram, and Viettel High Technology.
- ▷ We have added results for new algorithms from thirty returning developers: 20Face, 3divi, Canon Inc Chunghwa Telecom, Corsight, Decatur Industries, Deepglint, Dermalog, FaceTag, Fiberhome Telecommunication Technologies, GeoVision, ICM Airport Technics, Imagus Technology, InsightFace AI, Kakao Enterprise, Kookmin University, Line Corporation, N-Tech Lab, NotionTag Technologies, Realnetworks, Suprema ID, Taiwan-Certificate Authority, Toshiba, Tripleize, Trueface.ai, Veridas Digital Authentication, Visidon, VisionLabs, YooniK, and Yuan High-Tech Development.
- ▷ We have retired results for twenty algorithms per our policy to only list results for two algorithms per developer. Results for retired algorithms appear in prior versions of this report in the [archive](#).

2021-09-08 changes since 2021-08-02:

- ▷ We have added results for first algorithms from seven new developers: Griaule, SQIssoft, Qnap Security, Techsign, Smart Engines, Verihubs, and Wuhan Tianyu Information Industry.

- ▷ We have added results for new algorithms from sixteen returning developers: ADVANCE.AI, AuthenMetric, CloudSmart Consulting, Code Everest Pvt, Cognitec Systems, Thales Gemalto Cogent, Intel Research Group, Omnidarde, Oz Forensics, Rank One Computing, Samsung S1 Corp, Securif AI, Tevian, TigerIT Americas, Universidade de Coimbra, and Vigilant Solutions
- ▷ We have retired results for eleven algorithms per our policy to only list results for two algorithms per developer. Results for retired algorithms appear in prior versions of this report in the [archive](#).

2021-08-02 changes since 2021-06-25:

- ▷ We have added results for first algorithms from eight new developers: Bee the Data, Closeli Inc, Coretech Knowledge Inc, DeepSense (France), ioNetworks Inc, Kakao Pay Corp, Seventh Sense Artificial Intelligence, and SK Telecom.
- ▷ We have added results for new algorithms from fifteen returning developers: Alchera Inc, Adera Global PTE, Aware, Bresee Technology, Cyberlink Corp, Expasoft LLC, Fujitsu Research and Development Center, Gorilla Technology, Idemia, Neurotechnology, NEO Systems, NHN Corp, Paravision, Panasonic R+D Center Singapore, and Shenzhen University-Macau University of Science and Technology.
- ▷ We have retired results for twelve algorithms per our policy to only list results for two algorithms per developer. Results for retired algorithms appear in prior versions of this report in the [archive](#).

2021-06-25 changes since 2021-05-21:

- ▷ We have added results for first algorithms from six new developers: Alice Biometrics, BOE Technology Group, Fincore, Neosecu, Sodec App, and Yuntu Data and Technology.
- ▷ We have added results for new algorithms from seven returning developers: Incode Technologies, HyperVerge, Mobbeel Solutions, Guangzhou Pixel Solutions, Remark Holdings, Sensetime, and Vietnam Posts and Telecommunications Group.
- ▷ We have retired results for four algorithms per our policy to only list results for two algorithms per developer. Results for retired algorithms appear in prior versions of this report in the [archive](#).

2021-05-21 changes since 2021-04-26:

- ▷ We have added results for first algorithms from five new developers: Ekin Smart City Technologies, Suprema ID, Tripleize, Taiwan-Certificate Authority, and Vision Intelligence Center of Meituan.
- ▷ We have added results for new algorithms from eight returning developers: ID3 Technology, Imagus Technology, Momentum Digital, N-Tech Lab, NSENSE, Shanghai Jiao Tong University, Vision-Box, and Yuan High-Tech Development
- ▷ We have retired results for seven algorithms per our policy to only list results for two algorithms per developer. Results for retired algorithms appear in prior versions of this report in the [archive](#).

2021-04-26 changes since 2021-04-16:

- ▷ We have added results for first algorithms from three new developers: Quantasoft, Rendip, and NEO Systems.
- ▷ We have added results for new algorithms from four returning developers: 3Divi, Realnetworks, Veridas Digital Authentication Solutions, and Universidade de Coimbra.

- ▷ We have retired results for three algorithms per our policy to only list results for two algorithms per developer. Results for retired algorithms appear in prior versions of this report in the [archive](#).

2021-04-16 changes since 2021-03-19:

- ▷ We have added results for first algorithms from six new developers: 20Face, Beijing DeepSense Technologies, BitCenter UK, Enface, FaceTag, InsightFace AI, Line Corporation, Lema Labs, Nanjing Kiwi Network Technology, Omnidarde, Regula Forensics, and Suprema.
- ▷ We have added results for new algorithms from ten returning developers: CloudSmart Consulting, Dermalog, GeoVision, Neurotechnology, Panasonic R+D Center Singapore, Samsung S1, Securif AI, Trueface.ai, Vigilant Solutions, and Visidon.
- ▷ We have retired results for ten algorithms per our policy to only list results for two algorithms per developer. Results for retired algorithms appear in prior versions of this report in the [archive](#).

2021-03-19 changes since 2021-03-05:

- ▷ We have added results for first algorithms from six new developers: Ajou University, AuthenMetric, Code Everest, Corsight, Papilon Savunma, and NHN Corp
- ▷ We have added results for new algorithms from seven returning developers: Alchera, Deepglint, Fiber-home Telecommunication Technologies, Kakao Enterprise, Kookmin University, Megvii/Face++, and NotionTag Technologies.
- ▷ We have updated many of the hyperlinked HTML report-cards to include seven figures on demographic dependence. Figures of this kind first appeared, and are documented in, the December 2019 document, [NIST Interagency Report 8280](#) on demographic differentials in face recognition. The figures quantify false negative dependence on demographics using “visa-border” comparisons, and false positive dependence using comparisons of “application” photos that uniformly of quality and similar to visa photos.

2021-03-05 changes since 2021-01-19:

- ▷ We have added results for first algorithms from three new developers: IVA Cognitive, Mobbeel, and MoreDian Technology.
- ▷ We have added results for new algorithms from returning developers: Ability Enterprise - Andro Video, ACI Software, Adera Global, AnyVision, BioID Technologies, China Electronics Import-Export, Cognitec Systems, Fujitsu Research and Development Center, Glory, Guangzhou Pixel Solutions, Hengrui AI Technology, Incode Technologies, Intel Research, iQIYI, Mobai, Oz Forensics, Paravision, VisionLabs, and Xforward AI Technology.
- ▷ We have added a new “resources” tab to the main [webpage](#). It includes sortable columns for data related to speed, model size, storage, and memory consumption.
- ▷ We have retired results for 13 algorithms per our policy to only list results for two algorithms per developer. Results for retired algorithms appear in prior versions of this report in the [archive](#).

2021-01-19 changes since 2020-12-18:

- ▷ This report adds results for first algorithms from four developers: Herta Security, Irex AI, Shenzhen University-Macau University of Science and Technology, and Vietnam Posts and Telecommunications Group. See Table 7 for more information.
- ▷ The report also includes results for thirteen developers who have previously submitted algorithms: Bresee Technology, Canon (previously Canon Information Technology (Beijing)), Cyberlink, CSA IntelliCloud Technology, Dahua Technology, ID3 Technology, Imagus Technology (Vixvizon), Moontime Smart Technology, N-Tech Lab, Thales Cogent, Veridas Digital Authentication Solutions, Vocord, and Yuan High-Tech Development.
- ▷ We have retired results for ten algorithms per our policy to only list results for two algorithms per developer. Results for retired algorithms appear in prior versions of this report in the [archive](#).

2020-12-18 changes since 2020-10-09:

- ▷ This report adds results for first algorithms from ten developers: BitCenter UK, CloudSmart Consulting, Cubox, Institute of Computing Technology, Naver Corp, Minivision, NSENSE Corp, Viettel Group, Visage Technologies, and Xiamen University. See Table 7 for more information.
- ▷ The report also includes results for eighteen developers who have previously submitted algorithms: ADVANCE.AI, Awidit Systems, Chosun University, Dermalog, GeoVision, ICM Airport Technics, Idemia, Institute of Information Technologies, Kakao Enterprise, Neurotechnology, Panasonic R+D Center Singapore, Rank One Computing, Sensetime Group, Shanghai Jiao Tong University, TigerIT Americas LLC, Vigilant Solutions, Winsense, and YooniK
- ▷ We have retired results for twelve algorithms per our policy to only list results for two algorithms per developer. Results for retired algorithms appear in prior versions of this report in the [archive](#).

Changes since September 18, 2020:

- ▷ This report adds results for first algorithms from five developers: Aigen, Cortica, Kookmin University, Securif AI and Vinai.
- ▷ The report also includes results for three developers who have previously submitted algorithms: Fujitsu Laboratories, Hengrui AI, and X-Forward AI.
- ▷ In the per-algorithm report-cards linked from tables and the main webpage, we have added a chart to showing reduction in error rates over the course of FRVT i.e. from 2017 onwards for all algorithms supplied by that developer. Similarly we have added a chart showing error rate reductions for our test of protective face mask verification.
- ▷ We plan to continue evaluating algorithms on various mask datasets. We hold that algorithms should be capable of detecting masks and verifying identity of all combinations of masked and unmasked faces. We have accordingly increased the amount of time allowed to extract those features from 1.0 to 1.5 seconds.

Changes since August 25, 2020:

- ▷ This report adds results for first algorithms from eight new developers. Akurat Satu Indonesia, Cybercore, Decatur Industries, Innef Labs, Satellite Innovation/Eocortex, Expasoft, and Mobai.
- ▷ The report includes results for seven developers who have previously submitted algorithms: 3Divi, BioID Technologies, Incode Technologies, Innovatrics, iSAP Solution, Synology, and Tevian.

- ▷ We have retired results for five algorithms per our policy to only list results for two algorithms per developer. Results for retired algorithms appear in prior versions of this report in the [archive](#).

Changes since July 27, 2020:

- ▷ We have introduced per-algorithm report sheets. These are HTML documents linked from the accuracy tables in this report (i.e. Table 29) and on the FRVT 1:1 [homepage](#). The sheets contain interactive graphics allowing, for example, mouseover exploration of FNMR(T) and FMR(T). Some of their content had previously appeared in this document.
- ▷ This report adds results for algorithms from six new developers. ACI Software, Bresee Technology, Fiberhome Telecommunication Technologies, Imageware Systems, Oz Forensics, and Pensees.
- ▷ The report includes results for thirteen developers who have previously submitted algorithms: Canon Information Technology (Beijing), Cyberlink, Dahua Technology, Gorilla Technology, ID3 Technology, Intel Research Group, iQIYI Inc, Momentum Digital, Netbridge Technology, Tech5 SA, Shenzhen AiMall Tech, Vigilant Solutions, and VisionLabs.
- ▷ We have retired results for nine algorithms per our policy to only list results for two algorithms per developer. Results for retired algorithms appear in prior versions of this report in the [archive](#).

Changes since May 18, 2020:

- ▷ The report is the first FRVT update since the pandemic closed it from March to June 2020.
- ▷ This report includes results for algorithms from nine new developers: GeoVision Inc, Su Zhou NaZhi-TianDi Intelligent Technology, YooniK, AYF Technology, PXL Vision AG, Yuan High-Tech Development, Beihang University-ERCACAT, ICM Airport Technics, and Staqu Technologies
- ▷ This report includes results for algorithms from 15 returning developers Acer Incorporated, Antheus Technologia, Chosun University, Chunghwa Telecom, Idemia, Moontime Smart Technology, Neurotechnology, Guangzhou Pixel Solutions, Panasonic R+D Center Singapore, Rank One Computing, Scanovate, Shanghai Universiy - Shanghai Film Academy, Synesis, Trueface.ai, and Veridas Digital Authentication Solutions
- ▷ We have retired results for ten algorithms per our policy to only list results for two algorithms per developer. Results for retired algorithms appear in prior versions of this report in the [archive](#).
- ▷ We separated timing and other resource consumption from the main participation table. The new Table 18 includes template generation durations for four kinds of images, not just mugshots.
- ▷ We have published a separate report, [NIST Interagency Report 8311](#) on accuracy of pre-pandemic algorithms on subjects wearing face masks. We plan to track improvements in accuracy on masked images going forward. In particular, we invite submission of algorithms that can detect whether a person is wearing a mask, extract features from the full face or the exposed periocular region, and do appropriate comparison. We do not intend to evaluate algorithms that assume 100% of images will be of masked individuals.

Changes since March 25, 2020:

- ▷ The report is a maintenance release - it does not add any new algorithms, and FRVT has been closed to new algorithms since mid March 2020.
- ▷ We modified the primary accuracy summary, Table 29, as follows:

- ▷▷ For visa images, the column for FNMR at FMR = 0.0001 has been removed. The visa images are so highly controlled that the error rates for the most accurate algorithms are dominated by false rejection of very young children and by the presence of a few noisy greyscale images. For now, two visa columns remain: FNMR at $FMR = 10^{-6}$ and, for matched covariates, FNMR at $FMR = 10^{-4}$.
- ▷▷ We have inserted a new column labelled “BORDER” giving accuracy for comparison of moderately poor webcam border-crossing photos that exhibit pose variations, poor compression, and low contrast due to strong background illumination. The accuracies are the worst from all cooperative image datasets used in FRVT.
- ▷ Accordingly, we updated the failure-to-template rates in Table 38.
- ▷ We withdrew a figure showing how false matches are concentrated in certain visa images used in cross-comparison, because it didn’t attempt to include demographic information.

Changes since February 27, 2020:

- ▷ The report adds results algorithms from two new developers: Beijing Alleyes Technology, and the Chinese University of Hong Kong. Results for newly submitted algorithms from two other developers will appear in the next report.
- ▷ The report adds results for algorithms from thirteen returning developers: ASUSTek Computer, Aware, Cyberlink Corp, Gorilla Technology, Innovative Technology, Kakao Enterprise, Lomonosov Moscow State University, Panasonic R+D Center Singapore, Shenzhen AiMall Technology, Shenzhen Intellifusion Technologies, Synology, Tech5 SA, and Via Technologies.
- ▷ Per policy to only list results for two algorithms per developer, we have dropped results for algorithms from Aware, Cyberlink, Gorilla Technology, Kakao Enterprise, Lomonosov Moscow State University, Panasonic R+D Center Singapore, and Tech5 SA.

Changes since January 20, 2020:

- ▷ The report adds results for five new developers: Ability Enterprise (Andro Video), Chosun University, Fujitsu Research and Development Center, University of Coimbra, and Xforward AI Technology.
- ▷ The report adds results for algorithms from six returning developers: AlphaSSTG, Incode Technologies, Kneron, Shanghai Jiao Tong University, Vocord, and X-Laboratory.
- ▷ We have corrected template comparison timing numbers for algorithms submitted September 2019 to January 2020. The values reported previously were slower due to a software bug.
- ▷ We have dropped results for algorithms from Vocord and Incode per policy to only list results for two algorithms per developer.
- ▷ The [FRVT 1:1 homepage](#) has been updated with latest accuracy results.
- ▷ The [FRVT 1:N homepage](#) now includes an update to the September 2019 NIST Interagency Report 8271. The new report adds results for one-to-many search algorithms submitted to NIST from June 2019 to January 2020.

Changes since January 6, 2020:

- ▷ Section 2 has been updated to better describe the Visa and Border images. The caption for Table 29 has been updated to better relate the accuracy values to particular image comparisons.

- ▷ The report adds results for five new developers: Acer, Advance.AI, Expasoft, Netbridge Technology, and Videmo Intelligent Videoanalyse.
- ▷ The report adds results for algorithms from 7 returning developers: China Electronics Import-Export Corp, Intel Research Group, ITMO University, Neurotechnology, N-Tech Lab, Rokid, and VisionLabs.
- ▷ We have dropped results from this edition of the report per policy to only list results for two algorithms per developer: N-Tech Lab, Neurotechnology, ITMO, Visionlabs, and CEIEC.
- ▷ The [FRVT homepage](#) has been updated with latest accuracy results.

Changes since November 11, 2019:

- ▷ Table 18 has been updated to include runtime memory usage. This is the first time such a quantity has been reported. The value is the peak size of the resident set size logged during enrollment of single images.
- ▷ We have migrated summary results table to a new platform that supports sortable tables:
<https://pages.nist.gov/frvt/html/frvt11.html>
- ▷ The report adds results for four new developers: Antheus Technologia, BioID Technologies SA, Canon Information Tech. (Beijing), Samsung S1 (listed in the tables as S1), and Taiwan AI Labs.
- ▷ The report adds results for algorithms from 13 returning developers: Anke Investments, Chunghwa Telecom, Deepglint, Institute of Information Technologies, iQIYI, Kneron, Ping An Technology, Paravision, KanKan Ai, Rokid Corporation, Shanghai Universiy - Shanghai Film Academy, Veridas Digital Authentication Solutions, and Videonetics Technology.
- ▷ We have dropped results from this edition of the report per policy to only list results for two algorithms per developer: remarkai-000, veridas-001, sensetime-001, iit-000, anke-003, and everai-002. Results for these are available in prior editions of this report linked from the FRVT page.
- ▷ We issued [NIST Interagency Report 8280: FRVT Part 3: Demographics](#) on 2019-12-19. It includes results for many of the algorithms covered by this report.

Changes since October 16, 2019:

- ▷ The report adds results for ten new developers: Ai-Union Technology, ASUSTek Computer, DiDi ChuXing Technology, Innovative Technology, Luxand, MVision, Pyramid Cyber Security + Forensic, Scanovate, Shenzhen AiMall Tech, and TUPU Technology.
- ▷ The report adds results for 12 returning developers: CTBC Bank Glory Gorilla Technology Guangzhou Pixel Solutions Imagus Technology Incode Technologies Lomonosov Moscow State University Rank One Computing Samtech InfoNet Shanghai Ulucu Electronics Technology Synesis, and Winsense.
- ▷ We have dropped results from this edition of the report per policy to only list results for two algorithms per developer: glory-000, gorilla-002, incode-003, rankone-006, and synesis-004.
- ▷ Results for five recently submitted algorithms will appear in the next report.

Changes since September 11, 2019:

- ▷ The report adds results for five new participants: Awidit Systems (Awiros), Momentum Digital (Sertis), Trueface AI, Shanghai Jiao Tong University, and X-Laboratory.

- ▷ The report adds results for five new algorithms from returning developers: Cyberlink, Hengrui AI Technology, Idemia, Panasonic R+D Singapore, and Tevian. This causes three algorithm, to be de-listed from the report per policy to list results for two algorithms per developer.

Changes since July 31 2019:

- ▷ The HTML table on the [FRVT 1:1 homepage](#) has been updated to include a column for cross-domain Visa-Border verification. Results for this new dataset appeared in the July 29 report under the name "CrossEV" - these are now renamed "Visa-Border".
- ▷ The [FRVT 1:1 homepage](#) lists algorithms according to lowest mean rank accuracy:

$$\begin{aligned} &\text{Rank(FNMR}_{\text{VISA}} \text{ at FMR = 0.000001}) + \\ &\text{Rank(FNMR}_{\text{VISA-BORDER}} \text{ at FMR = 0.000001}) + \\ &\text{Rank(FNMR}_{\text{MUGSHOT}} \text{ at FMR = 0.00001 after 14 years}) + \\ &\text{Rank(FNMR}_{\text{WILD}} \text{ at FMR = 0.00001}) \end{aligned}$$

This ordering rewards high accuracy across all datasets.
- ▷ The main results in Table 29 is now in landscape format to accomodate extra columns for the Visa-Border set, and mugshot comparisons after at least 12 years.
- ▷ The report adds results for nine new participants: Alpha SSTG, Intel Research, ULSee, Chungwa Telecon, iSAP Solution, Rokid, Shenzhen EI Networks, CSA Intellicloud, Shenzhen Intellifusion Technologies.
- ▷ The reports adds results for six new algorithms from returning developers: Innovatrics, Dahua Technology, Tech5 SA, Intellivision, Nodeflux and Imperial College, London. One algorithm, from Imperial has been retired, per policy to list results for two algorithms per developer.
- ▷ The cross-country false match rate heatmaps have been replotted to reveal more structure by listing countries by region instead of alphabetically.
- ▷ The next version of this report will be posted around October 18, 2019.

Changes since July 3 2019:

- ▷ The HTML table on the [FRVT 1:1 homepage](#) has been updated to list the 20 most accurate developers rather than algorithms, choosing the most accurate algorithm from each developer based on visa and mugshot results. Also, the algorithms are ordered in terms of lowest mean rank across mugshot, visa and wild datasets, rewarding broad accuracy over a good result on one particular dataset.
- ▷ This report includes results for a new dataset - see the column labelled "visa-border" in Table 5. It compares a new set of high quality visa-like portraits with a set webcam border-crossing photos that exhibit moderately poor pose variations and background illumination. The two new sets are described in sections 2.2 and 2.4. The comparisons are "cross-domain" in that the algorithm must compare "visa" and "wild" images. Results for other algorithms will be added in future reports as they become available.
- ▷ This report adds results for algorithms from 9 developers submitted in early July 2019. These are from 3DiVi, Camvi, EverAI-Paravision, Facesoft, Farbar (F8), Institute of Information Technologies, Shanghai U. Film Academy, Via Technologies, and Ulucu Electronics Tech. Six of these are new participants.
- ▷ Several other algorithms have been submitted and are being evaluated. Results will be released in the next report, scheduled for September 5. That report will include results for new datasets.
- ▷ Older algorithms from Everai, Camvi and 3DiVi, have been retired, per the policy to list only two algorithms per developer.

Changes since June 20 2019:

- ▷ This report adds results for algorithms from 18 developers submitted in early June 2019. These are from CTBC Bank, Deep Glint, Thales Cogent, Ever AI Paravision, Gorilla Technology, Imagus, Incode, Kneron, N-Tech Lab, Neurotechnology, Notiontag Technologies, Star Hybrid, Videonetics, Vigilant Solutions, Winsense, Anke Investments, CEIEC, and DSK. Nine of these are new participants.

- ▷ Several other algorithms have been submitted and are being evaluated. Results will be released in the next report, scheduled for August 1.
- ▷ Older algorithms from Everai, Thales Cogent, Gorilla Technology, Incode, Neurotechnology, N-Tech Lab and Vigilant Solutions have been retired, per the policy to list only two algorithms per developer.

Changes since April 2019:

- ▷ This report adds results for nine algorithms from nine developers submitted in early June 2019. These are from Tencent Deepsea, Hengrui, Kedacom, Moontime, Guangzhou Pixel, Rank One Computing, Synesis, Sensetime and Vocord.
- ▷ Another 23 algorithms have been submitted and are being evaluated. Results will be released in the next report, scheduled for July 3.
- ▷ Older algorithms for Rank One, Synesis, and Vocord have been retired, per the policy to list only two algorithms per developer.

Changes since February 2019:

- ▷ This report adds results for 49 algorithms from 42 developers submitted in early March 2019.
- ▷ This report omits results for algorithms that we retired. We retired for three reasons: 1. The developer submitted a new algorithm, and we only list two. 2. The algorithm needs a GPU, and we no longer allow GPU-based algorithms. 3. Inoperable algorithms.
- ▷ Previous results for retired algorithms are available in older editions of this report linked [here](#).
- ▷ The mugshot database used from February 2017 to January 2019 has been replaced with an extract of the mugshot database documented in NIST Interagency Report 8238, November 2018. The new mugshot set is described in section [2.5](#) and is adopted because:
 - ▷▷ It has much better identity label integrity, so that false non-match rates are substantially lower than those reported in FRVT 1:1 reports to date - see Figure [114](#).
 - ▷▷ It includes images collected over a 17 year period such that ageing can be much better characterized - - see Figure [359](#).
- ▷ Using the new mugshot database, Figure [359](#) shows accuracy for four demographic groups identified in the biographic metadata that accompanies the data: black females, black males, white females and white males.
- ▷ The report added a figure (now moved to web) with results for the twenty human-difficult pairs used in the May 2018 paper [Face recognition accuracy of forensic examiners, superrecognizers, and face recognition algorithms](#) by Phillips et al. [1].
- ▷ The report uses an update to the wild image database that corrects some ground truth labels.
- ▷ Some results for the child exploitation database are not complete. They are typically updated less frequently than for other image sets.

Contents

ACKNOWLEDGMENTS	1
DISCLAIMER	1
INSTITUTIONAL REVIEW BOARD	1
1 METRICS	55
1.1 CORE ACCURACY	55
1.2 MULTI-TEMPLATE SCORING METHODOLOGY	55
2 DATASETS	56
2.1 VISA IMAGES	56
2.2 APPLICATION IMAGES	56
2.3 APPLICATION IMAGES WITH HEAD YAW	56
2.4 BORDER CROSSING IMAGES	57
2.5 MUGSHOT IMAGES	57
2.6 KIOSK IMAGES	57
2.7 WILD IMAGES	58
3 RESULTS	58
3.1 TEST GOALS	58
3.2 TEST DESIGN	59
3.3 FAILURE TO ENROLL	62
3.4 RECOGNITION ACCURACY	72
3.5 GENUINE DISTRIBUTION STABILITY	361
3.5.1 EFFECT OF BIRTH PLACE ON THE GENUINE DISTRIBUTION	361
3.5.2 EFFECT OF AGEING	401
3.5.3 EFFECT OF AGE ON GENUINE SUBJECTS	431
3.6 IMPOSTOR DISTRIBUTION STABILITY	472
3.6.1 EFFECT OF BIRTH PLACE ON THE IMPOSTOR DISTRIBUTION	472
3.6.2 EFFECT OF AGE ON IMPOSTORS	475

List of Tables

1 PARTICIPANT INFORMATION	24
2 PARTICIPANT INFORMATION	25
3 PARTICIPANT INFORMATION	26
4 PARTICIPANT INFORMATION	27
5 PARTICIPANT INFORMATION	28
6 PARTICIPANT INFORMATION	29
7 PARTICIPANT INFORMATION	30
8 ALGORITHM SUMMARY	31
9 ALGORITHM SUMMARY	32
10 ALGORITHM SUMMARY	33
11 ALGORITHM SUMMARY	34
12 ALGORITHM SUMMARY	35
13 ALGORITHM SUMMARY	36
14 ALGORITHM SUMMARY	37
15 ALGORITHM SUMMARY	38
16 ALGORITHM SUMMARY	39
17 ALGORITHM SUMMARY	40
18 ALGORITHM SUMMARY	41

19	FALSE NON-MATCH RATE	42
20	FALSE NON-MATCH RATE	43
21	FALSE NON-MATCH RATE	44
22	FALSE NON-MATCH RATE	45
23	FALSE NON-MATCH RATE	46
24	FALSE NON-MATCH RATE	47
25	FALSE NON-MATCH RATE	48
26	FALSE NON-MATCH RATE	49
27	FALSE NON-MATCH RATE	50
28	FALSE NON-MATCH RATE	51
29	FALSE NON-MATCH RATE	52
30	FAILURE TO ENROL RATES	63
31	FAILURE TO ENROL RATES	64
32	FAILURE TO ENROL RATES	65
33	FAILURE TO ENROL RATES	66
34	FAILURE TO ENROL RATES	67
35	FAILURE TO ENROL RATES	68
36	FAILURE TO ENROL RATES	69
37	FAILURE TO ENROL RATES	70
38	FAILURE TO ENROL RATES	71

List of Figures

1	PERFORMANCE SUMMARY: FNMR VS. TEMPLATE SIZE TRADEOFF	53
2	PERFORMANCE SUMMARY: FNMR VS. TEMPLATE TIME TRADEOFF	54
3	EXAMPLE IMAGES	58
	(A) VISA	58
	(B) MUGSHOT	58
	(C) WILD	58
	(D) BORDER	58
4	PERFORMANCE ON 20 HUMAN-DIFFICULT PAIRS	73
5	PERFORMANCE ON 20 HUMAN-DIFFICULT PAIRS	74
6	PERFORMANCE ON 20 HUMAN-DIFFICULT PAIRS	75
7	PERFORMANCE ON 20 HUMAN-DIFFICULT PAIRS	76
8	PERFORMANCE ON 20 HUMAN-DIFFICULT PAIRS	77
9	PERFORMANCE ON 20 HUMAN-DIFFICULT PAIRS	78
10	PERFORMANCE ON 20 HUMAN-DIFFICULT PAIRS	79
11	PERFORMANCE ON 20 HUMAN-DIFFICULT PAIRS	80
12	PERFORMANCE ON 20 HUMAN-DIFFICULT PAIRS	81
13	PERFORMANCE ON 20 HUMAN-DIFFICULT PAIRS	82
14	PERFORMANCE ON 20 HUMAN-DIFFICULT PAIRS	83
15	PERFORMANCE ON 20 HUMAN-DIFFICULT PAIRS	84
16	PERFORMANCE ON 20 HUMAN-DIFFICULT PAIRS	85
17	PERFORMANCE ON 20 HUMAN-DIFFICULT PAIRS	86
18	PERFORMANCE ON 20 HUMAN-DIFFICULT PAIRS	87
19	PERFORMANCE ON 20 HUMAN-DIFFICULT PAIRS	88
20	PERFORMANCE ON 20 HUMAN-DIFFICULT PAIRS	89
21	PERFORMANCE ON 20 HUMAN-DIFFICULT PAIRS	90
22	PERFORMANCE ON 20 HUMAN-DIFFICULT PAIRS	91
23	PERFORMANCE ON 20 HUMAN-DIFFICULT PAIRS	92
24	PERFORMANCE ON 20 HUMAN-DIFFICULT PAIRS	93
25	PERFORMANCE ON 20 HUMAN-DIFFICULT PAIRS	94
26	PERFORMANCE ON 20 HUMAN-DIFFICULT PAIRS	95
27	PERFORMANCE ON 20 HUMAN-DIFFICULT PAIRS	96
28	PERFORMANCE ON 20 HUMAN-DIFFICULT PAIRS	97

29	PERFORMANCE ON 20 HUMAN-DIFFICULT PAIRS	98
30	PERFORMANCE ON 20 HUMAN-DIFFICULT PAIRS	99
31	PERFORMANCE ON 20 HUMAN-DIFFICULT PAIRS	100
32	PERFORMANCE ON 20 HUMAN-DIFFICULT PAIRS	101
33	PERFORMANCE ON 20 HUMAN-DIFFICULT PAIRS	102
34	PERFORMANCE ON 20 HUMAN-DIFFICULT PAIRS	103
35	PERFORMANCE ON 20 HUMAN-DIFFICULT PAIRS	104
36	PERFORMANCE ON 20 HUMAN-DIFFICULT PAIRS	105
37	PERFORMANCE ON 20 HUMAN-DIFFICULT PAIRS	106
38	PERFORMANCE ON 20 HUMAN-DIFFICULT PAIRS	107
39	PERFORMANCE ON 20 HUMAN-DIFFICULT PAIRS	108
40	PERFORMANCE ON 20 HUMAN-DIFFICULT PAIRS	109
41	PERFORMANCE ON 20 HUMAN-DIFFICULT PAIRS	110
42	PERFORMANCE ON 20 HUMAN-DIFFICULT PAIRS	111
43	PERFORMANCE ON 20 HUMAN-DIFFICULT PAIRS	112
44	ERROR TRADEOFF CHARACTERISTIC: VISA IMAGES	113
45	ERROR TRADEOFF CHARACTERISTIC: VISA IMAGES	114
46	ERROR TRADEOFF CHARACTERISTIC: VISA IMAGES	115
47	ERROR TRADEOFF CHARACTERISTIC: VISA IMAGES	116
48	ERROR TRADEOFF CHARACTERISTIC: VISA IMAGES	117
49	ERROR TRADEOFF CHARACTERISTIC: VISA IMAGES	118
50	ERROR TRADEOFF CHARACTERISTIC: VISA IMAGES	119
51	ERROR TRADEOFF CHARACTERISTIC: VISA IMAGES	120
52	ERROR TRADEOFF CHARACTERISTIC: VISA IMAGES	121
53	ERROR TRADEOFF CHARACTERISTIC: VISA IMAGES	122
54	ERROR TRADEOFF CHARACTERISTIC: VISA IMAGES	123
55	ERROR TRADEOFF CHARACTERISTIC: VISA IMAGES	124
56	ERROR TRADEOFF CHARACTERISTIC: VISA IMAGES	125
57	ERROR TRADEOFF CHARACTERISTIC: VISA IMAGES	126
58	ERROR TRADEOFF CHARACTERISTIC: VISA IMAGES	127
59	ERROR TRADEOFF CHARACTERISTIC: VISA IMAGES	128
60	ERROR TRADEOFF CHARACTERISTIC: VISA IMAGES	129
61	ERROR TRADEOFF CHARACTERISTIC: VISA IMAGES	130
62	ERROR TRADEOFF CHARACTERISTIC: VISA IMAGES	131
63	ERROR TRADEOFF CHARACTERISTIC: VISA IMAGES	132
64	ERROR TRADEOFF CHARACTERISTIC: VISA IMAGES	133
65	ERROR TRADEOFF CHARACTERISTIC: VISA IMAGES	134
66	ERROR TRADEOFF CHARACTERISTIC: VISA IMAGES	135
67	ERROR TRADEOFF CHARACTERISTIC: VISA IMAGES	136
68	ERROR TRADEOFF CHARACTERISTIC: VISA IMAGES	137
69	ERROR TRADEOFF CHARACTERISTIC: VISA IMAGES	138
70	ERROR TRADEOFF CHARACTERISTIC: VISA IMAGES	139
71	ERROR TRADEOFF CHARACTERISTIC: VISA IMAGES	140
72	ERROR TRADEOFF CHARACTERISTIC: VISA IMAGES	141
73	ERROR TRADEOFF CHARACTERISTIC: VISA IMAGES	142
74	ERROR TRADEOFF CHARACTERISTIC: VISA IMAGES	143
75	ERROR TRADEOFF CHARACTERISTIC: VISA IMAGES	144
76	ERROR TRADEOFF CHARACTERISTIC: VISA IMAGES	145
77	ERROR TRADEOFF CHARACTERISTIC: VISA IMAGES	146
78	ERROR TRADEOFF CHARACTERISTIC: VISA IMAGES	147
79	ERROR TRADEOFF CHARACTERISTIC: VISA IMAGES	148
80	ERROR TRADEOFF CHARACTERISTIC: VISA IMAGES	149
81	ERROR TRADEOFF CHARACTERISTIC: VISA IMAGES	150
82	ERROR TRADEOFF CHARACTERISTIC: VISA IMAGES	151
83	ERROR TRADEOFF CHARACTERISTIC: VISA IMAGES	152
84	ERROR TRADEOFF CHARACTERISTIC: VISA IMAGES	153

85	ERROR TRADEOFF CHARACTERISTIC: VISA IMAGES	154
86	ERROR TRADEOFF CHARACTERISTIC: VISA IMAGES	155
87	ERROR TRADEOFF CHARACTERISTIC: VISA IMAGES	156
88	ERROR TRADEOFF CHARACTERISTIC: VISA IMAGES	157
89	ERROR TRADEOFF CHARACTERISTIC: VISA IMAGES	158
90	ERROR TRADEOFF CHARACTERISTIC: VISA IMAGES	159
91	ERROR TRADEOFF CHARACTERISTIC: MUGSHOT IMAGES	160
92	ERROR TRADEOFF CHARACTERISTIC: MUGSHOT IMAGES	161
93	ERROR TRADEOFF CHARACTERISTIC: MUGSHOT IMAGES	162
94	ERROR TRADEOFF CHARACTERISTIC: MUGSHOT IMAGES	163
95	ERROR TRADEOFF CHARACTERISTIC: MUGSHOT IMAGES	164
96	ERROR TRADEOFF CHARACTERISTIC: MUGSHOT IMAGES	165
97	ERROR TRADEOFF CHARACTERISTIC: MUGSHOT IMAGES	166
98	ERROR TRADEOFF CHARACTERISTIC: MUGSHOT IMAGES	167
99	ERROR TRADEOFF CHARACTERISTIC: MUGSHOT IMAGES	168
100	ERROR TRADEOFF CHARACTERISTIC: MUGSHOT IMAGES	169
101	ERROR TRADEOFF CHARACTERISTIC: MUGSHOT IMAGES	170
102	ERROR TRADEOFF CHARACTERISTIC: MUGSHOT IMAGES	171
103	ERROR TRADEOFF CHARACTERISTIC: MUGSHOT IMAGES	172
104	ERROR TRADEOFF CHARACTERISTIC: MUGSHOT IMAGES	173
105	ERROR TRADEOFF CHARACTERISTIC: MUGSHOT IMAGES	174
106	ERROR TRADEOFF CHARACTERISTIC: MUGSHOT IMAGES	175
107	ERROR TRADEOFF CHARACTERISTIC: MUGSHOT IMAGES	176
108	ERROR TRADEOFF CHARACTERISTIC: MUGSHOT IMAGES	177
109	ERROR TRADEOFF CHARACTERISTIC: MUGSHOT IMAGES	178
110	ERROR TRADEOFF CHARACTERISTIC: MUGSHOT IMAGES	179
111	ERROR TRADEOFF CHARACTERISTIC: MUGSHOT IMAGES	180
112	ERROR TRADEOFF CHARACTERISTIC: MUGSHOT IMAGES	181
113	ERROR TRADEOFF CHARACTERISTIC: MUGSHOT IMAGES	182
114	ERROR TRADEOFF CHARACTERISTIC: MUGSHOT IMAGES	183
115	ERROR TRADEOFF CHARACTERISTIC: WILD IMAGES	184
116	ERROR TRADEOFF CHARACTERISTIC: WILD IMAGES	185
117	ERROR TRADEOFF CHARACTERISTIC: WILD IMAGES	186
118	ERROR TRADEOFF CHARACTERISTIC: WILD IMAGES	187
119	ERROR TRADEOFF CHARACTERISTIC: WILD IMAGES	188
120	ERROR TRADEOFF CHARACTERISTIC: WILD IMAGES	189
121	ERROR TRADEOFF CHARACTERISTIC: WILD IMAGES	190
122	ERROR TRADEOFF CHARACTERISTIC: WILD IMAGES	191
123	ERROR TRADEOFF CHARACTERISTIC: WILD IMAGES	192
124	ERROR TRADEOFF CHARACTERISTIC: WILD IMAGES	193
125	ERROR TRADEOFF CHARACTERISTIC: WILD IMAGES	194
126	ERROR TRADEOFF CHARACTERISTIC: WILD IMAGES	195
127	ERROR TRADEOFF CHARACTERISTIC: WILD IMAGES	196
128	ERROR TRADEOFF CHARACTERISTIC: WILD IMAGES	197
129	ERROR TRADEOFF CHARACTERISTIC: WILD IMAGES	198
130	ERROR TRADEOFF CHARACTERISTIC: WILD IMAGES	199
131	ERROR TRADEOFF CHARACTERISTIC: WILD IMAGES	200
132	ERROR TRADEOFF CHARACTERISTIC: WILD IMAGES	201
133	ERROR TRADEOFF CHARACTERISTIC: WILD IMAGES	202
134	ERROR TRADEOFF CHARACTERISTIC: WILD IMAGES	203
135	FALSE MATCH RATES WITHIN AND ACROSS DEMOGRAPHIC GROUPS	204
136	FALSE MATCH RATES WITHIN AND ACROSS DEMOGRAPHIC GROUPS	205
137	FALSE MATCH RATES WITHIN AND ACROSS DEMOGRAPHIC GROUPS	206
138	FALSE MATCH RATES WITHIN AND ACROSS DEMOGRAPHIC GROUPS	207
139	FALSE MATCH RATES WITHIN AND ACROSS DEMOGRAPHIC GROUPS	208
140	FALSE MATCH RATES WITHIN AND ACROSS DEMOGRAPHIC GROUPS	209
141	FALSE MATCH RATES WITHIN AND ACROSS DEMOGRAPHIC GROUPS	210

142	FALSE MATCH RATES WITHIN AND ACROSS DEMOGRAPHIC GROUPS	211
143	FALSE MATCH RATES WITHIN AND ACROSS DEMOGRAPHIC GROUPS	212
144	FALSE MATCH RATES WITHIN AND ACROSS DEMOGRAPHIC GROUPS	213
145	FALSE MATCH RATES WITHIN AND ACROSS DEMOGRAPHIC GROUPS	214
146	FALSE MATCH RATES WITHIN AND ACROSS DEMOGRAPHIC GROUPS	215
147	FALSE MATCH RATES WITHIN AND ACROSS DEMOGRAPHIC GROUPS	216
148	FALSE MATCH RATES WITHIN AND ACROSS DEMOGRAPHIC GROUPS	217
149	FALSE MATCH RATES WITHIN AND ACROSS DEMOGRAPHIC GROUPS	218
150	FALSE MATCH RATES WITHIN AND ACROSS DEMOGRAPHIC GROUPS	219
151	FALSE MATCH RATES WITHIN AND ACROSS DEMOGRAPHIC GROUPS	220
152	FALSE MATCH RATES WITHIN AND ACROSS DEMOGRAPHIC GROUPS	221
153	FALSE MATCH RATES WITHIN AND ACROSS DEMOGRAPHIC GROUPS	222
154	FALSE MATCH RATES WITHIN AND ACROSS DEMOGRAPHIC GROUPS	223
155	FALSE MATCH RATES WITHIN AND ACROSS DEMOGRAPHIC GROUPS	224
156	FALSE MATCH RATES WITHIN AND ACROSS DEMOGRAPHIC GROUPS	225
157	SEX AND RACE EFFECTS: MUGSHOT IMAGES	226
158	SEX AND RACE EFFECTS: MUGSHOT IMAGES	227
159	SEX AND RACE EFFECTS: MUGSHOT IMAGES	228
160	SEX AND RACE EFFECTS: MUGSHOT IMAGES	229
161	SEX AND RACE EFFECTS: MUGSHOT IMAGES	230
162	SEX AND RACE EFFECTS: MUGSHOT IMAGES	231
163	SEX AND RACE EFFECTS: MUGSHOT IMAGES	232
164	SEX AND RACE EFFECTS: MUGSHOT IMAGES	233
165	SEX AND RACE EFFECTS: MUGSHOT IMAGES	234
166	SEX AND RACE EFFECTS: MUGSHOT IMAGES	235
167	SEX AND RACE EFFECTS: MUGSHOT IMAGES	236
168	SEX AND RACE EFFECTS: MUGSHOT IMAGES	237
169	SEX AND RACE EFFECTS: MUGSHOT IMAGES	238
170	SEX AND RACE EFFECTS: MUGSHOT IMAGES	239
171	SEX AND RACE EFFECTS: MUGSHOT IMAGES	240
172	SEX AND RACE EFFECTS: MUGSHOT IMAGES	241
173	SEX AND RACE EFFECTS: MUGSHOT IMAGES	242
174	SEX AND RACE EFFECTS: MUGSHOT IMAGES	243
175	SEX AND RACE EFFECTS: MUGSHOT IMAGES	244
176	SEX AND RACE EFFECTS: MUGSHOT IMAGES	245
177	SEX AND RACE EFFECTS: MUGSHOT IMAGES	246
178	SEX AND RACE EFFECTS: MUGSHOT IMAGES	247
179	SEX AND RACE EFFECTS: MUGSHOT IMAGES	248
180	SEX AND RACE EFFECTS: MUGSHOT IMAGES	249
181	SEX EFFECTS: VISA IMAGES	250
182	SEX EFFECTS: VISA IMAGES	251
183	SEX EFFECTS: VISA IMAGES	252
184	SEX EFFECTS: VISA IMAGES	253
185	SEX EFFECTS: VISA IMAGES	254
186	SEX EFFECTS: VISA IMAGES	255
187	SEX EFFECTS: VISA IMAGES	256
188	SEX EFFECTS: VISA IMAGES	257
189	SEX EFFECTS: VISA IMAGES	258
190	SEX EFFECTS: VISA IMAGES	259
191	SEX EFFECTS: VISA IMAGES	260
192	SEX EFFECTS: VISA IMAGES	261
193	SEX EFFECTS: VISA IMAGES	262
194	SEX EFFECTS: VISA IMAGES	263
195	SEX EFFECTS: VISA IMAGES	264
196	SEX EFFECTS: VISA IMAGES	265
197	SEX EFFECTS: VISA IMAGES	266
198	SEX EFFECTS: VISA IMAGES	267

199	SEX EFFECTS: VISA IMAGES	268
200	SEX EFFECTS: VISA IMAGES	269
201	SEX EFFECTS: VISA IMAGES	270
202	SEX EFFECTS: VISA IMAGES	271
203	SEX EFFECTS: VISA IMAGES	272
204	SEX EFFECTS: VISA IMAGES	273
205	SEX EFFECTS: VISA IMAGES	274
206	SEX EFFECTS: VISA IMAGES	275
207	SEX EFFECTS: VISA IMAGES	276
208	SEX EFFECTS: VISA IMAGES	277
209	SEX EFFECTS: VISA IMAGES	278
210	SEX EFFECTS: VISA IMAGES	279
211	SEX EFFECTS: VISA IMAGES	280
212	SEX EFFECTS: VISA IMAGES	281
213	SEX EFFECTS: VISA IMAGES	282
214	SEX EFFECTS: VISA IMAGES	283
215	SEX EFFECTS: VISA IMAGES	284
216	SEX EFFECTS: VISA IMAGES	285
217	SEX EFFECTS: VISA IMAGES	286
218	SEX EFFECTS: VISA IMAGES	287
219	SEX EFFECTS: VISA IMAGES	288
220	FALSE MATCH RATE CALIBRATION: MUGSHOT IMAGES	289
221	FALSE MATCH RATE CALIBRATION: MUGSHOT IMAGES	290
222	FALSE MATCH RATE CALIBRATION: MUGSHOT IMAGES	291
223	FALSE MATCH RATE CALIBRATION: MUGSHOT IMAGES	292
224	FALSE MATCH RATE CALIBRATION: MUGSHOT IMAGES	293
225	FALSE MATCH RATE CALIBRATION: MUGSHOT IMAGES	294
226	FALSE MATCH RATE CALIBRATION: MUGSHOT IMAGES	295
227	FALSE MATCH RATE CALIBRATION: MUGSHOT IMAGES	296
228	FALSE MATCH RATE CALIBRATION: MUGSHOT IMAGES	297
229	FALSE MATCH RATE CALIBRATION: MUGSHOT IMAGES	298
230	FALSE MATCH RATE CALIBRATION: MUGSHOT IMAGES	299
231	FALSE MATCH RATE CALIBRATION: MUGSHOT IMAGES	300
232	FALSE MATCH RATE CALIBRATION: MUGSHOT IMAGES	301
233	FALSE MATCH RATE CALIBRATION: MUGSHOT IMAGES	302
234	FALSE MATCH RATE CALIBRATION: MUGSHOT IMAGES	303
235	FALSE MATCH RATE CALIBRATION: MUGSHOT IMAGES	304
236	FALSE MATCH RATE CALIBRATION: MUGSHOT IMAGES	305
237	FALSE MATCH RATE CALIBRATION: MUGSHOT IMAGES	306
238	FALSE MATCH RATE CALIBRATION: MUGSHOT IMAGES	307
239	FALSE MATCH RATE CALIBRATION: MUGSHOT IMAGES	308
240	FALSE MATCH RATE CALIBRATION: MUGSHOT IMAGES	309
241	FALSE MATCH RATE CALIBRATION: MUGSHOT IMAGES	310
242	FALSE MATCH RATE CALIBRATION: MUGSHOT IMAGES	311
243	FALSE MATCH RATE CALIBRATION: MUGSHOT IMAGES	312
244	FALSE MATCH RATE CALIBRATION: VISA IMAGES	313
245	FALSE MATCH RATE CALIBRATION: VISA IMAGES	314
246	FALSE MATCH RATE CALIBRATION: VISA IMAGES	315
247	FALSE MATCH RATE CALIBRATION: VISA IMAGES	316
248	FALSE MATCH RATE CALIBRATION: VISA IMAGES	317
249	FALSE MATCH RATE CALIBRATION: VISA IMAGES	318
250	FALSE MATCH RATE CALIBRATION: VISA IMAGES	319
251	FALSE MATCH RATE CALIBRATION: VISA IMAGES	320
252	FALSE MATCH RATE CALIBRATION: VISA IMAGES	321
253	FALSE MATCH RATE CALIBRATION: VISA IMAGES	322
254	FALSE MATCH RATE CALIBRATION: VISA IMAGES	323
255	FALSE MATCH RATE CALIBRATION: VISA IMAGES	324

256	FALSE MATCH RATE CALIBRATION: VISA IMAGES	325
257	FALSE MATCH RATE CALIBRATION: VISA IMAGES	326
258	FALSE MATCH RATE CALIBRATION: VISA IMAGES	327
259	FALSE MATCH RATE CALIBRATION: VISA IMAGES	328
260	FALSE MATCH RATE CALIBRATION: VISA IMAGES	329
261	FALSE MATCH RATE CALIBRATION: VISA IMAGES	330
262	FALSE MATCH RATE CALIBRATION: VISA IMAGES	331
263	FALSE MATCH RATE CALIBRATION: VISA IMAGES	332
264	FALSE MATCH RATE CALIBRATION: VISA IMAGES	333
265	FALSE MATCH RATE CALIBRATION: VISA IMAGES	334
266	FALSE MATCH RATE CALIBRATION: VISA IMAGES	335
267	FALSE MATCH RATE CALIBRATION: VISA IMAGES	336
268	FALSE MATCH RATE CALIBRATION: VISA IMAGES	337
269	FALSE MATCH RATE CALIBRATION: VISA IMAGES	338
270	FALSE MATCH RATE CALIBRATION: VISA IMAGES	339
271	FALSE MATCH RATE CALIBRATION: VISA IMAGES	340
272	FALSE MATCH RATE CALIBRATION: VISA IMAGES	341
273	FALSE MATCH RATE CALIBRATION: VISA IMAGES	342
274	FALSE MATCH RATE CALIBRATION: VISA IMAGES	343
275	FALSE MATCH RATE CALIBRATION: VISA IMAGES	344
276	FALSE MATCH RATE CALIBRATION: VISA IMAGES	345
277	FALSE MATCH RATE CALIBRATION: VISA IMAGES	346
278	FALSE MATCH RATE CALIBRATION: VISA IMAGES	347
279	FALSE MATCH RATE CALIBRATION: VISA IMAGES	348
280	FALSE MATCH RATE CALIBRATION: VISA IMAGES	349
281	FALSE MATCH RATE CALIBRATION: VISA IMAGES	350
282	FALSE MATCH RATE CALIBRATION: VISA IMAGES	351
283	FALSE MATCH RATE CALIBRATION: VISA IMAGES	352
284	FALSE MATCH RATE CALIBRATION: VISA IMAGES	353
285	FALSE MATCH RATE CALIBRATION: VISA IMAGES	354
286	FALSE MATCH RATE CALIBRATION: VISA IMAGES	355
287	FALSE MATCH RATE CALIBRATION: VISA IMAGES	356
288	FALSE MATCH RATE CALIBRATION: VISA IMAGES	357
289	FALSE MATCH RATE CALIBRATION: VISA IMAGES	358
290	FALSE MATCH RATE CALIBRATION: VISA IMAGES	359
291	FALSE MATCH RATE CALIBRATION: VISA IMAGES	360
292	EFFECT OF COUNTRY OF BIRTH ON FNMR	362
293	EFFECT OF COUNTRY OF BIRTH ON FNMR	363
294	EFFECT OF COUNTRY OF BIRTH ON FNMR	364
295	EFFECT OF COUNTRY OF BIRTH ON FNMR	365
296	EFFECT OF COUNTRY OF BIRTH ON FNMR	366
297	EFFECT OF COUNTRY OF BIRTH ON FNMR	367
298	EFFECT OF COUNTRY OF BIRTH ON FNMR	368
299	EFFECT OF COUNTRY OF BIRTH ON FNMR	369
300	EFFECT OF COUNTRY OF BIRTH ON FNMR	370
301	EFFECT OF COUNTRY OF BIRTH ON FNMR	371
302	EFFECT OF COUNTRY OF BIRTH ON FNMR	372
303	EFFECT OF COUNTRY OF BIRTH ON FNMR	373
304	EFFECT OF COUNTRY OF BIRTH ON FNMR	374
305	EFFECT OF COUNTRY OF BIRTH ON FNMR	375
306	EFFECT OF COUNTRY OF BIRTH ON FNMR	376
307	EFFECT OF COUNTRY OF BIRTH ON FNMR	377
308	EFFECT OF COUNTRY OF BIRTH ON FNMR	378
309	EFFECT OF COUNTRY OF BIRTH ON FNMR	379
310	EFFECT OF COUNTRY OF BIRTH ON FNMR	380
311	EFFECT OF COUNTRY OF BIRTH ON FNMR	381
312	EFFECT OF COUNTRY OF BIRTH ON FNMR	382

313	EFFECT OF COUNTRY OF BIRTH ON FNMR	383
314	EFFECT OF COUNTRY OF BIRTH ON FNMR	384
315	EFFECT OF COUNTRY OF BIRTH ON FNMR	385
316	EFFECT OF COUNTRY OF BIRTH ON FNMR	386
317	EFFECT OF COUNTRY OF BIRTH ON FNMR	387
318	EFFECT OF COUNTRY OF BIRTH ON FNMR	388
319	EFFECT OF COUNTRY OF BIRTH ON FNMR	389
320	EFFECT OF COUNTRY OF BIRTH ON FNMR	390
321	EFFECT OF COUNTRY OF BIRTH ON FNMR	391
322	EFFECT OF COUNTRY OF BIRTH ON FNMR	392
323	EFFECT OF COUNTRY OF BIRTH ON FNMR	393
324	EFFECT OF COUNTRY OF BIRTH ON FNMR	394
325	EFFECT OF COUNTRY OF BIRTH ON FNMR	395
326	EFFECT OF COUNTRY OF BIRTH ON FNMR	396
327	EFFECT OF COUNTRY OF BIRTH ON FNMR	397
328	EFFECT OF COUNTRY OF BIRTH ON FNMR	398
329	EFFECT OF COUNTRY OF BIRTH ON FNMR	399
330	EFFECT OF COUNTRY OF BIRTH ON FNMR	400
331	ERROR TRADEOFF CHARACTERISTIC: MUGSHOT IMAGES	402
332	ERROR TRADEOFF CHARACTERISTIC: MUGSHOT IMAGES	403
333	ERROR TRADEOFF CHARACTERISTIC: MUGSHOT IMAGES	404
334	ERROR TRADEOFF CHARACTERISTIC: MUGSHOT IMAGES	405
335	ERROR TRADEOFF CHARACTERISTIC: MUGSHOT IMAGES	406
336	ERROR TRADEOFF CHARACTERISTIC: MUGSHOT IMAGES	407
337	ERROR TRADEOFF CHARACTERISTIC: MUGSHOT IMAGES	408
338	ERROR TRADEOFF CHARACTERISTIC: MUGSHOT IMAGES	409
339	ERROR TRADEOFF CHARACTERISTIC: MUGSHOT IMAGES	410
340	ERROR TRADEOFF CHARACTERISTIC: MUGSHOT IMAGES	411
341	ERROR TRADEOFF CHARACTERISTIC: MUGSHOT IMAGES	412
342	ERROR TRADEOFF CHARACTERISTIC: MUGSHOT IMAGES	413
343	ERROR TRADEOFF CHARACTERISTIC: MUGSHOT IMAGES	414
344	ERROR TRADEOFF CHARACTERISTIC: MUGSHOT IMAGES	415
345	ERROR TRADEOFF CHARACTERISTIC: MUGSHOT IMAGES	416
346	ERROR TRADEOFF CHARACTERISTIC: MUGSHOT IMAGES	417
347	ERROR TRADEOFF CHARACTERISTIC: MUGSHOT IMAGES	418
348	ERROR TRADEOFF CHARACTERISTIC: MUGSHOT IMAGES	419
349	ERROR TRADEOFF CHARACTERISTIC: MUGSHOT IMAGES	420
350	ERROR TRADEOFF CHARACTERISTIC: MUGSHOT IMAGES	421
351	ERROR TRADEOFF CHARACTERISTIC: MUGSHOT IMAGES	422
352	ERROR TRADEOFF CHARACTERISTIC: MUGSHOT IMAGES	423
353	ERROR TRADEOFF CHARACTERISTIC: MUGSHOT IMAGES	424
354	ERROR TRADEOFF CHARACTERISTIC: MUGSHOT IMAGES	425
355	ERROR TRADEOFF CHARACTERISTIC: MUGSHOT IMAGES	426
356	ERROR TRADEOFF CHARACTERISTIC: MUGSHOT IMAGES	427
357	ERROR TRADEOFF CHARACTERISTIC: MUGSHOT IMAGES	428
358	ERROR TRADEOFF CHARACTERISTIC: MUGSHOT IMAGES	429
359	ERROR TRADEOFF CHARACTERISTIC: MUGSHOT IMAGES	430
360	EFFECT OF SUBJECT AGE ON FNMR	432
361	EFFECT OF SUBJECT AGE ON FNMR	433
362	EFFECT OF SUBJECT AGE ON FNMR	434
363	EFFECT OF SUBJECT AGE ON FNMR	435
364	EFFECT OF SUBJECT AGE ON FNMR	436
365	EFFECT OF SUBJECT AGE ON FNMR	437
366	EFFECT OF SUBJECT AGE ON FNMR	438
367	EFFECT OF SUBJECT AGE ON FNMR	439
368	EFFECT OF SUBJECT AGE ON FNMR	440

369	EFFECT OF SUBJECT AGE ON FNMR	441
370	EFFECT OF SUBJECT AGE ON FNMR	442
371	EFFECT OF SUBJECT AGE ON FNMR	443
372	EFFECT OF SUBJECT AGE ON FNMR	444
373	EFFECT OF SUBJECT AGE ON FNMR	445
374	EFFECT OF SUBJECT AGE ON FNMR	446
375	EFFECT OF SUBJECT AGE ON FNMR	447
376	EFFECT OF SUBJECT AGE ON FNMR	448
377	EFFECT OF SUBJECT AGE ON FNMR	449
378	EFFECT OF SUBJECT AGE ON FNMR	450
379	EFFECT OF SUBJECT AGE ON FNMR	451
380	EFFECT OF SUBJECT AGE ON FNMR	452
381	EFFECT OF SUBJECT AGE ON FNMR	453
382	EFFECT OF SUBJECT AGE ON FNMR	454
383	EFFECT OF SUBJECT AGE ON FNMR	455
384	EFFECT OF SUBJECT AGE ON FNMR	456
385	EFFECT OF SUBJECT AGE ON FNMR	457
386	EFFECT OF SUBJECT AGE ON FNMR	458
387	EFFECT OF SUBJECT AGE ON FNMR	459
388	EFFECT OF SUBJECT AGE ON FNMR	460
389	EFFECT OF SUBJECT AGE ON FNMR	461
390	EFFECT OF SUBJECT AGE ON FNMR	462
391	EFFECT OF SUBJECT AGE ON FNMR	463
392	EFFECT OF SUBJECT AGE ON FNMR	464
393	EFFECT OF SUBJECT AGE ON FNMR	465
394	EFFECT OF SUBJECT AGE ON FNMR	466
395	EFFECT OF SUBJECT AGE ON FNMR	467
396	EFFECT OF SUBJECT AGE ON FNMR	468
397	EFFECT OF SUBJECT AGE ON FNMR	469
398	EFFECT OF SUBJECT AGE ON FNMR	470
399	IMPOSTOR COUNTS FOR CROSS COUNTRY FMR CALCULATIONS	474

	Location	Developer Name	Short Name	Seq. Num.	Validation Date
1	NL	20Face	20face-000	000	2021-04-12
2	NL	20Face	20face-001	001	2021-09-29
3	US	3Divi	3divi-006	006	2021-04-14
4	US	3Divi	3divi-007	007	2021-09-27
5	TH	ACI Software	acisw-007	007	2021-11-15
6	TH	ACI Software	acisw-008	008	2022-03-22
7	US	AFIS and Biometrics Consulting	afisbiometrics-000	000	2022-01-27
8	US	AFR Engine	afrengine-000	000	2022-09-29
9	TW	ASUSTek Computer Inc	asusaics-000	000	2019-10-24
10	TW	ASUSTek Computer Inc	asusaics-001	001	2020-02-25
11	CN	AYF Technology	ayftech-001	001	2020-07-06
12	TW	Ability Enterprise - Andro Video	androvideo-000	000	2021-01-25
13	TW	Acer Incorporated	acer-001	001	2020-06-30
14	TW	Acer Incorporated	acer-002	002	2021-11-10
15	SG	Adera Global PTE	ader-a-003	003	2021-07-12
16	SG	Adera Global PTE	ader-a-004	004	2022-11-14
17	SG	Advancegroup	advance-003	003	2021-08-05
18	SG	Advancegroup	advance-004	004	2022-09-06
19	TH	Ai First	aifirst-001	001	2019-11-21
20	TW	AiUnion Technology	aiunionface-000	000	2019-10-22
21	TH	Aigen	aigen-001	001	2020-10-06
22	TH	Aigen	aigen-002	002	2021-03-15
23	CN	Aiseemu Technology	aiseemu-001	001	2022-06-16
24	CN	Aiseemu Technology	aiseemu-002	002	2022-11-18
25	KR	Ajou University	ajou-001	001	2021-03-08
26	ID	Akurat Satu Indonesia	ptakuratsatu-000	000	2020-09-11
27	KR	Alchera Inc	alchera-004	004	2022-08-12
28	KR	Alchera Inc	alchera-005	005	2023-01-04
29	ID	Alfabeta	alfabeta-001	001	2021-12-02
30	ES	Alice Biometrics	alice-000	000	2021-06-15
31	RU	Alivia / Innovation Sys	isystems-001	001	2018-06-12
32	RU	Alivia / Innovation Sys	isystems-002	002	2018-10-18
33	IN	AllGoVision	allgovision-000	000	2019-03-01
34	CN	AlphaSSTG	alphaface-001	001	2019-09-03
35	CN	AlphaSSTG	alphaface-002	002	2020-02-20
36	GB	Amplified Group	amplifiedgroup-001	001	2019-03-01
37	CN	Anke Investments	anke-004	004	2019-06-27
38	CN	Anke Investments	anke-005	005	2019-11-21
39	BR	Antheus Technologia	antheus-000	000	2019-12-05
40	BR	Antheus Technologia	antheus-001	001	2020-06-25
41	GB	AnyVision	anyvision-004	004	2018-06-15
42	GB	AnyVision	anyvision-005	005	2021-02-03
43	US	Armatura LLC	armatura-001	001	2022-01-04
44	US	Armatura LLC	armatura-003	003	2023-01-13
45	CN	AuthenMetric	authenmetric-003	003	2021-08-09
46	CN	AuthenMetric	authenmetric-004	004	2022-01-03
47	US	Aware	aware-005	005	2020-02-27
48	US	Aware	aware-006	006	2021-07-03
49	IN	Awidit Systems	awiroos-001	001	2019-09-23
50	IN	Awidit Systems	awiroos-002	002	2020-10-28
51	CH	Aximetria	aximetria-001	001	2022-08-10
52	JP	Ayonix	ayonix-000	000	2017-06-22
53	CN	BÖE Technology Group	boetech-001	001	2021-06-22
54	CN	BOE Technology Group	boetech-002	002	2021-12-21
55	ES	Bee the Data	beethedata-000	000	2021-07-26
56	CN	Beihang University-ERCACAT	ercacat-001	001	2020-07-06
57	CN	Beijing Alleyes Technology	alleyes-000	000	2020-03-09
58	CN	Beijing DeepSense Technologies	deepsense-000	000	2021-03-19
59	CN	Beijing DeepSense Technologies	deepsense-001	001	2022-03-11
60	CN	Beijing Hisign Technology	hisign-001	001	2021-09-24
61	CN	Beijing Hisign Technology	hisign-002	002	2022-09-09
62	CN	Beijing Mendaxia Technology	mendaxiatech-000	000	2021-09-15
63	CN	Beijing Vion Technology Inc	vion-000	000	2018-10-19
64	KZ	Beyne.AI	beyneai-000	000	2022-01-03
65	CH	BioID Technologies SA	bioidtechswiss-001	001	2020-08-28
66	CH	BioID Technologies SA	bioidtechswiss-002	002	2021-02-17
67	IN	Biocube Matrics	biocube-001	001	2021-09-08
68	UK	BitCenter UK	farfaces-001	001	2021-04-09
69	CN	Bitmain	bm-001	001	2018-10-17
70	CN	Bresee Technology	bresee-001	001	2020-12-30

Table 1: Summary of participant information included in this report.

	Location	Developer Name	Short Name	Seq. Num.	Validation Date
71	CN	Bresee Technology	bresee-002	002	2021-06-30
72	VN	CMC Institute of Science and Technology	cist-001	001	2022-10-20
73	CN	CSA IntelliCloud Technology	intellicloudai-001	001	2019-08-13
74	CN	CSA IntelliCloud Technology	intellicloudai-002	002	2020-12-17
75	TW	CTBC Bank	ctbcbank-000	000	2019-06-28
76	TW	CTBC Bank	ctbcbank-001	001	2019-10-28
77	KR	CUDO Communication	cudocommunication-001	001	2021-10-20
78	US	Camvi Technologies	camvi-002	002	2018-10-19
79	US	Camvi Technologies	camvi-004	004	2019-07-12
80	JP	Canon Inc	canon-003	003	2021-09-15
81	JP	Canon Inc	canon-004	004	2022-04-25
82	CN	China Electronics Import-Export Corp	ceiec-003	003	2020-01-06
83	CN	China Electronics Import-Export Corp	ceiec-004	004	2021-01-18
84	CN	China University of Petroleum	upc-001	001	2019-06-05
85	CN	Chinese University of Hong Kong	cuhkee-001	001	2020-03-18
86	KR	Chosun University	chosun-001	001	2020-07-01
87	KR	Chosun University	chosun-002	002	2020-11-25
88	TW	Chunghwa Telecom	chtface-005	005	2022-03-09
89	TW	Chunghwa Telecom	chtface-006	006	2022-11-03
90	US	Clearview AI Inc	clearviewai-000	000	2021-09-22
91	CN	Closeli Inc	closeli-001	001	2021-07-15
92	US	CloudSmart Consulting LLC	csc-002	002	2021-03-24
93	US	CloudSmart Consulting LLC	csc-003	003	2021-08-26
94	TW	Cloudmatrix	cloudmatrix-001	001	2022-02-16
95	TW	Cloudmatrix	cloudmatrix-002	002	2022-10-17
96	CN	Cloudwalk - Hengrui AI Technology	cloudwalk-hr-003	003	2020-09-25
97	CN	Cloudwalk - Hengrui AI Technology	cloudwalk-hr-004	004	2021-02-10
98	CN	Cloudwalk - Moontime Smart Technology	cloudwalk-mt-005	005	2022-03-29
99	CN	Cloudwalk - Moontime Smart Technology	cloudwalk-mt-006	006	2022-10-20
100	IN	Code Everest Pvt	facex-001	001	2021-03-08
101	IN	Code Everest Pvt	facex-002	002	2021-08-24
102	KR	Codeline	codeline-000	000	2022-09-13
103	DE	Cognitec Systems GmbH	cognitec-003	003	2021-07-30
104	DE	Cognitec Systems GmbH	cognitec-004	004	2022-02-10
105	TW	Coretech Knowledge Inc	coretech-000	000	2021-07-12
106	TW	Coretech Knowledge Inc	coretech-001	001	2022-09-29
107	IL	Corsight	corsight-002	002	2021-09-01
108	IL	Corsight	corsight-003	003	2022-06-09
109	IL	Cortica	cor-001	001	2020-09-24
110	TW	Cu-Face	cu-face-002	002	2023-01-05
111	KR	Cubox	cubox-001	001	2020-12-07
112	KR	Cubox	cubox-002	002	2021-08-24
113	JP	Cybercore	cybercore-002	002	2022-04-25
114	JP	Cybercore	cybercore-003	003	2022-08-31
115	US	Cyberextruder	cyberextruder-003	003	2022-03-16
116	US	Cyberextruder	cyberextruder-004	004	2022-07-20
117	TW	Cyberlink Corp	cyberlink-009	009	2022-05-12
118	TW	Cyberlink Corp	cyberlink-010	010	2022-09-16
119	MX	DICIO	dicio-001	001	2022-03-22
120	CN	DSK	dsk-000	000	2019-06-28
121	CN	Dahua Technology	dahua-006	006	2020-12-30
122	CN	Dahua Technology	dahua-007	007	2021-12-20
123	IE	Daon	daon-000	000	2021-11-03
124	US	Decatur Industries Inc	decatur-000	000	2020-08-18
125	US	Decatur Industries Inc	decatur-001	001	2021-09-27
126	CN	Deepglint	deepglint-004	004	2021-09-17
127	CN	Deepglint	deepglint-005	005	2022-10-17
128	FR	Deepsense	dps-000	000	2021-07-16
129	DE	Dermalog	dermalog-010	010	2022-07-25
130	DE	Dermalog	dermalog-011	011	2022-12-12
131	CN	DiDi ChuXing Technology	didiglobalface-001	001	2019-10-23
132	CN	DiDi ChuXing Technology	didiglobalface-002	002	2023-01-09
133	IN	Digidata	didata-000	000	2022-01-27
134	IN	Digidata	didata-001	001	2022-06-10
135	GB	Digital Barriers	digitalbarriers-002	002	2019-03-01
136	TR	Ekin Smart City Technologies	ekin-002	002	2021-05-04
137	RU	Enface	enface-000	000	2021-04-09
138	RU	Enface	enface-001	001	2021-12-17
139	CH	Euronovate SA	euronovate-001	001	2021-11-15
140	RU	Expasoft LLC	expasoft-001	001	2020-09-03

Table 2: Summary of participant information included in this report.

	Location	Developer Name	Short Name	Seq. Num.	Validation Date
141	RU	Expasoft LLC	expasoft-002	002	2021-07-26
142	US	FRP LLC	frpkauai-001	001	2022-07-18
143	US	FRP LLC	frpkauai-002	002	2022-11-21
144	DE	FaceOnLive Inc	faceonlive-001	001	2021-11-23
145	DE	FaceOnLive Inc	faceonlive-002	002	2022-04-11
146	ES	FacePhi	facephi-000	000	2022-04-06
147	GB	FaceSoft	facesoft-000	000	2019-07-10
148	KR	FaceTag Co	facetag-000	000	2021-03-22
149	KR	FaceTag Co	facetag-002	002	2022-01-06
150	TW	FarBar Inc	f8-001	001	2019-07-11
151	TW	FarBar Inc	f8-002	002	2022-03-02
152	CN	Fiberhome Telecommunication Technologies	fiberhome-nanjing-003	003	2021-03-12
153	CN	Fiberhome Telecommunication Technologies	fiberhome-nanjing-004	004	2021-09-14
154	UK	Fincore Ltd	fincore-000	000	2021-06-07
155	KZ	First Credit Bureau Kazakhstan	firstcreditKZ-001	001	2022-08-22
156	CN	Fujitsu Research and Development Center	fujitsulab-002	002	2021-02-24
157	CN	Fujitsu Research and Development Center	fujitsulab-003	003	2021-07-12
158	US	Gemalto Cogent	cogent-007	007	2022-04-11
159	US	Gemalto Cogent	cogent-008	008	2023-01-03
160	TW	GeoVision Inc	geo-002	002	2021-04-01
161	TW	GeoVision Inc	geo-004	004	2022-02-10
162	JP	Glory	glory-004	004	2022-02-08
163	JP	Glory	glory-005	005	2022-07-08
164	TW	Gorilla Technology	gorilla-008	008	2021-11-08
165	TW	Gorilla Technology	gorilla-009	009	2022-12-14
166	US	Graymatics	graymatics-001	001	2022-01-13
167	US	Griaule	griaule-001	001	2022-05-31
168	US	Griaule	griaule-002	002	2022-12-02
169	CN	Guangzhou Pixel Solutions	pixelall-008	008	2022-06-16
170	CN	Guangzhou Pixel Solutions	pixelall-009	009	2022-10-26
171	CN	Hangzhuo Allu Network Information Technology	hzailu-002	002	2022-06-02
172	CN	Hangzhuo Allu Network Information Technology	hzailu-003	003	2022-10-11
173	ES	Herta Security	hertasecurity-001	001	2022-01-18
174	ES	Herta Security	hertasecurity-002	002	2022-09-02
175	CN	Hikvision Research Institute	hik-001	001	2019-03-01
176	IN	HyperVerge Inc	hyperverge-003	003	2022-04-11
177	IN	HyperVerge Inc	hyperverge-004	004	2022-12-14
178	AU	ICM Airport Technics	icm-003	003	2021-09-06
179	AU	ICM Airport Technics	icm-004	004	2022-09-07
180	FR	ID3 Technology	id3-006	006	2020-12-17
181	FR	ID3 Technology	id3-008	008	2021-11-10
182	CA	IMDS Software	imds-software-001	001	2022-07-06
183	RU	ITMO University	itmo-007	007	2020-01-06
184	RU	ITMO University	itmo-008	008	2021-11-19
185	RU	IVA Cognitive	ivacognitive-001	001	2021-01-29
186	FR	Idemia	idemia-008	008	2021-07-07
187	FR	Idemia	idemia-009	009	2022-07-27
188	US	Imageware Systems	iws-000	000	2020-08-12
189	GB	Imperial College London	imperial-000	000	2019-03-01
190	GB	Imperial College London	imperial-002	002	2019-08-28
191	US	Incode Technologies Inc	incode-010	010	2021-10-22
192	US	Incode Technologies Inc	incode-011	011	2022-08-10
193	IT	InfoCert	infocert-001	001	2022-09-08
194	IN	Innef Labs	innefulabs-000	000	2020-09-04
195	GB	Innovative Technology	innovativetechnologyltd-001	001	2019-10-22
196	GB	Innovative Technology	innovativetechnologyltd-002	002	2020-02-26
197	SK	Innovatrics	innovatrics-008	008	2021-12-15
198	SK	Innovatrics	innovatrics-009	009	2022-01-19
199	CN	InsightFace AI	insightface-001	001	2021-09-27
200	CN	InsightFace AI	insightface-003	003	2022-08-23
201	CN	Inspur (Beijing) Electronic Information Industry Co	inspur-000	000	2022-07-19
202	CN	Institute of Computing Technology	ichthtc-000	000	2020-11-29
203	RU	Institute of Information Technologies	iit-002	002	2019-12-04
204	RU	Institute of Information Technologies	iit-003	003	2020-12-01
205	IS	Intel Research Group	intelresearch-005	005	2022-02-13
206	IS	Intel Research Group	intelresearch-006	006	2022-12-19
207	KR	IntelliVIX	intellivix-002	002	2022-07-14
208	KR	IntelliVIX	intellivix-003	003	2022-12-12
209	AE	Intellibrain Technological Projects	g42-intellibrain-001	001	2022-07-27
210	US	Intellivision	intellivision-003	003	2022-03-07

Table 3: Summary of participant information included in this report.

	Location	Developer Name	Short Name	Seq. Num.	Validation Date
211	US	Intellivision	intellivision-004	004	2022-07-28
212	LU	Intema-LGL Group	intema-000	000	2022-07-15
213	LU	Intema-LGL Group	intema-001	001	2023-01-11
214	US	IrexAI	irex-000	000	2020-12-17
215	IL	Is It You	isityou-000	000	2017-06-26
216	MX	Jaak IT	jaakit-001	001	2022-05-20
217	KR	Kakao Enterprise	kakao-007	007	2022-01-12
218	KR	Kakao Enterprise	kakao-008	008	2022-05-12
219	KR	Kakao Pay Corp	kakaopay-001	001	2021-07-06
220	TH	Kasikorn Labs	kasikornlabs-000	000	2022-03-02
221	TH	Kasikorn Labs	kasikornlabs-002	002	2022-12-13
222	SG	Kedacom International Pte	kedacom-000	000	2019-06-03
223	US	Kneron Inc	kneron-003	003	2019-07-01
224	US	Kneron Inc	kneron-005	005	2020-02-21
225	US	KnowUTech LLC	knowutech-000	000	2022-02-13
226	KR	Kookmin University	kookmin-002	002	2021-03-05
227	KR	Korea Identification Inc	koreaid-001	001	2022-12-12
228	TH	Krungthai	krungthai-002	002	2022-06-21
229	CN	KuKe3D Technology	kuke3d-001	001	2021-10-28
230	CN	KuKe3D Technology	kuke3d-002	002	2022-04-14
231	MX	Lebentech Biometrics	lebentech-000	000	2022-02-16
232	IN	Lema Labs	lemalabs-001	001	2021-04-13
233	JP	Line Corporation	lineclova-002	002	2022-05-18
234	JP	Line Corporation	lineclova-003	003	2022-11-28
235	RU	Lomonosov Moscow State University	intsysmsu-001	001	2019-10-22
236	RU	Lomonosov Moscow State University	intsysmsu-002	002	2020-03-12
237	IN	Lookman Electroplast Industries	lookman-002	002	2018-06-13
238	IN	Lookman Electroplast Industries	lookman-004	004	2019-06-03
239	US	Luxand Inc	luxand-000	000	2019-11-07
240	RU	MVision	mvision-001	001	2019-11-12
241	IN	Mantra Softech India	mantra-000	000	2021-10-28
242	CN	Maxvision Technology	maxvision-002	002	2022-07-12
243	CN	Maxvision Technology	maxvision-003	003	2022-11-14
244	CN	Megvii/Face++	megvii-005	005	2022-03-28
245	CN	Megvii/Face++	megvii-006	006	2022-08-08
246	KR	Metsakuur	metsakuurcompany-001	001	2022-05-12
247	KR	Metsakuur	metsakuurcompany-002	002	2022-09-14
248	CN	Miaxis Biometrics	miaxis-001	001	2022-11-15
249	GB	MicroFocus	microfocus-001	001	2018-06-13
250	GB	MicroFocus	microfocus-002	002	2018-10-17
251	CN	Minivision	minivision-000	000	2020-10-28
252	NO	Mobai	mobai-000	000	2020-08-26
253	NO	Mobai	mobai-001	001	2021-02-17
254	ES	Mobbeel Solutions	mobbl-001	001	2021-06-16
255	ES	Mobbeel Solutions	mobbl-003	003	2022-04-19
256	KR	Mobipin Technology	mobipintech-000	000	2021-11-23
257	TH	Momentum Digital	sertis-000	000	2019-10-07
258	TH	Momentum Digital	sertis-002	002	2021-05-13
259	CN	MoreDian Technology	moreedian-000	000	2021-02-24
260	US	Mukh Technologies	mukh-001	001	2022-03-22
261	US	Mukh Technologies	mukh-002	002	2022-11-01
262	CN	Multi-Modality Intelligence	multimodality-000	000	2021-10-19
263	CN	Multi-Modality Intelligence	multimodality-001	001	2022-05-16
264	RU	N-Tech Lab	ntechlab-011	011	2021-09-13
265	RU	N-Tech Lab	ntechlab-012	012	2022-01-20
266	CA	NEO Systems	neosystems-004	004	2022-05-02
267	KR	NHN Corp	nhn-002	002	2021-07-15
268	KR	NHN Corp	nhn-003	003	2022-02-22
269	KR	NSENSE Corp	nsensecorp-003	003	2021-10-29
270	KR	NSENSE Corp	nsensecorp-004	004	2022-09-08
271	CN	Nanjing Kiwi Network Technology	kiwitech-000	000	2021-03-19
272	KR	Neosecu Co	openface-001	001	2021-06-15
273	TW	Netbridge Technology Incoporation	netbridgegetech-001	001	2020-01-08
274	TW	Netbridge Technology Incoporation	netbridgegetech-002	002	2020-08-11
275	LT	Neurotechnology	neurotechnology-013	013	2022-01-07
276	LT	Neurotechnology	neurotechnology-015	015	2022-06-07
277	ID	Nodeflux	nodeflux-002	002	2019-08-13
278	IN	NotionTag Technologies Private Limited	notionntag-001	001	2021-03-04
279	IN	NotionTag Technologies Private Limited	notionntag-002	002	2021-09-17
280	US	Omnigarde Ltd	omnigarde-001	001	2021-08-23

Table 4: Summary of participant information included in this report.

	Location	Developer Name	Short Name	Seq. Num.	Validation Date
281	US	Omnigarde Ltd	omnigarde-002	002	2022-01-19
282	KR	One More Security	omface-000	000	2021-12-15
283	KR	One More Security	omface-001	001	2022-10-21
284	UK	Onfido	onfido-000	000	2022-12-13
285	RU	Oz Forensics LLC	oz-003	003	2021-08-09
286	RU	Oz Forensics LLC	oz-004	004	2021-12-13
287	TW	PAPAGO Inc	papago-001	001	2022-07-19
288	ID	PT Autentika Digital Indonesia	autentika-000	000	2022-12-05
289	ID	PT Qlue Performa Indonesia	qluevision-001	001	2022-11-15
290	CH	PXL Vision AG	pxl-001	001	2020-06-30
291	TW	Palit Microsystems	palit-000	000	2022-05-16
292	TW	Palit Microsystems	palit-001	001	2022-09-26
293	SG	Panasonic R+D Center Singapore	psl-010	010	2022-04-19
294	SG	Panasonic R+D Center Singapore	psl-011	011	2022-10-06
295	US	Pangiam	pangiam-000	000	2022-04-04
296	TR	Papilon Savunma	papsav1923-002	002	2022-01-20
297	TR	Papilon Savunma	papsav1923-003	003	2022-11-25
298	US	Paravision (EverAI)	paravision-010	010	2022-02-02
299	US	Paravision (EverAI)	paravision-011	011	2022-12-12
300	SG	Pensees Pte	pensees-001	001	2020-08-17
301	IN	Pyramid Cyber Security + Forensic (P)	pyramid-000	000	2019-11-04
302	KZ	Qaz Biometric Systems	qazbs-000	000	2022-06-22
303	TW	Qnap Security	qnap-002	002	2022-04-15
304	TW	Qnap Security	qnap-003	003	2022-12-09
305	CZ	Quantasoft	quantasoft-003	003	2021-04-19
306	US	Rank One Computing	rankone-013	013	2022-07-09
307	US	Rank One Computing	rankone-014	014	2022-12-21
308	US	Realnetworks Inc	realnetworks-007	007	2022-06-14
309	US	Realnetworks Inc	realnetworks-008	008	2022-11-10
310	US	Regula Forensics	regula-000	000	2021-04-13
311	US	Regula Forensics	regula-001	001	2021-12-14
312	CN	Remark Holdings	remarkai-001	001	2019-03-01
313	CN	Remark Holdings	remarkai-003	003	2021-06-22
314	SG	Rendip	rendip-000	000	2021-04-19
315	UK	Reveal Media Ltd	revealmedia-005	005	2021-09-24
316	UK	Reveal Media Ltd	revealmedia-006	006	2022-01-26
317	CN	Rokid Corporation	rokid-000	000	2019-08-01
318	CN	Rokid Corporation	rokid-001	001	2019-12-13
319	KR	SK Telecom	sktelecom-000	000	2021-07-09
320	KR	SQIsoft	sqisoft-002	002	2021-11-03
321	KR	SQIsoft	sqisoft-003	003	2022-10-26
322	SA	STCON LLC	stcon-000	000	2022-11-02
323	DE	Saffe	saffe-001	001	2018-10-19
324	DE	Saffe	saffe-002	002	2019-03-01
325	JP	Saga Densan Center Co Ltd	sdc-000	000	2022-10-18
326	KR	Samsung S1 Corp	s1-005	005	2022-06-17
327	KR	Samsung S1 Corp	s1-006	006	2022-10-17
328	KR	Samsung-SDS	samsungsds-001	001	2022-04-18
329	KR	Samsung-SDS	samsungsds-002	002	2022-09-16
330	IN	Samtech InfoNet Limited	samtech-001	001	2019-10-15
331	RU	Satellite Innovation/Eocortex	eocortex-000	000	2020-08-26
332	IL	Scanovate	scanovate-002	002	2020-06-26
333	IL	Scanovate	scanovate-003	003	2021-11-15
334	RO	Securif AI	securifai-005	005	2022-05-16
335	RO	Securif AI	securifai-006	006	2022-11-14
336	CN	Sensetime Group	sensetime-007	007	2022-06-17
337	CN	Sensetime Group	sensetime-008	008	2023-01-04
338	SG	Seventh Sense Artificial Intelligence	seventhsense-001	001	2022-03-04
339	SG	Seventh Sense Artificial Intelligence	seventhsense-002	002	2022-10-17
340	US	Shaman Software	shaman-000	000	2017-12-05
341	US	Shaman Software	shaman-001	001	2018-01-13
342	CN	Shanghai Jiao Tong University	sjtu-003	003	2020-11-02
343	CN	Shanghai Jiao Tong University	sjtu-004	004	2021-05-13
344	CN	Shanghai Ulucu Electronics Technology	uluface-002	002	2019-07-10
345	CN	Shanghai Ulucu Electronics Technology	uluface-003	003	2019-11-12
346	CN	Shanghai University - Shanghai Film Academy	shu-002	002	2019-12-10
347	CN	Shanghai University - Shanghai Film Academy	shu-003	003	2020-06-24
348	CN	Shanghai Yitu Technology	yitu-003	003	2019-03-01
349	CN	Shenzhen AiMall Tech	aimall-002	002	2020-03-12
350	CN	Shenzhen AiMall Tech	aimall-003	003	2020-08-12

Table 5: Summary of participant information included in this report.

	Location	Developer Name	Short Name	Seq. Num.	Validation Date
351	CN	Shenzhen EI Networks	einetworks-000	000	2019-08-13
352	CN	Shenzhen Inst Adv Integrated Tech CAS	siat-002	002	2018-06-13
353	CN	Shenzhen Inst Adv Integrated Tech CAS	siat-005	005	2022-02-08
354	CN	Shenzhen Intellifusion Technologies	intellifusion-001	001	2019-08-22
355	CN	Shenzhen Intellifusion Technologies	intellifusion-002	002	2020-03-18
356	CN	Shenzhen University-Macau University of Science and Technology	sztu-000	000	2020-12-17
357	CN	Shenzhen University-Macau University of Science and Technology	sztu-001	001	2021-07-13
358	RU	Smart Engines	smartengines-000	000	2021-08-25
359	RU	Smart Engines	smartengines-001	001	2022-05-31
360	ES	Smartbiometrik	smartbiometrik-001	001	2022-05-16
361	TR	Smarvist Teknoloji	smartvist-000	000	2022-05-10
362	DE	Smilart	smilart-002	002	2018-02-06
363	DE	Smilart	smilart-003	003	2019-03-01
364	TR	Sodec App Inc	sodec-000	000	2021-06-02
365	IN	Staqu Technologies	stagu-000	000	2020-07-15
366	CN	Star Hybrid Limited	starhybrid-001	001	2019-06-19
367	CN	Su Zhou NaZhiTianDi intelligent technology	nazhai-000	000	2020-06-25
368	IN	Sukshi Technology Innovation	sukshi-000	000	2022-02-13
369	KR	Suprema AI Inc	suprema-003	003	2022-07-20
370	KR	Suprema AI Inc	suprema-004	004	2023-01-09
371	KR	Suprema ID Inc	supremaid-001	001	2021-05-04
372	KR	Suprema ID Inc	supremaid-002	002	2022-06-24
373	RU	Synesis	synesis-006	006	2019-10-10
374	RU	Synesis	synesis-007	007	2020-06-24
375	TW	Synology Inc	synology-000	000	2019-10-23
376	TW	Synology Inc	synology-002	002	2020-08-20
377	BR	T4isB	t4isb-000	000	2022-01-28
378	CN	TUPU Technology	tuputech-000	000	2019-10-11
379	TW	Taiwan AI Labs	ailabs-001	001	2019-12-18
380	TW	Taiwan-Certificate Authority Incorporation	twface-000	000	2021-05-14
381	TW	Taiwan-Certificate Authority Incorporation	twface-001	001	2021-09-14
382	CH	Tech5 SA	tech5-005	005	2020-07-24
383	CH	Tech5 SA	tech5-007	007	2022-12-30
384	TR	Techsign	techsign-000	000	2021-08-25
385	TR	Techsign	techsign-001	001	2022-07-01
386	CN	Tencent Deepsea Lab	deepsea-001	001	2019-06-03
387	RU	Tevian	tevian-007	007	2021-08-06
388	RU	Tevian	tevian-008	008	2021-12-06
389	US	TigerIT Americas LLC	tiger-005	005	2021-07-29
390	US	TigerIT Americas LLC	tiger-006	006	2021-12-13
391	RU	Tinkoff Bank	tinkoff-001	001	2021-05-13
392	CN	TongYi Transportation Technology	tongyi-005	005	2019-06-12
393	TW	Toppan ID Gate	toppanidgate-000	000	2021-09-28
394	JP	Toshiba	toshiba-004	004	2021-09-27
395	JP	Toshiba	toshiba-006	006	2022-06-29
396	ES	Touchless ID	touchlessid-000	000	2022-05-02
397	ES	Touchless ID	touchlessid-001	001	2022-09-21
398	JP	Tripleize	aize-001	001	2021-04-23
399	JP	Tripleize	aize-002	002	2021-10-08
400	VN	TrueID-VNG	trueidvng-001	001	2023-01-05
401	US	Trueface.ai	trueface-002	002	2021-03-29
402	US	Trueface.ai	trueface-003	003	2021-09-30
403	CN	TuringTech.vip	turingtechvip-001	001	2022-02-03
404	CN	TuringTech.vip	turingtechvip-002	002	2022-07-27
405	TR	Turkcell Technology	turkcell-000	000	2022-10-11
406	CN	ULSee Inc	ulsee-001	001	2019-07-31
407	TW	UXLabs	uxlabs-001	001	2022-09-19
408	FR	Unissey	unissey-002	002	2022-04-29
409	FR	Unissey	unissey-003	003	2022-12-19
410	PT	Universidade de Coimbra	visteam-004	004	2022-08-01
411	PT	Universidade de Coimbra	visteam-005	005	2023-01-04
412	UK	University of Surrey-CVSSP	surrey-cvssp-000	000	2022-03-25
413	UK	University of Surrey-CVSSP	surrey-cvssp-001	001	2022-09-22
414	US	VCognition	vcog-002	002	2017-06-12
415	ES	Veridas Digital Authentication Solutions S.L.	veridas-007	007	2021-09-02
416	ES	Veridas Digital Authentication Solutions S.L.	veridas-008	008	2022-10-17
417	UK	Veridium	veridium-000	000	2022-03-28
418	UK	Veridium	veridium-001	001	2022-11-03
419	KZ	Verigram	verigram-000	000	2021-09-06
420	KZ	Verigram	verigram-001	001	2022-03-09

Table 6: Summary of participant information included in this report.

	Location	Developer Name	Short Name	Seq. Num.	Validation Date
421	ID	Verihubs	verihubs-inteligensia-000	000	2021-07-27
422	ID	Verihubs	verihubs-inteligensia-001	001	2022-06-16
423	ID	Verijelas	verijelas-000	000	2022-08-01
424	TW	Via Technologies Inc	via-000	000	2019-07-08
425	TW	Via Technologies Inc	via-001	001	2020-01-08
426	DE	Videmo Intelligent Videoanalyse	videmo-001	001	2021-12-22
427	DE	Videmo Intelligent Videoanalyse	videmo-002	002	2022-08-31
428	IN	Videonetics Technology Pvt	videonetics-001	001	2019-06-19
429	IN	Videonetics Technology Pvt	videonetics-002	002	2019-11-21
430	VN	Vietnam Posts and Telecommunications Group	vnpt-004	004	2022-04-15
431	VN	Vietnam Posts and Telecommunications Group	vnpt-005	005	2022-08-24
432	VN	Viettel Group	vts-000	000	2020-11-04
433	VN	Viettel Group	vts-001	001	2022-04-20
434	VN	Viettel High Technology	viettelhightech-000	000	2021-08-04
435	US	Vigilant Solutions	vigilantsolutions-010	010	2021-04-07
436	US	Vigilant Solutions	vigilantsolutions-011	011	2021-08-07
437	VN	VinAI Research VietNam	vinai-000	000	2020-09-24
438	VN	VinBigData	vinbigdata-001	001	2022-01-06
439	VN	VinBigData	vinbigdata-002	002	2022-06-07
440	SE	Visage Technologies	visage-000	000	2020-12-09
441	FI	Visidon	vd-002	002	2021-04-12
442	FI	Visidon	vd-003	003	2021-10-12
443	CN	Vision Intelligence Center of Meituan	meituan-001	001	2022-03-25
444	CN	Vision Intelligence Center of Meituan	meituan-002	002	2022-09-14
445	PT	Vision-Box	visionbox-001	001	2019-03-01
446	PT	Vision-Box	visionbox-002	002	2021-04-29
447	RU	VisionLabs	visionlabs-010	010	2021-01-25
448	RU	VisionLabs	visionlabs-011	011	2021-10-13
449	AU	Vixvizon	vixvization-006	006	2022-08-11
450	AU	Vixvizon	vixvization-007	007	2023-01-17
451	RU	Vocord	vocord-009	009	2020-12-28
452	RU	Vocord	vocord-010	010	2021-12-20
453	US	Wicket	wicket-000	000	2022-02-14
454	CN	Winsense	winsense-001	001	2019-10-16
455	CN	Winsense	winsense-002	002	2020-11-20
456	MY	Wise AI SDN BHD	wiseai-001	001	2022-10-25
457	CN	Wuhan Tianyu Information Industry	wuhantianyu-001	001	2021-08-05
458	CN	X-Laboratory	x-laboratory-000	000	2019-09-03
459	CN	X-Laboratory	x-laboratory-001	001	2020-01-21
460	CN	Xforward AI Technology	xforwardai-001	001	2020-09-25
461	CN	Xforward AI Technology	xforwardai-002	002	2021-02-10
462	CN	Xiamen Meiya Pico Information	meiya-001	001	2019-03-01
463	CN	Xiamen University	xm-000	000	2020-10-19
464	PT	YooniK	yoonik-002	002	2021-09-06
465	PT	YooniK	yoonik-003	003	2022-01-06
466	TW	Yuan High-Tech Development	yuan-005	005	2022-06-22
467	TW	Yuan High-Tech Development	yuan-006	006	2022-12-14
468	CN	Yuntu Data and Technology	ytu-000	000	2021-06-16
469	CN	Zhuhai Yisheng Electronics Technology	yisheng-004	004	2018-06-12
470	CN	iQIYI Inc	iqface-000	000	2019-06-04
471	CN	iQIYI Inc	iqface-003	003	2021-02-23
472	TW	iSAP Solution Corporation	isap-001	001	2019-08-07
473	TW	iSAP Solution Corporation	isap-002	002	2020-09-01
474	TW	ioNetworks Inc	ionetworks-000	000	2021-07-20

Table 7: Summary of participant information included in this report.

ALGORITHM			CONFIG	LIBRARY	TEMPLATE						COMPARISON ⁴	
NAME		DATA	DATA	MEMORY	SIZE	GENERATION TIME (ms) ⁴				TIME (ns) ⁵		
		(KB) ¹	(KB) ²	(MB) ³	(B)	MUGSHOT	480x720	960x1440	1600x2400	3000x4500	GENUINE	IMPOSTOR
1	20face-000	117155	324083	²¹² 905	¹⁹⁹ 2048 ± 0	⁴² 232 ± 1	³⁰ 223 ± 1	²⁶ 226 ± 4	²² 222 ± 1	¹⁶ 224 ± 1	⁴⁴⁵ 44880 ± 134	⁴⁴³ 44462 ± 163
2	20face-001	226824	324119	³⁷¹ 1940	⁴³⁶ 4096 ± 0	⁵³ 279 ± 2	³⁷ 266 ± 1	²⁹ 266 ± 1	²⁸ 267 ± 1	²³ 267 ± 0	³⁵⁰ 5553 ± 54	³⁴⁸ 5541 ± 65
3	3divi-006	273866	52656	⁸⁹ 472	²⁹⁵ 2048 ± 0	²⁰⁹ 654 ± 1	¹⁷⁴ 651 ± 0	¹⁵⁷ 660 ± 1	¹⁴¹ 678 ± 2	¹³⁹ 759 ± 13	¹¹³ 775 ± 19	¹¹² 770 ± 22
4	3divi-007	483115	24723	²⁹⁴ 1285	¹⁴⁶ 2048 ± 0	¹⁸⁸ 615 ± 1	¹⁶¹ 616 ± 1	¹⁴⁴ 623 ± 1	¹²⁷ 644 ± 1	¹³⁰ 727 ± 5	¹⁰¹ 707 ± 31	¹⁰¹ 712 ± 25
5	acer-001	36650	66086	⁷⁴ 417	²⁸ 512 ± 0	³⁶ 199 ± 0	³³ 237 ± 28	²⁷ 229 ± 26	²⁷ 242 ± 37	²¹ 259 ± 21	²⁶² 2453 ± 44	²⁶³ 2461 ± 62
6	acer-002	43922	624858	³⁸ 187	²⁹⁹ 2048 ± 0	³¹ 184 ± 0	²³ 184 ± 0	¹⁷ 185 ± 0	¹⁴ 185 ± 0	¹³ 186 ± 0	³⁰³ 3370 ± 47	³⁰³ 3350 ± 54
7	acisw-007	267619	36111	⁵² 286	²³² 2048 ± 0	⁵⁸ 283 ± 0	⁴⁷ 293 ± 3	⁶² 414 ± 0	⁵⁴ 404 ± 0	⁵⁵ 484 ± 1	¹⁷³ 1316 ± 22	¹⁷³ 1297 ± 23
8	acisw-008	171703	39359	²⁸⁵ 1101	²¹⁰ 2048 ± 0	⁹⁶ 400 ± 1	⁶⁶ 362 ± 28	⁵⁰ 369 ± 9	³³ 300 ± 2	²⁸ 336 ± 5	¹⁷⁴ 1327 ± 19	¹⁷⁶ 1337 ± 32
9	adera-003	0	749778	²¹⁷ 917	⁴⁵⁷ 5120 ± 0	⁴⁴¹ 1381 ± 12	⁴¹⁰ 1385 ± 1	⁴⁰⁹ 1394 ± 1	³⁸⁴ 1401 ± 1	³³⁶ 1469 ± 1	²⁴⁶ 2148 ± 34	²⁴⁶ 2130 ± 32
10	adera-004	0	959123	³⁵⁵ 1748	⁴⁶⁰ 6144 ± 0	⁴⁰⁹ 1246 ± 1	³⁶⁴ 1204 ± 1	³⁵⁶ 1230 ± 2	³²¹ 1207 ± 2	²⁷¹ 1254 ± 1	²²⁰ 1840 ± 34	²¹⁹ 1828 ± 31
11	advance-003	258867	78699	¹⁰² 518	³²⁸ 2048 ± 0	¹⁷⁵ 586 ± 0	¹⁴⁸ 584 ± 0	¹²⁸ 583 ± 0	¹⁰⁸ 588 ± 0	⁸⁶ 591 ± 1	²¹⁹ 1813 ± 17	²¹⁵ 1788 ± 26
12	advance-004	803133	954494	¹⁴⁴ 679	¹¹⁰ 2048 ± 0	³⁶⁷ 1099 ± 20	³³⁸ 1107 ± 15	³¹⁹ 1093 ± 21	²⁸² 1103 ± 21	²⁴⁰ 1138 ± 21	²³² 1935 ± 35	²³⁴ 1936 ± 32
13	afisbiometrics-000	545886	32882	²⁵² 1088	³⁹ 512 ± 0	⁴⁰⁰ 1219 ± 1	³⁴⁴ 1135 ± 1	³³⁰ 1137 ± 2	²⁹⁴ 1137 ± 1	²⁴² 1147 ± 1	¹⁷⁹ 1400 ± 29	¹⁷⁷ 1357 ± 32
14	affrengine-000	151875	382842	³⁷ 177	⁴²² 4096 ± 0	¹⁶ 107 ± 0	¹³ 112 ± 0	³³ 284 ± 2	¹⁴⁹ 697 ± 2	⁴¹¹ 3299 ± 17	⁴⁵² 54329 ± 140	⁴⁵¹ 56195 ± 256
15	aifirst-001	224157	808777	⁹⁰ 485	²⁶⁴ 2048 ± 0	¹⁷⁷ 587 ± 2	¹⁴¹ 568 ± 2	¹²⁹ 584 ± 3	¹¹³ 601 ± 6	¹³⁷ 755 ± 5	¹⁵⁵ 1099 ± 14	¹⁵⁷ 1087 ± 45
16	aigen-001	256958	595227	²⁶⁷ 1136	²²⁵ 2048 ± 0	⁴⁶² 1448 ± 9	⁴³³ 1451 ± 8	⁴⁴⁰ 1759 ± 6	⁴³⁶ 2594 ± 4	⁴²³ 5691 ± 44	³¹⁹ 3772 ± 57	³¹⁸ 3736 ± 56
17	aigen-002	205300	1316138	²⁰⁶ 874	³¹⁹ 2048 ± 0	¹⁷⁶ 586 ± 24	¹⁴⁷ 582 ± 4	²⁴¹ 920 ± 4	⁴²¹ 1758 ± 5	⁴²² 5427 ± 17	³¹⁶ 3678 ± 44	³¹⁵ 3646 ± 48
18	ailabs-001	1054663	338989	²⁸⁴ 1252	²¹¹ 2048 ± 0	²¹⁵ 664 ± 4	²¹⁵ 774 ± 50	³³⁴ 1145 ± 12	⁴²⁷ 1972 ± 74	⁴¹⁹ 5205 ± 272	⁴⁶⁷ 104034 ± 661	⁴⁶⁷ 103415 ± 7722
19	aimall-002	370156	25210	³³² 1576	³⁰⁹ 2048 ± 0	²⁵² 776 ± 4	²⁷⁵ 927 ± 27	²⁴⁹ 940 ± 21	²³¹ 955 ± 34	¹⁹⁵ 1003 ± 75	⁴⁶³ 72811 ± 7399	⁴⁶¹ 71216 ± 6286
20	aimall-003	504324	171935	³⁶⁷ 1913	⁶⁷ 1024 ± 0	²¹² 662 ± 1	²⁰⁵ 740 ± 51	¹⁸⁸ 752 ± 62	¹⁶⁴ 741 ± 46	¹⁴⁸ 807 ± 47	⁴³⁷ 34565 ± 93	⁴³⁸ 34598 ± 118
21	aiseemu-001	0	1005354	⁴⁰⁸ 2697	⁴⁰⁷ 4096 ± 0	³⁴⁵ 1001 ± 1	³⁰⁹ 1017 ± 0	²⁸⁹ 1014 ± 5	²⁵⁹ 1022 ± 2	²¹⁴ 1059 ± 4	³³⁶ 4864 ± 25	³³⁷ 4855 ± 32
22	aiseemu-002	0	1216980	⁴²⁹ 3446	⁴²⁰ 4096 ± 0	⁴²³ 1298 ± 5	³⁹¹ 1303 ± 4	³⁸¹ 1313 ± 2	³⁶⁰ 1329 ± 0	²⁹⁹ 1348 ± 2	³³⁹ 4917 ± 37	³³⁸ 4916 ± 37
23	aiunionface-000	241642	840295	⁷¹ 402	¹¹⁹ 2048 ± 0	²⁰¹ 637 ± 13	²¹⁰ 754 ± 41	²⁹¹ 1025 ± 28	³⁰⁹ 1179 ± 29	³⁶⁴ 1639 ± 47	¹⁴⁹ 1072 ± 19	¹⁵⁵ 1080 ± 47
24	aize-001	268456	168970	³¹⁸ 1436	¹³⁶ 2048 ± 0	¹¹² 437 ± 10	⁹ 440 ± 8	¹¹⁶ 542 ± 17	¹⁶⁷ 756 ± 27	³⁵⁹ 1583 ± 53	²³⁴ 1937 ± 22	²²⁸ 1919 ± 23
25	aize-002	257106	182517	¹²² 586	¹⁵⁹ 2048 ± 0	¹²⁵ 467 ± 1	¹⁰⁵ 479 ± 1	¹⁸⁹ 756 ± 1	⁴⁰⁸ 1477 ± 1	⁴¹⁶ 4617 ± 41	⁶³ 597 ± 16	⁶⁹ 598 ± 14
26	ajou-001	363257	31734	⁸² 442	¹⁶² 2048 ± 0	¹⁴⁸ 530 ± 0	¹²⁸ 536 ± 0	¹¹¹ 535 ± 0	⁹⁶ 549 ± 0	⁸³ 577 ± 0	⁶⁴ 597 ± 19	⁶⁷ 596 ± 13
27	alchera-004	1001019	388616	²⁸⁹ 1270	²⁹⁷ 2048 ± 0	³³⁴ 975 ± 0	²⁸³ 955 ± 0	²⁶¹ 960 ± 0	²⁴⁴ 989 ± 0	²⁴³ 1152 ± 1	³¹¹ 3529 ± 54	³¹¹ 3530 ± 63
28	alchera-005	1001019	388616	²⁸⁷ 1268	²³¹ 2048 ± 0	³³² 969 ± 1	²⁹⁰ 987 ± 3	²⁷⁴ 985 ± 3	²⁴⁸ 998 ± 0	²⁴⁹ 1162 ± 2	³¹⁰ 3481 ± 59	³⁰⁷ 3422 ± 57
29	alfabeta-001	128232	21780	⁸ 73	²⁷ 512 ± 0	⁴⁸ 271 ± 0	⁴⁷ 276 ± 0	⁸⁰ 459 ± 2	²⁰⁶ 886 ± 2	³⁹⁵ 2547 ± 9	⁴³ 470 ± 25	⁴⁵ 458 ± 20
30	alice-000	1741293	19355	³⁵¹ 1732	⁴⁰⁴ 4096 ± 0	³²² 950 ± 2	²⁷⁷ 933 ± 1	²⁵³ 949 ± 1	²⁵⁷ 1011 ± 3	²⁷⁵ 1264 ± 8	⁴⁰⁴ 14975 ± 201	⁴⁰⁴ 14890 ± 229
31	alleyes-000	507636	997090	²⁰³ 857	²⁷⁹ 2048 ± 0	²⁵⁷ 784 ± 1	²⁸⁸ 970 ± 61	²⁶⁶ 974 ± 62	²²⁷ 943 ± 69	²¹² 1057 ± 23	¹⁷² 1298 ± 34	¹⁷⁴ 1303 ± 51
32	allgovision-000	172509	155862	¹¹⁴ 561	²³⁷ 2048 ± 0	⁹¹ 384 ± 8	⁷⁴ 395 ± 17	⁶¹ 413 ± 14	⁷² 471 ± 14	¹²³ 710 ± 21	⁴²⁷ 29903 ± 406	⁴²⁸ 29735 ± 194
33	alphaface-001	259849	81636	¹⁰⁵ 527	²⁹⁰ 2048 ± 0	¹⁸⁶ 612 ± 1	¹⁵⁷ 613 ± 3	¹⁴⁰ 612 ± 1	¹¹⁹ 619 ± 1	¹⁰⁵ 640 ± 2	¹⁴⁰ 1008 ± 10	¹⁴⁰ 1002 ± 19
34	alphaface-002	768995	70692	³¹⁷ 1434	²⁰⁹ 2048 ± 0	¹⁹⁶ 628 ± 2	²⁰⁷ 746 ± 19	¹⁸⁷ 751 ± 18	¹⁷² 779 ± 22	¹⁵³ 828 ± 40	¹³⁰ 945 ± 25	¹³¹ 935 ± 17
35	amplifiedgroup-001	0	47053	¹² 81	⁶⁶ 866 ± 2	¹³ 93 ± 0	-	-	-	-	⁴⁵⁵ 57803 ± 4210	⁴⁵² 56365 ± 1196
36	androvideo-000	174847	585063	⁷² 403	²⁵³ 2048 ± 0	⁵⁰ 277 ± 0	⁴⁵ 285 ± 0	³⁸ 314 ± 0	⁴⁴ 372 ± 1	⁹⁶ 620 ± 0	²⁸¹ 2860 ± 28	²⁸⁰ 2847 ± 22
37	anke-004	349388	410776	¹⁵⁴ 706	³⁷⁵ 2056 ± 0	¹⁹⁴ 625 ± 1	¹⁶⁴ 627 ± 2	¹⁴⁹ 635 ± 3	¹³² 653 ± 2	¹⁹¹ 982 ± 8	⁸⁴ 633 ± 22	⁸⁴ 632 ± 34
38	anke-005	328553	429160	²⁶⁵ 1134	³⁷⁴ 2056 ± 0	¹⁷⁸ 590 ± 2	¹⁵³ 594 ± 5	¹³⁷ 601 ± 3	¹²⁰ 638 ± 4	¹⁵² 821 ± 24	⁹⁵ 685 ± 19	⁹⁷ 687 ± 26
39	antheus-000	119453	41994	²⁰ 116	⁵² 520 ± 0	¹⁷ 109 ± 1	²⁸ 187 ± 1	²⁰ 189 ± 1	¹⁶ 195 ± 1	¹⁸ 236 ± 2	³⁶⁵ 6901 ± 268	³⁶⁵ 6936 ± 103
40	antheus-001	119453	41962	²¹ 118	⁵⁴ 520 ± 0	²⁰ 120 ± 1	³⁶ 265 ± 13	⁸⁴ 468 ± 22	³²⁴ 1223 ± 27	³⁹⁷ 2660 ± 87	³⁶¹ 6218 ± 47	³⁶⁰ 6216 ± 45
41	anyvision-004	401001	630797	²⁵⁶ 1102	⁷⁶ 1024 ± 0	⁸⁰ 355 ± 1	-	-	-	-	²²⁹ 1891 ± 51	²²⁰ 1829 ± 85
42	anyvision-005	190979	116595	²²⁵ 963	⁷⁸ 1024 ± 0	³⁴⁰ 985 ± 1	²⁹⁹ 997 ± 1	²⁸⁵ 1004 ± 1	²⁴⁶ 995 ± 1	¹⁹⁴ 995 ± 1	¹⁰⁶ 733 ± 14	¹⁰⁶ 733 ± 16
43	armatura-001	0	374608	²⁷¹ 1151	²⁵⁶ 2048 ± 0	²²⁶ 688 ± 1	¹⁸⁹ 689 ± 1	¹⁷¹ 693 ± 1	¹⁵³ 708 ± 3	¹³⁸ 756 ± 13	¹⁹ 270 ± 17	²² 268 ± 11
44	armatura-003	0	836082	³³³ 1577	⁴⁵⁹ 6144 ± 0	³⁵⁴ 1028 ± 1	³¹⁵ 1032 ± 1	²⁹⁴ 1027 ± 0	²⁶² 1036 ± 1	²⁰⁶ 1041 ± 3	⁴⁵¹ 51850 ± 56	⁴⁵⁰ 51835 ± 48

Notes

- 1 The configuration size does not capture static data included in libraries.
- 2 The library size is the combined total of all files provided in the submission lib folder. These libraries e.g. OpenCV may or may not be installed on any end user's platform natively and would not need to be installed with the algorithm. Some developers put neural network models in their libraries.
- 3 The memory usage is the peak resident set size reported by the ps system call during template generation.
- 4 The median template creation times are measured on Intel®Xeon®CPU E5-2630 v4 @ 2.20GHz processors.
- 5 The comparison durations, in nanoseconds, are estimated using std::chrono::high_resolution_clock which on the machine in (2) counts 1ns clock ticks. Precision is somewhat worse than that however. The ± value is the median absolute deviation times 1.48 for Normal consistency.

Table 8: Summary of algorithms and properties included in this report. The red superscripts give ranking for the quantity in that column.

	ALGORITHM	CONFIG	LIBRARY	TEMPLATE								COMPARISON ⁴		
	NAME	DATA	DATA	MEMORY	SIZE	MUGSHOT	480x720	960x1440	1600x2400	3000x4500	GENUINE	IMPOSTOR	TIME (ns) ⁵	
		(KB) ¹	(KB) ²	(MB) ³	(B)	MUGSHOT	480x720	960x1440	1600x2400	3000x4500	GENUINE	IMPOSTOR		
45	asusaics-000	257418	245320	129 605	204 2048 ± 0	135 484 ± 13	121 506 ± 21	213 850 ± 26	423 1789 ± 61	425 6305 ± 188	348 5455 ± 78	347 5422 ± 112		
46	asusaics-001	257418	245330	126 595	401 4096 ± 0	282 842 ± 17	307 1008 ± 20	402 1377 ± 28	435 2423 ± 90	429 7284 ± 277	375 8618 ± 42	375 8638 ± 136		
47	autentika-000	266093	3200425	372 1942	120 2048 ± 0	159 553 ± 1	155 605 ± 1	139 609 ± 2	115 608 ± 1	95 618 ± 2	464 72833 ± 577	462 71829 ± 541		
48	authenmetric-003	293599	39492	229 982	200 2048 ± 0	343 992 ± 1	305 1006 ± 1	284 1003 ± 2	252 1002 ± 1	204 1036 ± 1	210 1757 ± 19	210 1755 ± 19		
49	authenmetric-004	381165	39492	279 1214	168 2048 ± 0	307 910 ± 1	269 909 ± 1	238 915 ± 1	219 921 ± 2	185 950 ± 1	206 1724 ± 14	205 1691 ± 29		
50	aware-005	300017	26320	286 1265	99 1572 ± 0	301 886 ± 23	319 1038 ± 21	324 1121 ± 22	361 1337 ± 58	384 2195 ± 144	189 1475 ± 63	186 1427 ± 115		
51	aware-006	298543	14124	222 943	14 352 ± 0	385 1148 ± 3	349 1146 ± 2	348 1190 ± 2	346 1306 ± 20	374 1754 ± 84	271 2598 ± 42	271 2559 ± 60		
52	awiros-001	15499	87480	14 88	31 512 ± 0	14 97 ± 6	11 98 ± 4	12 138 ± 6	23 225 ± 7	78 556 ± 8	151 1079 ± 44	149 1050 ± 45		
53	awiros-002	289016	203723	115 562	294 2048 ± 0	130 479 ± 0	115 500 ± 0	110 534 ± 0	118 618 ± 0	182 946 ± 1	235 1966 ± 31	236 1957 ± 25		
54	aximetria-001	408902	487912	143 674	263 2048 ± 0	350 1013 ± 1	310 1023 ± 21	295 1029 ± 5	250 999 ± 2	226 1091 ± 5	330 4401 ± 94	329 4490 ± 80		
55	ayftech-001	195423	43580	163 731	42 512 ± 0	103 408 ± 23	103 476 ± 52	202 814 ± 108	425 1827 ± 384	421 5412 ± 1029	75 615 ± 16	125 885 ± 44		
56	ayonix-000	58505	5252	6 69	86 1036 ± 0	2 18 ± 2	-	-	-	-	77 621 ± 23	81 620 ± 26		
57	beethedata-000	227849	1087592	113 555	293 2048 ± 0	123 465 ± 0	101 467 ± 0	86 468 ± 0	71 467 ± 0	52 467 ± 0	243 2121 ± 34	244 2110 ± 38		
58	beyneai-000	256958	591433	262 1124	269 2048 ± 0	115 451 ± 8	93 449 ± 1	191 767 ± 7	418 1603 ± 25	417 4669 ± 124	317 3730 ± 57	316 3668 ± 54		
59	biocube-001	25030	6192987	86 458	429 4096 ± 0	57 282 ± 22	46 292 ± 24	108 521 ± 57	142 684 ± 59	280 1282 ± 68	418 21787 ± 96	418 21812 ± 109		
60	bioidtechswiss-001	1178769	120811	319 1455	18 512 ± 0	330 966 ± 4	382 1270 ± 270	375 1294 ± 96	388 1409 ± 157	378 1793 ± 79	272 2610 ± 25	272 2624 ± 32		
61	bioidtechswiss-002	744786	114842	234 993	41 512 ± 0	312 917 ± 2	276 930 ± 2	255 952 ± 2	228 947 ± 3	213 1058 ± 11	249 2177 ± 29	250 2170 ± 31		
62	bm-001	287734	38076	27 148	1 64 ± 0	113 444 ± 88	-	-	-	-	228 1887 ± 31	226 1877 ± 26		
63	boetech-001	261376	88710	309 1384	266 2048 ± 0	49 271 ± 1	38 268 ± 1	30 273 ± 0	31 286 ± 1	26 318 ± 1	460 68519 ± 1921	459 67648 ± 822		
64	boetech-002	294347	88710	324 1489	275 2048 ± 0	65 305 ± 4	50 296 ± 1	34 302 ± 1	34 313 ± 1	30 348 ± 2	461 68921 ± 2137	460 69473 ± 2104		
65	bresee-001	287880	23227	280 1214	144 2048 ± 0	402 1223 ± 3	367 1216 ± 1	384 1331 ± 1	327 1227 ± 1	305 1360 ± 1	440 37240 ± 655	440 37167 ± 584		
66	bresee-002	313627	30902	374 1956	167 2048 ± 0	244 743 ± 4	347 1143 ± 2	335 1146 ± 2	296 1148 ± 2	256 1176 ± 2	213 1778 ± 22	213 1775 ± 23		
67	camvi-002	236278	225285	165 737	74 1024 ± 0	220 677 ± 7	202 726 ± 36	217 869 ± 28	289 1129 ± 43	402 2785 ± 113	73 612 ± 26	73 603 ± 20		
68	camvi-004	280733	615819	218 919	130 2048 ± 0	247 759 ± 10	241 861 ± 17	275 986 ± 34	342 1279 ± 51	404 2891 ± 158	131 948 ± 40	132 963 ± 31		
69	canon-003	2550850	101378	457 5472	462 6180 ± 0	412 1263 ± 3	379 1263 ± 1	371 1283 ± 1	354 1320 ± 1	341 1482 ± 2	334 4783 ± 17	332 4780 ± 19		
70	canon-004	2399160	114188	459 5956	463 6200 ± 0	321 948 ± 4	282 955 ± 3	260 959 ± 3	237 977 ± 3	219 1064 ± 2	371 7172 ± 63	370 7169 ± 51		
71	ceiec-003	260371	88707	78 430	154 2048 ± 0	269 817 ± 4	256 883 ± 57	228 897 ± 60	212 899 ± 72	181 944 ± 72	256 2256 ± 38	256 2241 ± 54		
72	ceiec-004	263476	67011	73 408	238 2048 ± 0	353 1024 ± 1	312 1027 ± 1	293 1027 ± 1	261 1030 ± 1	209 1055 ± 1	222 1844 ± 26	221 1836 ± 20		
73	chosun-001	765615	707	93 491	315 2048 ± 0	256 783 ± 2	230 826 ± 4	439 1662 ± 13	440 3679 ± 67	436 11694 ± 243	137 998 ± 25	147 1035 ± 11		
74	chosun-002	234001	31875	83 450	320 2048 ± 0	44 248 ± 3	39 273 ± 3	434 1495 ± 14	441 7920 ± 90	437 80302 ± 1349	79 623 ± 17	86 634 ± 13		
75	chtface-005	408364	311100	313 1412	138 2048 ± 0	70 322 ± 0	54 316 ± 1	40 325 ± 2	36 324 ± 1	43 411 ± 2	230 1907 ± 19	227 1898 ± 23		
76	chtface-006	733645	610439	393 2417	229 2048 ± 0	146 522 ± 1	122 514 ± 1	112 536 ± 2	99 561 ± 1	119 693 ± 2	240 2034 ± 41	241 2049 ± 29		
77	cist-001	0	300551	119 583	149 2048 ± 0	333 972 ± 0	290 977 ± 1	271 981 ± 0	240 983 ± 0	217 1061 ± 0	287 2947 ± 20	286 2940 ± 22		
78	clearviewai-000	342491	211852	414 2750	257 2048 ± 0	451 1402 ± 1	420 1403 ± 1	417 1412 ± 1	391 1420 ± 1	320 1418 ± 1	195 1592 ± 37	193 1561 ± 37		
79	cloesli-001	420342	9851	176 773	416 4096 ± 0	281 839 ± 1	233 843 ± 1	217 841 ± 1	193 845 ± 1	163 865 ± 1	347 5404 ± 17	346 5400 ± 25		
80	cloudmatrix-001	10390	542121	45 249	128 2048 ± 0	19 114 ± 1	14 117 ± 0	11 118 ± 0	10 123 ± 1	11 169 ± 1	448 50263 ± 212	447 50243 ± 237		
81	cloudmatrix-002	256635	693318	239 1030	284 2048 ± 0	95 395 ± 1	75 398 ± 1	57 399 ± 1	52 402 ± 1	47 437 ± 20	447 49578 ± 120	446 49602 ± 180		
82	cloudwalk-hr-003	383739	144263	232 984	377 2057 ± 0	183 606 ± 0	150 588 ± 0	133 594 ± 0	117 612 ± 1	-	367 6982 ± 80	366 6972 ± 84		
83	cloudwalk-hr-004	502916	520169	312 1394	331 2049 ± 0	294 873 ± 1	250 877 ± 1	222 876 ± 1	204 879 ± 1	174 902 ± 3	389 11652 ± 127	389 11608 ± 123		
84	cloudwalk-mt-005	846026	573253	421 2928	261 2048 ± 0	389 1179 ± 3	363 1200 ± 3	353 1209 ± 3	326 1226 ± 5	268 1229 ± 3	396 12525 ± 225	395 12394 ± 152		
85	cloudwalk-mt-006	563322	480071	417 2836	314 2048 ± 0	444 1385 ± 0	414 1392 ± 1	411 1398 ± 1	383 1397 ± 4	330 1444 ± 2	302 3364 ± 96	301 3324 ± 83		
86	codeline-000	361659	138388	277 1188	186 2048 ± 0	463 1453 ± 0	435 1456 ± 2	428 1456 ± 0	400 1457 ± 0	342 1483 ± 1	247 2171 ± 69	252 2194 ± 84		
87	cogent-007	621565	72316	366 1884	62 550 ± 0	432 1329 ± 2	402 1333 ± 5	389 1337 ± 4	364 1353 ± 5	314 1390 ± 4	31 355 ± 8	34 367 ± 14		
88	cogent-008	856817	73587	385 2173	61 550 ± 0	455 1412 ± 1	425 1419 ± 2	420 1426 ± 3	396 1437 ± 3	338 1476 ± 1	39 436 ± 14	42 441 ± 23		

Notes

- 1 The configuration size does not capture static data included in libraries.
- 2 The library size is the combined total of all files provided in the submission lib folder. These libraries e.g. OpenCV may or may not be installed on any end user's platform natively and would not need to be installed with the algorithm. Some developers put neural network models in their libraries.
- 3 The memory usage is the peak resident set size reported by the ps system call during template generation.
- 4 The median template creation times are measured on Intel®Xeon®CPU E5-2630 v4 @ 2.20GHz processors.
- 5 The comparison durations, in nanoseconds, are estimated using std::chrono::high_resolution_clock which on the machine in (2) counts 1ns clock ticks. Precision is somewhat worse than that however. The ± value is the median absolute deviation times 1.48 for Normal consistency.

Table 9: Summary of algorithms and properties included in this report. The red superscripts give ranking for the quantity in that column.

	ALGORITHM	CONFIG	LIBRARY	TEMPLATE								COMPARISON ⁴									
				NAME	DATA	DATA	MEMORY	SIZE	GENERATION TIME (ms) ⁴				TIME (ns) ⁵								
									(KB) ¹	(KB) ²	(MB) ³	(B)	MUGSHOT	480x720	960x1440	1600x2400	3000x4500	GENUINE	IMPOSTOR		
89	cognitec-003	471458	62502	192	817	336	2052 ± 0	85	366 ± 9	79	403 ± 9	59	408 ± 9	58	424 ± 9	60	509 ± 13	307	3417 ± 51	309	3433 ± 53
90	cognitec-004	705645	62678	121	585	338	2052 ± 0	120	463 ± 9	113	497 ± 9	100	504 ± 10	87	521 ± 10	97	631 ± 12	293	3028 ± 197	294	3059 ± 238
91	cor-001	1194948	11240	283	1249	380	2060 ± 0	234	699 ± 3	242	863 ± 76	216	865 ± 80	200	872 ± 89	186	952 ± 39	470	270145 ± 2259	470	282686 ± 11788
92	coretech-000	186423	43964	70	393	21	512 ± 0	182	602 ± 15	175	659 ± 12	331	1139 ± 24	297	1149 ± 25	250	1165 ± 23	27	333 ± 14	28	321 ± 13
93	coretech-001	235361	305490	328	1524	187	2048 ± 0	225	688 ± 7	192	695 ± 7	218	870 ± 17	203	879 ± 15	167	877 ± 15	80	625 ± 25	89	641 ± 25
94	corsight-002	1474921	32093	378	2061	382	2080 ± 0	421	1290 ± 1	387	1287 ± 1	372	1290 ± 1	347	1307 ± 2	313	1388 ± 4	422	24953 ± 637	421	24263 ± 578
95	corsight-003	1413063	32198	339	1637	383	2080 ± 0	397	1202 ± 2	362	1190 ± 5	351	1199 ± 3	328	1236 ± 3	300	1349 ± 7	426	28754 ± 434	427	28279 ± 446
96	csc-002	0	519768	307	1376	58	544 ± 0	127	473 ± 0	112	494 ± 0	90	481 ± 1	78	490 ± 1	63	514 ± 5	34	367 ± 11	35	371 ± 10
97	csc-003	0	400435	337	1609	57	544 ± 0	139	499 ± 0	117	500 ± 1	98	502 ± 0	84	508 ± 1	71	535 ± 4	37	393 ± 8	37	397 ± 7
98	ctcbcbank-000	257208	599238	117	570	313	2048 ± 0	165	568 ± 43	156	606 ± 38	170	690 ± 53	154	711 ± 50	154	831 ± 51	312	3551 ± 87	334	4805 ± 209
99	ctcbcbank-001	275511	599238	127	603	208	2048 ± 0	206	652 ± 35	217	781 ± 30	221	875 ± 43	211	898 ± 51	202	1030 ± 47	320	3926 ± 45	319	3924 ± 56
100	cu-face-002	812008	38655	164	735	424	4096 ± 0	362	1054 ± 1	323	1059 ± 0	308	1060 ± 0	272	1063 ± 1	221	1070 ± 0	454	57287 ± 1750	454	57027 ± 945
101	cubox-001	369627	75427	137	649	163	2048 ± 0	304	907 ± 1	262	902 ± 1	233	903 ± 0	218	917 ± 0	178	931 ± 0	176	1379 ± 37	183	1417 ± 38
102	cubox-002	542254	90975	375	1964	267	2048 ± 0	314	921 ± 1	269	921 ± 1	242	922 ± 1	223	933 ± 1	196	1003 ± 1	238	2008 ± 72	238	1969 ± 57
103	cudocommunication-001	385258	341277	249	1077	148	2048 ± 0	316	925 ± 1	272	923 ± 1	246	928 ± 1	222	932 ± 0	188	964 ± 1	267	2534 ± 20	269	2537 ± 20
104	cuhkee-001	787853	74917	400	2515	334	2052 ± 0	337	977 ± 31	-	-	-	-	-	-	-	-	273	2719 ± 60	277	2783 ± 56
105	cybercore-002	166096	7374	403	2564	288	2048 ± 0	137	489 ± 1	116	500 ± 4	97	500 ± 1	82	499 ± 2	70	528 ± 1	394	12389 ± 123	394	12352 ± 112
106	cybercore-003	289176	7969	447	4310	419	4096 ± 0	283	844 ± 2	239	855 ± 4	215	864 ± 4	199	862 ± 4	168	878 ± 2	354	5744 ± 41	355	5737 ± 31
107	cyberextruder-003	253300	12354	80	437	33	512 ± 0	93	390 ± 1	71	388 ± 1	55	393 ± 1	50	399 ± 1	46	435 ± 1	10	198 ± 4	11	189 ± 8
108	cyberextruder-004	169301	12354	63	349	2	128 ± 0	38	206 ± 0	28	208 ± 0	24	209 ± 0	20	229 ± 0	24	249 ± 1	5	145 ± 14	6	155 ± 14
109	cyberlink-009	588443	102201	344	1704	449	4164 ± 0	443	1384 ± 2	417	1395 ± 2	410	1398 ± 2	385	1401 ± 2	334	1456 ± 2	22	299 ± 17	25	304 ± 16
110	cyberlink-010	1590818	102180	433	3672	469	8260 ± 0	413	1265 ± 2	394	1314 ± 5	374	1294 ± 2	340	1273 ± 2	288	1305 ± 2	44	476 ± 23	47	472 ± 14
111	dahua-006	831641	119261	453	5068	109	2048 ± 0	449	1398 ± 2	419	1397 ± 1	414	1404 ± 1	386	1402 ± 1	317	1402 ± 1	18	249 ± 13	19	250 ± 11
112	dahua-007	1578737	119418	464	7237	414	4096 ± 0	448	1393 ± 2	409	1373 ± 1	403	1378 ± 1	374	1378 ± 1	309	1379 ± 2	35	367 ± 102	39	434 ± 108
113	daon-000	280726	2307	377	2013	381	2065 ± 0	162	562 ± 3	145	581 ± 5	193	791 ± 9	190	838 ± 15	210	1055 ± 32	407	16052 ± 88	407	16041 ± 85
114	decatur-000	350495	171271	213	907	444	4100 ± 0	352	1024 ± 2	-	-	-	-	-	-	-	-	388	11439 ± 80	388	11418 ± 112
115	decatur-001	342866	253734	325	1507	341	2052 ± 0	369	1103 ± 2	324	1064 ± 2	311	1063 ± 2	273	1067 ± 2	222	1084 ± 2	72	610 ± 19	71	602 ± 8
116	deepglint-004	1073382	261571	424	3084	234	2048 ± 0	465	1470 ± 1	439	1474 ± 1	433	1485 ± 1	406	1474 ± 1	345	1492 ± 2	358	5961 ± 34	358	5955 ± 29
117	deepglint-005	960326	213877	423	2947	155	2048 ± 0	454	1408 ± 1	427	1431 ± 2	419	1424 ± 3	393	1424 ± 3	332	1446 ± 2	364	6765 ± 38	363	6765 ± 40
118	deepsea-001	147497	336250	65	358	73	1024 ± 0	197	630 ± 7	209	752 ± 37	186	746 ± 30	159	727 ± 32	151	820 ± 32	181	1401 ± 37	188	1467 ± 50
119	deepsense-000	357113	936618	465	7618	166	2048 ± 0	213	664 ± 3	173	645 ± 1	158	660 ± 2	144	687 ± 2	149	808 ± 3	45	480 ± 22	46	459 ± 34
120	deepsense-001	73173	1288355	454	5314	35	512 ± 0	382	1142 ± 2	352	1164 ± 3	347	1183 ± 3	319	1201 ± 3	294	1323 ± 2	260	2356 ± 35	260	2354 ± 42
121	dermalog-010	0	525908	237	1023	20	512 ± 0	200	635 ± 0	171	640 ± 1	151	639 ± 4	129	647 ± 3	118	691 ± 5	41	444 ± 13	31	341 ± 26
122	dermalog-011	0	278395	157	715	3	128 ± 0	76	343 ± 0	61	345 ± 0	43	347 ± 0	39	351 ± 0	34	363 ± 0	23	299 ± 19	21	253 ± 14
123	dicio-001	61751	119517	11	77	51	520 ± 0	152	538 ± 0	140	563 ± 10	237	915 ± 3	424	1800 ± 7	420	5286 ± 30	277	2818 ± 20	278	2807 ± 31
124	didiglobalface-001	259849	70680	104	527	276	2048 ± 0	185	612 ± 1	168	633 ± 3	148	634 ± 3	130	650 ± 15	111	666 ± 4	133	973 ± 20	134	988 ± 20
125	didiglobalface-002	260054	161508	194	826	255	2048 ± 0	193	622 ± 1	167	633 ± 1	154	642 ± 2	134	659 ± 4	129	726 ± 15	56	560 ± 10	59	567 ± 13
126	digidata-000	133370	30249	48	257	145	2048 ± 0	84	361 ± 0	64	360 ± 0	48	361 ± 0	42	363 ± 0	36	380 ± 0	242	2084 ± 37	240	2039 ± 42
127	digidata-001	254564	33036	66	367	268	2048 ± 0	161	559 ± 1	138	561 ± 1	122	562 ± 1	100	564 ± 1	91	602 ± 1	385	10308 ± 102	385	10301 ± 121
128	digitalbarriers-002	83002	598577	370	1930	367	2056 ± 0	39	209 ± 11	34	250 ± 19	60	411 ± 37	179	808 ± 72	385	2236 ± 123	397	13409 ± 228	397	13267 ± 206
129	dps-000	0	2211812	243	1058	397	4096 ± 0	288	868 ± 2	259	893 ± 6	425	1445 ± 9	438	2910 ± 38	431	9345 ± 17	188	1473 ± 37	189	1479 ± 37
130	dsk-000	11967	782905	47	252	23	512 ± 0	64	304 ± 47	55	317 ± 33	283	1001 ± 96	437	2660 ± 170	434	10451 ± 832	370	7152 ± 115	368	7134 ± 111
131	einetworks-000	372608	219883	209	880	355	2056 ± 0	204	645 ± 3	-	-	-	-	-	-	-	-	337	4876 ± 66	341	5156 ± 77
132	ekin-002	51434	278	23	139	391	3072 ± 0	394	1186 ± 13	360	1180 ± 12	344	1181 ± 11	316	1191 ± 11	263	1207 ± 8	328	4294 ± 80	350	5569 ± 112

Notes
 1 The configuration size does not capture static data included in libraries.
 2 The library size is the combined total of all files provided in the submission lib folder. These libraries e.g. OpenCV may or may not be installed on any end user's platform natively and would not need to be installed with the algorithm. Some developers put neural network models in their libraries.
 3 The memory usage is the peak resident set size reported by the ps system call during template generation.
 4 The median template creation times are measured on Intel®Xeon®CPU E5-2630 v4 @ 2.20GHz processors.
 5 The comparison durations, in nanoseconds, are estimated using std::chrono::high_resolution_clock which on the machine in (2) counts 1ns clock ticks. Precision is somewhat worse than that however. The ± value is the median absolute deviation times 1.48 for Normal consistency.

	ALGORITHM	CONFIG	LIBRARY	TEMPLATE								COMPARISON ⁴										
				NAME	DATA	DATA	MEMORY	SIZE	GENERATION TIME (ms) ⁴				TIME (ns) ⁵									
									(KB) ¹	(KB) ²	(MB) ³	(B)	MUGSHOT	480x720	960x1440	1600x2400	3000x4500	GENUINE	IMPOSTOR			
133	enface-000		369598	153781	139	662	68	1024 ± 0	160	555 ± 4	137	558 ± 4	162	669 ± 6	243	987 ± 15	388	2349 ± 54	368	7059 ± 62	367	6980 ± 65
134	enface-001		370710	173609	142	670	75	1024 ± 0	157	550 ± 4	136	555 ± 3	161	668 ± 7	238	981 ± 15	392	2416 ± 59	363	6734 ± 68	364	6766 ± 69
135	eocortex-000		255937	59432	43	224	311	2048 ± 0	66	305 ± 22	59	341 ± 25	74	440 ± 47	69	464 ± 45	61	513 ± 44	129	923 ± 11	130	918 ± 11
136	ercacat-001		811623	58012	416	2816	337	2052 ± 0	360	1052 ± 3	-	-	-	-	-	-	269	2551 ± 62	266	2501 ± 81		
137	euronovate-001		0	1774966	300	1308	90	1177 ± 0	356	1034 ± 2	353	1165 ± 3	339	1160 ± 3	307	1177 ± 3	252	1172 ± 2	466	81294 ± 591	466	81631 ± 931
138	expasoft-001		39057	983064	25	142	244	2048 ± 0	9	70 ± 0	74 ± 0	77 ± 0	673 ± 0	574 ± 0	201	1660 ± 35	202	1676 ± 48				
139	expasoft-002		38760	59825	33	168	185	2048 ± 0	5	34 ± 0	34 ± 0	34 ± 0	234 ± 0	234 ± 0	377	8870 ± 78	377	8838 ± 77				
140	f8-001		272977	19668	290	1276	281	2048 ± 0	277	822 ± 39	-	-	-	-	-	-	406	15262 ± 139	406	15277 ± 212		
141	f8-002		28278	215616	13	83	265	2048 ± 0	63	39 ± 0	441 ± 0	675 ± 0	18	197 ± 1	121	702 ± 1	403	14765 ± 131	403	14790 ± 133		
142	faceonline-001		0	71529	55	302	369	2056 ± 0	28	179 ± 0	20	179 ± 0	21	190 ± 0	21	217 ± 0	29	343 ± 1	147	1064 ± 37	146	1033 ± 35
143	faceonline-002		155220	141019	235	995	202	2048 ± 0	255	783 ± 1	222	797 ± 2	194	794 ± 2	180	809 ± 3	173	901 ± 2	398	13798 ± 197	398	13743 ± 127
144	facephi-000		148904	5219	468	11481	196	2048 ± 0	289	871 ± 2	253	881 ± 3	224	880 ± 4	208	888 ± 4	184	949 ± 12	326	4067 ± 53	325	4047 ± 53
145	facesoft-000		370120	10612	181	796	245	2048 ± 0	218	675 ± 18	179	669 ± 3	167	686 ± 3	139	675 ± 5	115	687 ± 2	255	2239 ± 28	258	2277 ± 96
146	facetag-000		1232331	4022	227	965	65	684 ± 0	79	355 ± 17	67	369 ± 8	278	989 ± 33	434	2408 ± 91	430	7930 ± 316	462	72003 ± 625	463	71912 ± 612
147	facetag-002		819806	4021	160	726	242	2048 ± 0	154	544 ± 1	132	544 ± 0	114	542 ± 0	95	545 ± 0	77	554 ± 0	207	1730 ± 25	207	1733 ± 25
148	facex-001		305074	930372	422	2931	178	2048 ± 0	107	422 ± 4	89	434 ± 4	107	520 ± 7	163	737 ± 13	367	1670 ± 27	225	1871 ± 23	223	1846 ± 29
149	facex-002		305074	928334	425	3095	129	2048 ± 0	108	426 ± 5	87	429 ± 4	105	516 ± 8	161	730 ± 12	373	1738 ± 36	83	631 ± 25	79	614 ± 19
150	farfaces-001		346494	44581	49	261	37	512 ± 0	390	1179 ± 1	359	1180 ± 1	343	1180 ± 0	313	1185 ± 1	264	1209 ± 2	122	855 ± 25	121	860 ± 31
151	fiberhome-nanjing-003		352895	1482309	199	845	206	2048 ± 0	378	1136 ± 7	343	1134 ± 4	329	1132 ± 3	295	1139 ± 3	244	1154 ± 5	154	1097 ± 38	156	1083 ± 42
152	fiberhome-nanjing-004		443779	1482313	242	1048	408	4096 ± 0	429	1321 ± 5	392	1304 ± 3	380	1307 ± 2	350	1308 ± 3	296	1326 ± 5	170	1276 ± 40	171	1265 ± 38
153	fincore-000		256615	19409	109	535	135	2048 ± 0	143	508 ± 3	120	505 ± 0	101	508 ± 1	86	513 ± 2	72	535 ± 1	211	1765 ± 31	211	1763 ± 22
154	firstcreditKZ-001		553811	24803	259	1112	322	2048 ± 0	265	808 ± 0	300	997 ± 0	310	1061 ± 1	306	1174 ± 1	377	1774 ± 54	126	904 ± 20	127	903 ± 23
155	frpkauai-001		507771	24807	248	1076	153	2048 ± 0	228	689 ± 1	191	691 ± 0	174	697 ± 2	157	714 ± 6	142	775 ± 31	109	752 ± 29	111	764 ± 23
156	frpkauai-002		519141	24803	260	1112	220	2048 ± 0	262	799 ± 0	297	987 ± 0	302	1046 ± 1	301	1163 ± 2	376	1769 ± 4	127	907 ± 20	126	886 ± 28
157	fujitsulab-002		0	1088887	338	1613	446	4104 ± 0	405	1237 ± 2	370	1222 ± 2	357	1236 ± 1	331	1251 ± 2	297	1327 ± 2	278	2836 ± 25	279	2809 ± 44
158	fujitsulab-003		662263	318209	463	6907	447	4104 ± 0	325	951 ± 20	278	941 ± 19	254	952 ± 19	236	971 ± 20	207	1045 ± 21	280	2855 ± 16	281	2849 ± 19
159	g42-intelibrain-001		1031335	235521	473	25628	9	269 ± 0	336	976 ± 6	289	975 ± 1	275	1068 ± 3	306	1362 ± 8	356	5878 ± 96	357	5865 ± 71		
160	geo-002		369903	98667	236	1018	183	2048 ± 0	258	791 ± 1	220	793 ± 0	195	794 ± 0	174	795 ± 1	145	803 ± 1	306	3407 ± 45	308	3422 ± 65
161	geo-004		168980	107714	292	1280	223	2048 ± 0	414	1268 ± 1	385	1279 ± 1	368	1274 ± 0	335	1259 ± 1	285	1296 ± 1	143	1023 ± 20	145	1028 ± 22
162	glory-004		0	999639	386	2181	452	4182 ± 0	227	688 ± 0	212	759 ± 1	250	941 ± 1	429	2134 ± 4	432	9360 ± 47	340	4982 ± 66	339	4990 ± 63
163	glory-005		0	999999	395	2428	451	4182 ± 0	236	703 ± 1	219	789 ± 0	265	972 ± 1	431	2200 ± 25	433	9679 ± 22	344	5224 ± 93	343	5176 ± 81
164	gorilla-008		450175	707000	358	1789	470	8338 ± 0	181	595 ± 1	151	590 ± 0	136	600 ± 1	122	621 ± 2	126	720 ± 9	332	4530 ± 44	330	4524 ± 38
165	gorilla-009		329584	297395	302	1312	453	4242 ± 0	303	899 ± 2	271	922 ± 1	231	901 ± 3	220	924 ± 4	203	1032 ± 12	259	2294 ± 74	259	2301 ± 66
166	graymatics-001		13095	70406	22	127	421	4096 ± 0	33	191 ± 1	26	203 ± 1	132	592 ± 5	420	1698 ± 9	428	7150 ± 34	442	39874 ± 309	441	39762 ± 295
167	griaule-001		0	412061	288	1269	333	2052 ± 0	387	1164 ± 1	334	1096 ± 5	320	1099 ± 4	292	1136 ± 2	348	1509 ± 2	323	3948 ± 23	322	3957 ± 32
168	griaule-002		0	1320474	361	1815	349	2052 ± 0	276	822 ± 1	273	924 ± 4	236	907 ± 1	265	1038 ± 21	326	1430 ± 9	324	4005 ± 32	324	4012 ± 31
169	hertasecurity-001		0	944427	276	1183	32	512 ± 0	78	346 ± 0	60	345 ± 0	45	349 ± 0	40	354 ± 0	37	388 ± 0	212	1770 ± 45	206	1726 ± 48
170	hertasecurity-002		0	944582	275	1177	17	512 ± 0	134	484 ± 7	104	478 ± 3	89	480 ± 3	81	495 ± 3	68	520 ± 3	258	2289 ± 40	257	2267 ± 48
171	hik-001		667866	9290	461	6597	94	1408 ± 0	205	651 ± 0	178	667 ± 8	164	677 ± 16	143	686 ± 13	133	737 ± 12	47	488 ± 19	48	477 ± 22
172	hisign-001		732412	167488	330	1553	385	2080 ± 0	425	1306 ± 1	396	1320 ± 1	382	1315 ± 1	352	1312 ± 1	299	1325 ± 1	11	201 ± 10	9	185 ± 13
173	hisign-002		1014906	102652	382	2123	384	2080 ± 0	260	797 ± 0	223	800 ± 5	197	800 ± 0	176	801 ± 0	146	803 ± 1	17	232 ± 11	13	207 ± 11
174	hyperverge-003		1167779	282156	413	2748	80	1024 ± 0	469	1477 ± 2	440	1503 ± 3	436	1520 ± 3	413	1525 ± 4	357	1565 ± 3	57	566 ± 11	57	561 ± 8
175	hyperverge-004		4924393	282156	440	3907	205	2048 ± 0	467	1471 ± 2	428	1434 ± 1	426	1446 ± 6	398	1445 ± 3	344	1491 ± 3	136	996 ± 10	138	1000 ± 19
176	hzailu-002		1515880	74047	450	4715	336	2056 ± 0	386	1150 ± 5	342	1127 ± 6	326	1129 ± 7	293	1137 ± 7	254	1172 ± 3	152	1079 ± 53	151	1070 ± 31

Notes

- 1 The configuration size does not capture static data included in libraries.
- 2 The library size is the combined total of all files provided in the submission lib folder. These libraries e.g. OpenCV may or may not be installed on any end user's platform natively and would not need to be installed with the algorithm. Some developers put neural network models in their libraries.
- 3 The memory usage is the peak resident set size reported by the ps system call during template generation.
- 4 The median template creation times are measured on Intel®Xeon®CPU E5-2630 v4 @ 2.20GHz processors.
- 5 The comparison durations, in nanoseconds, are estimated using std::chrono::high_resolution_clock which on the machine in (2) counts 1ns clock ticks. Precision is somewhat worse than that however. The ± value is the median absolute deviation times 1.48 for Normal consistency.

Table 11: Summary of algorithms and properties included in this report. The red superscripts give ranking for the quantity in that column.

ALGORITHM			CONFIG	LIBRARY	TEMPLATE						COMPARISON ⁴										
NAME		DATA	DATA	MEMORY	SIZE	GENERATION TIME (ms) ⁴				TIME (ns) ⁵											
		(KB) ¹	(KB) ²	(MB) ³	(B)	MUGSHOT	480x720	960x1440	1600x2400	3000x4500	GENUINE	IMPOSTOR									
177	hzailu-003	1923030	222185	451	4817	393	3080 ± 0	446	1389 ± 5	401	1331 ± 7	387	1334 ± 2	363	1349 ± 6	323	1424 ± 8	190	1483 ± 35	187	1464 ± 31
178	icm-003	1513988	940	95	500	228	2048 ± 0	221	681 ± 6	180	672 ± 4	179	714 ± 11	189	837 ± 41	310	1381 ± 131	421	24351 ± 161	420	24227 ± 146
179	icm-004	2012129	1089	241	1040	171	2048 ± 0	108	419 ± 6	80	407 ± 6	79	454 ± 15	114	603 ± 51	352	1527 ± 235	402	14730 ± 154	402	14521 ± 152
180	ichttc-000	172459	1471004	359	1805	291	2048 ± 0	75	338 ± 11	58	338 ± 9	71	437 ± 16	151	705 ± 24	371	1719 ± 44	346	5284 ± 63	345	5290 ± 54
181	id3-006	210116	7706	230	982	53	520 ± 0	222	683 ± 0	328	1088 ± 1	349	1192 ± 1	322	1209 ± 1	276	1270 ± 1	349	5547 ± 34	349	5563 ± 34
182	id3-008	242416	8151	246	1068	8	264 ± 0	271	819 ± 0	366	1209 ± 2	378	1297 ± 2	359	1329 ± 1	328	1433 ± 1	352	5658 ± 44	353	5624 ± 40
183	idemia-008	374017	69922	278	1194	13	348 ± 0	117	457 ± 1	99	461 ± 0	74	466 ± 1	62	513 ± 10	296	3080 ± 41	292	3046 ± 56		
184	idemia-009	1066728	70572	409	2702	64	636 ± 0	398	1207 ± 1	368	1218 ± 1	354	1222 ± 2	323	1222 ± 3	278	1280 ± 10	353	5664 ± 84	352	5597 ± 90
185	iit-002	259579	52070	162	731	140	2048 ± 0	144	514 ± 1	124	531 ± 2	119	547 ± 1	104	583 ± 1	131	733 ± 2	144	1023 ± 7	141	1011 ± 66
186	iit-003	261288	53791	193	817	289	2048 ± 0	132	482 ± 0	110	493 ± 0	102	509 ± 0	93	541 ± 0	109	661 ± 0	26	324 ± 17	29	326 ± 8
187	imds-software-001	373399	352623	174	772	174	2048 ± 0	122	465 ± 1	285	958 ± 6	328	1131 ± 5	291	1134 ± 2	233	1119 ± 10	391	11885 ± 120	390	11779 ± 174
188	imperial-000	370120	10623	182	796	115	2048 ± 0	217	669 ± 1	184	675 ± 3	166	683 ± 17	140	676 ± 2	116	689 ± 2	244	2130 ± 32	242	2052 ± 100
189	imperial-002	472327	16134	362	1826	194	2048 ± 0	167	569 ± 1	146	581 ± 15	128	575 ± 5	103	576 ± 2	85	588 ± 3	257	2278 ± 90	247	2131 ± 44
190	incode-010	627808	21014	405	2628	227	2048 ± 0	392	1180 ± 2	356	1178 ± 1	345	1182 ± 1	311	1184 ± 1	266	1221 ± 1	164	1164 ± 32	163	1144 ± 32
191	incode-011	477280	21781	347	1708	114	2048 ± 0	291	872 ± 0	249	875 ± 0	227	881 ± 1	210	892 ± 1	179	939 ± 0	157	1117 ± 31	159	1109 ± 37
192	infocert-001	1204340	38972	323	1483	300	2048 ± 0	295	874 ± 1	257	891 ± 1	304	1050 ± 5	405	1473 ± 2	409	3174 ± 8	342	5055 ± 108	340	5008 ± 100
193	ineffulabs-000	370588	162172	81	439	188	2048 ± 0	347	1006 ± 3	311	1025 ± 3	296	1030 ± 4	266	1041 ± 2	238	1135 ± 3	355	5782 ± 41	356	5741 ± 45
194	innovativetechnologyltd-001	177232	335757	60	341	272	2048 ± 0	111	433 ± 7	92	446 ± 8	72	439 ± 4	63	452 ± 4	56	485 ± 7	227	1877 ± 42	231	1924 ± 97
195	innovativetechnologyltd-002	173939	372324	215	912	218	2048 ± 0	210	661 ± 2	203	726 ± 4	270	981 ± 27	247	997 ± 40	141	766 ± 3	221	1841 ± 50	225	1857 ± 59
196	innovatrics-008	307323	59842	315	1424	56	538 ± 0	254	778 ± 6	213	767 ± 3	192	770 ± 3	177	803 ± 3	159	853 ± 10	291	3021 ± 66	274	2673 ± 88
197	innovatrics-009	624485	105187	368	1917	448	4136 ± 0	374	1116 ± 1	337	1107 ± 5	322	1104 ± 5	284	1110 ± 5	241	1146 ± 6	341	5051 ± 54	331	4733 ± 102
198	insightface-001	776777	16606	435	3852	303	2048 ± 0	436	1366 ± 2	407	1368 ± 3	398	1372 ± 3	373	1375 ± 5	311	1386 ± 4	158	1119 ± 29	158	1108 ± 34
199	insightface-003	1016917	26668	326	1515	236	2048 ± 0	364	1073 ± 0	329	1092 ± 2	314	1070 ± 1	279	1082 ± 1	227	1101 ± 1	62	597 ± 16	66	595 ± 17
200	inspur-000	364844	91926	187	808	428	4096 ± 0	437	1367 ± 1	400	1331 ± 2	396	1368 ± 2	404	1465 ± 1	381	1861 ± 3	383	9831 ± 37	382	9860 ± 40
201	intelllicloudai-001	220831	868246	138	655	157	2048 ± 0	126	468 ± 2	96	456 ± 1	82	466 ± 3	80	492 ± 1	98	632 ± 2	140	1056 ± 4	150	1051 ± 72
202	intelllicloudai-002	259047	58559	431	3584	443	4100 ± 0	284	847 ± 1	236	847 ± 2	212	849 ± 1	195	853 ± 1	169	878 ± 4	118	822 ± 28	117	818 ± 23
203	intellifusion-001	271872	289387	170	762	226	2048 ± 0	248	764 ± 38	216	774 ± 39	196	797 ± 42	178	803 ± 34	147	805 ± 33	156	1112 ± 28	160	1128 ± 41
204	intellifusion-002	762731	385841	221	941	409	4096 ± 0	322	950 ± 2	335	1096 ± 42	316	1088 ± 33	304	1168 ± 31	251	1171 ± 10	205	1713 ± 57	201	1665 ± 87
205	intellivision-003	64023	133748	185	799	358	2056 ± 0	98	407 ± 3	76	398 ± 2	65	418 ± 2	62	450 ± 1	87	591 ± 4	386	11069 ± 56	386	11066 ± 75
206	intellivision-004	117727	131310	101	515	361	2056 ± 0	72	330 ± 0	57	330 ± 0	44	347 ± 0	45	382 ± 0	64	514 ± 0	387	11197 ± 63	387	11165 ± 72
207	intellivix-002	361566	116162	274	1172	164	2048 ± 0	327	956 ± 0	281	947 ± 6	268	976 ± 0	241	984 ± 4	224	1089 ± 1	429	30096 ± 128	431	31287 ± 140
208	intellivix-003	234409	116167	298	1299	177	2048 ± 0	305	908 ± 0	268	916 ± 1	248	930 ± 0	233	961 ± 1	237	1129 ± 3	428	30025 ± 137	430	31190 ± 131
209	intelresearch-005	398137	85290	272	1158	169	2048 ± 0	431	1328 ± 1	403	1334 ± 2	391	1344 ± 2	365	1356 ± 2	321	1423 ± 4	331	4524 ± 87	328	4461 ± 74
210	intelresearch-006	445223	101126	238	1028	122	2048 ± 0	313	918 ± 1	252	881 ± 0	227	892 ± 0	216	913 ± 1	197	1008 ± 3	360	6137 ± 410	359	6024 ± 109
211	intema-000	1532392	19488	254	1097	46	513 ± 0	349	1010 ± 0	302	1001 ± 4	281	994 ± 0	248	993 ± 5	211	1056 ± 1	128	910 ± 29	129	906 ± 32
212	intema-001	1122562	19536	320	1460	47	513 ± 0	434	1354 ± 1	395	1318 ± 5	388	1336 ± 4	358	1328 ± 2	307	1375 ± 0	134	977 ± 31	133	980 ± 31
213	intsysmsu-001	384409	172480	180	789	217	2048 ± 0	187	614 ± 2	160	615 ± 2	155	642 ± 2	162	750 ± 3	247	1159 ± 4	78	621 ± 8	75	611 ± 31
214	intsysmsu-002	765921	172298	179	786	70	1024 ± 0	180	593 ± 1	221	793 ± 2	207	827 ± 1	201	875 ± 104	284	1293 ± 3	52	549 ± 25	55	548 ± 29
215	ionetworks-000	287609	51236	64	351	246	2048 ± 0	110	430 ± 0	90	435 ± 0	70	433 ± 0	60	432 ± 0	49	444 ± 0	366	6913 ± 102	369	7150 ± 160
216	iqface-000	268819	596337	153	704	455	4750 ± 32	153	538 ± 26	111	494 ± 2	117	543 ± 3	162	734 ± 4	315	1393 ± 4	473	636433 ± 38446	473	632654 ± 85615
217	iqface-003	370803	963398	191	817	456	4763 ± 37	147	529 ± 1	120	532 ± 2	135	599 ± 8	194	850 ± 2	368	1694 ± 2	472	575924 ± 2601	472	576653 ± 2051
218	irex-000	741899	47419	380	2086	395	3080 ± 0	286	852 ± 2	238	850 ± 1	220	874 ± 2	225	939 ± 1	270	1249 ± 5	12	201 ± 11	15	208 ± 8
219	isap-001	99049	204201	1	18	437	4096 ± 0	1	0 ± 0	-	-	-	-	-	-	-	42	459 ± 17	43	456 ± 11	
220	isap-002	256765	49931	53	288	273	2048 ± 0	251	769 ± 3	313	1027 ± 2	223	877 ± 2	170	761 ± 1	175	912 ± 2	294	3045 ± 94	288	2973 ± 66

Notes

- 1 The configuration size does not capture static data included in libraries.
- 2 The library size is the combined total of all files provided in the submission lib folder. These libraries e.g. OpenCV may or may not be installed on any end user's platform natively and would not need to be installed with the algorithm. Some developers put neural network models in their libraries.
- 3 The memory usage is the peak resident set size reported by the ps system call during template generation.
- 4 The median template creation times are measured on Intel®Xeon®CPU E5-2630 v4 @ 2.20GHz processors.
- 5 The comparison durations, in nanoseconds, are estimated using std::chrono::high_resolution_clock which on the machine in (2) counts 1ns clock ticks. Precision is somewhat worse than that however. The ± value is the median absolute deviation times 1.48 for Normal consistency.

Table 12: Summary of algorithms and properties included in this report. The red superscripts give ranking for the quantity in that column.

	ALGORITHM	CONFIG	LIBRARY	TEMPLATE								COMPARISON ⁴					
				NAME		DATA		MEMORY		SIZE		GENERATION TIME (ms) ⁴				TIME (ns) ⁵	
				(KB) ¹	(KB) ²	(MB) ³	(B)	MUGSHOT	480x720	960x1440	1600x2400	3000x4500	GENUINE	IMPOSTOR			
221	isityou-000	48010	36621	17	110	471	19200 ± 0	18	113 ± 5	-	-	-	-	469	237517 ± 1318	469	237374 ± 1279
222	isystems-001	274621	639268	253	1091	310	2048 ± 0	59	291 ± 9	-	-	-	-	54	557 ± 16	58	564 ± 22
223	isystems-002	358984	803389	335	1595	161	2048 ± 0	275	822 ± 8	-	-	-	-	108	749 ± 31	85	632 ± 28
224	itmo-007	415979	245376	389	2199	323	2048 ± 0	243	741 ± 2	-	-	-	-	268	2551 ± 50	268	2529 ± 80
225	itmo-008	726866	318238	308	1377	417	4096 ± 0	363	1060 ± 1	322	1058 ± 1	307	1059 ± 1	277	1072 ± 4	229	1104 ± 1
226	ivacognitive-001	256958	62791	224	947	165	2048 ± 0	422	1292 ± 3	388	1289 ± 4	373	1292 ± 4	343	1292 ± 3	292	1321 ± 4
227	iws-000	30875	3063	10	77	36	512 ± 0	51	277 ± 5	44	283 ± 1	96	494 ± 3	242	984 ± 3	405	2987 ± 39
228	jaakit-001	99024	24754	46	251	27	512 ± 0	10	76 ± 0	8	77 ± 0	89	70 ± 0	7	81 ± 0	79	93 ± 0
229	kakao-007	526993	129545	443	3953	324	2048 ± 0	326	952 ± 1	286	961 ± 1	259	958 ± 1	235	962 ± 1	190	968 ± 1
230	kakao-008	734583	104820	437	3876	176	2048 ± 0	377	1135 ± 3	350	1148 ± 3	336	1150 ± 3	299	1156 ± 1	265	1175 ± 1
231	kakaopay-001	397864	179869	146	684	434	4096 ± 0	114	448 ± 0	130	542 ± 0	115	542 ± 0	94	542 ± 0	74	553 ± 0
232	kasikornlabs-000	256471	61000	149	693	197	2048 ± 0	306	908 ± 36	251	878 ± 22	263	969 ± 39	310	1184 ± 54	390	2382 ± 145
233	kasikornlabs-002	256431	61063	169	757	254	2048 ± 0	311	917 ± 35	265	907 ± 13	262	963 ± 13	355	1320 ± 45	396	2629 ± 178
234	kedacom-000	245292	37401	472	23574	12	292 ± 0	141	506 ± 3	135	547 ± 10	142	614 ± 9	106	588 ± 10	110	665 ± 24
235	kiwitech-000	369711	21375	188	808	230	2048 ± 0	179	591 ± 0	152	594 ± 0	134	595 ± 1	112	596 ± 0	92	609 ± 0
236	kneron-003	58366	1747	39	188	270	2048 ± 0	55	281 ± 3	43	280 ± 1	39	315 ± 13	43	365 ± 7	267	1224 ± 30
237	kneron-005	375374	13633	85	457	156	2048 ± 0	145	518 ± 2	123	522 ± 4	121	556 ± 5	168	757 ± 19	375	1760 ± 25
238	knowutech-000	808045	32886	299	1303	99	1536 ± 0	456	1419 ± 2	408	1372 ± 1	401	1377 ± 1	378	1382 ± 2	312	1386 ± 2
239	kookmin-002	371771	30734	190	827	121	2048 ± 0	358	1038 ± 2	320	1047 ± 1	301	1045 ± 1	271	1061 ± 1	231	1116 ± 1
240	koreaid-001	256261	20152	360	1811	158	2048 ± 0	90	384 ± 2	72	390 ± 1	76	444 ± 2	97	556 ± 6	144	795 ± 5
241	krungthai-002	2360957	15033	273	1171	241	2048 ± 0	67	308 ± 0	53	314 ± 5	35	309 ± 0	35	319 ± 0	33	362 ± 0
242	kuke3d-001	403462	68786	107	530	432	4096 ± 0	268	814 ± 2	225	811 ± 2	201	814 ± 2	181	814 ± 1	156	834 ± 1
243	kuke3d-002	270544	1227855	189	809	250	2048 ± 0	140	504 ± 3	119	504 ± 1	103	511 ± 1	89	523 ± 2	84	585 ± 1
244	lebentech-000	0	10360	18	110	19	512 ± 0	322	± 0	22	± 0	122	± 0	123	± 0	110	801 ± 42
245	lemalabs-001	748400	198794	412	2738	125	2048 ± 0	266	810 ± 0	226	812 ± 0	200	813 ± 0	183	819 ± 0	158	844 ± 1
246	lineclova-002	475779	406756	304	1353	137	2048 ± 0	419	1284 ± 1	384	1275 ± 2	369	1275 ± 1	339	1273 ± 2	279	1281 ± 2
247	lineclova-003	585149	410482	349	1726	283	2048 ± 0	459	1444 ± 1	430	1438 ± 1	422	1439 ± 2	397	1440 ± 1	331	1446 ± 2
248	lookman-002	138200	25410	470	16518	60	548 ± 0	20	173 ± 1	-	-	-	-	71	610 ± 19	78	612 ± 22
249	lookman-004	244775	37401	471	23548	59	548 ± 0	142	507 ± 5	133	545 ± 12	141	613 ± 12	109	590 ± 11	106	656 ± 16
250	luxand-000	0	57908	306	1366	87	1040 ± 0	100	407 ± 23	88	433 ± 11	75	444 ± 14	68	464 ± 14	80	562 ± 25
251	mantra-000	471458	62566	167	749	350	2052 ± 0	104	413 ± 18	109	487 ± 19	95	494 ± 18	85	511 ± 18	89	598 ± 19
252	maxvision-002	171894	60623	365	1863	102	2048 ± 0	25	172 ± 0	19	171 ± 0	16	172 ± 0	13	174 ± 0	15	221 ± 0
253	maxvision-003	234062	61252	391	2292	219	2048 ± 0	128	474 ± 0	102	468 ± 0	87	471 ± 0	73	475 ± 0	67	519 ± 0
254	megvii-005	1378009	44038	445	4036	336	2049 ± 0	428	1319 ± 5	376	1247 ± 6	359	1240 ± 2	330	1245 ± 2	286	1298 ± 3
255	megvii-006	1554938	44038	448	4354	332	2049 ± 0	420	1287 ± 3	386	1286 ± 0	408	1393 ± 5	353	1319 ± 1	303	1360 ± 1
256	meituan-001	615387	333249	257	1106	152	2048 ± 0	351	1017 ± 4	306	1008 ± 3	288	1010 ± 2	256	1010 ± 3	198	1011 ± 4
257	meituan-002	686111	244091	387	2191	411	4096 ± 0	361	1052 ± 0	327	1086 ± 1	312	1064 ± 2	270	1060 ± 5	218	1063 ± 1
258	meiya-001	280055	264913	97	507	329	2049 ± 0	192	622 ± 12	-	-	-	-	373	8356 ± 615	373	8134 ± 97
259	mendaxiatech-000	1941475	45484	428	3195	438	4097 ± 0	407	1243 ± 2	377	1255 ± 1	399	1373 ± 2	417	1598 ± 3	398	2689 ± 8
260	metsakurcompany-001	445177	1091558	331	1572	366	2056 ± 0	169	578 ± 1	149	587 ± 3	130	590 ± 1	133	659 ± 1	160	854 ± 1
261	metsakurcompany-002	0	957558	231	983	360	2056 ± 0	338	980 ± 1	292	978 ± 1	267	976 ± 2	253	1005 ± 1	228	1103 ± 2
262	maxis-001	0	215019	57	322	43	512 ± 0	52	279 ± 0	42	278 ± 0	32	278 ± 1	30	285 ± 0	25	297 ± 0
263	microfocus-001	104524	27242	40	190	5	256 ± 0	47	264 ± 18	-	-	-	-	16	215 ± 8	17	217 ± 10
264	microfocus-002	96288	27362	36	176	4	256 ± 0	45	259 ± 18	-	-	-	-	28	337 ± 34	18	230 ± 25

Notes

- 1 The configuration size does not capture static data included in libraries.
- 2 The library size is the combined total of all files provided in the submission lib folder. These libraries e.g. OpenCV may or may not be installed on any end user's platform natively and would not need to be installed with the algorithm. Some developers put neural network models in their libraries.
- 3 The memory usage is the peak resident set size reported by the ps system call during template generation.
- 4 The median template creation times are measured on Intel®Xeon®CPU E5-2630 v4 @ 2.20GHz processors.
- 5 The comparison durations, in nanoseconds, are estimated using std::chrono::high_resolution_clock which on the machine in (2) counts 1ns clock ticks. Precision is somewhat worse than that however. The ± value is the median absolute deviation times 1.48 for Normal consistency.

Table 13: Summary of algorithms and properties included in this report. The red superscripts give ranking for the quantity in that column.

	ALGORITHM	CONFIG	LIBRARY	TEMPLATE								COMPARISON ⁴									
				NAME	DATA	DATA	MEMORY	SIZE	GENERATION TIME (ms) ⁴				TIME (ns) ⁵								
									(KB) ¹	(KB) ²	(MB) ³	(B)	MUGSHOT	480x720	960x1440	1600x2400	3000x4500	GENUINE	IMPOSTOR		
265	minivision-000	836697	16597	444	4013	398	4096 ± 0	357	1035 ± 1	317	1033 ± 2	298	1035 ± 1	263	1037 ± 1	215	1059 ± 2	264	2466 ± 26	262	2460 ± 25
266	mobai-000	365451	80573	178	786	458	6144 ± 0	249	766 ± 8	244	869 ± 6	352	1205 ± 31	426	1867 ± 45	414	3549 ± 190	408	16458 ± 333	408	16423 ± 1473
267	mobai-001	265297	60164	108	534	103	2048 ± 0	184	612 ± 3	159	614 ± 3	169	687 ± 9	205	886 ± 31	370	1707 ± 103	177	1386 ± 25	178	1377 ± 26
268	mobbl-001	231160	58706	42	223	190	2048 ± 0	30	183 ± 32	24	184 ± 25	47	354 ± 76	185	823 ± 396	401	2781 ± 1166	390	11832 ± 109	391	11851 ± 88
269	mobbl-003	172248	60960	51	270	212	2048 ± 0	214	664 ± 6	176	661 ± 5	160	663 ± 5	138	665 ± 6	117	691 ± 5	395	12506 ± 111	396	12509 ± 100
270	mobilpintech-000	370514	303291	263	1130	133	2048 ± 0	408	1245 ± 1	371	1234 ± 1	365	1264 ± 1	368	1360 ± 1	369	1707 ± 1	401	14506 ± 214	401	14433 ± 197
271	moreedian-000	525259	21374	220	932	179	2048 ± 0	232	694 ± 0	193	698 ± 0	175	699 ± 0	150	700 ± 0	125	713 ± 1	216	1803 ± 11	214	1779 ± 23
272	mukh-001	866223	451194	340	1637	72	1024 ± 0	439	1375 ± 17	412	1390 ± 12	415	1406 ± 8	380	1394 ± 10	304	1360 ± 11	38	433 ± 14	40	435 ± 14
273	mukh-002	693809	454936	258	1109	126	2048 ± 0	331	968 ± 1	270	921 ± 12	257	957 ± 2	230	954 ± 6	187	953 ± 5	74	612 ± 13	76	611 ± 17
274	multimodality-000	0	503924	314	1417	141	2048 ± 0	105	416 ± 0	85	420 ± 0	67	423 ± 0	59	427 ± 0	51	463 ± 0	121	848 ± 25	115	800 ± 28
275	multimodality-001	185719	545045	310	1388	412	4096 ± 0	396	1190 ± 2	354	1169 ± 2	340	1165 ± 2	303	1167 ± 2	257	1177 ± 2	184	1424 ± 35	180	1384 ± 42
276	mvision-001	227502	149531	159	723	15	512 ± 0	230	691 ± 21	194	702 ± 19	173	697 ± 24	152	708 ± 29	124	710 ± 27	159	1123 ± 40	165	1154 ± 38
277	nazhiai-000	547484	16141	410	2716	282	2048 ± 0	222	683 ± 3	188	687 ± 2	209	835 ± 27	192	840 ± 31	157	834 ± 34	254	2230 ± 34	248	2133 ± 81
278	neosystems-004	243546	352623	106	529	123	2048 ± 0	71	324 ± 0	198	711 ± 3	206	827 ± 7	197	854 ± 2	176	916 ± 2	400	14437 ± 176	400	14355 ± 173
279	netbridge-tech-001	133108	205875	98	508	403	4096 ± 0	12	85 ± 1	10	83 ± 0	9	84 ± 0	9	92 ± 0	9	113 ± 4	378	9280 ± 74	378	9446 ± 512
280	netbridge-tech-002	257687	49931	54	299	213	2048 ± 0	280	838 ± 6	234	838 ± 2	210	839 ± 1	191	839 ± 3	161	859 ± 3	284	2893 ± 65	293	3050 ± 123
281	neurotechnology-013	474749	85552	420	2894	48	514 ± 0	344	1000 ± 1	304	1006 ± 2	290	1022 ± 2	269	1053 ± 2	258	1195 ± 8	210	109 ± 4	110	110 ± 4
282	neurotechnology-015	474782	86045	402	2564	49	515 ± 0	355	1028 ± 3	316	1033 ± 3	305	1055 ± 4	280	1097 ± 4	287	1304 ± 18	4130	130 ± 2	4130	130 ± 4
283	nhn-002	363471	817674	141	667	412	4096 ± 0	380	1141 ± 3	345	1138 ± 2	332	1141 ± 2	298	1151 ± 6	261	1203 ± 2	453	56608 ± 579	453	56549 ± 606
284	nhn-003	933665	432730	321	1464	399	4096 ± 0	403	1229 ± 2	378	1261 ± 1	364	1263 ± 3	343	1279 ± 2	308	1375 ± 3	449	50560 ± 105	448	50592 ± 142
285	nodeflux-002	774668	690213	88	466	147	2048 ± 0	238	708 ± 4	197	709 ± 4	180	716 ± 5	158	716 ± 7	132	736 ± 3	309	3475 ± 62	306	3408 ± 143
286	notiontag-001	92753	427967	116	566	63	584 ± 0	317	929 ± 35	330	1092 ± 39	442	3709 ± 81	442	10233 ± 180	-	443	43636 ± 286	442	43724 ± 330	
287	notiontag-002	271987	967207	418	2840	388	2120 ± 0	116	453 ± 2	95	453 ± 3	78	453 ± 3	64	458 ± 2	53	471 ± 3	416	20278 ± 194	416	20195 ± 186
288	nsensecorp-003	199895	117041	156	710	218	2048 ± 0	211	661 ± 0	177	664 ± 0	159	662 ± 1	135	659 ± 1	108	659 ± 0	444	44658 ± 51	444	44654 ± 72
289	nsensecorp-004	513276	139178	341	1663	104	2048 ± 0	458	1433 ± 0	431	1445 ± 7	427	1450 ± 3	410	1487 ± 5	-	261	2388 ± 42	261	2385 ± 63	
290	ntechlab-011	786933	209458	462	6867	91	1280 ± 0	384	1148 ± 2	424	1142 ± 1	338	1159 ± 1	312	1185 ± 1	283	1290 ± 3	7	179 ± 11	8	173 ± 11
291	ntechlab-012	570796	212350	456	5451	390	2560 ± 0	427	1309 ± 1	399	1323 ± 1	385	1331 ± 1	369	1360 ± 1	335	1460 ± 3	15	211 ± 8	15	211 ± 7
292	omface-000	45945	844976	29	150	69	1024 ± 0	32	185 ± 1	27	206 ± 2	22	203 ± 1	15	195 ± 1	14	193 ± 1	46	481 ± 42	44	456 ± 20
293	omface-001	146370	1799745	26	145	71	1024 ± 0	34	194 ± 2	29	222 ± 2	23	209 ± 0	19	216 ± 1	17	233 ± 1	410	18369 ± 19	410	18366 ± 32
294	omnigarde-001	200523	32882	87	464	25	512 ± 0	318	941 ± 0	255	883 ± 1	226	886 ± 1	209	891 ± 1	171	898 ± 0	182	1405 ± 31	179	1379 ± 26
295	omnigarde-002	368860	32882	168	757	81	1024 ± 0	424	1303 ± 1	375	1246 ± 1	362	1249 ± 1	333	1253 ± 1	274	1261 ± 1	275	2272 ± 34	275	2686 ± 32
296	onfido-000	273478	959781	214	908	118	2048 ± 0	118	459 ± 17	94	451 ± 15	77	451 ± 14	67	462 ± 15	59	505 ± 18	198	1617 ± 50	199	1637 ± 53
297	openface-001	0	40111	16	100	278	2048 ± 0	22	148 ± 1	16	154 ± 0	49	365 ± 3	56	409 ± 9	94	616 ± 31	70	608 ± 14	74	604 ± 13
298	oz-003	484147	519652	469	11949	353	2053 ± 0	438	1375 ± 12	411	1388 ± 3	441	1773 ± 16	428	2039 ± 6	410	3209 ± 5	465	73905 ± 456	465	73892 ± 444
299	oz-004	373982	1075452	466	8071	354	2053 ± 0	279	832 ± 7	246	871 ± 6	230	899 ± 10	278	1078 ± 12	361	1608 ± 10	457	61654 ± 418	456	61749 ± 450
300	palit-000	428754	144958	305	1355	413	4096 ± 0	168	570 ± 1	143	578 ± 1	126	576 ± 3	105	583 ± 1	93	614 ± 1	253	2227 ± 16	255	2226 ± 16
301	palit-001	173886	145564	120	583	259	2048 ± 0	40	227 ± 0	31	224 ± 1	25	224 ± 1	25	229 ± 3	22	262 ± 2	160	1150 ± 16	161	1135 ± 23
302	pangiam-000	464252	24512	442	3919	107	2048 ± 0	195	627 ± 5	162	618 ± 4	143	615 ± 3	121	620 ± 3	104	639 ± 3	3	118 ± 7	3	113 ± 7
303	papago-001	669274	52817	392	2341	160	2048 ± 0	416	1272 ± 6	390	1296 ± 7	377	1295 ± 6	344	1281 ± 3	298	1345 ± 3	405	15236 ± 169	405	15184 ± 142
304	papsav1923-002	491185	24727	266	1136	344	2052 ± 0	259	792 ± 1	291	978 ± 1	299	1042 ± 1	300	1158 ± 1	365	1641 ± 19	165	1209 ± 29	167	1206 ± 38
305	papsav1923-003	515576	24803	261	1112	207	2048 ± 0	261	797 ± 0	295	987 ± 1	300	1043 ± 1	308	1178 ± 1	379	1809 ± 7	125	903 ± 26	128	905 ± 34
306	paravision-010	688291	205854	383	2150	439	4100 ± 0	199	634 ± 0	170	635 ± 0	150	635 ± 0	124	635 ± 0	101	635 ± 1	194	1577 ± 35	195	1571 ± 32
307	paravision-011	781138	95589	394	2420	440	4100 ± 0	285	852 ± 0	245	871 ± 1	214	858 ± 1	196	854 ± 0	166	873 ± 1	197	1608 ± 35	197	1625 ± 32
308	pensees-001	1619431	408932	369	1922	467	8200 ± 0	371	1108 ± 3	432	1448 ± 17	421	1439 ± 10	403	1464 ± 5	356	1546 ± 9	298	3151 ± 34	298	3143 ± 25

Notes

1 The configuration size does not capture static data included in libraries.

2 The library size is the combined total of all files provided in the submission lib folder. These libraries e.g. OpenCV may or may not be installed on any end user's platform natively and would not need to be installed with the algorithm. Some developers put neural network models in their libraries.

3 The memory usage is the peak resident set size reported by the ps system call during template generation.

4 The median template creation times are measured on Intel®Xeon®CPU E5-2630 v4 @ 2.20GHz processors.

5 The comparison durations, in nanoseconds, are estimated using std::chrono::high_resolution_clock which on the machine in (2) counts 1ns clock ticks. Precision is somewhat worse than that however. The ± value is the median absolute deviation times 1.48 for Normal consistency.

	ALGORITHM	CONFIG	LIBRARY	TEMPLATE								COMPARISON ⁴									
				NAME	DATA	DATA	MEMORY	SIZE	GENERATION TIME (ms) ⁴				TIME (ns) ⁵								
									(KB) ¹	(KB) ²	(MB) ³	(B)	MUGSHOT	480x720	960x1440	1600x2400	3000x4500	GENUINE	IMPOSTOR		
309	pixelall-008	0	992249	354	1741	465	8192 ± 0	466	1471 ± 3	422	1405 ± 4	416	1409 ± 4	390	1413 ± 3	325	1426 ± 4	215	1799 ± 50	218	1807 ± 48
310	pixelall-009	0	1009114	350	1731	466	8192 ± 0	473	1484 ± 3	418	1395 ± 3	412	1400 ± 4	378	1391 ± 3	327	1433 ± 3	223	1848 ± 13	222	1842 ± 19
311	psl-010	411027	591157	455	5361	450	4168 ± 0	453	1403 ± 9	415	1393 ± 3	406	1392 ± 3	381	1395 ± 3	316	1396 ± 3	30	354 ± 53	30	329 ± 29
312	psl-011	814579	606050	452	4984	468	8248 ± 0	430	1324 ± 2	398	1323 ± 8	383	1326 ± 8	356	1324 ± 8	293	1322 ± 4	203	1680 ± 37	204	1688 ± 40
313	ptakuratsatu-000	0	585434	303	1347	55	538 ± 0	296	875 ± 3	243	863 ± 48	247	928 ± 9	232	958 ± 17	220	1066 ± 26	357	5900 ± 103	354	5687 ± 167
314	pxl-001	110116	78231	32	168	29	512 ± 0	15	101 ± 5	12	104 ± 5	19	189 ± 12	55	408 ± 27	337	1470 ± 144	351	5598 ± 45	351	5590 ± 68
315	pyramid-000	372608	219883	184	804	365	2056 ± 0	172	583 ± 2	-	-	-	-	-	-	369	7147 ± 59	371	7586 ± 425		
316	qazbs-000	362015	805258	202	856	106	2048 ± 0	426	1307 ± 1	374	1243 ± 0	361	1248 ± 9	332	1253 ± 1	277	1270 ± 0	343	5181 ± 62	342	5167 ± 93
317	qluevision-001	173605	205230	69	376	464	8192 ± 0	41	229 ± 1	32	230 ± 1	28	231 ± 1	26	233 ± 1	19	239 ± 1	304	3374 ± 38	304	3365 ± 41
318	qnap-002	346963	33284	151	700	150	2048 ± 0	273	821 ± 1	229	824 ± 1	205	824 ± 1	188	826 ± 1	155	832 ± 1	20	293 ± 13	23	287 ± 17
319	qnap-003	245476	61427	173	770	247	2048 ± 0	92	387 ± 0	73	393 ± 0	56	393 ± 0	49	393 ± 1	41	400 ± 2	91	683 ± 20	90	651 ± 17
320	quantasoft-003	370518	211354	244	1058	203	2048 ± 0	198	632 ± 2	169	634 ± 0	146	632 ± 0	123	631 ± 1	100	634 ± 0	13	201 ± 7	12	203 ± 8
321	rankone-013	0	228729	28	149	7	261 ± 0	229	690 ± 5	181	672 ± 1	178	712 ± 1	173	780 ± 1	232	1118 ± 3	32	356 ± 23	26	304 ± 23
322	rankone-014	0	243130	30	163	6	261 ± 0	235	701 ± 1	196	705 ± 0	183	732 ± 1	175	800 ± 1	230	1113 ± 1	25	306 ± 16	20	251 ± 13
323	realnetworks-007	570797	101527	426	3137	371	2056 ± 0	433	1348 ± 2	405	1358 ± 11	395	1363 ± 10	376	1386 ± 9	350	1517 ± 6	55	559 ± 31	53	539 ± 35
324	realnetworks-008	73346	75421	67	369	363	2056 ± 0	62	296 ± 3	48	294 ± 3	46	353 ± 4	41	361 ± 5	57	485 ± 5	51	539 ± 31	54	543 ± 29
325	regula-000	262444	29384	131	610	170	2048 ± 0	395	1187 ± 1	341	1126 ± 1	327	1129 ± 0	290	1132 ± 1	248	1159 ± 1	49	491 ± 16	50	500 ± 22
326	regula-001	256075	25980	228	976	113	2048 ± 0	418	1284 ± 1	369	1220 ± 1	355	1222 ± 1	325	1226 ± 1	272	1255 ± 1	33	361 ± 10	32	342 ± 25
327	remarkai-001	241857	868314	161	730	352	2052 ± 0	278	831 ± 6	237	849 ± 18	306	1055 ± 25	317	1198 ± 34	351	1519 ± 38	168	1229 ± 20	116	805 ± 56
328	remarkai-003	280516	58559	439	3896	441	4100 ± 0	341	986 ± 1	298	993 ± 1	279	992 ± 1	249	999 ± 3	199	1019 ± 2	115	787 ± 20	113	793 ± 22
329	rendip-000	0	437653	145	682	192	2048 ± 0	121	464 ± 2	97	458 ± 0	88	473 ± 0	75	483 ± 1	79	556 ± 4	58	576 ± 13	60	573 ± 11
330	revealmedia-005	293933	202465	172	763	442	4100 ± 0	109	428 ± 0	86	428 ± 0	69	430 ± 0	61	433 ± 0	48	442 ± 0	239	2023 ± 38	239	2009 ± 26
331	revealmedia-006	293933	200912	166	741	346	2052 ± 0	89	381 ± 0	68	381 ± 0	52	382 ± 0	46	384 ± 0	39	394 ± 0	82	626 ± 35	70	600 ± 2
332	rökid-000	258612	396624	281	1218	372	2056 ± 0	155	546 ± 3	131	542 ± 2	118	545 ± 1	88	522 ± 3	81	563 ± 4	308	3457 ± 62	310	3463 ± 77
333	rökid-001	641223	413733	247	1071	379	2060 ± 0	308	911 ± 2	261	901 ± 5	229	899 ± 2	213	900 ± 3	172	901 ± 3	301	3345 ± 50	302	3346 ± 149
334	s1-005	482369	95685	269	1137	292	2048 ± 0	346	1001 ± 0	303	1002 ± 0	286	1004 ± 0	254	1008 ± 0	201	1029 ± 2	81	626 ± 74	62	589 ± 14
335	s1-006	482372	95681	268	1137	175	2048 ± 0	324	951 ± 0	284	956 ± 0	258	957 ± 0	234	962 ± 0	192	983 ± 0	97	696 ± 23	99	696 ± 29
336	saffe-001	85973	62488	34	168	92	1280 ± 0	54	281 ± 1	-	-	-	-	-	-	169	1274 ± 19	172	1277 ± 26		
337	saffe-002	260622	28285	201	855	189	2048 ± 0	270	817 ± 11	224	805 ± 15	199	809 ± 19	182	815 ± 29	150	813 ± 23	102	717 ± 7	102	714 ± 29
338	samsungsds-001	1189592	147444	438	3893	435	4096 ± 0	379	1140 ± 3	348	1145 ± 4	390	1344 ± 5	371	1366 ± 5	349	1514 ± 7	450	51559 ± 773	449	51721 ± 1003
339	samsungsds-002	1040732	147475	396	2431	364	2056 ± 0	376	1118 ± 1	355	1175 ± 12	397	1372 ± 6	357	1324 ± 2	343	1489 ± 4	438	35803 ± 266	439	36181 ± 674
340	samtech-001	288082	219883	128	605	359	2056 ± 0	60	294 ± 3	-	-	-	-	-	-	372	7694 ± 59	372	7678 ± 91		
341	scanovate-002	256986	457227	200	850	131	2048 ± 0	233	696 ± 32	199	713 ± 33	185	738 ± 28	171	779 ± 32	253	1172 ± 53	292	3021 ± 38	296	3120 ± 163
342	scanovate-003	135585	89469	186	808	184	2048 ± 0	173	585 ± 1	158	613 ± 12	131	591 ± 1	116	610 ± 2	114	684 ± 1	285	2926 ± 22	285	2925 ± 20
343	sdc-000	256814	481583	177	786	214	2048 ± 0	309	913 ± 14	264	906 ± 9	333	1142 ± 19	422	1774 ± 45	418	4719 ± 222	436	32645 ± 93	437	32653 ± 112
344	securifai-005	252532	81777	103	525	274	2048 ± 0	440	1377 ± 2	404	1355 ± 1	393	1353 ± 0	366	1357 ± 0	302	1356 ± 0	226	1873 ± 25	224	1847 ± 35
345	securifai-006	452474	81856	175	773	428	4096 ± 0	365	1090 ± 2	318	1086 ± 3	283	1093 ± 1	225	1090 ± 2	305	3376 ± 42	305	3399 ± 40		
346	sensetime-007	765353	37533	458	5699	83	1028 ± 0	445	1386 ± 41	397	1323 ± 2	392	1347 ± 2	370	1366 ± 2	360	1593 ± 8	186	1460 ± 29	185	1425 ± 26
347	sensetime-008	1176483	60067	460	5976	82	1028 ± 0	471	1479 ± 31	429	1436 ± 4	432	1482 ± 4	412	1525 ± 5	366	1669 ± 2	171	1283 ± 51	169	1240 ± 47
348	sertis-000	265572	68770	76	427	258	2048 ± 0	246	754 ± 0	211	759 ± 0	190	764 ± 0	169	760 ± 0	140	763 ± 0	191	1497 ± 29	196	1582 ± 38
349	sertis-002	460790	68929	311	1391	286	2048 ± 0	393	1181 ± 1	357	1178 ± 0	346	1183 ± 0	315	1187 ± 0	265	1221 ± 0	153	1086 ± 32	153	1076 ± 31
350	seventhSense-001	369850	3183365	190	811	343	2052 ± 0	411	1255 ± 2	389	1294 ± 15	370	1277 ± 3	341	1275 ± 2	281	1288 ± 3	233	1936 ± 26	235	1943 ± 34
351	seventhSense-002	452197	1567903	223	944	351	2052 ± 0	410	1252 ± 1	388	1271 ± 1	366	1269 ± 1	338	1272 ± 1	282	1290 ± 1	245	2131 ± 45	245	2123 ± 45
352	shaman-000	0	120033	96	507	410	4096 ± 0	207	653 ± 16	-	-	-	-	-	-	36	380 ± 25	36	379 ± 31		

Notes

- 1 The configuration size does not capture static data included in libraries.
- 2 The library size is the combined total of all files provided in the submission lib folder. These libraries e.g. OpenCV may or may not be installed on any end user's platform natively and would not need to be installed with the algorithm. Some developers put neural network models in their libraries.
- 3 The memory usage is the peak resident set size reported by the ps system call during template generation.
- 4 The median template creation times are measured on Intel®Xeon®CPU E5-2630 v4 @ 2.20GHz processors.
- 5 The comparison durations, in nanoseconds, are estimated using std::chrono::high_resolution_clock which on the machine in (2) counts 1ns clock ticks. Precision is somewhat worse than that however. The ± value is the median absolute deviation times 1.48 for Normal consistency.

Table 15: Summary of algorithms and properties included in this report. The red superscripts give ranking for the quantity in that column.

	ALGORITHM	CONFIG	LIBRARY	TEMPLATE								COMPARISON ⁴		
				NAME	DATA		MEMORY	SIZE	GENERATION TIME (ms) ⁴				TIME (ns) ⁵	
					(KB) ¹	(KB) ²			(B)	MUGSHOT	480x720	960x1440	1600x2400	3000x4500
353	shaman-001	0	174446	¹⁰⁰ 511	⁴²³ 4096 ± 0	⁶¹ 294 ± 2	-	-	-	-	-	-	⁸⁶ 635 ± 19	⁴¹ 441 ± 25
354	shu-002	731250	148309	²¹⁰ 890	⁴⁰⁰ 4096 ± 0	²⁴⁵ 751 ± 2	²¹⁴ 769 ± 4	²⁴³ 922 ± 4	³⁹⁵ 1431 ± 9	⁴¹³ 3489 ± 47	⁴⁷⁴ 2930763 ± 47355	⁴⁷⁴ 2929759 ± 39149	-	-
355	shu-003	428774	146940	⁹⁹ 511	¹¹⁶ 2048 ± 0	²⁷² 820 ± 6	²³¹ 828 ± 3	²⁵¹ 941 ± 9	³⁴⁹ 1308 ± 15	⁴⁰⁶ 3045 ± 44	²⁶⁶ 2506 ± 26	²⁶⁷ 2512 ± 38	-	-
356	siat-002	486842	7738	³⁹⁷ 2434	³⁴⁸ 2052 ± 0	¹⁷⁰ 579 ± 0	-	-	-	-	-	-	¹¹² 769 ± 13	¹⁰⁹ 750 ± 13
357	siat-005	380936	16935	²⁹⁷ 1298	²⁸⁰ 2048 ± 0	⁹⁸ 403 ± 0	⁷⁸ 400 ± 0	⁵⁸ 401 ± 0	⁵³ 403 ± 1	⁴⁵ 422 ± 7	⁵⁹ 577 ± 13	⁶¹ 580 ± 17	-	-
358	sjtu-003	480795	148243	¹¹¹ 538	²⁰¹ 2048 ± 0	²⁷⁴ 821 ± 2	²²⁷ 820 ± 2	²⁴⁴ 923 ± 3	³¹⁸ 1201 ± 3	³⁸⁹ 2373 ± 9	¹⁹³ 1560 ± 20	¹⁹² 1560 ± 14	-	-
359	sjtu-004	1953267	241108	⁴¹¹ 2727	⁴⁵⁴ 4608 ± 0	⁴⁰⁴ 1236 ± 2	³⁶⁵ 1209 ± 2	³⁷⁶ 1294 ± 4	⁴¹⁵ 1554 ± 5	⁴⁰⁰ 2738 ± 8	²⁹⁵ 3057 ± 14	²⁹⁵ 3070 ± 20	-	-
360	sktelecom-000	527132	298496	³⁰¹ 1311	⁹⁶ 1536 ± 0	³⁷³ 1110 ± 1	³³⁹ 1113 ± 1	³²³ 1114 ± 1	²⁸⁵ 1120 ± 1	²⁴⁵ 1155 ± 1	⁴²⁵ 26583 ± 128	⁴²⁴ 26508 ± 126	-	-
361	smartbiometrik-001	30875	92620	⁷ 71	³⁰ 512 ± 0	¹⁹¹ 620 ± 7	¹⁶³ 625 ± 7	¹⁵² 640 ± 4	¹⁶⁰ 728 ± 6	²⁰⁸ 1047 ± 8	⁹⁹ 703 ± 31	¹⁰⁰ 710 ± 40	-	-
362	smartengines-000	1711	3025	⁴ 50	¹¹ 288 ± 0	²⁴ 168 ± 1	²¹ 180 ± 1	¹⁸ 188 ± 3	²⁰ 217 ± 3	²⁴ 275 ± 1	⁹ 197 ± 5	⁷ 167 ± 11	-	-
363	smartengines-001	7095	4601	³ 46	¹⁰ 288 ± 0	⁷⁴ 333 ± 89	⁸¹ 408 ± 1	⁶⁸ 423 ± 1	⁶⁵ 460 ± 2	⁷⁶ 553 ± 5	⁶ 153 ± 11	⁵ 143 ± 13	-	-
364	smartvist-000	5959	134084	³¹ 165	³⁴ 512 ± 0	⁸ 59 ± 0	⁶ 56 ± 0	⁵ 56 ± 0	⁶ 58 ± 0	⁶ 90 ± 1	¹⁸⁵ 1435 ± 31	¹⁸⁴ 1422 ± 48	-	-
365	smilart-002	111826	87805	⁵⁰ 263	⁷⁹ 1024 ± 0	²⁷ 176 ± 16	-	-	-	-	⁴¹¹ 18784 ± 136	⁴¹² 18795 ± 151	-	-
366	smilart-003	67339	91670	⁴¹ 192	²⁶ 512 ± 0	²⁹ 180 ± 12	²² 181 ± 10	³⁷ 313 ± 22	¹³⁷ 665 ± 49	³⁸⁶ 2299 ± 196	¹⁷⁸ 1395 ± 74	¹⁴⁴ 1027 ± 66	-	-
367	sodec-000	836592	13142	⁴²⁷ 3186	⁴¹³ 4096 ± 0	³⁵⁹ 1041 ± 2	³¹⁴ 1032 ± 1	²⁹⁷ 1035 ± 1	²⁶⁴ 1037 ± 2	²¹⁶ 1061 ± 2	²¹⁴ 1794 ± 37	²¹² 1775 ± 23	-	-
368	sqisoft-002	278039	386291	¹⁴⁰ 666	³⁷⁶ 2056 ± 0	¹²⁴ 466 ± 8	¹⁰⁰ 466 ± 2	⁸⁵ 468 ± 11	⁶⁶ 461 ± 6	⁵⁴ 472 ± 4	¹¹⁰ 758 ± 11	¹¹⁰ 760 ± 23	-	-
369	sqisoft-003	362737	607964	¹⁸⁵ 805	³⁶² 2056 ± 0	²⁰² 638 ± 2	¹⁸² 674 ± 7	¹⁸¹ 718 ± 17	¹³⁶ 665 ± 6	¹²⁷ 720 ± 6	¹²⁰ 844 ± 11	¹²⁰ 844 ± 23	-	-
370	stauq-000	879661	624676	²⁴⁵ 1064	⁴³³ 4096 ± 0	²⁶⁷ 813 ± 25	-	-	-	-	²⁸⁸ 2979 ± 31	²⁹¹ 3007 ± 75	-	-
371	starhybrid-001	100509	289356	¹⁹⁸ 845	³²⁷ 2048 ± 0	⁸² 358 ± 82	⁶³ 355 ± 49	⁵¹ 379 ± 58	⁵¹ 401 ± 79	³⁸ 393 ± 67	¹⁵⁰ 1075 ± 51	¹⁵⁴ 1078 ± 53	-	-
372	stcon-000	408095	49619	²⁶⁴ 1131	⁷⁷ 1024 ± 0	¹⁹⁰ 617 ± 1	¹⁶⁶ 632 ± 4	¹⁴⁷ 634 ± 1	¹²⁸ 645 ± 2	¹¹³ 676 ± 6	⁴⁰ 437 ± 10	³⁸ 434 ± 11	-	-
373	sukshi-000	94035	688738	⁶⁸ 372	⁴⁷³ 32768 ± 0	¹⁰¹ 407 ± 11	⁸² 413 ± 8	⁹⁹ 504 ± 8	¹⁴⁵ 689 ± 11	³⁵⁸ 1574 ± 28	³⁸² 9817 ± 50	³⁸¹ 9787 ± 62	-	-
374	suprema-003	498231	116054	²⁸² 1239	¹⁹⁵ 2048 ± 0	⁴⁶¹ 1448 ± 1	⁴²⁴ 1417 ± 4	⁴¹⁸ 1418 ± 3	³⁹² 1421 ± 4	³³³ 1451 ± 5	²⁵⁰ 2201 ± 10	²⁵³ 2198 ± 13	-	-
375	suprema-004	1430475	116085	³⁹⁰ 2272	⁴⁰² 4096 ± 0	⁴⁷⁰ 1478 ± 2	⁴³⁸ 1472 ± 2	⁴³¹ 1469 ± 1	⁴⁰⁷ 1476 ± 1	³⁴⁶ 1496 ± 1	³⁰⁰ 3201 ± 14	³⁰⁰ 3202 ± 22	-	-
376	supremaid-001	258193	23479	¹¹² 541	¹³² 2048 ± 0	¹²⁹ 479 ± 1	¹⁰⁶ 481 ± 0	⁹¹ 481 ± 0	⁷⁷ 490 ± 0	⁶⁹ 522 ± 0	¹⁰⁰ 704 ± 19	⁹¹ 652 ± 19	-	-
377	supremaid-002	256273	23899	⁵⁹ 335	²⁹⁸ 2048 ± 0	¹³³ 483 ± 0	¹¹⁸ 501 ± 0	⁹⁴ 488 ± 0	⁸³ 503 ± 0	⁸² 565 ± 0	²³⁷ 1990 ± 19	²³⁰ 1923 ± 29	-	-
378	surrey-cvssp-000	158030	70795	²⁰⁸ 879	³¹⁶ 2048 ± 0	³⁸¹ 1141 ± 3	³⁵¹ 1157 ± 3	³³⁷ 1158 ± 4	³⁰² 1163 ± 3	²⁶⁹ 1245 ± 3	³⁸⁰ 9557 ± 143	³⁷⁹ 9602 ± 186	-	-
379	surrey-cvssp-001	900280	76392	³⁴⁶ 1707	²⁷³ 2048 ± 0	⁴⁰¹ 1221 ± 1	³⁷² 1238 ± 2	³⁵⁸ 1240 ± 0	³²⁹ 1243 ± 0	²⁷³ 1257 ± 0	⁴¹³ 18970 ± 161	⁴¹³ 18999 ± 176	-	-
380	synesis-006	731941	21817	³²² 1472	⁴⁴⁹ 4104 ± 0	¹⁵⁶ 549 ± 1	¹³⁴ 546 ± 1	¹²⁰ 552 ± 1	⁹⁸ 558 ± 2	¹⁰³ 639 ± 28	⁹⁸ 697 ± 32	⁹⁸ 688 ± 31	-	-
381	synesis-007	1442961	24145	³⁹⁸ 2443	³⁹⁴ 3080 ± 0	³⁹⁹ 1215 ± 5	³⁸¹ 1268 ± 30	³⁷⁹ 1306 ± 67	³⁵¹ 1311 ± 58	³²² 1423 ± 52	⁹² 684 ± 32	⁹⁶ 686 ± 25	-	-
382	synology-000	221021	25809	⁸⁴ 453	³⁰⁵ 2048 ± 0	¹⁰² 407 ± 14	⁸³ 415 ± 14	¹⁷² 694 ± 31	³⁸² 1396 ± 58	⁴¹⁵ 4568 ± 211	⁴¹⁵ 19720 ± 203	⁴¹⁴ 19767 ± 379	-	-
383	synology-002	256713	25943	⁹² 488	²¹⁶ 2048 ± 0	³⁰² 886 ± 4	²⁵⁸ 892 ± 3	²⁴⁰ 920 ± 2	²⁵¹ 1000 ± 5	²⁹⁰ 1317 ± 12	¹⁸⁷ 1466 ± 32	¹⁹⁰ 1496 ± 45	-	-
384	sztu-000	338637	15871	²⁹⁵ 1298	³⁰⁴ 2048 ± 0	¹⁵⁰ 531 ± 0	¹²⁵ 532 ± 0	¹⁰⁹ 533 ± 0	⁹⁰ 537 ± 0	⁷³ 548 ± 0	⁶⁰ 585 ± 11	⁶⁴ 592 ± 13	-	-
385	sztu-001	338650	15871	²⁹⁶ 1298	²⁶⁰ 2048 ± 0	¹⁵¹ 535 ± 0	¹²⁹ 537 ± 0	¹¹³ 538 ± 0	⁹² 540 ± 0	⁷⁵ 553 ± 0	⁶⁶ 599 ± 10	⁶⁸ 598 ± 10	-	-
386	t4isb-000	234227	115237	⁶¹ 343	³⁰¹ 2048 ± 0	³⁴⁸ 1006 ± 5	³⁰¹ 1001 ± 1	²⁸⁷ 1006 ± 1	²⁵⁵ 1009 ± 1	²⁰⁰ 1022 ± 2	³¹⁵ 3586 ± 34	³¹² 3534 ± 34	-	-
387	tech5-005	1178769	120517	³¹⁶ 1426	¹⁶ 512 ± 0	⁴¹⁵ 1272 ± 109	³¹⁸ 1038 ± 63	³⁰³ 1046 ± 39	²⁸⁶ 1124 ± 38	³⁰¹ 1351 ± 44	²⁷⁰ 2573 ± 37	²⁷⁰ 2545 ± 32	-	-
388	tech5-007	0	340324	⁴⁰⁷ 2643	³⁸ 512 ± 0	⁴³⁵ 1360 ± 0	⁴⁰⁶ 1366 ± 0	⁴⁰⁰ 1376 ± 0	³⁷² 1373 ± 0	³²⁹ 1438 ± 6	⁵⁰ 538 ± 19	⁵¹ 516 ± 22	-	-
389	techsign-000	0	1101622	³⁷³ 1955	¹⁸² 2048 ± 0	⁸⁶ 366 ± 1	⁷⁷ 398 ± 1	³⁴¹ 1172 ± 3	⁴³⁹ 3065 ± 18	⁴³⁵ 10460 ± 65	³³³ 4758 ± 112	³³³ 4789 ± 93	-	-
390	techsign-001	0	586983	³⁵³ 1741	³⁰⁸ 2048 ± 0	²⁵² 772 ± 35	²¹⁸ 788 ± 23	¹⁹⁸ 802 ± 42	²²⁹ 949 ± 10	³¹⁹ 1409 ± 26	⁶¹ 592 ± 11	⁶⁵ 592 ± 13	-	-
391	tevian-007	779934	19523	³⁴⁸ 1714	⁸⁵ 1032 ± 0	¹⁷¹ 583 ± 1	¹⁴⁴ 579 ± 0	¹²⁷ 580 ± 0	¹⁰⁷ 588 ± 1	¹⁰² 636 ± 0	³³⁸ 4894 ± 65	³³⁶ 4841 ± 83	-	-
392	tevian-008	847177	19519	⁴³⁰ 3490	⁸⁴ 1032 ± 0	²⁹⁹ 884 ± 2	²⁶³ 903 ± 1	²³² 903 ± 1	²¹⁵ 911 ± 1	¹⁸³ 946 ± 1	³³⁵ 4828 ± 40	³³⁵ 4811 ± 41	-	-
393	tiger-005	342866	253734	³²⁹ 1531	³⁴² 2052 ± 0	³⁶⁶ 1097 ± 2	³²⁵ 1065 ± 2	³¹³ 1066 ± 2	²⁷⁴ 1067 ± 3	²²³ 1088 ± 3	⁷⁶ 620 ± 19	⁸⁰ 615 ± 16	-	-
394	tiger-006	421186	394688	¹⁵⁵ 707	³³⁵ 2052 ± 0	⁴⁴⁷ 1392 ± 16	⁴²³ 1411 ± 10	⁴²⁴ 1444 ± 10	⁴¹⁴ 1531 ± 11	³⁸⁰ 1848 ± 10	²¹⁸ 1810 ± 20	²¹⁷ 1801 ± 13	-	-
395	tinkoff-001	274660	389272	¹²⁵ 592	²³⁵ 2048 ± 0	³⁸⁸ 1176 ± 3	³⁵⁸ 1179 ± 3	³⁴² 1178 ± 3	³⁰⁵ 1169 ± 2	²⁶⁰ 1203 ± 3	³²⁹ 4361 ± 74	³²⁷ 4364 ± 75	-	-
396	tongyi-005	1140701	138919	³⁸¹ 2121	³⁸⁷ 2089 ± 0	²³ 165 ± 1	-	-	-	-	⁴¹² 18924 ± 65	⁴¹⁵ 20158 ± 103	-	-

Notes

1 The configuration size does not capture static data included in libraries.

2 The library size is the combined total of all files provided in the submission lib folder. These libraries e.g. OpenCV may or may not be installed on any end user's platform natively and would not need to be installed with the algorithm. Some developers put neural network models in their libraries.

3 The memory usage is the peak resident set size reported by the ps system call during template generation.

4 The median template creation times are measured on Intel®Xeon®CPU E5-2630 v4 @ 2.20GHz processors.

5 The comparison durations, in nanoseconds, are estimated using std::chrono::high_resolution_clock which on the machine in (2) counts 1ns clock ticks. Precision is somewhat worse than that however. The ± value is the median absolute deviation times 1.48 for Normal consistency.

ALGORITHM		CONFIG	LIBRARY	TEMPLATE								COMPARISON ⁴		
NAME		DATA	DATA	MEMORY	SIZE	GENERATION TIME (ms) ⁴				TIME (ns) ⁵				
	(KB) ¹	(KB) ²	(MB) ³	(B)	MUGSHOT	480x720	960x1440	1600x2400	3000x4500	GENUINE	IMPOSTOR			
397	toppanidgate-000	671181	711850	357 1786	405 4096 ± 0	310 915 ± 1	267 916 ± 1	239 916 ± 1	217 917 ± 1	177 917 ± 1	423 25262 ± 84	422 25264 ± 97		
398	toshiba-004	599297	27880	336 1595	370 2056 ± 0	460 1447 ± 3	434 1453 ± 2	429 1457 ± 9	401 1457 ± 3	340 1479 ± 4	141 1020 ± 25	137 998 ± 32		
399	toshiba-006	599566	44078	334 1588	373 2056 ± 0	472 1481 ± 16	441 1515 ± 7	435 1506 ± 6	411 1521 ± 2	355 1546 ± 30	142 1022 ± 17	143 1022 ± 23		
400	touchlessid-000	92561	64467	158 716	111 2048 ± 0	68 309 ± 5	51 305 ± 2	36 312 ± 5	29 277 ± 4	31 349 ± 17	434 31935 ± 292	435 31958 ± 243		
401	touchlessid-001	255274	14355	110 537	127 2048 ± 0	77 344 ± 1	62 347 ± 1	63 414 ± 3	111 595 ± 10	372 1732 ± 61	217 1806 ± 35	216 1800 ± 35		
402	trueface-002	253947	123116	91 486	101 2000 ± 0	83 360 ± 0	65 361 ± 0	66 423 ± 0	110 590 ± 1	-	8 192 ± 14	10 186 ± 19		
403	trueface-003	346530	24308	441 3915	139 2048 ± 0	370 1107 ± 22	185 677 ± 3	184 732 ± 7	214 905 ± 5	-	1 103 ± 11	2 112 ± 29		
404	trueidvng-001	766071	37721	342 1692	461 6144 ± 0	335 975 ± 1	294 985 ± 1	277 989 ± 1	208 1016 ± 1	236 1128 ± 2	439 37129 ± 216	464 72067 ± 305		
405	tuputech-000	11476	17185	2 33	312 2048 ± 0	21 122 ± 4	15 120 ± 1	13 142 ± 2	17 196 ± 5	42 411 ± 14	420 23893 ± 406	423 25279 ± 406		
406	turingtechvip-001	399874	54535	133 617	243 2048 ± 0	442 1384 ± 4	413 1391 ± 1	407 1393 ± 1	389 1411 ± 1	339 1476 ± 2	208 1733 ± 19	208 1734 ± 20		
407	turingtechvip-002	167556	140995	207 876	249 2048 ± 0	474 1493 ± 2	393 1306 ± 1	404 1382 ± 1	362 1337 ± 1	324 1426 ± 3	399 13819 ± 103	399 13807 ± 137		
408	turkcell-000	271083	133553	136 637	193 2048 ± 0	372 1110 ± 1	332 1094 ± 0	321 1103 ± 0	288 1126 ± 1	259 1201 ± 1	282 2866 ± 23	283 2873 ± 40		
409	twface-000	661735	11782	404 2610	321 2048 ± 0	290 871 ± 1	247 873 ± 1	219 873 ± 2	202 876 ± 2	170 898 ± 1	192 1504 ± 29	191 1510 ± 34		
410	twface-001	671511	11782	419 2855	134 2048 ± 0	315 923 ± 1	274 925 ± 2	245 926 ± 1	221 929 ± 2	180 940 ± 2	180 1400 ± 32	181 1402 ± 37		
411	ulsee-001	370519	57261	-	142 2048 ± 0	208 654 ± 2	-	-	-	-	359 6065 ± 94	361 6228 ± 77		
412	uluface-002	0	480761	251 1088	221 2048 ± 0	293 873 ± 42	240 855 ± 9	269 978 ± 24	336 1271 ± 40	387 2333 ± 68	414 19207 ± 1114	411 18501 ± 274		
413	uluface-003	97357	529422	285 1264	392 3072 ± 0	329 965 ± 11	287 968 ± 10	315 1087 ± 20	377 1387 ± 36	394 2469 ± 86	424 26057 ± 195	426 26865 ± 566		
414	unissey-002	0	1443765	171 763	426 4096 ± 0	242 736 ± 1	208 752 ± 1	280 994 ± 1	394 1426 ± 1	412 3331 ± 2	393 12308 ± 91	393 12302 ± 137		
415	unissey-003	0	814526	135 618	431 4096 ± 0	239 718 ± 1	206 744 ± 0	256 956 ± 1	387 1403 ± 1	407 3055 ± 2	196 1594 ± 20	194 1570 ± 44		
416	upc-001	0	89914	250 1077	88 1052 ± 0	158 551 ± 15	195 703 ± 56	182 724 ± 51	166 751 ± 49	162 863 ± 33	297 3114 ± 44	299 3165 ± 97		
417	uxlabs-001	291127	39378	152 700	406 4096 ± 0	94 395 ± 0	70 387 ± 0	54 388 ± 0	48 390 ± 0	40 396 ± 0	224 1863 ± 31	229 1921 ± 45		
418	vcog-002	3229434	118946	432 3666	474 61504 ± 5	81 357 ± 25	-	-	-	-	471 296154 ± 3077	471 296436 ± 4183		
419	vd-002	254498	34389	148 688	50 516 ± 0	224 684 ± 5	186 679 ± 4	163 676 ± 5	147 693 ± 5	136 754 ± 5	24 300 ± 14	27 319 ± 32		
420	vd-003	254505	44051	150 696	347 2052 ± 0	231 691 ± 5	190 690 ± 5	165 683 ± 4	146 691 ± 5	128 722 ± 5	139 1003 ± 11	139 1001 ± 7		
421	veridas-007	355105	891492	401 2527	240 2048 ± 0	292 872 ± 9	248 875 ± 8	363 1261 ± 18	432 2238 ± 38	426 6374 ± 147	90 655 ± 16	93 660 ± 19		
422	veridas-008	1100495	1190915	467 8932	317 2048 ± 0	320 944 ± 12	280 945 ± 11	386 1334 ± 27	433 2382 ± 48	427 6959 ± 172	103 723 ± 14	105 731 ± 16		
423	veridium-000	0	47198	15 98	472 29399 ± 2045	11 79 ± 0	9 80 ± 0	10 89 ± 0	8 90 ± 0	8 111 ± 0	459 64880 ± 171	458 64697 ± 247		
424	veridium-001	0	40561	24 142	389 2489 ± 0	7 44 ± 0	5 45 ± 0	4 48 ± 0	4 50 ± 0	4 72 ± 0	458 63417 ± 1061	457 63225 ± 2133		
425	verigram-000	256209	7798	363 1842	287 2048 ± 0	263 807 ± 1	228 821 ± 1	264 972 ± 2	367 1358 ± 3	403 2848 ± 13	167 1222 ± 17	168 1219 ± 17		
426	verigram-001	282155	11773	2638	252 2048 ± 0	216 664 ± 2	183 675 ± 2	208 833 ± 4	320 1202 ± 7	399 2733 ± 32	202 1664 ± 60	200 1648 ± 56		
427	verihubs-inteligensia-000	209562	51877	77 427	173 2048 ± 0	164 567 ± 0	442 1558 ± 8	438 1560 ± 8	416 1568 ± 8	362 1621 ± 8	419 22351 ± 91	419 22371 ± 81		
428	verihubs-inteligensia-001	216524	59196	79 437	108 2048 ± 0	162 564 ± 0	139 562 ± 0	123 566 ± 1	101 566 ± 0	90 600 ± 0	417 21770 ± 84	417 21735 ± 102		
429	verijelas-000	254540	10322	352 1736	224 2048 ± 0	69 321 ± 0	56 325 ± 1	42 329 ± 0	38 335 ± 5	32 360 ± 0	384 10267 ± 143	384 10218 ± 109		
430	via-000	124422	11151	226 964	233 2048 ± 0	237 707 ± 8	204 740 ± 5	234 906 ± 41	226 941 ± 40	205 1040 ± 5	132 966 ± 28	142 1021 ± 44		
431	via-001	370255	11151	343 1697	239 2048 ± 0	328 964 ± 3	308 1011 ± 3	292 1026 ± 4	267 1045 ± 3	239 1137 ± 28	135 983 ± 31	135 989 ± 40		
432	videmo-001	212051	95063	56 304	124 2048 ± 0	35 199 ± 0	17 164 ± 0	14 164 ± 0	11 164 ± 0	10 165 ± 0	21 296 ± 17	24 288 ± 16		
433	videmo-002	212053	32963	58 332	285 2048 ± 0	31 199 ± 0	18 169 ± 0	15 169 ± 0	12 170 ± 0	12 170 ± 0	14 209 ± 7	14 208 ± 8		
434	videonetics-001	30875	5963	5 61	24 512 ± 0	46 262 ± 3	40 273 ± 1	73 439 ± 3	184 820 ± 3	391 2393 ± 43	161 1153 ± 38	162 1142 ± 65		
435	videonetics-002	121981	6289	19 115	345 2052 ± 0	56 282 ± 5	49 295 ± 1	104 513 ± 4	260 1029 ± 3	408 3151 ± 46	166 1219 ± 57	170 1262 ± 56		
436	viettelhightech-000	259471	215557	75 419	326 2048 ± 0	119 461 ± 1	98 461 ± 2	81 461 ± 1	70 467 ± 2	58 494 ± 0	65 599 ± 11	63 591 ± 13		
437	vigilantsolutions-010	348798	49973	197 840	98 1548 ± 0	189 615 ± 0	165 631 ± 0	145 632 ± 0	125 636 ± 0	107 659 ± 0	48 490 ± 13	49 488 ± 11		
438	vigilantsolutions-011	255661	49973	124 591	97 1548 ± 0	97 402 ± 0	84 418 ± 0	64 418 ± 0	57 422 ± 0	50 445 ± 0	29 339 ± 20	33 366 ± 37		
439	vinai-000	402391	866522	240 1032	262 2048 ± 0	368 1099 ± 1	333 1095 ± 1	317 1093 ± 1	281 1099 ± 1	234 1126 ± 1	280 2996 ± 20	290 2993 ± 26		
440	vinbigdata-001	271405	44746	123 589	251 2048 ± 0	430 1400 ± 5	416 1393 ± 2	405 1391 ± 2	379 1393 ± 1	318 1404 ± 1	175 1351 ± 50	175 1310 ± 38		

Notes

- 1 The configuration size does not capture static data included in libraries.
 - 2 The library size is the combined total of all files provided in the submission lib folder. These libraries e.g. OpenCV may or may not be installed on any end user's platform natively and would not need to be installed with the algorithm. Some developers put neural network models in their libraries.
 - 3 The memory usage is the peak resident set size reported by the ps system call during template generation.
 - 4 The median template creation times are measured on Intel®Xeon®CPU E5-2630 v4 @ 2.20GHz processors.
 - 5 The comparison durations, in nanoseconds, are estimated using std::chrono::high_resolution_clock which on the machine in (2) counts 1ns clock ticks. Precision is somewhat worse than that however. The \pm value is the median absolute deviation times 1.48 for Normal consistency.

	ALGORITHM	CONFIG	LIBRARY	TEMPLATE								COMPARISON ⁴			
				NAME		DATA		MEMORY	SIZE	GENERATION TIME (ms) ⁴				TIME (ns) ⁵	
				(KB) ¹	(KB) ²	(MB) ³	(B)			MUGSHOT	480x720	960x1440	1600x2400	3000x4500	GENUINE
441	vinbigdata-002	256322	138864	130 ⁶⁰⁶	117 ^{2048 ± 0}	166 ^{569 ± 2}	142 ^{572 ± 1}	124 ^{571 ± 1}	102 ^{572 ± 1}	88 ^{596 ± 1}	248 ^{2175 ± 44}	249 ^{2160 ± 53}			
442	vion-000	228219	7533	94 ⁴⁹⁸	339 ^{2052 ± 0}	73 ^{333 ± 1}	-	-	-	-	441 ^{39839 ± 3561}	425 ^{26830 ± 2241}			
443	visage-000	49218	70150	9 ⁷³	40 ^{512 ± 0}	4 ^{27 ± 0}	2 ^{27 ± 0}	2 ^{31 ± 0}	338 ^{± 0}	3 ^{63 ± 0}	252 ^{2220 ± 14}	254 ^{2218 ± 14}			
444	visionbox-001	256869	190645	118 ⁵⁷⁹	308 ^{2048 ± 0}	339 ^{983 ± 7}	331 ^{1093 ± 46}	394 ^{1360 ± 68}	430 ^{2181 ± 105}	424 ^{5955 ± 281}	163 ^{1161 ± 22}	164 ^{1154 ± 20}			
445	visionbox-002	259063	135281	132 ⁶¹²	378 ^{2059 ± 0}	131 ^{482 ± 1}	108 ^{482 ± 0}	92 ^{484 ± 1}	79 ^{492 ± 1}	66 ^{517 ± 3}	236 ^{1969 ± 44}	233 ^{1931 ± 42}			
446	visionlabs-010	1067280	19357	211 ⁹⁰²	45 ^{513 ± 0}	240 ^{730 ± 0}	200 ^{717 ± 1}	176 ^{709 ± 0}	155 ^{713 ± 1}	134 ^{739 ± 0}	69 ^{600 ± 41}	82 ^{626 ± 35}			
447	visionlabs-011	1067280	19353	204 ⁸⁶²	44 ^{513 ± 0}	241 ^{731 ± 1}	201 ^{717 ± 1}	177 ^{710 ± 1}	156 ^{714 ± 1}	135 ^{741 ± 1}	53 ^{556 ± 26}	56 ^{559 ± 25}			
448	visteam-004	61594	35369	35 ¹⁶⁸	318 ^{2048 ± 0}	63 ^{303 ± 5}	52 ^{313 ± 6}	31 ^{278 ± 4}	32 ^{288 ± 4}	35 ^{377 ± 7}	322 ^{3936 ± 72}	321 ^{3938 ± 79}			
449	visteam-005	288140	35427	62 ³⁴⁸	222 ^{2048 ± 0}	375 ^{1117 ± 6}	336 ^{1106 ± 6}	309 ^{1060 ± 4}	276 ^{1071 ± 4}	246 ^{1156 ± 8}	321 ^{3932 ± 97}	321 ^{3932 ± 71}			
450	vixvizion-006	594053	396294	216 ⁹¹⁴	181 ^{2048 ± 0}	297 ^{876 ± 9}	232 ^{828 ± 3}	204 ^{817 ± 1}	180 ^{825 ± 2}	165 ^{871 ± 1}	68 ^{600 ± 23}	77 ^{611 ± 25}			
451	vixvizion-007	594053	470119	293 ¹²⁸²	191 ^{2048 ± 0}	300 ^{885 ± 35}	233 ^{828 ± 1}	203 ^{816 ± 1}	187 ^{825 ± 1}	164 ^{870 ± 1}	67 ^{600 ± 28}	72 ^{602 ± 34}			
452	vnpt-004	370110	240841	233 ⁹⁸⁸	296 ^{2048 ± 0}	406 ^{1238 ± 1}	373 ^{1241 ± 1}	360 ^{1242 ± 2}	348 ^{1307 ± 2}	347 ^{1505 ± 2}	325 ^{4047 ± 48}	323 ^{4008 ± 108}			
453	vnpt-005	560630	240888	270 ¹¹⁴¹	143 ^{2048 ± 0}	452 ^{1403 ± 0}	421 ^{1404 ± 6}	413 ^{1403 ± 6}	399 ^{1456 ± 0}	363 ^{1630 ± 10}	313 ^{3562 ± 23}	313 ^{3554 ± 29}			
454	vocord-009	1380132	201560	446 ⁴¹⁶²	100 ^{1920 ± 0}	468 ^{1472 ± 2}	437 ^{1472 ± 1}	419 ^{1549 ± 1}	419 ^{1667 ± 2}	383 ^{2064 ± 2}	241 ^{2052 ± 50}	241 ^{2056 ± 39}			
455	vocord-010	902552	206873	436 ³⁸⁵⁸	89 ^{1088 ± 0}	464 ^{1459 ± 2}	436 ^{1459 ± 1}	430 ^{1463 ± 2}	409 ^{1484 ± 1}	353 ^{1535 ± 3}	274 ^{2724 ± 31}	273 ^{2653 ± 45}			
456	vts-000	256589	169760	345 ¹⁷⁰⁴	105 ^{2048 ± 0}	136 ^{486 ± 1}	107 ^{481 ± 0}	93 ^{484 ± 0}	76 ^{485 ± 1}	65 ^{517 ± 0}	468 ^{124209 ± 352}	468 ^{123652 ± 358}			
457	vts-001	293000	475743	134 ⁶¹⁸	307 ^{2048 ± 0}	219 ^{676 ± 1}	187 ^{683 ± 6}	168 ^{687 ± 3}	148 ^{695 ± 2}	122 ^{709 ± 2}	381 ^{9620 ± 44}	380 ^{9618 ± 54}			
458	wicket-000	826392	641802	379 ²⁰⁷¹	248 ^{2048 ± 0}	457 ^{1419 ± 2}	426 ^{1429 ± 3}	423 ^{1444 ± 4}	402 ^{1460 ± 3}	354 ^{1537 ± 6}	456 ^{60976 ± 232}	455 ^{61096 ± 323}			
459	winsense-001	264428	32035	219 ⁹²²	93 ^{1280 ± 0}	250 ^{766 ± 7}	321 ^{1058 ± 47}	272 ^{983 ± 97}	268 ^{1053 ± 119}	291 ^{1320 ± 84}	199 ^{1631 ± 28}	237 ^{1964 ± 171}			
460	winsense-002	281379	25780	356 ¹⁷⁸¹	277 ^{2048 ± 0}	138 ^{494 ± 2}	114 ^{498 ± 1}	106 ^{519 ± 1}	91 ^{537 ± 1}	99 ^{634 ± 1}	204 ^{1683 ± 8}	203 ^{1685 ± 7}			
461	wiseai-001	189467	60781	44 ²⁴⁵	323 ^{2048 ± 0}	43 ^{240 ± 0}	35 ^{251 ± 0}	41 ^{328 ± 1}	37 ^{327 ± 0}	27 ^{332 ± 0}	279 ^{2850 ± 29}	282 ^{2852 ± 31}			
462	wuhantianyu-001	465118	66457	205 ⁸⁶⁶	302 ^{2048 ± 0}	203 ^{642 ± 1}	172 ^{642 ± 1}	156 ^{644 ± 0}	131 ^{652 ± 0}	120 ^{697 ± 0}	379 ^{9502 ± 151}	383 ^{9920 ± 253}			
463	x-laboratory-000	520020	197310	327 ¹⁵²⁴	368 ^{2056 ± 0}	264 ^{808 ± 7}	260 ^{897 ± 113}	238 ^{907 ± 103}	207 ^{886 ± 103}	112 ^{673 ± 39}	104 ^{725 ± 19}	108 ^{749 ± 34}			
464	x-laboratory-001	625140	398792	364 ¹⁸⁴⁴	357 ^{2056 ± 0}	174 ^{586 ± 2}	134 ^{596 ± 5}	138 ^{603 ± 6}	120 ^{620 ± 7}	143 ^{793 ± 14}	117 ^{813 ± 28}	122 ^{872 ± 32}			
465	xforwardai-001	340100	51163	384 ²¹⁷³	198 ^{2048 ± 0}	391 ^{1180 ± 2}	361 ^{1182 ± 1}	350 ^{1194 ± 1}	314 ^{1186 ± 2}	262 ^{1203 ± 1}	114 ^{779 ± 17}	114 ^{797 ± 13}			
466	xforwardai-002	707715	51163	376 ¹⁹⁸⁹	430 ^{4096 ± 0}	319 ^{944 ± 1}	279 ^{942 ± 1}	252 ^{943 ± 4}	224 ^{935 ± 1}	189 ^{967 ± 1}	183 ^{1406 ± 8}	182 ^{1405 ± 13}			
467	xm-000	578041	148920	147 ⁶⁸⁸	340 ^{2052 ± 0}	298 ^{878 ± 2}	254 ^{882 ± 1}	276 ^{988 ± 2}	334 ^{1258 ± 3}	393 ^{2434 ± 7}	200 ^{1634 ± 17}	198 ^{1632 ± 20}			
468	yisheng-004	486351	38653	291 ¹²⁷⁹	396 ^{3704 ± 0}	87 ^{378 ± 12}	-	-	-	-	96 ^{693 ± 137}	52 ^{526 ± 34}			
469	yitu-003	1525719	138919	434 ³⁷³⁷	386 ^{2082 ± 0}	287 ^{860 ± 0}	-	-	-	-	409 ^{18305 ± 71}	409 ^{18286 ± 62}			
470	yoonik-002	453720	265415	415 ²⁷⁵⁵	172 ^{2048 ± 0}	383 ^{1145 ± 4}	340 ^{1123 ± 2}	325 ^{1124 ± 2}	287 ^{1125 ± 2}	235 ^{1126 ± 3}	111 ^{761 ± 32}	107 ^{736 ± 32}			
471	yoonik-003	346691	265415	388 ²¹⁹⁶	151 ^{2048 ± 0}	342 ^{991 ± 3}	293 ^{980 ± 1}	273 ^{984 ± 4}	239 ^{982 ± 1}	193 ^{983 ± 1}	93 ^{684 ± 45}	94 ^{678 ± 41}			
472	ytu-000	1477360	44032	399 ²⁴⁸⁴	180 ^{2048 ± 0}	149 ^{530 ± 0}	127 ^{533 ± 0}	153 ^{640 ± 0}	198 ^{861 ± 2}	382 ^{1949 ± 8}	432 ^{31797 ± 131}	433 ^{31794 ± 133}			
473	yuan-005	258312	145564	196 ⁸³⁹	112 ^{2048 ± 0}	88 ^{381 ± 0}	69 ^{386 ± 0}	53 ^{387 ± 2}	47 ^{390 ± 4}	44 ^{421 ± 3}	162 ^{1156 ± 8}	166 ^{1196 ± 26}			
474	yuan-006	1622733	145572	449 ⁴³⁶⁵	427 ^{4096 ± 0}	417 ^{1280 ± 2}	380 ^{1268 ± 1}	367 ^{1273 ± 0}	337 ^{1272 ± 2}	289 ^{1306 ± 3}	251 ^{2202 ± 19}	251 ^{2190 ± 20}			

Notes

- 1 The configuration size does not capture static data included in libraries.
- 2 The library size is the combined total of all files provided in the submission lib folder. These libraries e.g. OpenCV may or may not be installed on any end user's platform natively and would not need to be installed with the algorithm. Some developers put neural network models in their libraries.
- 3 The memory usage is the peak resident set size reported by the ps system call during template generation.
- 4 The median template creation times are measured on Intel®Xeon®CPU E5-2630 v4 @ 2.20GHz processors.
- 5 The comparison durations, in nanoseconds, are estimated using std::chrono::high_resolution_clock which on the machine in (2) counts 1ns clock ticks. Precision is somewhat worse than that however. The ± value is the median absolute deviation times 1.48 for Normal consistency.

Table 18: Summary of algorithms and properties included in this report. The red superscripts give ranking for the quantity in that column.

	Algorithm	FALSE NON-MATCH RATE (FNMR)										LESS CONSTRAINED, NON-COOP.					
		CONSTRAINED, COOPERATIVE								WILD							
		Name	VISAMC	VISA	MUGSHOT	MUGSHOT12+YRS	VISABORDER	BORDER	BORDER	1E-05							
	FMR	0.0001	1E-06	1E-05	1E-05	1E-06	1E-06	1E-06	1E-05	0.0001							
1	20face-000	0.1268	415	0.1828	411	0.1748	419	0.2768	419	0.1765	403	0.1864	306	0.0927	340	0.0405	296
2	20face-001	0.0521	392	0.0732	393	0.1414	417	0.2549	418	0.0769	380	0.1354	297	0.0419	297	0.0295	186
3	3divi-006	0.0064	203	0.0094	202	0.0047	186	0.0066	189	0.0091	195	0.0191	163	0.0113	162	0.0289	156
4	3divi-007	0.0024	69	0.0038	73	0.0028	78	0.0034	74	0.0046	109	0.0101	92	0.0082	111	0.0300	200
5	acer-001	0.0294	373	0.0504	375	0.0240	366	0.0463	368	0.0436	359	0.0622	263	0.0360	290	0.0307	216
6	acer-002	0.0169	338	0.0262	338	0.0103	301	0.0167	310	0.0182	293	0.0281	203	0.0159	215	0.0297	192
7	acisw-007	0.4276	444	0.5493	446	0.8425	460	0.9185	460	0.8424	443	0.9976	428	0.9930	446	0.4963	443
8	acisw-008	0.0100	269	0.0147	266	0.0094	297	0.0126	268	0.1740	402	0.6651	364	0.4545	393	0.0925	379
9	ader-a-003	0.0043	139	0.0059	136	0.0036	136	0.0043	116	0.0076	167	0.0151	129	0.0128	182	0.0989	380
10	ader-a-004	0.0014	24	0.0022	24	0.0035	132	0.0050	141	0.0023	12	0.0212	175	0.0058	56	0.0278	44
11	advance-003	0.0060	195	0.0087	193	0.0052	201	0.0067	190	0.0389	352	0.4914	346	0.1291	346	0.0508	328
12	advance-004	0.0083	247	0.0101	218	0.0037	143	0.0054	152	0.0051	121	0.3555	335	0.1088	344	0.1635	399
13	afisbiometrics-000	0.0051	157	0.0073	161	0.0030	98	0.0050	142	0.0044	104	0.0077	55	0.0057	53	0.0282	102
14	afrengine-000	0.6244	464	0.7336	463	0.8318	459	0.9083	458	0.8122	440	0.9980	430	0.9895	444	0.6480	450
15	aifirst-001	0.0119	295	0.0170	286	0.0084	278	0.0127	273	0.0131	252	0.0212	174	0.0138	191	0.0432	311
16	aigen-001	0.0124	303	0.0219	316	0.0143	336	0.0217	333	0.0236	318	0.8960	395	0.3255	378	0.0681	354
17	aigen-002	0.0192	350	0.0343	355	0.0256	367	0.0402	362	0.0389	351	0.9196	399	0.3876	387	0.1096	385
18	ailabs-001	0.0158	331	0.0276	343	0.0192	352	0.0317	353	0.0352	346	0.0608	260	0.0434	300	0.0338	261
19	aimall-002	0.0119	297	0.0167	284	0.0224	361	0.0411	364	0.0233	316	0.0373	234	0.0235	262	0.0327	248
20	aimall-003	0.0033	107	0.0041	82	0.0033	124	0.0035	86	0.0056	134	0.0109	99	0.0087	122	0.0312	226
21	aiseemu-001	0.0021	54	0.0029	46	0.0027	64	0.0033	69	0.0038	80	0.0339	223	0.0057	54	0.0282	93
22	aiseemu-002	0.0023	67	0.0032	53	0.0026	50	0.0027	32	0.0036	73	0.0439	241	0.0057	50	0.0280	78
23	aiunionface-000	0.0104	274	0.0154	275	0.0082	275	0.0122	263	0.0141	259	0.0243	188	0.0169	220	0.0306	213
24	aize-001	0.0223	358	0.0344	356	0.0199	353	0.0313	352	0.0367	348	0.0522	253	0.0359	289	0.0446	316
25	aize-002	0.0210	355	0.0327	351	0.0280	371	0.0489	372	0.0504	366	0.0692	268	0.0434	299	0.0854	374
26	ajou-001	0.0093	260	0.0147	265	0.0071	251	0.0126	269	0.0173	290	0.0274	198	0.0186	236	0.0348	266
27	alchera-004	0.0035	116	0.0052	126	0.0028	85	0.0039	102	0.0029	32	0.0075	51	0.0044	18	0.0304	208
28	alchera-005	0.0027	79	0.0040	78	0.0026	46	0.0030	50	0.0025	18	0.0055	21	0.0040	13	0.0306	215
29	alfabeta-001	0.4867	451	0.5831	449	0.6855	445	0.8156	447	0.8253	442	0.7765	380	0.6416	409	0.3427	431
30	alice-000	0.0119	298	0.0192	304	0.0106	307	0.0170	311	0.0167	281	0.0265	195	0.0150	209	0.0288	144
31	alleyes-000	0.0058	186	0.0090	197	0.0055	212	0.0087	231	0.0068	155	0.0105	98	0.0076	99	0.0282	101
32	allgovision-000	0.0346	382	0.0527	379	0.0232	363	0.0339	354	0.0372	350	0.0620	262	0.0443	303	0.0607	342
33	alphaface-001	0.0065	205	0.0097	210	0.0039	152	0.0063	184	0.0083	181	-	-	-	-	0.0280	80
34	alphaface-002	0.0052	162	0.0075	166	0.0030	91	0.0044	121	1.0000	465	0.0115	105	0.0084	116	0.0279	66
35	amplifiedgroup-001	0.5034	453	0.5848	450	0.6973	448	0.8316	448	0.7807	437	0.7724	378	0.6354	406	0.4250	438
36	androvideo-000	0.0243	362	0.0438	370	0.0239	365	0.0365	359	0.0483	364	0.1870	307	0.0635	323	0.1163	388
37	anke-004	0.0080	239	0.0154	274	0.0073	253	0.0112	255	0.0102	222	0.0178	156	0.0118	170	0.0288	148
38	anke-005	0.0070	214	0.0109	230	0.0059	223	0.0094	238	0.0105	224	0.0142	120	0.0102	142	0.0289	155
39	antheus-000	0.2564	429	0.3776	432	0.7240	449	0.8699	453	0.8899	450	0.9872	417	0.9483	434	0.7668	454
40	antheus-001	0.1311	416	0.2306	418	0.5113	437	0.6797	439	0.8748	449	0.9908	422	0.9649	439	0.7586	453
41	anyvision-004	0.0267	367	0.0385	366	0.0258	368	0.0487	371	0.0234	317	0.0301	209	0.0191	239	0.0470	321
42	anyvision-005	0.0023	66	0.0037	72	0.0027	74	0.0035	82	0.0049	117	0.0084	69	0.0069	84	0.0285	119
43	armatura-001	0.0033	105	0.0042	91	0.0031	102	0.0037	94	0.0056	133	0.0110	100	0.0092	128	0.0815	371
44	armatura-003	0.0020	49	0.0029	45	0.0026	55	0.0028	37	0.0025	19	0.0049	11	0.0043	17	0.0292	176

Table 19: FNMR is the proportion of mated comparisons below a threshold set to achieve the FMR given in the header on the fourth row. FMR is the proportion of impostor comparisons at or above that threshold. The light grey values give rank over all algorithms in that column. The pink columns use only same-sex impostors; others are selected regardless of demographics. The exception, in the green column, uses “matched-covariates” i.e. impostors of the same sex, age group, and country of birth. The second pink column includes effects of extended ageing. Missing entries for border, visa, mugshot and wild images generally mean the algorithm did not run to completion. The VISA columns compare images described in section 2.1. The MUGSHOT columns compare images described in section 2.5. The VISA-BORDER column compare images described in section 2.2 with those of section 2.4. The BORDER column compares images described in section 2.4. The WILD columns compare images described in section 2.7.

	Algorithm	FALSE NON-MATCH RATE (FNMR)										LESS CONSTRAINED, NON-COOP.					
		CONSTRAINED, COOPERATIVE								WILD							
		Name	VISAMC	VISA	MUGSHOT	MUGSHOT12+YRS	VISABORDER	BORDER	BORDER								
	FMR	0.0001	1E-06	1E-05	1E-05	1E-05	1E-06	1E-06	1E-05	0.0001							
45	asusaics-000	0.0125	305	0.0209	312	0.0085	280	0.0134	281	0.0143	263	0.7189	368	0.0285	274	0.0295	184
46	asusaics-001	0.0125	307	0.0210	313	0.0085	282	0.0134	282	0.0143	264	0.7437	372	0.0289	276	0.0295	183
47	autentika-000	0.1415	418	0.1916	413	0.4130	431	0.5521	431	0.4217	424	0.9998	443	0.9954	448	0.3183	429
48	authenmetric-003	0.0036	122	0.0053	128	0.0039	157	0.0051	143	0.0095	208	0.9930	424	0.5932	403	0.0290	160
49	authenmetric-004	0.0027	80	0.0042	90	0.0033	119	0.0036	91	0.0083	184	0.9879	418	0.4058	389	0.0290	165
50	aware-005	0.0457	389	0.0643	387	0.0603	400	0.1094	403	0.0613	373	0.1075	289	0.0491	307	0.0314	231
51	aware-006	0.0487	390	0.0819	396	0.0529	394	0.1090	401	0.1011	391	0.1058	286	0.0502	310	0.0317	237
52	awiros-001	0.4044	442	0.4622	438	0.5530	439	0.6518	436	0.2008	407	0.1994	310	0.1386	351	0.5584	446
53	awiros-002	0.1990	423	0.2561	420	0.3319	425	0.4411	425	0.3821	422	0.9938	425	0.2634	368	0.0997	381
54	aximetria-001	0.0111	285	0.0186	299	0.0110	313	0.0148	297	0.0170	285	0.3928	338	0.2090	361	0.0409	301
55	ayftech-001	0.0946	409	0.1941	414	0.2438	421	0.3625	421	0.1558	399	0.1589	301	0.0936	341	0.0785	363
56	ayonix-000	0.4351	446	0.4872	440	0.6150	444	0.7510	444	0.6557	432	0.6361	360	0.4981	395	0.3635	433
57	beethedata-000	0.0127	310	0.0195	305	0.0092	291	0.0157	303	0.0171	287	0.0306	210	0.0204	249	0.0285	121
58	beyneai-000	0.0071	220	0.0107	228	0.0104	304	0.0131	279	0.0170	286	0.9837	414	0.6171	405	0.0597	341
59	biocube-001	0.5596	459	0.6834	458	0.7700	456	0.8712	454	0.8446	444	0.9661	410	0.7922	420	0.2377	414
60	bioittechswiss-001	0.0054	170	0.0072	157	0.0069	244	0.0124	266	0.0060	141	0.0094	83	0.0065	75	0.0313	230
61	bioittechswiss-002	0.0049	150	0.0067	150	0.0064	232	0.0116	258	0.0067	154	0.0117	107	0.0086	119	0.0279	56
62	bm-001	0.7431	468	0.9494	469	0.9586	464	0.9843	464	0.9049	452	0.9021	398	0.8395	426	0.9935	464
63	boetech-001	0.0662	402	0.0802	395	0.0493	392	0.0791	391	0.0682	377	0.1074	288	0.0758	331	0.1719	401
64	boetech-002	0.0535	395	0.0565	383	0.0114	321	0.0136	284	0.0403	353	0.0650	264	0.0606	321	0.1697	400
65	bresee-001	0.0085	248	0.0143	262	0.0086	284	0.0153	300	0.0108	228	0.0168	146	0.0115	167	0.0355	279
66	bresee-002	0.0079	237	0.0101	216	0.0065	235	0.0079	215	0.0129	247	0.0263	194	0.0224	259	0.0327	249
67	camvi-002	0.0125	306	0.0221	318	0.0089	288	0.0145	295	0.0142	260	0.2650	324	0.0166	219	0.0288	143
68	camvi-004	0.0171	342	0.0316	350	0.0042	168	0.0049	139	0.0097	215	0.6636	363	0.0141	196	0.0284	109
69	canon-003	0.0041	138	0.0059	135	0.0030	90	0.0040	104	0.0040	87	0.0073	48	0.0059	61	0.0274	20
70	canon-004	0.0052	161	0.0091	200	0.0033	123	0.0058	167	0.0037	75	0.0770	272	0.0494	308	0.0267	2
71	ceiec-003	0.0071	222	0.0107	225	0.0061	229	0.0079	218	0.0160	273	0.0316	212	0.0260	270	0.0308	222
72	ceiec-004	0.0038	130	0.0051	119	0.0045	180	0.0053	147	0.0062	147	0.3939	339	0.0104	148	0.0325	245
73	chosun-001	0.0525	393	0.0936	398	0.0742	405	0.1263	408	0.0978	390	1.0000	456	0.9354	432	0.4446	440
74	chosun-002	0.0390	384	0.0646	388	0.0339	383	0.0576	382	0.0455	363	0.6904	366	0.1746	358	0.0696	356
75	chtface-005	0.0033	104	0.0049	114	0.0029	87	0.0041	108	0.0044	103	0.0317	213	0.0066	78	0.0306	214
76	chtface-006	0.0029	88	0.0043	92	0.0026	59	0.0034	79	0.0040	88	0.2701	325	0.0065	74	0.0305	212
77	cist-001	0.0046	144	0.0065	149	0.0042	169	0.0063	183	0.9675	459	0.9997	441	0.9994	455	0.0407	298
78	clearviewai-000	0.0010	8	0.0019	17	0.0024	20	0.0028	38	0.0030	35	0.0058	25	0.0050	29	0.0271	5
79	closeli-001	0.0136	313	0.0163	279	0.0039	155	0.0054	151	0.0072	160	1.0000	450	0.0094	132	0.0318	238
80	cloudmatrix-001	0.0668	403	0.1141	402	0.0539	395	0.0905	396	0.3509	419	0.9819	413	0.9010	429	0.0636	346
81	cloudmatrix-002	0.0075	230	0.0113	235	0.0084	279	0.0120	260	0.9248	455	0.9997	440	0.9985	454	0.0358	280
82	cloudwalk-hr-003	0.0026	76	0.0041	81	0.0040	162	0.0058	166	0.0060	145	0.9992	433	0.0094	130	0.7206	452
83	cloudwalk-hr-004	0.0009	6	0.0018	13	0.0034	127	0.0028	44	0.0052	123	0.9992	434	0.0093	129	0.1625	398
84	cloudwalk-mt-005	0.0006	2	0.0009	2	0.0025	36	0.0022	9	0.0017	2	0.9286	402	0.5956	404	0.0287	136
85	cloudwalk-mt-006	0.0006	1	0.0006	1	0.0023	12	0.0019	1	0.0016	1	0.0032	1	0.0030	2	0.0290	162
86	codeline-000	0.0057	178	0.0079	177	0.0037	140	0.0053	150	0.2721	413	1.0000	451	0.9763	441	0.0273	13
87	cogent-007	0.0022	62	0.0038	75	0.0028	82	0.0031	56	0.0040	90	0.0082	63	0.0067	79	0.0438	314
88	cogent-008	0.0015	28	0.0027	41	0.0023	14	0.0025	21	0.0033	54	0.0063	32	0.0055	47	0.0281	84

Table 20: FNMR is the proportion of mated comparisons below a threshold set to achieve the FMR given in the header on the fourth row. FMR is the proportion of impostor comparisons at or above that threshold. The light grey values give rank over all algorithms in that column. The pink columns use only same-sex impostors; others are selected regardless of demographics. The exception, in the green column, uses “matched-covariates” i.e. impostors of the same sex, age group, and country of birth. The second pink column includes effects of extended ageing. Missing entries for border, visa, mugshot and wild images generally mean the algorithm did not run to completion. The VISA columns compare images described in section 2.1. The MUGSHOT columns compare images described in section 2.5. The VISA-BORDER column compare images described in section 2.2 with those of section 2.4. The BORDER column compares images described in section 2.4. The WILD columns compare images described in section 2.7.

Algorithm	FALSE NON-MATCH RATE (FNMR)										
	CONSTRAINED, COOPERATIVE								LESS CONSTRAINED, NON-COOP.		
	Name	VISAMC	VISA	MUGSHOT	MUGSHOT12+YRS	VISABORDER	BORDER	BORDER	WILD		
FMR	0.0001	1E-06	1E-05	1E-05	1E-06	1E-06	1E-06	1E-05	0.0001		
89 cognitec-003	0.0038	128	0.0052	123	0.0054	210	0.0057	163	0.0225	311	0.0416
90 cognitec-004	0.0036	119	0.0053	127	0.0053	203	0.0056	159	0.0098	216	0.0202
91 cor-001	0.0075	232	0.0113	234	0.0055	214	0.0084	223	0.0091	197	0.0148
92 coretech-000	0.7699	470	1.0000	475	1.0000	470	-	1.0000	468	1.0000	466
93 coretech-001	0.0052	158	0.0067	152	0.0083	277	0.0092	235	0.0346	345	0.1363
94 corsight-002	0.0053	164	0.0068	154	0.0030	95	0.0041	109	0.0039	84	0.0079
95 corsight-003	0.0026	77	0.0040	79	0.0028	79	0.0045	124	0.0035	71	0.0059
96 csc-002	0.0099	267	0.0132	252	0.0077	260	0.0142	292	0.0126	246	0.0195
97 csc-003	0.0053	165	0.0065	147	0.0037	141	0.0047	130	0.0074	162	0.0124
98 ctbcbank-000	0.0168	337	0.0250	331	0.0146	338	0.0224	335	0.0211	308	0.8964
99 ctbcbank-001	0.0155	328	0.0235	326	0.0148	343	0.0243	340	0.0207	305	0.9279
100 cu-face-002	0.0105	279	0.0116	237	0.0650	402	0.0568	379	0.0271	331	0.0139
101 cubox-001	0.0064	204	0.0080	179	0.0037	138	0.0055	155	0.0060	142	0.0111
102 cubox-002	0.0034	115	0.0041	83	0.0025	33	0.0025	24	0.0033	53	0.0064
103 cudocommunication-001	0.4777	449	1.0000	473	0.4373	432	0.5360	428	1.0000	466	1.0000
104 cuhkee-001	0.0036	121	0.0045	104	0.0031	108	0.0046	127	0.0051	122	0.0095
105 cybercore-002	0.0092	258	0.0119	240	0.0049	192	0.0072	196	0.9105	454	1.0000
106 cybercore-003	0.0155	329	0.0164	280	0.0032	115	0.0033	73	0.0024	13	0.9719
107 cyberextruder-003	0.0109	282	0.0169	285	0.0071	249	0.0112	256	0.0165	279	0.0410
108 cyberextruder-004	0.0118	294	0.0181	295	0.0081	272	0.0133	280	0.0191	300	0.0329
109 cyberlink-009	0.0018	42	0.0027	40	0.0047	182	0.0046	125	0.0040	93	0.0086
110 cyberlink-010	0.0011	15	0.0019	18	0.0041	164	0.0041	105	0.0039	82	0.1829
111 dahua-006	0.0027	78	0.0039	77	0.0031	105	0.0039	103	0.0039	83	0.0067
112 dahua-007	0.0017	37	0.0023	26	0.0026	53	0.0032	62	0.0033	49	0.0060
113 daon-000	0.0095	264	0.0117	239	0.0068	240	0.0077	210	0.0092	201	0.0174
114 decatur-000	0.0714	404	0.1115	401	0.0608	401	0.1106	404	0.0866	384	1.0000
115 decatur-001	0.0424	386	0.0711	391	0.0237	364	0.0458	367	0.0447	361	1.0000
116 deepglint-004	0.0025	74	0.0034	61	0.0039	156	0.0061	179	0.0050	118	0.0091
117 deepglint-005	0.0052	159	0.0059	139	0.0030	92	0.0031	57	0.0033	57	0.7620
118 deepsea-001	0.0136	314	0.0215	315	0.0142	335	0.0214	332	0.0163	277	0.0250
119 deepsense-000	0.0145	322	0.0265	339	0.0113	319	0.0196	325	0.0151	267	0.0215
120 deepsense-001	0.0013	22	0.0019	15	0.0024	25	0.0025	22	0.0027	27	0.0115
121 dermalog-010	0.0030	92	0.0041	85	0.0034	128	0.0037	96	0.0075	163	0.5181
122 dermalog-011	0.0045	142	0.0062	143	0.0035	131	0.0059	171	0.0057	136	0.2242
123 dicio-001	0.5486	458	0.6442	453	0.7516	452	0.8607	450	0.8678	448	0.8268
124 didiglobalface-001	0.0055	173	0.0092	201	0.0030	94	0.0045	123	0.0088	190	0.0119
125 didiglobalface-002	0.0033	108	0.0051	121	0.0026	54	0.0034	81	0.0033	52	0.0085
126 digidata-000	0.0967	410	0.1410	407	0.2596	422	0.3462	420	0.0293	335	0.0363
127 digidata-001	0.0224	359	0.0352	358	0.0330	380	0.0570	381	0.0109	230	0.0481
128 digitalbarriers-002	0.3360	438	0.3690	430	0.0877	409	0.1557	409	0.0971	389	0.0951
129 dps-000	0.0115	290	0.0176	292	0.0149	345	0.0185	320	0.0173	289	0.0275
130 dsk-000	0.1526	420	0.2169	417	0.3787	427	0.5426	430	0.3115	415	0.3089
131 einetworks-000	0.0099	268	0.0180	294	0.0088	287	0.0140	289	0.0130	248	0.0225
132 ekin-002	0.1168	413	0.2042	416	0.1530	418	0.2524	417	0.1777	404	0.2773

Table 21: FNMR is the proportion of mated comparisons below a threshold set to achieve the FMR given in the header on the fourth row. FMR is the proportion of impostor comparisons at or above that threshold. The light grey values give rank over all algorithms in that column. The pink columns use only same-sex impostors; others are selected regardless of demographics. The exception, in the green column, uses “matched-covariates” i.e. impostors of the same sex, age group, and country of birth. The second pink column includes effects of extended ageing. Missing entries for border, visa, mugshot and wild images generally mean the algorithm did not run to completion. The VISA columns compare images described in section 2.1. The MUGSHOT columns compare images described in section 2.5. The VISA-BORDER column compare images described in section 2.2 with those of section 2.4. The BORDER column compares images described in section 2.4. The WILD columns compare images described in section 2.7.

Algorithm	FALSE NON-MATCH RATE (FNMR)									
	CONSTRAINED, COOPERATIVE								LESS CONSTRAINED, NON-COOP.	
	Name	VISAMC	VISA	MUGSHOT	MUGSHOT12+YRS	VISABORDER	BORDER	BORDER	WILD	
FMR	0.0001	1E-06	1E-05	1E-05	1E-06	1E-06	1E-06	1E-05	0.0001	
133	enface-000	0.0028	85	0.0049	115	0.0043	171	0.0072	194	0.0058
134	enface-001	0.0072	225	0.0107	226	0.0071	246	0.0138	286	0.0068
135	eocortex-000	0.3485	439	0.6943	459	0.1122	410	0.1574	410	0.2155
136	ercacat-001	0.0036	124	0.0044	98	0.0033	118	0.0047	131	0.0106
137	euronovate-001	0.2786	432	0.3608	429	0.4489	434	0.6105	435	0.5010
138	expasoft-001	0.0328	379	0.0488	372	0.0211	358	0.0342	356	0.0629
139	expasoft-002	0.0170	340	0.0274	341	0.0787	408	0.0768	390	0.1629
140	f8-001	0.0249	363	0.0336	353	0.0178	350	0.0232	336	0.0303
141	f8-002	0.0340	381	0.0591	386	0.0213	360	0.0374	360	0.0452
142	faceonlive-001	0.0269	369	0.0359	361	0.0387	386	0.0721	388	0.0246
143	faceonlive-002	0.0121	299	0.0135	255	0.0033	120	0.0041	107	0.0037
144	facephi-000	0.0044	140	0.0059	137	0.0047	183	0.0057	164	0.0088
145	facesoft-000	0.0085	249	0.0112	232	0.0064	233	0.0107	251	0.0091
146	facetag-000	0.2836	433	0.4081	435	0.2933	424	0.4303	424	0.3448
147	facetag-002	0.0098	266	0.0147	267	0.0064	234	0.0110	253	0.0116
148	facex-001	1.0000	474	1.0000	476	1.0000	469	-	1.0000	467
149	facex-002	0.0803	406	0.1404	406	0.1283	413	0.1979	414	0.1440
150	farfaces-001	0.4890	452	0.5860	451	0.5650	440	0.7268	442	0.8015
151	fiberhome-nanjing-003	0.0090	252	0.0139	259	0.0082	274	0.0144	293	0.0110
152	fiberhome-nanjing-004	0.0037	127	0.0056	134	0.0031	103	0.0043	115	0.0043
153	fincore-000	0.0309	377	0.0502	374	0.0281	372	0.0510	375	0.0521
154	firstcreditKZ-001	0.0024	72	0.0034	58	0.0024	30	0.0024	17	0.0034
155	frpkauai-001	0.0023	64	0.0035	68	0.0026	43	0.0030	53	0.0040
156	frpkauai-002	0.0024	70	0.0035	66	0.0024	28	0.0024	15	0.0033
157	fujitsulab-002	0.0091	257	0.0124	247	0.0105	305	0.0156	301	0.0169
158	fujitsulab-003	0.0045	143	0.0065	148	0.0057	218	0.0083	221	0.0080
159	g42-intelibrain-001	0.0006	3	0.0009	3	0.0037	139	0.0044	118	0.0030
160	geo-002	0.0171	343	0.0187	300	0.0035	130	0.0051	145	0.0064
161	geo-004	0.0030	90	0.0041	80	0.0025	39	0.0030	49	0.0035
162	glory-004	0.0077	236	0.0123	244	0.0074	257	0.0098	246	0.0122
163	glory-005	0.0056	175	0.0076	167	0.0054	211	0.0072	197	0.0075
164	gorilla-008	0.0058	187	0.0091	198	0.0049	191	0.0079	217	0.0079
165	gorilla-009	0.0049	148	0.0072	159	0.0038	145	0.0056	160	0.0065
166	graymatrics-001	0.1039	411	0.1620	410	0.1344	415	0.1917	413	0.1648
167	griaule-001	0.0057	177	0.0078	173	0.0045	179	0.0065	187	0.0070
168	griaule-002	0.0021	55	0.0032	54	0.0025	42	0.0027	33	0.0034
169	hertasecurity-001	0.0249	364	0.0309	348	0.0105	306	0.0161	305	0.0245
170	hertasecurity-002	0.0206	354	0.0315	349	0.0060	226	0.0078	213	0.0253
171	hik-001	0.0096	265	0.0125	249	0.0093	296	0.0164	308	0.0108
172	hisign-001	0.0036	120	0.0050	117	0.0034	125	0.0046	126	0.0079
173	hisign-002	0.0029	86	0.0044	100	0.0027	70	0.0032	67	0.0028
174	hyperverge-003	0.0019	46	0.0030	49	0.0025	34	0.0029	47	0.0027
175	hyperverge-004	0.0072	227	0.0116	238	0.0040	160	0.0071	193	0.0058
176	hzailu-002	0.0051	156	0.0072	158	0.0038	151	0.0055	156	0.0040

Table 22: FNMR is the proportion of mated comparisons below a threshold set to achieve the FMR given in the header on the fourth row. FMR is the proportion of impostor comparisons at or above that threshold. The light grey values give rank over all algorithms in that column. The pink columns use only same-sex impostors; others are selected regardless of demographics. The exception, in the green column, uses “matched-covariates” i.e. impostors of the same sex, age group, and country of birth. The second pink column includes effects of extended ageing. Missing entries for border, visa, mugshot and wild images generally mean the algorithm did not run to completion. The VISA columns compare images described in section 2.1. The MUGSHOT columns compare images described in section 2.5. The VISA-BORDER column compare images described in section 2.2 with those of section 2.4. The BORDER column compares images described in section 2.4. The WILD columns compare images described in section 2.7.

	Algorithm	FALSE NON-MATCH RATE (FNMR)										LESS CONSTRAINED, NON-COOP.					
		CONSTRAINED, COOPERATIVE								WILD							
		Name	VISAMC	VISA	MUGSHOT	MUGSHOT12+YRS	VISABORDER	BORDER	BORDER	1E-06	1E-05						
FMR		0.0001	1E-06	1E-05	1E-05	1E-05	1E-06	1E-06	1E-05		0.0001						
177	hzailu-003	0.0178	345	0.0291	346	0.0031	109	0.0042	113	0.0035	65	0.0061	31	0.0052	34	0.0524	332
178	icm-003	0.0138	316	0.0222	320	0.0149	344	0.0282	347	0.0227	312	0.0384	235	0.0257	267	0.0333	255
179	icm-004	0.0079	238	0.0120	241	0.0074	255	0.0107	250	0.0091	198	0.0281	204	0.0128	183	0.0315	233
180	icthtc-000	0.0260	366	0.0396	367	0.0207	357	0.0339	355	0.0291	334	0.0474	247	0.0346	285	0.0459	319
181	id3-006	0.0072	226	0.0103	219	0.0049	193	0.0074	202	0.0095	206	0.0165	144	0.0119	174	0.9938	465
182	id3-008	0.0039	131	0.0055	131	0.0032	113	0.0042	111	0.0081	177	0.0155	135	0.0134	187	0.8856	458
183	idemria-008	0.0023	65	0.0032	55	0.0023	15	0.0028	35	0.0034	64	0.0067	40	0.0056	49	0.0290	164
184	idemria-009	0.0022	60	0.0030	50	0.0022	7	0.0023	14	0.0023	11	0.0046	7	0.0039	10	0.0285	118
185	iit-002	0.0111	287	0.0177	293	0.0085	281	0.0140	288	0.0193	301	0.0332	219	0.0260	269	0.1373	391
186	iit-003	0.0082	246	0.0151	272	0.0053	205	0.0084	224	0.0122	242	0.0199	169	0.0137	189	0.0407	299
187	imds-software-001	0.0126	308	0.0228	321	0.0130	332	0.0221	334	0.0231	314	0.0469	246	0.0199	247	0.0365	283
188	imperial-000	0.0067	208	0.0108	229	0.0080	269	0.0134	283	0.0087	188	0.0581	256	0.0102	143	0.0281	86
189	imperial-002	0.0058	185	0.0081	182	0.0055	213	0.0085	227	0.0083	182	0.0157	136	0.0103	144	0.0273	15
190	incode-010	0.0041	136	0.0063	144	0.0028	83	0.0043	114	0.0047	112	0.0077	56	0.0061	67	0.0296	191
191	incode-011	0.0032	98	0.0044	97	0.0026	57	0.0034	78	0.0032	45	0.0359	228	0.0140	194	0.0295	187
192	infocert-001	0.0105	278	0.0172	287	0.0078	263	0.0125	267	0.0159	271	0.1573	300	0.0565	317	0.0307	218
193	innefulabs-000	0.0122	301	0.0199	308	0.0112	318	0.0197	326	0.0222	310	0.0372	233	0.0271	272	0.0348	268
194	innovativetechnologyltd-001	0.0578	398	0.0938	399	0.0501	393	0.0981	397	0.0592	372	0.0779	273	0.0422	298	0.0449	318
195	innovativetechnologyltd-002	0.0451	388	0.0716	392	0.0541	396	0.1009	399	0.0506	367	0.0682	266	0.0371	291	0.0804	369
196	innovatrics-008	0.0047	146	0.0064	146	0.0038	148	0.0052	146	0.0053	125	0.0088	77	0.0069	86	0.0287	134
197	innovatrics-009	0.0022	57	0.0031	52	0.0028	76	0.0032	65	0.0034	60	0.1165	293	0.0326	280	0.0279	57
198	insightface-001	0.0009	7	0.0014	4	0.0027	63	0.0024	16	0.0035	69	0.0070	44	0.0065	73	0.0279	62
199	insightface-003	0.0015	29	0.0021	21	0.0045	178	0.0034	80	0.1298	393	1.0000	475	0.9407	433	0.0277	38
200	inspur-000	0.0060	194	0.0078	172	0.7415	451	0.9093	459	0.2838	414	0.9996	437	0.9976	452	0.0283	106
201	intellicloudai-001	0.0142	319	0.0234	325	0.0092	293	0.0145	294	0.0162	275	0.0371	232	0.0171	222	0.0409	302
202	intellicloudai-002	0.0059	191	0.0085	189	0.0060	227	0.0069	192	0.0108	227	0.2477	322	0.0171	221	0.0303	207
203	intellifusion-001	0.0072	223	0.0094	203	0.0056	217	0.0085	228	0.0111	234	0.0212	176	0.0143	199	0.0289	153
204	intellifusion-002	0.0059	190	0.0077	168	0.0040	161	0.0074	201	0.0085	186	0.5352	352	0.0104	149	0.0305	211
205	intellivision-003	0.1177	414	0.2006	415	0.0760	406	0.1244	407	0.1069	392	0.1431	299	0.0839	334	0.0829	373
206	intellivision-004	0.0271	370	0.0559	382	0.0294	378	0.0503	374	0.0327	342	0.0461	244	0.0293	279	0.0645	348
207	intellivix-002	0.0062	199	0.0085	188	0.0039	154	0.0056	158	0.0060	144	0.3464	332	0.0857	337	0.0289	154
208	intellivix-003	0.0075	231	0.0125	248	0.0052	202	0.0091	234	0.0066	152	0.0297	207	0.0096	135	0.0286	131
209	intelresearch-005	0.0016	33	0.0023	27	0.0028	75	0.0034	76	0.0042	100	0.0084	67	0.0066	77	0.0290	163
210	intelresearch-006	0.0010	11	0.0015	8	0.0026	62	0.0028	41	0.0032	47	0.8123	384	0.4742	394	0.0291	170
211	intema-000	0.0012	16	0.0017	12	0.0023	8	0.0022	10	0.0022	9	0.0172	149	0.0061	66	0.0279	61
212	intema-001	0.0010	10	0.0014	6	0.0021	3	0.0020	5	0.0019	6	0.0037	4	0.0030	3	0.0282	96
213	intsyssmu-001	0.9543	473	0.9888	471	0.9923	465	-		0.9977	460	0.9955	426	0.9892	443	0.7871	456
214	intsyssmu-002	0.0130	311	0.0254	333	0.0137	333	0.0267	345	0.0160	272	0.0267	197	0.0145	202	0.0289	157
215	ionetworks-000	0.0060	196	0.0087	190	0.0044	173	0.0058	169	0.0080	176	0.0144	124	0.0112	159	0.0319	240
216	iqface-000	0.0091	255	0.0143	261	0.0075	258	0.0110	254	0.0171	288	0.2234	315	0.0359	287	0.0381	289
217	iqface-003	0.0058	188	0.0079	176	0.0051	199	0.0058	170	0.0104	223	0.0200	170	0.0193	241	0.0402	294
218	irex-000	0.0052	160	0.0099	212	0.0056	216	0.0083	222	0.0137	257	0.0163	142	0.0078	101	0.0285	122
219	isap-001	0.5092	454	0.6588	455	0.6899	447	0.7978	445	0.7200	433	0.7253	369	0.5373	399	0.1931	405
220	isap-002	0.0114	289	0.0186	298	0.0087	285	0.0151	299	0.0156	270	0.5134	348	0.0333	281	0.0354	278

Table 23: FNMR is the proportion of mated comparisons below a threshold set to achieve the FMR given in the header on the fourth row. FMR is the proportion of impostor comparisons at or above that threshold. The light grey values give rank over all algorithms in that column. The pink columns use only same-sex impostors; others are selected regardless of demographics. The exception, in the green column, uses “matched-covariates” i.e. impostors of the same sex, age group, and country of birth. The second pink column includes effects of extended ageing. Missing entries for border, visa, mugshot and wild images generally mean the algorithm did not run to completion. The VISA columns compare images described in section 2.1. The MUGSHOT columns compare images described in section 2.5. The VISA-BORDER column compare images described in section 2.2 with those of section 2.4. The BORDER column compares images described in section 2.4. The WILD columns compare images described in section 2.7.

	Algorithm	FALSE NON-MATCH RATE (FNMR)									
		CONSTRAINED, COOPERATIVE								LESS CONSTRAINED, NON-COOP.	
		Name	VISAMC	VISA	MUGSHOT	MUGSHOT12+YRS	VISABORDER	BORDER	BORDER	WILD	
	FMR	0.0001	1E-06	1E-05	1E-05	1E-05	1E-06	1E-06	1E-05	0.0001	
221	isityou-000	0.5682	460	0.7033	461	1.0000	475	-	1.0000	476	1.0000
222	isystems-001	0.0149	325	0.0245	329	0.0138	334	0.0210	330	0.0209	307
223	isystems-002	0.0118	292	0.0182	296	0.0111	315	0.0162	306	0.0166	280
224	itmo-007	0.0080	240	0.0125	250	0.0107	308	0.0185	318	0.0167	282
225	itmo-008	0.0090	253	0.0150	270	0.0058	220	0.0059	173	0.0187	296
226	ivacognitive-001	0.0189	348	0.0351	357	0.0123	328	0.0235	337	0.0198	303
227	iws-000	0.4824	450	0.5801	448	0.6859	446	0.8155	446	0.8251	441
228	jaakit-001	0.5830	461	0.7146	462	0.8173	458	0.8893	456	0.8950	451
229	kakao-007	0.0019	47	0.0028	43	0.0024	19	0.0026	26	0.0033	51
230	kakao-008	0.0011	13	0.0018	14	0.0023	9	0.0023	12	0.0021	8
231	kakaopay-001	0.0152	327	0.0252	332	0.0145	337	0.0270	346	0.0232	315
232	kasikornlabs-000	0.0112	288	0.0184	297	0.0086	283	0.0137	285	0.0130	250
233	kasikornlabs-002	0.0069	213	0.0091	199	0.0048	187	0.0063	182	0.0076	166
234	kedacom-000	0.0055	171	0.0081	181	0.0111	317	0.0120	261	0.0415	355
235	kiwitech-000	0.0076	233	0.0105	222	0.0081	273	0.0128	275	0.0096	210
236	kneron-003	0.0542	397	0.0902	397	0.0346	384	0.0562	378	0.0919	387
237	kneron-005	0.0157	330	0.0259	335	0.0126	331	0.0212	331	0.0406	354
238	knowutech-000	0.0039	132	0.0055	132	0.0028	86	0.0042	110	0.0042	98
239	kookmin-002	0.0054	168	0.0077	170	0.0043	170	0.0065	186	0.0123	244
240	koreaid-001	0.0031	94	0.0045	103	0.0026	52	0.0032	63	0.0043	101
241	krungthai-002	0.0105	276	0.0161	276	0.0091	290	0.0141	290	0.7350	435
242	kuke3d-001	0.0058	183	0.0104	221	0.0083	276	0.0093	237	0.0270	330
243	kuke3d-002	0.0077	235	0.0135	256	0.0069	243	0.0098	245	0.0111	233
244	lebentech-000	0.5940	462	0.7032	460	0.8854	461	0.9511	461	0.9089	453
245	lemalabs-001	0.0111	286	0.0175	290	0.0088	286	0.0142	291	0.0143	261
246	lineclova-002	0.0021	52	0.0035	63	0.0025	32	0.0027	31	0.0041	94
247	lineclova-003	0.0018	44	0.0030	48	0.0028	84	0.0031	58	0.0041	95
248	lookman-002	0.0297	375	0.0547	381	0.0339	382	0.0562	377	0.0614	374
249	lookman-004	0.0074	229	0.0099	214	0.0124	330	0.0149	298	0.0430	358
250	luxand-000	0.2056	424	0.2814	422	0.4053	429	0.5365	429	0.3497	418
251	mantra-000	0.0037	125	0.0052	125	0.0054	208	0.0056	161	0.0097	214
252	maxvision-002	0.0070	217	0.0107	224	0.0061	228	0.0093	236	0.0080	173
253	maxvision-003	0.0056	174	0.0083	186	0.0038	149	0.0060	174	0.0061	146
254	megvii-005	0.0010	9	0.0015	7	0.0026	51	0.0031	61	0.0019	5
255	megvii-006	0.0011	12	0.0016	9	0.0026	58	0.0033	72	0.0025	17
256	meituan-001	0.0164	335	0.1886	412	0.0025	35	0.0026	25	0.0030	38
257	meituan-002	0.0017	35	0.0025	32	0.0024	22	0.0023	11	0.0024	16
258	meiya-001	0.0171	341	0.0275	342	0.0159	347	0.0261	344	0.0311	339
259	mendaxiatech-000	0.0027	81	0.0036	69	0.0029	88	0.0036	92	0.0031	43
260	metsakuurcompany-001	0.0068	212	0.0087	194	0.0068	241	0.0078	212	0.0095	207
261	metsakuurcompany-002	0.0048	147	0.0071	155	0.0030	97	0.0043	117	0.0032	48
262	maxis-001	0.0068	210	0.0099	213	0.0059	224	0.0097	244	0.0096	212
263	microfocus-001	0.4482	447	0.5524	447	0.7256	450	0.8416	449	0.7301	434
264	microfocus-002	0.3605	440	0.5057	442	0.5783	442	0.7223	441	0.5909	429

Table 24: FNMR is the proportion of mated comparisons below a threshold set to achieve the FMR given in the header on the fourth row. FMR is the proportion of impostor comparisons at or above that threshold. The light grey values give rank over all algorithms in that column. The pink columns use only same-sex impostors; others are selected regardless of demographics. The exception, in the green column, uses “matched-covariates” i.e. impostors of the same sex, age group, and country of birth. The second pink column includes effects of extended ageing. Missing entries for border, visa, mugshot and wild images generally mean the algorithm did not run to completion. The VISA columns compare images described in section 2.1. The MUGSHOT columns compare images described in section 2.5. The VISA-BORDER column compare images described in section 2.2 with those of section 2.4. The BORDER column compares images described in section 2.4. The WILD columns compare images described in section 2.7.

	Algorithm	FALSE NON-MATCH RATE (FNMR)										LESS CONSTRAINED, NON-COOP.					
		CONSTRAINED, COOPERATIVE								WILD							
		Name	VISAMC	VISA	MUGSHOT	MUGSHOT12+YRS	VISABORDER	BORDER	BORDER								
	FMR	0.0001	1E-06	1E-05	1E-05	1E-06	1E-06	1E-06	1E-05		0.0001						
265	minivision-000	0.0033	103	0.0048	113	0.0038	147	0.0049	135	0.0055	130	0.0094	85	0.0079	105	0.0273	12
266	mobai-000	0.0360	383	0.0439	371	0.0372	385	0.0700	386	0.0367	349	0.0939	279	0.0795	333	0.2640	424
267	mobai-001	0.0199	352	0.0219	317	0.0047	184	0.0061	176	0.0093	204	0.0174	151	0.0138	192	0.1045	382
268	mobbl-001	0.3208	434	0.4375	436	0.5680	441	0.7193	440	0.6282	430	0.5783	356	0.3984	388	0.1866	404
269	mobbl-003	0.0087	250	0.0134	254	0.0062	230	0.0087	230	0.0099	217	0.0197	166	0.0122	179	0.0312	227
270	mobipintech-000	0.0090	254	0.0149	268	0.0039	159	0.0057	162	0.0115	238	0.0465	245	0.0182	231	0.0315	234
271	moreedian-000	0.3874	441	0.4912	441	0.9988	467	-	0.9990	462	0.9999	444	0.9998	457	0.4788	441	
272	mukh-001	0.0170	339	0.0285	344	0.0225	362	0.0405	363	0.0272	332	0.0950	280	0.0291	278	0.0301	202
273	mukh-002	0.0269	368	0.0357	360	0.0435	390	0.0799	392	0.0143	262	0.0213	177	0.0122	178	0.0345	262
274	multimodality-000	0.0034	112	0.0047	109	0.0036	137	0.0044	120	0.0077	168	0.9976	429	0.4456	392	0.0287	135
275	multimodality-001	0.0029	89	0.0042	88	0.0031	101	0.0035	83	0.0038	78	0.0071	45	0.0059	62	0.0281	85
276	mvision-001	0.0191	349	0.0233	323	0.0204	355	0.0356	358	0.0198	304	0.0337	221	0.0242	263	0.0431	310
277	nazhiai-000	0.0040	135	0.0059	138	0.0036	133	0.0048	133	0.0057	135	0.0125	113	0.0083	113	0.0275	27
278	neosystems-004	0.0279	372	0.0495	373	0.0289	374	0.0585	384	0.0439	360	0.9621	408	0.1296	347	0.0333	257
279	netbridge-tech-001	0.4749	448	0.6599	456	0.4438	433	0.5676	432	0.4491	425	1.0000	449	0.9541	435	0.1098	386
280	netbridge-tech-002	0.0101	271	0.0166	283	0.0077	261	0.0127	272	0.0133	253	0.8215	386	0.0523	313	0.0351	274
281	neurotechnology-013	0.0032	100	0.0045	102	0.0026	61	0.0036	87	0.0037	76	0.0068	43	0.0052	37	0.0278	48
282	neurotechnology-015	0.0022	58	0.0036	71	0.0024	18	0.0028	40	0.0030	36	0.0052	15	0.0041	14	0.0276	33
283	nhn-002	0.0068	211	0.0096	208	0.0057	219	0.0087	232	0.0136	256	0.0253	193	0.0186	237	0.0302	204
284	nhn-003	0.0033	102	0.0048	112	0.0027	68	0.0038	98	0.0036	74	0.0198	167	0.0071	89	0.0285	127
285	nodeflux-002	0.0186	347	0.0340	354	0.0261	369	0.0451	366	0.0548	370	1.0000	454	1.0000	461	0.0299	196
286	notiontag-001	0.6846	466	0.8006	466	0.3955	428	0.5247	427	0.8669	446	0.8313	390	0.6362	407	0.2221	411
287	notiontag-002	0.0066	207	0.0089	195	0.0045	177	0.0061	177	0.0077	169	0.0137	118	0.0104	147	0.0299	195
288	nsensecorp-003	0.0251	365	0.0295	347	0.0212	359	0.0305	350	0.0131	251	0.2139	314	0.0141	197	0.0872	376
289	nsensecorp-004	0.1370	417	0.1397	405	0.0066	237	0.0094	239	1.0000	469	1.0000	472	1.0000	467	0.0805	370
290	ntechlab-011	0.0012	18	0.0019	16	0.0024	23	0.0028	45	0.0029	34	0.0055	19	0.0047	24	0.0288	145
291	ntechlab-012	0.0011	14	0.0016	10	0.0023	16	0.0030	51	0.0026	21	0.0050	14	0.0043	16	0.0280	76
292	omface-000	0.2573	430	0.3835	433	0.3590	426	0.4903	426	0.3956	423	0.5003	347	0.2595	365	0.2400	415
293	omface-001	0.0137	315	0.0212	314	0.0114	323	0.0187	321	0.0174	291	1.0000	462	0.0214	255	0.0789	365
294	omnigarde-001	0.0168	336	0.0260	336	0.0203	354	0.0402	361	0.0243	322	0.0327	215	0.0177	225	0.0288	142
295	omnigarde-002	0.0033	111	0.0046	107	0.0027	72	0.0039	100	0.0041	96	0.0076	52	0.0059	65	0.0278	51
296	onfido-000	0.1472	419	0.2881	423	0.0335	381	0.0731	389	0.0515	368	0.9915	423	0.9579	436	0.0731	360
297	openface-001	0.1804	421	0.2921	424	0.2878	423	0.3906	423	0.2054	409	0.2338	320	0.1549	355	0.2445	416
298	oz-003	0.0095	263	0.0143	260	0.0054	209	0.0077	209	0.0096	211	0.0175	154	0.0118	171	0.0288	149
299	oz-004	0.0033	109	0.0049	116	0.0038	150	0.0055	154	0.0081	178	0.0163	143	0.0142	198	0.0329	251
300	palit-000	0.0062	197	0.0084	187	0.0039	153	0.0055	153	0.0055	131	0.4610	344	0.2468	363	0.0280	74
301	palit-001	0.0050	151	0.0068	153	0.0032	116	0.0047	132	0.0045	106	0.0110	101	0.0058	60	0.0287	138
302	pangiam-000	0.0031	95	0.0043	95	0.0026	45	0.0030	55	0.0038	79	0.0071	46	0.0061	70	0.0424	307
303	papago-001	0.0067	209	0.0096	209	0.0051	200	0.0077	208	0.0071	158	0.0126	114	0.0086	120	0.0816	372
304	papsav1923-002	0.0021	56	0.0034	60	0.0026	47	0.0030	54	0.0048	113	0.0093	82	0.0086	118	0.0312	228
305	papsav1923-003	0.0025	75	0.0035	62	0.0024	31	0.0025	19	0.0034	59	0.0066	38	0.0058	59	0.0281	89
306	paravision-010	0.0012	19	0.0021	20	0.0022	6	0.0021	7	0.0027	26	0.0055	20	0.0050	30	0.0288	150
307	paravision-011	0.0008	4	0.0020	19	0.0021	4	0.0020	4	0.0026	22	0.0053	16	0.0049	28	0.0289	158
308	pensees-001	0.0087	251	0.0133	253	0.0071	248	0.0122	265	0.0145	265	0.0252	192	0.0195	244	0.0283	105

Table 25: FNMR is the proportion of mated comparisons below a threshold set to achieve the FMR given in the header on the fourth row. FMR is the proportion of impostor comparisons at or above that threshold. The light grey values give rank over all algorithms in that column. The pink columns use only same-sex impostors; others are selected regardless of demographics. The exception, in the green column, uses “matched-covariates” i.e. impostors of the same sex, age group, and country of birth. The second pink column includes effects of extended ageing. Missing entries for border, visa, mugshot and wild images generally mean the algorithm did not run to completion. The VISA columns compare images described in section 2.1. The MUGSHOT columns compare images described in section 2.5. The VISA-BORDER column compare images described in section 2.2 with those of section 2.4. The BORDER column compares images described in section 2.4. The WILD columns compare images described in section 2.7.

Algorithm	FALSE NON-MATCH RATE (FNMR)																
	CONSTRAINED, COOPERATIVE											LESS CONSTRAINED, NON-COOP.					
	Name	VISAMC	VISA	MUGSHOT	MUGSHOT12+YRS	VISABORDER	BORDER	BORDER	WILD								
	FMR	0.0001	1E-06	1E-05	1E-05	1E-06	1E-06	1E-05	0.0001	0.0001	0.0001						
309	pixelall-008	0.0015	27	0.0023	29	0.0034	129	0.0049	134	0.0031	42	0.0057	23	0.0052	33	0.0278	43
310	pixelall-009	0.0018	41	0.0025	33	0.0024	27	0.0026	27	0.0031	44	0.3475	333	0.0053	40	0.0276	31
311	psl-010	0.0017	39	0.0035	65	0.0023	10	0.0025	18	0.0035	68	0.0104	94	0.0052	36	0.0282	91
312	psl-011	0.0013	23	0.0026	35	0.0021	1	0.0021	6	0.0024	14	0.0047	8	0.0035	7	0.0285	123
313	ptakuratsatu-000	0.0060	193	0.0089	196	0.0070	245	0.0104	249	0.0096	213	0.0152	131	0.0100	138	0.0284	110
314	pxl-001	0.0488	391	0.0752	394	0.0586	399	0.1087	400	0.0946	388	0.1065	287	0.0625	322	0.1088	384
315	pyramid-000	0.0136	312	0.0233	324	0.0117	325	0.0192	323	0.0185	295	0.0322	214	0.0206	251	0.0304	210
316	qazbs-000	0.0058	182	0.0083	185	0.0046	181	0.0072	195	0.0130	249	0.0244	189	0.0196	245	0.0297	193
317	qluevision-001	0.0223	357	0.0419	369	0.0205	356	0.0343	357	0.0327	343	0.8762	393	0.7413	417	0.0460	320
318	qnap-002	0.0122	300	0.0191	302	0.0075	259	0.0095	242	0.0146	266	0.0281	205	0.0184	233	0.0352	276
319	qnap-003	0.0637	400	0.0657	389	0.0058	221	0.0078	211	0.0082	180	0.9985	432	0.9658	440	0.0287	137
320	quantasoft-003	0.0081	243	0.0113	233	0.0056	215	0.0076	205	0.0091	199	0.0161	140	0.0107	153	0.0414	304
321	rankone-013	0.0028	83	0.0041	84	0.0026	48	0.0033	70	0.0028	31	0.0055	22	0.0040	12	0.0291	169
322	rankone-014	0.0016	34	0.0021	22	0.0024	17	0.0027	30	0.0022	10	0.0047	9	0.0035	5	0.0293	177
323	realnetworks-007	0.0031	96	0.0051	120	0.0028	81	0.0035	84	0.0048	114	0.0091	79	0.0074	95	0.0279	54
324	realnetworks-008	0.0022	61	0.0039	76	0.0038	144	0.0045	122	0.0055	128	0.0100	91	0.0080	108	0.0292	173
325	regula-000	0.0184	346	0.0376	365	0.0103	302	0.0185	317	0.0120	240	0.9983	431	0.0231	260	0.0273	16
326	regula-001	0.0072	224	0.0107	227	0.0102	300	0.0179	315	0.0123	245	0.0333	220	0.0174	223	0.0295	182
327	remarkai-001	0.0144	320	0.0256	334	0.0102	299	0.0159	304	0.0162	276	0.0582	257	0.0185	235	0.0308	221
328	remarkai-003	0.0047	145	0.0063	145	0.0033	122	0.0049	137	0.0054	126	0.0100	90	0.0072	92	0.0275	28
329	rendip-000	0.0055	172	0.0077	169	0.0048	189	0.0060	175	0.0080	174	0.0142	122	0.0110	158	0.0433	312
330	revealmedia-005	0.0050	152	0.0074	165	0.0050	195	0.0068	191	0.0075	165	0.0124	111	0.0104	150	0.3960	435
331	revealmedia-006	0.0040	134	0.0067	151	0.0041	166	0.0056	157	0.0056	132	0.0085	71	0.0068	81	0.0278	50
332	rokid-000	0.0093	261	0.0145	263	0.0073	254	0.0102	248	0.0164	278	0.0280	202	0.0214	254	0.0857	375
333	rokid-001	0.0105	277	0.0162	277	0.0094	298	0.0163	307	0.0181	292	0.0276	201	0.0165	218	0.0325	246
334	s1-005	0.0024	73	0.0036	70	0.0025	41	0.0029	48	0.0026	23	0.0048	10	0.0038	9	0.0359	281
335	s1-006	0.0029	87	0.0044	96	0.0028	77	0.0033	68	0.0035	67	0.0073	47	0.0044	19	0.0367	284
336	saffe-001	0.4339	445	0.5261	444	0.7539	454	0.8736	455	0.7977	438	0.9810	412	0.7435	418	0.3887	434
337	saffe-002	0.0119	296	0.0206	309	0.0107	311	0.0177	313	0.0244	323	0.9998	442	0.2785	370	0.0308	220
338	samsungsd-001	0.0015	31	0.0026	36	0.0023	13	0.0023	13	0.0024	15	0.1660	302	0.0536	314	0.0282	90
339	samsungsd-002	0.0017	40	0.0027	39	0.0023	11	0.0022	8	0.0021	7	0.0043	6	0.0036	8	0.0283	103
340	samtech-001	0.0197	351	0.0365	362	0.0146	341	0.0241	339	0.0238	321	0.0394	236	0.0251	265	0.0337	258
341	scanovate-002	0.0175	344	0.0355	359	0.0146	339	0.0286	348	0.0269	329	0.0301	208	0.0178	227	0.0301	203
342	scanovate-003	0.0054	167	0.0080	180	0.0054	206	0.0072	199	0.0312	340	0.0599	258	0.0568	318	0.0283	104
343	sdc-000	0.0303	376	0.0526	378	0.0572	398	0.1094	402	0.0867	385	0.6230	358	0.3682	384	0.1201	390
344	securifai-005	0.0125	304	0.0190	301	0.0080	270	0.0126	270	0.0134	254	0.9861	415	0.9205	430	0.0329	250
345	securifai-006	0.0140	318	0.0196	306	0.0067	239	0.0102	247	0.0113	236	0.9888	419	0.9239	431	0.0346	264
346	sensetime-007	0.0012	20	0.0022	23	0.0021	5	0.0020	3	0.0018	3	0.0034	2	0.0029	1	0.0280	71
347	sensetime-008	0.0008	5	0.0014	5	0.0021	2	0.0020	2	0.0018	4	0.0036	3	0.0033	4	0.0284	116
348	sertis-000	0.0118	293	0.0208	311	0.0080	266	0.0127	271	0.0110	232	0.0176	155	0.0114	164	0.0285	125
349	sertis-002	0.0049	149	0.0061	140	0.0039	158	0.0061	180	0.0055	129	0.0099	89	0.0070	88	0.0281	82
350	seventhSense-001	0.0034	114	0.0047	110	0.0025	40	0.0031	60	0.0029	33	0.0338	222	0.0109	155	0.0279	55
351	seventhSense-002	0.0036	123	0.0050	118	0.0028	80	0.0036	88	0.0035	66	0.0811	274	0.0183	232	0.0278	47
352	shaman-000	0.9297	472	0.9774	470	0.9990	468	-	0.9999	463	1.0000	452	0.9999	459	0.9575	462	

Table 26: FNMR is the proportion of mated comparisons below a threshold set to achieve the FMR given in the header on the fourth row. FMR is the proportion of impostor comparisons at or above that threshold. The light grey values give rank over all algorithms in that column. The pink columns use only same-sex impostors; others are selected regardless of demographics. The exception, in the green column, uses “matched-covariates” i.e. impostors of the same sex, age group, and country of birth. The second pink column includes effects of extended ageing. Missing entries for border, visa, mugshot and wild images generally mean the algorithm did not run to completion. The VISA columns compare images described in section 2.1. The MUGSHOT columns compare images described in section 2.5. The VISA-BORDER column compare images described in section 2.2 with those of section 2.4. The BORDER column compares images described in section 2.4. The WILD columns compare images described in section 2.7.

Algorithm	FALSE NON-MATCH RATE (FNMR)																
	CONSTRAINED, COOPERATIVE																
	Name	VISAMC	VISA	MUGSHOT	MUGSHOT12+YRS	VISABORDER	BORDER	BORDER	WILD	LESS CONSTRAINED, NON-COOP.							
	FMR	0.0001	1E-06	1E-05	1E-05	1E-06	1E-06	1E-05	0.0001								
353	shaman-001	0.3346	437	0.4616	437	0.2368	420	0.3723	422	0.3574	420	0.3527	334	0.2304	362	0.1498	395
354	shu-002	-	0.0079	178	0.0146	340	0.0308	351	1.0000	464	0.0183	158	0.0115	166	0.0284	112	
355	shu-003	0.0028	82	0.0041	86	0.0050	194	0.0088	233	0.0081	179	0.0133	117	0.0094	131	0.0283	108
356	siat-002	0.0091	256	0.0126	251	0.0109	312	0.0190	322	0.0276	333	0.0516	252	0.0464	306	0.0520	330
357	siat-005	0.0021	50	0.0038	74	0.0059	222	0.0049	138	0.0742	378	0.9623	409	0.6801	410	0.0279	59
358	situ-003	0.0017	38	0.0033	56	0.0030	96	0.0037	95	0.0058	137	0.0104	95	0.0081	109	0.0284	117
359	situ-004	0.0014	25	0.0025	31	0.0027	65	0.0028	46	0.0046	107	0.0086	74	0.0073	93	0.0272	8
360	sktelecom-000	0.0038	129	0.0054	129	0.0031	99	0.0051	144	0.0042	97	0.3418	330	0.0061	69	0.0293	179
361	smartbiometrik-001	0.5485	457	0.6442	452	0.7550	455	0.8611	452	0.8677	447	0.8270	389	0.7030	412	0.3144	428
362	smartengines-000	0.6240	463	0.7562	464	0.9552	463	0.9784	463	0.9515	458	0.9288	404	0.8200	423	0.8037	457
363	smartengines-001	0.6434	465	0.7666	465	0.9446	462	0.9750	462	0.9387	457	0.9556	407	0.8647	428	0.7748	455
364	smartvist-000	0.0912	407	0.1587	409	0.1163	412	0.1841	411	0.1397	396	0.9372	405	0.7107	415	0.0779	362
365	smilart-002	0.2440	426	0.3532	428	-	-	-	-	0.3785	421	0.4145	341	0.2611	367	-	-
366	smilart-003	0.6944	467	0.8836	467	0.0695	404	0.1193	406	0.0894	386	0.1221	294	0.0737	330	0.1190	389
367	sodec-000	0.0033	110	0.0044	101	0.0040	163	0.0053	149	0.0054	127	0.0096	87	0.0080	106	0.0274	18
368	sqisoft-002	0.0082	245	0.0124	245	0.0051	198	0.0086	229	0.0102	221	0.0183	159	0.0122	177	0.0287	139
369	sqisoft-003	0.0041	137	0.0055	130	0.0026	44	0.0032	66	0.0039	85	1.0000	460	1.0000	475	0.0295	185
370	stagu-000	0.0139	317	0.0208	310	0.0104	303	0.0145	296	0.0156	269	0.8063	383	0.1408	352	0.0332	254
371	starhybrid-001	0.0108	280	0.0138	257	0.0081	271	0.0113	257	0.0152	268	0.0265	196	0.0189	238	0.0350	272
372	stcon-000	0.0040	133	0.0056	133	0.0031	106	0.0047	129	0.0048	115	0.9863	416	0.3562	382	0.0300	201
373	sukshi-000	0.5409	455	0.6612	457	0.4556	435	0.6567	437	0.9296	456	0.8898	394	0.7384	416	0.6892	451
374	suprema-003	0.0028	84	0.0041	87	0.0034	126	0.0039	101	0.0030	39	0.3095	329	0.0580	320	0.0284	111
375	suprema-004	0.0024	68	0.0035	67	0.0032	112	0.0036	89	0.0028	28	0.0053	17	0.0045	21	0.0281	83
376	supremaid-001	0.0053	166	0.0073	164	0.0045	176	0.0066	188	0.0099	219	0.0186	160	0.0148	206	0.0352	275
377	supremaid-002	0.0063	201	0.0094	204	0.0044	172	0.0062	181	0.0072	161	0.0229	185	0.0095	134	0.0345	263
378	surrey-cvssp-000	0.9084	471	0.9909	472	0.9923	466	0.9950	465	0.9981	461	0.9994	435	0.9979	453	0.9389	459
379	surrey-cvssp-001	1.0000	476	1.0000	474	0.0077	262	0.0079	216	0.0266	328	0.3822	337	0.0551	316	1.0000	468
380	synesys-006	0.0070	215	0.0096	207	0.0107	309	0.0166	309	-	-	0.0128	116	0.0089	123	0.0292	172
381	synesis-007	0.0050	154	0.0073	162	0.0062	231	0.0076	204	-	-	0.0105	96	0.0080	107	0.0288	141
382	synology-000	0.0149	324	0.0238	327	0.0148	342	0.0261	342	0.0221	309	0.0331	217	0.0209	252	0.0330	252
383	synology-002	0.0104	275	0.0153	273	0.0107	310	0.0184	316	0.0189	298	0.2032	311	0.0180	228	0.0312	225
384	sztu-000	0.0092	259	0.0139	258	0.0091	289	0.0201	328	0.0136	255	0.0685	267	0.0118	173	0.0270	4
385	sztu-001	0.0031	93	0.0043	94	0.0025	37	0.0028	43	0.0051	119	0.0113	103	0.0089	124	0.0275	21
386	t4isb-000	0.0058	181	0.0087	192	0.0041	167	0.0064	185	0.0083	183	0.0157	137	0.0103	145	0.0282	97
387	tech5-005	0.0054	169	0.0072	156	0.0069	242	0.0122	264	0.0060	143	0.0094	84	0.0066	76	0.0349	270
388	tech5-007	0.0020	48	0.0029	44	0.0024	21	0.0028	36	0.0034	62	0.8622	392	0.5335	398	0.0280	67
389	techsign-000	0.0325	378	0.0511	376	0.0435	389	0.0710	387	0.0746	379	0.1104	290	0.0841	335	0.0639	347
390	techsign-001	0.0110	283	0.0196	307	0.0067	238	0.0120	262	0.0087	189	0.2475	321	0.0883	339	0.0299	197
391	tevian-007	0.0019	45	0.0027	38	0.0032	114	0.0041	106	0.0045	105	0.0086	73	0.0078	102	0.0310	224
392	tevian-008	0.0012	21	0.0017	11	0.0033	117	0.0042	112	0.0042	99	0.0081	61	0.0068	82	0.0290	161
393	tiger-005	0.0624	399	0.2450	419	0.0292	376	0.0556	376	0.0430	357	1.0000	446	0.9964	449	0.0278	45
394	tiger-006	0.0066	206	0.0101	217	0.0050	197	0.0075	203	0.0089	193	0.0158	138	0.0117	169	0.0290	168
395	tinkoff-001	0.0145	321	0.0244	328	0.0318	379	0.0636	385	0.0236	319	1.0000	476	0.0339	283	0.0563	339
396	tongyi-005	0.0073	228	0.0146	264	0.0187	351	0.0421	365	0.0161	274	0.0215	178	0.0149	208	0.0399	293

Table 27: FNMR is the proportion of mated comparisons below a threshold set to achieve the FMR given in the header on the fourth row. FMR is the proportion of impostor comparisons at or above that threshold. The light grey values give rank over all algorithms in that column. The pink columns use only same-sex impostors; others are selected regardless of demographics. The exception, in the green column, uses “matched-covariates” i.e. impostors of the same sex, age group, and country of birth. The second pink column includes effects of extended ageing. Missing entries for border, visa, mugshot and wild images generally mean the algorithm did not run to completion. The VISA columns compare images described in section 2.1. The MUGSHOT columns compare images described in section 2.5. The VISA-BORDER column compare images described in section 2.2 with those of section 2.4. The BORDER column compares images described in section 2.4. The WILD columns compare images described in section 2.7.

Algorithm	Name	FALSE NON-MATCH RATE (FNMR)										LESS CONSTRAINED, NON-COOP.					
		CONSTRAINED, COOPERATIVE								WILD							
		VISAMC	VISA	MUGSHOT	MUGSHOT12+YRS	VISABORDER	BORDER	BORDER	1E-05	0.0001							
FMR		0.0001	1E-06	1E-05	1E-05	1E-06	1E-06	1E-05									
397	toppanidgate-000	0.0021	51	0.0033	57	0.0026	49	0.0028	39	0.0039	86	0.0075	50	0.0068	80	0.0376	288
398	toshiba-004	0.0030	91	0.0042	89	0.0025	38	0.0027	34	0.0034	61	0.0063	33	0.0053	43	0.0278	42
399	toshiba-006	0.0022	63	0.0035	64	0.0024	26	0.0025	23	0.0027	25	0.7425	371	0.3070	376	0.0275	25
400	touchlessid-000	0.3296	436	0.4804	439	0.4111	430	0.6026	434	0.5324	428	0.9996	438	0.9964	450	0.2521	420
401	touchlessid-001	0.0076	234	0.0104	220	0.0680	403	0.0842	394	0.1358	394	1.0000	448	0.9995	456	0.0499	326
402	trueface-002	0.0060	192	0.0096	206	0.0048	188	0.0061	178	0.0112	235	0.0198	168	0.0155	213	0.0793	367
403	trueface-003	0.0070	216	0.0094	205	0.0053	204	0.0081	219	0.0122	241	0.0217	180	0.0159	216	0.0785	364
404	trueidvng-001	0.0063	200	0.0077	171	0.0033	121	0.0044	119	0.0046	108	0.0086	75	0.0069	85	0.0628	344
405	tuputech-000	0.3218	435	0.3696	431	-	-	-	-	0.3237	416	0.4304	342	0.2973	375	0.9415	460
406	turingtechvip-001	0.0330	380	0.0540	380	0.0458	391	0.1007	398	0.4715	426	0.9286	403	0.8448	427	0.4035	437
407	turingtechvip-002	0.0126	309	0.0163	278	0.0092	294	0.0118	259	0.2264	411	1.0000	466	0.9925	445	0.2144	409
408	turkcell-000	0.1134	412	0.1288	404	0.0770	407	0.1112	405	0.2570	412	1.0000	445	0.9999	458	0.9556	461
409	twface-000	0.0051	155	0.0072	160	0.0041	165	0.0058	165	0.0071	159	0.0153	132	0.0100	137	0.0276	32
410	twface-001	0.0036	117	0.0051	122	0.0031	107	0.0038	97	0.0049	116	0.0091	81	0.0075	96	0.0277	36
411	ulsee-001	0.0151	326	0.0246	330	0.0113	320	0.0185	319	0.0187	297	0.6766	365	0.0181	230	0.0316	236
412	ultinous-000	0.2343	425	0.3484	427	-	-	-	-	-	-	-	-	-	-	-	
413	ultinous-001	0.2485	427	0.4003	434	-	-	-	-	-	-	-	-	-	-	-	
414	uluface-002	0.0081	242	0.0123	243	0.0071	247	0.0095	243	0.0107	226	1.0000	468	0.0140	195	0.0444	315
415	uluface-003	0.0100	270	0.0150	269	0.0079	264	0.0128	274	-	-	-	-	-	0.0635	345	
416	unissey-002	0.0094	262	0.0151	271	0.0079	265	0.0110	252	0.0114	237	0.4424	343	0.1914	359	0.0420	306
417	unissey-003	0.0057	176	0.0082	183	0.0047	185	0.0082	220	0.0067	153	0.5179	350	0.2863	373	0.0288	146
418	upc-001	0.0234	360	0.0519	377	0.0291	375	0.0490	373	0.0294	336	0.2316	319	0.0389	294	0.0314	232
419	uxlabs-001	0.0534	394	0.0570	384	0.0118	326	0.0131	278	0.0237	320	0.0399	237	0.0288	275	0.0876	377
420	vcog-002	0.7522	469	0.9033	468	-	-	-	-	-	-	-	-	-	-	-	
421	vd-002	0.0429	387	0.0704	390	0.0569	397	0.0844	395	0.0801	381	0.0937	277	0.0577	319	0.0556	338
422	vd-003	0.0199	353	0.0222	319	0.0115	324	0.0130	277	0.0138	258	0.0239	187	0.0177	226	0.0389	290
423	veridas-007	0.0063	202	0.0083	184	0.0044	174	0.0058	168	0.0080	175	0.0152	130	0.0120	176	0.0284	113
424	veridas-008	0.0032	99	0.0045	105	0.0030	93	0.0033	71	0.0085	187	0.0206	173	0.0143	200	0.0288	147
425	veridium-000	0.0726	405	0.1248	403	0.5226	438	0.6652	438	0.6425	431	0.8150	385	0.7989	422	0.4988	444
426	veridium-001	0.0274	371	0.0368	364	0.0292	377	0.0475	369	0.0488	365	0.0673	265	0.0463	305	0.0800	368
427	verigram-000	0.0032	97	0.0043	93	0.0031	100	0.0034	75	0.0093	203	0.0175	153	0.0164	217	0.0276	29
428	verigram-001	0.0032	101	0.0044	99	0.0027	66	0.0032	64	0.0030	37	0.9995	436	0.9953	447	0.0276	34
429	verihubs-inteligensia-000	0.0070	218	0.0098	211	0.0048	190	0.0076	207	0.0092	200	0.0160	139	0.0117	168	0.0283	107
430	verihubs-inteligensia-001	0.0071	219	0.0114	236	0.0050	196	0.0076	206	0.0096	209	0.0165	145	0.0114	165	0.0282	94
431	verijelas-000	0.2488	428	0.3431	426	0.4861	436	0.6004	433	0.0811	382	0.1148	291	0.0440	301	0.0524	333
432	via-000	0.0216	356	0.0365	363	0.0177	349	0.0287	349	0.0296	337	0.0572	255	0.0290	277	0.0349	269
433	via-001	0.0149	323	0.0229	322	0.0114	322	0.0177	314	0.0183	294	0.4056	340	0.0176	224	0.0373	286
434	videmo-001	0.0295	374	0.0417	368	0.0164	348	0.0261	343	0.0355	347	0.0603	259	0.0442	302	0.1473	392
435	videmo-002	0.0158	332	0.0288	345	0.0149	346	0.0249	341	0.0230	313	0.3429	331	0.1468	353	0.0294	181
436	videonetics-001	0.5483	456	0.6446	454	0.7517	453	0.8607	451	0.8664	445	0.8255	387	0.6956	411	0.2986	425
437	videonetics-002	0.4274	443	0.5329	445	0.6081	443	0.7438	443	0.7775	436	0.7297	370	0.5756	401	0.1976	407
438	viettelhightech-000	0.0117	291	0.0166	282	0.0110	314	0.0198	327	0.0167	283	0.0249	190	0.0158	214	0.0409	303
439	vigilantsolutions-010	0.0109	281	0.0164	281	0.0074	256	0.0095	241	0.0209	306	0.0365	231	0.0233	261	0.0277	37
440	vigilantsolutions-011	0.0124	302	0.0176	291	0.0073	252	0.0095	240	0.0196	302	0.0360	229	0.0221	257	0.0274	17

Table 28: FNMR is the proportion of mated comparisons below a threshold set to achieve the FMR given in the header on the fourth row. FMR is the proportion of impostor comparisons at or above that threshold. The light grey values give rank over all algorithms in that column. The pink columns use only same-sex impostors; others are selected regardless of demographics. The exception, in the green column, uses “matched-covariates” i.e. impostors of the same sex, age group, and country of birth. The second pink column includes effects of extended ageing. Missing entries for border, visa, mugshot and wild images generally mean the algorithm did not run to completion. The VISA columns compare images described in section 2.1. The MUGSHOT columns compare images described in section 2.5. The VISA-BORDER column compare images described in section 2.2 with those of section 2.4. The BORDER column compares images described in section 2.4. The WILD columns compare images described in section 2.7.

	Algorithm	FALSE NON-MATCH RATE (FNMR)															
		CONSTRAINED, COOPERATIVE								LESS CONSTRAINED, NON-COOP.							
		Name	VISAMC	VISA	MUGSHOT	MUGSHOT12+YRS	VISABORDER	BORDER	BORDER	WILD							
FMR		0.0001	1E-06	1E-05	1E-05	1E-05	1E-06	1E-06	1E-05	0.0001							
441	vinal-000	0.0081	241	0.0124	246	0.0045	175	0.0072	198	0.0089	192	0.1814	304	0.0112	160	0.0274	19
442	vinbigdata-001	0.2576	431	0.2763	421	0.1404	416	0.1988	415	0.1407	397	0.1150	292	0.0703	328	0.9767	463
443	vinbigdata-002	0.0102	272	0.0175	289	0.0071	250	0.0084	225	0.0090	194	0.8017	382	0.3134	377	0.0304	209
444	vion-000	0.0419	385	0.0590	385	0.0422	388	0.0478	370	0.0581	371	0.0968	284	0.0847	336	0.2479	417
445	visage-000	0.0933	408	0.1441	408	0.1316	414	0.2416	416	0.1395	395	0.1920	308	0.1001	343	0.0500	327
446	visionbox-001	0.0159	333	0.0270	340	0.0111	316	0.0173	312	0.0190	299	0.0315	211	0.0205	250	0.0389	291
447	visionbox-002	0.0058	180	0.0079	175	0.0060	225	0.0074	200	0.0084	185	0.0149	127	0.0113	163	0.0447	317
448	visionlabs-010	0.0017	36	0.0024	30	0.0026	56	0.0030	52	0.0033	55	0.0061	30	0.0052	35	0.0282	99
449	visionlabs-011	0.0012	17	0.0022	25	0.0024	29	0.0026	28	0.0028	29	0.0053	18	0.0046	23	0.0280	73
450	visteam-004	0.0541	396	0.5202	443	0.0406	387	0.0827	393	0.1879	405	0.1795	303	0.0347	286	0.0289	152
451	visteam-005	0.0235	361	0.0333	352	0.0265	370	0.0583	383	0.0341	344	0.0524	254	0.0259	268	0.0292	171
452	vixvzion-006	0.0082	244	0.0122	242	0.0093	295	0.0194	324	0.0099	218	0.0169	147	0.0108	154	0.0268	3
453	vixvzion-007	0.0110	284	0.0191	303	0.0080	268	0.0157	302	0.0101	220	0.0190	161	0.0118	172	0.0273	14
454	vnpt-004	0.0058	184	0.0078	174	0.0037	142	0.0053	148	0.0051	120	0.4640	345	0.1384	350	0.0275	24
455	vnpt-005	0.0036	118	0.0052	124	0.0027	67	0.0031	59	0.0036	72	0.0066	39	0.0056	48	0.0286	130
456	vocord-009	0.0022	59	0.0029	47	0.0036	134	0.0046	128	0.0052	124	0.0098	88	0.0086	121	0.0284	115
457	vocord-010	0.0024	71	0.0031	51	0.0036	135	0.0049	140	0.0025	20	0.0065	35	0.0040	11	0.0280	70
458	vts-000	0.0103	273	0.0174	288	0.0080	267	0.0129	276	0.0250	326	0.0450	243	0.0372	292	0.0596	340
459	vts-001	0.0033	106	0.0048	111	0.0027	69	0.0036	90	0.0032	46	0.6519	362	0.3563	383	0.0338	260
460	wicket-000	0.0018	43	0.0028	42	0.0024	24	0.0027	29	0.0031	41	0.7968	381	0.4340	391	0.0323	243
461	winsense-001	0.0062	198	0.0099	215	0.0092	292	0.0210	329	0.0093	202	0.0144	125	0.0098	136	0.0320	241
462	winsense-002	0.0050	153	0.0073	163	0.0038	146	0.0059	172	0.0064	149	0.0118	109	0.0084	115	0.0307	217
463	wiseai-001	0.0658	401	0.0964	400	0.7743	457	0.8956	457	0.1967	406	0.7526	375	0.3419	379	0.5780	447
464	wuhantianyu-001	0.0163	334	0.0262	337	0.0281	373	0.0569	380	0.0316	341	0.0486	249	0.0344	284	0.0324	244
465	x-laboratory-000	0.0071	221	0.0106	223	0.0123	329	0.0138	287	0.0419	356	0.5629	354	0.2852	372	0.0295	188
466	x-laboratory-001	0.0059	189	0.0110	231	0.0054	207	0.0078	214	0.0094	205	0.0142	121	0.0100	139	0.0294	180
467	xforwardai-001	0.0021	53	0.0034	59	0.0027	71	0.0028	42	0.0046	110	0.0088	78	0.0079	104	0.0281	88
468	xforwardai-002	0.0016	32	0.0023	28	0.0026	60	0.0025	20	0.0040	91	0.0081	62	0.0074	94	0.0282	92
469	xm-000	0.0015	26	0.0026	37	0.0031	104	0.0038	99	0.0058	138	0.0105	97	0.0082	112	0.0282	98
470	yisheng-004	0.1988	422	0.3329	425	0.1147	411	0.1849	412	0.2044	408	-	-	-	-	0.0908	378
471	yitu-003	0.0015	30	0.0026	34	0.0066	236	0.0085	226	0.0064	150	0.0114	104	0.0103	146	0.0325	247
472	yoonik-002	0.0052	163	0.0062	142	0.0029	89	0.0034	77	0.0615	375	0.1279	296	0.1166	345	0.0549	336
473	yoonik-003	0.0034	113	0.0047	108	0.0032	111	0.0037	93	0.0816	383	0.2033	312	0.1601	356	0.0699	357
474	ytu-000	0.0057	179	0.0087	191	0.0121	327	0.0238	338	0.0047	111	0.0078	57	0.0059	64	0.0286	132
475	yuan-005	0.0037	126	0.0046	106	0.0027	73	0.0035	85	0.0033	50	0.2706	326	0.0876	338	0.0288	151
476	yuan-006	0.0045	141	0.0062	141	0.0032	110	0.0049	136	0.0038	81	0.0084	68	0.0049	27	0.0273	11

Table 29: FNMR is the proportion of mated comparisons below a threshold set to achieve the FMR given in the header on the fourth row. FMR is the proportion of impostor comparisons at or above that threshold. The light grey values give rank over all algorithms in that column. The pink columns use only same-sex impostors; others are selected regardless of demographics. The exception, in the green column, uses “matched-covariates” i.e. impostors of the same sex, age group, and country of birth. The second pink column includes effects of extended ageing. Missing entries for border, visa, mugshot and wild images generally mean the algorithm did not run to completion. The VISA columns compare images described in section 2.1. The MUGSHOT columns compare images described in section 2.5. The VISA-BORDER column compare images described in section 2.2 with those of section 2.4. The BORDER column compares images described in section 2.4. The WILD columns compare images described in section 2.7.

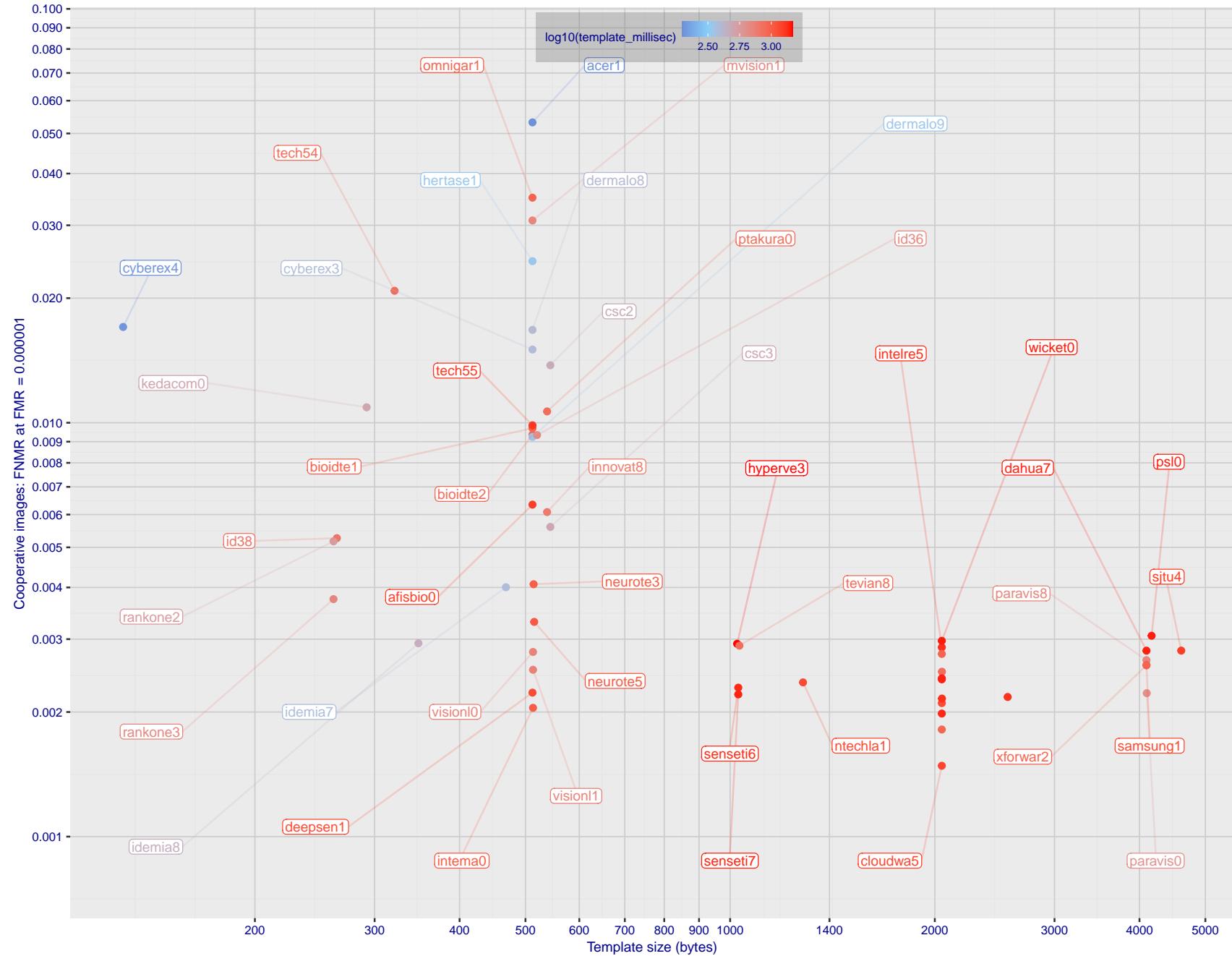


Figure 1: The points show false non-match rates (FNMR) versus the size of the encoded template. FNMR is the geometric mean of FNMR values for visa and mugshot images (from Figs. 90 and 114) at the false match rate (FMR) given in the y-axis label. The color of the points encodes template generation time - which spans at least one order of magnitude. Durations are measured on a single core of a c. 2016 Intel Xeon CPU E5-2630 v4 running at 2.20GHz. Algorithms with poor FNMR are omitted.

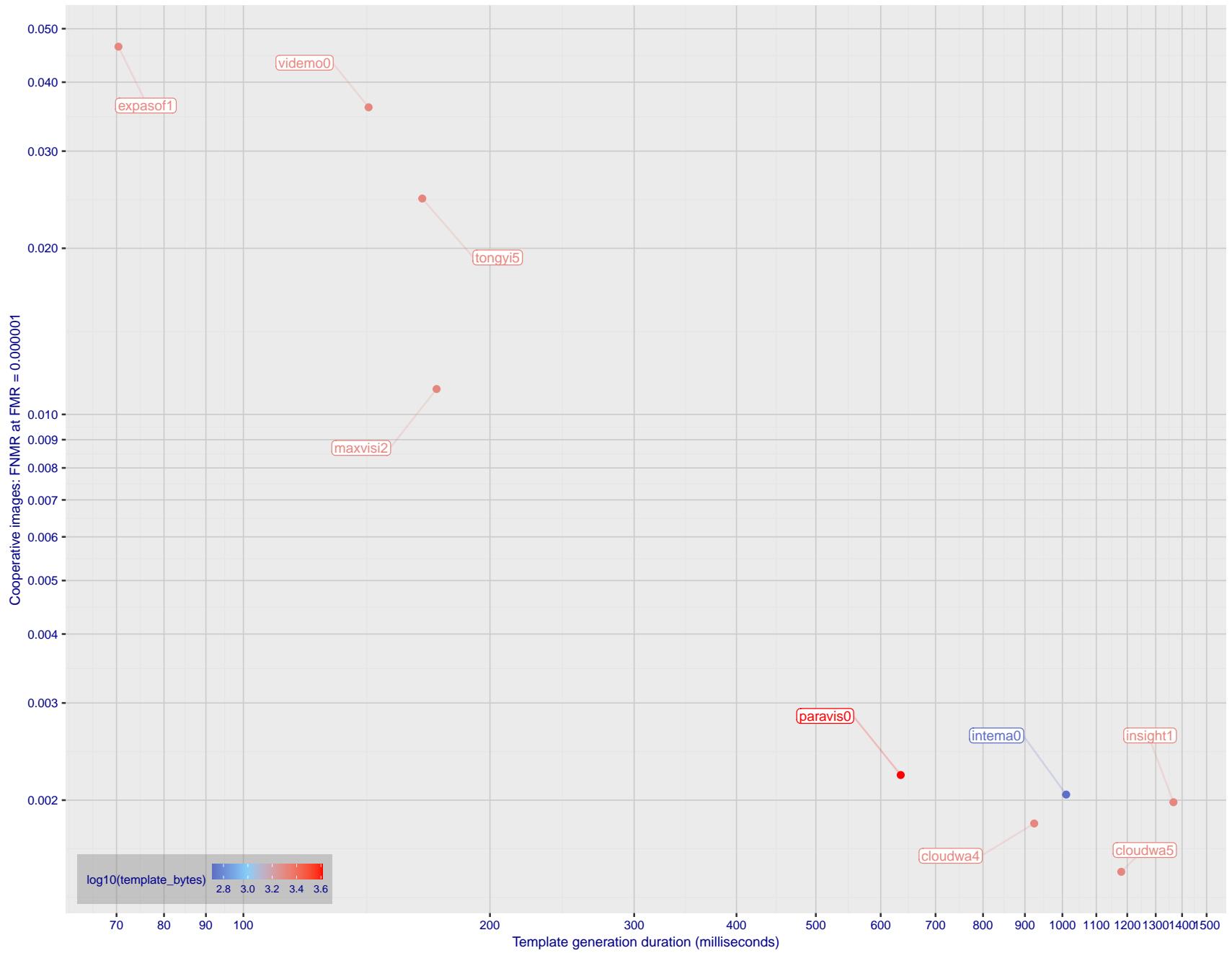


Figure 2: The points show false non-match rates (FNMR) versus the duration of the template generation operation. FNMR is the geometric mean of FNMR values for visa and mugshot images (from Figs. 90 and 114) at a false match rate (FMR) given in the y-axis label. Template generation time is a median estimated over 640 x 480 pixel portraits. It is measured on a single core of a c. 2016 Intel Xeon CPU E5-2630 v4 running at 2.20GHz. The color of the points encodes template size - which span two orders of magnitude. Algorithms with poor FNMR are omitted.

1 Metrics

1.1 Core accuracy

Given a vector of N genuine scores, u , the false non-match rate (FNMR) is computed as the proportion below some threshold, T:

$$\text{FNMR}(T) = 1 - \frac{1}{N} \sum_{i=1}^N H(u_i - T) \quad (1)$$

where $H(x)$ is the unit step function, and $H(0)$ taken to be 1.

Similarly, given a vector of N impostor scores, v , the false match rate (FMR) is computed as the proportion above T:

$$\text{FMR}(T) = \frac{1}{N} \sum_{i=1}^N H(v_i - T) \quad (2)$$

The threshold, T, can take on any value. We typically generate a set of thresholds from quantiles of the observed impostor scores, v , as follows. Given some interesting false match rate range, $[\text{FMR}_L, \text{FMR}_U]$, we form a vector of K thresholds corresponding to FMR measurements evenly spaced on a logarithmic scale

$$T_k = Q_v(1 - \text{FMR}_k) \quad (3)$$

where Q is the quantile function, and FMR_k comes from

$$\log_{10} \text{FMR}_k = \log_{10} \text{FMR}_L + \frac{k}{K} [\log_{10} \text{FMR}_U - \log_{10} \text{FMR}_L] \quad (4)$$

Error tradeoff characteristics are plots of FNMR(T) vs. FMR(T). These are plotted with $\text{FMR}_U \rightarrow 1$ and FMR_L as low as is sustained by the number of impostor comparisons, N. This is somewhat higher than the “rule of three” limit $3/N$ because samples are not independent, due to re-use of images.

1.2 Multi-template scoring methodology

There are some scenarios when one or more people exist and are detected in an image, and some of the proposed test images include $K > 1$ persons for some images and situations where the subject of interest may or may not be the foreground face (largest face in the image). The NIST FRVT 1:1 API supports this by allowing generation of multiple templates representing each person detected in an image. When this occurs, NIST will match all templates generated from the enrollment image with all templates generated from the verification image and use the **maximum** similarity score across all template comparisons. This scoring approach will be used in our calculation of FMR and FNMR (this applies to both genuine and imposter comparisons).

2 Datasets

2.1 Visa images

- ▷ The number of images is on the order of 10^5 .
- ▷ The number of subjects is on the order of 10^5 .
- ▷ The number of subjects with two images is on the order of 10^4 .
- ▷ The images have geometry in reasonable conformance with the ISO/IEC 19794-5 Full Frontal image type. Pose is generally excellent.
- ▷ The images are of size 252x300 pixels. The mean interocular distance (IOD) is 69 pixels.
- ▷ The images are of subjects from greater than 100 countries, with significant imbalance due to visa issuance patterns.
- ▷ The images are of subjects of all ages, including children, again with imbalance due to visa issuance demand.
- ▷ Many of the images are live capture. A substantial number of the images are photographs of paper photographs.
- ▷ When these images are input to the algorithm, they are labelled as being of type "ISO" - see Table 4 of the FRVT API.

2.2 Application images

- ▷ The number of images is on the order of 10^6 .
- ▷ The number of subjects is on the order of 10^6 .
- ▷ The number of subjects with two images is on the order of 10^6 .
- ▷ The images have geometry in good conformance with the ISO/IEC 19794-5 Full Frontal image type. Pose is generally excellent.
- ▷ The images are of size 300x300 pixels. The mean interocular distance (IOD) is 61 pixels.
- ▷ The images are of subjects from greater than 100 countries, with significant imbalance due to population and immigration patterns.
- ▷ The images are of subjects of adults.
- ▷ All of the images are live capture.
- ▷ When these images are input to the algorithm, they are labelled as being of type "ISO" - see Table 4 of the FRVT API.

2.3 Application images with head yaw

- ▷ The number of images is on the order of 10^5 .
- ▷ The number of subjects is on the order of 10^5 .
- ▷ The number of subjects with two images is on the order of 10^5 .
- ▷ The images have geometry in good conformance with the ISO/IEC 19794-5 Full Frontal image type *except* the yaw angle is between 25 and 85 degrees. Our pose estimates are approximate, with an angular error that increases with yaw. The angular estimates will be improved over time.
- ▷ The images are of size 300x300 pixels. The mean interocular distance (IOD), if frontal, would be about pixels, but reduces with cosine of yaw.
- ▷ The images are of subjects from greater than 100 countries, with significant imbalance due to population and immigration patterns.

- ▷ The images are of subjects of adults.
- ▷ All of the images are live capture.
- ▷ When these images are input to the algorithm, they are labelled as being of type "WILD" - see Table 4 of the FRVT API.

2.4 Border crossing images

- ▷ The number of images is on the order of 10^6 .
- ▷ The number of subjects is on the order of 10^6 .
- ▷ The number of subjects with two images is on the order of 10^6 .
- ▷ The images are taken with a camera oriented by an attendant toward a cooperating subject. This is done under time constraints so there are roll, pitch and yaw angle variations. Also background illumination is sometimes strong, so the face is under-exposed. There is some perspective distortion due to close range images. Some faces are partially cropped.
- ▷ The images have mean IOD of 38 pixels.
- ▷ The images are of subjects of adults and children aged 12 or above.
- ▷ The images are of subjects from greater than 100 countries, with significant imbalance due to population and immigration patterns.
- ▷ The images are all live capture.
- ▷ When these images are input to the algorithm, they are labelled as being of type "WILD" - see Table 4 of the FRVT API.

2.5 Mugshot images

- ▷ The number of images is on the order of 10^6 .
- ▷ The number of subjects is on the order of 10^6 .
- ▷ The number of subjects with two images is on the order of 10^6 .
- ▷ The images have geometry in reasonable conformance with the ISO/IEC 19794-5 Full Frontal image type.
- ▷ The images are of variable sizes. The median IOD is 105 pixels. The mean IOD is 113 pixels. The 1-st, 5-th, 10-th, 25-th, 75-th, 90-th and 99-th percentiles are 34, 58, 70, 87, 121, 161 and 297 pixels.
- ▷ The images are of subjects from the United States.
- ▷ The images are of adults.
- ▷ The images are all live capture.
- ▷ When these images are input to the algorithm, they are labelled as being of type "mugshot" - see Table 4 of the FRVT API.

2.6 Kiosk images

- ▷ The number of images is on the order of 10^6 .
- ▷ The number of subjects is on the order of 10^5 .
- ▷ The number of subjects with multiple images is the order of 10^5 .

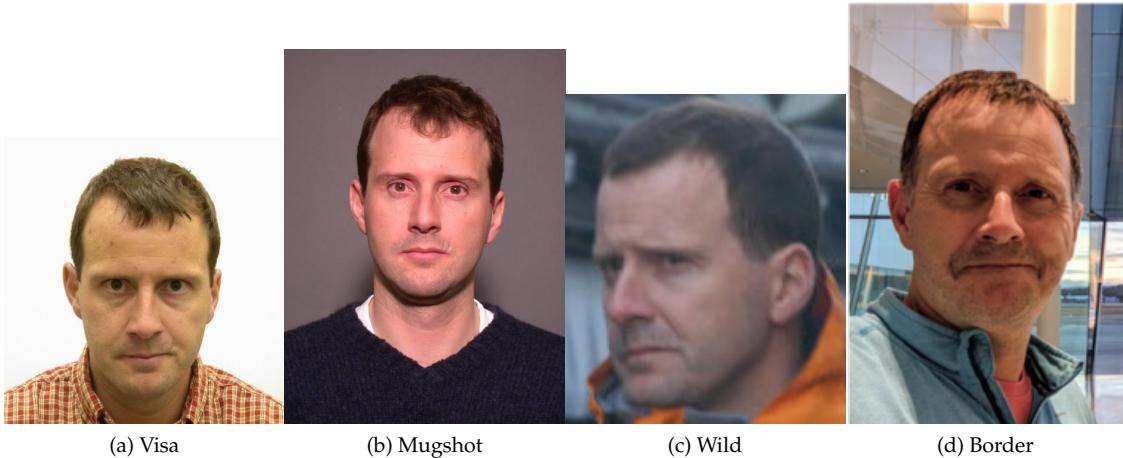


Figure 3: The figure gives simulated samples of image types used in this report.

- ▷ The images are taken at kiosk equipped with a camera intended to capture a centered face. However the images have specific quality defects arising from the camera triggering before the subject looks at it. These are downward pitch of the face relative to the optical axis; cropping of the forehead; and cropping of left or right part of the face. Partial cropping affects perhaps 10% of the images. Resolution does not vary widely.
 - ▷ The images are of adults.
 - ▷ The images have mean IOD of 44 pixels, with maximum below 75, and minimum when both eyes are present above 25 pixels.
 - ▷ All of the images are live capture, none are scanned.
 - ▷ When these images are input to the algorithm, they are labelled as being of type "WILD" - see Table 4 of the FRVT API.

2.7 Wild images

- ▷ The number of images is on the order of 10^5 .
 - ▷ The number of subjects is on the order of 10^4 .
 - ▷ The number of subjects with two images on the order of 10^4 .
 - ▷ The images include many photojournalism-style images. Images are given to the algorithm using a variable but generally tight crop of the head. Resolution varies very widely. The images are very unconstrained, with wide yaw and pitch pose variation. Faces can be occluded, including hair and hands.
 - ▷ The images are of adults.
 - ▷ All of the images are live capture, none are scanned.
 - ▷ When these images are input to the algorithm, they are labelled as being of type "WILD" - see Table 4 of the FRVT API.

3 Results

3.1 Test goals

- To state absolute accuracy for different kinds of images, including those with and without subject cooperation.

- ▷ To state comparative accuracy, across algorithms.

3.2 Test design

Method: For visa images:

- ▷ The comparisons are of visa photos against visa photos.
- ▷ The number of genuine comparisons is on the order of 10^4 .
- ▷ The number of impostor comparisons is on the order of 10^{10} .
- ▷ The comparisons are fully zero-effort, meaning impostors are paired without attention to sex, age or other covariates. However, later analysis is conducted on subsets.
- ▷ The number of persons is on the order of 10^5 .
- ▷ The number of images used to make a template is one.
- ▷ The number of templates used to make each comparison score is two corresponding to simple one-to-one verification.

Method: For mugshot images:

- ▷ The comparisons are of mugshot photos against mugshot photos.
- ▷ The number of genuine comparisons is on the order of 10^6 .
- ▷ The number of impostor comparisons is on the order of 10^8 .
- ▷ The impostors are paired by sex, but not by age or other covariates.
- ▷ The number of persons is on the order of 10^6 .
- ▷ The number of images used to make a template is one.
- ▷ The number of templates used to make each comparison score is two, corresponding to simple one-to-one verification.

Method: For visa-border comparisons:

- ▷ The comparisons are of visa-like frontals against border crossing webcam photos.
- ▷ The number of genuine comparisons is on the order of 10^6 .
- ▷ The number of impostor comparisons is on the order of 10^8 .
- ▷ The impostors are paired by sex, but not by age or other covariates.
- ▷ The number of persons is on the order of 10^6 .
- ▷ The number of images used to make a template is one.
- ▷ The number of templates used to make each comparison score is two, corresponding to simple one-to-one verification.

Method: For visa-border non-frontal yaw comparisons:

- ▷ The comparisons are of visa-like images with yaw 25 to 85 degrees against border crossing webcam photos.
- ▷ The number of genuine comparisons is on the order of 10^5 .
- ▷ The number of impostor comparisons is on the order of 10^8 .
- ▷ The impostors are paired by sex, but not by age or other covariates.

- ▷ The number of persons is on the order of 10^5 .
- ▷ The number of images used to make a template is one.
- ▷ The number of templates used to make each comparison score is two, corresponding to simple one-to-one verification.

Method: For kiosk-border comparisons:

- ▷ The comparisons are of visa-like frontals against kiosk-style photos.
- ▷ The number of genuine comparisons is on the order of 10^6 .
- ▷ The number of impostor comparisons is on the order of 10^8 .
- ▷ The impostors are paired by sex, but not by age or other covariates.
- ▷ The number of persons is on the order of 10^5 .
- ▷ The number of images used to make a template is one.
- ▷ The number of templates used to make each comparison score is two, corresponding to simple one-to-one verification.

Method: For border-border comparisons:

- ▷ The comparisons are of border crossing webcam photos.
- ▷ The number of genuine comparisons is on the order of 10^6 .
- ▷ The number of impostor comparisons is on the order of 10^8 .
- ▷ The impostors are paired by sex, but not by age or other covariates.
- ▷ The number of persons is on the order of 10^6 .
- ▷ The number of images used to make a template is one.
- ▷ The number of templates used to make each comparison score is two corresponding to simple one-to-one verification.

Method: For wild images:

- ▷ The comparisons are of wild photos against wild photos.
- ▷ The number of genuine comparisons is on the order of 10^6 .
- ▷ The number of impostor comparisons is on the order of 10^8 .
- ▷ The comparisons are fully zero-effort, meaning impostors are paired without attention to sex, age or other covariates.
- ▷ The number of persons is on the order of 10^4 .
- ▷ The number of images used to make a template is one.
- ▷ The number of templates used to make each comparison score is two corresponding to simple one-to-one verification.

Method: For child exploitation images:

- ▷ The comparisons are of unconstrained child exploitation photos against others of the same type.
- ▷ The number of genuine comparisons is on the order of 10^4 .
- ▷ The number of impostor comparisons is on the order of 10^7 .

- ▷ The comparisons are fully zero-effort, meaning impostors are paired without attention to sex, age or other covariates.
- ▷ The number of persons is on the order of 10^3 .
- ▷ The number of images used to make 1 template is 1.
- ▷ The number of templates used to make each comparison score is two corresponding to simple one-to-one verification.
- ▷ We produce two performance statements. First, is a DET as used for visa and mugshot images. The second is a cumulative match characteristic (CMC) summarizing a simulated one-to-many search process. This is done as follows.
 - We regard M enrollment templates as items in a gallery.
 - These M templates come from $M > N$ individuals, because multiple images of a subject are present in the gallery under separate identifiers.
 - We regard the verification templates as search templates.
 - For each search we compute the rank of the highest scoring mate.
 - This process should properly be conducted with a 1:N algorithm, such as those tested in NIST IR 8009. We use the 1:1 algorithms in a simulated 1:N mode here to a) better reflect what a child exploitation analyst does, and b) to show algorithm efficacy is better than that revealed in the verification DETs.

3.3 Failure to enroll

	Algorithm	Failure to Enrol Rate ¹											
		APPLICATION		BORDER		KIOSK		MUGSHOT		VISA			
Name	SEC. 2.2	SEC. 2.4	SEC. 2.6	SEC. 2.5	SEC. 2.1	SEC. 2.7							
1	20face-000	0.0000	278	0.0008	235	0.0217	171	0.0000	137	0.0004	272	0.0004	199
2	20face-001	0.0000	272	0.0008	236	0.0000	3	0.0000	136	0.0004	271	0.0004	198
3	3divi-006	0.0000	290	0.0007	203	0.0214	169	0.0001	252	0.0002	137	0.0005	259
4	3divi-007	0.0000	299	0.0007	204	0.0214	168	0.0001	253	0.0002	138	0.0005	260
5	acer-001	0.0000	247	0.0011	295	-	452	0.0001	220	0.0004	294	0.0004	215
6	acer-002	0.0000	390	0.0008	228	0.0191	148	0.0003	345	0.0004	287	0.0011	316
7	acisw-007	0.0000	63	0.0000	43	0.0000	53	0.0000	13	0.0000	59	0.0000	31
8	acisw-008	0.0000	281	0.0009	260	0.0173	132	0.0004	371	0.0004	196	0.0007	291
9	adera-003	0.0000	373	0.0034	393	0.0403	252	0.0003	350	0.0005	386	0.0505	437
10	adera-004	0.0000	276	0.0008	225	0.0202	154	0.0003	358	0.0004	244	0.0003	160
11	advance-003	0.0000	363	0.0012	305	0.0247	189	0.0001	279	0.0004	336	0.0011	314
12	advance-004	0.0001	425	0.0010	286	0.0157	123	0.0008	417	0.0006	402	0.0222	417
13	afisbiometrics-000	0.0000	302	0.0008	220	0.0213	166	0.0000	135	0.0004	289	0.0003	192
14	afrengine-000	0.0000	257	0.0015	327	0.0254	198	0.0008	416	0.0004	223	0.0265	425
15	aifirst-001	0.0000	82	0.0000	61	-	445	0.0000	28	0.0000	71	0.0000	104
16	aigen-001	0.0000	45	0.0000	19	-	383	0.0000	49	0.0000	114	0.0000	26
17	aigen-002	0.0000	116	0.0000	67	0.0000	9	0.0000	97	0.0000	36	0.0000	54
18	ailabs-001	0.0000	258	0.0090	434	-	341	0.0007	409	0.0005	361	0.0016	329
19	aimall-002	0.0000	374	0.0043	411	-	406	0.0012	428	0.0005	381	0.0005	268
20	aimall-003	0.0000	349	0.0012	312	-	387	0.0004	364	0.0005	357	0.0004	229
21	aiseemu-001	0.0000	88	0.0000	59	0.0000	48	0.0000	22	0.0000	75	0.0000	44
22	aiseemu-002	0.0000	85	0.0000	60	0.0000	45	0.0000	30	0.0000	72	0.0000	49
23	aiunionface-000	0.0000	40	0.0000	20	-	405	0.0000	53	0.0000	112	0.0000	108
24	aize-001	0.0001	426	0.0040	406	0.0652	269	0.0026	450	0.0022	454	0.0058	372
25	aize-002	0.0000	187	0.0014	323	0.0230	183	0.0005	394	0.0004	269	0.0071	378
26	ajou-001	0.0000	224	0.0020	352	-	381	0.0001	255	0.0004	341	0.0045	360
27	alchera-004	0.0000	216	0.0009	257	0.0228	180	0.0001	285	0.0004	230	0.0003	174
28	alchera-005	0.0000	314	0.0009	258	0.0228	179	0.0001	286	0.0004	222	0.0003	179
29	alfabeta-001	0.0005	447	0.0650	468	0.2142	301	0.0024	446	0.0018	449	0.1071	457
30	alice-000	0.0000	76	0.0006	176	0.0133	106	0.0000	154	0.0004	216	0.0004	231
31	alleyes-000	0.0000	206	0.0010	274	-	429	0.0002	297	0.0004	317	0.0004	240
32	allgvision-000	0.0007	452	0.0062	427	-	348	0.0026	449	0.0052	465	0.0131	398
33	alphaface-001	0.0000	277	0.0012	302	-	320	0.0000	208	0.0004	315	0.0004	210
34	alphaface-002	0.0000	229	0.0012	299	-	391	0.0000	206	0.0004	319	0.0004	204
35	amplifiedgroup-001	0.0114	468	0.1023	471	-	466	0.0189	470	0.0279	473	0.1390	465
36	androvideo-000	0.0000	24	0.0000	31	-	397	0.0000	61	0.0000	101	0.0002	123
37	anke-004	0.0000	213	0.0011	291	-	416	0.0001	267	0.0004	327	0.0006	283
38	anke-005	0.0000	255	0.0012	303	-	336	0.0001	280	0.0004	334	0.0007	289
39	antheus-000	0.0000	126	0.0000	64	-	330	0.0000	96	0.0000	39	0.0242	421
40	antheus-001	0.0000	6	0.0000	12	-	431	0.0000	45	0.0000	88	0.0242	420
41	anyvision-004	0.0000	361	0.0017	340	-	327	0.0001	281	0.0004	277	0.0080	382
42	anyvision-005	0.0000	241	0.0013	313	-	463	0.0000	171	0.0004	215	0.0004	233
43	armatura-001	0.0000	381	0.0021	359	0.0257	201	0.0005	387	0.0005	367	0.0357	434
44	armatura-003	0.0000	259	0.0012	307	0.0333	231	0.0004	368	0.0004	259	0.0008	299
45	asusaics-000	0.0000	102	0.0000	49	-	444	0.0000	17	0.0000	84	0.0000	51
46	asusaics-001	0.0000	127	0.0000	65	-	331	0.0000	95	0.0000	38	0.0000	63
47	autentika-000	0.0000	29	0.0000	30	0.0000	26	0.0000	56	0.0000	106	0.0000	19
48	authenmetric-003	0.0000	109	0.0000	70	0.0000	8	0.0000	103	0.0000	31	0.0000	60
49	authenmetric-004	0.0000	193	0.0000	103	0.0000	12	0.0000	89	0.0000	22	0.0000	101
50	aware-005	0.0000	340	0.0020	350	-	328	0.0001	296	0.0004	321	0.0011	310
51	aware-006	0.0000	298	0.0009	254	0.0249	192	0.0000	175	0.0004	275	0.0006	279
52	awiros-001	0.0039	456	0.0369	461	-	363	0.0386	471	0.0872	476	0.3415	470
53	awiros-002	0.0000	392	0.0038	403	-	360	0.0007	408	0.0012	439	0.0208	413
54	aximetria-001	0.0000	336	0.0010	287	0.0217	172	0.0001	295	0.0004	270	0.0024	340
55	ayftech-001	0.0002	439	0.0046	415	-	448	0.0043	459	0.0011	423	0.0091	387
56	ayonix-000	0.0053	460	0.0341	458	-	340	0.0113	468	0.0137	470	0.1194	461
57	beethedata-000	0.0005	446	0.0042	410	0.0366	239	0.0002	309	0.0010	418	0.0006	272
58	beyneai-000	0.0000	112	0.0000	68	0.0000	10	0.0000	100	0.0000	34	0.0000	56

Table 30: FTE is the proportion of failed template generation attempts. Failures can occur because the software throws an exception, or because the software electively refuses to process the input image. This would typically occur if a face is not detected. FTE is measured as the number of function calls that give EITHER a non-zero error code OR that give a “small” template. This is defined as one whose size is less than 0.3 times the median template size for that algorithm. This second rule is needed because some algorithms incorrectly fail to return a non-zero error code when template generation fails.

A hyphen “-” indicates the dataset was not produced.¹ The effects of FTE are included in the accuracy results of this report by regarding any template comparison involving a failed template to produce a low similarity score. Thus higher FTE results in higher FNMR and lower FMR.

	Algorithm	Failure to Enrol Rate ¹											
		APPLICATION	BORDER	KIOSK	MUGSHOT	VISA	WILD	SEC. 2.2	SEC. 2.4	SEC. 2.6	SEC. 2.5	SEC. 2.1	SEC. 2.7
59	biocube-001	0.0006	450	0.0391	462	0.1207	292	0.0015	434	0.0020	452	0.0253	424
60	biodtechswiss-001	0.0000	271	0.0007	199	-	313	0.0000	163	0.0004	306	0.0025	342
61	biodtechswiss-002	0.0000	250	0.0007	202	-	435	0.0000	165	0.0004	299	0.0005	269
62	bm-001	0.0000	134	0.0000	82	-	324	0.0000	124	0.0000	43	0.0000	67
63	boetech-001	0.0087	464	0.0272	452	0.2117	299	0.0032	455	0.0160	471	0.0946	452
64	boetech-002	0.0087	465	0.0272	453	0.2117	298	0.0032	456	0.0160	472	0.0946	453
65	bressee-001	0.0000	280	0.0010	282	-	372	0.0002	308	0.0003	167	0.0003	137
66	bressee-002	0.0000	371	0.0020	356	0.0219	174	0.0008	410	0.0004	251	0.0031	351
67	camvi-002	0.0000	26	0.0000	33	-	398	0.0000	59	0.0000	102	0.0000	20
68	camvi-004	0.0000	149	0.0000	116	-	312	0.0000	111	0.0000	54	0.0000	74
69	canon-003	0.0000	265	0.0008	218	0.0234	186	0.0000	198	0.0004	292	0.0003	182
70	canon-004	0.0000	296	0.0008	219	0.0234	187	0.0000	196	0.0004	288	0.0003	185
71	ceiec-003	0.0000	167	0.0013	320	-	359	0.0001	234	0.0004	302	0.0004	203
72	ceiec-004	0.0000	59	0.0008	233	-	475	0.0000	168	0.0004	226	0.0004	241
73	chosun-001	0.0000	15	0.0000	5	-	419	0.0000	37	0.0000	96	0.0000	14
74	chosun-002	0.0000	93	0.0000	53	-	453	0.0000	25	0.0000	79	0.0000	45
75	chtface-005	0.0000	108	0.0017	337	0.0320	222	0.0000	184	0.0004	311	0.0020	337
76	chtface-006	0.0000	125	0.0017	336	0.0320	221	0.0000	183	0.0004	312	0.0020	338
77	cist-001	0.0000	9	0.0005	170	0.0087	87	0.0000	38	0.0000	91	0.0000	1
78	clearviewai-000	0.0000	227	0.0003	133	0.0081	84	0.0000	186	0.0003	154	0.0003	136
79	closeli-001	0.0000	1	0.0000	13	0.0000	35	0.0000	42	0.0000	86	0.0001	120
80	cloudmatrix-001	0.0000	326	0.0028	373	0.0225	178	0.0001	223	0.0004	204	0.0004	225
81	cloudmatrix-002	0.0000	318	0.0028	372	0.0225	177	0.0001	225	0.0004	208	0.0004	224
82	cloudwalk-hr-003	0.0000	256	0.0008	238	-	338	0.0001	238	0.0004	213	0.0113	393
83	cloudwalk-hr-004	0.0000	210	0.0011	298	-	415	0.0004	366	0.0003	188	0.0129	397
84	cloudwalk-mt-005	0.0000	238	0.0005	162	0.0130	105	0.0003	341	0.0004	325	0.0004	214
85	cloudwalk-mt-006	0.0000	284	0.0006	178	0.0158	124	0.0002	321	0.0004	320	0.0004	211
86	codeline-000	0.0000	61	0.0000	46	0.0000	52	0.0000	11	0.0000	57	0.0000	29
87	cogent-007	0.0000	370	0.0000	112	0.0000	56	0.0000	172	0.0000	124	0.0001	117
88	cogent-008	0.0000	95	0.0010	288	0.0304	216	0.0000	187	0.0004	200	0.0003	153
89	cognitec-003	0.0001	416	0.0194	447	0.0820	287	0.0003	356	0.0005	364	0.0039	357
90	cognitec-004	0.0001	417	0.0037	402	0.0580	263	0.0003	355	0.0005	365	0.0035	352
91	cor-001	0.0000	231	0.0006	181	-	470	0.0002	335	0.0004	280	0.0004	255
92	coretech-000	0.0000	200	0.0000	101	0.0000	15	0.0000	81	0.0000	25	0.0000	94
93	coretech-001	0.0000	413	0.0033	390	0.0677	274	0.0005	392	0.0011	430	0.0027	345
94	corsight-002	0.0000	274	0.0005	173	0.0152	118	0.0001	270	0.0004	262	0.0003	183
95	corsight-003	0.0000	251	0.0006	188	0.0175	133	0.0001	260	0.0004	273	0.0003	188
96	csc-002	0.0015	455	0.0033	387	-	321	0.0006	403	0.0006	405	0.0968	455
97	csc-003	0.0015	454	0.0033	386	0.0445	258	0.0006	402	0.0006	406	0.0968	454
98	ctcbcbank-000	0.0001	420	0.0051	420	-	399	0.0011	426	0.0019	450	0.0868	448
99	ctcbcbank-001	0.0000	393	0.0036	401	-	370	0.0005	388	0.0010	417	0.0844	445
100	cu-face-002	0.0000	41	0.0000	21	0.0000	29	0.0000	52	0.0000	113	0.0000	15
101	cubox-001	0.0000	18	0.0000	4	-	422	0.0000	31	0.0000	98	0.0000	9
102	cubox-002	0.0000	320	0.0006	184	0.0159	126	0.0002	336	0.0005	385	0.0016	328
103	cudocommunication-001	0.0000	188	0.0000	105	0.0000	11	0.0000	87	0.0000	19	0.0000	107
104	cuhkee-001	0.0000	212	0.0011	297	-	417	0.0000	133	0.0004	266	0.1278	463
105	cybercore-002	0.0000	375	0.0001	122	0.0014	63	0.0002	302	0.0002	133	0.0018	333
106	cybercore-003	0.0000	313	0.0003	136	0.0060	72	0.0005	393	0.0003	156	0.0192	412
107	cyberextruder-003	0.0000	377	0.0077	432	0.0887	289	0.0001	291	0.0006	400	0.0009	305
108	cyberextruder-004	0.0000	372	0.0097	435	0.1025	291	0.0001	284	0.0007	407	0.0213	414
109	cyberlink-009	0.0000	177	0.0004	153	0.0106	93	0.0000	130	0.0003	168	0.0002	132
110	cyberlink-010	0.0000	36	0.0004	152	0.0106	94	0.0000	127	0.0003	169	0.0002	130
111	dahua-006	0.0000	172	0.0000	111	-	366	0.0000	190	0.0003	184	0.0000	89
112	dahua-007	0.0000	173	0.0000	110	0.0000	58	0.0000	191	0.0003	183	0.0000	88
113	daon-000	0.0000	398	0.0028	376	0.0577	262	0.0014	432	0.0015	443	0.0030	350
114	decatur-000	0.0000	335	0.0020	349	-	342	0.0004	376	0.0005	354	0.0236	418
115	decatur-001	0.0000	219	0.0009	263	0.0194	149	0.0001	241	0.0004	250	0.0004	244
116	deepglint-004	0.0000	289	0.0005	157	0.0130	104	0.0002	332	0.0004	218	0.0003	161

Table 31: FTE is the proportion of failed template generation attempts. Failures can occur because the software throws an exception, or because the software electively refuses to process the input image. This would typically occur if a face is not detected. FTE is measured as the number of function calls that give EITHER a non-zero error code OR that give a “small” template. This is defined as one whose size is less than 0.3 times the median template size for that algorithm. This second rule is needed because some algorithms incorrectly fail to return a non-zero error code when template generation fails.

A hyphen “-” indicates the dataset was not produced.¹ The effects of FTE are included in the accuracy results of this report by regarding any template comparison involving a failed template to produce a low similarity score. Thus higher FTE results in higher FNMR and lower FMR.

	Algorithm	Failure to Enrol Rate ¹											
		APPLICATION	BORDER	KIOSK	MUGSHOT	VISA	WILD						
	Name	SEC. 2.2	SEC. 2.4	SEC. 2.6	SEC. 2.5	SEC. 2.1	SEC. 2.7						
117	deepglint-005	0.0000	350	0.0019	344	0.0438	257	0.0006	399	0.0006	404	0.0028	349
118	deepsea-001	0.0000	37	0.0000	23	-	407	0.0000	55	0.0000	111	0.0000	16
119	deepsense-000	0.0000	54	0.0006	189	-	393	0.0000	152	0.0004	195	0.0003	163
120	deepsense-001	0.0000	196	0.0006	191	0.0191	147	0.0000	157	0.0004	197	0.0003	180
121	dermalog-010	0.0000	388	0.0031	383	0.0148	115	0.0006	397	0.0003	145	0.0002	121
122	dermalog-011	0.0000	408	0.0005	158	0.0116	98	0.0001	221	0.0003	151	0.0002	122
123	dicio-001	0.0005	449	0.0649	466	0.2136	300	0.0024	444	0.0012	434	0.0935	450
124	didiglobalface-001	0.0000	226	0.0012	300	-	388	0.0000	207	0.0004	318	0.0004	205
125	didiglobalface-002	0.0000	236	0.0012	301	0.0247	191	0.0000	205	0.0004	316	0.0004	206
126	digidata-000	0.0000	207	0.0023	363	0.0375	245	0.0004	380	0.0006	397	0.0006	274
127	digidata-001	0.0000	242	0.0023	365	0.0375	246	0.0004	379	0.0006	396	0.0006	276
128	digitalbarriers-002	0.0001	429	0.0045	413	-	423	0.0028	452	0.0027	458	0.0071	377
129	dps-000	0.0000	2	0.0000	14	0.0000	36	0.0000	41	0.0000	85	0.0000	4
130	dsk-000	0.0000	129	0.0000	63	-	333	0.0000	93	0.0000	40	0.0000	61
131	einetworks-000	0.0000	391	0.0017	338	-	441	0.0002	323	0.0005	377	0.0008	302
132	ekin-002	0.0000	124	0.0000	115	0.0004	61	0.0000	131	0.0000	123	0.0019	335
133	enface-000	0.0000	22	0.0012	310	0.0305	218	0.0000	179	0.0004	274	0.0004	227
134	enface-001	0.0000	135	0.0012	309	0.0304	217	0.0000	164	0.0004	261	0.0004	216
135	eocortex-000	0.0095	466	0.0602	465	-	430	0.0094	466	0.0059	466	0.1405	466
136	ercacat-001	0.0000	178	0.0005	166	-	354	0.0000	180	0.0003	171	0.0002	126
137	euronovate-001	0.0255	472	0.0102	437	0.0517	261	0.0021	441	0.0004	347	0.2451	468
138	expasoft-001	0.0000	175	0.0000	86	-	367	0.0000	66	0.0000	14	0.0000	84
139	expasoft-002	0.0000	143	0.0000	74	0.0000	1	0.0000	110	0.0000	48	0.0000	69
140	f8-001	0.0003	442	0.0059	425	-	454	0.0035	457	0.0030	463	0.0087	385
141	f8-002	0.0000	414	0.0150	445	0.0685	278	0.0005	382	0.0013	441	0.0883	449
142	faceonlive-001	0.0000	404	0.0029	380	0.0481	259	0.0013	430	0.0011	424	0.0160	403
143	faceonlive-002	0.0002	437	0.0009	266	0.0075	78	0.0008	413	0.0008	414	0.0083	383
144	facephi-000	0.0000	100	0.0004	140	0.0090	88	0.0001	268	0.0004	207	0.0003	165
145	facesoft-000	0.0000	73	0.0000	39	-	459	0.0000	9	0.0000	64	0.0000	39
146	facetag-000	0.0000	97	0.0000	51	0.0000	42	0.0000	19	0.0000	81	0.0000	52
147	facetag-002	0.0000	122	0.0000	66	0.0000	6	0.0000	94	0.0000	37	0.0000	62
148	facex-001	0.0001	436	0.0360	459	-	418	0.0047	461	0.0027	460	0.1109	459
149	facex-002	0.0001	435	0.0360	460	0.2663	303	0.0047	462	0.0027	459	0.1109	458
150	farfaces-001	0.0000	389	0.0007	201	0.0061	73	0.0003	352	0.0003	161	0.0006	284
151	fiberhome-nanjing-003	0.0000	32	0.0004	145	-	403	0.0000	64	0.0003	149	0.0001	112
152	fiberhome-nanjing-004	0.0000	103	0.0004	146	-	443	0.0000	16	0.0003	148	0.0001	113
153	fincore-000	0.0000	309	0.0008	240	0.0185	141	0.0001	216	0.0004	304	0.0006	277
154	firstcreditKZ-001	0.0000	353	0.0019	346	0.0321	225	0.0000	201	0.0004	265	0.0007	285
155	frpkauai-001	0.0000	345	0.0024	368	0.0360	237	0.0001	224	0.0004	332	0.0007	294
156	frpkauai-002	0.0000	356	0.0019	348	0.0321	224	0.0000	202	0.0004	256	0.0007	287
157	fujitsulab-002	0.0000	81	0.0009	250	-	449	0.0001	277	0.0003	147	0.0003	144
158	fujitsulab-003	0.0000	105	0.0008	224	0.0166	130	0.0001	266	0.0001	128	0.0003	139
159	g42-intellibrain-001	0.0000	106	0.0000	71	0.0000	7	0.0000	101	0.0000	30	0.0000	57
160	geo-002	0.0000	285	0.0015	326	0.0332	229	0.0001	214	0.0004	333	0.0017	332
161	geo-004	0.0000	268	0.0005	172	0.0138	109	0.0001	254	0.0004	240	0.0009	306
162	glory-004	0.0000	330	0.0020	355	0.0345	232	0.0001	273	0.0004	329	0.0167	405
163	glory-005	0.0000	327	0.0020	354	0.0345	233	0.0001	272	0.0004	328	0.0167	404
164	gorilla-008	0.0000	240	0.0009	269	0.0259	202	0.0001	239	0.0004	308	0.0004	218
165	gorilla-009	0.0000	304	0.0010	277	0.0276	210	0.0001	228	0.0004	290	0.0004	212
166	graymatics-001	0.0000	203	0.0010	270	0.0210	162	0.0001	289	0.0004	243	0.0006	281
167	griaule-001	0.0000	72	0.0012	311	0.0366	240	0.0000	149	0.0004	298	0.0005	263
168	griaule-002	0.0000	142	0.0007	206	0.0209	160	0.0000	200	0.0004	252	0.0004	200
169	hertasecurity-001	0.0000	123	0.0000	118	0.0000	59	0.0000	142	0.0001	125	0.0002	131
170	hertasecurity-002	0.0000	159	0.0000	94	0.0000	22	0.0000	139	0.0000	120	0.0000	77
171	hik-001	0.0000	148	0.0000	119	-	315	0.0000	112	0.0000	53	0.0000	75
172	hisign-001	0.0000	199	0.0000	100	0.0000	14	0.0000	82	0.0000	26	0.0000	95
173	hisign-002	0.0000	319	0.0006	185	0.0150	116	0.0001	275	0.0003	181	0.0005	266
174	hyperverge-003	0.0000	14	0.0008	222	0.0210	163	0.0002	337	0.0004	249	0.0004	243

Table 32: FTE is the proportion of failed template generation attempts. Failures can occur because the software throws an exception, or because the software electively refuses to process the input image. This would typically occur if a face is not detected. FTE is measured as the number of function calls that give EITHER a non-zero error code OR that give a “small” template. This is defined as one whose size is less than 0.3 times the median template size for that algorithm. This second rule is needed because some algorithms incorrectly fail to return a non-zero error code when template generation fails.

A hyphen “-” indicates the dataset was not produced.¹ The effects of FTE are included in the accuracy results of this report by regarding any template comparison involving a failed template to produce a low similarity score. Thus higher FTE results in higher FNMR and lower FMR.

	Algorithm	Failure to Enrol Rate ¹											
		APPLICATION	BORDER	KIOSK	MUGSHOT	VISA	WILD	SEC. 2.2	SEC. 2.4	SEC. 2.6	SEC. 2.5	SEC. 2.1	SEC. 2.7
175	hyperverge-004	0.0000	230	0.0008	237	0.0218	173	0.0002	325	0.0004	263	0.0004	230
176	hzailiu-002	0.0000	380	0.0015	329	0.0424	253	0.0003	357	0.0005	380	0.0075	379
177	hzailiu-003	0.0000	292	0.0004	141	0.0081	85	0.0002	303	0.0003	173	0.0003	158
178	icm-003	0.0000	68	0.0001	121	0.0023	64	0.0000	8	0.0000	119	0.0000	109
179	icm-004	0.0000	399	0.0033	392	0.0698	279	0.0006	401	0.0010	422	0.0026	344
180	icthtc-000	0.0001	434	0.0047	418	-	389	0.0028	453	0.0029	461	0.0086	384
181	id3-006	0.0000	348	0.0009	268	-	382	0.0004	370	0.0005	375	0.0008	300
182	id3-008	0.0000	44	0.0006	187	0.0184	138	0.0001	288	0.0004	202	0.0003	138
183	idemia-008	0.0000	204	0.0004	154	0.0078	82	0.0000	140	0.0003	174	0.0003	154
184	idemia-009	0.0000	128	0.0004	150	0.0077	80	0.0000	143	0.0003	175	0.0003	157
185	iit-002	0.0000	396	0.0021	358	-	433	0.0009	422	0.0005	388	0.0443	435
186	iit-003	0.0000	315	0.0008	239	-	353	0.0000	170	0.0004	203	0.0069	376
187	imds-software-001	0.0000	62	0.0000	44	0.0000	54	0.0000	14	0.0000	58	0.0000	30
188	imperial-000	0.0000	28	0.0000	29	-	395	0.0000	57	0.0000	104	0.0000	17
189	imperial-002	0.0000	77	0.0000	34	-	468	0.0000	3	0.0000	68	0.0000	35
190	incode-010	0.0000	342	0.0009	256	0.0255	200	0.0002	311	0.0004	232	0.0007	295
191	incode-011	0.0000	343	0.0009	255	0.0255	199	0.0002	310	0.0004	233	0.0007	296
192	infocert-001	0.0000	364	0.0059	426	0.0424	254	0.0001	246	0.0006	392	0.0018	334
193	innefulabs-000	0.0000	294	0.0024	367	-	361	0.0003	353	0.0005	371	0.0004	226
194	innovativetechnologyltd-001	0.0001	433	0.0050	419	-	425	0.0024	447	0.0025	457	0.0055	369
195	innovativetechnologyltd-002	0.0000	352	0.0046	414	-	450	0.0057	465	0.0005	373	0.0247	423
196	innovatrics-008	0.0000	234	0.0009	261	0.0204	155	0.0000	177	0.0004	193	0.0003	186
197	innovatrics-009	0.0000	152	0.0005	156	0.0142	112	0.0000	78	0.0000	122	0.0000	110
198	insightface-001	0.0000	25	0.0000	32	0.0000	27	0.0000	60	0.0000	103	0.0000	21
199	insightface-003	0.0000	205	0.0000	99	0.0000	17	0.0000	84	0.0000	28	0.0000	98
200	inspur-000	0.0000	183	0.0000	109	0.0000	18	0.0000	91	0.0000	17	0.0000	91
201	intellicloudai-001	0.0000	133	0.0000	83	-	325	0.0000	118	0.0000	42	0.0001	118
202	intellicloudai-002	0.0000	3	0.0008	229	-	428	0.0000	169	0.0004	201	0.0012	319
203	intellifusion-001	0.0000	244	0.0005	168	-	447	0.0001	235	0.0003	180	0.0005	265
204	intellifusion-002	0.0000	166	0.0000	117	-	358	0.0000	123	0.0000	10	0.0001	119
205	intellivision-003	0.0000	293	0.0012	306	0.0308	220	0.0003	347	0.0004	348	0.0185	410
206	intellivision-004	0.0000	297	0.0011	292	0.0266	207	0.0002	338	0.0004	343	0.0179	408
207	intellivix-002	0.0000	113	0.0009	267	0.0184	139	0.0000	99	0.0000	33	0.0000	55
208	intellivix-003	0.0000	21	0.0000	1	0.0000	33	0.0000	34	0.0000	100	0.0000	11
209	intelresearch-005	0.0000	248	0.0006	180	0.0144	113	0.0000	155	0.0004	229	0.0003	164
210	intelresearch-006	0.0000	153	0.0000	114	0.0004	62	0.0000	128	0.0004	217	0.0003	184
211	intemta-000	0.0000	52	0.0005	160	0.0126	101	0.0000	189	0.0004	210	0.0003	152
212	intemta-001	0.0000	217	0.0004	149	0.0106	95	0.0000	126	0.0003	189	0.0003	173
213	intsysmsu-001	0.0000	31	0.0010	279	-	402	0.0001	258	0.0004	283	0.0004	236
214	intsysmsu-002	0.0000	39	0.0010	278	-	409	0.0001	257	0.0004	284	0.0004	235
215	ionetworks-000	0.0000	150	0.0016	334	0.0387	248	0.0004	361	0.0005	362	0.0004	246
216	iqface-000	0.0000	141	0.0000	75	-	308	0.0000	108	0.0000	47	0.0000	70
217	iqface-003	0.0000	394	0.0076	431	-	442	0.0006	396	0.0005	389	0.0069	375
218	irex-000	0.0000	360	0.0009	265	-	439	0.0000	185	0.0005	356	0.0003	181
219	isap-001	0.0000	71	0.0000	40	-	460	0.0000	10	0.0000	63	0.0000	40
220	isap-002	0.0000	163	0.0000	89	-	379	0.0000	75	0.0000	7	0.0000	79
221	isityou-000	0.0068	463	0.0316	456	-	469	0.0023	443	0.0010	420	0.0663	442
222	isystems-001	0.0000	403	0.0035	398	-	462	0.0010	423	0.0007	408	0.0128	396
223	isystems-002	0.0000	402	0.0035	397	-	411	0.0010	424	0.0007	409	0.0128	395
224	itm0-007	0.0000	179	0.0009	249	-	355	0.0003	359	0.0000	16	0.0004	217
225	itm0-008	0.0000	194	0.0135	442	0.1239	293	0.0024	448	0.0000	23	0.0836	444
226	ivacognitive-001	0.0000	323	0.0011	294	-	396	0.0001	226	0.0004	335	0.0011	311
227	iws-000	0.0005	448	0.0650	469	-	394	0.0024	445	0.0012	435	0.0936	451
228	jaakit-001	0.0008	453	0.0858	470	0.2713	304	0.0042	458	0.0021	453	0.1062	456
229	kakao-007	0.0000	58	0.0007	192	0.0165	129	0.0001	248	0.0004	225	0.0097	390
230	kakao-008	0.0000	190	0.0009	252	0.0209	161	0.0001	250	0.0004	220	0.0097	391
231	kakaopay-001	0.0000	321	0.0013	318	0.0322	226	0.0001	232	0.0004	337	0.0078	381
232	kasikornlabs-000	0.0000	409	0.0035	396	0.0713	282	0.0004	377	0.0012	438	0.0270	427

Table 33: FTE is the proportion of failed template generation attempts. Failures can occur because the software throws an exception, or because the software electively refuses to process the input image. This would typically occur if a face is not detected. FTE is measured as the number of function calls that give EITHER a non-zero error code OR that give a “small” template. This is defined as one whose size is less than 0.3 times the median template size for that algorithm. This second rule is needed because some algorithms incorrectly fail to return a non-zero error code when template generation fails.

A hyphen “-” indicates the dataset was not produced.¹ The effects of FTE are included in the accuracy results of this report by regarding any template comparison involving a failed template to produce a low similarity score. Thus higher FTE results in higher FNMR and lower FMR.

	Algorithm	Failure to Enrol Rate ¹											
		APPLICATION	BORDER	KIOSK	MUGSHOT	VISA	WILD	SEC. 2.2	SEC. 2.4	SEC. 2.6	SEC. 2.5	SEC. 2.1	SEC. 2.7
233	kasikornlabs-002	0.0000	407	0.0033	388	0.0698	280	0.0004	373	0.0012	432	0.0269	426
234	kedacom-000	0.0000	30	0.0000	27	-	401	0.0000	65	0.0000	107	0.0000	24
235	kiwitech-000	0.0000	275	0.0009	247	-	316	0.0004	375	0.0005	360	0.0004	248
236	kneron-003	0.0239	470	0.0306	454	-	413	0.0044	460	0.0016	447	0.1823	467
237	kneron-005	0.0000	405	0.0226	448	-	334	0.0006	395	0.0005	368	0.0097	389
238	knowutech-000	0.0000	305	0.0008	221	0.0215	170	0.0000	174	0.0004	291	0.0003	193
239	kokmin-002	0.0000	174	0.0000	87	-	362	0.0000	68	0.0000	13	0.0000	86
240	koreaid-001	0.0000	195	0.0023	366	0.0371	243	0.0000	197	0.0005	353	0.0027	346
241	krungthai-002	0.0000	208	0.0005	163	0.0111	97	0.0002	324	0.0003	187	0.0005	256
242	kuke3d-001	0.0000	10	0.0000	7	0.0000	40	0.0000	40	0.0000	93	0.0000	3
243	kuke3d-002	0.0000	17	0.0000	3	0.0000	32	0.0000	32	0.0000	97	0.0000	8
244	lebentech-000	0.0042	457	0.0029	382	0.0252	196	0.0051	464	0.0066	467	0.0154	402
245	lemalabs-001	0.0000	84	0.0005	171	0.0141	110	0.0002	320	0.0004	206	0.0004	208
246	lineclova-002	0.0000	158	0.0007	193	0.0181	136	0.0000	73	0.0000	4	0.0000	106
247	lineclova-003	0.0000	384	0.0023	362	0.0700	281	0.0002	339	0.0005	355	0.0038	354
248	lookman-002	0.0000	91	0.0000	55	-	456	0.0000	26	0.0000	78	0.0000	47
249	lookman-004	0.0000	186	0.0000	106	-	347	0.0000	88	0.0000	18	0.0000	100
250	luxand-000	0.0000	156	0.0000	95	-	374	0.0000	80	0.0000	3	0.0000	83
251	mantra-000	0.0001	418	0.0041	409	0.0680	277	0.0003	351	0.0004	346	0.0037	353
252	maxvision-002	0.0000	245	0.0009	245	0.0229	182	0.0002	299	0.0004	264	0.0004	252
253	maxvision-003	0.0000	223	0.0009	244	0.0229	181	0.0002	300	0.0004	267	0.0004	251
254	megvii-005	0.0000	263	0.0010	271	0.0206	158	0.0002	330	0.0004	313	0.0011	312
255	megvii-006	0.0000	270	0.0010	272	0.0206	157	0.0002	331	0.0004	314	0.0011	313
256	meituan-001	0.0000	262	0.0014	322	0.0295	213	0.0001	262	0.0004	297	0.0013	324
257	meituan-002	0.0000	214	0.0013	317	0.0251	195	0.0001	261	0.0004	296	0.0020	336
258	meiya-001	0.0000	400	0.0028	377	-	464	0.0004	378	0.0010	421	0.0025	341
259	mendaxiatech-000	0.0000	308	0.0010	273	0.0206	156	0.0002	333	0.0004	310	0.0011	315
260	metsakuurcompany-001	0.0000	110	0.0011	290	0.0208	159	0.0002	329	0.0004	224	0.0003	177
261	metsakuurcompany-002	0.0000	145	0.0000	77	0.0000	2	0.0000	107	0.0000	50	0.0000	72
262	maxis-001	0.0000	303	0.0013	314	0.0262	205	0.0001	290	0.0003	155	0.0003	191
263	microfocus-001	0.0001	432	0.0053	423	-	368	0.0008	414	0.0016	445	0.0220	416
264	microfocus-002	0.0001	431	0.0053	422	-	317	0.0008	415	0.0016	446	0.0220	415
265	minivision-000	0.0000	34	0.0000	25	-	400	0.0000	63	0.0000	109	0.0000	23
266	mobai-000	0.0000	367	0.0114	439	-	412	0.0003	354	0.0012	437	0.1242	462
267	mobai-001	0.0000	333	0.0040	405	-	436	0.0001	269	0.0012	436	0.0523	439
268	mobbl-001	0.0000	395	0.0052	421	0.0678	275	0.0002	306	0.0005	378	0.0181	409
269	mobbl-003	0.0000	406	0.0029	381	0.0633	268	0.0002	326	0.0009	416	0.0026	343
270	mobipintech-000	0.0000	5	0.0000	11	0.0000	39	0.0000	46	0.0000	87	0.0000	7
271	moreedian-000	0.0000	288	0.0009	248	-	377	0.0004	374	0.0005	359	0.0004	249
272	mukh-001	0.0000	66	0.0010	280	0.0154	121	0.0001	265	0.0003	141	0.0010	307
273	mukh-002	0.0000	64	0.0022	361	0.0513	260	0.0002	304	0.0004	254	0.0016	330
274	multimodality-000	0.0000	87	0.0000	58	0.0000	47	0.0000	24	0.0000	73	0.0000	42
275	multimodality-001	0.0000	13	0.0009	243	0.0259	203	0.0000	35	0.0000	95	0.0000	12
276	mvision-001	0.0000	157	0.0000	96	-	375	0.0000	79	0.0000	2	0.0000	82
277	nazhiai-000	0.0000	57	0.0000	47	-	473	0.0000	15	0.0000	56	0.0000	32
278	neosystems-004	0.0000	201	0.0000	98	0.0000	16	0.0000	85	0.0000	27	0.0000	97
279	netbridgeotech-001	0.0000	146	0.0000	78	-	310	0.0000	106	0.0000	51	0.0000	73
280	netbridgeotech-002	0.0000	89	0.0000	56	-	451	0.0000	21	0.0000	76	0.0000	41
281	neurotechnology-013	0.0000	83	0.0008	241	0.0185	140	0.0000	132	0.0001	126	0.0004	222
282	neurotechnology-015	0.0000	130	0.0004	142	0.0082	86	0.0000	117	0.0000	121	0.0003	140
283	nhn-002	0.0000	33	0.0004	155	0.0091	89	0.0000	167	0.0003	153	0.0003	141
284	nhn-003	0.0000	346	0.0000	22	0.0000	30	0.0001	294	0.0004	300	0.0010	308
285	nodeflux-002	0.0000	312	0.0261	451	-	351	0.0008	412	0.0005	372	0.0008	303
286	notiontag-001	0.0000	99	0.0000	50	-	438	0.0027	451	0.0000	82	0.0132	399
287	notiontag-002	0.0000	46	0.0000	18	0.0000	24	0.0000	51	0.0000	115	0.0000	28
288	nsensecorp-003	0.0000	42	0.0000	120	0.0002	60	0.0000	156	0.0007	411	0.0150	400
289	nsensecorp-004	0.0406	473	0.0035	395	0.0181	135	0.0016	436	0.0760	475	0.0509	438
290	ntechlab-011	0.0000	107	0.0003	126	0.0057	70	0.0000	194	0.0004	191	0.0003	168

Table 34: FTE is the proportion of failed template generation attempts. Failures can occur because the software throws an exception, or because the software electively refuses to process the input image. This would typically occur if a face is not detected. FTE is measured as the number of function calls that give EITHER a non-zero error code OR that give a “small” template. This is defined as one whose size is less than 0.3 times the median template size for that algorithm. This second rule is needed because some algorithms incorrectly fail to return a non-zero error code when template generation fails.

A hyphen “-” indicates the dataset was not produced.¹ The effects of FTE are included in the accuracy results of this report by regarding any template comparison involving a failed template to produce a low similarity score. Thus higher FTE results in higher FNMR and lower FMR.

	Algorithm	Failure to Enrol Rate ¹										
		Name	APPLICATION		BORDER		KIOSK		MUGSHOT		VISA	WILD
			SEC. 2.2	SEC. 2.4	SEC. 2.6	SEC. 2.5	SEC. 2.1	SEC. 2.7				
291	ntechlab-012	0.0000	137	0.0003	127	0.0057	69	0.0000	195	0.0004	192	0.0003 170
292	omface-000	0.0000	161	0.0000	93	0.0000	21	0.0000	71	0.0000	6	0.1160 460
293	omface-001	0.0000	114	0.0000	113	0.0000	57	0.0000	98	0.0000	35	0.0000 105
294	omnigarde-001	0.0000	279	0.0008	216	0.0213	164	0.0000	162	0.0004	278	0.0003 190
295	omnigarde-002	0.0000	243	0.0008	215	0.0213	165	0.0000	159	0.0004	281	0.0003 187
296	onfido-000	0.0000	401	0.0040	404	0.0804	286	0.0004	363	0.0012	433	0.0052 368
297	openface-001	0.0000	378	0.0104	438	0.0668	270	0.0004	369	0.0006	403	0.0856 447
298	oz-003	0.0000	92	0.0002	124	0.0042	66	0.0000	125	0.0003	140	0.0002 124
299	oz-004	0.0000	383	0.0003	131	0.0041	65	0.0000	134	0.0002	130	0.0006 273
300	palit-000	0.0000	235	0.0005	164	0.0134	108	0.0002	313	0.0004	228	0.0004 237
301	palit-001	0.0000	291	0.0007	214	0.0201	153	0.0002	314	0.0004	219	0.0004 238
302	pangiam-000	0.0000	67	0.0021	360	0.0364	238	0.0001	212	0.0005	358	0.0095 388
303	papago-001	0.0000	325	0.0008	223	0.0159	127	0.0002	340	0.0004	253	0.0190 411
304	papsav1923-002	0.0000	269	0.0018	343	0.0268	208	0.0000	181	0.0004	293	0.0004 223
305	papsav1923-003	0.0000	354	0.0019	347	0.0321	223	0.0000	204	0.0004	258	0.0007 286
306	paravision-010	0.0000	202	0.0010	276	0.0201	152	0.0001	245	0.0004	198	0.0003 194
307	paravision-011	0.0000	120	0.0010	275	0.0201	151	0.0001	247	0.0004	199	0.0003 189
308	pensees-001	0.0000	249	0.0000	52	-	437	0.0000	20	0.0000	80	0.0000 53
309	pixelall-008	0.0000	171	0.0008	231	0.0247	190	0.0000	69	0.0000	12	0.0000 90
310	pixelall-009	0.0000	7	0.0000	9	0.0000	37	0.0000	44	0.0000	89	0.0000 5
311	psl-010	0.0000	215	0.0004	144	0.0095	90	0.0000	120	0.0004	194	0.0003 155
312	psl-011	0.0000	246	0.0003	128	0.0063	75	0.0000	119	0.0003	176	0.0003 150
313	ptakuratsatu-000	0.0000	220	0.0007	212	-	404	0.0001	213	0.0003	163	0.0003 156
314	pxl-001	0.0000	415	0.0044	412	-	465	0.0005	386	0.0022	455	0.0323 430
315	pyramid-000	0.0001	428	0.0041	408	-	350	0.0005	385	0.0007	410	0.0015 327
316	qazbs-000	0.0000	96	0.0009	253	0.0265	206	0.0000	151	0.0004	248	0.0003 196
317	qluevision-001	0.0000	358	0.0008	226	0.0153	119	0.0008	411	0.0004	352	0.0041 358
318	qnap-002	0.0000	397	0.0033	385	0.0761	284	0.0004	365	0.0002	129	0.0017 331
319	qnap-003	0.0000	155	0.0016	332	0.0402	251	0.0000	199	0.0001	127	0.0003 142
320	quantasoft-003	0.0000	368	0.0015	330	0.0355	235	0.0005	384	0.0006	399	0.0088 386
321	rankone-013	0.0000	198	0.0005	161	0.0126	102	0.0000	145	0.0003	144	0.0003 145
322	rankone-014	0.0000	180	0.0005	159	0.0129	103	0.0000	147	0.0002	131	0.0002 134
323	realnetworks-007	0.0000	316	0.0013	319	0.0425	255	0.0000	129	0.0004	257	0.0004 242
324	realnetworks-008	0.0000	228	0.0002	125	0.0045	67	0.0000	122	0.0002	139	0.0003 149
325	regula-000	0.0000	12	0.0000	6	0.0000	31	0.0000	36	0.0000	94	0.0000 13
326	regula-001	0.0000	11	0.0000	8	0.0000	41	0.0000	39	0.0000	92	0.0000 2
327	remarkai-001	0.0000	50	0.0000	16	-	392	0.0000	48	0.0000	117	0.0000 111
328	remarkai-003	0.0000	239	0.0007	200	0.0187	142	0.0000	182	0.0004	214	0.0004 228
329	rendip-000	0.0000	355	0.0016	333	0.0293	212	0.0002	312	0.0004	344	0.0013 325
330	revealmedia-005	0.0000	362	0.0007	207	0.0189	144	0.0009	421	0.0004	351	0.0076 380
331	revealmedia-006	0.0000	118	0.0009	262	0.0238	188	0.0001	263	0.0004	305	0.0004 253
332	rokid-000	0.0000	47	0.0072	429	-	384	0.0001	249	0.0005	370	0.0354 433
333	rokid-001	0.0000	151	0.0013	316	-	319	0.0000	104	0.0000	55	0.0007 292
334	s1-005	0.0000	121	0.0004	147	0.0120	100	0.0001	229	0.0002	132	0.0050 366
335	s1-006	0.0000	182	0.0003	129	0.0074	77	0.0001	222	0.0002	134	0.0050 367
336	saffe-001	0.0000	51	0.0000	15	-	390	0.0000	47	0.0000	118	0.0000 25
337	saffe-002	0.0000	49	0.0000	17	-	386	0.0000	50	0.0000	116	0.0000 27
338	samsungsds-001	0.0000	20	0.0005	167	0.0146	114	0.0001	244	0.0003	182	0.0003 195
339	samsungsds-002	0.0000	94	0.0004	148	0.0119	99	0.0001	243	0.0003	172	0.0003 167
340	samtech-001	0.0001	427	0.0032	384	-	432	0.0004	372	0.0008	412	0.0013 322
341	scanovate-002	0.0000	339	0.0018	342	-	323	0.0000	209	0.0004	340	0.0008 301
342	scanovate-003	0.0000	334	0.0233	449	0.3371	306	0.0006	398	0.0004	350	0.0007 293
343	sdc-000	0.0000	412	0.0035	394	0.0678	276	0.0005	391	0.0011	427	0.0028 348
344	securifai-005	0.0000	139	0.0000	80	0.0000	5	0.0000	115	0.0000	45	0.0000 65
345	securifai-006	0.0000	70	0.0000	42	0.0000	49	0.0000	6	0.0000	62	0.0000 38
346	sensetime-007	0.0000	19	0.0004	143	0.0106	92	0.0000	166	0.0003	162	0.0002 129
347	sensetime-008	0.0000	4	0.0007	211	0.0250	193	0.0000	121	0.0003	186	0.0003 135
348	sertis-000	0.0000	56	0.0007	205	-	471	0.0000	210	0.0004	241	0.0004 213

Table 35: FTE is the proportion of failed template generation attempts. Failures can occur because the software throws an exception, or because the software electively refuses to process the input image. This would typically occur if a face is not detected. FTE is measured as the number of function calls that give EITHER a non-zero error code OR that give a “small” template. This is defined as one whose size is less than 0.3 times the median template size for that algorithm. This second rule is needed because some algorithms incorrectly fail to return a non-zero error code when template generation fails.

A hyphen “-” indicates the dataset was not produced.¹ The effects of FTE are included in the accuracy results of this report by regarding any template comparison involving a failed template to produce a low similarity score. Thus higher FTE results in higher FNMR and lower FMR.

	Algorithm	Failure to Enrol Rate ¹											
		Name	APPLICATION		BORDER		KIOSK		MUGSHOT		VISA		
			SEC. 2.2	SEC. 2.4	SEC. 2.6	SEC. 2.5	SEC. 2.1	SEC. 2.7					
349	sertis-002	0.0000	115	0.0007	196	0.0152	117	0.0000	203	0.0004	237	0.0004	209
350	seventhsense-001	0.0000	254	0.0006	190	0.0184	137	0.0001	217	0.0004	276	0.0003	169
351	seventhsense-002	0.0000	192	0.0003	139	0.0076	79	0.0000	211	0.0004	190	0.0003	151
352	shaman-000	0.0000	154	0.0000	97	-	371	0.0000	77	0.0000	1	0.0000	81
353	shaman-001	0.0000	38	0.0000	24	-	410	0.0000	54	0.0000	110	0.0000	103
354	shu-002	0.0000	332	0.0010	283	-	457	0.0005	383	0.0004	330	0.0007	290
355	shu-003	0.0000	170	0.0007	195	-	365	0.0001	219	0.0003	157	0.0004	250
356	siat-002	0.0000	282	0.0012	308	-	373	0.0000	178	0.0004	255	0.0048	364
357	siat-005	0.0000	74	0.0000	38	0.0000	55	0.0000	1	0.0000	65	0.0000	33
358	sjtu-003	0.0000	16	0.0005	174	-	420	0.0000	188	0.0003	152	0.0003	166
359	sjtu-004	0.0000	184	0.0000	108	0.0000	19	0.0000	92	0.0003	150	0.0000	93
360	sktelecom-000	0.0000	286	0.0008	232	0.0190	145	0.0000	192	0.0004	286	0.0013	323
361	smartbiometrik-001	0.0005	445	0.0649	467	0.2147	302	0.0017	437	0.0008	413	0.0123	394
362	smartengines-000	0.0066	462	0.0150	444	0.1656	295	0.0022	442	0.0013	440	0.0826	443
363	smartengines-001	0.0003	441	0.0073	430	0.0714	283	0.0007	405	0.0005	374	0.0169	406
364	smartvist-000	0.0000	55	0.0026	371	0.0357	236	0.0002	298	0.0011	429	0.0152	401
365	smilart-002	0.0000	410	0.0036	399	-	376	-	473	0.0011	426	-	473
366	smilart-003	0.0003	440	0.0100	436	-	426	0.0014	431	0.0013	442	0.0555	440
367	sodec-000	0.0000	8	0.0000	10	0.0000	38	0.0000	43	0.0000	90	0.0000	6
368	sqisoft-002	0.0000	181	0.0003	135	0.0078	81	0.0000	146	0.0003	185	0.0003	148
369	sqisoft-003	0.0000	132	0.0003	137	0.0078	83	0.0000	148	0.0003	166	0.0003	147
370	staqu-000	0.0000	147	0.0000	73	-	307	0.0000	105	0.0000	52	0.0000	68
371	starhybrid-001	0.0001	430	0.0033	391	-	332	0.0009	420	0.0023	456	0.0044	359
372	stcon-000	0.0000	287	0.0017	341	0.0301	215	0.0000	161	0.0003	170	0.0002	133
373	sukshi-000	0.0000	27	0.0000	28	0.0000	25	0.0000	58	0.0000	105	0.0000	18
374	suprema-003	0.0000	301	0.0008	234	0.0231	184	0.0000	141	0.0004	235	0.0003	178
375	suprema-004	0.0000	260	0.0014	321	0.0299	214	0.0000	144	0.0004	238	0.0003	175
376	supremaid-001	0.0000	225	0.0020	351	0.0330	228	0.0001	256	0.0004	342	0.0045	361
377	supremaid-002	0.0000	307	0.0020	353	0.0330	227	0.0001	259	0.0004	339	0.0045	362
378	surrey-cvssp-000	0.0000	101	0.0000	48	0.0000	43	0.0000	18	0.0000	83	0.0000	50
379	surrey-cvssp-001	0.0173	469	0.0007	197	0.0179	134	0.0011	427	0.0015	444	0.0038	356
380	synesis-006	0.0000	185	0.0003	138	-	346	0.0000	193	0.0003	143	0.0002	128
381	synesis-007	0.0000	261	0.0013	315	-	343	0.0002	328	0.0004	260	0.0005	258
382	synology-000	0.0000	176	0.0000	85	-	369	0.0000	67	0.0000	15	0.0000	85
383	synology-002	0.0000	144	0.0000	76	-	309	0.0000	109	0.0000	49	0.0000	71
384	sztu-000	0.0000	90	0.0000	54	-	455	0.0000	27	0.0000	77	0.0000	46
385	sztu-001	0.0000	79	0.0000	36	0.0000	50	0.0000	2	0.0000	69	0.0000	36
386	t4isb-000	0.0000	140	0.0000	79	0.0000	4	0.0000	114	0.0000	46	0.0000	64
387	tech5-005	0.0000	221	0.0007	213	-	408	0.0000	160	0.0004	309	0.0049	365
388	tech5-007	0.0000	222	0.0014	324	0.0305	219	0.0000	153	0.0004	231	0.0004	254
389	techsign-000	0.0007	451	0.0334	457	0.2093	297	0.0020	440	0.0011	425	0.0170	407
390	techsign-001	0.0000	295	0.0008	242	0.0253	197	0.0002	316	0.0004	268	0.0004	232
391	tevian-007	0.0000	253	0.0015	331	0.0429	256	0.0002	322	0.0004	295	0.0008	298
392	tevian-008	0.0000	264	0.0006	177	0.0109	96	0.0000	158	0.0003	159	0.0004	234
393	tiger-005	0.0000	237	0.0009	264	0.0194	150	0.0001	240	0.0004	246	0.0004	245
394	tiger-006	0.0000	344	0.0011	296	0.0396	249	0.0001	287	0.0004	349	0.0009	304
395	tinkoff-001	0.0000	331	0.0008	230	0.0171	131	0.0001	278	0.0004	247	0.0014	326
396	tongyi-005	0.0000	169	0.0000	88	-	364	0.0000	70	0.0000	11	0.0000	87
397	toppanidgate-000	0.0000	252	0.0008	227	0.0232	185	0.0004	362	0.0004	282	0.0005	270
398	toshiba-004	0.0000	80	0.0000	62	0.0000	44	0.0000	29	0.0000	70	0.0000	48
399	toshiba-006	0.0000	317	0.0004	151	0.0050	68	0.0001	282	0.0003	158	0.0003	146
400	touchlessid-000	0.0042	458	0.0133	441	0.2009	296	0.0018	439	0.0032	464	0.0457	436
401	touchlessid-001	0.0000	189	0.0036	400	0.0923	290	0.0000	86	0.0000	20	0.0000	99
402	trueface-002	0.0000	337	0.0046	417	-	329	0.0003	343	0.0005	383	0.0330	432
403	trueface-003	0.0000	328	0.0046	416	0.0397	250	0.0003	342	0.0005	384	0.0330	431
404	trueidvng-001	0.0000	322	0.0020	357	0.0385	247	0.0002	318	0.0005	369	0.0241	419
405	tuputech-000	0.0003	443	0.0116	440	-	427	-	472	0.0081	469	0.6383	471
406	turingtechvip-001	0.0001	422	0.0007	209	0.0061	74	0.0007	404	0.0006	394	0.0057	370

Table 36: FTE is the proportion of failed template generation attempts. Failures can occur because the software throws an exception, or because the software electively refuses to process the input image. This would typically occur if a face is not detected. FTE is measured as the number of function calls that give EITHER a non-zero error code OR that give a “small” template. This is defined as one whose size is less than 0.3 times the median template size for that algorithm. This second rule is needed because some algorithms incorrectly fail to return a non-zero error code when template generation fails.

A hyphen “-” indicates the dataset was not produced.¹ The effects of FTE are included in the accuracy results of this report by regarding any template comparison involving a failed template to produce a low similarity score. Thus higher FTE results in higher FNMR and lower FMR.

	Algorithm	Failure to Enrol Rate ¹											
		APPLICATION	BORDER	KIOSK	MUGSHOT	VISA	WILD	SEC. 2.2	SEC. 2.4	SEC. 2.6	SEC. 2.5	SEC. 2.1	SEC. 2.7
407	turingtechvip-002	0.0001	423	0.0017	339	0.0097	91	0.0007	406	0.0006	393	0.0057	371
408	turkcell-000	0.0110	467	0.0234	450	0.0350	234	0.0103	467	0.0306	474	0.7213	472
409	twface-000	0.0000	86	0.0000	57	0.0000	46	0.0000	23	0.0000	74	0.0000	43
410	twface-001	0.0000	23	0.0000	2	0.0000	34	0.0000	33	0.0000	99	0.0000	10
411	ulsee-001	0.0000	136	0.0000	81	-	326	0.0000	113	0.0000	44	0.0001	114
412	ultinous-000	-	474	-	476	-	356	-	476	0.0003	164	-	474
413	ultinous-001	-	475	-	475	-	345	-	475	0.0003	165	-	476
414	uluface-002	0.0000	131	0.0000	84	-	322	0.0000	116	0.0000	41	0.0000	66
415	uluface-003	0.0000	117	0.0001	123	-	344	0.0002	301	0.0002	135	0.0244	422
416	unissey-002	0.0000	160	0.0000	92	0.0000	20	0.0000	72	0.0000	5	0.0000	76
417	unissey-003	0.0000	60	0.0008	217	0.0191	146	0.0001	242	0.0004	227	0.0005	257
418	upc-001	0.0000	382	0.0003	132	-	440	0.0003	346	0.0003	177	0.0011	309
419	uxlabs-001	0.0000	35	0.0000	26	0.0000	28	0.0000	62	0.0000	108	0.0000	22
420	vcog-002	-	476	-	474	-	352	-	474	0.0019	451	-	475
421	vd-002	0.0000	162	0.0000	90	1.0000	380	0.0000	76	0.0000	8	0.0000	78
422	vd-003	0.0001	424	0.0041	407	0.0676	273	0.0030	454	0.0029	462	0.0060	373
423	veridas-007	0.0000	379	0.0026	370	0.0595	264	0.0001	274	0.0005	363	0.0006	280
424	veridas-008	0.0000	376	0.0026	369	0.0595	265	0.0001	271	0.0005	366	0.0006	278
425	veridium-000	0.0061	461	0.5956	472	0.2889	305	0.0050	463	0.0009	415	0.3133	469
426	veridium-001	0.0001	421	0.0087	433	0.1615	294	0.0014	433	0.0006	391	0.0284	428
427	verigram-000	0.0000	347	0.0068	428	0.0822	288	0.0003	360	0.0005	379	0.0004	220
428	verigram-001	0.0000	329	0.0003	134	0.0060	71	0.0002	327	0.0003	179	0.0004	219
429	verihubs-inteligensia-000	0.0000	273	0.0029	378	0.0669	271	0.0001	230	0.0004	307	0.0003	162
430	verihubs-inteligensia-001	0.0000	310	0.0029	379	0.0669	272	0.0001	227	0.0004	303	0.0003	159
431	verijelas-000	0.0000	218	0.0023	364	0.0375	244	0.0004	381	0.0006	398	0.0006	275
432	via-000	0.0000	65	0.0000	45	-	476	0.0000	12	0.0000	60	0.0001	115
433	via-001	0.0000	69	0.0000	41	-	458	0.0000	7	0.0000	61	0.0001	116
434	videmo-001	0.0000	365	0.0170	446	0.0332	230	0.0010	425	0.0011	431	0.0847	446
435	videmo-002	0.0000	168	0.0006	186	0.0189	143	0.0001	251	0.0004	212	0.0003	172
436	videonetics-001	0.0004	444	0.0309	455	-	421	0.0015	435	0.0010	419	0.0112	392
437	videonetics-002	0.0000	351	0.0459	464	-	446	0.0006	400	0.0005	387	0.0013	320
438	viettelhightech-000	0.0000	387	0.0019	345	0.0368	241	0.0007	407	0.0005	382	0.0024	339
439	vigilantsolutions-010	0.0000	366	0.0028	374	0.0609	266	0.0001	233	0.0004	209	0.0005	261
440	vigilantsolutions-011	0.0000	369	0.0028	375	0.0609	267	0.0001	231	0.0004	205	0.0005	262
441	vinai-000	0.0000	78	0.0000	35	-	467	0.0000	4	0.0000	67	0.0000	34
442	vinbigdata-001	0.0000	165	0.0000	91	0.0000	23	0.0000	74	0.0000	9	0.0000	80
443	vinbigdata-002	0.0000	98	0.0015	328	0.0250	194	0.0000	173	0.0004	326	0.0012	318
444	vion-000	0.0050	459	0.0392	463	-	461	0.0130	469	0.0078	468	0.1389	464
445	visage-000	0.0000	385	0.0054	424	-	318	0.0009	419	0.0006	395	0.0064	374
446	visionbox-001	0.0000	411	0.0033	389	-	424	0.0005	390	0.0011	428	0.0028	347
447	visionbox-002	0.0000	138	0.0017	335	0.0270	209	0.0000	176	0.0004	345	0.0046	363
448	visionlabs-010	0.0000	359	0.0009	251	-	472	0.0001	283	0.0004	279	0.0006	282
449	visionlabs-011	0.0000	164	0.0006	183	0.0156	122	0.0001	236	0.0004	211	0.0004	202
450	visteam-004	0.0000	306	0.0010	285	0.0225	176	0.0001	264	0.0004	236	0.0006	271
451	visteam-005	0.0000	300	0.0010	284	0.0224	175	0.0001	237	0.0004	234	0.0005	267
452	vixvizioni-006	0.0000	75	0.0000	37	0.0000	51	0.0000	5	0.0000	66	0.0000	37
453	vixvizioni-007	0.0000	191	0.0000	104	0.0000	13	0.0000	90	0.0000	21	0.0000	102
454	vnpt-004	0.0000	283	0.0006	179	0.0160	128	0.0002	307	0.0004	242	0.0003	171
455	vnpt-005	0.0000	119	0.0006	175	0.0154	120	0.0002	317	0.0004	239	0.0003	176
456	vocord-009	0.0000	211	0.0006	182	-	414	0.0001	292	0.0003	146	0.0003	143
457	vocord-010	0.0000	341	0.0005	169	0.0141	111	0.0002	319	0.0003	178	0.0004	221
458	vts-000	0.0000	357	0.0011	293	-	378	0.0001	293	0.0004	338	0.0013	321
459	vts-001	0.0000	43	0.0003	130	0.0073	76	0.0000	138	0.0003	142	0.0002	125
460	wicket-000	0.0000	232	0.0009	246	0.0260	204	0.0000	150	0.0004	245	0.0004	207
461	winsense-001	0.0000	197	0.0000	102	-	349	0.0000	83	0.0000	24	0.0000	96
462	winsense-002	0.0000	104	0.0000	72	-	337	0.0000	102	0.0000	29	0.0000	58
463	wiseai-001	0.0001	419	0.0137	443	0.0768	285	0.0018	438	0.0018	448	0.0624	441
464	wuhantianyu-001	0.0000	53	0.0007	198	0.0159	125	0.0001	215	0.0004	285	0.0002	127

Table 37: FTE is the proportion of failed template generation attempts. Failures can occur because the software throws an exception, or because the software electively refuses to process the input image. This would typically occur if a face is not detected. FTE is measured as the number of function calls that give EITHER a non-zero error code OR that give a “small” template. This is defined as one whose size is less than 0.3 times the median template size for that algorithm. This second rule is needed because some algorithms incorrectly fail to return a non-zero error code when template generation fails.

A hyphen “-” indicates the dataset was not produced.¹ The effects of FTE are included in the accuracy results of this report by regarding any template comparison involving a failed template to produce a low similarity score. Thus higher FTE results in higher FNMR and lower FMR.

	Algorithm	Failure to Enrol Rate ¹											
		Name		APPLICATION	BORDER	KIOSK	MUGSHOT	VISA	WILD				
		Name	SEC. 2.2	SEC. 2.4	SEC. 2.6	SEC. 2.5	SEC. 2.1	SEC. 2.7					
465	x-laboratory-000	0.0247	471	0.0000	107	-	357	0.0005	389	0.0002	136	0.0000	92
466	x-laboratory-001	0.0000	209	0.0012	304	-	434	0.0001	276	0.0004	331	0.0007	288
467	xforwardai-001	0.0000	266	0.0007	210	-	311	0.0003	349	0.0004	322	0.0004	201
468	xforwardai-002	0.0000	233	0.0007	208	-	474	0.0003	348	0.0004	324	0.0004	197
469	xm-000	0.0000	48	0.0007	194	-	385	0.0001	218	0.0003	160	0.0004	247
470	yisheng-004	0.0002	438	-	473	-	335	0.0013	429	0.0006	401	0.0321	429
471	yitu-003	0.0000	111	0.0000	69	-	339	0.0009	418	0.0000	32	0.0000	59
472	yoonik-002	0.0000	338	0.0010	281	0.0284	211	0.0003	344	0.0006	390	0.0005	264
473	yoonik-003	0.0000	324	0.0009	259	0.0214	167	0.0002	305	0.0004	301	0.0008	297
474	ytu-000	0.0000	267	0.0010	289	-	314	0.0002	334	0.0004	323	0.0011	317
475	yuan-005	0.0000	311	0.0005	165	0.0134	107	0.0002	315	0.0004	221	0.0004	239
476	yuan-006	0.0000	386	0.0014	325	0.0369	242	0.0004	367	0.0005	376	0.0038	355

Table 38: FTE is the proportion of failed template generation attempts. Failures can occur because the software throws an exception, or because the software electively refuses to process the input image. This would typically occur if a face is not detected. FTE is measured as the number of function calls that give EITHER a non-zero error code OR that give a “small” template. This is defined as one whose size is less than 0.3 times the median template size for that algorithm. This second rule is needed because some algorithms incorrectly fail to return a non-zero error code when template generation fails.

A hyphen “-” indicates the dataset was not produced. ¹The effects of FTE are included in the accuracy results of this report by regarding any template comparison involving a failed template to produce a low similarity score. Thus higher FTE results in higher FNMR and lower FMR.

3.4 Recognition accuracy

Core algorithm accuracy is stated via:

▷ **Cooperative subjects**

- The summary table of Figure 29;
- The visa image DETs of Figure 90;
- The mugshot DETs of Figure 114;
- The mugshot ageing profiles of Figure 359;
- The human-difficult pairs of Figure 43

▷ **Non-cooperative subjects**

- The photojournalism DET of Figure 134

Figure 291 shows dependence of false match rate on algorithm score threshold. This allows a deployer to set a threshold to target a particular false match rate appropriate to the security objectives of the application.

Figure 243 likewise shows FMR(T) but for mugshots, and specially four subsets of the population.

Note that in both the mugshot and visa sets false match rates vary with the ethnicity, age, and sex, of the enrollee and impostor. For example figure 156 summarizes FMR for impostors paired from four groups black females, black males, white females, white males.

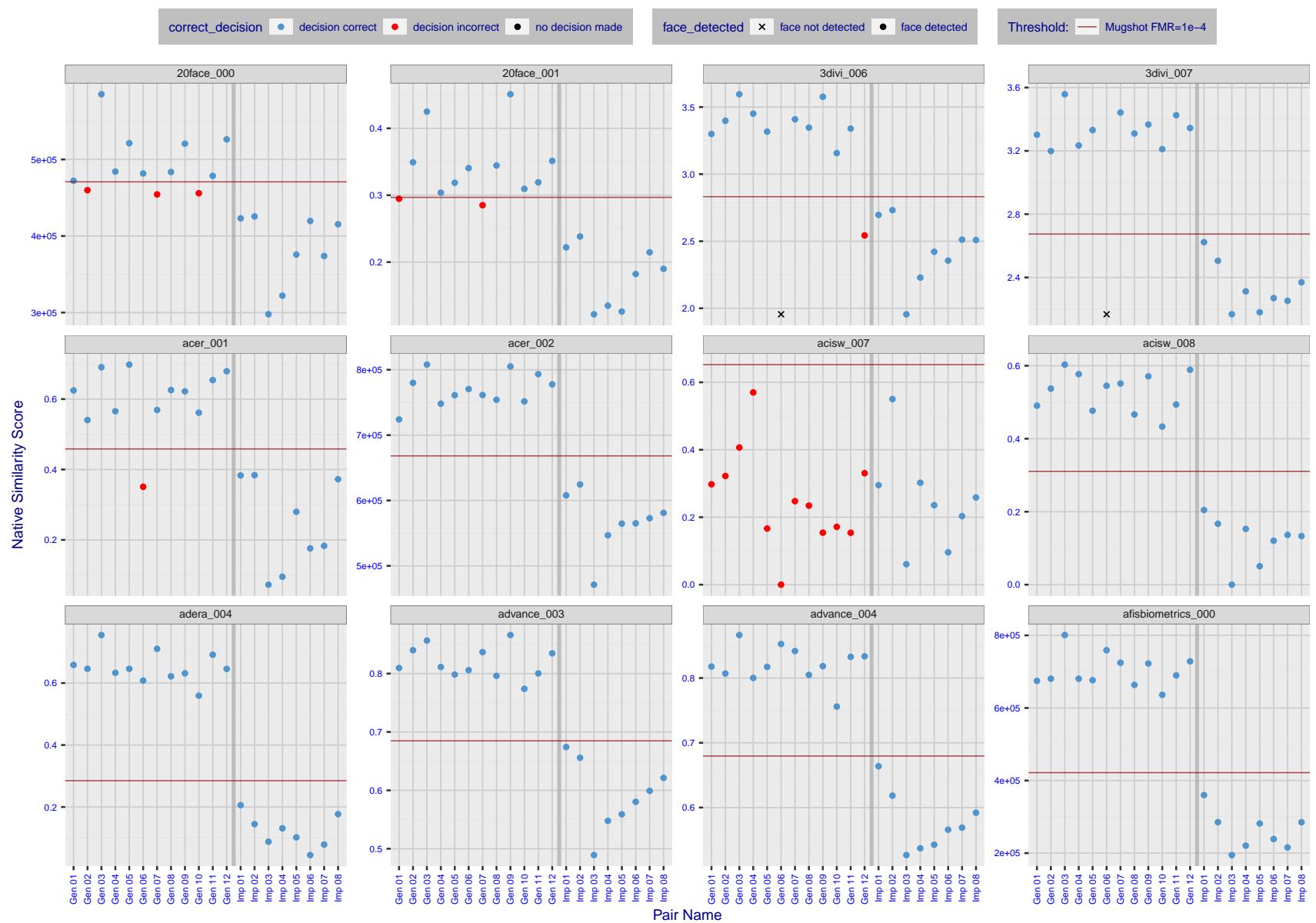


Figure 4: The figure shows algorithms' similarity scores for 12 genuine and 8 impostor image pairs used in a May 2018 paper by Phillips et al. ([1]). The threshold (red horizontal line) is a value calibrated to give $FMR = 0.0001$ on mugshot images. Points above the threshold correspond to pairs determined to be genuine, and points below the threshold correspond to pairs determined to be impostors. If the determined class (genuine or impostor) matches the real class, points will be blue; if not, red. An X represents face detection failure in either of the images in the pair. Note that the sample size ($n=20$) is small, and the figure may change substantially if larger or different sets are used. The images can be viewed on p. 13 of the Appendix, where Gen 01 corresponds to Same-Identity Pair 1, Gen 02 corresponds to Same-Identity Pair 2, and so on.

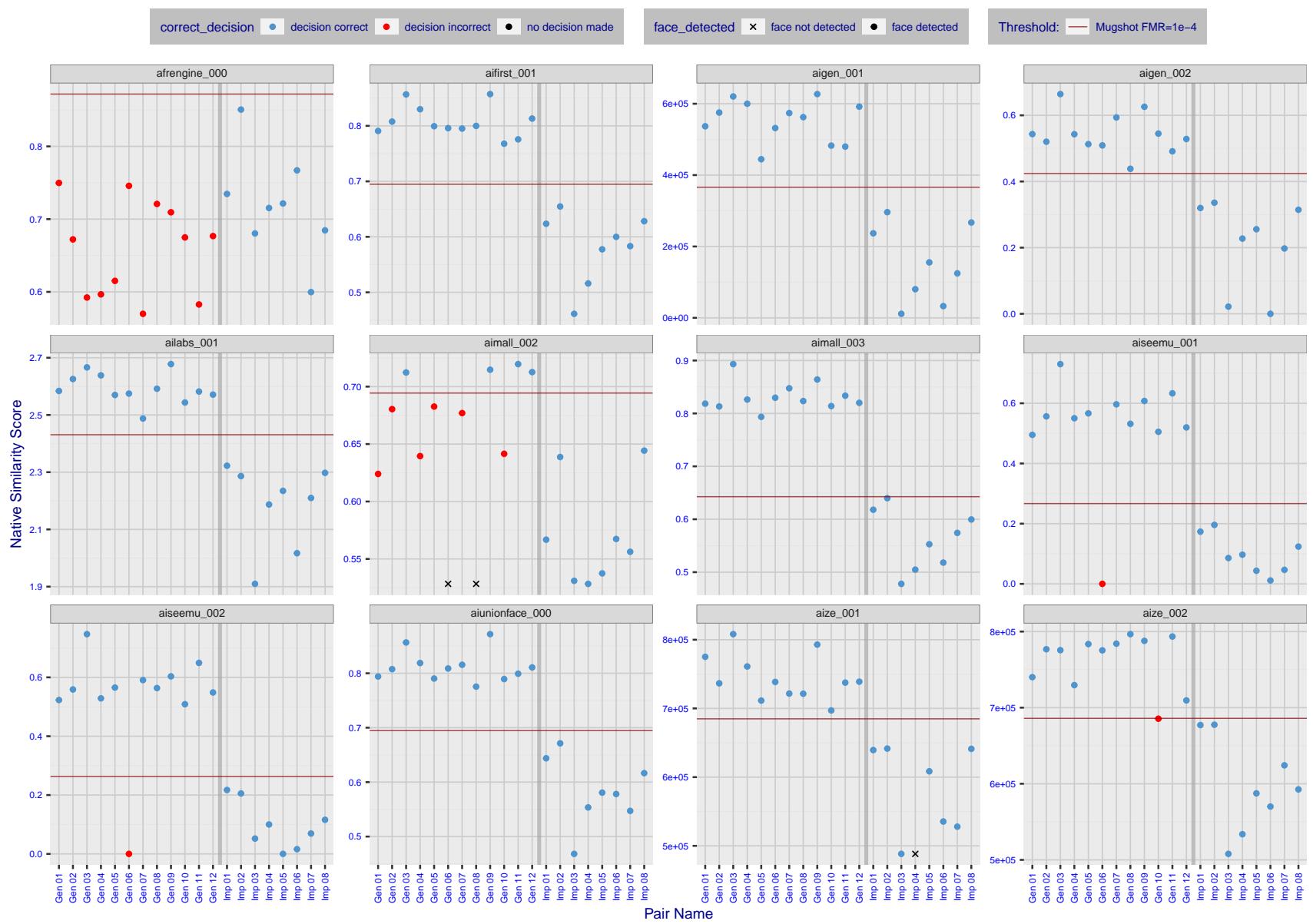


Figure 5: The figure shows algorithms' similarity scores for 12 genuine and 8 impostor image pairs used in a May 2018 paper by Phillips et al. ([1]). The threshold (red horizontal line) is a value calibrated to give $FMR = 0.0001$ on mugshot images. Points above the threshold correspond to pairs determined to be genuine, and points below the threshold correspond to pairs determined to be impostors. If the determined class (genuine or impostor) matches the real class, points will be blue; if not, red. An X represents face detection failure in either of the images in the pair. Note that the sample size ($n=20$) is small, and the figure may change substantially if larger or different sets are used. The images can be viewed on p. 13 of the Appendix, where Gen 01 corresponds to Same-Identity Pair 1, Gen 02 corresponds to Same-Identity Pair 2, and so on.

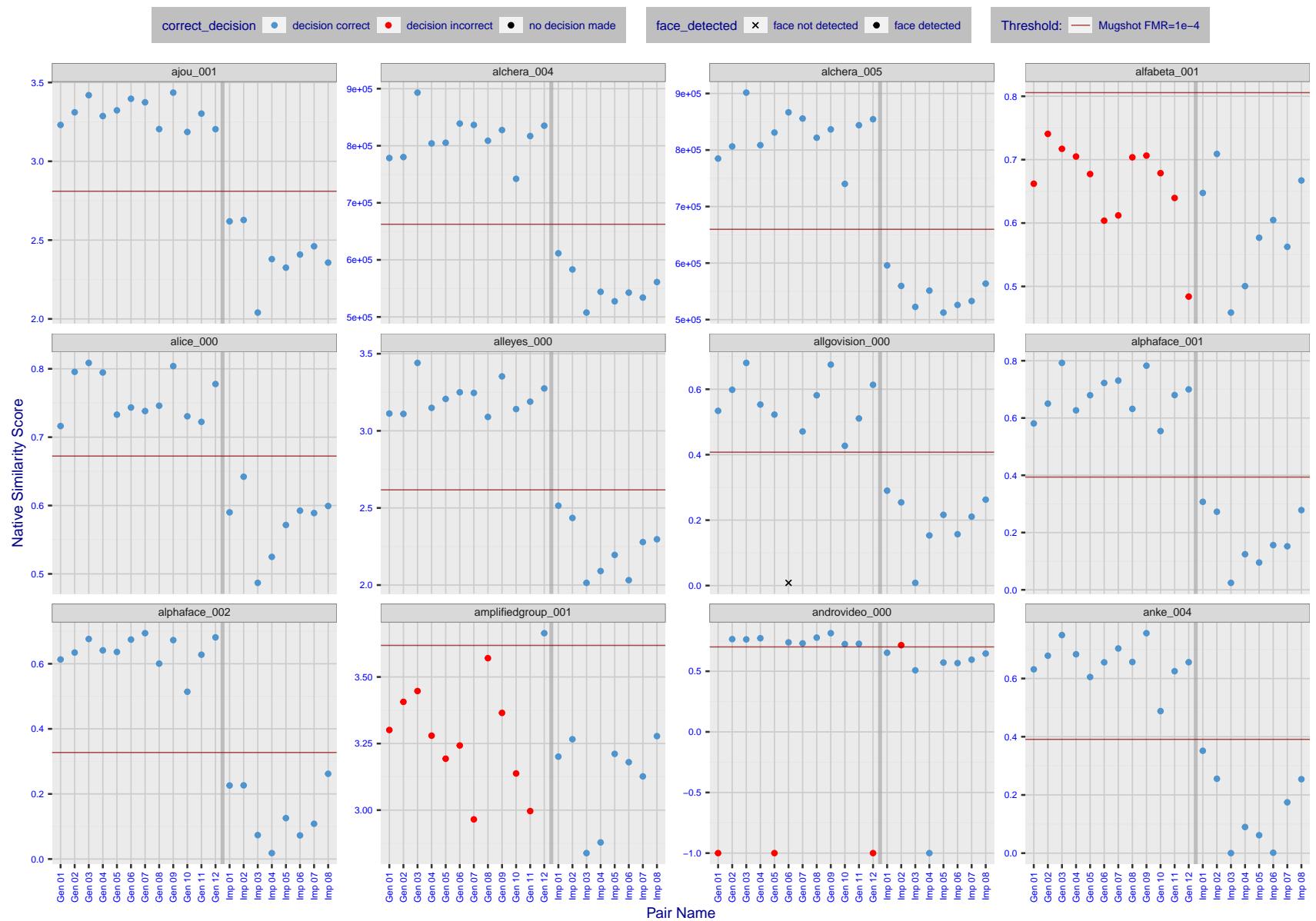


Figure 6: The figure shows algorithms' similarity scores for 12 genuine and 8 impostor image pairs used in a May 2018 paper by Phillips et al. ([1]). The threshold (red horizontal line) is a value calibrated to give $FMR = 0.0001$ on mugshot images. Points above the threshold correspond to pairs determined to be genuine, and points below the threshold correspond to pairs determined to be impostors. If the determined class (genuine or impostor) matches the real class, points will be blue; if not, red. An X represents face detection failure in either of the images in the pair. Note that the sample size ($n=20$) is small, and the figure may change substantially if larger or different sets are used. The images can be viewed on p. 13 of the Appendix, where Gen 01 corresponds to Same-Identity Pair 1, Gen 02 corresponds to Same-Identity Pair 2, and so on.

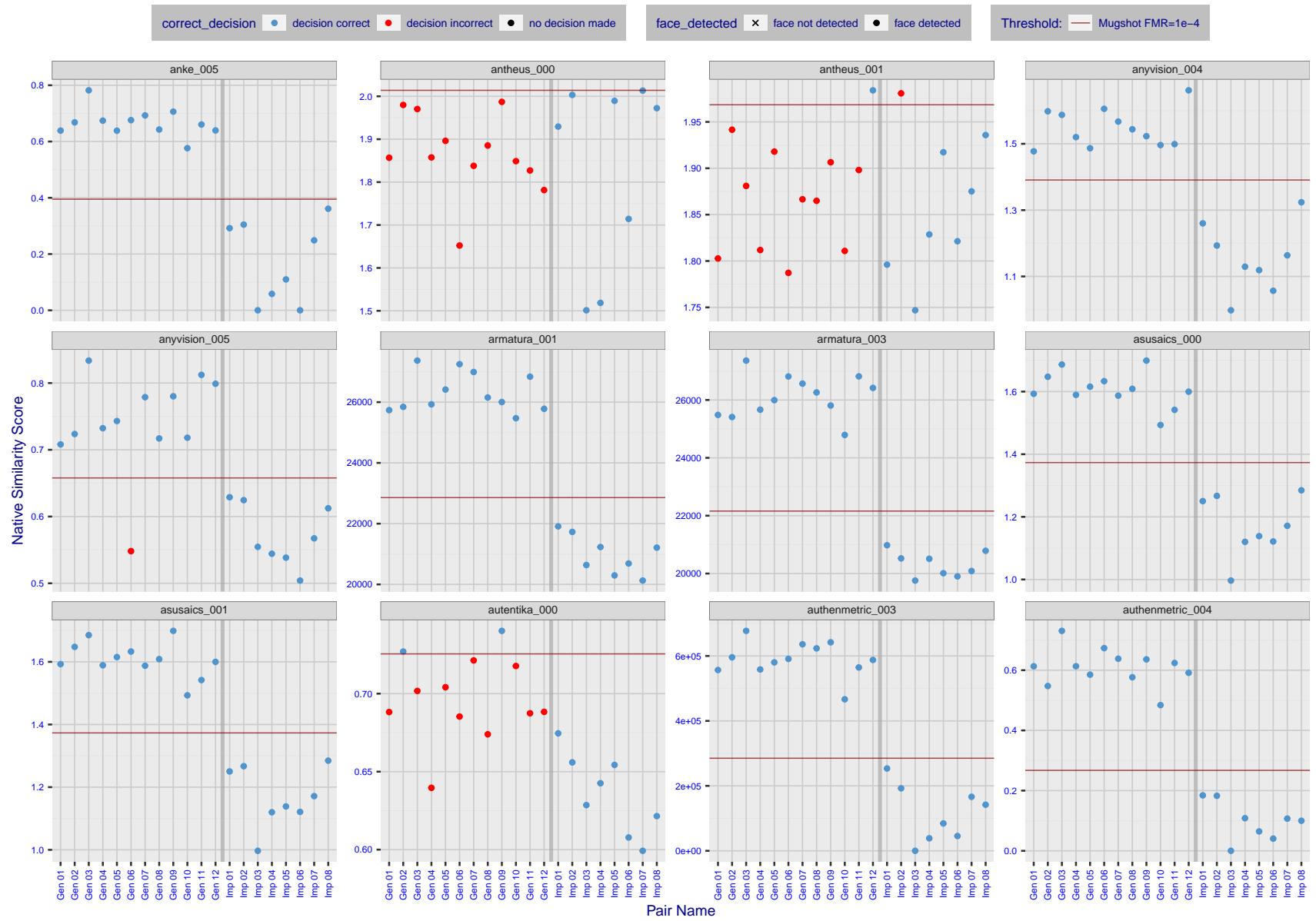


Figure 7: The figure shows algorithms' similarity scores for 12 genuine and 8 impostor image pairs used in a May 2018 paper by Phillips et al. ([1]). The threshold (red horizontal line) is a value calibrated to give $FMR = 0.0001$ on mugshot images. Points above the threshold correspond to pairs determined to be genuine, and points below the threshold correspond to pairs determined to be impostors. If the determined class (genuine or impostor) matches the real class, points will be blue; if not, red. An X represents face detection failure in either of the images in the pair. Note that the sample size ($n=20$) is small, and the figure may change substantially if larger or different sets are used. The images can be viewed on p. 13 of the Appendix, where Gen 01 corresponds to Same-Identity Pair 1, Gen 02 corresponds to Same-Identity Pair 2, and so on.

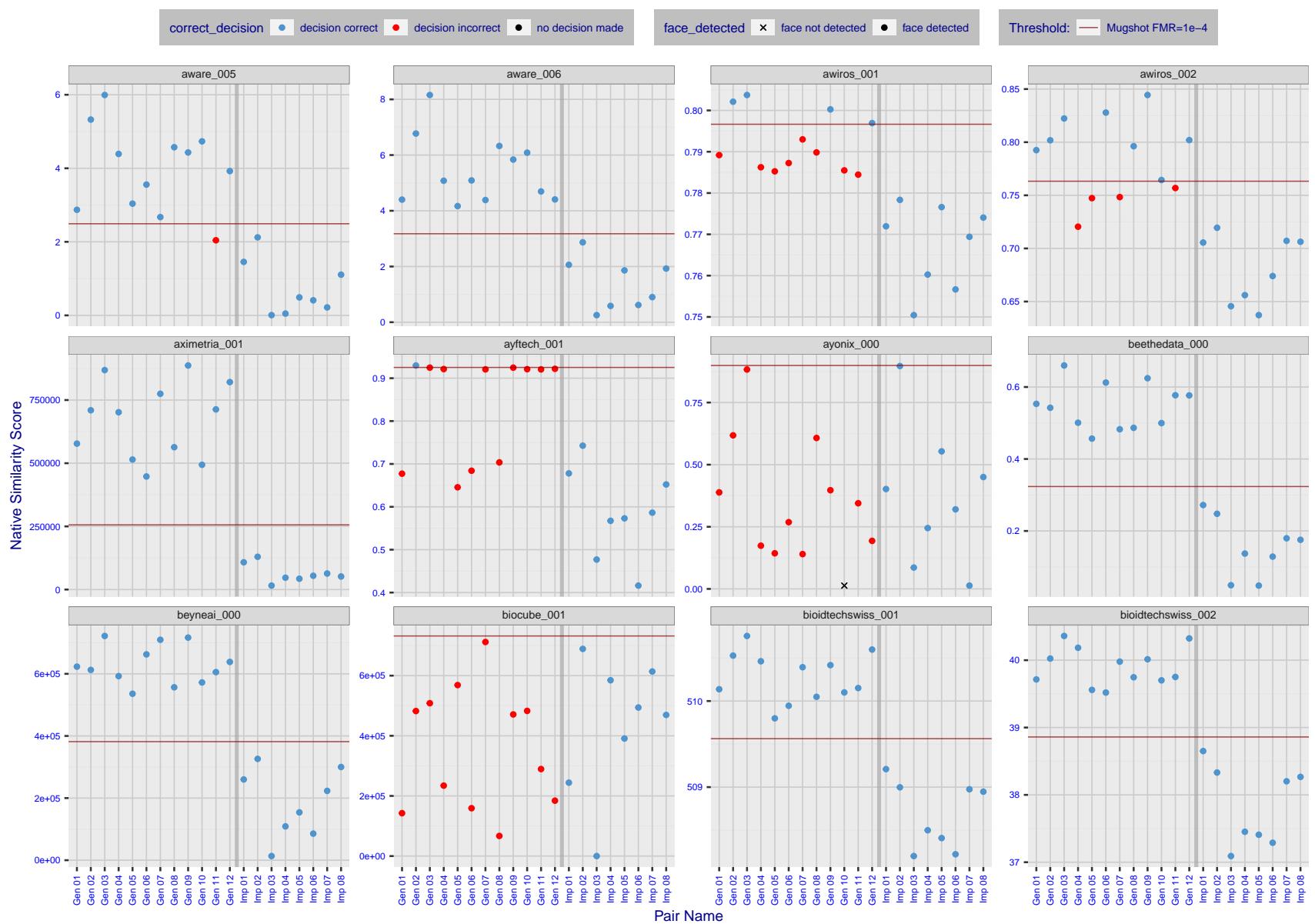


Figure 8: The figure shows algorithms' similarity scores for 12 genuine and 8 impostor image pairs used in a May 2018 paper by Phillips et al. ([1]). The threshold (red horizontal line) is a value calibrated to give $FMR = 0.0001$ on mugshot images. Points above the threshold correspond to pairs determined to be genuine, and points below the threshold correspond to pairs determined to be impostors. If the determined class (genuine or impostor) matches the real class, points will be blue; if not, red. An X represents face detection failure in either of the images in the pair. Note that the sample size ($n=20$) is small, and the figure may change substantially if larger or different sets are used. The images can be viewed on p. 13 of the Appendix, where Gen 01 corresponds to Same-Identity Pair 1, Gen 02 corresponds to Same-Identity Pair 2, and so on.

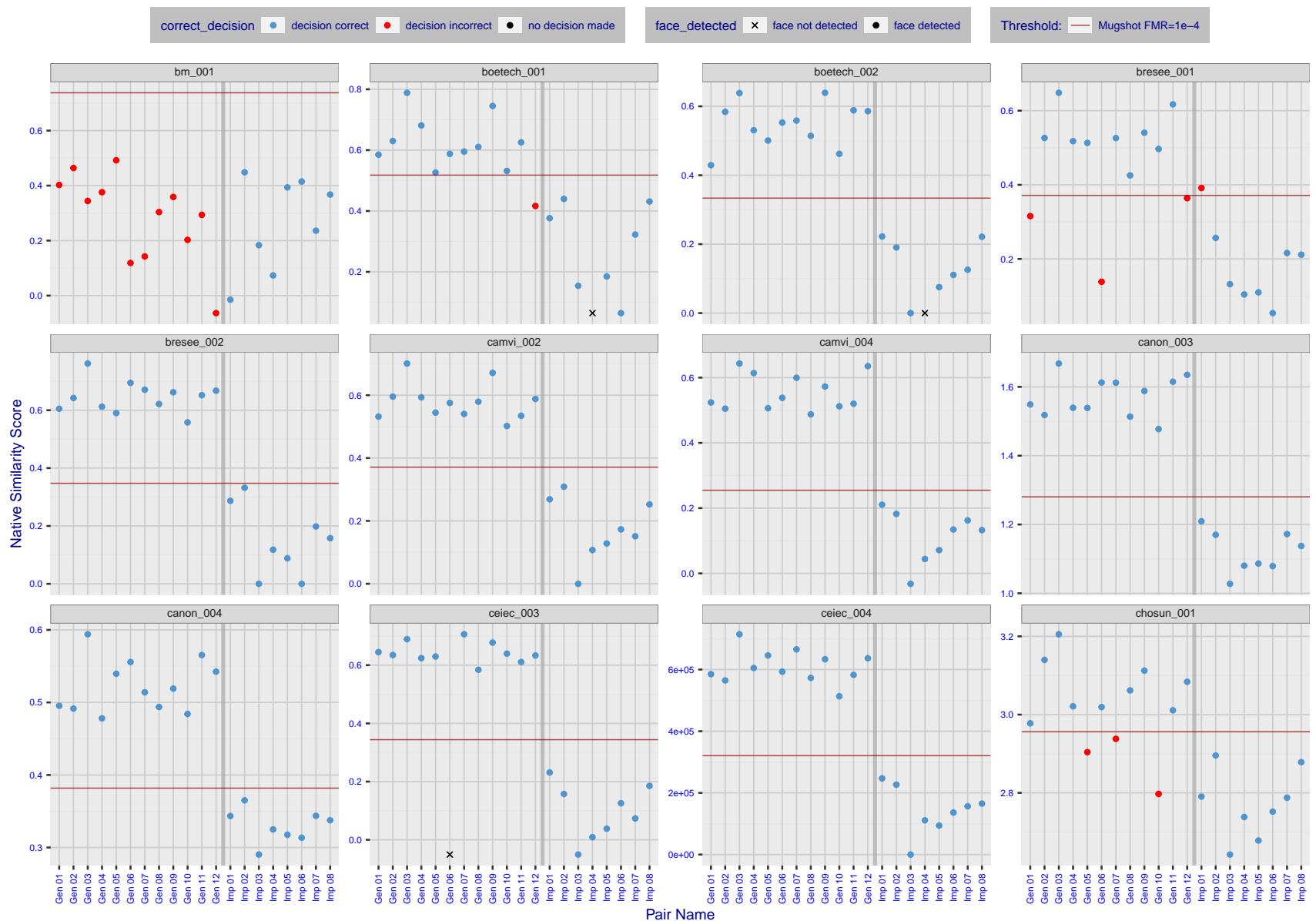


Figure 9: The figure shows algorithms' similarity scores for 12 genuine and 8 impostor image pairs used in a May 2018 paper by Phillips et al. ([1]). The threshold (red horizontal line) is a value calibrated to give $FMR = 0.0001$ on mugshot images. Points above the threshold correspond to pairs determined to be genuine, and points below the threshold correspond to pairs determined to be impostors. If the determined class (genuine or impostor) matches the real class, points will be blue; if not, red. An X represents face detection failure in either of the images in the pair. Note that the sample size ($n=20$) is small, and the figure may change substantially if larger or different sets are used. The images can be viewed on p. 13 of the Appendix, where Gen 01 corresponds to Same-Identity Pair 1, Gen 02 corresponds to Same-Identity Pair 2, and so on.

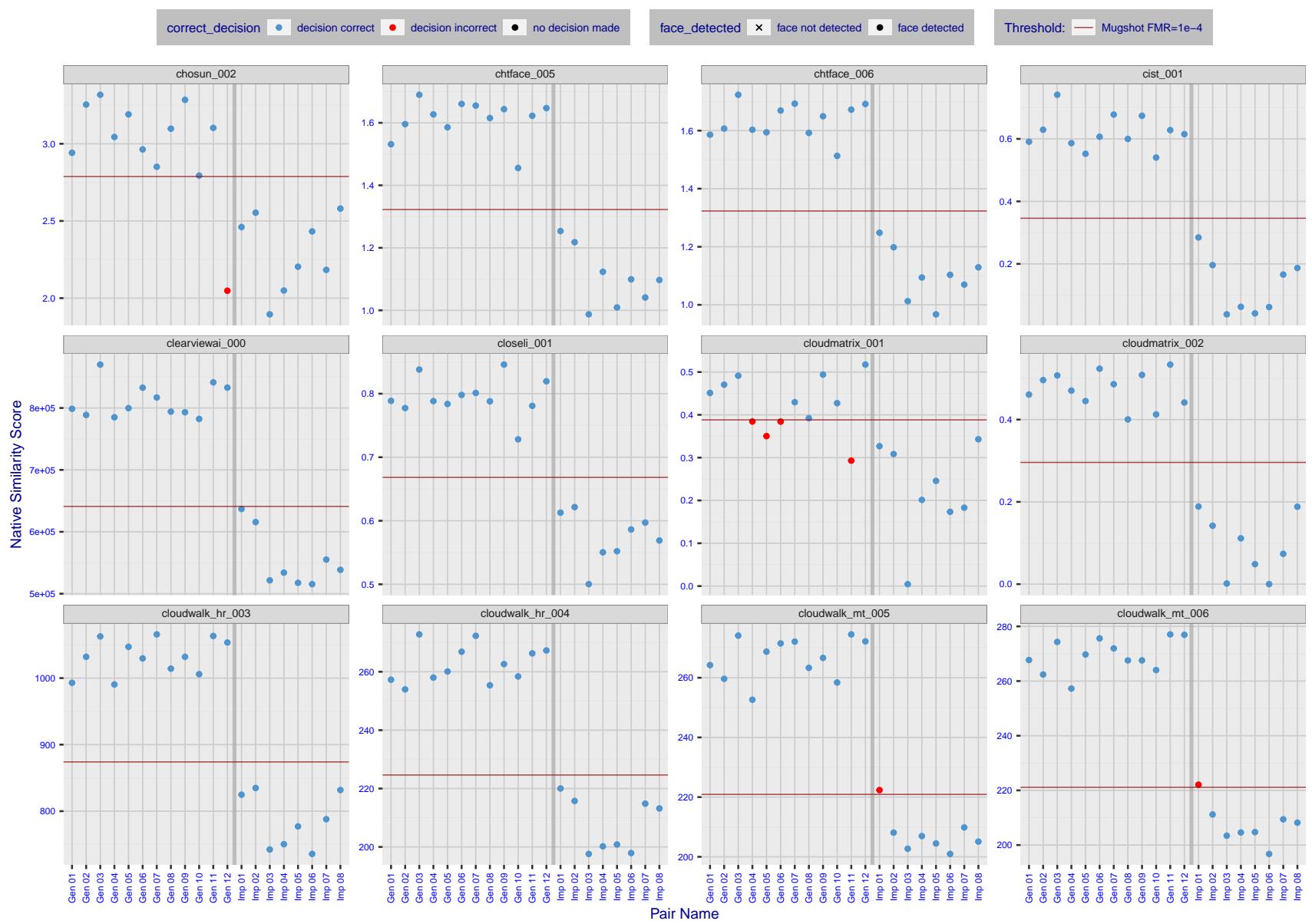


Figure 10: The figure shows algorithms' similarity scores for 12 genuine and 8 impostor image pairs used in a May 2018 paper by Phillips et al. ([1]). The threshold (red horizontal line) is a value calibrated to give $FMR = 0.0001$ on mugshot images. Points above the threshold correspond to pairs determined to be genuine, and points below the threshold correspond to pairs determined to be impostors. If the determined class (genuine or impostor) matches the real class, points will be blue; if not, red. An X represents face detection failure in either of the images in the pair. Note that the sample size ($n=20$) is small, and the figure may change substantially if larger or different sets are used. The images can be viewed on p. 13 of the Appendix, where Gen 01 corresponds to Same-Identity Pair 1, Gen 02 corresponds to Same-Identity Pair 2, and so on.

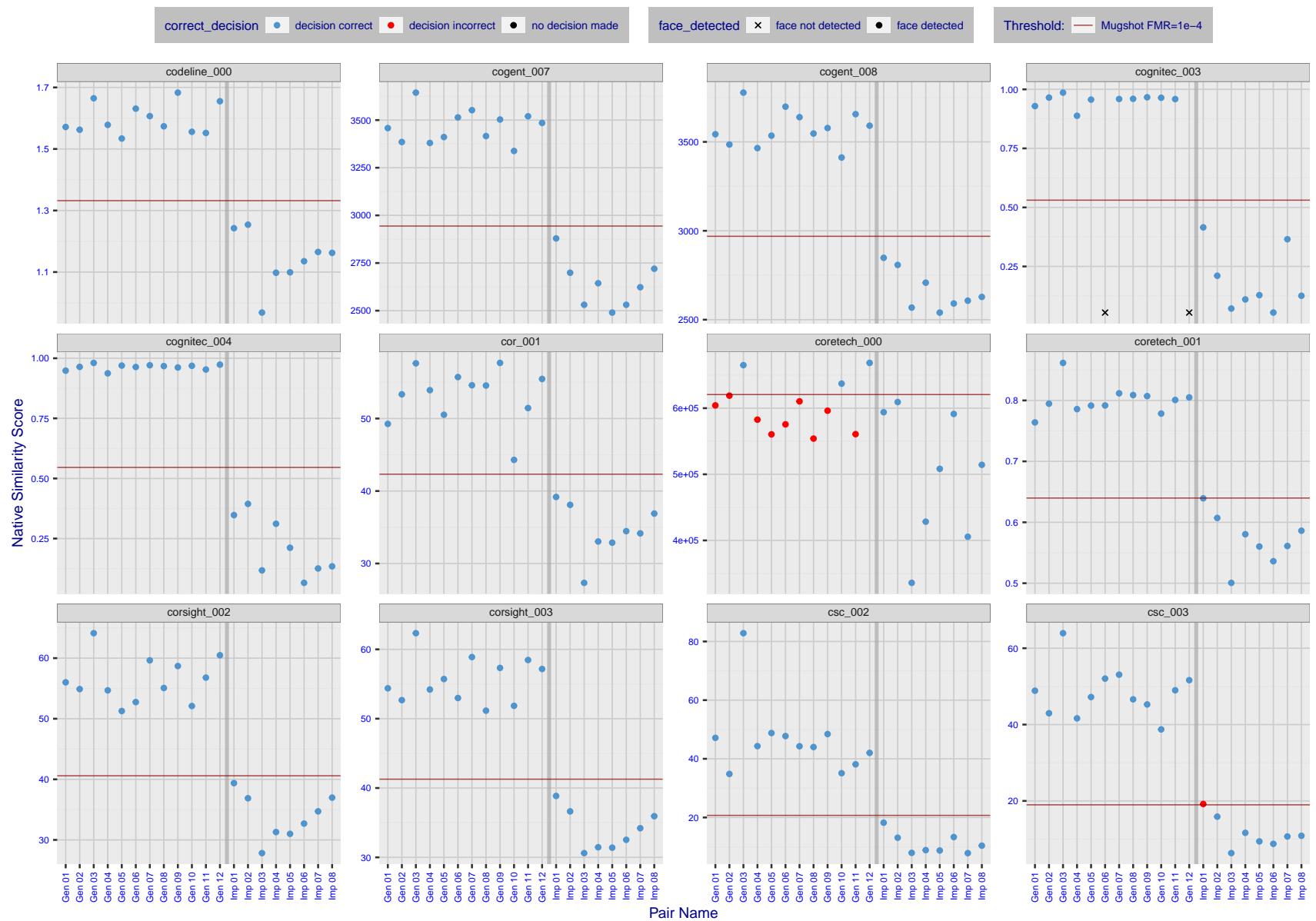


Figure 11: The figure shows algorithms' similarity scores for 12 genuine and 8 impostor image pairs used in a May 2018 paper by Phillips et al. ([1]). The threshold (red horizontal line) is a value calibrated to give $FMR = 0.0001$ on mugshot images. Points above the threshold correspond to pairs determined to be genuine, and points below the threshold correspond to pairs determined to be impostors. If the determined class (genuine or impostor) matches the real class, points will be blue; if not, red. An X represents face detection failure in either of the images in the pair. Note that the sample size ($n=20$) is small, and the figure may change substantially if larger or different sets are used. The images can be viewed on p. 13 of the Appendix, where Gen 01 corresponds to Same-Identity Pair 1, Gen 02 corresponds to Same-Identity Pair 2, and so on.

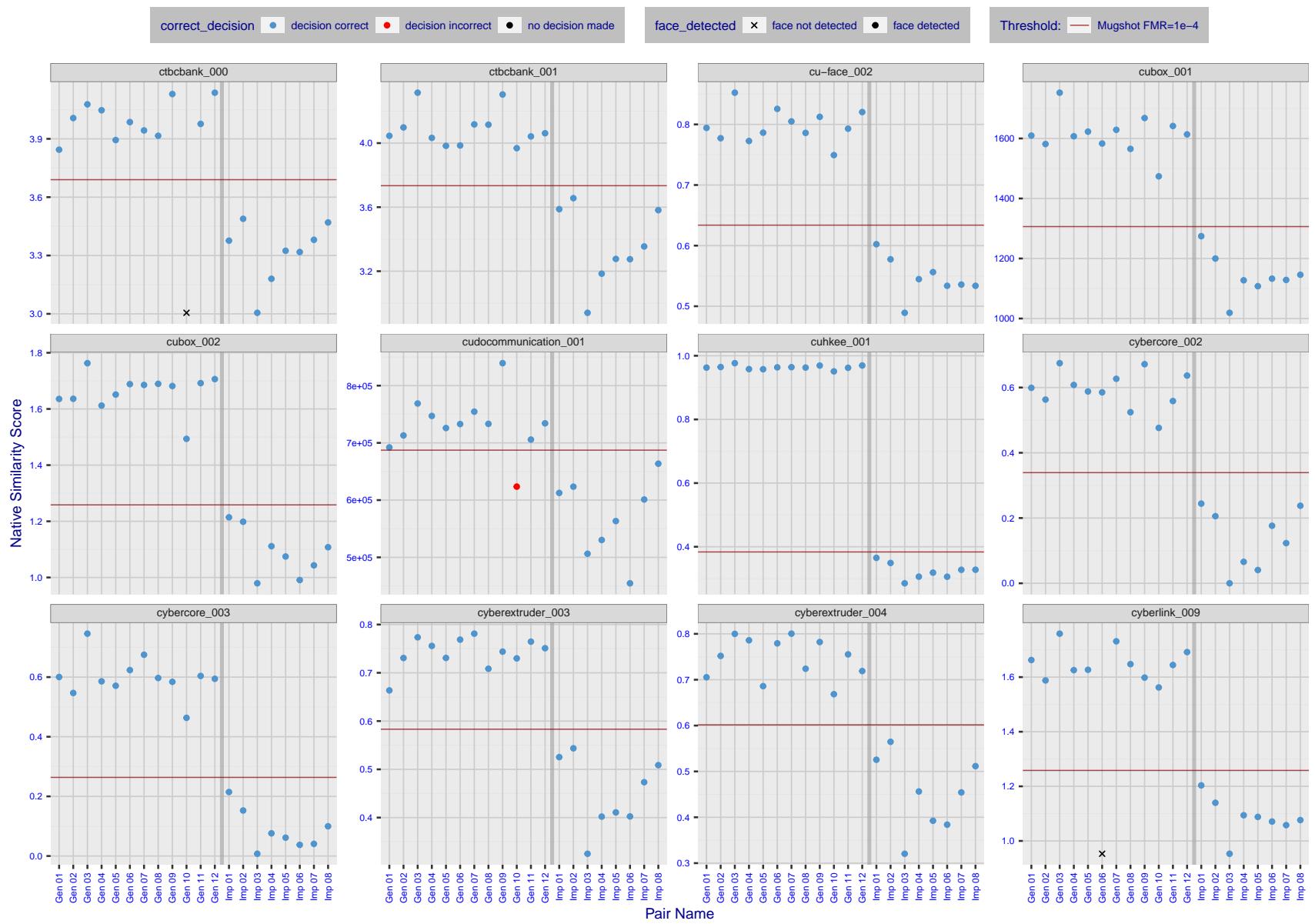


Figure 12: The figure shows algorithms' similarity scores for 12 genuine and 8 impostor image pairs used in a May 2018 paper by Phillips et al. ([1]). The threshold (red horizontal line) is a value calibrated to give $FMR = 0.0001$ on mugshot images. Points above the threshold correspond to pairs determined to be genuine, and points below the threshold correspond to pairs determined to be impostors. If the determined class (genuine or impostor) matches the real class, points will be blue; if not, red. An X represents face detection failure in either of the images in the pair. Note that the sample size ($n=20$) is small, and the figure may change substantially if larger or different sets are used. The images can be viewed on p. 13 of the Appendix, where Gen 01 corresponds to Same-Identity Pair 1, Gen 02 corresponds to Same-Identity Pair 2, and so on.

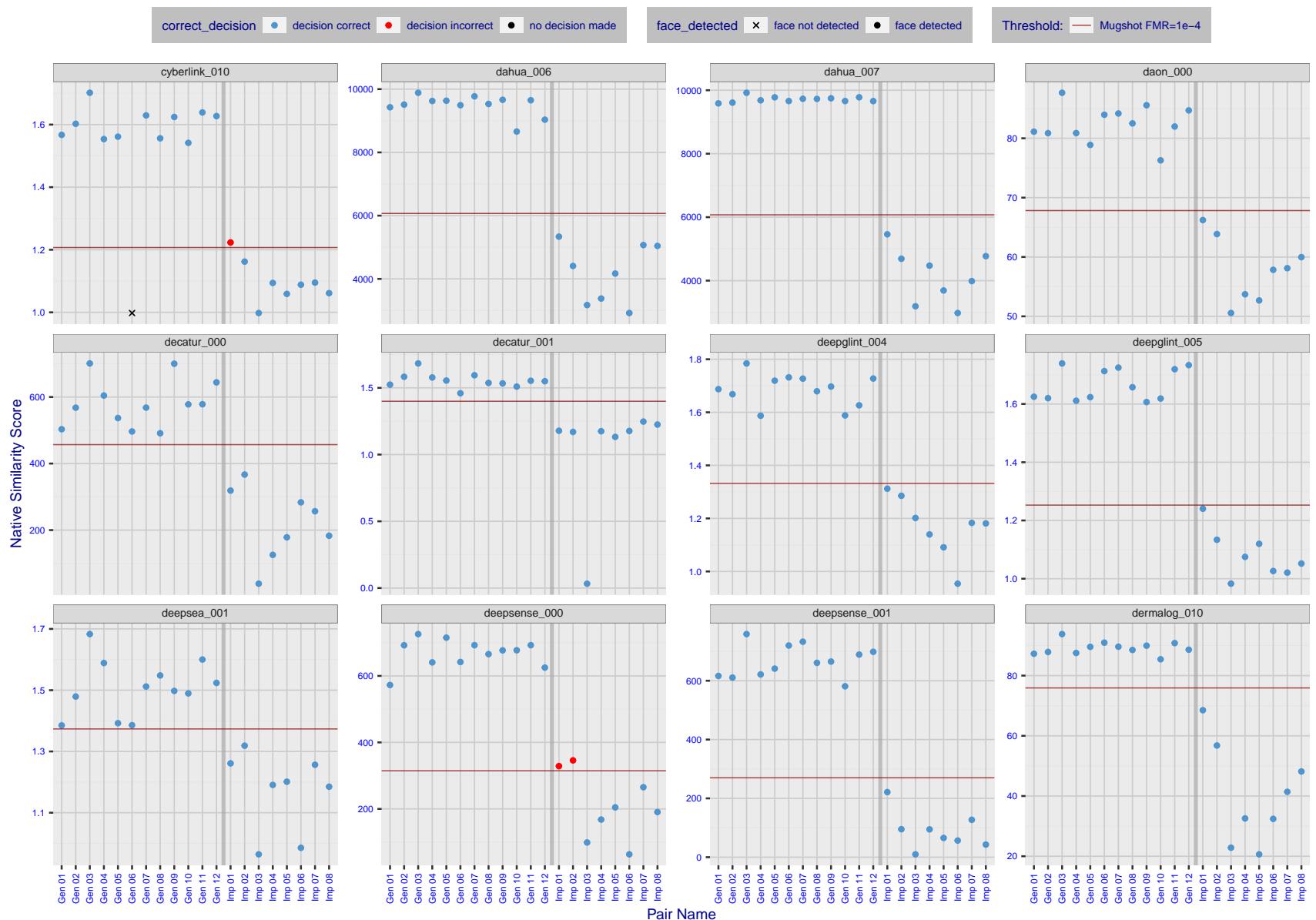


Figure 13: The figure shows algorithms' similarity scores for 12 genuine and 8 impostor image pairs used in a May 2018 paper by Phillips et al. ([1]). The threshold (red horizontal line) is a value calibrated to give $FMR = 0.0001$ on mugshot images. Points above the threshold correspond to pairs determined to be genuine, and points below the threshold correspond to pairs determined to be impostors. If the determined class (genuine or impostor) matches the real class, points will be blue; if not, red. An X represents face detection failure in either of the images in the pair. Note that the sample size ($n=20$) is small, and the figure may change substantially if larger or different sets are used. The images can be viewed on p. 13 of the Appendix, where Gen 01 corresponds to Same-Identity Pair 1, Gen 02 corresponds to Same-Identity Pair 2, and so on.

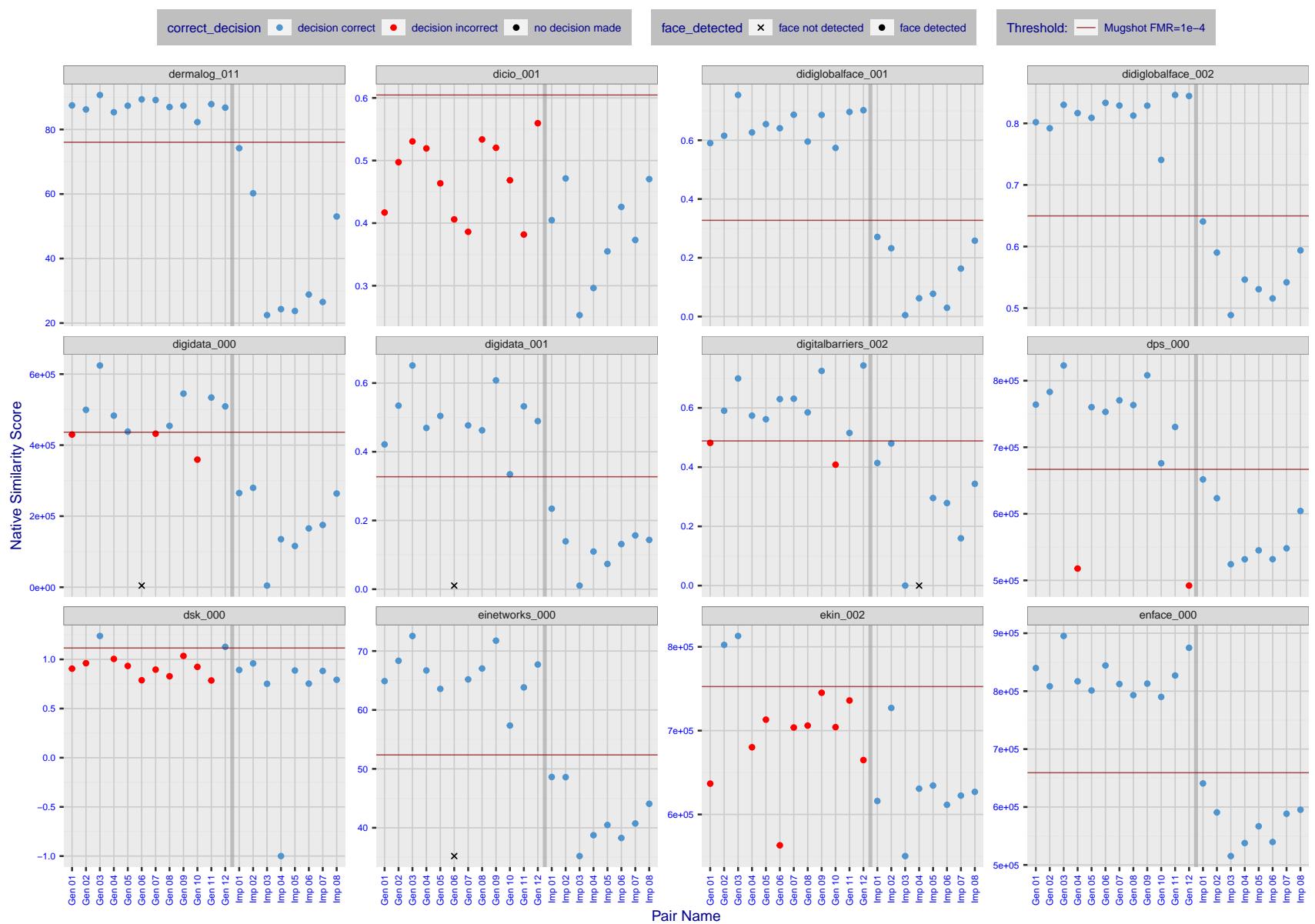


Figure 14: The figure shows algorithms' similarity scores for 12 genuine and 8 impostor image pairs used in a May 2018 paper by Phillips et al. ([1]). The threshold (red horizontal line) is a value calibrated to give $FMR = 0.0001$ on mugshot images. Points above the threshold correspond to pairs determined to be genuine, and points below the threshold correspond to pairs determined to be impostors. If the determined class (genuine or impostor) matches the real class, points will be blue; if not, red. An X represents face detection failure in either of the images in the pair. Note that the sample size ($n=20$) is small, and the figure may change substantially if larger or different sets are used. The images can be viewed on p. 13 of the Appendix, where Gen 01 corresponds to Same-Identity Pair 1, Gen 02 corresponds to Same-Identity Pair 2, and so on.

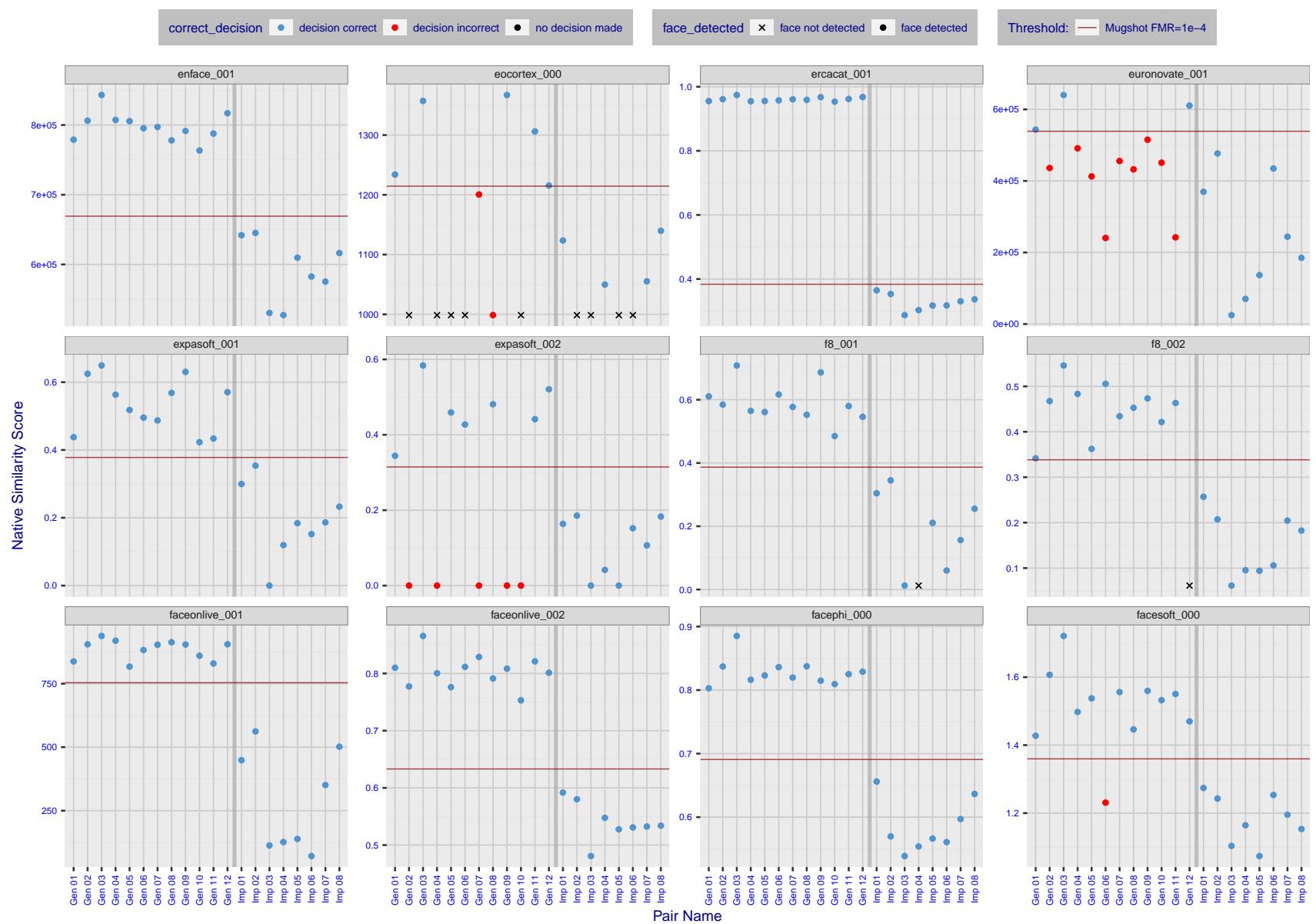


Figure 15: The figure shows algorithms' similarity scores for 12 genuine and 8 impostor image pairs used in a May 2018 paper by Phillips et al. ([1]). The threshold (red horizontal line) is a value calibrated to give $FMR = 0.0001$ on mugshot images. Points above the threshold correspond to pairs determined to be genuine, and points below the threshold correspond to pairs determined to be impostors. If the determined class (genuine or impostor) matches the real class, points will be blue; if not, red. An X represents face detection failure in either of the images in the pair. Note that the sample size ($n=20$) is small, and the figure may change substantially if larger or different sets are used. The images can be viewed on p. 13 of the Appendix, where Gen 01 corresponds to Same-Identity Pair 1, Gen 02 corresponds to Same-Identity Pair 2, and so on.

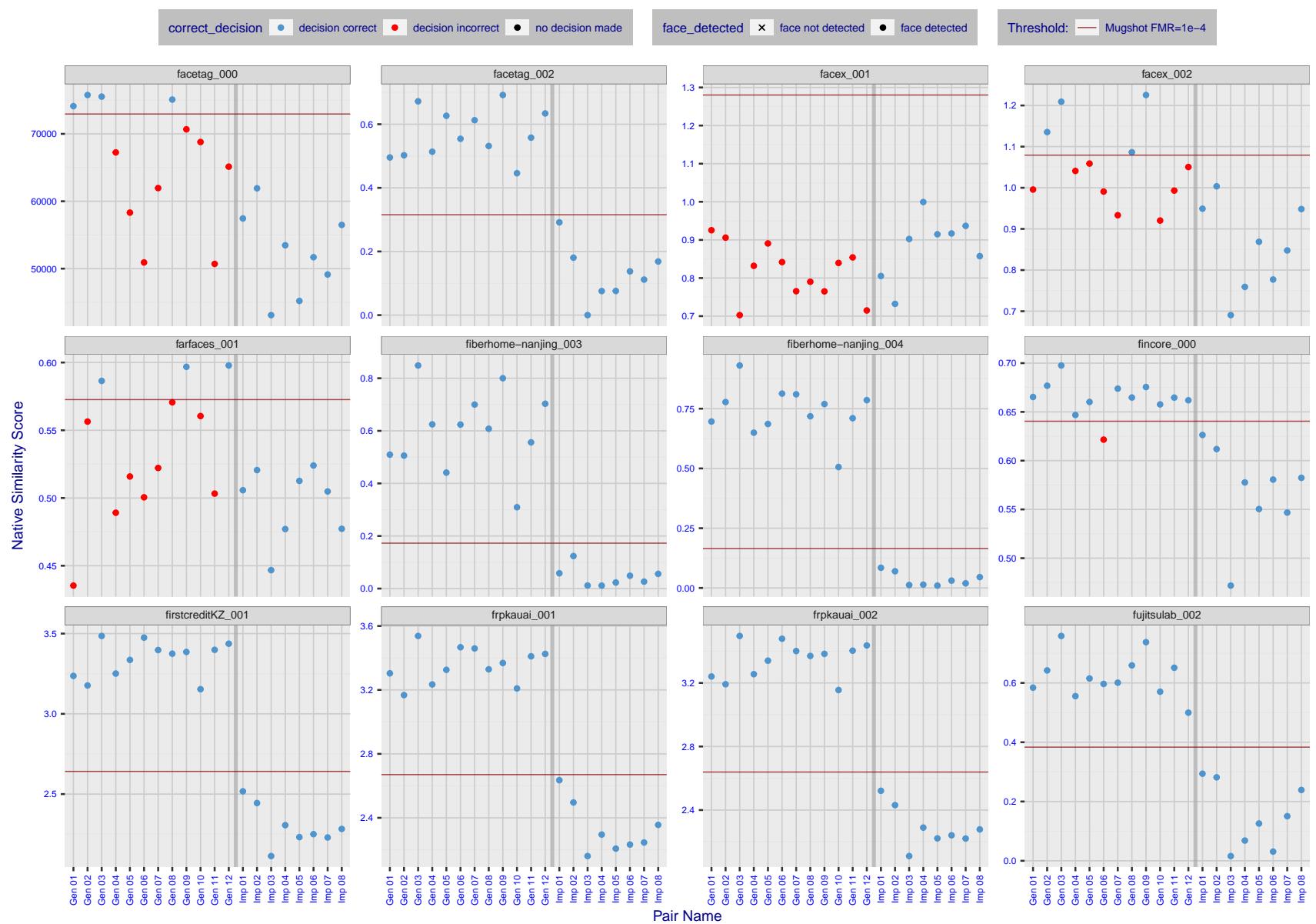


Figure 16: The figure shows algorithms' similarity scores for 12 genuine and 8 impostor image pairs used in a May 2018 paper by Phillips et al. ([1]). The threshold (red horizontal line) is a value calibrated to give $FMR = 0.0001$ on mugshot images. Points above the threshold correspond to pairs determined to be genuine, and points below the threshold correspond to pairs determined to be impostors. If the determined class (genuine or impostor) matches the real class, points will be blue; if not, red. An X represents face detection failure in either of the images in the pair. Note that the sample size ($n=20$) is small, and the figure may change substantially if larger or different sets are used. The images can be viewed on p. 13 of the Appendix, where Gen 01 corresponds to Same-Identity Pair 1, Gen 02 corresponds to Same-Identity Pair 2, and so on.

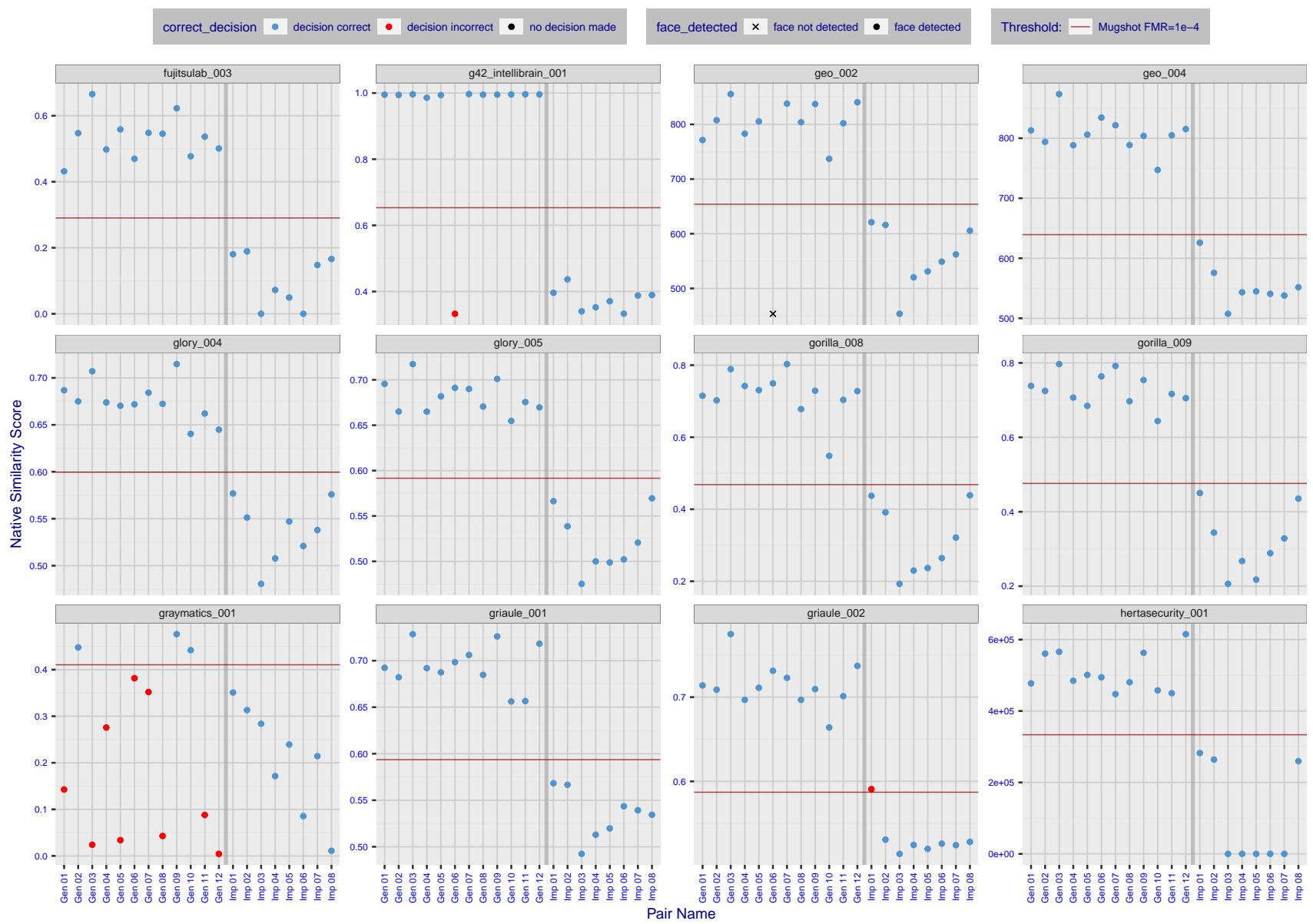


Figure 17: The figure shows algorithms' similarity scores for 12 genuine and 8 impostor image pairs used in a May 2018 paper by Phillips et al. ([1]). The threshold (red horizontal line) is a value calibrated to give $FMR = 0.0001$ on mugshot images. Points above the threshold correspond to pairs determined to be genuine, and points below the threshold correspond to pairs determined to be impostors. If the determined class (genuine or impostor) matches the real class, points will be blue; if not, red. An X represents face detection failure in either of the images in the pair. Note that the sample size ($n=20$) is small, and the figure may change substantially if larger or different sets are used. The images can be viewed on p. 13 of the Appendix, where Gen 01 corresponds to Same-Identity Pair 1, Gen 02 corresponds to Same-Identity Pair 2, and so on.

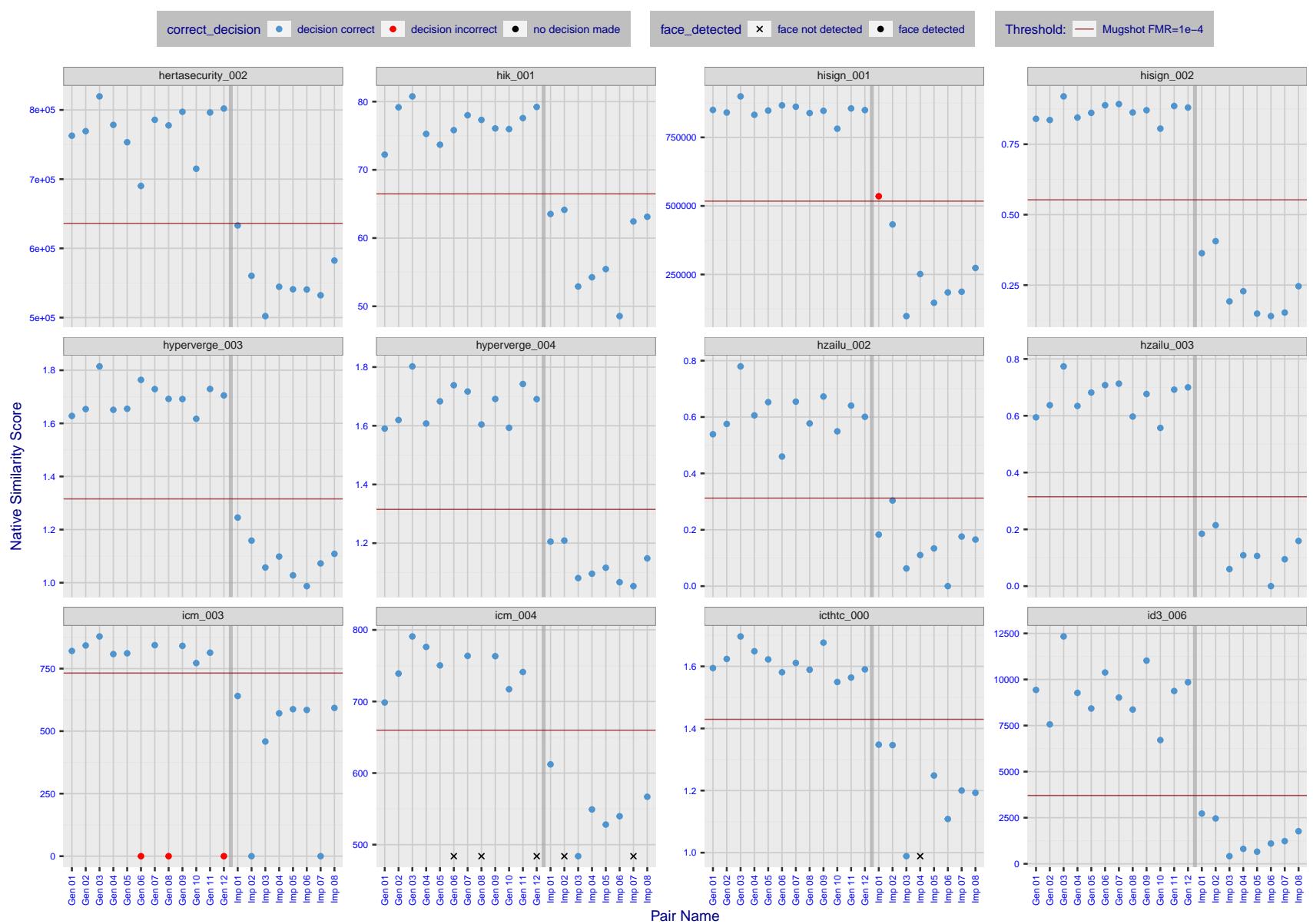


Figure 18: The figure shows algorithms' similarity scores for 12 genuine and 8 impostor image pairs used in a May 2018 paper by Phillips et al. ([1]). The threshold (red horizontal line) is a value calibrated to give $FMR = 0.0001$ on mugshot images. Points above the threshold correspond to pairs determined to be genuine, and points below the threshold correspond to pairs determined to be impostors. If the determined class (genuine or impostor) matches the real class, points will be blue; if not, red. An X represents face detection failure in either of the images in the pair. Note that the sample size ($n=20$) is small, and the figure may change substantially if larger or different sets are used. The images can be viewed on p. 13 of the Appendix, where Gen 01 corresponds to Same-Identity Pair 1, Gen 02 corresponds to Same-Identity Pair 2, and so on.

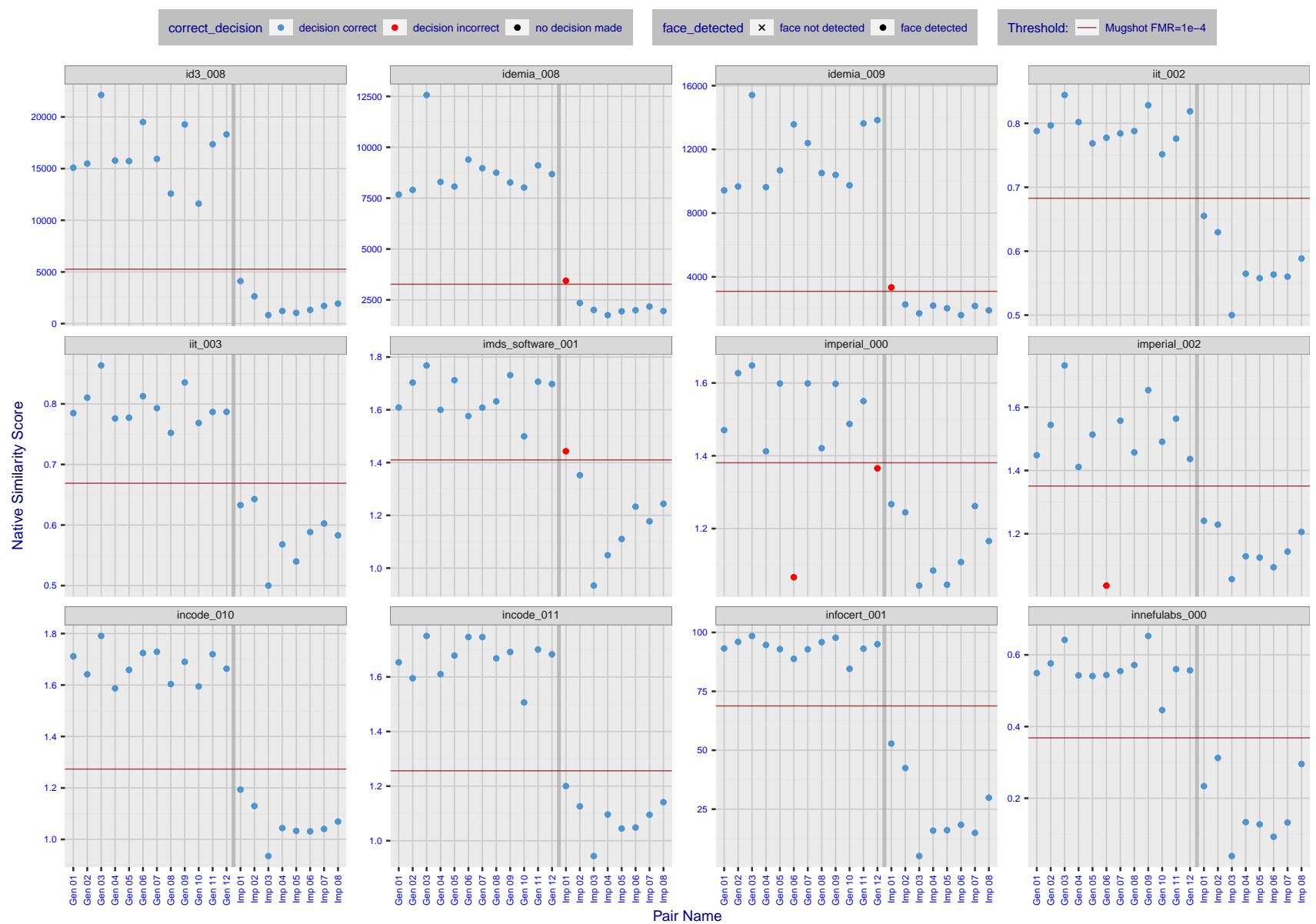


Figure 19: The figure shows algorithms' similarity scores for 12 genuine and 8 impostor image pairs used in a May 2018 paper by Phillips et al. ([1]). The threshold (red horizontal line) is a value calibrated to give $FMR = 0.0001$ on mugshot images. Points above the threshold correspond to pairs determined to be genuine, and points below the threshold correspond to pairs determined to be impostors. If the determined class (genuine or impostor) matches the real class, points will be blue; if not, red. An X represents face detection failure in either of the images in the pair. Note that the sample size ($n=20$) is small, and the figure may change substantially if larger or different sets are used. The images can be viewed on p. 13 of the Appendix, where Gen 01 corresponds to Same-Identity Pair 1, Gen 02 corresponds to Same-Identity Pair 2, and so on.

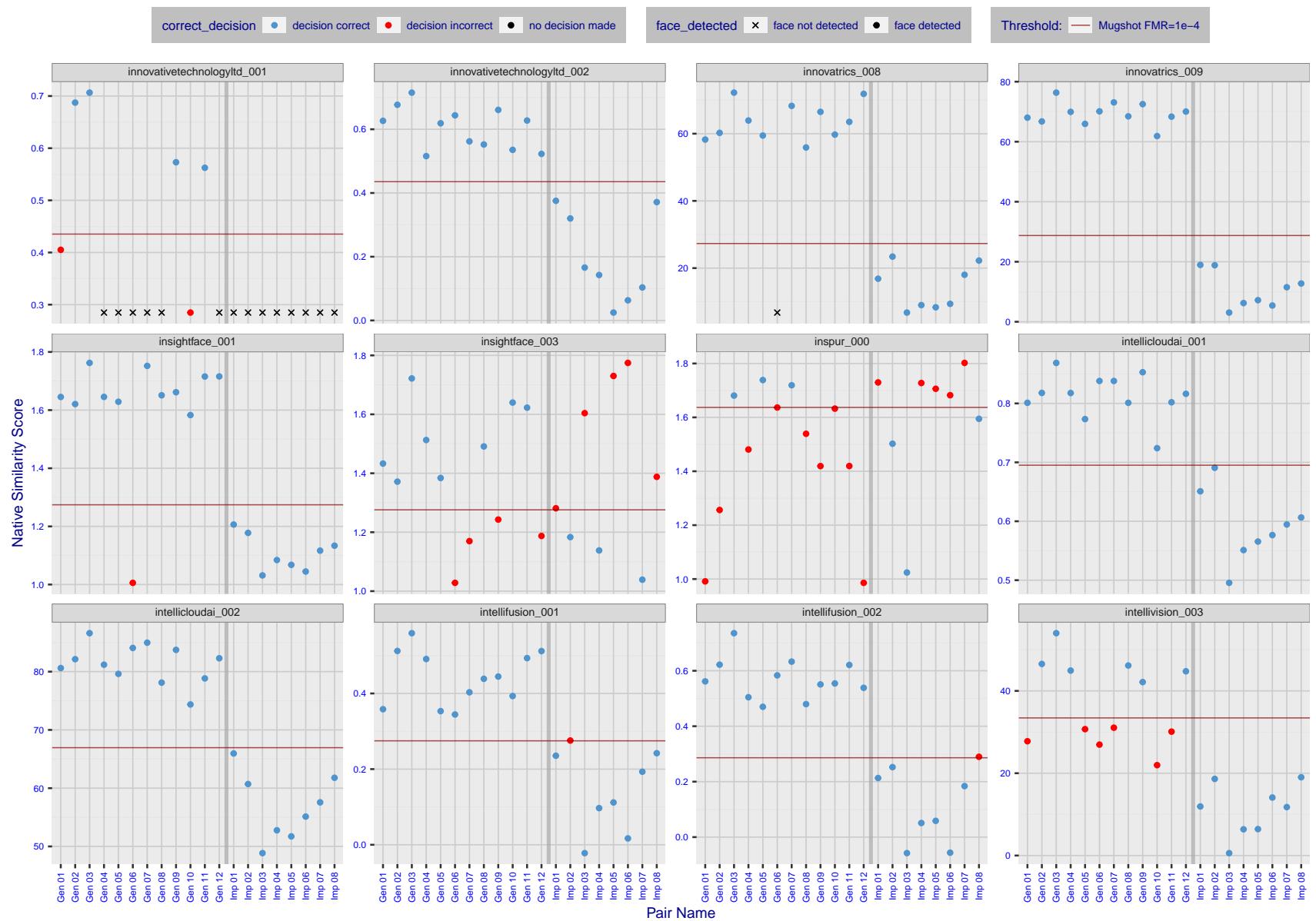


Figure 20: The figure shows algorithms' similarity scores for 12 genuine and 8 impostor image pairs used in a May 2018 paper by Phillips et al. ([1]). The threshold (red horizontal line) is a value calibrated to give $FMR = 0.0001$ on mugshot images. Points above the threshold correspond to pairs determined to be genuine, and points below the threshold correspond to pairs determined to be impostors. If the determined class (genuine or impostor) matches the real class, points will be blue; if not, red. An X represents face detection failure in either of the images in the pair. Note that the sample size ($n=20$) is small, and the figure may change substantially if larger or different sets are used. The images can be viewed on p. 13 of the Appendix, where Gen 01 corresponds to Same-Identity Pair 1, Gen 02 corresponds to Same-Identity Pair 2, and so on.

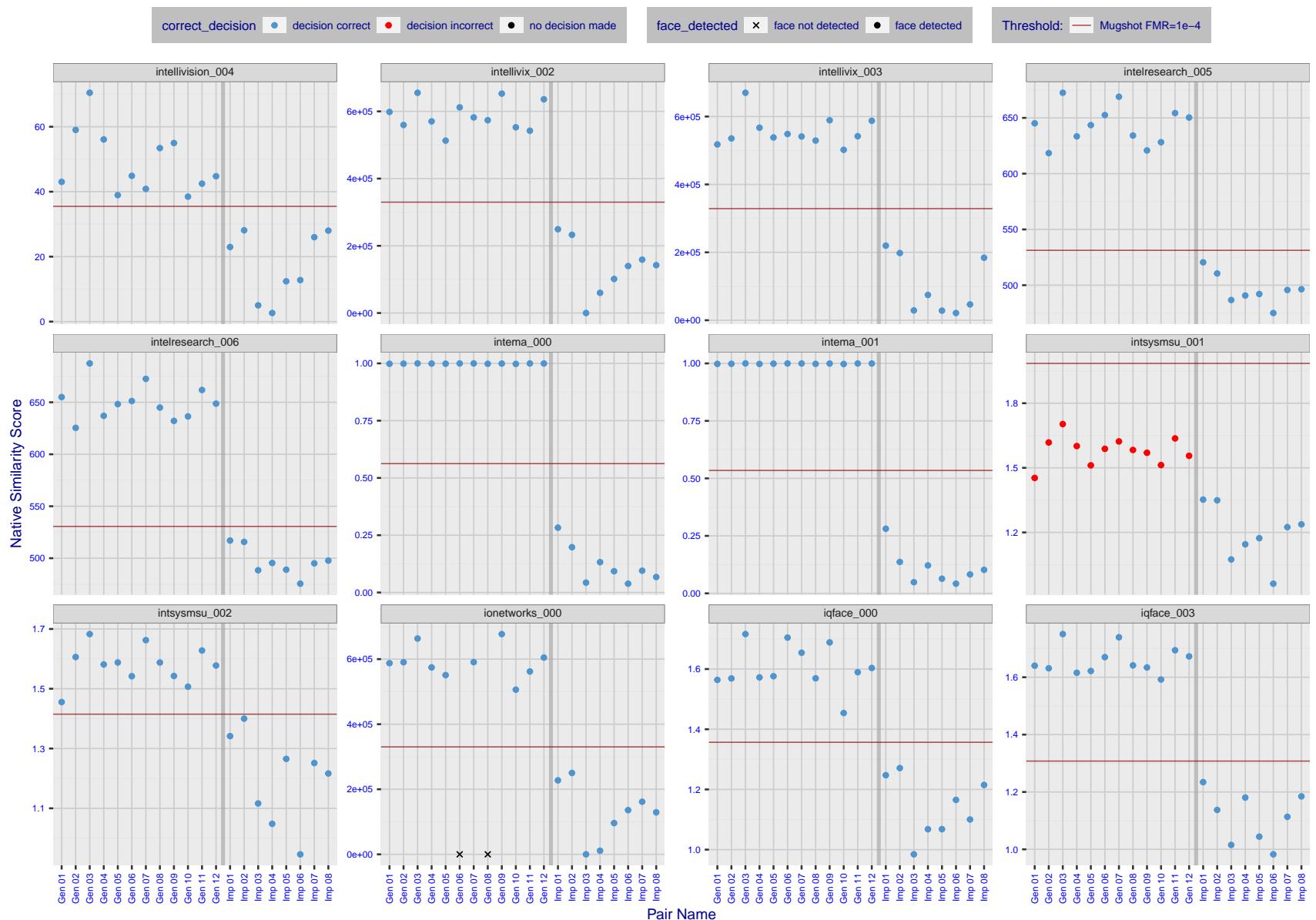


Figure 21: The figure shows algorithms' similarity scores for 12 genuine and 8 impostor image pairs used in a May 2018 paper by Phillips et al. ([1]). The threshold (red horizontal line) is a value calibrated to give $FMR = 0.0001$ on mugshot images. Points above the threshold correspond to pairs determined to be genuine, and points below the threshold correspond to pairs determined to be impostors. If the determined class (genuine or impostor) matches the real class, points will be blue; if not, red. An X represents face detection failure in either of the images in the pair. Note that the sample size ($n=20$) is small, and the figure may change substantially if larger or different sets are used. The images can be viewed on p. 13 of the Appendix, where Gen 01 corresponds to Same-Identity Pair 1, Gen 02 corresponds to Same-Identity Pair 2, and so on.

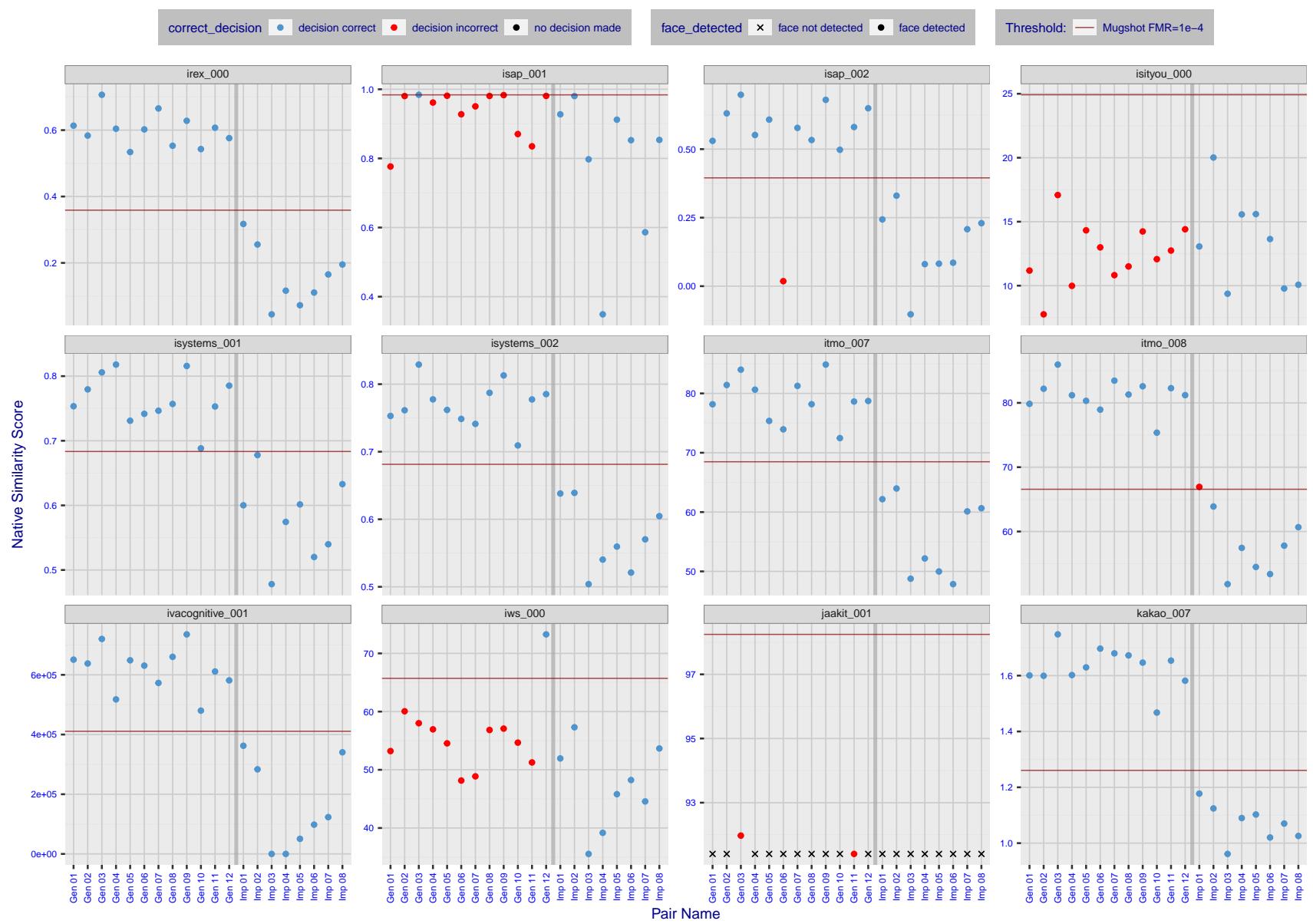


Figure 22: The figure shows algorithms' similarity scores for 12 genuine and 8 impostor image pairs used in a May 2018 paper by Phillips et al. ([1]). The threshold (red horizontal line) is a value calibrated to give $FMR = 0.0001$ on mugshot images. Points above the threshold correspond to pairs determined to be genuine, and points below the threshold correspond to pairs determined to be impostors. If the determined class (genuine or impostor) matches the real class, points will be blue; if not, red. An X represents face detection failure in either of the images in the pair. Note that the sample size ($n=20$) is small, and the figure may change substantially if larger or different sets are used. The images can be viewed on p. 13 of the Appendix, where Gen 01 corresponds to Same-Identity Pair 1, Gen 02 corresponds to Same-Identity Pair 2, and so on.

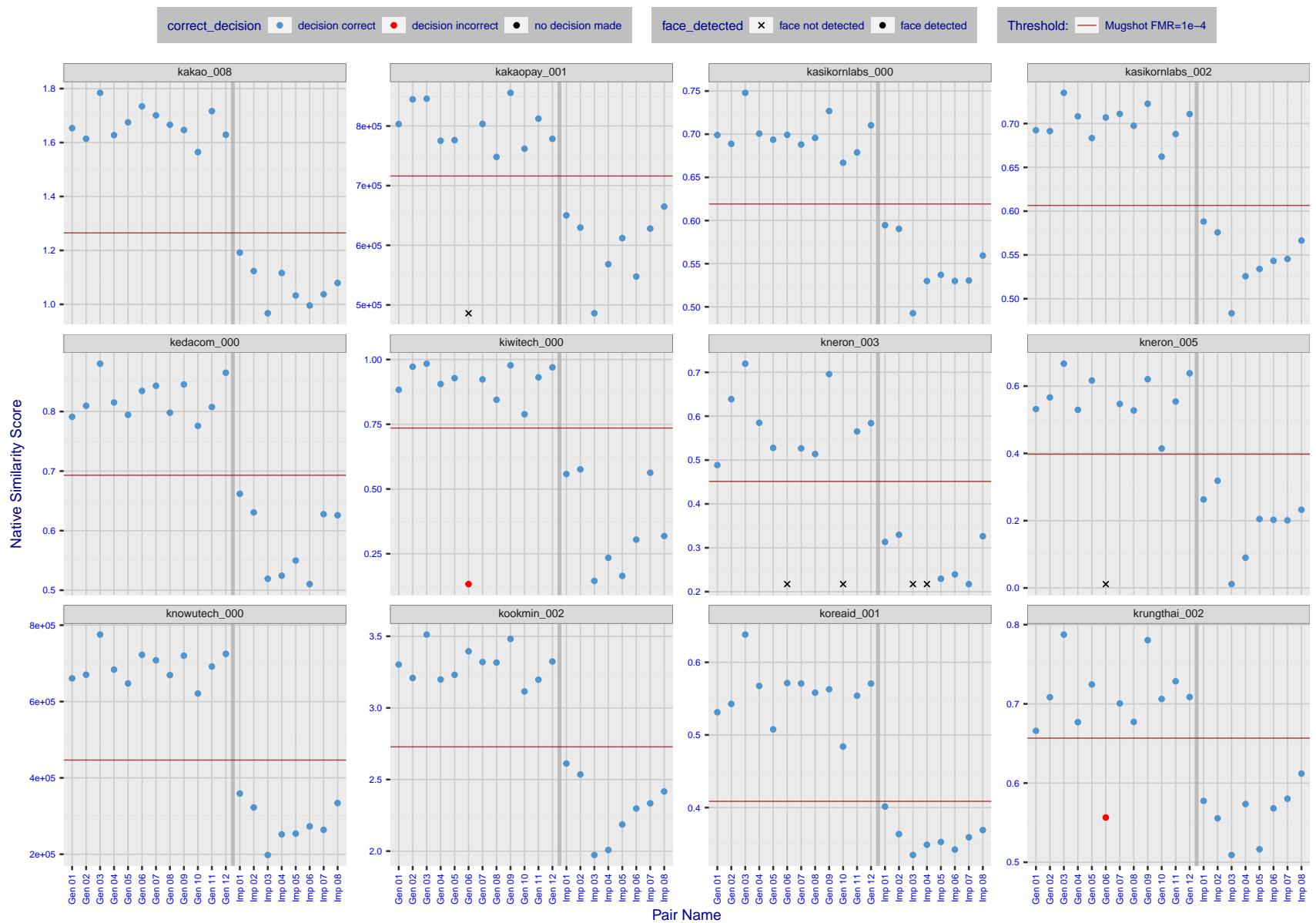


Figure 23: The figure shows algorithms' similarity scores for 12 genuine and 8 impostor image pairs used in a May 2018 paper by Phillips et al. ([1]). The threshold (red horizontal line) is a value calibrated to give $FMR = 0.0001$ on mugshot images. Points above the threshold correspond to pairs determined to be genuine, and points below the threshold correspond to pairs determined to be impostors. If the determined class (genuine or impostor) matches the real class, points will be blue; if not, red. An X represents face detection failure in either of the images in the pair. Note that the sample size ($n=20$) is small, and the figure may change substantially if larger or different sets are used. The images can be viewed on p. 13 of the Appendix, where Gen 01 corresponds to Same-Identity Pair 1, Gen 02 corresponds to Same-Identity Pair 2, and so on.

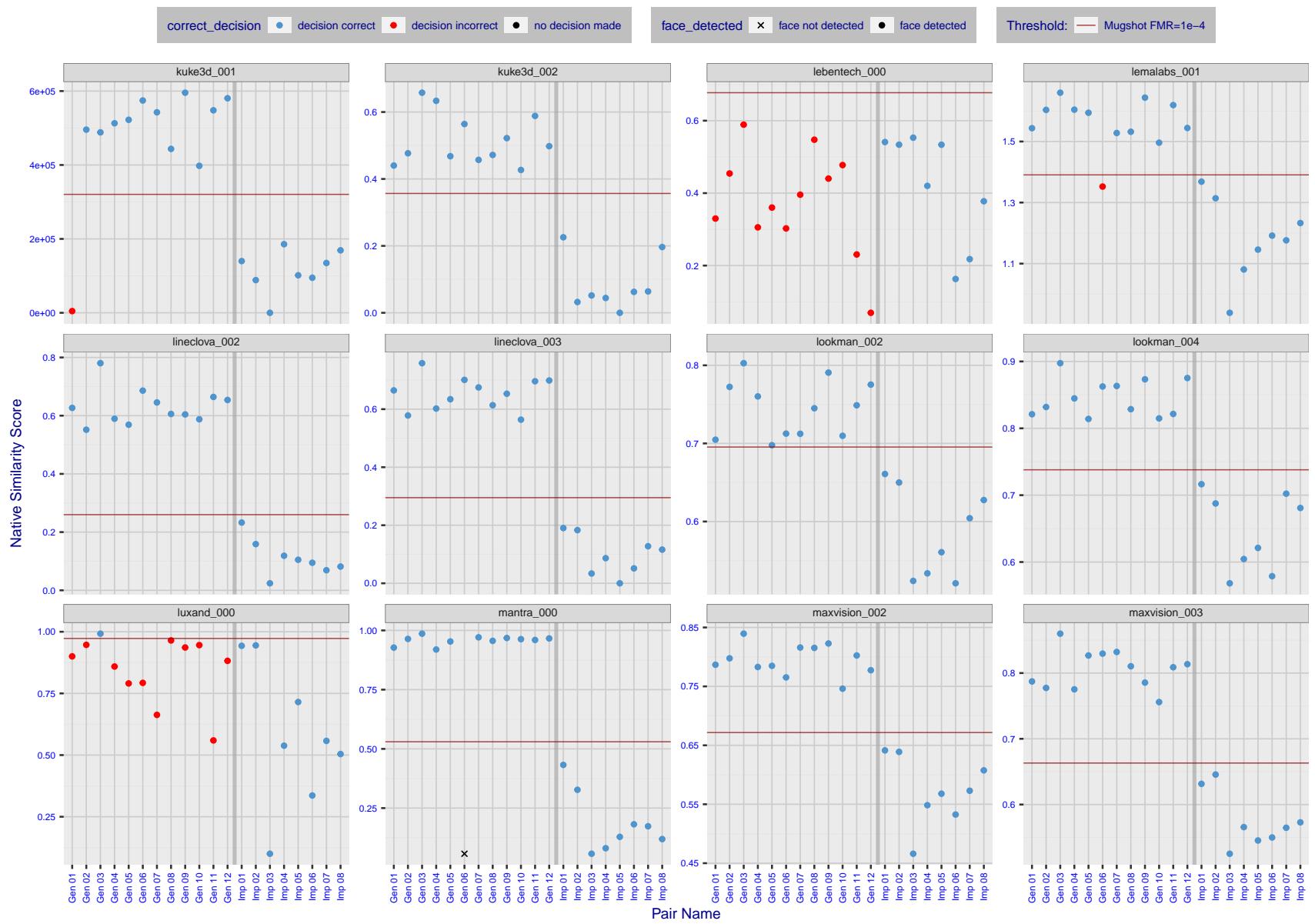


Figure 24: The figure shows algorithms' similarity scores for 12 genuine and 8 impostor image pairs used in a May 2018 paper by Phillips et al. ([1]). The threshold (red horizontal line) is a value calibrated to give $FMR = 0.0001$ on mugshot images. Points above the threshold correspond to pairs determined to be genuine, and points below the threshold correspond to pairs determined to be impostors. If the determined class (genuine or impostor) matches the real class, points will be blue; if not, red. An X represents face detection failure in either of the images in the pair. Note that the sample size ($n=20$) is small, and the figure may change substantially if larger or different sets are used. The images can be viewed on p. 13 of the Appendix, where Gen 01 corresponds to Same-Identity Pair 1, Gen 02 corresponds to Same-Identity Pair 2, and so on.

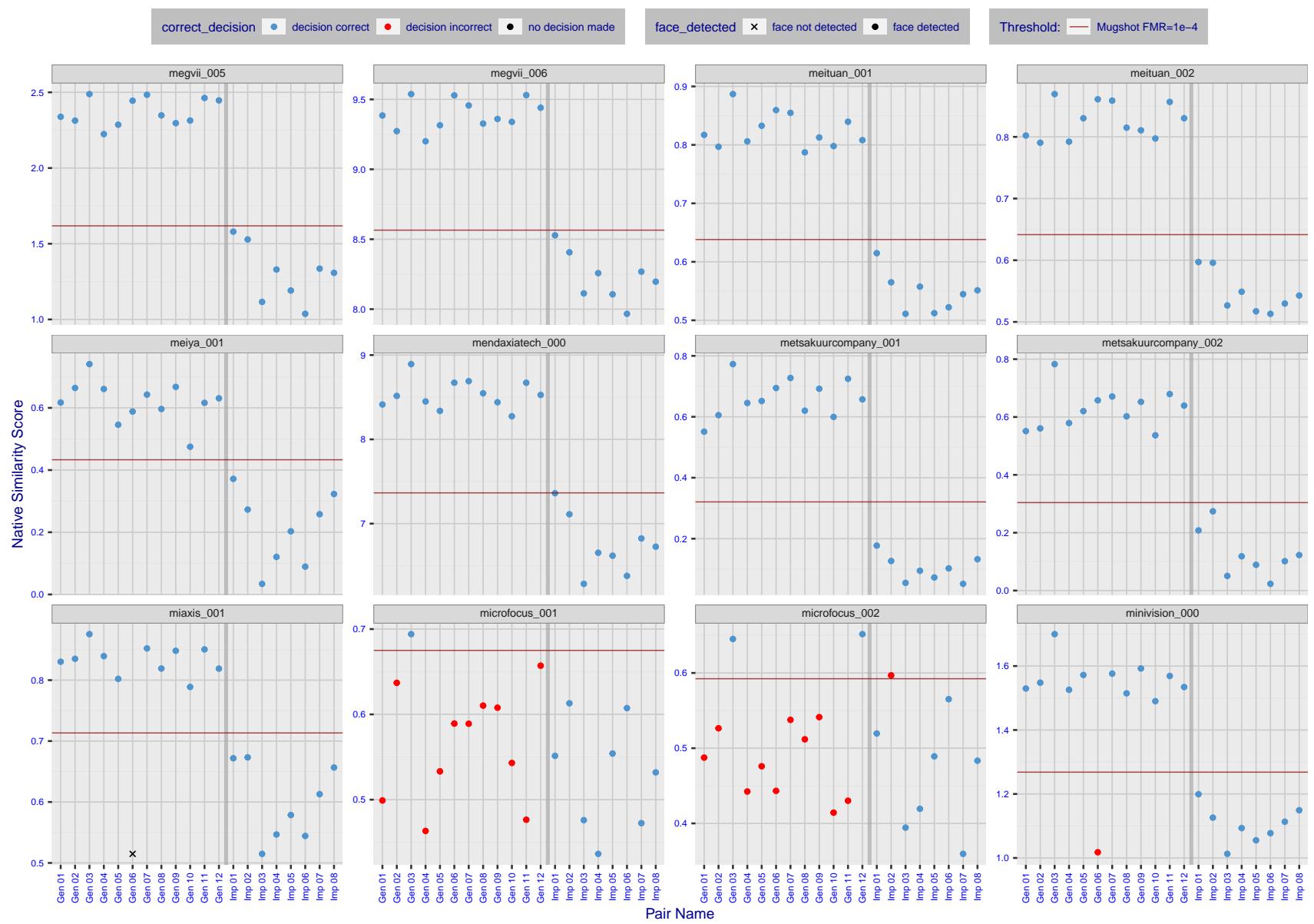


Figure 25: The figure shows algorithms' similarity scores for 12 genuine and 8 impostor image pairs used in a May 2018 paper by Phillips et al. ([1]). The threshold (red horizontal line) is a value calibrated to give $FMR = 0.0001$ on mugshot images. Points above the threshold correspond to pairs determined to be genuine, and points below the threshold correspond to pairs determined to be impostors. If the determined class (genuine or impostor) matches the real class, points will be blue; if not, red. An X represents face detection failure in either of the images in the pair. Note that the sample size ($n=20$) is small, and the figure may change substantially if larger or different sets are used. The images can be viewed on p. 13 of the Appendix, where Gen 01 corresponds to Same-Identity Pair 1, Gen 02 corresponds to Same-Identity Pair 2, and so on.

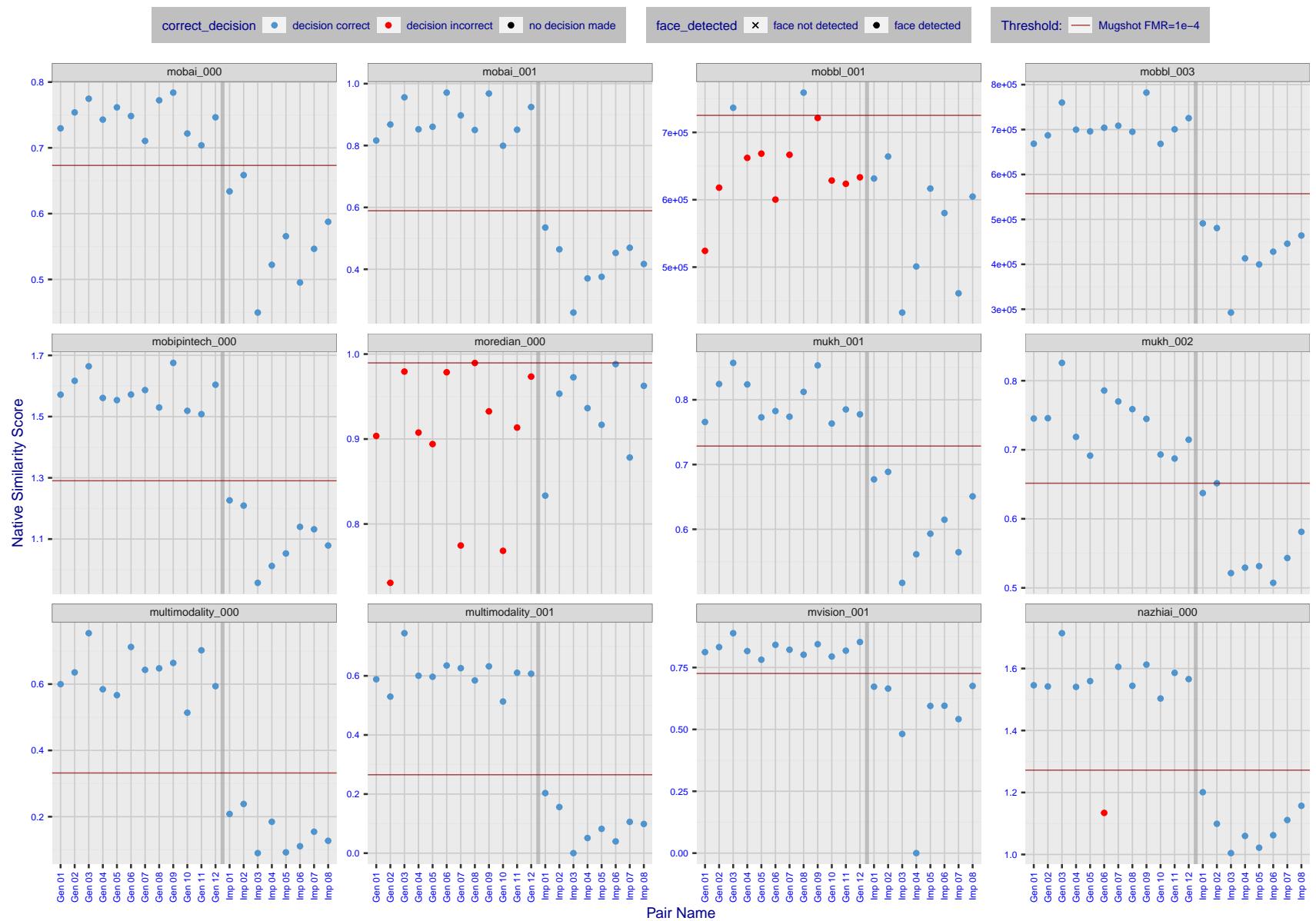


Figure 26: The figure shows algorithms' similarity scores for 12 genuine and 8 impostor image pairs used in a May 2018 paper by Phillips et al. ([1]). The threshold (red horizontal line) is a value calibrated to give $FMR = 0.0001$ on mugshot images. Points above the threshold correspond to pairs determined to be genuine, and points below the threshold correspond to pairs determined to be impostors. If the determined class (genuine or impostor) matches the real class, points will be blue; if not, red. An X represents face detection failure in either of the images in the pair. Note that the sample size ($n=20$) is small, and the figure may change substantially if larger or different sets are used. The images can be viewed on p. 13 of the Appendix, where Gen 01 corresponds to Same-Identity Pair 1, Gen 02 corresponds to Same-Identity Pair 2, and so on.

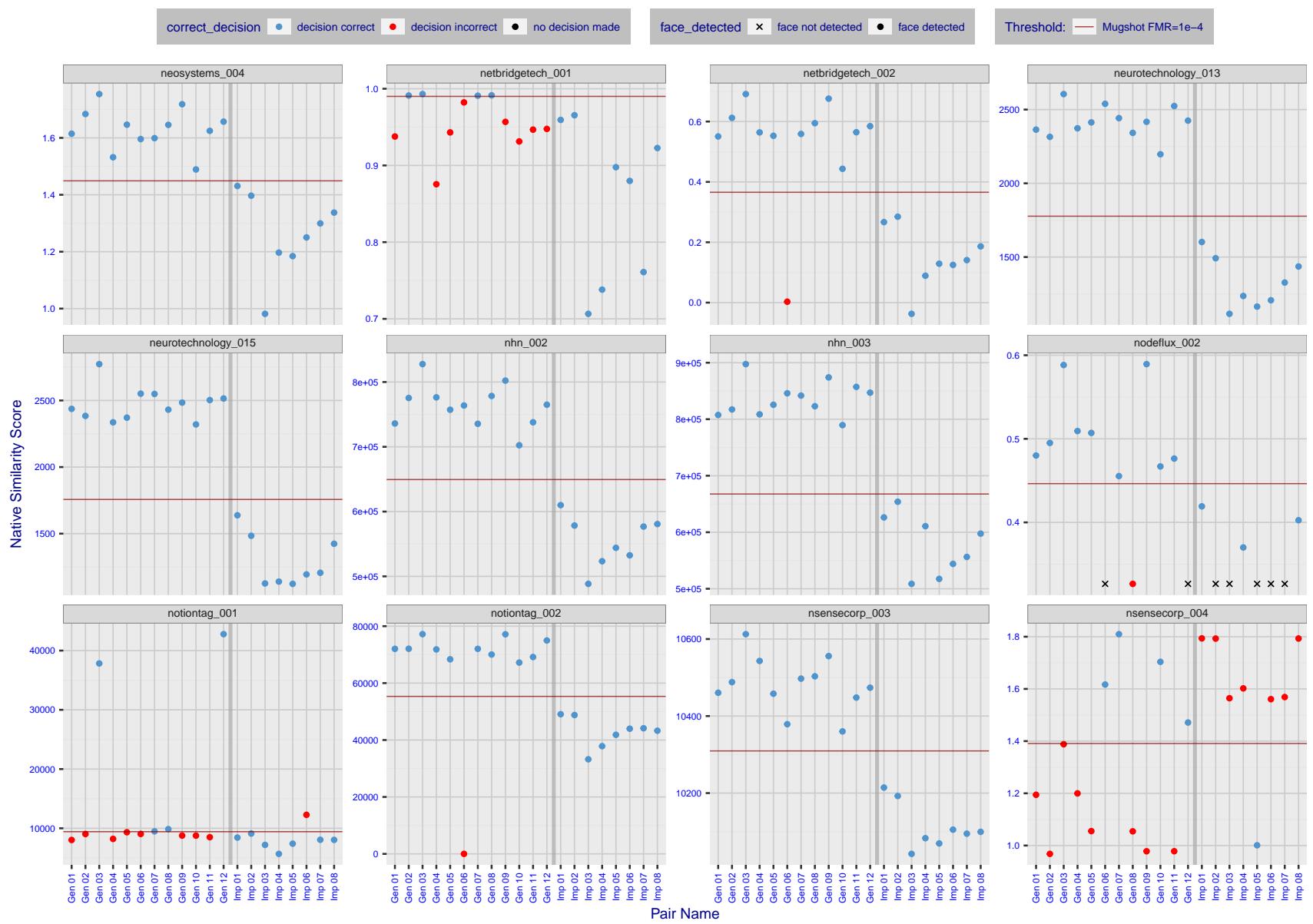


Figure 27: The figure shows algorithms' similarity scores for 12 genuine and 8 impostor image pairs used in a May 2018 paper by Phillips et al. ([1]). The threshold (red horizontal line) is a value calibrated to give $FMR = 0.0001$ on mugshot images. Points above the threshold correspond to pairs determined to be genuine, and points below the threshold correspond to pairs determined to be impostors. If the determined class (genuine or impostor) matches the real class, points will be blue; if not, red. An X represents face detection failure in either of the images in the pair. Note that the sample size ($n=20$) is small, and the figure may change substantially if larger or different sets are used. The images can be viewed on p. 13 of the Appendix, where Gen 01 corresponds to Same-Identity Pair 1, Gen 02 corresponds to Same-Identity Pair 2, and so on.

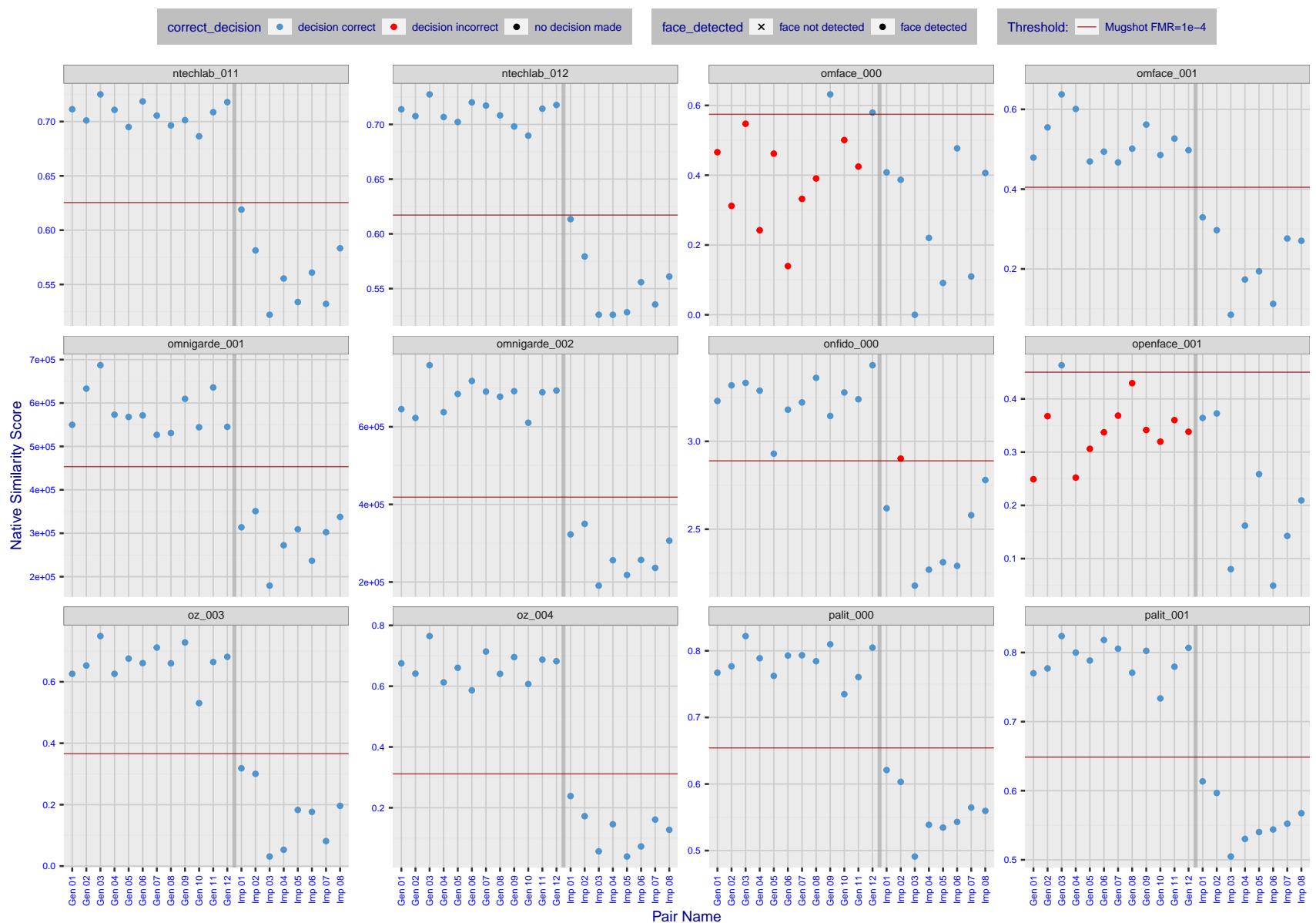


Figure 28: The figure shows algorithms' similarity scores for 12 genuine and 8 impostor image pairs used in a May 2018 paper by Phillips et al. ([1]). The threshold (red horizontal line) is a value calibrated to give $FMR = 0.0001$ on mugshot images. Points above the threshold correspond to pairs determined to be genuine, and points below the threshold correspond to pairs determined to be impostors. If the determined class (genuine or impostor) matches the real class, points will be blue; if not, red. An X represents face detection failure in either of the images in the pair. Note that the sample size ($n=20$) is small, and the figure may change substantially if larger or different sets are used. The images can be viewed on p. 13 of the Appendix, where Gen 01 corresponds to Same-Identity Pair 1, Gen 02 corresponds to Same-Identity Pair 2, and so on.

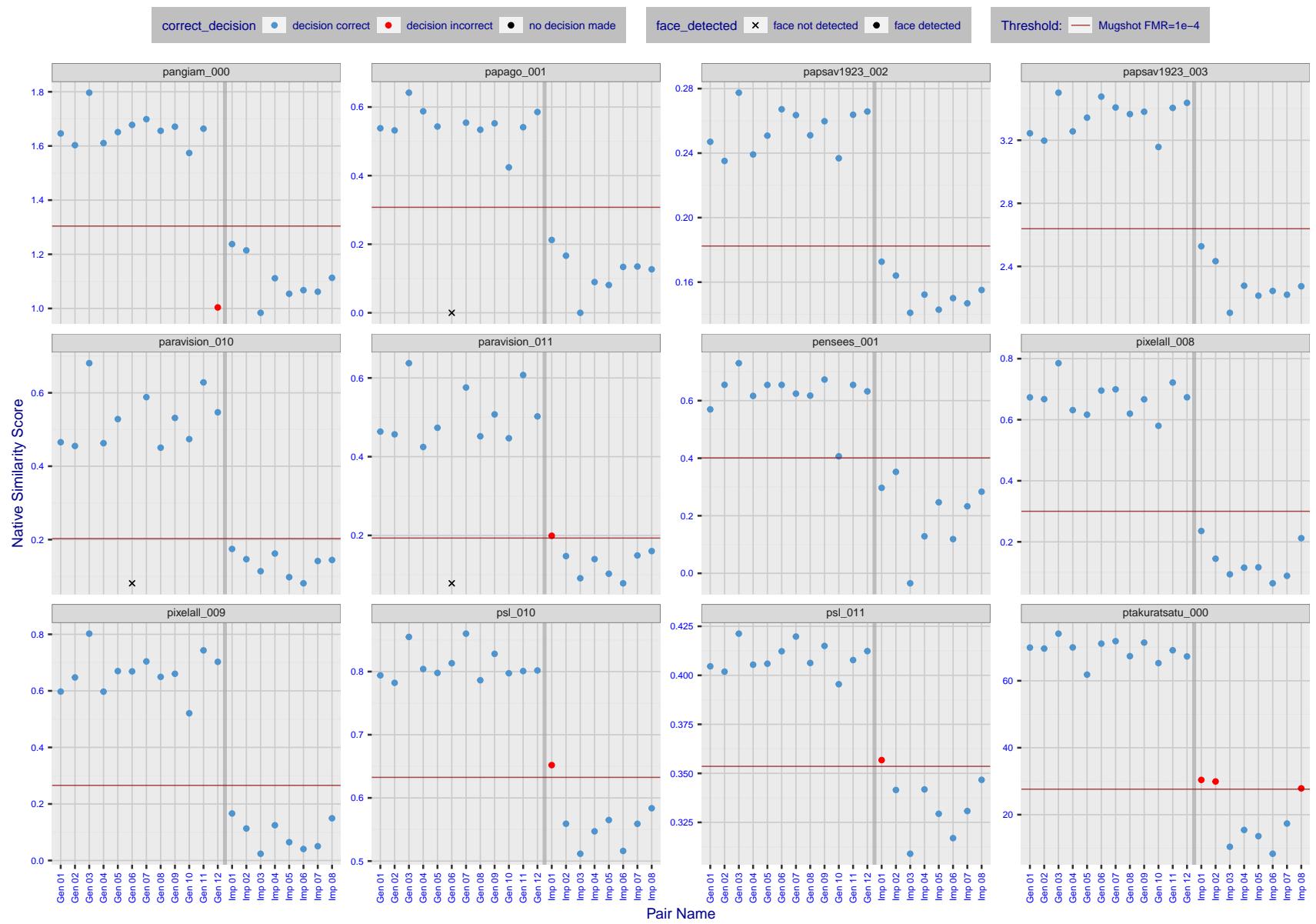


Figure 29: The figure shows algorithms' similarity scores for 12 genuine and 8 impostor image pairs used in a May 2018 paper by Phillips et al. ([1]). The threshold (red horizontal line) is a value calibrated to give $FMR = 0.0001$ on mugshot images. Points above the threshold correspond to pairs determined to be genuine, and points below the threshold correspond to pairs determined to be impostors. If the determined class (genuine or impostor) matches the real class, points will be blue; if not, red. An X represents face detection failure in either of the images in the pair. Note that the sample size ($n=20$) is small, and the figure may change substantially if larger or different sets are used. The images can be viewed on p. 13 of the Appendix, where Gen 01 corresponds to Same-Identity Pair 1, Gen 02 corresponds to Same-Identity Pair 2, and so on.

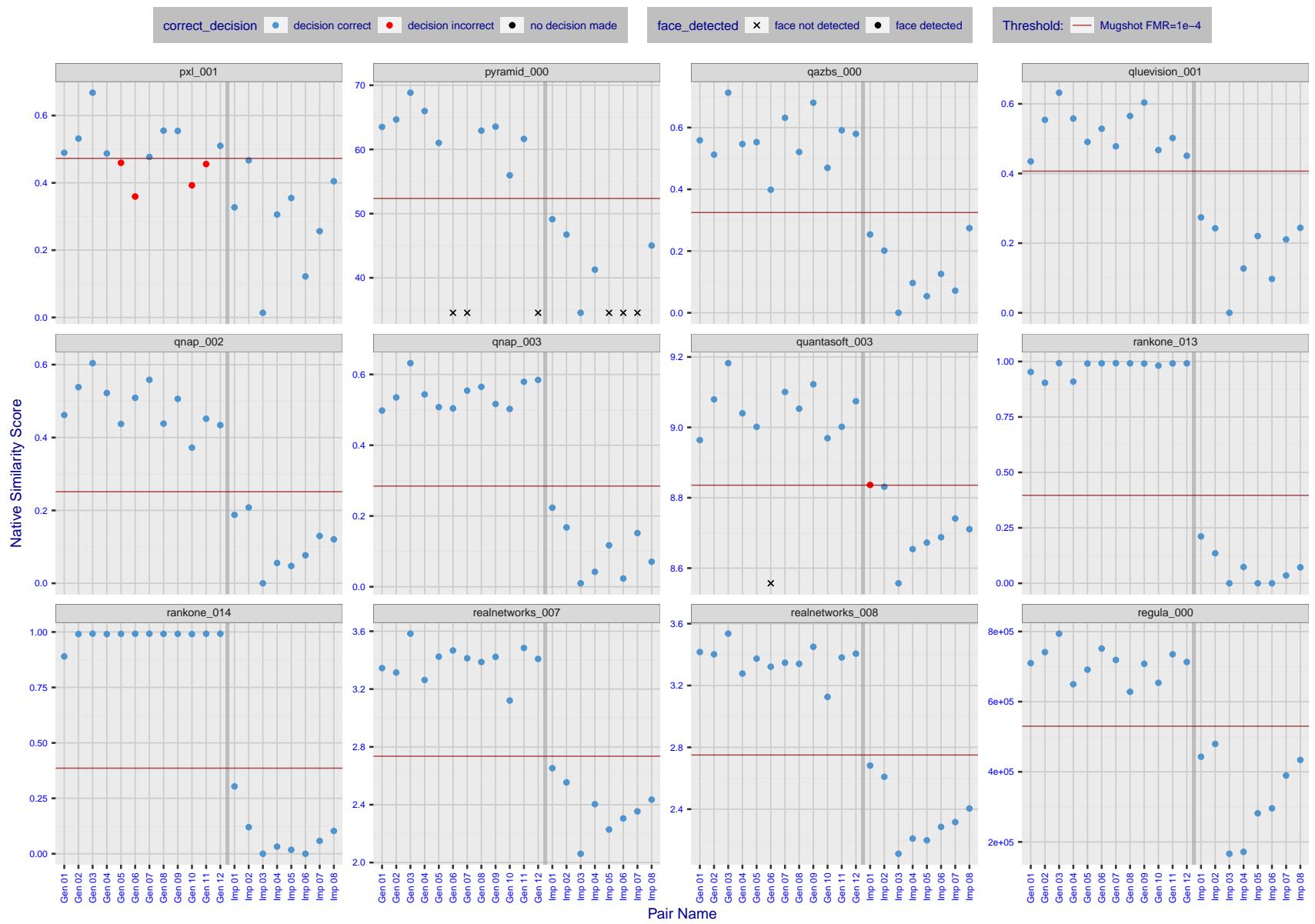


Figure 30: The figure shows algorithms' similarity scores for 12 genuine and 8 impostor image pairs used in a May 2018 paper by Phillips et al. ([1]). The threshold (red horizontal line) is a value calibrated to give $FMR = 0.0001$ on mugshot images. Points above the threshold correspond to pairs determined to be genuine, and points below the threshold correspond to pairs determined to be impostors. If the determined class (genuine or impostor) matches the real class, points will be blue; if not, red. An X represents face detection failure in either of the images in the pair. Note that the sample size ($n=20$) is small, and the figure may change substantially if larger or different sets are used. The images can be viewed on p. 13 of the Appendix, where Gen 01 corresponds to Same-Identity Pair 1, Gen 02 corresponds to Same-Identity Pair 2, and so on.

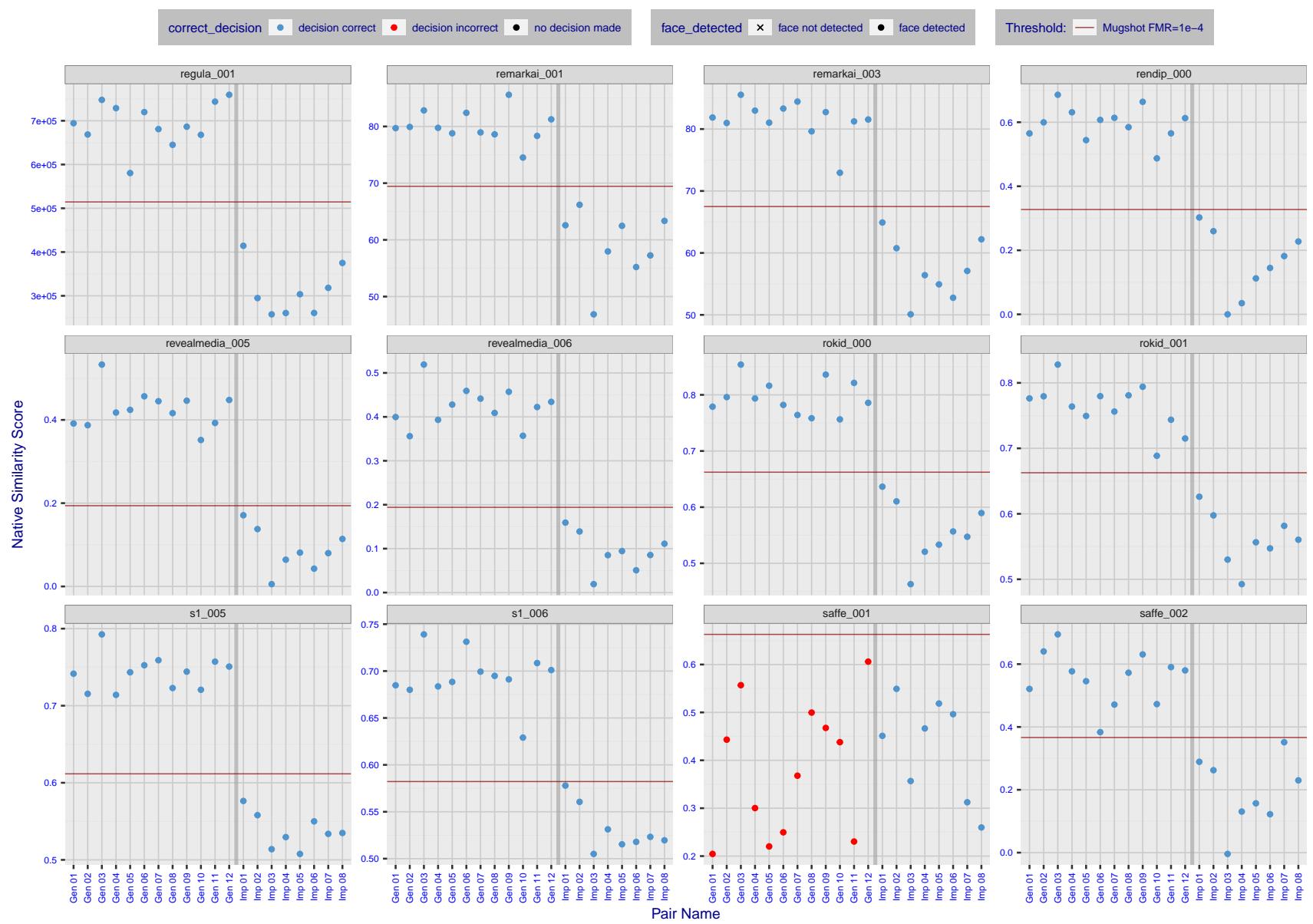


Figure 31: The figure shows algorithms' similarity scores for 12 genuine and 8 impostor image pairs used in a May 2018 paper by Phillips et al. ([1]). The threshold (red horizontal line) is a value calibrated to give $FMR = 0.0001$ on mugshot images. Points above the threshold correspond to pairs determined to be genuine, and points below the threshold correspond to pairs determined to be impostors. If the determined class (genuine or impostor) matches the real class, points will be blue; if not, red. An X represents face detection failure in either of the images in the pair. Note that the sample size ($n=20$) is small, and the figure may change substantially if larger or different sets are used. The images can be viewed on p. 13 of the Appendix, where Gen 01 corresponds to Same-Identity Pair 1, Gen 02 corresponds to Same-Identity Pair 2, and so on.

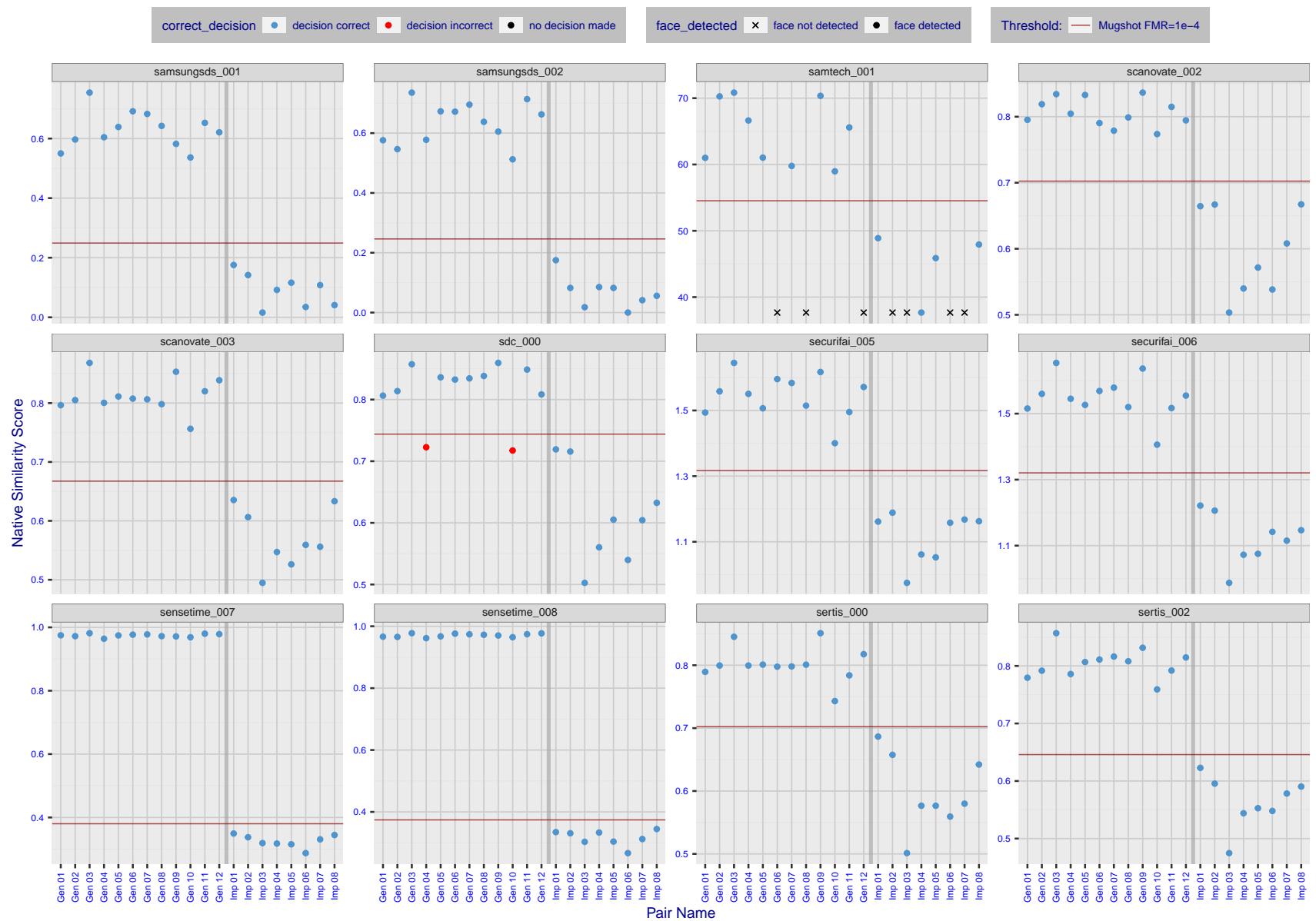


Figure 32: The figure shows algorithms' similarity scores for 12 genuine and 8 impostor image pairs used in a May 2018 paper by Phillips et al. ([1]). The threshold (red horizontal line) is a value calibrated to give $FMR = 0.0001$ on mugshot images. Points above the threshold correspond to pairs determined to be genuine, and points below the threshold correspond to pairs determined to be impostors. If the determined class (genuine or impostor) matches the real class, points will be blue; if not, red. An X represents face detection failure in either of the images in the pair. Note that the sample size ($n=20$) is small, and the figure may change substantially if larger or different sets are used. The images can be viewed on p. 13 of the Appendix, where Gen 01 corresponds to Same-Identity Pair 1, Gen 02 corresponds to Same-Identity Pair 2, and so on.

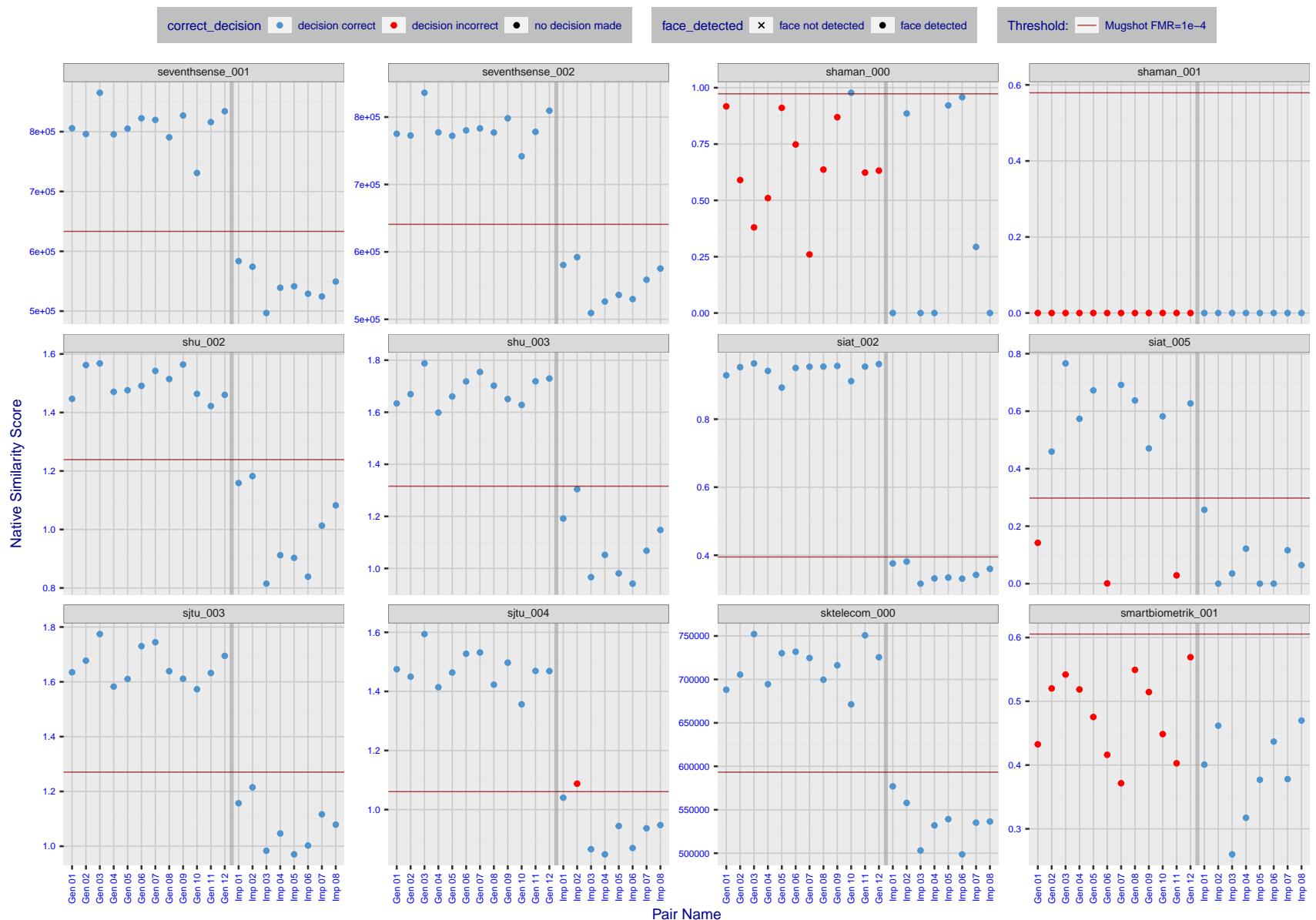


Figure 33: The figure shows algorithms' similarity scores for 12 genuine and 8 impostor image pairs used in a May 2018 paper by Phillips et al. ([1]). The threshold (red horizontal line) is a value calibrated to give $FMR = 0.0001$ on mugshot images. Points above the threshold correspond to pairs determined to be genuine, and points below the threshold correspond to pairs determined to be impostors. If the determined class (genuine or impostor) matches the real class, points will be blue; if not, red. An X represents face detection failure in either of the images in the pair. Note that the sample size ($n=20$) is small, and the figure may change substantially if larger or different sets are used. The images can be viewed on p. 13 of the Appendix, where Gen 01 corresponds to Same-Identity Pair 1, Gen 02 corresponds to Same-Identity Pair 2, and so on.

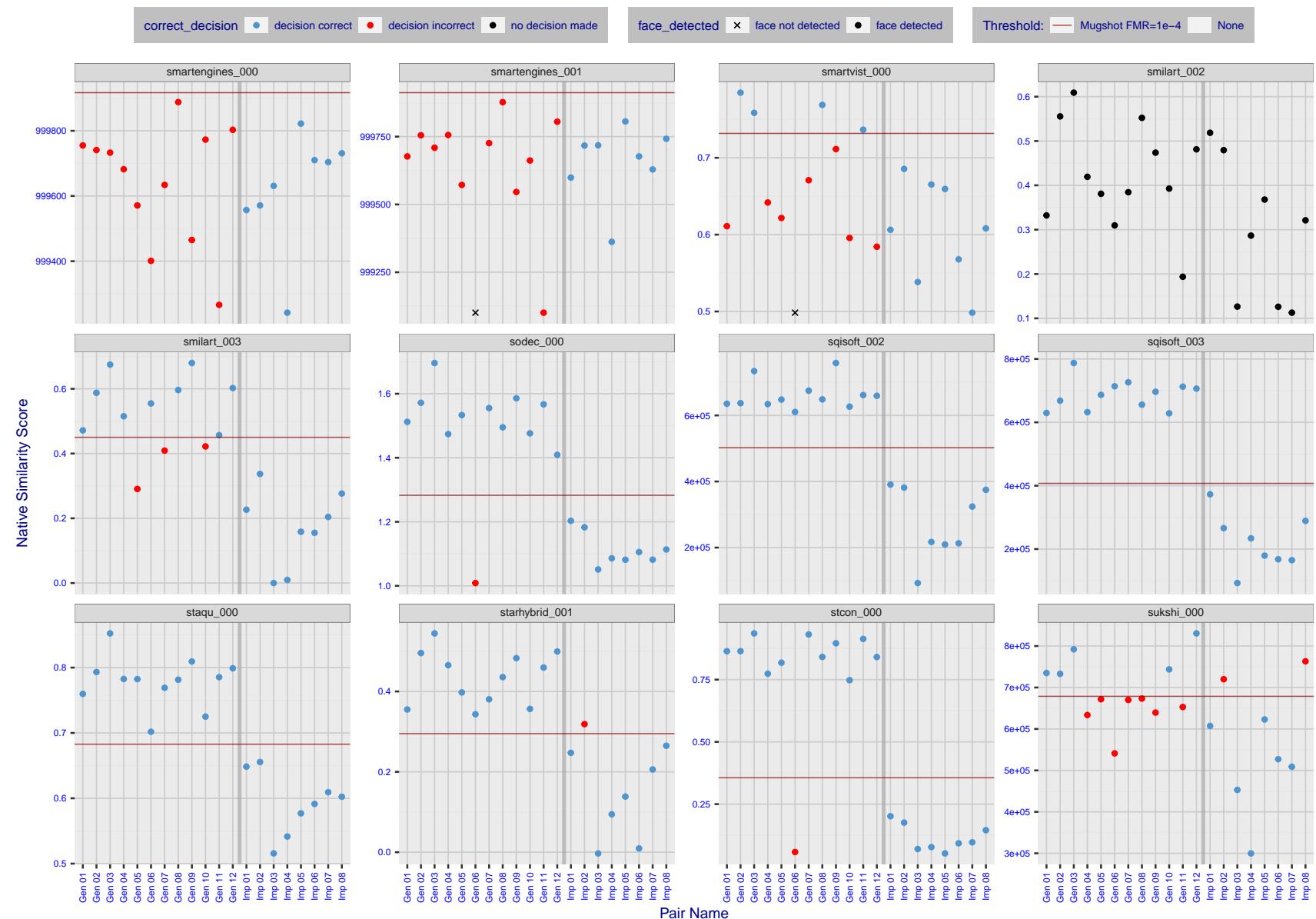


Figure 34: The figure shows algorithms' similarity scores for 12 genuine and 8 impostor image pairs used in a May 2018 paper by Phillips et al. ([1]). The threshold (red horizontal line) is a value calibrated to give $FMR = 0.0001$ on mugshot images. Points above the threshold correspond to pairs determined to be genuine, and points below the threshold correspond to pairs determined to be impostors. If the determined class (genuine or impostor) matches the real class, points will be blue; if not, red. An X represents face detection failure in either of the images in the pair. Note that the sample size ($n=20$) is small, and the figure may change substantially if larger or different sets are used. The images can be viewed on p. 13 of the Appendix, where Gen 01 corresponds to Same-Identity Pair 1, Gen 02 corresponds to Same-Identity Pair 2, and so on.

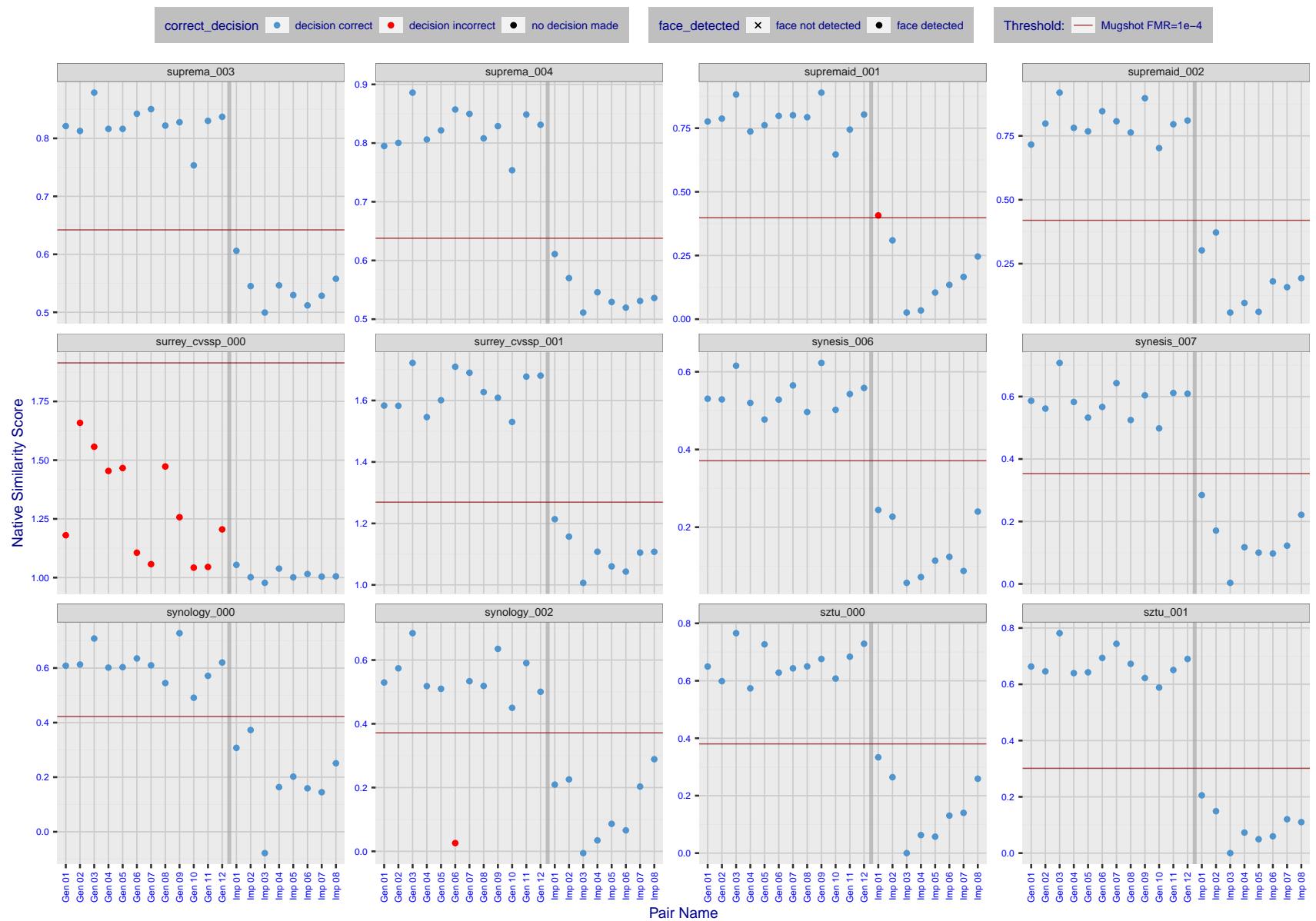


Figure 35: The figure shows algorithms' similarity scores for 12 genuine and 8 impostor image pairs used in a May 2018 paper by Phillips et al. ([1]). The threshold (red horizontal line) is a value calibrated to give $FMR = 0.0001$ on mugshot images. Points above the threshold correspond to pairs determined to be genuine, and points below the threshold correspond to pairs determined to be impostors. If the determined class (genuine or impostor) matches the real class, points will be blue; if not, red. An X represents face detection failure in either of the images in the pair. Note that the sample size ($n=20$) is small, and the figure may change substantially if larger or different sets are used. The images can be viewed on p. 13 of the Appendix, where Gen 01 corresponds to Same-Identity Pair 1, Gen 02 corresponds to Same-Identity Pair 2, and so on.

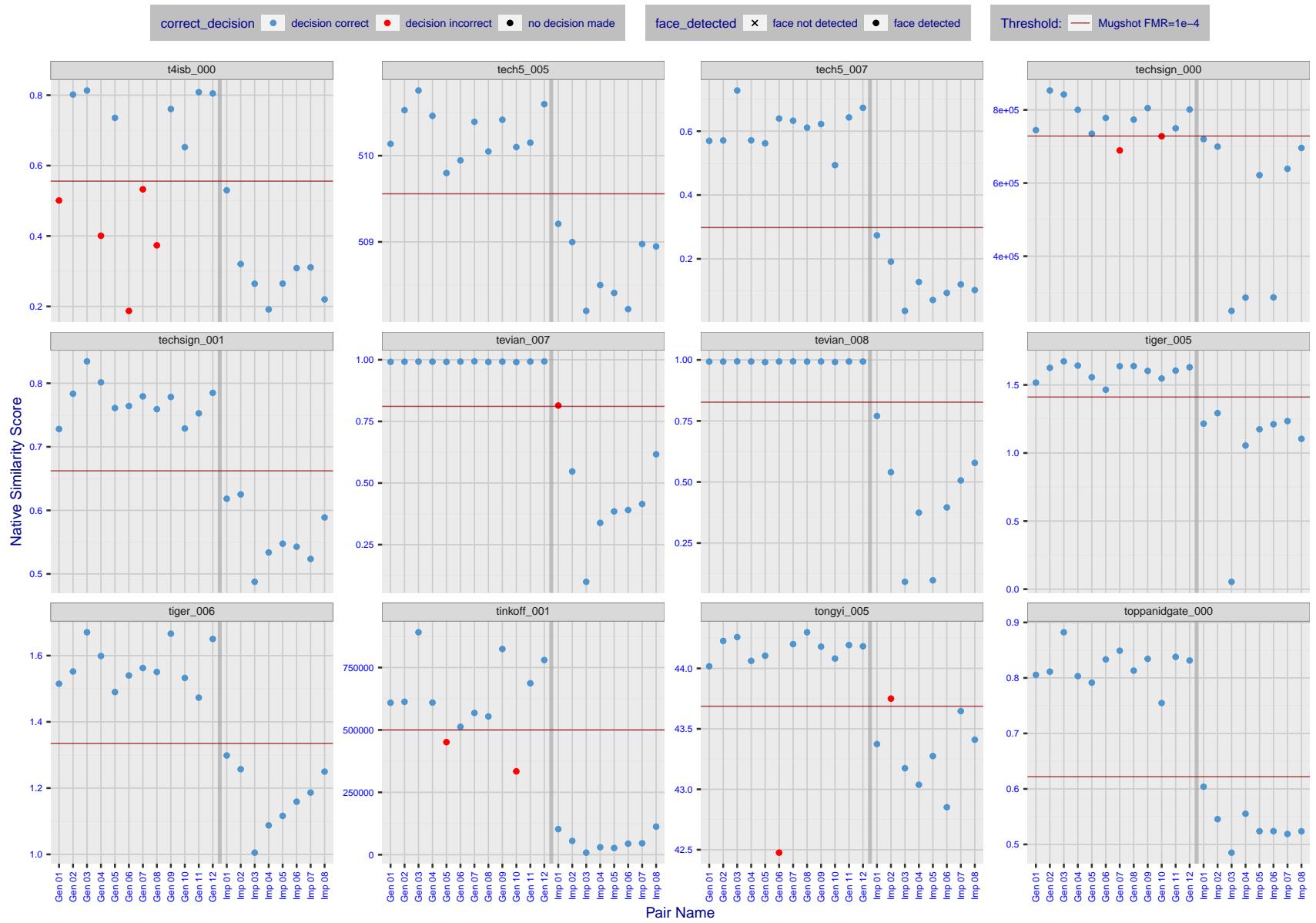


Figure 36: The figure shows algorithms' similarity scores for 12 genuine and 8 impostor image pairs used in a May 2018 paper by Phillips et al. ([1]). The threshold (red horizontal line) is a value calibrated to give $FMR = 0.0001$ on mugshot images. Points above the threshold correspond to pairs determined to be genuine, and points below the threshold correspond to pairs determined to be impostors. If the determined class (genuine or impostor) matches the real class, points will be blue; if not, red. An X represents face detection failure in either of the images in the pair. Note that the sample size ($n=20$) is small, and the figure may change substantially if larger or different sets are used. The images can be viewed on p. 13 of the Appendix, where Gen 01 corresponds to Same-Identity Pair 1, Gen 02 corresponds to Same-Identity Pair 2, and so on.

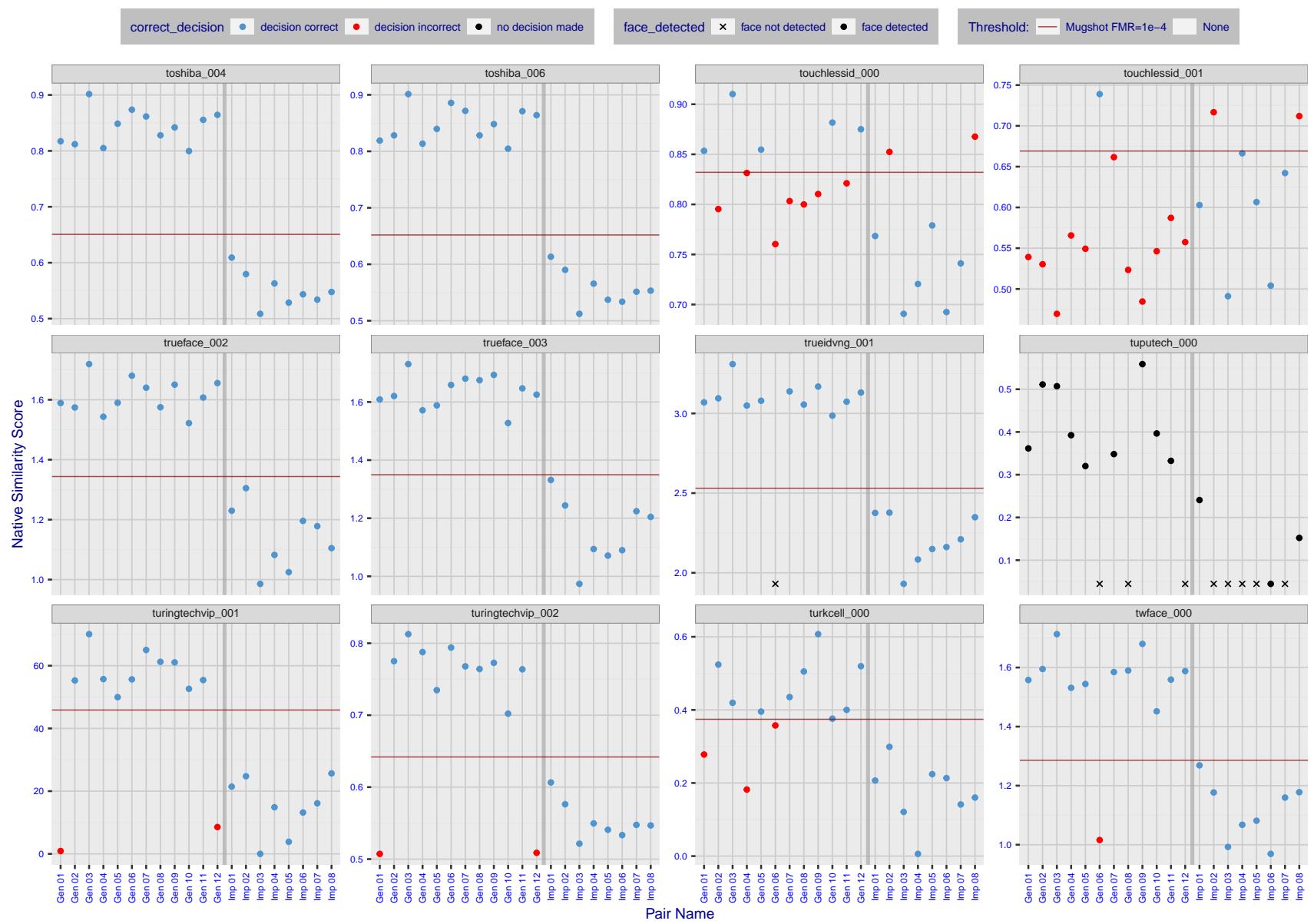


Figure 37: The figure shows algorithms' similarity scores for 12 genuine and 8 impostor image pairs used in a May 2018 paper by Phillips et al. ([1]). The threshold (red horizontal line) is a value calibrated to give $FMR = 0.0001$ on mugshot images. Points above the threshold correspond to pairs determined to be genuine, and points below the threshold correspond to pairs determined to be impostors. If the determined class (genuine or impostor) matches the real class, points will be blue; if not, red. An X represents face detection failure in either of the images in the pair. Note that the sample size ($n=20$) is small, and the figure may change substantially if larger or different sets are used. The images can be viewed on p. 13 of the Appendix, where Gen 01 corresponds to Same-Identity Pair 1, Gen 02 corresponds to Same-Identity Pair 2, and so on.

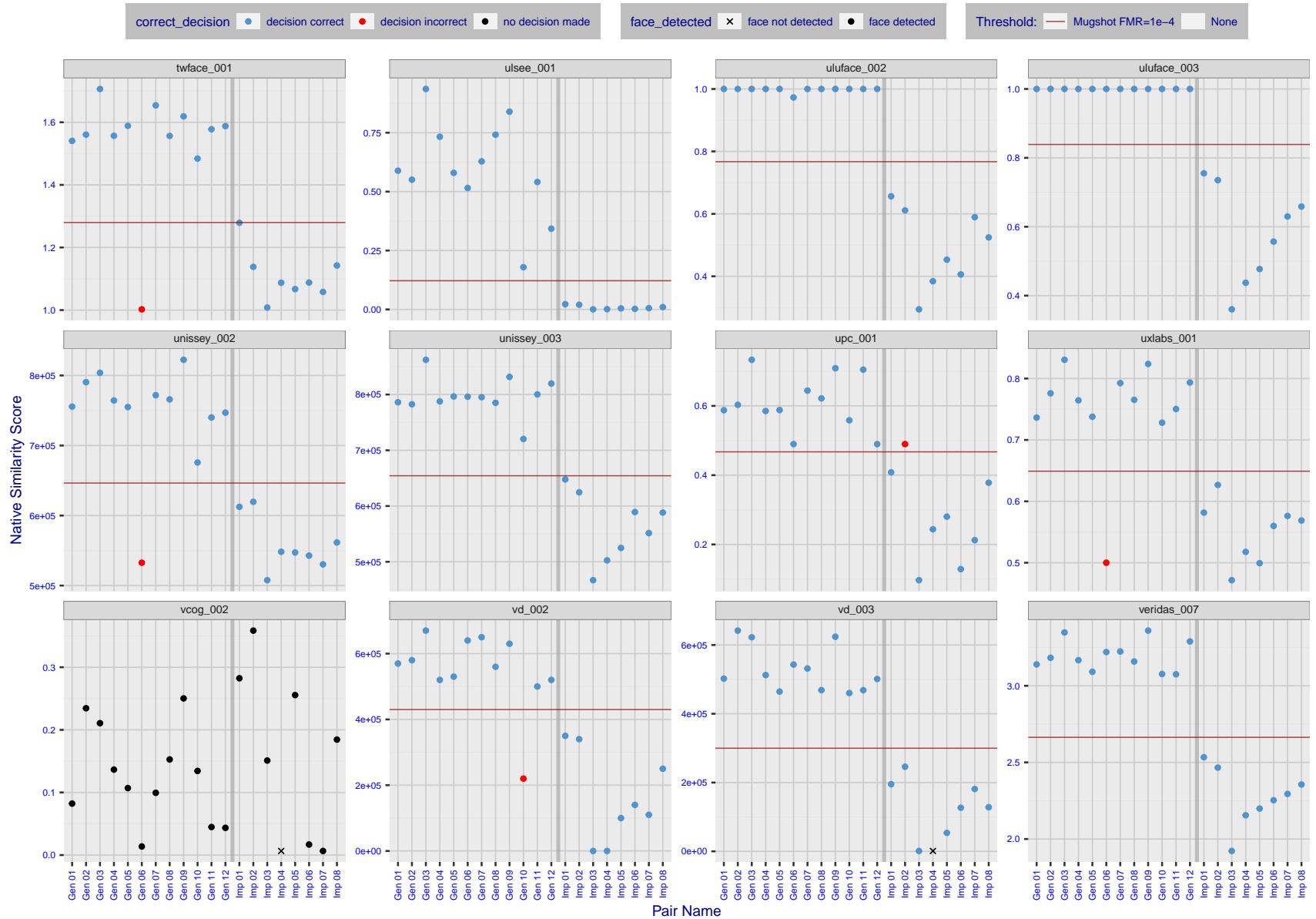


Figure 38: The figure shows algorithms' similarity scores for 12 genuine and 8 impostor image pairs used in a May 2018 paper by Phillips et al. ([1]). The threshold (red horizontal line) is a value calibrated to give $FMR = 0.0001$ on mugshot images. Points above the threshold correspond to pairs determined to be genuine, and points below the threshold correspond to pairs determined to be impostors. If the determined class (genuine or impostor) matches the real class, points will be blue; if not, red. An X represents face detection failure in either of the images in the pair. Note that the sample size ($n=20$) is small, and the figure may change substantially if larger or different sets are used. The images can be viewed on p. 13 of the Appendix, where Gen 01 corresponds to Same-Identity Pair 1, Gen 02 corresponds to Same-Identity Pair 2, and so on.

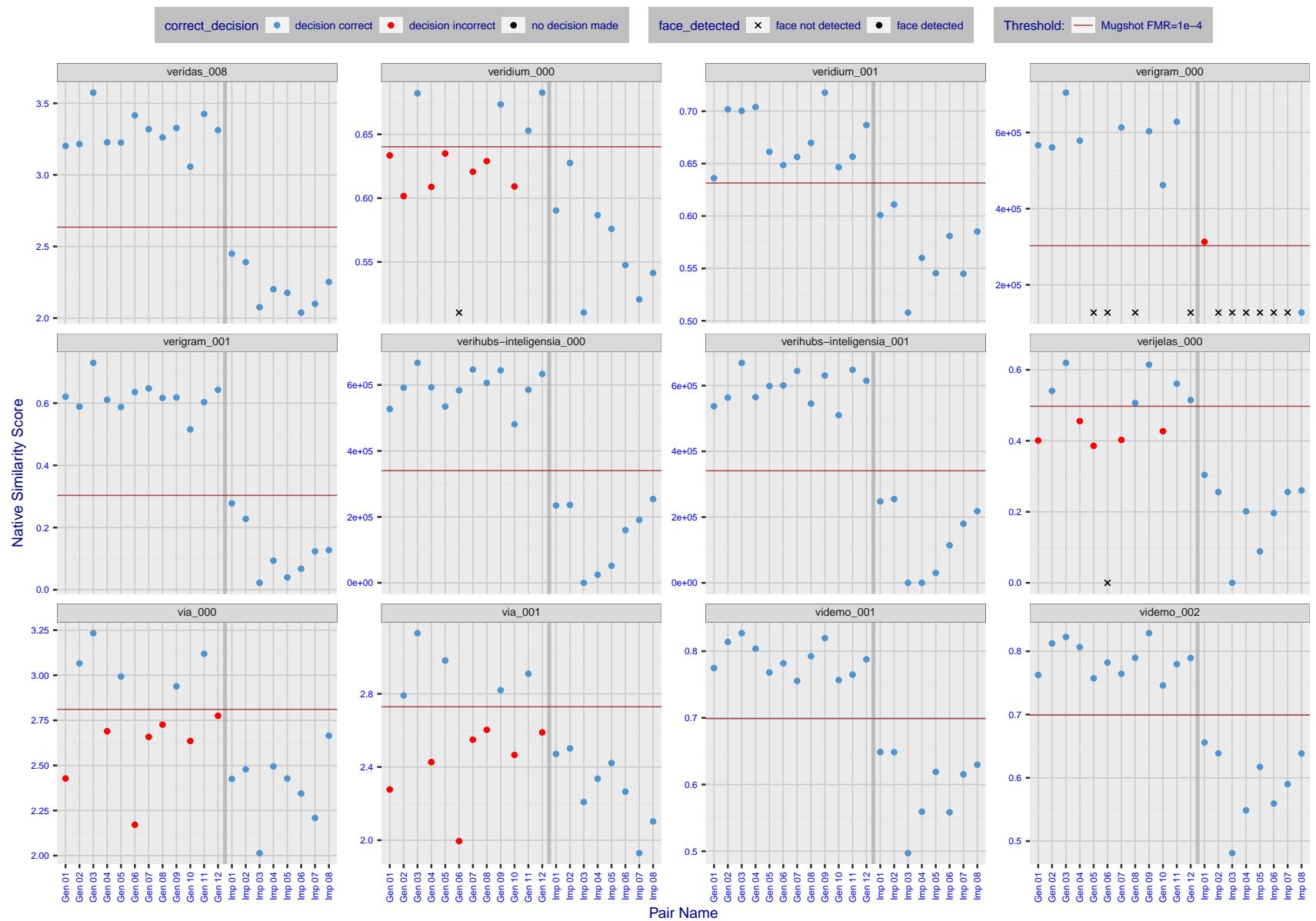


Figure 39: The figure shows algorithms' similarity scores for 12 genuine and 8 impostor image pairs used in a May 2018 paper by Phillips et al. ([1]). The threshold (red horizontal line) is a value calibrated to give $FMR = 0.0001$ on mugshot images. Points above the threshold correspond to pairs determined to be genuine, and points below the threshold correspond to pairs determined to be impostors. If the determined class (genuine or impostor) matches the real class, points will be blue; if not, red. An X represents face detection failure in either of the images in the pair. Note that the sample size ($n=20$) is small, and the figure may change substantially if larger or different sets are used. The images can be viewed on p. 13 of the Appendix, where Gen 01 corresponds to Same-Identity Pair 1, Gen 02 corresponds to Same-Identity Pair 2, and so on.

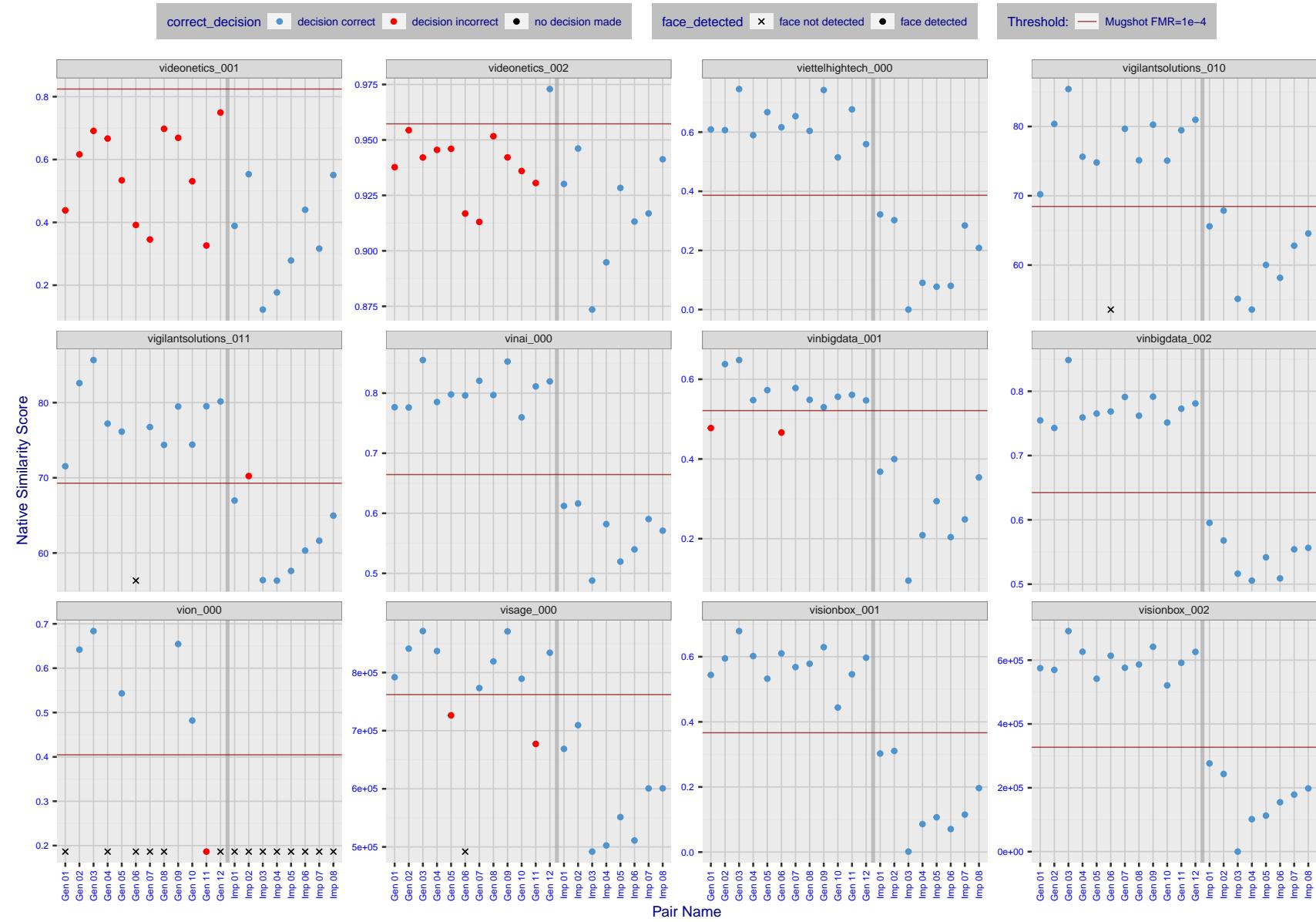


Figure 40: The figure shows algorithms' similarity scores for 12 genuine and 8 impostor image pairs used in a May 2018 paper by Phillips et al. ([1]). The threshold (red horizontal line) is a value calibrated to give $FMR = 0.0001$ on mugshot images. Points above the threshold correspond to pairs determined to be genuine, and points below the threshold correspond to pairs determined to be impostors. If the determined class (genuine or impostor) matches the real class, points will be blue; if not, red. An X represents face detection failure in either of the images in the pair. Note that the sample size ($n=20$) is small, and the figure may change substantially if larger or different sets are used. The images can be viewed on p. 13 of the Appendix, where Gen 01 corresponds to Same-Identity Pair 1, Gen 02 corresponds to Same-Identity Pair 2, and so on.

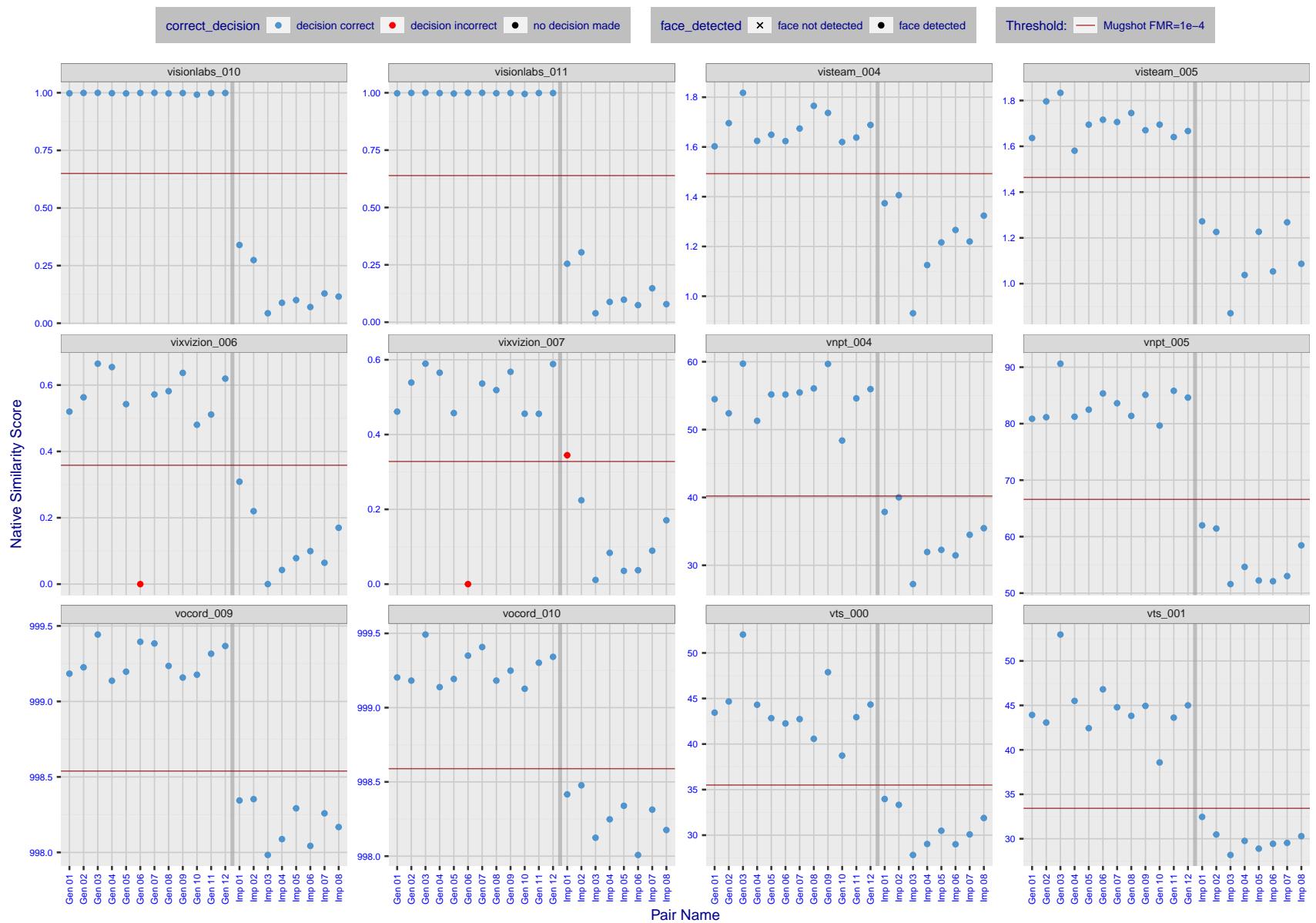


Figure 41: The figure shows algorithms' similarity scores for 12 genuine and 8 impostor image pairs used in a May 2018 paper by Phillips et al. ([1]). The threshold (red horizontal line) is a value calibrated to give $FMR = 0.0001$ on mugshot images. Points above the threshold correspond to pairs determined to be genuine, and points below the threshold correspond to pairs determined to be impostors. If the determined class (genuine or impostor) matches the real class, points will be blue; if not, red. An X represents face detection failure in either of the images in the pair. Note that the sample size ($n=20$) is small, and the figure may change substantially if larger or different sets are used. The images can be viewed on p. 13 of the Appendix, where Gen 01 corresponds to Same-Identity Pair 1, Gen 02 corresponds to Same-Identity Pair 2, and so on.

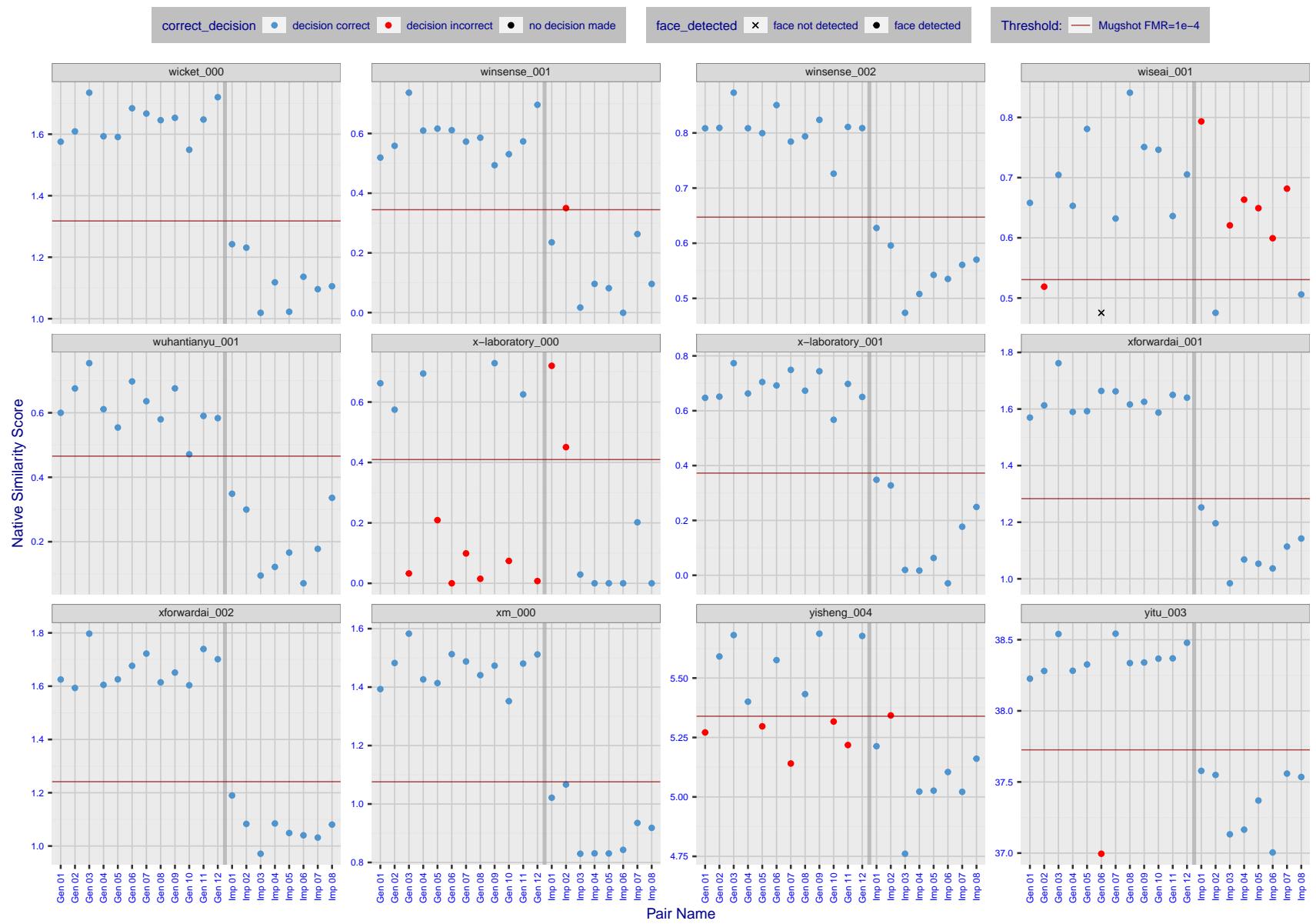


Figure 42: The figure shows algorithms' similarity scores for 12 genuine and 8 impostor image pairs used in a May 2018 paper by Phillips et al. ([1]). The threshold (red horizontal line) is a value calibrated to give $FMR = 0.0001$ on mugshot images. Points above the threshold correspond to pairs determined to be genuine, and points below the threshold correspond to pairs determined to be impostors. If the determined class (genuine or impostor) matches the real class, points will be blue; if not, red. An X represents face detection failure in either of the images in the pair. Note that the sample size ($n=20$) is small, and the figure may change substantially if larger or different sets are used. The images can be viewed on p. 13 of the Appendix, where Gen 01 corresponds to Same-Identity Pair 1, Gen 02 corresponds to Same-Identity Pair 2, and so on.

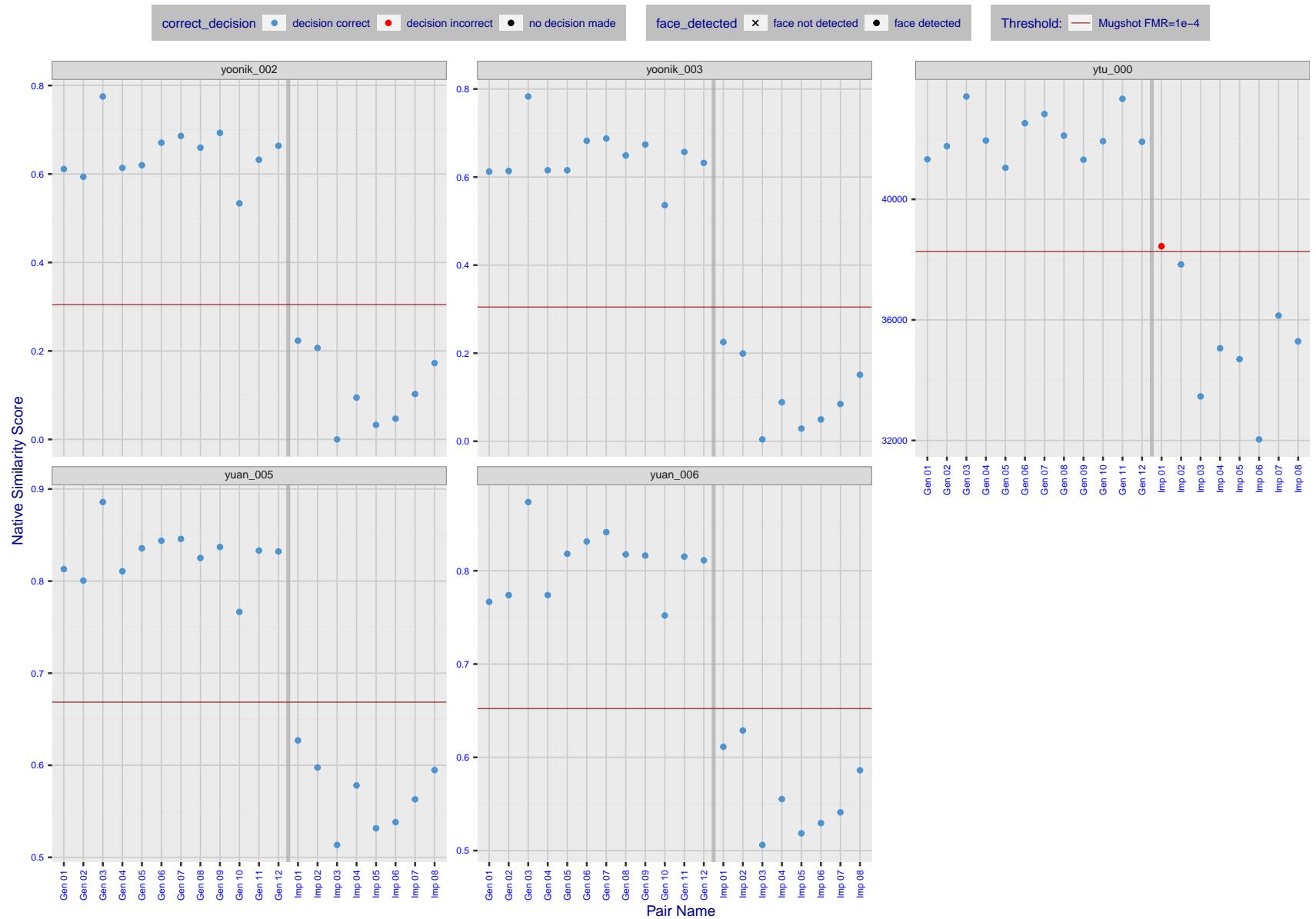


Figure 43: The figure shows algorithms' similarity scores for 12 genuine and 8 impostor image pairs used in a May 2018 paper by Phillips et al. ([1]). The threshold (red horizontal line) is a value calibrated to give $FMR = 0.0001$ on mugshot images. Points above the threshold correspond to pairs determined to be genuine, and points below the threshold correspond to pairs determined to be impostors. If the determined class (genuine or impostor) matches the real class, points will be blue; if not, red. An X represents face detection failure in either of the images in the pair. Note that the sample size ($n=20$) is small, and the figure may change substantially if larger or different sets are used. The images can be viewed on p. 13 of the Appendix, where Gen 01 corresponds to Same-Identity Pair 1, Gen 02 corresponds to Same-Identity Pair 2, and so on.

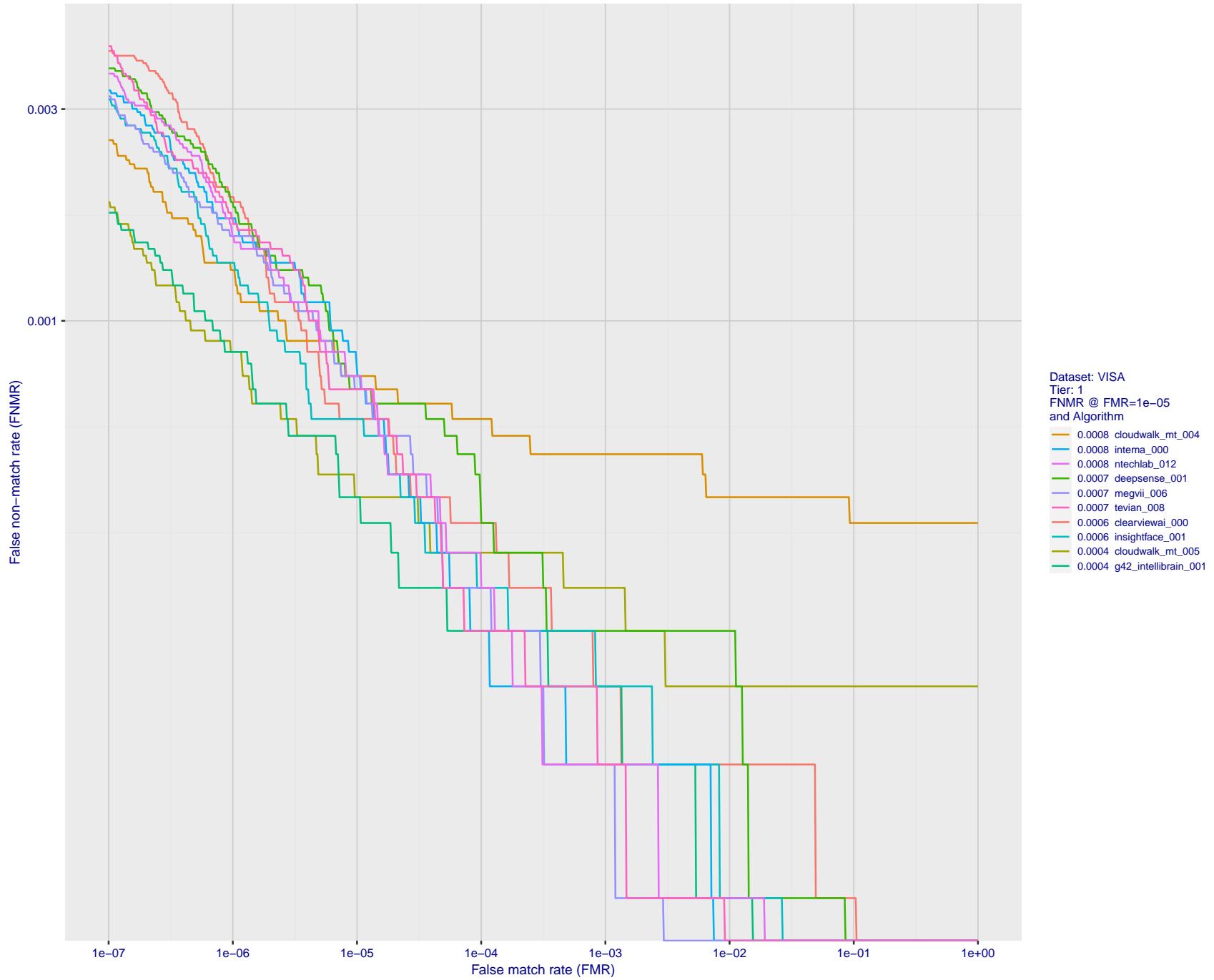


Figure 44: For the visa images, detection error tradeoff (DET) characteristics showing false non-match rate vs. false match rate plotted parametrically on threshold, T . The scales are logarithmic in order to show many decades of FMR.

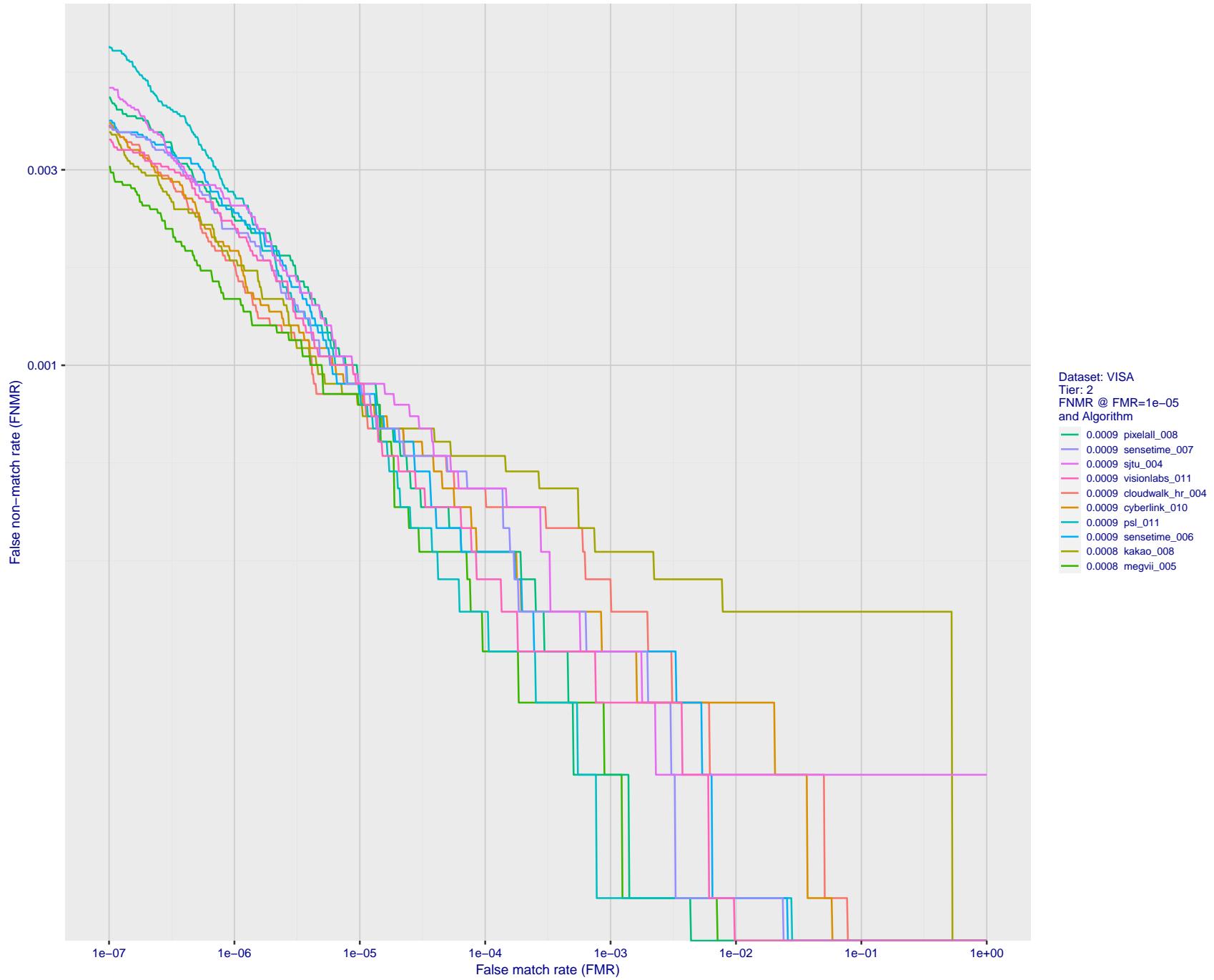


Figure 45: For the visa images, detection error tradeoff (DET) characteristics showing false non-match rate vs. false match rate plotted parametrically on threshold, T . The scales are logarithmic in order to show many decades of FMR.

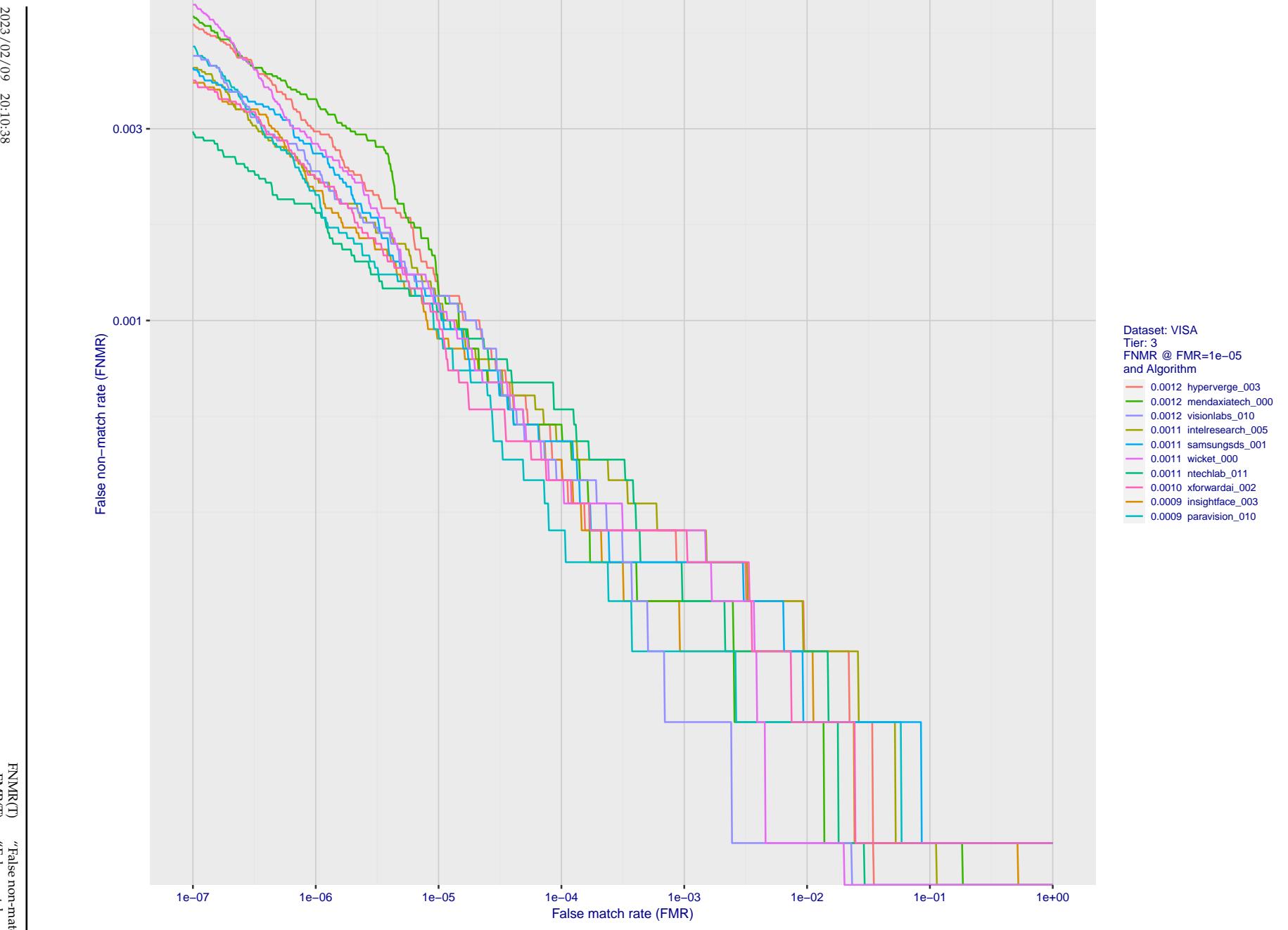


Figure 46: For the visa images, detection error tradeoff (DET) characteristics showing false non-match rate vs. false match rate plotted parametrically on threshold, T . The scales are logarithmic in order to show many decades of FMR.

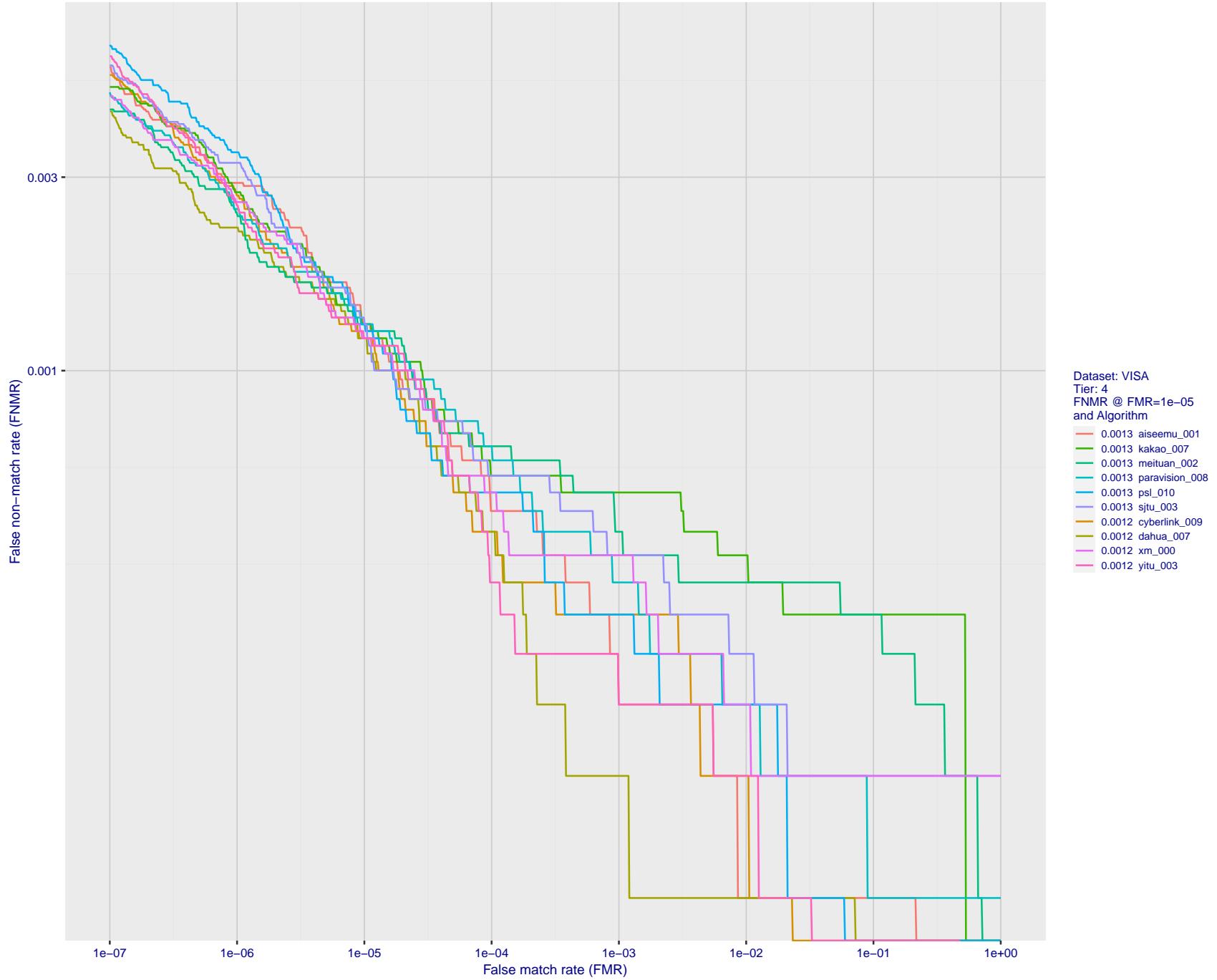


Figure 47: For the visa images, detection error tradeoff (DET) characteristics showing false non-match rate vs. false match rate plotted parametrically on threshold, T . The scales are logarithmic in order to show many decades of FMR.

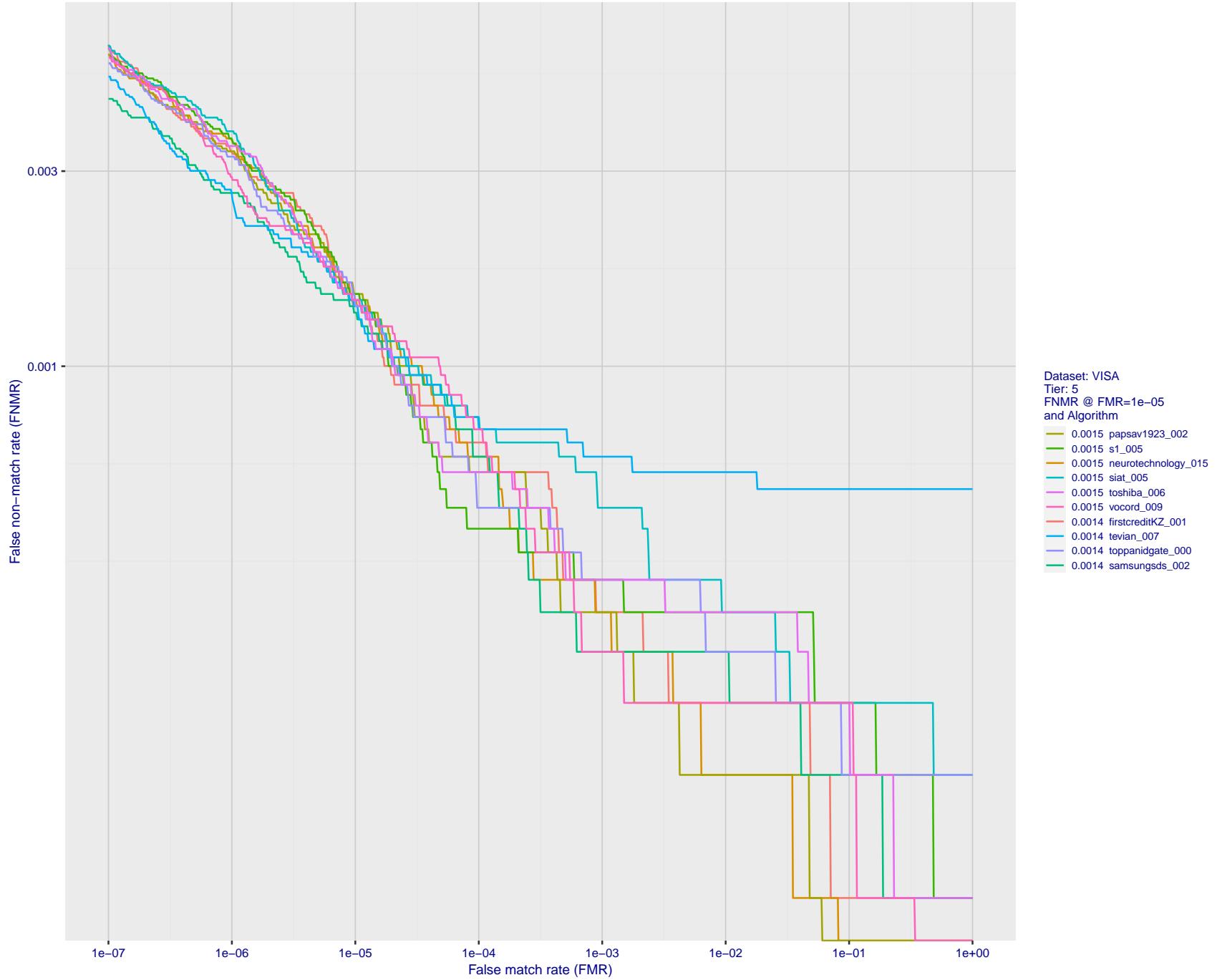


Figure 48: For the visa images, detection error tradeoff (DET) characteristics showing false non-match rate vs. false match rate plotted parametrically on threshold, T . The scales are logarithmic in order to show many decades of FMR.

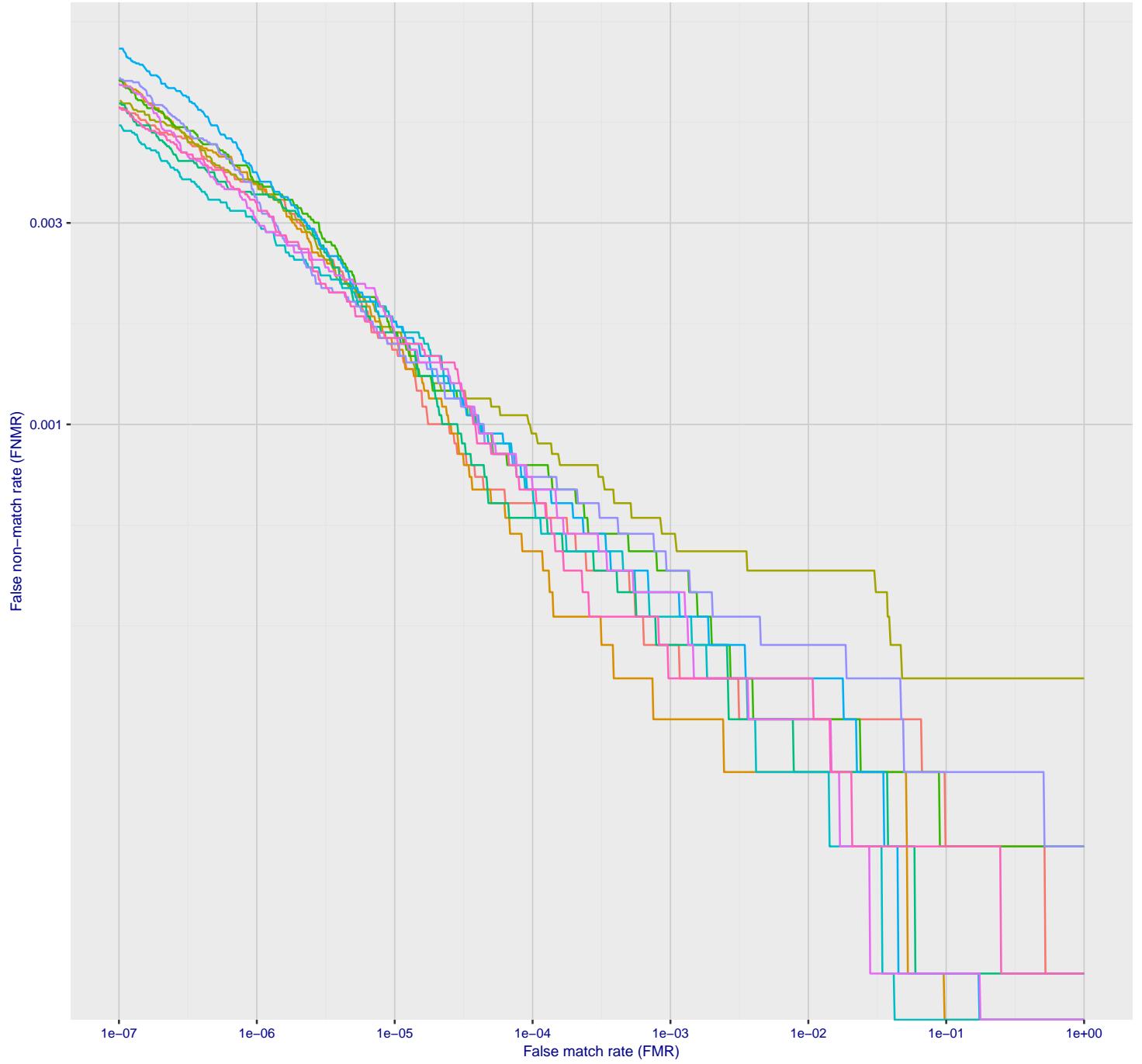


Figure 49: For the visa images, detection error tradeoff (DET) characteristics showing false non-match rate vs. false match rate plotted parametrically on threshold, T . The scales are logarithmic in order to show many decades of FMR.

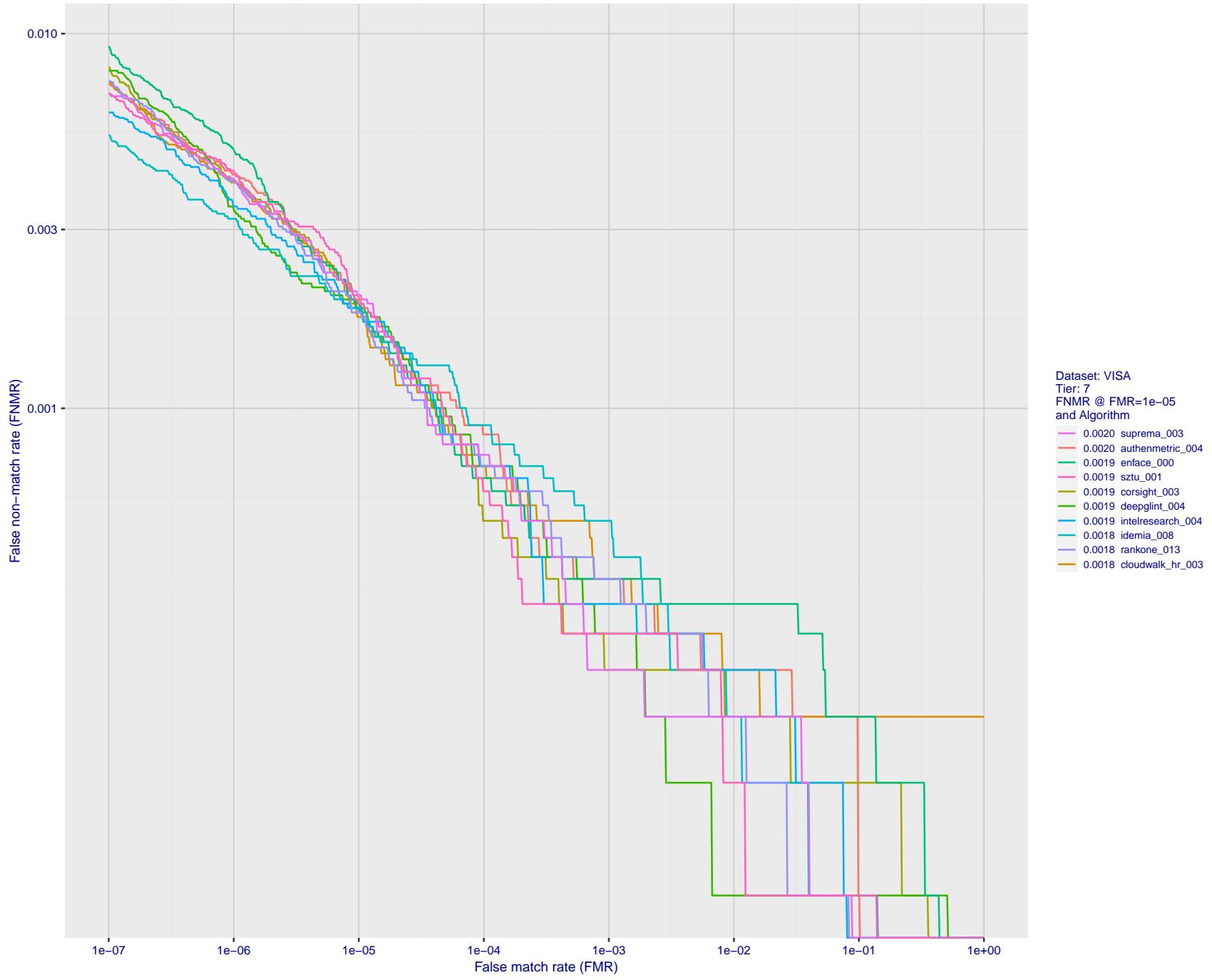


Figure 50: For the visa images, detection error tradeoff (DET) characteristics showing false non-match rate vs. false match rate plotted parametrically on threshold, T . The scales are logarithmic in order to show many decades of FMR.

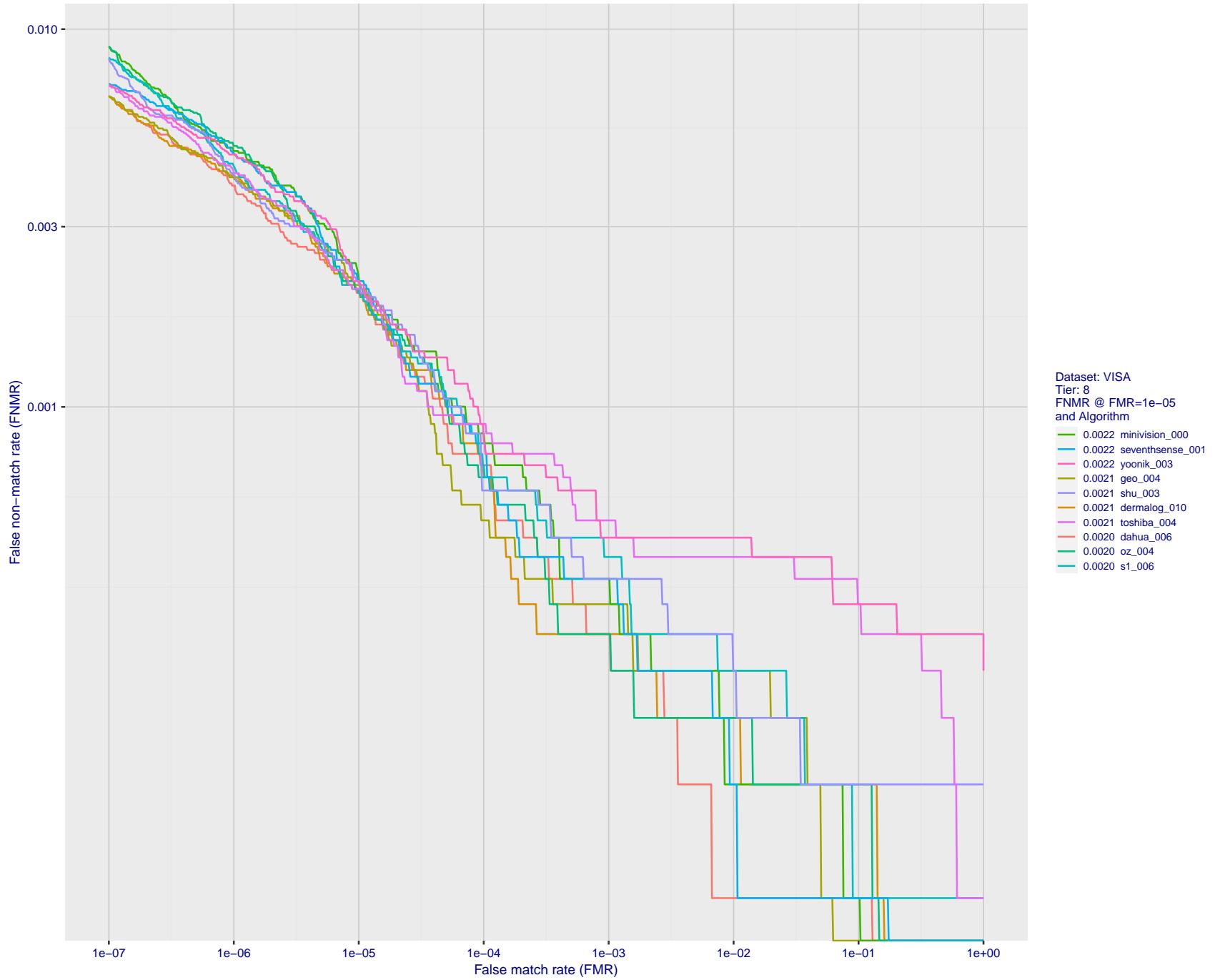


Figure 51: For the visa images, detection error tradeoff (DET) characteristics showing false non-match rate vs. false match rate plotted parametrically on threshold, T . The scales are logarithmic in order to show many decades of FMR.

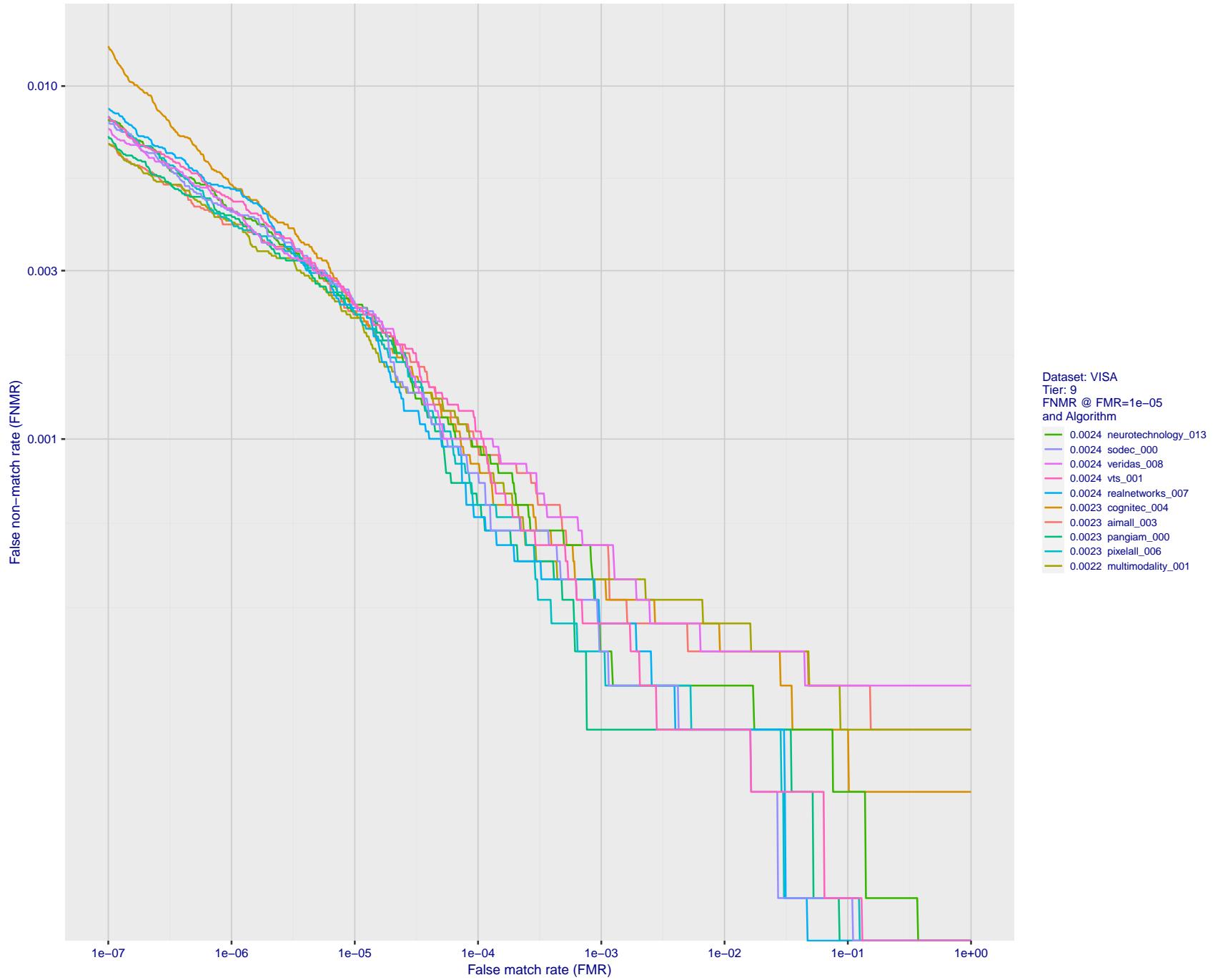


Figure 52: For the visa images, detection error tradeoff (DET) characteristics showing false non-match rate vs. false match rate plotted parametrically on threshold, T . The scales are logarithmic in order to show many decades of FMR.

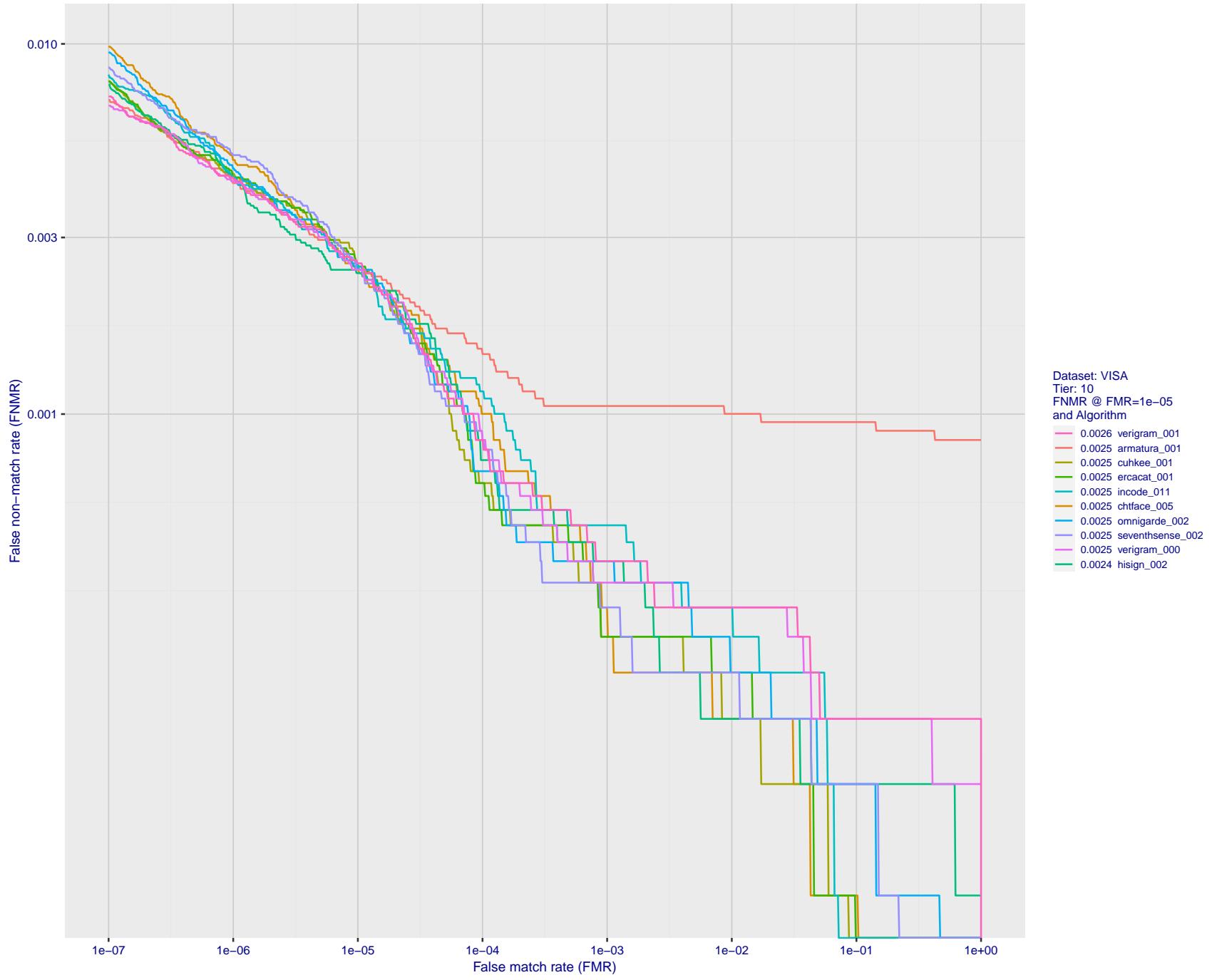


Figure 53: For the visa images, detection error tradeoff (DET) characteristics showing false non-match rate vs. false match rate plotted parametrically on threshold, T . The scales are logarithmic in order to show many decades of FMR.

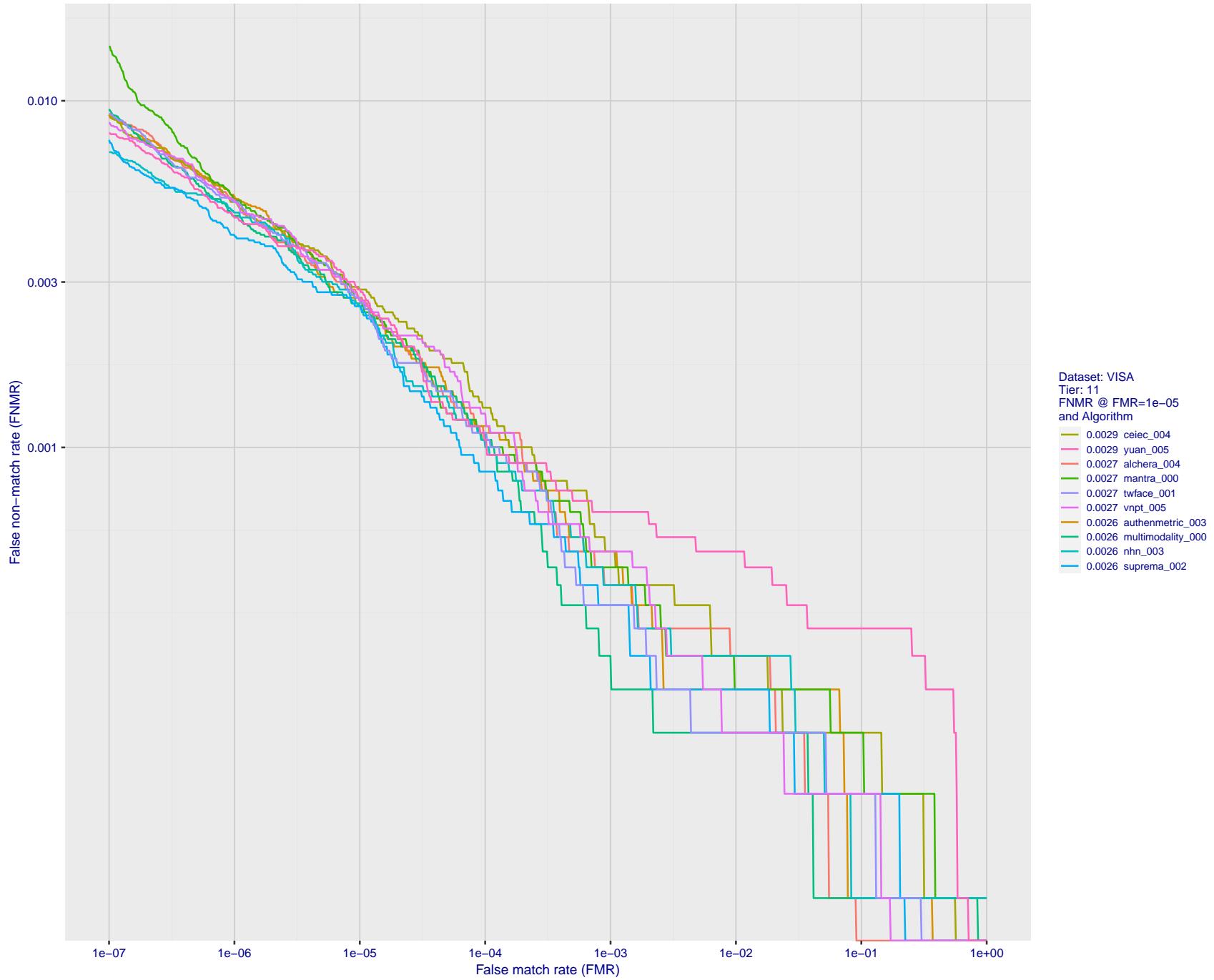


Figure 54: For the visa images, detection error tradeoff (DET) characteristics showing false non-match rate vs. false match rate plotted parametrically on threshold, T . The scales are logarithmic in order to show many decades of FMR.

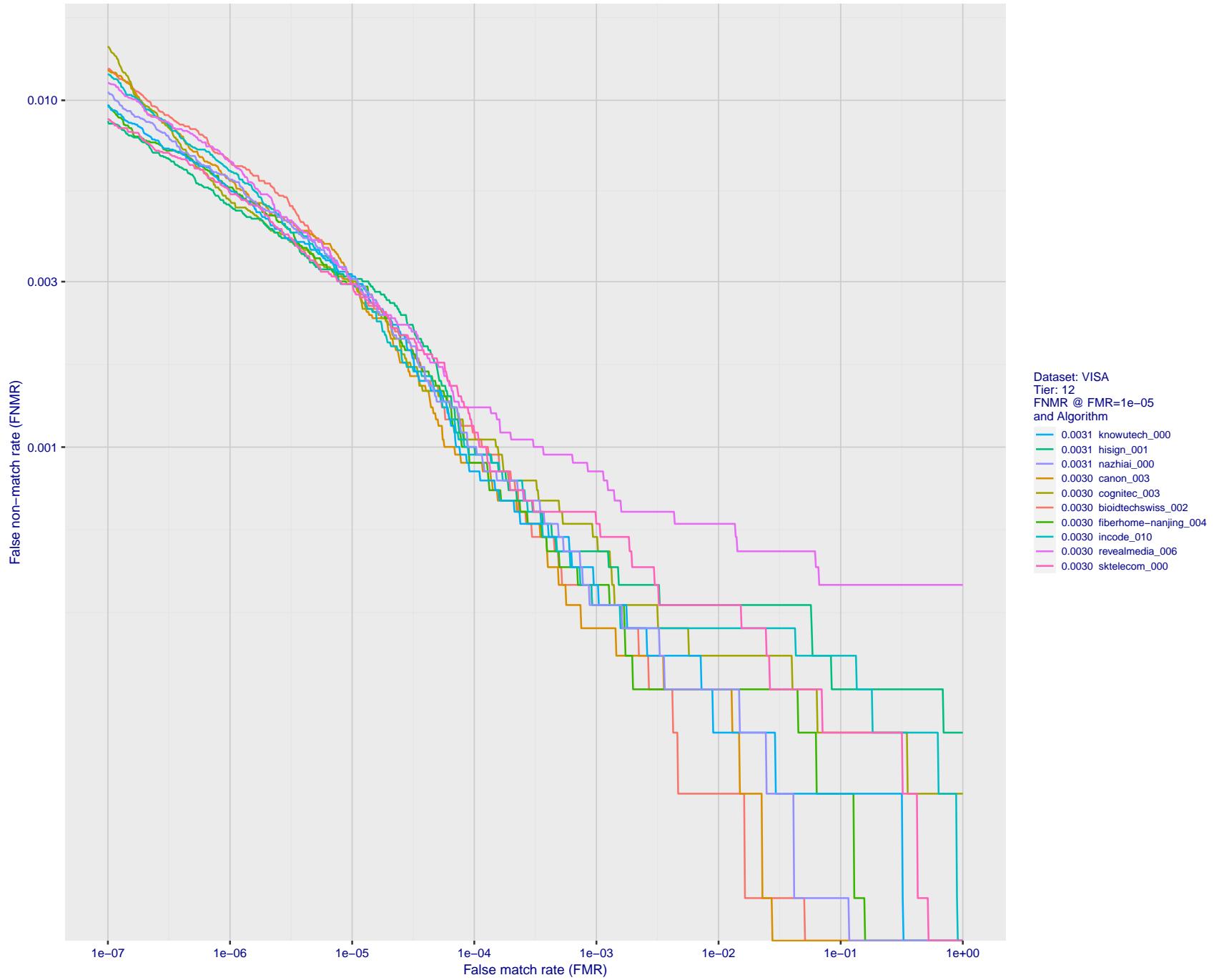


Figure 55: For the visa images, detection error tradeoff (DET) characteristics showing false non-match rate vs. false match rate plotted parametrically on threshold, T . The scales are logarithmic in order to show many decades of FMR.

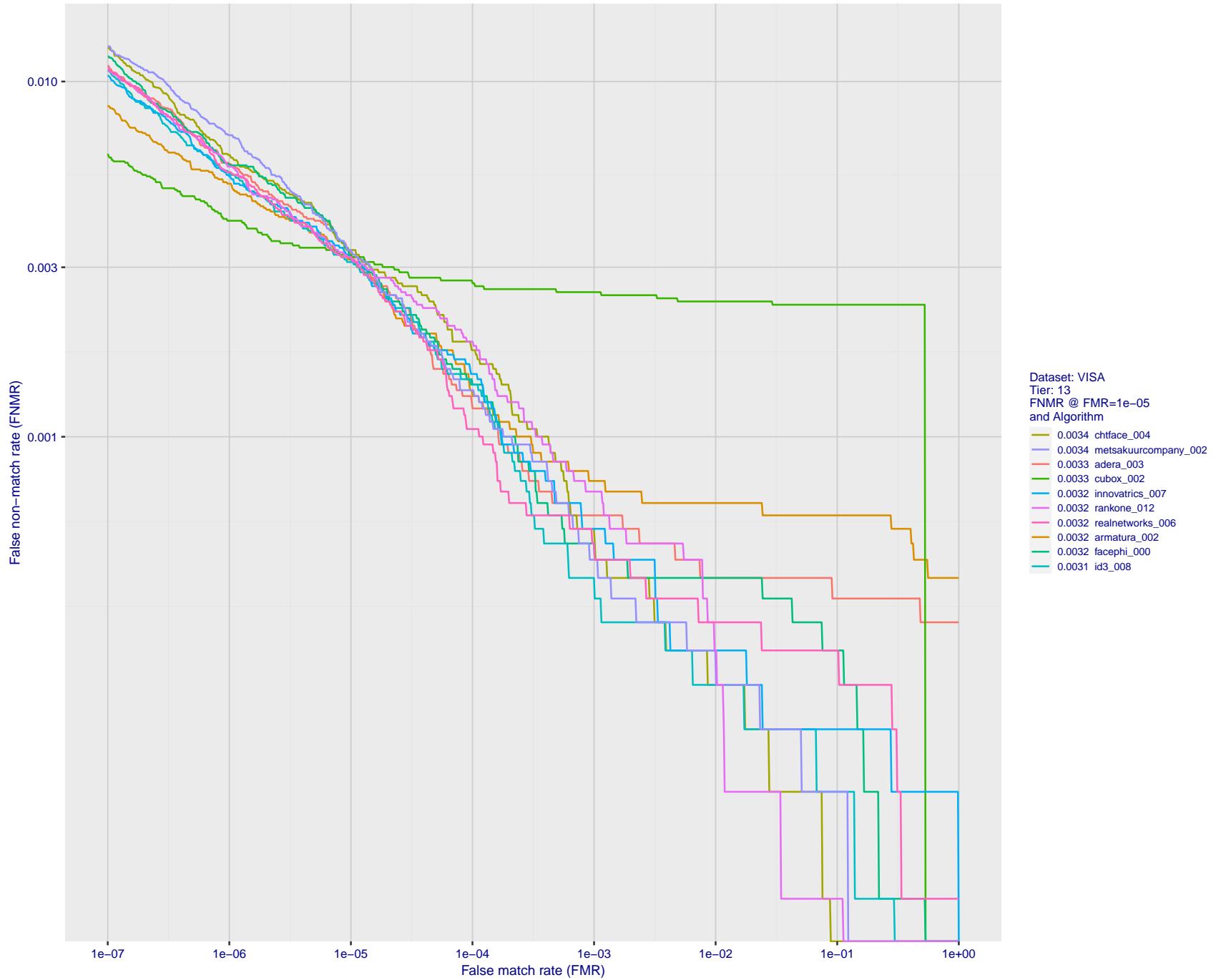


Figure 56: For the visa images, detection error tradeoff (DET) characteristics showing false non-match rate vs. false match rate plotted parametrically on threshold, T . The scales are logarithmic in order to show many decades of FMR.

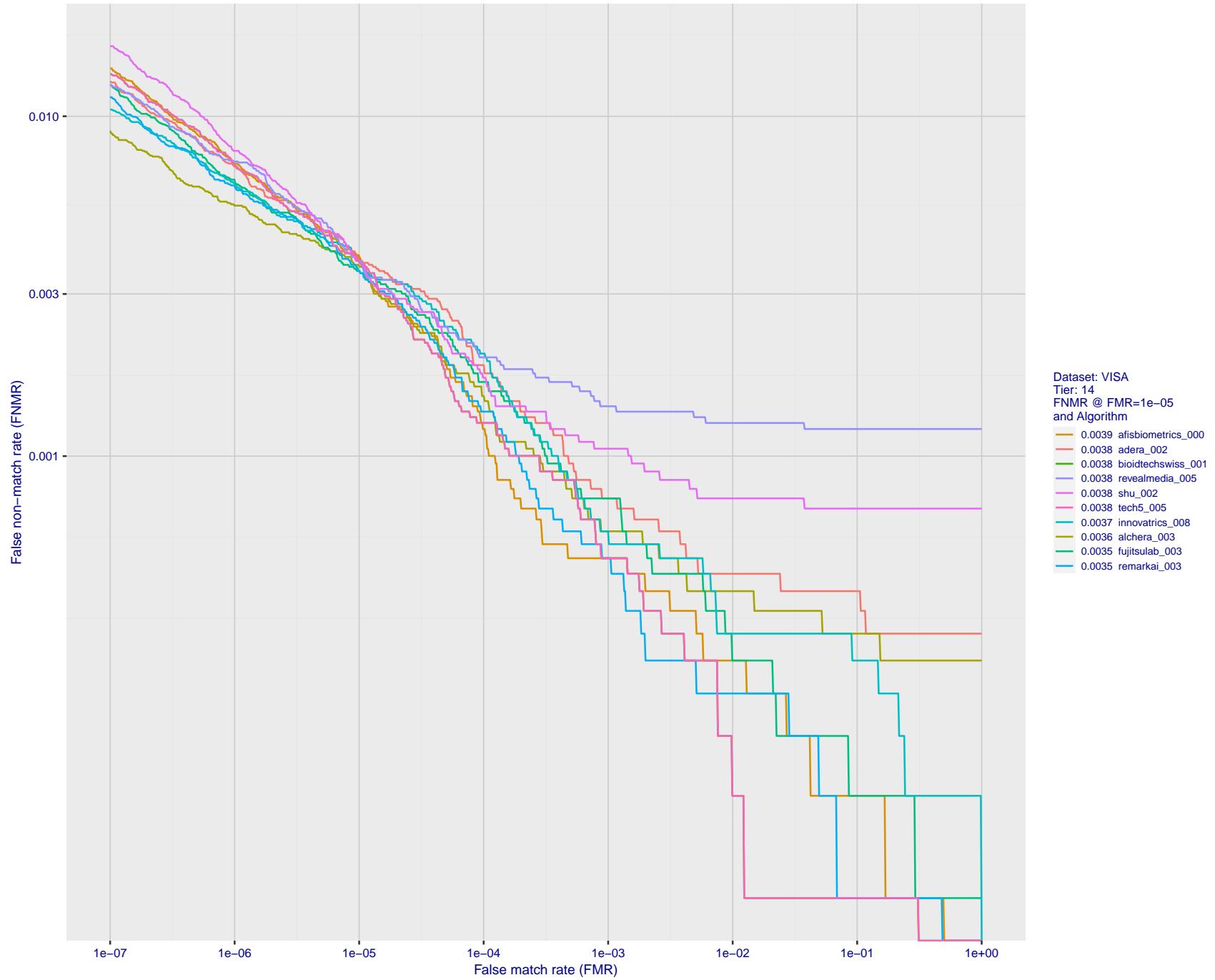


Figure 57: For the visa images, detection error tradeoff (DET) characteristics showing false non-match rate vs. false match rate plotted parametrically on threshold, T . The scales are logarithmic in order to show many decades of FMR.

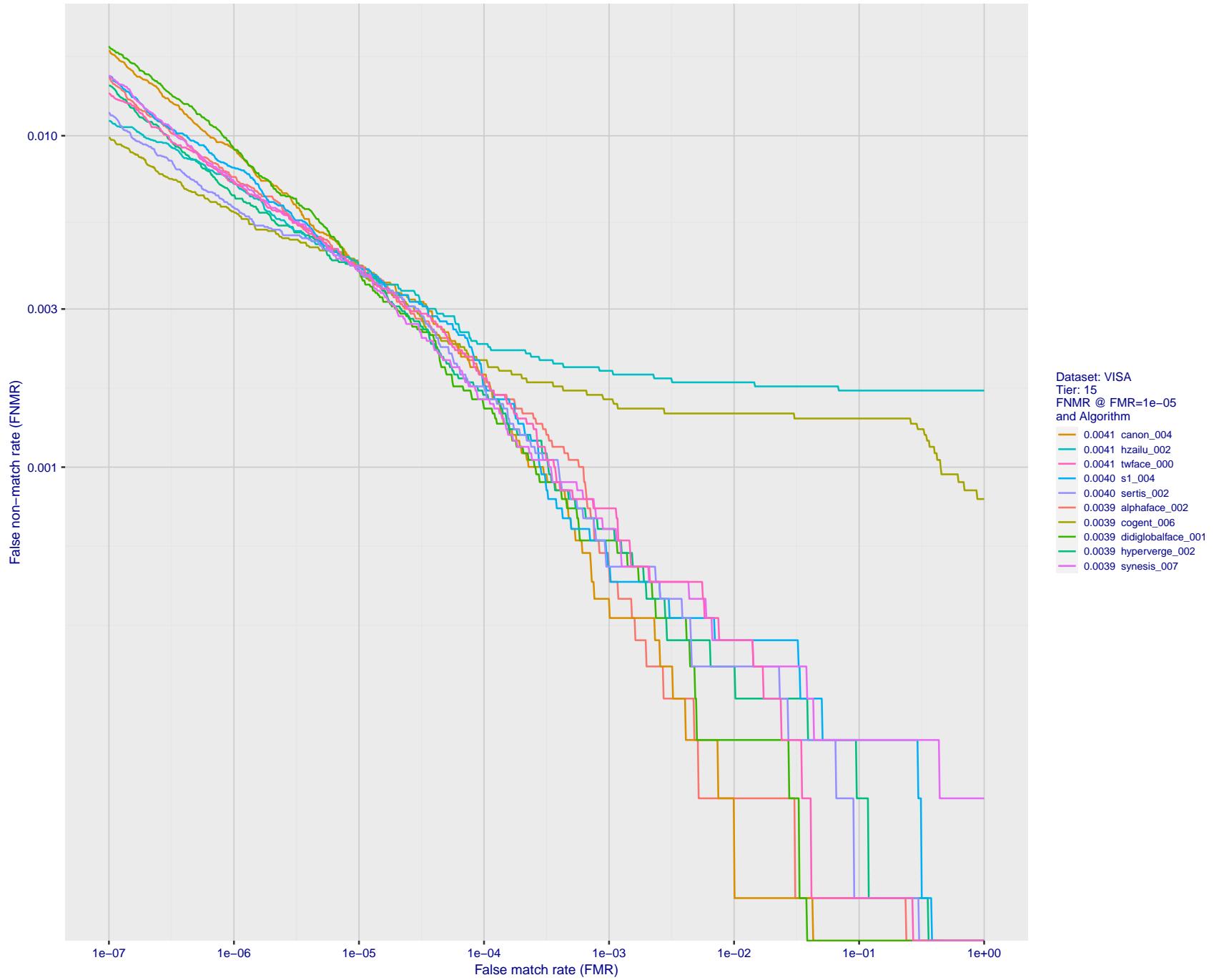


Figure 58: For the visa images, detection error tradeoff (DET) characteristics showing false non-match rate vs. false match rate plotted parametrically on threshold, T . The scales are logarithmic in order to show many decades of FMR.

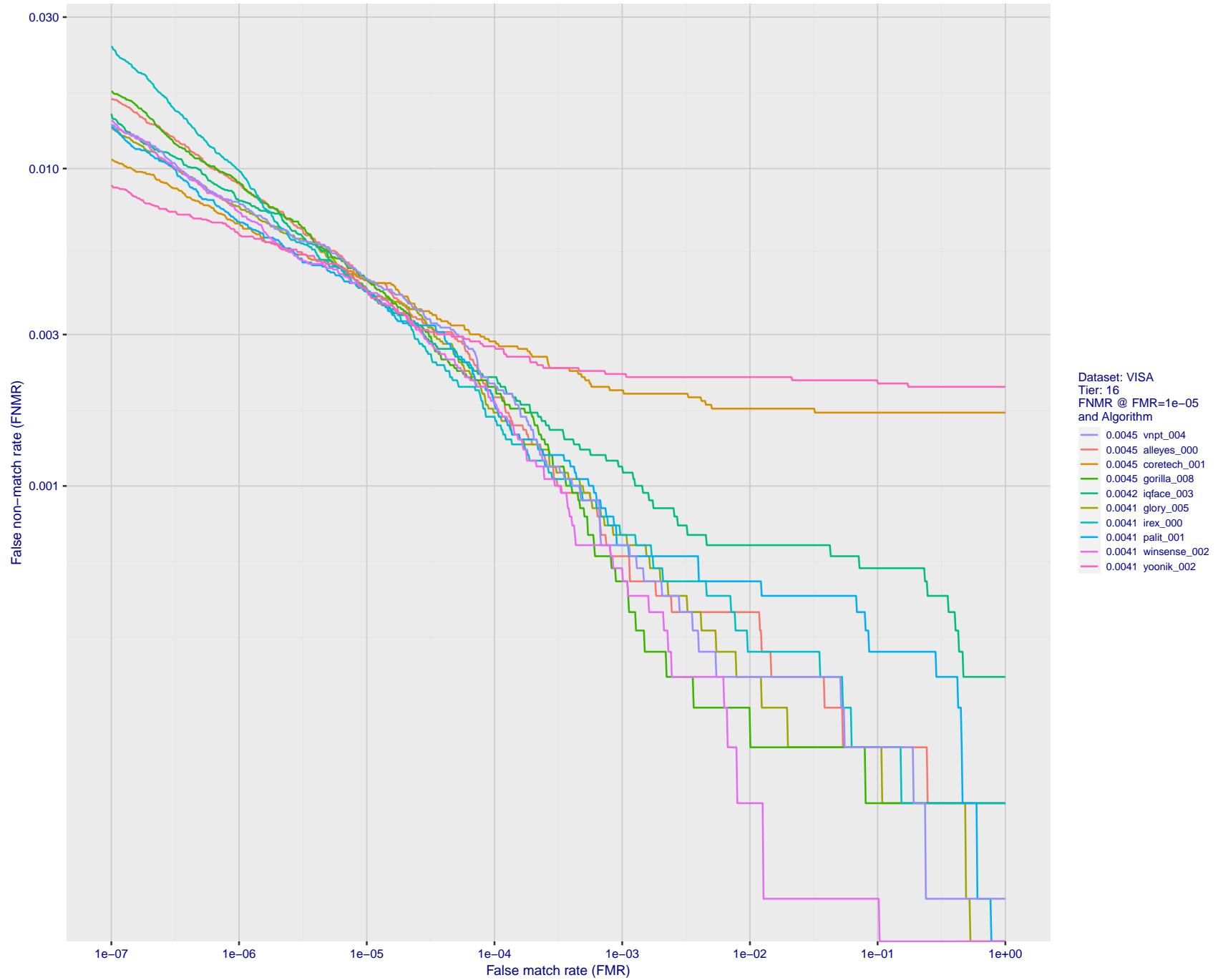


Figure 59: For the visa images, detection error tradeoff (DET) characteristics showing false non-match rate vs. false match rate plotted parametrically on threshold, T . The scales are logarithmic in order to show many decades of FMR.

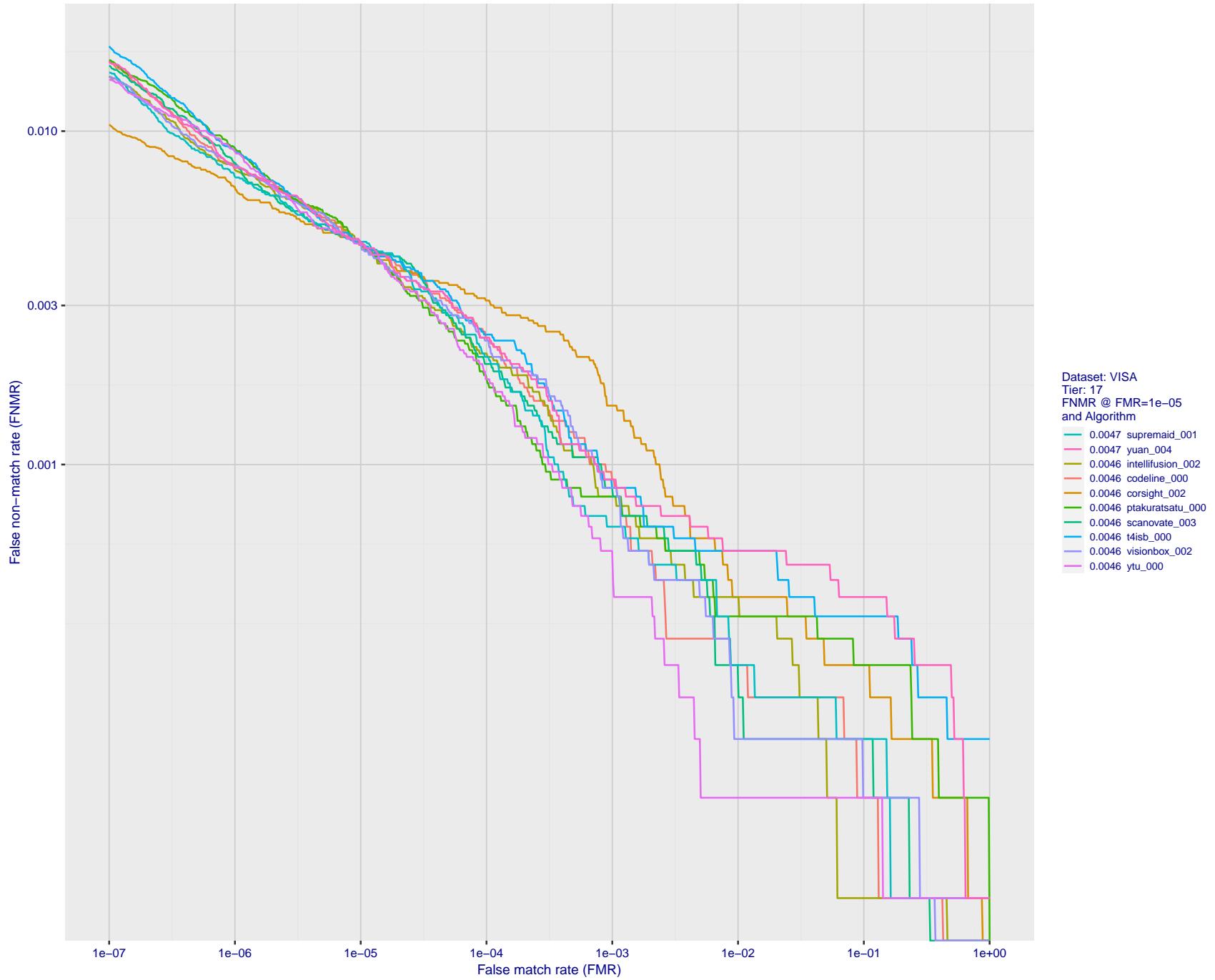


Figure 60: For the visa images, detection error tradeoff (DET) characteristics showing false non-match rate vs. false match rate plotted parametrically on threshold, T . The scales are logarithmic in order to show many decades of FMR.

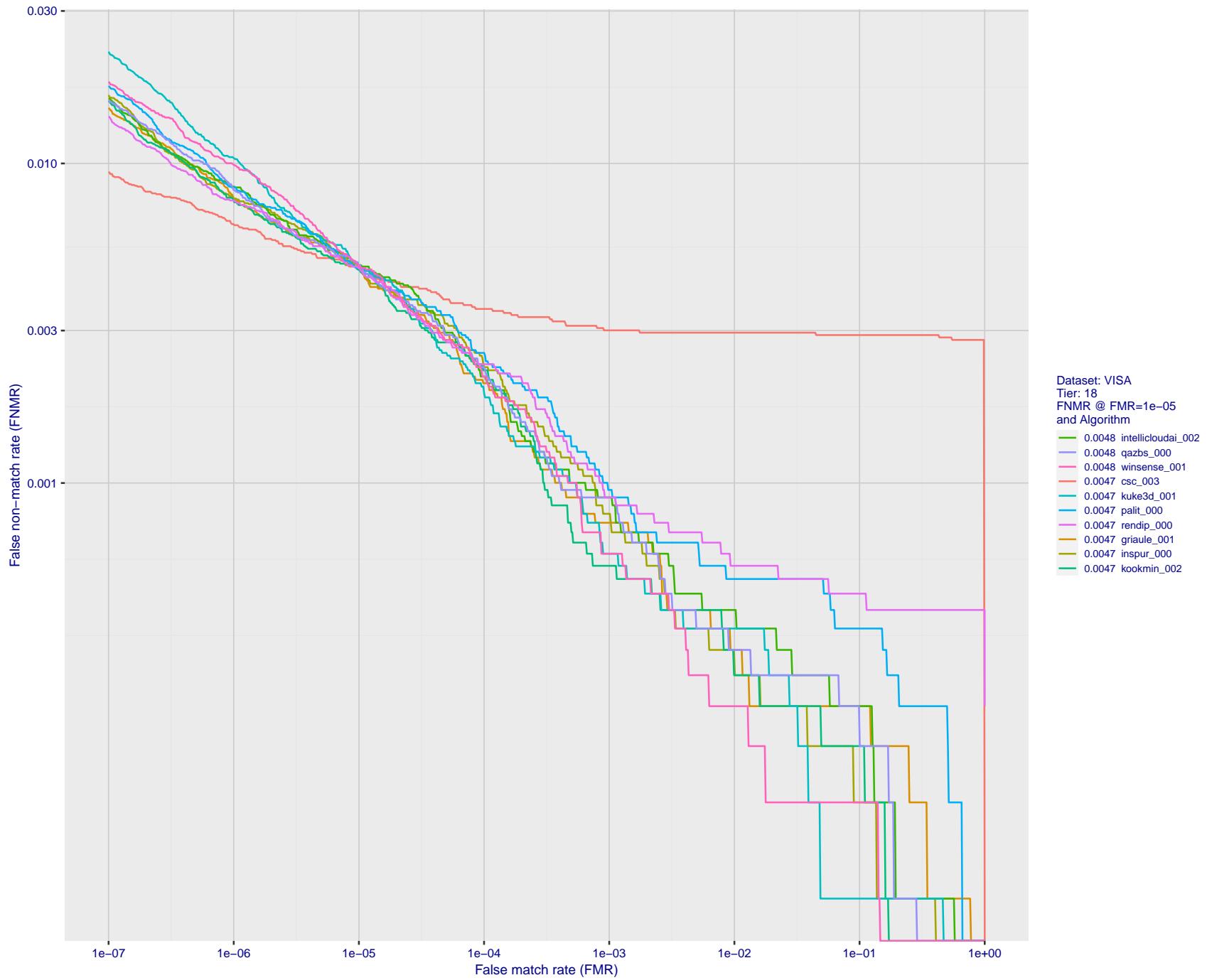


Figure 61: For the visa images, detection error tradeoff (DET) characteristics showing false non-match rate vs. false match rate plotted parametrically on threshold, T . The scales are logarithmic in order to show many decades of FMR.

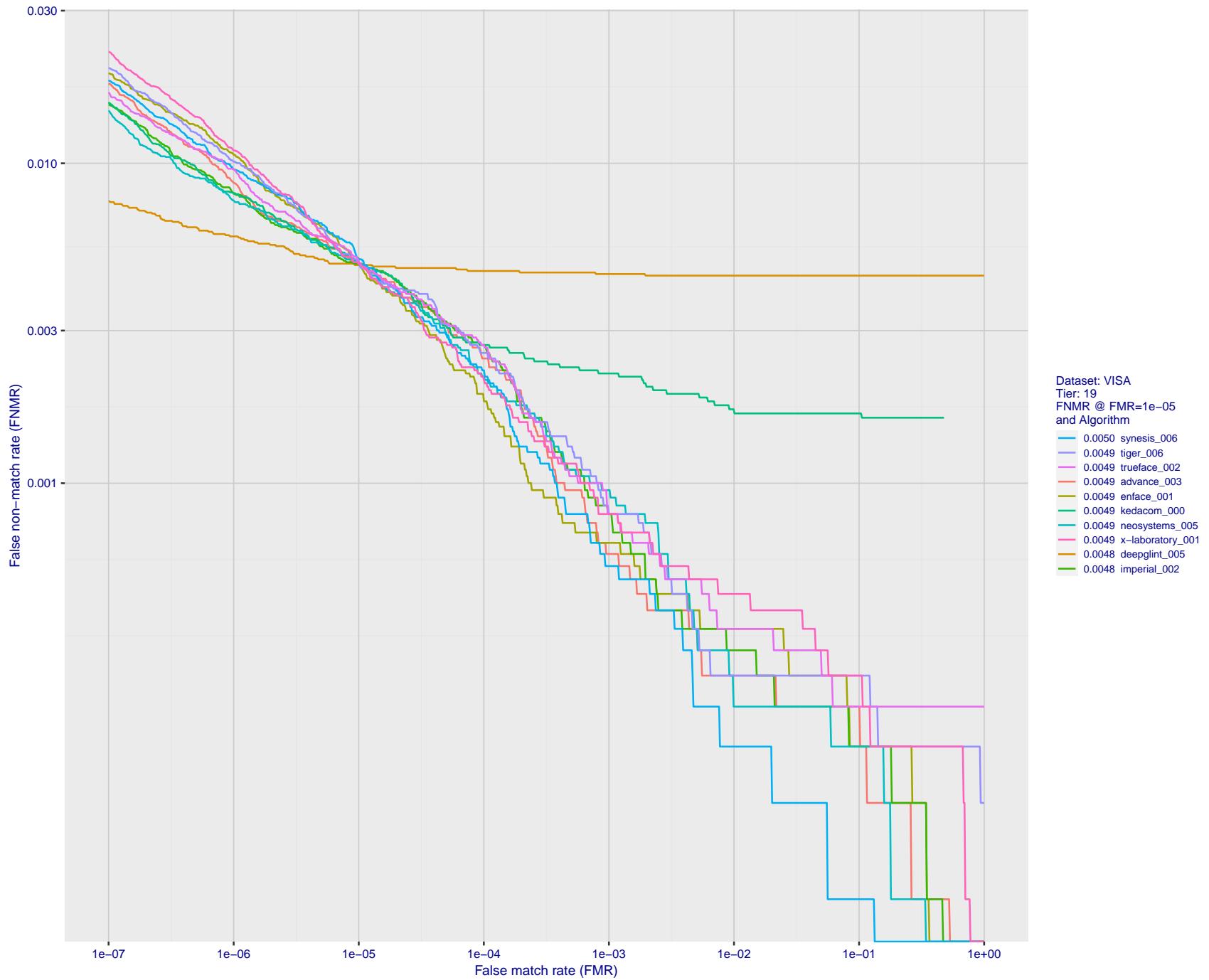


Figure 62: For the visa images, detection error tradeoff (DET) characteristics showing false non-match rate vs. false match rate plotted parametrically on threshold, T . The scales are logarithmic in order to show many decades of FMR.

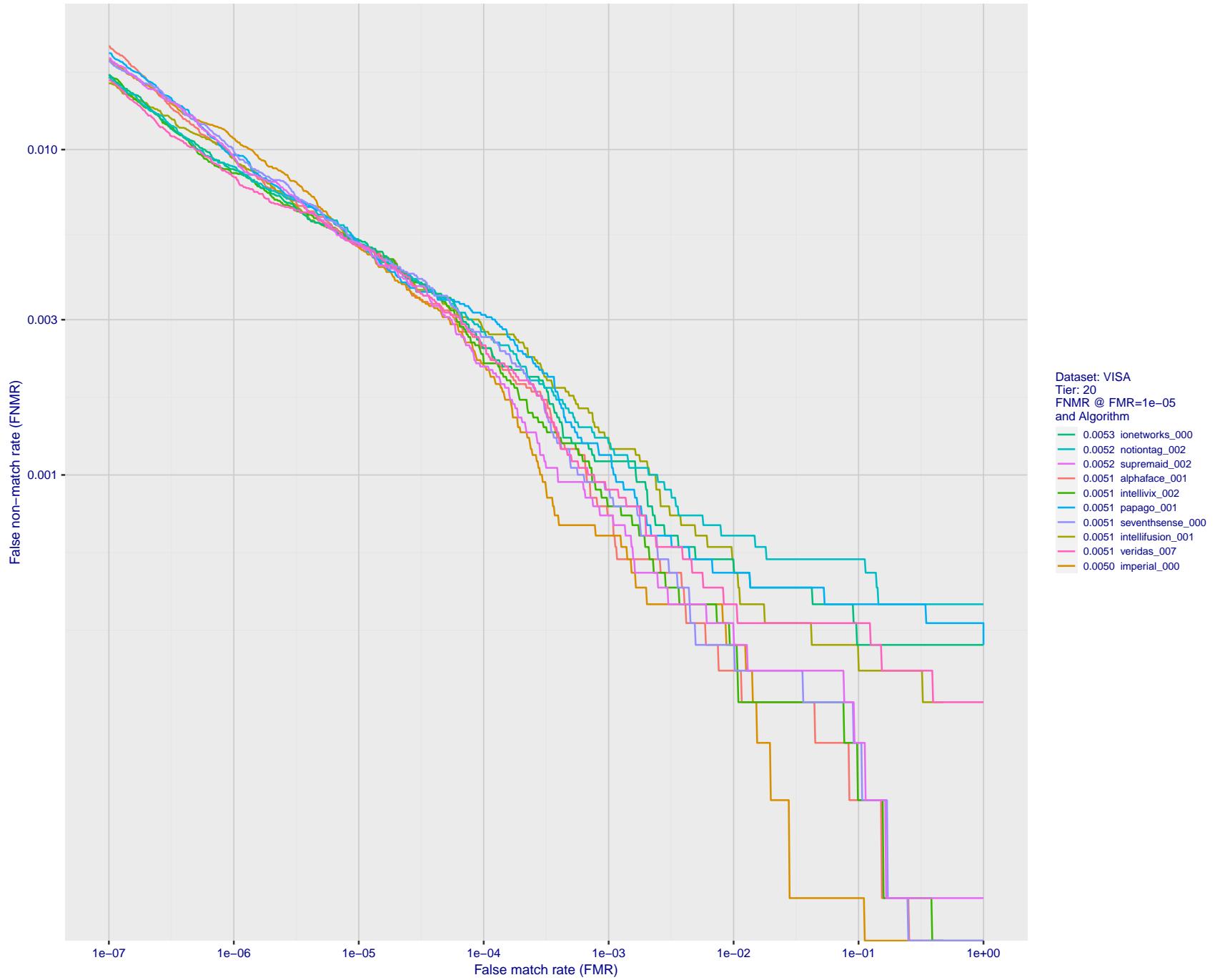


Figure 63: For the visa images, detection error tradeoff (DET) characteristics showing false non-match rate vs. false match rate plotted parametrically on threshold, T . The scales are logarithmic in order to show many decades of FMR.

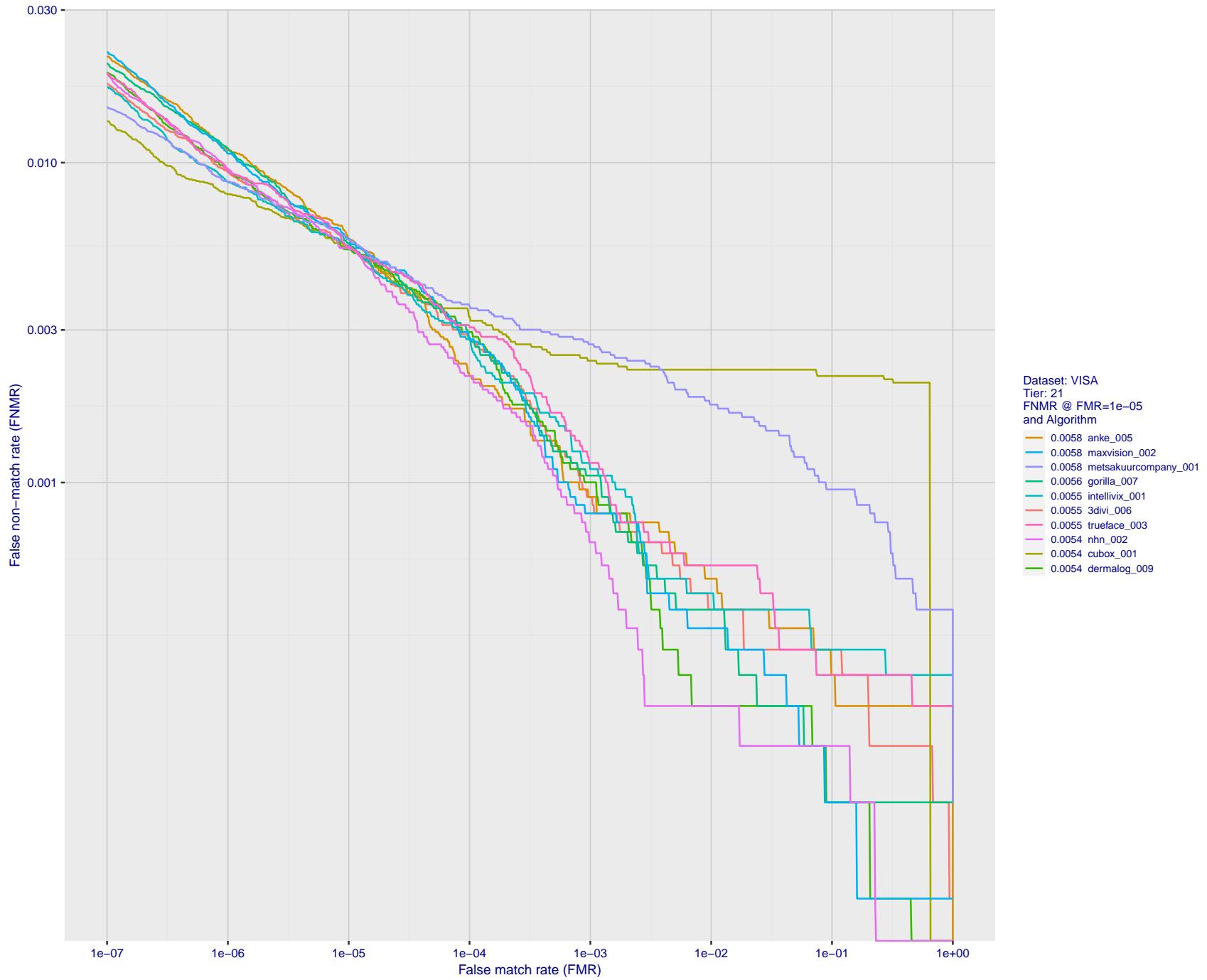


Figure 64: For the visa images, detection error tradeoff (DET) characteristics showing false non-match rate vs. false match rate plotted parametrically on threshold, T . The scales are logarithmic in order to show many decades of FMR.

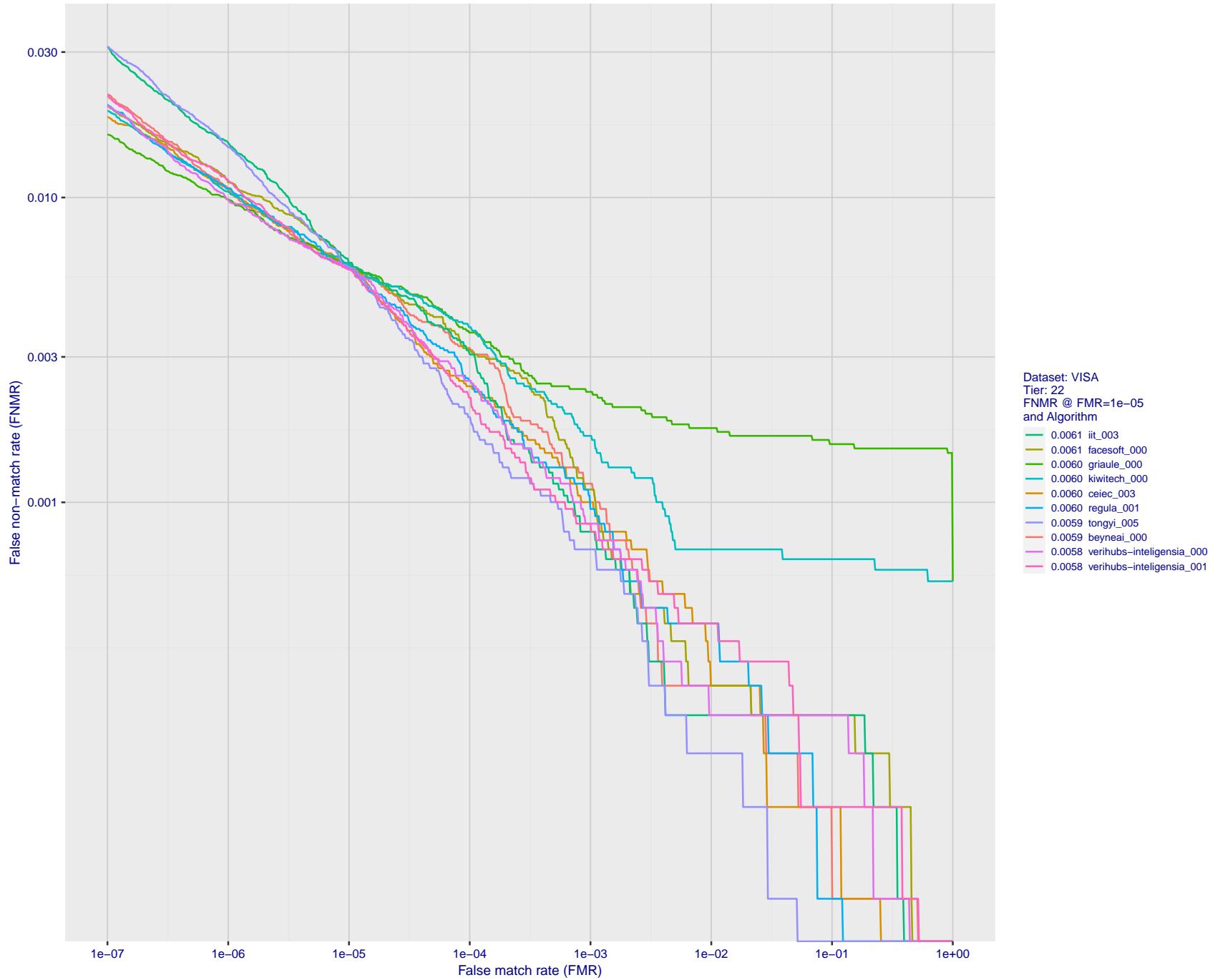


Figure 65: For the visa images, detection error tradeoff (DET) characteristics showing false non-match rate vs. false match rate plotted parametrically on threshold, T . The scales are logarithmic in order to show many decades of FMR.

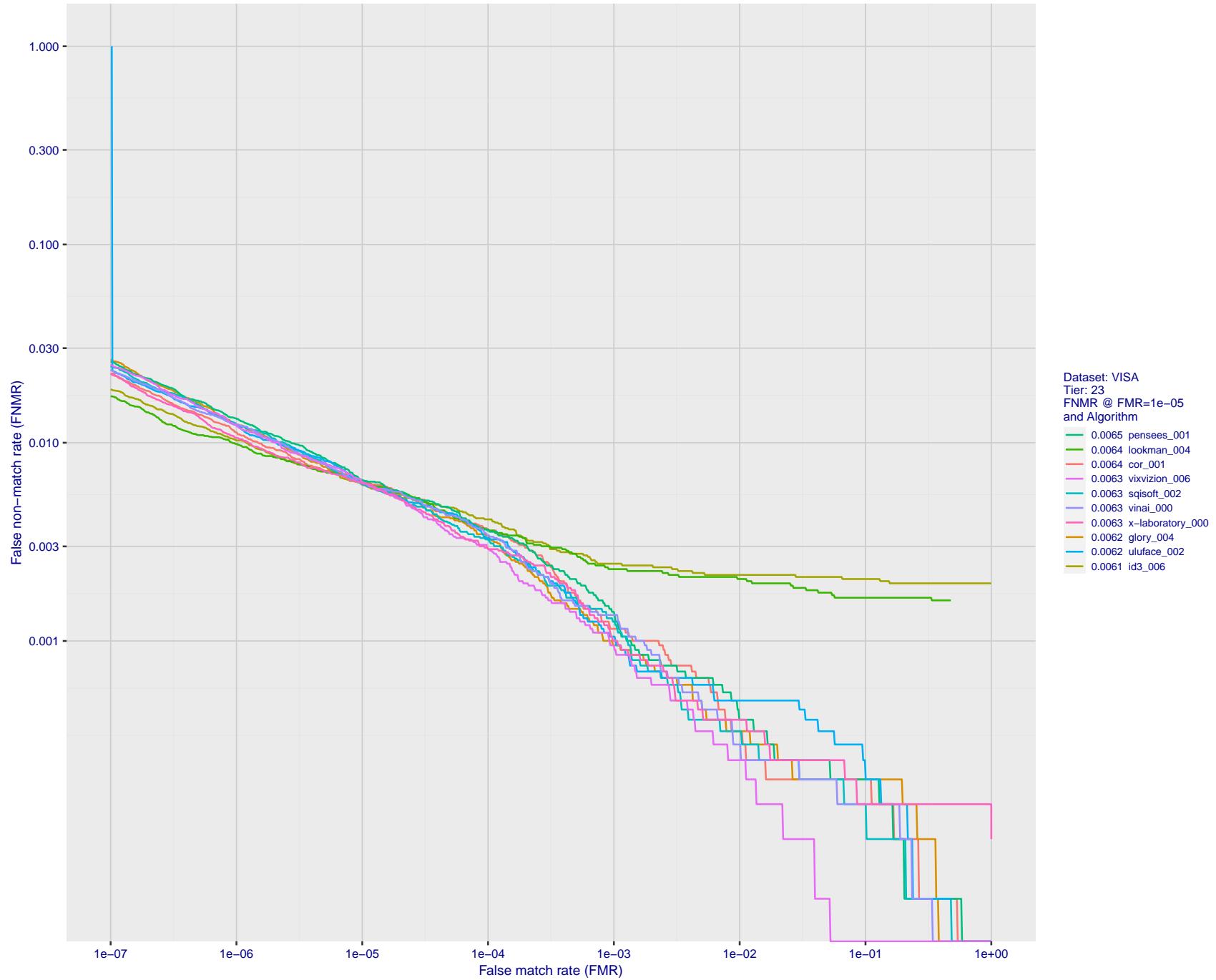


Figure 66: For the visa images, detection error tradeoff (DET) characteristics showing false non-match rate vs. false match rate plotted parametrically on threshold, T . The scales are logarithmic in order to show many decades of FMR.

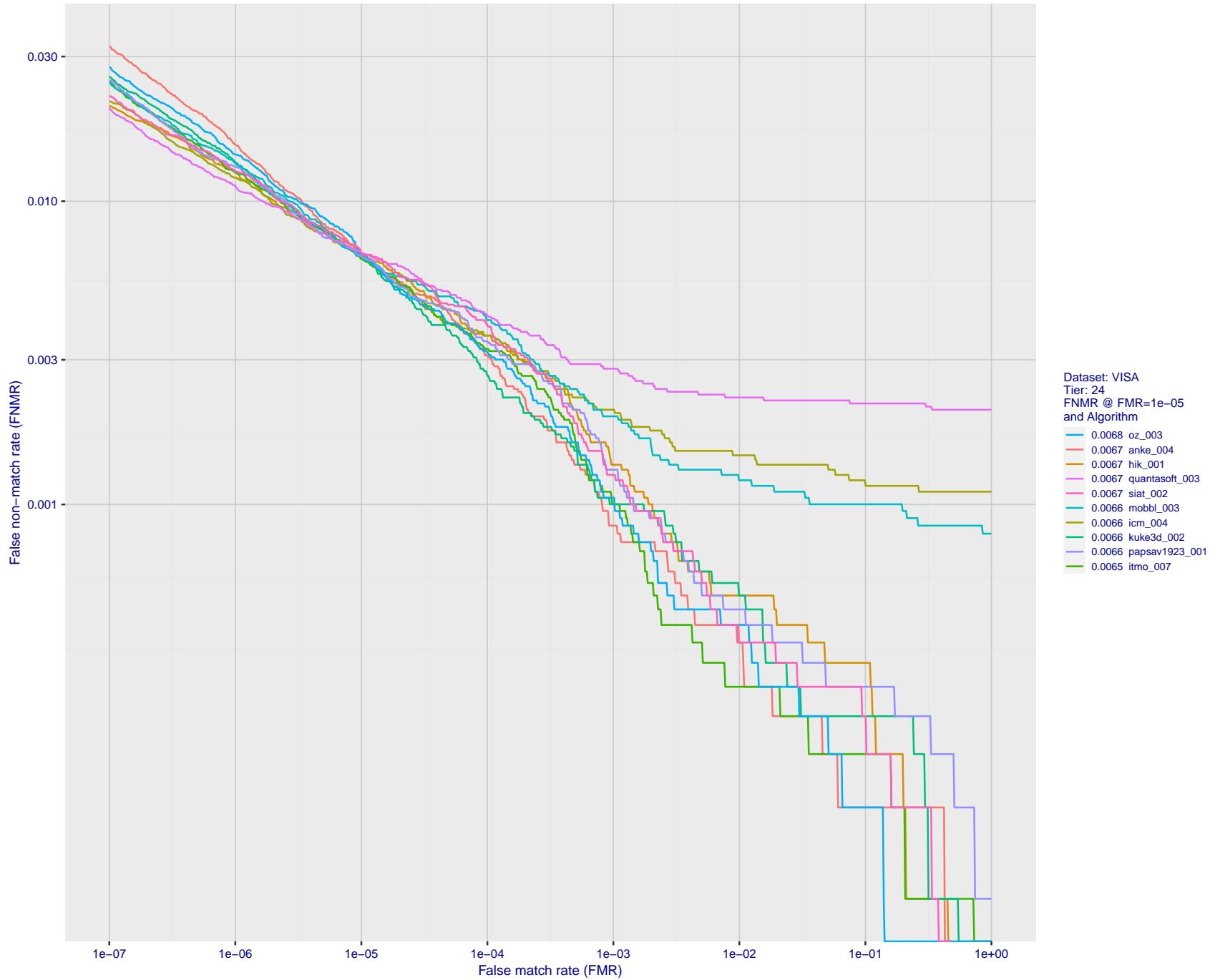


Figure 67: For the visa images, detection error tradeoff (DET) characteristics showing false non-match rate vs. false match rate plotted parametrically on threshold, T . The scales are logarithmic in order to show many decades of FMR.

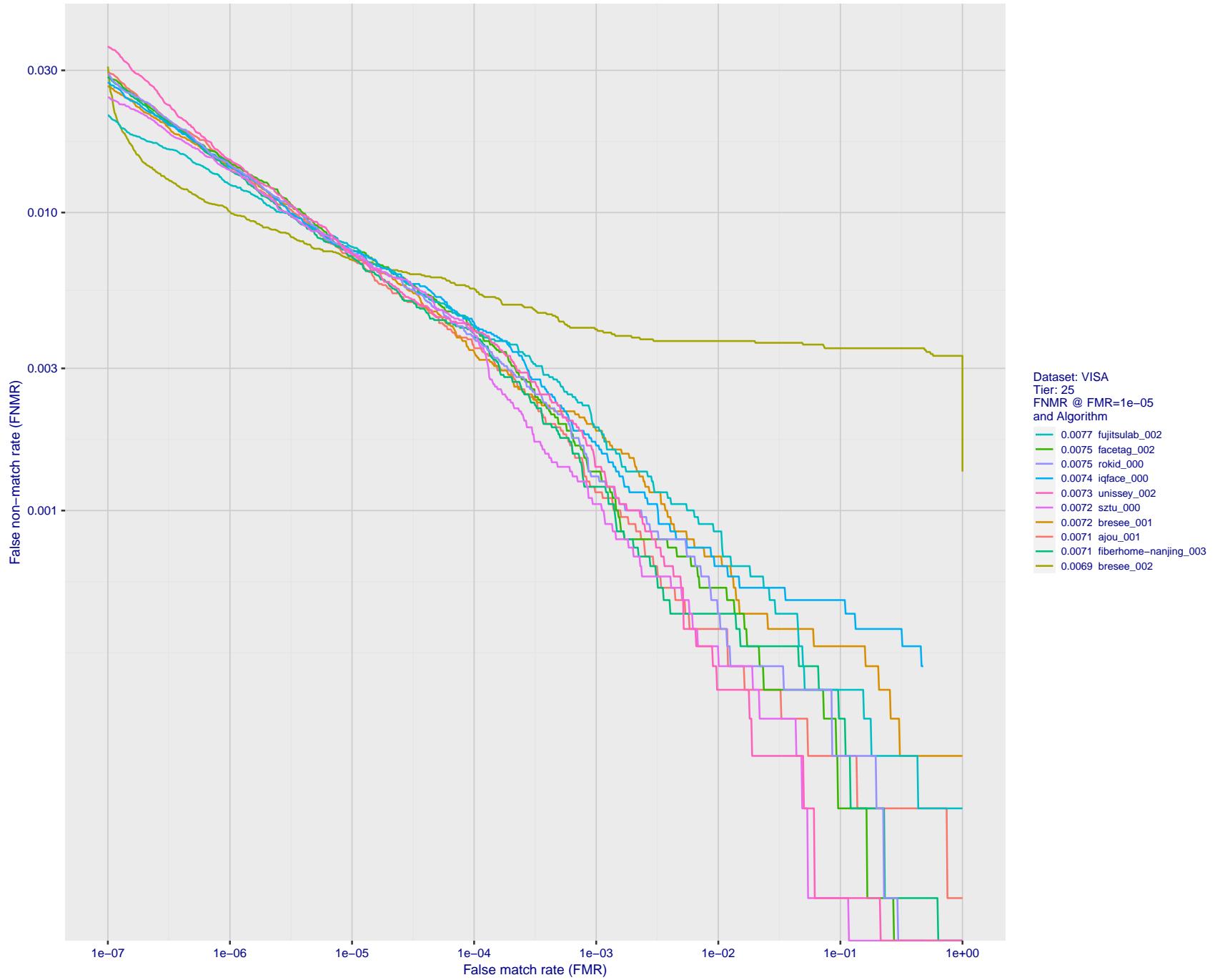


Figure 68: For the visa images, detection error tradeoff (DET) characteristics showing false non-match rate vs. false match rate plotted parametrically on threshold, T . The scales are logarithmic in order to show many decades of FMR.

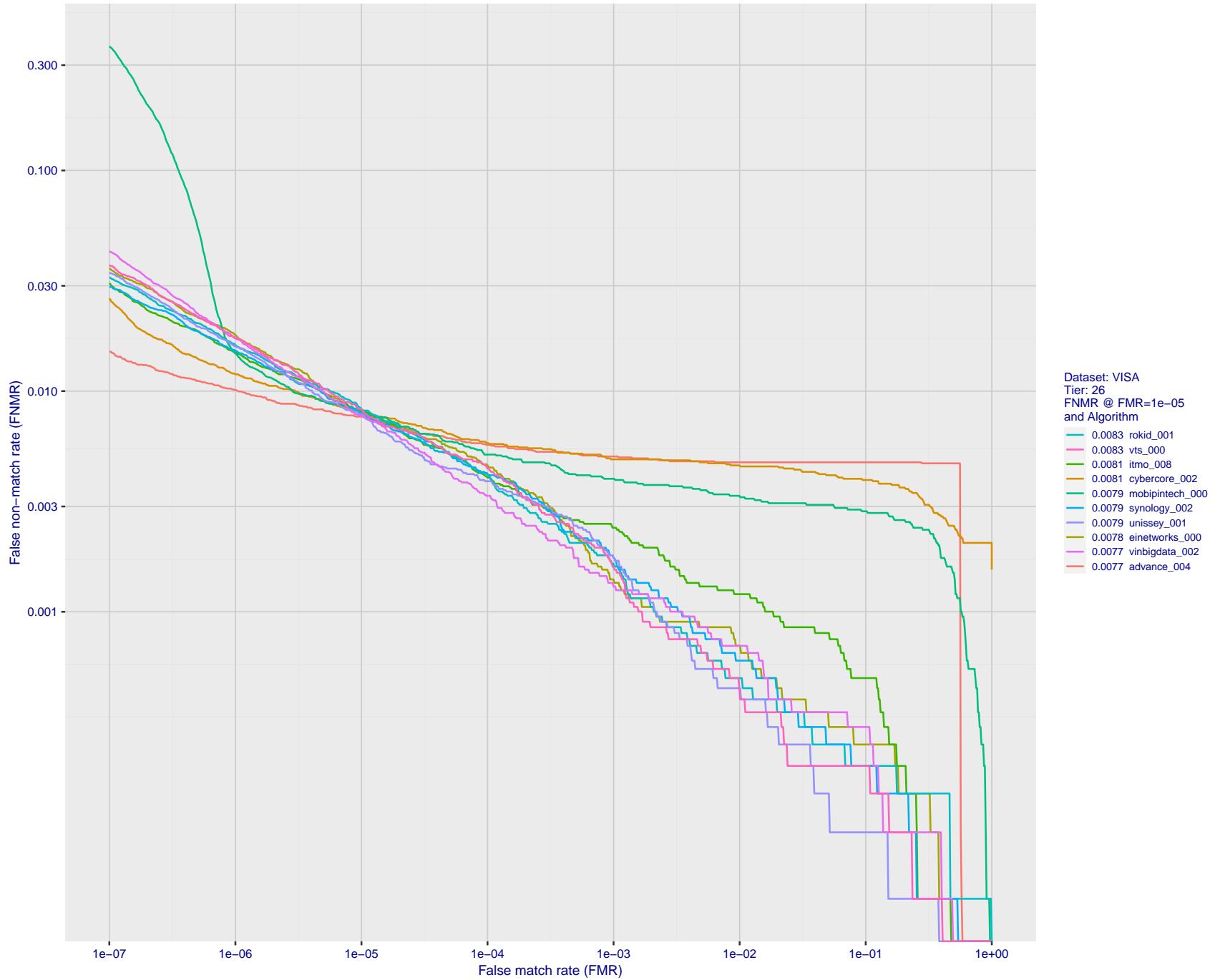


Figure 69: For the visa images, detection error tradeoff (DET) characteristics showing false non-match rate vs. false match rate plotted parametrically on threshold, T . The scales are logarithmic in order to show many decades of FMR.

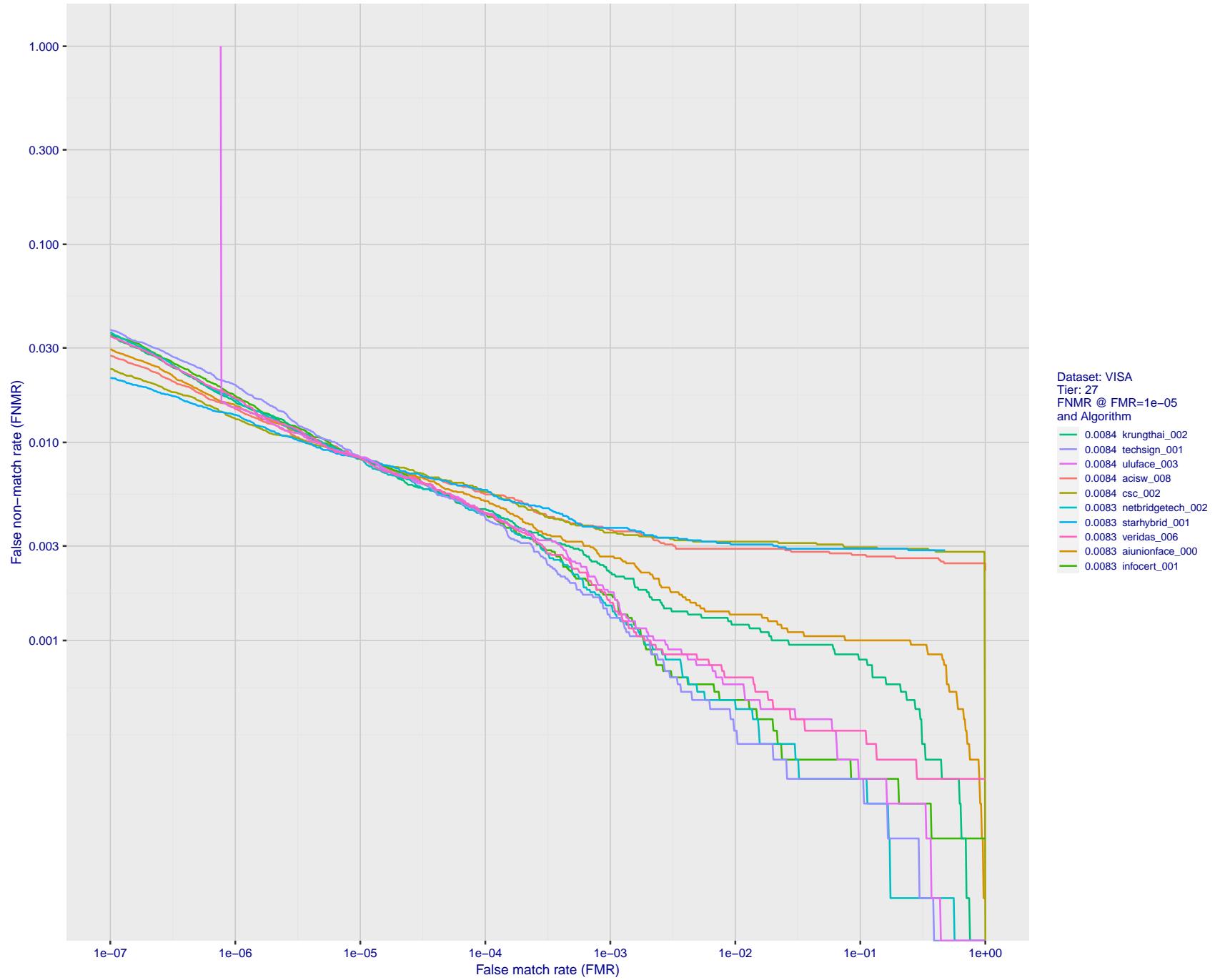


Figure 70: For the visa images, detection error tradeoff (DET) characteristics showing false non-match rate vs. false match rate plotted parametrically on threshold, T . The scales are logarithmic in order to show many decades of FMR.

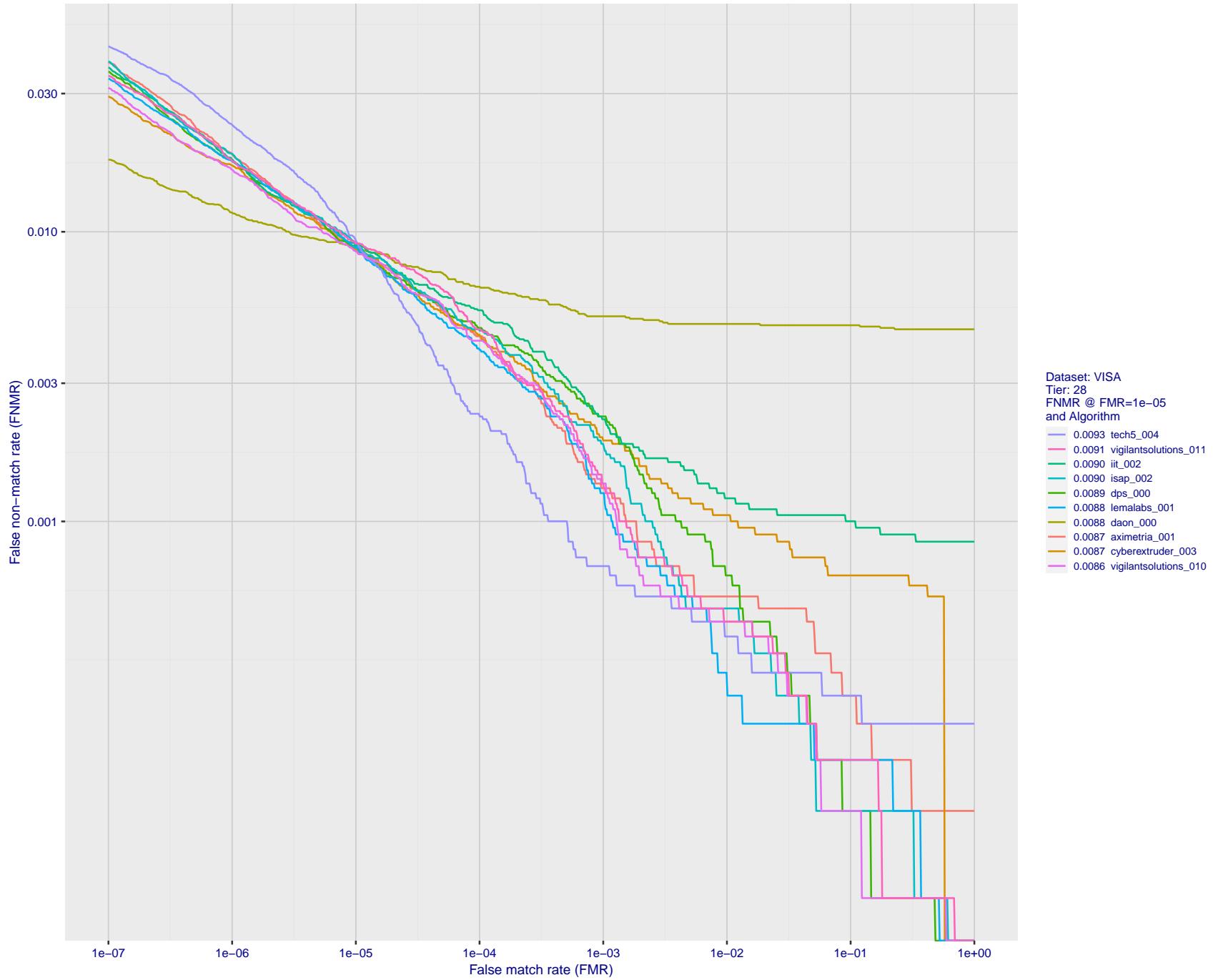


Figure 71: For the visa images, detection error tradeoff (DET) characteristics showing false non-match rate vs. false match rate plotted parametrically on threshold, T . The scales are logarithmic in order to show many decades of FMR.

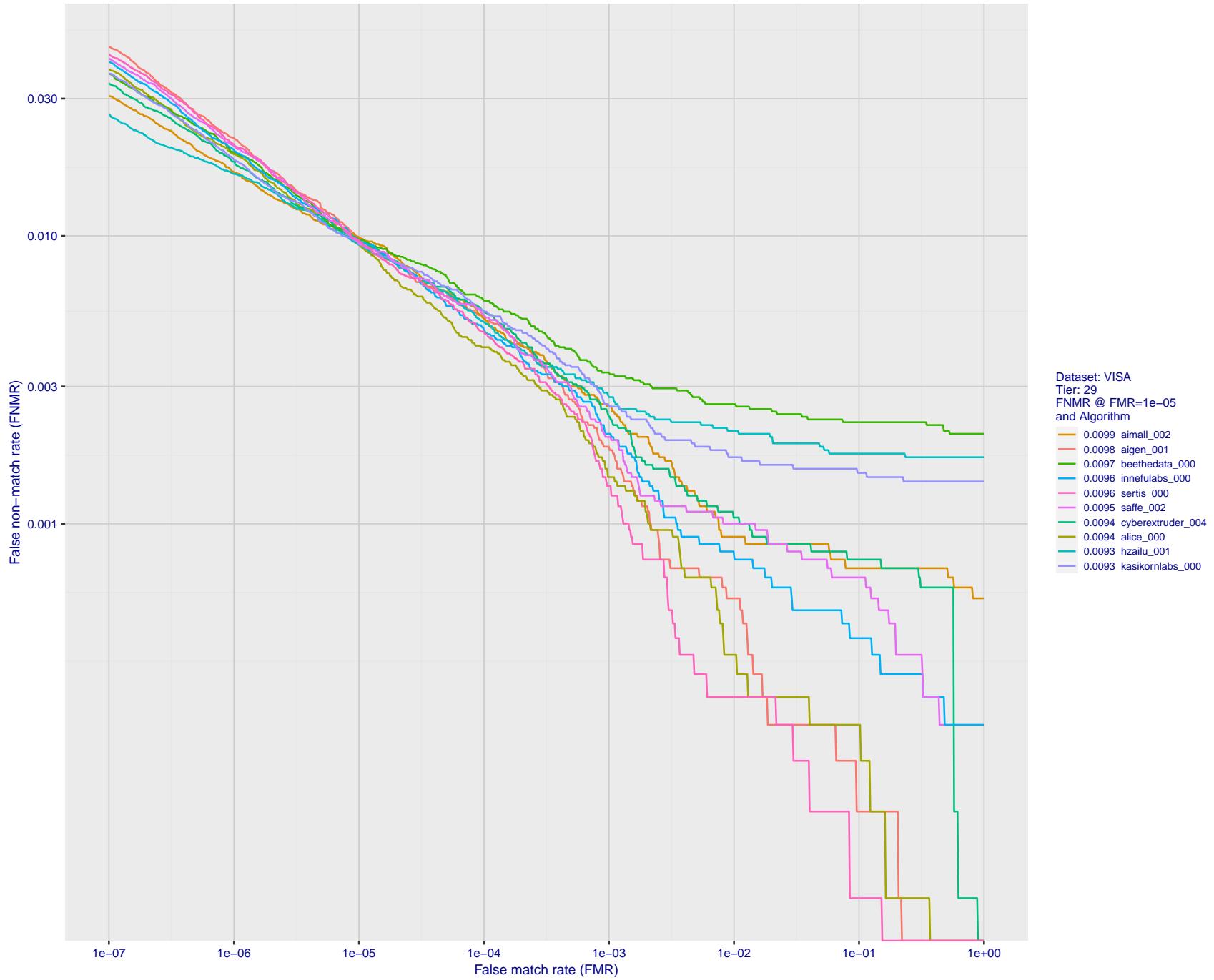


Figure 72: For the visa images, detection error tradeoff (DET) characteristics showing false non-match rate vs. false match rate plotted parametrically on threshold, T . The scales are logarithmic in order to show many decades of FMR.

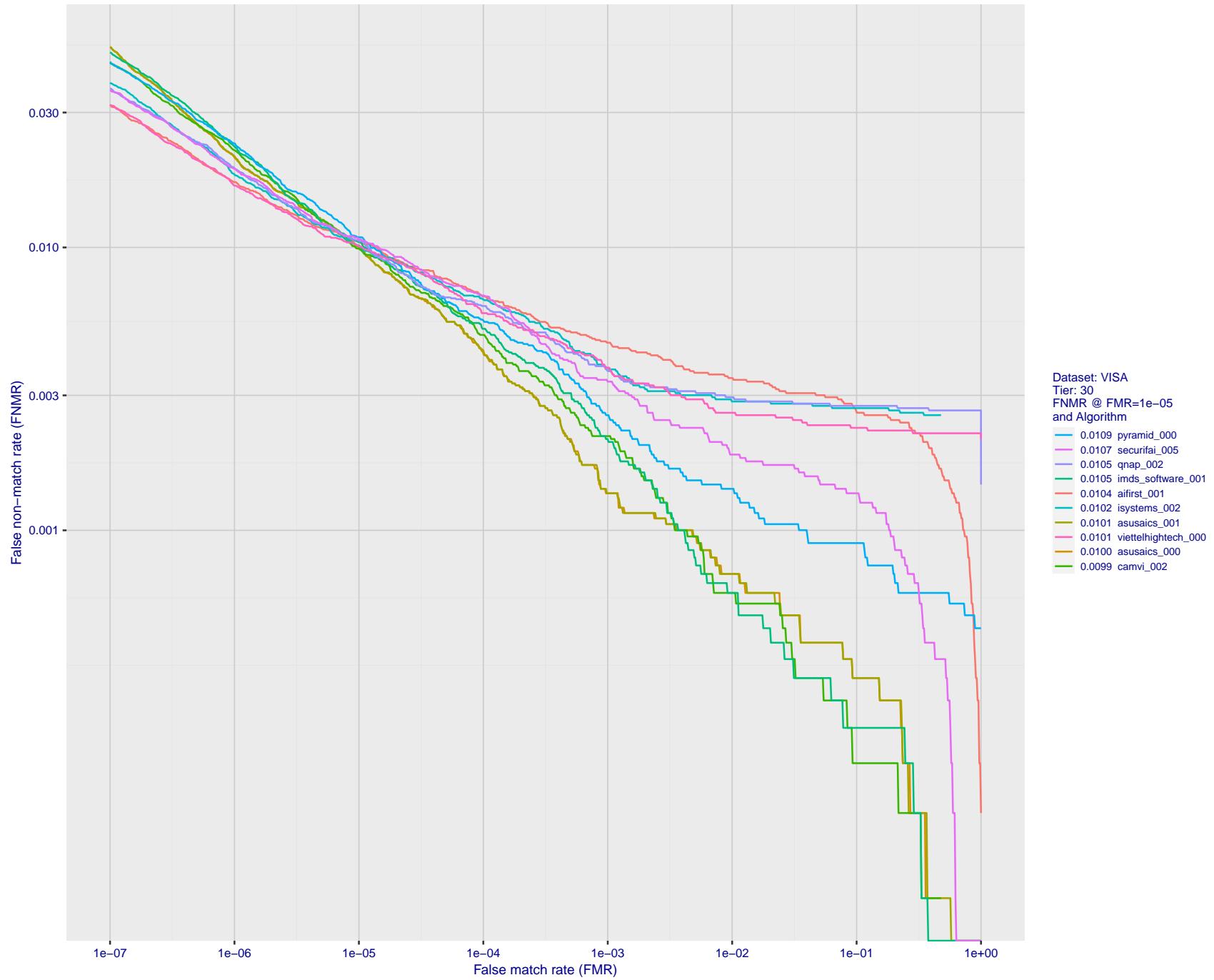


Figure 73: For the visa images, detection error tradeoff (DET) characteristics showing false non-match rate vs. false match rate plotted parametrically on threshold, T . The scales are logarithmic in order to show many decades of FMR.

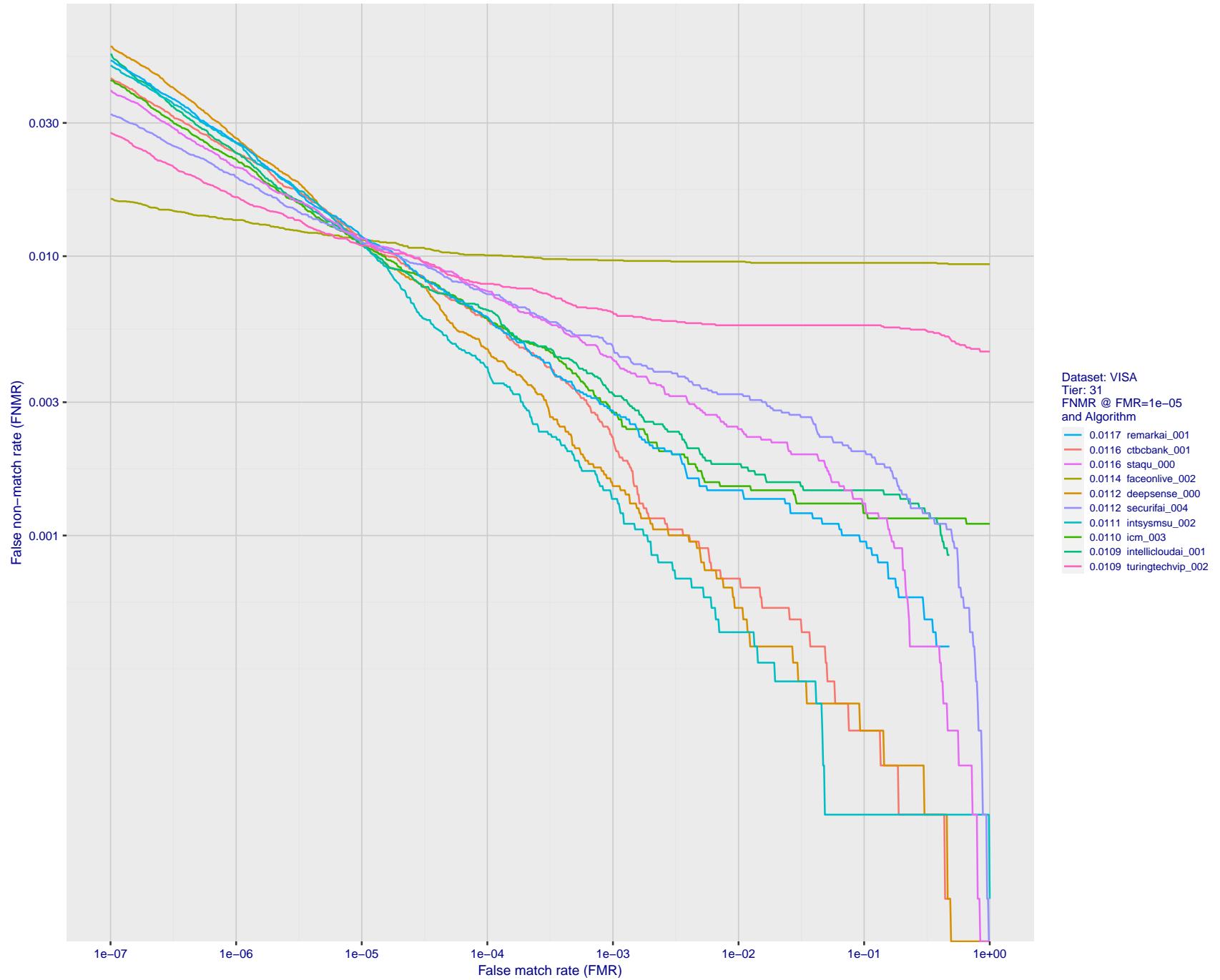


Figure 74: For the visa images, detection error tradeoff (DET) characteristics showing false non-match rate vs. false match rate plotted parametrically on threshold, T . The scales are logarithmic in order to show many decades of FMR.

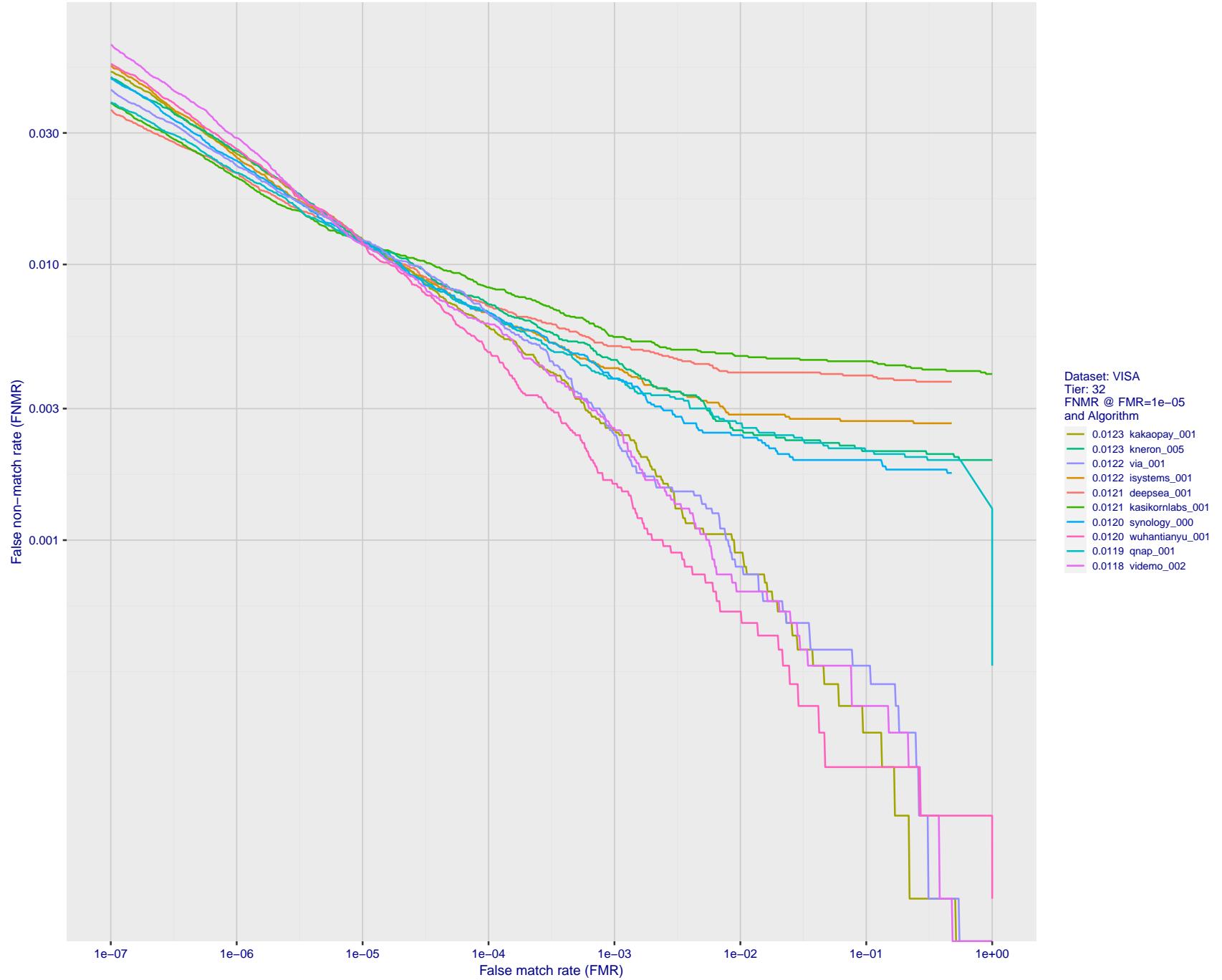


Figure 75: For the visa images, detection error tradeoff (DET) characteristics showing false non-match rate vs. false match rate plotted parametrically on threshold, T . The scales are logarithmic in order to show many decades of FMR.

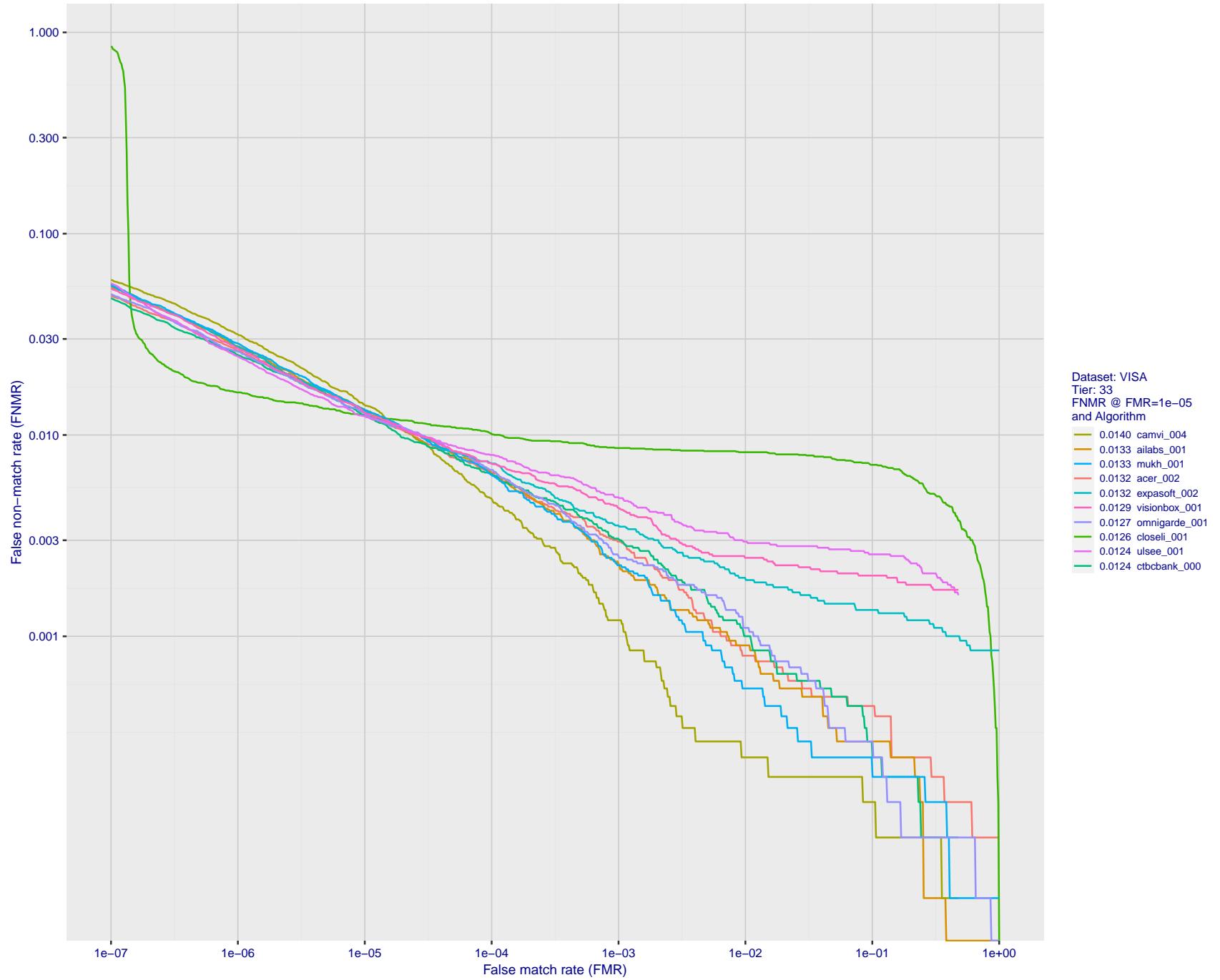


Figure 76: For the visa images, detection error tradeoff (DET) characteristics showing false non-match rate vs. false match rate plotted parametrically on threshold, T . The scales are logarithmic in order to show many decades of FMR.

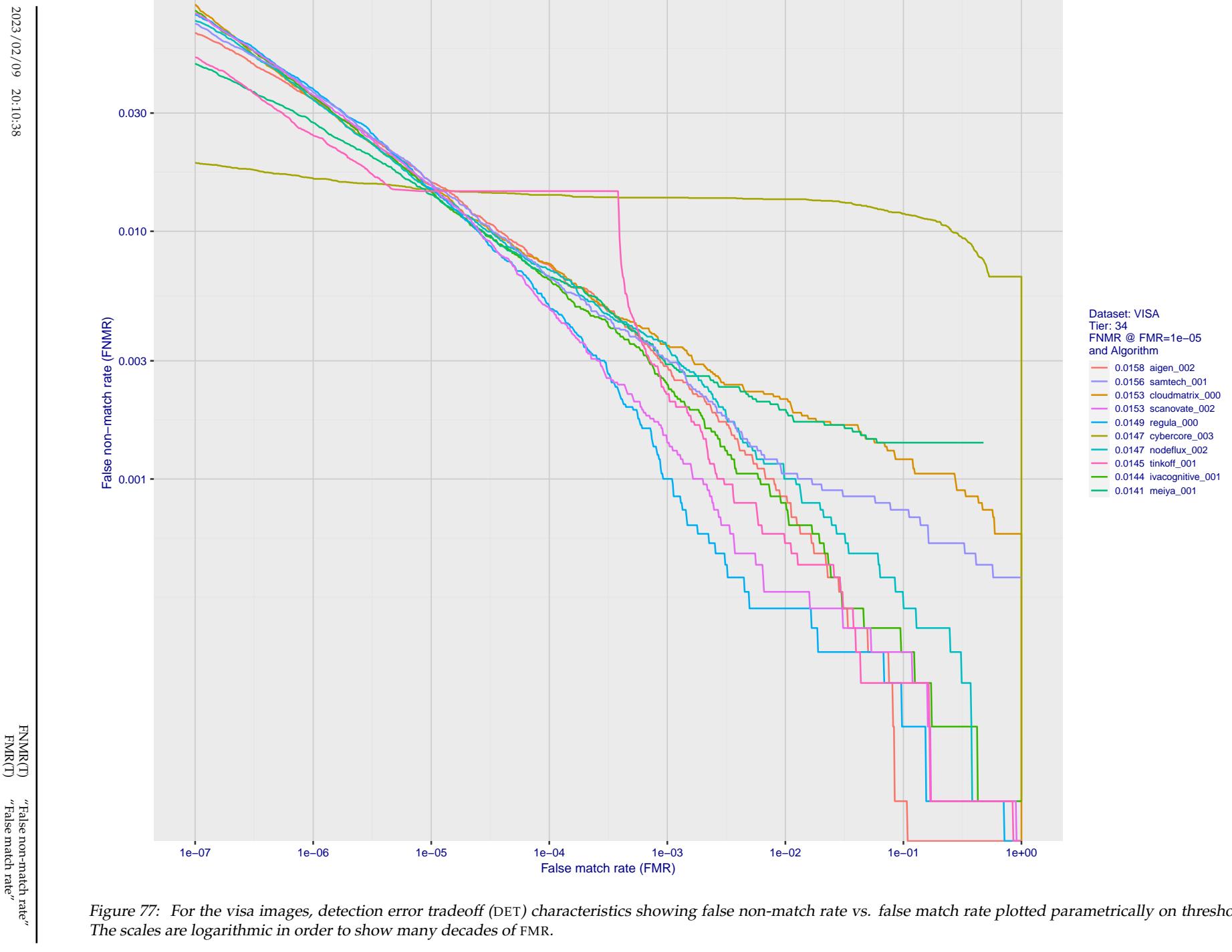


Figure 77: For the visa images, detection error tradeoff (DET) characteristics showing false non-match rate vs. false match rate plotted parametrically on threshold, T . The scales are logarithmic in order to show many decades of FMR.

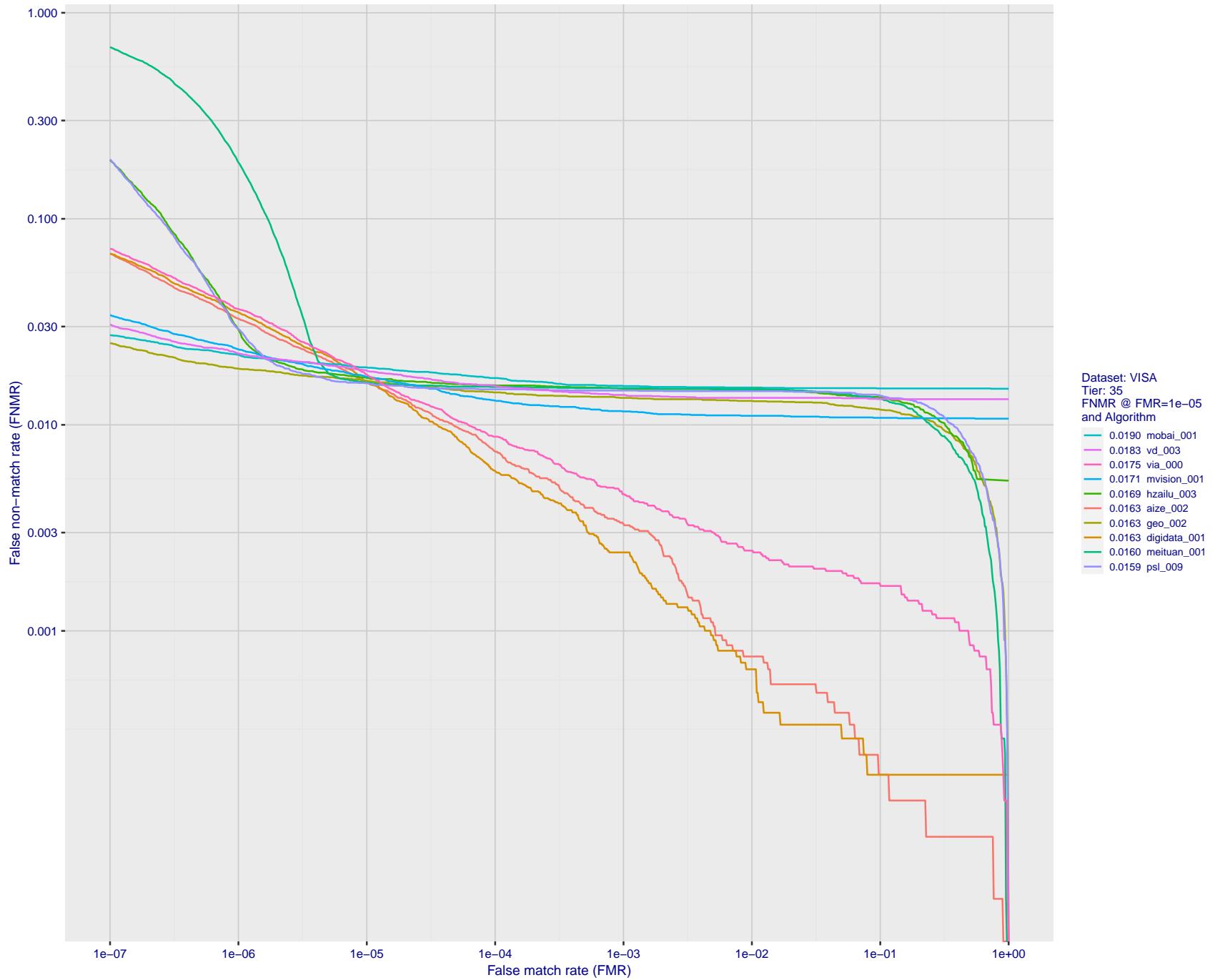


Figure 78: For the visa images, detection error tradeoff (DET) characteristics showing false non-match rate vs. false match rate plotted parametrically on threshold, T . The scales are logarithmic in order to show many decades of FMR.

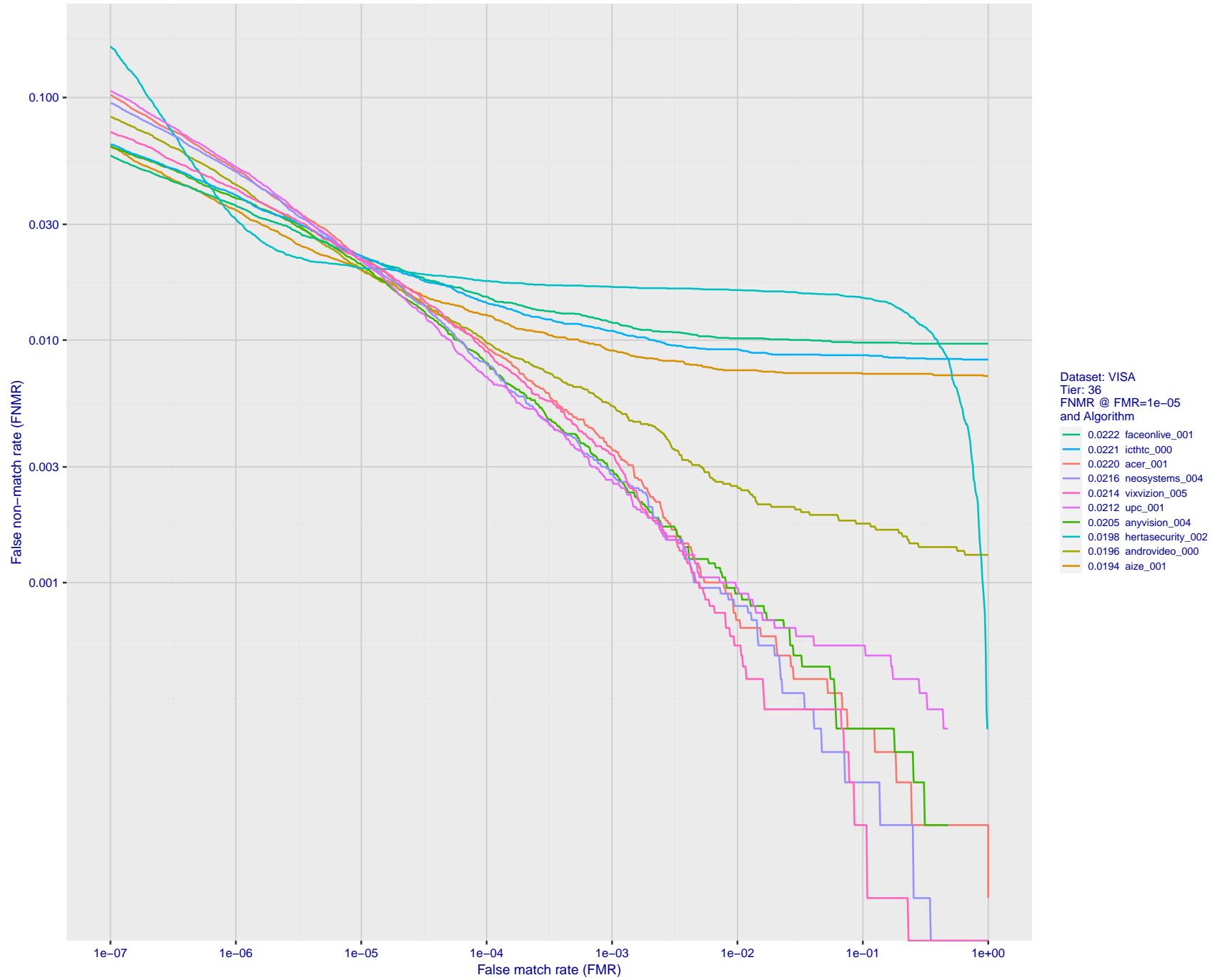


Figure 79: For the visa images, detection error tradeoff (DET) characteristics showing false non-match rate vs. false match rate plotted parametrically on threshold, T . The scales are logarithmic in order to show many decades of FMR.

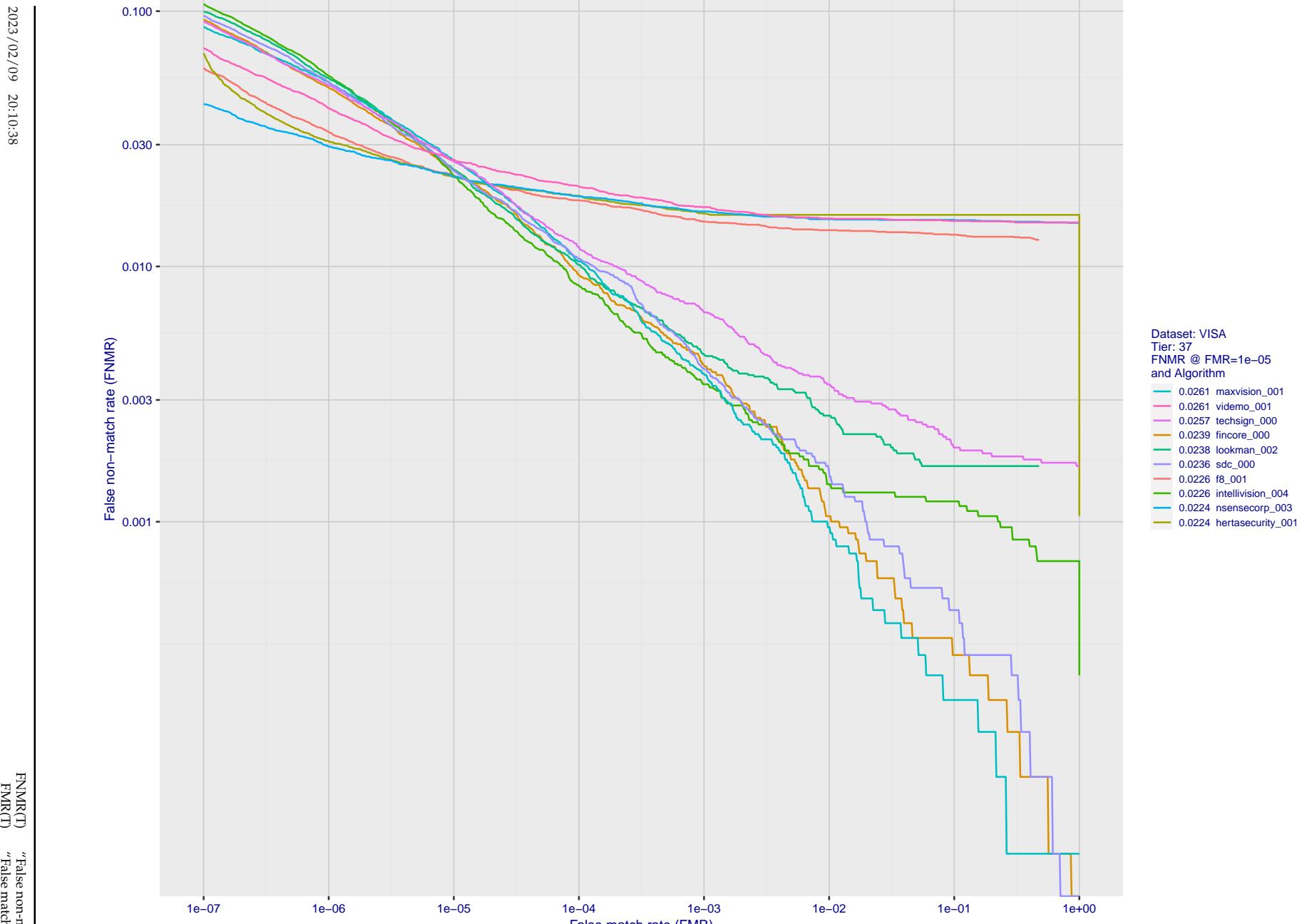


Figure 80: For the visa images, detection error tradeoff (DET) characteristics showing false non-match rate vs. false match rate plotted parametrically on threshold, T . The scales are logarithmic in order to show many decades of FMR.

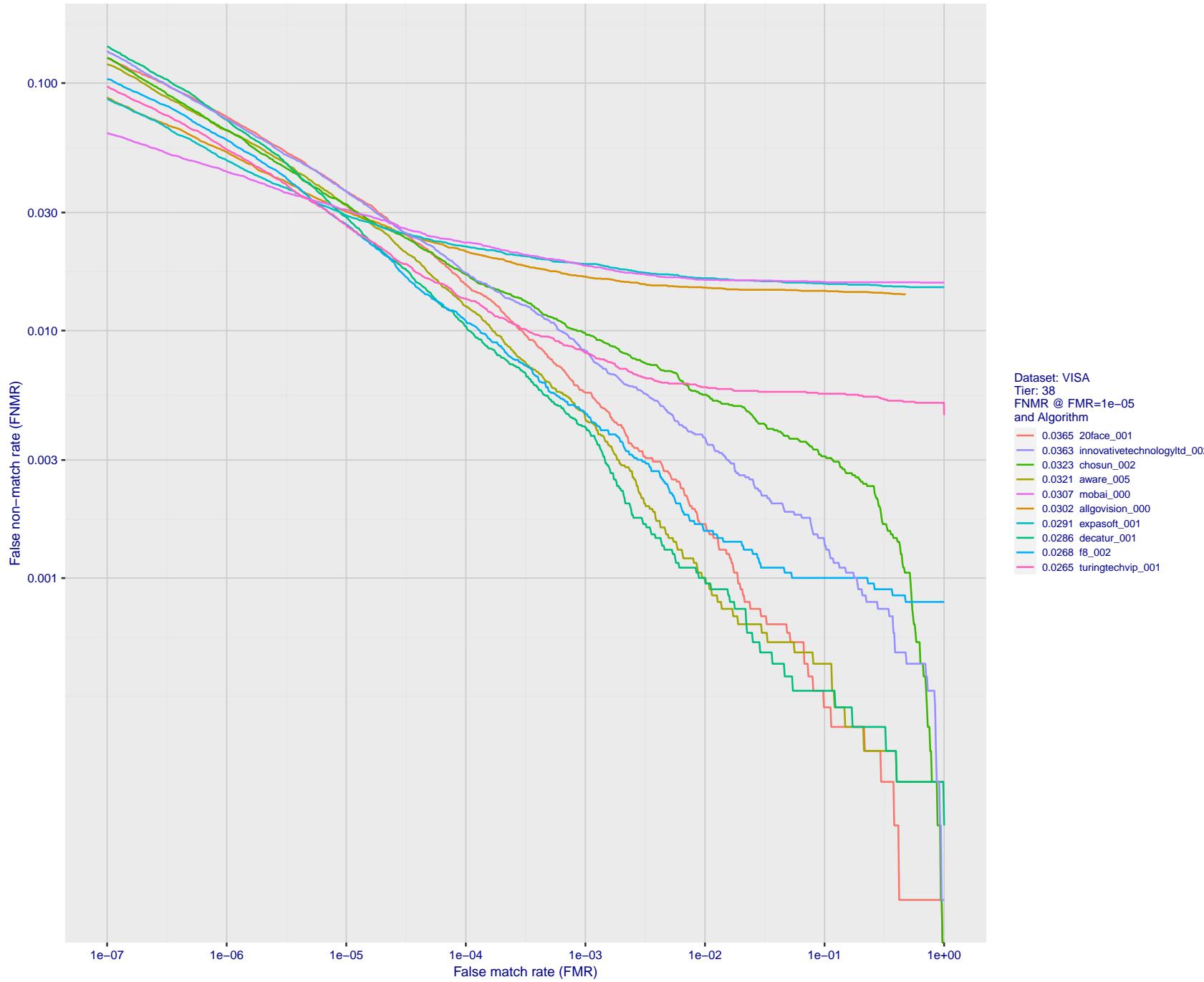


Figure 81: For the visa images, detection error tradeoff (DET) characteristics showing false non-match rate vs. false match rate plotted parametrically on threshold, T . The scales are logarithmic in order to show many decades of FMR.

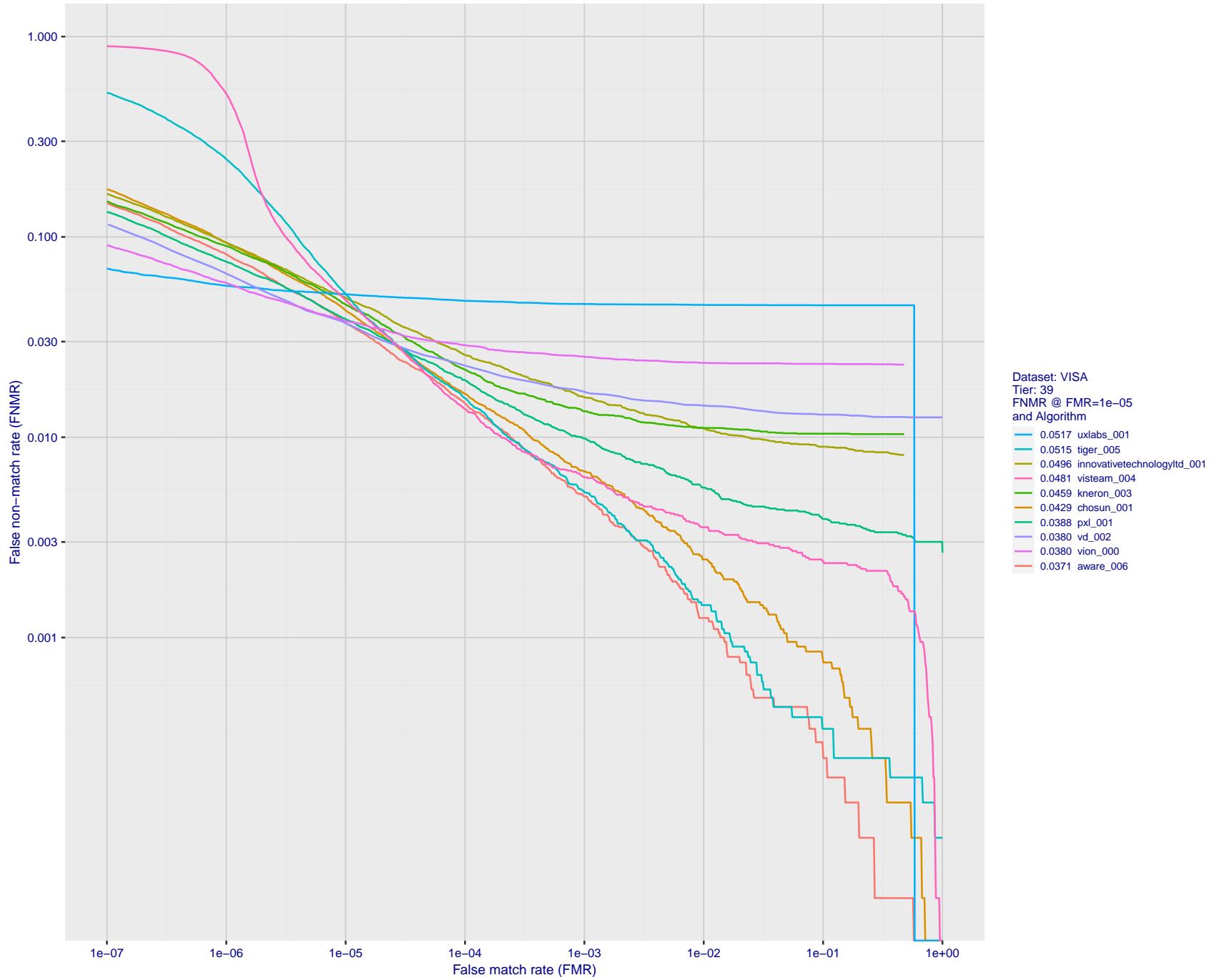


Figure 82: For the visa images, detection error tradeoff (DET) characteristics showing false non-match rate vs. false match rate plotted parametrically on threshold, T . The scales are logarithmic in order to show many decades of FMR.

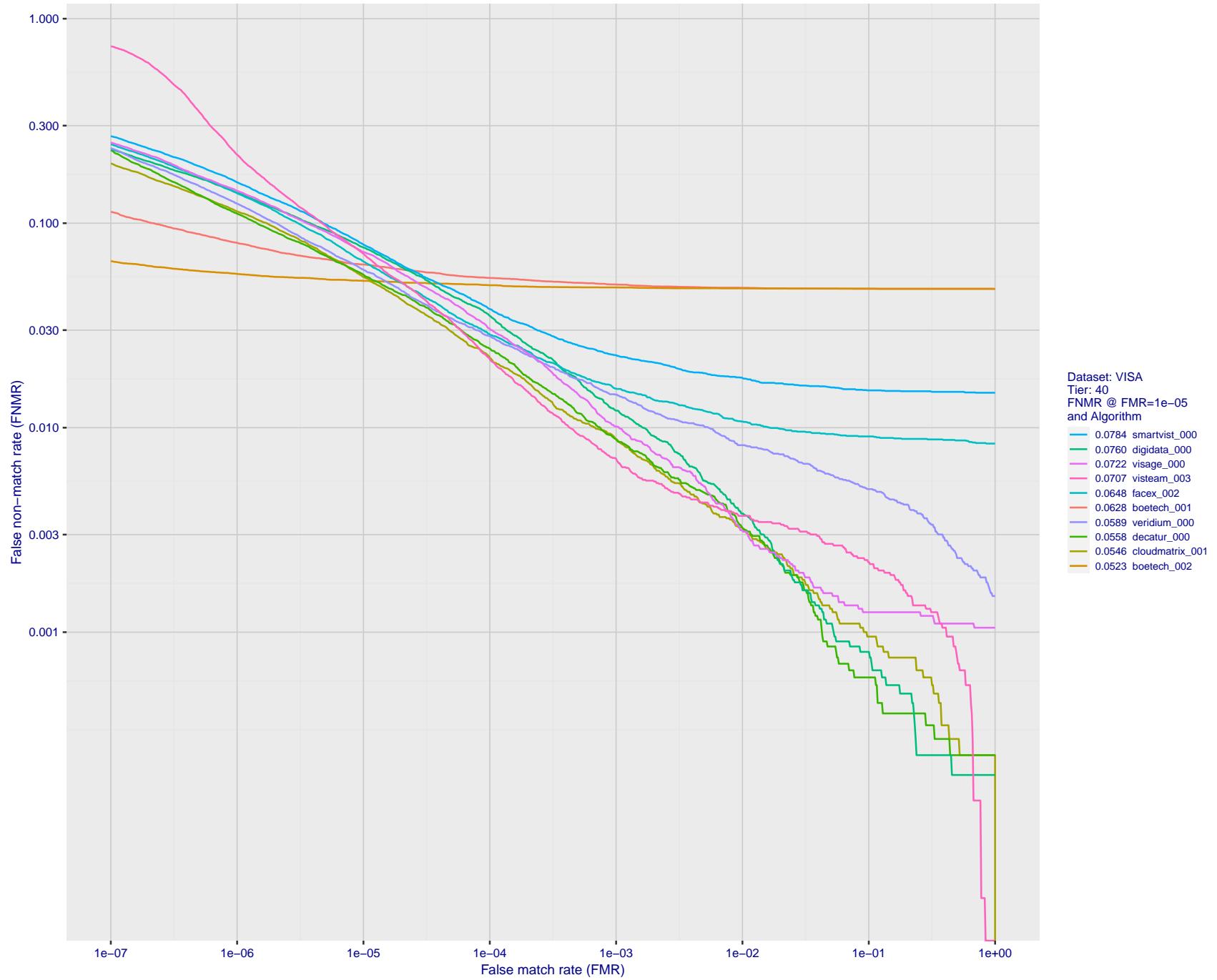


Figure 83: For the visa images, detection error tradeoff (DET) characteristics showing false non-match rate vs. false match rate plotted parametrically on threshold, T . The scales are logarithmic in order to show many decades of FMR.

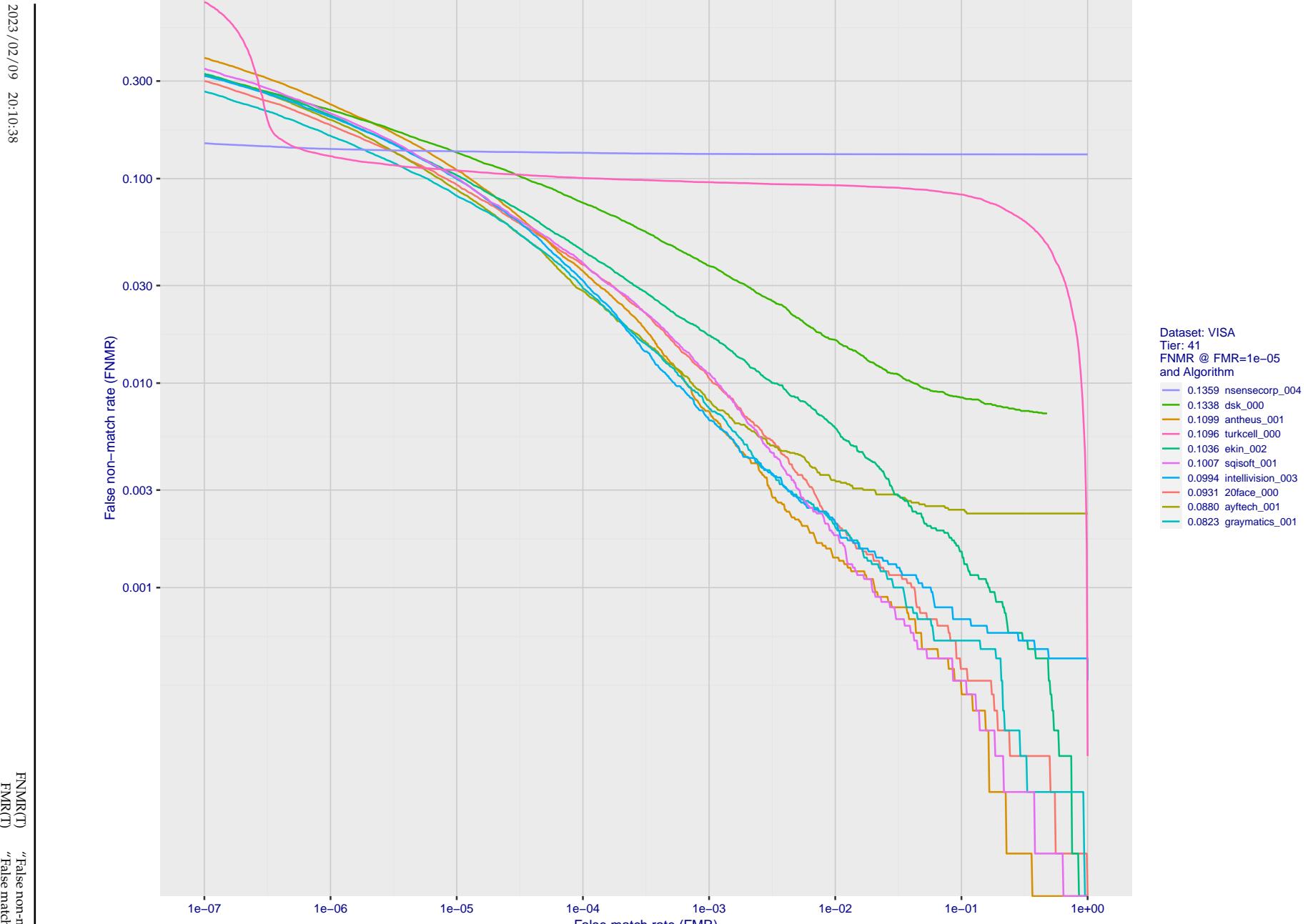


Figure 84: For the visa images, detection error tradeoff (DET) characteristics showing false non-match rate vs. false match rate plotted parametrically on threshold, T . The scales are logarithmic in order to show many decades of FMR.

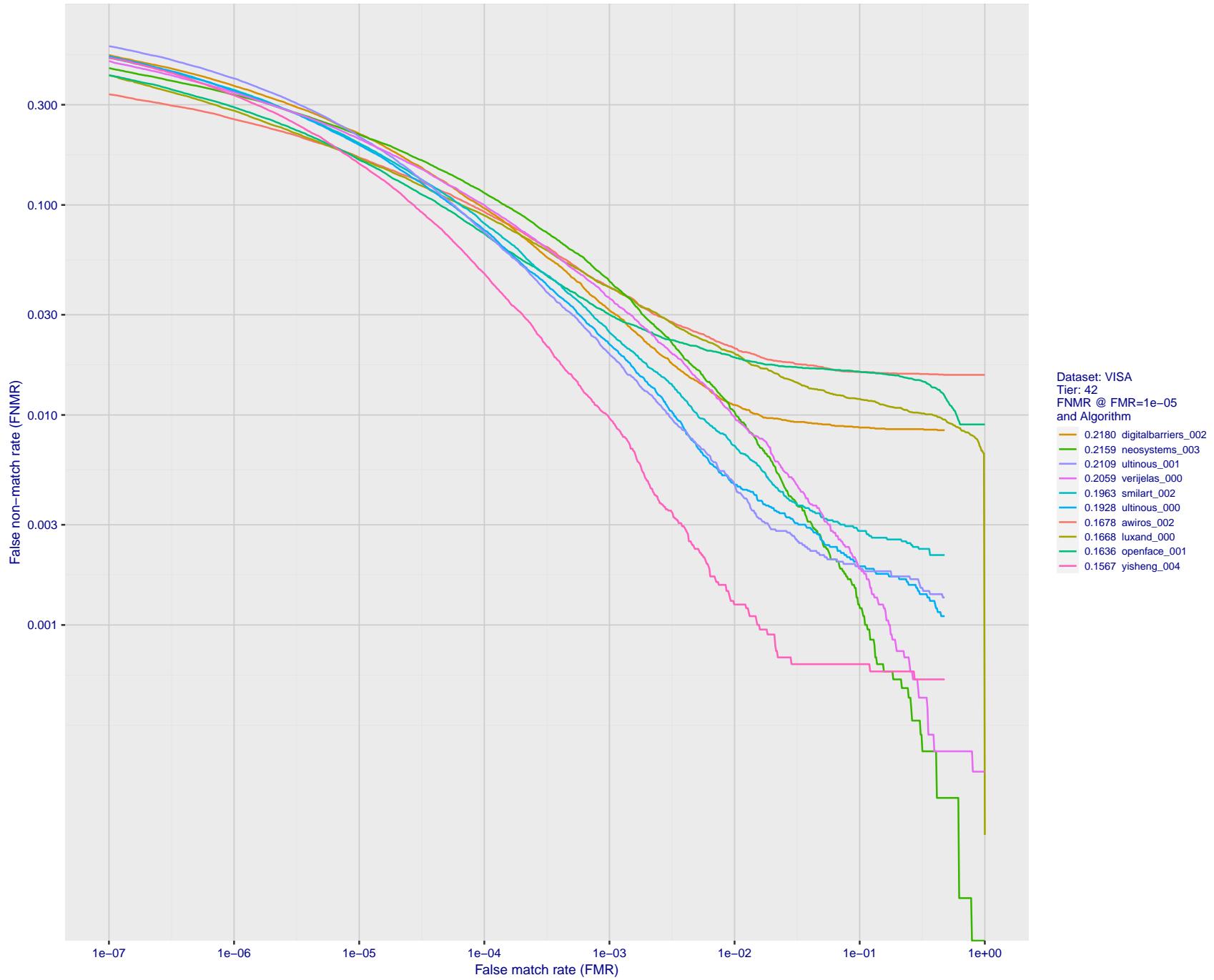


Figure 85: For the visa images, detection error tradeoff (DET) characteristics showing false non-match rate vs. false match rate plotted parametrically on threshold, T . The scales are logarithmic in order to show many decades of FMR.

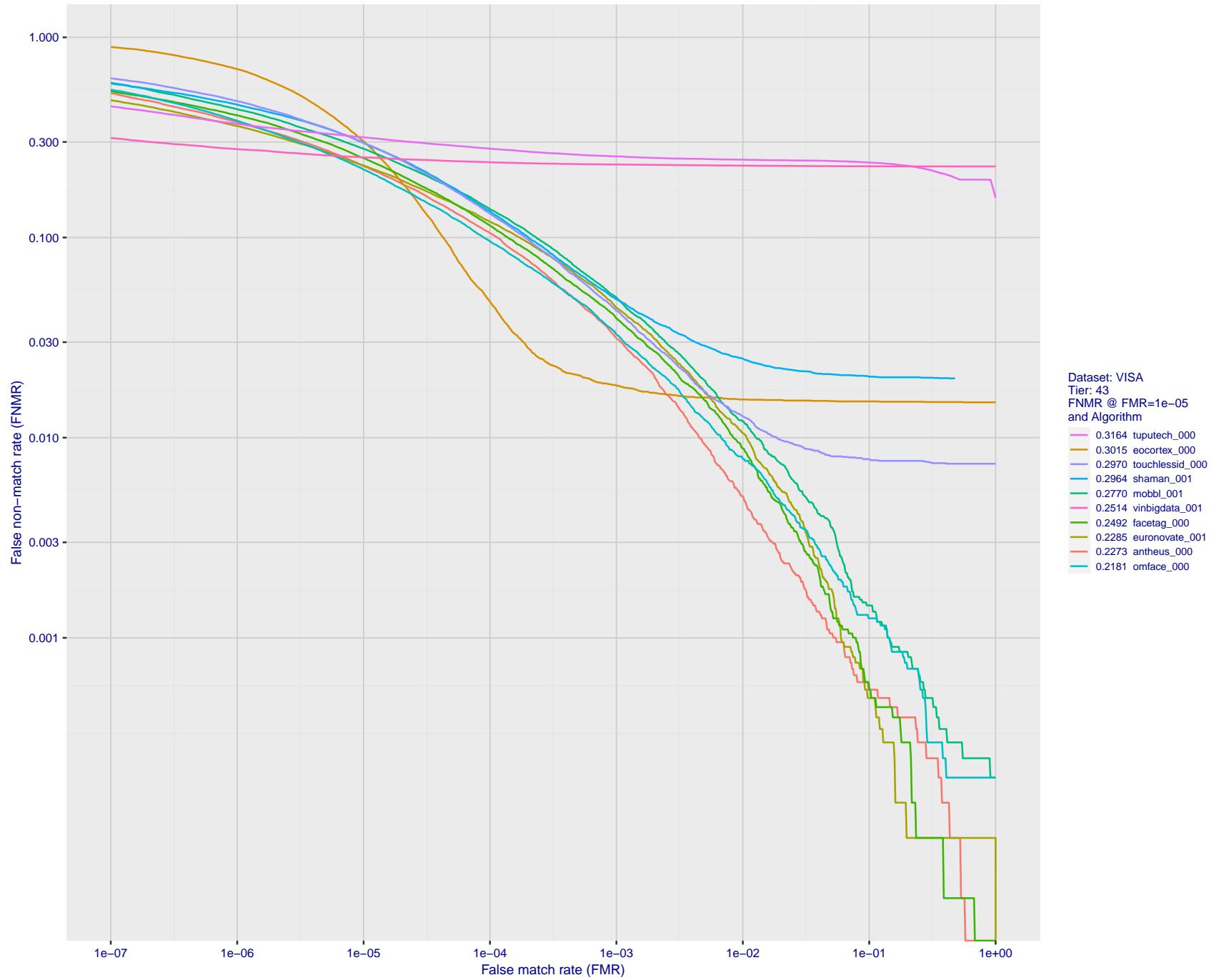


Figure 86: For the visa images, detection error tradeoff (DET) characteristics showing false non-match rate vs. false match rate plotted parametrically on threshold, T . The scales are logarithmic in order to show many decades of FMR.

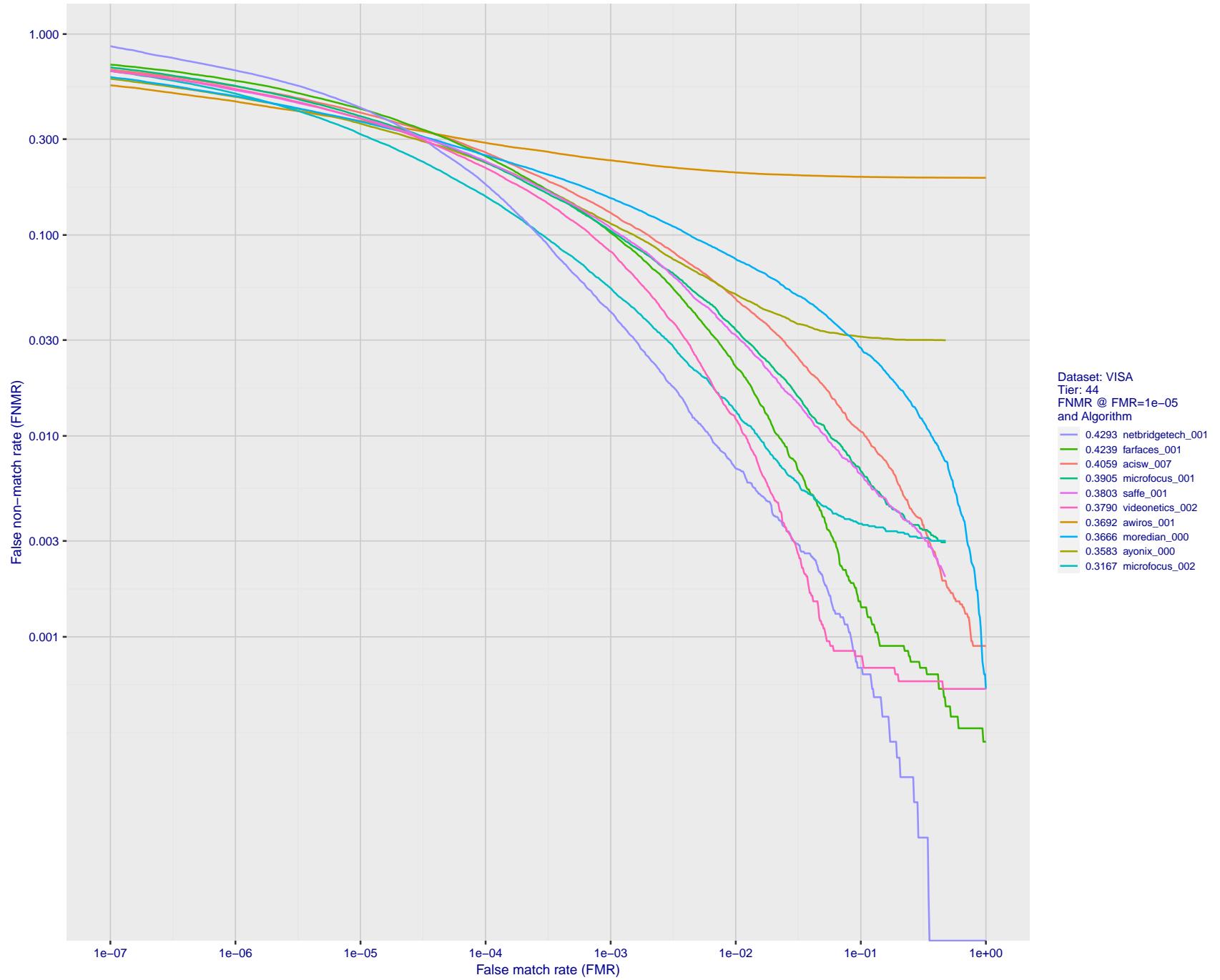


Figure 87: For the visa images, detection error tradeoff (DET) characteristics showing false non-match rate vs. false match rate plotted parametrically on threshold, T . The scales are logarithmic in order to show many decades of FMR.

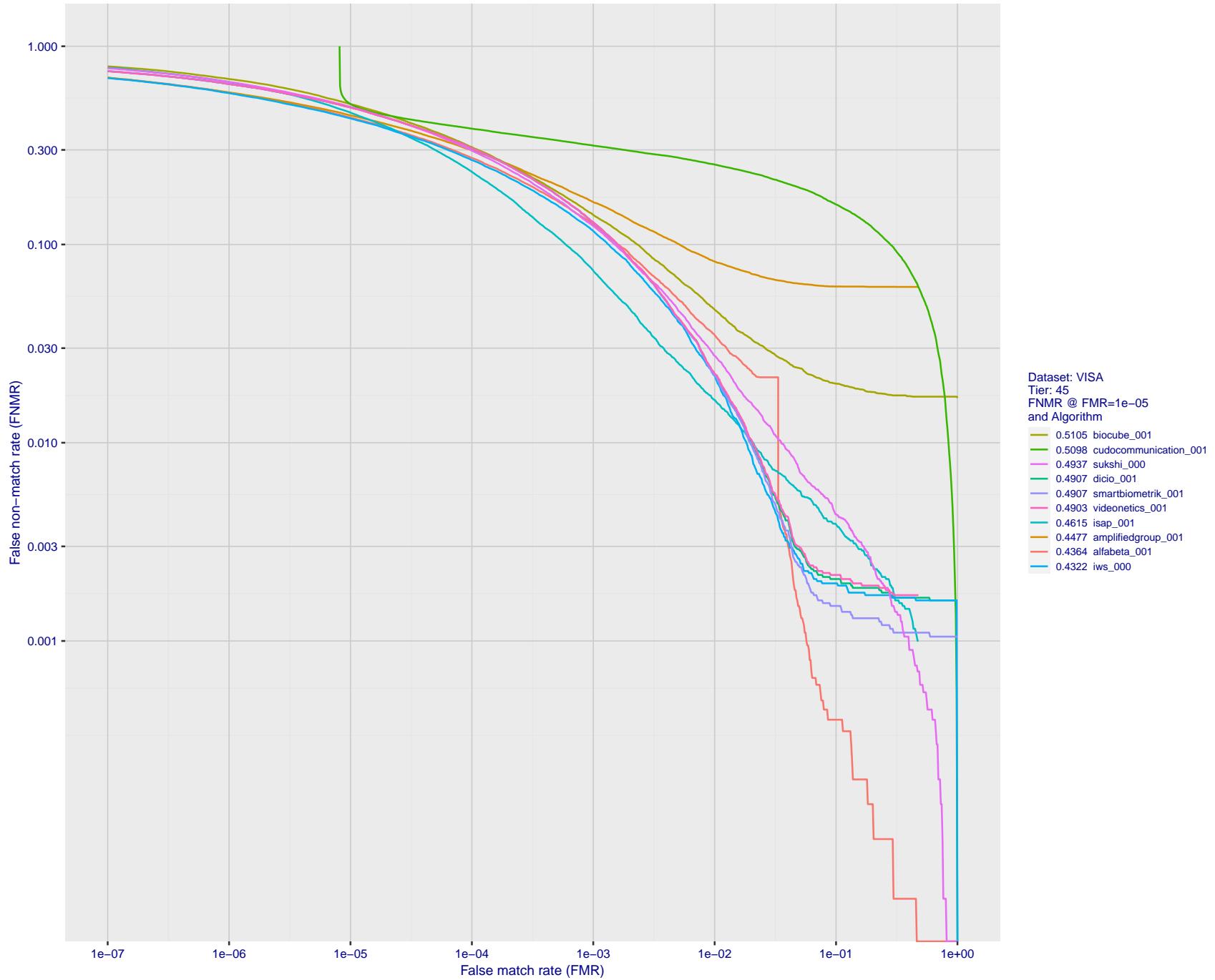


Figure 88: For the visa images, detection error tradeoff (DET) characteristics showing false non-match rate vs. false match rate plotted parametrically on threshold, T . The scales are logarithmic in order to show many decades of FMR.

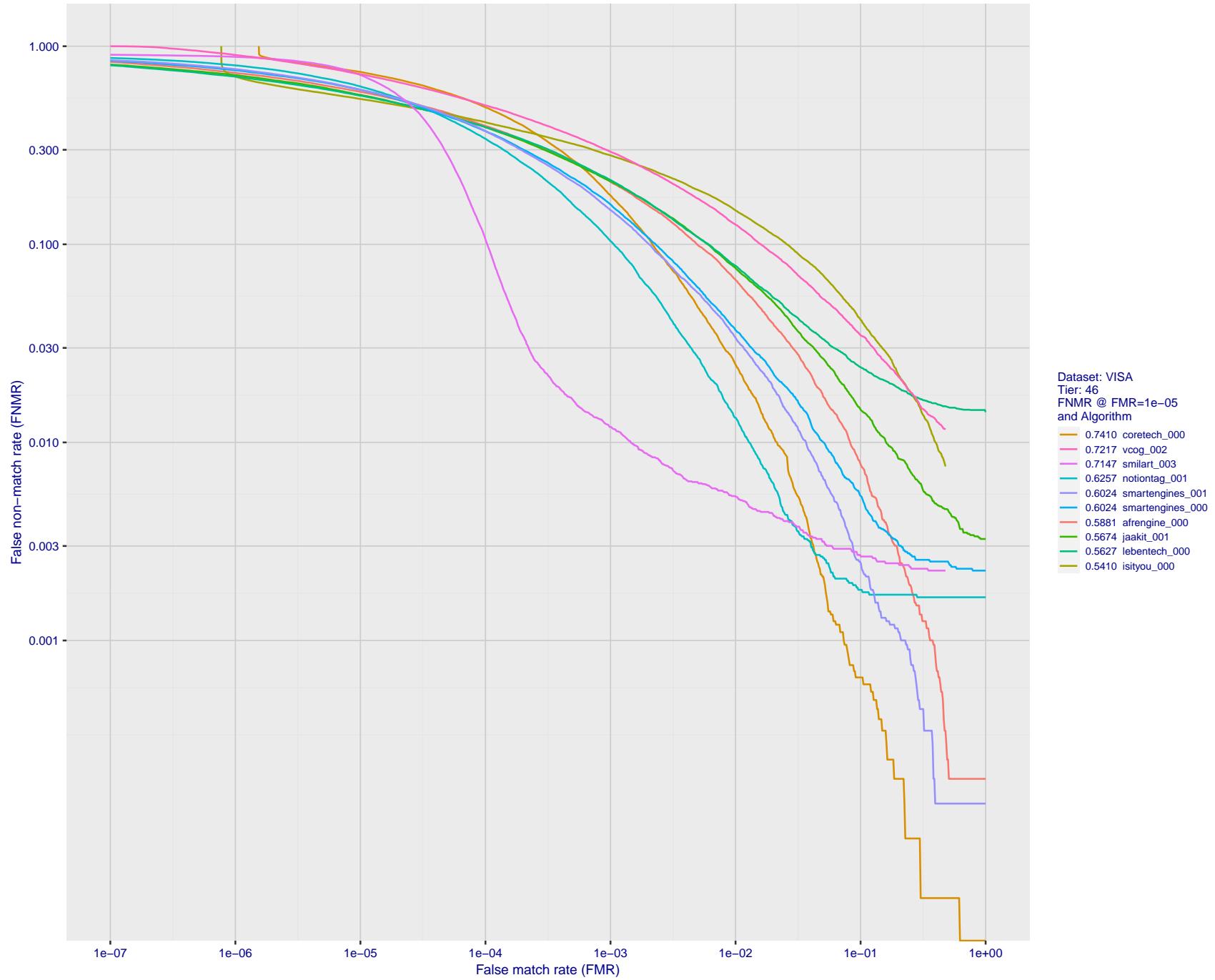


Figure 89: For the visa images, detection error tradeoff (DET) characteristics showing false non-match rate vs. false match rate plotted parametrically on threshold, T . The scales are logarithmic in order to show many decades of FMR.

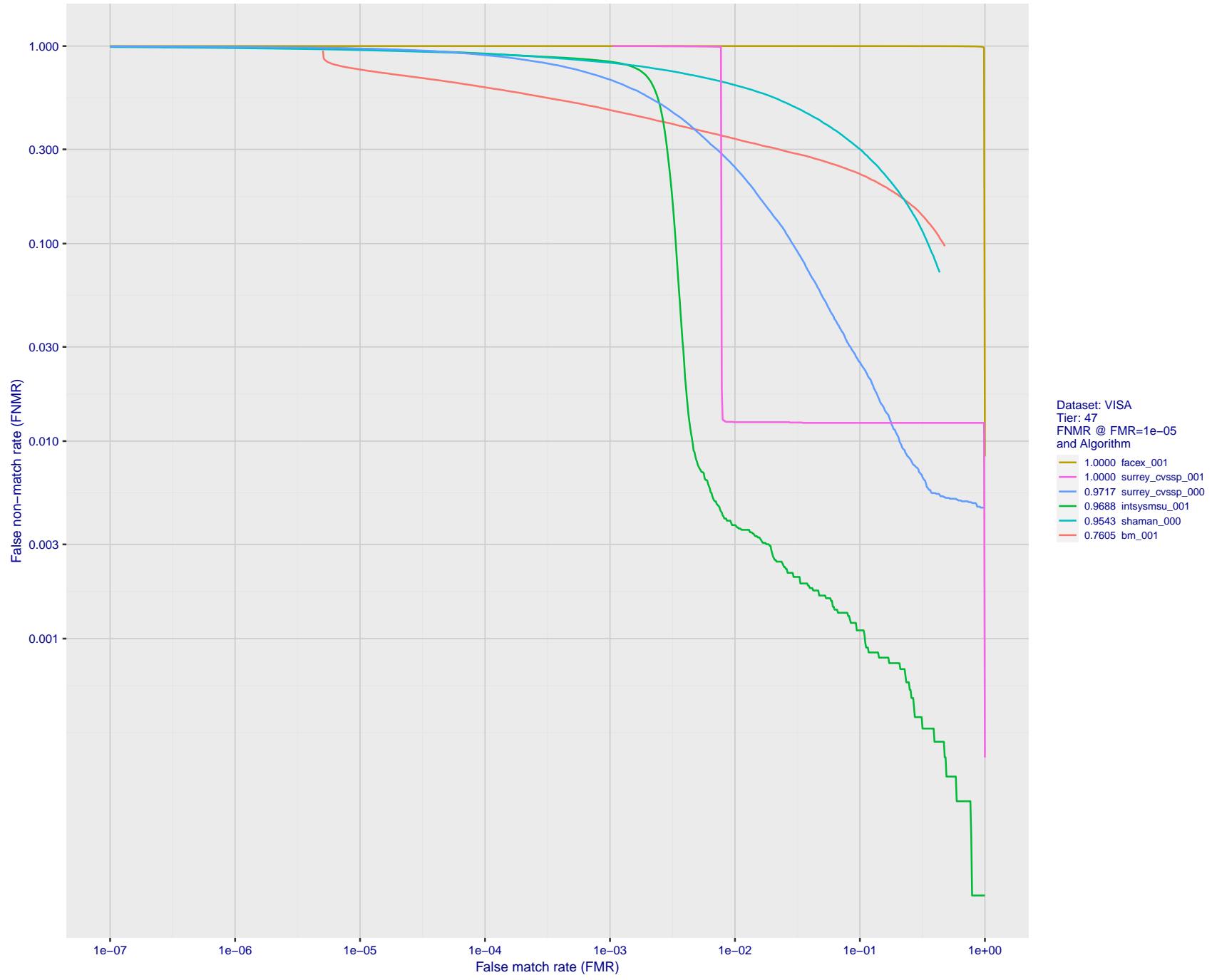


Figure 90: For the visa images, detection error tradeoff (DET) characteristics showing false non-match rate vs. false match rate plotted parametrically on threshold, T . The scales are logarithmic in order to show many decades of FMR.

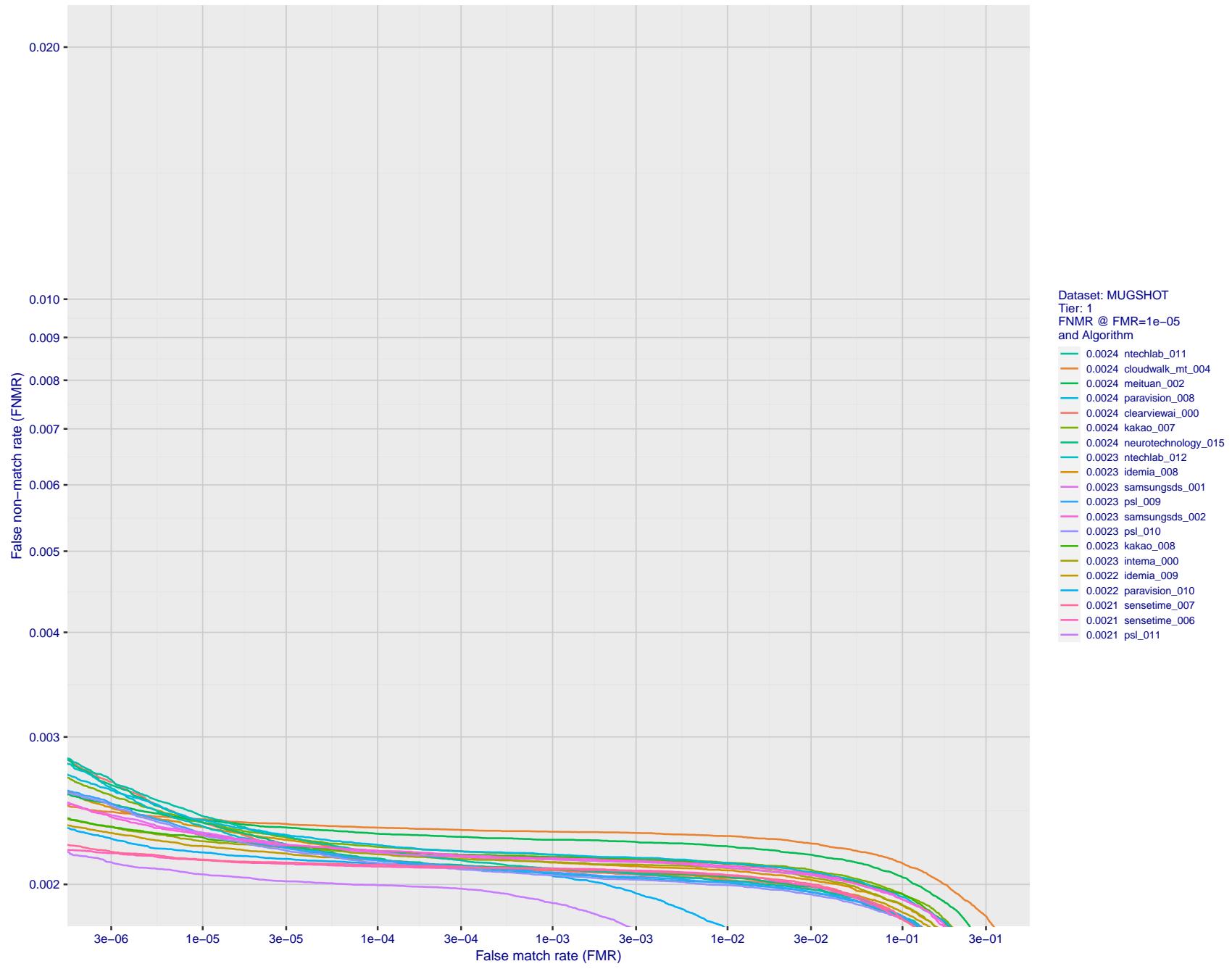


Figure 91: For the mugshot images, detection error tradeoff (DET) characteristics showing false non-match rate vs. false match rate plotted parametrically on threshold, T. The scales are logarithmic in order to show decades of FMR.

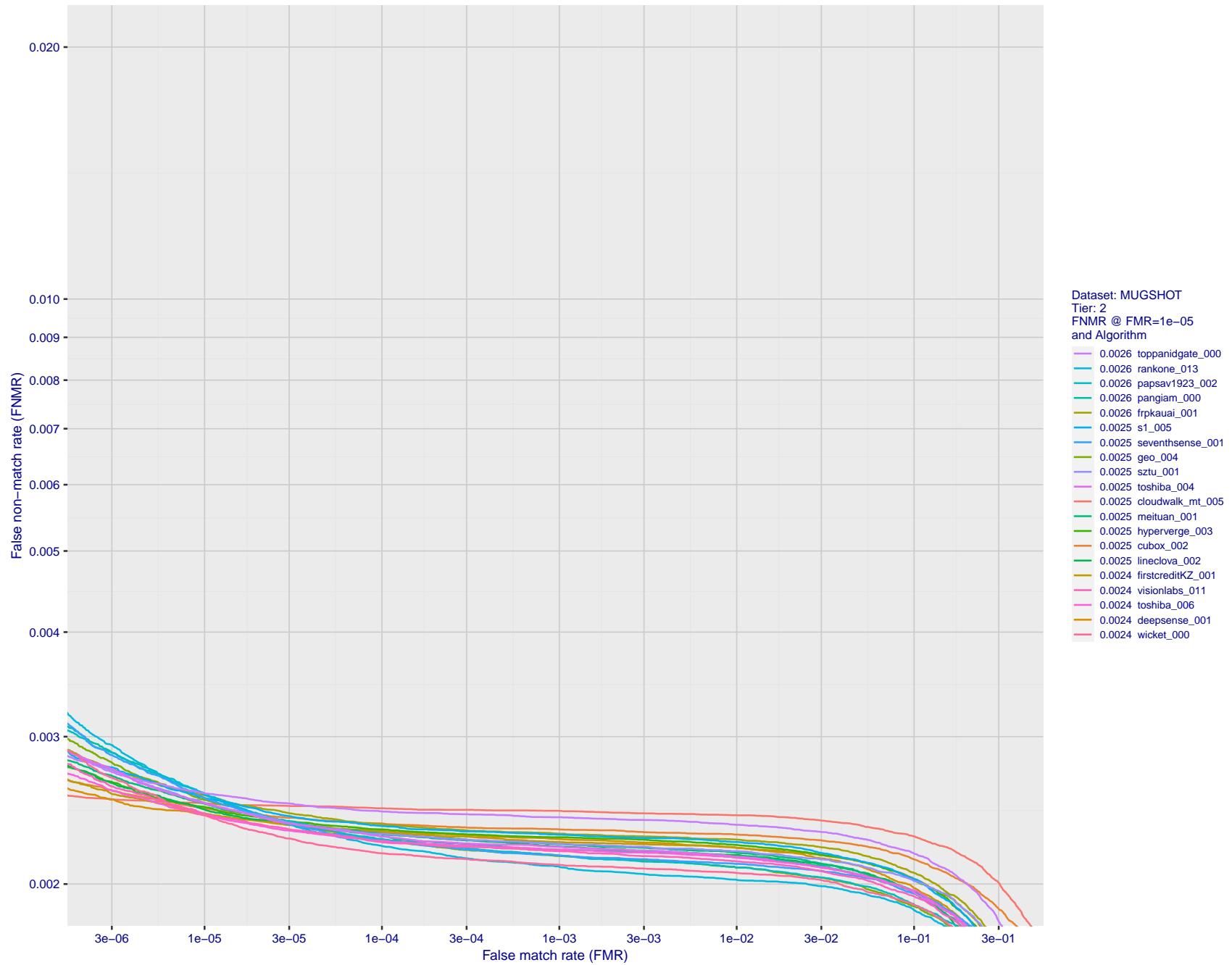


Figure 92: For the mugshot images, detection error tradeoff (DET) characteristics showing false non-match rate vs. false match rate plotted parametrically on threshold, T . The scales are logarithmic in order to show decades of FMR.

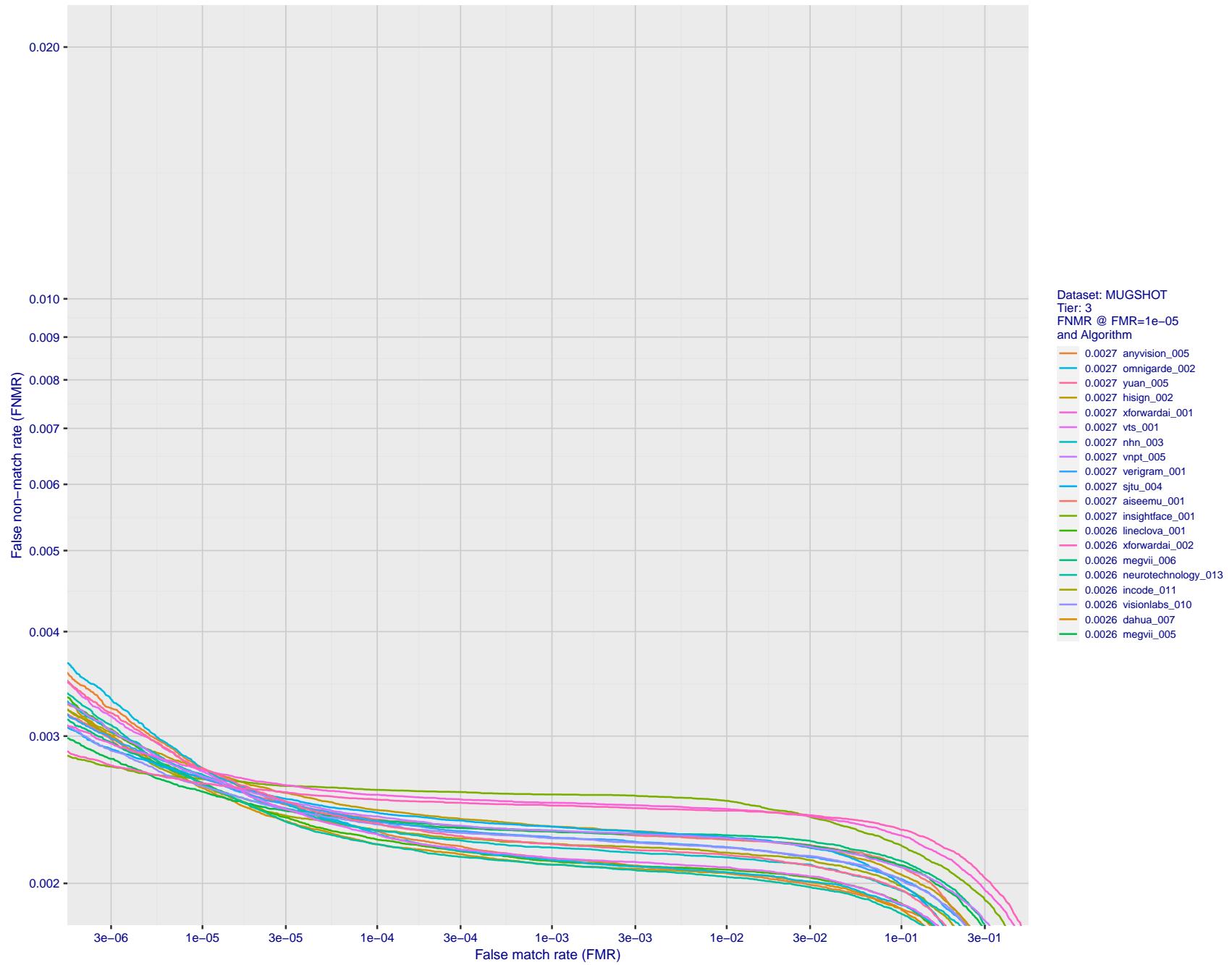


Figure 93: For the mugshot images, detection error tradeoff (DET) characteristics showing false non-match rate vs. false match rate plotted parametrically on threshold, T . The scales are logarithmic in order to show decades of FMR.

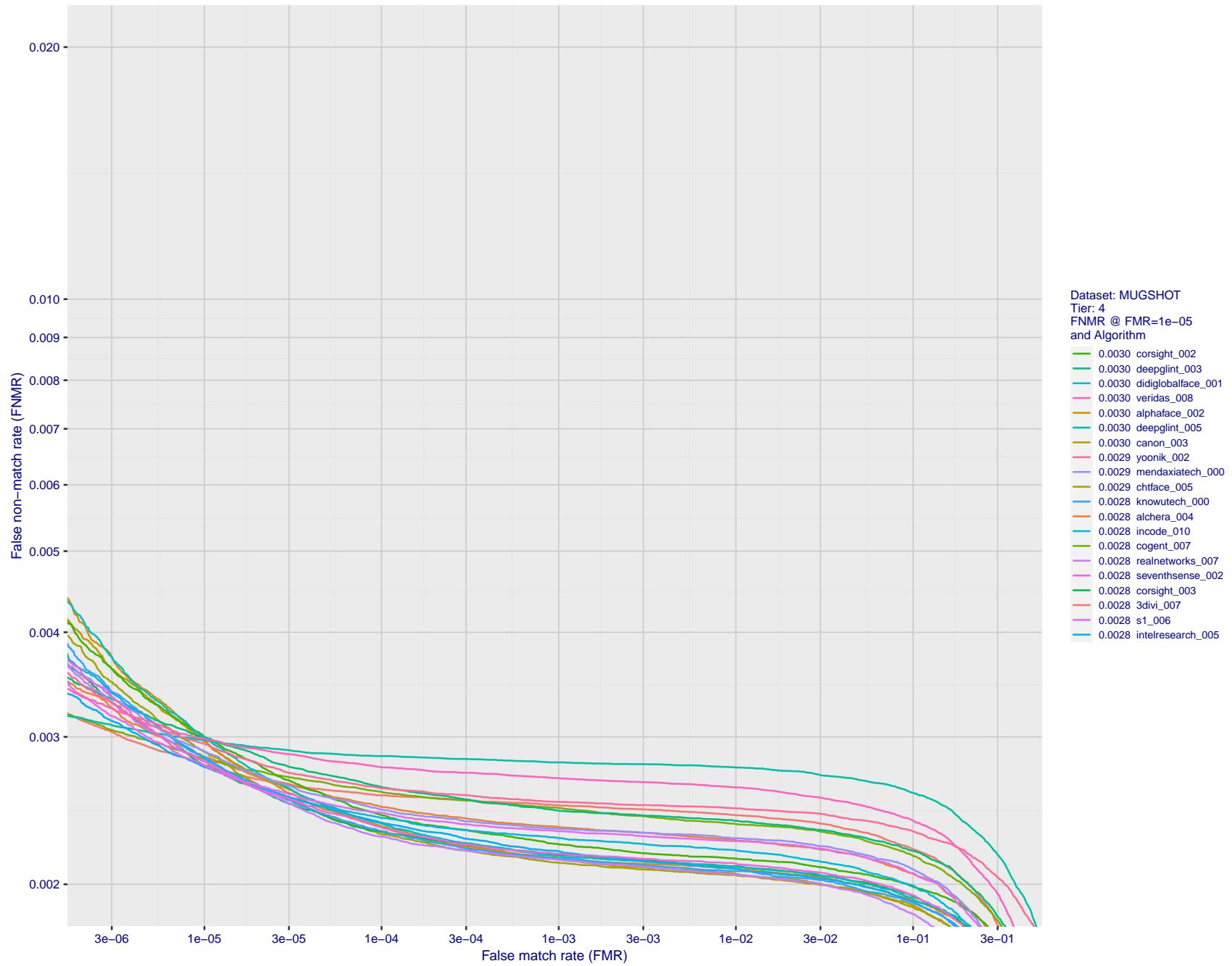


Figure 94: For the mugshot images, detection error tradeoff (DET) characteristics showing false non-match rate vs. false match rate plotted parametrically on threshold, T . The scales are logarithmic in order to show decades of FMR.

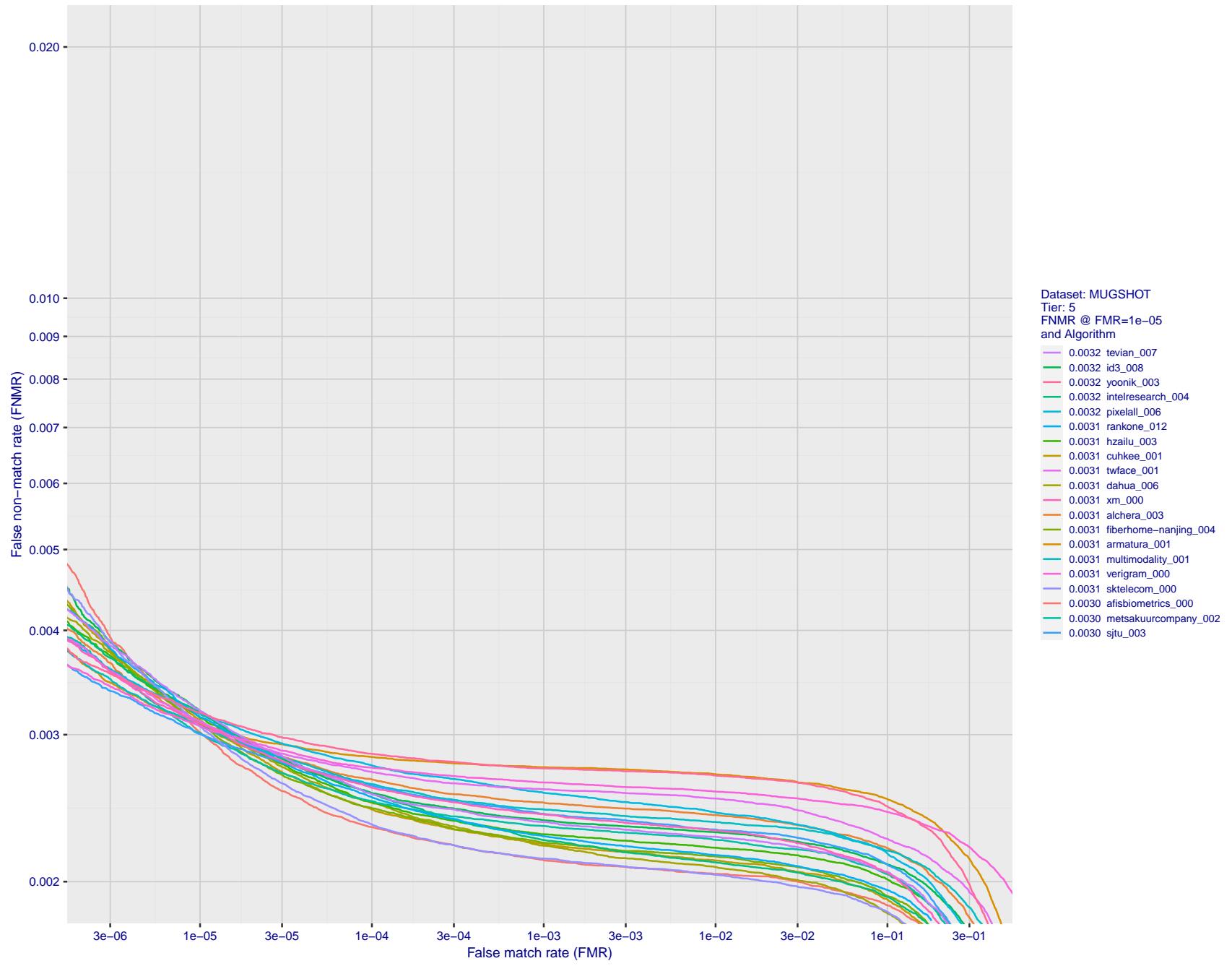


Figure 95: For the mugshot images, detection error tradeoff (DET) characteristics showing false non-match rate vs. false match rate plotted parametrically on threshold, T . The scales are logarithmic in order to show decades of FMR.

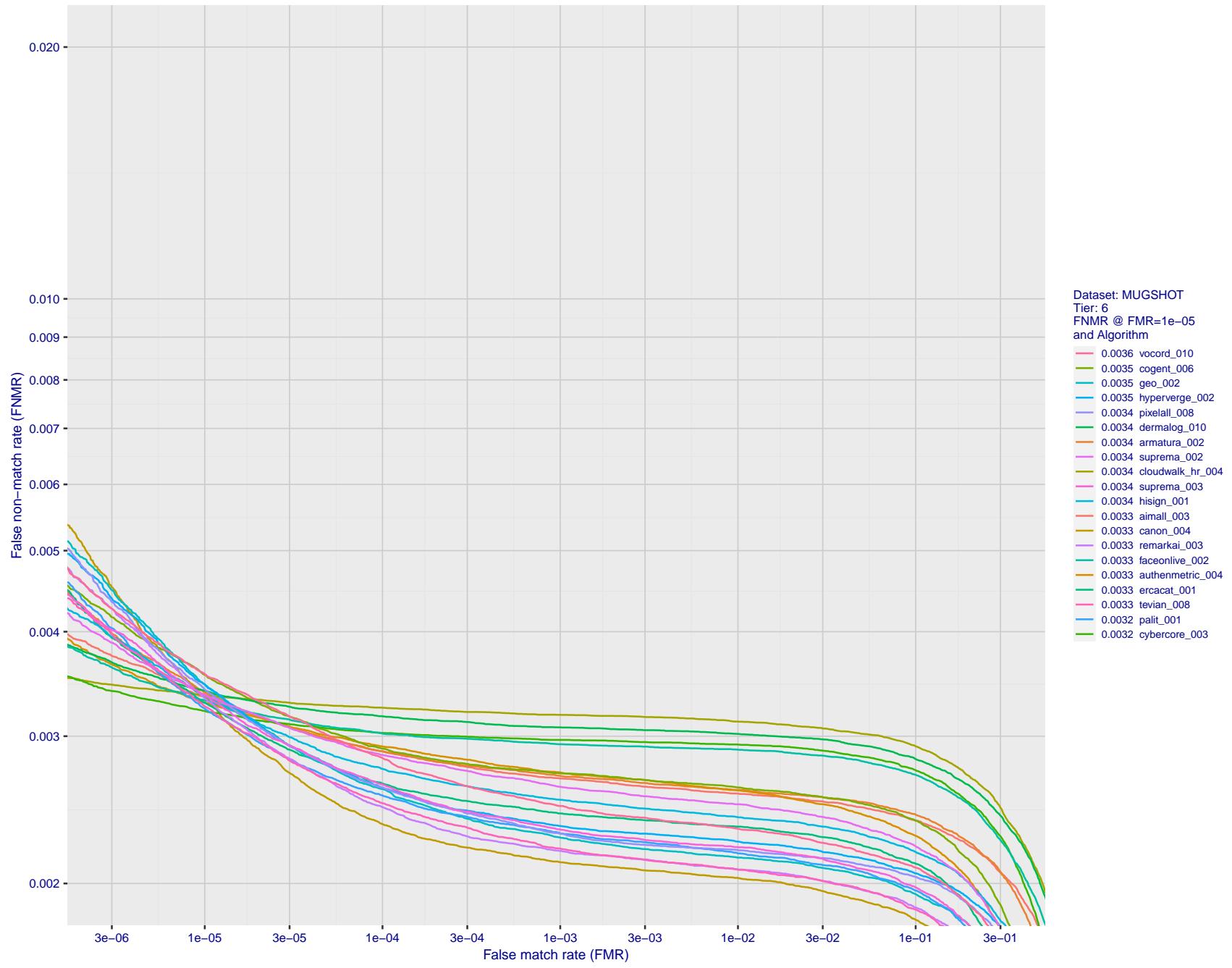


Figure 96: For the mugshot images, detection error tradeoff (DET) characteristics showing false non-match rate vs. false match rate plotted parametrically on threshold, T . The scales are logarithmic in order to show decades of FMR.

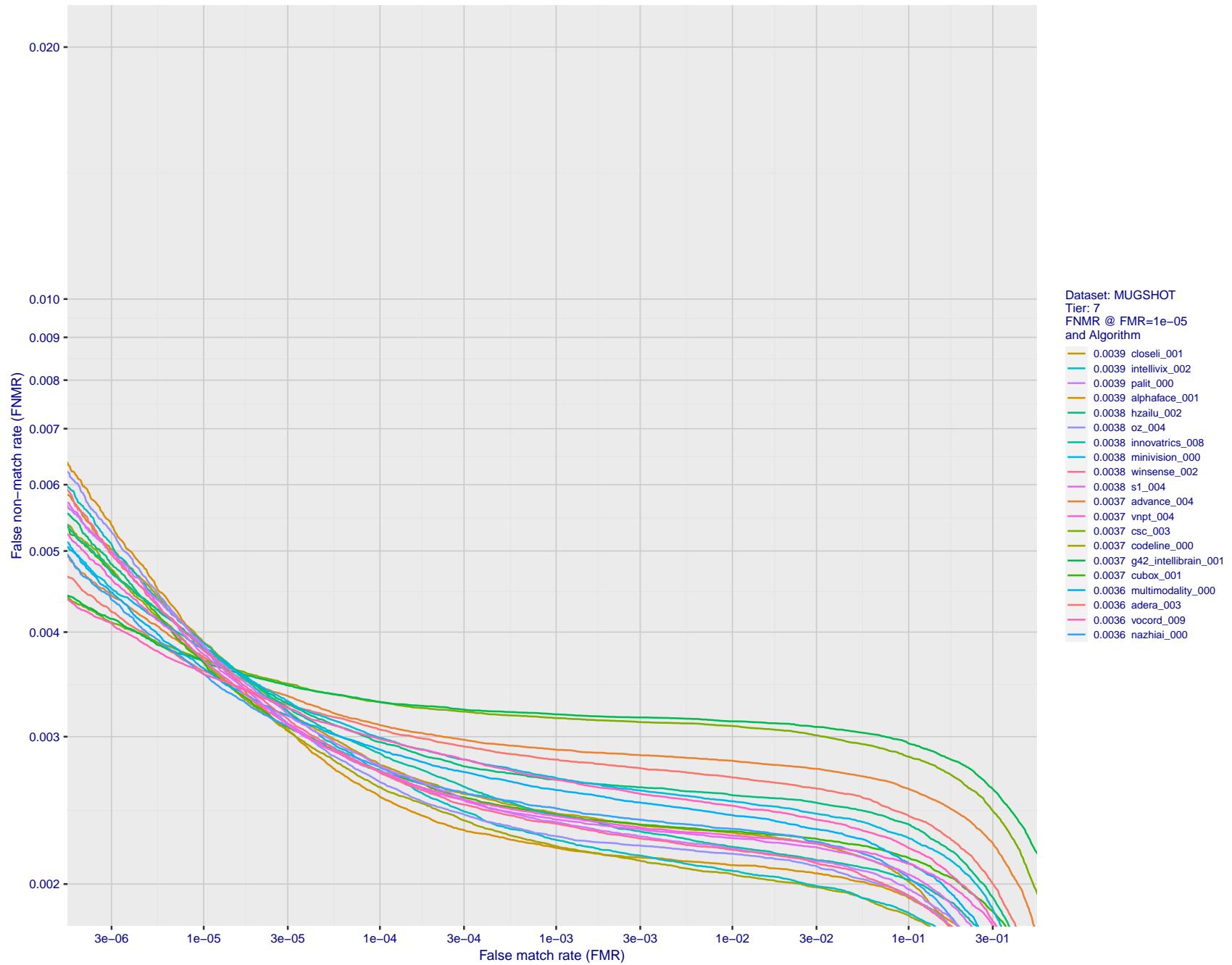


Figure 97: For the mugshot images, detection error tradeoff (DET) characteristics showing false non-match rate vs. false match rate plotted parametrically on threshold, T . The scales are logarithmic in order to show decades of FMR.

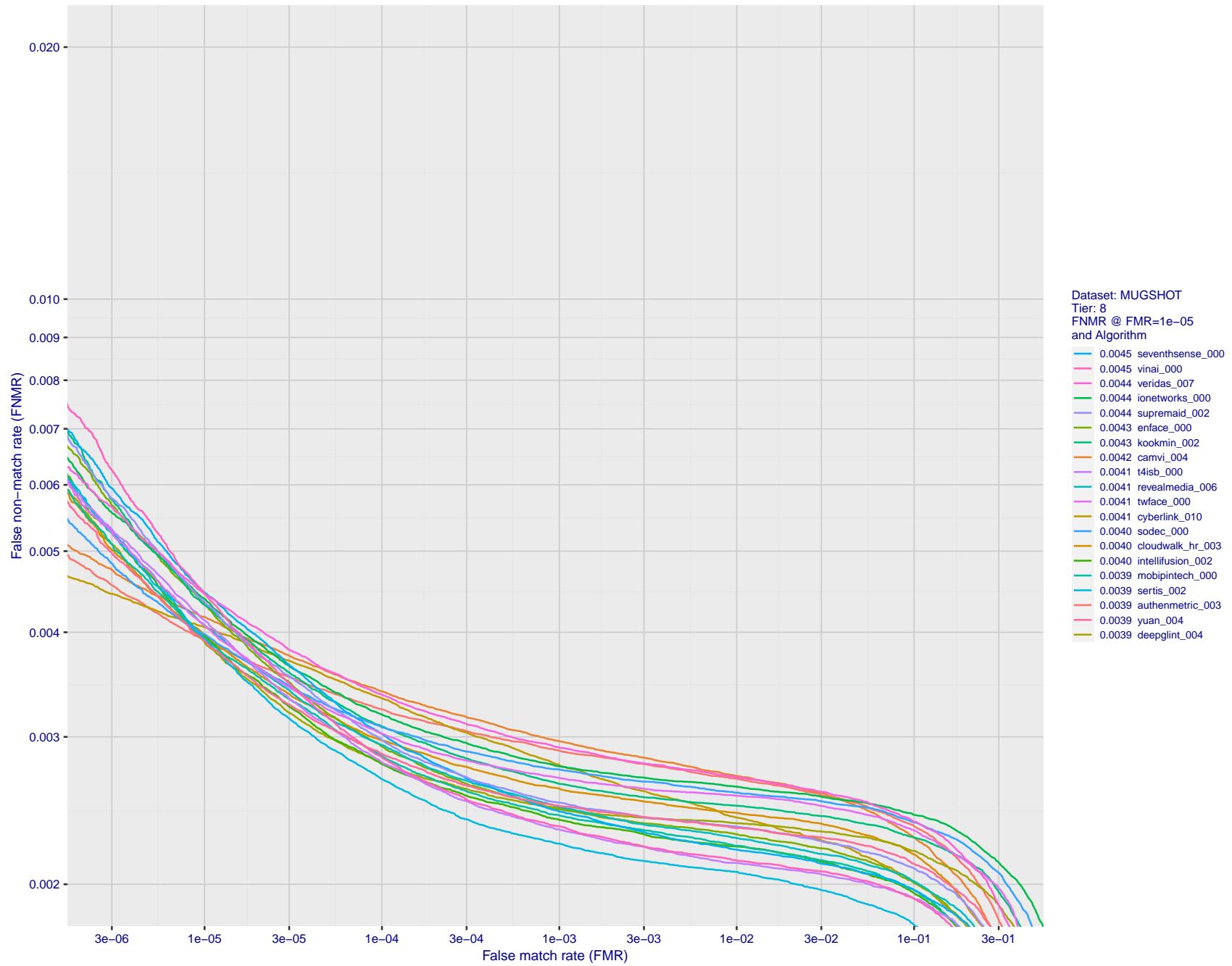


Figure 98: For the mugshot images, detection error tradeoff (DET) characteristics showing false non-match rate vs. false match rate plotted parametrically on threshold, T . The scales are logarithmic in order to show decades of FMR.

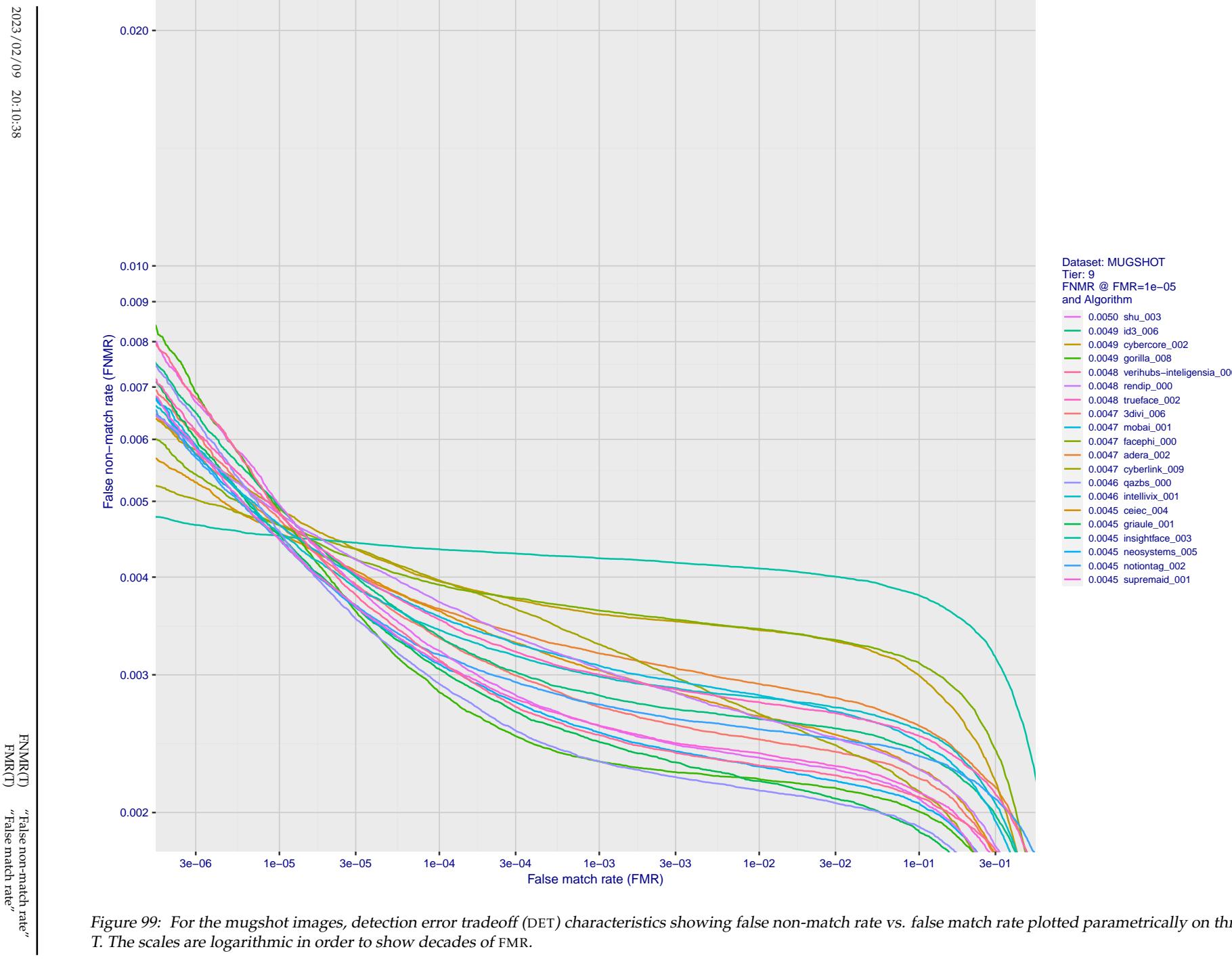


Figure 99: For the mugshot images, detection error tradeoff (DET) characteristics showing false non-match rate vs. false match rate plotted parametrically on threshold, T . The scales are logarithmic in order to show decades of FMR.

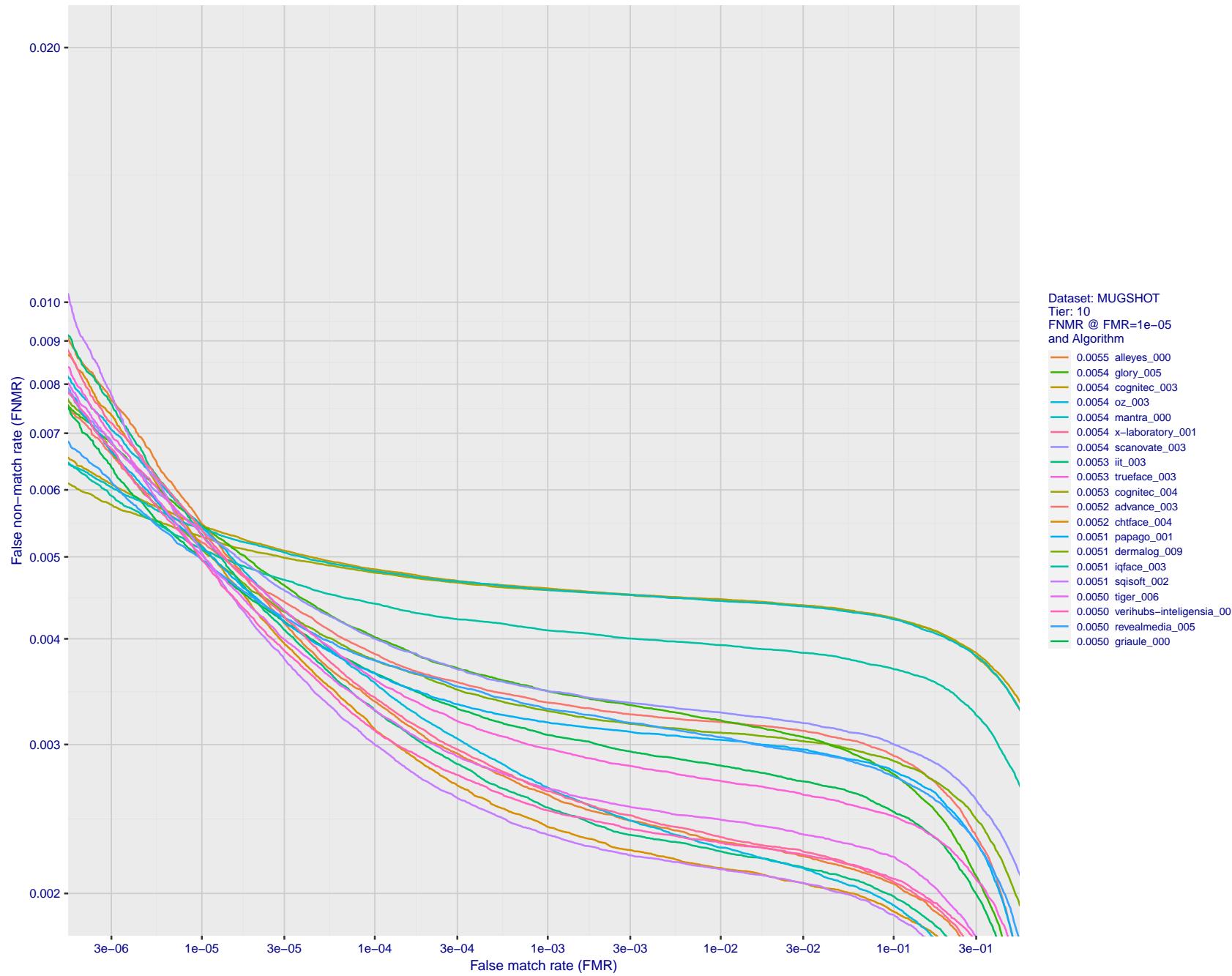


Figure 100: For the mugshot images, detection error tradeoff (DET) characteristics showing false non-match rate vs. false match rate plotted parametrically on threshold, T . The scales are logarithmic in order to show decades of FMR.

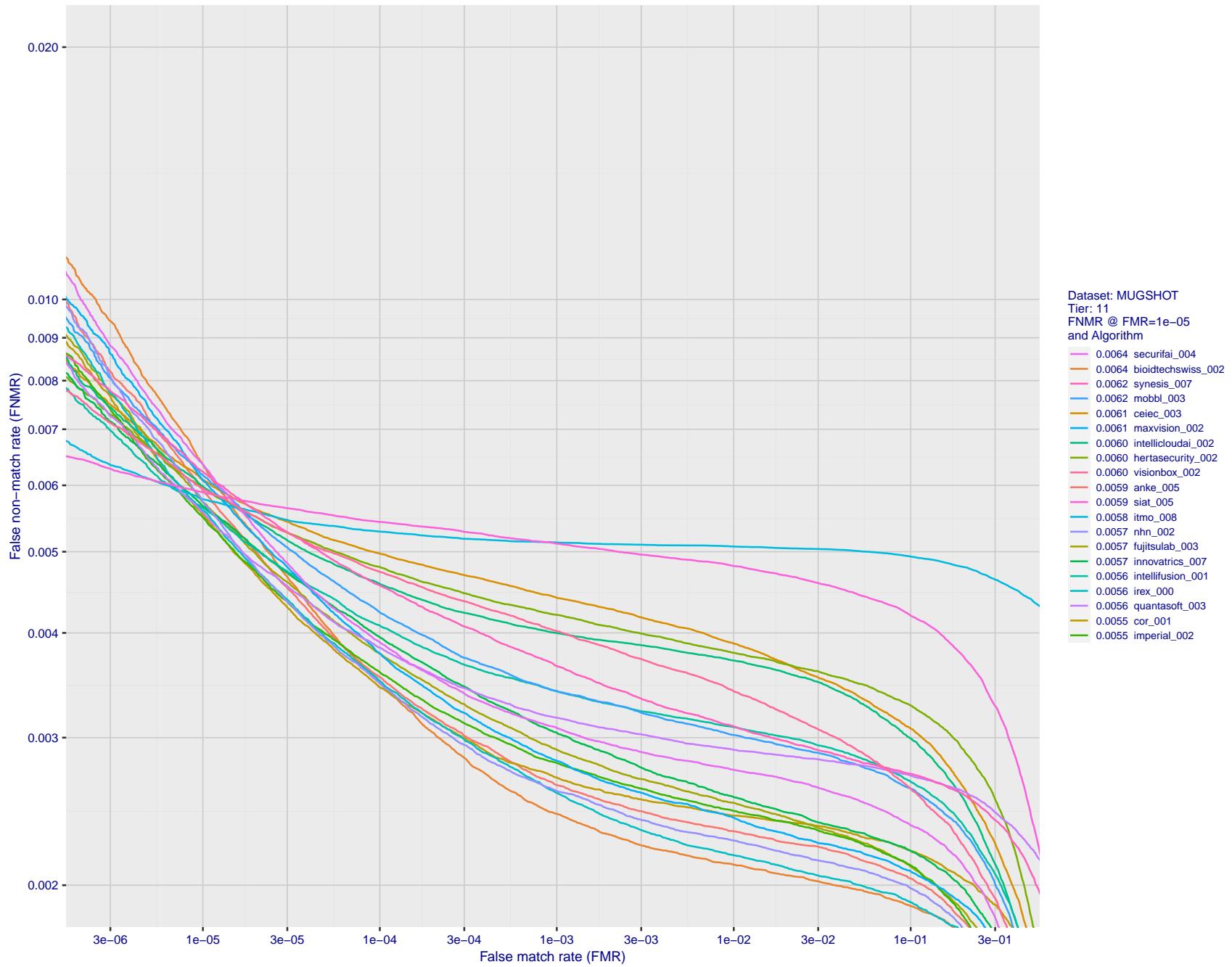
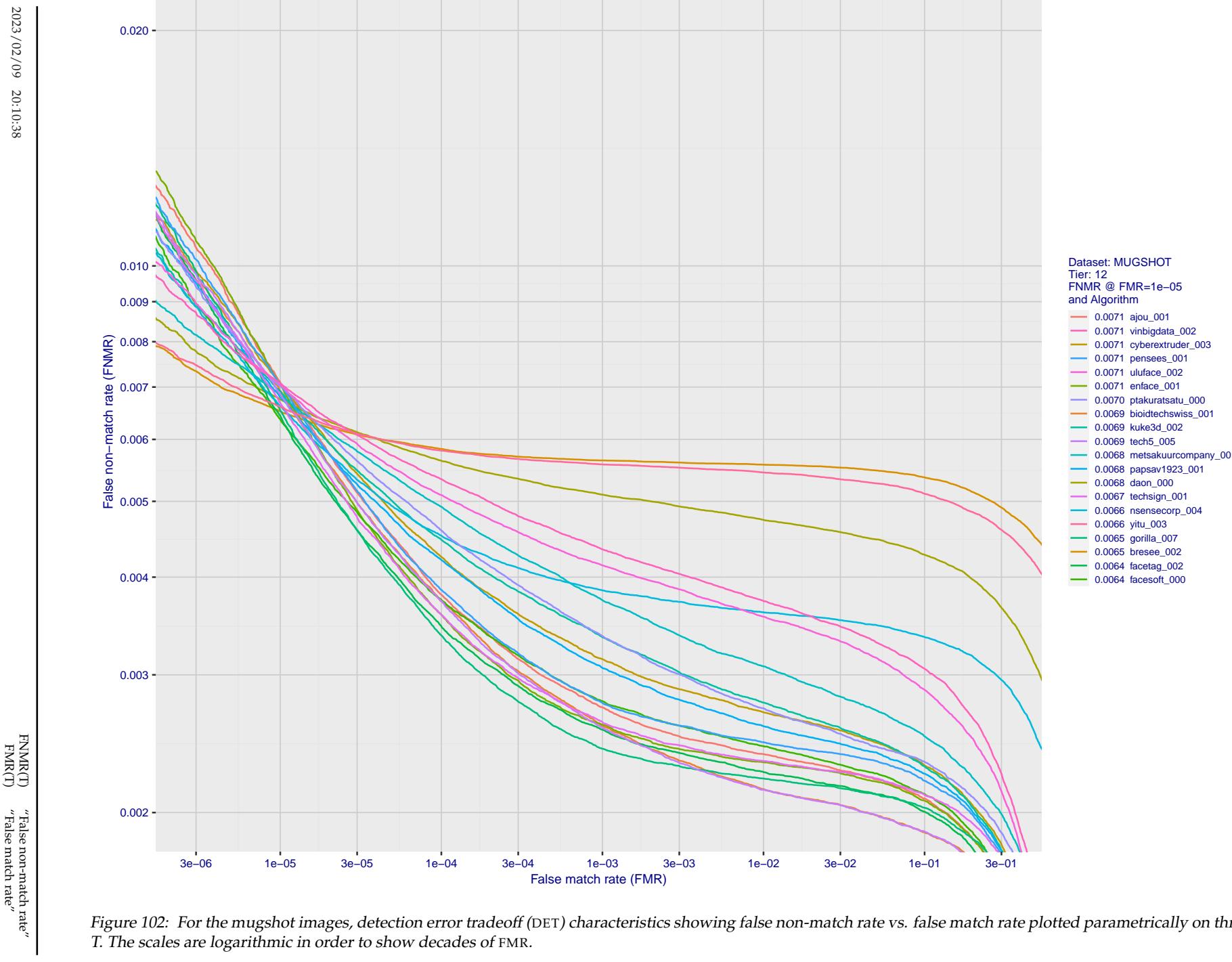


Figure 101: For the mugshot images, detection error tradeoff (DET) characteristics showing false non-match rate vs. false match rate plotted parametrically on threshold, T . The scales are logarithmic in order to show decades of FMR.



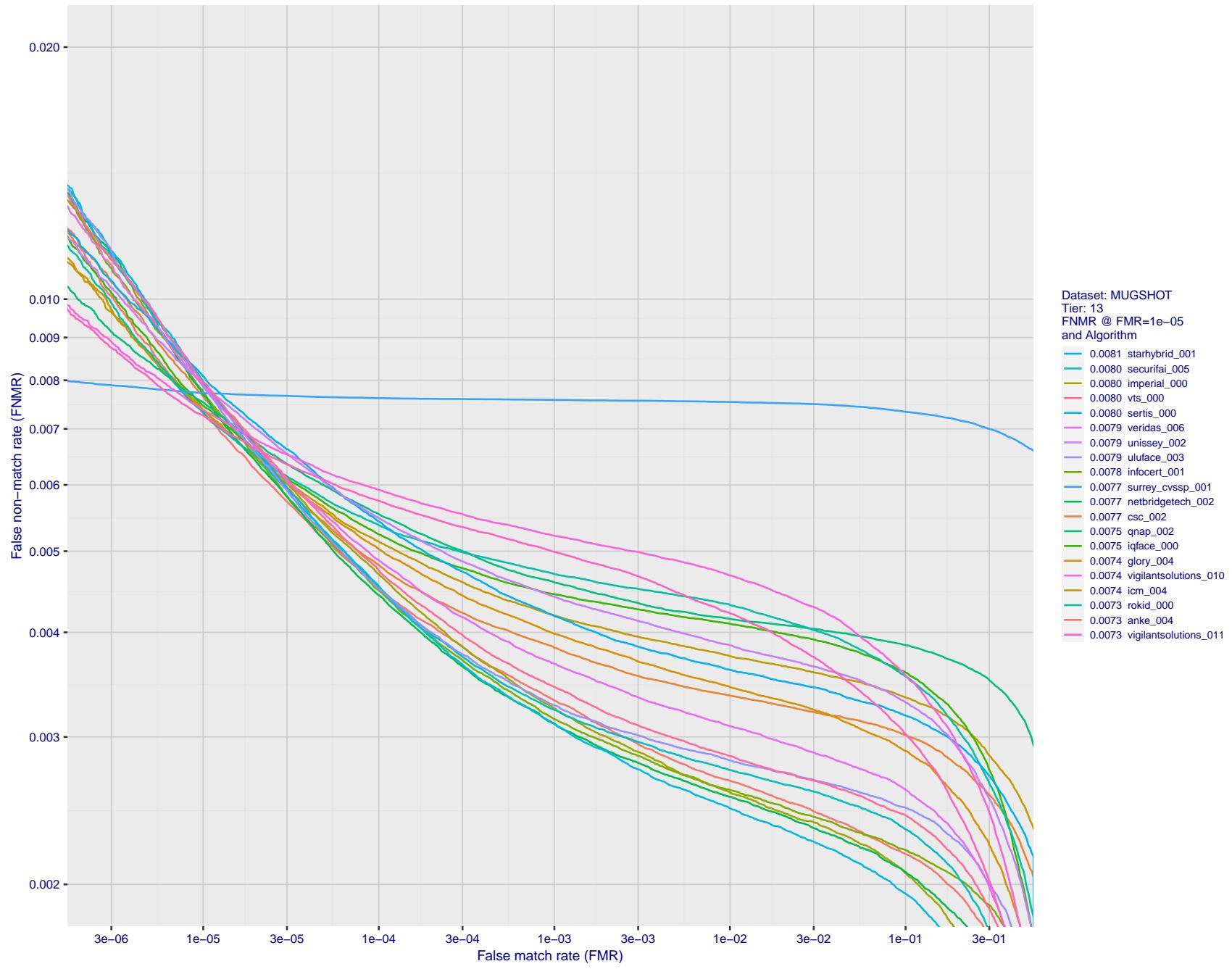


Figure 103: For the mugshot images, detection error tradeoff (DET) characteristics showing false non-match rate vs. false match rate plotted parametrically on threshold, T . The scales are logarithmic in order to show decades of FMR.

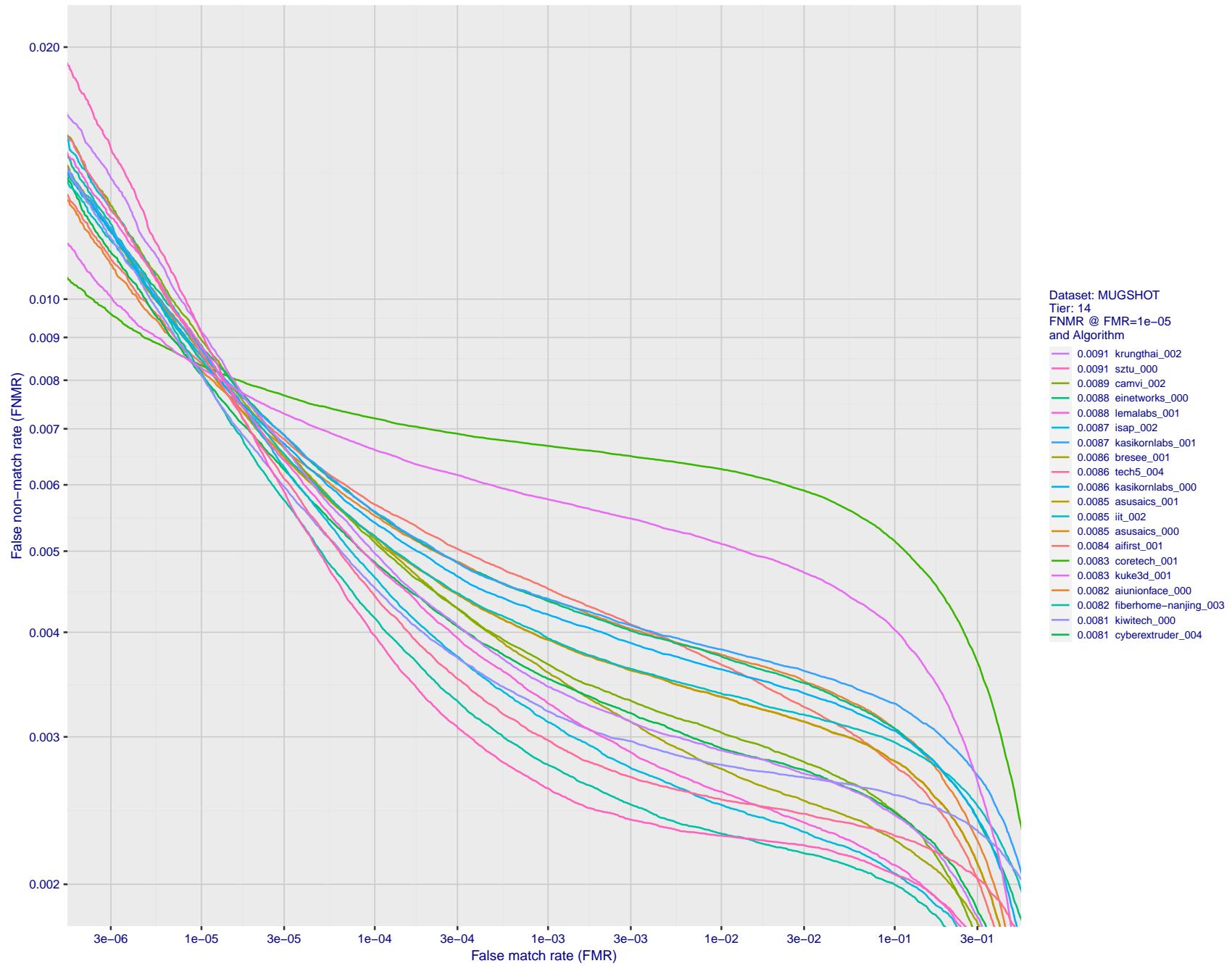


Figure 104: For the mugshot images, detection error tradeoff (DET) characteristics showing false non-match rate vs. false match rate plotted parametrically on threshold, T. The scales are logarithmic in order to show decades of FMR.

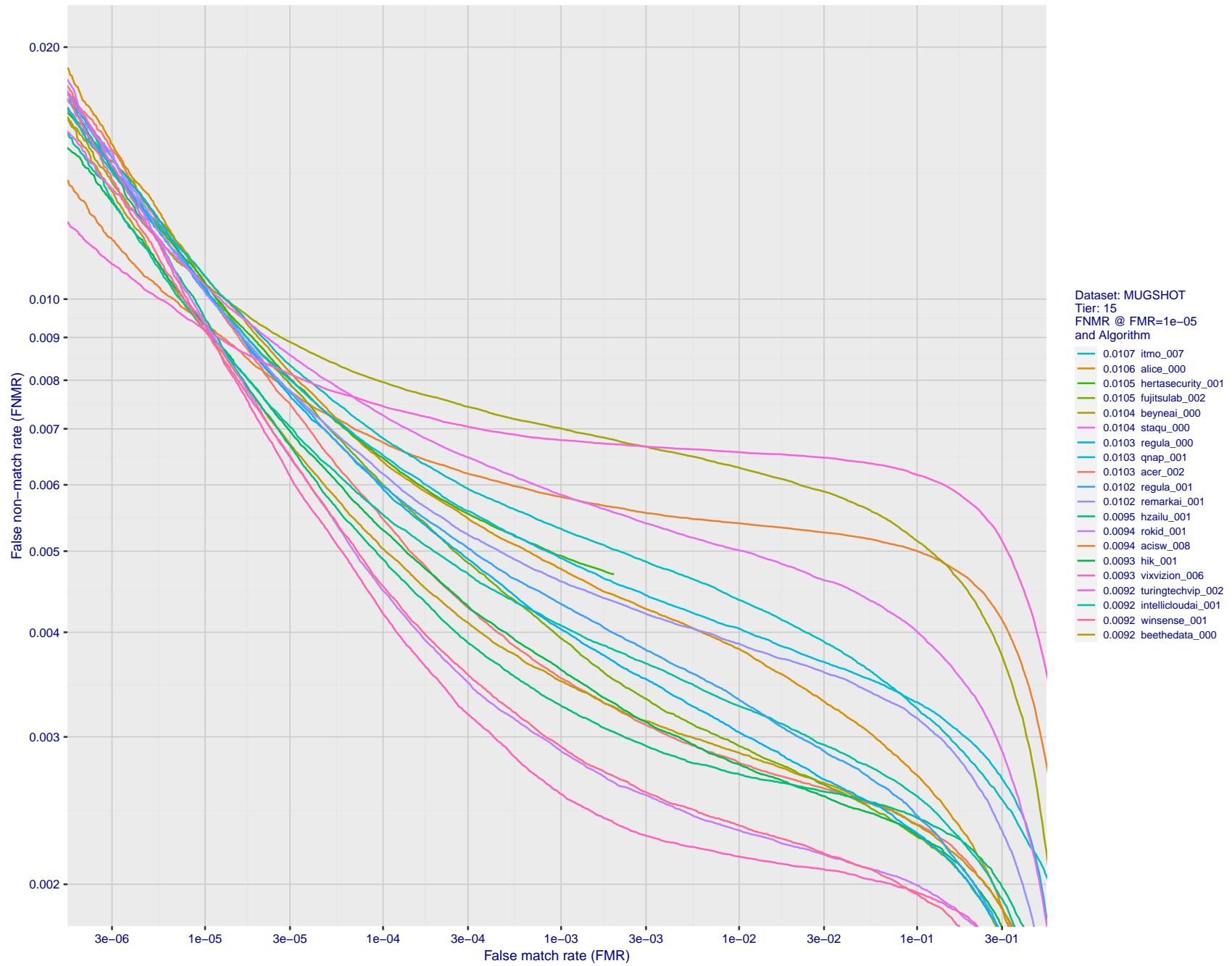


Figure 105: For the mugshot images, detection error tradeoff (DET) characteristics showing false non-match rate vs. false match rate plotted parametrically on threshold, T . The scales are logarithmic in order to show decades of FMR.

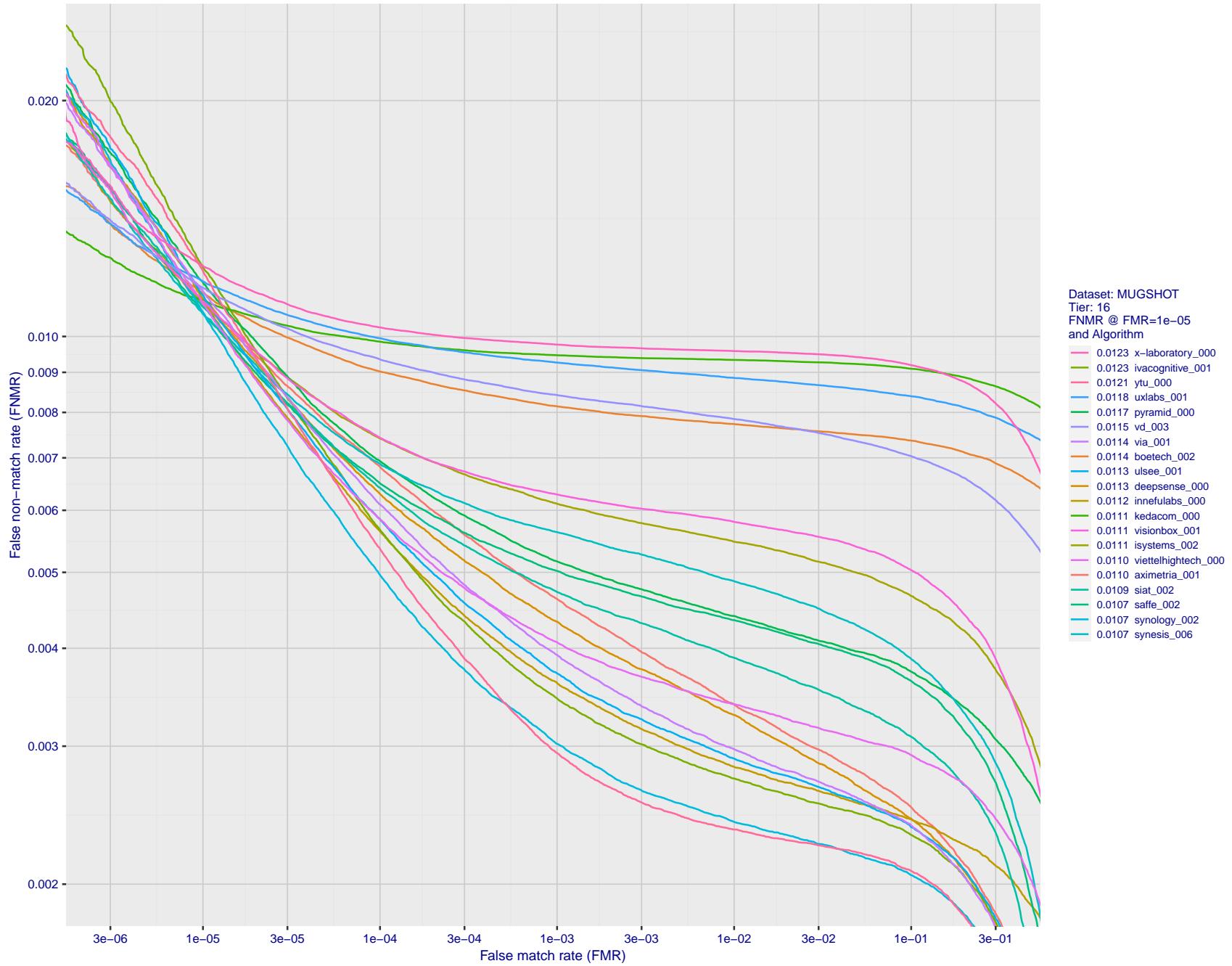


Figure 106: For the mugshot images, detection error tradeoff (DET) characteristics showing false non-match rate vs. false match rate plotted parametrically on threshold, T . The scales are logarithmic in order to show decades of FMR.

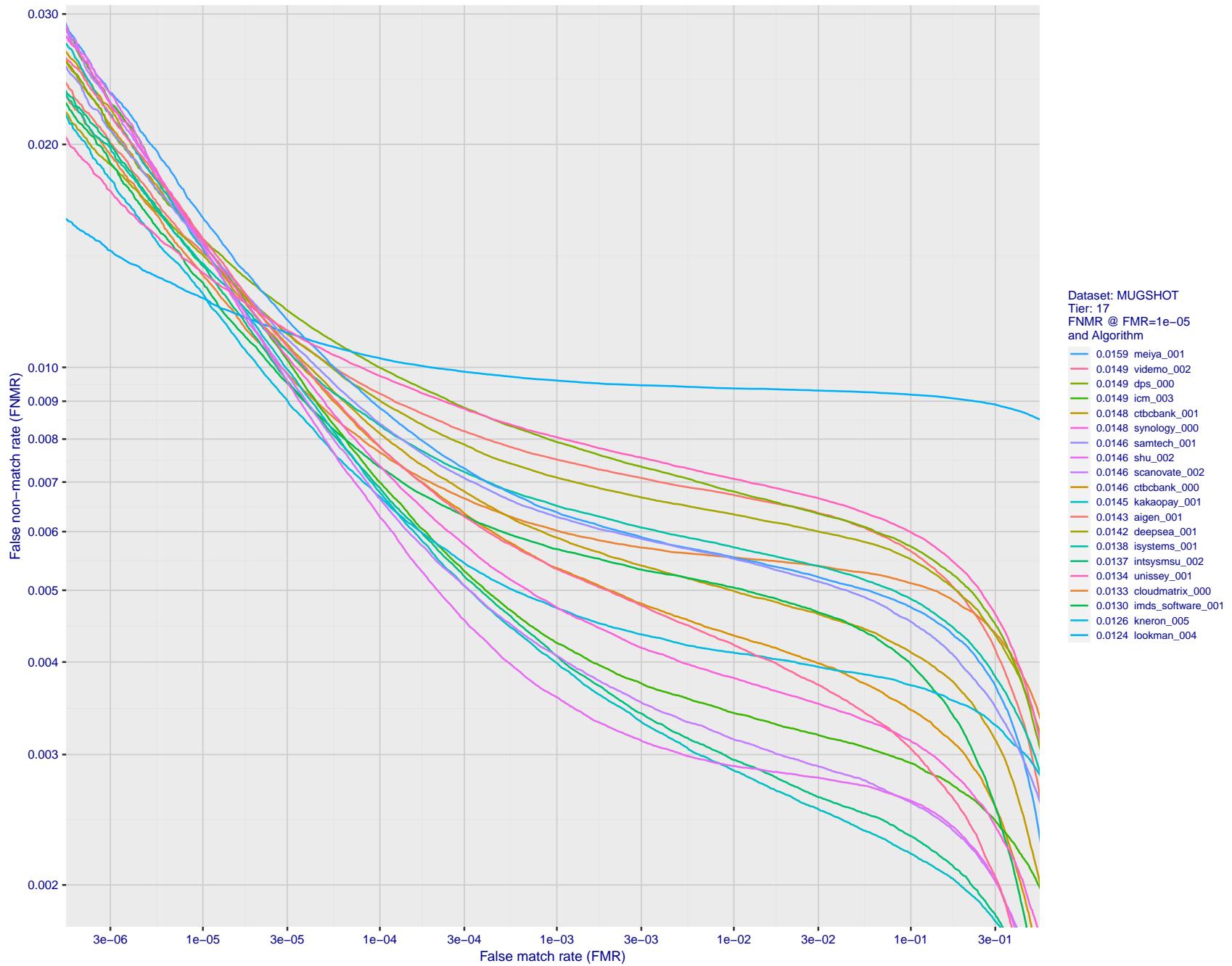


Figure 107: For the mugshot images, detection error tradeoff (DET) characteristics showing false non-match rate vs. false match rate plotted parametrically on threshold, T . The scales are logarithmic in order to show decades of FMR.

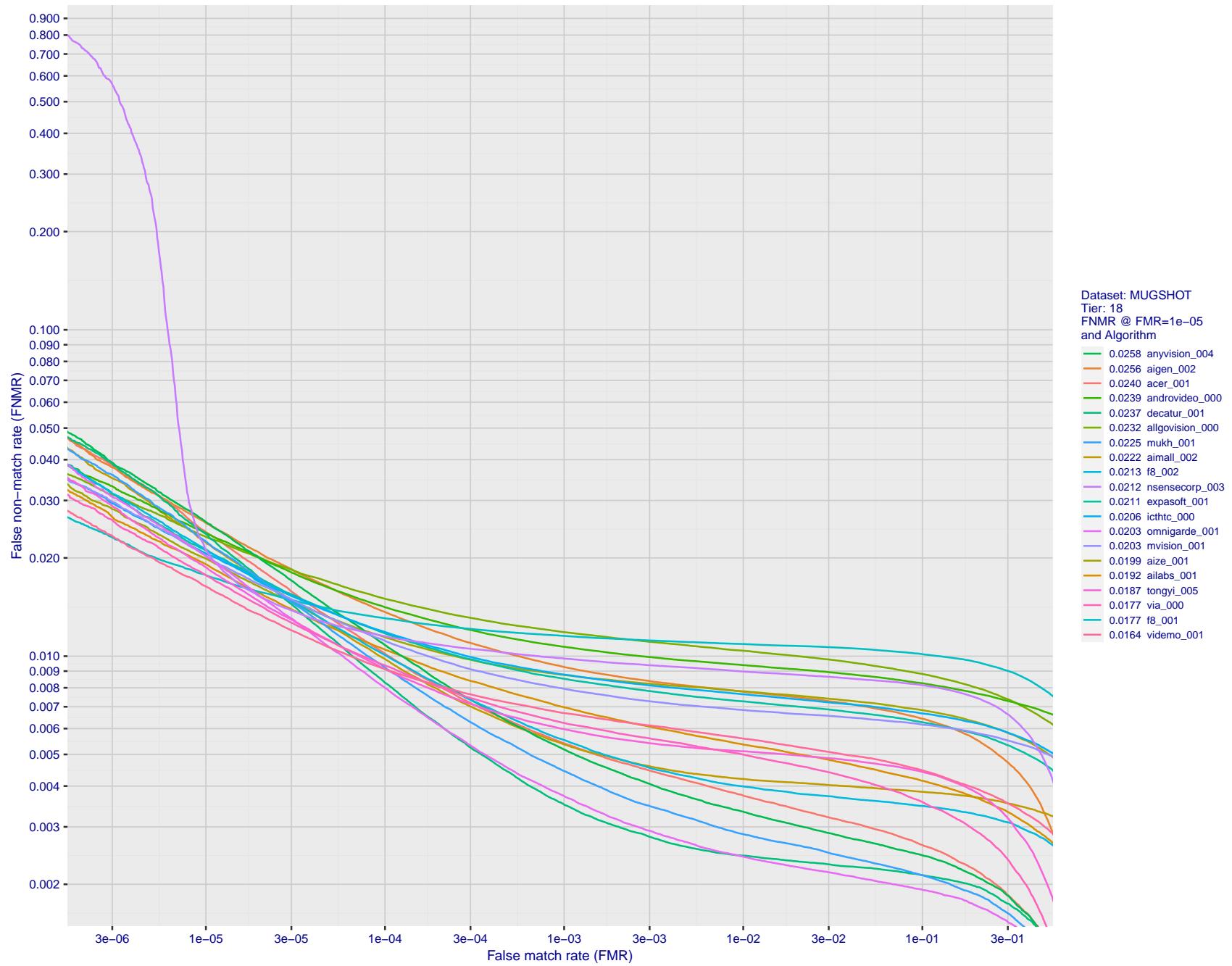


Figure 108: For the mugshot images, detection error tradeoff (DET) characteristics showing false non-match rate vs. false match rate plotted parametrically on threshold, T . The scales are logarithmic in order to show decades of FMR.

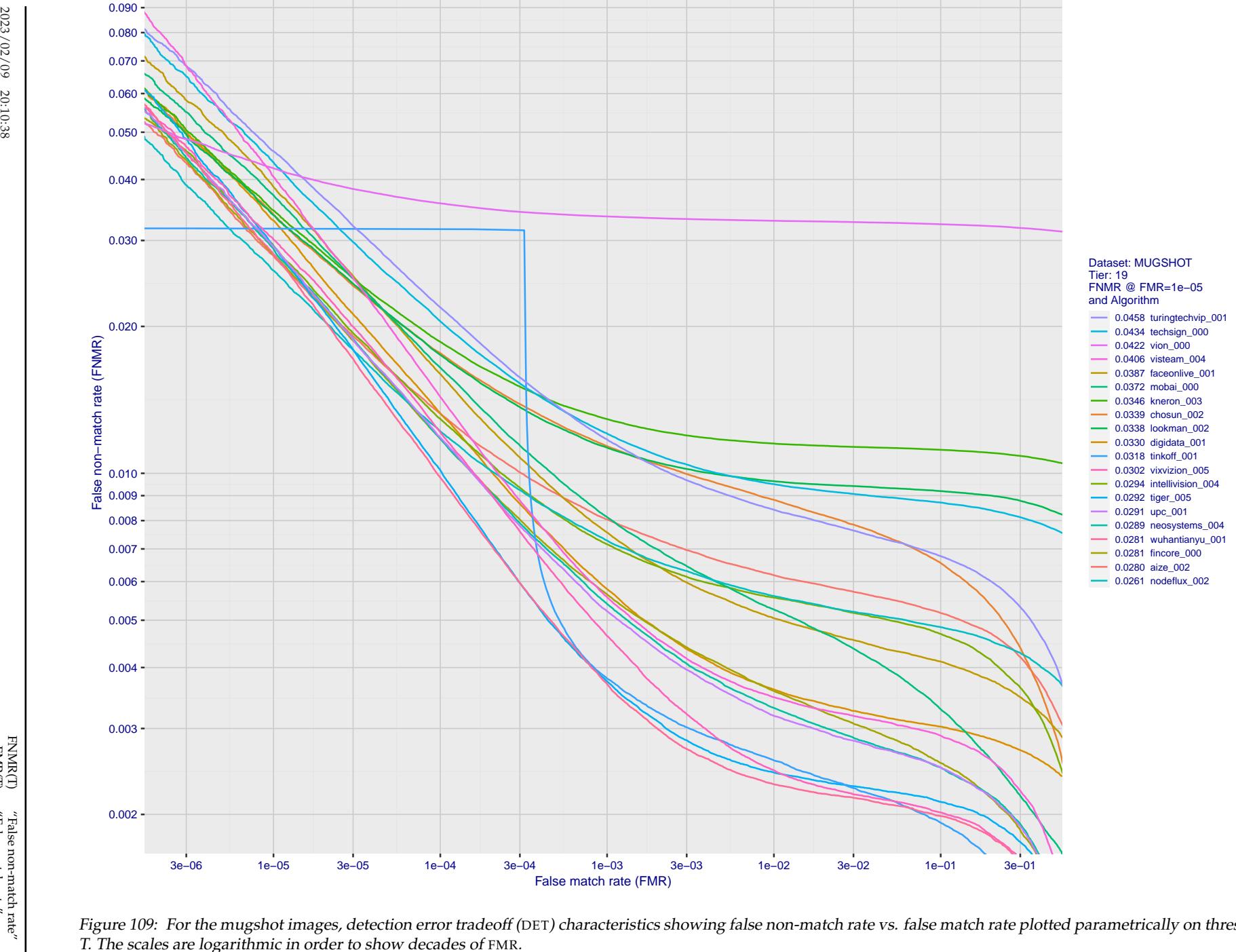


Figure 109: For the mugshot images, detection error tradeoff (DET) characteristics showing false non-match rate vs. false match rate plotted parametrically on threshold, T . The scales are logarithmic in order to show decades of FMR.

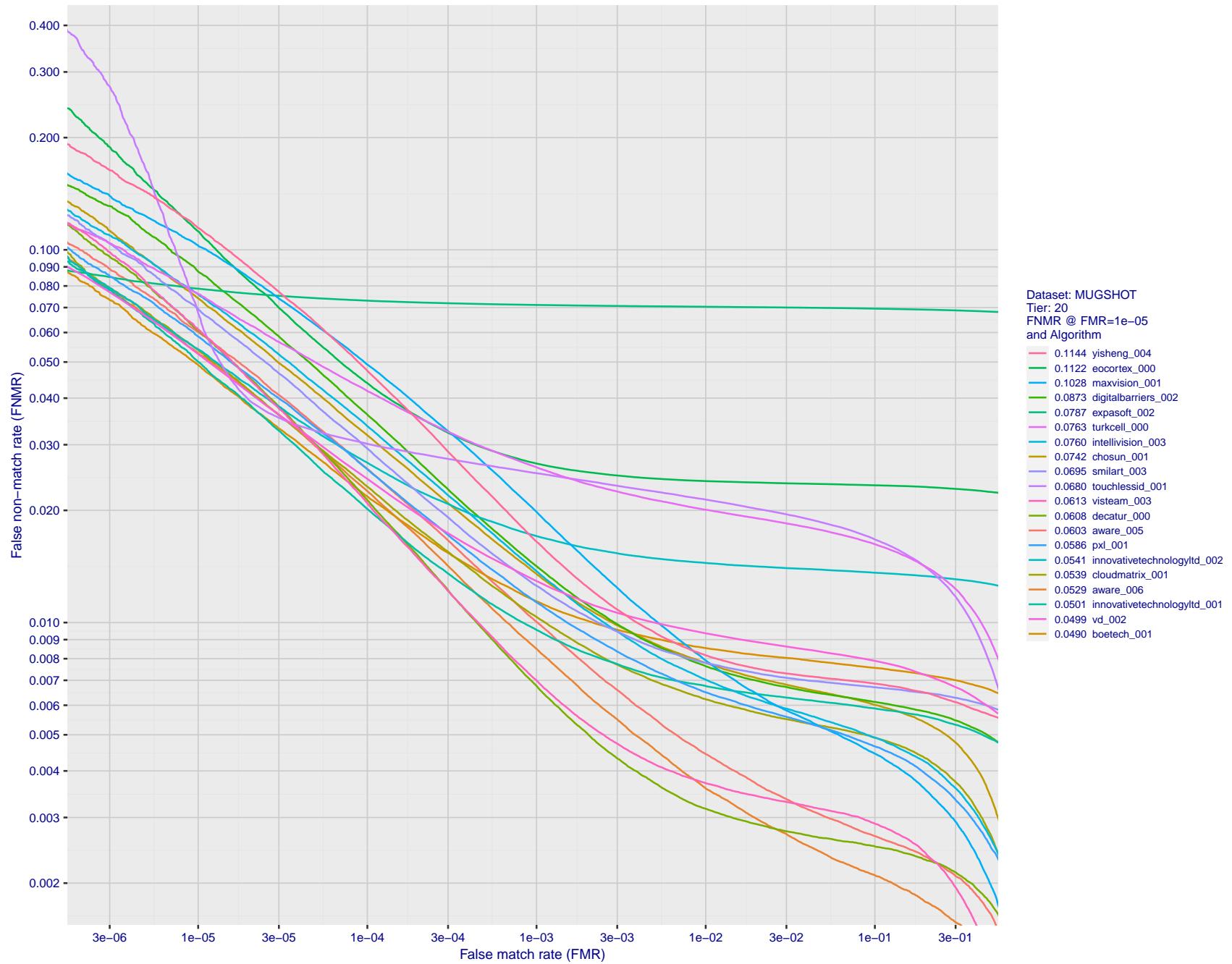


Figure 110: For the mugshot images, detection error tradeoff (DET) characteristics showing false non-match rate vs. false match rate plotted parametrically on threshold, T . The scales are logarithmic in order to show decades of FMR.

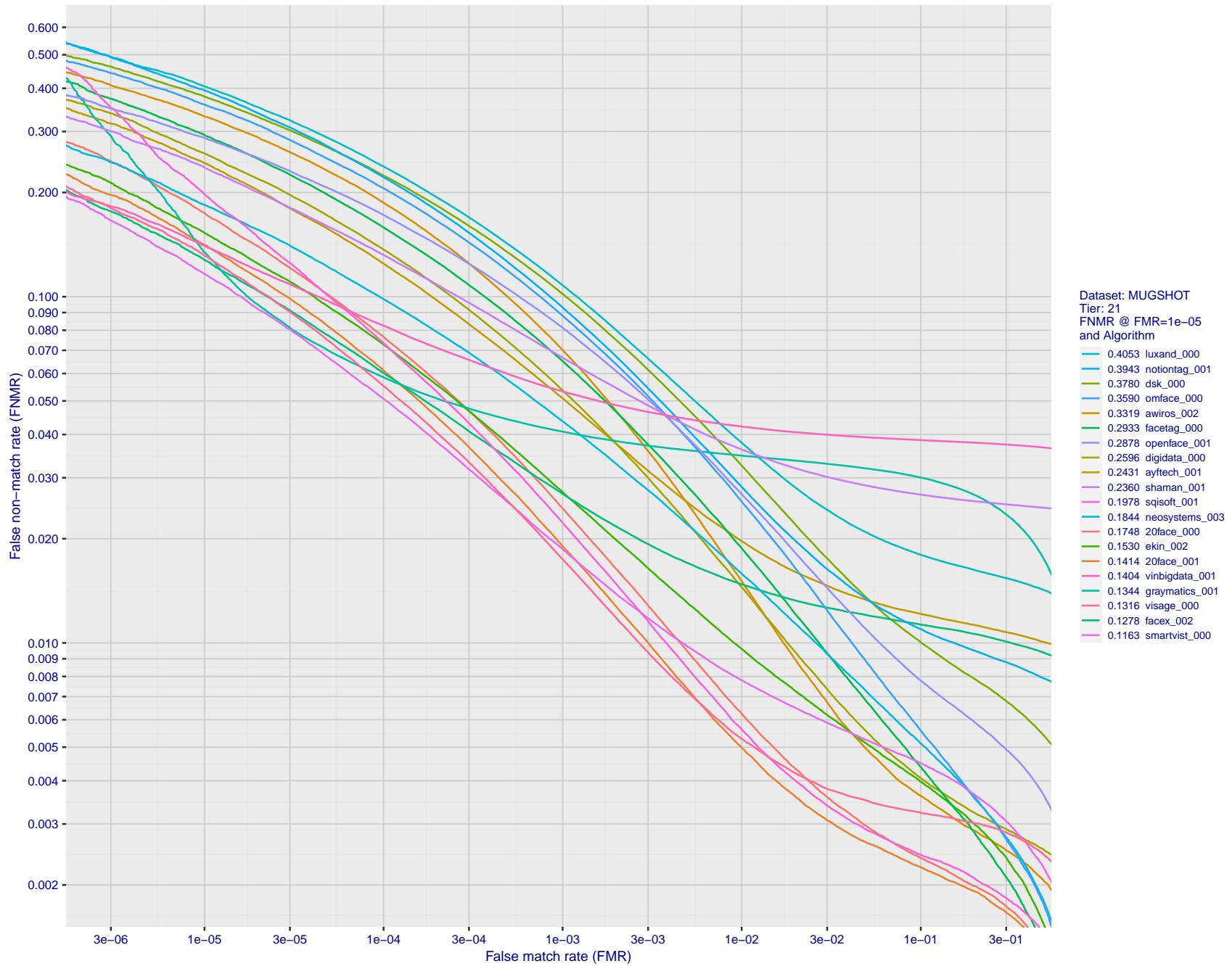


Figure 111: For the mugshot images, detection error tradeoff (DET) characteristics showing false non-match rate vs. false match rate plotted parametrically on threshold, T . The scales are logarithmic in order to show decades of FMR.

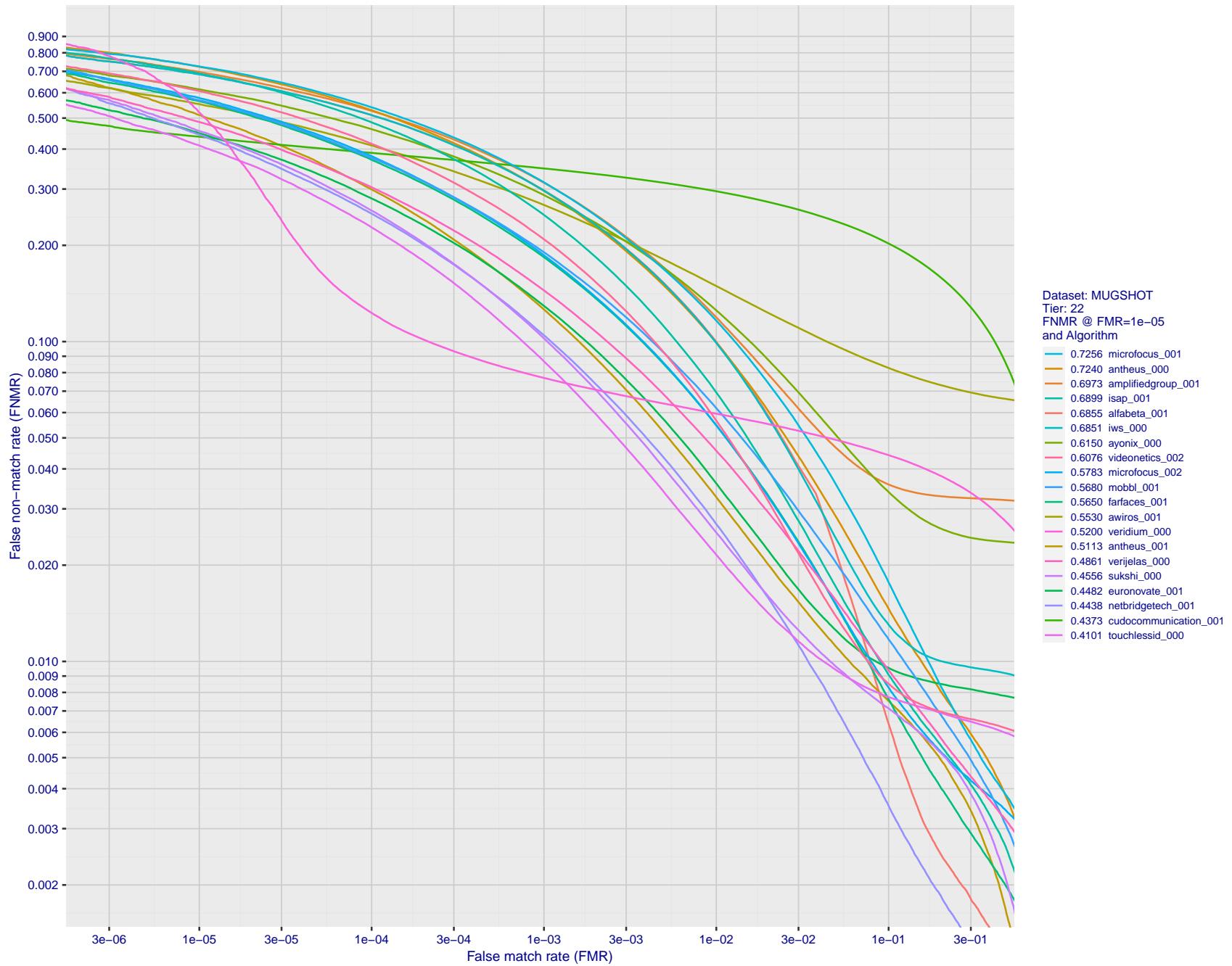


Figure 112: For the mugshot images, detection error tradeoff (DET) characteristics showing false non-match rate vs. false match rate plotted parametrically on threshold, T . The scales are logarithmic in order to show decades of FMR.

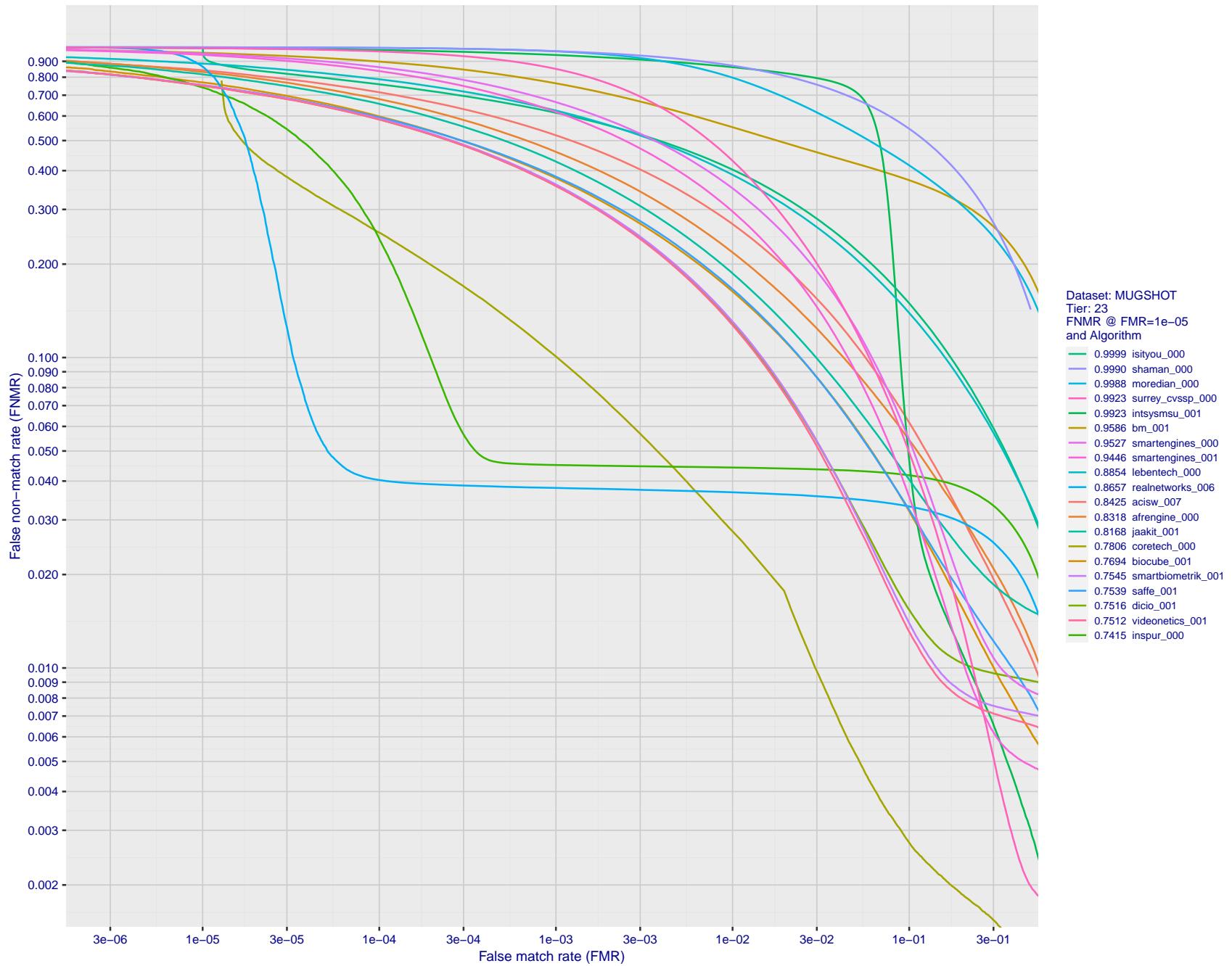


Figure 113: For the mugshot images, detection error tradeoff (DET) characteristics showing false non-match rate vs. false match rate plotted parametrically on threshold, T. The scales are logarithmic in order to show decades of FMR.

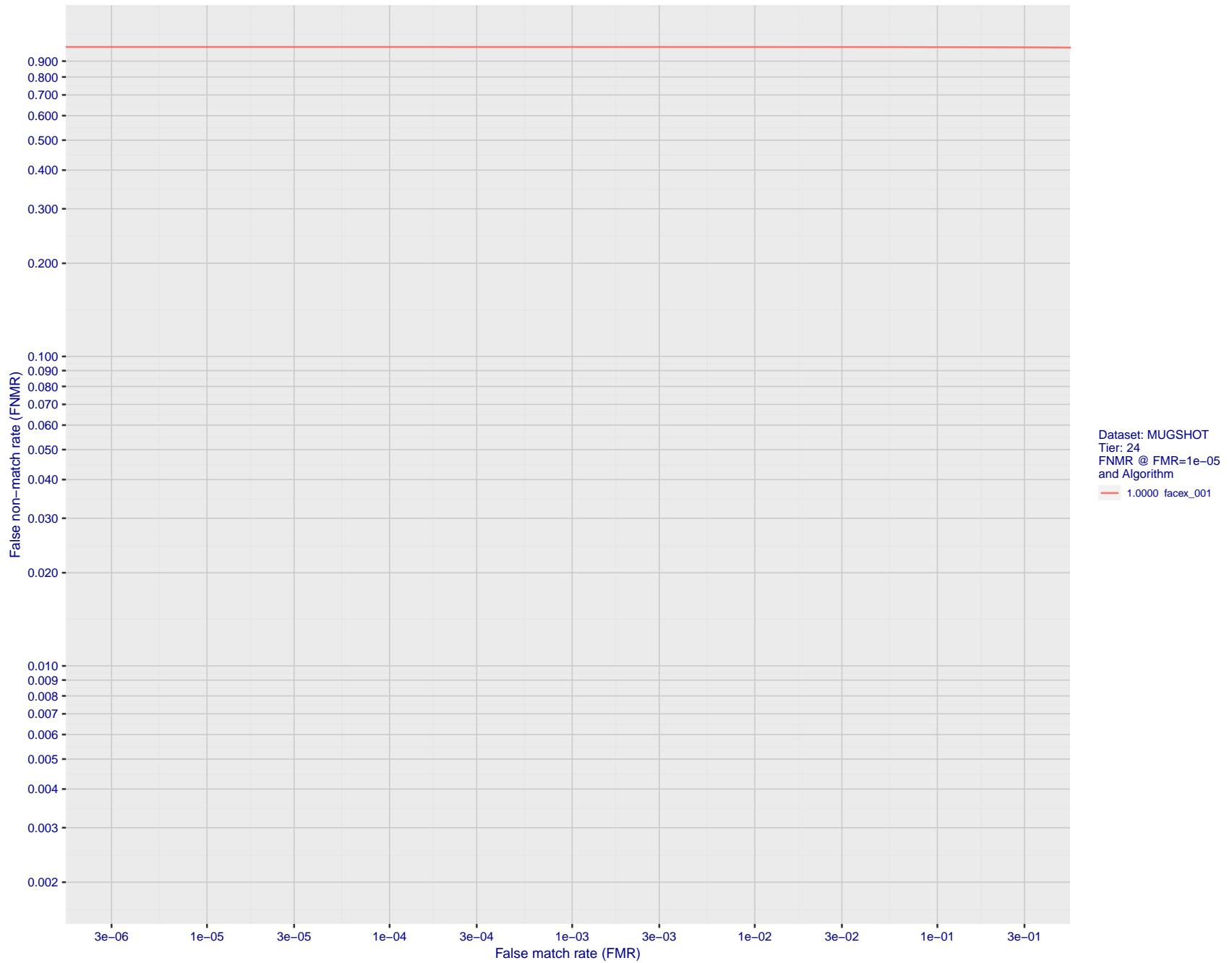


Figure 114: For the mugshot images, detection error tradeoff (DET) characteristics showing false non-match rate vs. false match rate plotted parametrically on threshold, T . The scales are logarithmic in order to show decades of FMR.

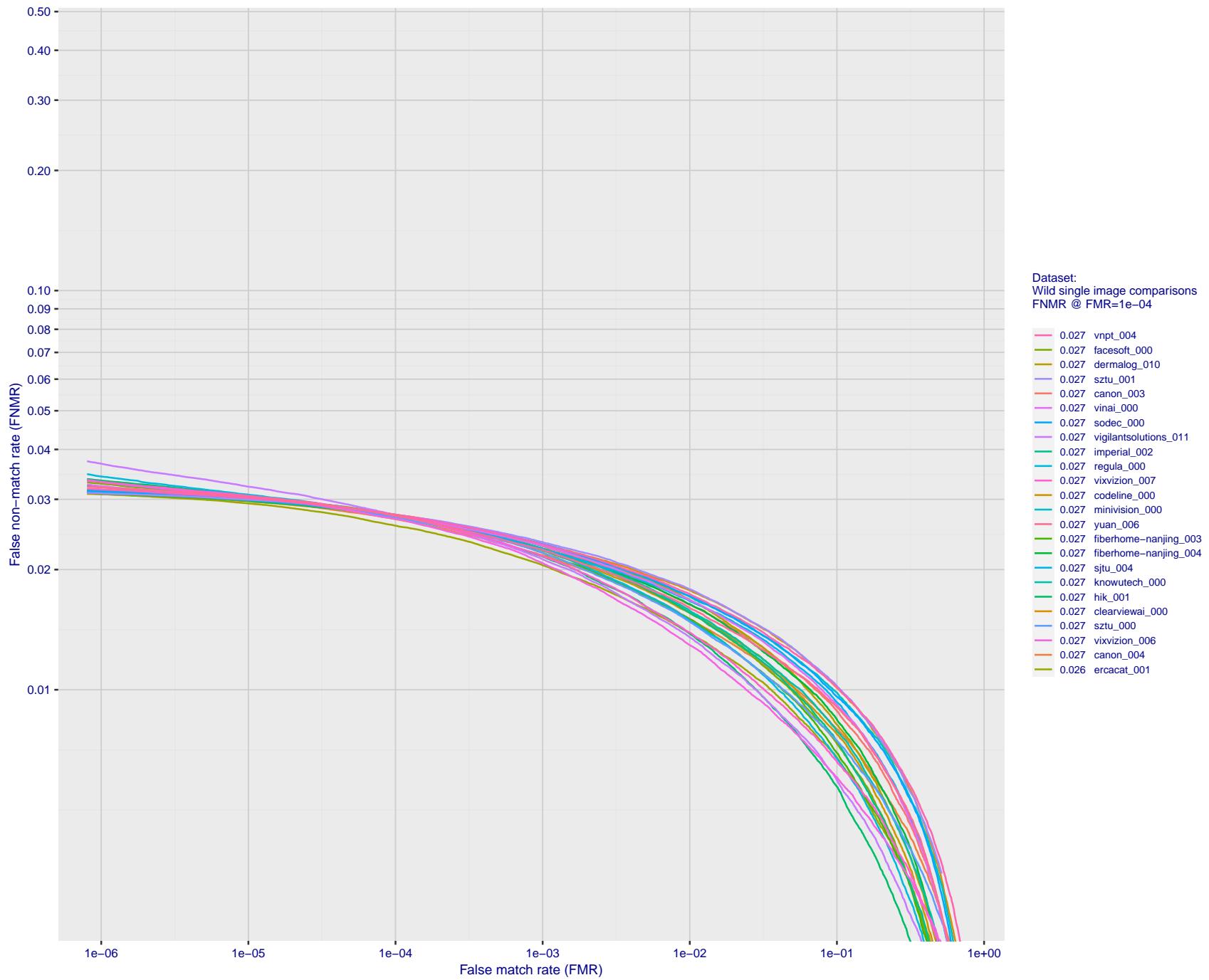


Figure 115: For the 2018 wild image comparisons, detection error tradeoff (DET) characteristics showing false non-match rate vs. false match rate plotted parametrically on threshold, T . The scales are logarithmic in order to show several decades of FMR.

2023/02/09 20:10:38

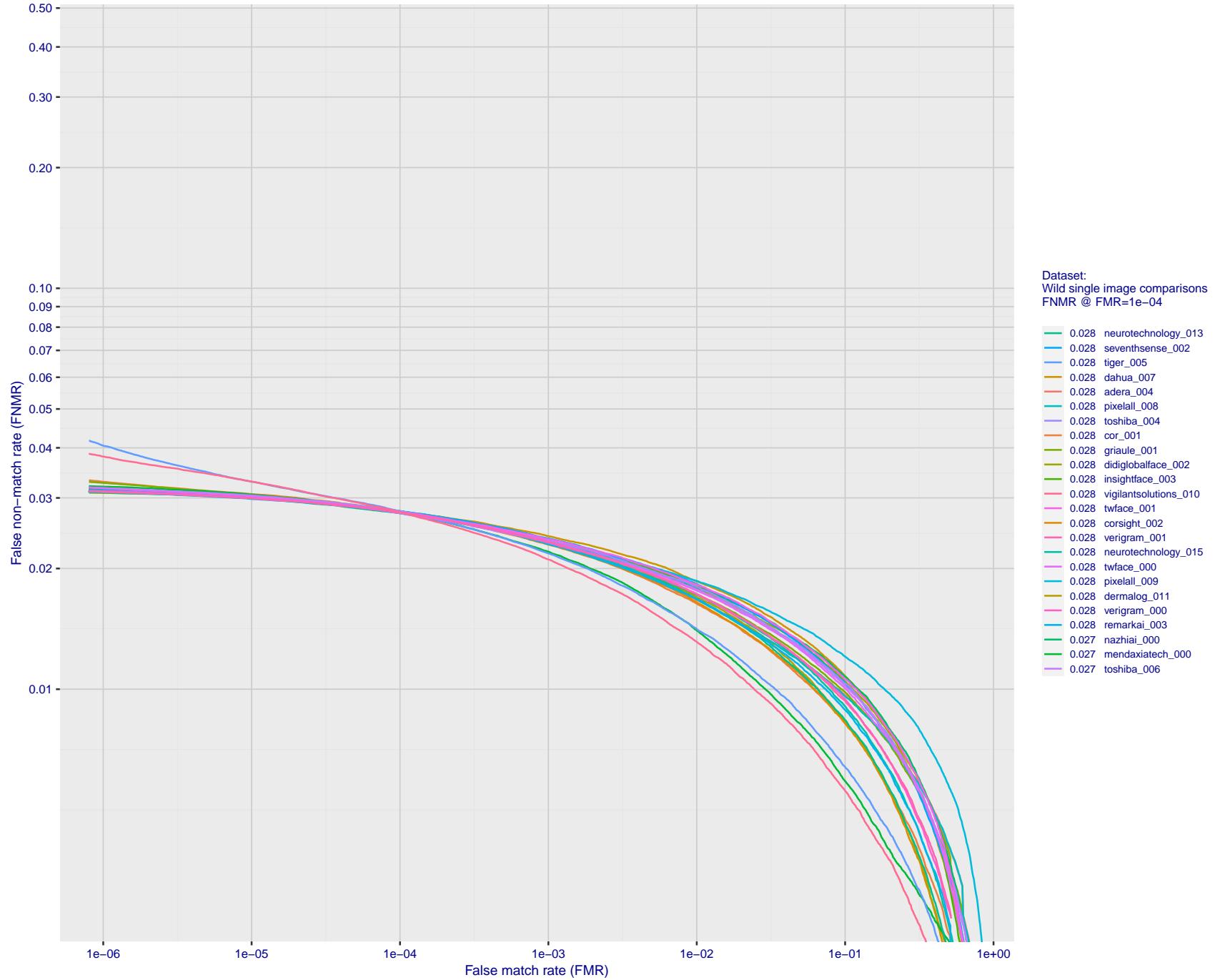


Figure 116: For the 2018 wild image comparisons, detection error tradeoff (DET) characteristics showing false non-match rate vs. false match rate plotted parametrically on threshold, T . The scales are logarithmic in order to show several decades of FMR.

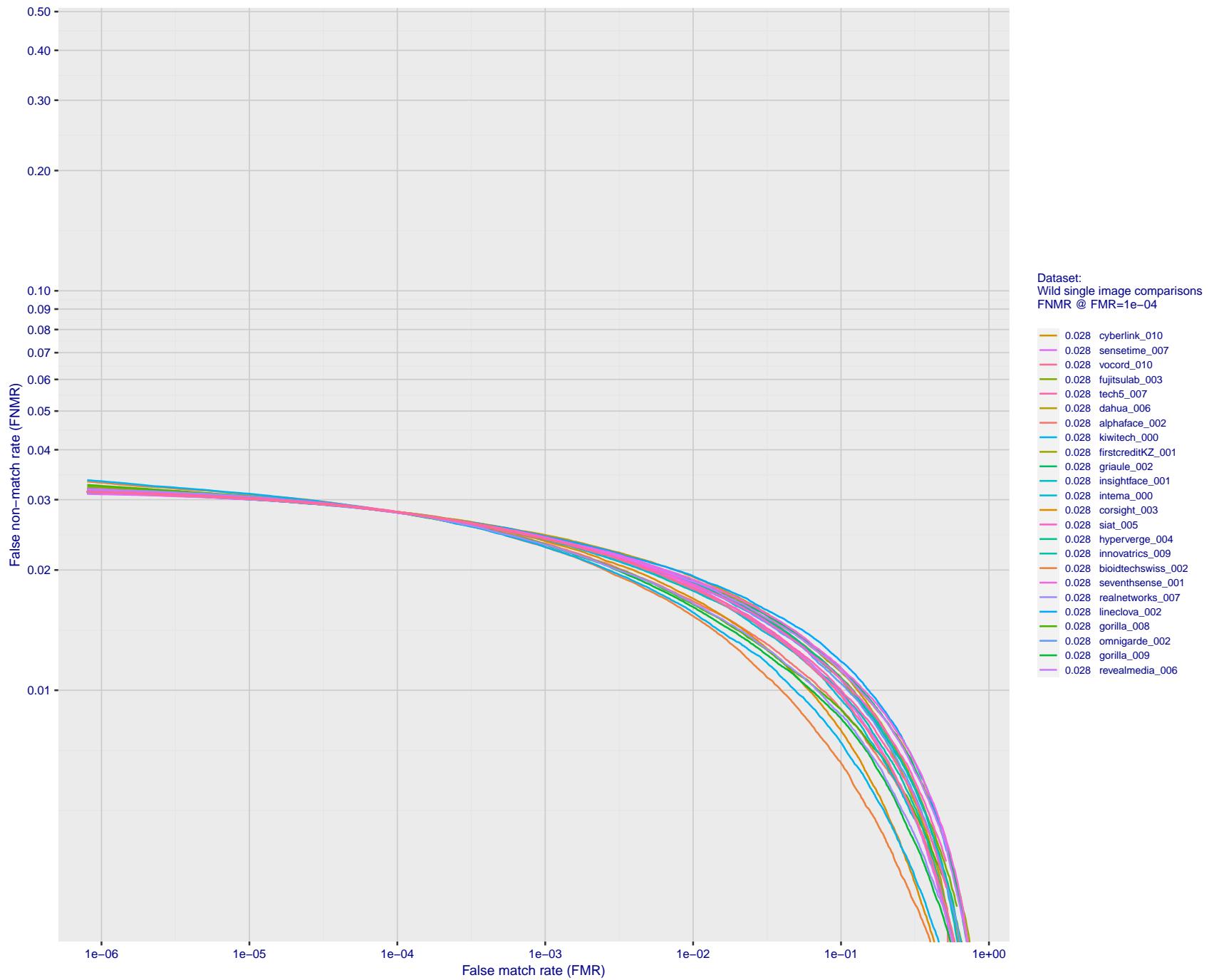


Figure 117: For the 2018 wild image comparisons, detection error tradeoff (DET) characteristics showing false non-match rate vs. false match rate plotted parametrically on threshold, T . The scales are logarithmic in order to show several decades of FMR.

2023/02/09 20:10:38

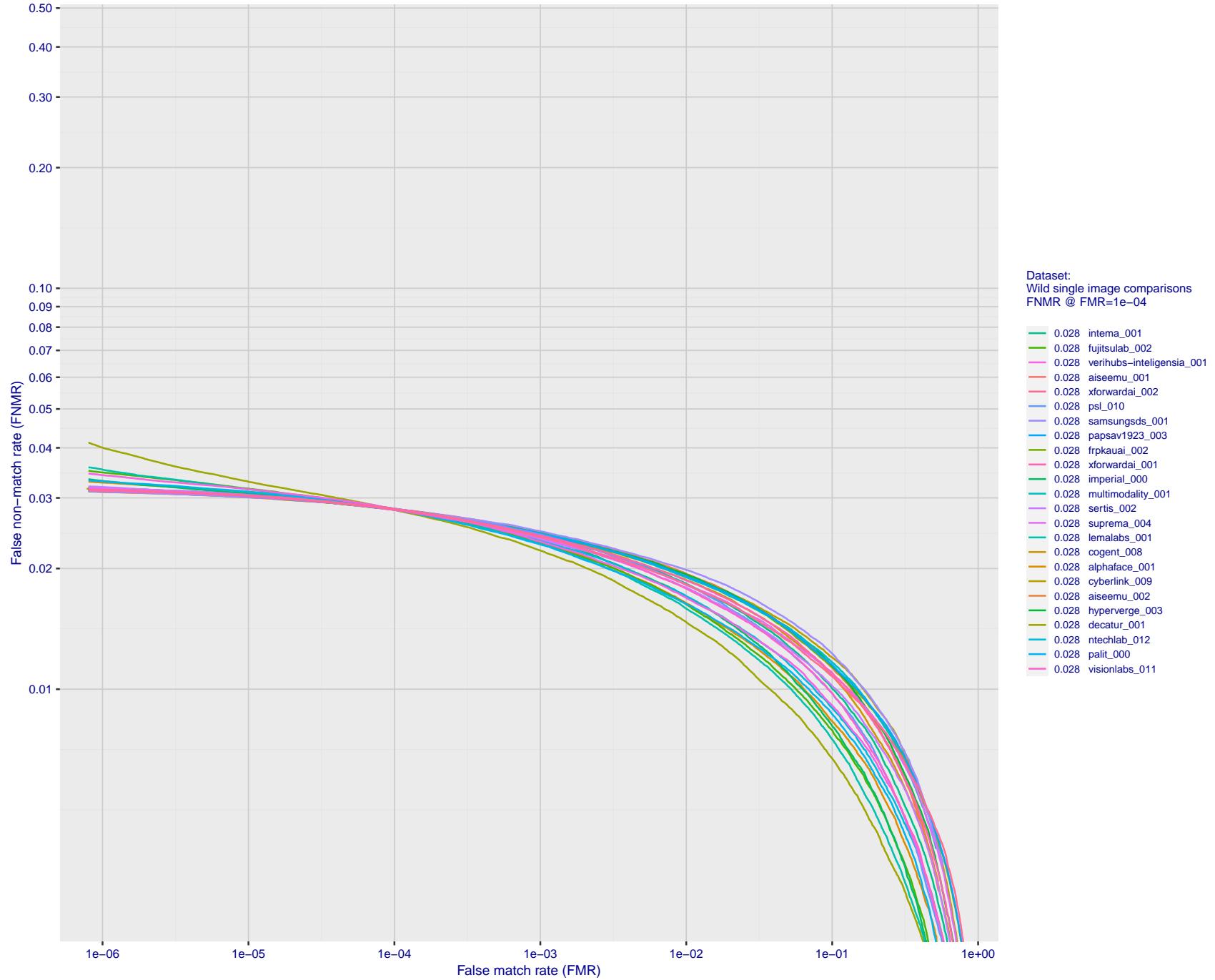


Figure 118: For the 2018 wild image comparisons, detection error tradeoff (DET) characteristics showing false non-match rate vs. false match rate plotted parametrically on threshold, T. The scales are logarithmic in order to show several decades of FMR.

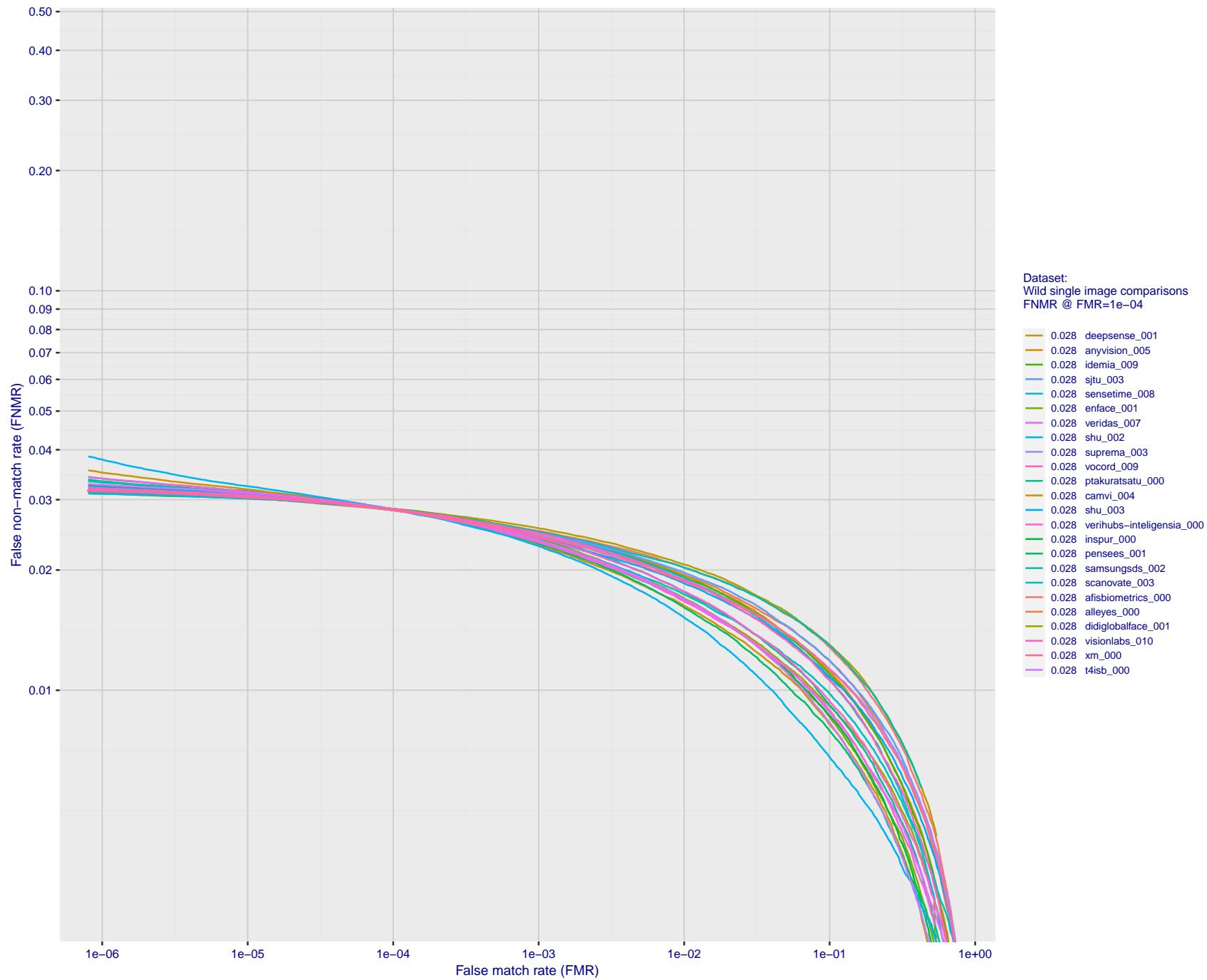


Figure 119: For the 2018 wild image comparisons, detection error tradeoff (DET) characteristics showing false non-match rate vs. false match rate plotted parametrically on threshold, T. The scales are logarithmic in order to show several decades of FMR.

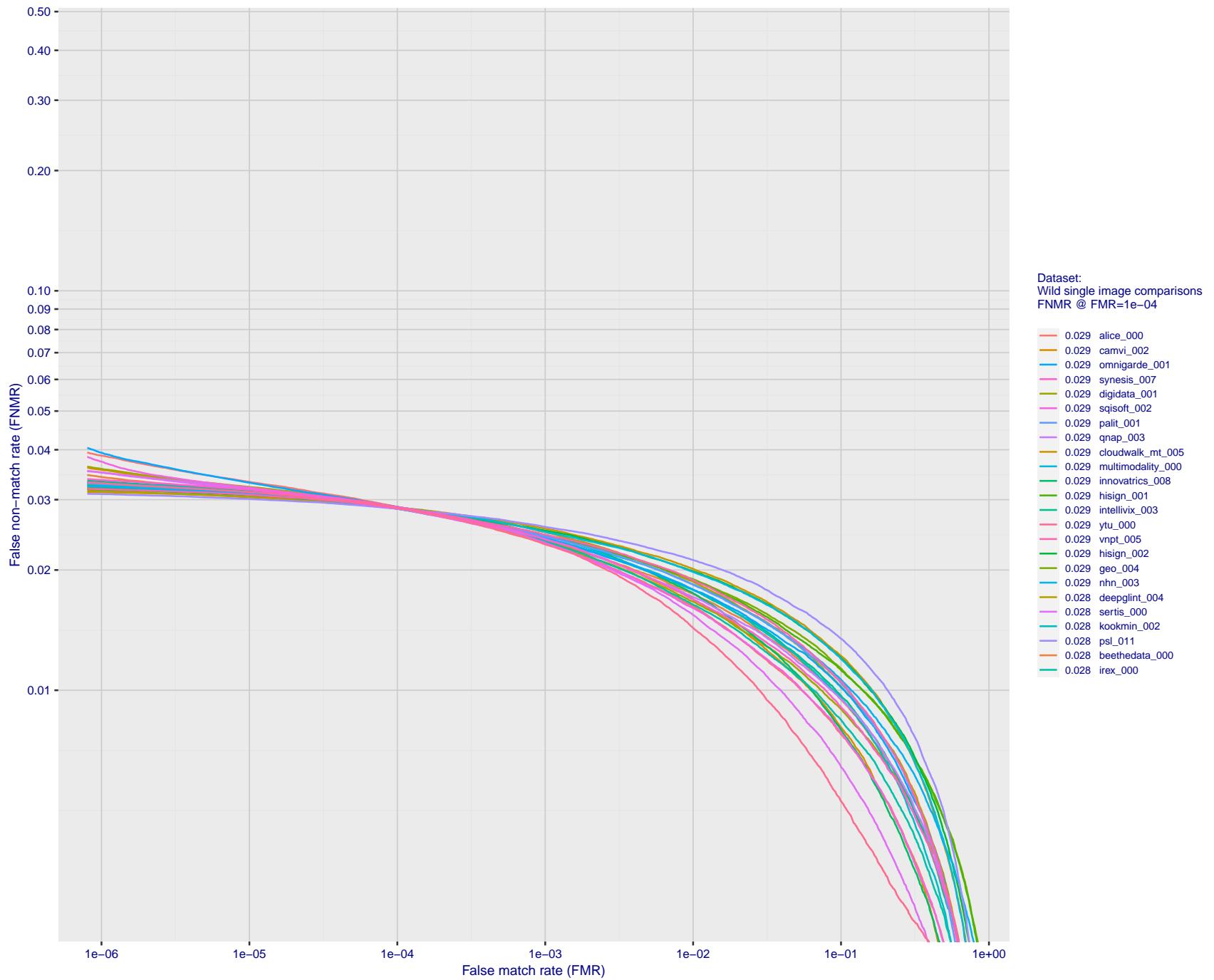


Figure 120: For the 2018 wild image comparisons, detection error tradeoff (DET) characteristics showing false non-match rate vs. false match rate plotted parametrically on threshold, T . The scales are logarithmic in order to show several decades of FMR.

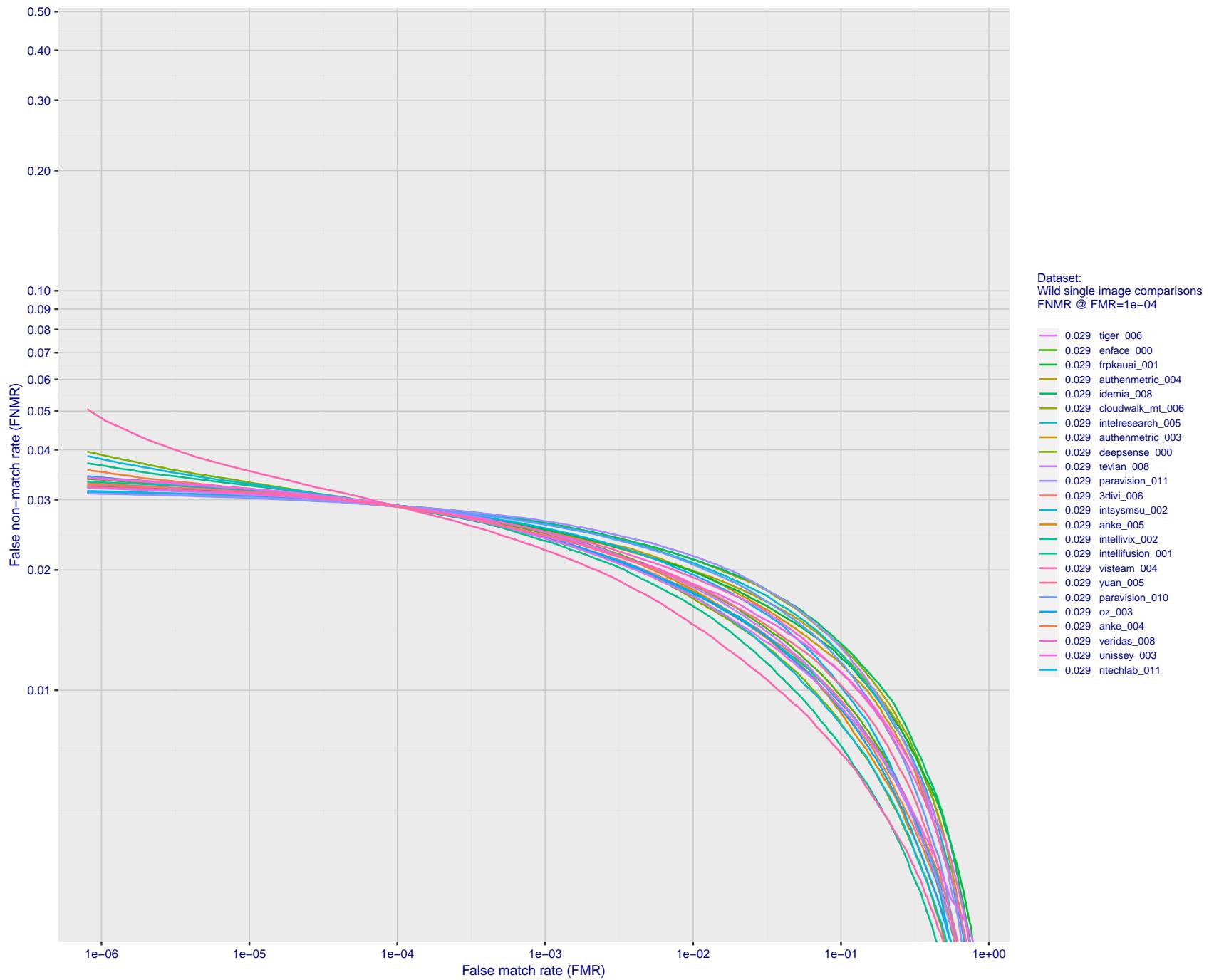


Figure 121: For the 2018 wild image comparisons, detection error tradeoff (DET) characteristics showing false non-match rate vs. false match rate plotted parametrically on threshold, T . The scales are logarithmic in order to show several decades of FMR.

2023/02/09 20:10:38

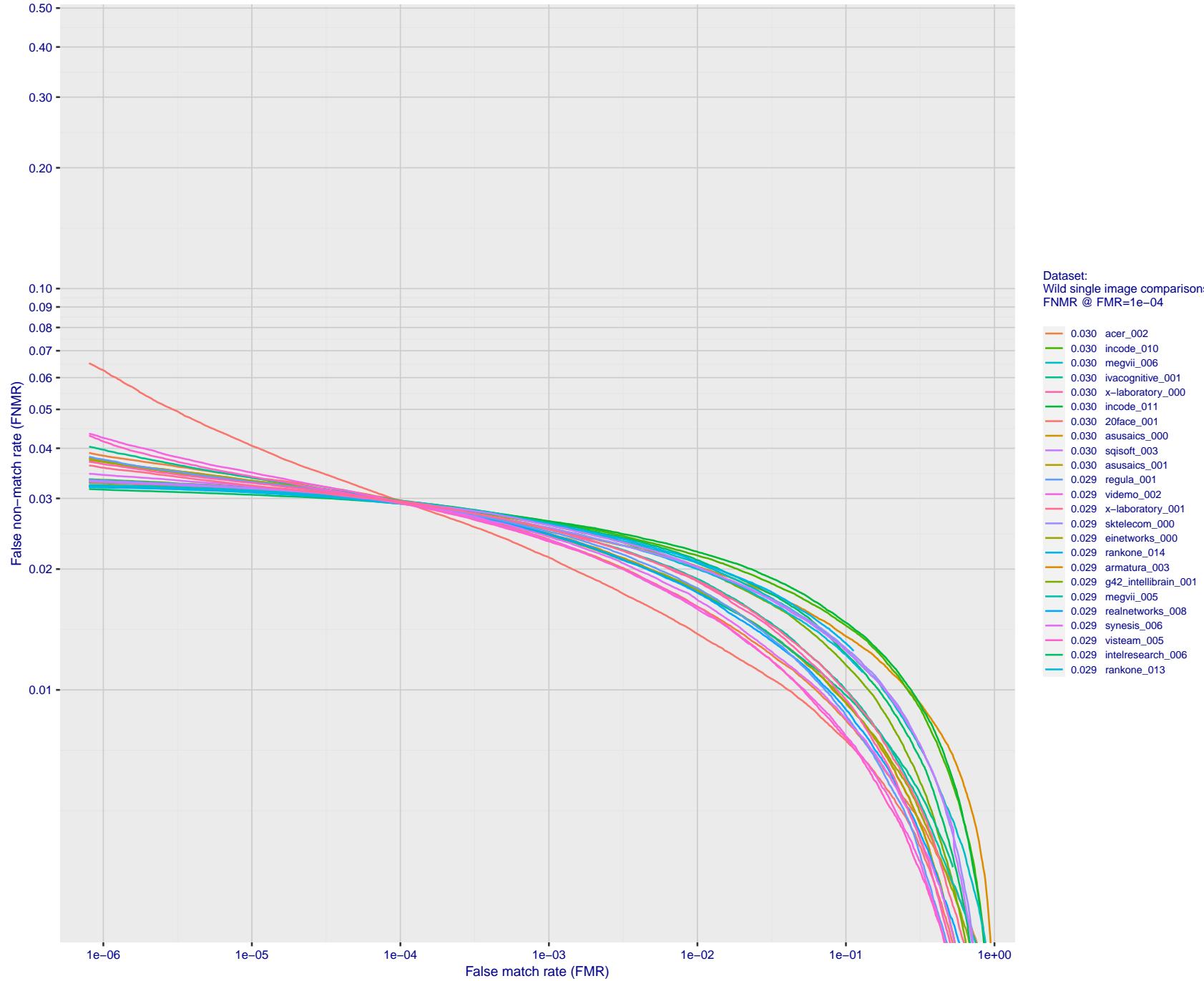


Figure 122: For the 2018 wild image comparisons, detection error tradeoff (DET) characteristics showing false non-match rate vs. false match rate plotted parametrically on threshold, T. The scales are logarithmic in order to show several decades of FMR.

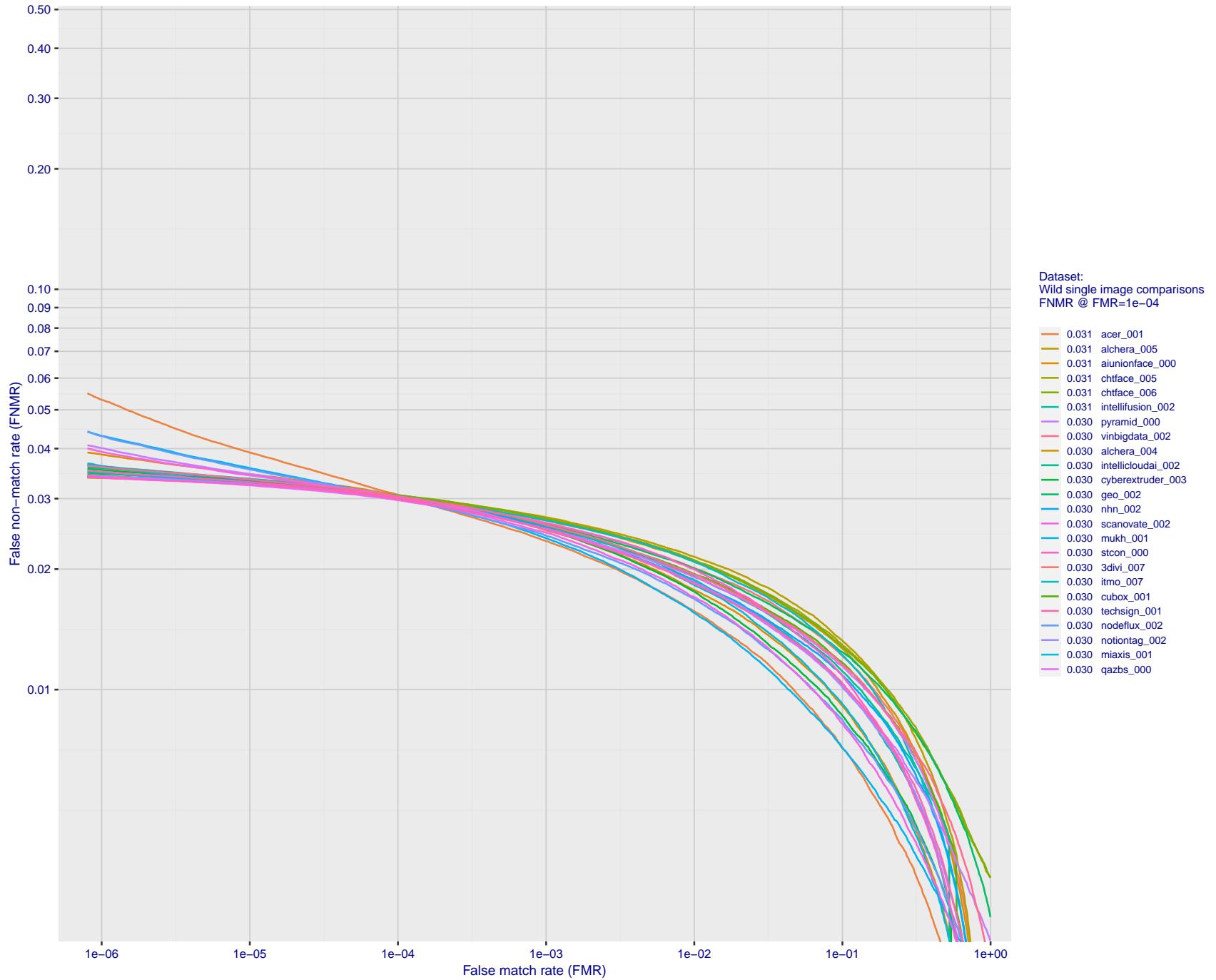


Figure 123: For the 2018 wild image comparisons, detection error tradeoff (DET) characteristics showing false non-match rate vs. false match rate plotted parametrically on threshold, T . The scales are logarithmic in order to show several decades of FMR.

2023/02/09 20:10:38

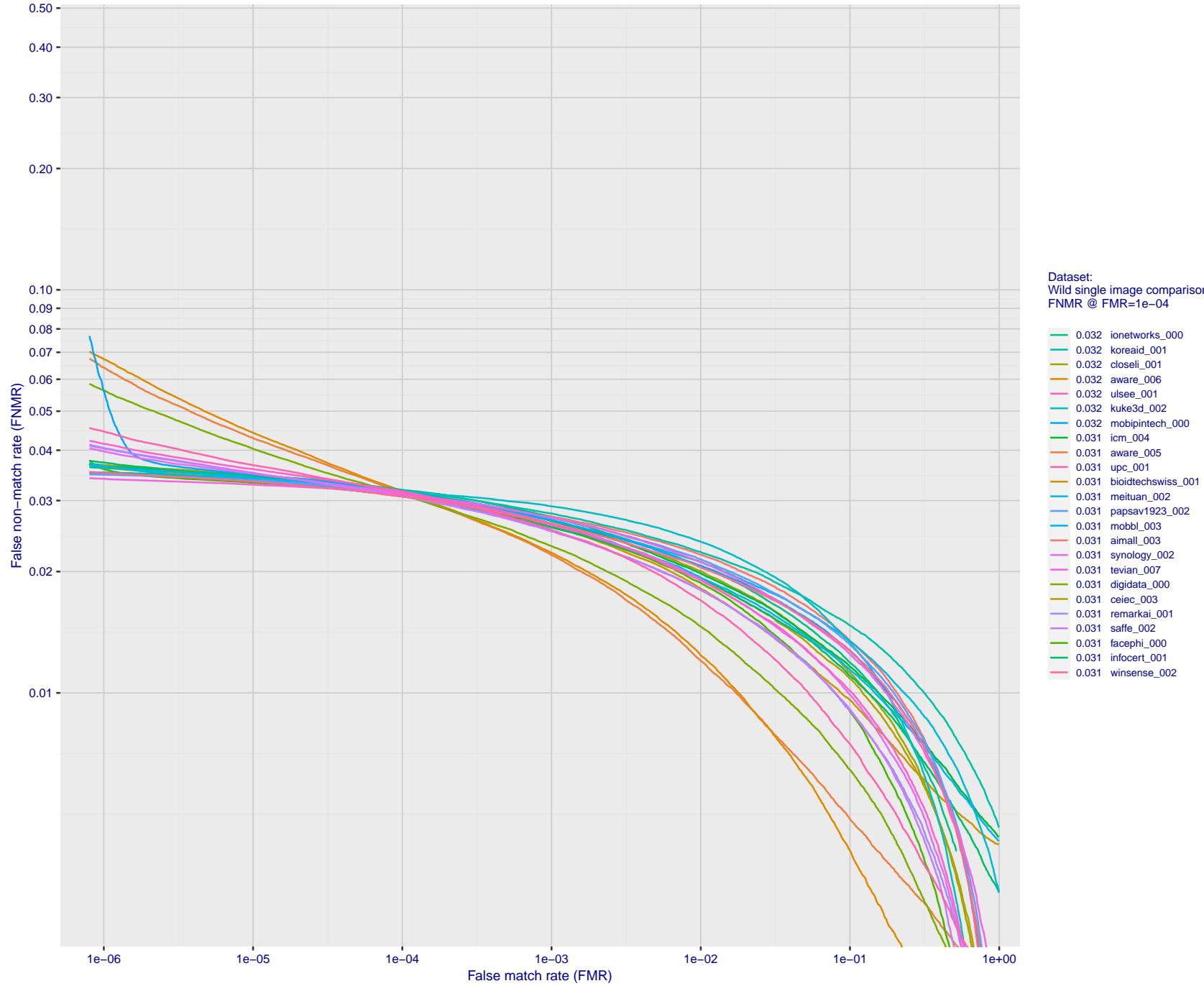


Figure 124: For the 2018 wild image comparisons, detection error tradeoff (DET) characteristics showing false non-match rate vs. false match rate plotted parametrically on threshold, T . The scales are logarithmic in order to show several decades of FMR.

2023/02/09 20:10:38

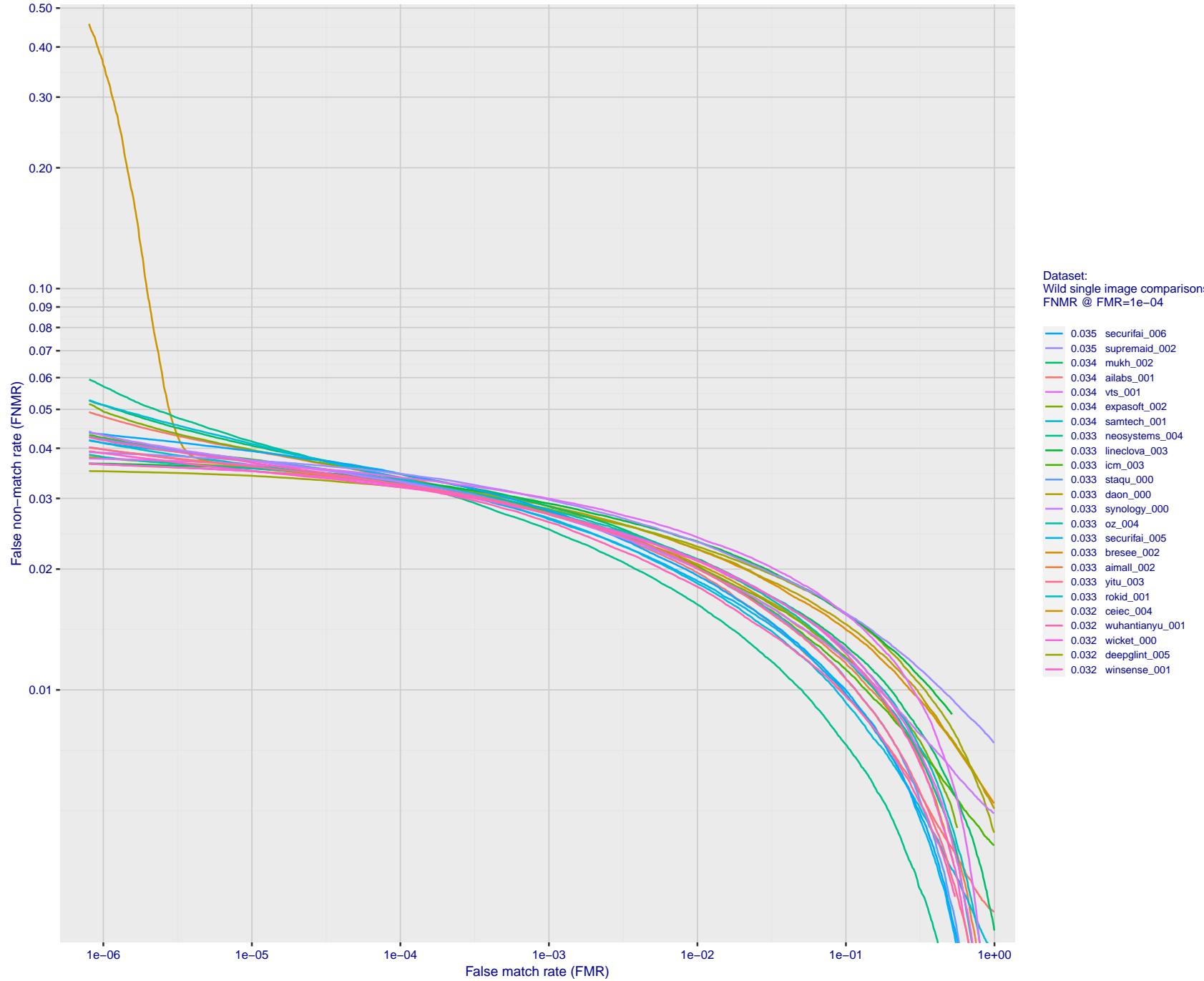


Figure 125: For the 2018 wild image comparisons, detection error tradeoff (DET) characteristics showing false non-match rate vs. false match rate plotted parametrically on threshold, T . The scales are logarithmic in order to show several decades of FMR.

2023/02/09 20:10:38

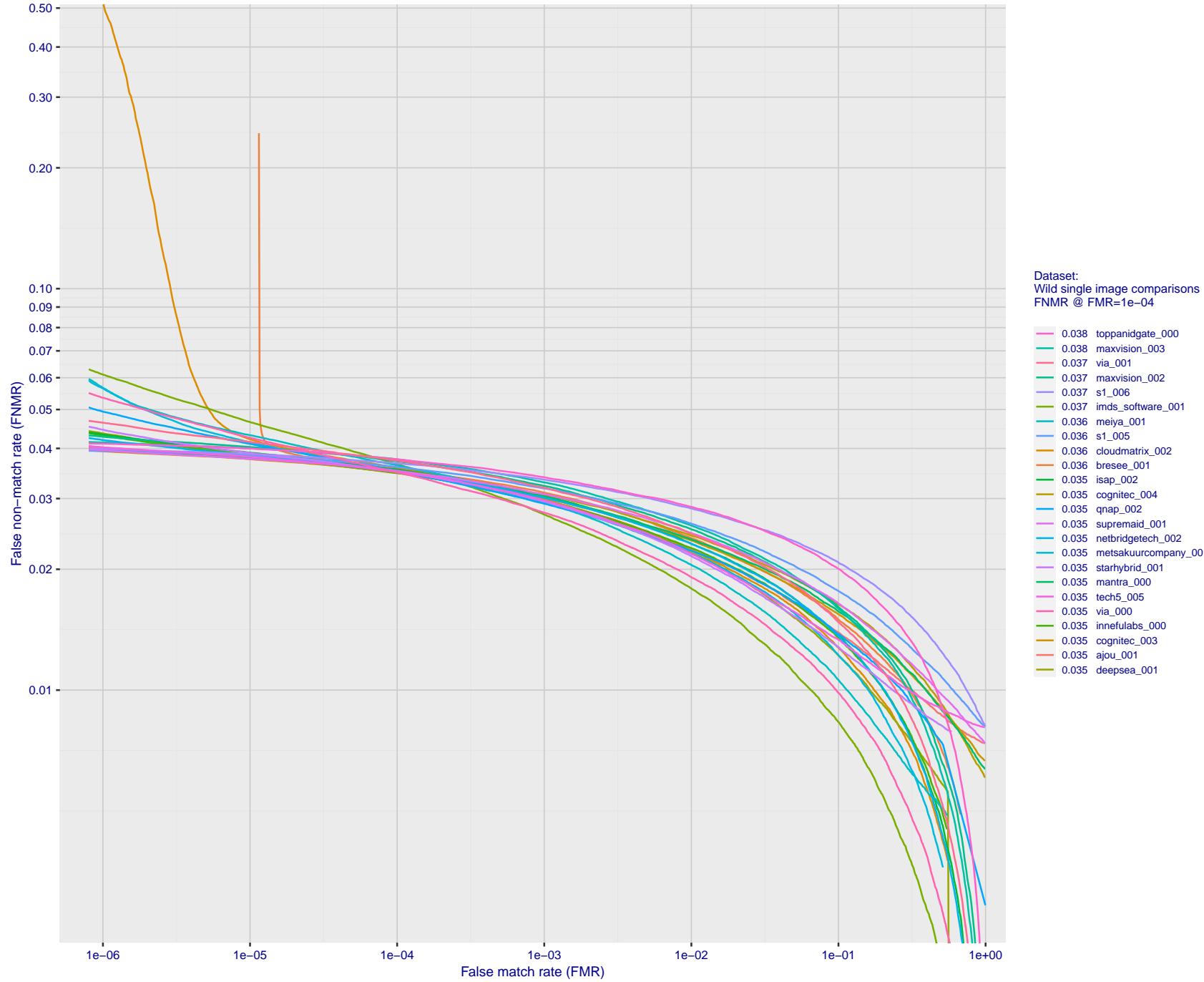


Figure 126: For the 2018 wild image comparisons, detection error tradeoff (DET) characteristics showing false non-match rate vs. false match rate plotted parametrically on threshold, T. The scales are logarithmic in order to show several decades of FMR.

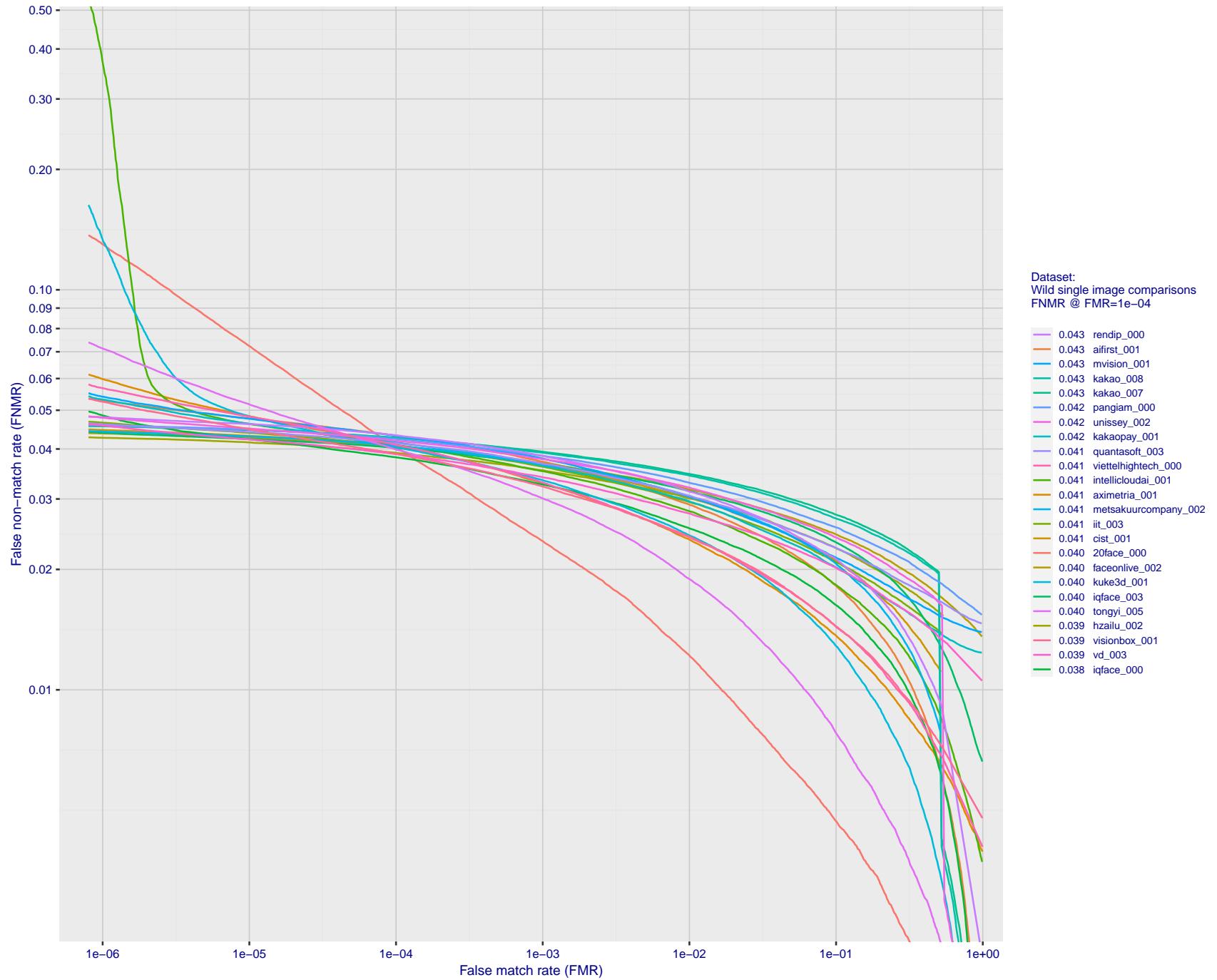


Figure 127: For the 2018 wild image comparisons, detection error tradeoff (DET) characteristics showing false non-match rate vs. false match rate plotted parametrically on threshold, T . The scales are logarithmic in order to show several decades of FMR.

2023/02/09 20:10:38

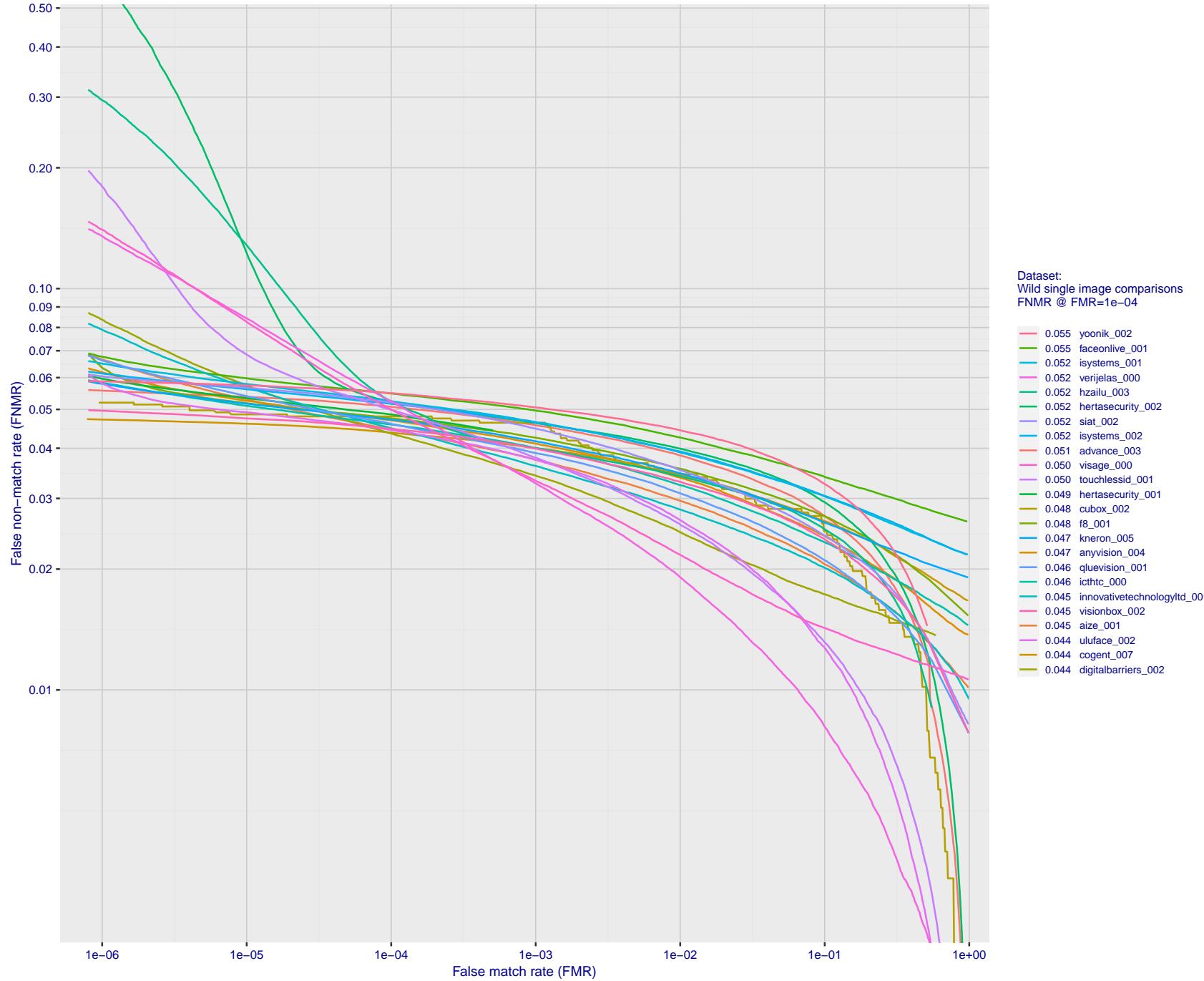


Figure 128: For the 2018 wild image comparisons, detection error tradeoff (DET) characteristics showing false non-match rate vs. false match rate plotted parametrically on threshold, T . The scales are logarithmic in order to show several decades of FMR.

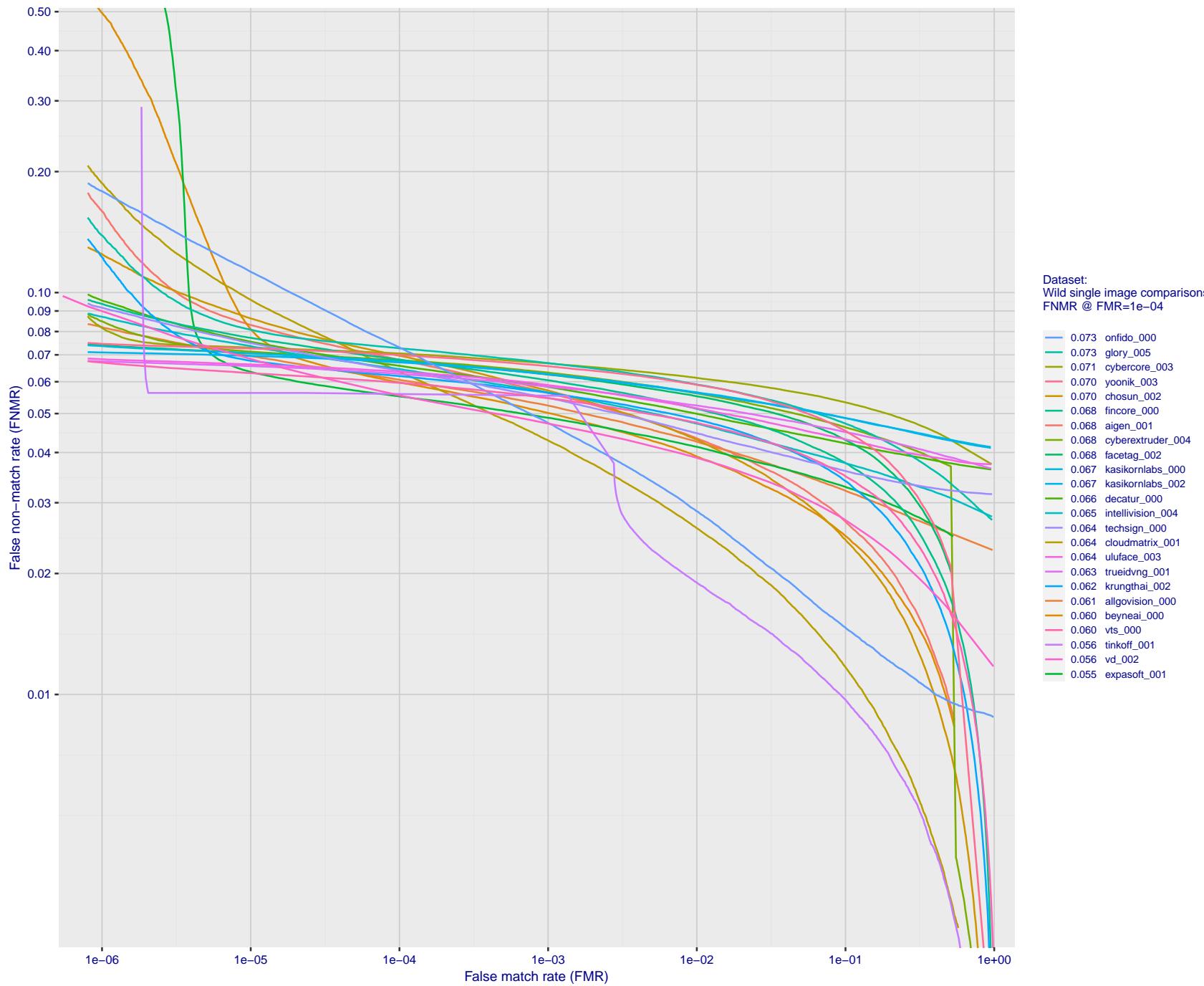


Figure 129: For the 2018 wild image comparisons, detection error tradeoff (DET) characteristics showing false non-match rate vs. false match rate plotted parametrically on threshold, T . The scales are logarithmic in order to show several decades of FMR.

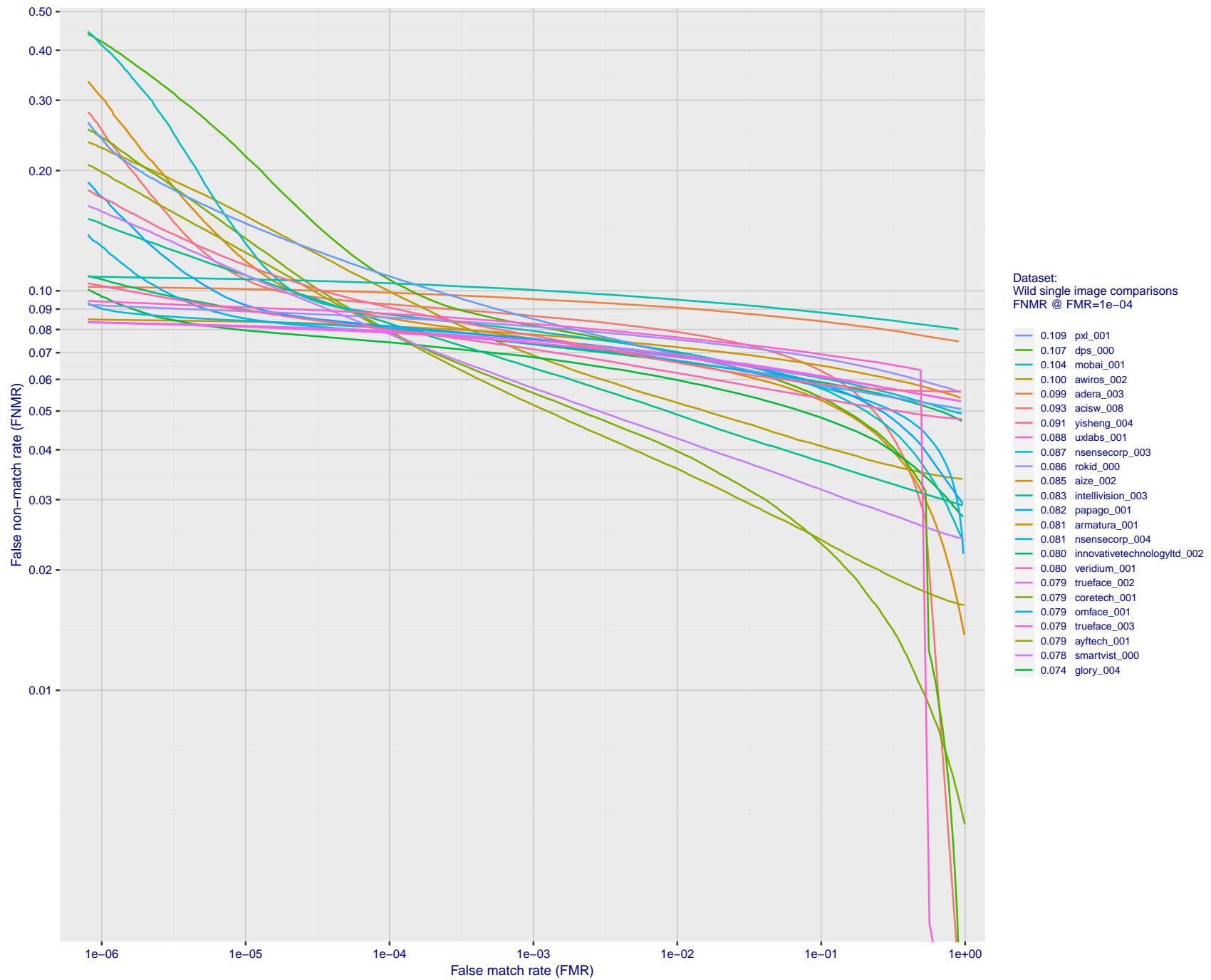


Figure 130: For the 2018 wild image comparisons, detection error tradeoff (DET) characteristics showing false non-match rate vs. false match rate plotted parametrically on threshold, T. The scales are logarithmic in order to show several decades of FMR.

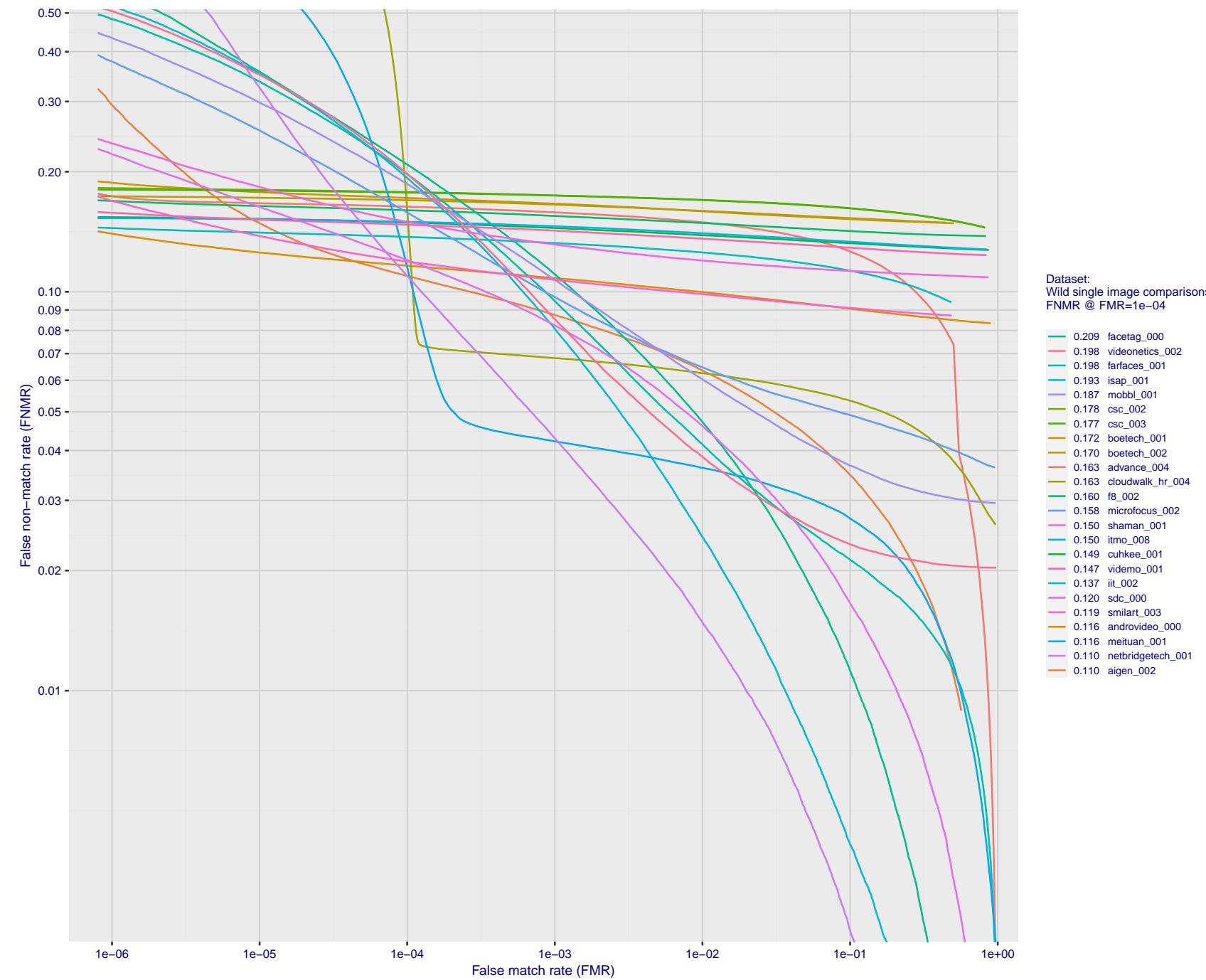


Figure 131: For the 2018 wild image comparisons, detection error tradeoff (DET) characteristics showing false non-match rate vs. false match rate plotted parametrically on threshold, T. The scales are logarithmic in order to show several decades of FMR.

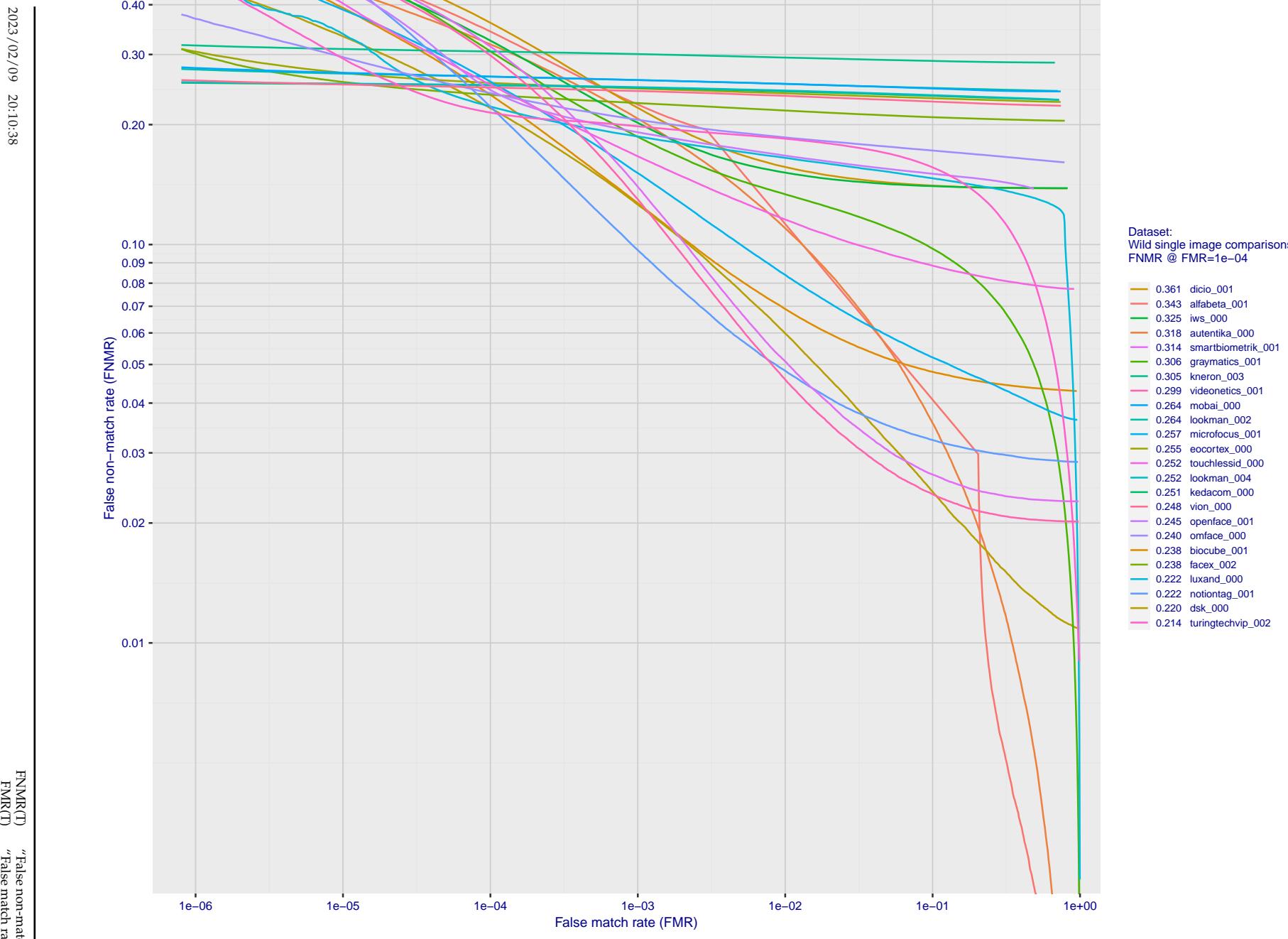


Figure 132: For the 2018 wild image comparisons, detection error tradeoff (DET) characteristics showing false non-match rate vs. false match rate plotted parametrically on threshold, T . The scales are logarithmic in order to show several decades of FMR.

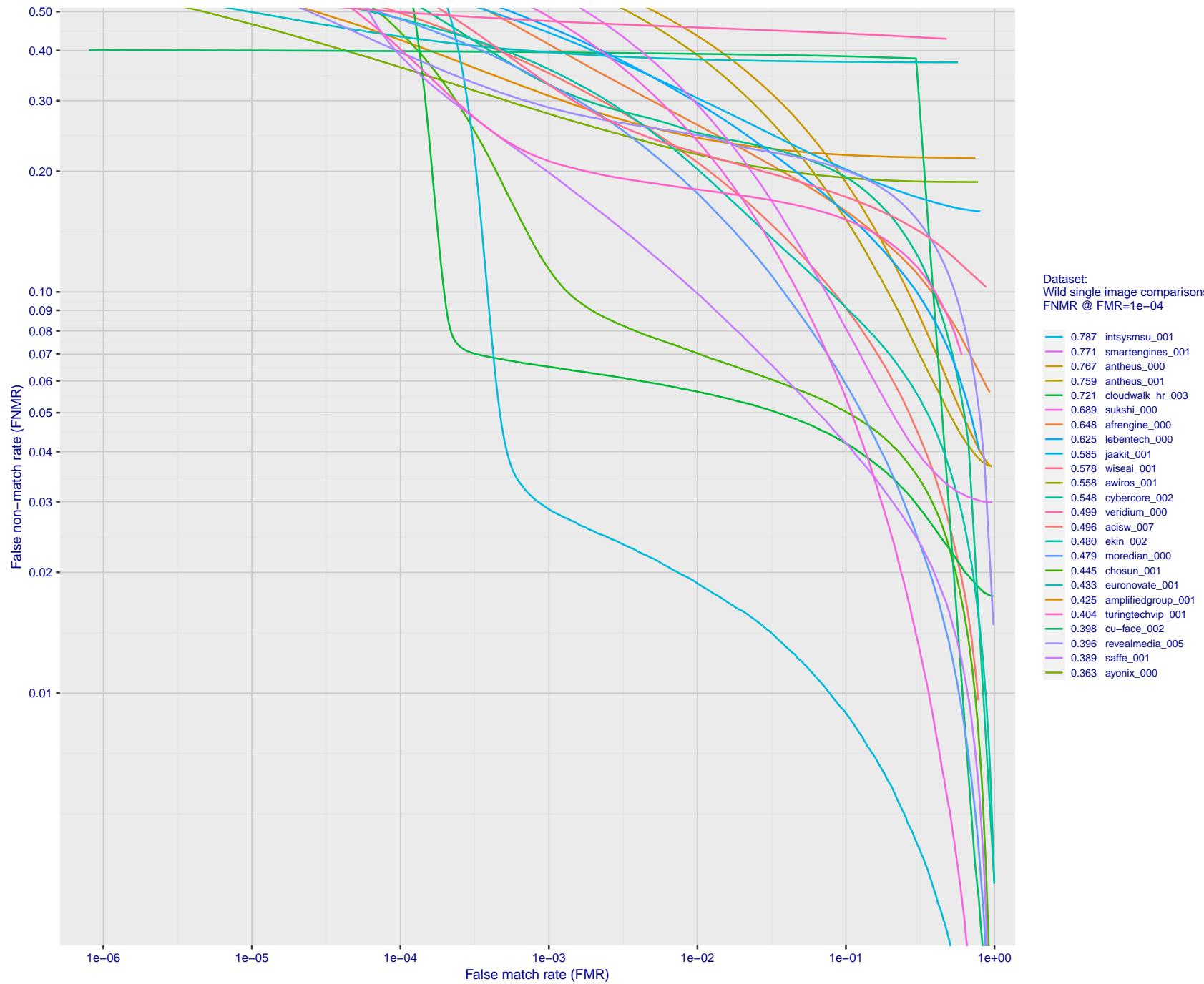


Figure 133: For the 2018 wild image comparisons, detection error tradeoff (DET) characteristics showing false non-match rate vs. false match rate plotted parametrically on threshold, T. The scales are logarithmic in order to show several decades of FMR.

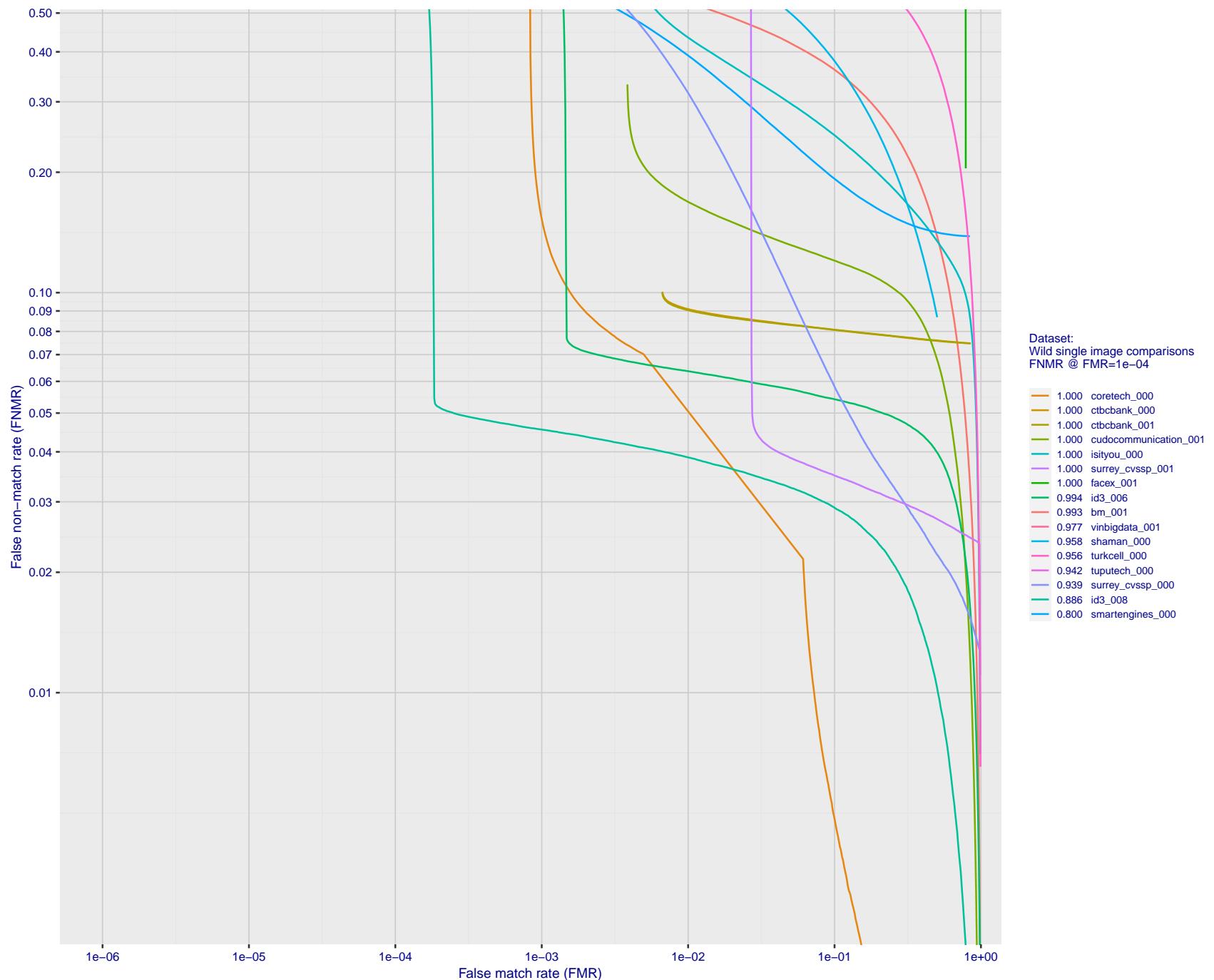


Figure 134: For the 2018 wild image comparisons, detection error tradeoff (DET) characteristics showing false non-match rate vs. false match rate plotted parametrically on threshold, T . The scales are logarithmic in order to show several decades of FMR.

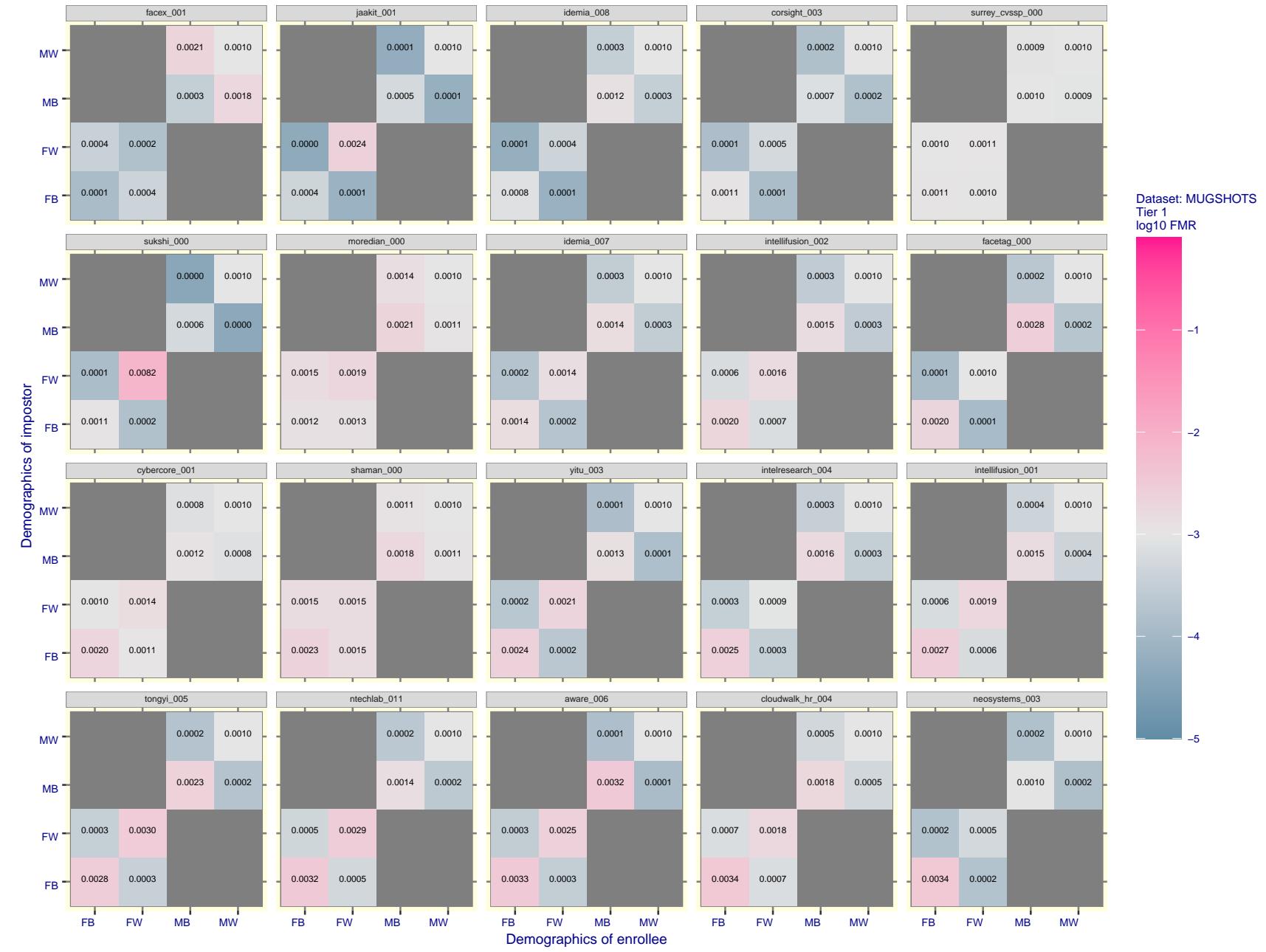


Figure 135: For the mugshot images, FMR for same-sex impostor pairs of images annotated with codes for black female, black male, white female, white male. The threshold is set for each algorithm to give FMR = 0.001 for white males which is the demographic that usually gives the lowest FMR. This means the top right box is the same color in all panels. The panels are sorted over multiple pages in order of FMR on black females, which is the demographic that usually gives the highest FMR.

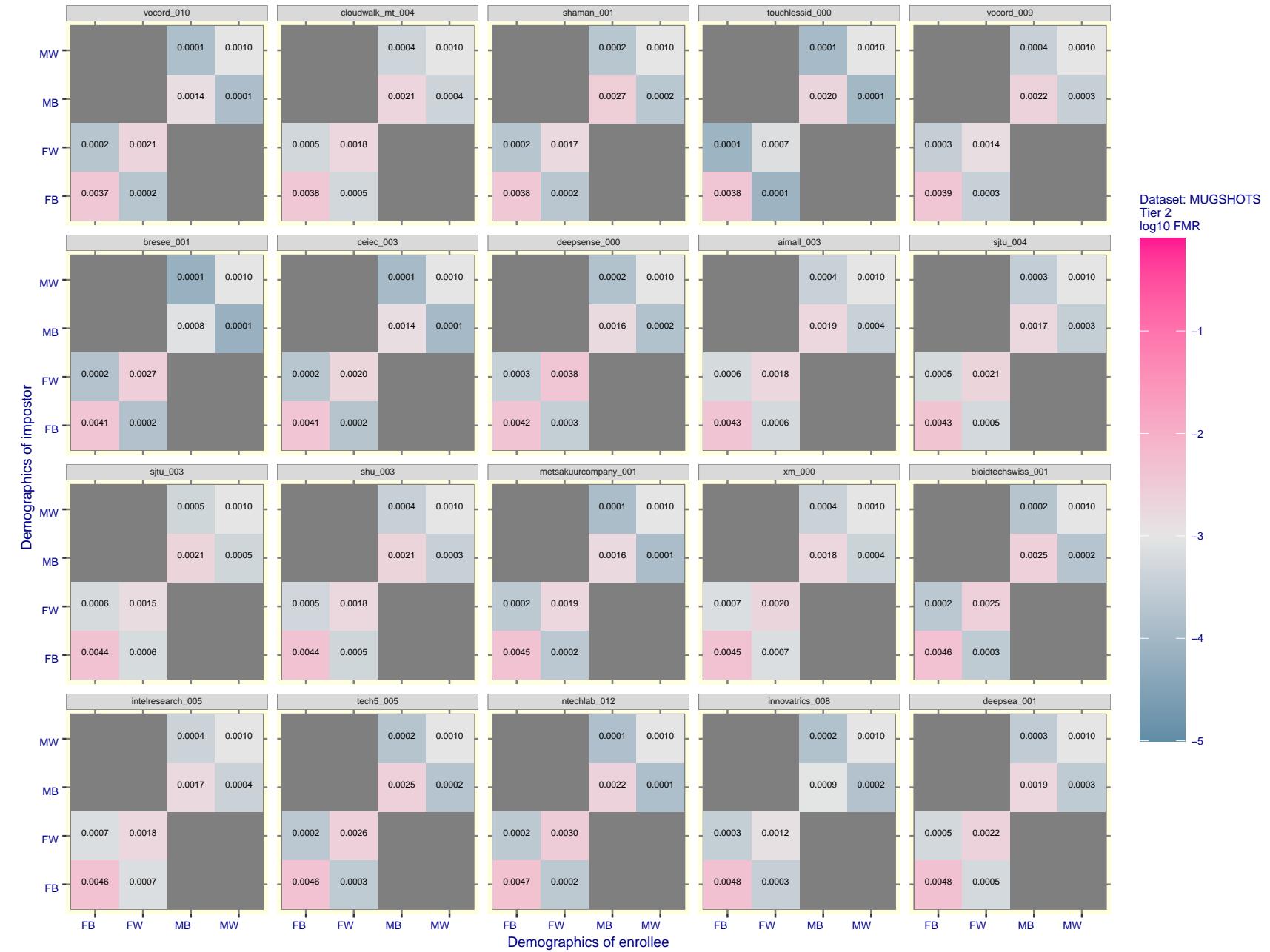


Figure 136: For the mugshot images, FMR for same-sex impostor pairs of images annotated with codes for black female, black male, white female, white male. The threshold is set for each algorithm to give FMR = 0.001 for white males which is the demographic that usually gives the lowest FMR. This means the top right box is the same color in all panels. The panels are sorted over multiple pages in order of FMR on black females, which is the demographic that usually gives the highest FMR.

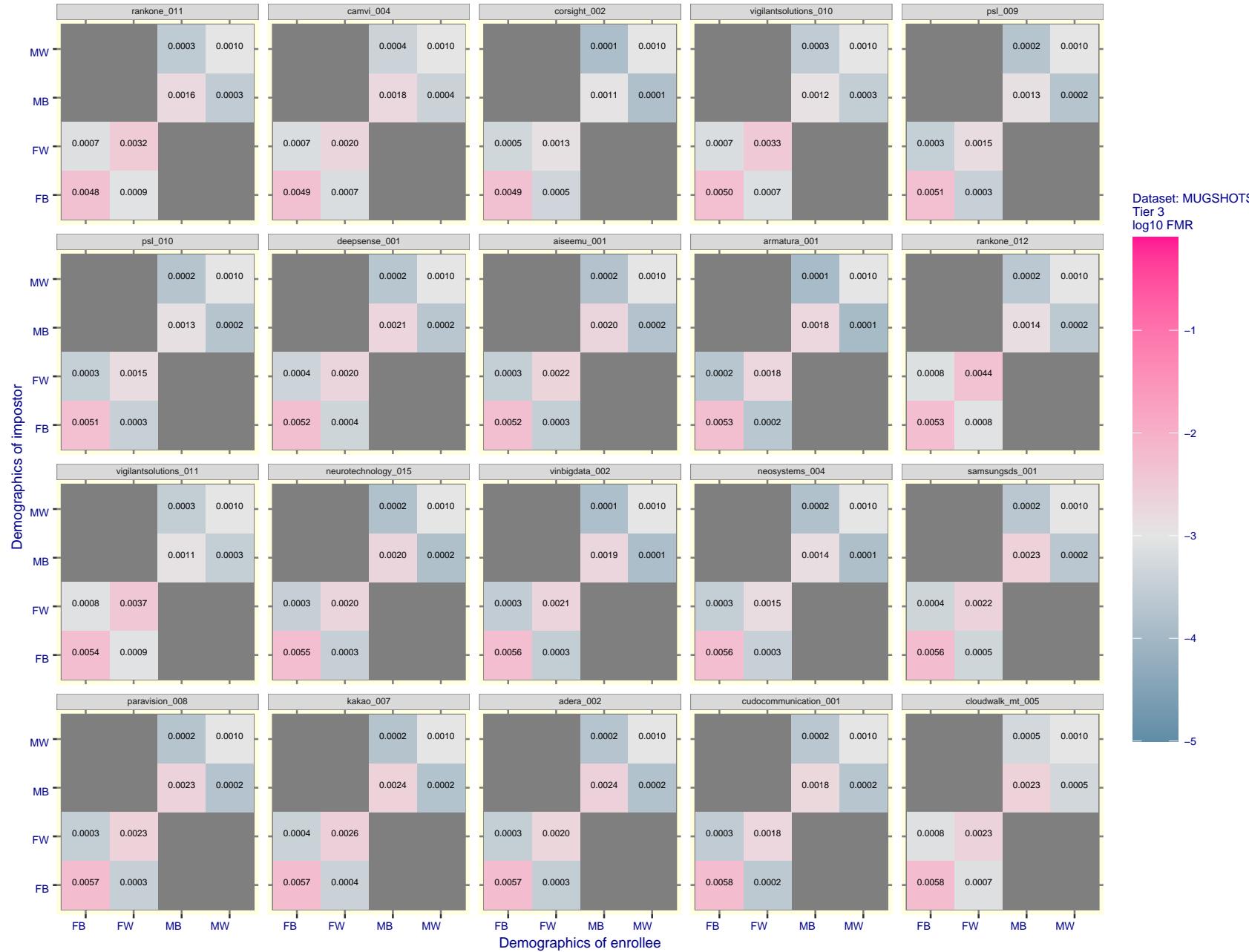


Figure 137: For the mugshot images, FMR for same-sex impostor pairs of images annotated with codes for black female, black male, white female, white male. The threshold is set for each algorithm to give $FMR = 0.001$ for white males which is the demographic that usually gives the lowest FMR. This means the top right box is the same color in all panels. The panels are sorted over multiple pages in order of FMR on black females, which is the demographic that usually gives the highest FMR.

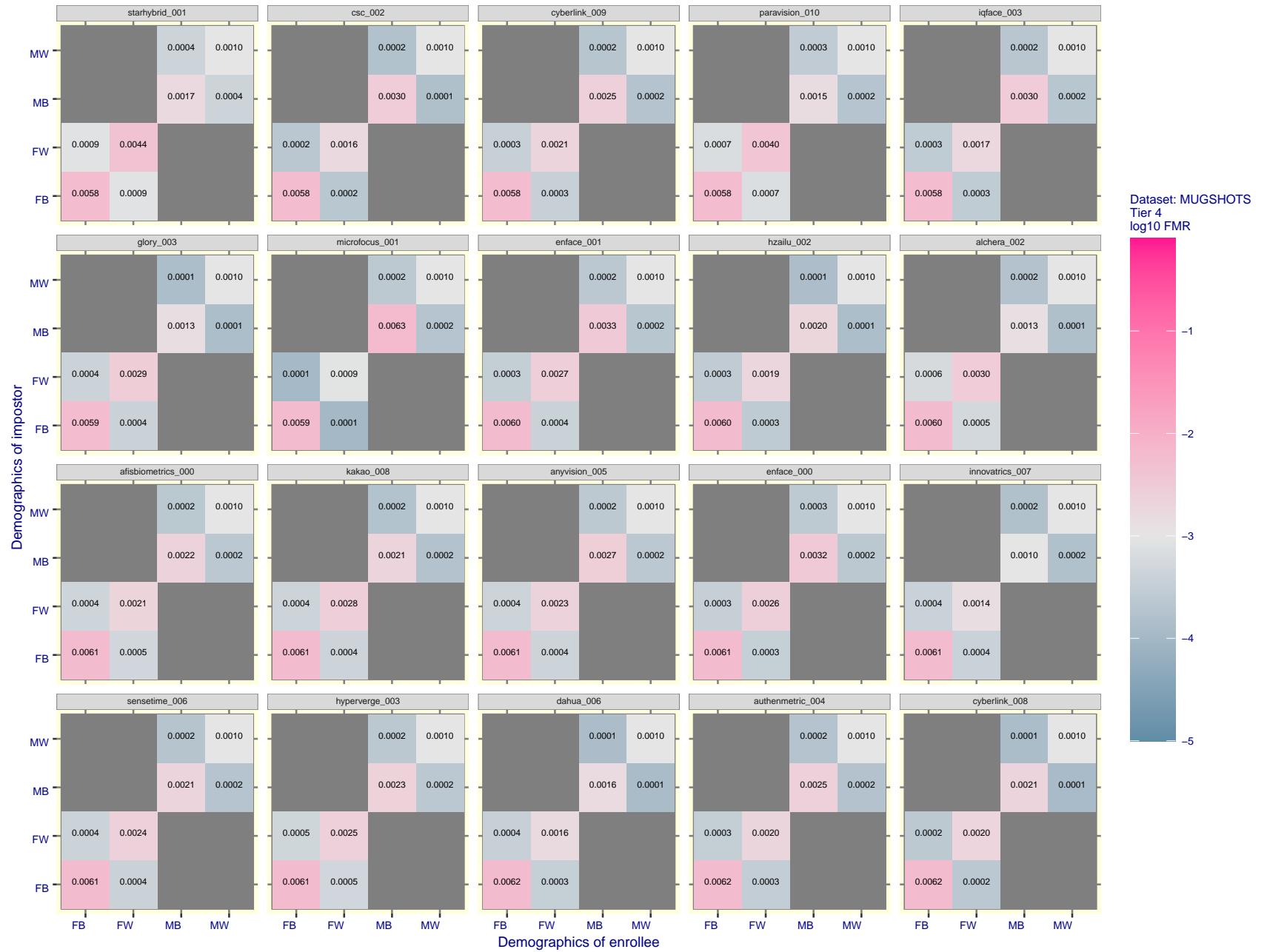


Figure 138: For the mugshot images, FMR for same-sex impostor pairs of images annotated with codes for black female, black male, white female, white male. The threshold is set for each algorithm to give $\text{FMR} = 0.001$ for white males which is the demographic that usually gives the lowest FMR. This means the top right box is the same color in all panels. The panels are sorted over multiple pages in order of FMR on black females, which is the demographic that usually gives the highest FMR.

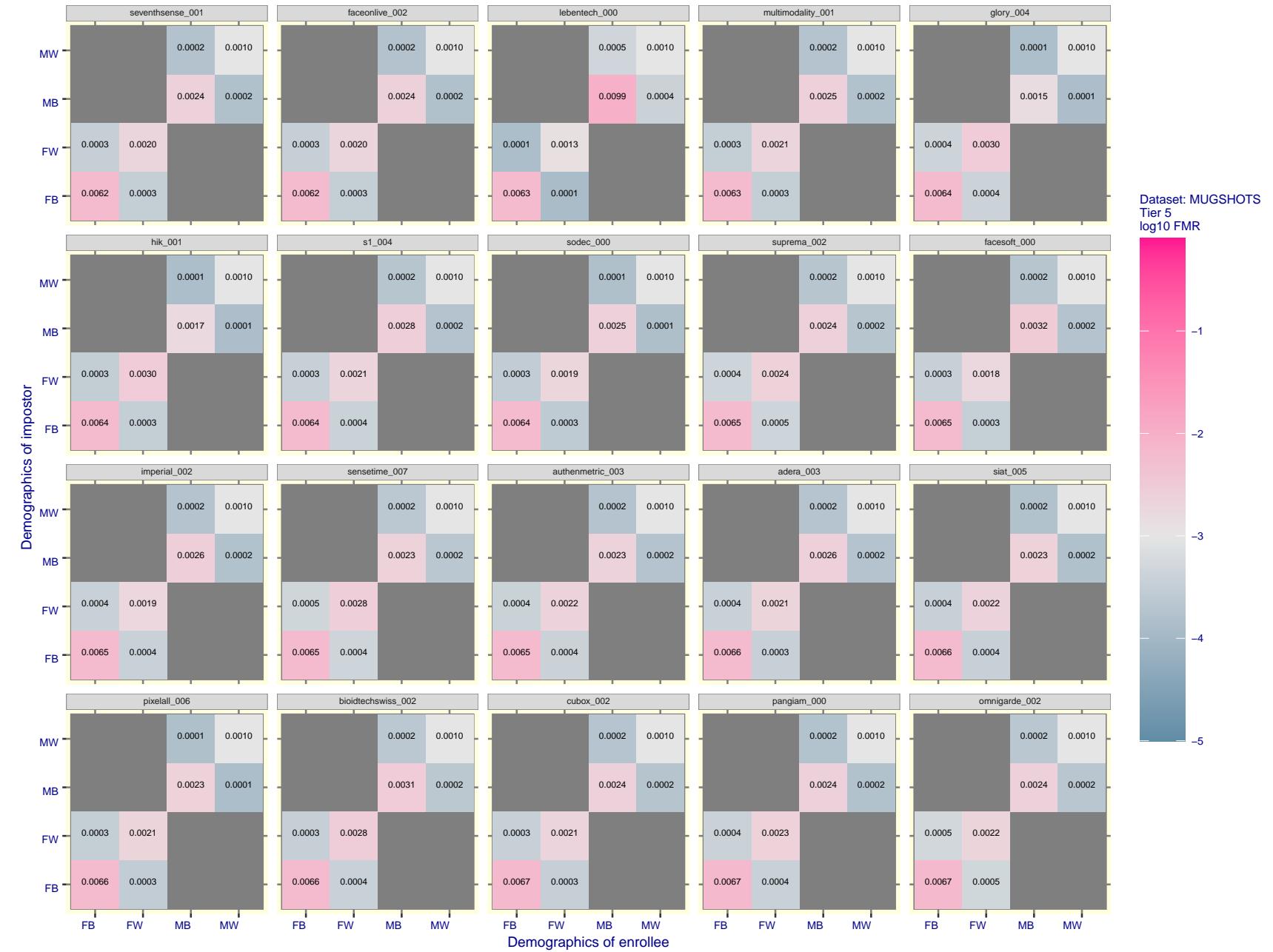


Figure 139: For the mugshot images, FMR for same-sex impostor pairs of images annotated with codes for black female, black male, white female, white male. The threshold is set for each algorithm to give $\text{FMR} = 0.001$ for white males which is the demographic that usually gives the lowest FMR. This means the top right box is the same color in all panels. The panels are sorted over multiple pages in order of FMR on black females, which is the demographic that usually gives the highest FMR.

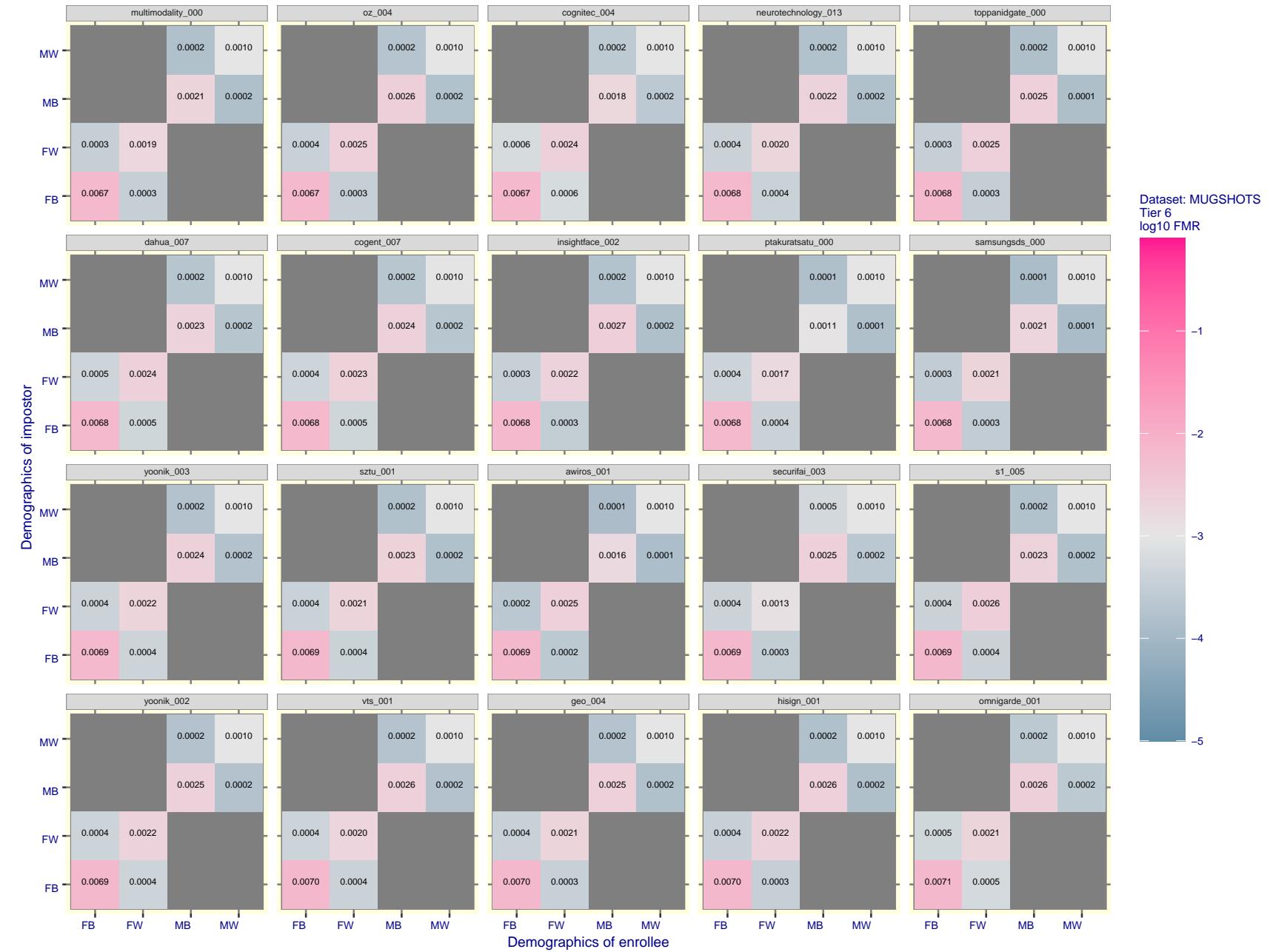


Figure 140: For the mugshot images, FMR for same-sex impostor pairs of images annotated with codes for black female, black male, white female, white male. The threshold is set for each algorithm to give $\text{FMR} = 0.001$ for white males which is the demographic that usually gives the lowest FMR. This means the top right box is the same color in all panels. The panels are sorted over multiple pages in order of FMR on black females, which is the demographic that usually gives the highest FMR.

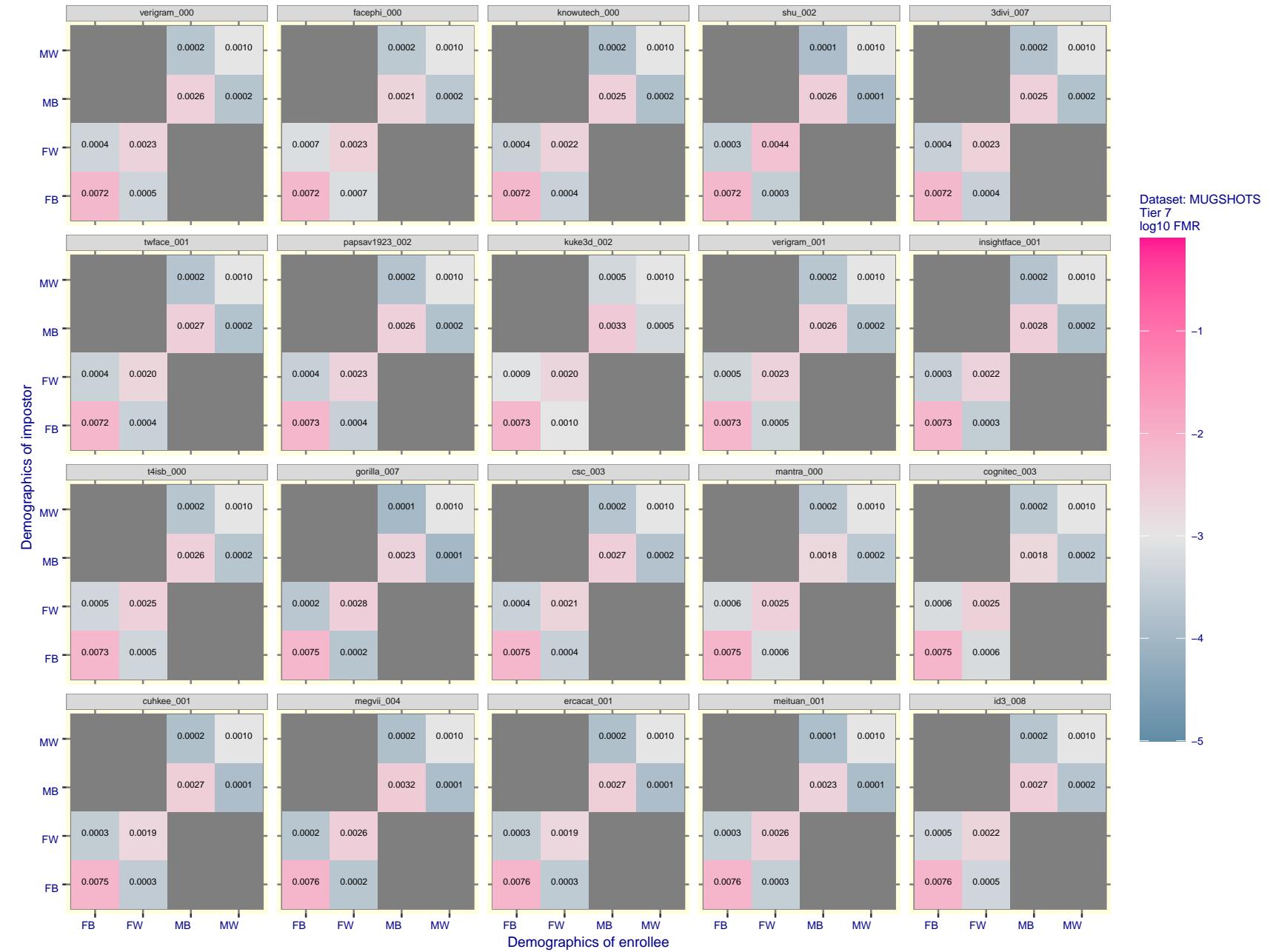


Figure 141: For the mugshot images, FMR for same-sex impostor pairs of images annotated with codes for black female, black male, white female, white male. The threshold is set for each algorithm to give $FMR = 0.001$ for white males which is the demographic that usually gives the lowest FMR. This means the top right box is the same color in all panels. The panels are sorted over multiple pages in order of FMR on black females, which is the demographic that usually gives the highest FMR.

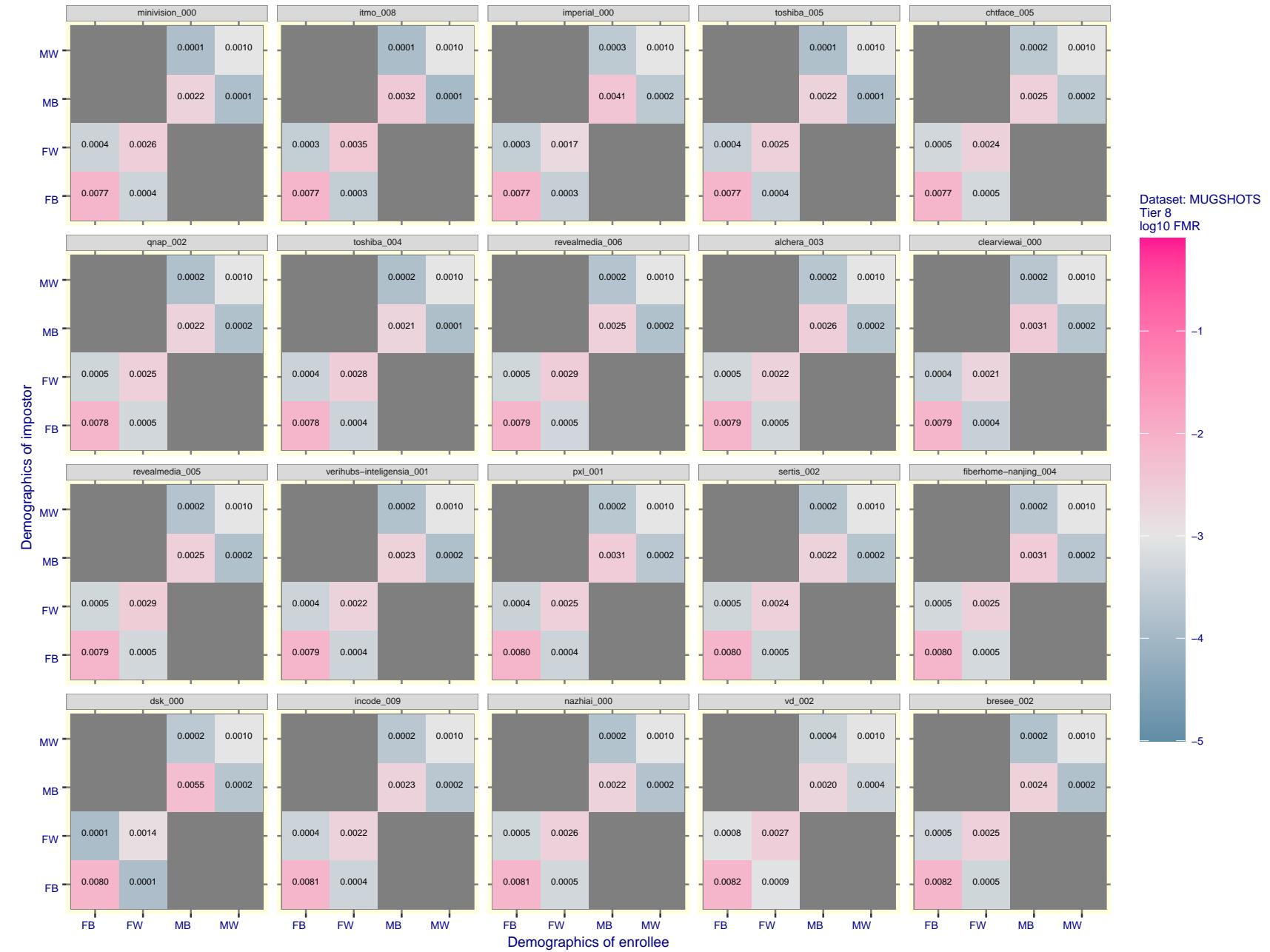


Figure 142: For the mugshot images, FMR for same-sex impostor pairs of images annotated with codes for black female, black male, white female, white male. The threshold is set for each algorithm to give $FMR = 0.001$ for white males which is the demographic that usually gives the lowest FMR. This means the top right box is the same color in all panels. The panels are sorted over multiple pages in order of FMR on black females, which is the demographic that usually gives the highest FMR.

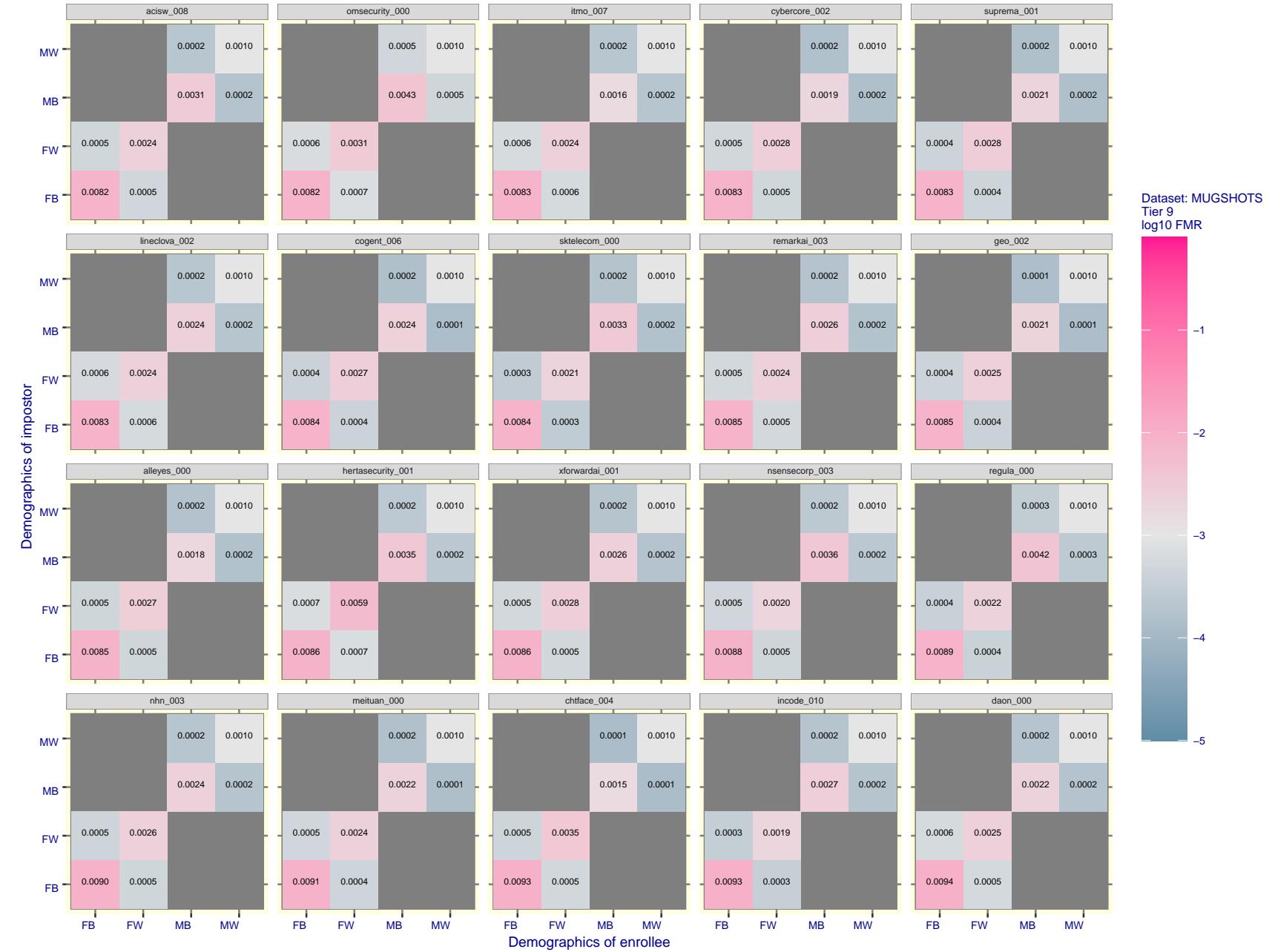


Figure 143: For the mugshot images, FMR for same-sex impostor pairs of images annotated with codes for black female, black male, white female, white male. The threshold is set for each algorithm to give FMR = 0.001 for white males which is the demographic that usually gives the lowest FMR. This means the top right box is the same color in all panels. The panels are sorted over multiple pages in order of FMR on black females, which is the demographic that usually gives the highest FMR.

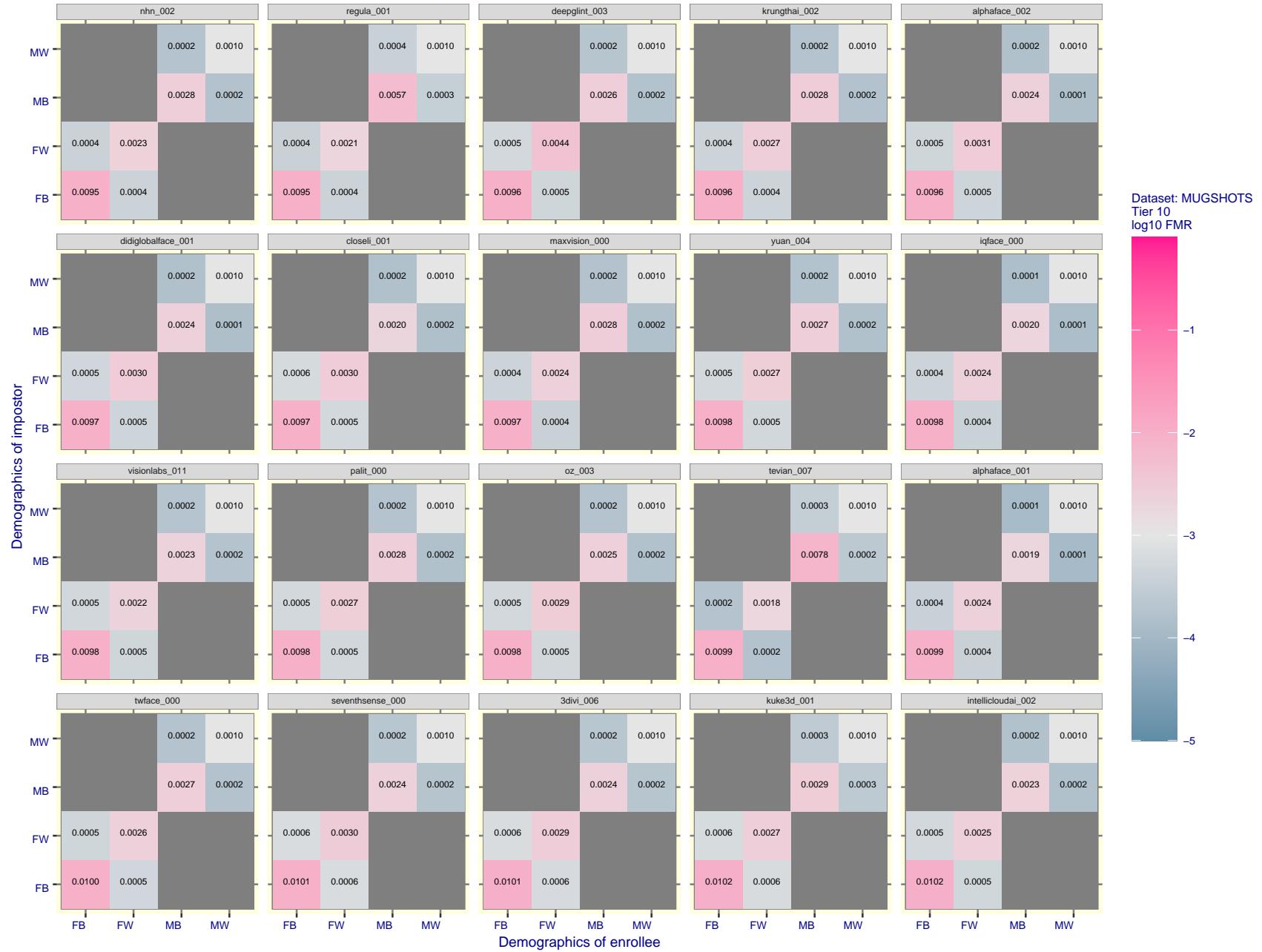


Figure 144: For the mugshot images, FMR for same-sex impostor pairs of images annotated with codes for black female, black male, white female, white male. The threshold is set for each algorithm to give FMR = 0.001 for white males which is the demographic that usually gives the lowest FMR. This means the top right box is the same color in all panels. The panels are sorted over multiple pages in order of FMR on black females, which is the demographic that usually gives the highest FMR.

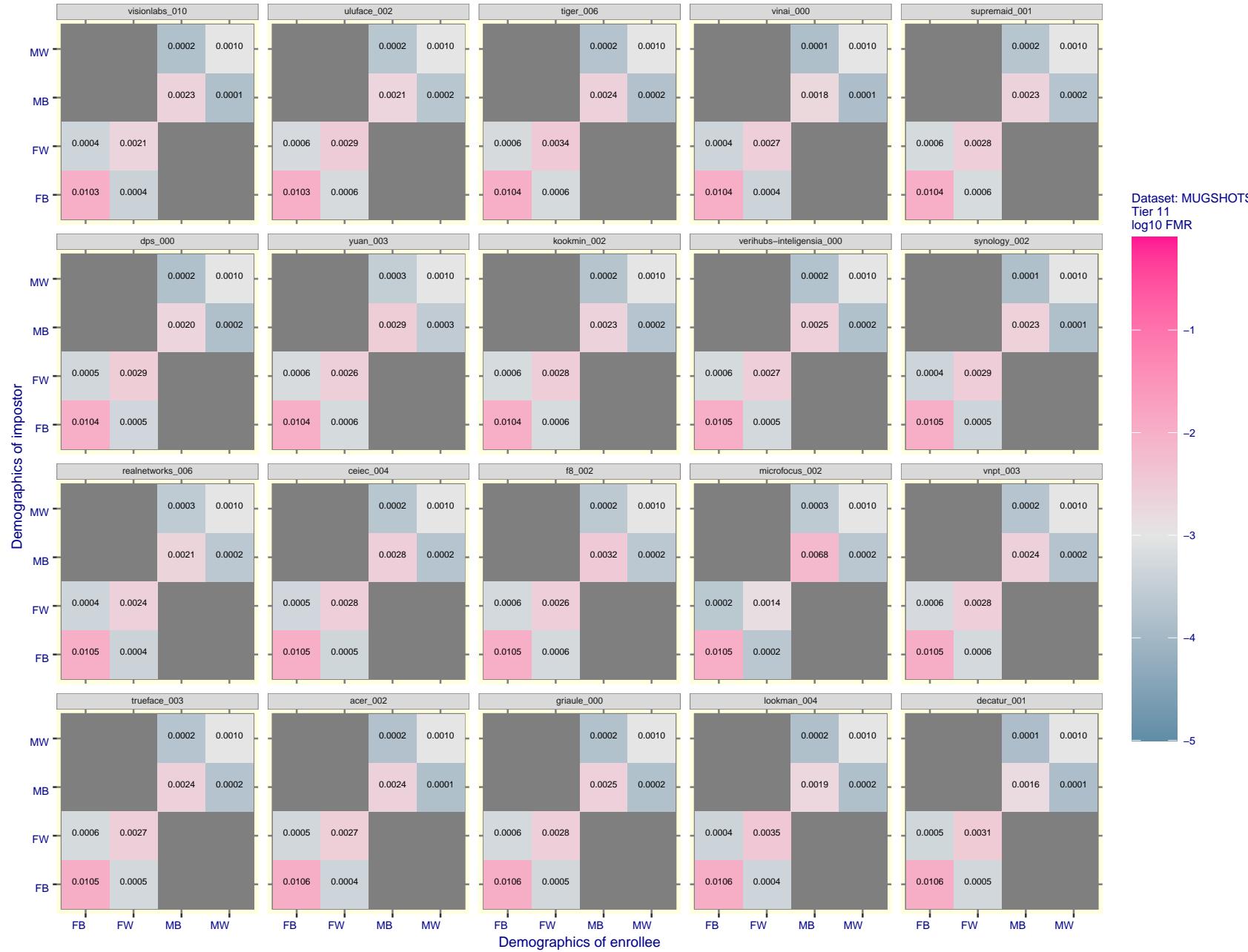


Figure 145: For the mugshot images, FMR for same-sex impostor pairs of images annotated with codes for black female, black male, white female, white male. The threshold is set for each algorithm to give $FMR = 0.001$ for white males which is the demographic that usually gives the lowest FMR. This means the top right box is the same color in all panels. The panels are sorted over multiple pages in order of FMR on black females, which is the demographic that usually gives the highest FMR.



Figure 146: For the mugshot images, FMR for same-sex impostor pairs of images annotated with codes for black female, black male, white female, white male. The threshold is set for each algorithm to give FMR = 0.001 for white males which is the demographic that usually gives the lowest FMR. This means the top right box is the same color in all panels. The panels are sorted over multiple pages in order of FMR on black females, which is the demographic that usually gives the highest FMR.

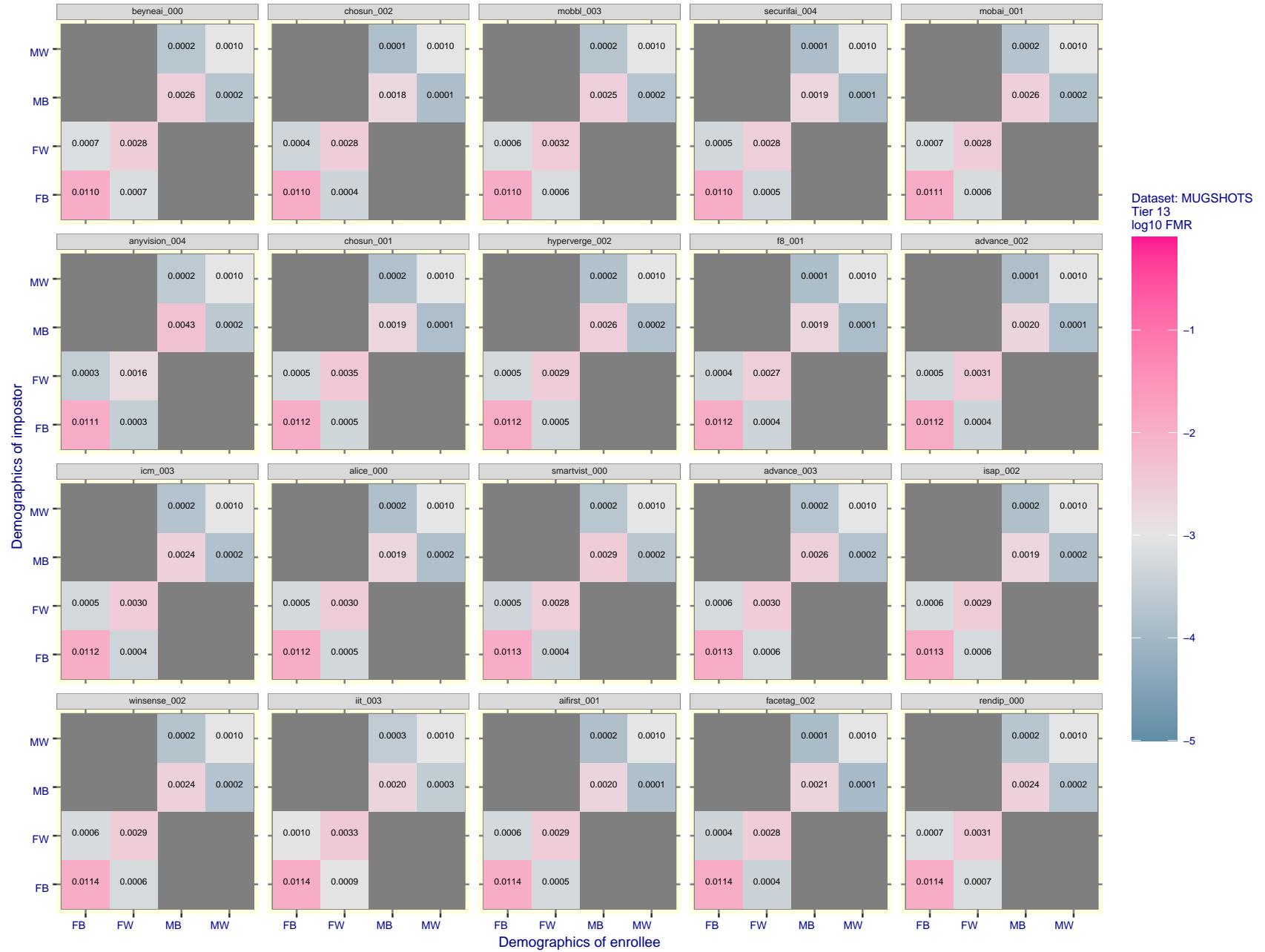


Figure 147: For the mugshot images, FMR for same-sex impostor pairs of images annotated with codes for black female, black male, white female, white male. The threshold is set for each algorithm to give FMR = 0.001 for white males which is the demographic that usually gives the lowest FMR. This means the top right box is the same color in all panels. The panels are sorted over multiple pages in order of FMR on black females, which is the demographic that usually gives the highest FMR.

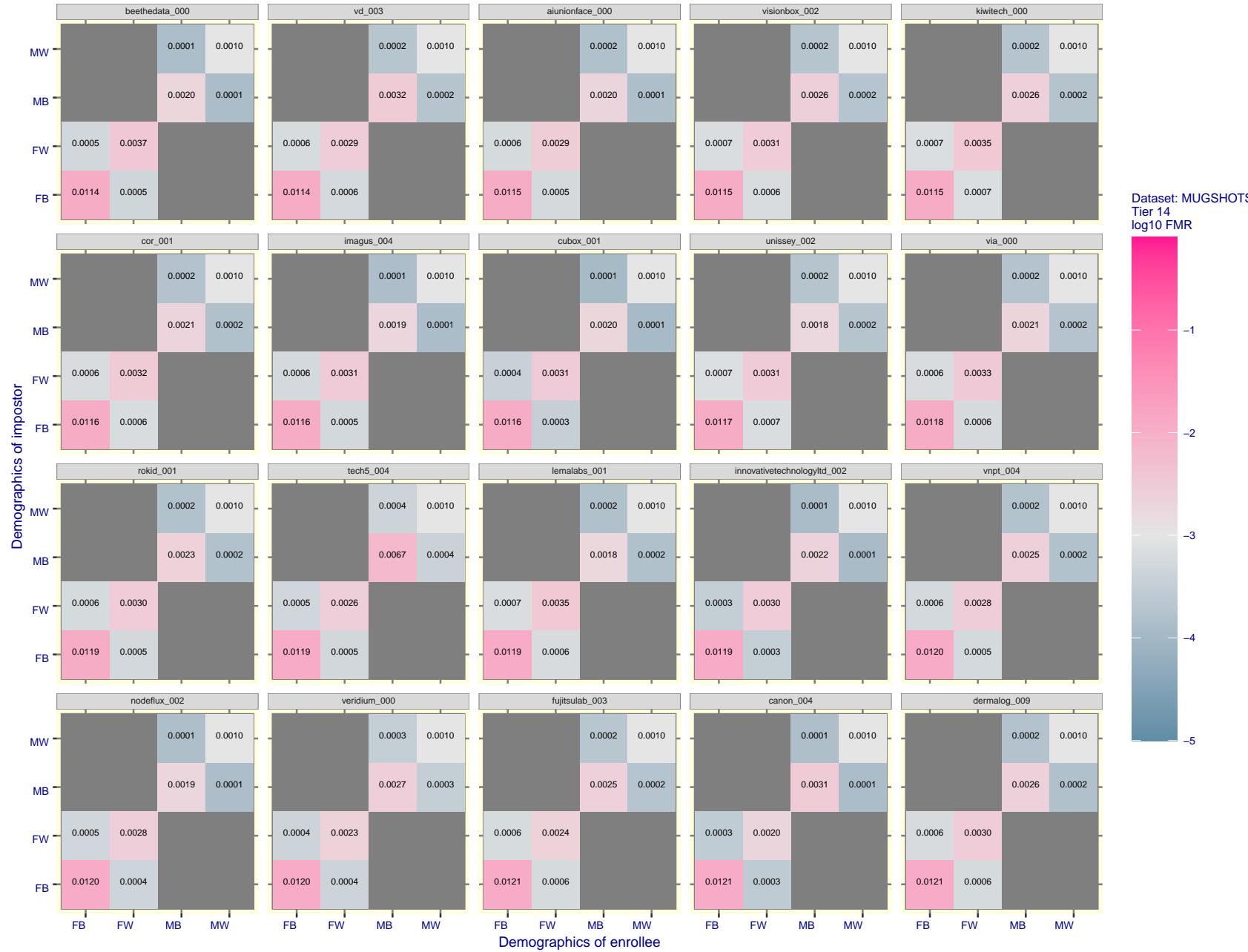


Figure 148: For the mugshot images, FMR for same-sex impostor pairs of images annotated with codes for black female, black male, white female, white male. The threshold is set for each algorithm to give FMR = 0.001 for white males which is the demographic that usually gives the lowest FMR. This means the top right box is the same color in all panels. The panels are sorted over multiple pages in order of FMR on black females, which is the demographic that usually gives the highest FMR.

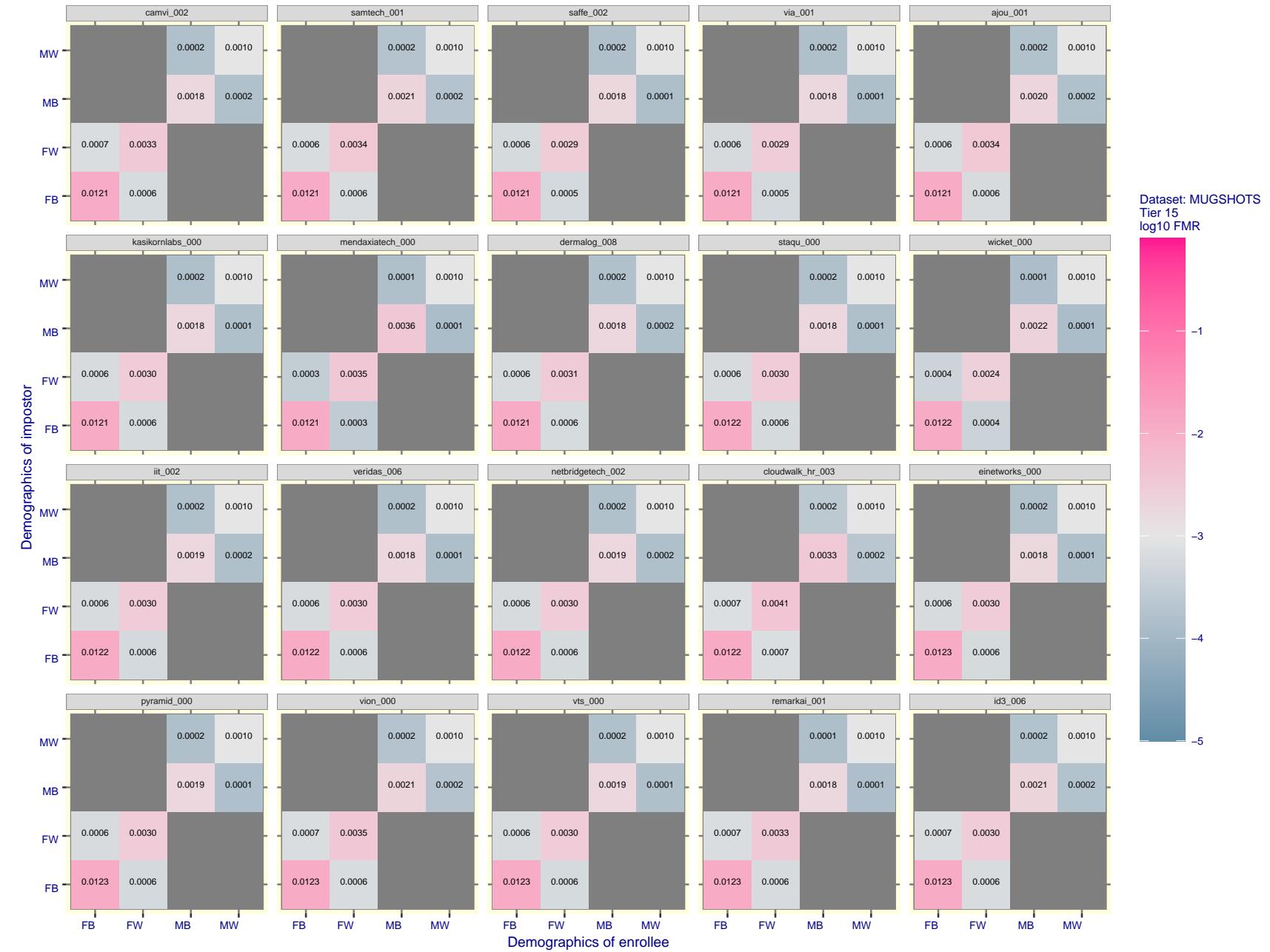


Figure 149: For the mugshot images, FMR for same-sex impostor pairs of images annotated with codes for black female, black male, white female, white male. The threshold is set for each algorithm to give FMR = 0.001 for white males which is the demographic that usually gives the lowest FMR. This means the top right box is the same color in all panels. The panels are sorted over multiple pages in order of FMR on black females, which is the demographic that usually gives the highest FMR.

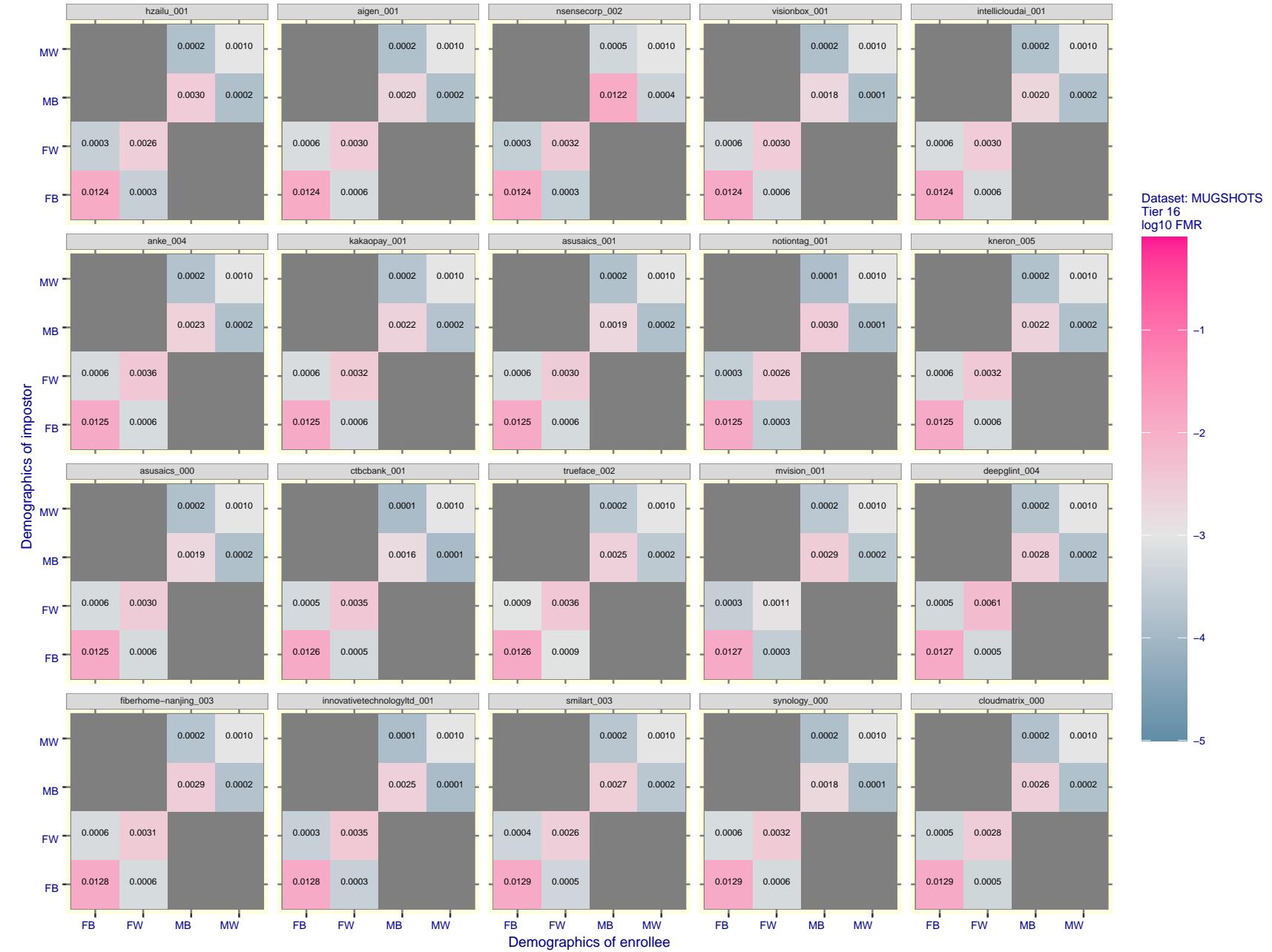


Figure 150: For the mugshot images, FMR for same-sex impostor pairs of images annotated with codes for black female, black male, white female, white male. The threshold is set for each algorithm to give $\text{FMR} = 0.001$ for white males which is the demographic that usually gives the lowest FMR. This means the top right box is the same color in all panels. The panels are sorted over multiple pages in order of FMR on black females, which is the demographic that usually gives the highest FMR.

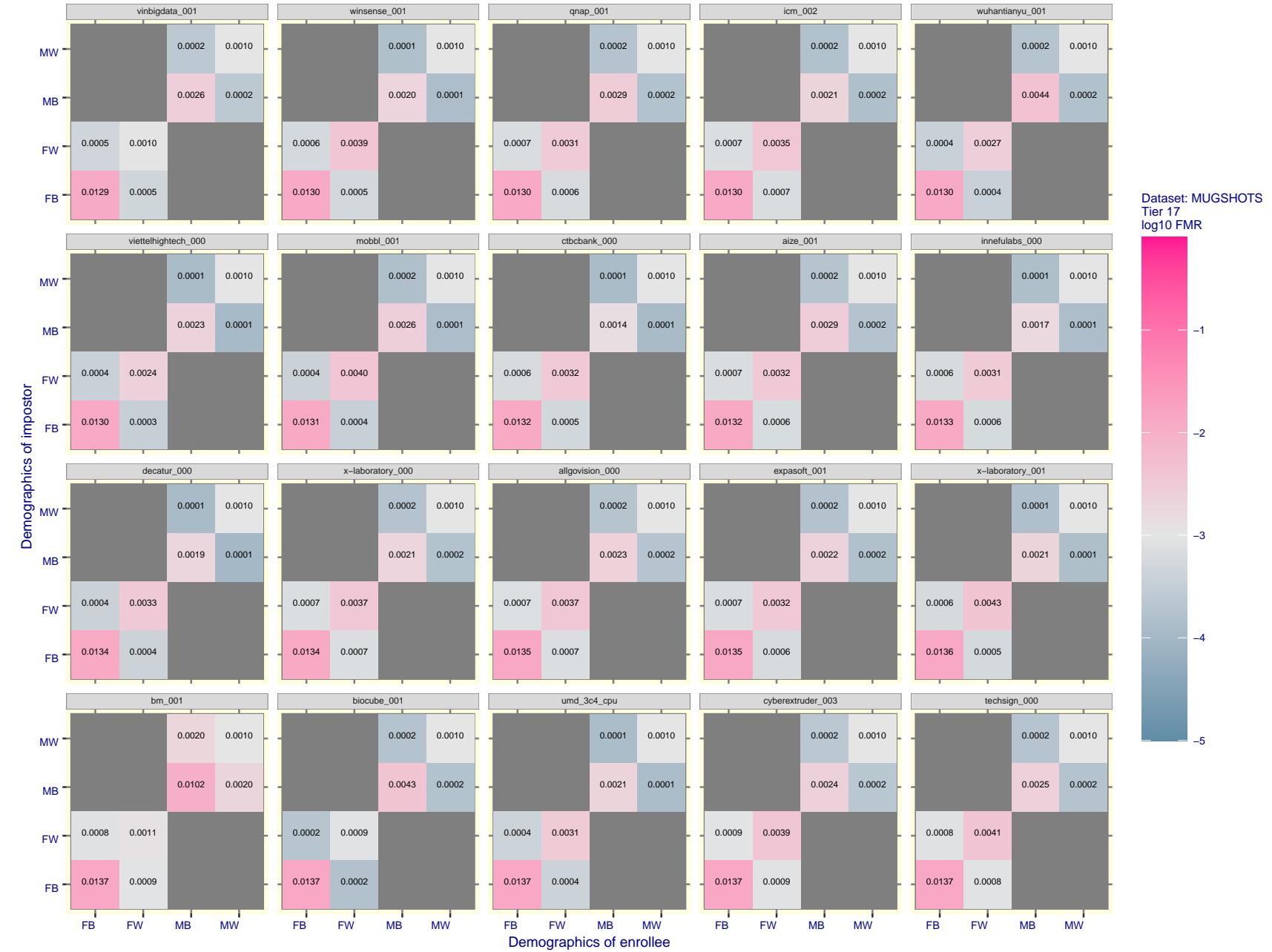


Figure 151: For the mugshot images, FMR for same-sex impostor pairs of images annotated with codes for black female, black male, white female, white male. The threshold is set for each algorithm to give $FMR = 0.001$ for white males which is the demographic that usually gives the lowest FMR. This means the top right box is the same color in all panels. The panels are sorted over multiple pages in order of FMR on black females, which is the demographic that usually gives the highest FMR.

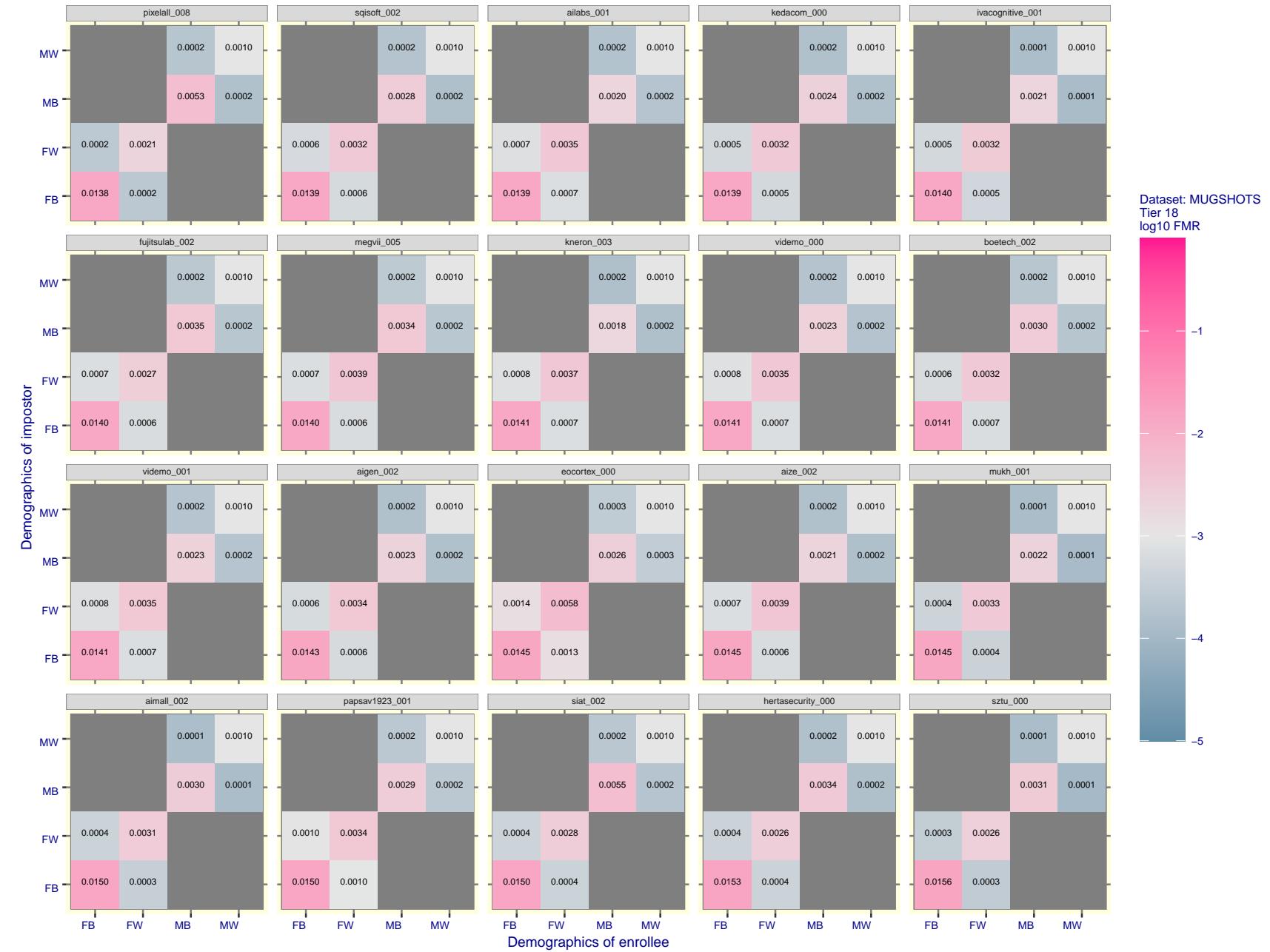


Figure 152: For the mugshot images, FMR for same-sex impostor pairs of images annotated with codes for black female, black male, white female, white male. The threshold is set for each algorithm to give $FMR = 0.001$ for white males which is the demographic that usually gives the lowest FMR. This means the top right box is the same color in all panels. The panels are sorted over multiple pages in order of FMR on black females, which is the demographic that usually gives the highest FMR.

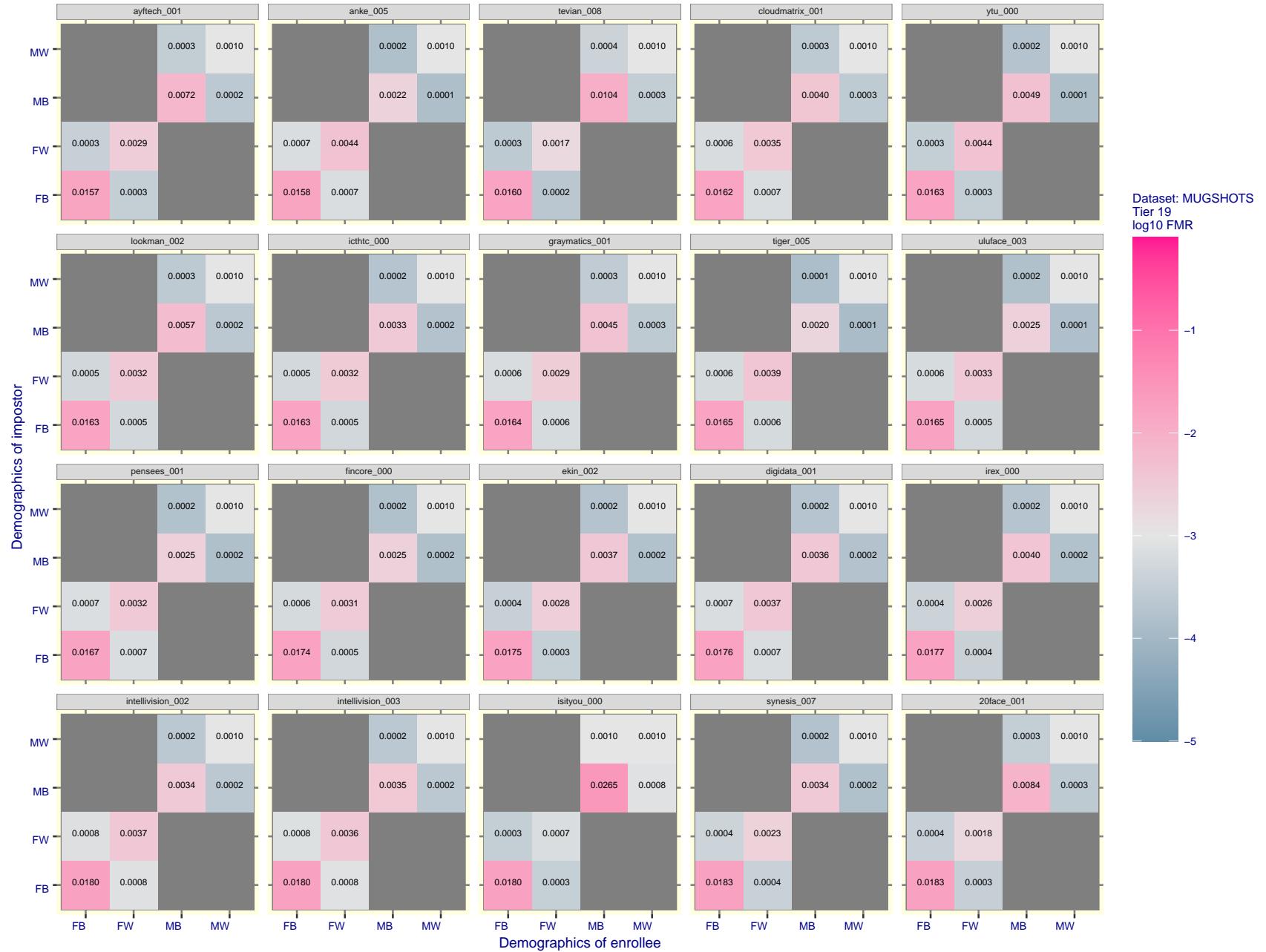


Figure 153: For the mugshot images, FMR for same-sex impostor pairs of images annotated with codes for black female, black male, white female, white male. The threshold is set for each algorithm to give $FMR = 0.001$ for white males which is the demographic that usually gives the lowest FMR. This means the top right box is the same color in all panels. The panels are sorted over multiple pages in order of FMR on black females, which is the demographic that usually gives the highest FMR.

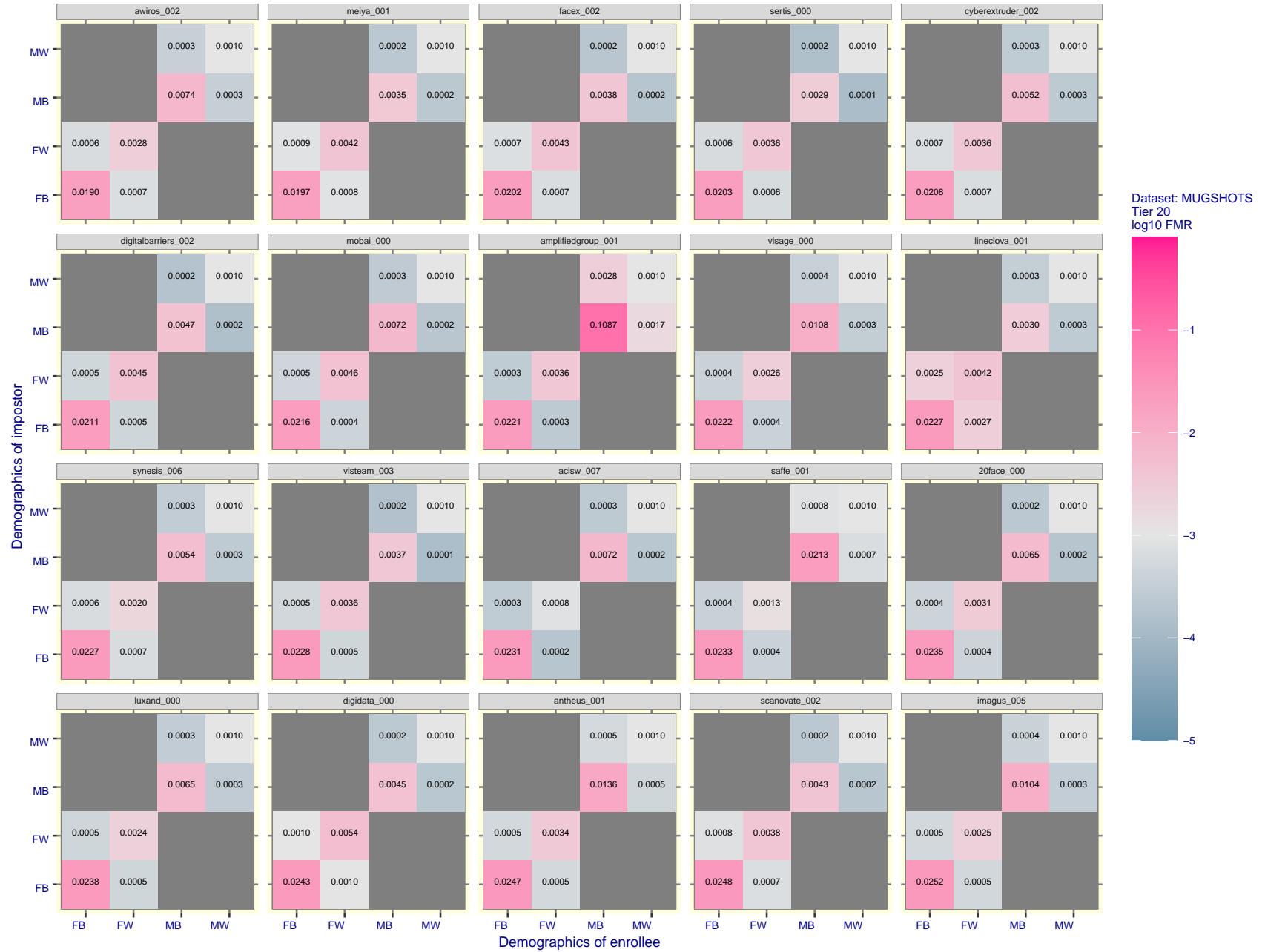


Figure 154: For the mugshot images, FMR for same-sex impostor pairs of images annotated with codes for black female, black male, white female, white male. The threshold is set for each algorithm to give FMR = 0.001 for white males which is the demographic that usually gives the lowest FMR. This means the top right box is the same color in all panels. The panels are sorted over multiple pages in order of FMR on black females, which is the demographic that usually gives the highest FMR.



Figure 155: For the mugshot images, FMR for same-sex impostor pairs of images annotated with codes for black female, black male, white female, white male. The threshold is set for each algorithm to give FMR = 0.001 for white males which is the demographic that usually gives the lowest FMR. This means the top right box is the same color in all panels. The panels are sorted over multiple pages in order of FMR on black females, which is the demographic that usually gives the highest FMR.

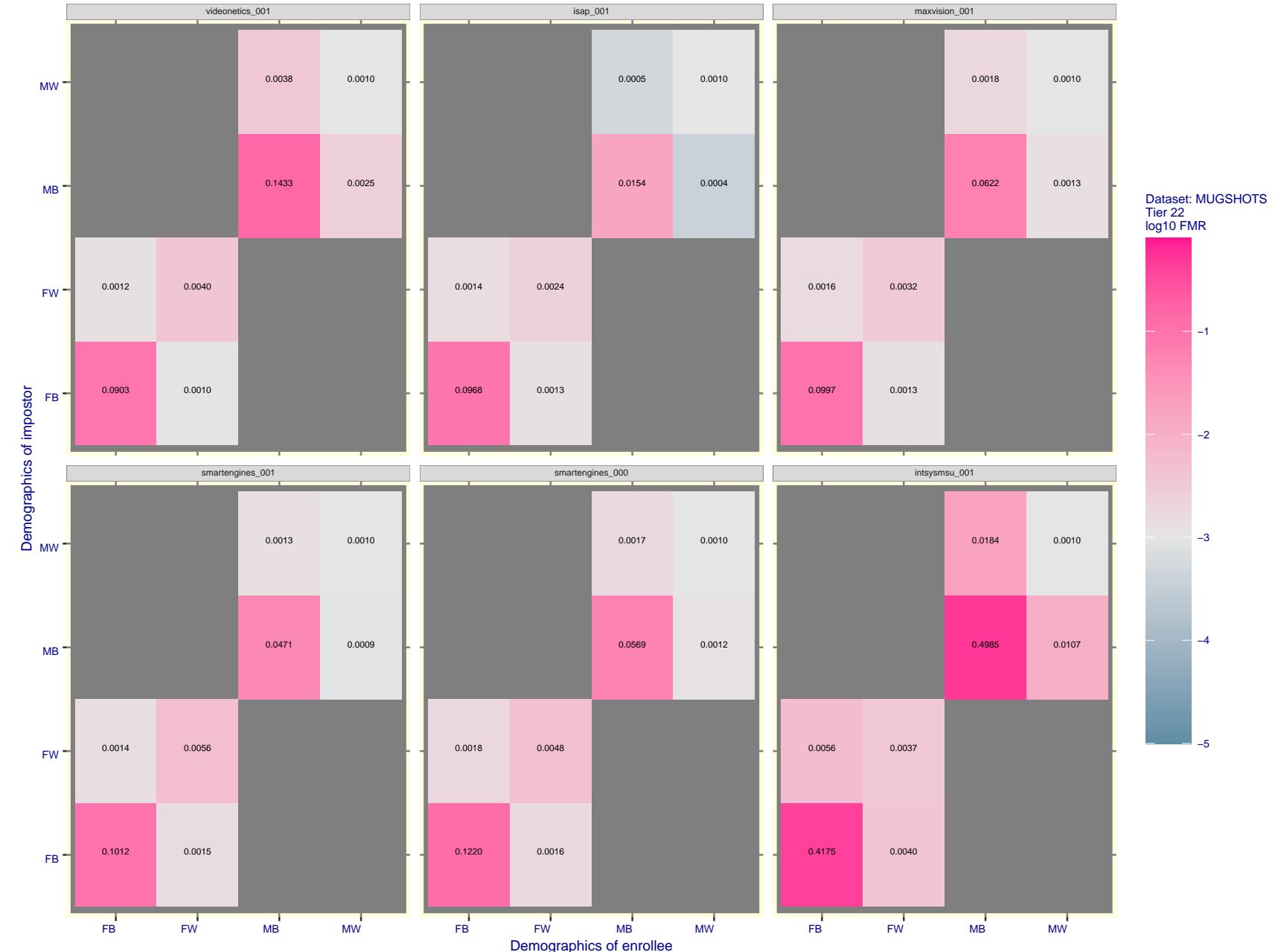


Figure 156: For the mugshot images, FMR for same-sex impostor pairs of images annotated with codes for black female, black male, white female, white male. The threshold is set for each algorithm to give $\text{FMR} = 0.001$ for white males which is the demographic that usually gives the lowest FMR. This means the top right box is the same color in all panels. The panels are sorted over multiple pages in order of FMR on black females, which is the demographic that usually gives the highest FMR.

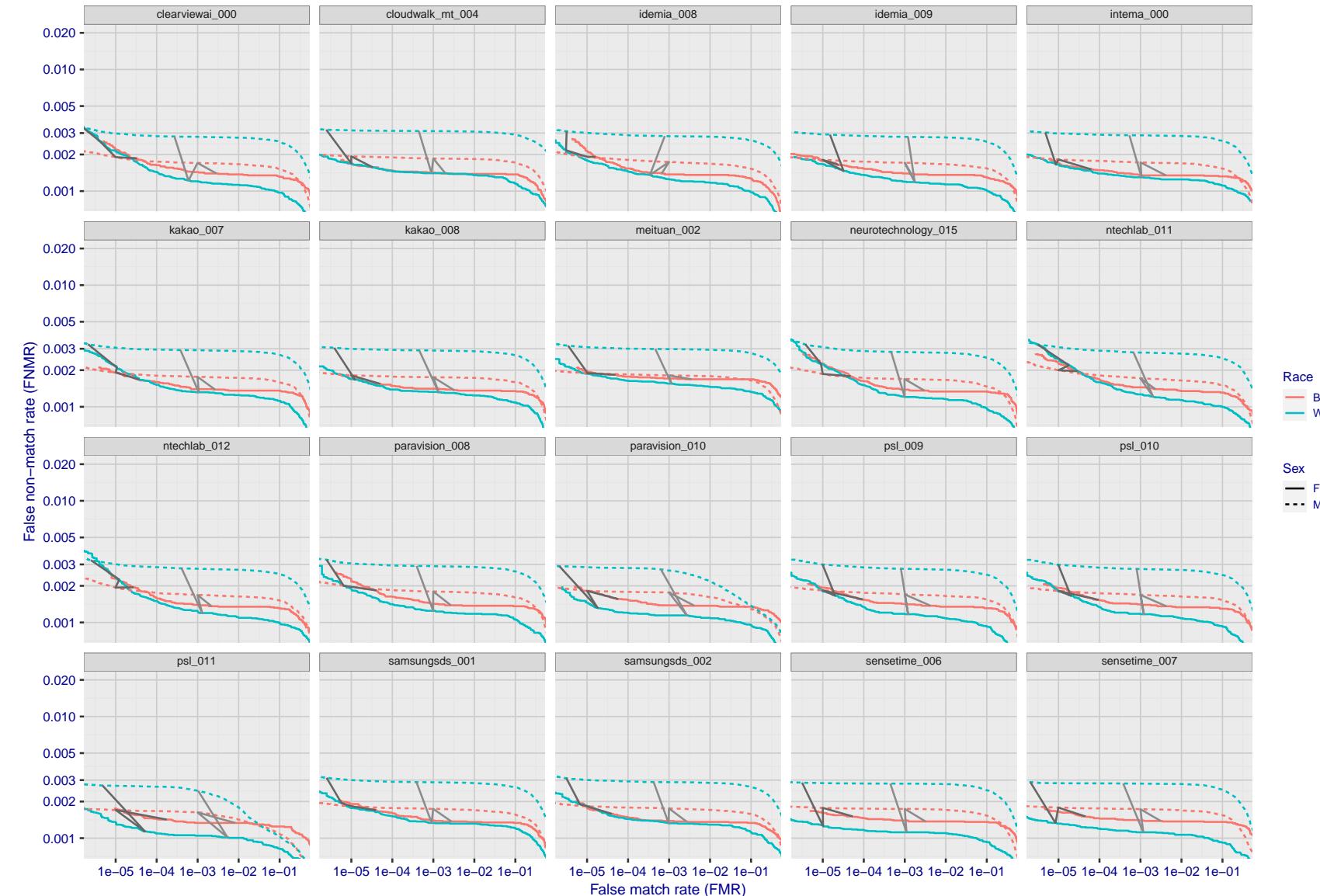


Figure 157: For the mugshot images, error tradeoff characteristics for white females, black females, black males and white males. The Z-shaped grey lines correspond to fixed thresholds, showing both FNMR and FMR vary at one T value. Note: Many of the plots will naively be read as saying women gives worse error rates than men because the solid traces lie above the dotted ones. However, this is misleading and incomplete: The grey lines show the traces reveal horizontal shifts. Thus for the cogent-003 algorithm FNMR for men is higher than for women at a fixed threshold but, at the same time, FMR is higher for women - see Figure 243. As access control systems almost always operate at a fixed threshold, the naive interpretation is incorrect.

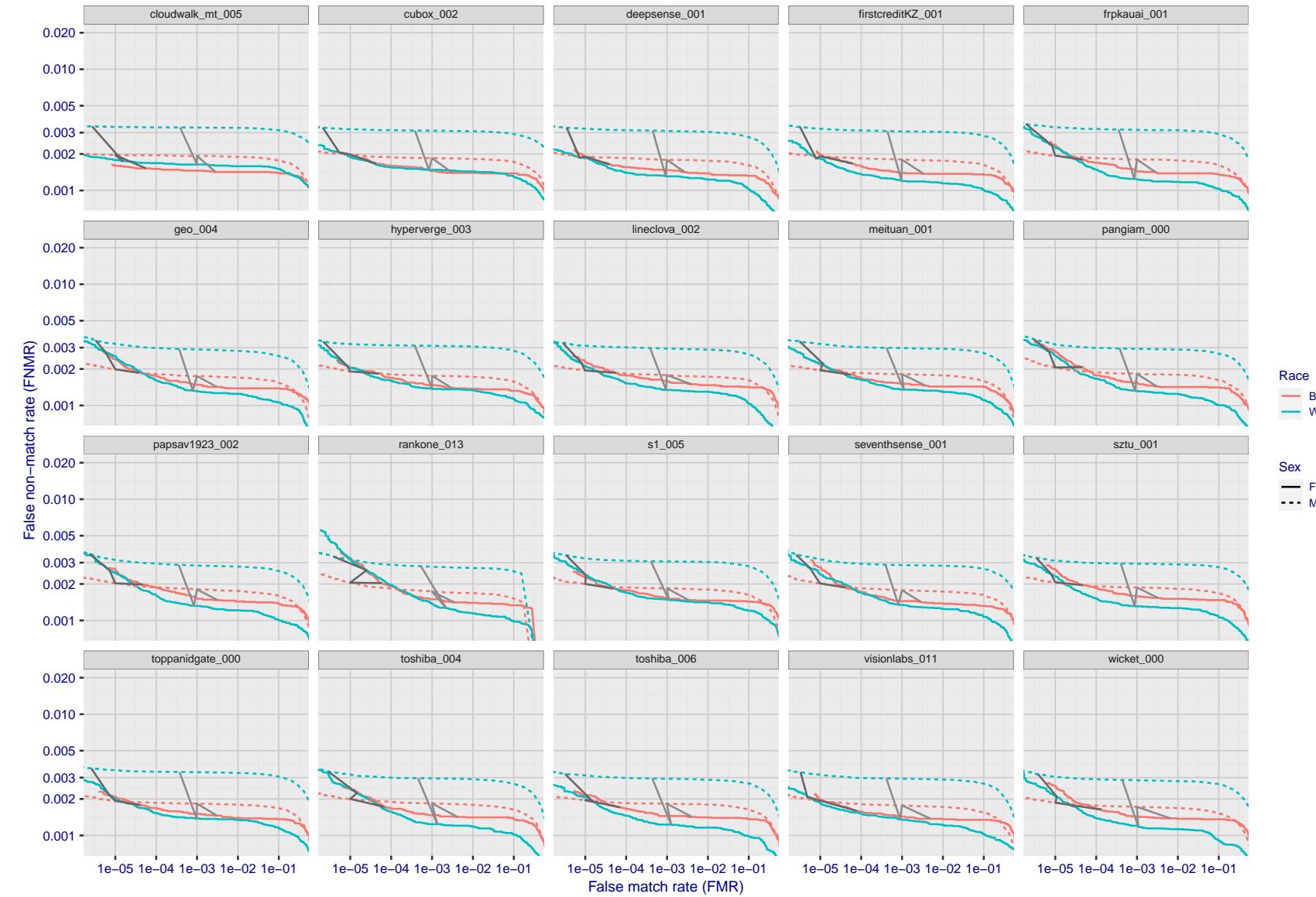


Figure 158: For the mugshot images, error tradeoff characteristics for white females, black females, black males and white males. The Z-shaped grey lines correspond to fixed thresholds, showing both FNMR and FMR vary at one T value. Note: Many of the plots will naively be read as saying women gives worse error rates than men because the solid traces lie above the dotted ones. However, this is misleading and incomplete: The grey lines show the traces reveal horizontal shifts. Thus for the cogent-003 algorithm FNMR for men is higher than for women at a fixed threshold but, at the same time, FMR is higher for women - see Figure 243. As access control systems almost always operate at a fixed threshold, the naive interpretation is incorrect.

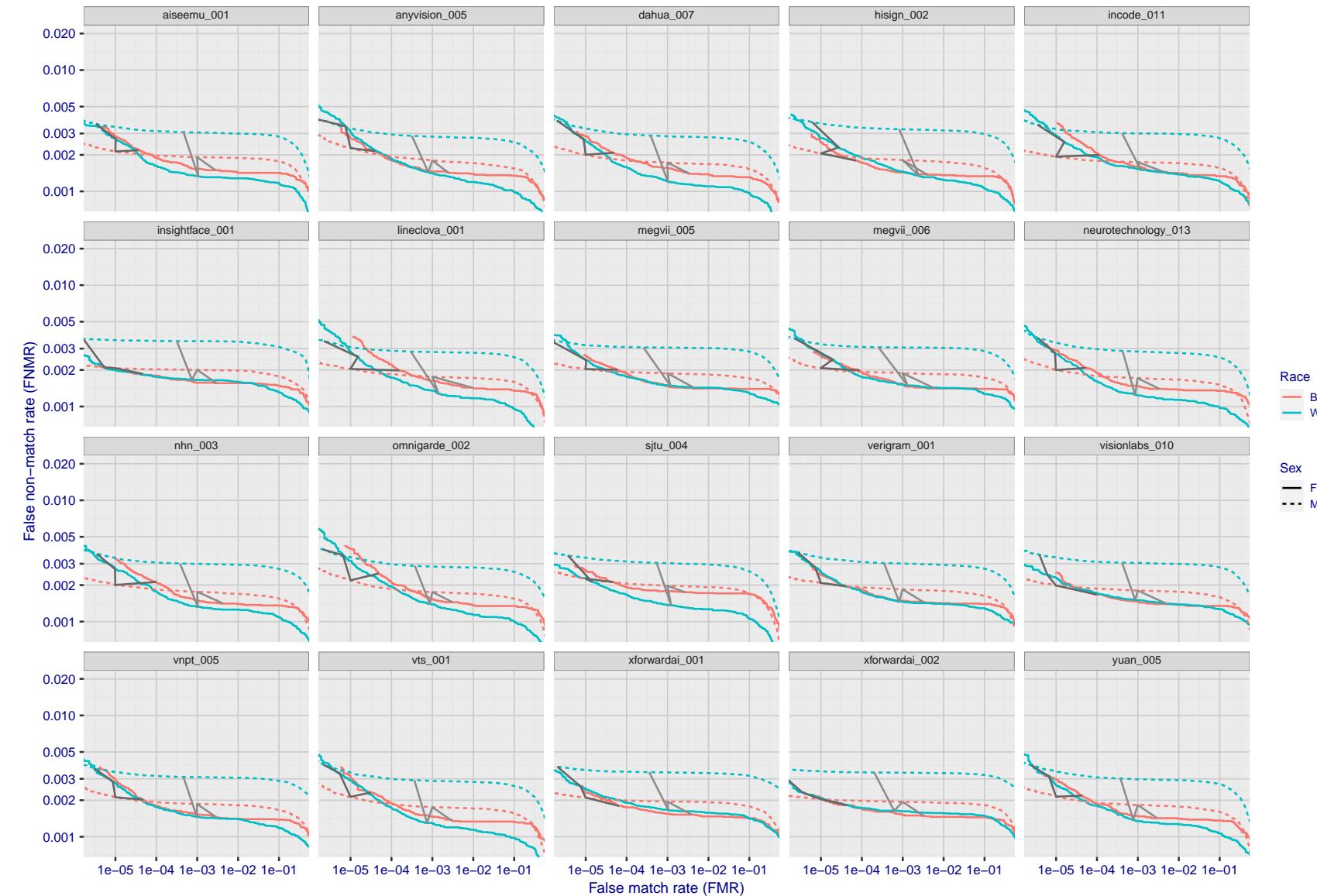


Figure 159: For the mugshot images, error tradeoff characteristics for white females, black females, black males and white males. The Z-shaped grey lines correspond to fixed thresholds, showing both FNMR and FMR vary at one T value. Note: Many of the plots will naively be read as saying women gives worse error rates than men because the solid traces lie above the dotted ones. However, this is misleading and incomplete: The grey lines show the traces reveal horizontal shifts. Thus for the cogent-003 algorithm FNMR for men is higher than for women at a fixed threshold but, at the same time, FMR is higher for women - see Figure 243. As access control systems almost always operate at a fixed threshold, the naive interpretation is incorrect.

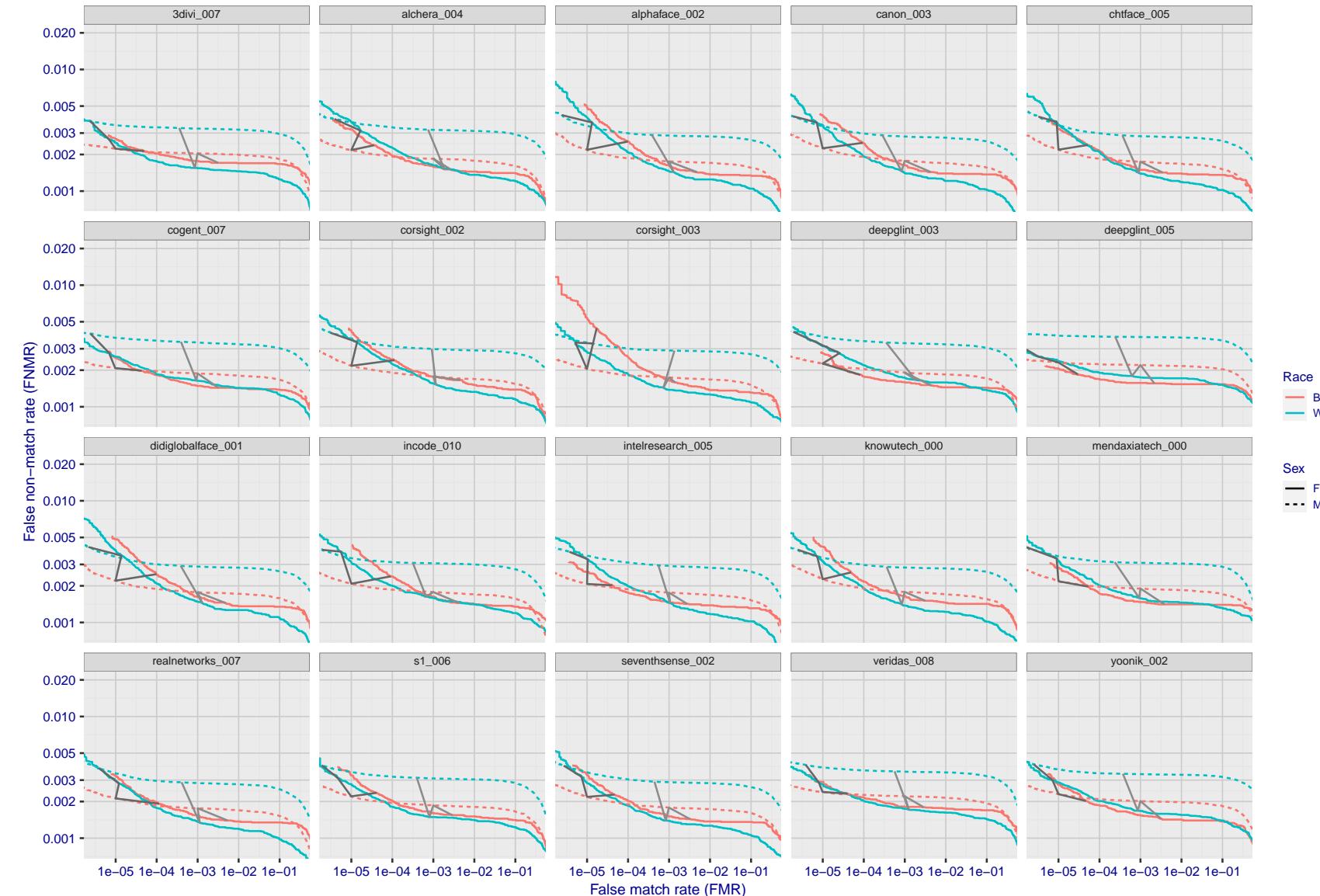


Figure 160: For the mugshot images, error tradeoff characteristics for white females, black females, black males and white males. The Z-shaped grey lines correspond to fixed thresholds, showing both FNMR and FMR vary at one T value. Note: Many of the plots will naively be read as saying women gives worse error rates than men because the solid traces lie above the dotted ones. However, this is misleading and incomplete: The grey lines show the traces reveal horizontal shifts. Thus for the cogent-003 algorithm FNMR for men is higher than for women at a fixed threshold but, at the same time, FMR is higher for women - see Figure 243. As access control systems almost always operate at a fixed threshold, the naive interpretation is incorrect.

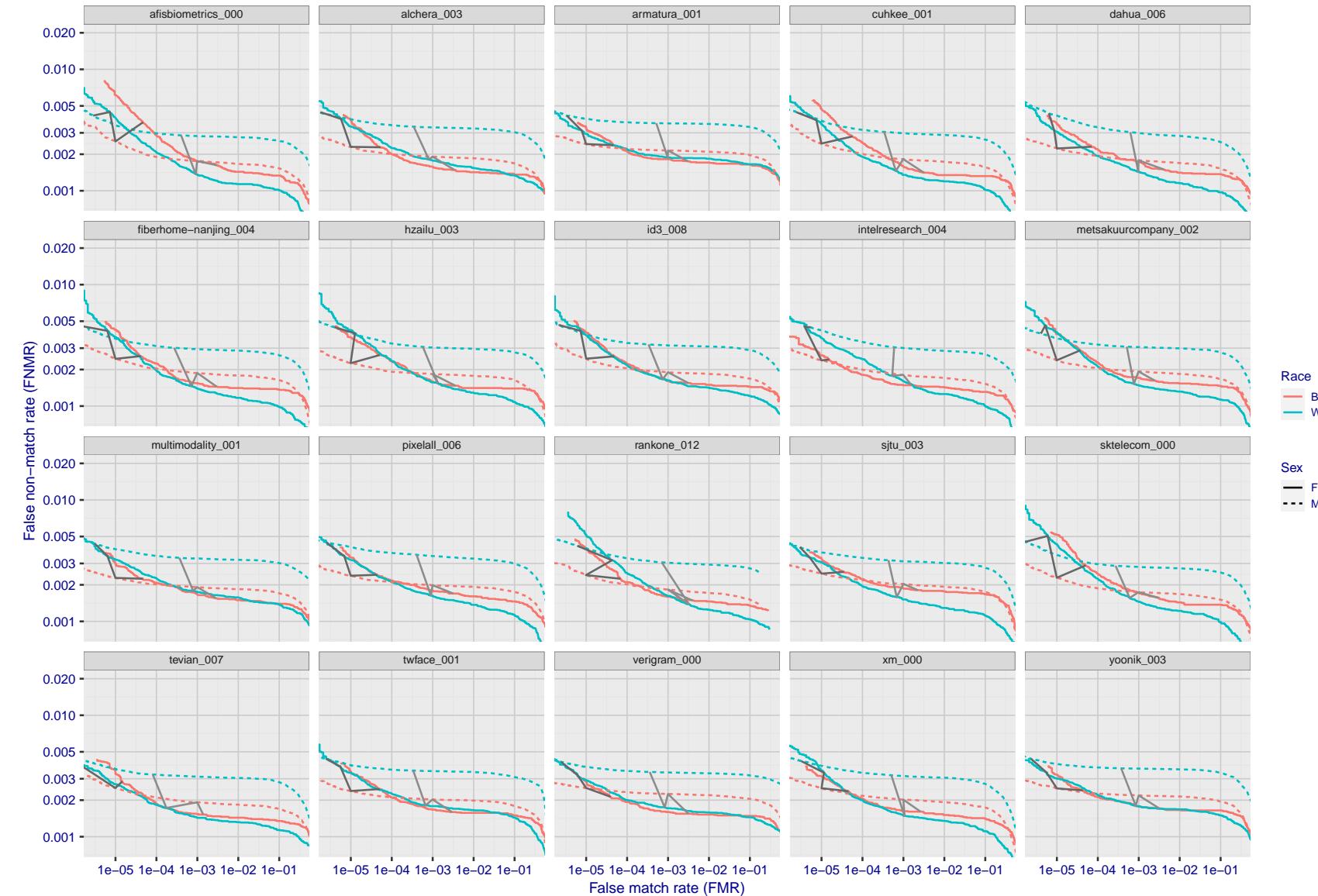


Figure 161: For the mugshot images, error tradeoff characteristics for white females, black females, black males and white males. The Z-shaped grey lines correspond to fixed thresholds, showing both FNMR and FMR vary at one T value. Note: Many of the plots will naively be read as saying women gives worse error rates than men because the solid traces lie above the dotted ones. However, this is misleading and incomplete: The grey lines show the traces reveal horizontal shifts. Thus for the cogent-003 algorithm FNMR for men is higher than for women at a fixed threshold but, at the same time, FMR is higher for women - see Figure 243. As access control systems almost always operate at a fixed threshold, the naive interpretation is incorrect.

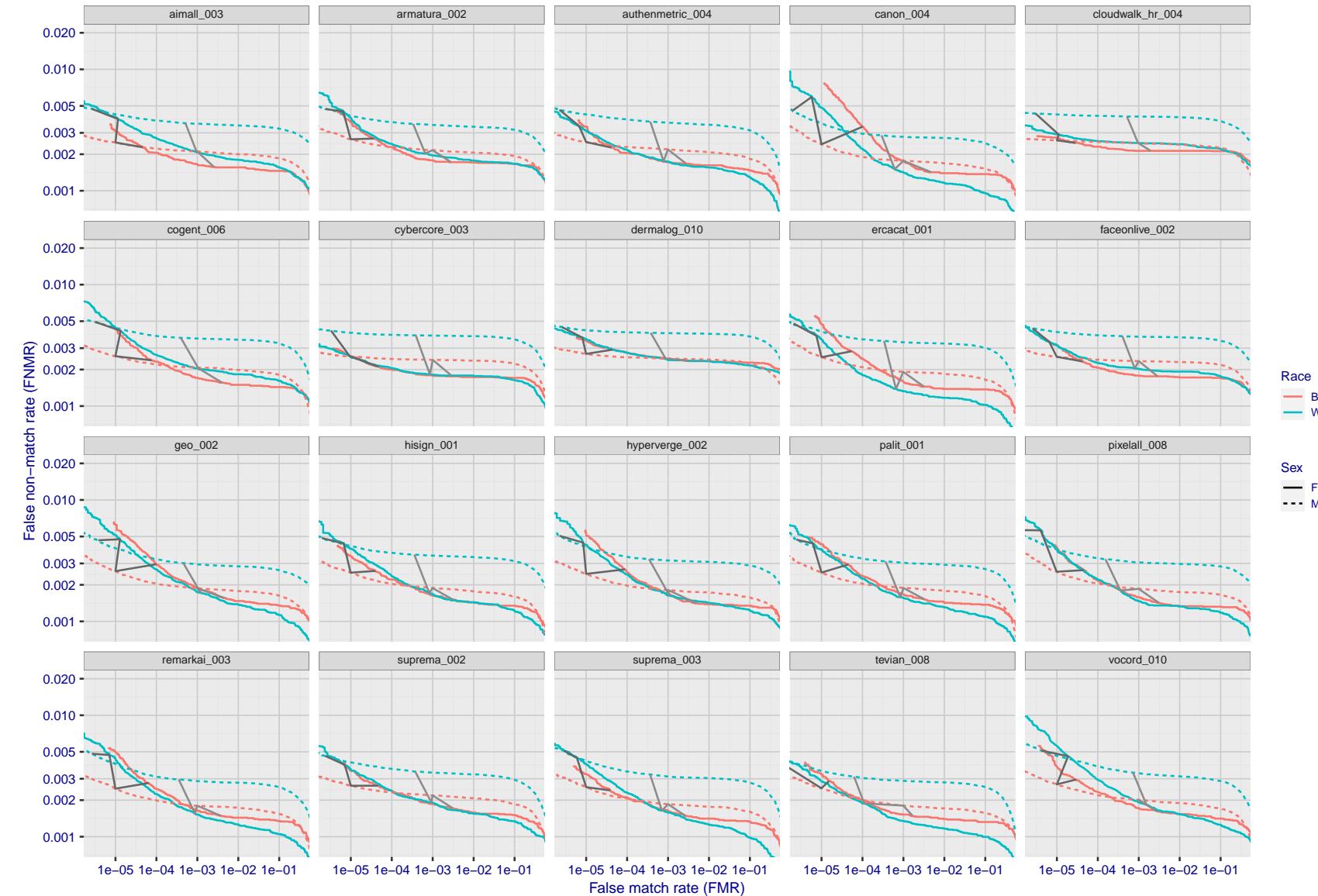


Figure 162: For the mugshot images, error tradeoff characteristics for white females, black females, black males and white males. The Z-shaped grey lines correspond to fixed thresholds, showing both FNMR and FMR vary at one T value. Note: Many of the plots will naively be read as saying women gives worse error rates than men because the solid traces lie above the dotted ones. However, this is misleading and incomplete: The grey lines show the traces reveal horizontal shifts. Thus for the cogent-003 algorithm FNMR for men is higher than for women at a fixed threshold but, at the same time, FMR is higher for women - see Figure 243. As access control systems almost always operate at a fixed threshold, the naive interpretation is incorrect.

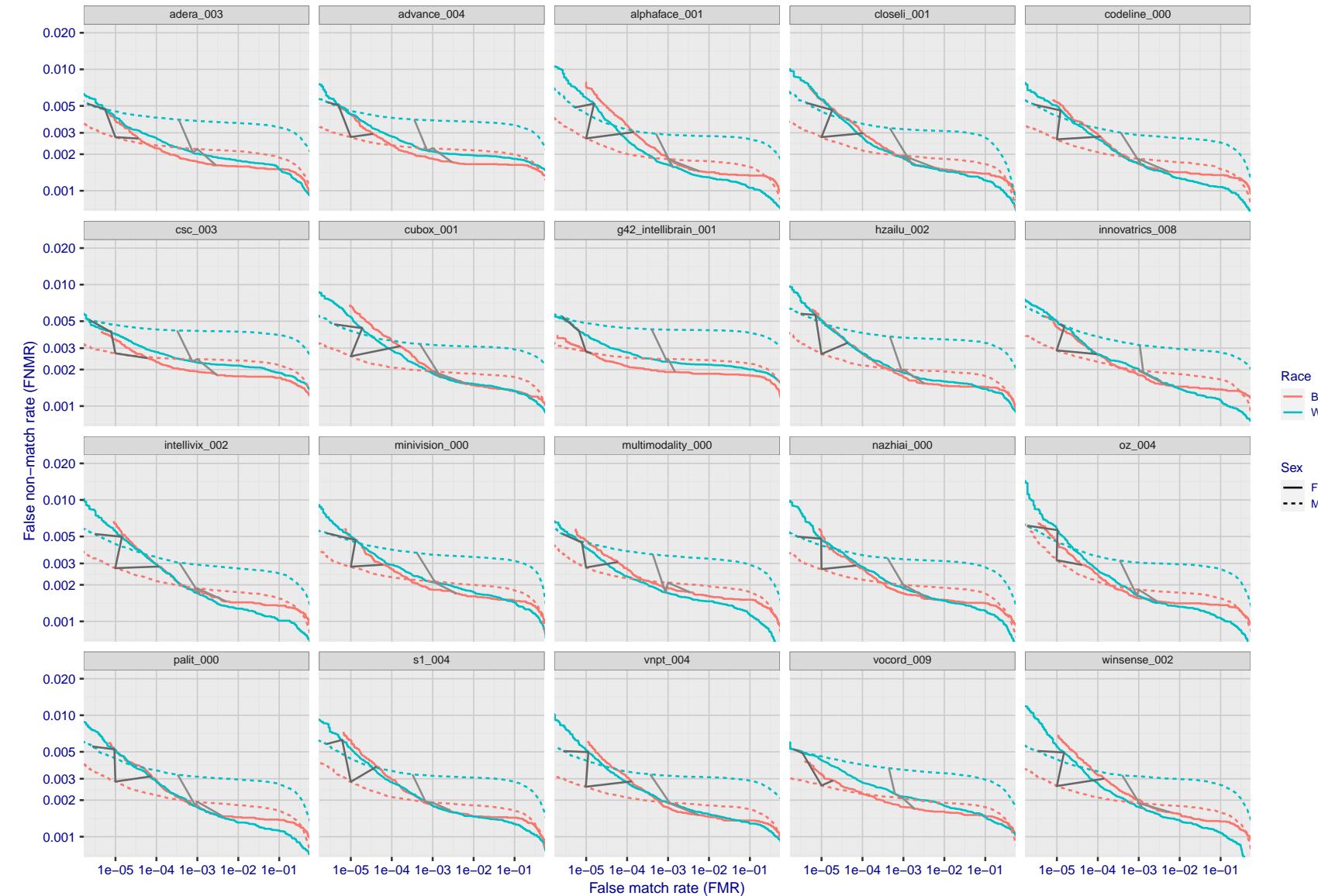


Figure 163: For the mugshot images, error tradeoff characteristics for white females, black females, black males and white males. The Z-shaped grey lines correspond to fixed thresholds, showing both FNMR and FMR vary at one T value. Note: Many of the plots will naively be read as saying women gives worse error rates than men because the solid traces lie above the dotted ones. However, this is misleading and incomplete: The grey lines show the traces reveal horizontal shifts. Thus for the cogent-003 algorithm FNMR for men is higher than for women at a fixed threshold but, at the same time, FMR is higher for women - see Figure 243. As access control systems almost always operate at a fixed threshold, the naive interpretation is incorrect.

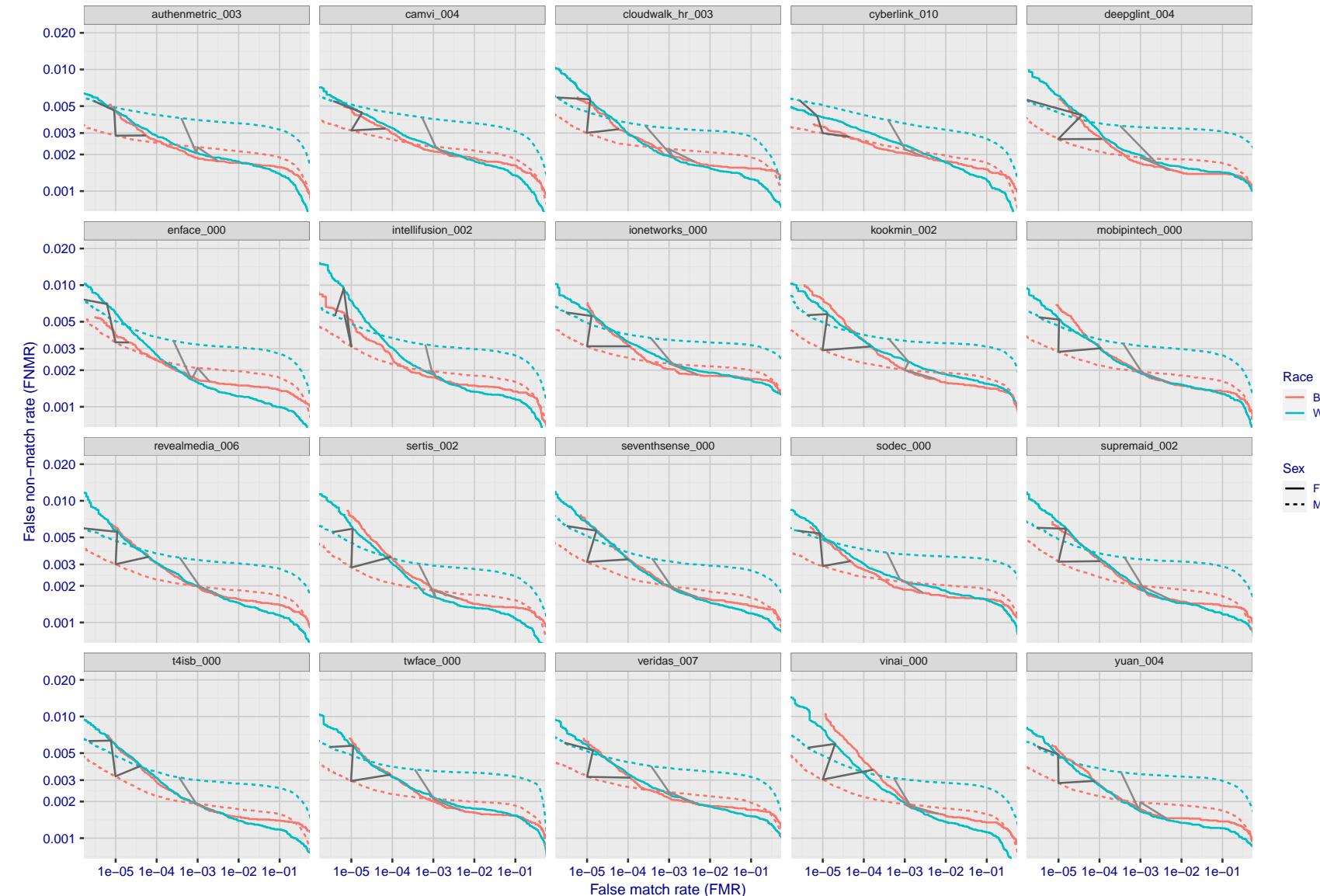


Figure 164: For the mugshot images, error tradeoff characteristics for white females, black females, black males and white males. The Z-shaped grey lines correspond to fixed thresholds, showing both FNMR and FMR vary at one T value. Note: Many of the plots will naively be read as saying women gives worse error rates than men because the solid traces lie above the dotted ones. However, this is misleading and incomplete: The grey lines show the traces reveal horizontal shifts. Thus for the cogent-003 algorithm FNMR for men is higher than for women at a fixed threshold but, at the same time, FMR is higher for women - see Figure 243. As access control systems almost always operate at a fixed threshold, the naive interpretation is incorrect.

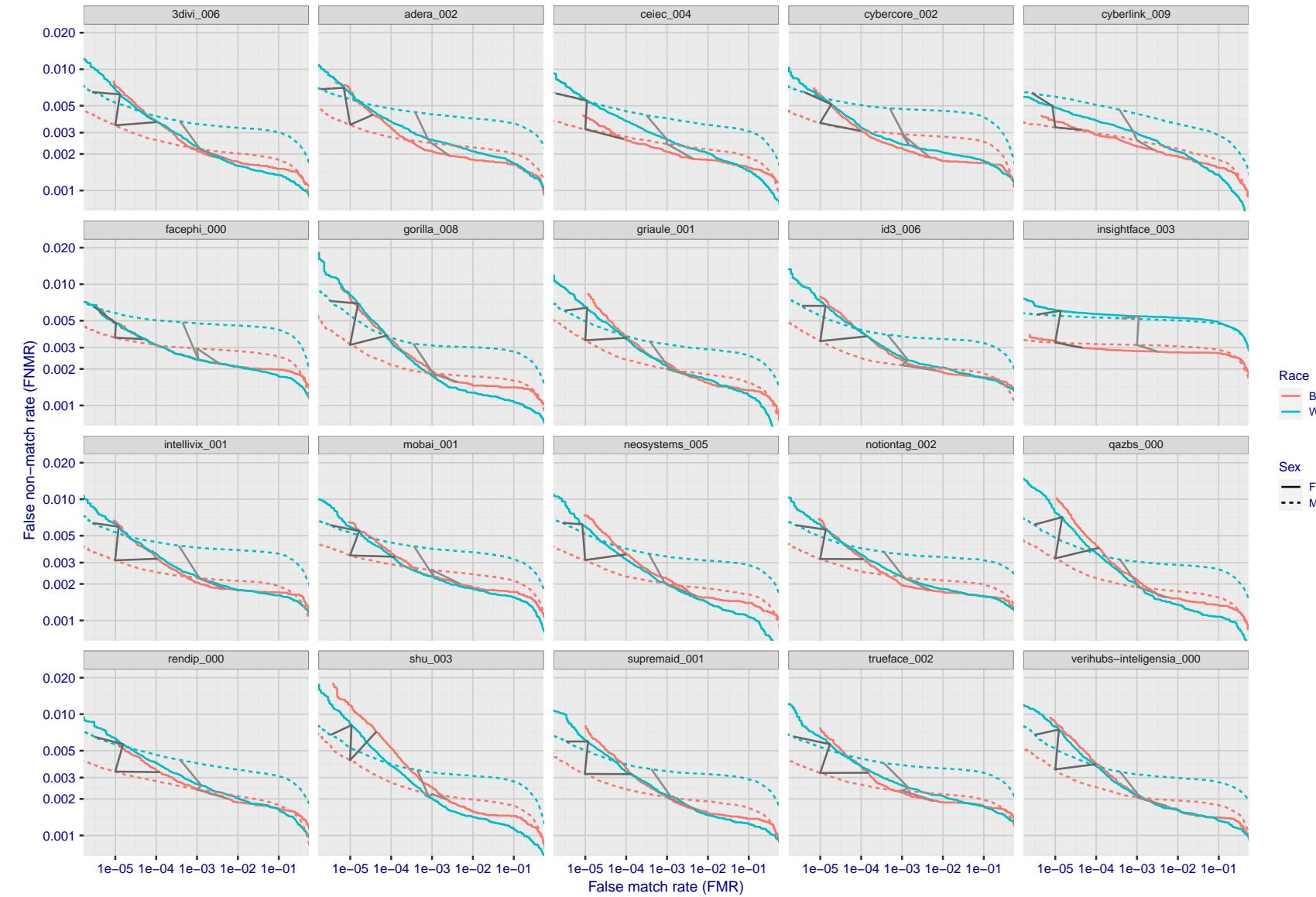


Figure 165: For the mugshot images, error tradeoff characteristics for white females, black females, black males and white males. The Z-shaped grey lines correspond to fixed thresholds, showing both FNMR and FMR vary at one T value. Note: Many of the plots will naively be read as saying women gives worse error rates than men because the solid traces lie above the dotted ones. However, this is misleading and incomplete: The grey lines show the traces reveal horizontal shifts. Thus for the cogent-003 algorithm FNMR for men is higher than for women at a fixed threshold but, at the same time, FMR is higher for women - see Figure 243. As access control systems almost always operate at a fixed threshold, the naive interpretation is incorrect.

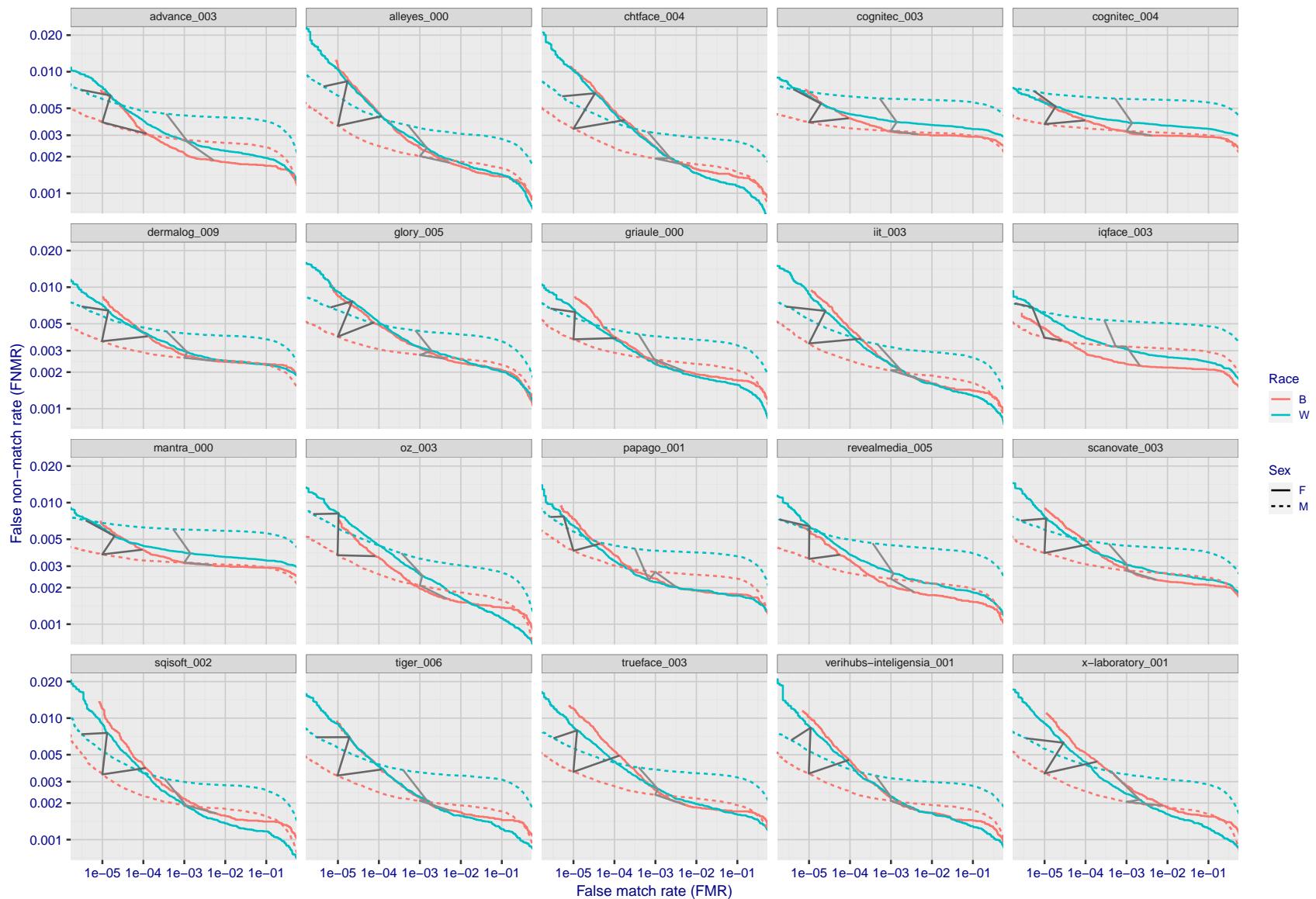


Figure 166: For the mugshot images, error tradeoff characteristics for white females, black females, black males and white males. The Z-shaped grey lines correspond to fixed thresholds, showing both FNMR and FMR vary at one T value. Note: Many of the plots will naively be read as saying women gives worse error rates than men because the solid traces lie above the dotted ones. However, this is misleading and incomplete: The grey lines show the traces reveal horizontal shifts. Thus for the cogent-003 algorithm FNMR for men is higher than for women at a fixed threshold but, at the same time, FMR is higher for women - see Figure 243. As access control systems almost always operate at a fixed threshold, the naive interpretation is incorrect.

2023/02/09 20:10:38

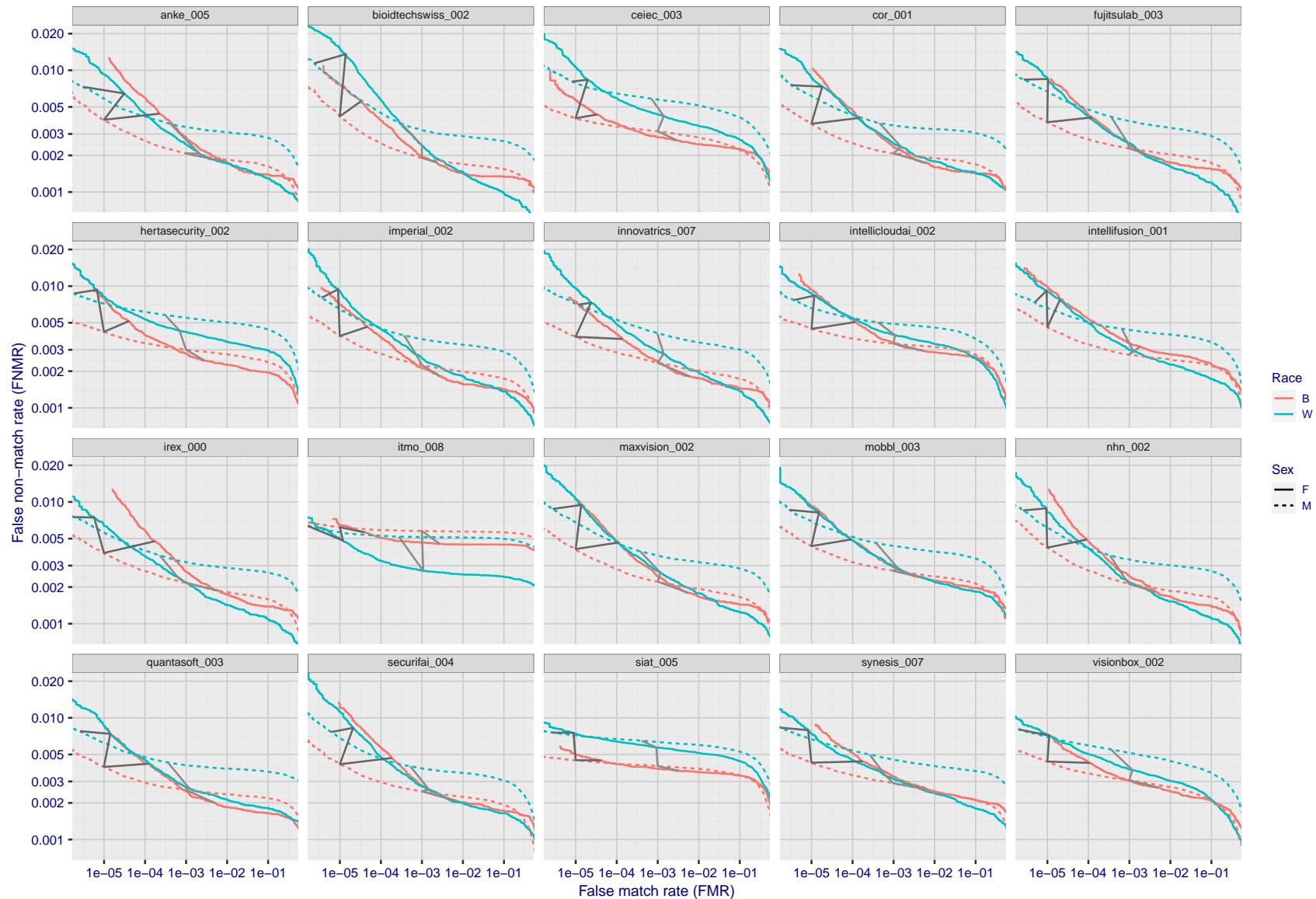


Figure 167: For the mugshot images, error tradeoff characteristics for white females, black females, black males and white males. The Z-shaped grey lines correspond to fixed thresholds, showing both FNMR and FMR vary at one T value. Note: Many of the plots will naively be read as saying women gives worse error rates than men because the solid traces lie above the dotted ones. However, this is misleading and incomplete: The grey lines show the traces reveal horizontal shifts. Thus for the cogent-003 algorithm FNMR for men is higher than for women at a fixed threshold but, at the same time, FMR is higher for women - see Figure 243. As access control systems almost always operate at a fixed threshold, the naive interpretation is incorrect.

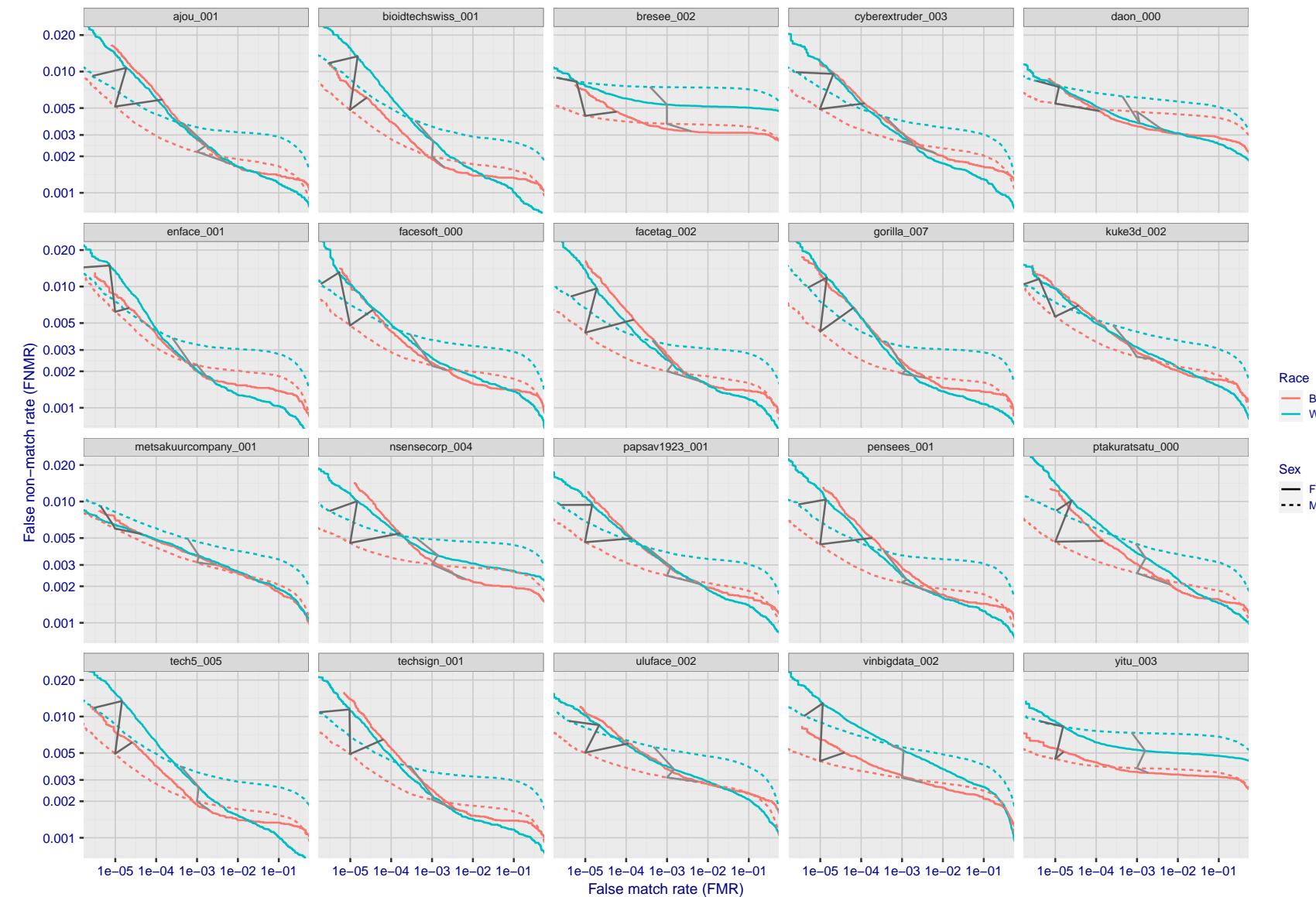


Figure 168: For the mugshot images, error tradeoff characteristics for white females, black females, black males and white males. The Z-shaped grey lines correspond to fixed thresholds, showing both FNMR and FMR vary at one T value. Note: Many of the plots will naively be read as saying women gives worse error rates than men because the solid traces lie above the dotted ones. However, this is misleading and incomplete: The grey lines show the traces reveal horizontal shifts. Thus for the cogent-003 algorithm FNMR for men is higher than for women at a fixed threshold but, at the same time, FMR is higher for women - see Figure 243. As access control systems almost always operate at a fixed threshold, the naive interpretation is incorrect.

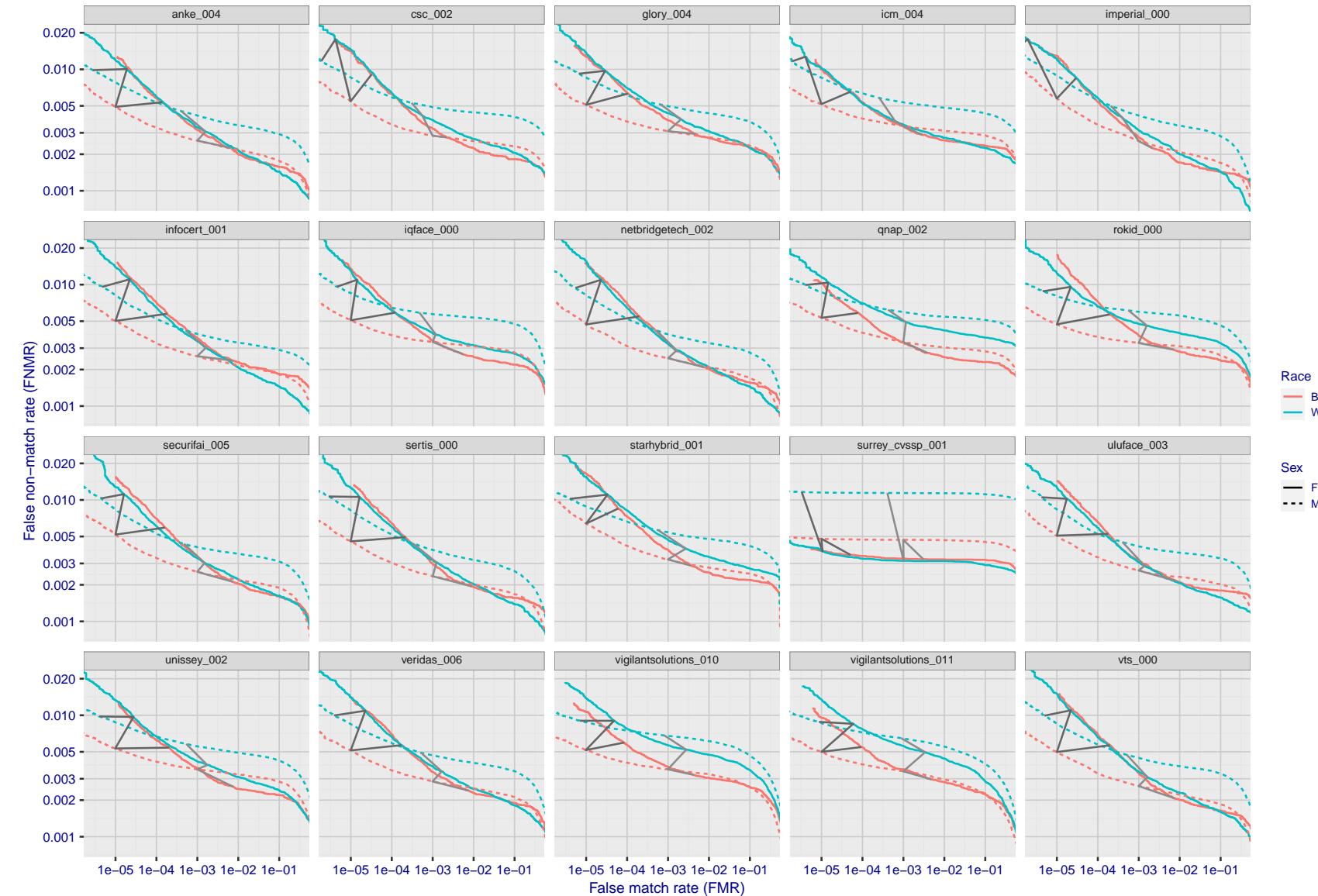


Figure 169: For the mugshot images, error tradeoff characteristics for white females, black females, black males and white males. The Z-shaped grey lines correspond to fixed thresholds, showing both FNMR and FMR vary at one T value. Note: Many of the plots will naively be read as saying women gives worse error rates than men because the solid traces lie above the dotted ones. However, this is misleading and incomplete: The grey lines show the traces reveal horizontal shifts. Thus for the cogent-003 algorithm FNMR for men is higher than for women at a fixed threshold but, at the same time, FMR is higher for women - see Figure 243. As access control systems almost always operate at a fixed threshold, the naive interpretation is incorrect.

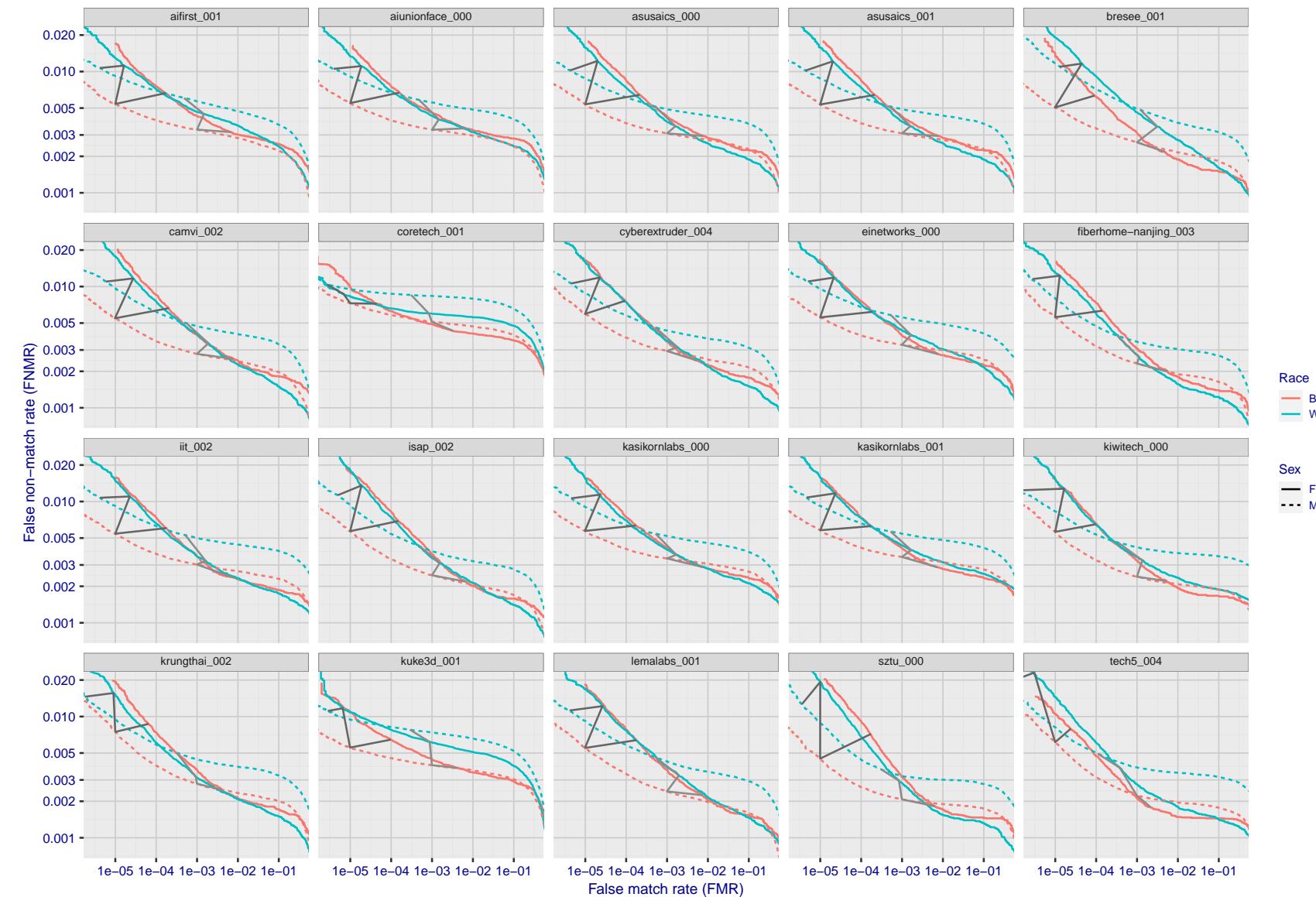


Figure 170: For the mugshot images, error tradeoff characteristics for white females, black females, black males and white males. The Z-shaped grey lines correspond to fixed thresholds, showing both FNMR and FMR vary at one T value. Note: Many of the plots will naively be read as saying women gives worse error rates than men because the solid traces lie above the dotted ones. However, this is misleading and incomplete: The grey lines show the traces reveal horizontal shifts. Thus for the cogent-003 algorithm FNMR for men is higher than for women at a fixed threshold but, at the same time, FMR is higher for women - see Figure 243. As access control systems almost always operate at a fixed threshold, the naive interpretation is incorrect.

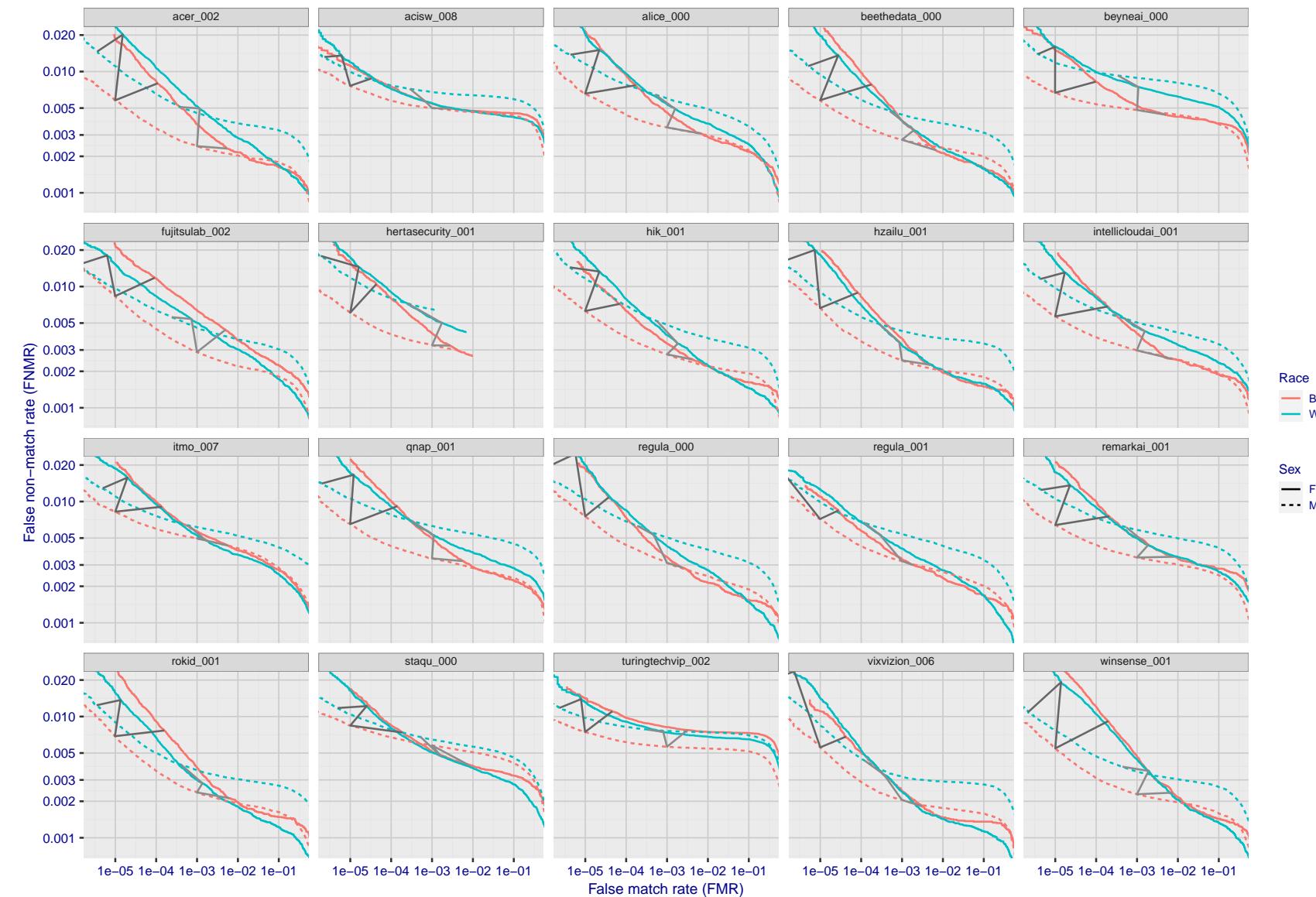


Figure 171: For the mugshot images, error tradeoff characteristics for white females, black females, black males and white males. The Z-shaped grey lines correspond to fixed thresholds, showing both FNMR and FMR vary at one T value. Note: Many of the plots will naively be read as saying women gives worse error rates than men because the solid traces lie above the dotted ones. However, this is misleading and incomplete: The grey lines show the traces reveal horizontal shifts. Thus for the cogent-003 algorithm FNMR for men is higher than for women at a fixed threshold but, at the same time, FMR is higher for women - see Figure 243. As access control systems almost always operate at a fixed threshold, the naive interpretation is incorrect.

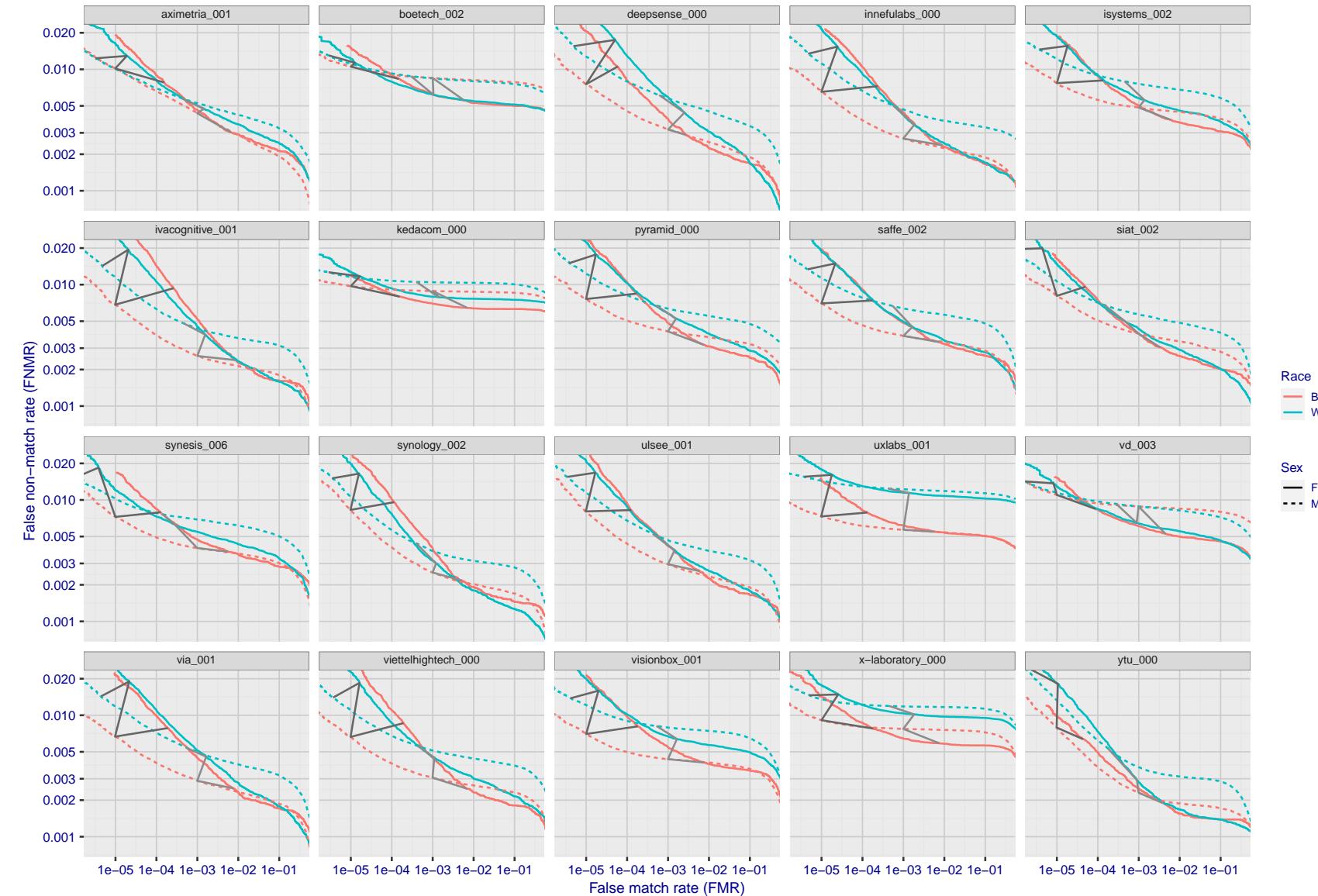


Figure 172: For the mugshot images, error tradeoff characteristics for white females, black females, black males and white males. The Z-shaped grey lines correspond to fixed thresholds, showing both FNMR and FMR vary at one T value. Note: Many of the plots will naively be read as saying women gives worse error rates than men because the solid traces lie above the dotted ones. However, this is misleading and incomplete: The grey lines show the traces reveal horizontal shifts. Thus for the cogent-003 algorithm FNMR for men is higher than for women at a fixed threshold but, at the same time, FMR is higher for women - see Figure 243. As access control systems almost always operate at a fixed threshold, the naive interpretation is incorrect.

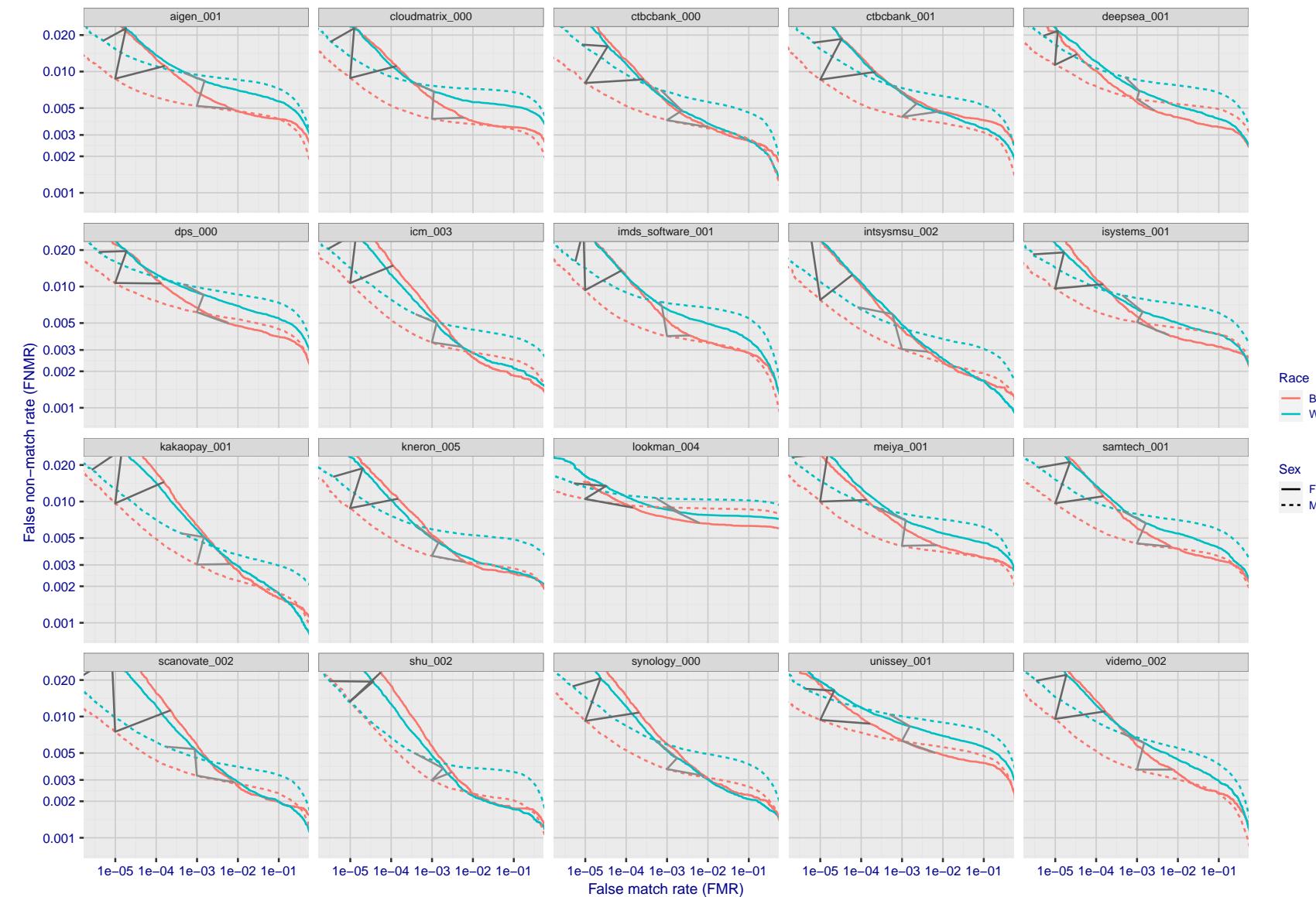


Figure 173: For the mugshot images, error tradeoff characteristics for white females, black females, black males and white males. The Z-shaped grey lines correspond to fixed thresholds, showing both FNMR and FMR vary at one T value. Note: Many of the plots will naively be read as saying women gives worse error rates than men because the solid traces lie above the dotted ones. However, this is misleading and incomplete: The grey lines show the traces reveal horizontal shifts. Thus for the cogent-003 algorithm FNMR for men is higher than for women at a fixed threshold but, at the same time, FMR is higher for women - see Figure 243. As access control systems almost always operate at a fixed threshold, the naive interpretation is incorrect.

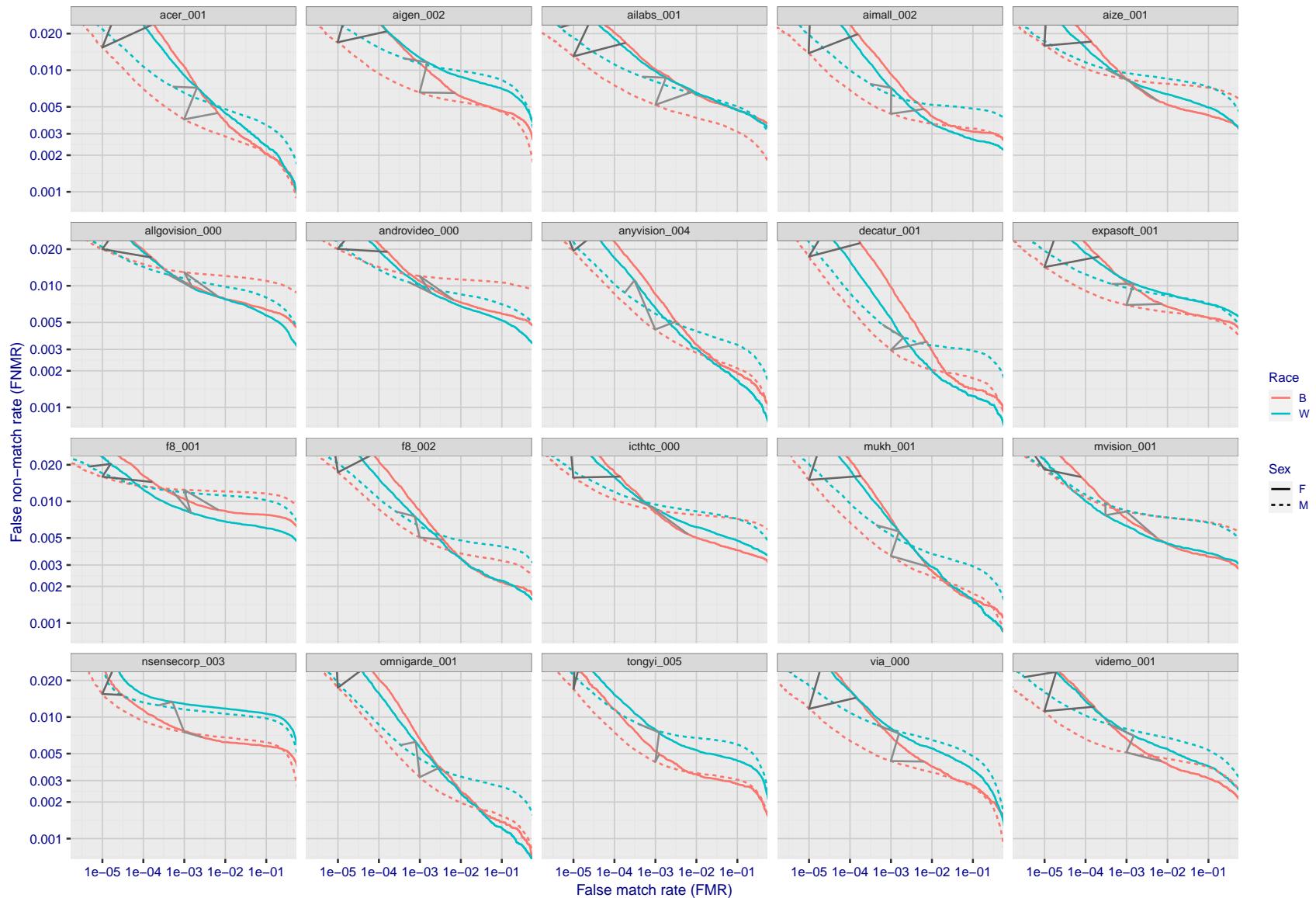


Figure 174: For the mugshot images, error tradeoff characteristics for white females, black females, black males and white males. The Z-shaped grey lines correspond to fixed thresholds, showing both FNMR and FMR vary at one T value. Note: Many of the plots will naively be read as saying women gives worse error rates than men because the solid traces lie above the dotted ones. However, this is misleading and incomplete: The grey lines show the traces reveal horizontal shifts. Thus for the cogent-003 algorithm FNMR for men is higher than for women at a fixed threshold but, at the same time, FMR is higher for women - see Figure 243. As access control systems almost always operate at a fixed threshold, the naive interpretation is incorrect.

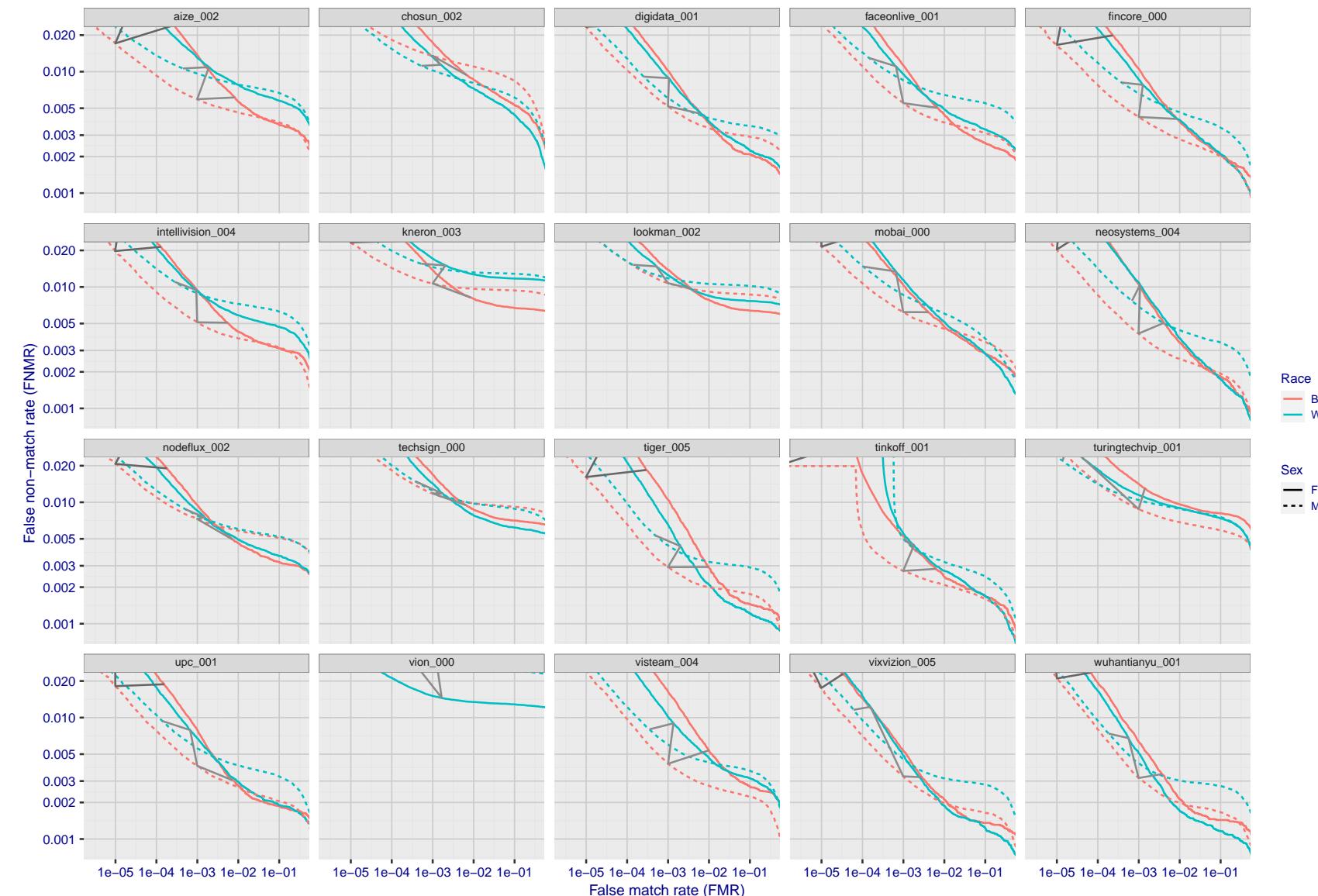


Figure 175: For the mugshot images, error tradeoff characteristics for white females, black females, black males and white males. The Z-shaped grey lines correspond to fixed thresholds, showing both FNMR and FMR vary at one T value. Note: Many of the plots will naively be read as saying women gives worse error rates than men because the solid traces lie above the dotted ones. However, this is misleading and incomplete: The grey lines show the traces reveal horizontal shifts. Thus for the cogent-003 algorithm FNMR for men is higher than for women at a fixed threshold but, at the same time, FMR is higher for women - see Figure 243. As access control systems almost always operate at a fixed threshold, the naive interpretation is incorrect.

2023/02/09 20:10:38

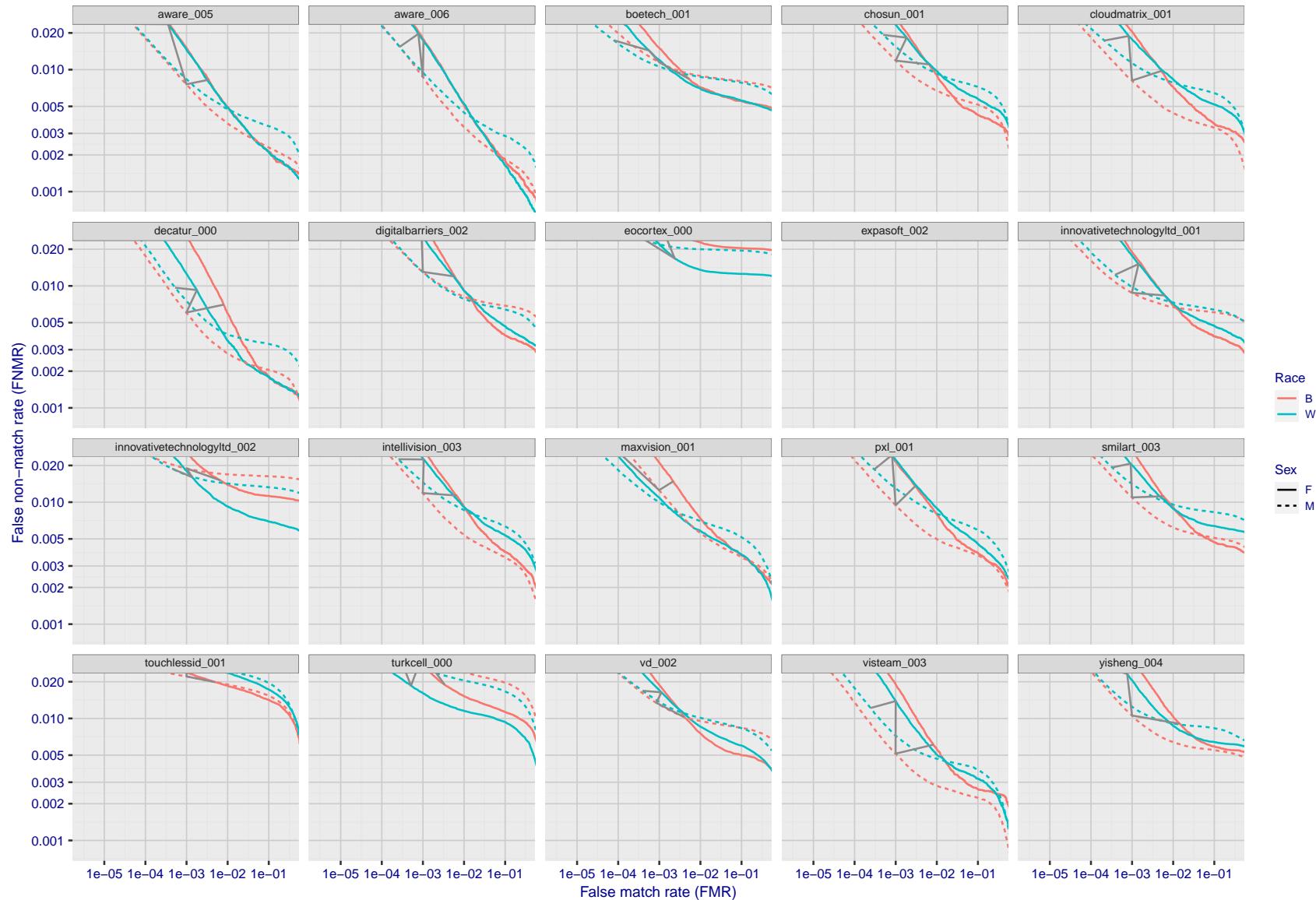


Figure 176: For the mugshot images, error tradeoff characteristics for white females, black females, black males and white males. The Z-shaped grey lines correspond to fixed thresholds, showing both FNMR and FMR vary at one T value. Note: Many of the plots will naively be read as saying women gives worse error rates than men because the solid traces lie above the dotted ones. However, this is misleading and incomplete: The grey lines show the traces reveal horizontal shifts. Thus for the cogent-003 algorithm FNMR for men is higher than for women at a fixed threshold but, at the same time, FMR is higher for women - see Figure 243. As access control systems almost always operate at a fixed threshold, the naive interpretation is incorrect.

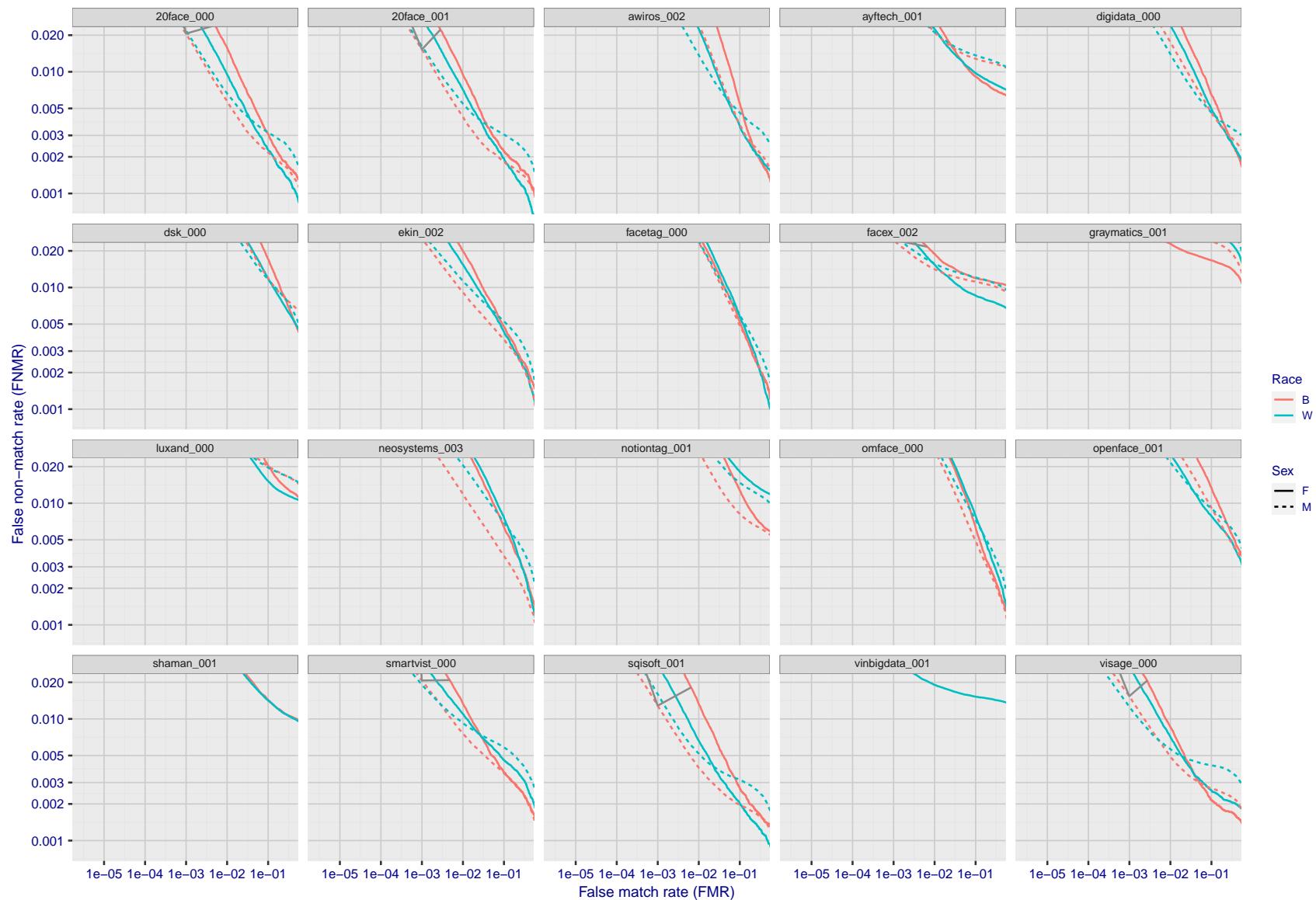


Figure 177: For the mugshot images, error tradeoff characteristics for white females, black females, black males and white males. The Z-shaped grey lines correspond to fixed thresholds, showing both FNMR and FMR vary at one T value. Note: Many of the plots will naively be read as saying women gives worse error rates than men because the solid traces lie above the dotted ones. However, this is misleading and incomplete: The grey lines show the traces reveal horizontal shifts. Thus for the cogent-003 algorithm FNMR for men is higher than for women at a fixed threshold but, at the same time, FMR is higher for women - see Figure 243. As access control systems almost always operate at a fixed threshold, the naive interpretation is incorrect.

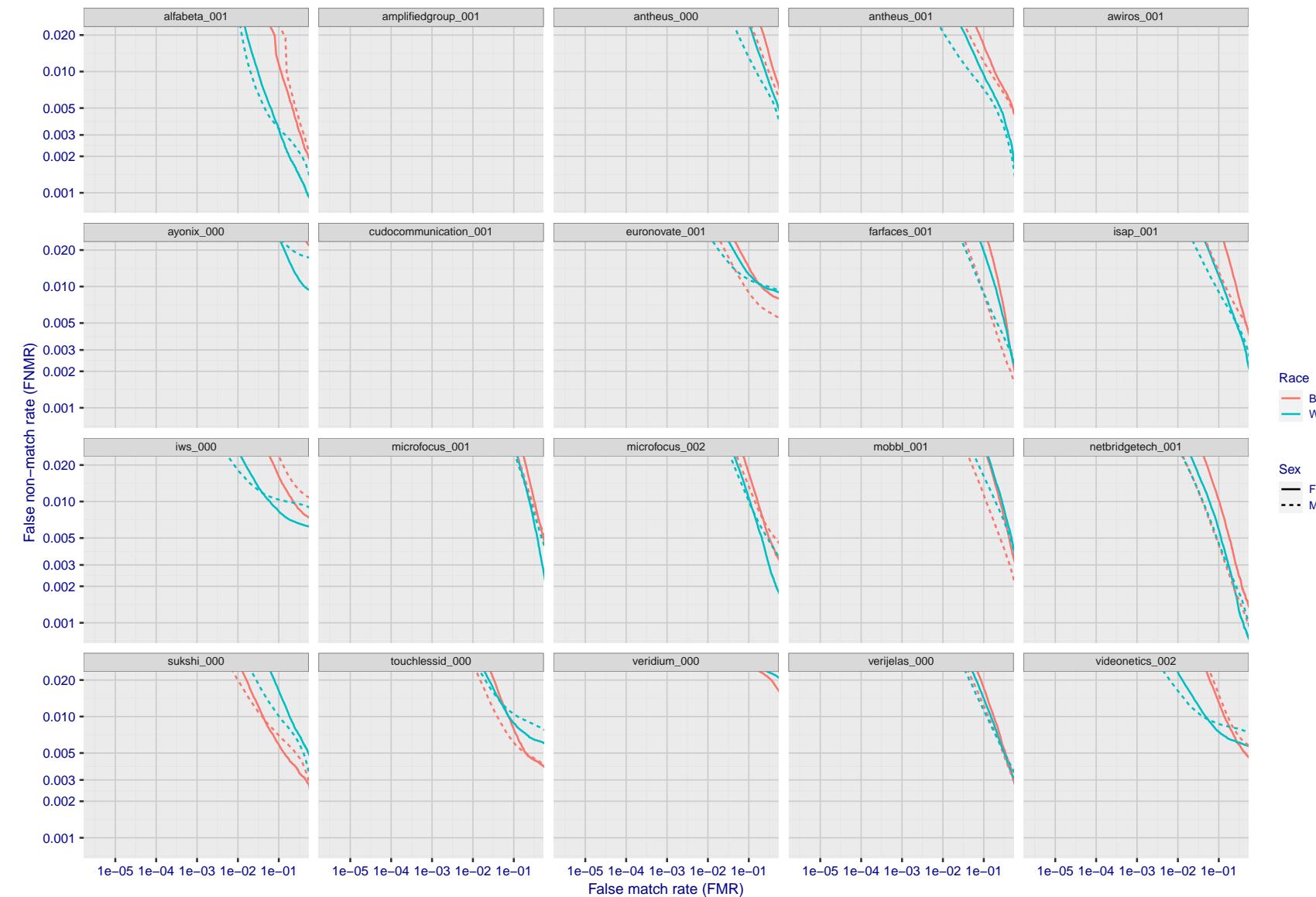


Figure 178: For the mugshot images, error tradeoff characteristics for white females, black females, black males and white males. The Z-shaped grey lines correspond to fixed thresholds, showing both FNMR and FMR vary at one T value. Note: Many of the plots will naively be read as saying women gives worse error rates than men because the solid traces lie above the dotted ones. However, this is misleading and incomplete: The grey lines show the traces reveal horizontal shifts. Thus for the cogent-003 algorithm FNMR for men is higher than for women at a fixed threshold but, at the same time, FMR is higher for women - see Figure 243. As access control systems almost always operate at a fixed threshold, the naive interpretation is incorrect.

2023/02/09 20:10:38

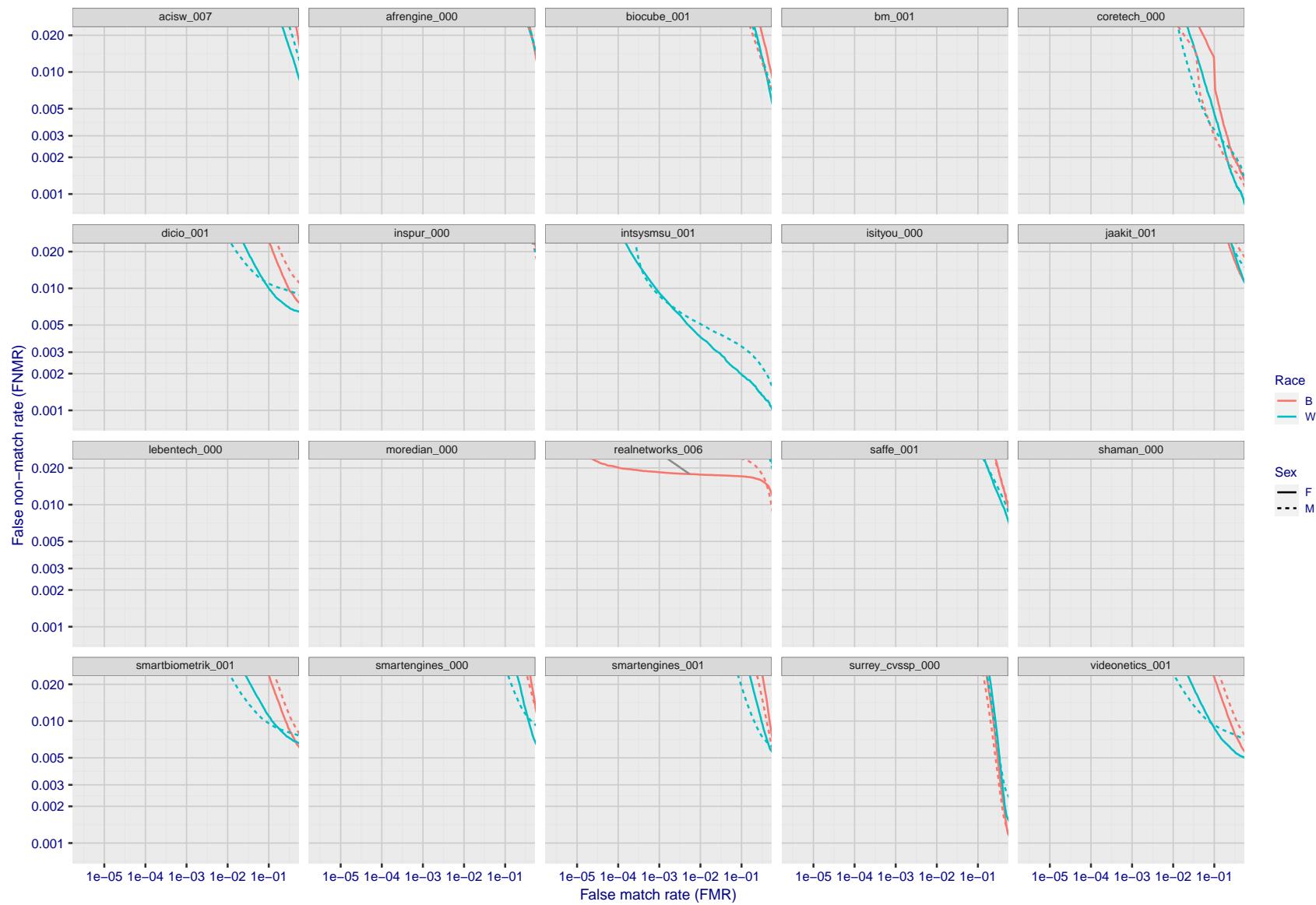


Figure 179: For the mugshot images, error tradeoff characteristics for white females, black females, black males and white males. The Z-shaped grey lines correspond to fixed thresholds, showing both FNMR and FMR vary at one T value. Note: Many of the plots will naively be read as saying women gives worse error rates than men because the solid traces lie above the dotted ones. However, this is misleading and incomplete: The grey lines show the traces reveal horizontal shifts. Thus for the cogent-003 algorithm FNMR for men is higher than for women at a fixed threshold but, at the same time, FMR is higher for women - see Figure 243. As access control systems almost always operate at a fixed threshold, the naive interpretation is incorrect.

FNMR(T)"False non-match rate"
"False match rate"

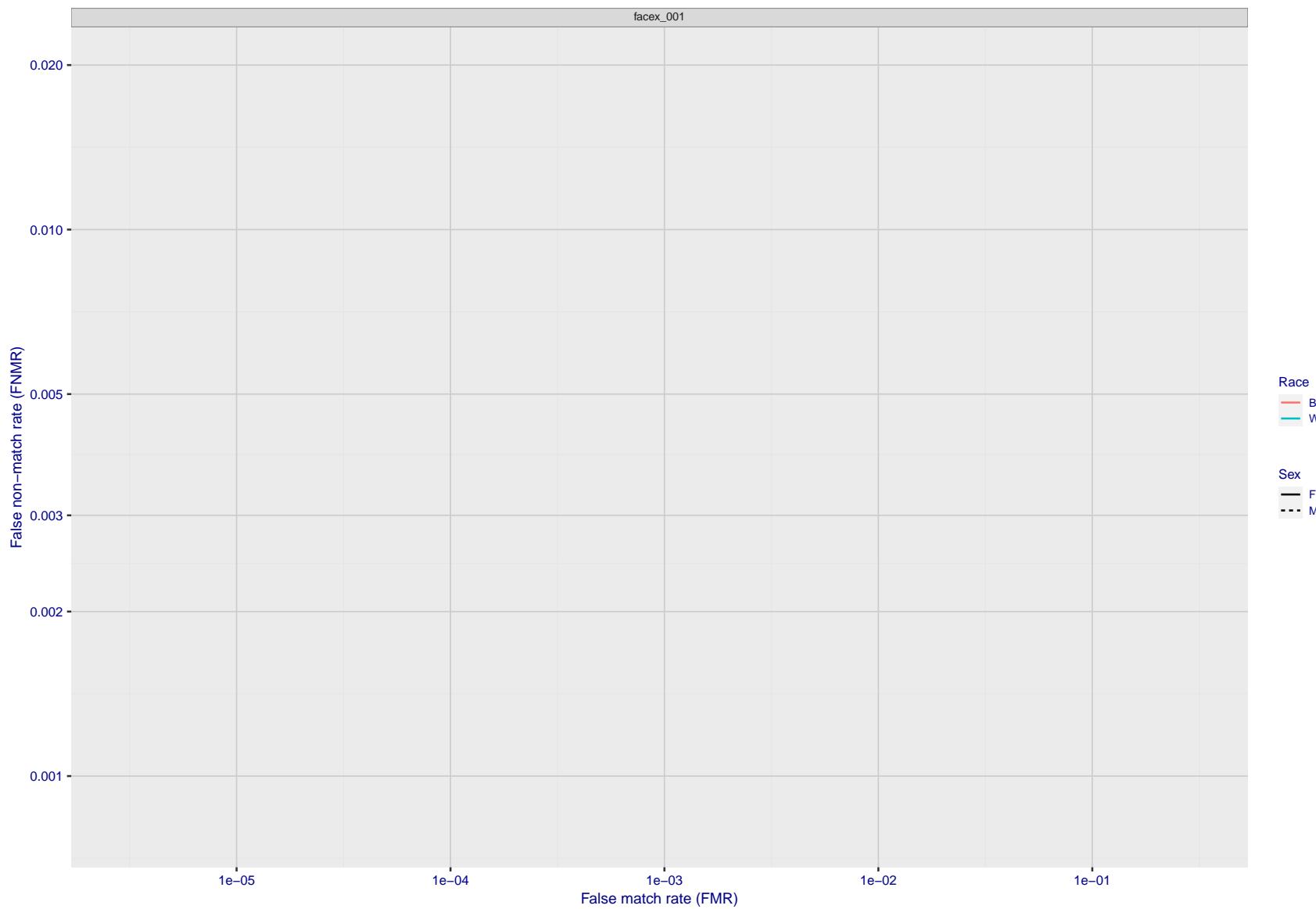


Figure 180: For the mugshot images, error tradeoff characteristics for white females, black females, black males and white males. The Z-shaped grey lines correspond to fixed thresholds, showing both FNMR and FMR vary at one T value. Note: Many of the plots will naively be read as saying women gives worse error rates than men because the solid traces lie above the dotted ones. However, this is misleading and incomplete: The grey lines show the traces reveal horizontal shifts. Thus for the cogent-003 algorithm FNMR for men is higher than for women at a fixed threshold but, at the same time, FMR is higher for women - see Figure 243. As access control systems almost always operate at a fixed threshold, the naive interpretation is incorrect.

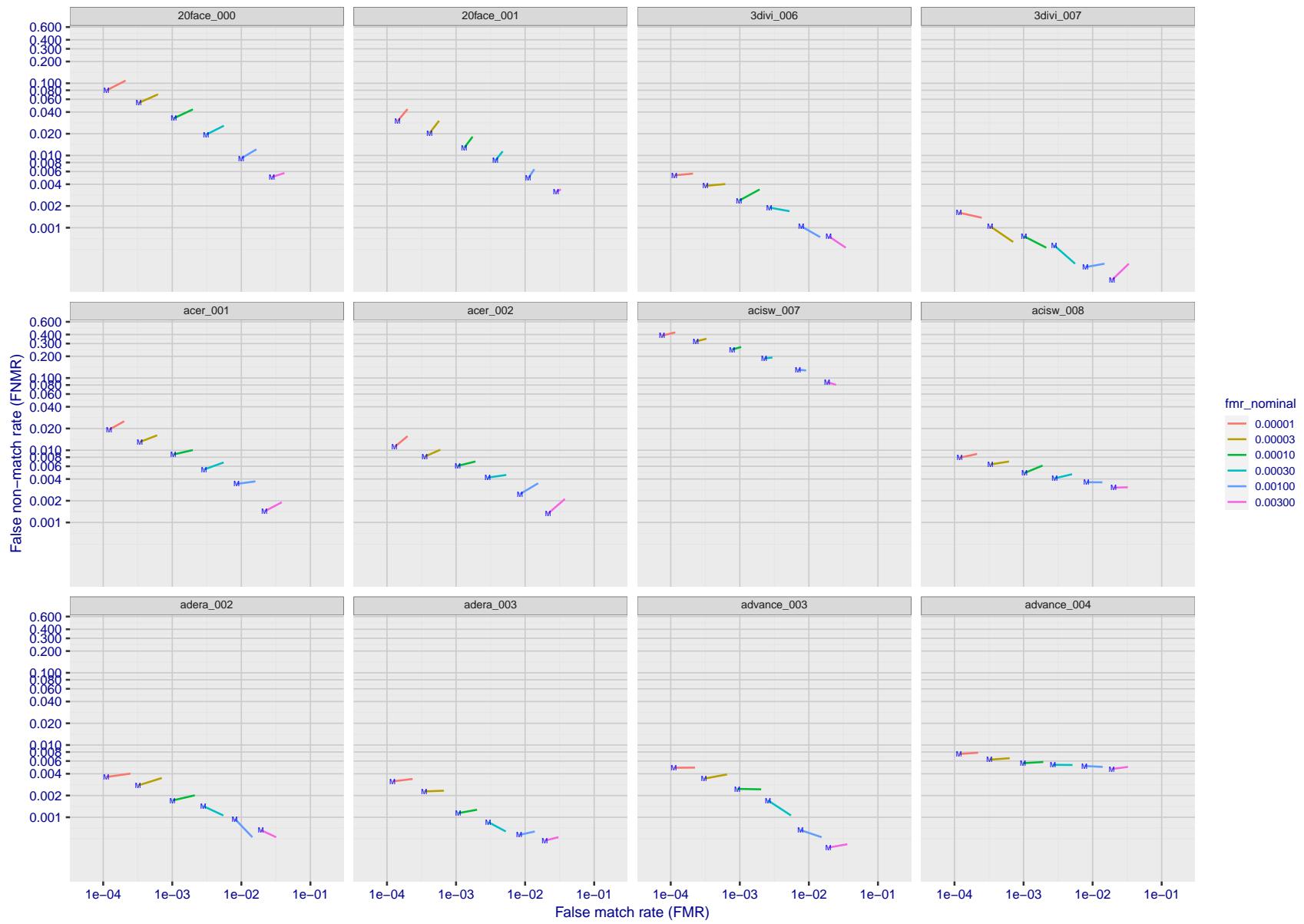


Figure 181: For the visa images, FNMR and FMR at six operating points along the DET characteristic. At each point a line is drawn between $(FMR, FNMR)_{MALE}$ and $(FMR, FNMR)_{FEMALE}$ showing how which sex has lower FMR and/or FNMR. The "M" label denotes male, the other end of the line corresponds to female. The six operating thresholds are selected to give the nominal false match rates given in the legend, and are computed over all impostor pairs regardless of age, sex, and place of birth. The plotted FMR values are broadly an order of magnitude larger than the nominal rates because FMR is computed over demographically-matched impostor pairs i.e individuals of the same sex, from the same geographic region (see section 3.6.1), and the same age group (see section 3.6.2).

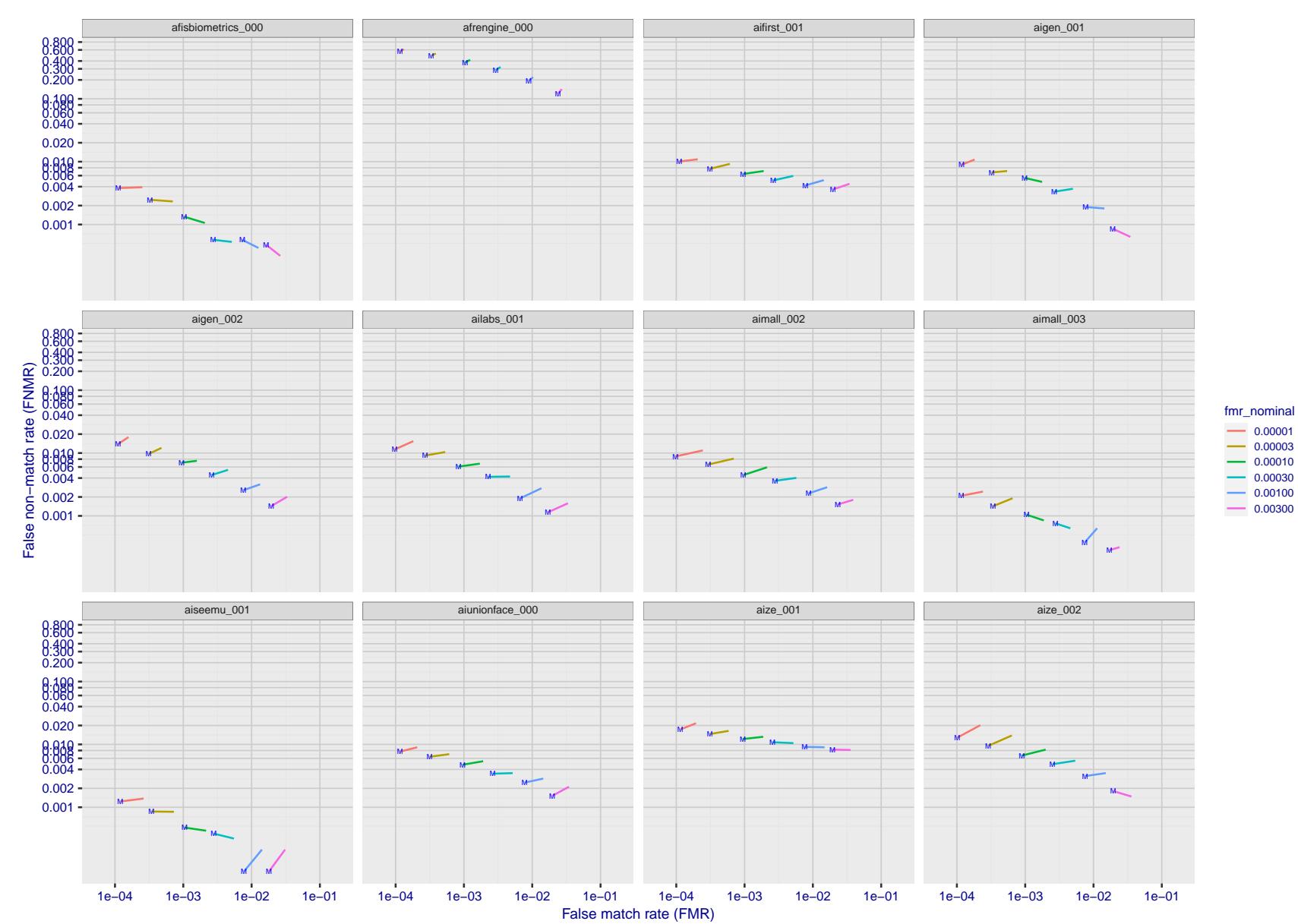


Figure 182: For the visa images, FNMR and FMR at six operating points along the DET characteristic. At each point a line is drawn between $(FMR, FNMR)_{MALE}$ and $(FMR, FNMR)_{FEMALE}$ showing how which sex has lower FMR and/or FNMR. The "M" label denotes male, the other end of the line corresponds to female. The six operating thresholds are selected to give the nominal false match rates given in the legend, and are computed over all impostor pairs regardless of age, sex, and place of birth. The plotted FMR values are broadly an order of magnitude larger than the nominal rates because FMR is computed over demographically-matched impostor pairs i.e individuals of the same sex, from the same geographic region (see section 3.6.1), and the same age group (see section 3.6.2).

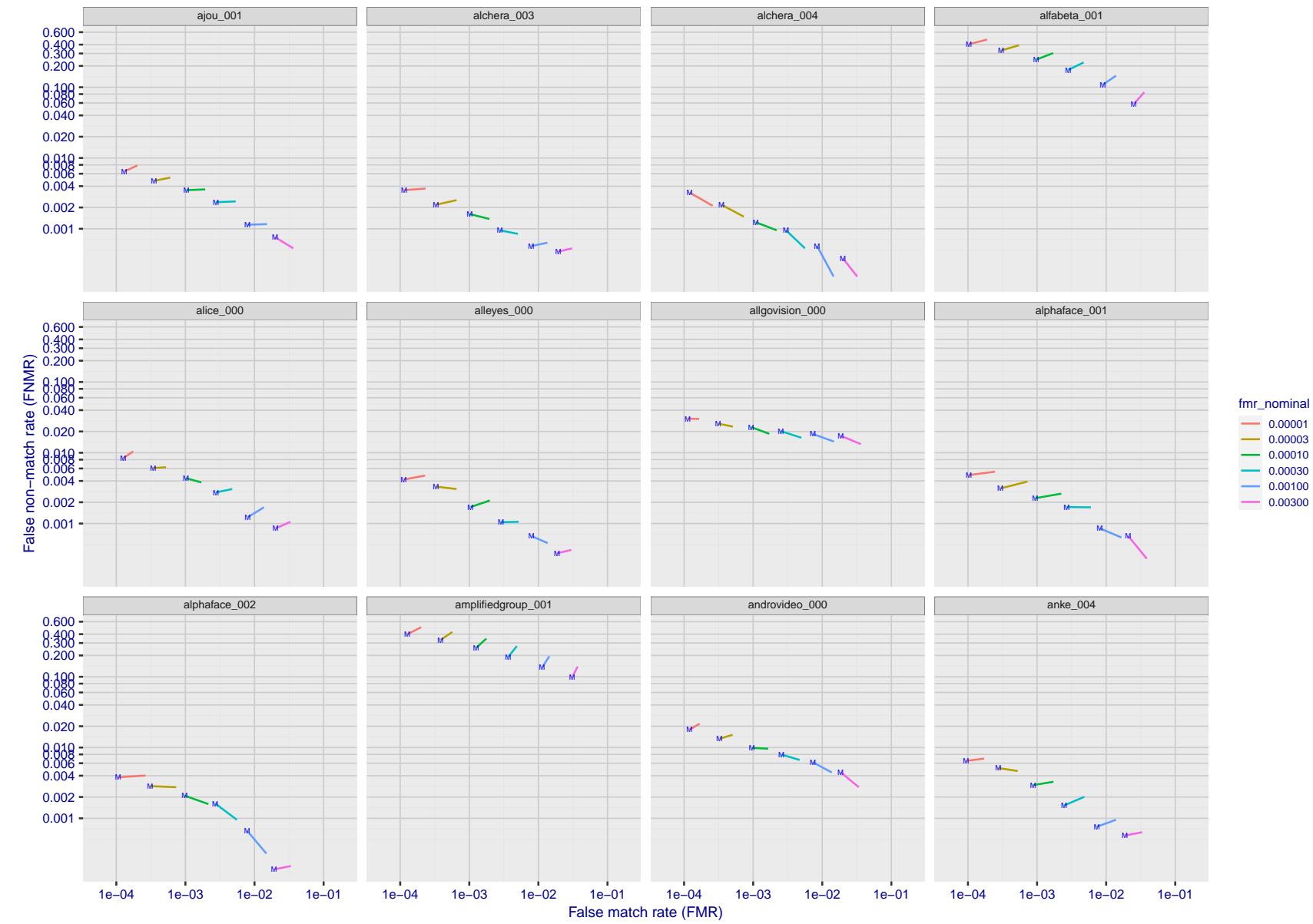


Figure 183: For the visa images, FNMR and FMR at six operating points along the DET characteristic. At each point a line is drawn between $(FMR, FNMR)_{MALE}$ and $(FMR, FNMR)_{FEMALE}$ showing how which sex has lower FMR and/or FNMR. The "M" label denotes male, the other end of the line corresponds to female. The six operating thresholds are selected to give the nominal false match rates given in the legend, and are computed over all impostor pairs regardless of age, sex, and place of birth. The plotted FMR values are broadly an order of magnitude larger than the nominal rates because FMR is computed over demographically-matched impostor pairs i.e individuals of the same sex, from the same geographic region (see section 3.6.1), and the same age group (see section 3.6.2).

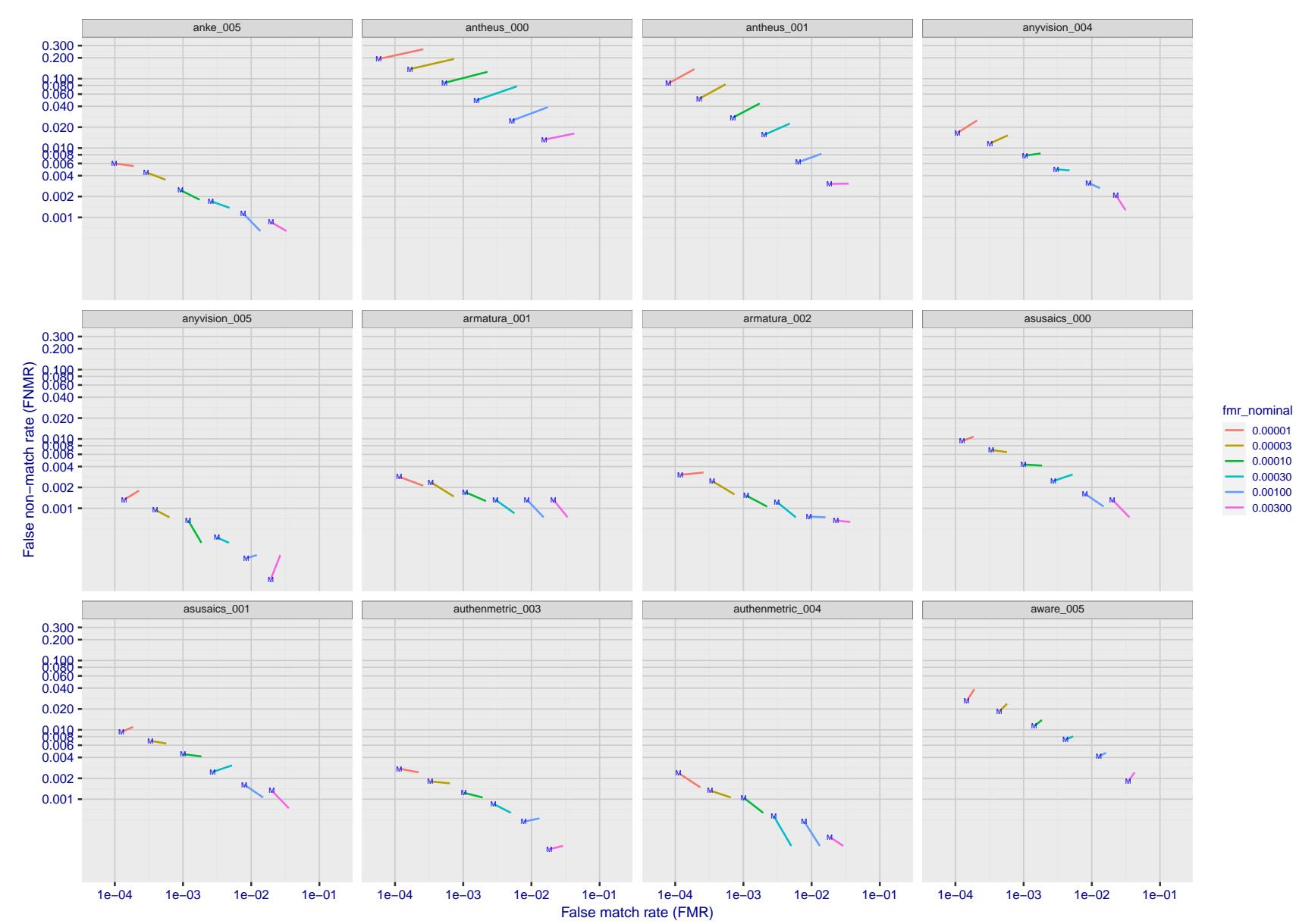


Figure 184: For the visa images, FNMR and FMR at six operating points along the DET characteristic. At each point a line is drawn between $(FMR, FNMR)_{MALE}$ and $(FMR, FNMR)_{FEMALE}$ showing how which sex has lower FMR and/or FNMR. The "M" label denotes male, the other end of the line corresponds to female. The six operating thresholds are selected to give the nominal false match rates given in the legend, and are computed over all impostor pairs regardless of age, sex, and place of birth. The plotted FMR values are broadly an order of magnitude larger than the nominal rates because FMR is computed over demographically-matched impostor pairs i.e individuals of the same sex, from the same geographic region (see section 3.6.1), and the same age group (see section 3.6.2).

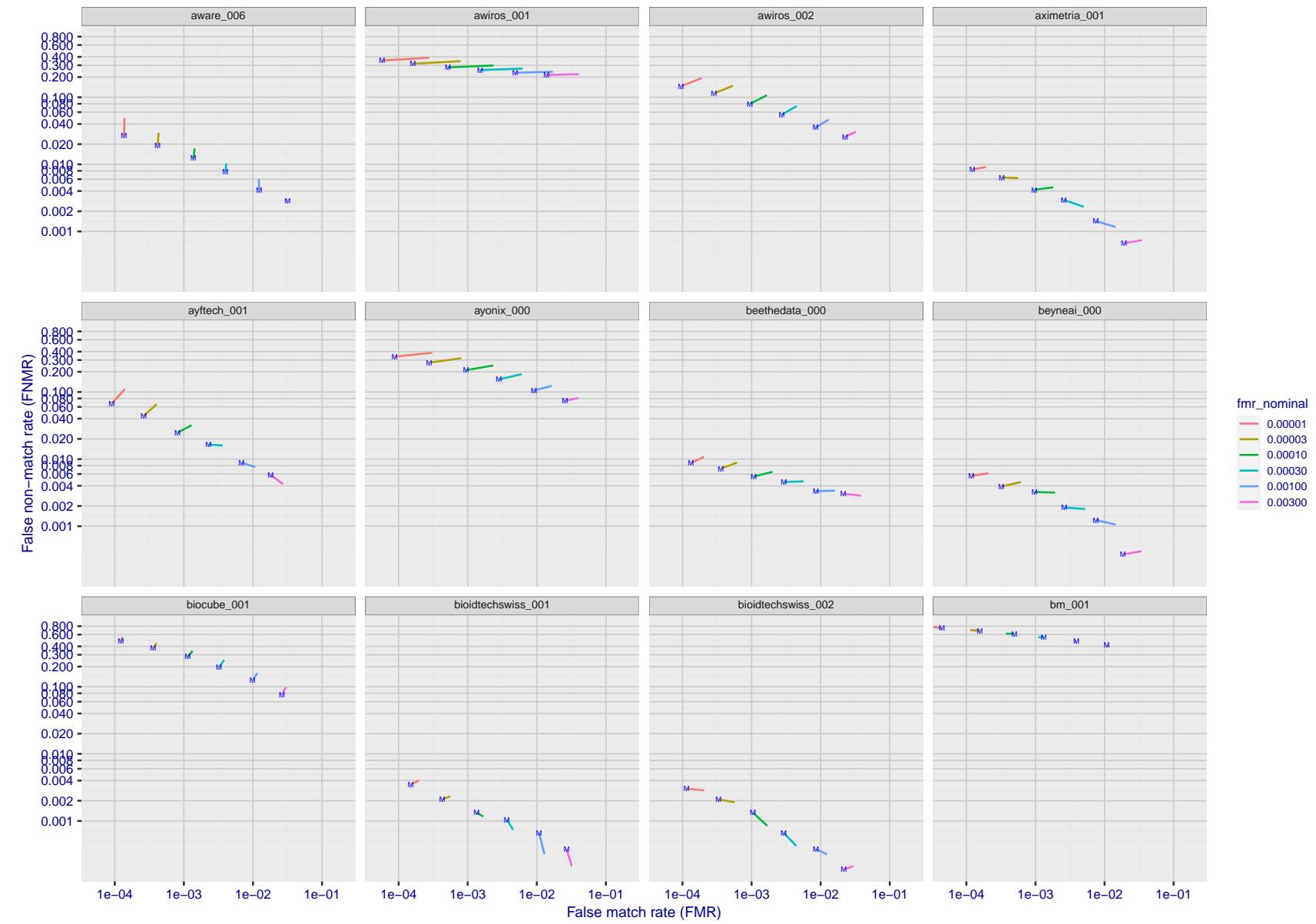


Figure 185: For the visa images, FNMR and FMR at six operating points along the DET characteristic. At each point a line is drawn between $(FMR, FNMR)_{MALE}$ and $(FMR, FNMR)_{FEMALE}$ showing how which sex has lower FMR and/or FNMR. The "M" label denotes male, the other end of the line corresponds to female. The six operating thresholds are selected to give the nominal false match rates given in the legend, and are computed over all impostor pairs regardless of age, sex, and place of birth. The plotted FMR values are broadly an order of magnitude larger than the nominal rates because FMR is computed over demographically-matched impostor pairs i.e individuals of the same sex, from the same geographic region (see section 3.6.1), and the same age group (see section 3.6.2).

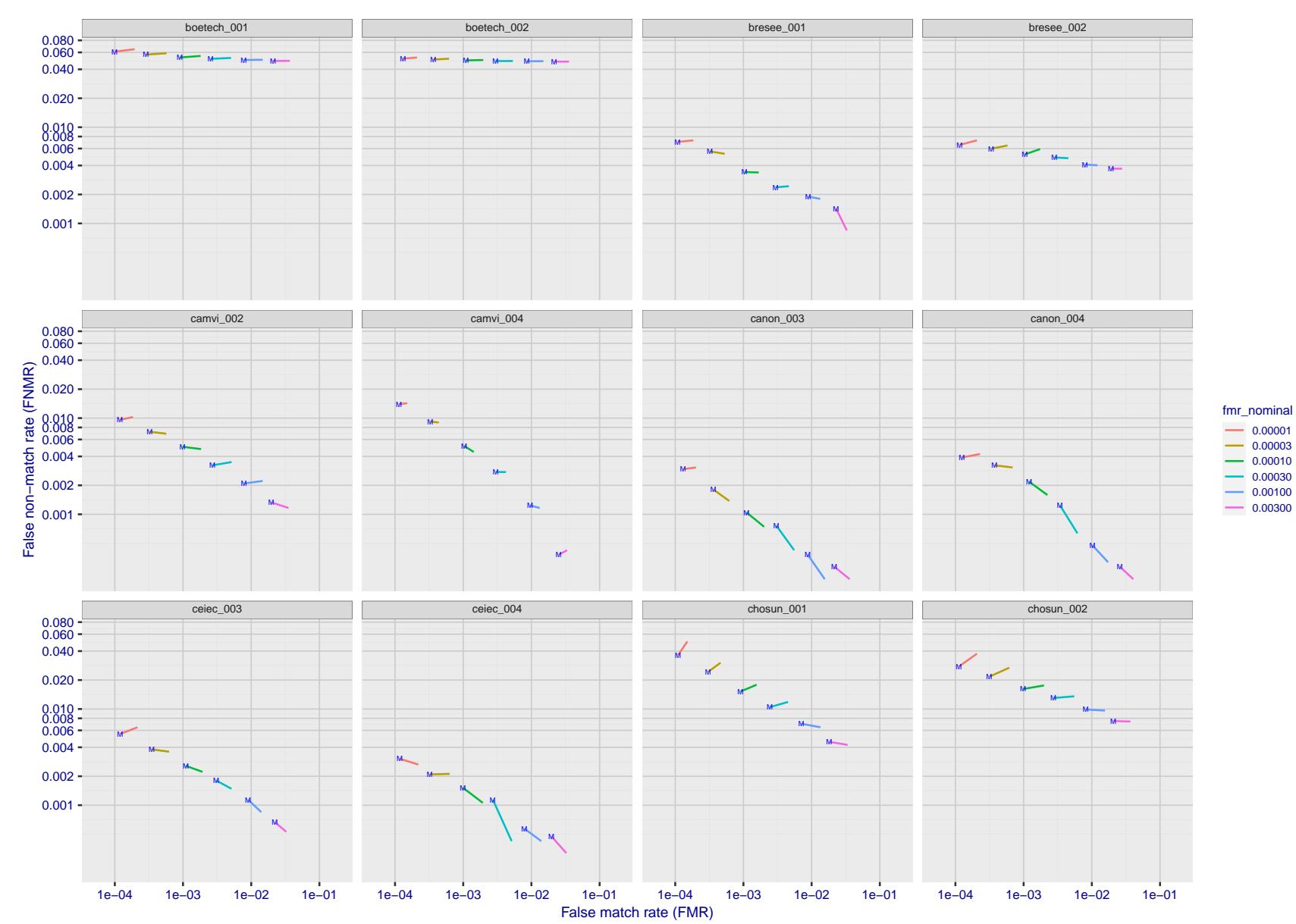


Figure 186: For the visa images, FNMR and FMR at six operating points along the DET characteristic. At each point a line is drawn between $(FMR, FNMR)_{MALE}$ and $(FMR, FNMR)_{FEMALE}$ showing how which sex has lower FMR and/or FNMR. The "M" label denotes male, the other end of the line corresponds to female. The six operating thresholds are selected to give the nominal false match rates given in the legend, and are computed over all impostor pairs regardless of age, sex, and place of birth. The plotted FMR values are broadly an order of magnitude larger than the nominal rates because FMR is computed over demographically-matched impostor pairs i.e individuals of the same sex, from the same geographic region (see section 3.6.1), and the same age group (see section 3.6.2).

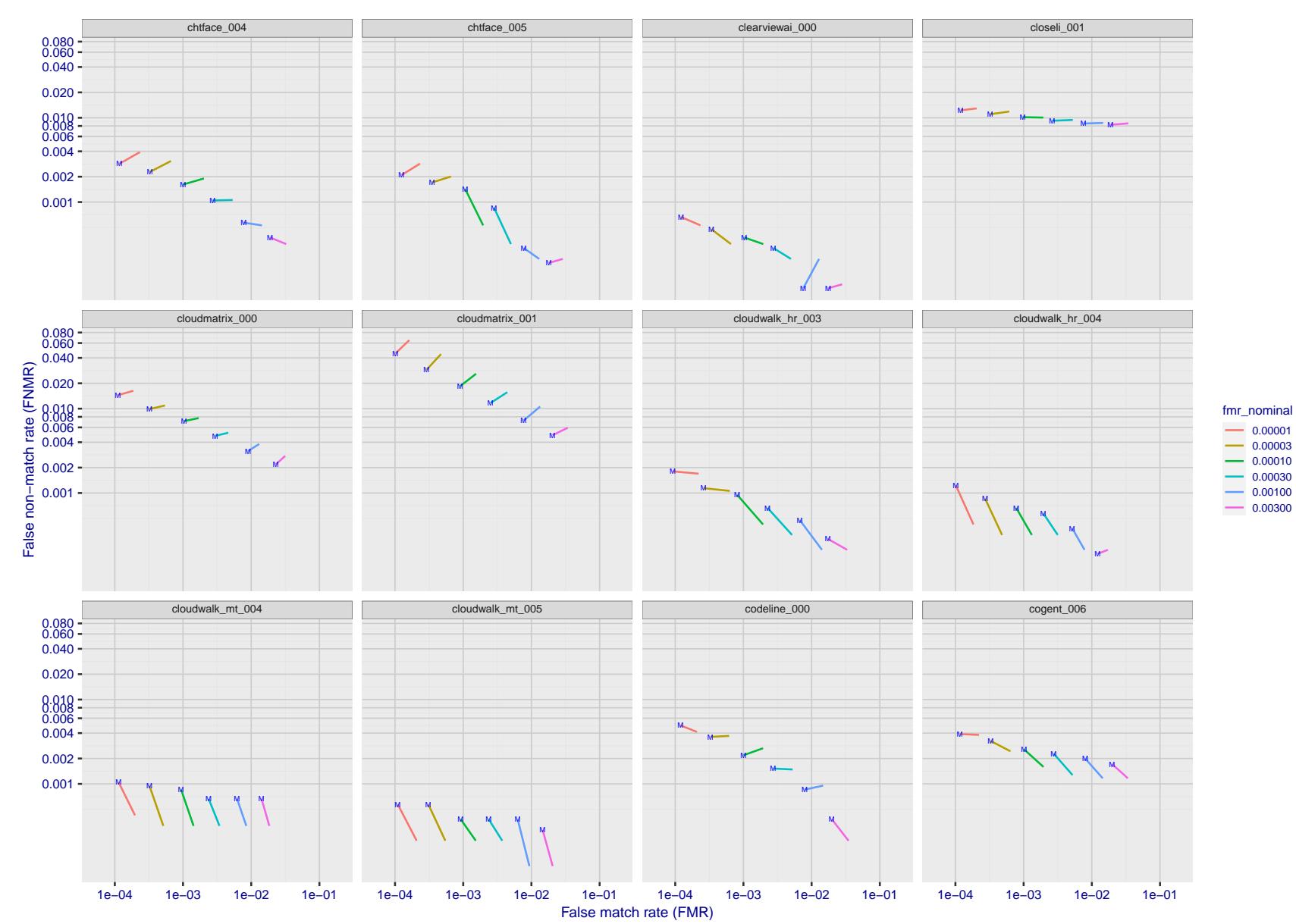


Figure 187: For the visa images, FNMR and FMR at six operating points along the DET characteristic. At each point a line is drawn between $(FMR, FNMR)_{MALE}$ and $(FMR, FNMR)_{FEMALE}$ showing how which sex has lower FMR and/or FNMR. The "M" label denotes male, the other end of the line corresponds to female. The six operating thresholds are selected to give the nominal false match rates given in the legend, and are computed over all impostor pairs regardless of age, sex, and place of birth. The plotted FMR values are broadly an order of magnitude larger than the nominal rates because FMR is computed over demographically-matched impostor pairs i.e individuals of the same sex, from the same geographic region (see section 3.6.1), and the same age group (see section 3.6.2).

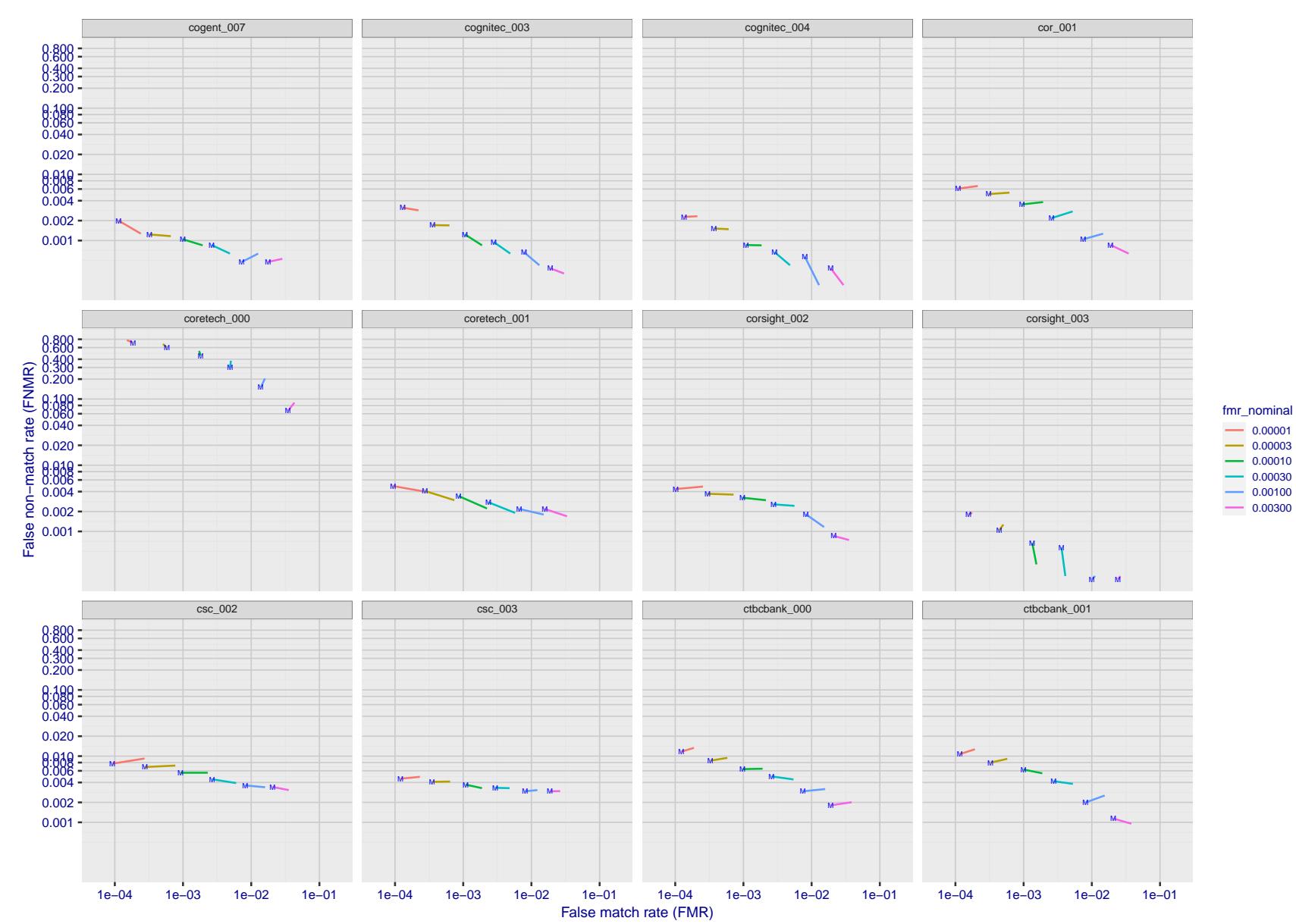


Figure 188: For the visa images, FNMR and FMR at six operating points along the DET characteristic. At each point a line is drawn between $(FMR, FNMR)_{MALE}$ and $(FMR, FNMR)_{FEMALE}$ showing how which sex has lower FMR and/or FNMR. The "M" label denotes male, the other end of the line corresponds to female. The six operating thresholds are selected to give the nominal false match rates given in the legend, and are computed over all impostor pairs regardless of age, sex, and place of birth. The plotted FMR values are broadly an order of magnitude larger than the nominal rates because FMR is computed over demographically-matched impostor pairs i.e individuals of the same sex, from the same geographic region (see section 3.6.1), and the same age group (see section 3.6.2).

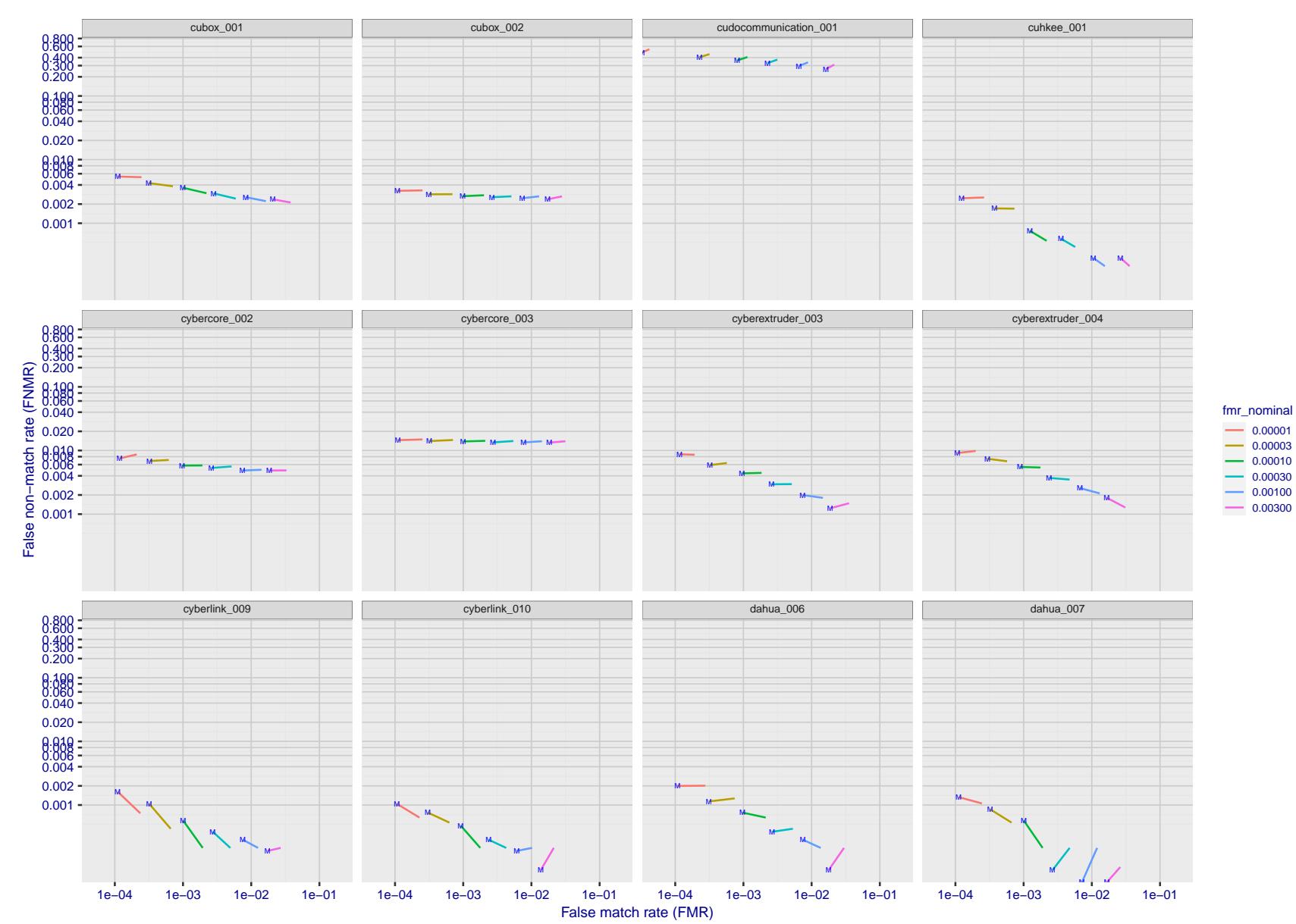


Figure 189: For the visa images, FNMR and FMR at six operating points along the DET characteristic. At each point a line is drawn between $(FMR, FNMR)_{MALE}$ and $(FMR, FNMR)_{FEMALE}$ showing how which sex has lower FMR and/or FNMR. The "M" label denotes male, the other end of the line corresponds to female. The six operating thresholds are selected to give the nominal false match rates given in the legend, and are computed over all impostor pairs regardless of age, sex, and place of birth. The plotted FMR values are broadly an order of magnitude larger than the nominal rates because FMR is computed over demographically-matched impostor pairs i.e individuals of the same sex, from the same geographic region (see section 3.6.1), and the same age group (see section 3.6.2).

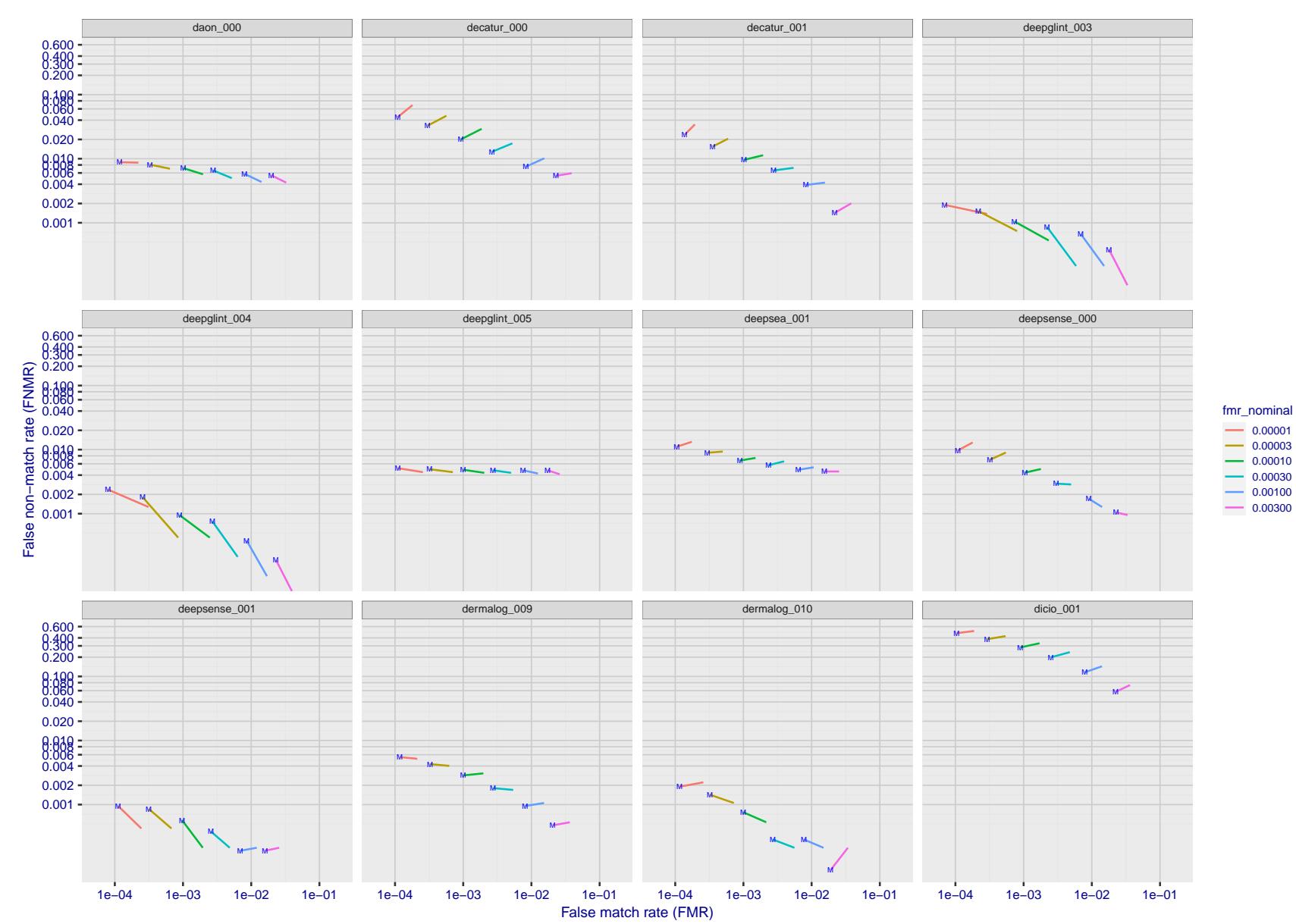


Figure 190: For the visa images, FNMR and FMR at six operating points along the DET characteristic. At each point a line is drawn between $(FMR, FNMR)_{MALE}$ and $(FMR, FNMR)_{FEMALE}$ showing how which sex has lower FMR and/or FNMR. The "M" label denotes male, the other end of the line corresponds to female. The six operating thresholds are selected to give the nominal false match rates given in the legend, and are computed over all impostor pairs regardless of age, sex, and place of birth. The plotted FMR values are broadly an order of magnitude larger than the nominal rates because FMR is computed over demographically-matched impostor pairs i.e individuals of the same sex, from the same geographic region (see section 3.6.1), and the same age group (see section 3.6.2).

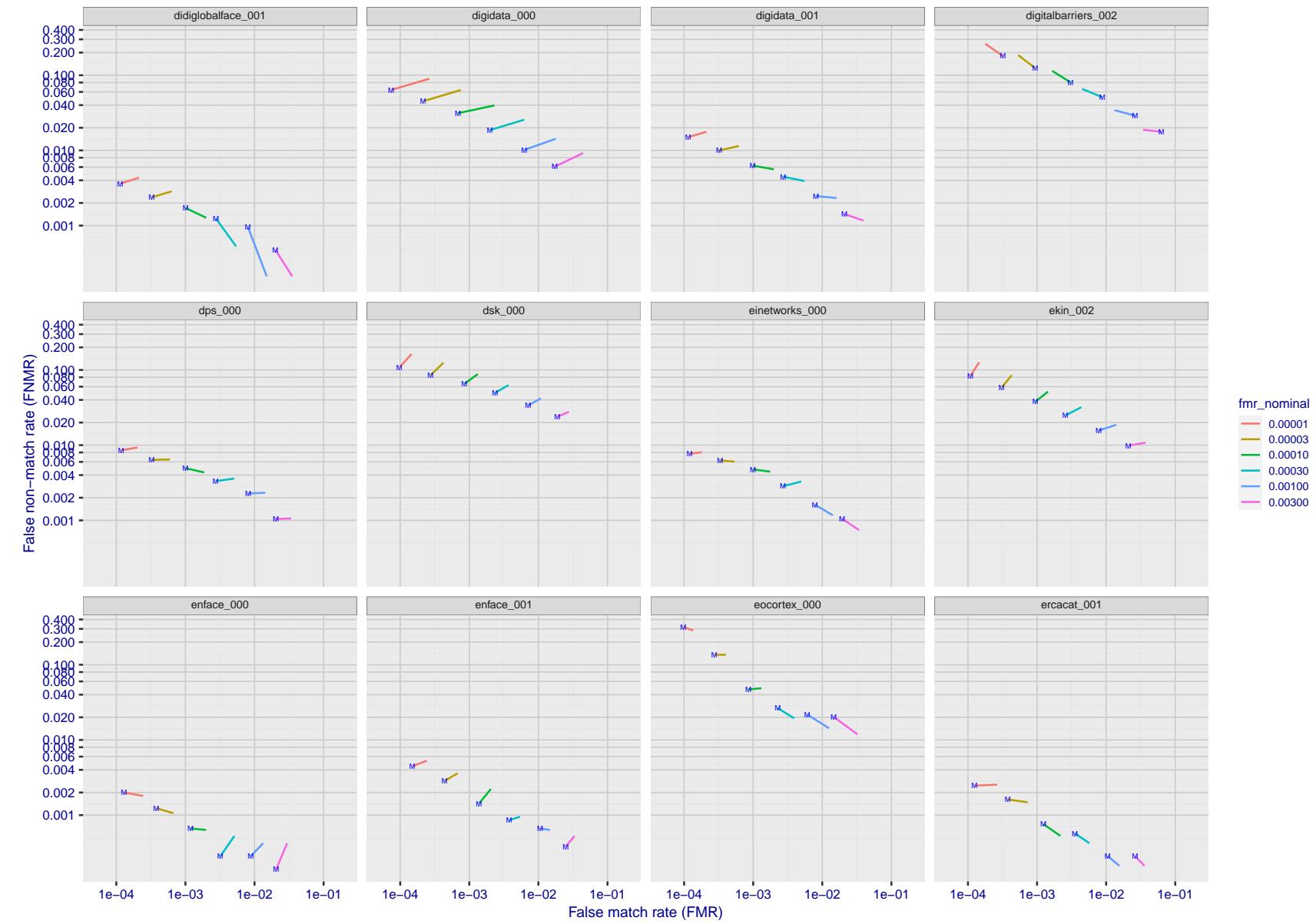


Figure 191: For the visa images, FNMR and FMR at six operating points along the DET characteristic. At each point a line is drawn between $(FMR, FNMR)_{MALE}$ and $(FMR, FNMR)_{FEMALE}$ showing how which sex has lower FMR and/or FNMR. The "M" label denotes male, the other end of the line corresponds to female. The six operating thresholds are selected to give the nominal false match rates given in the legend, and are computed over all impostor pairs regardless of age, sex, and place of birth. The plotted FMR values are broadly an order of magnitude larger than the nominal rates because FMR is computed over demographically-matched impostor pairs i.e individuals of the same sex, from the same geographic region (see section 3.6.1), and the same age group (see section 3.6.2).

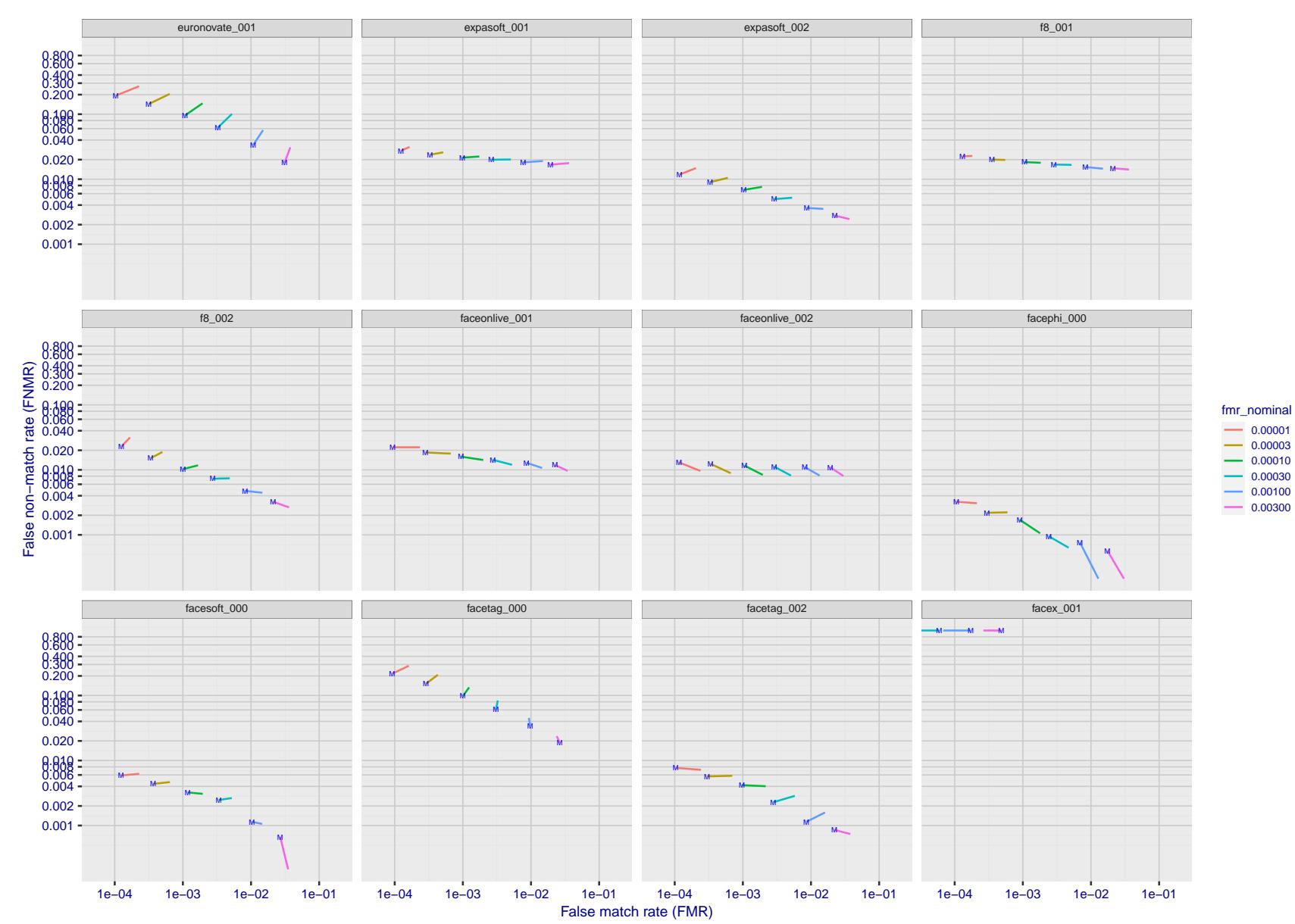


Figure 192: For the visa images, FNMR and FMR at six operating points along the DET characteristic. At each point a line is drawn between $(FMR, FNMR)_{MALE}$ and $(FMR, FNMR)_{FEMALE}$ showing how which sex has lower FMR and/or FNMR. The "M" label denotes male, the other end of the line corresponds to female. The six operating thresholds are selected to give the nominal false match rates given in the legend, and are computed over all impostor pairs regardless of age, sex, and place of birth. The plotted FMR values are broadly an order of magnitude larger than the nominal rates because FMR is computed over demographically-matched impostor pairs i.e individuals of the same sex, from the same geographic region (see section 3.6.1), and the same age group (see section 3.6.2).

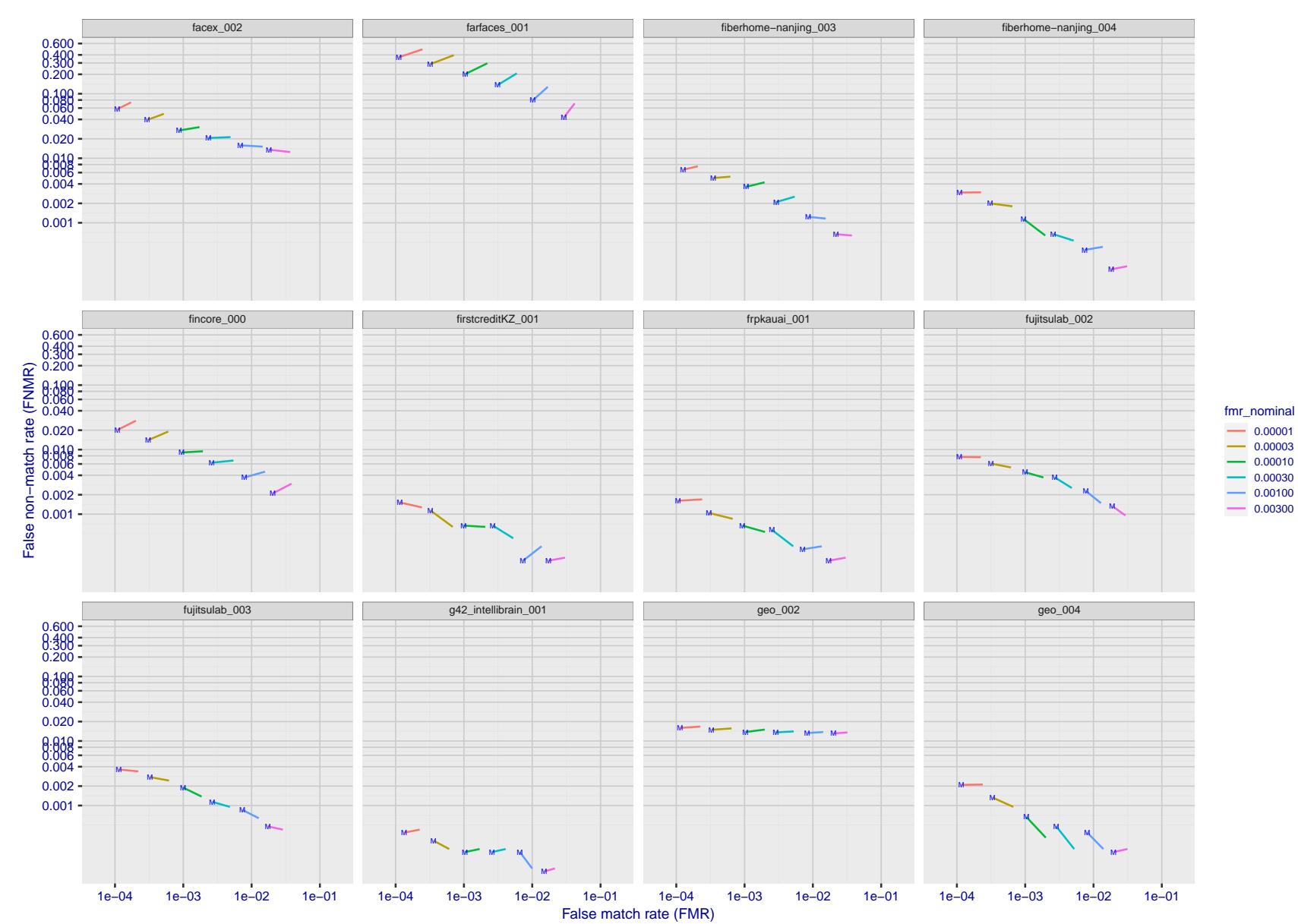


Figure 193: For the visa images, FNMR and FMR at six operating points along the DET characteristic. At each point a line is drawn between $(FMR, FNMR)_{MALE}$ and $(FMR, FNMR)_{FEMALE}$ showing how which sex has lower FMR and/or FNMR. The "M" label denotes male, the other end of the line corresponds to female. The six operating thresholds are selected to give the nominal false match rates given in the legend, and are computed over all impostor pairs regardless of age, sex, and place of birth. The plotted FMR values are broadly an order of magnitude larger than the nominal rates because FMR is computed over demographically-matched impostor pairs i.e individuals of the same sex, from the same geographic region (see section 3.6.1), and the same age group (see section 3.6.2).

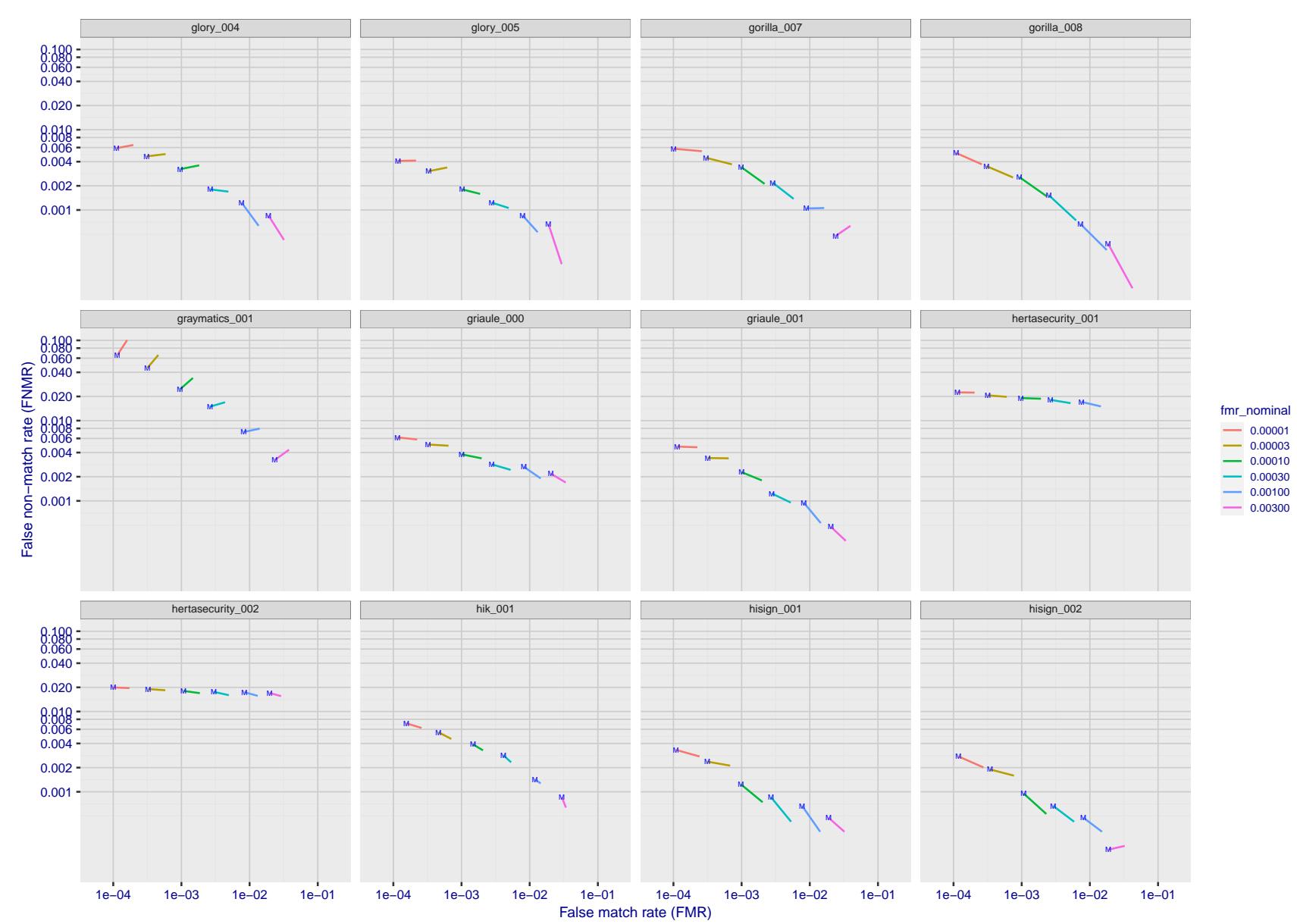


Figure 194: For the visa images, FNMR and FMR at six operating points along the DET characteristic. At each point a line is drawn between $(FMR, FNMR)_{MALE}$ and $(FMR, FNMR)_{FEMALE}$ showing how which sex has lower FMR and/or FNMR. The "M" label denotes male, the other end of the line corresponds to female. The six operating thresholds are selected to give the nominal false match rates given in the legend, and are computed over all impostor pairs regardless of age, sex, and place of birth. The plotted FMR values are broadly an order of magnitude larger than the nominal rates because FMR is computed over demographically-matched impostor pairs i.e individuals of the same sex, from the same geographic region (see section 3.6.1), and the same age group (see section 3.6.2).

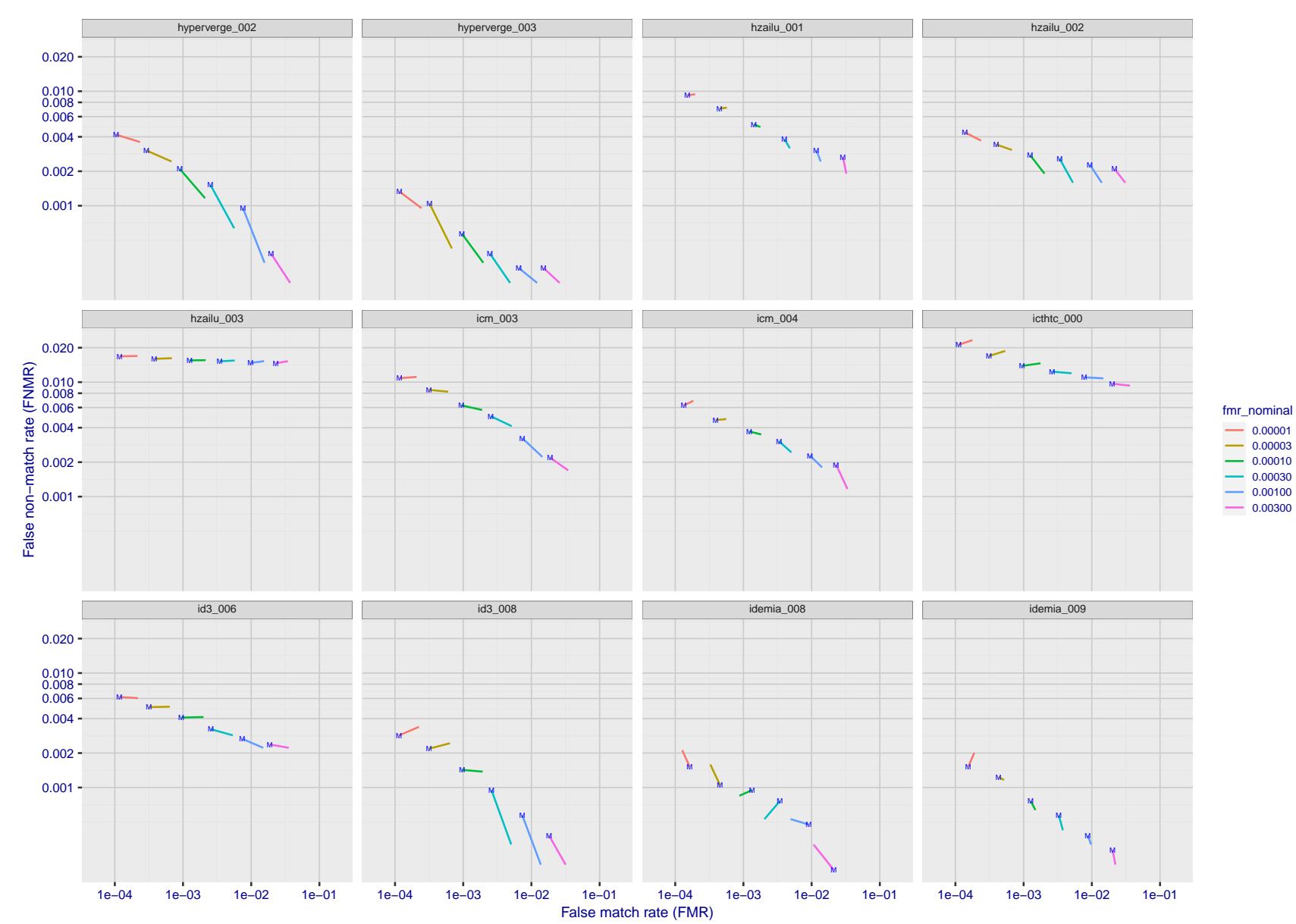


Figure 195: For the visa images, FNMR and FMR at six operating points along the DET characteristic. At each point a line is drawn between $(FMR, FNMR)_{MALE}$ and $(FMR, FNMR)_{FEMALE}$ showing how which sex has lower FMR and/or FNMR. The "M" label denotes male, the other end of the line corresponds to female. The six operating thresholds are selected to give the nominal false match rates given in the legend, and are computed over all impostor pairs regardless of age, sex, and place of birth. The plotted FMR values are broadly an order of magnitude larger than the nominal rates because FMR is computed over demographically-matched impostor pairs i.e individuals of the same sex, from the same geographic region (see section 3.6.1), and the same age group (see section 3.6.2).

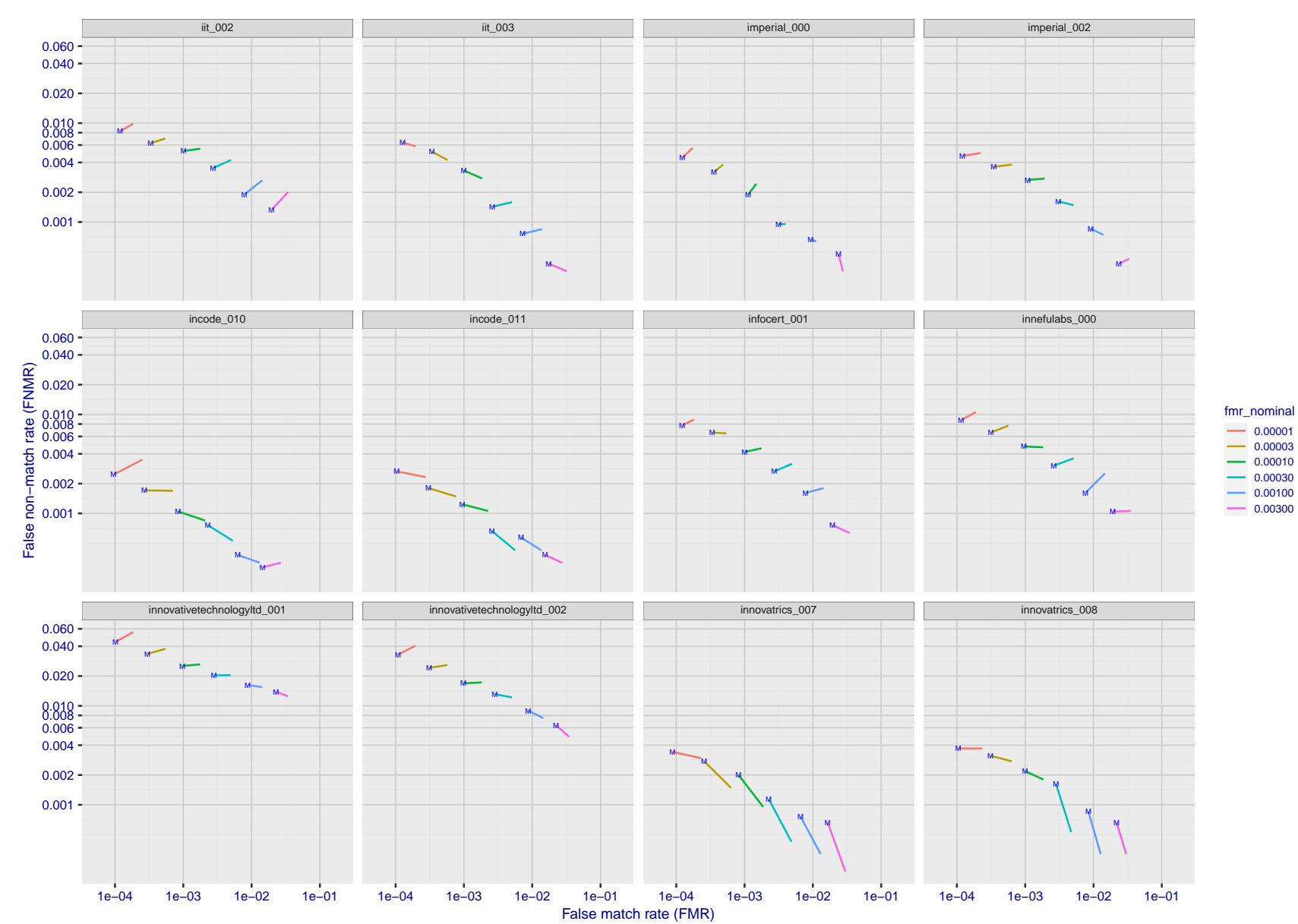


Figure 196: For the visa images, FNMR and FMR at six operating points along the DET characteristic. At each point a line is drawn between $(FMR, FNMR)_{MALE}$ and $(FMR, FNMR)_{FEMALE}$ showing how which sex has lower FMR and/or FNMR. The "M" label denotes male, the other end of the line corresponds to female. The six operating thresholds are selected to give the nominal false match rates given in the legend, and are computed over all impostor pairs regardless of age, sex, and place of birth. The plotted FMR values are broadly an order of magnitude larger than the nominal rates because FMR is computed over demographically-matched impostor pairs i.e individuals of the same sex, from the same geographic region (see section 3.6.1), and the same age group (see section 3.6.2).

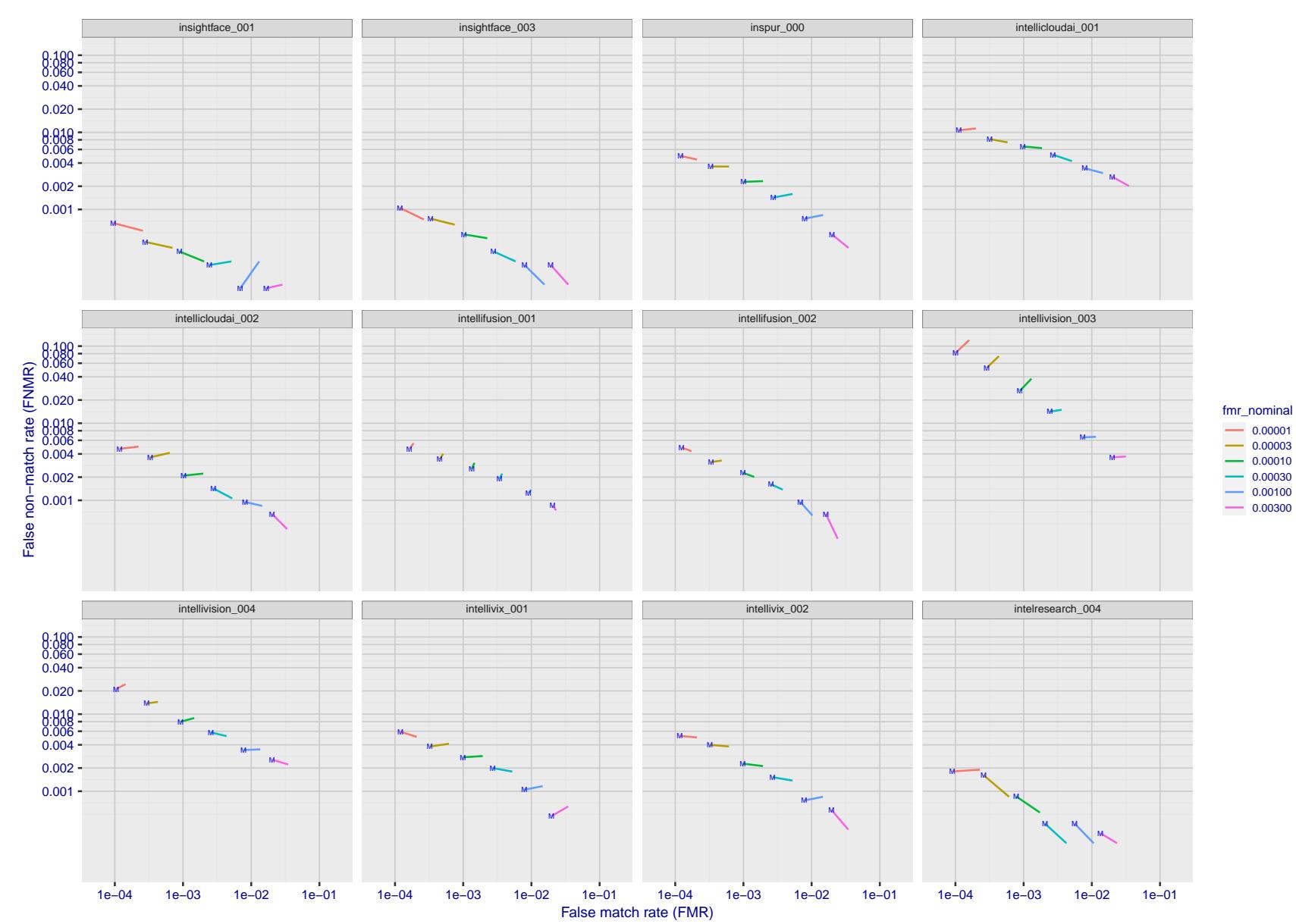


Figure 197: For the visa images, FNMR and FMR at six operating points along the DET characteristic. At each point a line is drawn between $(FMR, FNMR)_{MALE}$ and $(FMR, FNMR)_{FEMALE}$ showing how which sex has lower FMR and/or FNMR. The "M" label denotes male, the other end of the line corresponds to female. The six operating thresholds are selected to give the nominal false match rates given in the legend, and are computed over all impostor pairs regardless of age, sex, and place of birth. The plotted FMR values are broadly an order of magnitude larger than the nominal rates because FMR is computed over demographically-matched impostor pairs i.e individuals of the same sex, from the same geographic region (see section 3.6.1), and the same age group (see section 3.6.2).

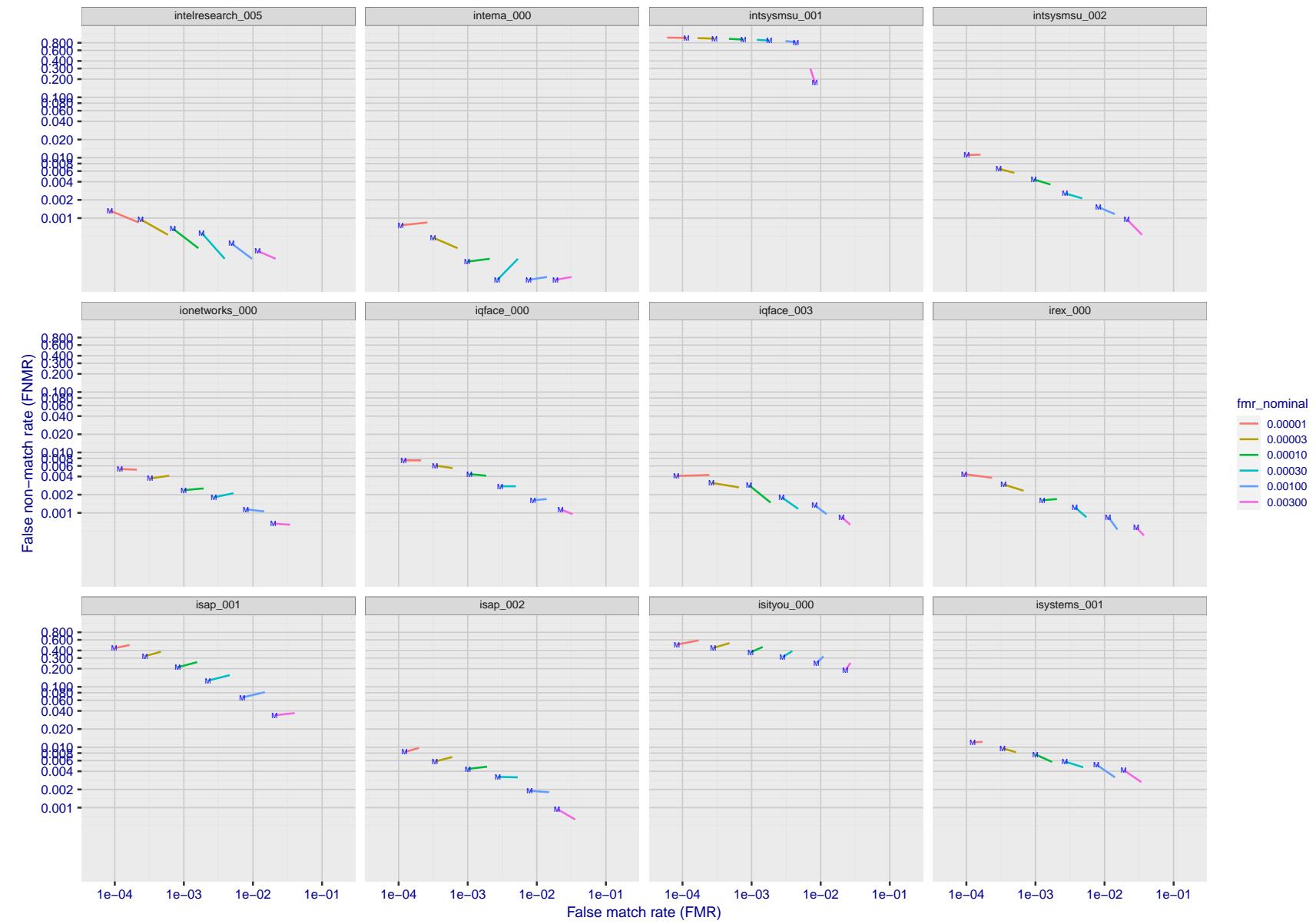


Figure 198: For the visa images, FNMR and FMR at six operating points along the DET characteristic. At each point a line is drawn between $(FMR, FNMR)_{MALE}$ and $(FMR, FNMR)_{FEMALE}$ showing how which sex has lower FMR and/or FNMR. The "M" label denotes male, the other end of the line corresponds to female. The six operating thresholds are selected to give the nominal false match rates given in the legend, and are computed over all impostor pairs regardless of age, sex, and place of birth. The plotted FMR values are broadly an order of magnitude larger than the nominal rates because FMR is computed over demographically-matched impostor pairs i.e individuals of the same sex, from the same geographic region (see section 3.6.1), and the same age group (see section 3.6.2).

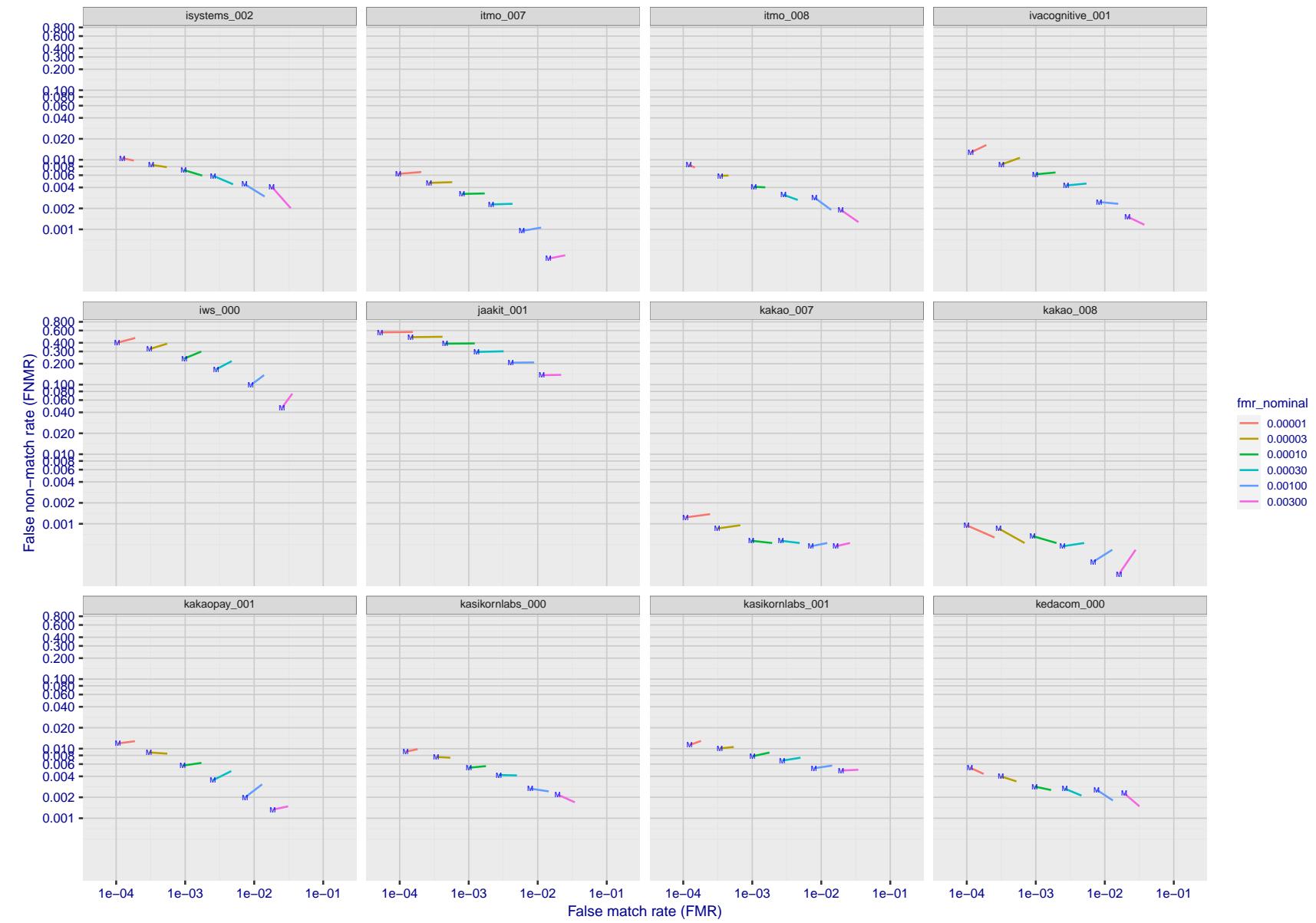


Figure 199: For the visa images, FNMR and FMR at six operating points along the DET characteristic. At each point a line is drawn between $(FMR, FNMR)_{MALE}$ and $(FMR, FNMR)_{FEMALE}$ showing how which sex has lower FMR and/or FNMR. The "M" label denotes male, the other end of the line corresponds to female. The six operating thresholds are selected to give the nominal false match rates given in the legend, and are computed over all impostor pairs regardless of age, sex, and place of birth. The plotted FMR values are broadly an order of magnitude larger than the nominal rates because FMR is computed over demographically-matched impostor pairs i.e individuals of the same sex, from the same geographic region (see section 3.6.1), and the same age group (see section 3.6.2).

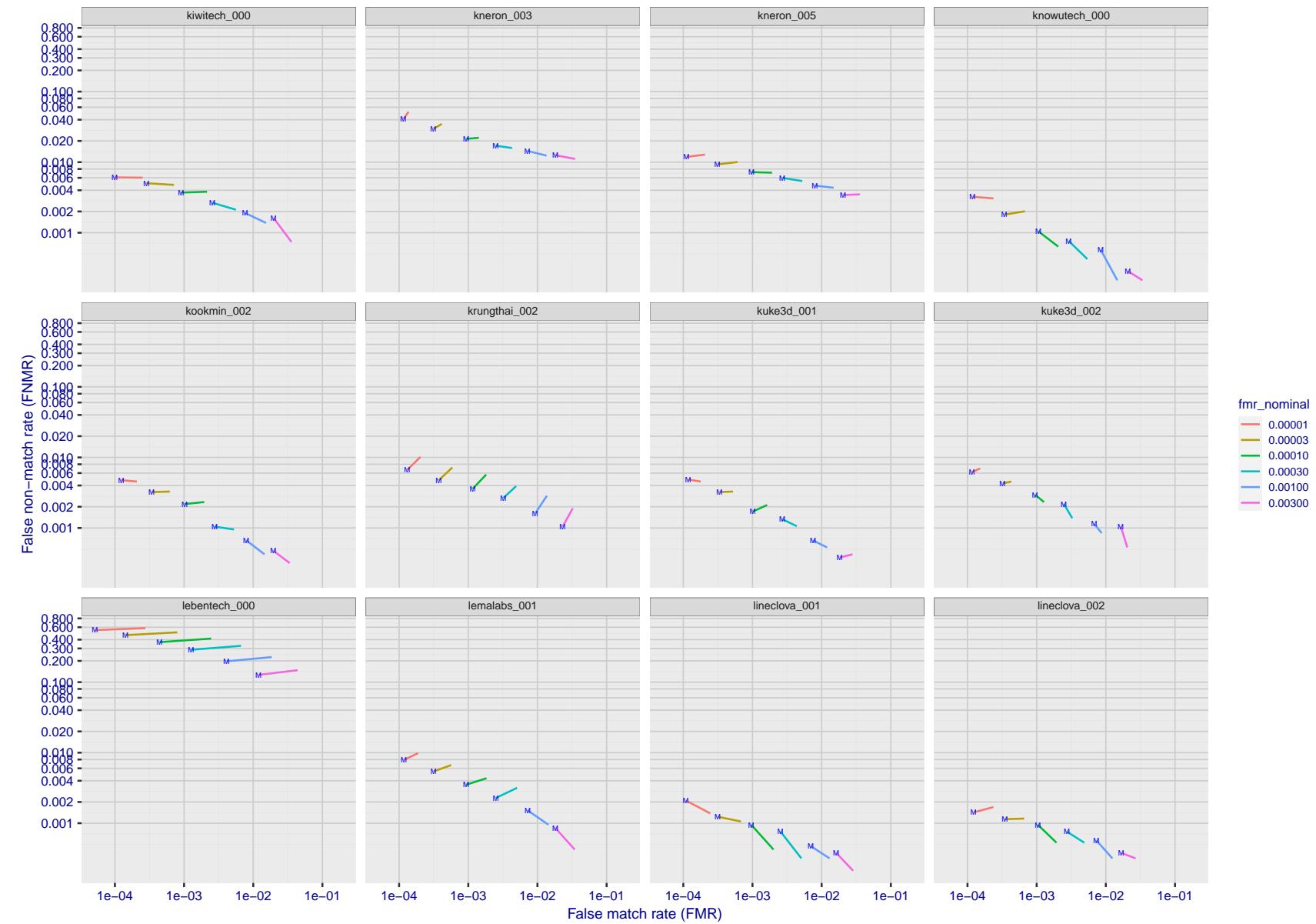


Figure 200: For the visa images, FNMR and FMR at six operating points along the DET characteristic. At each point a line is drawn between $(FMR, FNMR)_{MALE}$ and $(FMR, FNMR)_{FEMALE}$ showing how which sex has lower FMR and/or FNMR. The "M" label denotes male, the other end of the line corresponds to female. The six operating thresholds are selected to give the nominal false match rates given in the legend, and are computed over all impostor pairs regardless of age, sex, and place of birth. The plotted FMR values are broadly an order of magnitude larger than the nominal rates because FMR is computed over demographically-matched impostor pairs i.e individuals of the same sex, from the same geographic region (see section 3.6.1), and the same age group (see section 3.6.2).

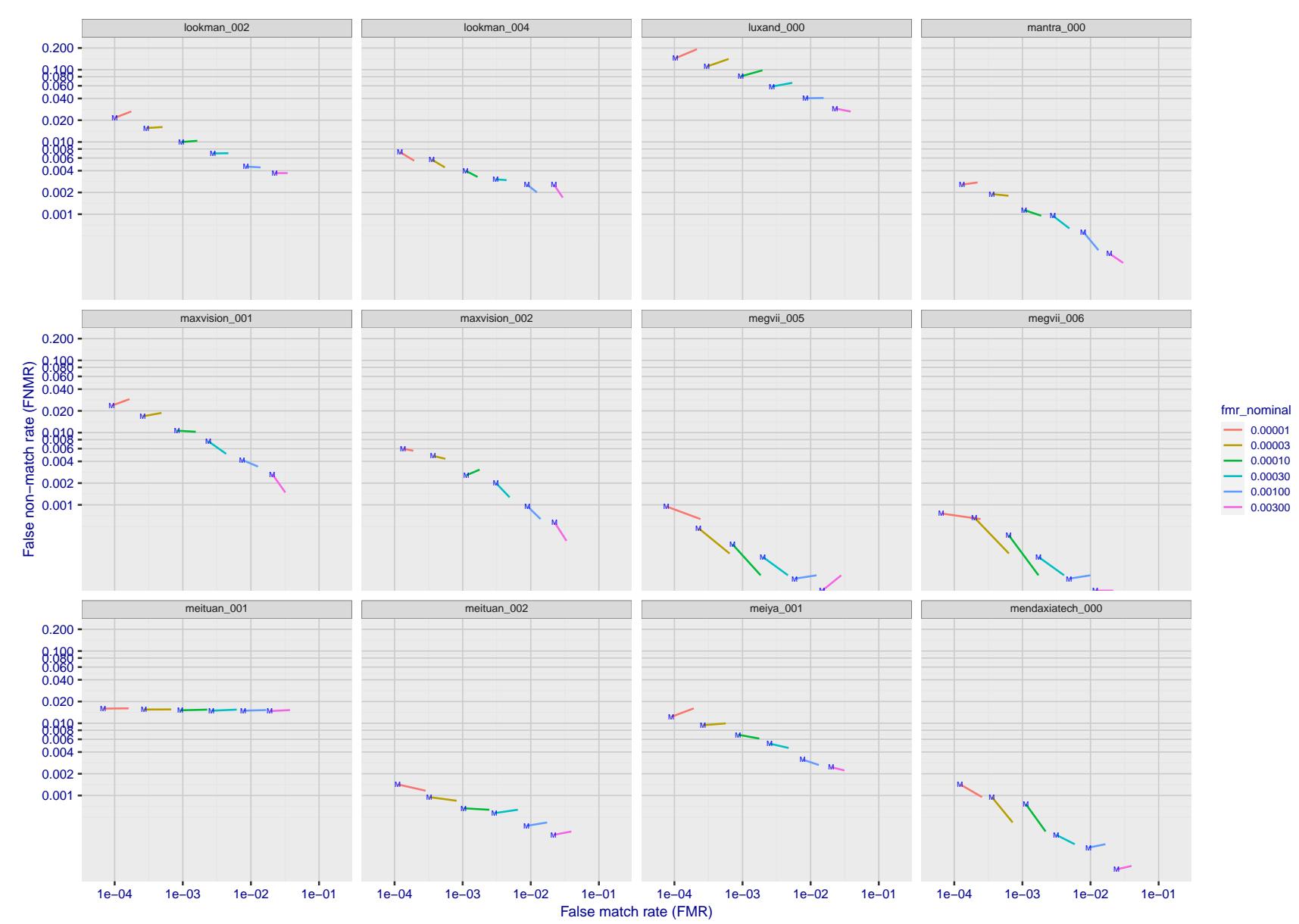


Figure 201: For the visa images, FNMR and FMR at six operating points along the DET characteristic. At each point a line is drawn between $(FMR, FNMR)_{MALE}$ and $(FMR, FNMR)_{FEMALE}$ showing how which sex has lower FMR and/or FNMR. The "M" label denotes male, the other end of the line corresponds to female. The six operating thresholds are selected to give the nominal false match rates given in the legend, and are computed over all impostor pairs regardless of age, sex, and place of birth. The plotted FMR values are broadly an order of magnitude larger than the nominal rates because FMR is computed over demographically-matched impostor pairs i.e individuals of the same sex, from the same geographic region (see section 3.6.1), and the same age group (see section 3.6.2).

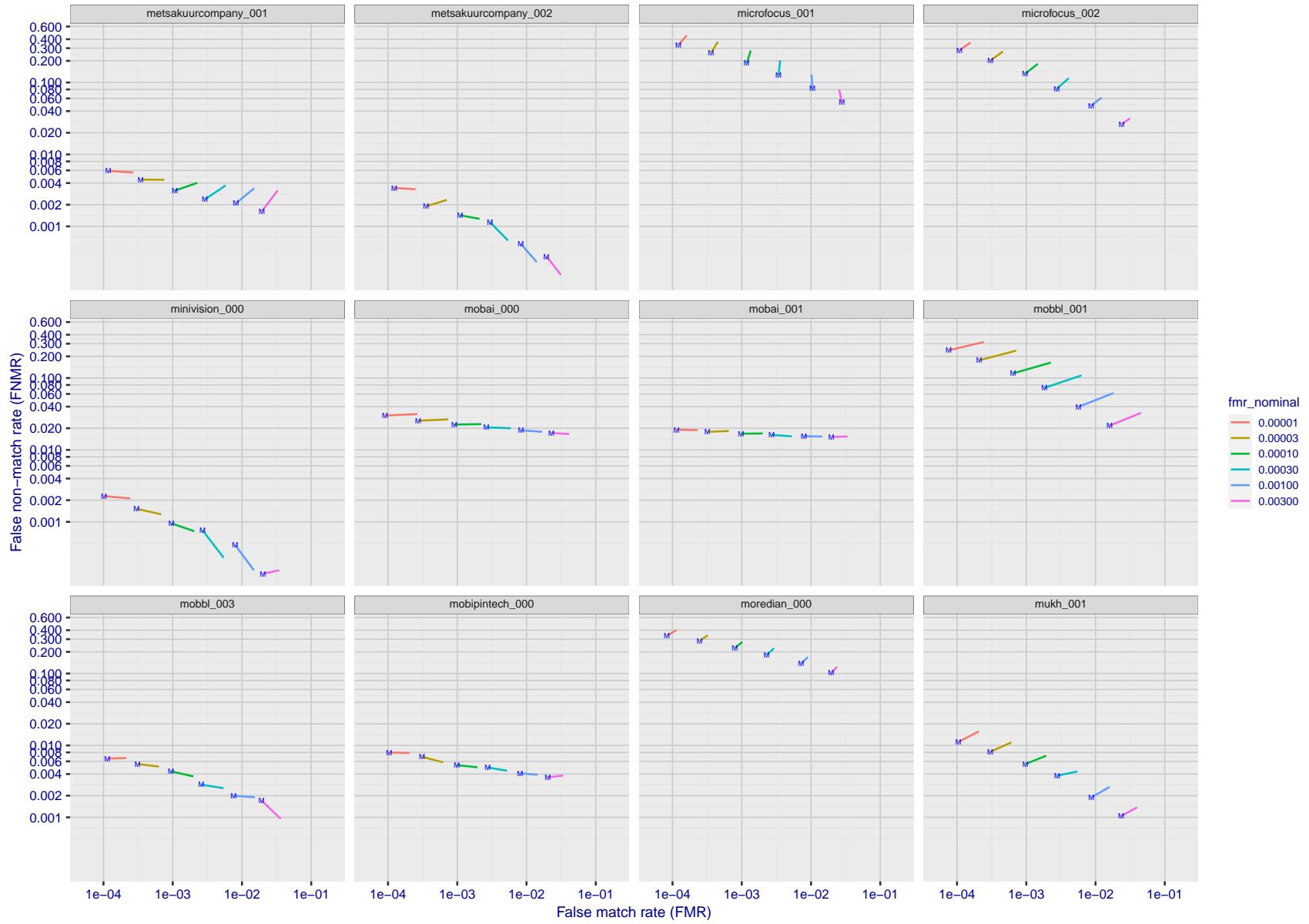


Figure 202: For the visa images, FNMR and FMR at six operating points along the DET characteristic. At each point a line is drawn between $(FMR, FNMR)_{MALE}$ and $(FMR, FNMR)_{FEMALE}$ showing how which sex has lower FMR and/or FNMR. The "M" label denotes male, the other end of the line corresponds to female. The six operating thresholds are selected to give the nominal false match rates given in the legend, and are computed over all impostor pairs regardless of age, sex, and place of birth. The plotted FMR values are broadly an order of magnitude larger than the nominal rates because FMR is computed over demographically-matched impostor pairs i.e individuals of the same sex, from the same geographic region (see section 3.6.1), and the same age group (see section 3.6.2).

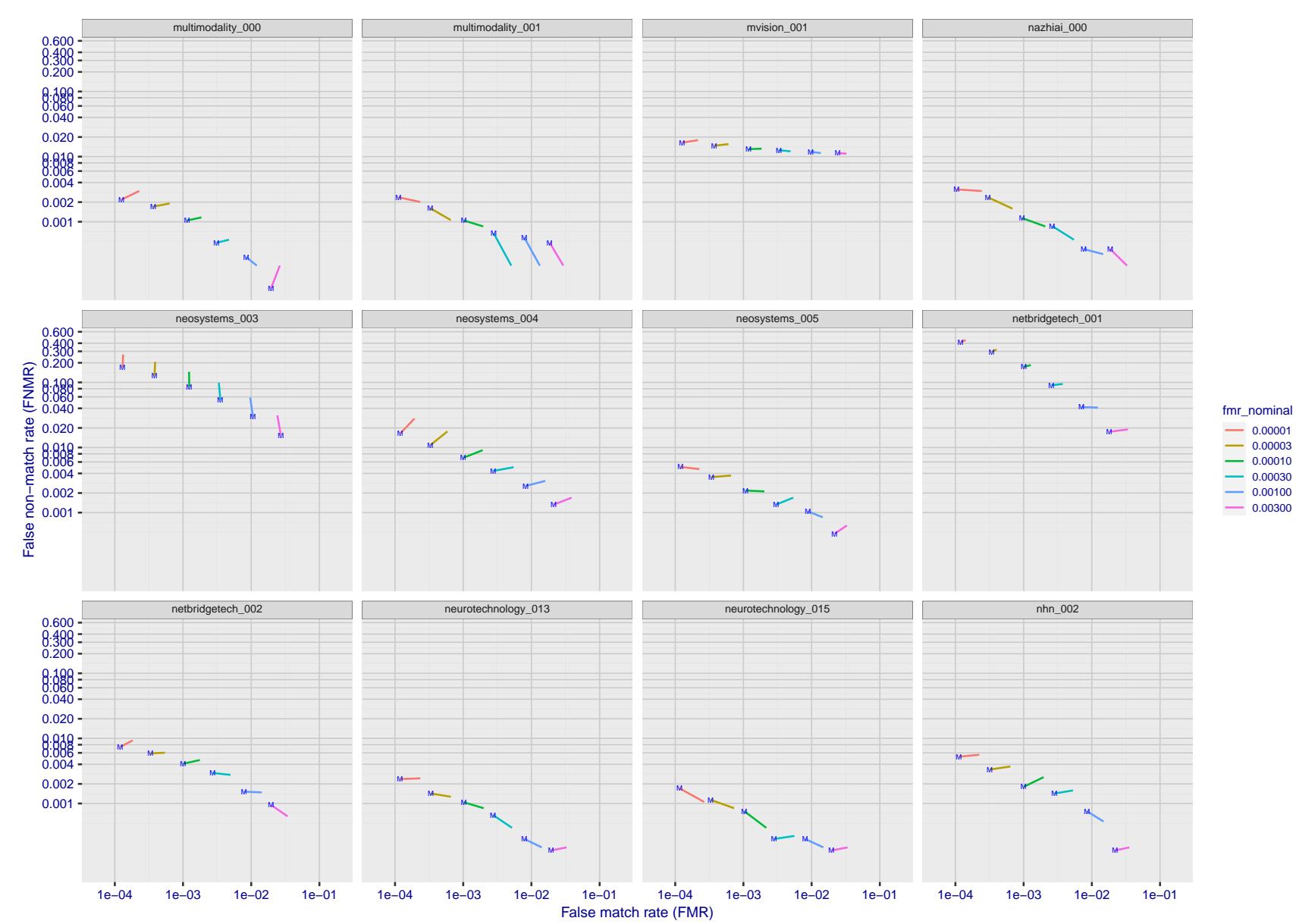


Figure 203: For the visa images, FNMR and FMR at six operating points along the DET characteristic. At each point a line is drawn between $(FMR, FNMR)_{MALE}$ and $(FMR, FNMR)_{FEMALE}$ showing how which sex has lower FMR and/or FNMR. The "M" label denotes male, the other end of the line corresponds to female. The six operating thresholds are selected to give the nominal false match rates given in the legend, and are computed over all impostor pairs regardless of age, sex, and place of birth. The plotted FMR values are broadly an order of magnitude larger than the nominal rates because FMR is computed over demographically-matched impostor pairs i.e individuals of the same sex, from the same geographic region (see section 3.6.1), and the same age group (see section 3.6.2).

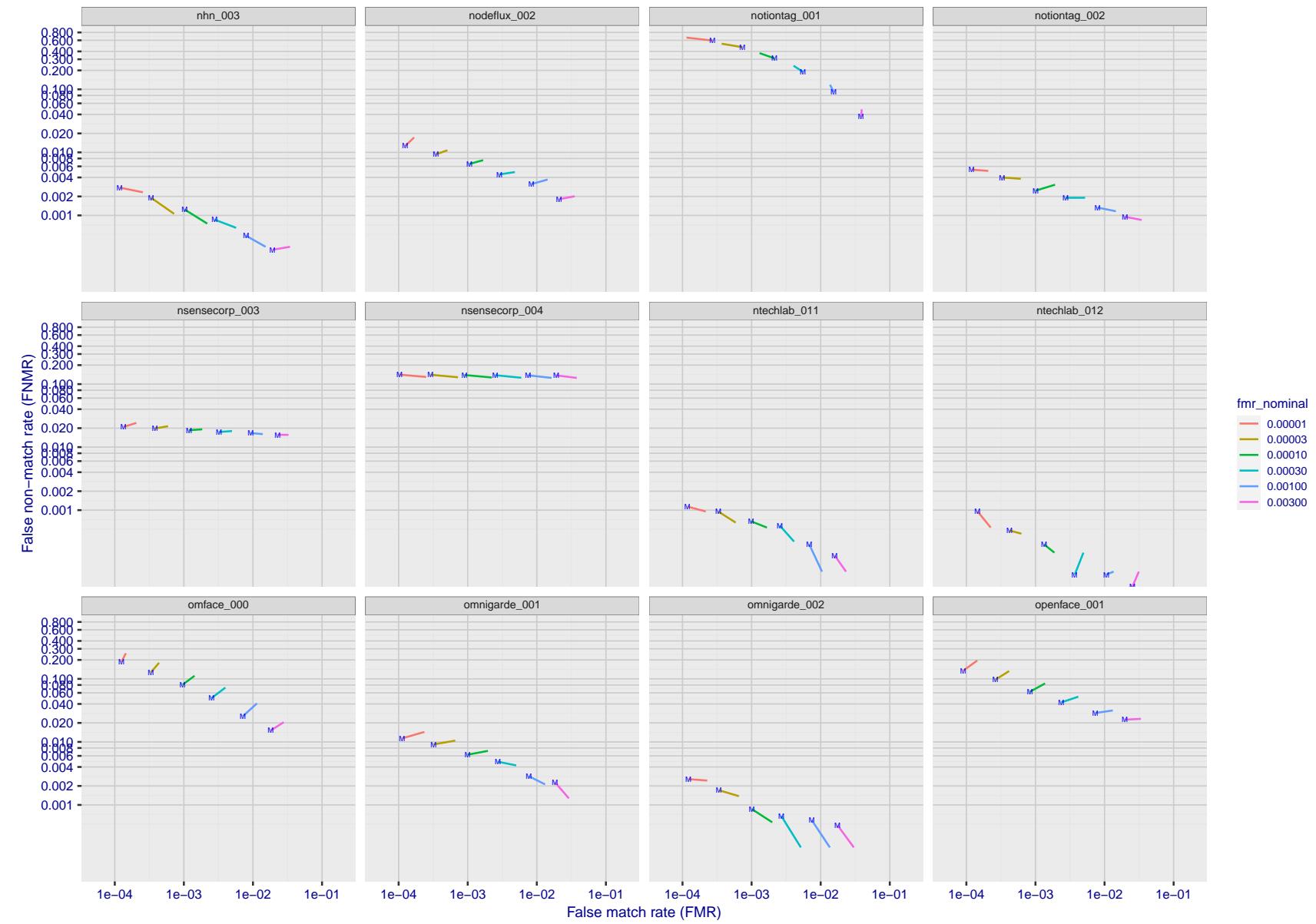


Figure 204: For the visa images, FNMR and FMR at six operating points along the DET characteristic. At each point a line is drawn between $(FMR, FNMR)_{MALE}$ and $(FMR, FNMR)_{FEMALE}$ showing how which sex has lower FMR and/or FNMR. The "M" label denotes male, the other end of the line corresponds to female. The six operating thresholds are selected to give the nominal false match rates given in the legend, and are computed over all impostor pairs regardless of age, sex, and place of birth. The plotted FMR values are broadly an order of magnitude larger than the nominal rates because FMR is computed over demographically-matched impostor pairs i.e individuals of the same sex, from the same geographic region (see section 3.6.1), and the same age group (see section 3.6.2).

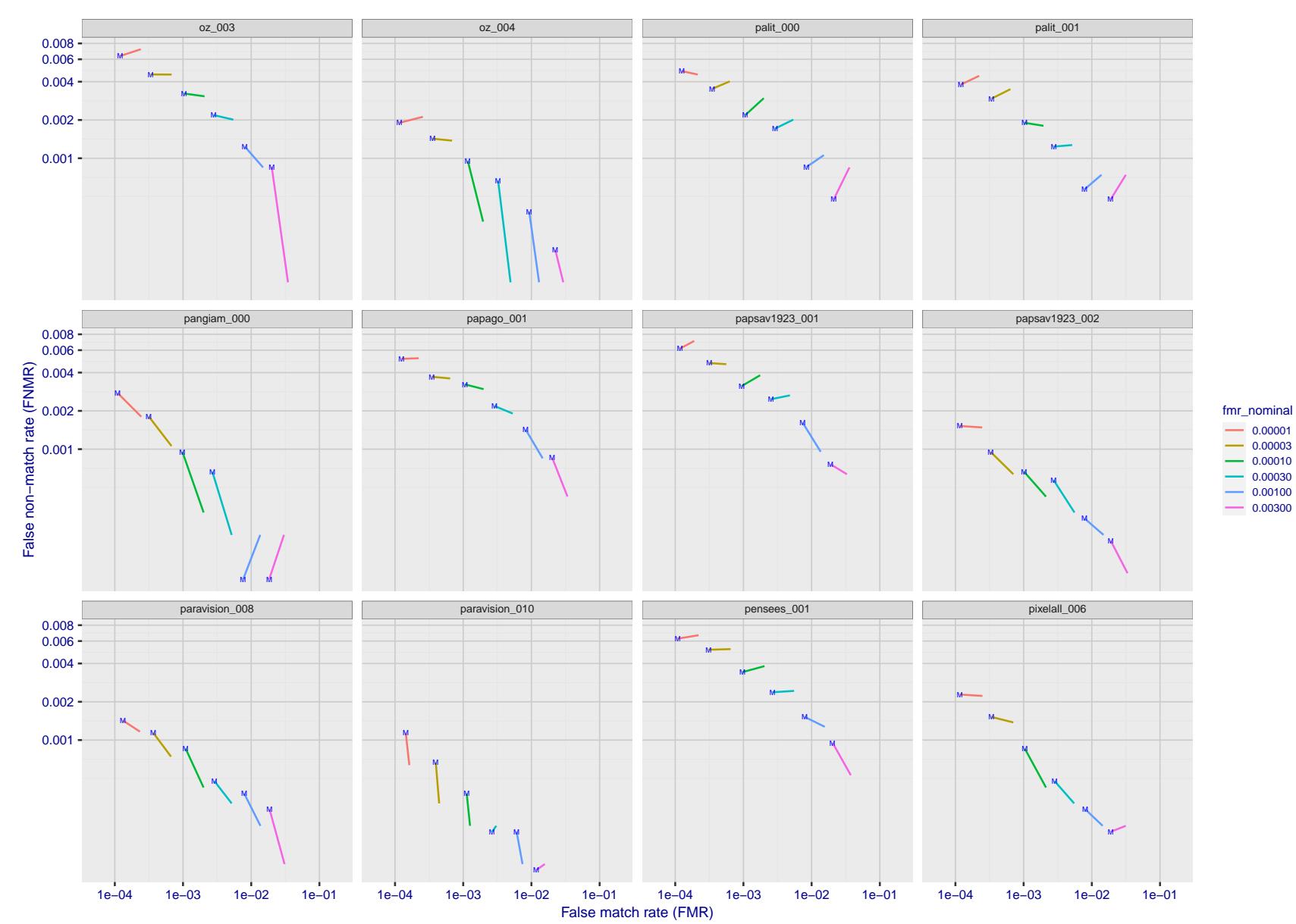


Figure 205: For the visa images, FNMR and FMR at six operating points along the DET characteristic. At each point a line is drawn between $(FMR, FNMR)_{MALE}$ and $(FMR, FNMR)_{FEMALE}$ showing how which sex has lower FMR and/or FNMR. The "M" label denotes male, the other end of the line corresponds to female. The six operating thresholds are selected to give the nominal false match rates given in the legend, and are computed over all impostor pairs regardless of age, sex, and place of birth. The plotted FMR values are broadly an order of magnitude larger than the nominal rates because FMR is computed over demographically-matched impostor pairs i.e individuals of the same sex, from the same geographic region (see section 3.6.1), and the same age group (see section 3.6.2).

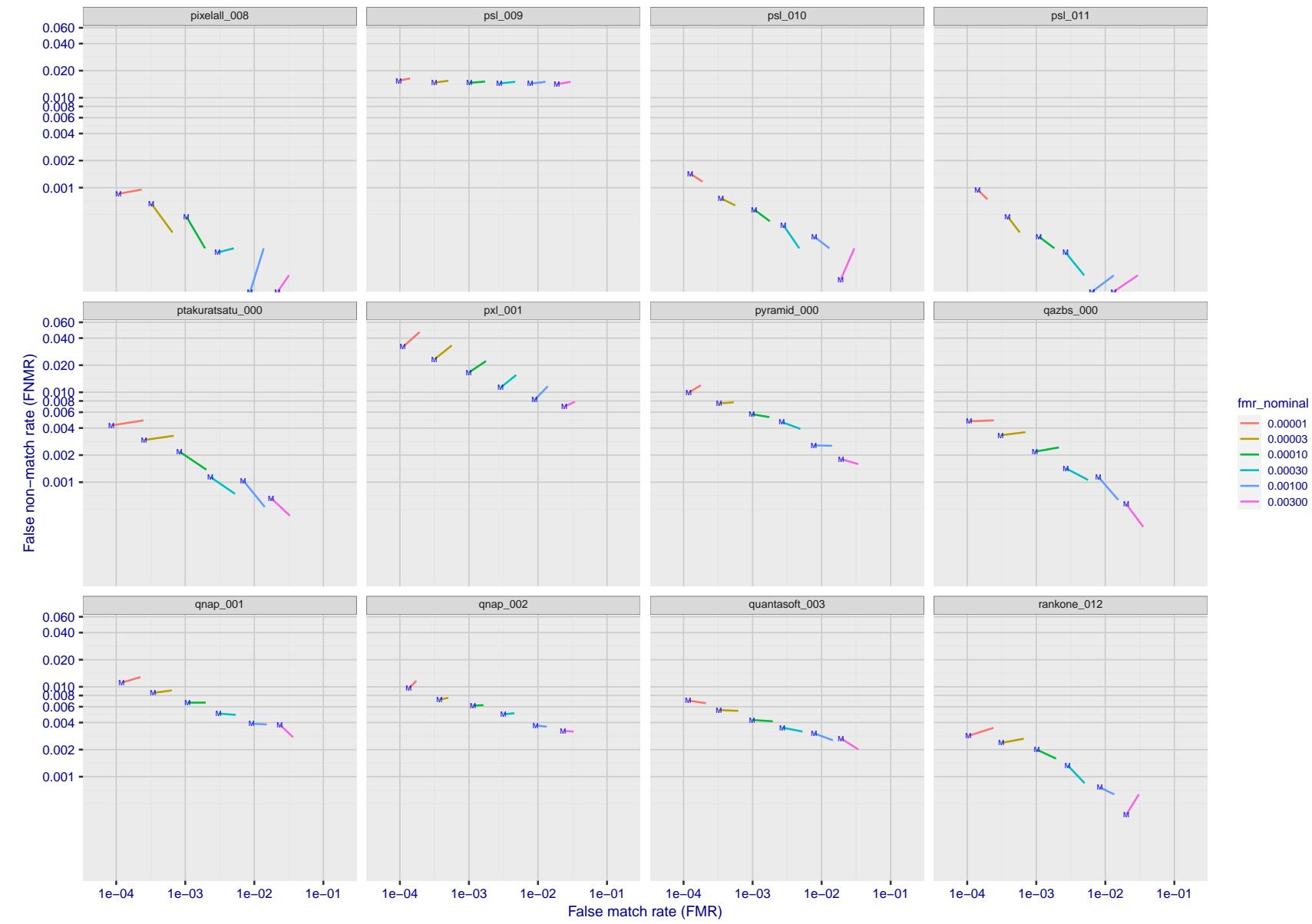


Figure 206: For the visa images, FNMR and FMR at six operating points along the DET characteristic. At each point a line is drawn between $(FMR, FNMR)_{MALE}$ and $(FMR, FNMR)_{FEMALE}$ showing how which sex has lower FMR and/or FNMR. The "M" label denotes male, the other end of the line corresponds to female. The six operating thresholds are selected to give the nominal false match rates given in the legend, and are computed over all impostor pairs regardless of age, sex, and place of birth. The plotted FMR values are broadly an order of magnitude larger than the nominal rates because FMR is computed over demographically-matched impostor pairs i.e individuals of the same sex, from the same geographic region (see section 3.6.1), and the same age group (see section 3.6.2).

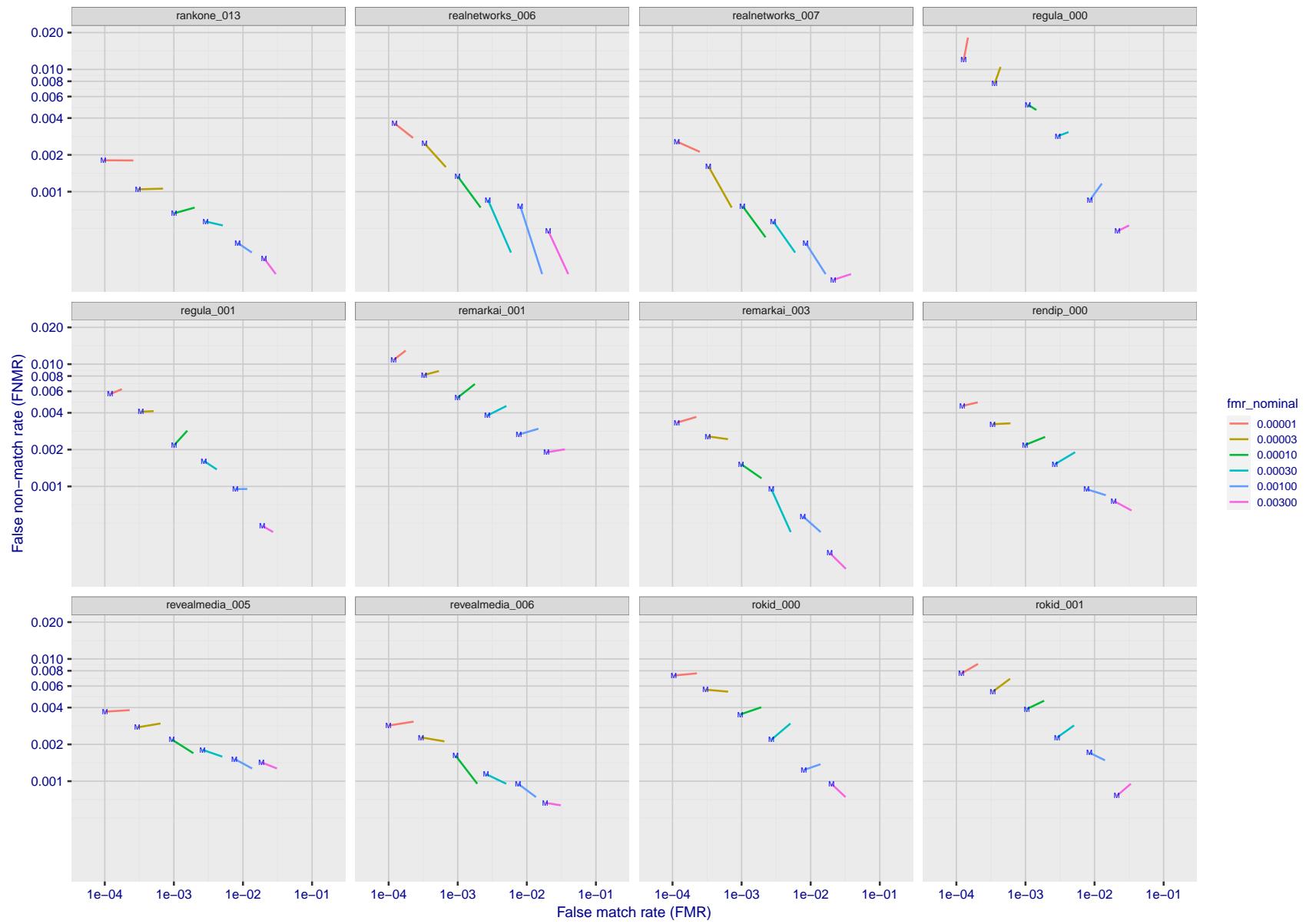


Figure 207: For the visa images, FNMR and FMR at six operating points along the DET characteristic. At each point a line is drawn between $(FMR, FNMR)_{MALE}$ and $(FMR, FNMR)_{FEMALE}$ showing how which sex has lower FMR and/or FNMR. The "M" label denotes male, the other end of the line corresponds to female. The six operating thresholds are selected to give the nominal false match rates given in the legend, and are computed over all impostor pairs regardless of age, sex, and place of birth. The plotted FMR values are broadly an order of magnitude larger than the nominal rates because FMR is computed over demographically-matched impostor pairs i.e individuals of the same sex, from the same geographic region (see section 3.6.1), and the same age group (see section 3.6.2).

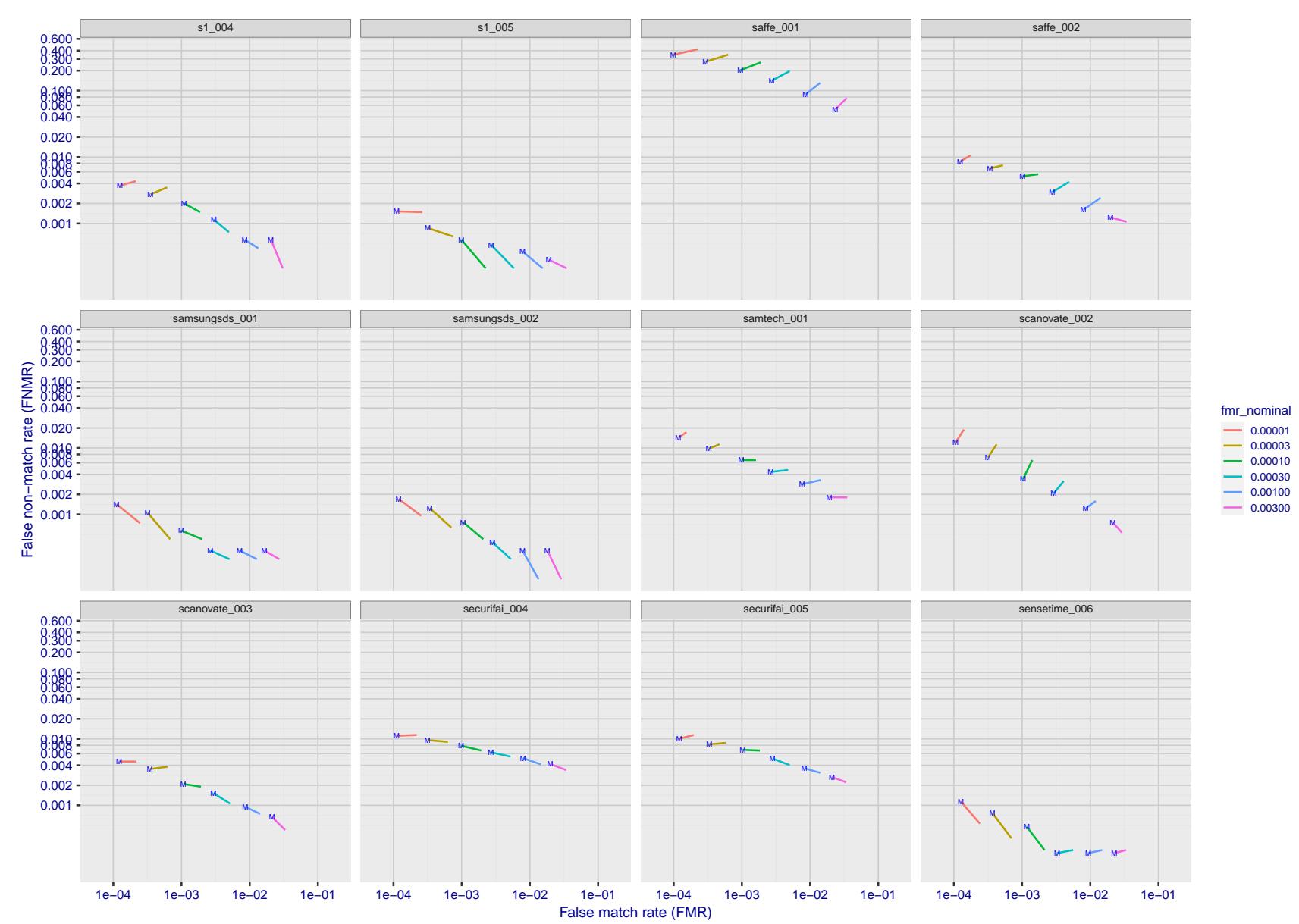


Figure 208: For the visa images, FNMR and FMR at six operating points along the DET characteristic. At each point a line is drawn between $(FMR, FNMR)_{MALE}$ and $(FMR, FNMR)_{FEMALE}$ showing how which sex has lower FMR and/or FNMR. The "M" label denotes male, the other end of the line corresponds to female. The six operating thresholds are selected to give the nominal false match rates given in the legend, and are computed over all impostor pairs regardless of age, sex, and place of birth. The plotted FMR values are broadly an order of magnitude larger than the nominal rates because FMR is computed over demographically-matched impostor pairs i.e individuals of the same sex, from the same geographic region (see section 3.6.1), and the same age group (see section 3.6.2).

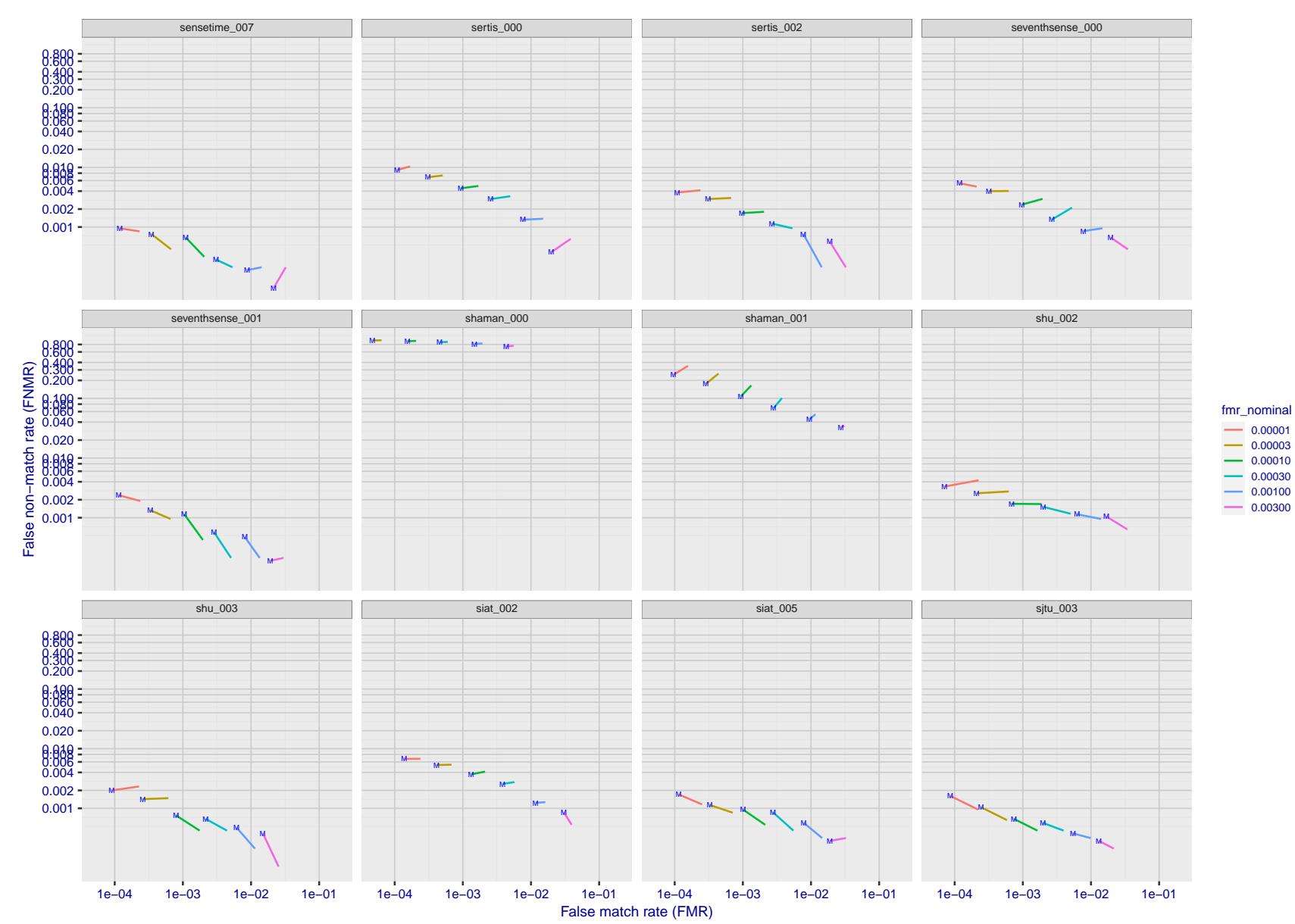


Figure 209: For the visa images, FNMR and FMR at six operating points along the DET characteristic. At each point a line is drawn between $(FMR, FNMR)_{MALE}$ and $(FMR, FNMR)_{FEMALE}$ showing how which sex has lower FMR and/or FNMR. The "M" label denotes male, the other end of the line corresponds to female. The six operating thresholds are selected to give the nominal false match rates given in the legend, and are computed over all impostor pairs regardless of age, sex, and place of birth. The plotted FMR values are broadly an order of magnitude larger than the nominal rates because FMR is computed over demographically-matched impostor pairs i.e individuals of the same sex, from the same geographic region (see section 3.6.1), and the same age group (see section 3.6.2).

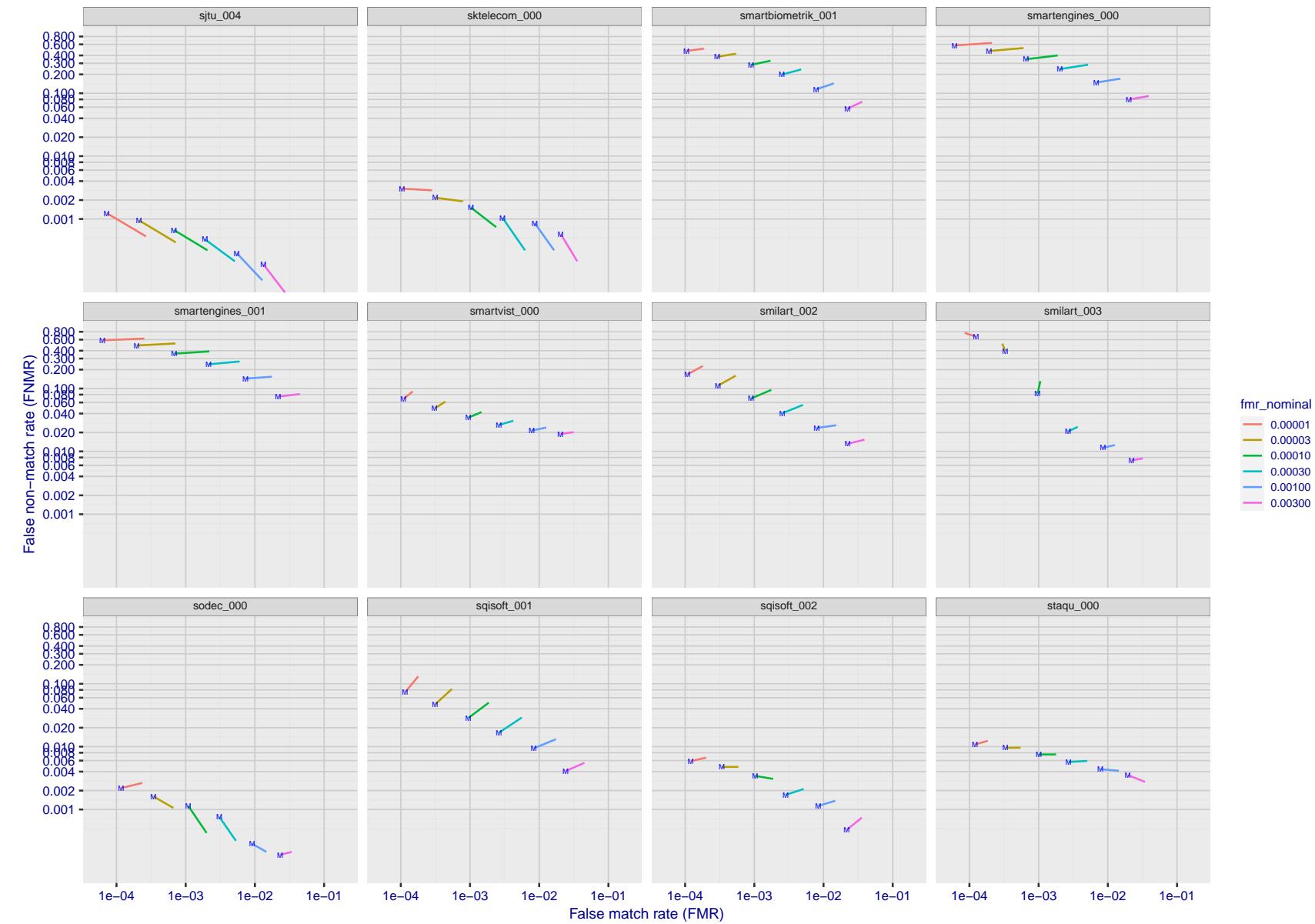


Figure 210: For the visa images, FNMR and FMR at six operating points along the DET characteristic. At each point a line is drawn between $(FMR, FNMR)_{MALE}$ and $(FMR, FNMR)_{FEMALE}$ showing how which sex has lower FMR and/or FNMR. The "M" label denotes male, the other end of the line corresponds to female. The six operating thresholds are selected to give the nominal false match rates given in the legend, and are computed over all impostor pairs regardless of age, sex, and place of birth. The plotted FMR values are broadly an order of magnitude larger than the nominal rates because FMR is computed over demographically-matched impostor pairs i.e individuals of the same sex, from the same geographic region (see section 3.6.1), and the same age group (see section 3.6.2).

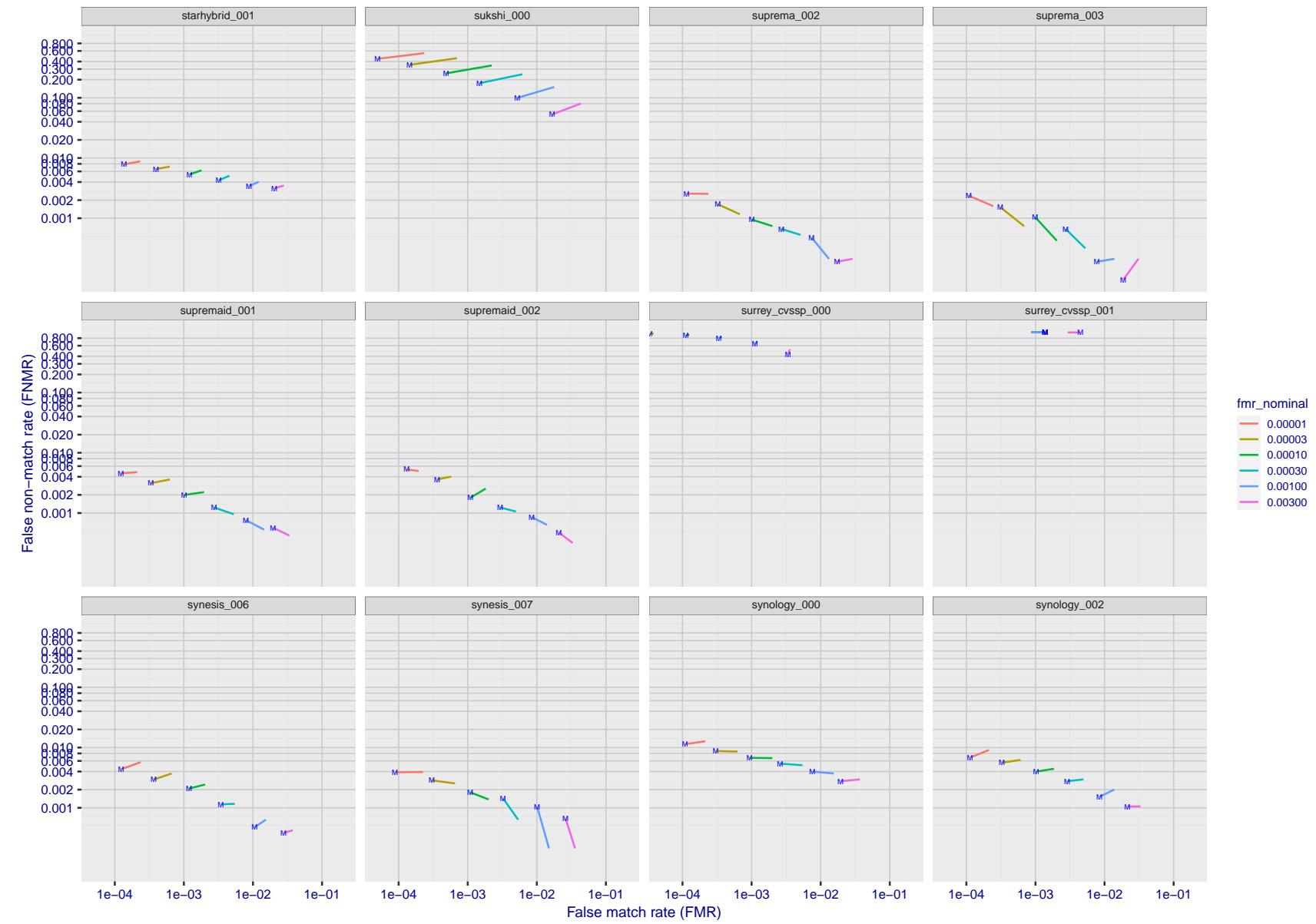


Figure 211: For the visa images, FNMR and FMR at six operating points along the DET characteristic. At each point a line is drawn between $(FMR, FNMR)_{MALE}$ and $(FMR, FNMR)_{FEMALE}$ showing how which sex has lower FMR and/or FNMR. The "M" label denotes male, the other end of the line corresponds to female. The six operating thresholds are selected to give the nominal false match rates given in the legend, and are computed over all impostor pairs regardless of age, sex, and place of birth. The plotted FMR values are broadly an order of magnitude larger than the nominal rates because FMR is computed over demographically-matched impostor pairs i.e individuals of the same sex, from the same geographic region (see section 3.6.1), and the same age group (see section 3.6.2).

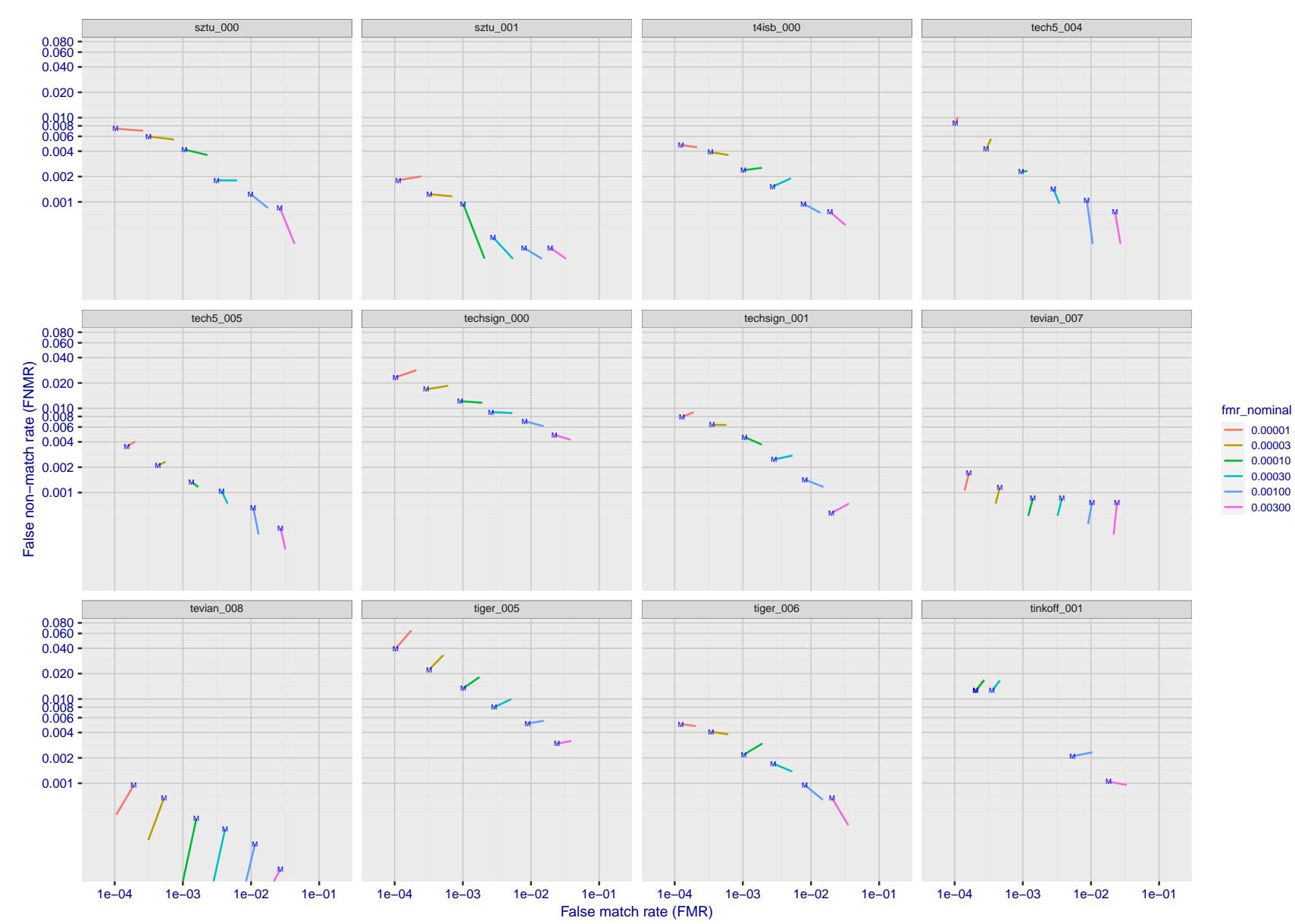


Figure 212: For the visa images, FNMR and FMR at six operating points along the DET characteristic. At each point a line is drawn between $(FMR, FNMR)_{MALE}$ and $(FMR, FNMR)_{FEMALE}$ showing how which sex has lower FMR and/or FNMR. The "M" label denotes male, the other end of the line corresponds to female. The six operating thresholds are selected to give the nominal false match rates given in the legend, and are computed over all impostor pairs regardless of age, sex, and place of birth. The plotted FMR values are broadly an order of magnitude larger than the nominal rates because FMR is computed over demographically-matched impostor pairs i.e individuals of the same sex, from the same geographic region (see section 3.6.1), and the same age group (see section 3.6.2).

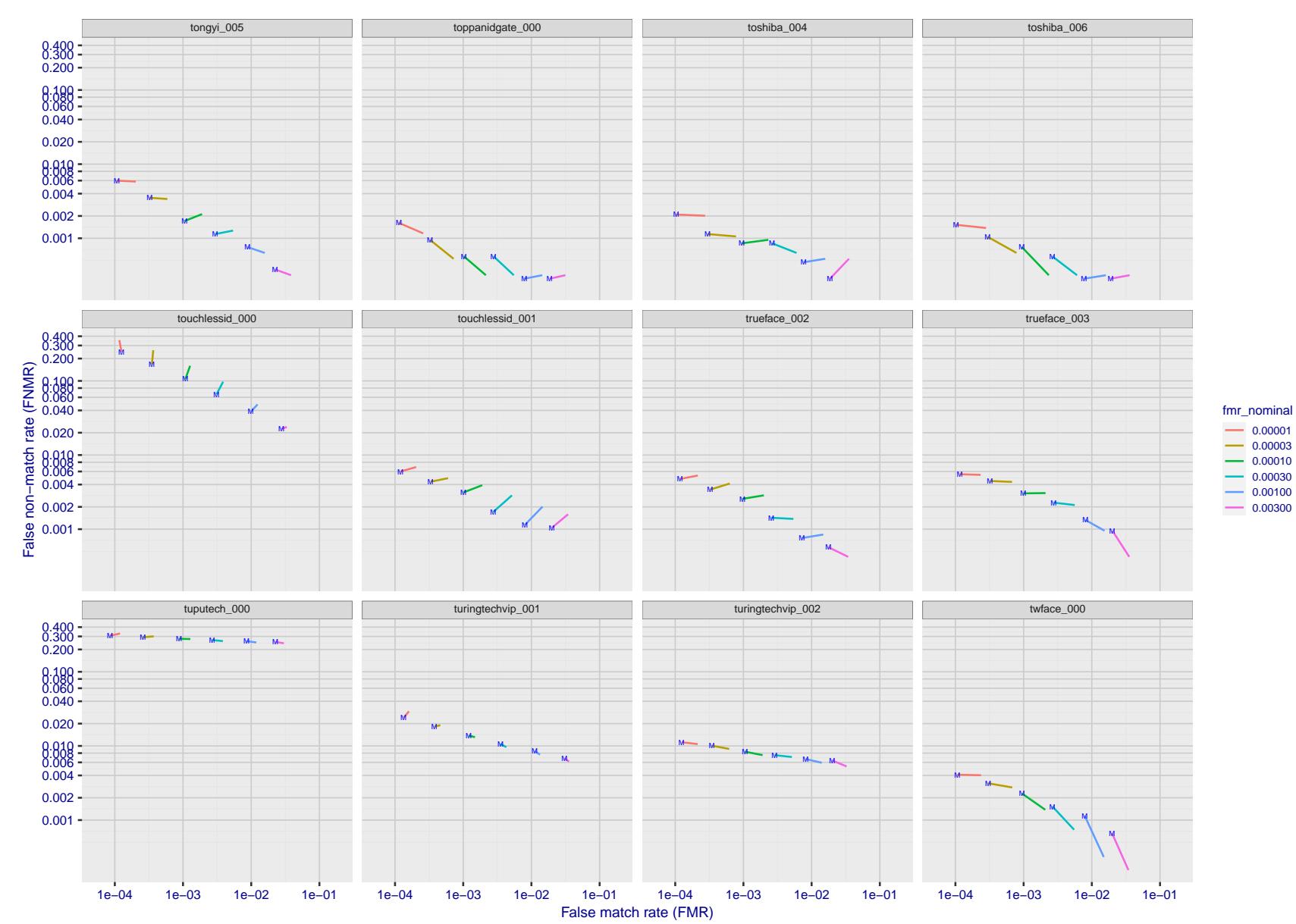


Figure 213: For the visa images, FNMR and FMR at six operating points along the DET characteristic. At each point a line is drawn between $(FMR, FNMR)_{MALE}$ and $(FMR, FNMR)_{FEMALE}$ showing how which sex has lower FMR and/or FNMR. The "M" label denotes male, the other end of the line corresponds to female. The six operating thresholds are selected to give the nominal false match rates given in the legend, and are computed over all impostor pairs regardless of age, sex, and place of birth. The plotted FMR values are broadly an order of magnitude larger than the nominal rates because FMR is computed over demographically-matched impostor pairs i.e individuals of the same sex, from the same geographic region (see section 3.6.1), and the same age group (see section 3.6.2).

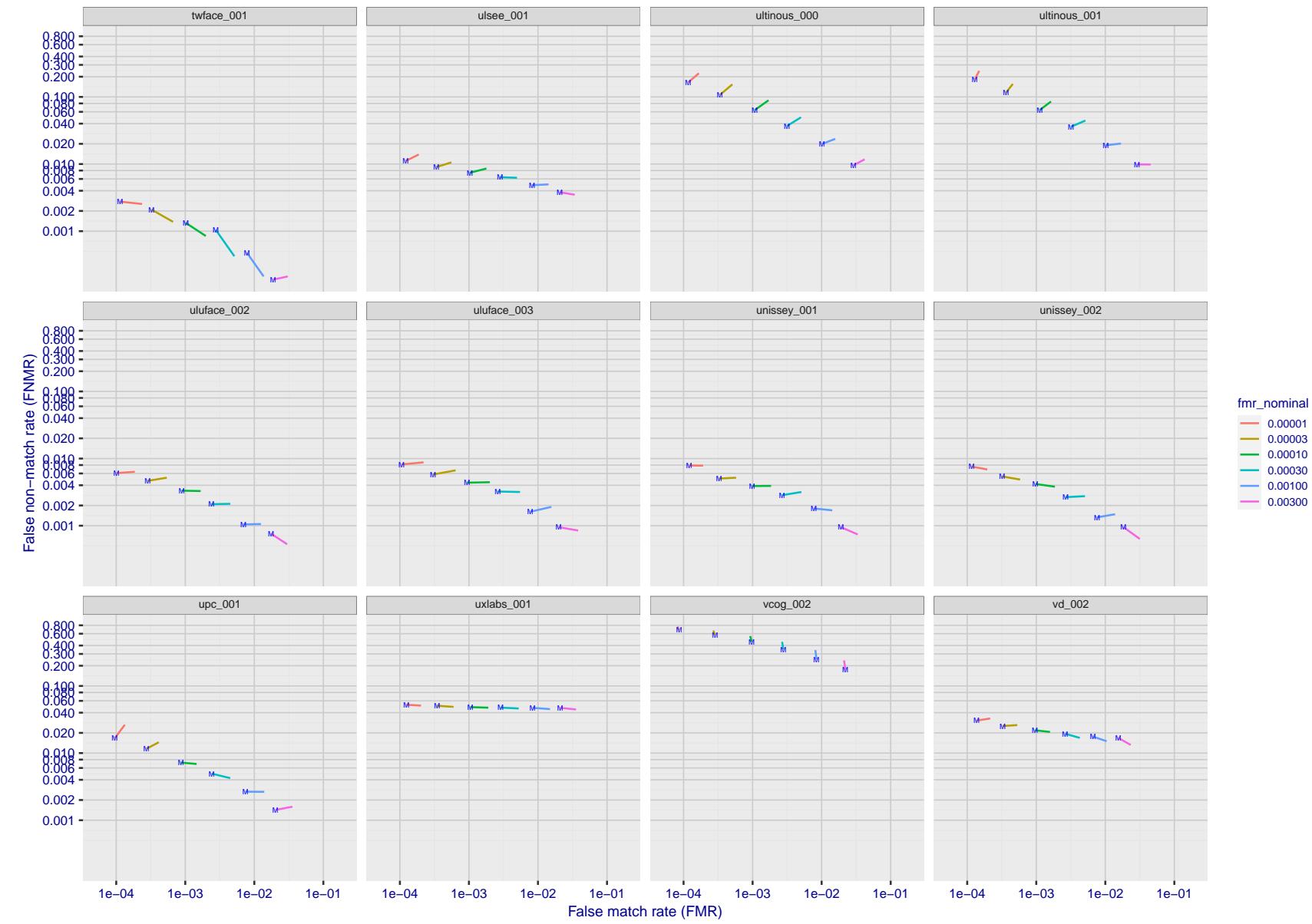


Figure 214: For the visa images, FNMR and FMR at six operating points along the DET characteristic. At each point a line is drawn between $(FMR, FNMR)_{MALE}$ and $(FMR, FNMR)_{FEMALE}$ showing how which sex has lower FMR and/or FNMR. The "M" label denotes male, the other end of the line corresponds to female. The six operating thresholds are selected to give the nominal false match rates given in the legend, and are computed over all impostor pairs regardless of age, sex, and place of birth. The plotted FMR values are broadly an order of magnitude larger than the nominal rates because FMR is computed over demographically-matched impostor pairs i.e individuals of the same sex, from the same geographic region (see section 3.6.1), and the same age group (see section 3.6.2).

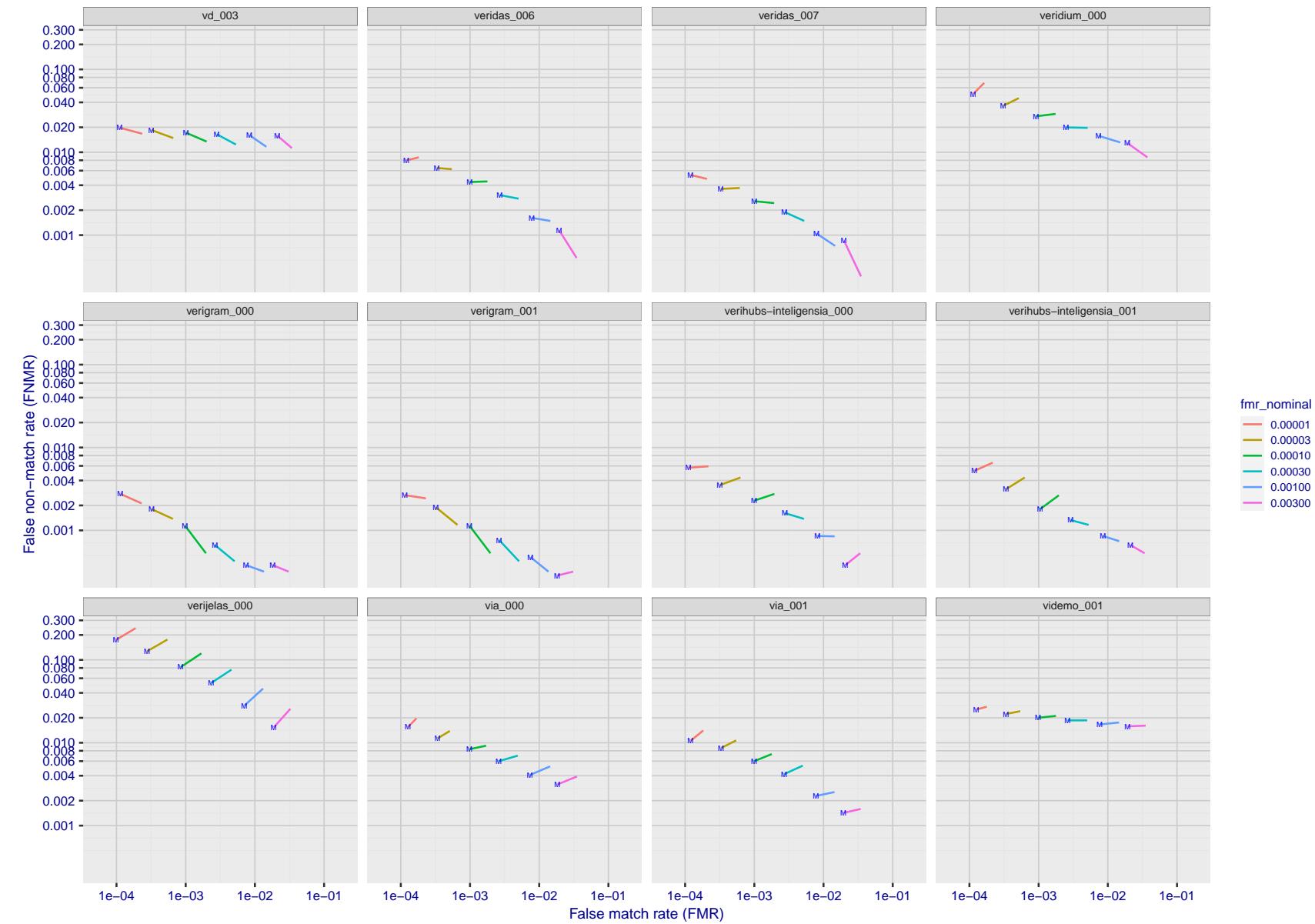


Figure 215: For the visa images, FNMR and FMR at six operating points along the DET characteristic. At each point a line is drawn between $(FMR, FNMR)_{MALE}$ and $(FMR, FNMR)_{FEMALE}$ showing how which sex has lower FMR and/or FNMR. The "M" label denotes male, the other end of the line corresponds to female. The six operating thresholds are selected to give the nominal false match rates given in the legend, and are computed over all impostor pairs regardless of age, sex, and place of birth. The plotted FMR values are broadly an order of magnitude larger than the nominal rates because FMR is computed over demographically-matched impostor pairs i.e individuals of the same sex, from the same geographic region (see section 3.6.1), and the same age group (see section 3.6.2).

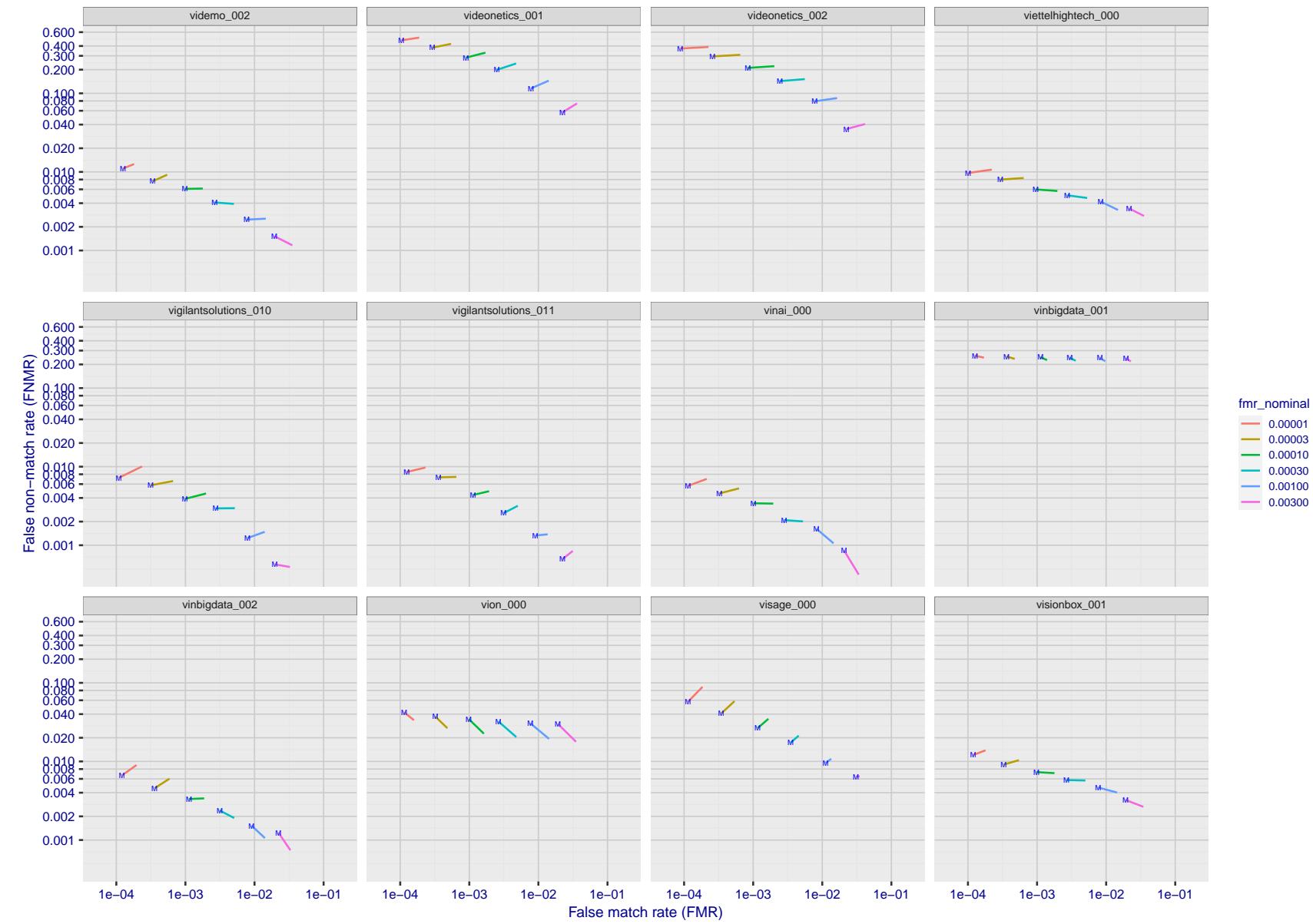


Figure 216: For the visa images, FNMR and FMR at six operating points along the DET characteristic. At each point a line is drawn between $(FMR, FNMR)_{MALE}$ and $(FMR, FNMR)_{FEMALE}$ showing how which sex has lower FMR and/or FNMR. The "M" label denotes male, the other end of the line corresponds to female. The six operating thresholds are selected to give the nominal false match rates given in the legend, and are computed over all impostor pairs regardless of age, sex, and place of birth. The plotted FMR values are broadly an order of magnitude larger than the nominal rates because FMR is computed over demographically-matched impostor pairs i.e individuals of the same sex, from the same geographic region (see section 3.6.1), and the same age group (see section 3.6.2).

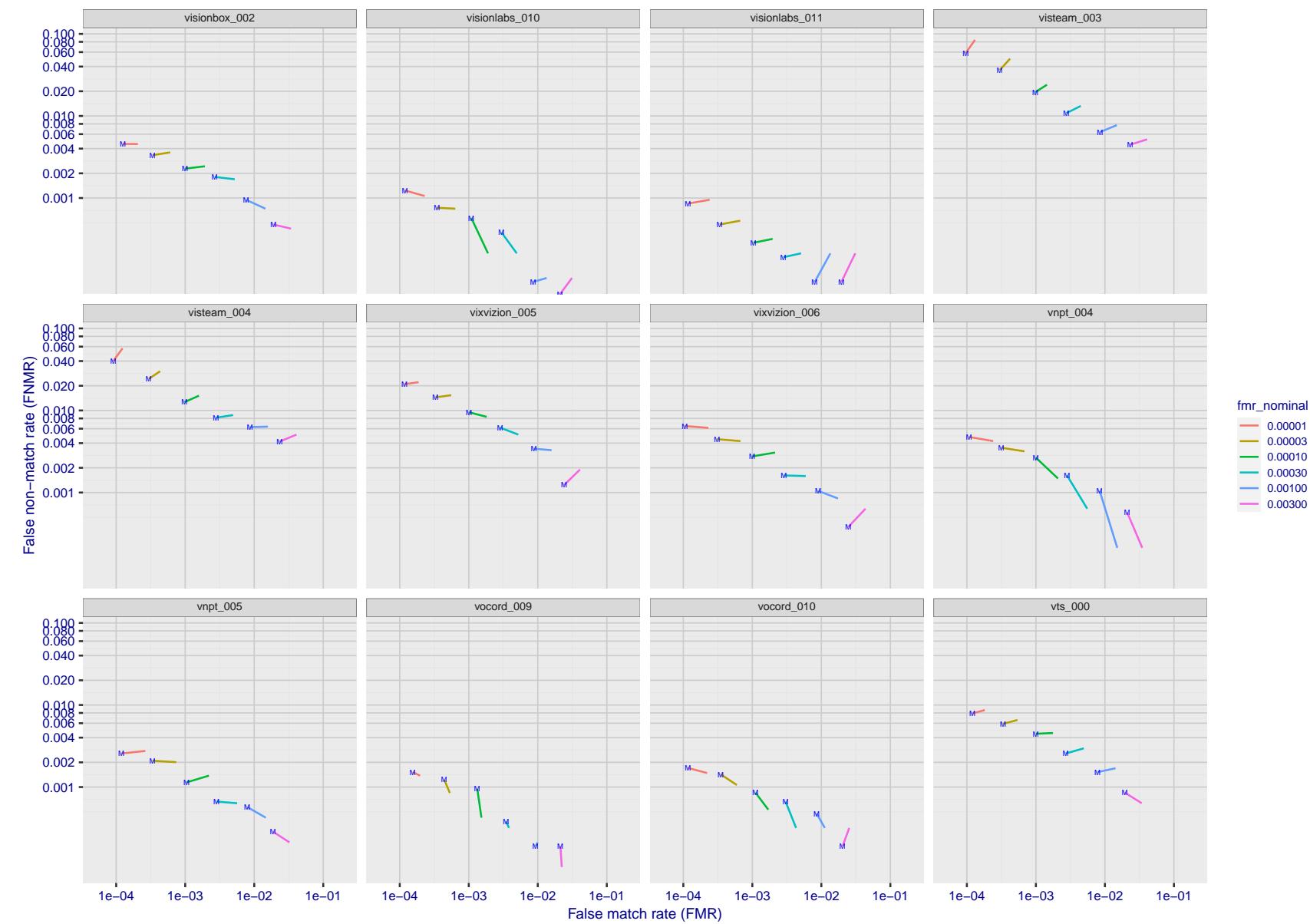


Figure 217: For the visa images, FNMR and FMR at six operating points along the DET characteristic. At each point a line is drawn between $(FMR, FNMR)_{MALE}$ and $(FMR, FNMR)_{FEMALE}$ showing how which sex has lower FMR and/or FNMR. The "M" label denotes male, the other end of the line corresponds to female. The six operating thresholds are selected to give the nominal false match rates given in the legend, and are computed over all impostor pairs regardless of age, sex, and place of birth. The plotted FMR values are broadly an order of magnitude larger than the nominal rates because FMR is computed over demographically-matched impostor pairs i.e individuals of the same sex, from the same geographic region (see section 3.6.1), and the same age group (see section 3.6.2).

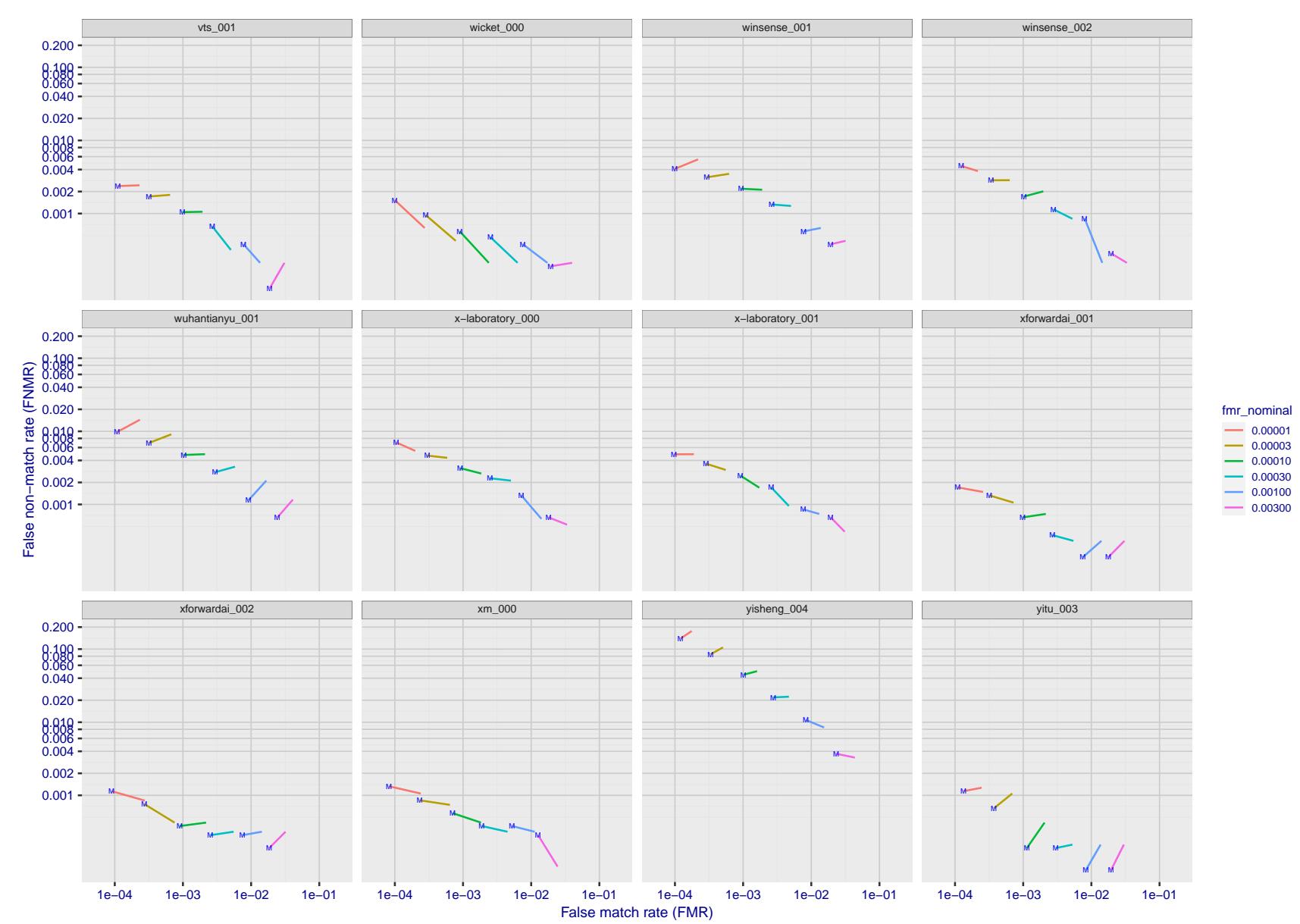


Figure 218: For the visa images, FNMR and FMR at six operating points along the DET characteristic. At each point a line is drawn between $(FMR, FNMR)_{MALE}$ and $(FMR, FNMR)_{FEMALE}$ showing how which sex has lower FMR and/or FNMR. The "M" label denotes male, the other end of the line corresponds to female. The six operating thresholds are selected to give the nominal false match rates given in the legend, and are computed over all impostor pairs regardless of age, sex, and place of birth. The plotted FMR values are broadly an order of magnitude larger than the nominal rates because FMR is computed over demographically-matched impostor pairs i.e individuals of the same sex, from the same geographic region (see section 3.6.1), and the same age group (see section 3.6.2).

2023/02/09 20:10:38

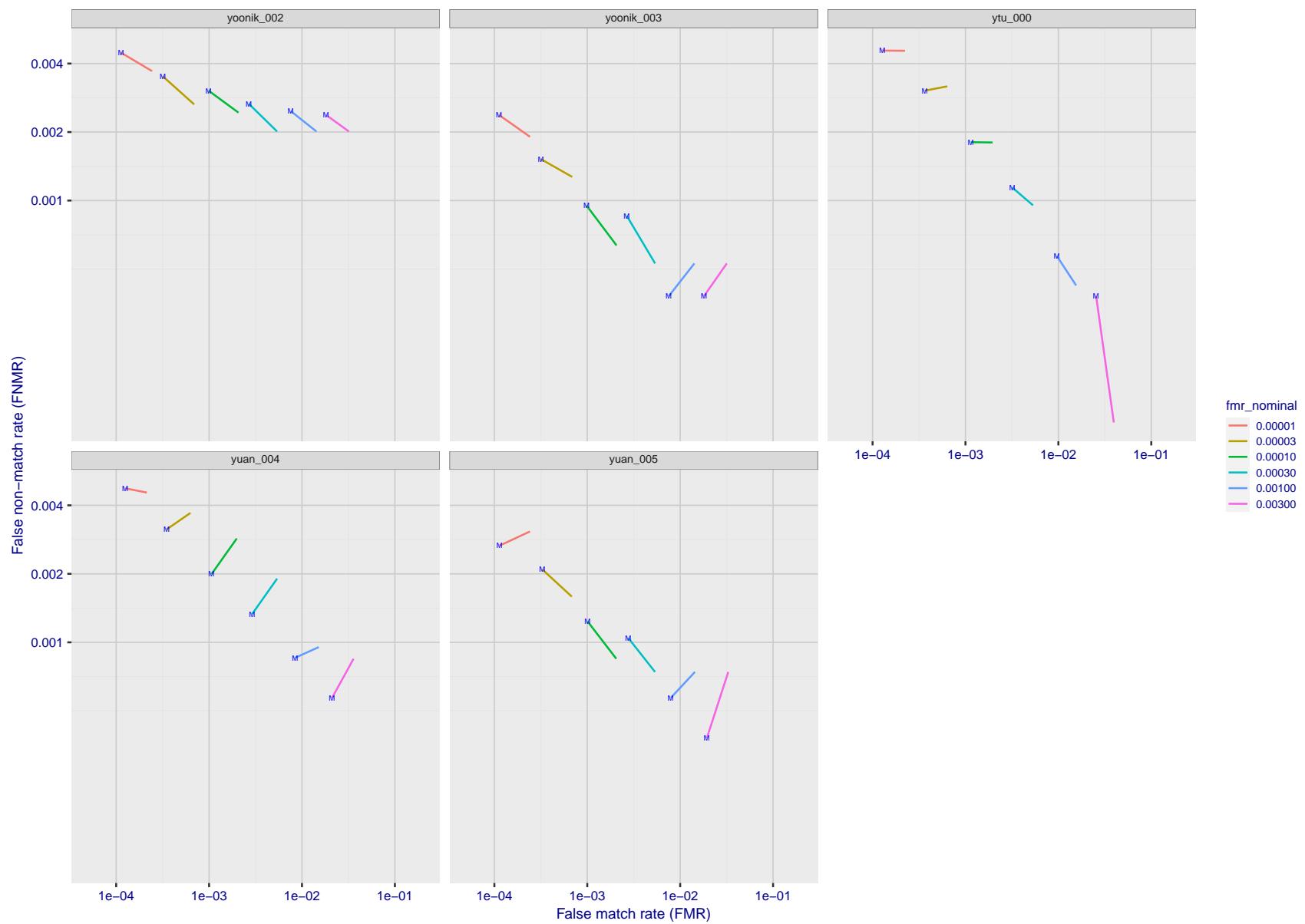


Figure 219: For the visa images, FNMR and FMR at six operating points along the DET characteristic. At each point a line is drawn between $(FMR, FNMR)_{MALE}$ and $(FMR, FNMR)_{FEMALE}$ showing how which sex has lower FMR and/or FNMR. The "M" label denotes male, the other end of the line corresponds to female. The six operating thresholds are selected to give the nominal false match rates given in the legend, and are computed over all impostor pairs regardless of age, sex, and place of birth. The plotted FMR values are broadly an order of magnitude larger than the nominal rates because FMR is computed over demographically-matched impostor pairs i.e individuals of the same sex, from the same geographic region (see section 3.6.1), and the same age group (see section 3.6.2).

FNMR(T)
FMR(T)
"False non-match rate"
"False match rate"

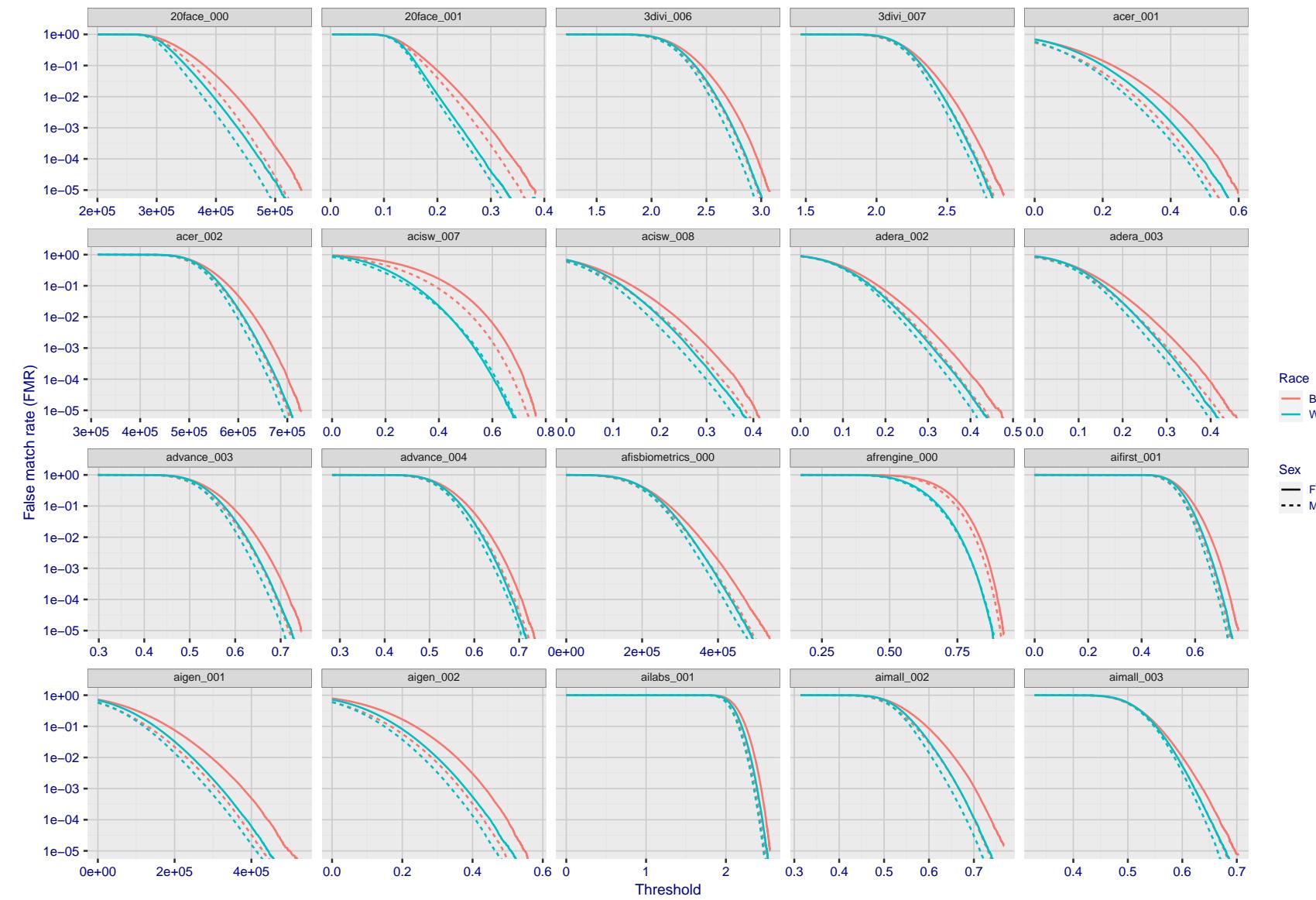


Figure 220: For the mugshot images, the false match calibration curves show false match rate vs. threshold. Separate curves appear for white females, black females, black males and white males.

2023/02/09 20:10:38

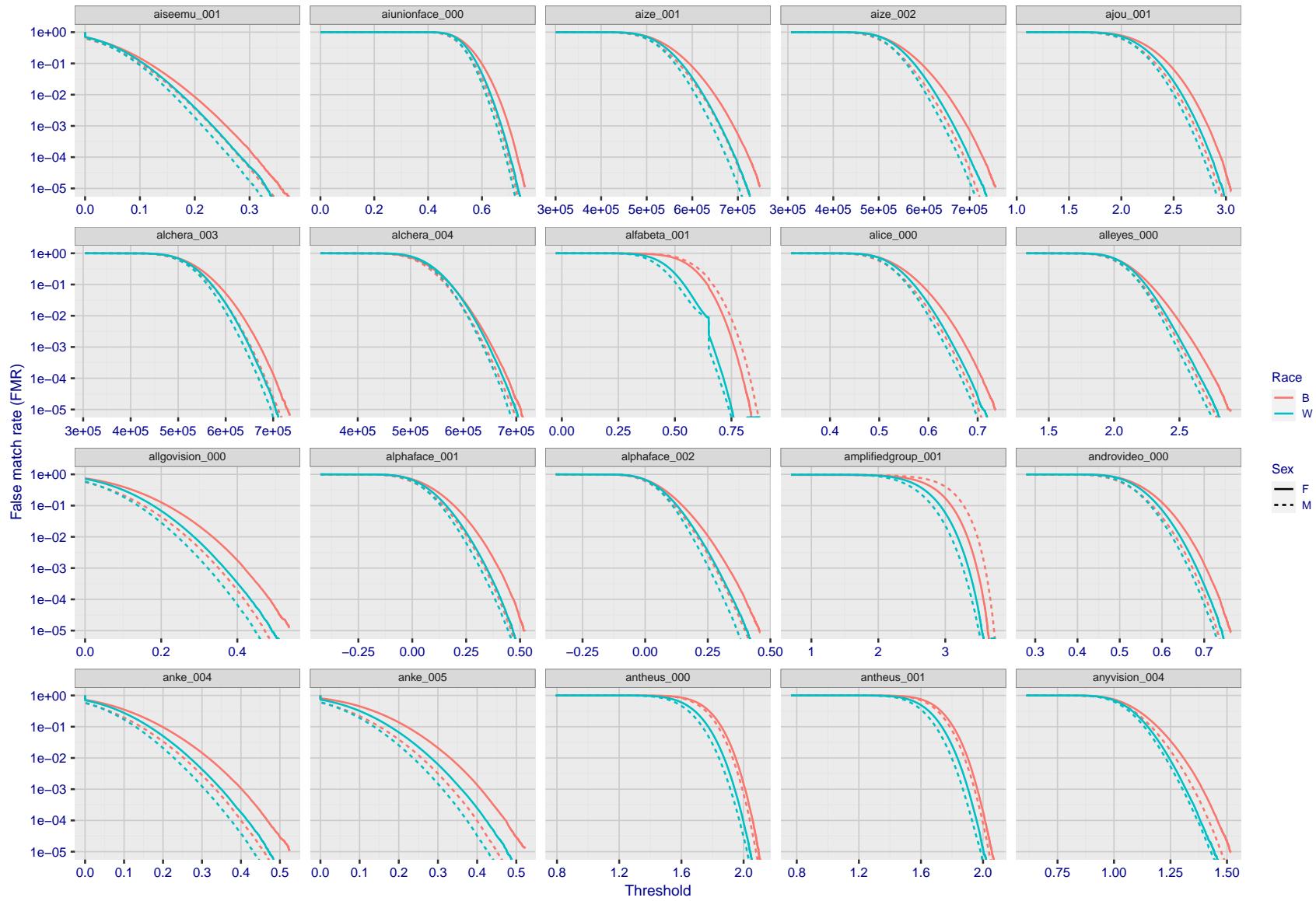


Figure 221: For the mugshot images, the false match calibration curves show false match rate vs. threshold. Separate curves appear for white females, black females, black males and white males.

2023/02/09 20:10:38

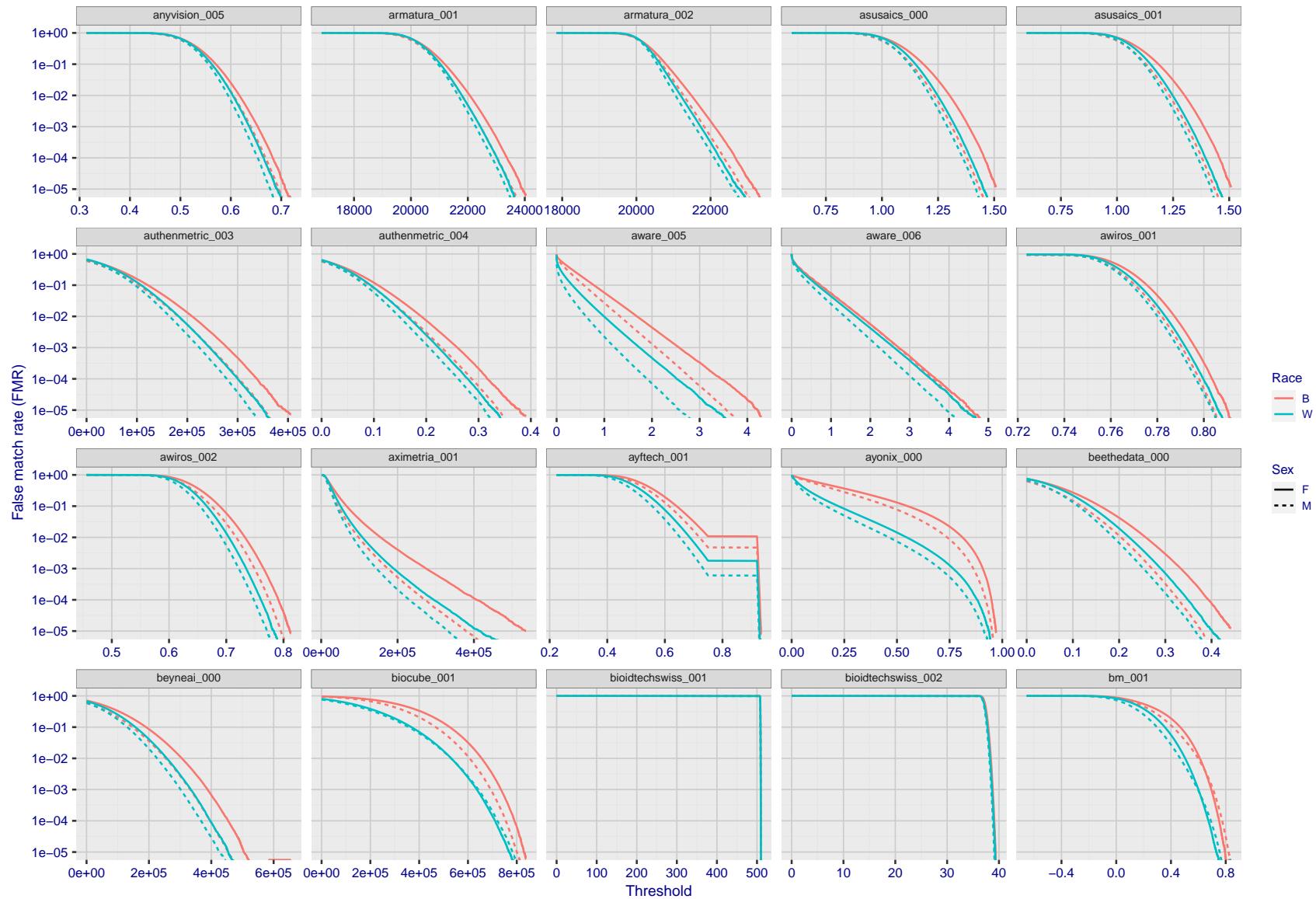


Figure 222: For the mugshot images, the false match calibration curves show false match rate vs. threshold. Separate curves appear for white females, black females, black males and white males.

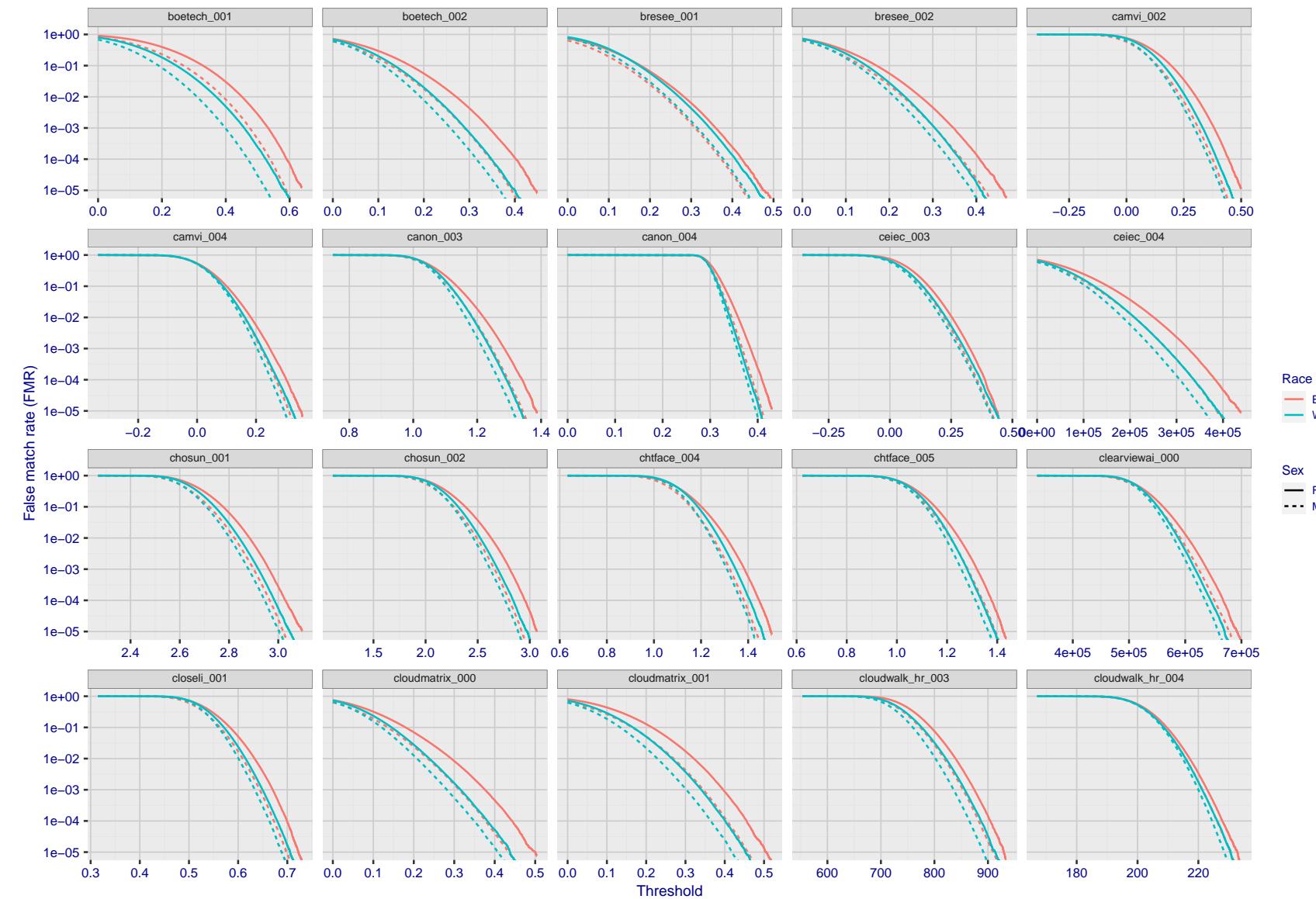


Figure 223: For the mugshot images, the false match calibration curves show false match rate vs. threshold. Separate curves appear for white females, black females, black males and white males.

2023/02/09 20:10:38

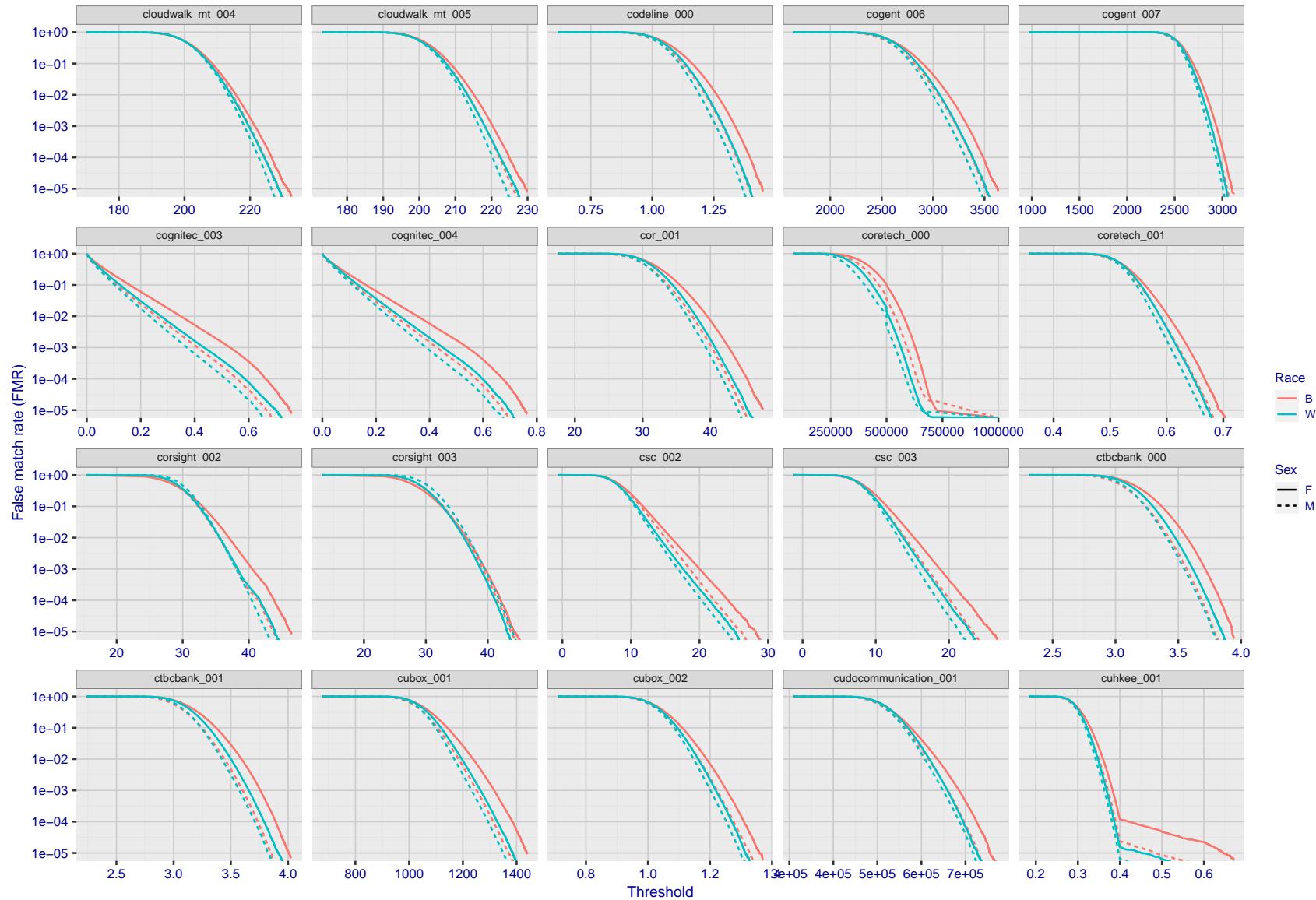


Figure 224: For the mugshot images, the false match calibration curves show false match rate vs. threshold. Separate curves appear for white females, black females, black males and white males.

2023/02/09 20:10:38

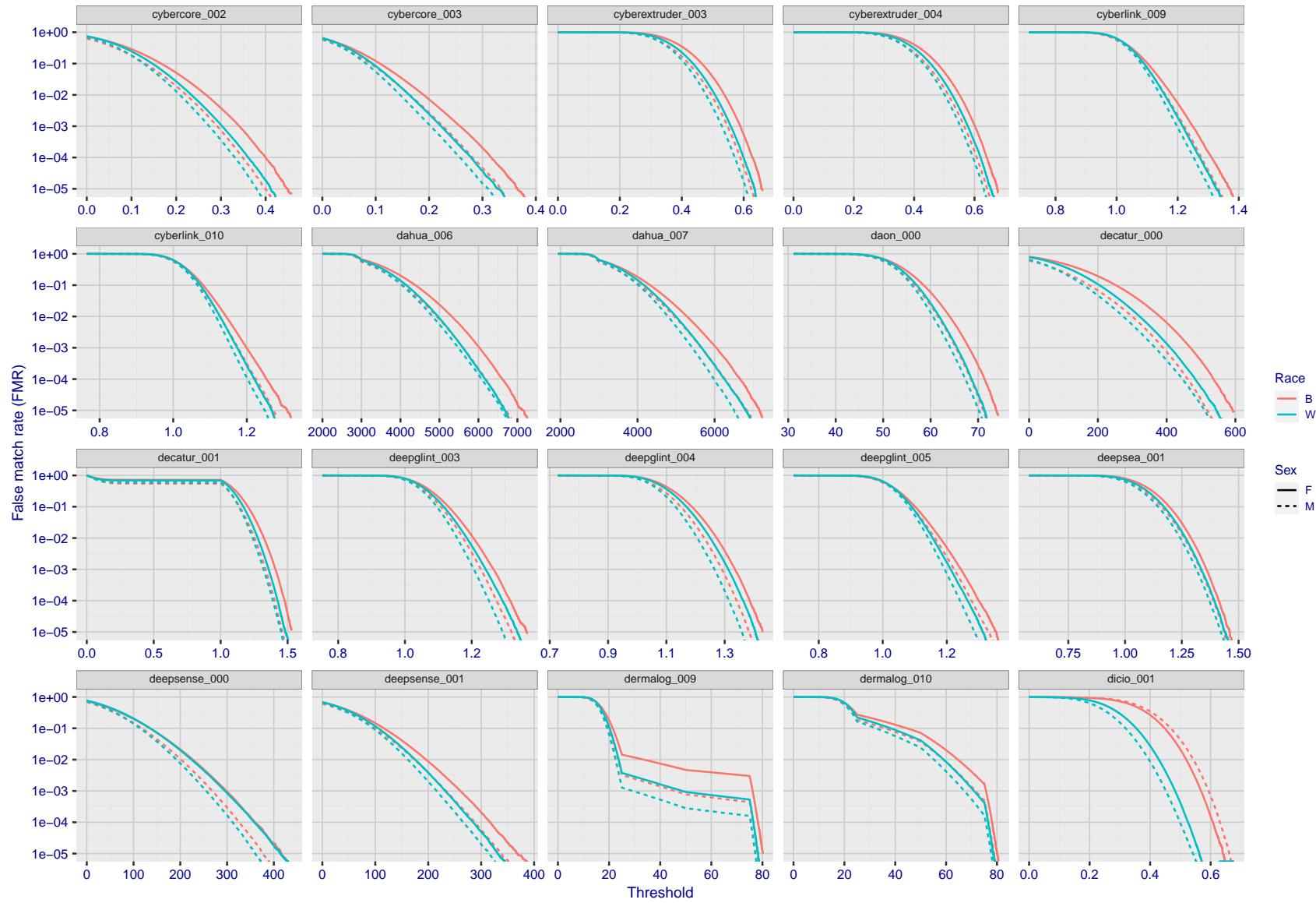


Figure 225: For the mugshot images, the false match calibration curves show false match rate vs. threshold. Separate curves appear for white females, black females, black males and white males.

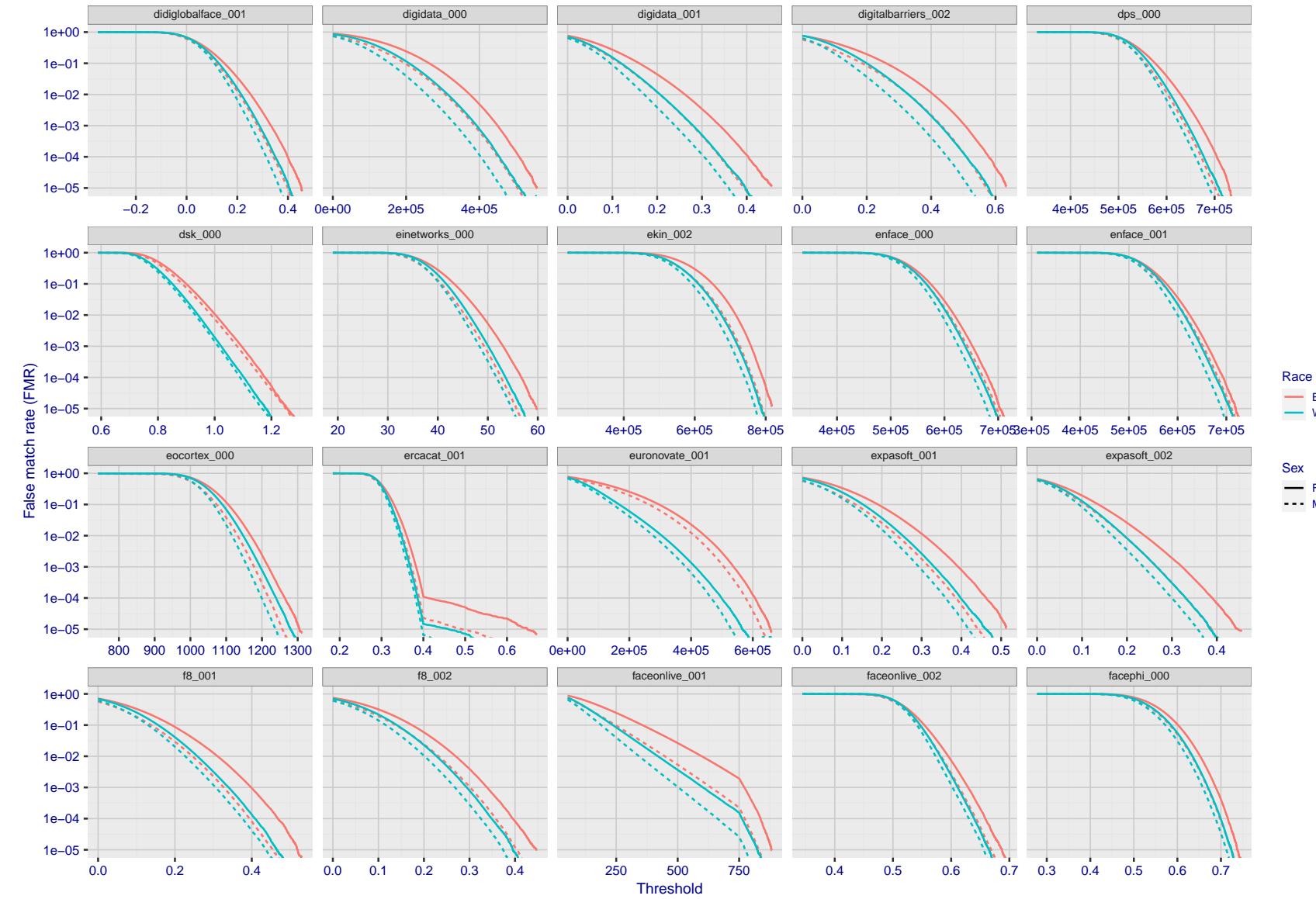


Figure 226: For the mugshot images, the false match calibration curves show false match rate vs. threshold. Separate curves appear for white females, black females, black males and white males.

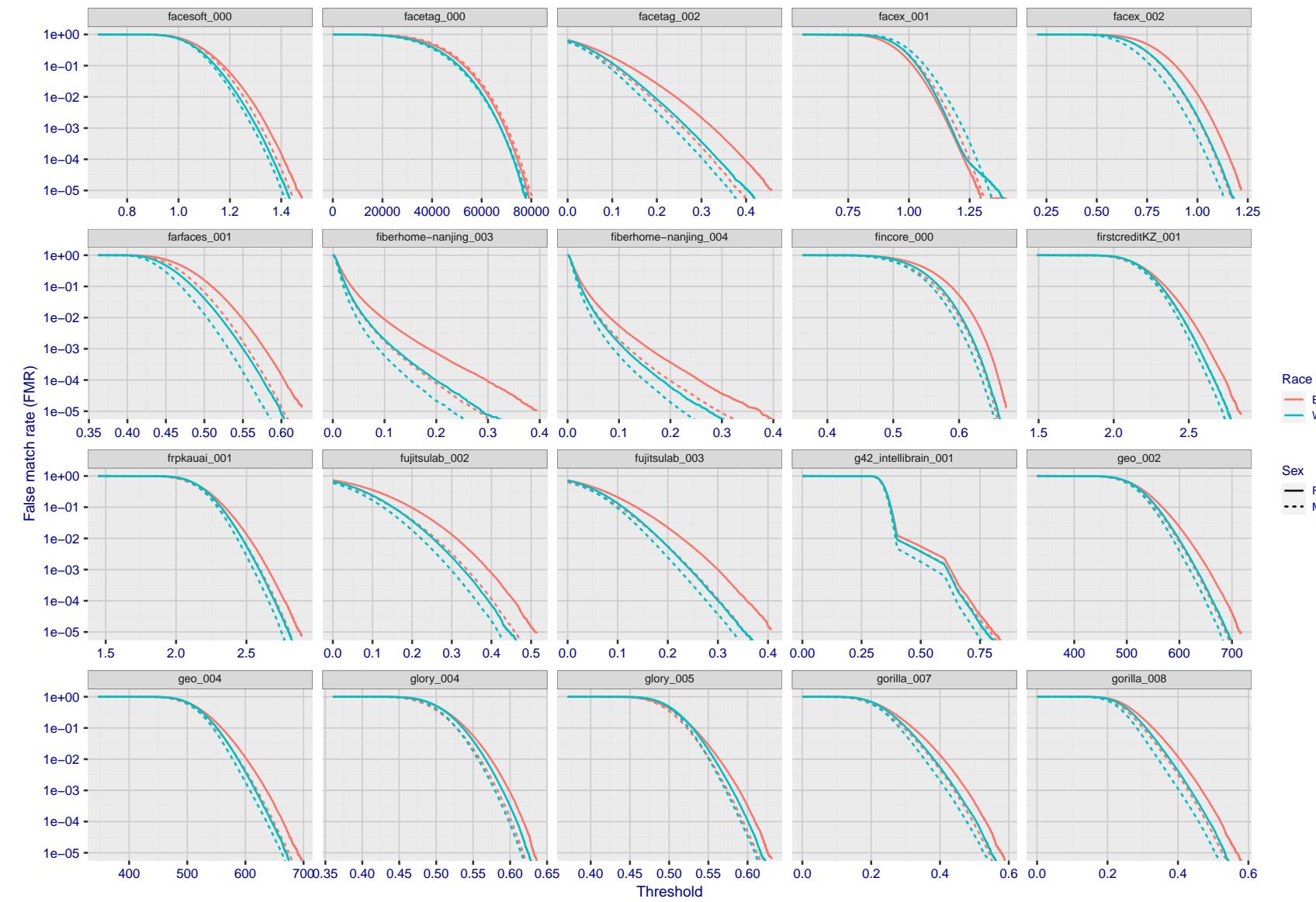


Figure 227: For the mugshot images, the false match calibration curves show false match rate vs. threshold. Separate curves appear for white females, black females, black males and white males.

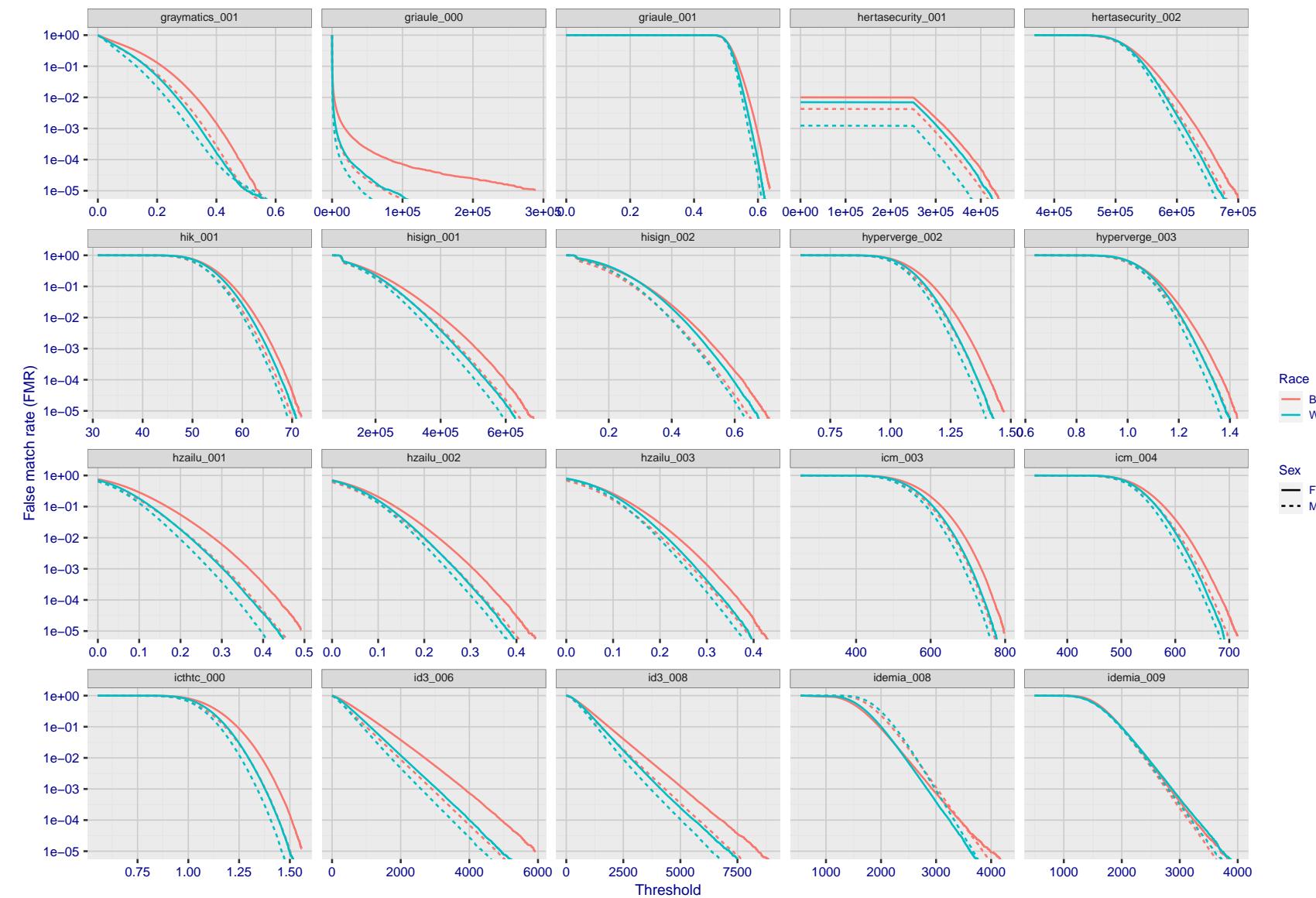
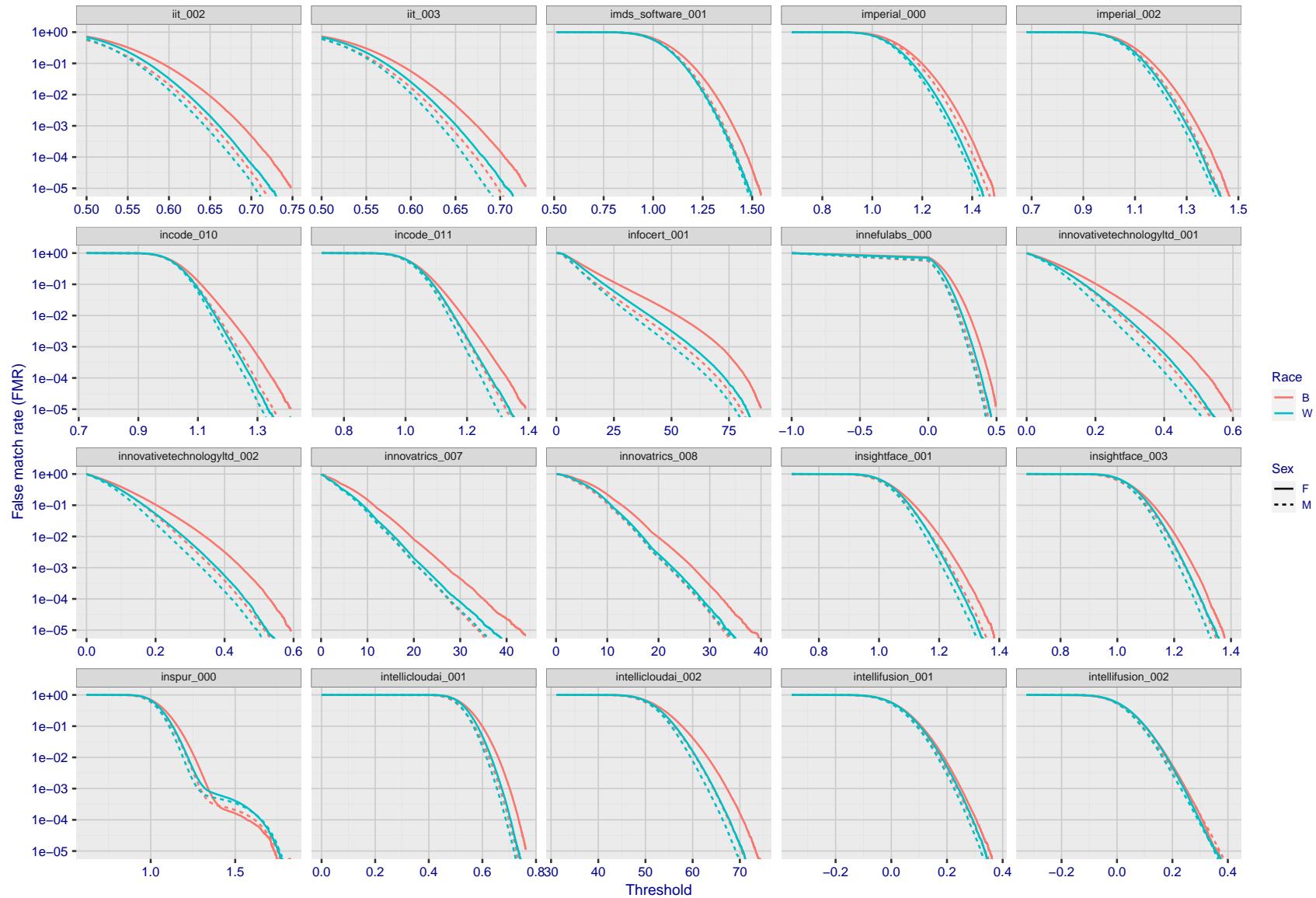


Figure 228: For the mugshot images, the false match calibration curves show false match rate vs. threshold. Separate curves appear for white females, black females, black males and white males.

2023/02/09 20:10:38



FNMR(T)
"False non-match rate"
"False match rate"

Figure 229: For the mugshot images, the false match calibration curves show false match rate vs. threshold. Separate curves appear for white females, black females, black males and white males.

2023/02/09 20:10:38

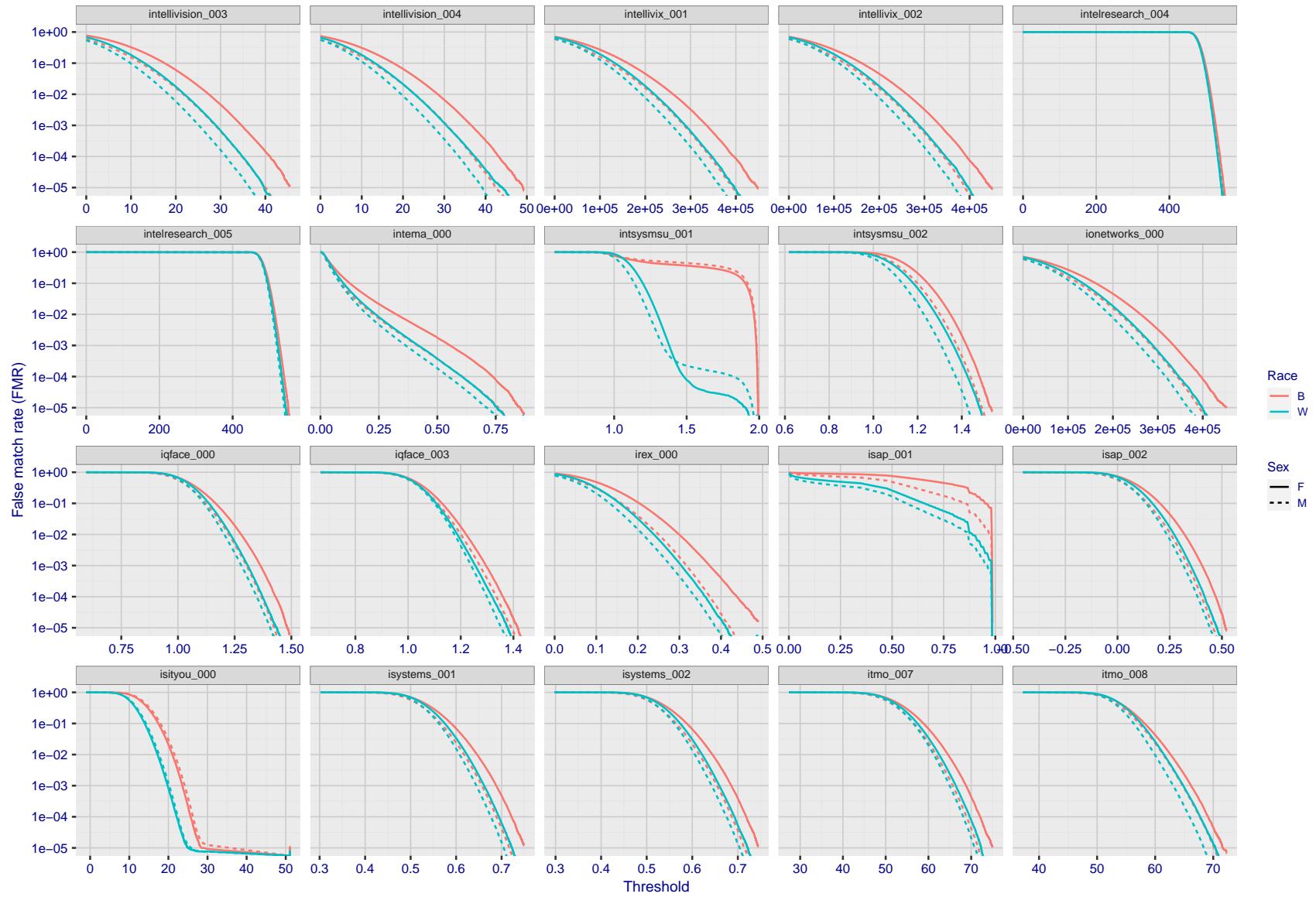


Figure 230: For the mugshot images, the false match calibration curves show false match rate vs. threshold. Separate curves appear for white females, black females, black males and white males.

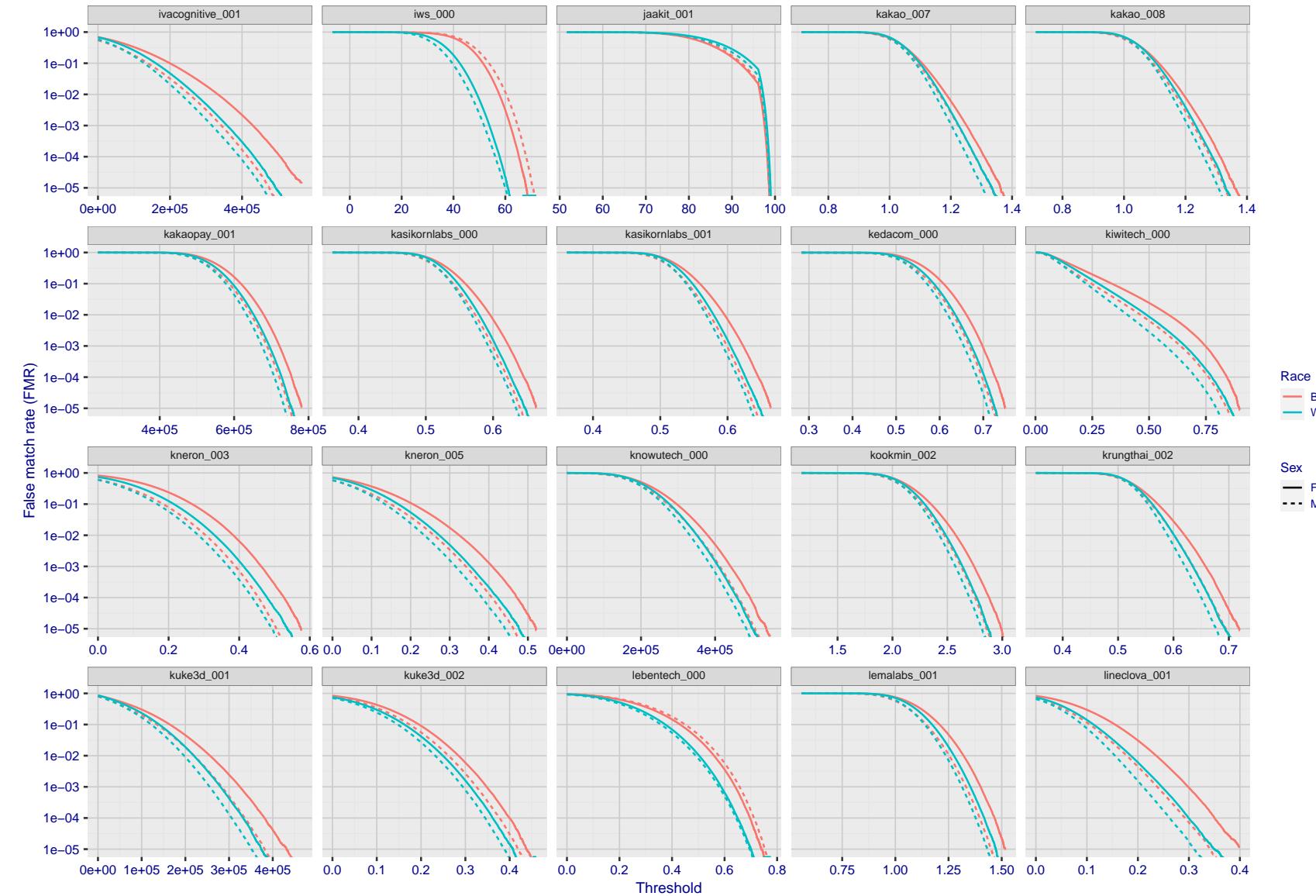


Figure 231: For the mugshot images, the false match calibration curves show false match rate vs. threshold. Separate curves appear for white females, black females, black males and white males.

2023/02/09 20:10:38

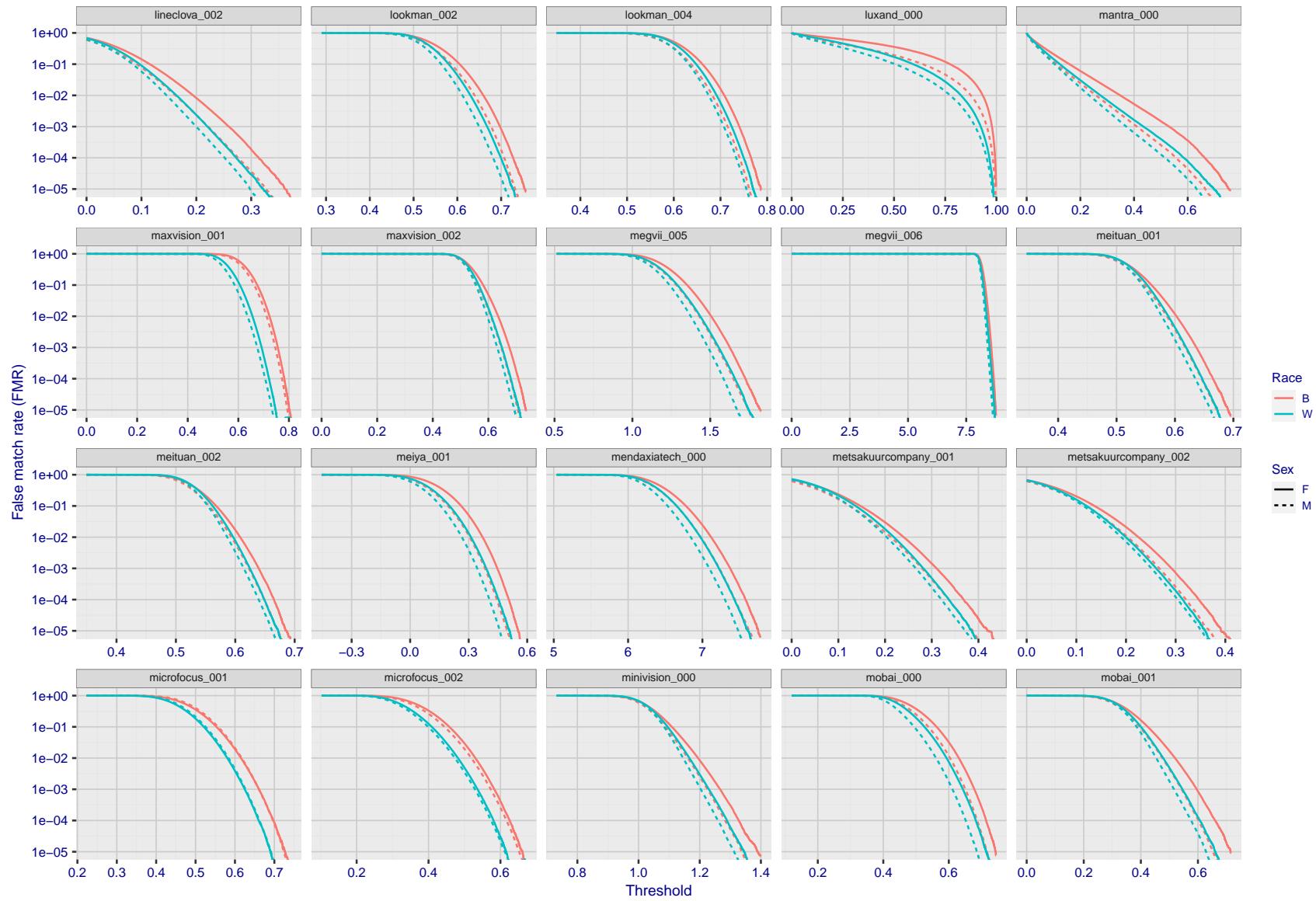


Figure 232: For the mugshot images, the false match calibration curves show false match rate vs. threshold. Separate curves appear for white females, black females, black males and white males.

2023/02/09 20:10:38

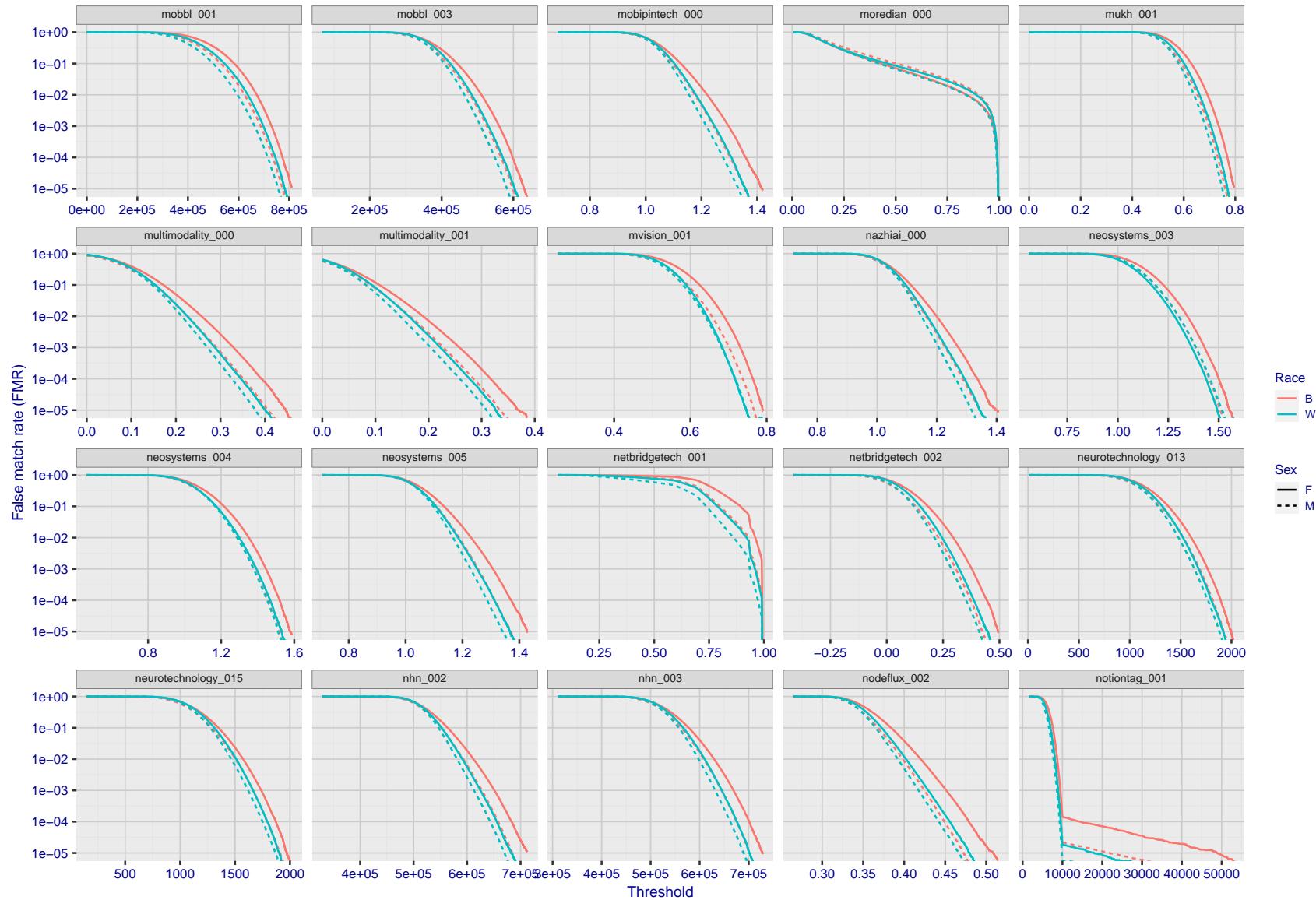


Figure 233: For the mugshot images, the false match calibration curves show false match rate vs. threshold. Separate curves appear for white females, black females, black males and white males.

2023/02/09 20:10:38

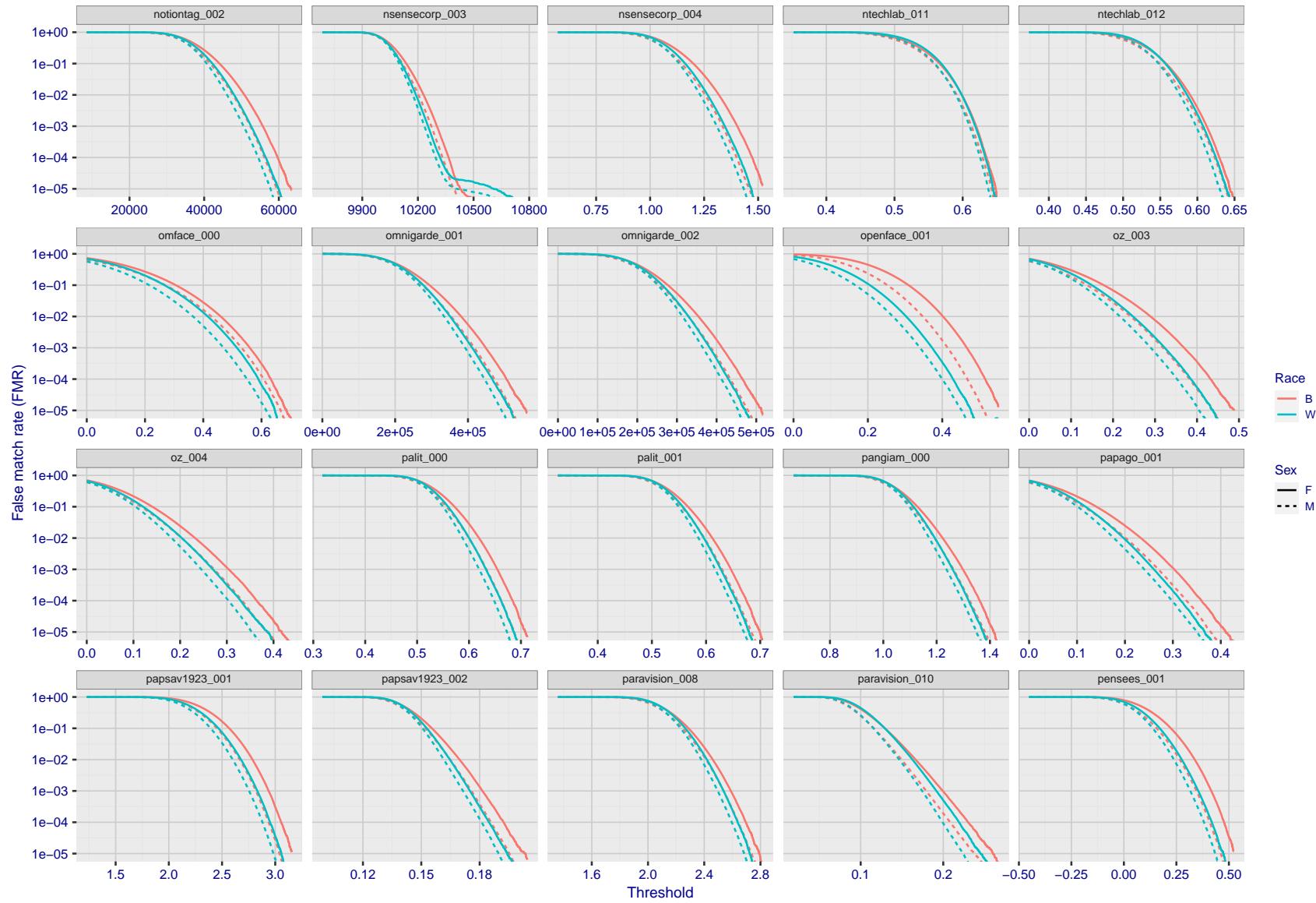


Figure 234: For the mugshot images, the false match calibration curves show false match rate vs. threshold. Separate curves appear for white females, black females, black males and white males.

2023/02/09 20:10:38

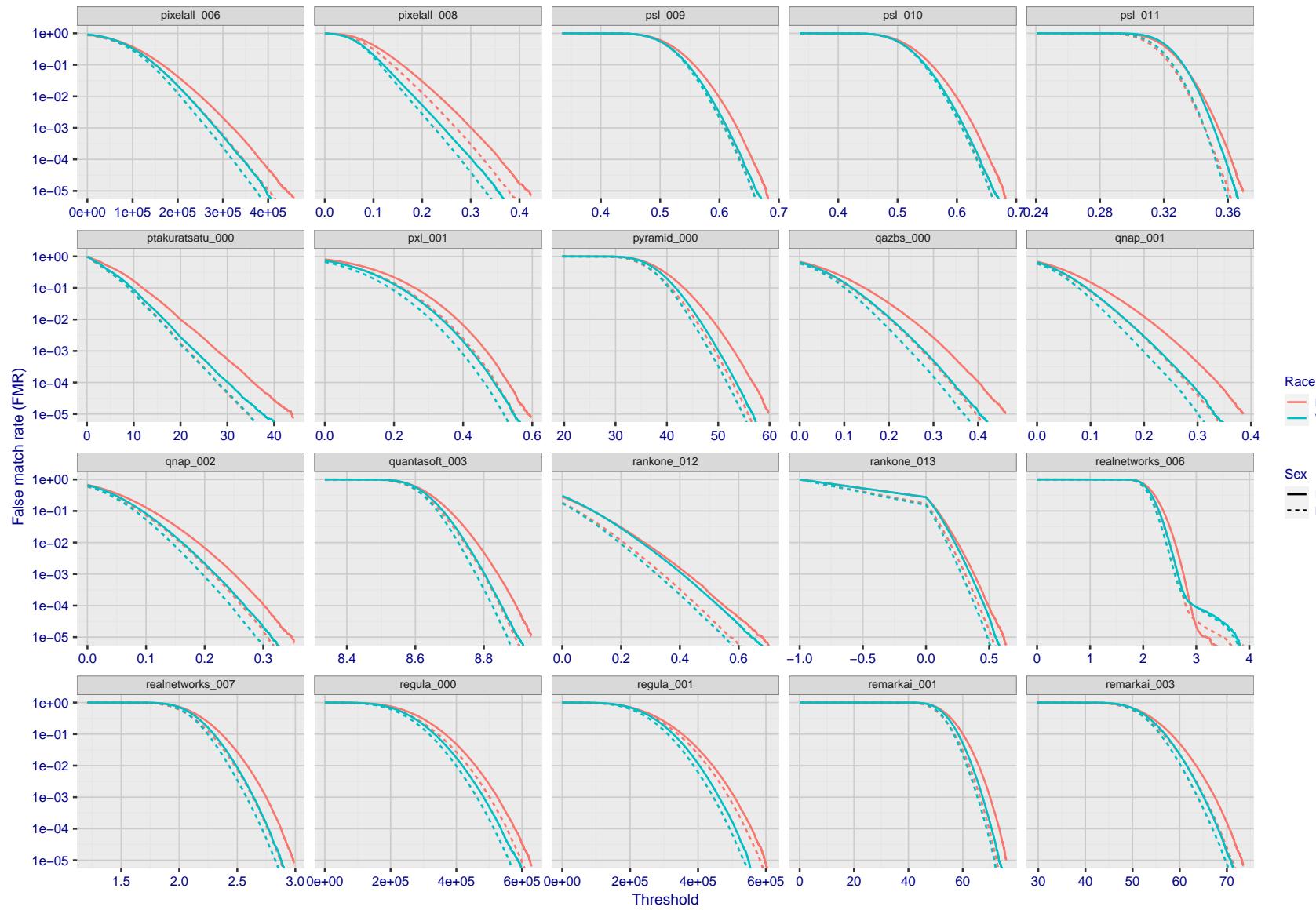


Figure 235: For the mugshot images, the false match calibration curves show false match rate vs. threshold. Separate curves appear for white females, black females, black males and white males.

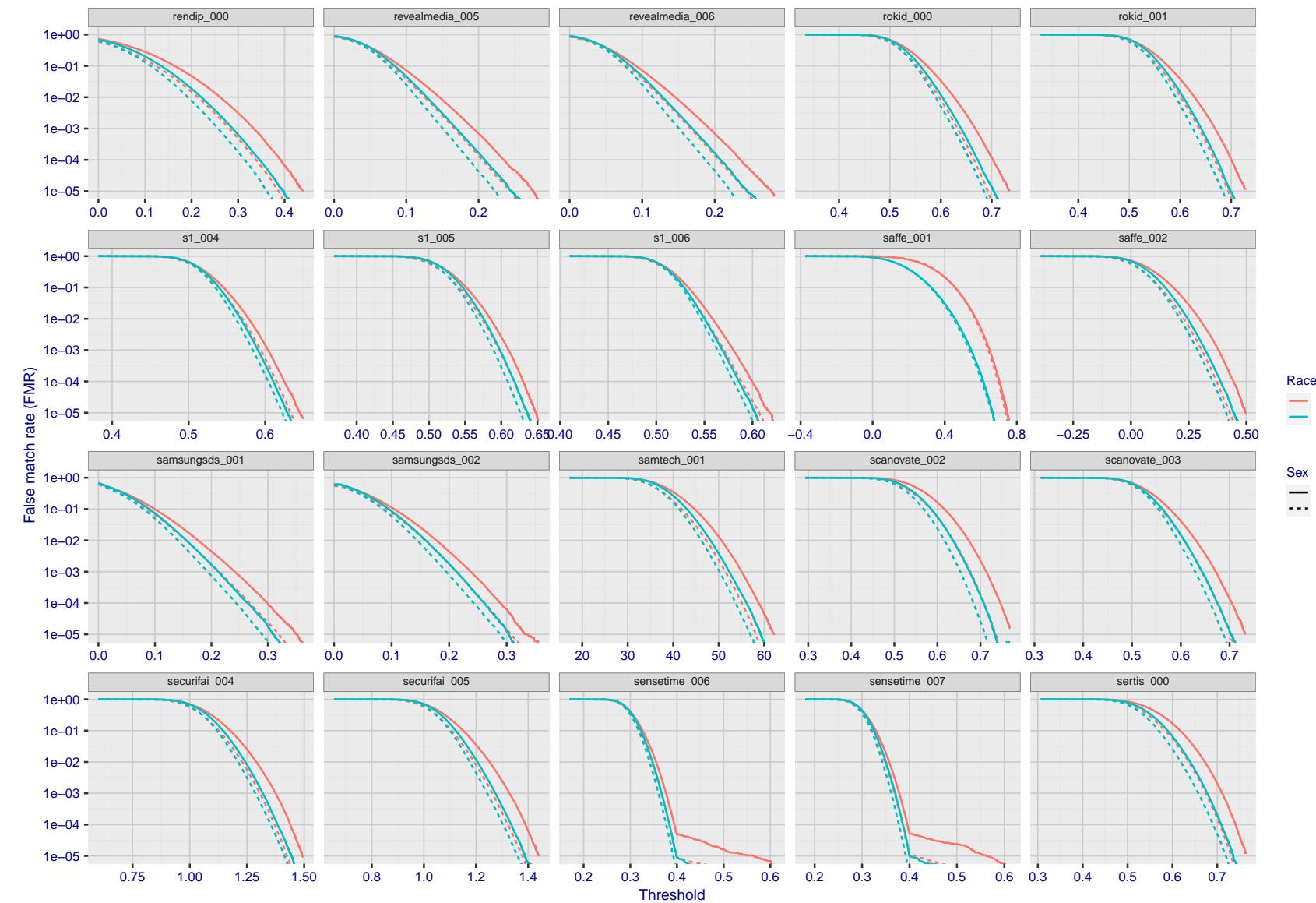
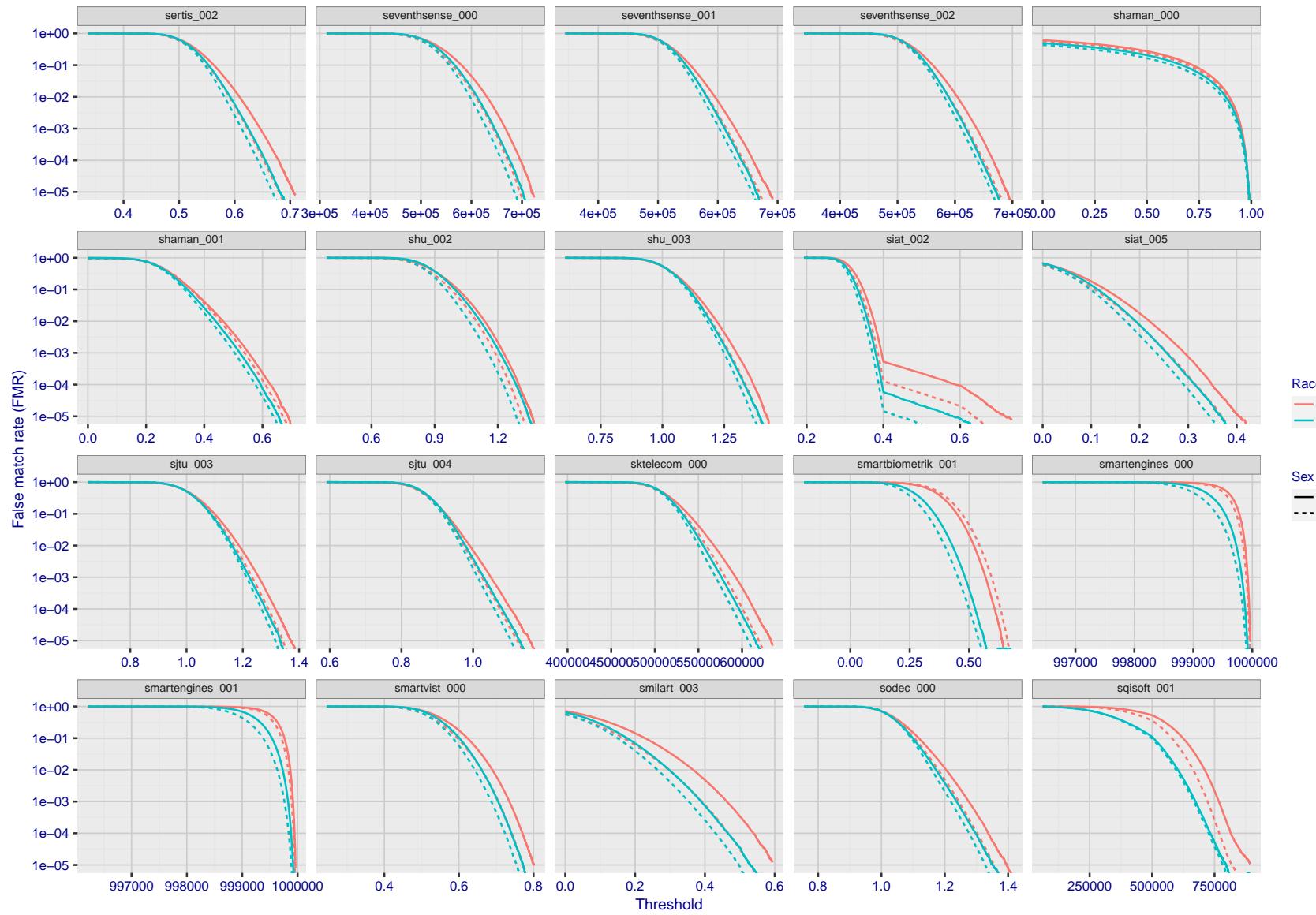


Figure 236: For the mugshot images, the false match calibration curves show false match rate vs. threshold. Separate curves appear for white females, black females, black males and white males.

2023/02/09 20:10:38



FNMR(T)
"False non-match rate"
"False match rate"

Figure 237: For the mugshot images, the false match calibration curves show false match rate vs. threshold. Separate curves appear for white females, black females, black males and white males.

2023/02/09 20:10:38

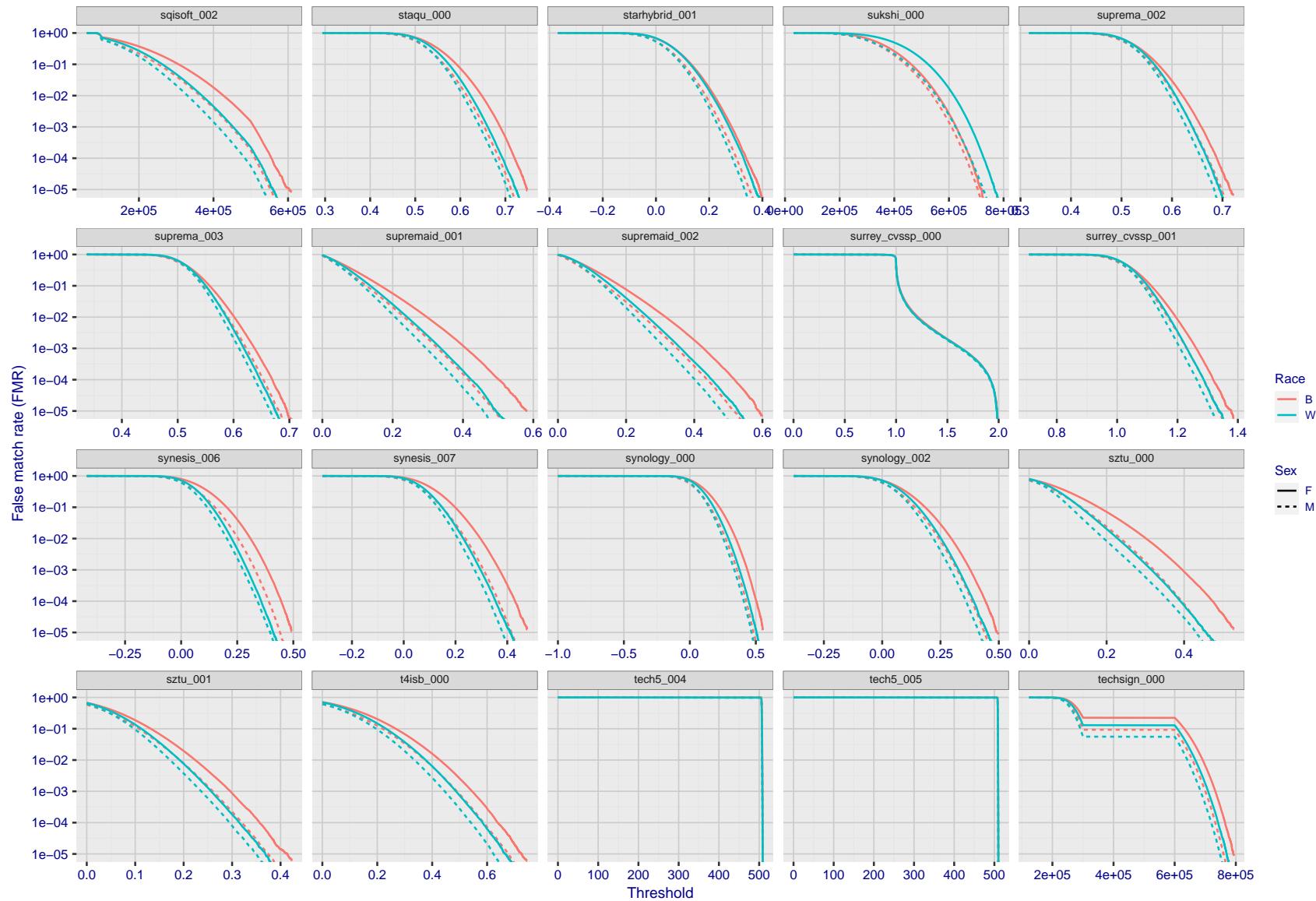


Figure 238: For the mugshot images, the false match calibration curves show false match rate vs. threshold. Separate curves appear for white females, black females, black males and white males.

FNMR(T)
"False non-match rate"
"False match rate"

2023/02/09 20:10:38

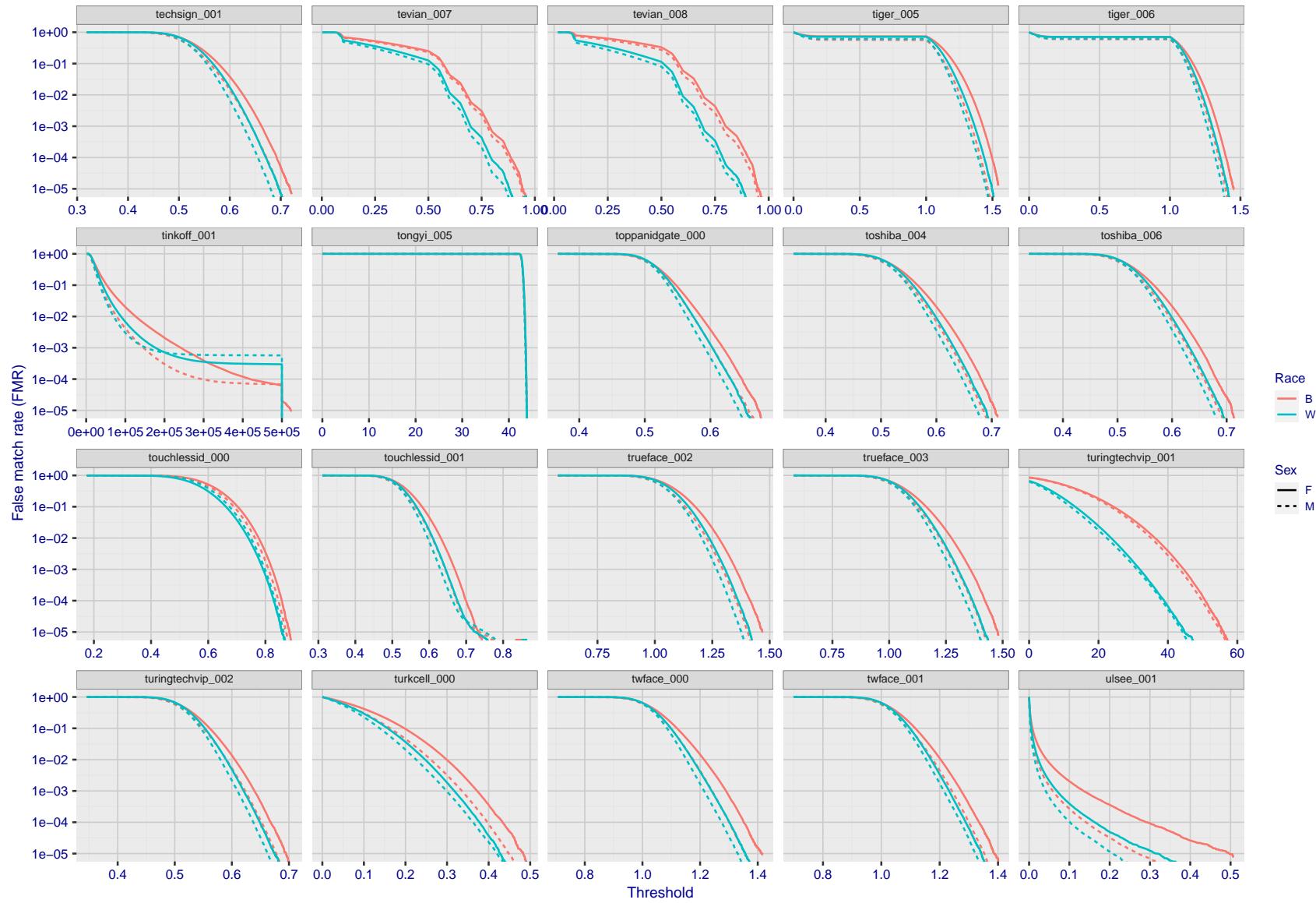


Figure 239: For the mugshot images, the false match calibration curves show false match rate vs. threshold. Separate curves appear for white females, black females, black males and white males.

2023/02/09 20:10:38

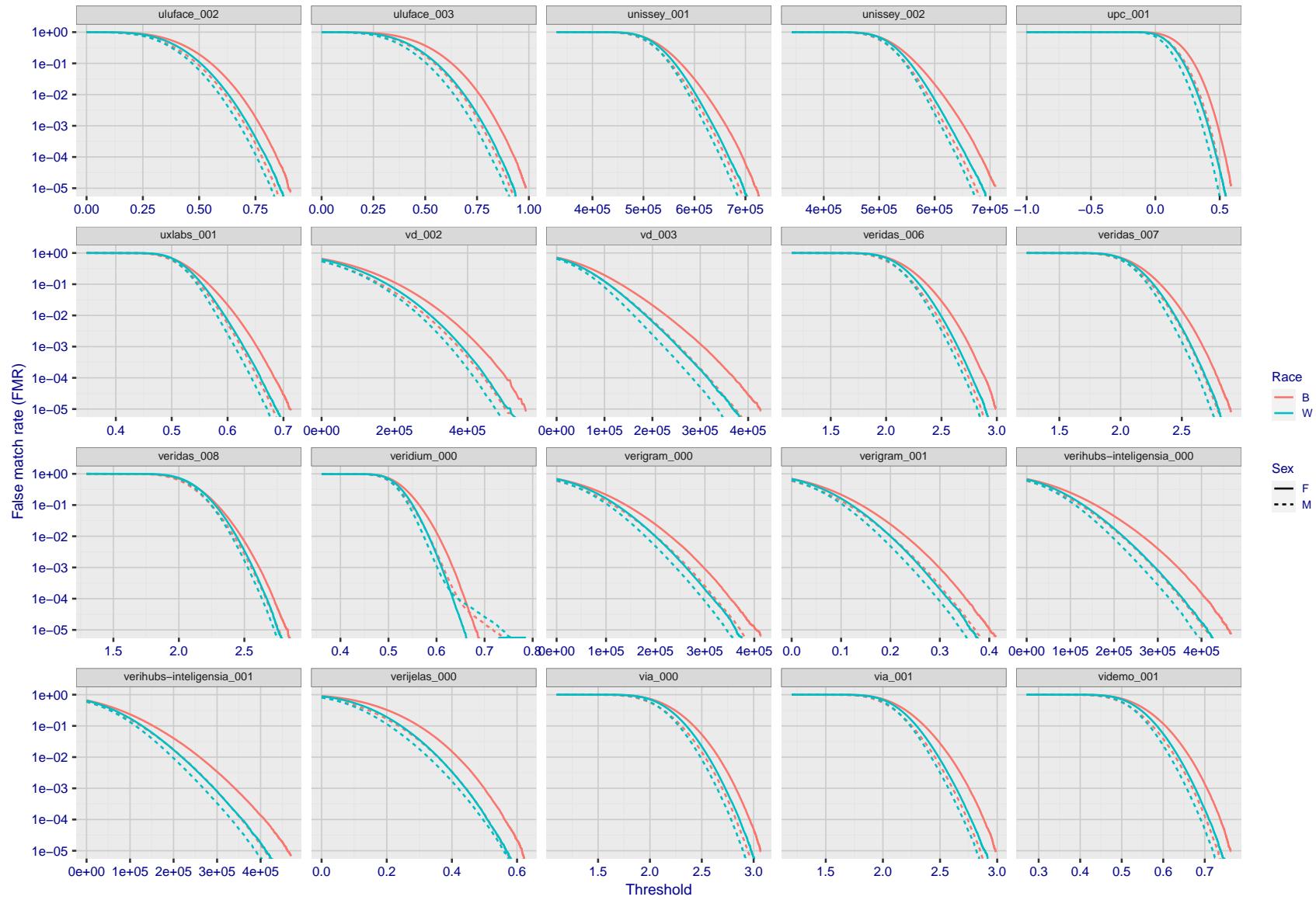


Figure 240: For the mugshot images, the false match calibration curves show false match rate vs. threshold. Separate curves appear for white females, black females, black males and white males.

FNMR(T)

"False non-match rate"

FMR(T)

"False match rate"

2023/02/09 20:10:38

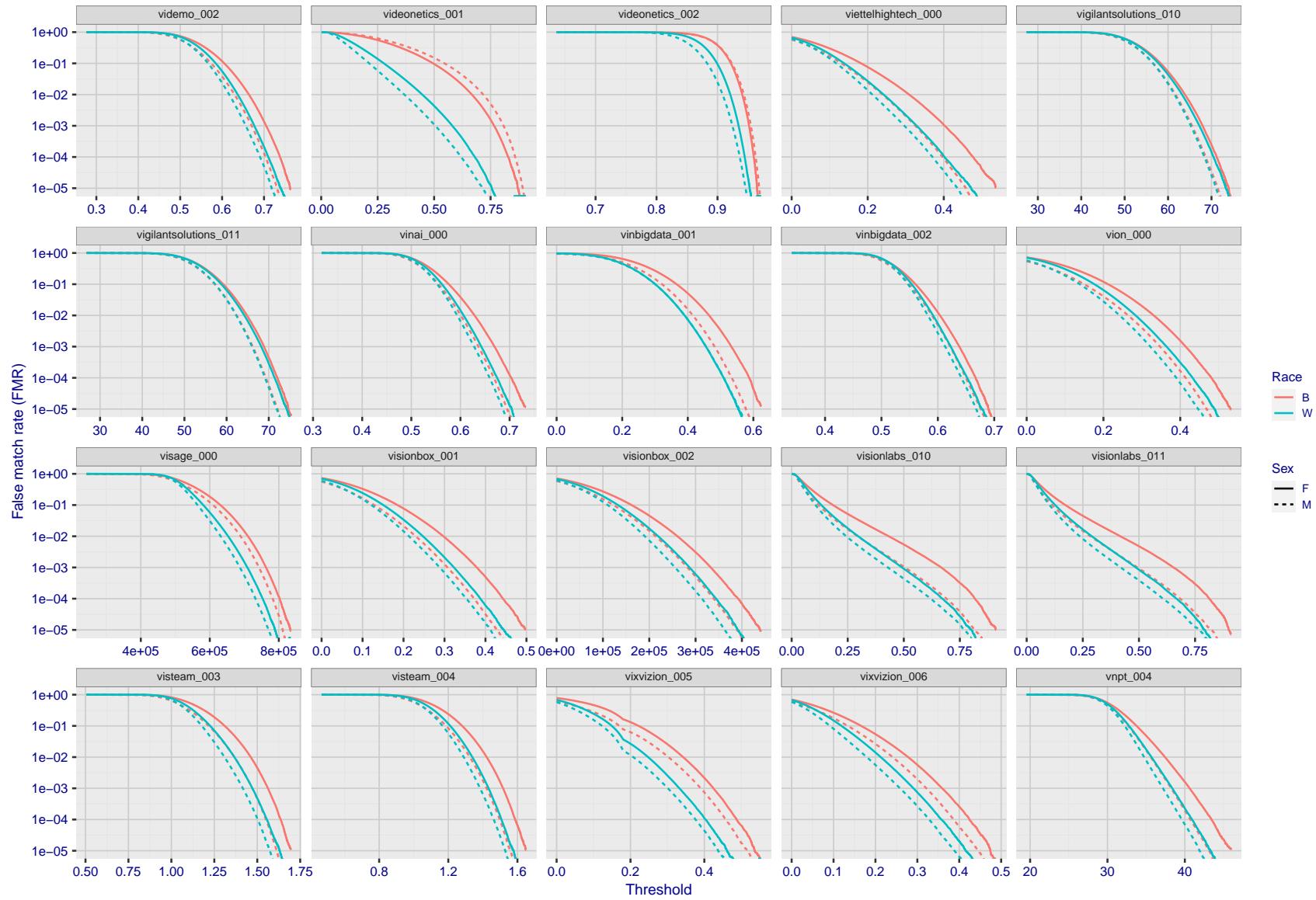


Figure 241: For the mugshot images, the false match calibration curves show false match rate vs. threshold. Separate curves appear for white females, black females, black males and white males.

2023/02/09 20:10:38

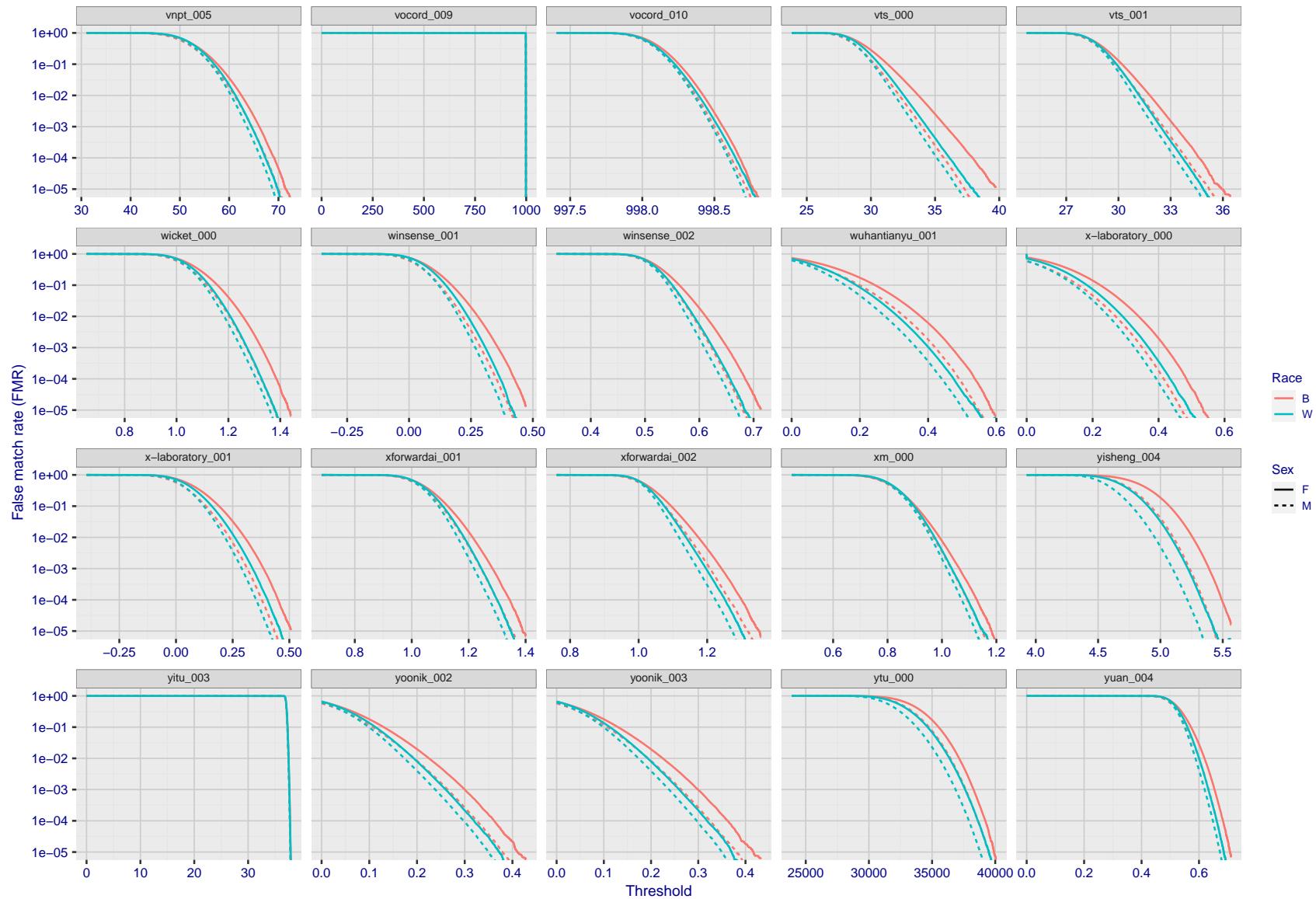


Figure 242: For the mugshot images, the false match calibration curves show false match rate vs. threshold. Separate curves appear for white females, black females, black males and white males.

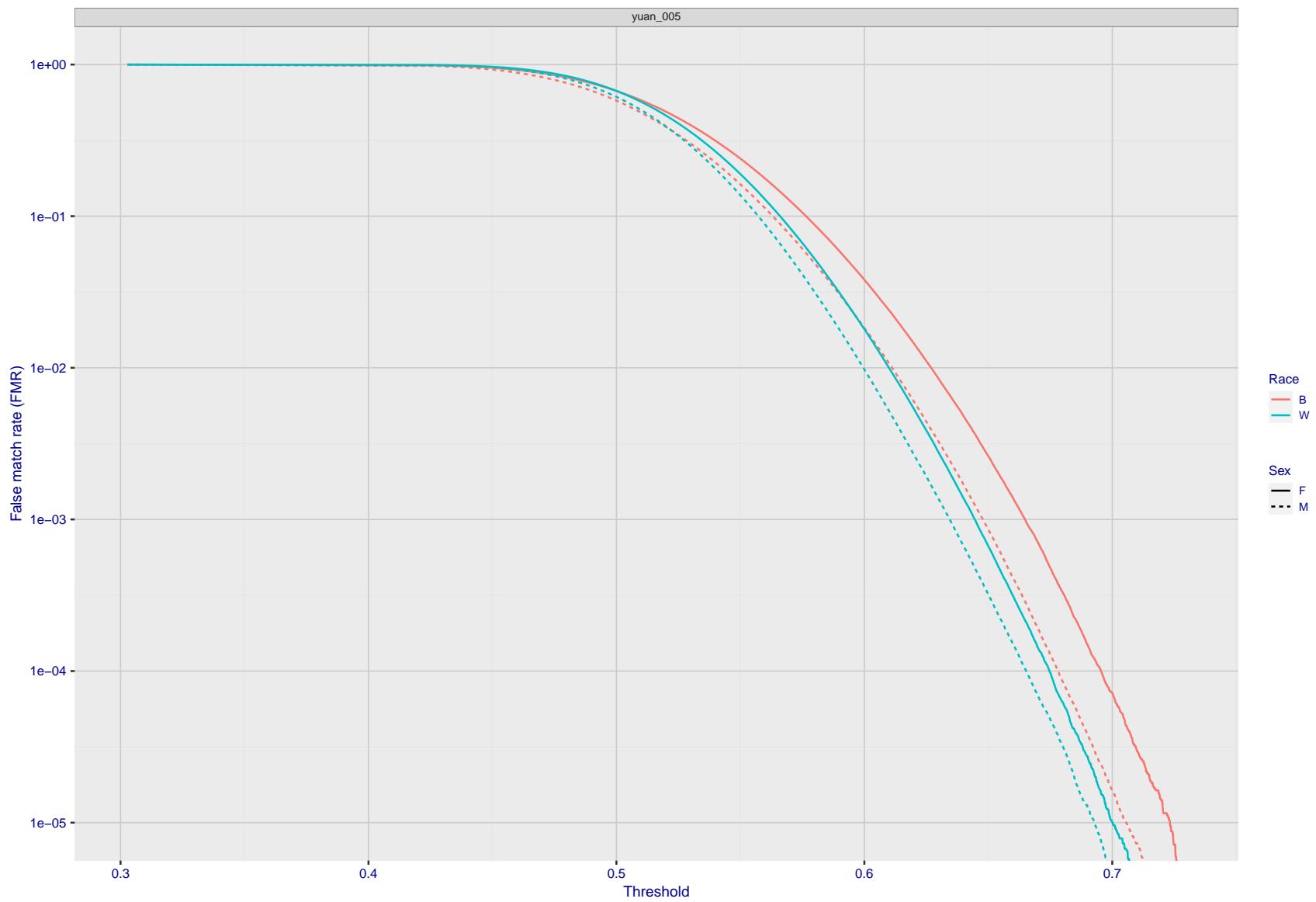


Figure 243: For the mugshot images, the false match calibration curves show false match rate vs. threshold. Separate curves appear for white females, black females, black males and white males.



Figure 244: For the visa images, the false match calibration curves show FMR vs. threshold, T . The blue (lower) curves are for zero-effort impostors (i.e. comparing all images against all). The red (upper) curves are for persons of the same-sex, same-age, and same national-origin. This shows that FMR is underestimated (by a factor of 10 or more) by using a zero-effort impostor calculation to calibrate T . As shown later (sec. 3.6), FMR is higher for demographic-matched impostors.

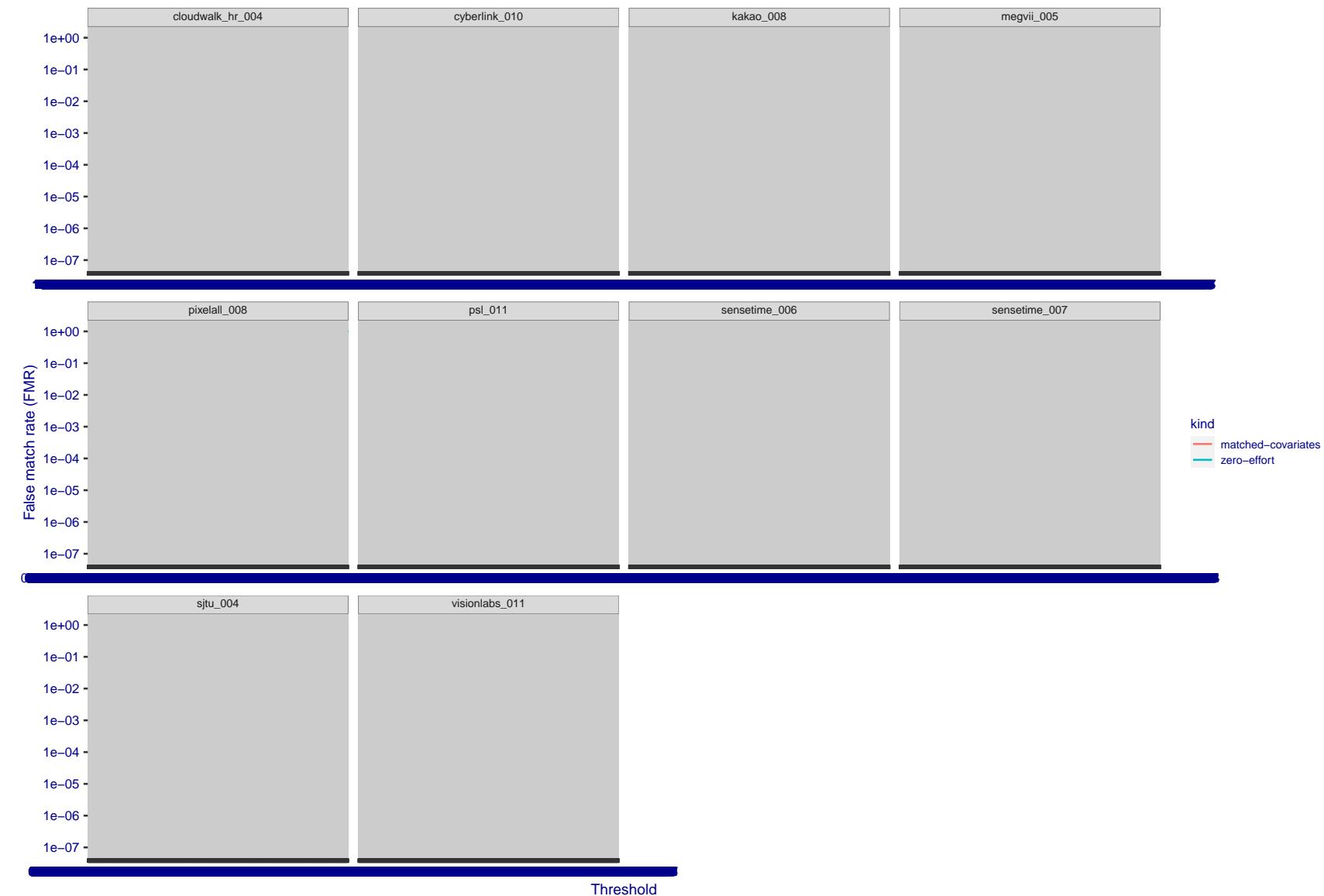


Figure 245: For the visa images, the false match calibration curves show FMR vs. threshold, T . The blue (lower) curves are for zero-effort impostors (i.e. comparing all images against all). The red (upper) curves are for persons of the same-sex, same-age, and same national-origin. This shows that FMR is underestimated (by a factor of 10 or more) by using a zero-effort impostor calculation to calibrate T . As shown later (sec. 3.6), FMR is higher for demographic-matched impostors.

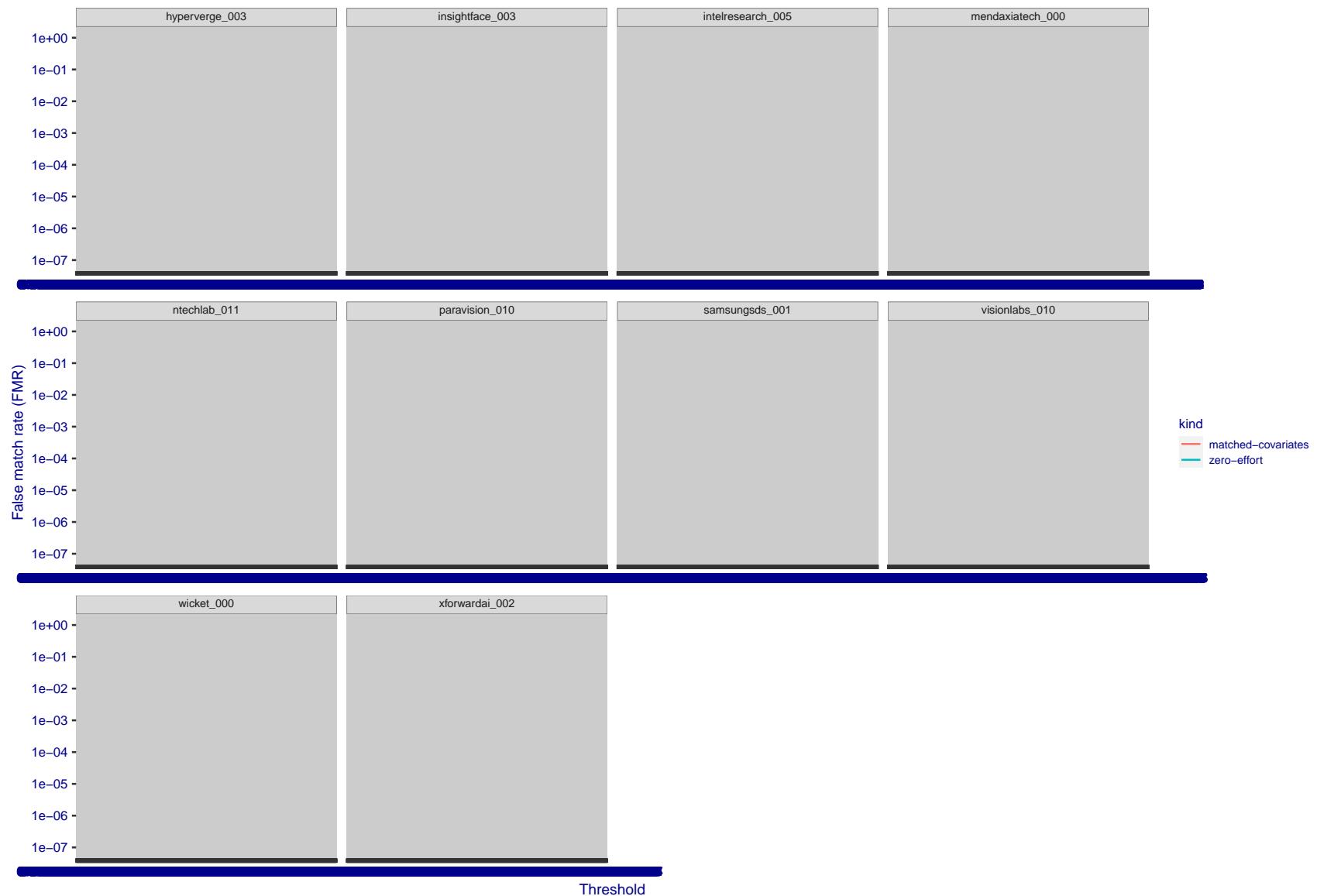


Figure 246: For the visa images, the false match calibration curves show FMR vs. threshold, T . The blue (lower) curves are for zero-effort impostors (i.e. comparing all images against all). The red (upper) curves are for persons of the same-sex, same-age, and same national-origin. This shows that FMR is underestimated (by a factor of 10 or more) by using a zero-effort impostor calculation to calibrate T . As shown later (sec. 3.6), FMR is higher for demographic-matched impostors.

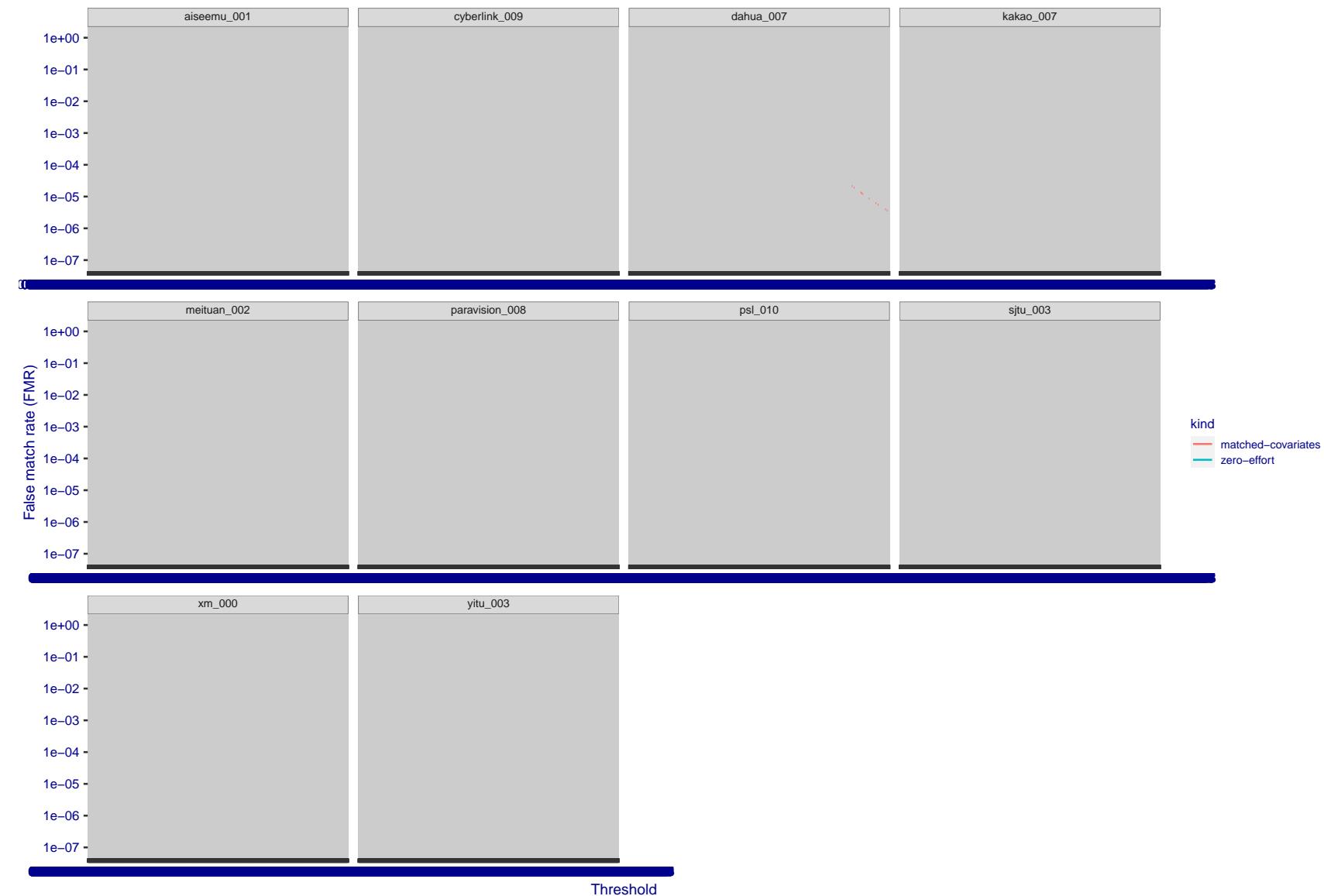


Figure 247: For the visa images, the false match calibration curves show FMR vs. threshold, T . The blue (lower) curves are for zero-effort impostors (i.e. comparing all images against all). The red (upper) curves are for persons of the same-sex, same-age, and same national-origin. This shows that FMR is underestimated (by a factor of 10 or more) by using a zero-effort impostor calculation to calibrate T . As shown later (sec. 3.6), FMR is higher for demographic-matched impostors.

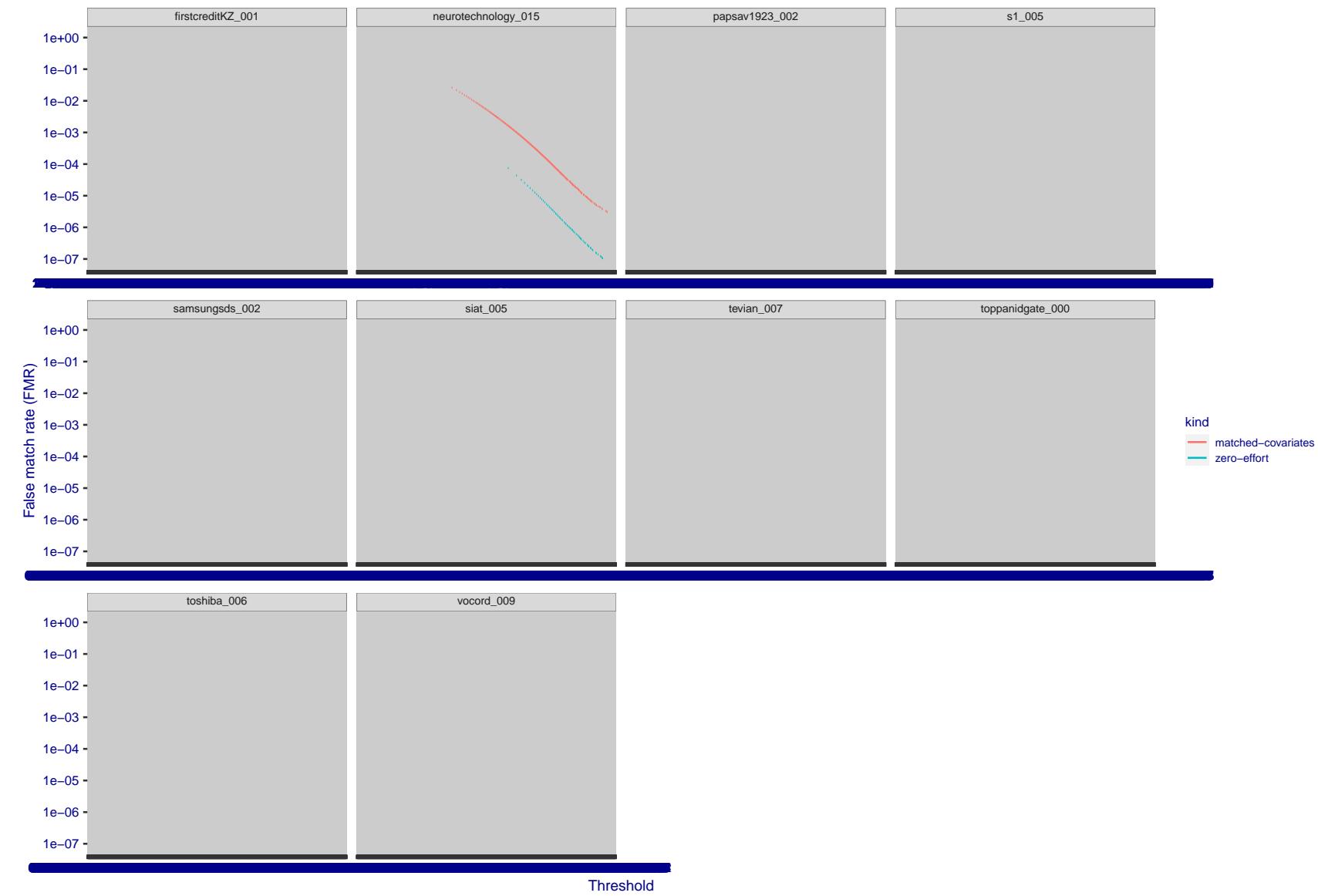


Figure 248: For the visa images, the false match calibration curves show FMR vs. threshold, T . The blue (lower) curves are for zero-effort impostors (i.e. comparing all images against all). The red (upper) curves are for persons of the same-sex, same-age, and same national-origin. This shows that FMR is underestimated (by a factor of 10 or more) by using a zero-effort impostor calculation to calibrate T . As shown later (sec. 3.6), FMR is higher for demographic-matched impostors.

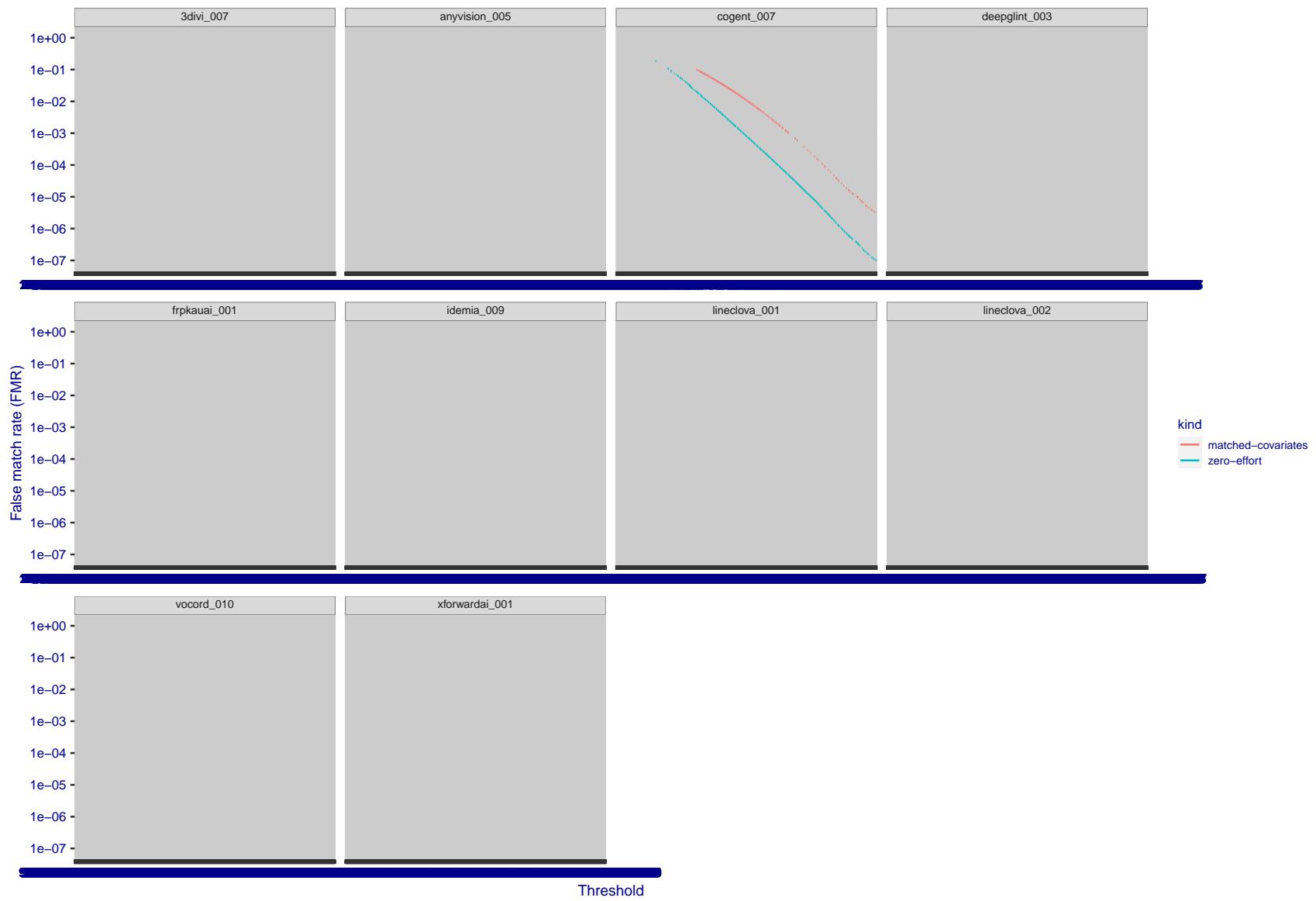


Figure 249: For the visa images, the false match calibration curves show FMR vs. threshold, T . The blue (lower) curves are for zero-effort impostors (i.e. comparing all images against all). The red (upper) curves are for persons of the same-sex, same-age, and same national-origin. This shows that FMR is underestimated (by a factor of 10 or more) by using a zero-effort impostor calculation to calibrate T . As shown later (sec. 3.6), FMR is higher for demographic-matched impostors.

2023/02/09 20:10:38

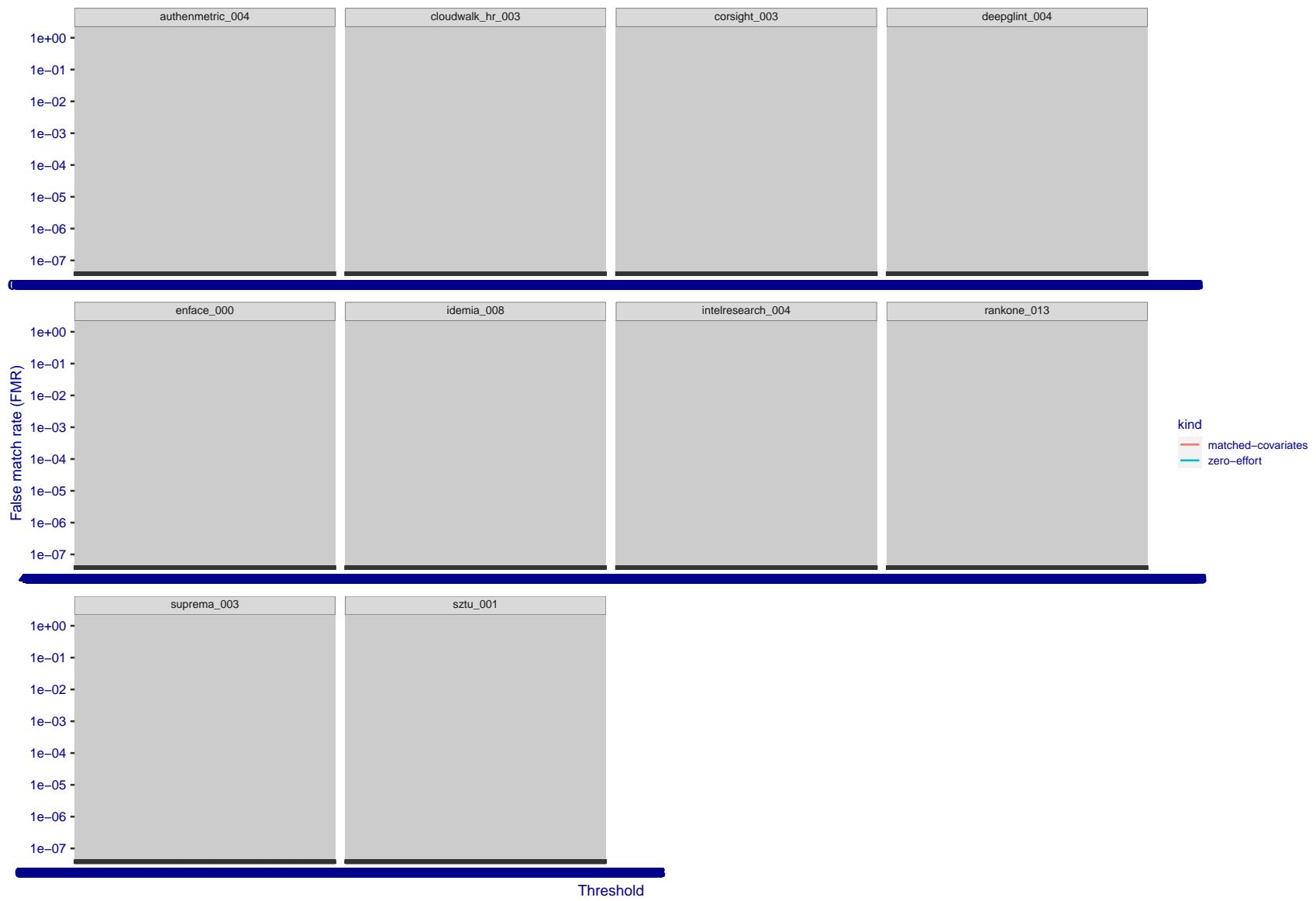


Figure 250: For the visa images, the false match calibration curves show FMR vs. threshold, T . The blue (lower) curves are for zero-effort impostors (i.e. comparing all images against all). The red (upper) curves are for persons of the same-sex, same-age, and same national-origin. This shows that FMR is underestimated (by a factor of 10 or more) by using a zero-effort impostor calculation to calibrate T . As shown later (sec. 3.6), FMR is higher for demographic-matched impostors.

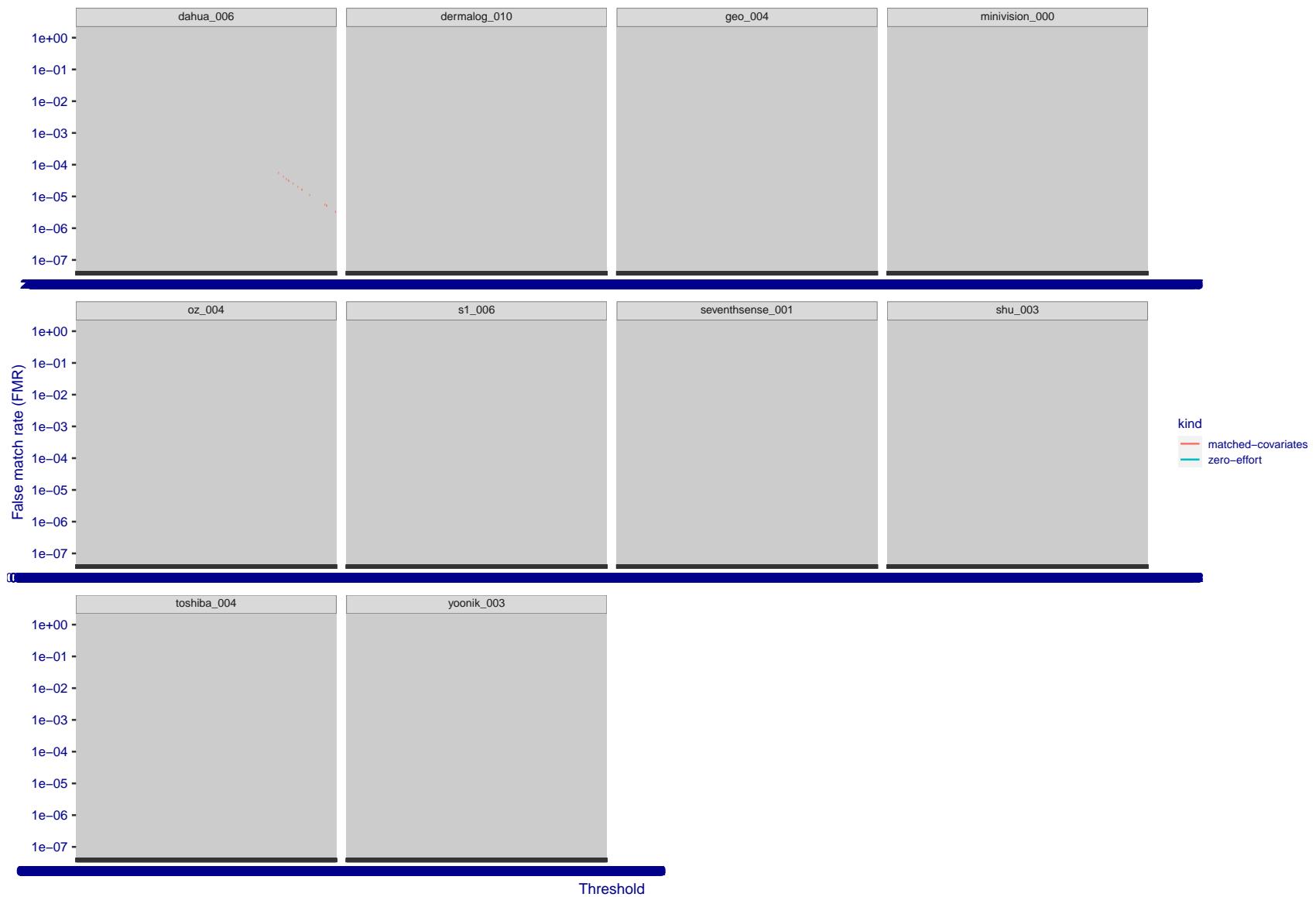


Figure 251: For the visa images, the false match calibration curves show FMR vs. threshold, T . The blue (lower) curves are for zero-effort impostors (i.e. comparing all images against all). The red (upper) curves are for persons of the same-sex, same-age, and same national-origin. This shows that FMR is underestimated (by a factor of 10 or more) by using a zero-effort impostor calculation to calibrate T . As shown later (sec. 3.6), FMR is higher for demographic-matched impostors.

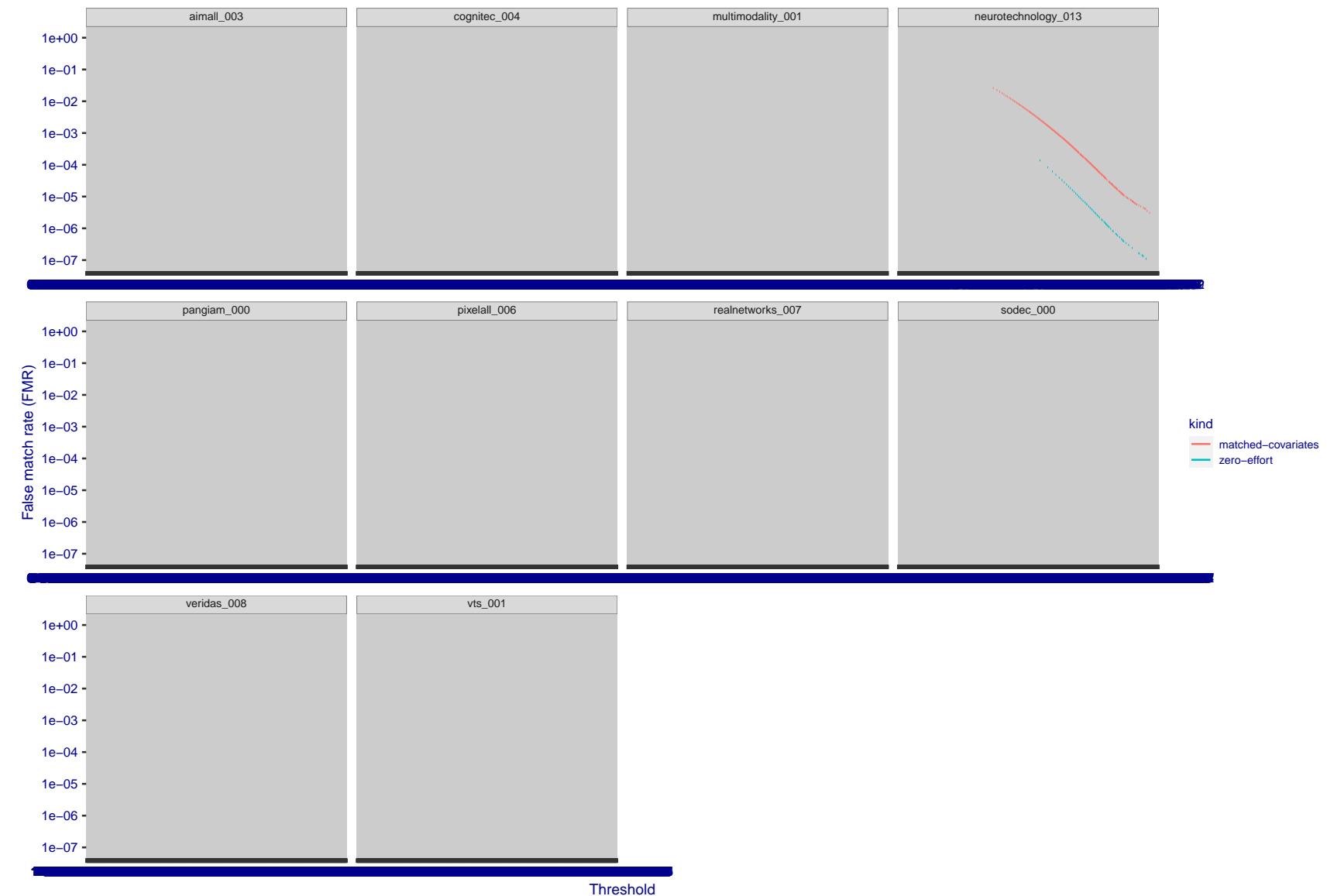


Figure 252: For the visa images, the false match calibration curves show FMR vs. threshold, T . The blue (lower) curves are for zero-effort impostors (i.e. comparing all images against all). The red (upper) curves are for persons of the same-sex, same-age, and same national-origin. This shows that FMR is underestimated (by a factor of 10 or more) by using a zero-effort impostor calculation to calibrate T . As shown later (sec. 3.6), FMR is higher for demographic-matched impostors.

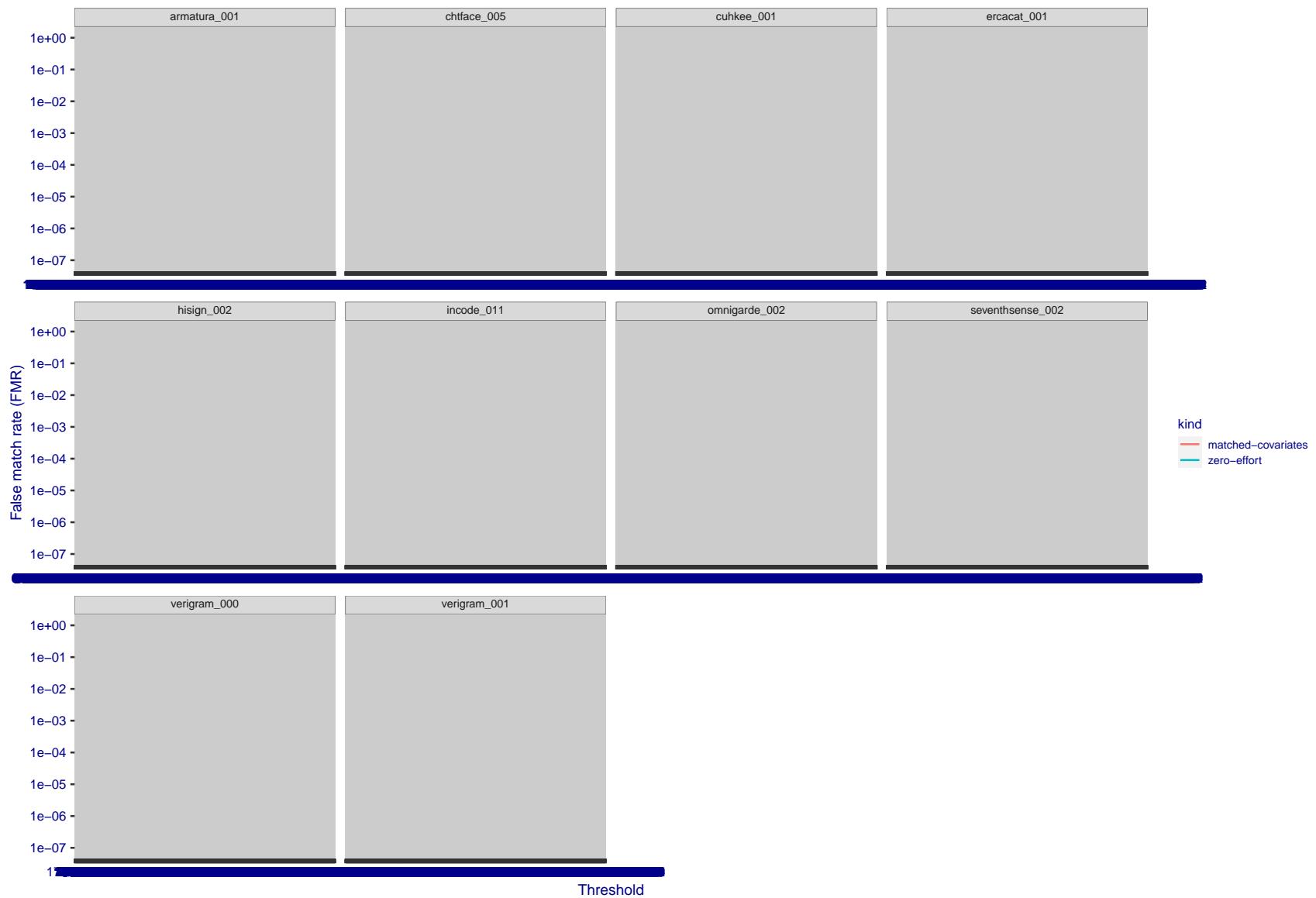


Figure 253: For the visa images, the false match calibration curves show FMR vs. threshold, T . The blue (lower) curves are for zero-effort impostors (i.e. comparing all images against all). The red (upper) curves are for persons of the same-sex, same-age, and same national-origin. This shows that FMR is underestimated (by a factor of 10 or more) by using a zero-effort impostor calculation to calibrate T . As shown later (sec. 3.6), FMR is higher for demographic-matched impostors.

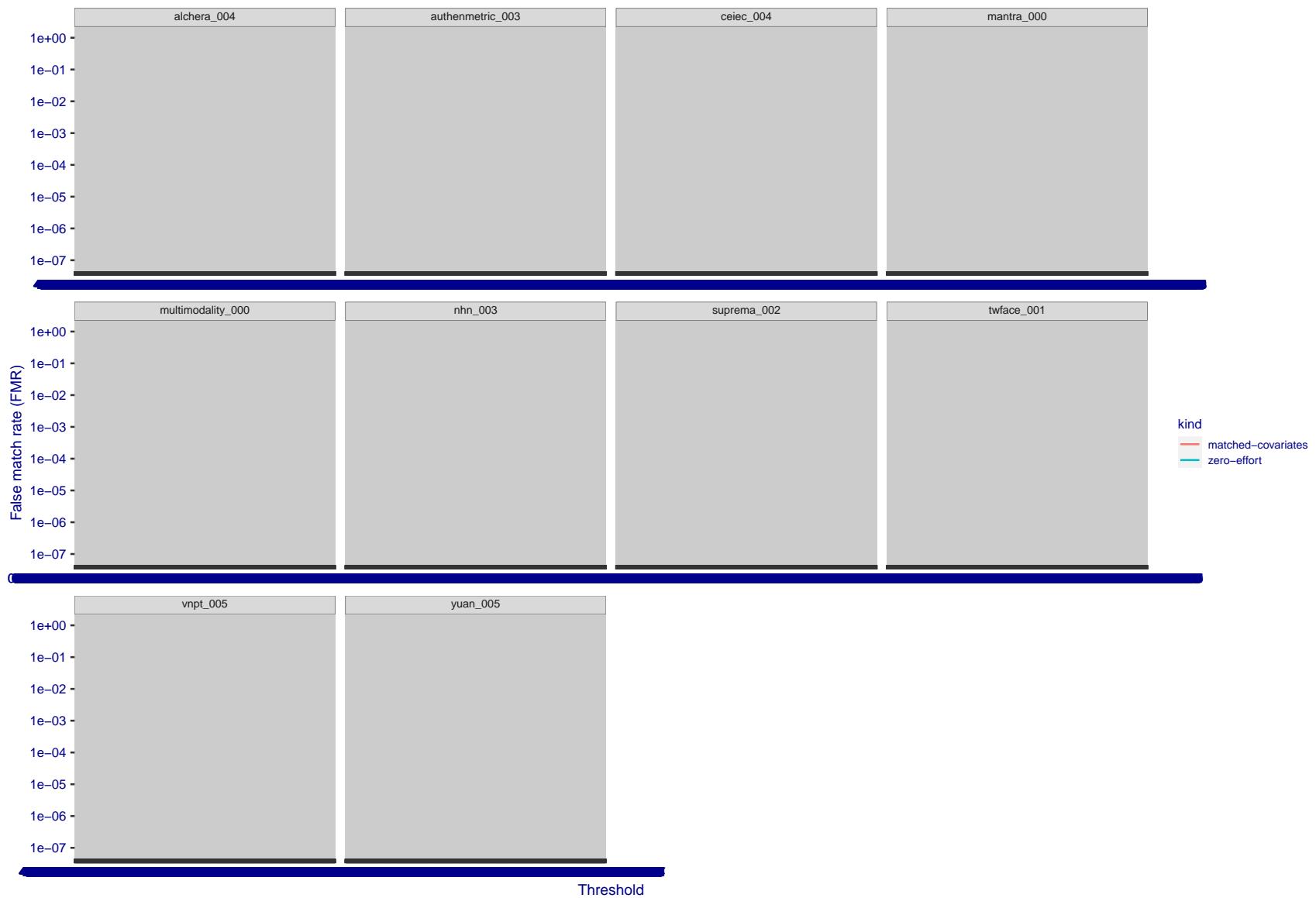


Figure 254: For the visa images, the false match calibration curves show FMR vs. threshold, T . The blue (lower) curves are for zero-effort impostors (i.e. comparing all images against all). The red (upper) curves are for persons of the same-sex, same-age, and same national-origin. This shows that FMR is underestimated (by a factor of 10 or more) by using a zero-effort impostor calculation to calibrate T . As shown later (sec. 3.6), FMR is higher for demographic-matched impostors.



Figure 255: For the visa images, the false match calibration curves show FMR vs. threshold, T . The blue (lower) curves are for zero-effort impostors (i.e. comparing all images against all). The red (upper) curves are for persons of the same-sex, same-age, and same national-origin. This shows that FMR is underestimated (by a factor of 10 or more) by using a zero-effort impostor calculation to calibrate T . As shown later (sec. 3.6), FMR is higher for demographic-matched impostors.

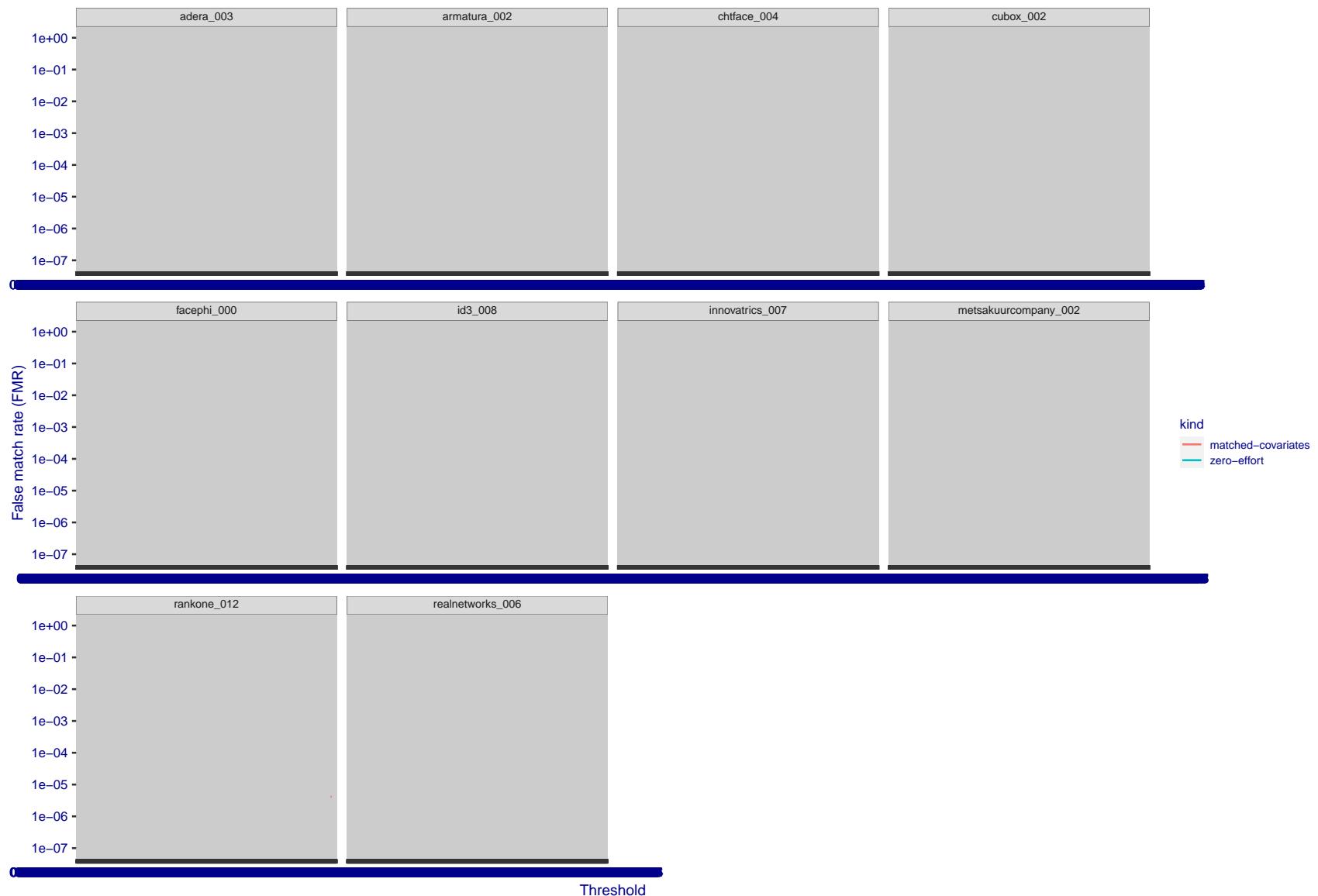


Figure 256: For the visa images, the false match calibration curves show FMR vs. threshold, T . The blue (lower) curves are for zero-effort impostors (i.e. comparing all images against all). The red (upper) curves are for persons of the same-sex, same-age, and same national-origin. This shows that FMR is underestimated (by a factor of 10 or more) by using a zero-effort impostor calculation to calibrate T . As shown later (sec. 3.6), FMR is higher for demographic-matched impostors.

2023/02/09 20:10:38

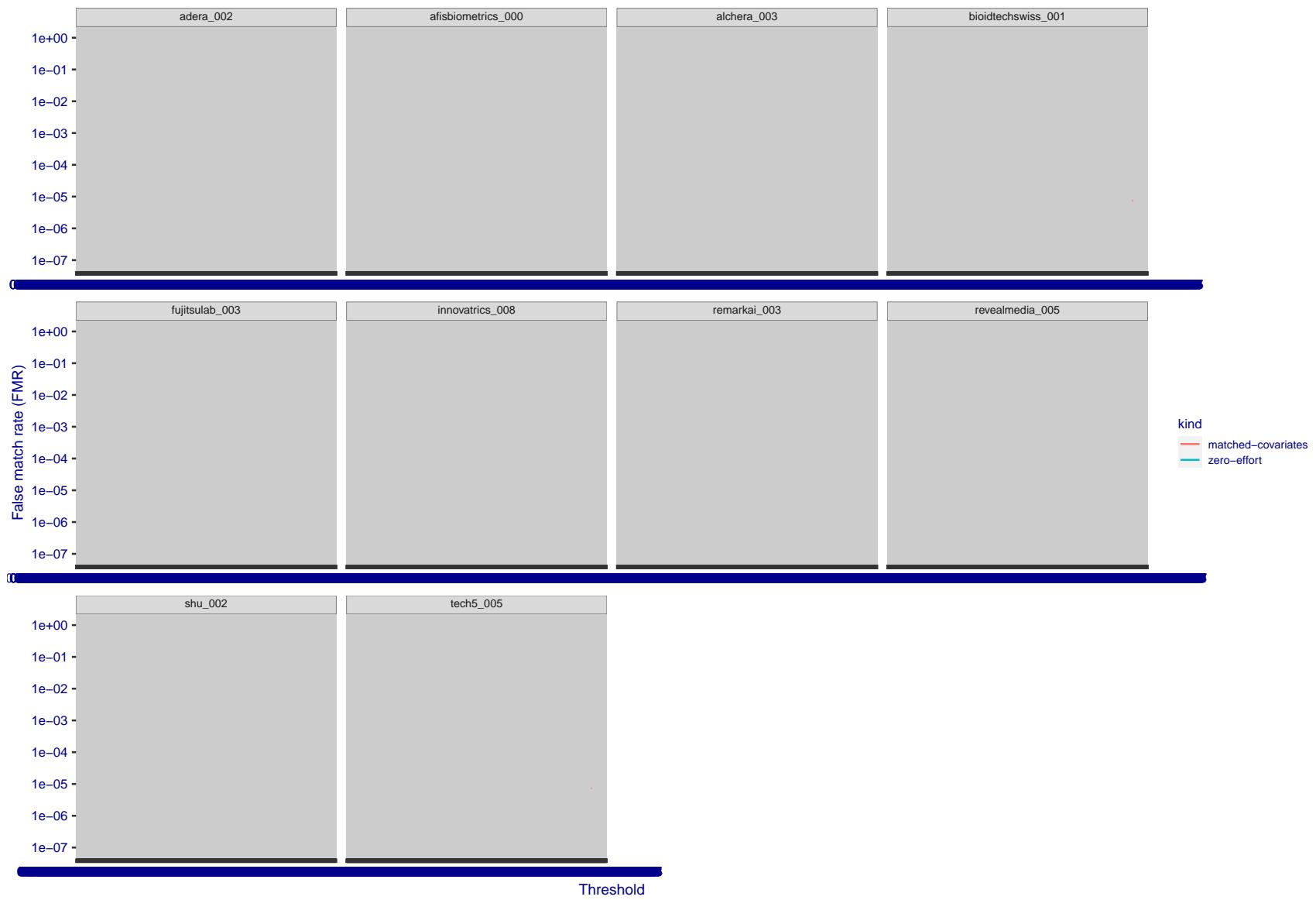


Figure 257: For the visa images, the false match calibration curves show FMR vs. threshold, T . The blue (lower) curves are for zero-effort impostors (i.e. comparing all images against all). The red (upper) curves are for persons of the same-sex, same-age, and same national-origin. This shows that FMR is underestimated (by a factor of 10 or more) by using a zero-effort impostor calculation to calibrate T . As shown later (sec. 3.6), FMR is higher for demographic-matched impostors.

FNMR(T)"False non-match rate"
"False match rate"

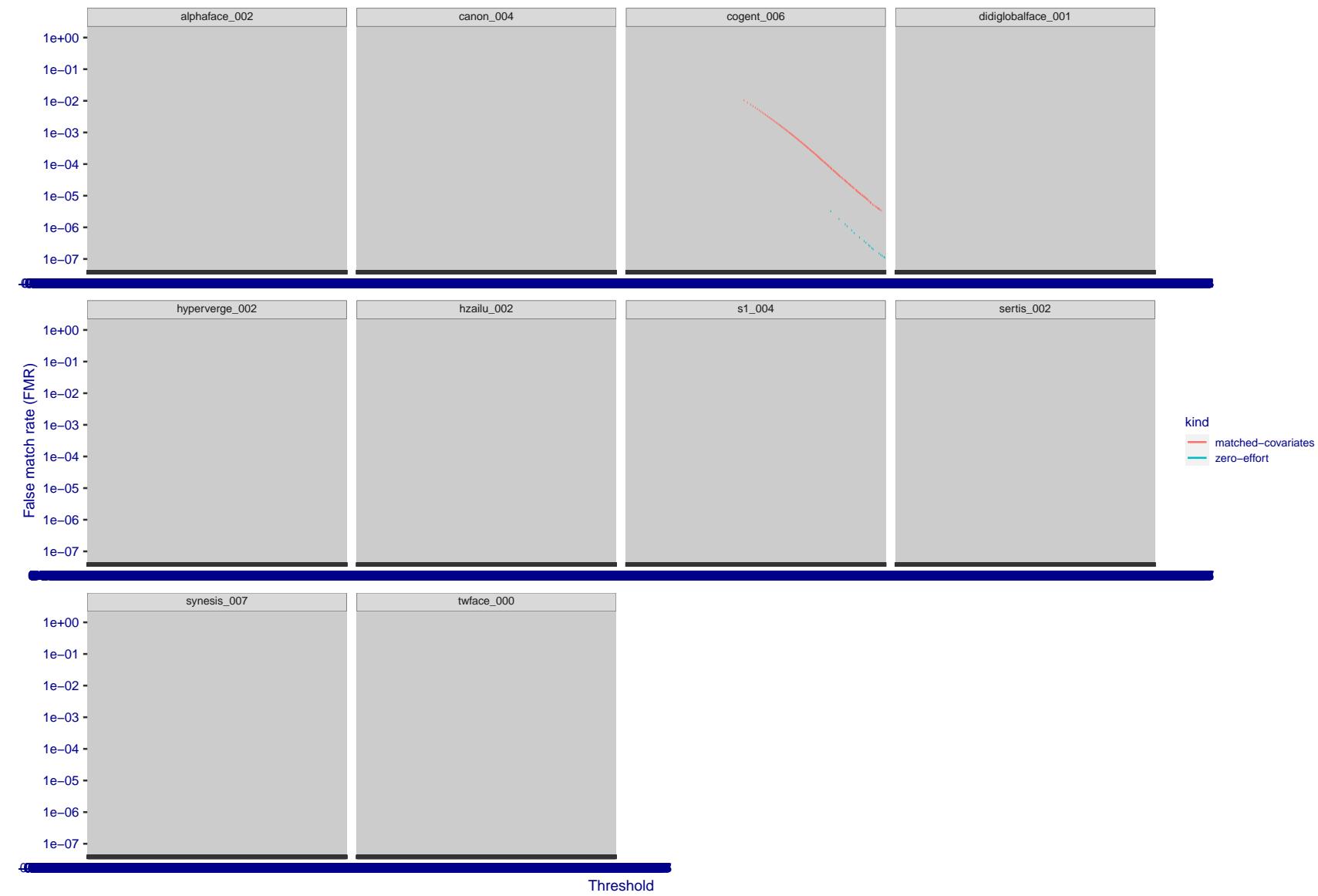


Figure 258: For the visa images, the false match calibration curves show FMR vs. threshold, T . The blue (lower) curves are for zero-effort impostors (i.e. comparing all images against all). The red (upper) curves are for persons of the same-sex, same-age, and same national-origin. This shows that FMR is underestimated (by a factor of 10 or more) by using a zero-effort impostor calculation to calibrate T . As shown later (sec. 3.6), FMR is higher for demographic-matched impostors.

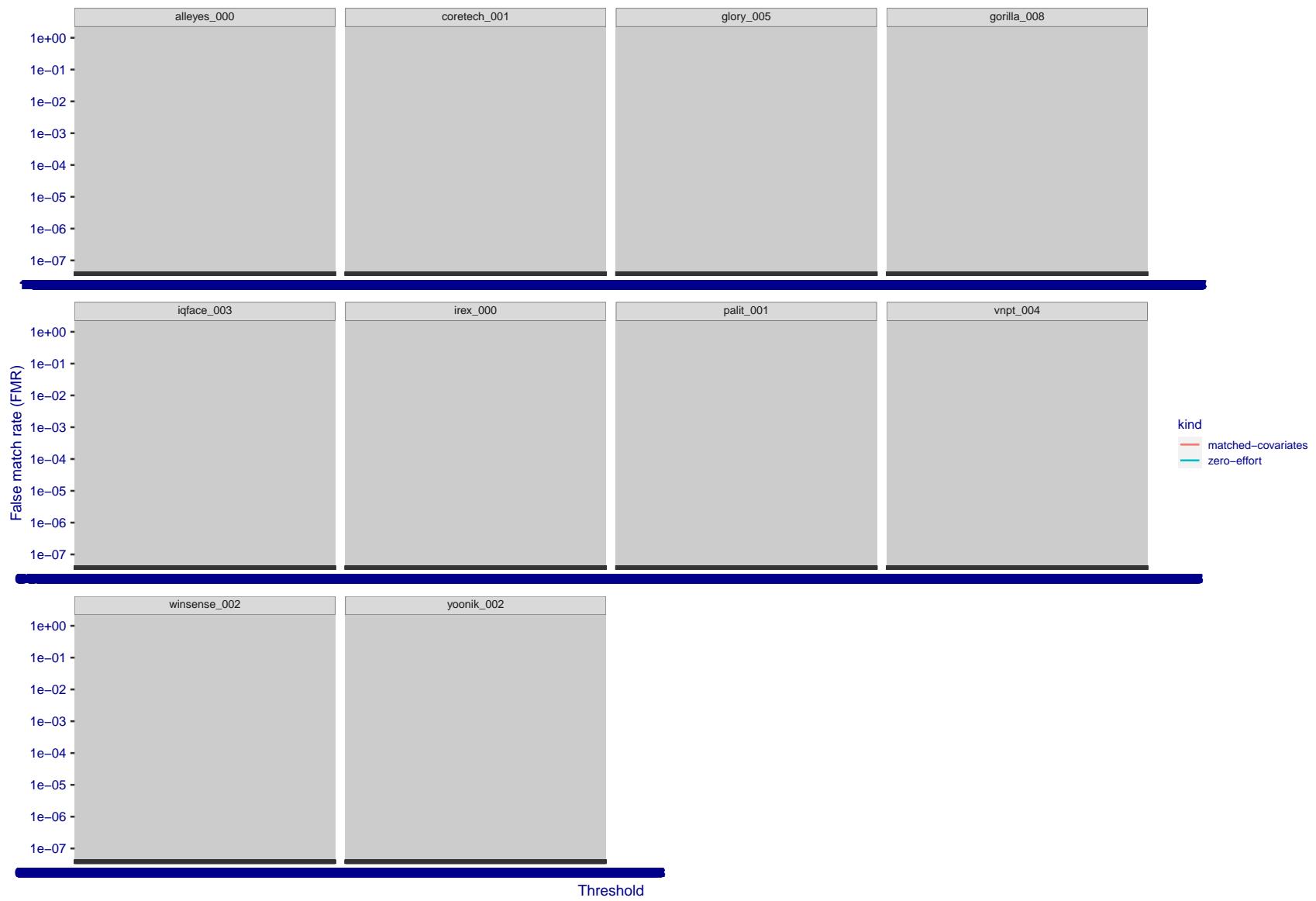


Figure 259: For the visa images, the false match calibration curves show FMR vs. threshold, T . The blue (lower) curves are for zero-effort impostors (i.e. comparing all images against all). The red (upper) curves are for persons of the same-sex, same-age, and same national-origin. This shows that FMR is underestimated (by a factor of 10 or more) by using a zero-effort impostor calculation to calibrate T . As shown later (sec. 3.6), FMR is higher for demographic-matched impostors.

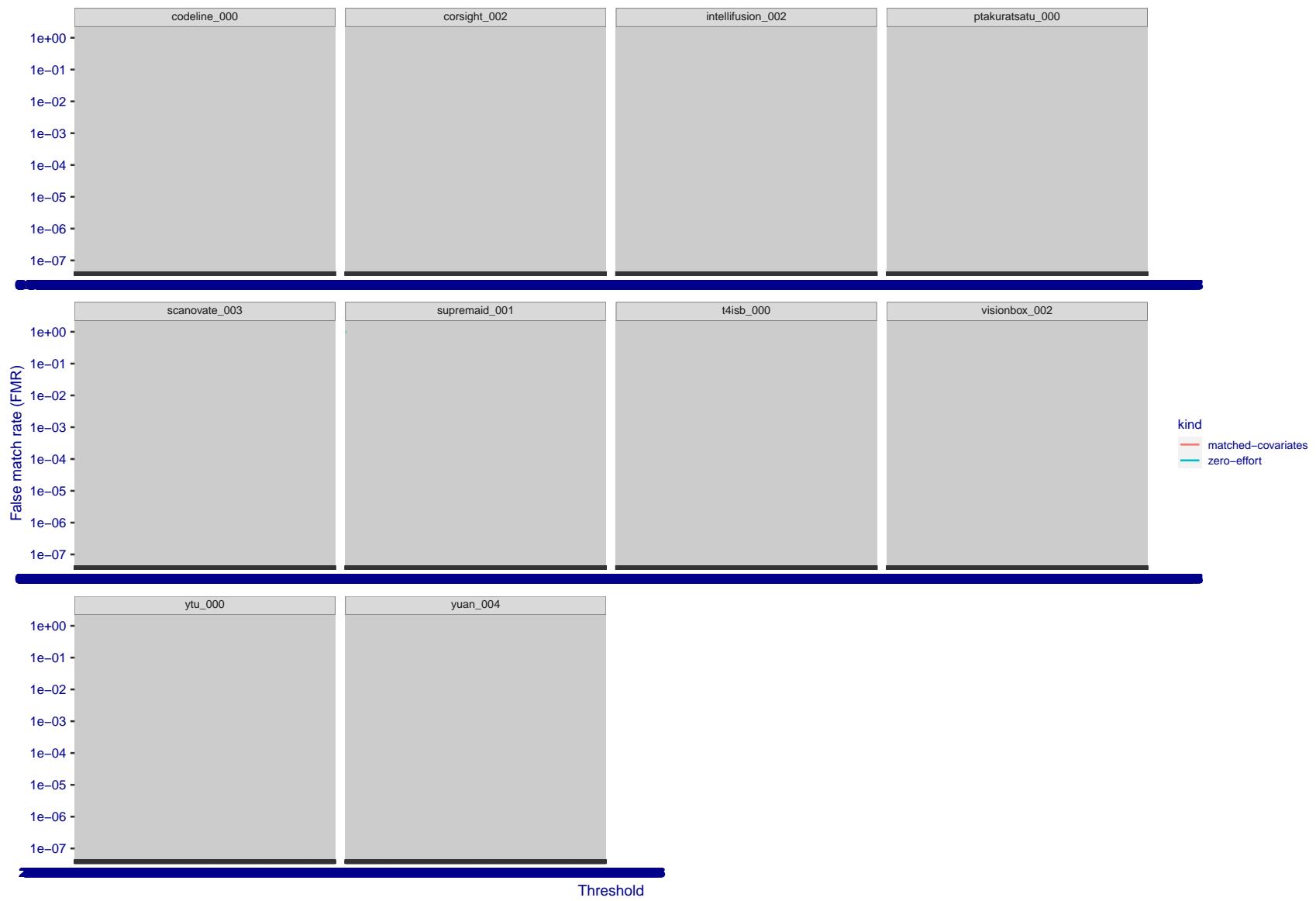


Figure 260: For the visa images, the false match calibration curves show FMR vs. threshold, T . The blue (lower) curves are for zero-effort impostors (i.e. comparing all images against all). The red (upper) curves are for persons of the same-sex, same-age, and same national-origin. This shows that FMR is underestimated (by a factor of 10 or more) by using a zero-effort impostor calculation to calibrate T . As shown later (sec. 3.6), FMR is higher for demographic-matched impostors.

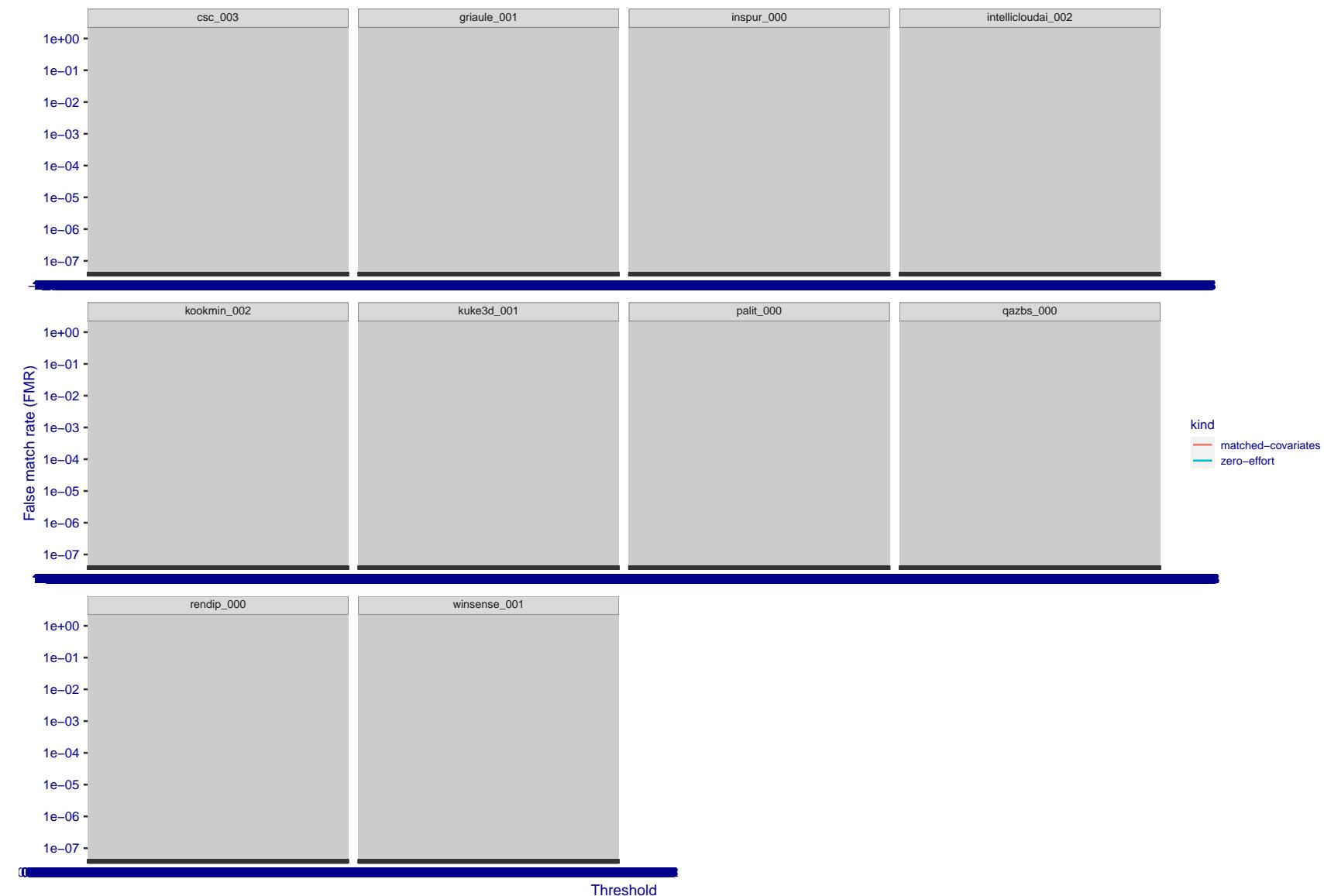


Figure 261: For the visa images, the false match calibration curves show FMR vs. threshold, T . The blue (lower) curves are for zero-effort impostors (i.e. comparing all images against all). The red (upper) curves are for persons of the same-sex, same-age, and same national-origin. This shows that FMR is underestimated (by a factor of 10 or more) by using a zero-effort impostor calculation to calibrate T . As shown later (sec. 3.6), FMR is higher for demographic-matched impostors.

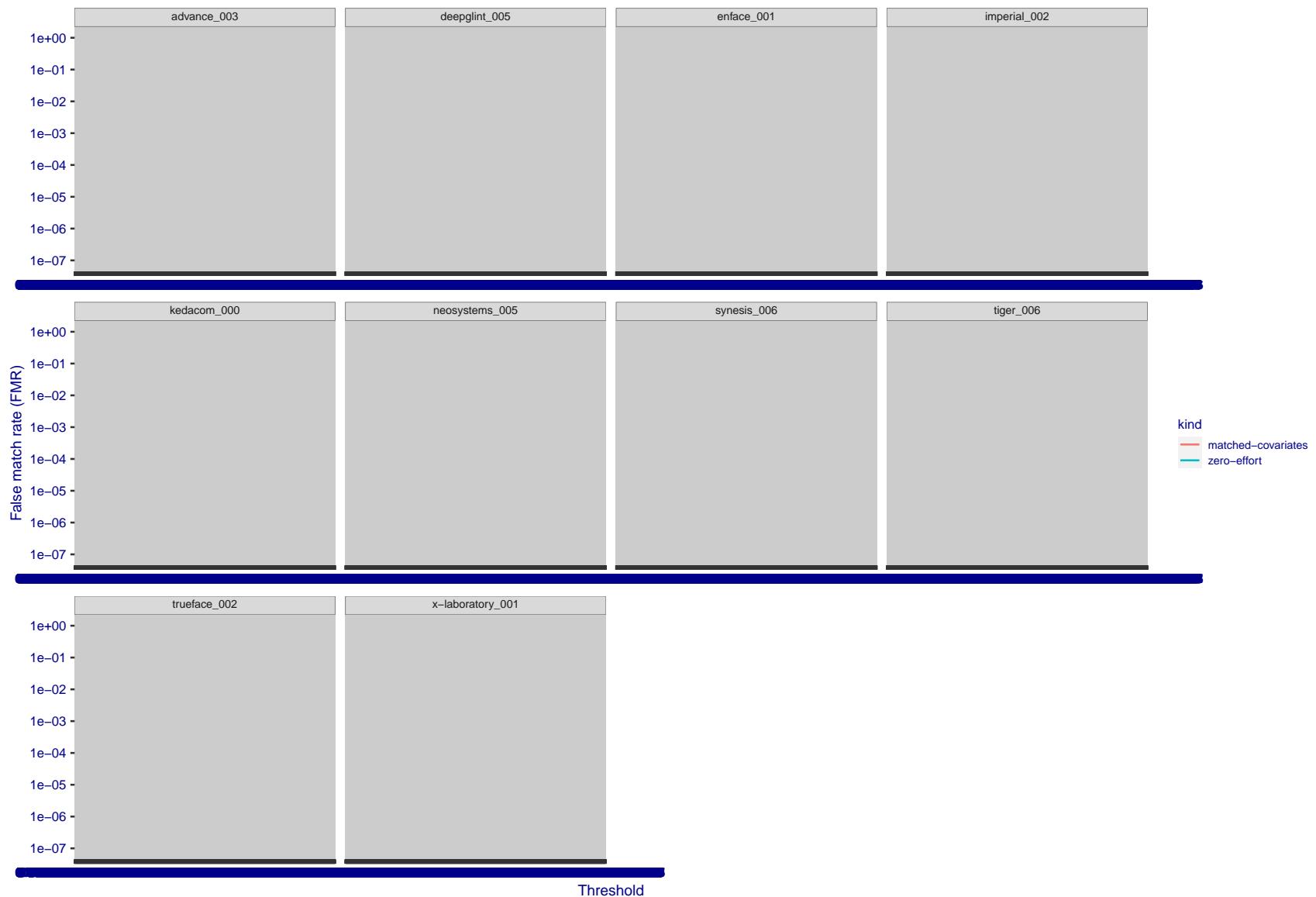


Figure 262: For the visa images, the false match calibration curves show FMR vs. threshold, T . The blue (lower) curves are for zero-effort impostors (i.e. comparing all images against all). The red (upper) curves are for persons of the same-sex, same-age, and same national-origin. This shows that FMR is underestimated (by a factor of 10 or more) by using a zero-effort impostor calculation to calibrate T . As shown later (sec. 3.6), FMR is higher for demographic-matched impostors.

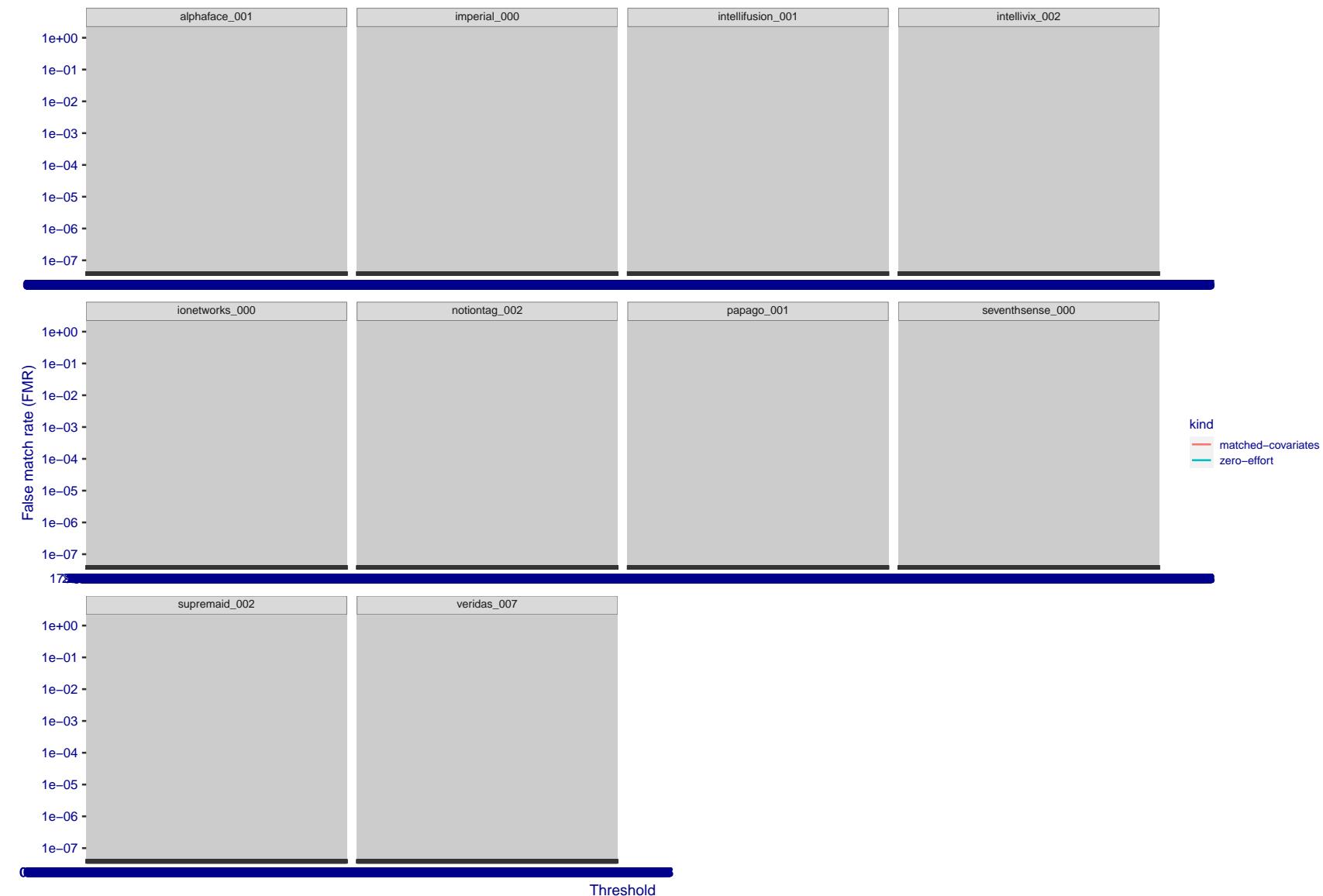


Figure 263: For the visa images, the false match calibration curves show FMR vs. threshold, T . The blue (lower) curves are for zero-effort impostors (i.e. comparing all images against all). The red (upper) curves are for persons of the same-sex, same-age, and same national-origin. This shows that FMR is underestimated (by a factor of 10 or more) by using a zero-effort impostor calculation to calibrate T . As shown later (sec. 3.6), FMR is higher for demographic-matched impostors.

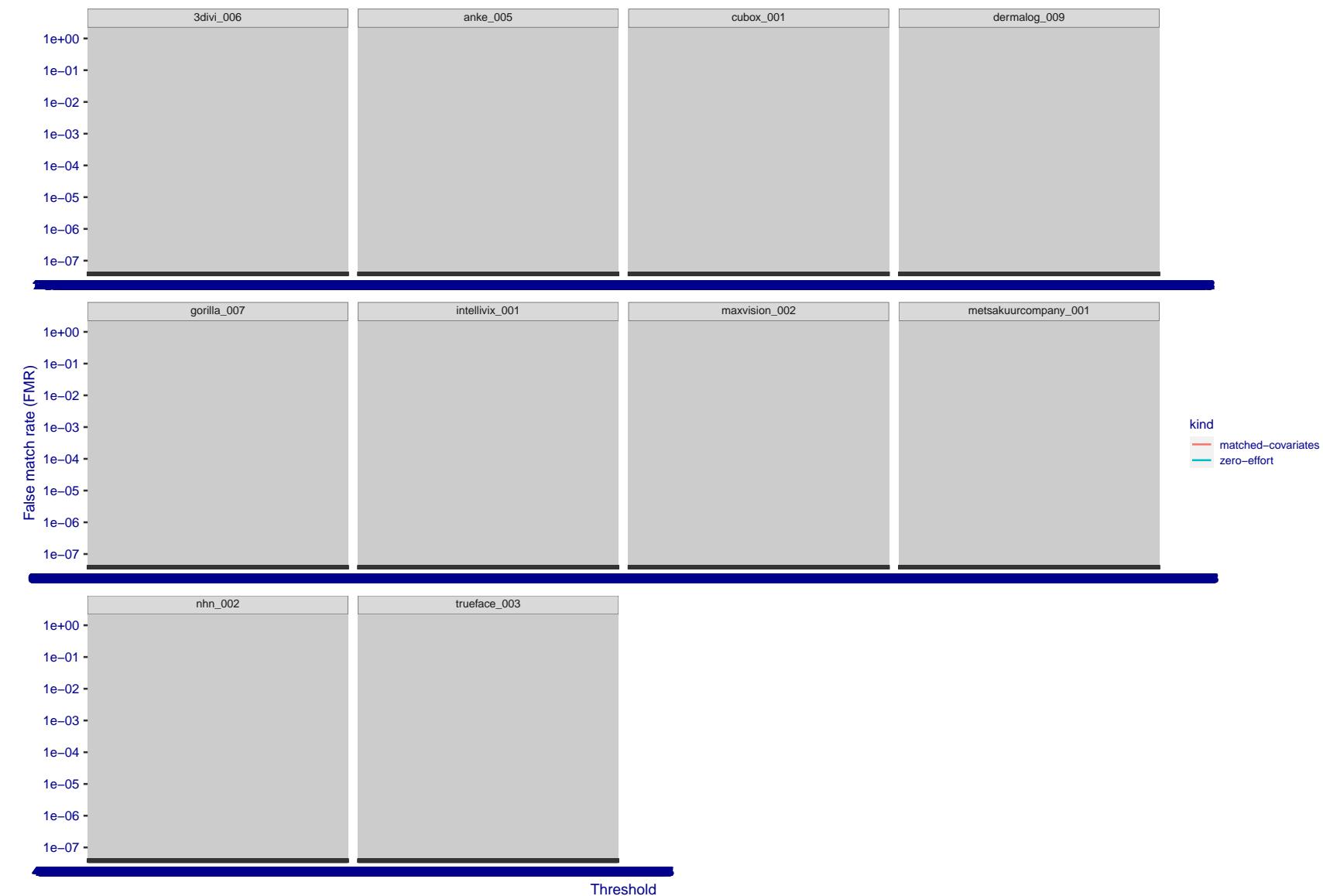


Figure 264: For the visa images, the false match calibration curves show FMR vs. threshold, T . The blue (lower) curves are for zero-effort impostors (i.e. comparing all images against all). The red (upper) curves are for persons of the same-sex, same-age, and same national-origin. This shows that FMR is underestimated (by a factor of 10 or more) by using a zero-effort impostor calculation to calibrate T . As shown later (sec. 3.6), FMR is higher for demographic-matched impostors.

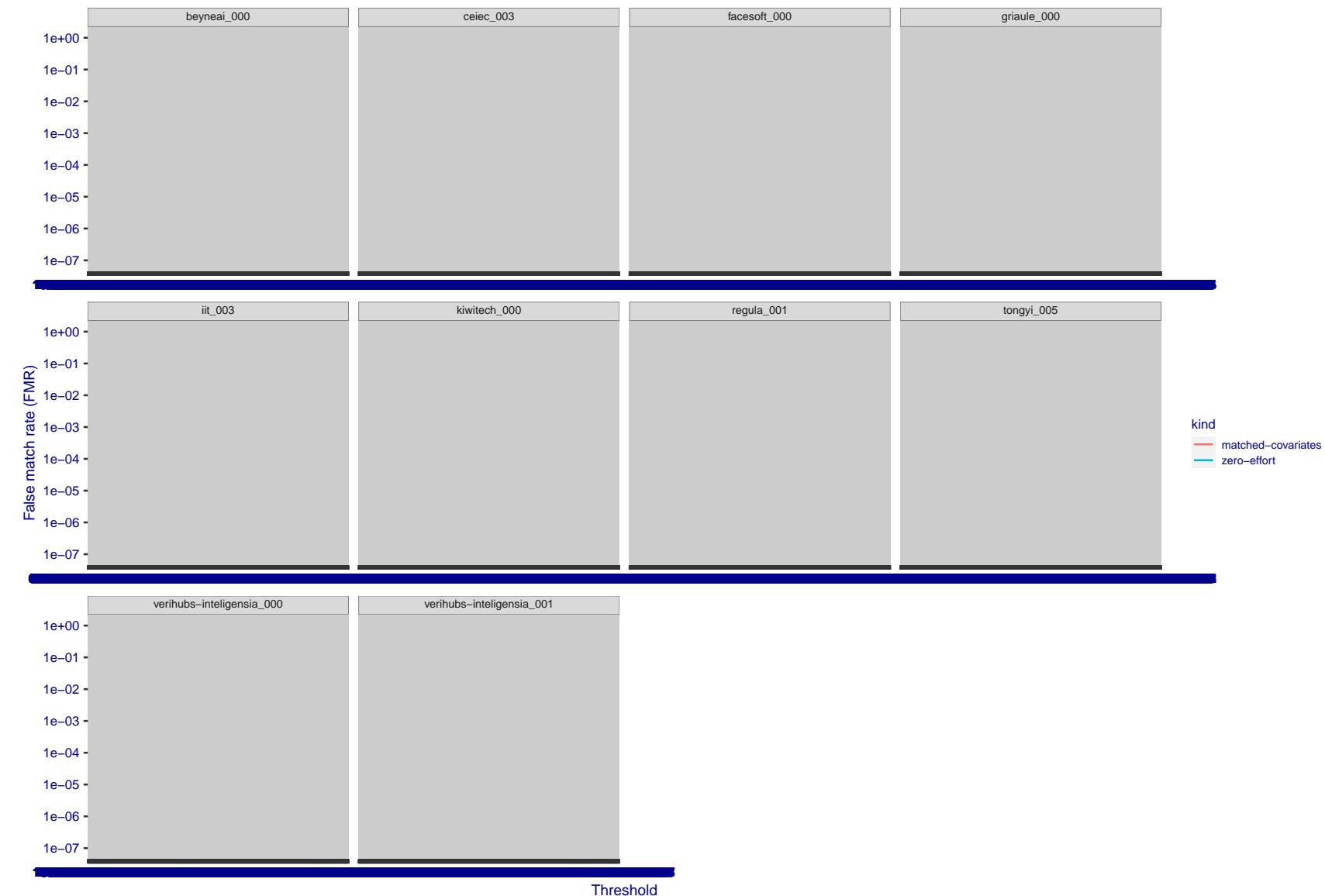


Figure 265: For the visa images, the false match calibration curves show FMR vs. threshold, T . The blue (lower) curves are for zero-effort impostors (i.e. comparing all images against all). The red (upper) curves are for persons of the same-sex, same-age, and same national-origin. This shows that FMR is underestimated (by a factor of 10 or more) by using a zero-effort impostor calculation to calibrate T . As shown later (sec. 3.6), FMR is higher for demographic-matched impostors.

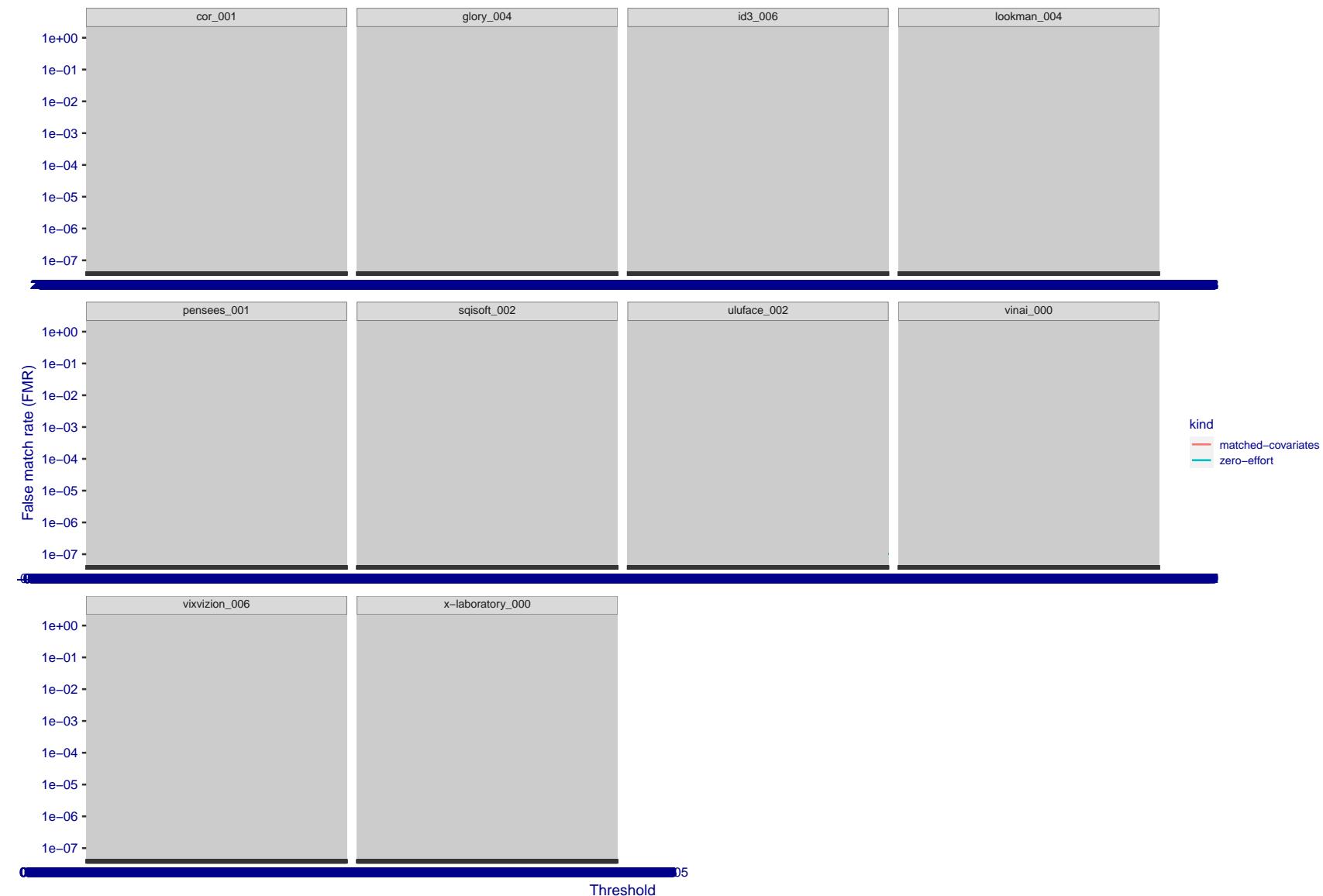


Figure 266: For the visa images, the false match calibration curves show FMR vs. threshold, T . The blue (lower) curves are for zero-effort impostors (i.e. comparing all images against all). The red (upper) curves are for persons of the same-sex, same-age, and same national-origin. This shows that FMR is underestimated (by a factor of 10 or more) by using a zero-effort impostor calculation to calibrate T . As shown later (sec. 3.6), FMR is higher for demographic-matched impostors.

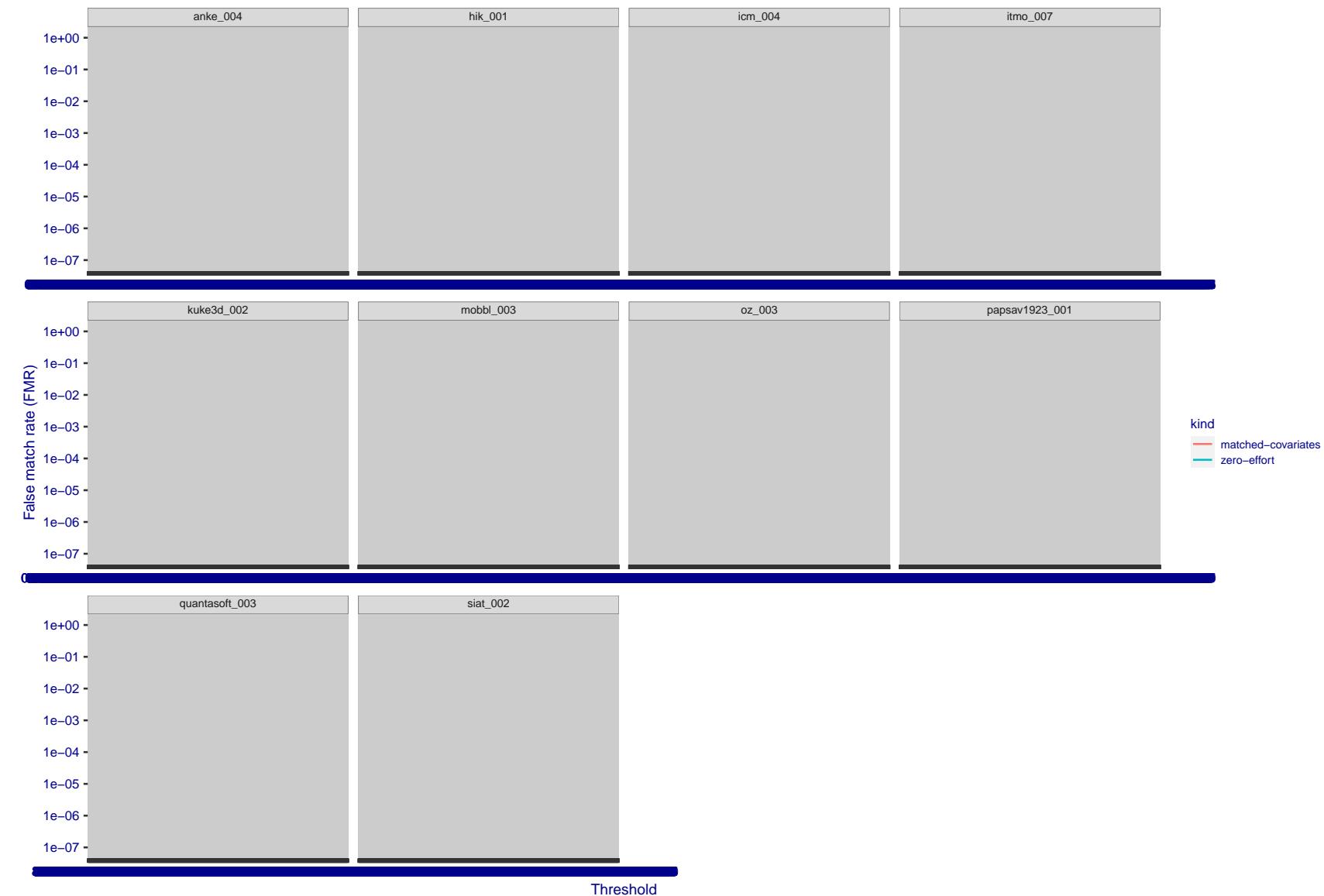


Figure 267: For the visa images, the false match calibration curves show FMR vs. threshold, T . The blue (lower) curves are for zero-effort impostors (i.e. comparing all images against all). The red (upper) curves are for persons of the same-sex, same-age, and same national-origin. This shows that FMR is underestimated (by a factor of 10 or more) by using a zero-effort impostor calculation to calibrate T . As shown later (sec. 3.6), FMR is higher for demographic-matched impostors.

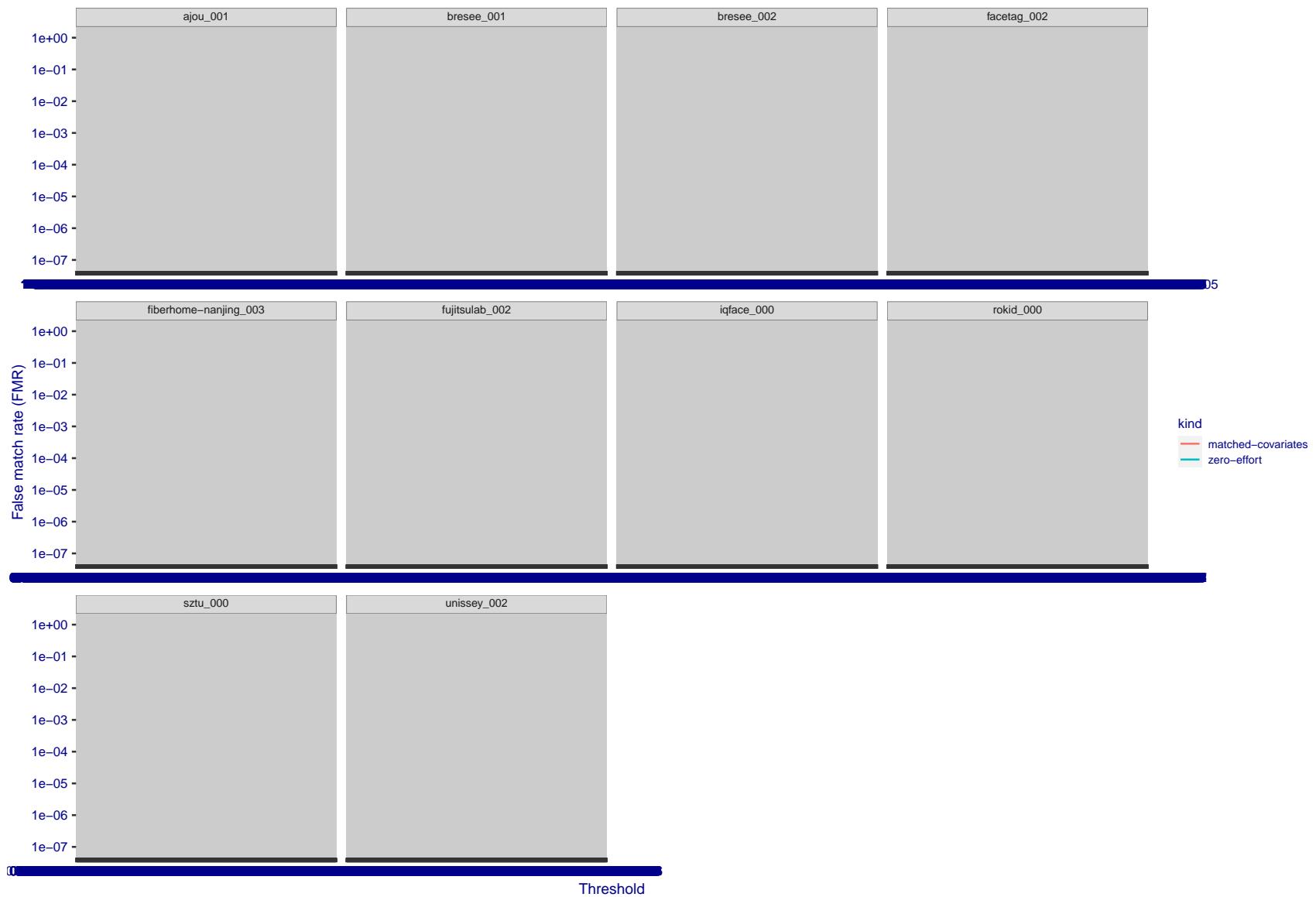


Figure 268: For the visa images, the false match calibration curves show FMR vs. threshold, T . The blue (lower) curves are for zero-effort impostors (i.e. comparing all images against all). The red (upper) curves are for persons of the same-sex, same-age, and same national-origin. This shows that FMR is underestimated (by a factor of 10 or more) by using a zero-effort impostor calculation to calibrate T . As shown later (sec. 3.6), FMR is higher for demographic-matched impostors.

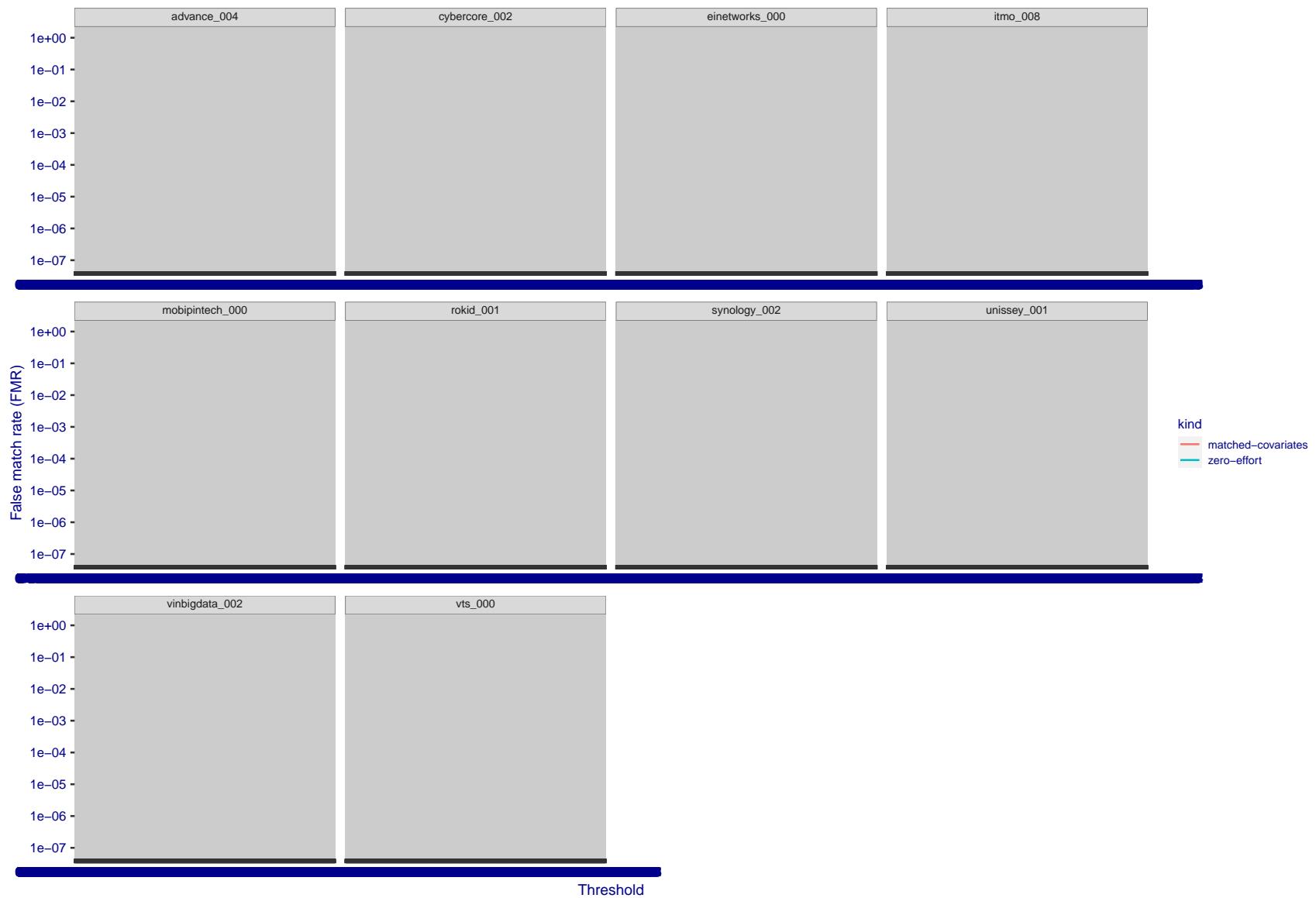


Figure 269: For the visa images, the false match calibration curves show FMR vs. threshold, T . The blue (lower) curves are for zero-effort impostors (i.e. comparing all images against all). The red (upper) curves are for persons of the same-sex, same-age, and same national-origin. This shows that FMR is underestimated (by a factor of 10 or more) by using a zero-effort impostor calculation to calibrate T . As shown later (sec. 3.6), FMR is higher for demographic-matched impostors.

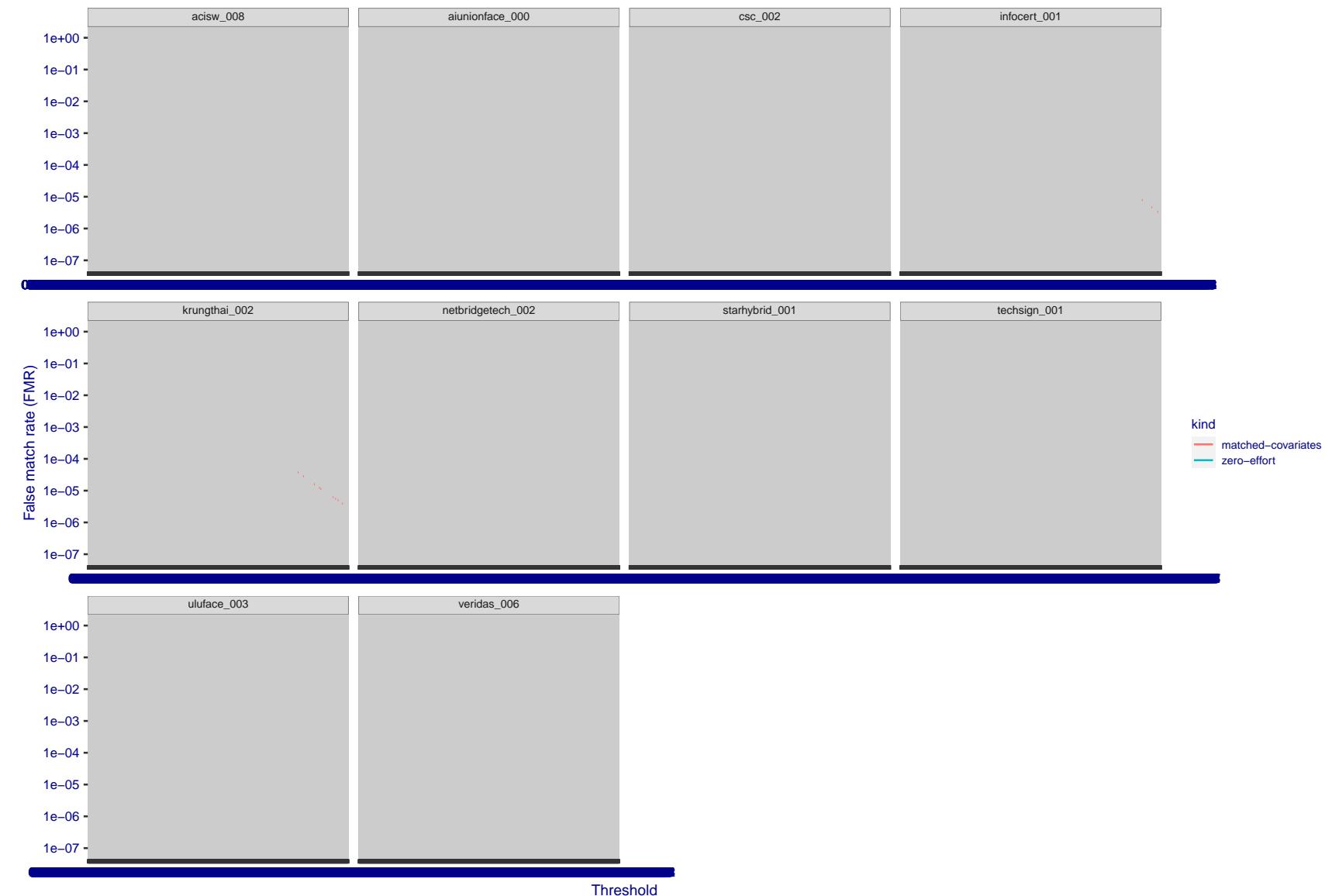


Figure 270: For the visa images, the false match calibration curves show FMR vs. threshold, T . The blue (lower) curves are for zero-effort impostors (i.e. comparing all images against all). The red (upper) curves are for persons of the same-sex, same-age, and same national-origin. This shows that FMR is underestimated (by a factor of 10 or more) by using a zero-effort impostor calculation to calibrate T . As shown later (sec. 3.6), FMR is higher for demographic-matched impostors.

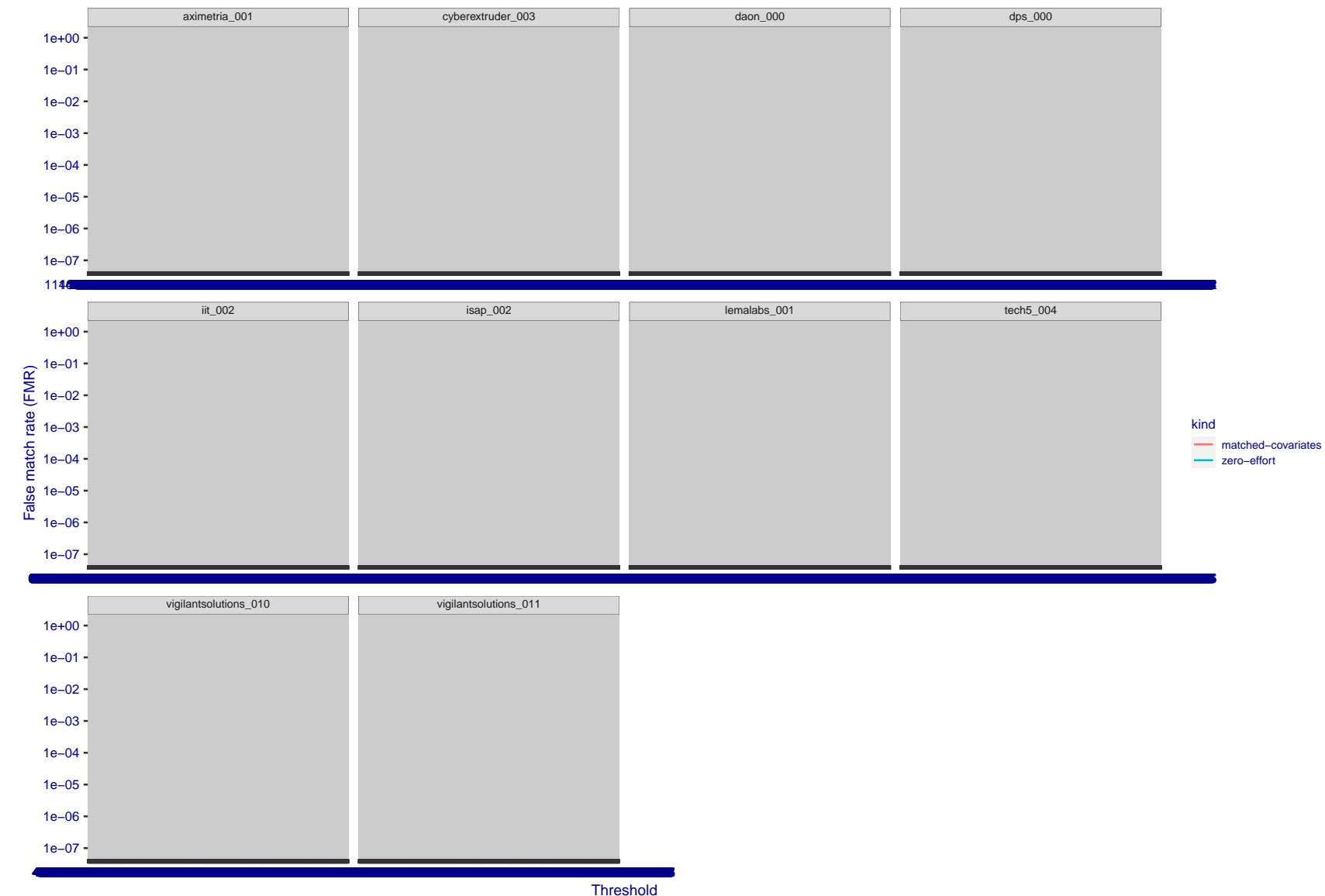


Figure 271: For the visa images, the false match calibration curves show FMR vs. threshold, T . The blue (lower) curves are for zero-effort impostors (i.e. comparing all images against all). The red (upper) curves are for persons of the same-sex, same-age, and same national-origin. This shows that FMR is underestimated (by a factor of 10 or more) by using a zero-effort impostor calculation to calibrate T . As shown later (sec. 3.6), FMR is higher for demographic-matched impostors.

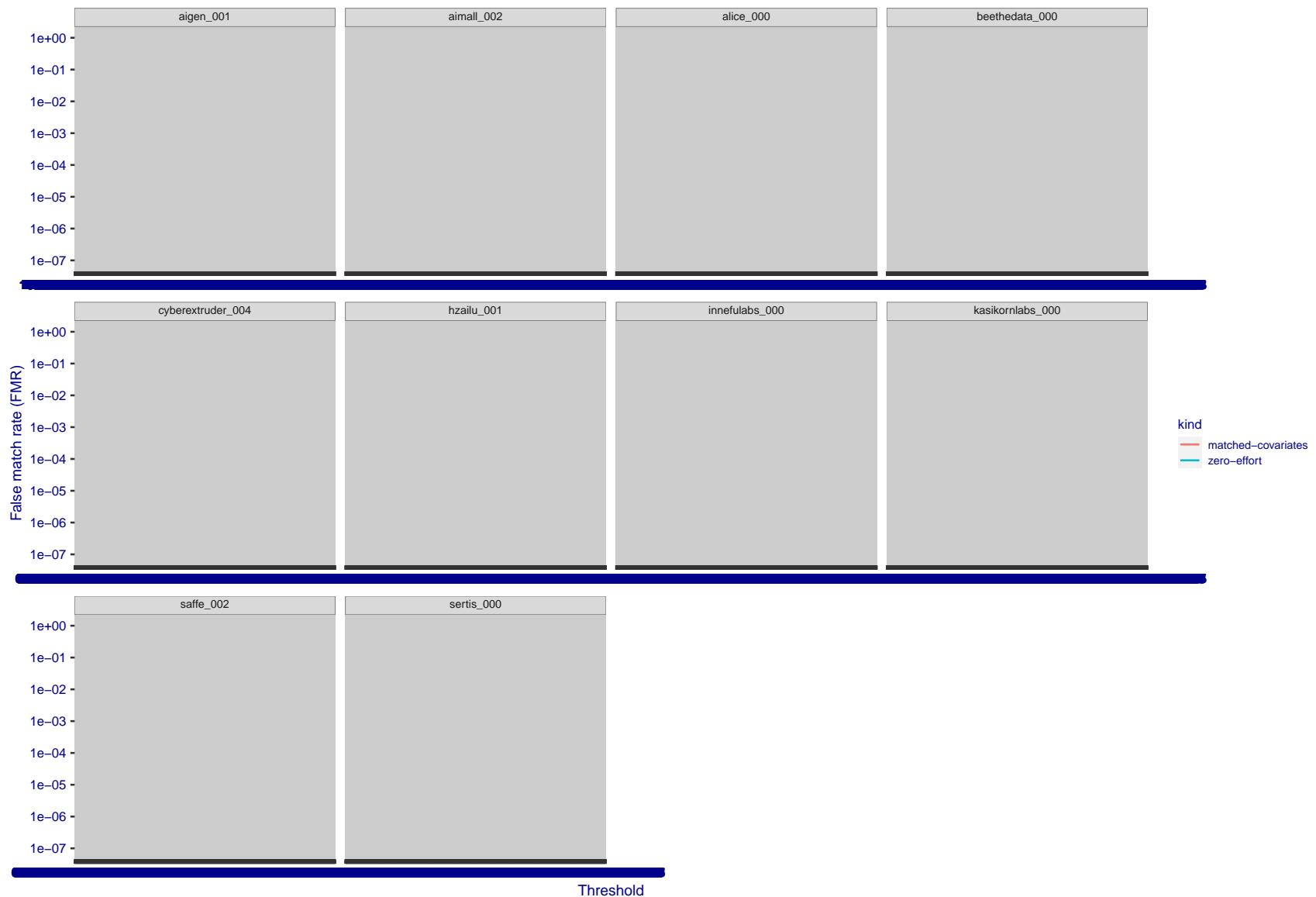


Figure 272: For the visa images, the false match calibration curves show FMR vs. threshold, T . The blue (lower) curves are for zero-effort impostors (i.e. comparing all images against all). The red (upper) curves are for persons of the same-sex, same-age, and same national-origin. This shows that FMR is underestimated (by a factor of 10 or more) by using a zero-effort impostor calculation to calibrate T . As shown later (sec. 3.6), FMR is higher for demographic-matched impostors.

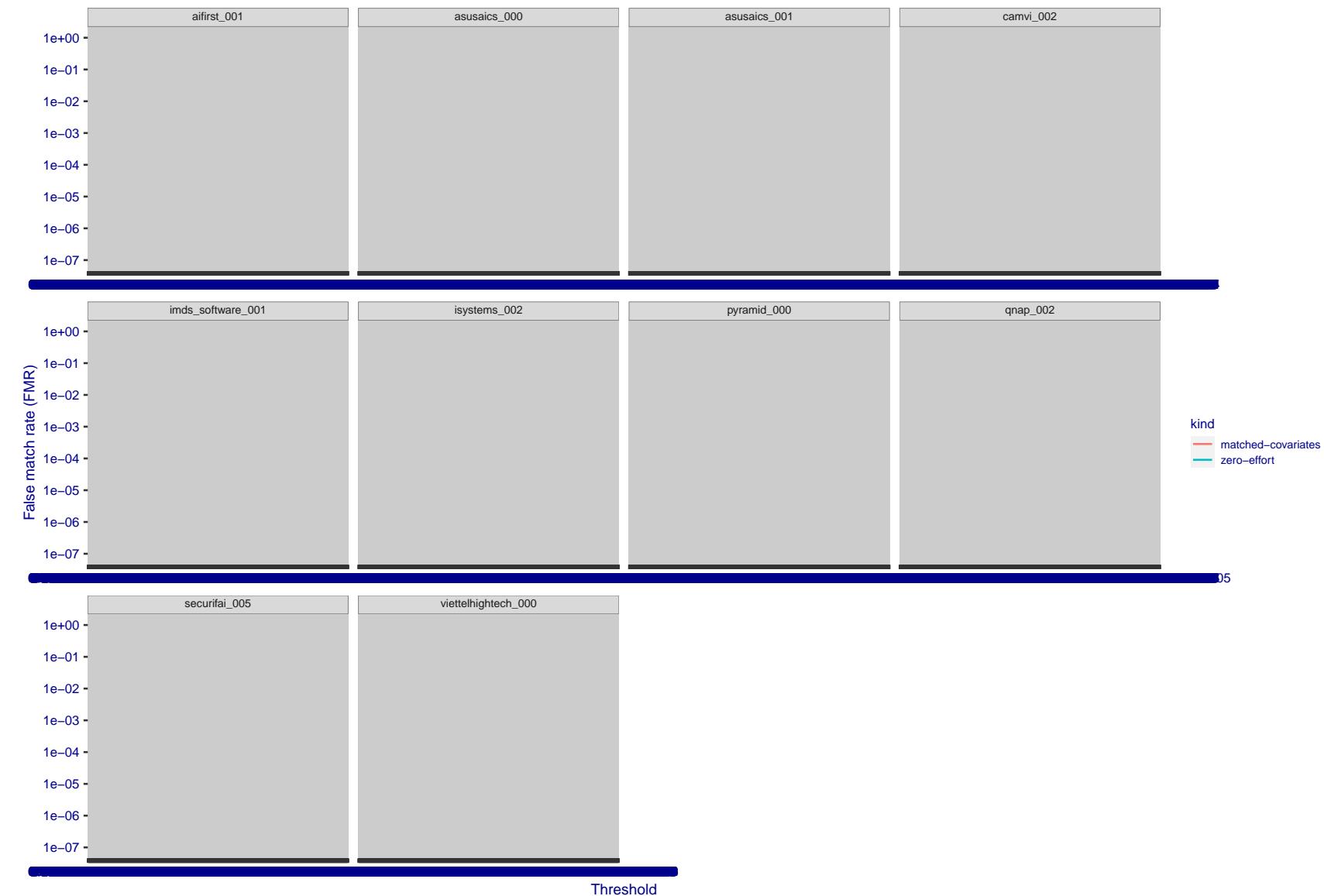


Figure 273: For the visa images, the false match calibration curves show FMR vs. threshold, T . The blue (lower) curves are for zero-effort impostors (i.e. comparing all images against all). The red (upper) curves are for persons of the same-sex, same-age, and same national-origin. This shows that FMR is underestimated (by a factor of 10 or more) by using a zero-effort impostor calculation to calibrate T . As shown later (sec. 3.6), FMR is higher for demographic-matched impostors.

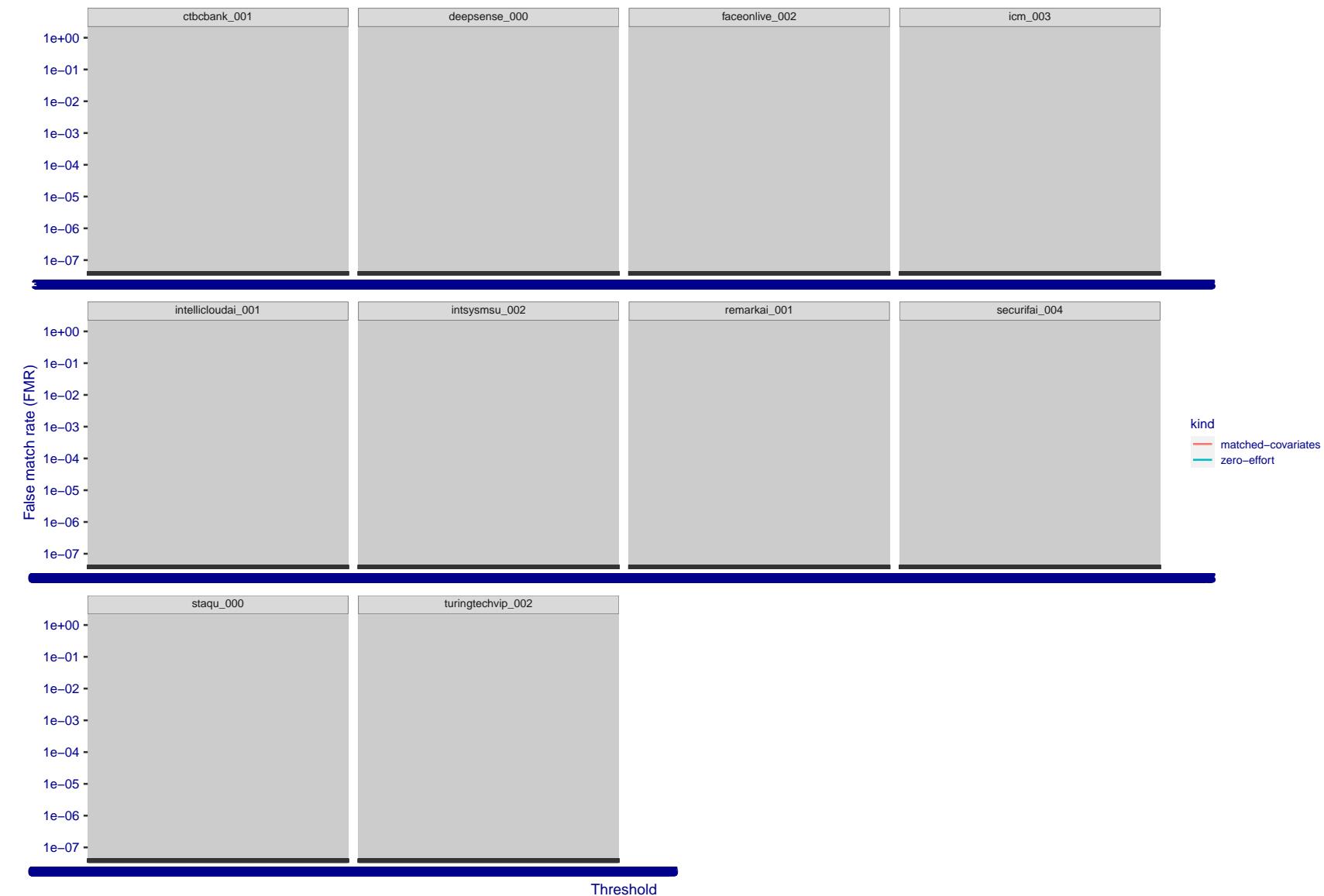


Figure 274: For the visa images, the false match calibration curves show FMR vs. threshold, T . The blue (lower) curves are for zero-effort impostors (i.e. comparing all images against all). The red (upper) curves are for persons of the same-sex, same-age, and same national-origin. This shows that FMR is underestimated (by a factor of 10 or more) by using a zero-effort impostor calculation to calibrate T . As shown later (sec. 3.6), FMR is higher for demographic-matched impostors.

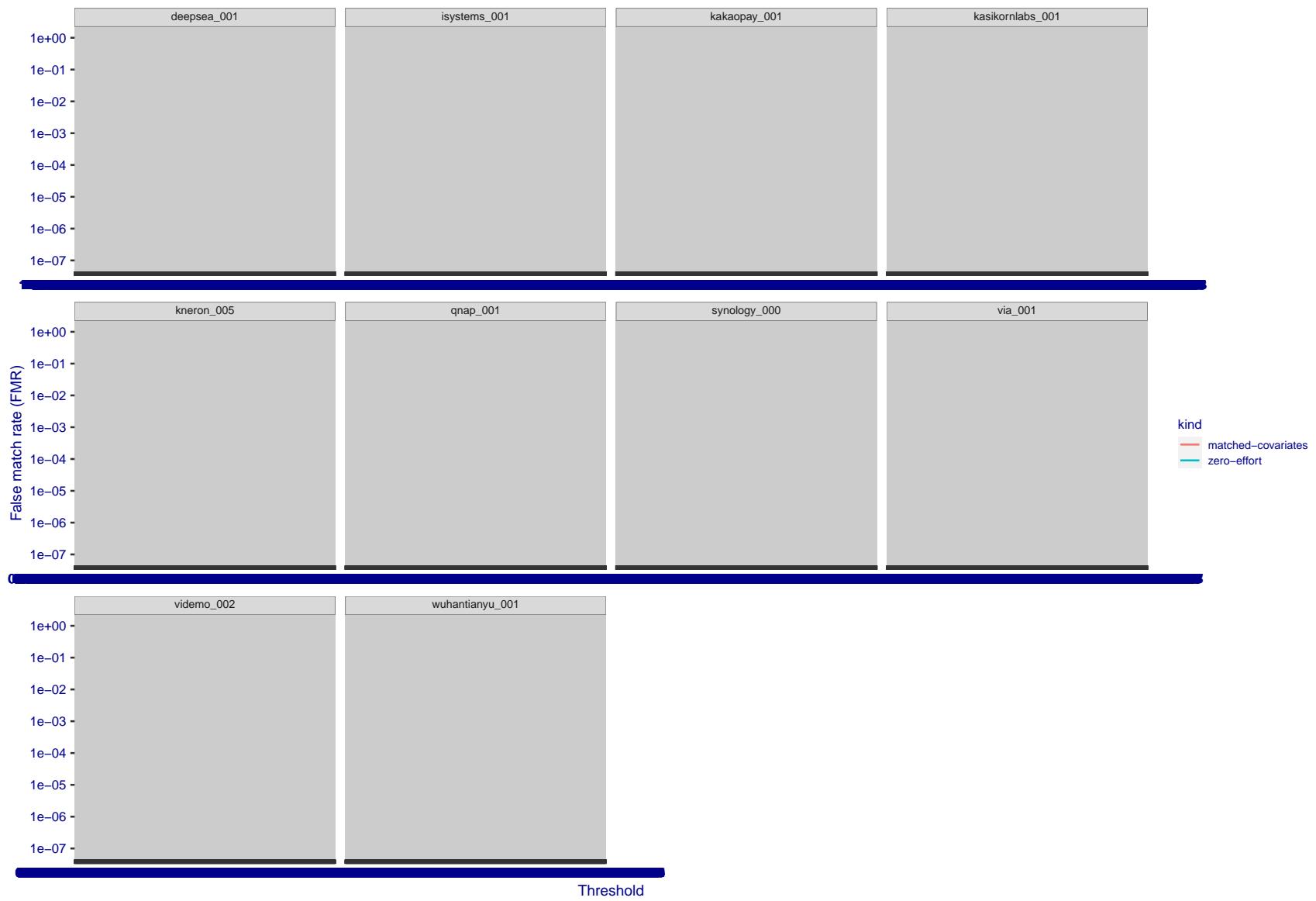


Figure 275: For the visa images, the false match calibration curves show FMR vs. threshold, T . The blue (lower) curves are for zero-effort impostors (i.e. comparing all images against all). The red (upper) curves are for persons of the same-sex, same-age, and same national-origin. This shows that FMR is underestimated (by a factor of 10 or more) by using a zero-effort impostor calculation to calibrate T . As shown later (sec. 3.6), FMR is higher for demographic-matched impostors.

2023/02/09 20:10:38

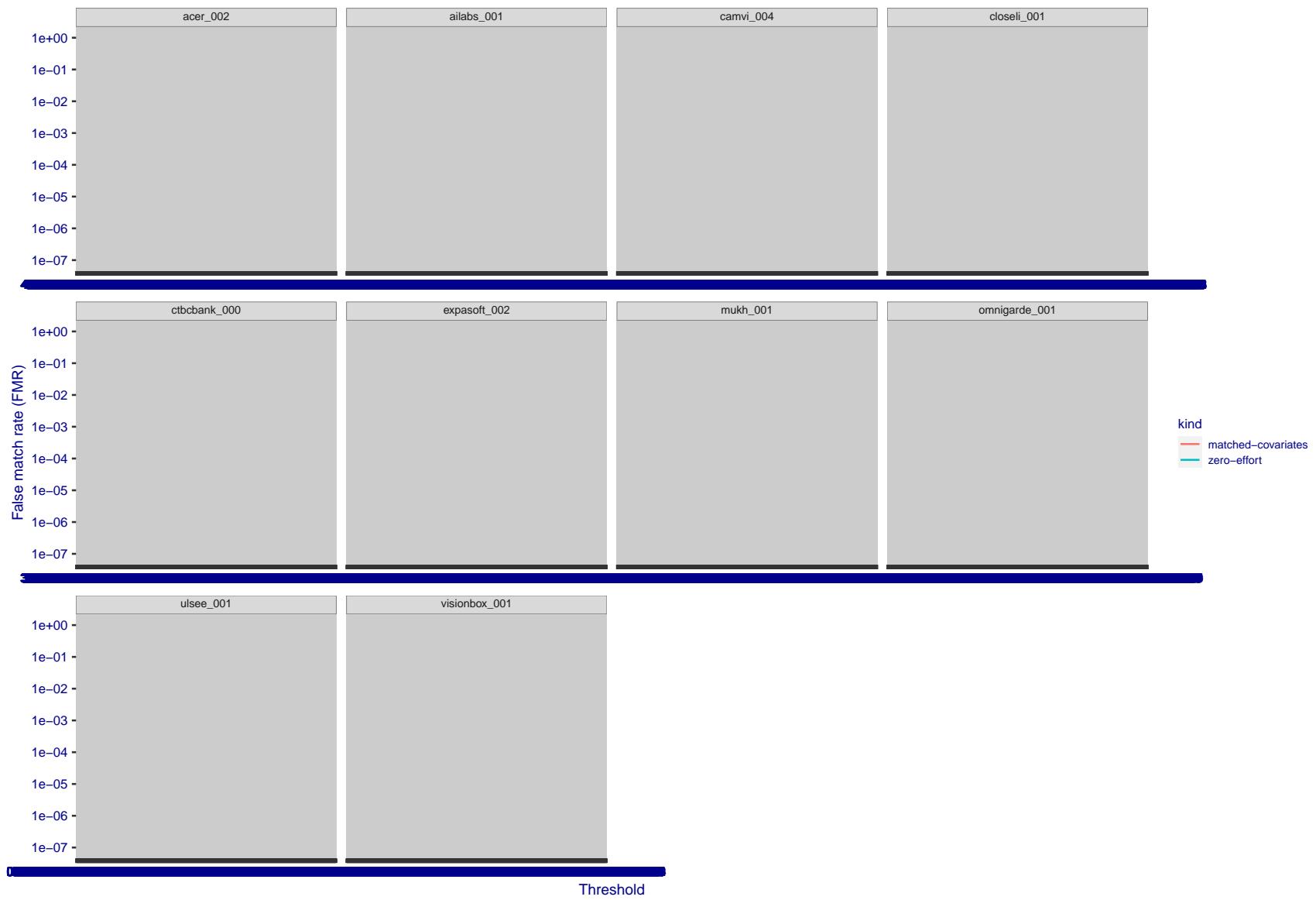


Figure 276: For the visa images, the false match calibration curves show FMR vs. threshold, T . The blue (lower) curves are for zero-effort impostors (i.e. comparing all images against all). The red (upper) curves are for persons of the same-sex, same-age, and same national-origin. This shows that FMR is underestimated (by a factor of 10 or more) by using a zero-effort impostor calculation to calibrate T . As shown later (sec. 3.6), FMR is higher for demographic-matched impostors.

2023/02/09 20:10:38

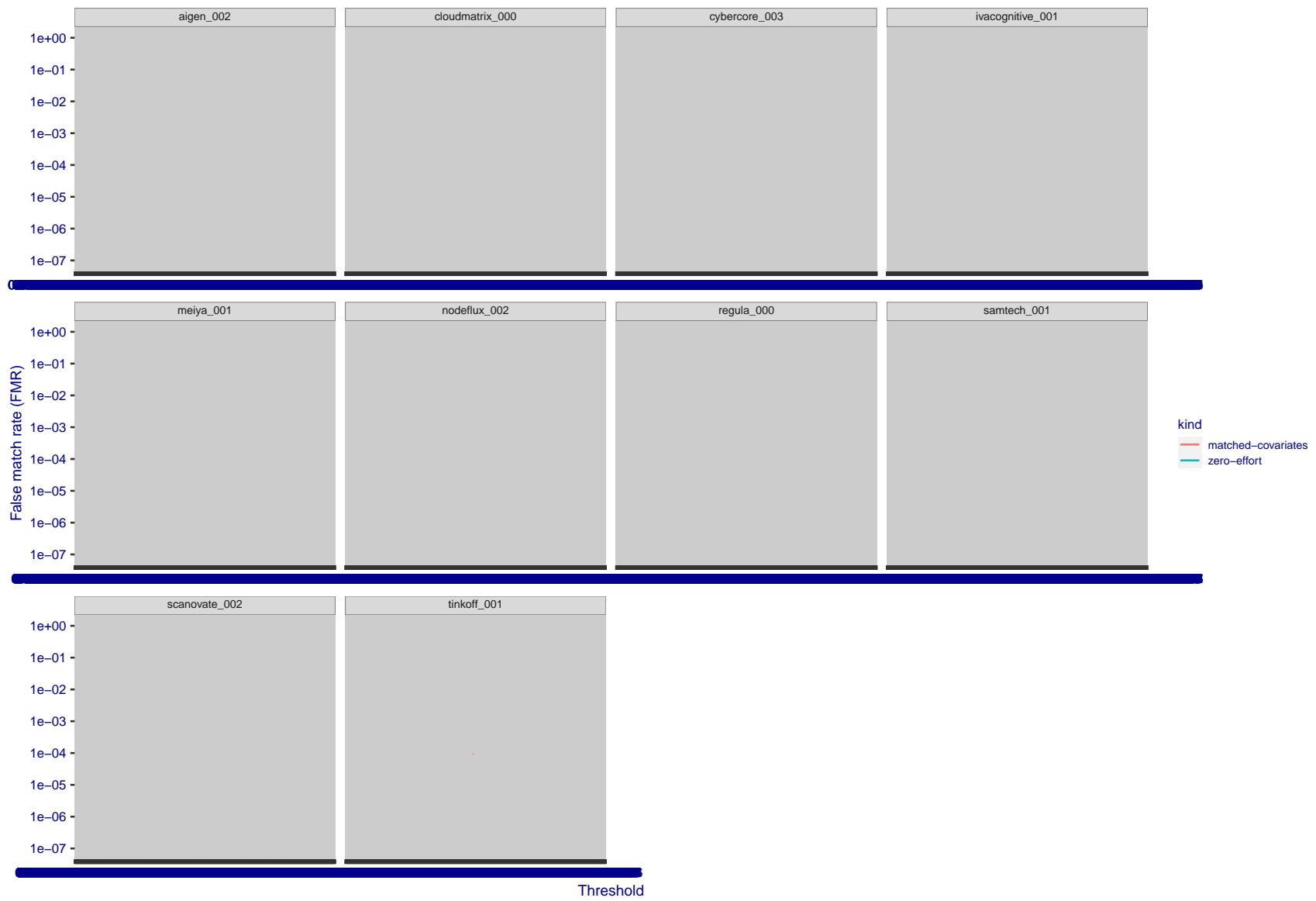


Figure 277: For the visa images, the false match calibration curves show FMR vs. threshold, T . The blue (lower) curves are for zero-effort impostors (i.e. comparing all images against all). The red (upper) curves are for persons of the same-sex, same-age, and same national-origin. This shows that FMR is underestimated (by a factor of 10 or more) by using a zero-effort impostor calculation to calibrate T . As shown later (sec. 3.6), FMR is higher for demographic-matched impostors.

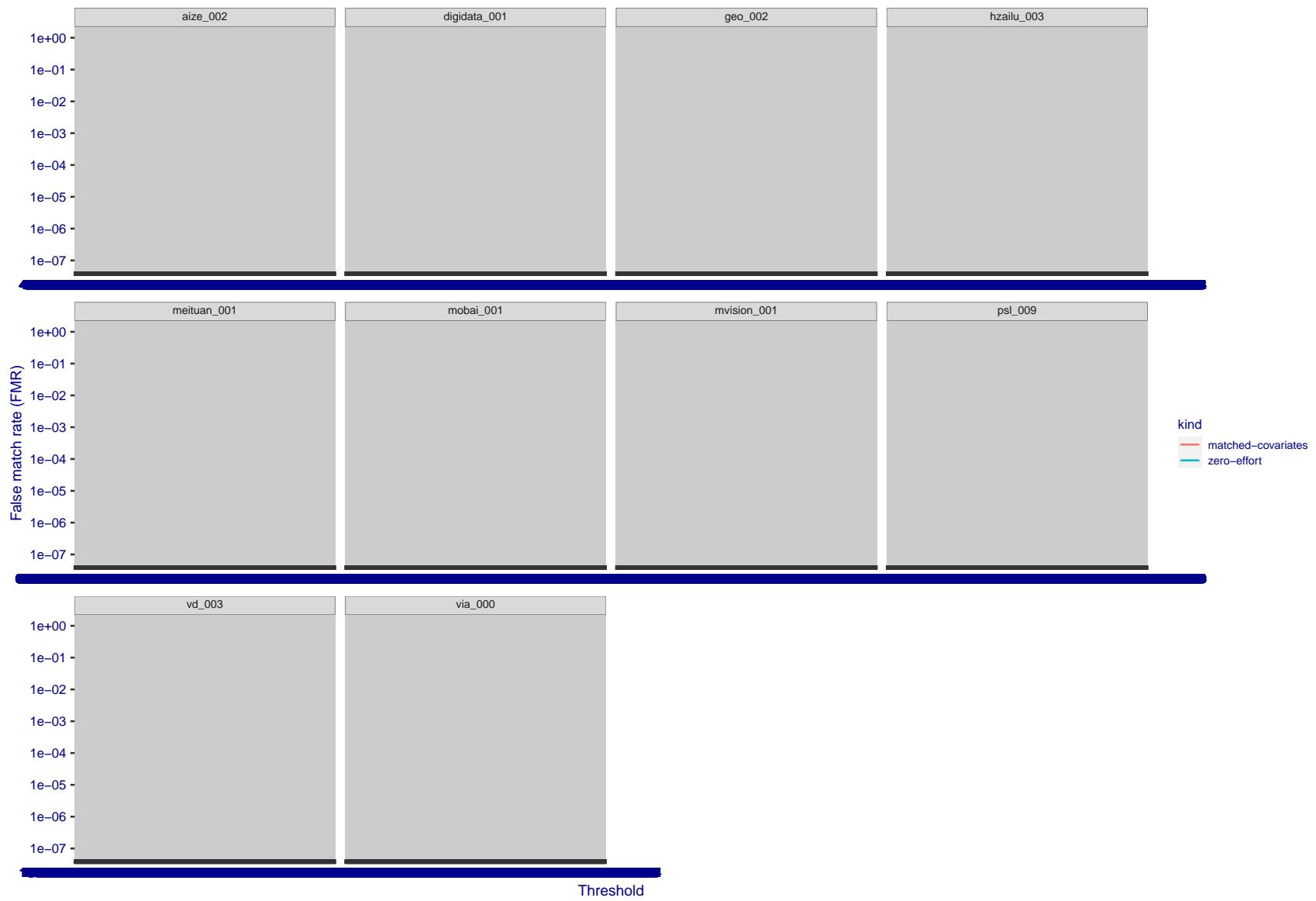


Figure 278: For the visa images, the false match calibration curves show FMR vs. threshold, T . The blue (lower) curves are for zero-effort impostors (i.e. comparing all images against all). The red (upper) curves are for persons of the same-sex, same-age, and same national-origin. This shows that FMR is underestimated (by a factor of 10 or more) by using a zero-effort impostor calculation to calibrate T . As shown later (sec. 3.6), FMR is higher for demographic-matched impostors.

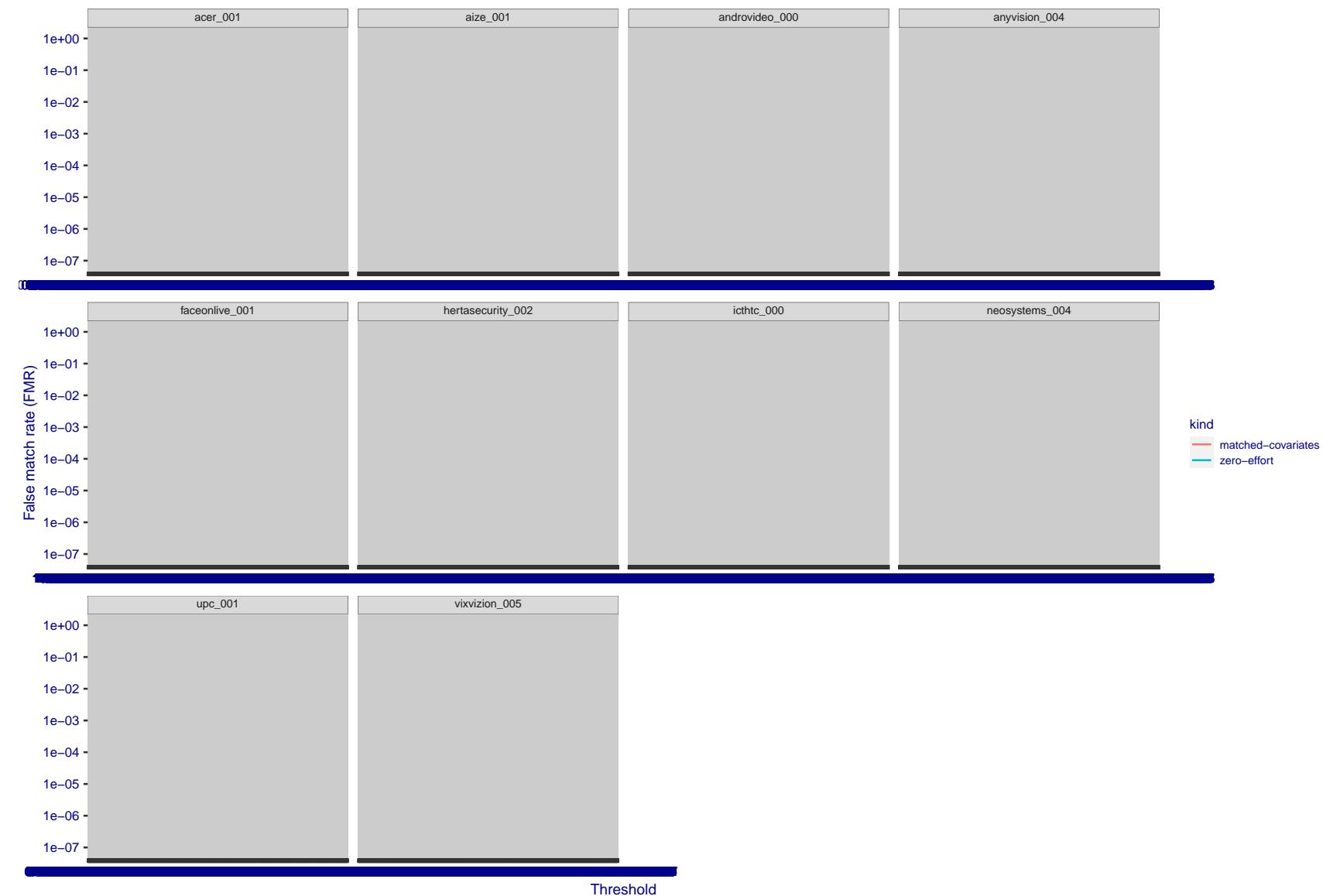


Figure 279: For the visa images, the false match calibration curves show FMR vs. threshold, T . The blue (lower) curves are for zero-effort impostors (i.e. comparing all images against all). The red (upper) curves are for persons of the same-sex, same-age, and same national-origin. This shows that FMR is underestimated (by a factor of 10 or more) by using a zero-effort impostor calculation to calibrate T . As shown later (sec. 3.6), FMR is higher for demographic-matched impostors.

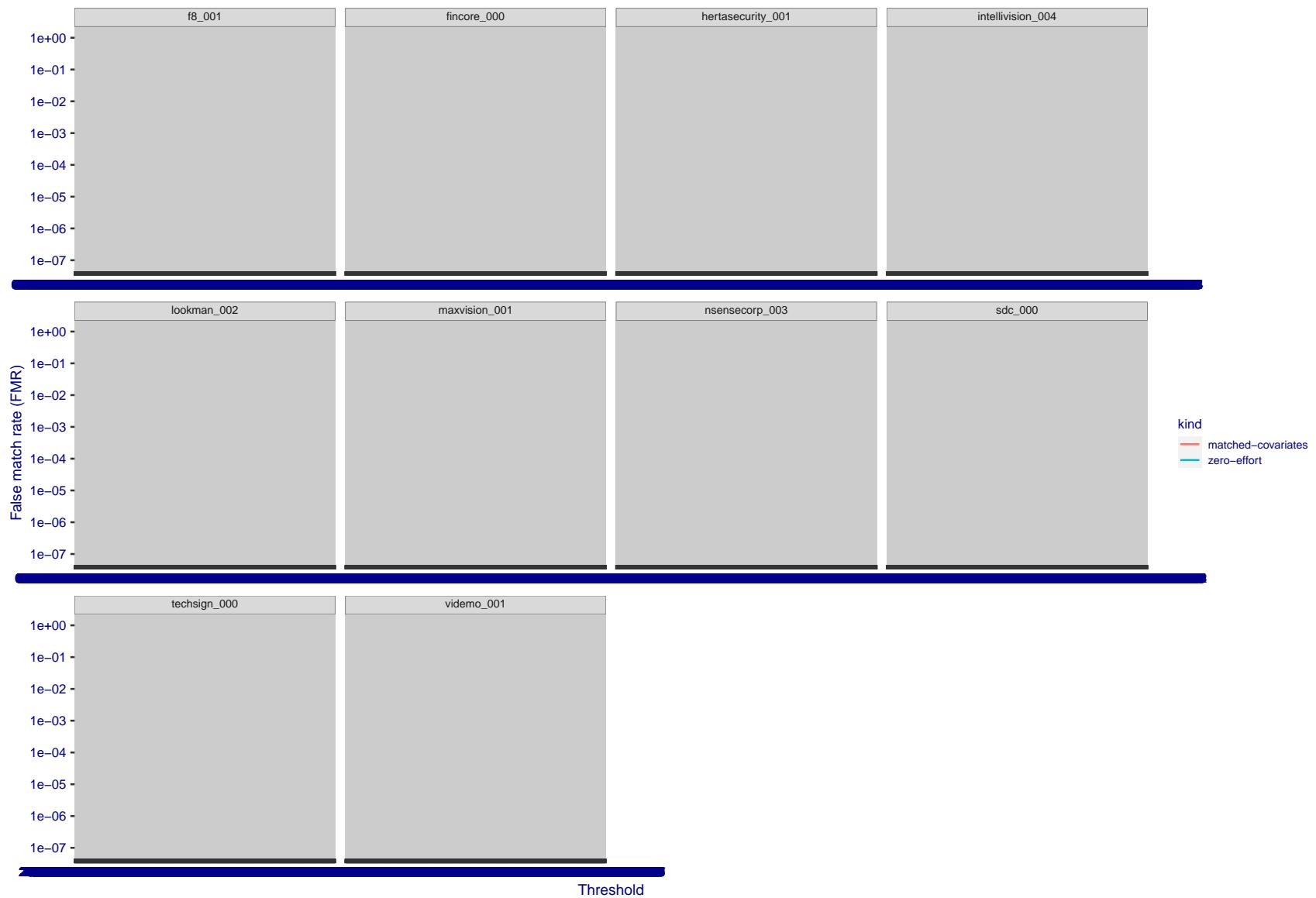


Figure 280: For the visa images, the false match calibration curves show FMR vs. threshold, T . The blue (lower) curves are for zero-effort impostors (i.e. comparing all images against all). The red (upper) curves are for persons of the same-sex, same-age, and same national-origin. This shows that FMR is underestimated (by a factor of 10 or more) by using a zero-effort impostor calculation to calibrate T . As shown later (sec. 3.6), FMR is higher for demographic-matched impostors.

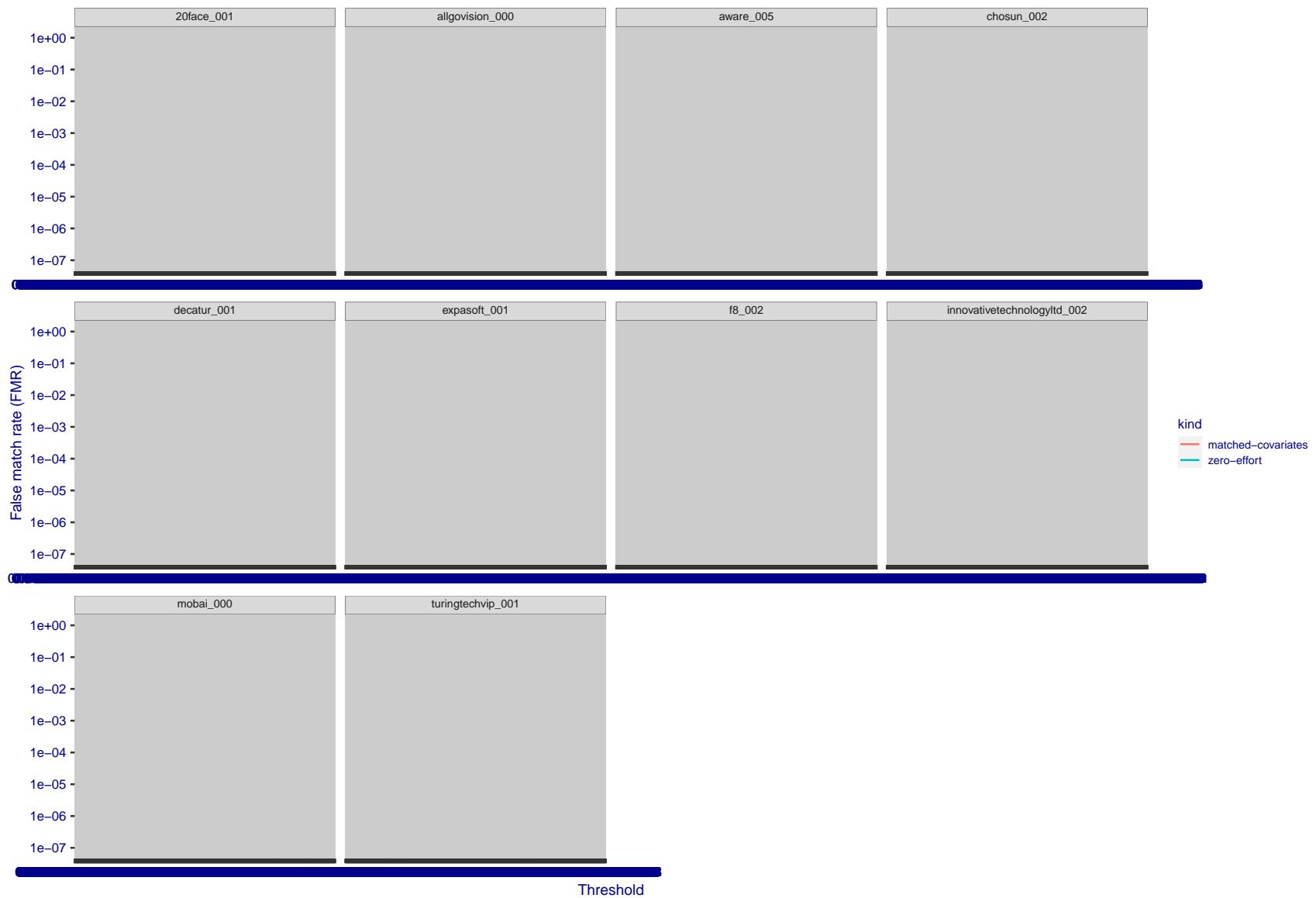


Figure 281: For the visa images, the false match calibration curves show FMR vs. threshold, T . The blue (lower) curves are for zero-effort impostors (i.e. comparing all images against all). The red (upper) curves are for persons of the same-sex, same-age, and same national-origin. This shows that FMR is underestimated (by a factor of 10 or more) by using a zero-effort impostor calculation to calibrate T . As shown later (sec. 3.6), FMR is higher for demographic-matched impostors.

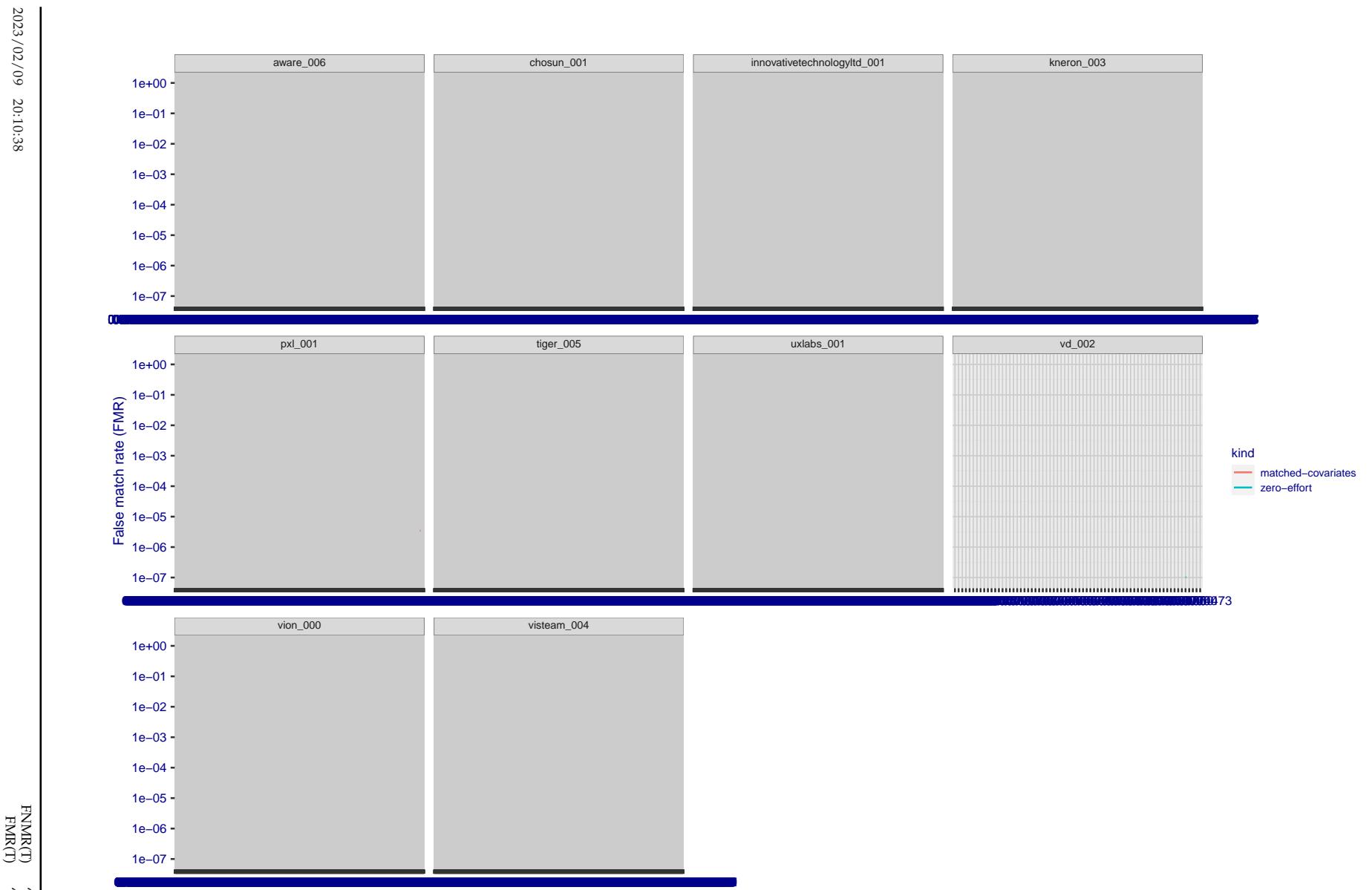


Figure 282: For the visa images, the false match calibration curves show FMR vs. threshold, T . The blue (lower) curves are for zero-effort impostors (i.e. comparing all images against all). The red (upper) curves are for persons of the same-sex, same-age, and same national-origin. This shows that FMR is underestimated (by a factor of 10 or more) by using a zero-effort impostor calculation to calibrate T . As shown later (sec. 3.6), FMR is higher for demographic-matched impostors.



Figure 283: For the visa images, the false match calibration curves show FMR vs. threshold, T . The blue (lower) curves are for zero-effort impostors (i.e. comparing all images against all). The red (upper) curves are for persons of the same-sex, same-age, and same national-origin. This shows that FMR is underestimated (by a factor of 10 or more) by using a zero-effort impostor calculation to calibrate T . As shown later (sec. 3.6), FMR is higher for demographic-matched impostors.

2023/02/09 20:10:38

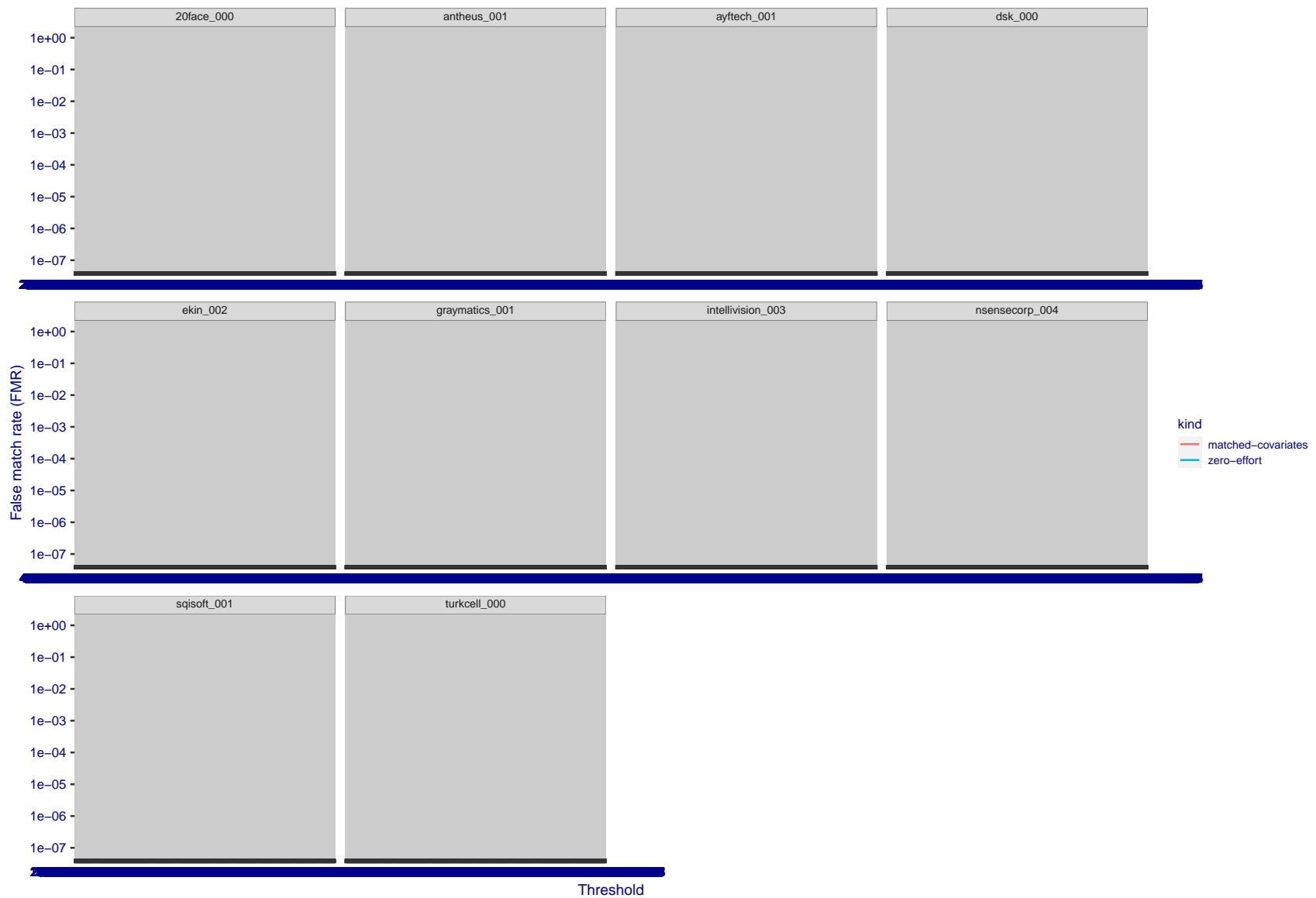


Figure 284: For the visa images, the false match calibration curves show FMR vs. threshold, T . The blue (lower) curves are for zero-effort impostors (i.e. comparing all images against all). The red (upper) curves are for persons of the same-sex, same-age, and same national-origin. This shows that FMR is underestimated (by a factor of 10 or more) by using a zero-effort impostor calculation to calibrate T . As shown later (sec. 3.6), FMR is higher for demographic-matched impostors.



Figure 285: For the visa images, the false match calibration curves show FMR vs. threshold, T . The blue (lower) curves are for zero-effort impostors (i.e. comparing all images against all). The red (upper) curves are for persons of the same-sex, same-age, and same national-origin. This shows that FMR is underestimated (by a factor of 10 or more) by using a zero-effort impostor calculation to calibrate T . As shown later (sec. 3.6), FMR is higher for demographic-matched impostors.

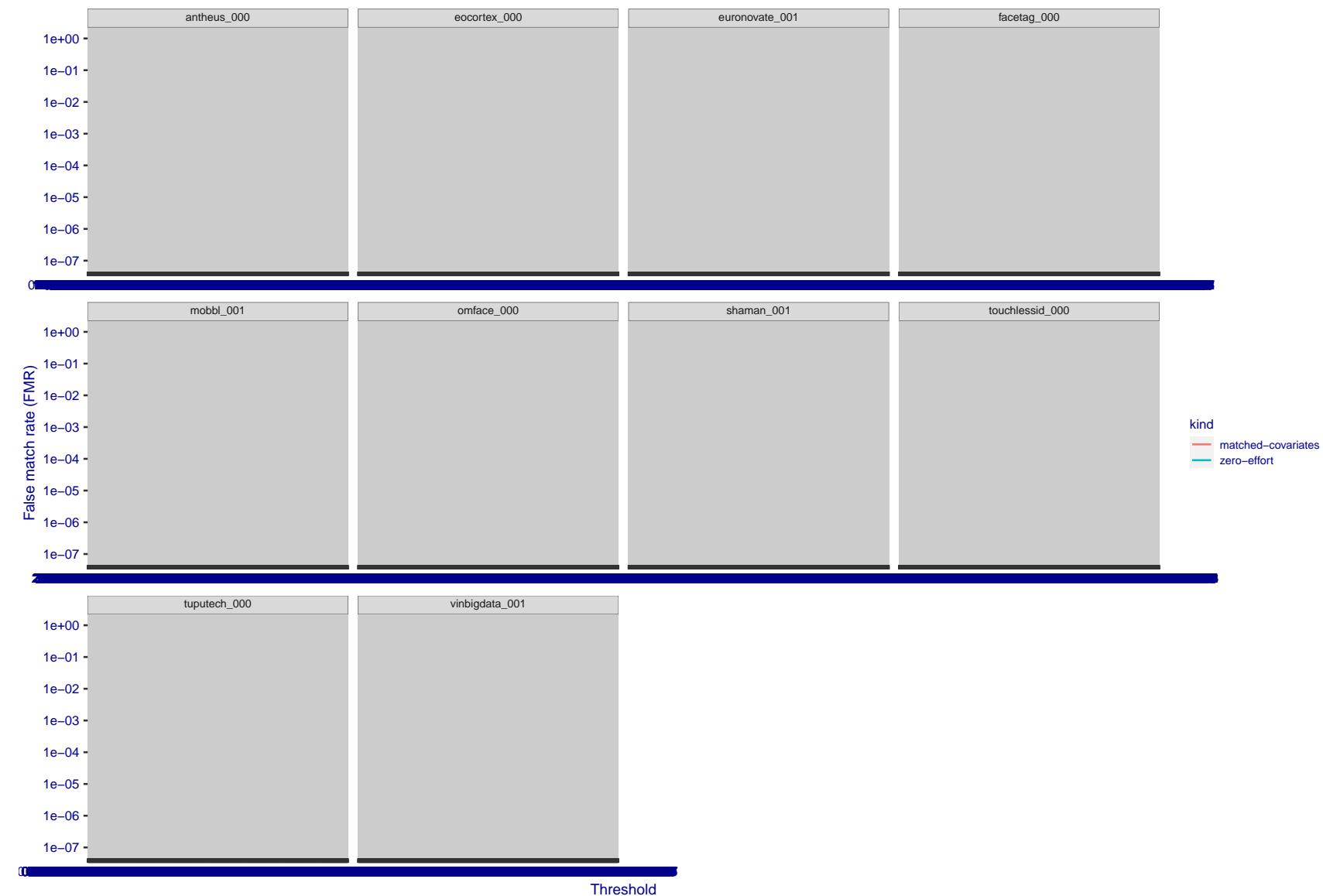


Figure 286: For the visa images, the false match calibration curves show FMR vs. threshold, T . The blue (lower) curves are for zero-effort impostors (i.e. comparing all images against all). The red (upper) curves are for persons of the same-sex, same-age, and same national-origin. This shows that FMR is underestimated (by a factor of 10 or more) by using a zero-effort impostor calculation to calibrate T . As shown later (sec. 3.6), FMR is higher for demographic-matched impostors.

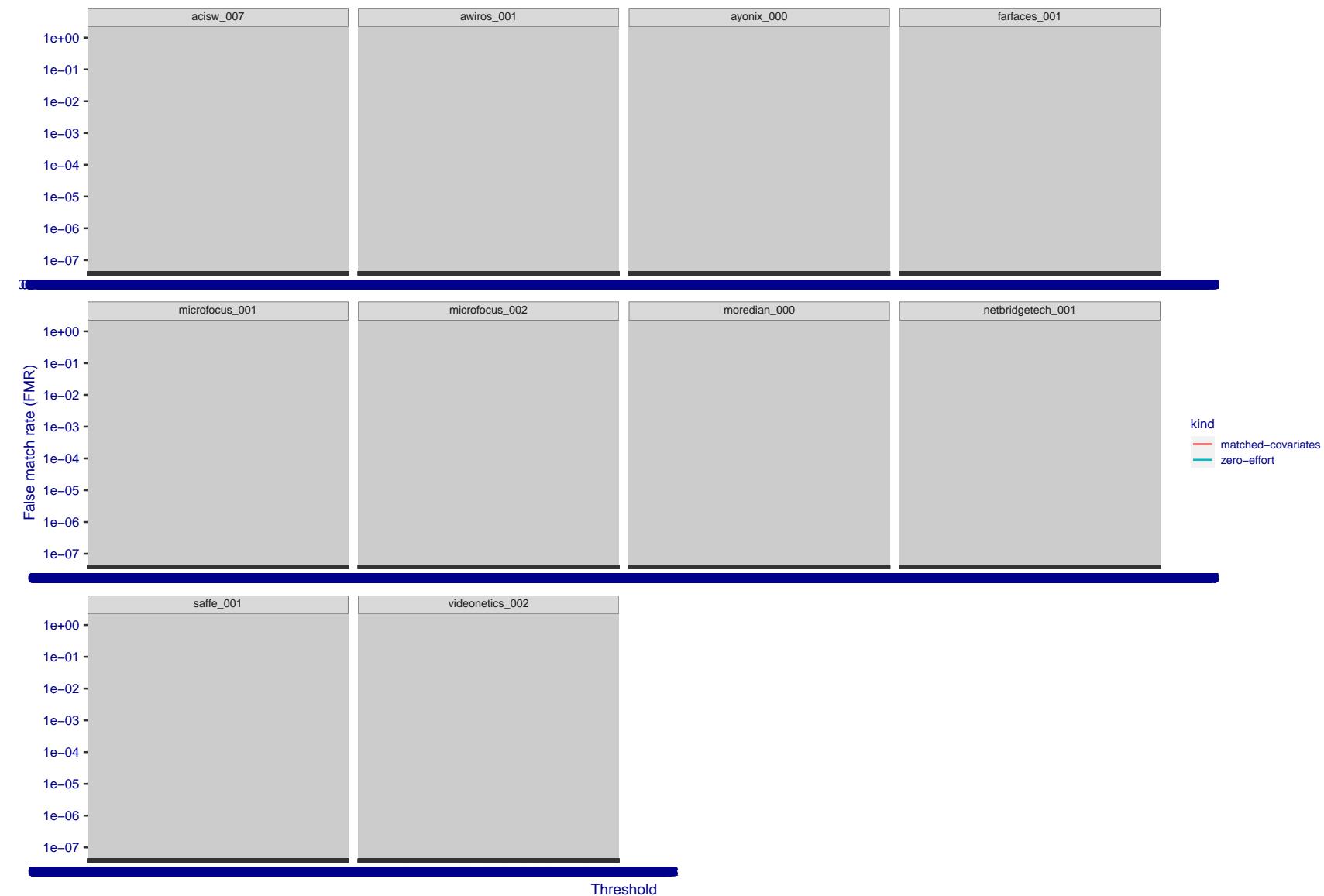


Figure 287: For the visa images, the false match calibration curves show FMR vs. threshold, T . The blue (lower) curves are for zero-effort impostors (i.e. comparing all images against all). The red (upper) curves are for persons of the same-sex, same-age, and same national-origin. This shows that FMR is underestimated (by a factor of 10 or more) by using a zero-effort impostor calculation to calibrate T . As shown later (sec. 3.6), FMR is higher for demographic-matched impostors.

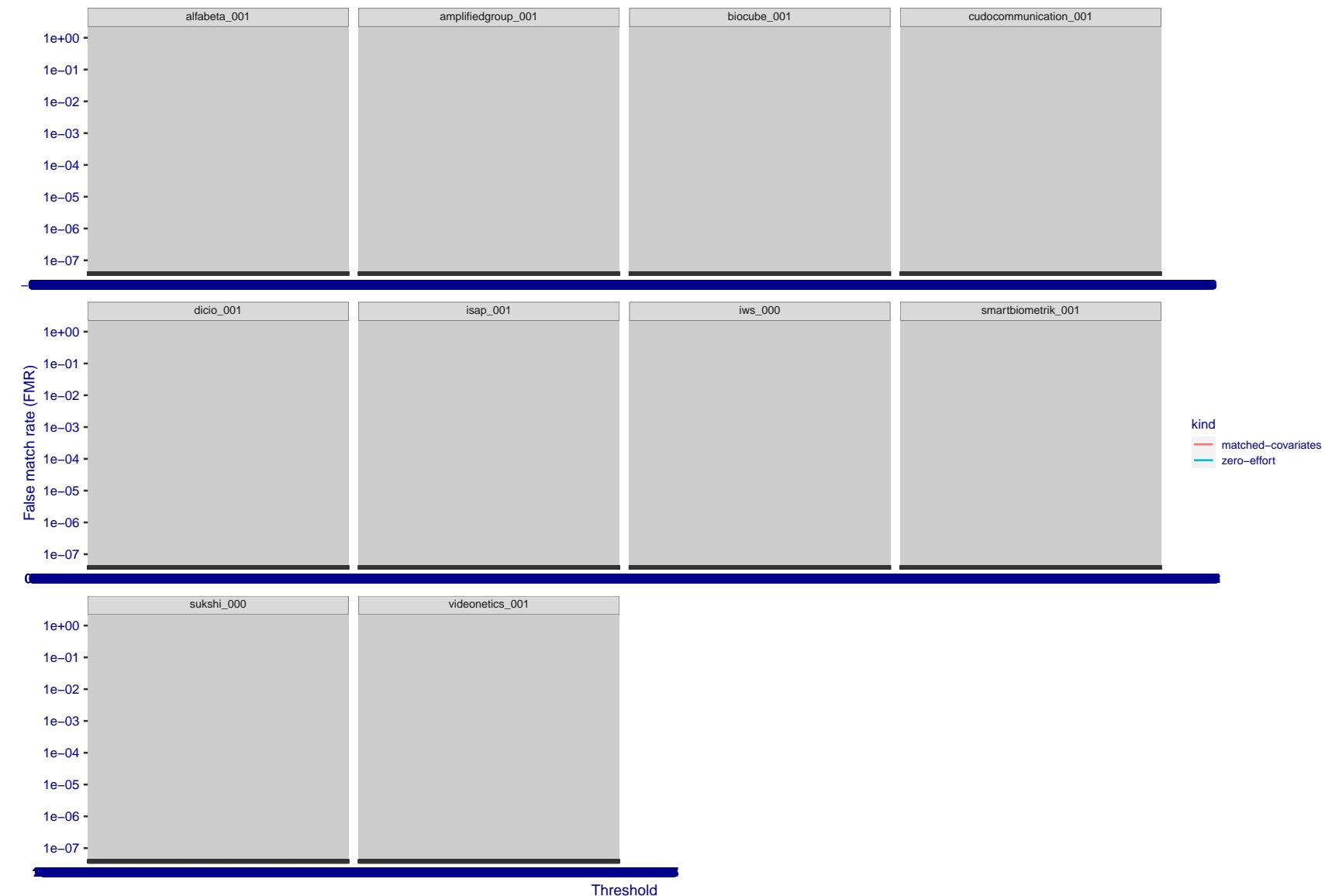


Figure 288: For the visa images, the false match calibration curves show FMR vs. threshold, T . The blue (lower) curves are for zero-effort impostors (i.e. comparing all images against all). The red (upper) curves are for persons of the same-sex, same-age, and same national-origin. This shows that FMR is underestimated (by a factor of 10 or more) by using a zero-effort impostor calculation to calibrate T . As shown later (sec. 3.6), FMR is higher for demographic-matched impostors.

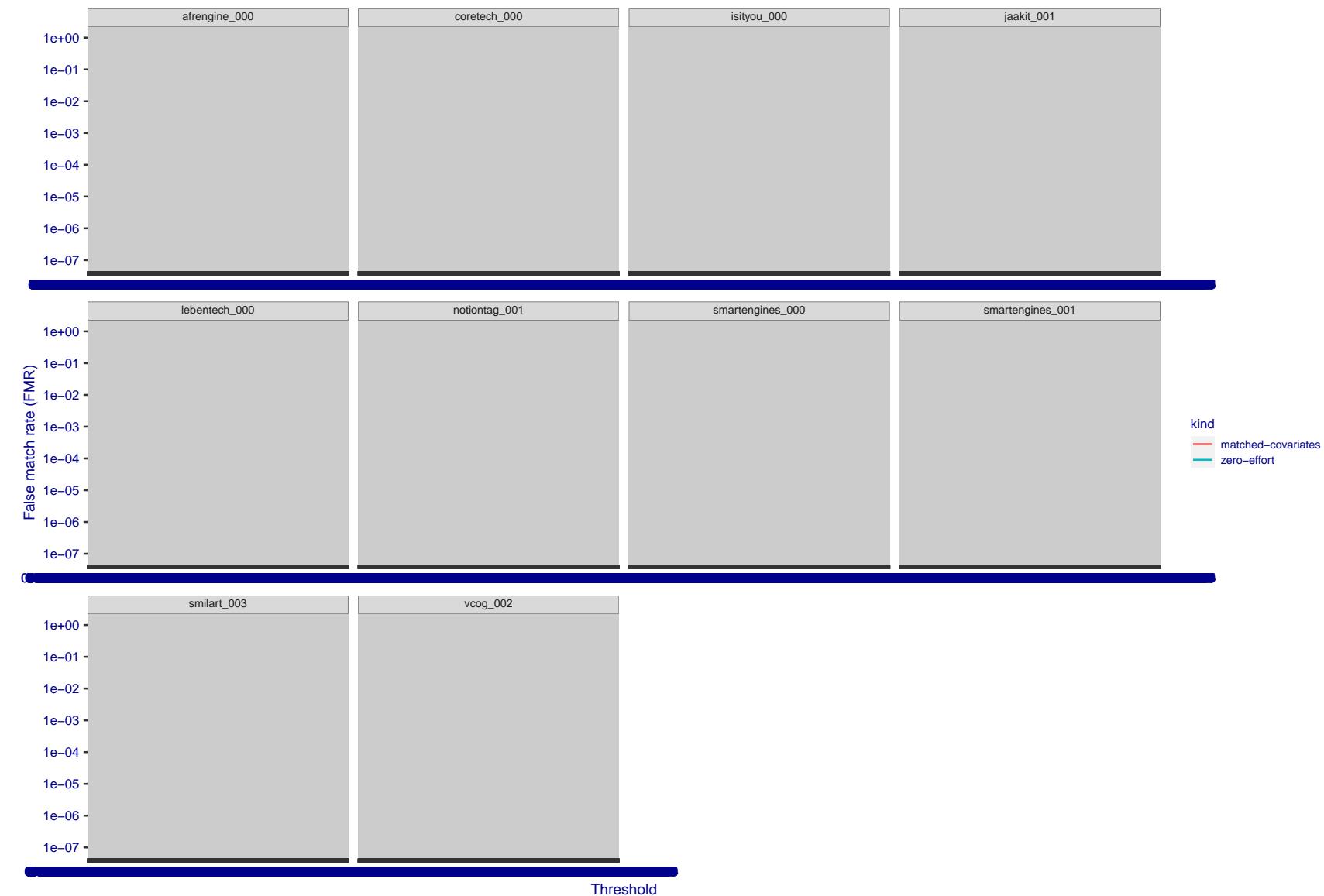


Figure 289: For the visa images, the false match calibration curves show FMR vs. threshold, T . The blue (lower) curves are for zero-effort impostors (i.e. comparing all images against all). The red (upper) curves are for persons of the same-sex, same-age, and same national-origin. This shows that FMR is underestimated (by a factor of 10 or more) by using a zero-effort impostor calculation to calibrate T . As shown later (sec. 3.6), FMR is higher for demographic-matched impostors.

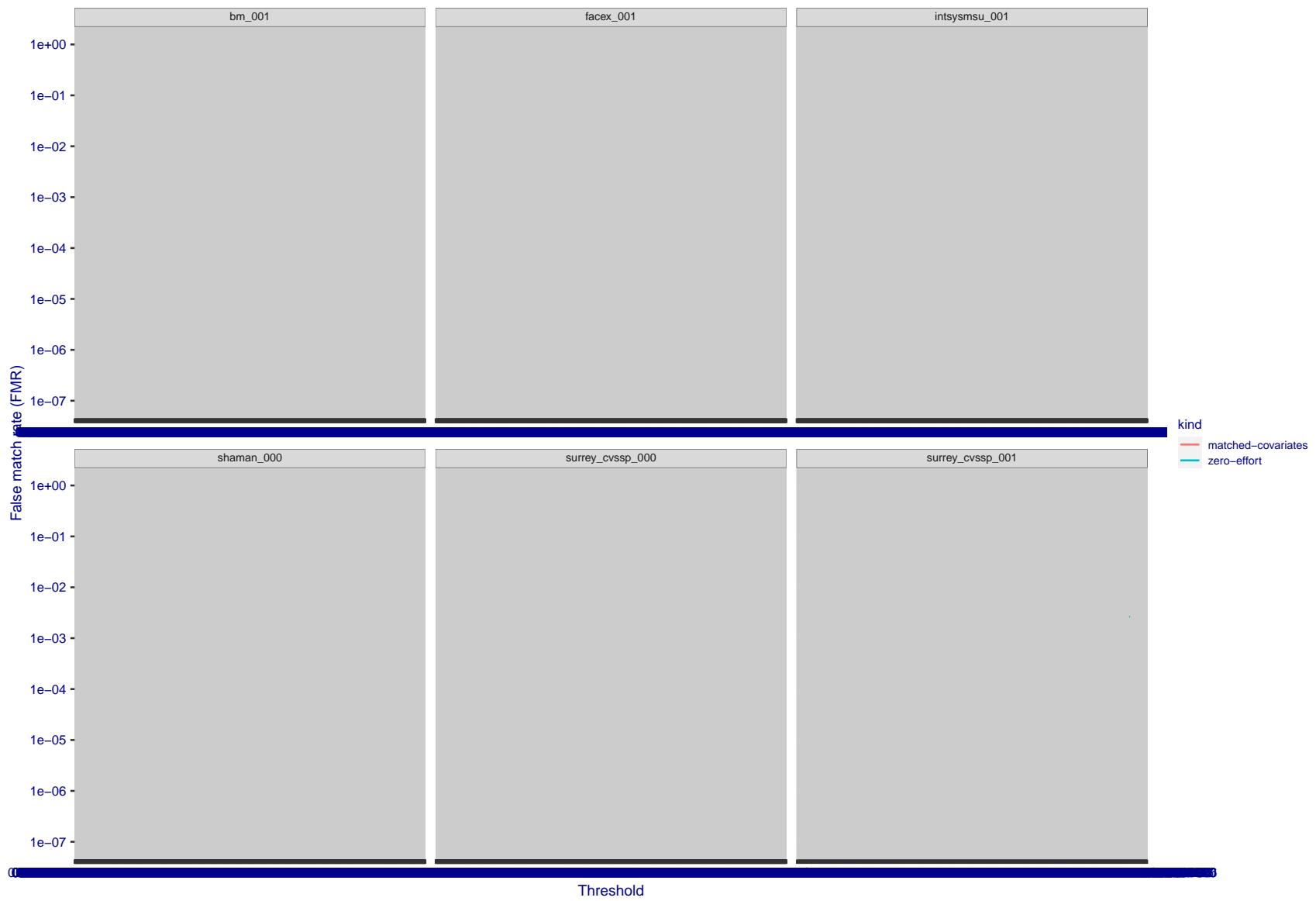


Figure 290: For the visa images, the false match calibration curves show FMR vs. threshold, T . The blue (lower) curves are for zero-effort impostors (i.e. comparing all images against all). The red (upper) curves are for persons of the same-sex, same-age, and same national-origin. This shows that FMR is underestimated (by a factor of 10 or more) by using a zero-effort impostor calculation to calibrate T . As shown later (sec. 3.6), FMR is higher for demographic-matched impostors.

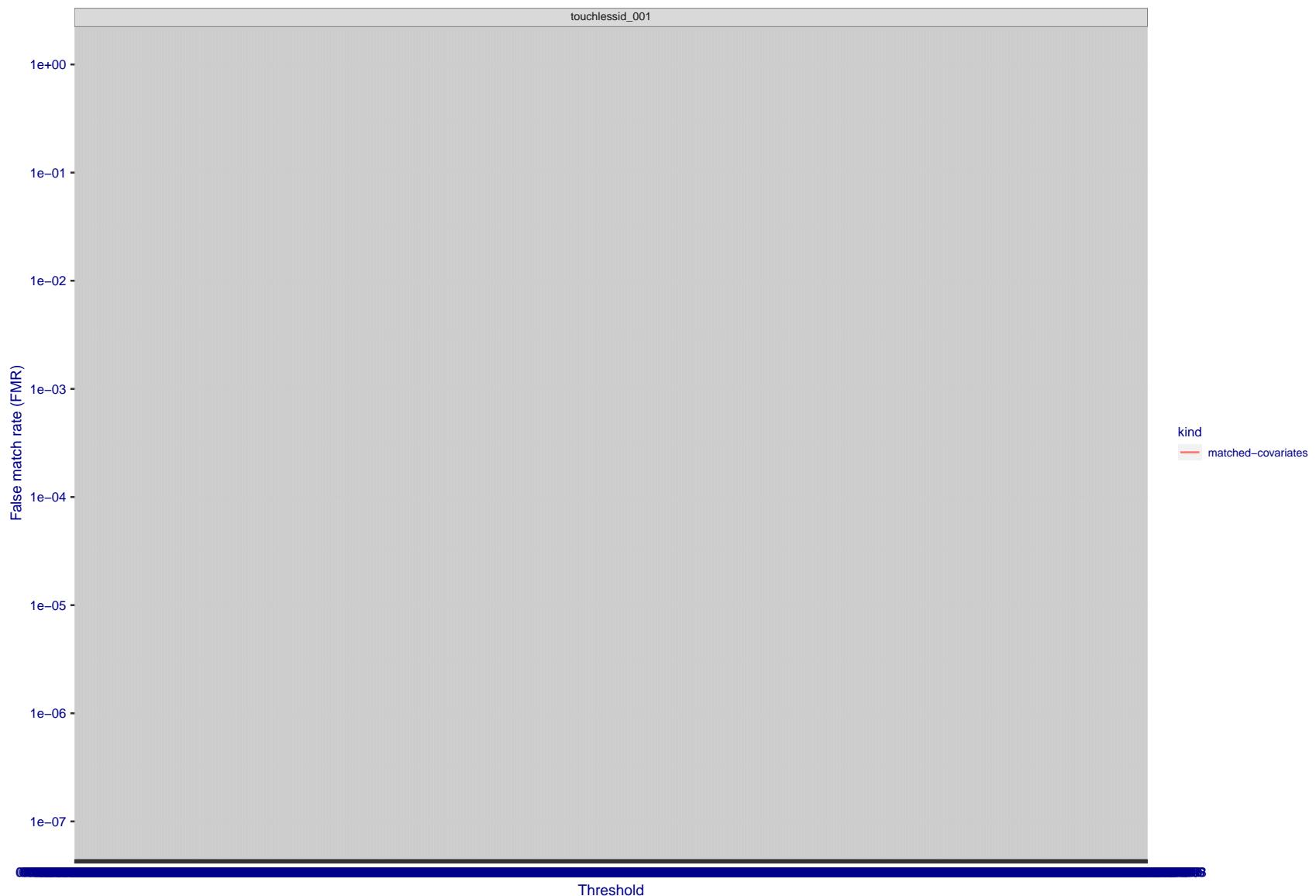


Figure 291: For the visa images, the false match calibration curves show FMR vs. threshold, T . The blue (lower) curves are for zero-effort impostors (i.e. comparing all images against all). The red (upper) curves are for persons of the same-sex, same-age, and same national-origin. This shows that FMR is underestimated (by a factor of 10 or more) by using a zero-effort impostor calculation to calibrate T . As shown later (sec. 3.6), FMR is higher for demographic-matched impostors.

3.5 Genuine distribution stability

3.5.1 Effect of birth place on the genuine distribution

Background: Both skin tone and bone structure vary geographically. Prior studies have reported variations in FNMR and FMR.

Goal: To measure false non-match rate (FNMR) variation with country of birth.

Methods: Thresholds are determined that give $FMR = \{0.001, 0.0001\}$ over the entire impostor set. Then FNMR is measured over 1000 bootstrap replications of the genuine scores. Only those countries with at least 140 individuals are included in the analysis.

Results: Figure 330 shows FNMR by country of birth for the two thresholds.

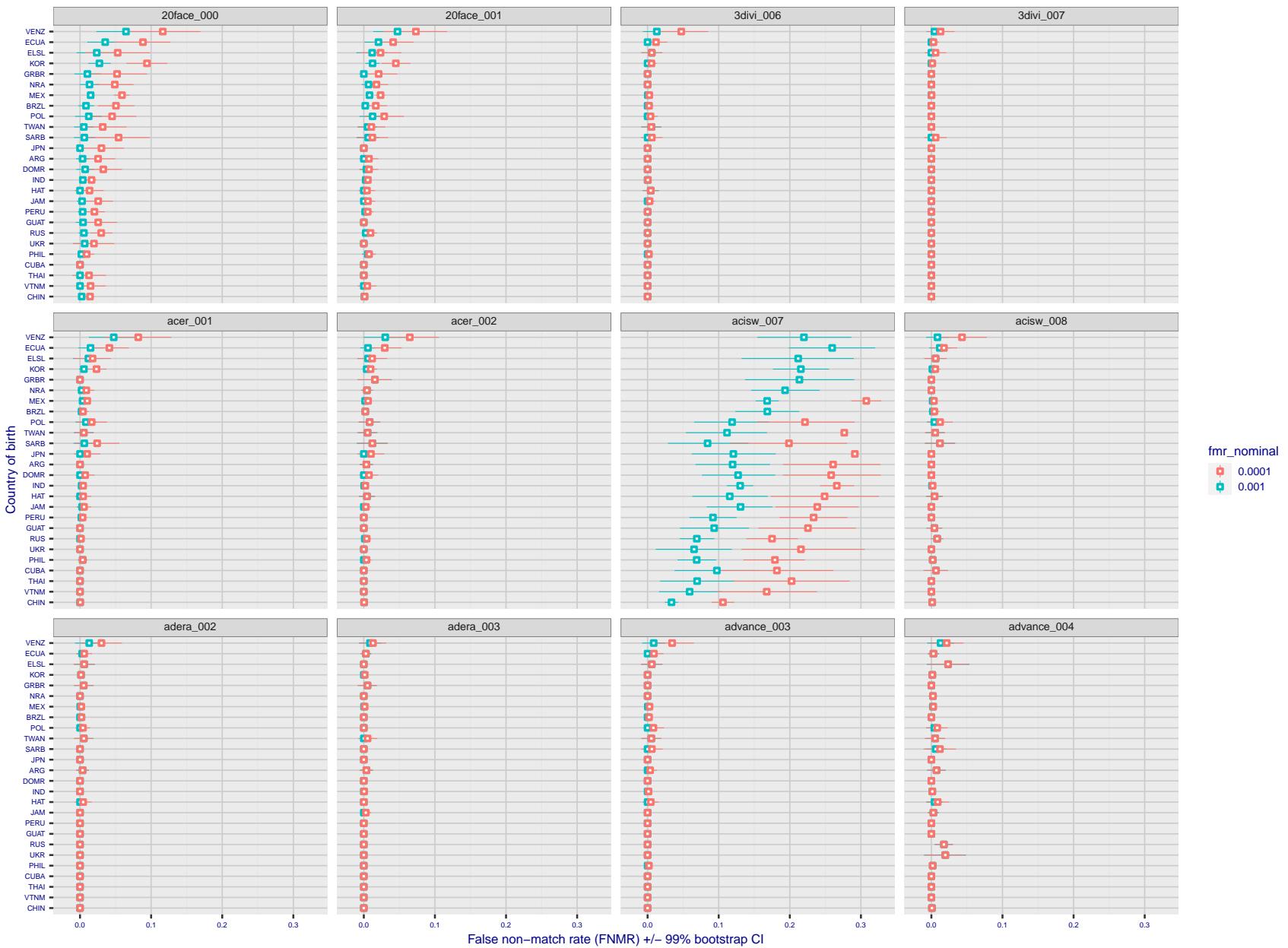


Figure 292: For the visa images, the dots show FNMR by country of birth for two globally set operating thresholds corresponding to $FMR = \{0.001, 0.0001\}$ computed over all on the order of 10^{10} impostor scores. The FMR in each bin will vary also - see subsequent impostor heatmaps in sec. 3.6.1. The figures shows an order of magnitude variation in FNMR across country of birth; these effects are likely due quality variations, then demographics like age and race. The error rates in some cases are zero, and in others the DET is flat so the error rates at the two thresholds are identical. The lines span 1% and 99% of bootstrap replicated FNMR estimates.

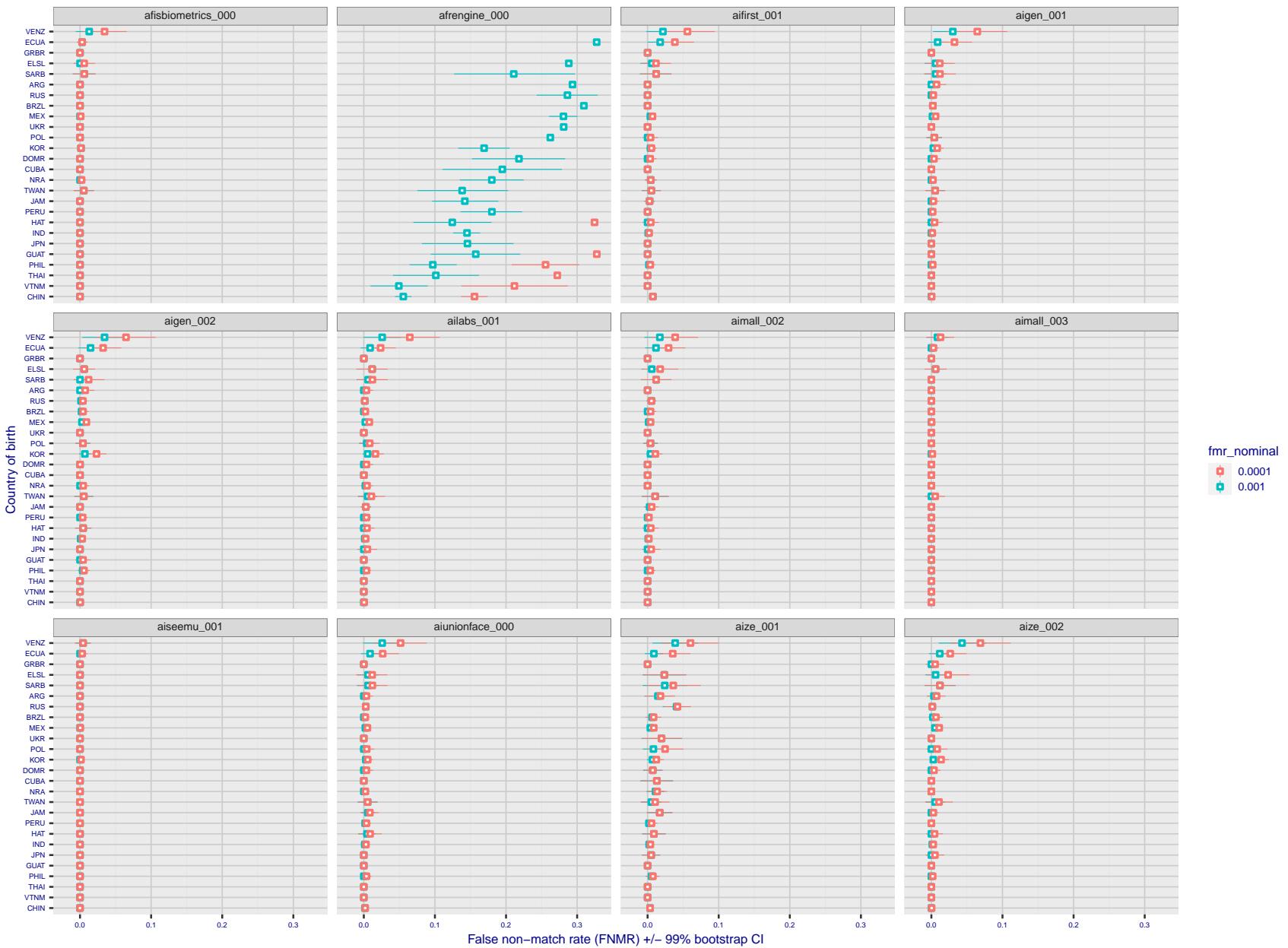


Figure 293: For the visa images, the dots show FNMR by country of birth for two globally set operating thresholds corresponding to $FMR = \{0.001, 0.0001\}$ computed over all on the order of 10^{10} impostor scores. The FMR in each bin will vary also - see subsequent impostor heatmaps in sec. 3.6.1. The figures shows an order of magnitude variation in FNMR across country of birth; these effects are likely due quality variations, then demographics like age and race. The error rates in some cases are zero, and in others the DET is flat so the error rates at the two thresholds are identical. The lines span 1% and 99% of bootstrap replicated FNMR estimates.

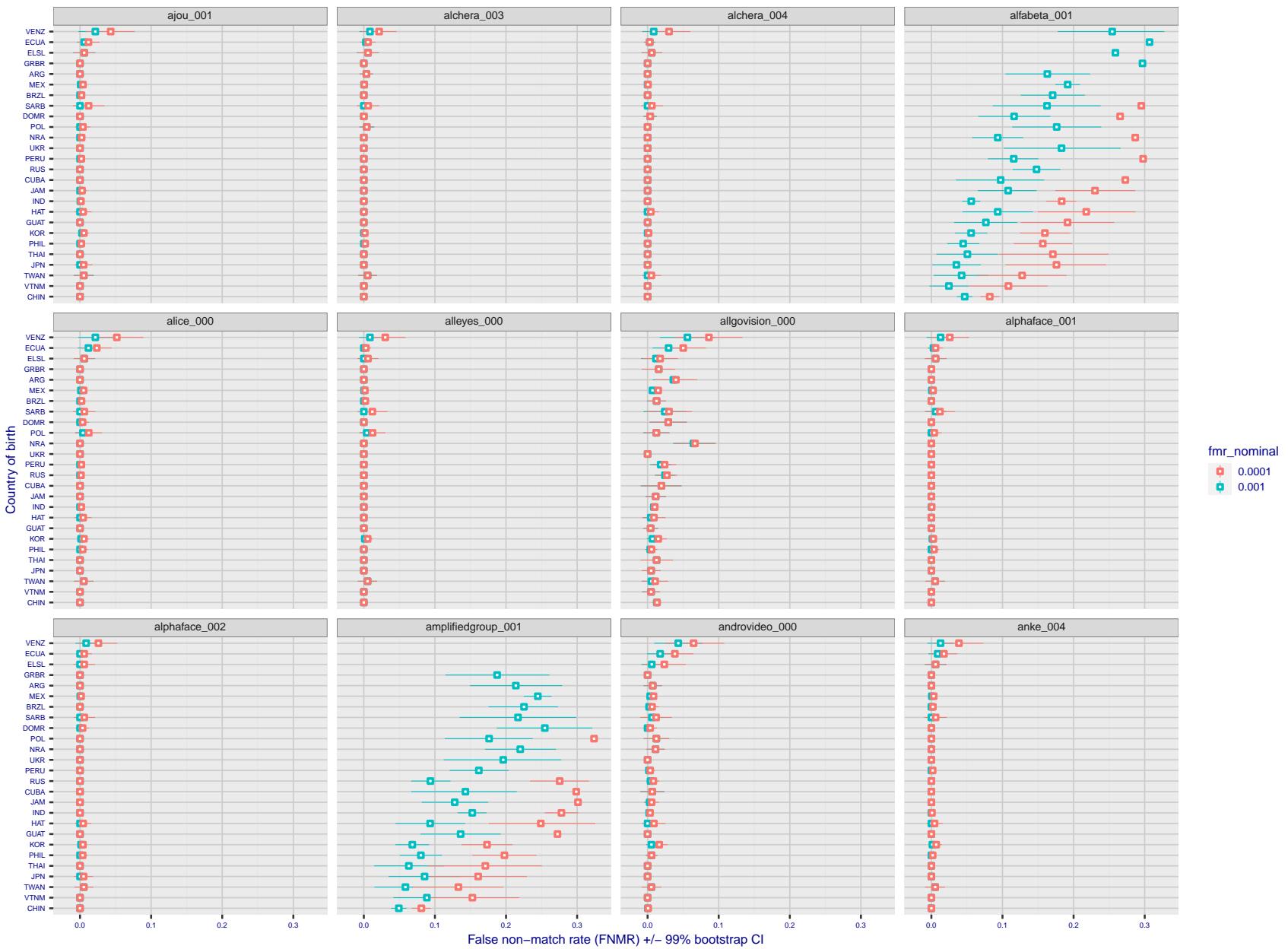


Figure 294: For the visa images, the dots show FNMR by country of birth for two globally set operating thresholds corresponding to $FMR = \{0.001, 0.0001\}$ computed over all on the order of 10^{10} impostor scores. The FMR in each bin will vary also - see subsequent impostor heatmaps in sec. 3.6.1. The figures shows an order of magnitude variation in FNMR across country of birth; these effects are likely due quality variations, then demographics like age and race. The error rates in some cases are zero, and in others the DET is flat so the error rates at the two thresholds are identical. The lines span 1% and 99% of bootstrap replicated FNMR estimates.

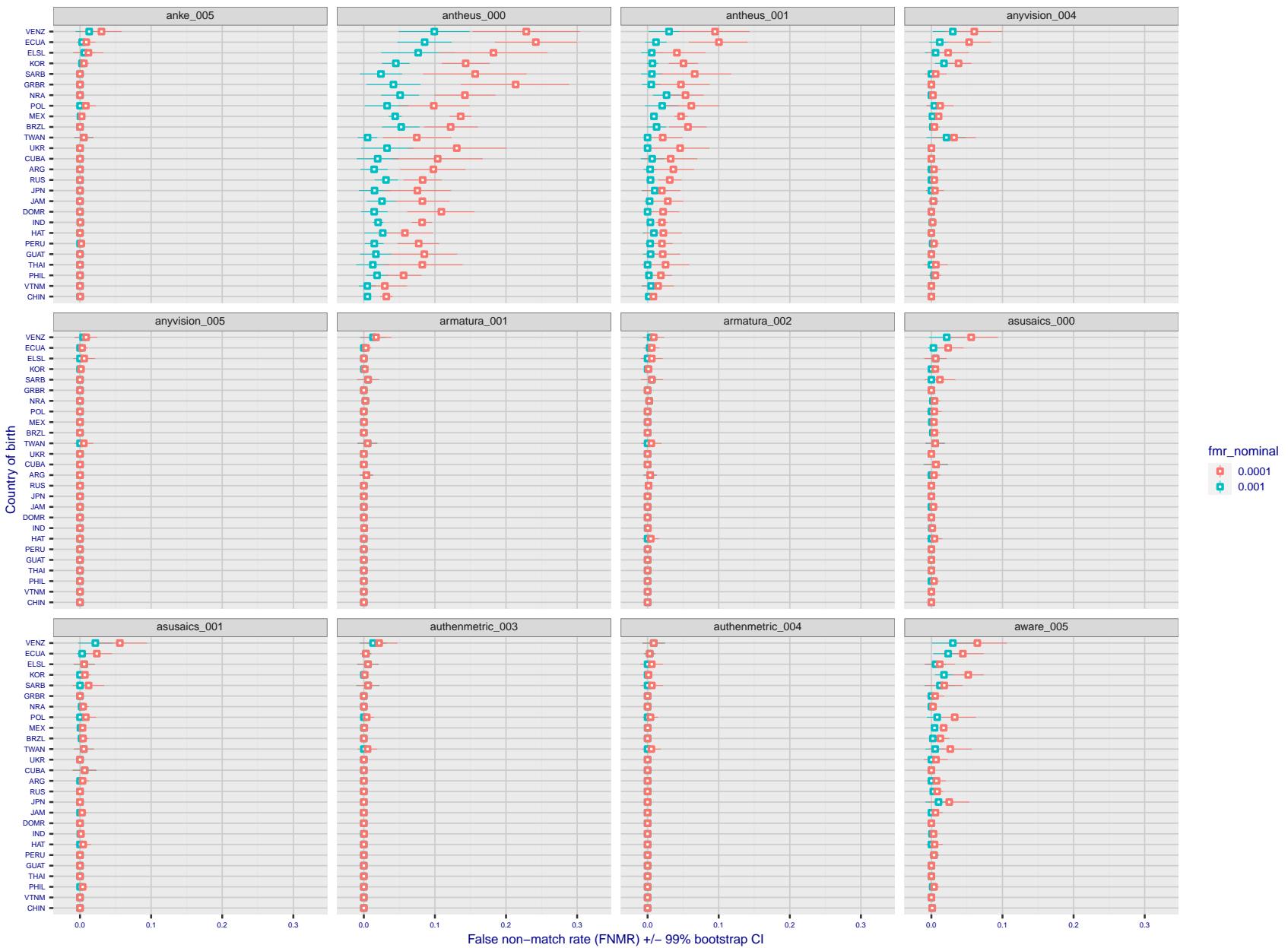


Figure 295: For the visa images, the dots show FNMR by country of birth for two globally set operating thresholds corresponding to $FMR = \{0.001, 0.0001\}$ computed over all on the order of 10^{10} impostor scores. The FMR in each bin will vary also - see subsequent impostor heatmaps in sec. 3.6.1. The figures shows an order of magnitude variation in FNMR across country of birth; these effects are likely due quality variations, then demographics like age and race. The error rates in some cases are zero, and in others the DET is flat so the error rates at the two thresholds are identical. The lines span 1% and 99% of bootstrap replicated FNMR estimates.

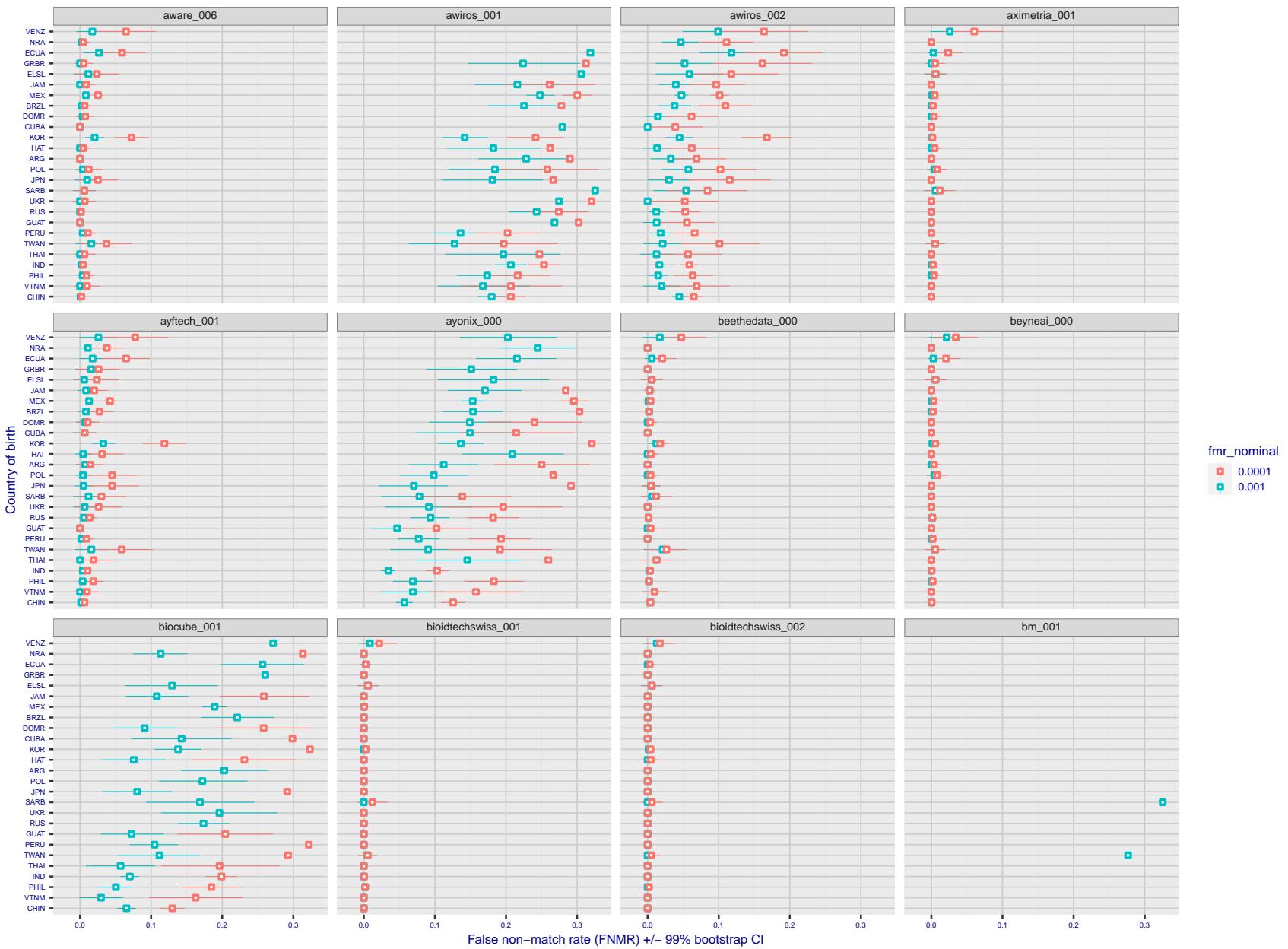


Figure 296: For the visa images, the dots show FNMR by country of birth for two globally set operating thresholds corresponding to $FMR = \{0.001, 0.0001\}$ computed over all on the order of 10^{10} impostor scores. The FMR in each bin will vary also - see subsequent impostor heatmaps in sec. 3.6.1. The figures shows an order of magnitude variation in FNMR across country of birth; these effects are likely due quality variations, then demographics like age and race. The error rates in some cases are zero, and in others the DET is flat so the error rates at the two thresholds are identical. The lines span 1% and 99% of bootstrap replicated FNMR estimates.

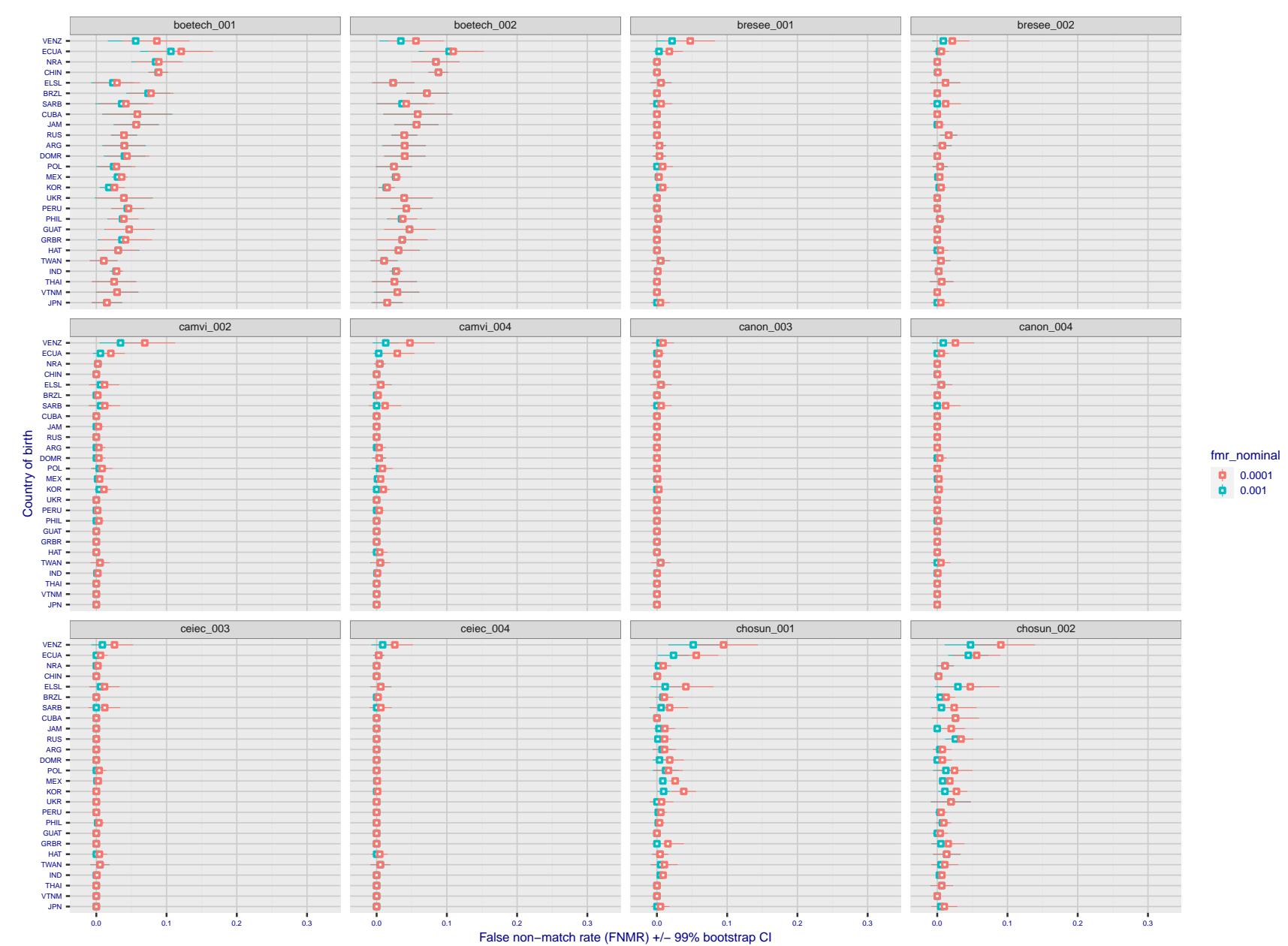


Figure 297: For the visa images, the dots show FNMR by country of birth for two globally set operating thresholds corresponding to $FMR = \{0.001, 0.0001\}$ computed over all on the order of 10^{10} impostor scores. The FMR in each bin will vary also - see subsequent impostor heatmaps in sec. 3.6.1. The figures shows an order of magnitude variation in FNMR across country of birth; these effects are likely due quality variations, then demographics like age and race. The error rates in some cases are zero, and in others the DET is flat so the error rates at the two thresholds are identical. The lines span 1% and 99% of bootstrap replicated FNMR estimates.

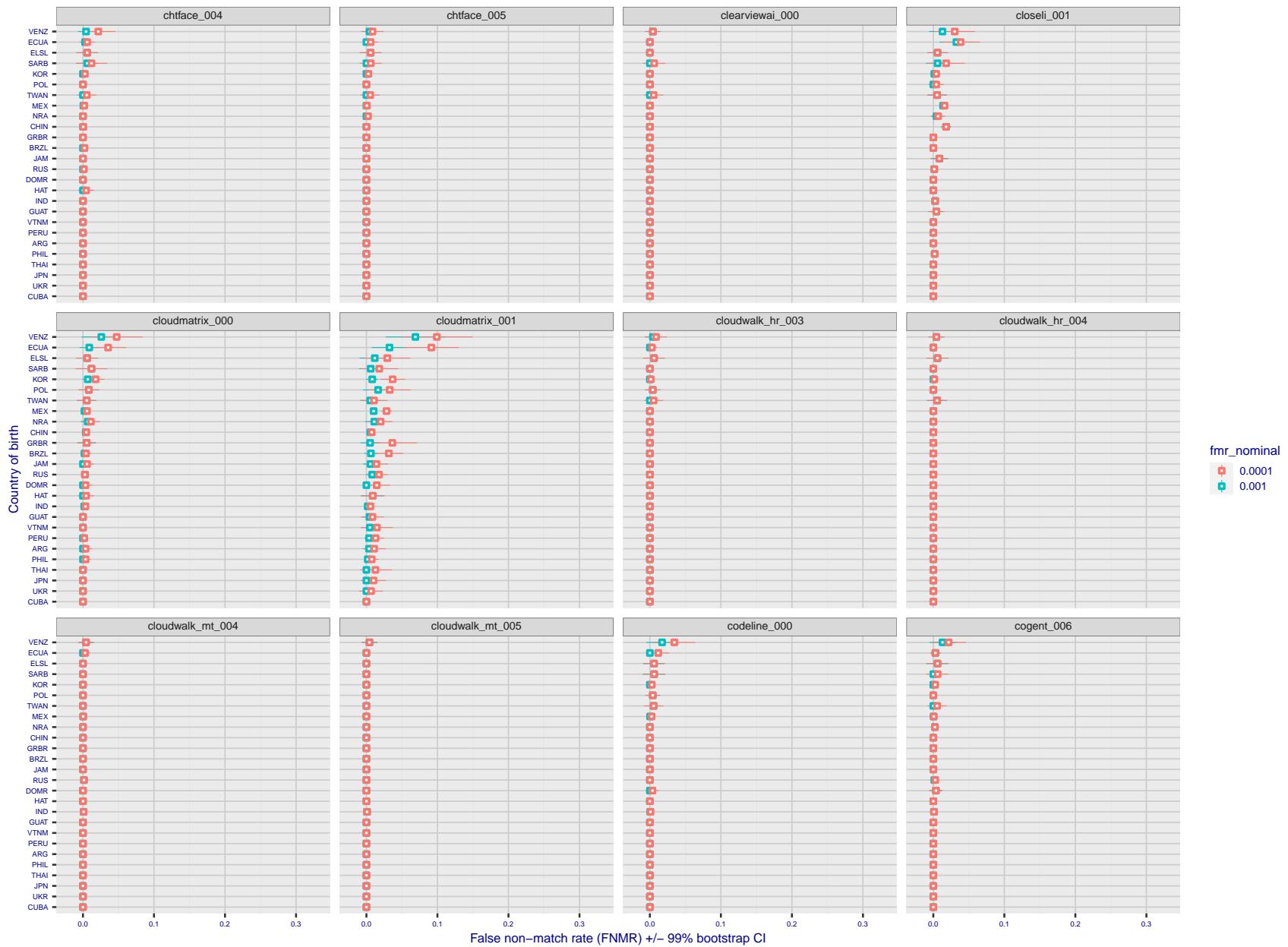


Figure 298: For the visa images, the dots show FNMR by country of birth for two globally set operating thresholds corresponding to $FMR = \{0.001, 0.0001\}$ computed over all on the order of 10^{10} impostor scores. The FMR in each bin will vary also - see subsequent impostor heatmaps in sec. 3.6.1. The figures shows an order of magnitude variation in FNMR across country of birth; these effects are likely due quality variations, then demographics like age and race. The error rates in some cases are zero, and in others the DET is flat so the error rates at the two thresholds are identical. The lines span 1% and 99% of bootstrap replicated FNMR estimates.

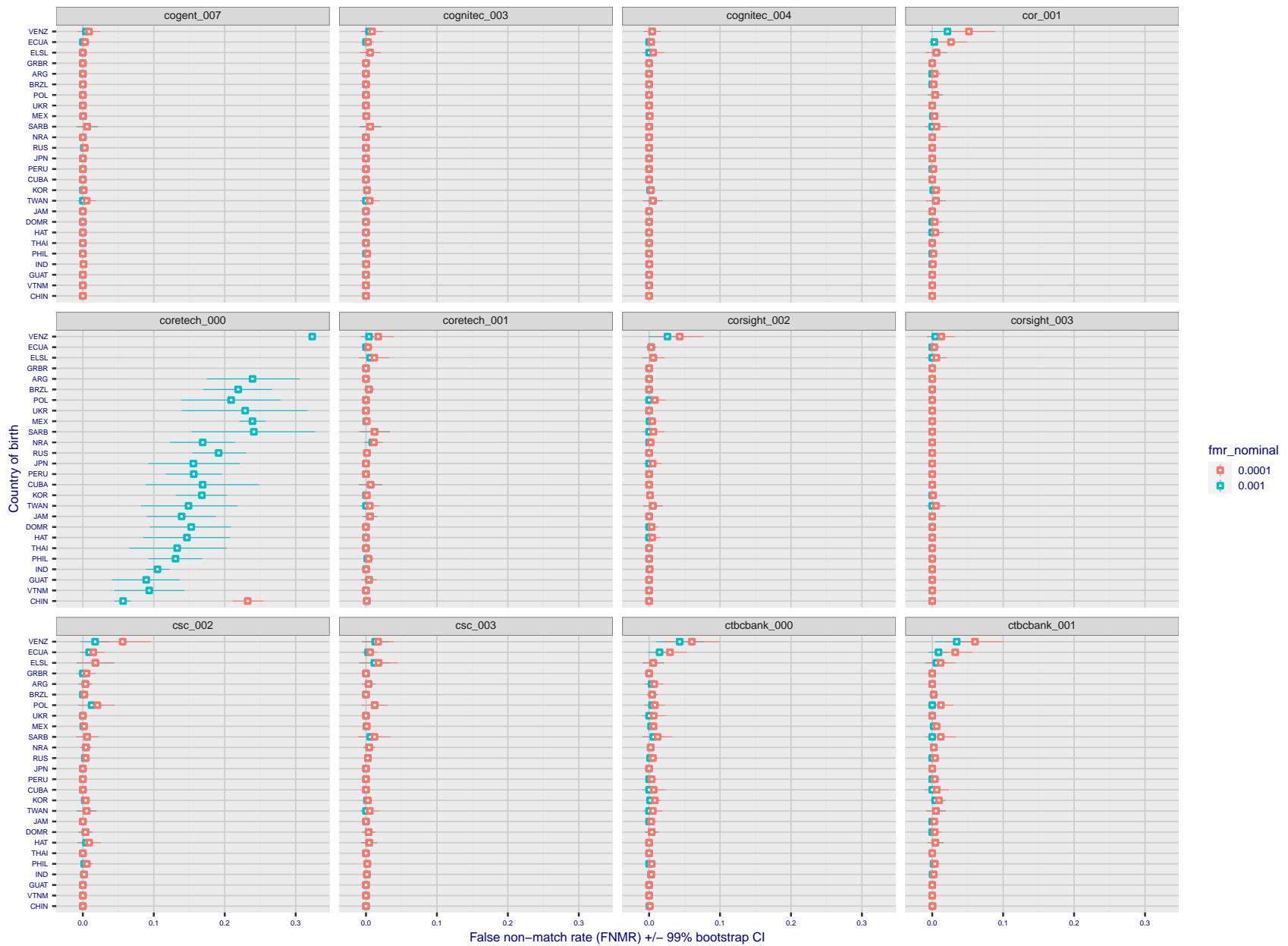


Figure 299: For the visa images, the dots show FNMR by country of birth for two globally set operating thresholds corresponding to $FMR = \{0.001, 0.0001\}$ computed over all on the order of 10^{10} impostor scores. The FMR in each bin will vary also - see subsequent impostor heatmaps in sec. 3.6.1. The figures shows an order of magnitude variation in FNMR across country of birth; these effects are likely due quality variations, then demographics like age and race. The error rates in some cases are zero, and in others the DET is flat so the error rates at the two thresholds are identical. The lines span 1% and 99% of bootstrap replicated FNMR estimates.

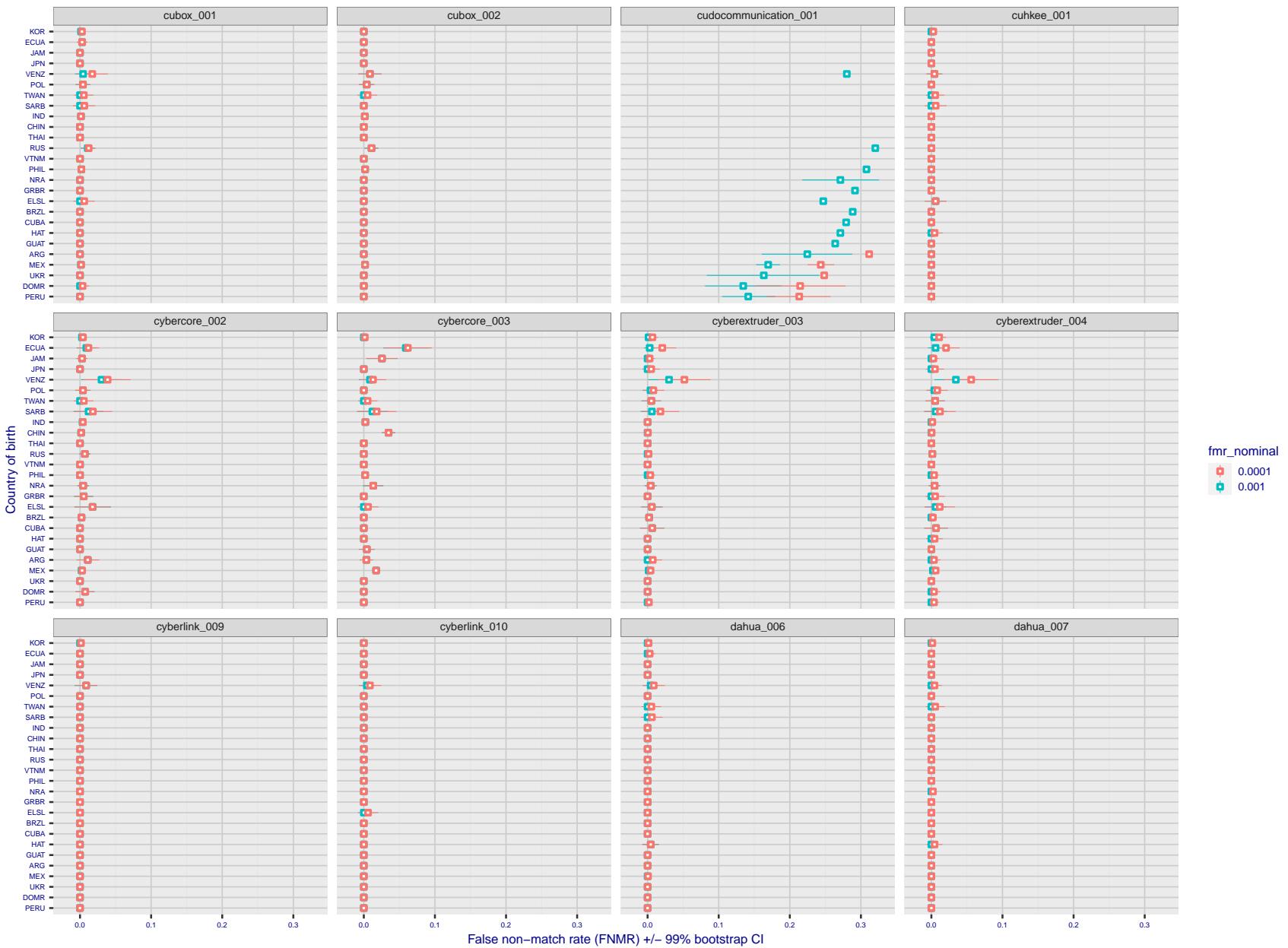


Figure 300: For the visa images, the dots show FNMR by country of birth for two globally set operating thresholds corresponding to $FMR = \{0.001, 0.0001\}$ computed over all on the order of 10^{10} impostor scores. The FMR in each bin will vary also - see subsequent impostor heatmaps in sec. 3.6.1. The figures shows an order of magnitude variation in FNMR across country of birth; these effects are likely due quality variations, then demographics like age and race. The error rates in some cases are zero, and in others the DET is flat so the error rates at the two thresholds are identical. The lines span 1% and 99% of bootstrap replicated FNMR estimates.

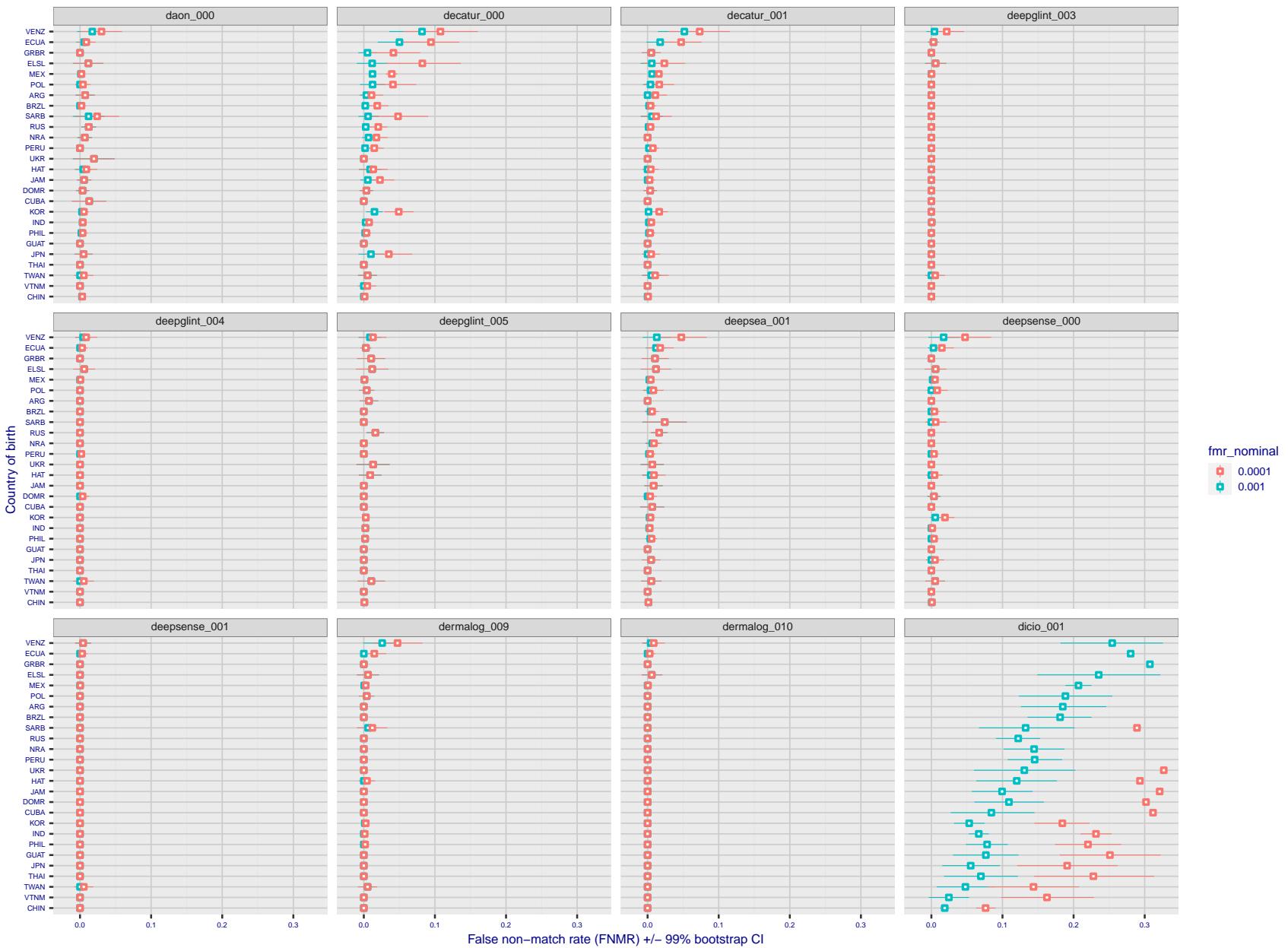


Figure 301: For the visa images, the dots show FNMR by country of birth for two globally set operating thresholds corresponding to $FMR = \{0.001, 0.0001\}$ computed over all on the order of 10^{10} impostor scores. The FMR in each bin will vary also - see subsequent impostor heatmaps in sec. 3.6.1. The figures shows an order of magnitude variation in FNMR across country of birth; these effects are likely due quality variations, then demographics like age and race. The error rates in some cases are zero, and in others the DET is flat so the error rates at the two thresholds are identical. The lines span 1% and 99% of bootstrap replicated FNMR estimates.

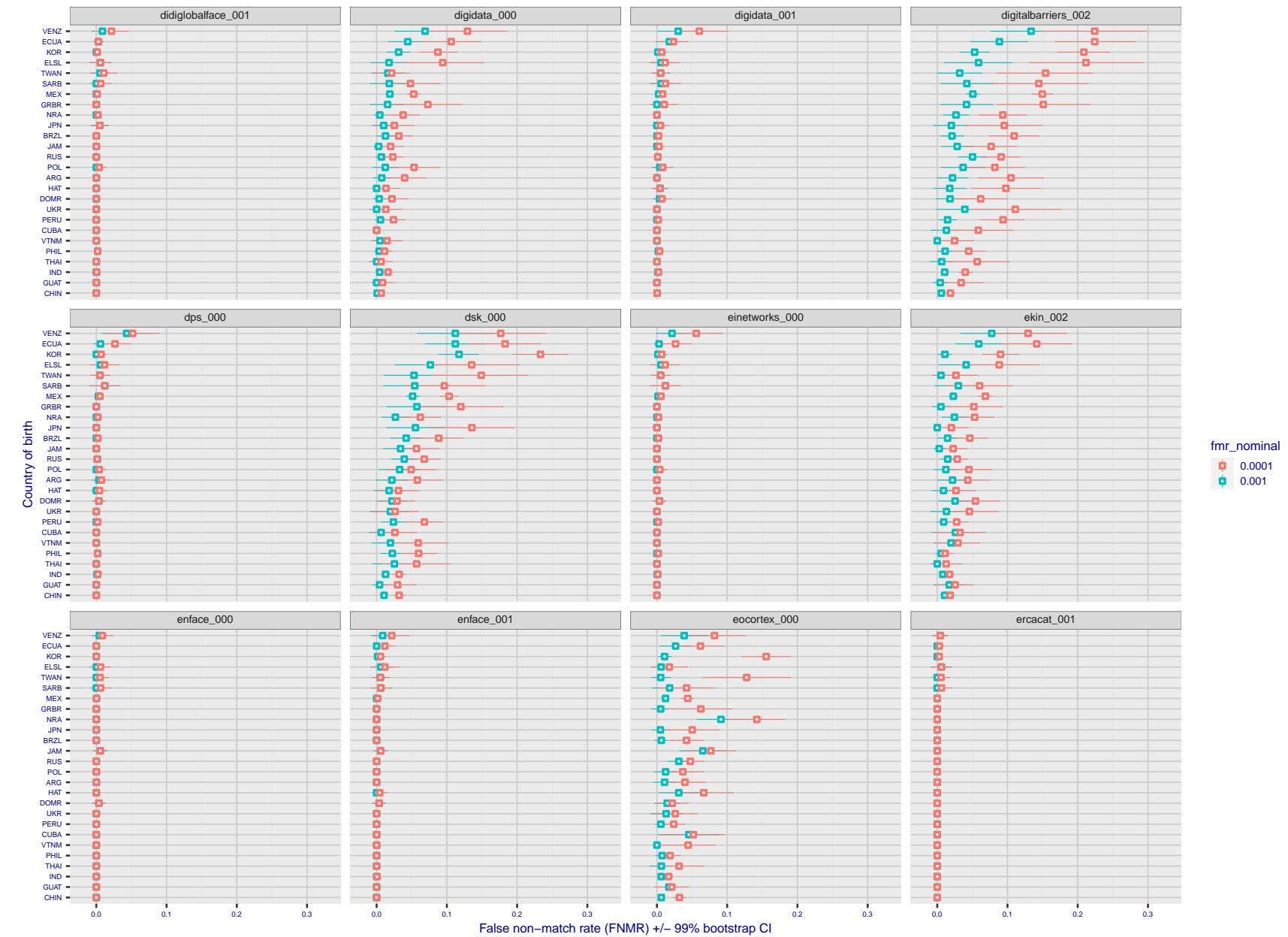


Figure 302: For the visa images, the dots show FNMR by country of birth for two globally set operating thresholds corresponding to $FMR = \{0.001, 0.0001\}$ computed over all on the order of 10^{10} impostor scores. The FMR in each bin will vary also - see subsequent impostor heatmaps in sec. 3.6.1. The figures shows an order of magnitude variation in FNMR across country of birth; these effects are likely due quality variations, then demographics like age and race. The error rates in some cases are zero, and in others the DET is flat so the error rates at the two thresholds are identical. The lines span 1% and 99% of bootstrap replicated FNMR estimates.

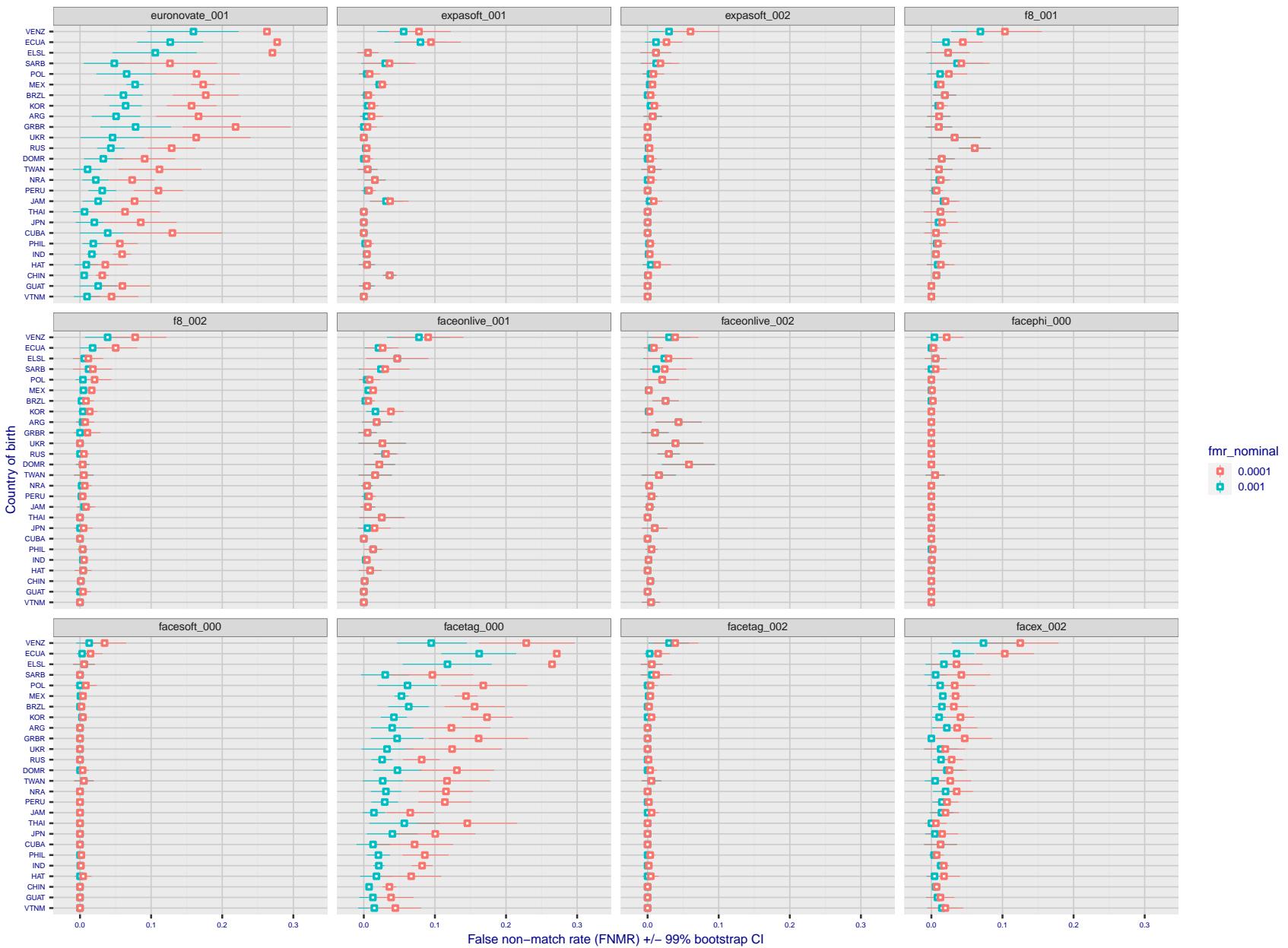


Figure 303: For the visa images, the dots show FNMR by country of birth for two globally set operating thresholds corresponding to $FMR = \{0.001, 0.0001\}$ computed over all on the order of 10^{10} impostor scores. The FMR in each bin will vary also - see subsequent impostor heatmaps in sec. 3.6.1. The figures shows an order of magnitude variation in FNMR across country of birth; these effects are likely due quality variations, then demographics like age and race. The error rates in some cases are zero, and in others the DET is flat so the error rates at the two thresholds are identical. The lines span 1% and 99% of bootstrap replicated FNMR estimates.

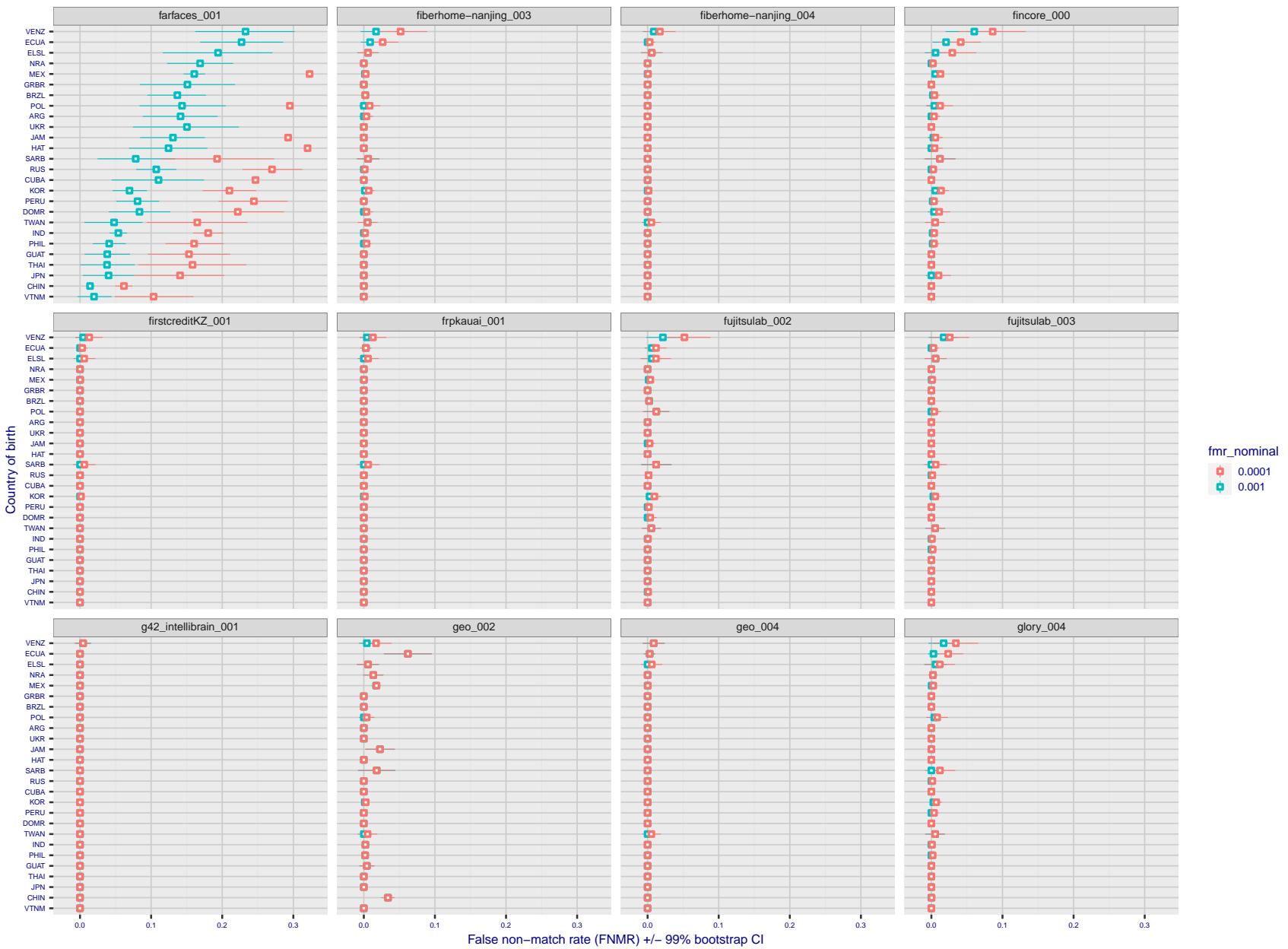


Figure 304: For the visa images, the dots show FNMR by country of birth for two globally set operating thresholds corresponding to $FMR = \{0.001, 0.0001\}$ computed over all on the order of 10^{10} impostor scores. The FMR in each bin will vary also - see subsequent impostor heatmaps in sec. 3.6.1. The figures shows an order of magnitude variation in FNMR across country of birth; these effects are likely due quality variations, then demographics like age and race. The error rates in some cases are zero, and in others the DET is flat so the error rates at the two thresholds are identical. The lines span 1% and 99% of bootstrap replicated FNMR estimates.

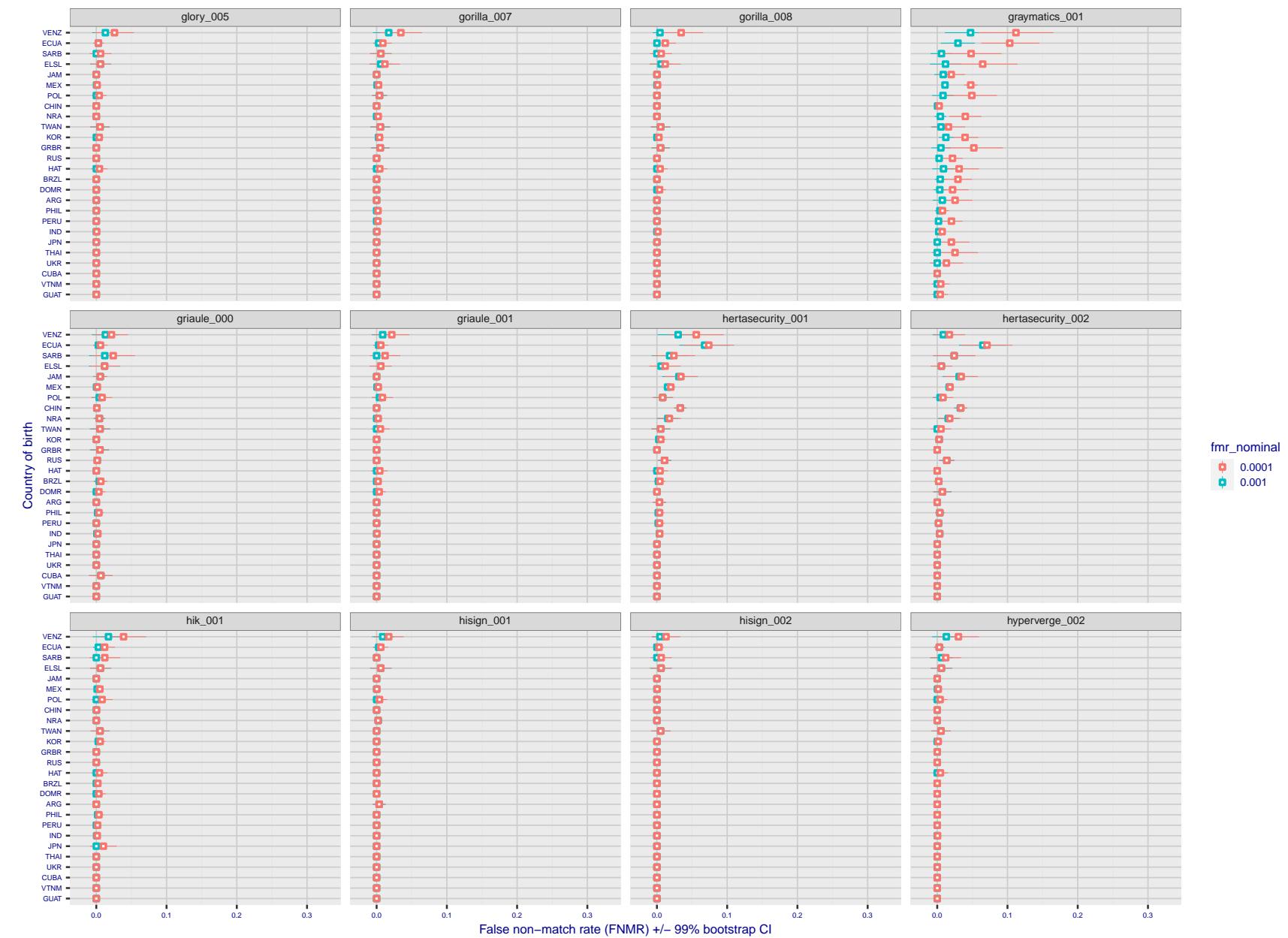


Figure 305: For the visa images, the dots show FNMR by country of birth for two globally set operating thresholds corresponding to $FMR = \{0.001, 0.0001\}$ computed over all on the order of 10^{10} impostor scores. The FMR in each bin will vary also - see subsequent impostor heatmaps in sec. 3.6.1. The figures shows an order of magnitude variation in FNMR across country of birth; these effects are likely due quality variations, then demographics like age and race. The error rates in some cases are zero, and in others the DET is flat so the error rates at the two thresholds are identical. The lines span 1% and 99% of bootstrap replicated FNMR estimates.

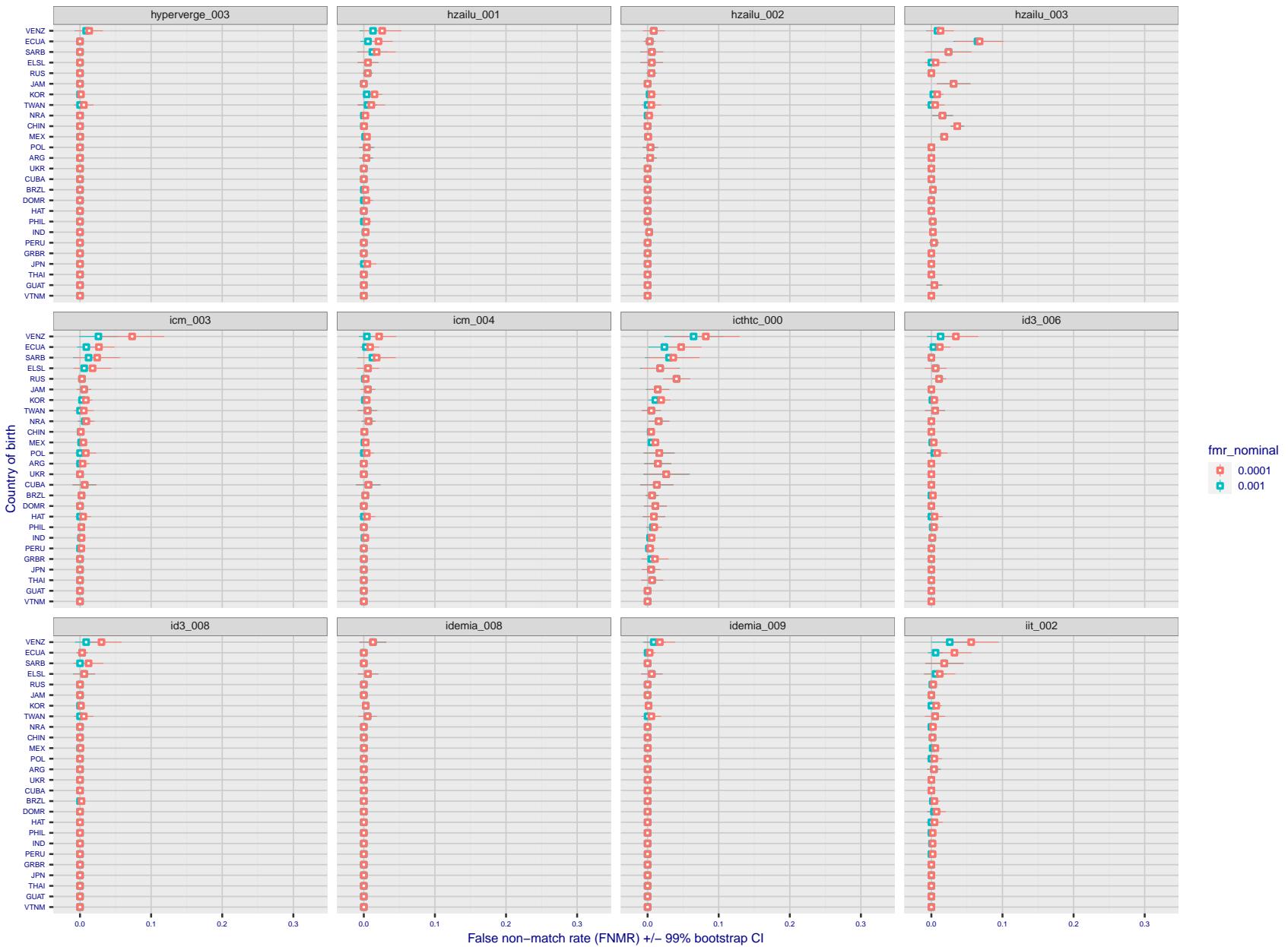


Figure 306: For the visa images, the dots show FNMR by country of birth for two globally set operating thresholds corresponding to $FMR = \{0.001, 0.0001\}$ computed over all on the order of 10^{10} impostor scores. The FMR in each bin will vary also - see subsequent impostor heatmaps in sec. 3.6.1. The figures shows an order of magnitude variation in FNMR across country of birth; these effects are likely due quality variations, then demographics like age and race. The error rates in some cases are zero, and in others the DET is flat so the error rates at the two thresholds are identical. The lines span 1% and 99% of bootstrap replicated FNMR estimates.

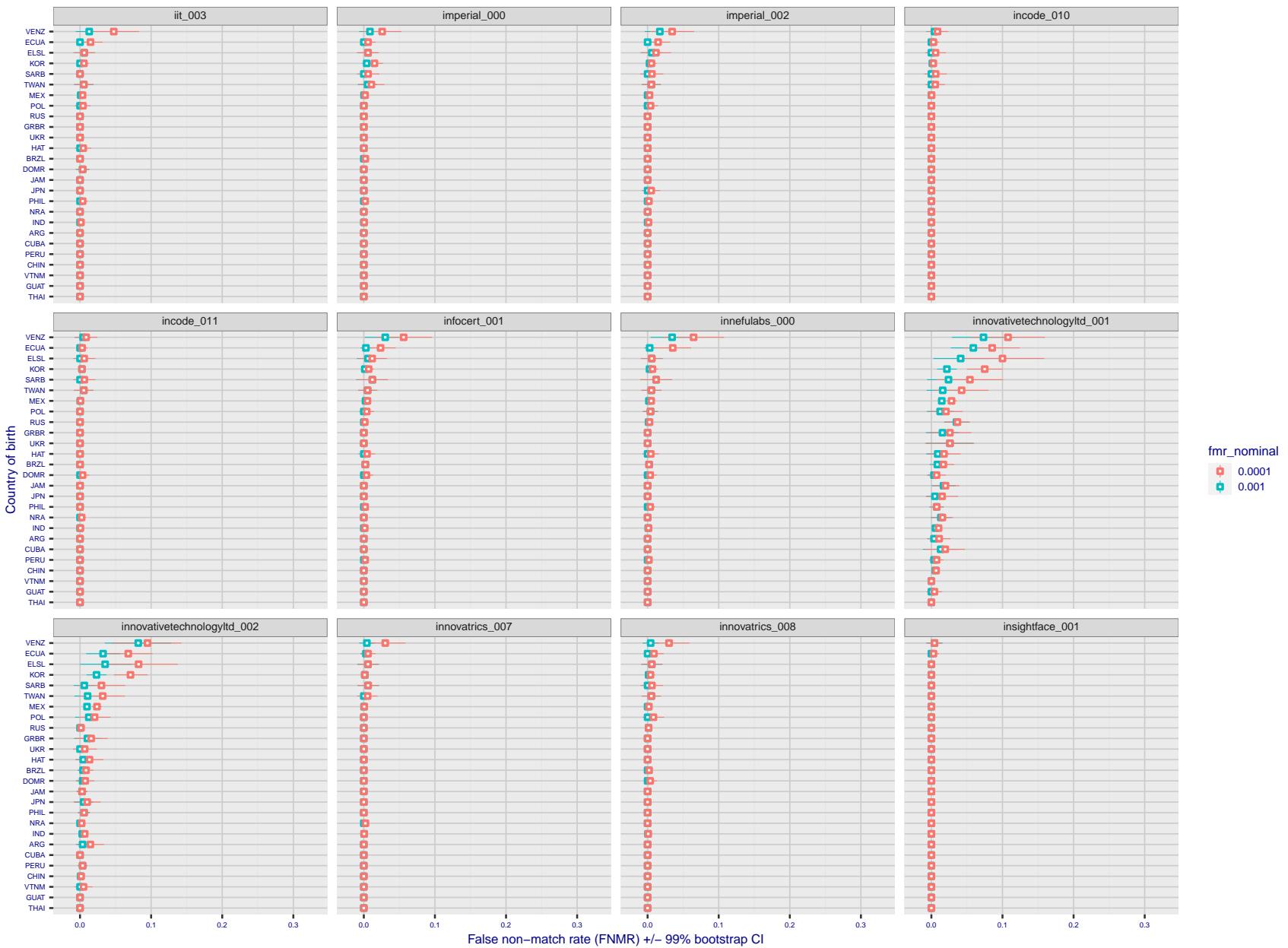


Figure 307: For the visa images, the dots show FNMR by country of birth for two globally set operating thresholds corresponding to $FMR = \{0.001, 0.0001\}$ computed over all on the order of 10^{10} impostor scores. The FMR in each bin will vary also - see subsequent impostor heatmaps in sec. 3.6.1. The figures shows an order of magnitude variation in FNMR across country of birth; these effects are likely due quality variations, then demographics like age and race. The error rates in some cases are zero, and in others the DET is flat so the error rates at the two thresholds are identical. The lines span 1% and 99% of bootstrap replicated FNMR estimates.

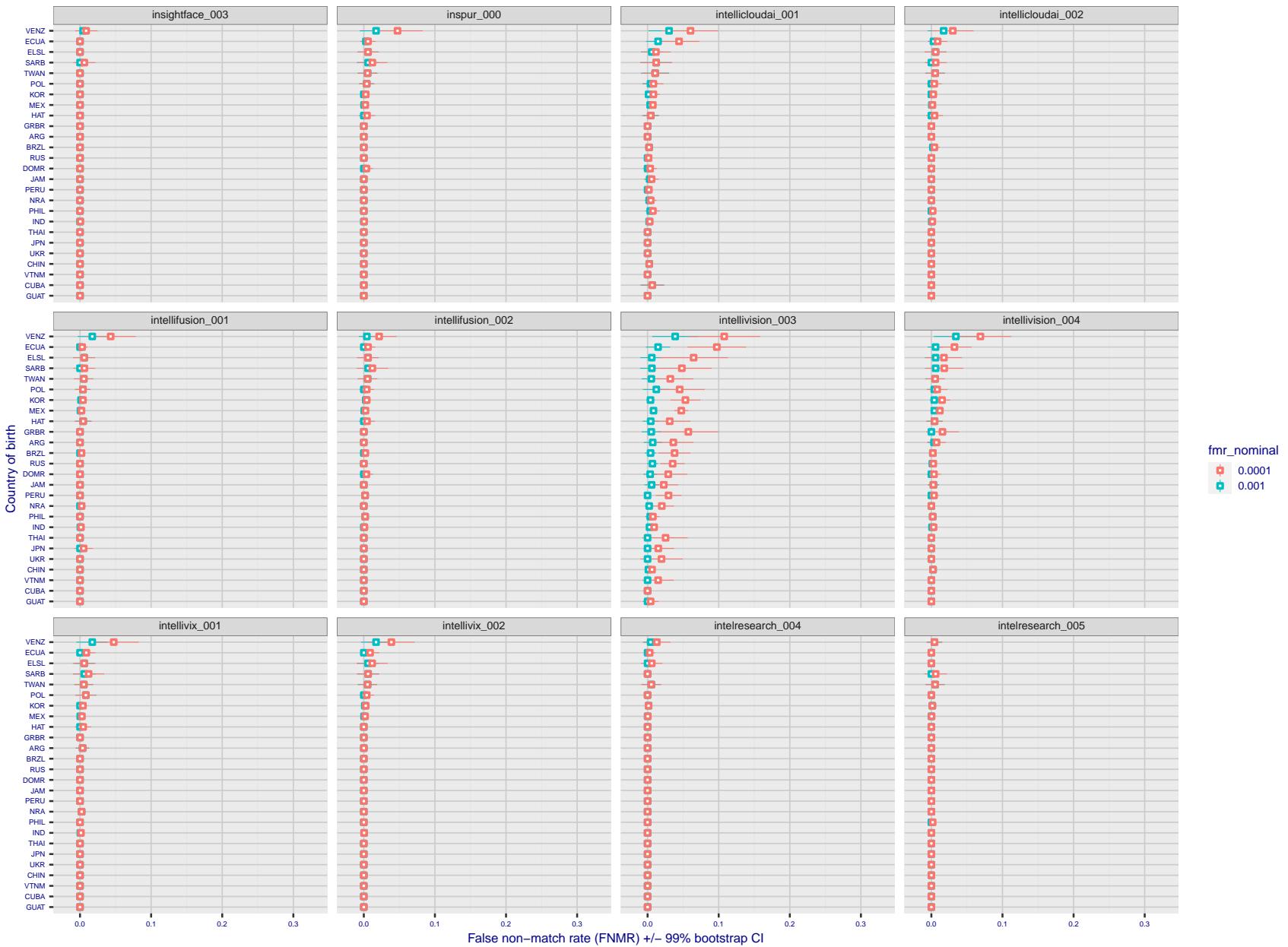


Figure 308: For the visa images, the dots show FNMR by country of birth for two globally set operating thresholds corresponding to $FMR = \{0.001, 0.0001\}$ computed over all on the order of 10^{10} impostor scores. The FMR in each bin will vary also - see subsequent impostor heatmaps in sec. 3.6.1. The figures shows an order of magnitude variation in FNMR across country of birth; these effects are likely due quality variations, then demographics like age and race. The error rates in some cases are zero, and in others the DET is flat so the error rates at the two thresholds are identical. The lines span 1% and 99% of bootstrap replicated FNMR estimates.

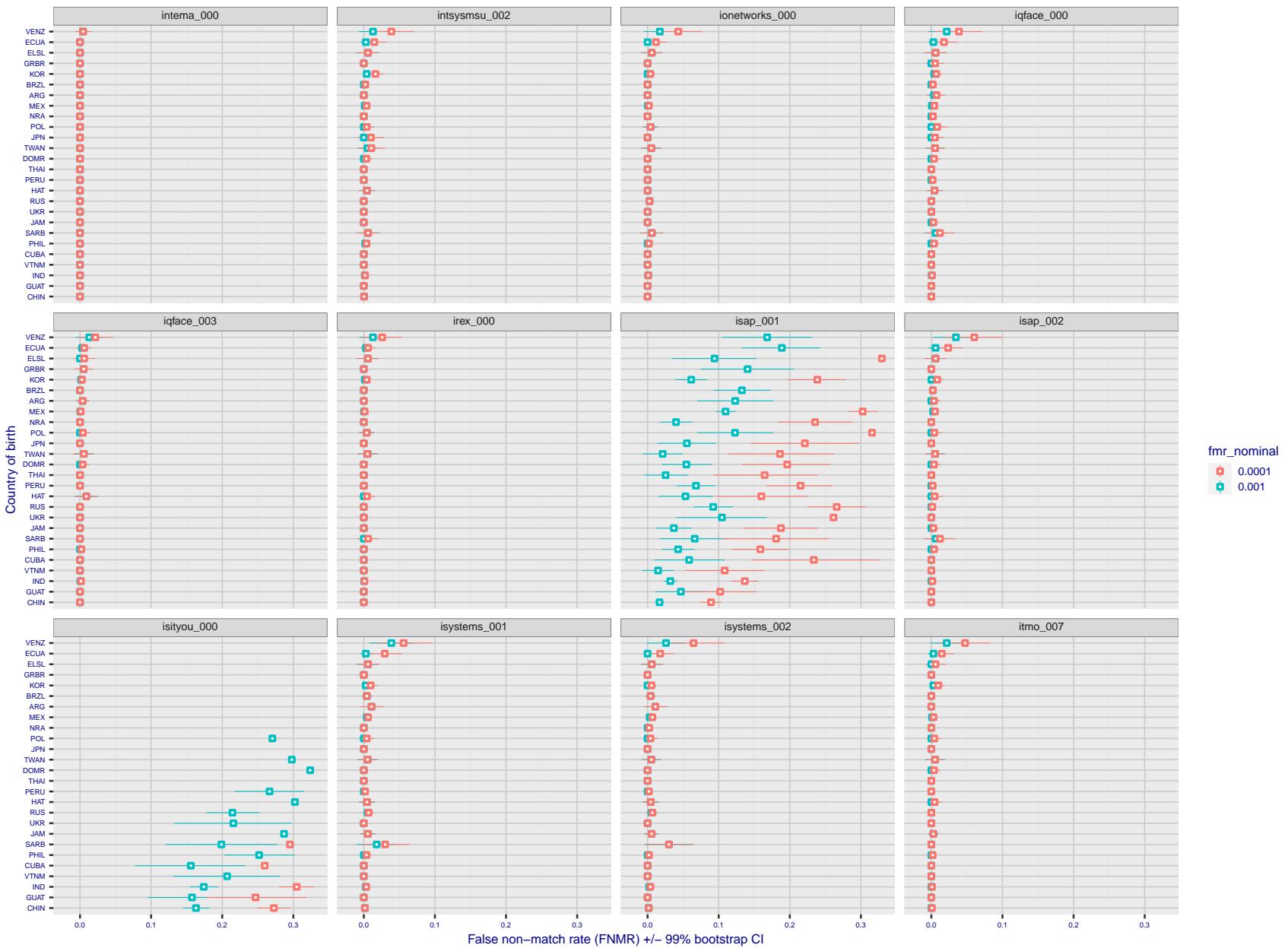


Figure 309: For the visa images, the dots show FNMR by country of birth for two globally set operating thresholds corresponding to $FMR = \{0.001, 0.0001\}$ computed over all on the order of 10^{10} impostor scores. The FMR in each bin will vary also - see subsequent impostor heatmaps in sec. 3.6.1. The figures shows an order of magnitude variation in FNMR across country of birth; these effects are likely due quality variations, then demographics like age and race. The error rates in some cases are zero, and in others the DET is flat so the error rates at the two thresholds are identical. The lines span 1% and 99% of bootstrap replicated FNMR estimates.

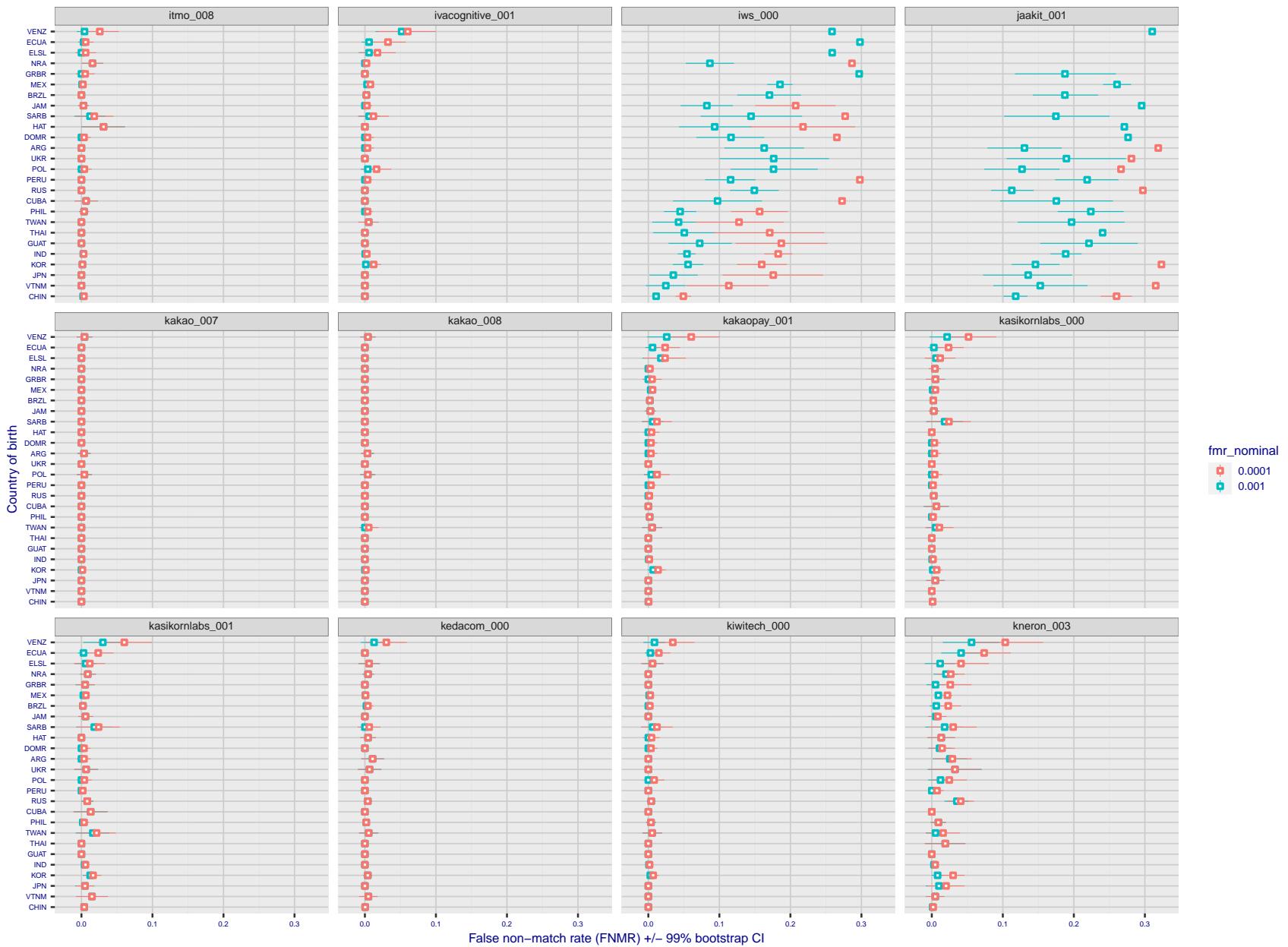


Figure 310: For the visa images, the dots show FNMR by country of birth for two globally set operating thresholds corresponding to $FMR = \{0.001, 0.0001\}$ computed over all on the order of 10^{10} impostor scores. The FMR in each bin will vary also - see subsequent impostor heatmaps in sec. 3.6.1. The figures shows an order of magnitude variation in FNMR across country of birth; these effects are likely due quality variations, then demographics like age and race. The error rates in some cases are zero, and in others the DET is flat so the error rates at the two thresholds are identical. The lines span 1% and 99% of bootstrap replicated FNMR estimates.

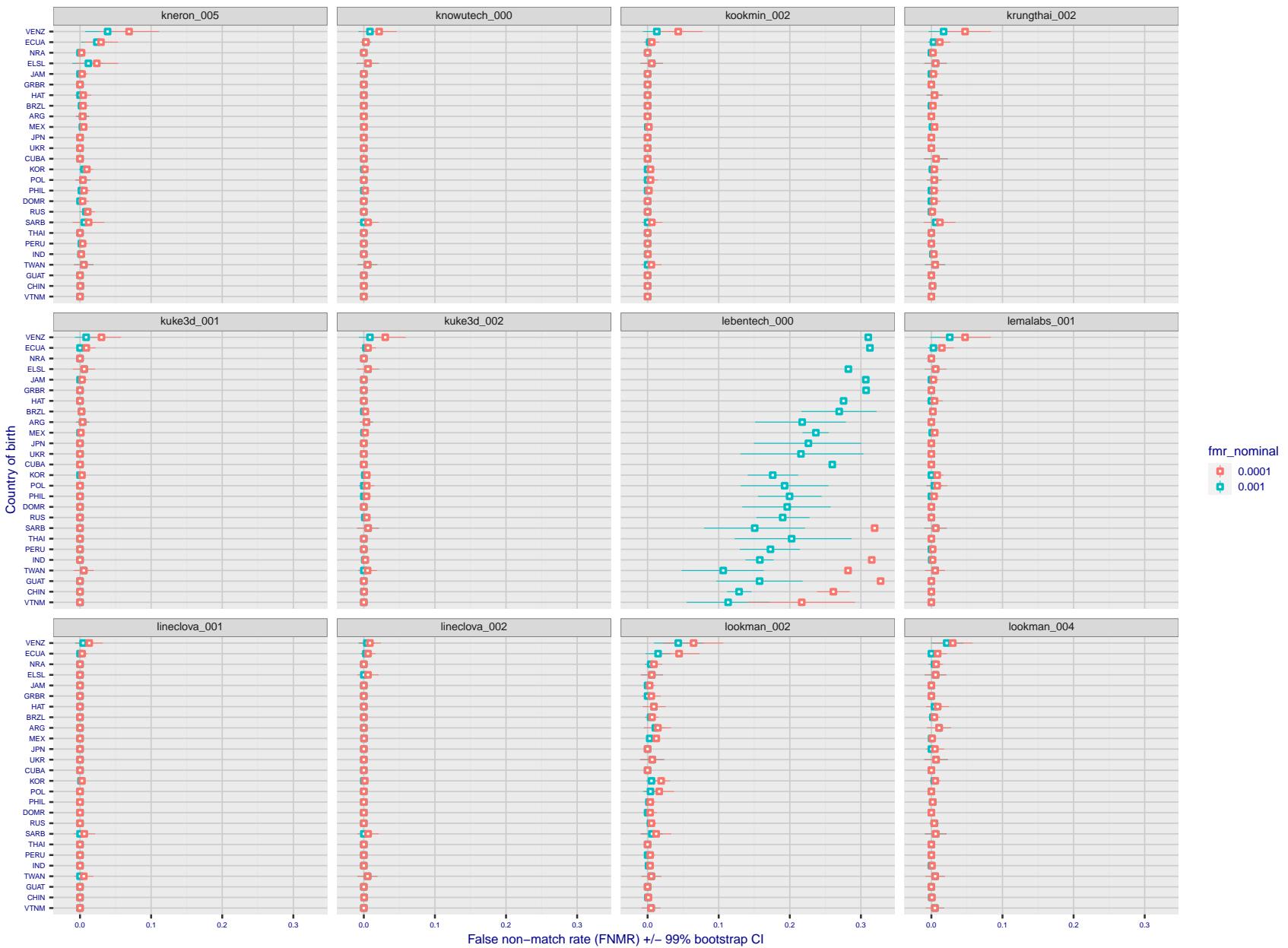


Figure 311: For the visa images, the dots show FNMR by country of birth for two globally set operating thresholds corresponding to $FMR = \{0.001, 0.0001\}$ computed over all on the order of 10^{10} impostor scores. The FMR in each bin will vary also - see subsequent impostor heatmaps in sec. 3.6.1. The figures shows an order of magnitude variation in FNMR across country of birth; these effects are likely due quality variations, then demographics like age and race. The error rates in some cases are zero, and in others the DET is flat so the error rates at the two thresholds are identical. The lines span 1% and 99% of bootstrap replicated FNMR estimates.

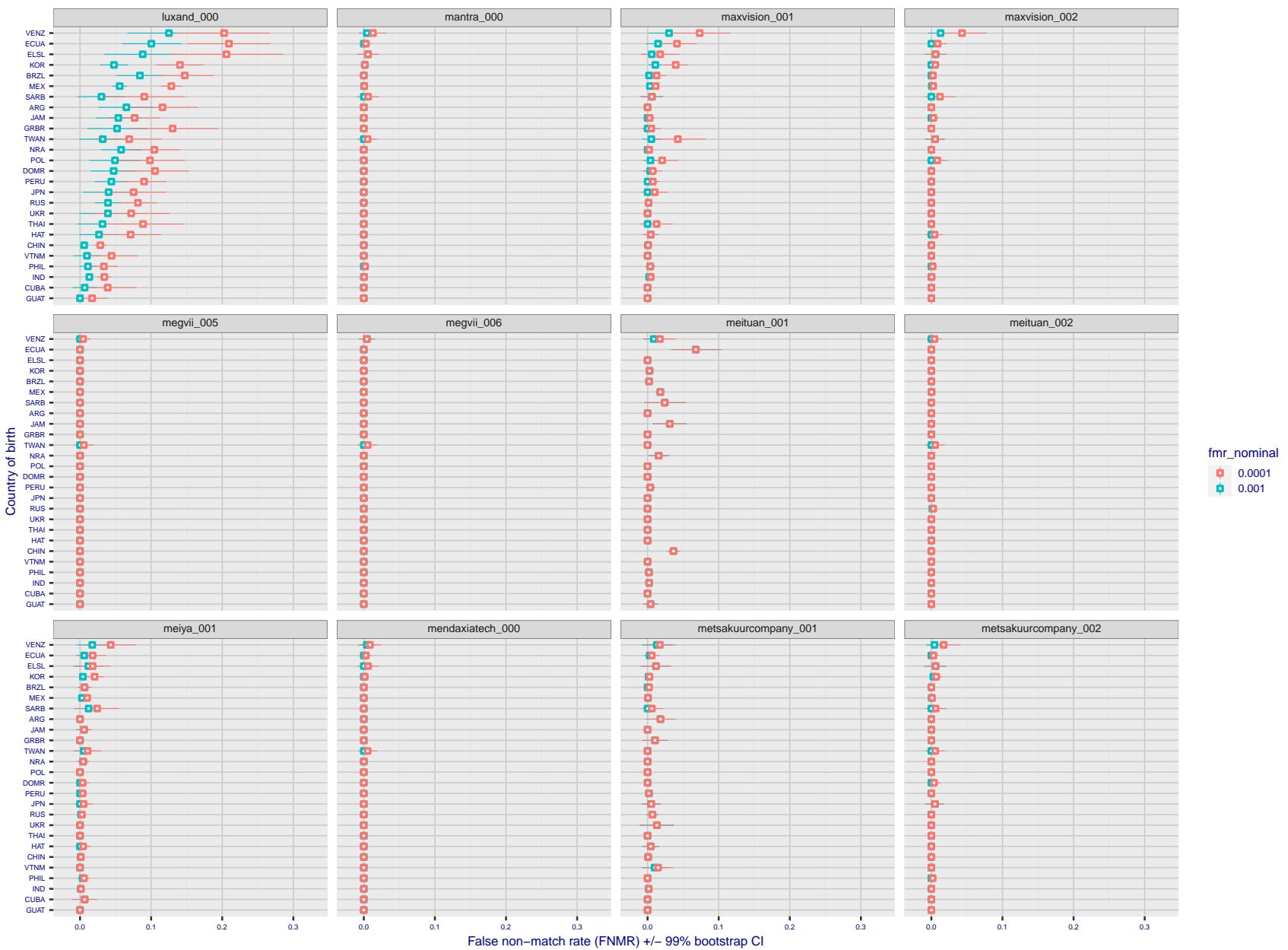


Figure 312: For the visa images, the dots show FNMR by country of birth for two globally set operating thresholds corresponding to $FMR = \{0.001, 0.0001\}$ computed over all on the order of 10^{10} impostor scores. The FMR in each bin will vary also - see subsequent impostor heatmaps in sec. 3.6.1. The figures shows an order of magnitude variation in FNMR across country of birth; these effects are likely due quality variations, then demographics like age and race. The error rates in some cases are zero, and in others the DET is flat so the error rates at the two thresholds are identical. The lines span 1% and 99% of bootstrap replicated FNMR estimates.

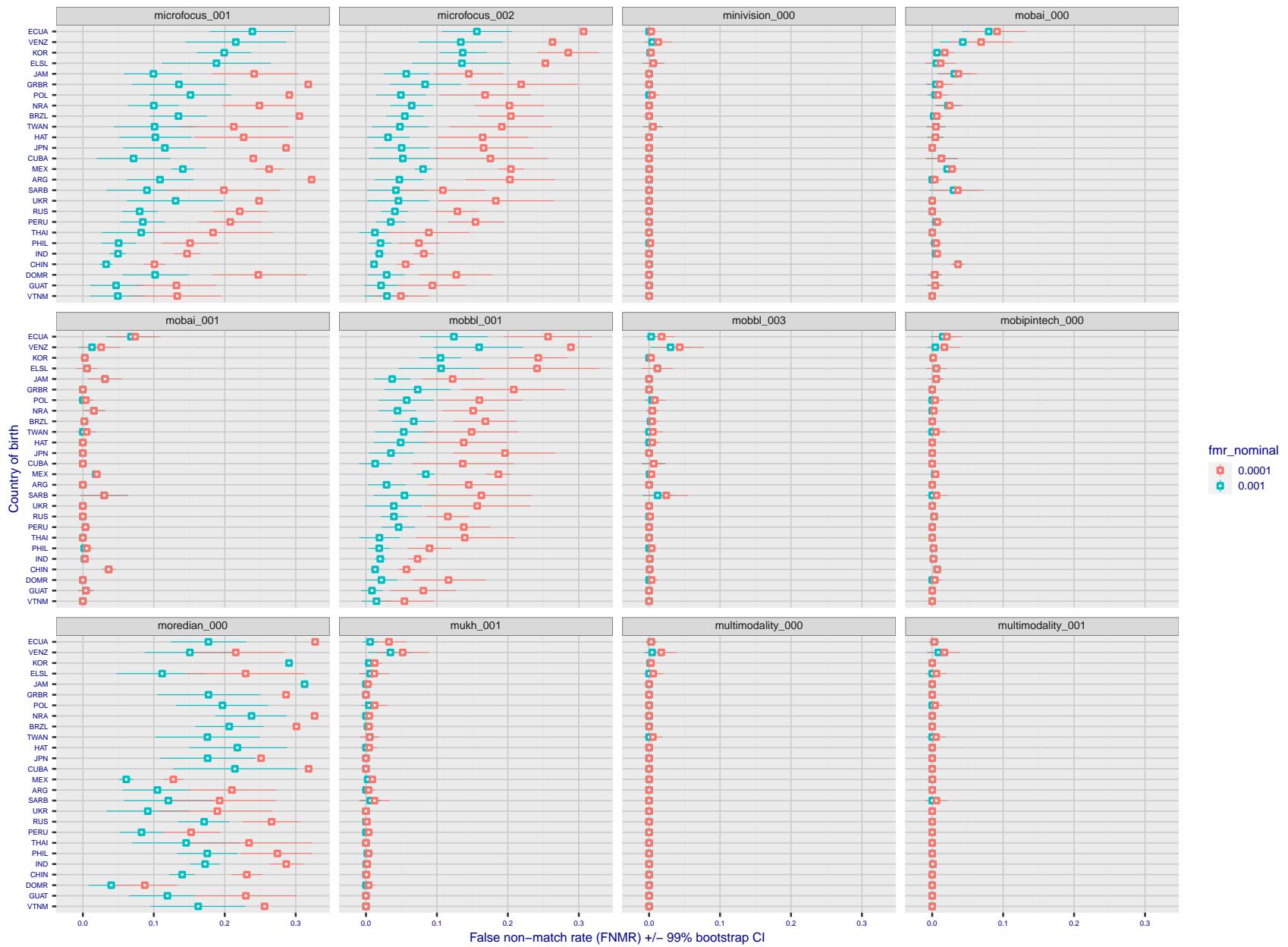


Figure 313: For the visa images, the dots show FNMR by country of birth for two globally set operating thresholds corresponding to $FMR = \{0.001, 0.0001\}$ computed over all on the order of 10^{10} impostor scores. The FMR in each bin will vary also - see subsequent impostor heatmaps in sec. 3.6.1. The figures shows an order of magnitude variation in FNMR across country of birth; these effects are likely due quality variations, then demographics like age and race. The error rates in some cases are zero, and in others the DET is flat so the error rates at the two thresholds are identical. The lines span 1% and 99% of bootstrap replicated FNMR estimates.

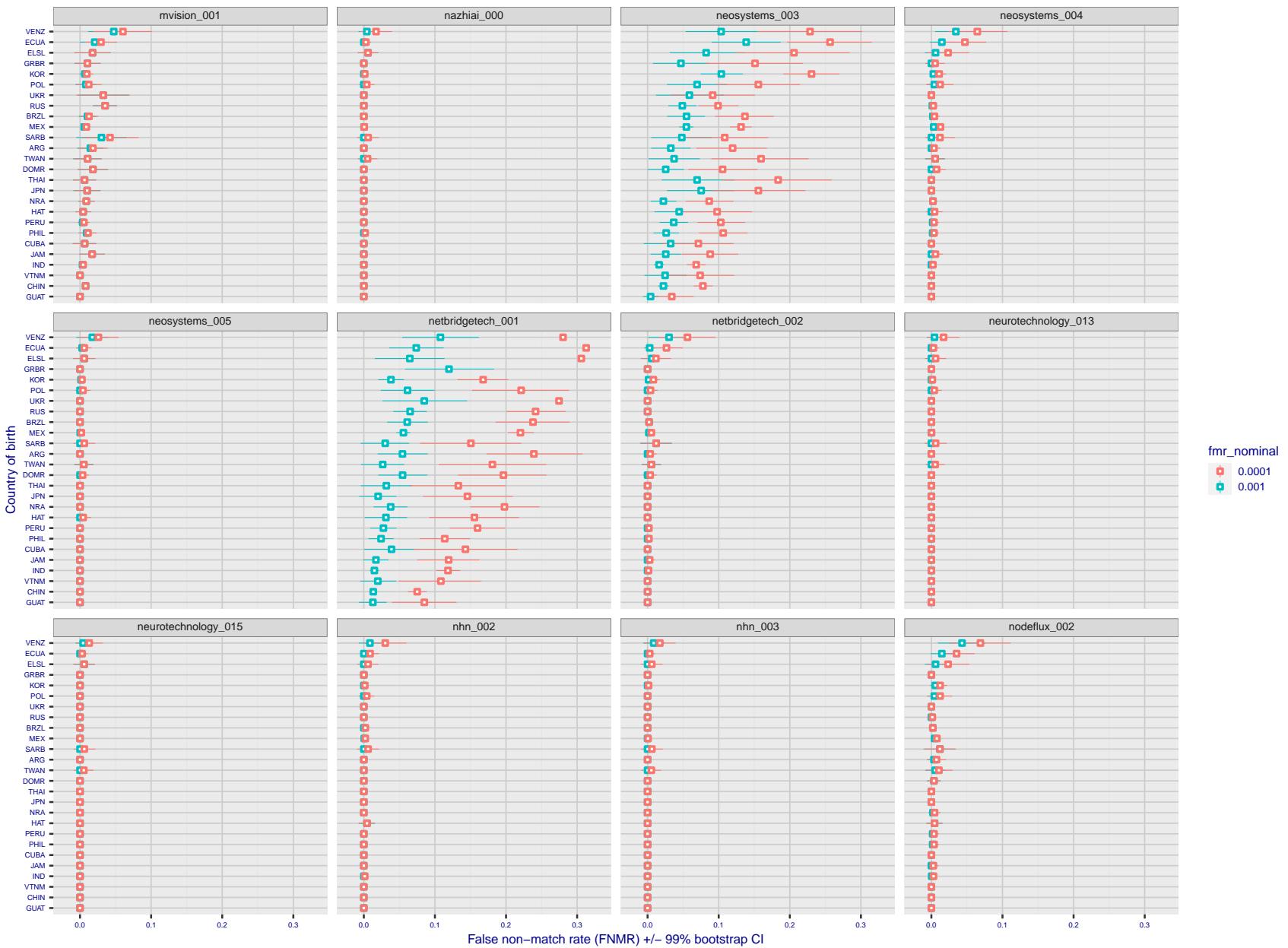


Figure 314: For the visa images, the dots show FNMR by country of birth for two globally set operating thresholds corresponding to $FMR = \{0.001, 0.0001\}$ computed over all on the order of 10^{10} impostor scores. The FMR in each bin will vary also - see subsequent impostor heatmaps in sec. 3.6.1. The figures shows an order of magnitude variation in FNMR across country of birth; these effects are likely due quality variations, then demographics like age and race. The error rates in some cases are zero, and in others the DET is flat so the error rates at the two thresholds are identical. The lines span 1% and 99% of bootstrap replicated FNMR estimates.

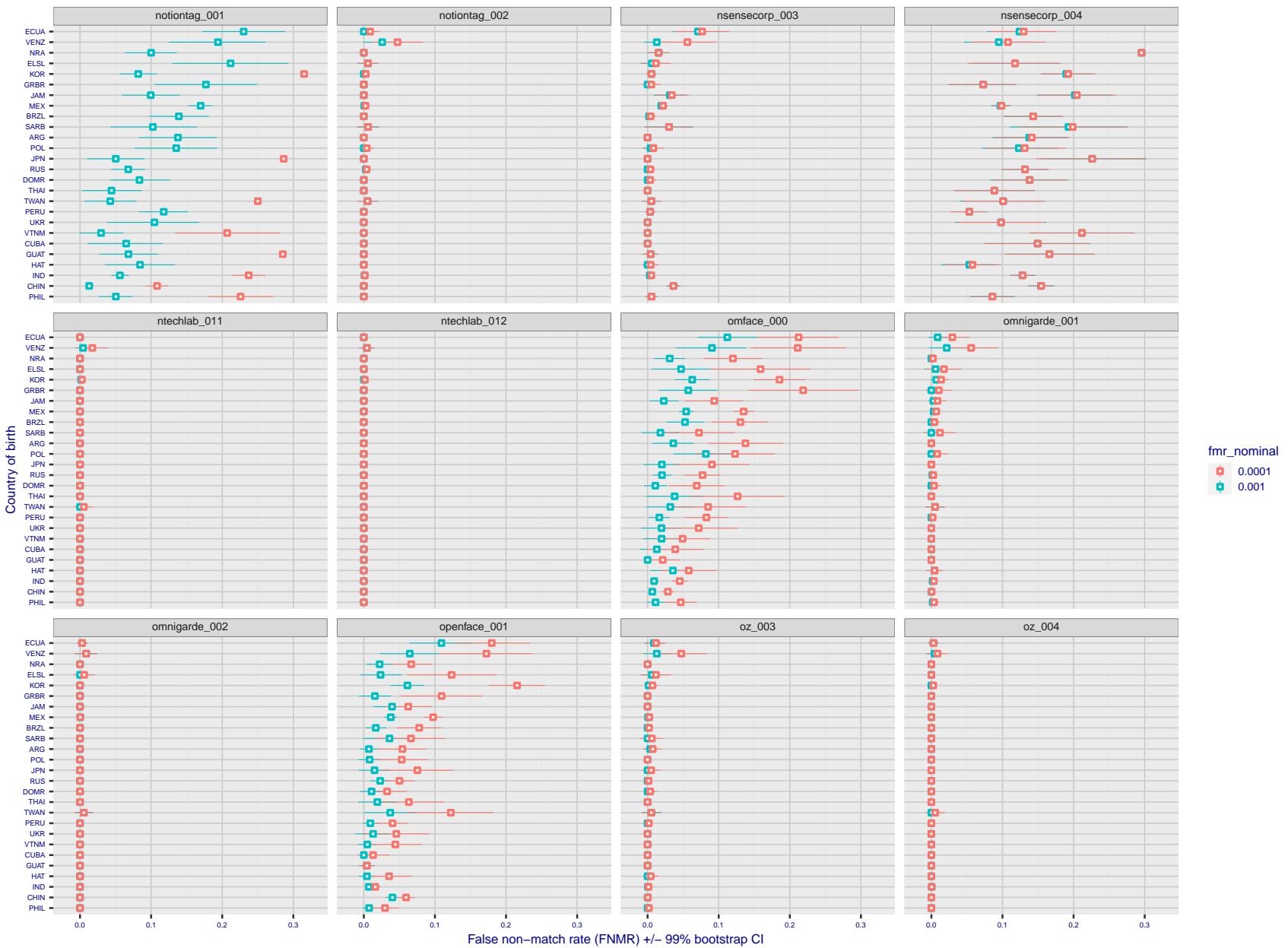


Figure 315: For the visa images, the dots show FNMR by country of birth for two globally set operating thresholds corresponding to $FMR = \{0.001, 0.0001\}$ computed over all on the order of 10^{10} impostor scores. The FMR in each bin will vary also - see subsequent impostor heatmaps in sec. 3.6.1. The figures shows an order of magnitude variation in FNMR across country of birth; these effects are likely due quality variations, then demographics like age and race. The error rates in some cases are zero, and in others the DET is flat so the error rates at the two thresholds are identical. The lines span 1% and 99% of bootstrap replicated FNMR estimates.

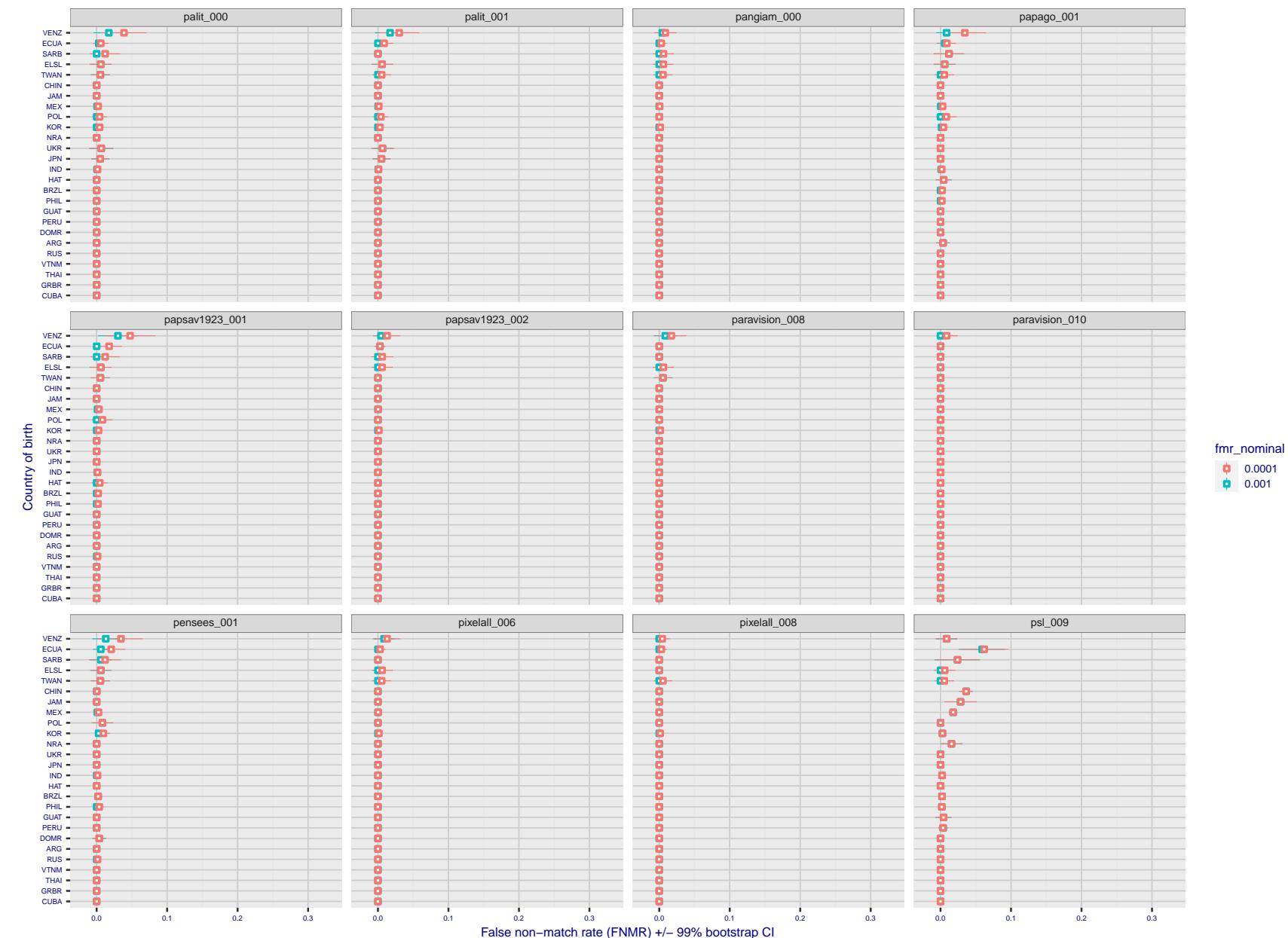


Figure 316: For the visa images, the dots show FNMR by country of birth for two globally set operating thresholds corresponding to $FMR = \{0.001, 0.0001\}$ computed over all on the order of 10^{10} impostor scores. The FMR in each bin will vary also - see subsequent impostor heatmaps in sec. 3.6.1. The figures shows an order of magnitude variation in FNMR across country of birth; these effects are likely due quality variations, then demographics like age and race. The error rates in some cases are zero, and in others the DET is flat so the error rates at the two thresholds are identical. The lines span 1% and 99% of bootstrap replicated FNMR estimates.

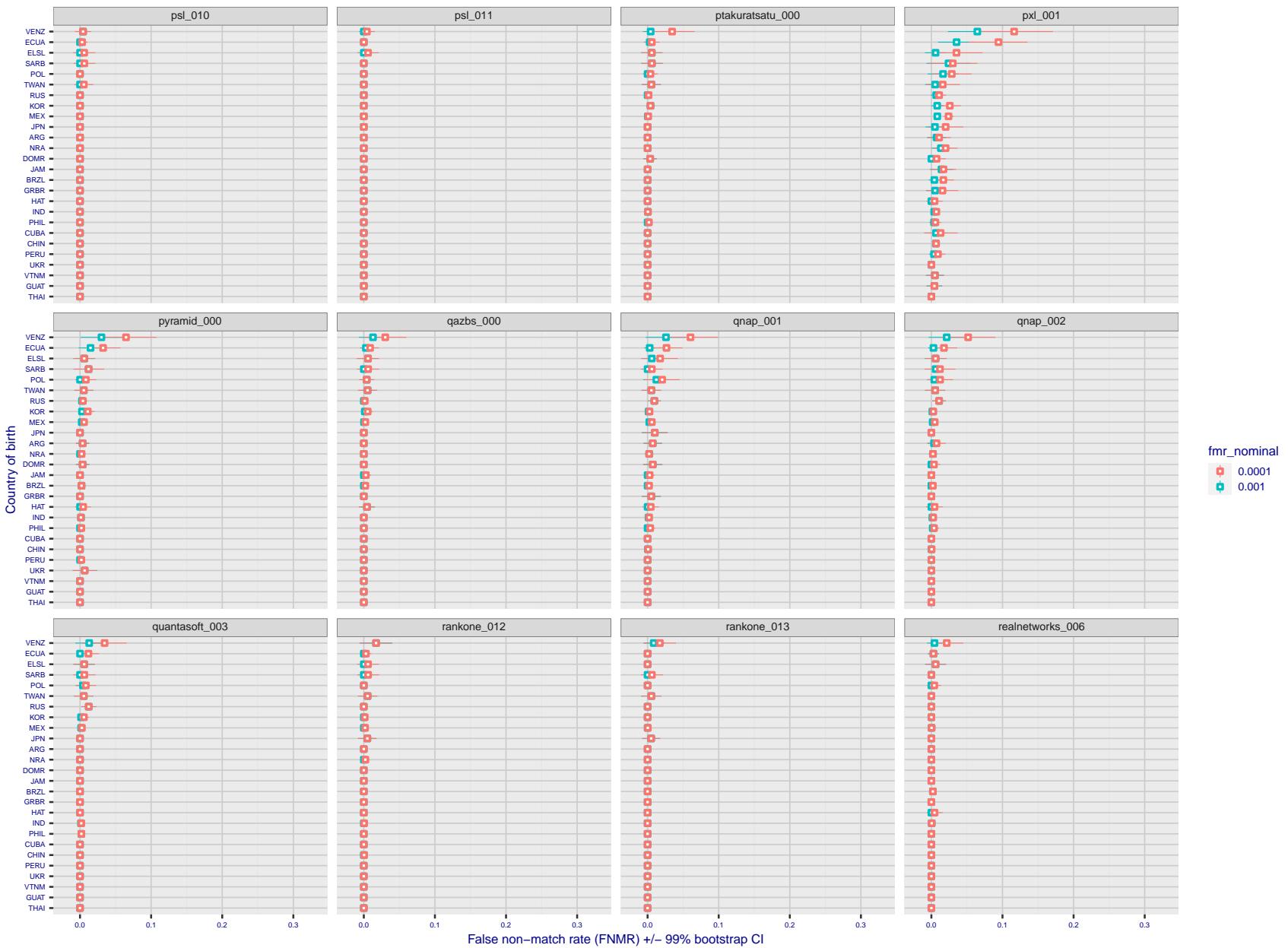


Figure 317: For the visa images, the dots show FNMR by country of birth for two globally set operating thresholds corresponding to $FMR = \{0.001, 0.0001\}$ computed over all on the order of 10^{10} impostor scores. The FMR in each bin will vary also - see subsequent impostor heatmaps in sec. 3.6.1. The figures shows an order of magnitude variation in FNMR across country of birth; these effects are likely due quality variations, then demographics like age and race. The error rates in some cases are zero, and in others the DET is flat so the error rates at the two thresholds are identical. The lines span 1% and 99% of bootstrap replicated FNMR estimates.

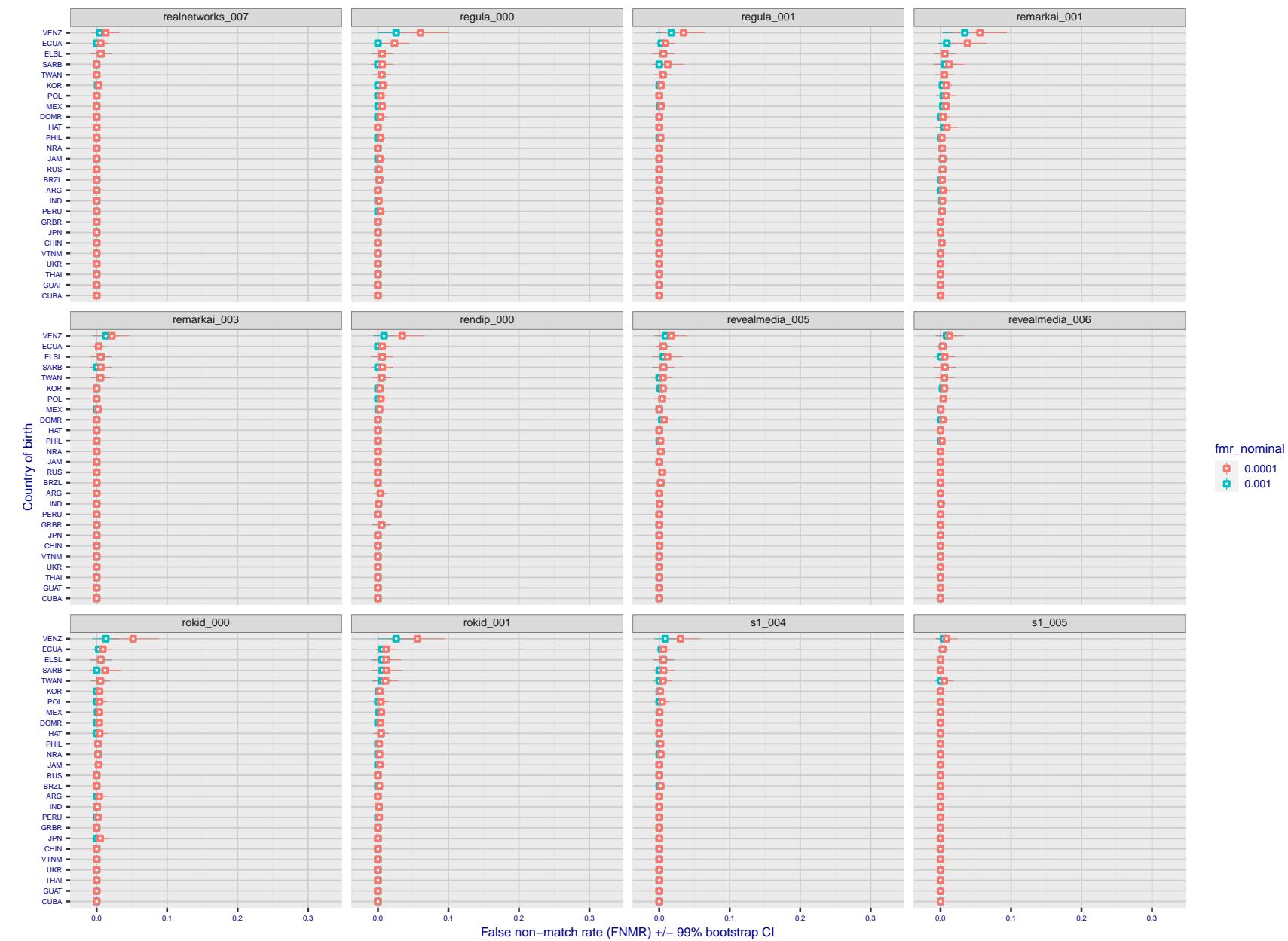


Figure 318: For the visa images, the dots show FNMR by country of birth for two globally set operating thresholds corresponding to $FMR = \{0.001, 0.0001\}$ computed over all on the order of 10^{10} impostor scores. The FMR in each bin will vary also - see subsequent impostor heatmaps in sec. 3.6.1. The figures shows an order of magnitude variation in FNMR across country of birth; these effects are likely due quality variations, then demographics like age and race. The error rates in some cases are zero, and in others the DET is flat so the error rates at the two thresholds are identical. The lines span 1% and 99% of bootstrap replicated FNMR estimates.

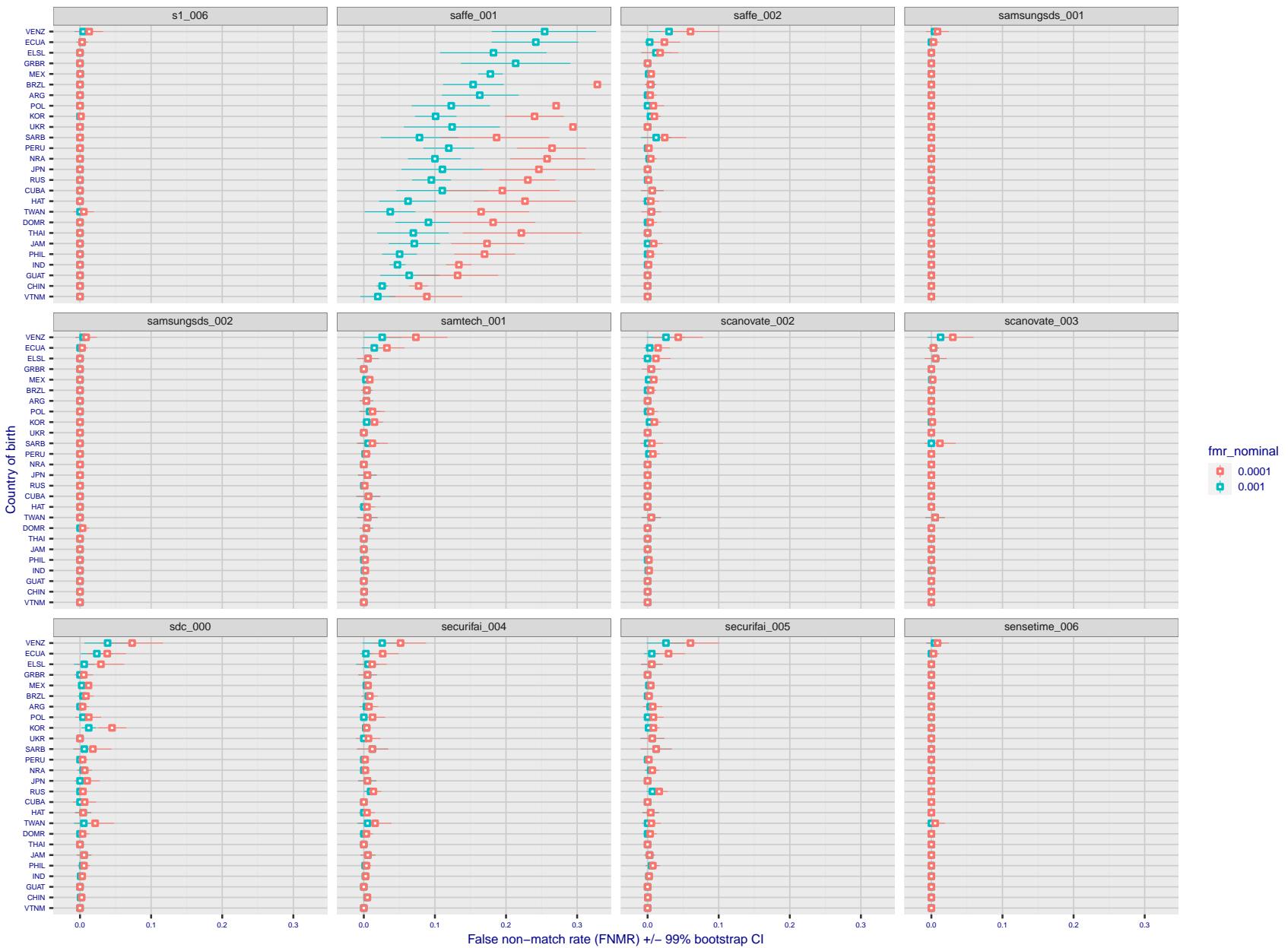


Figure 319: For the visa images, the dots show FNMR by country of birth for two globally set operating thresholds corresponding to $FMR = \{0.001, 0.0001\}$ computed over all on the order of 10^{10} impostor scores. The FMR in each bin will vary also - see subsequent impostor heatmaps in sec. 3.6.1. The figures shows an order of magnitude variation in FNMR across country of birth; these effects are likely due quality variations, then demographics like age and race. The error rates in some cases are zero, and in others the DET is flat so the error rates at the two thresholds are identical. The lines span 1% and 99% of bootstrap replicated FNMR estimates.

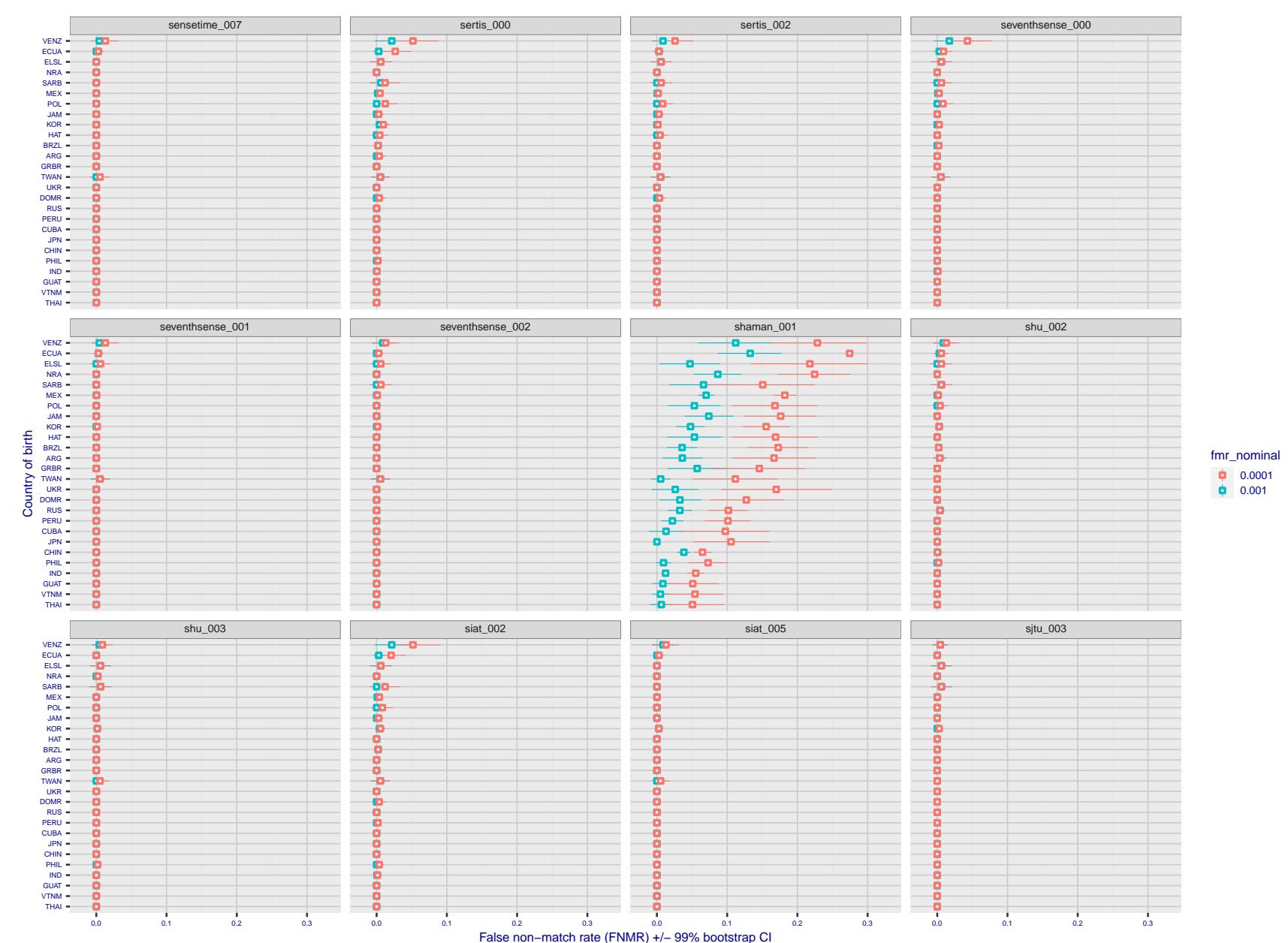


Figure 320: For the visa images, the dots show FNMR by country of birth for two globally set operating thresholds corresponding to $FMR = \{0.001, 0.0001\}$ computed over all on the order of 10^{10} impostor scores. The FMR in each bin will vary also - see subsequent impostor heatmaps in sec. 3.6.1. The figures shows an order of magnitude variation in FNMR across country of birth; these effects are likely due quality variations, then demographics like age and race. The error rates in some cases are zero, and in others the DET is flat so the error rates at the two thresholds are identical. The lines span 1% and 99% of bootstrap replicated FNMR estimates.

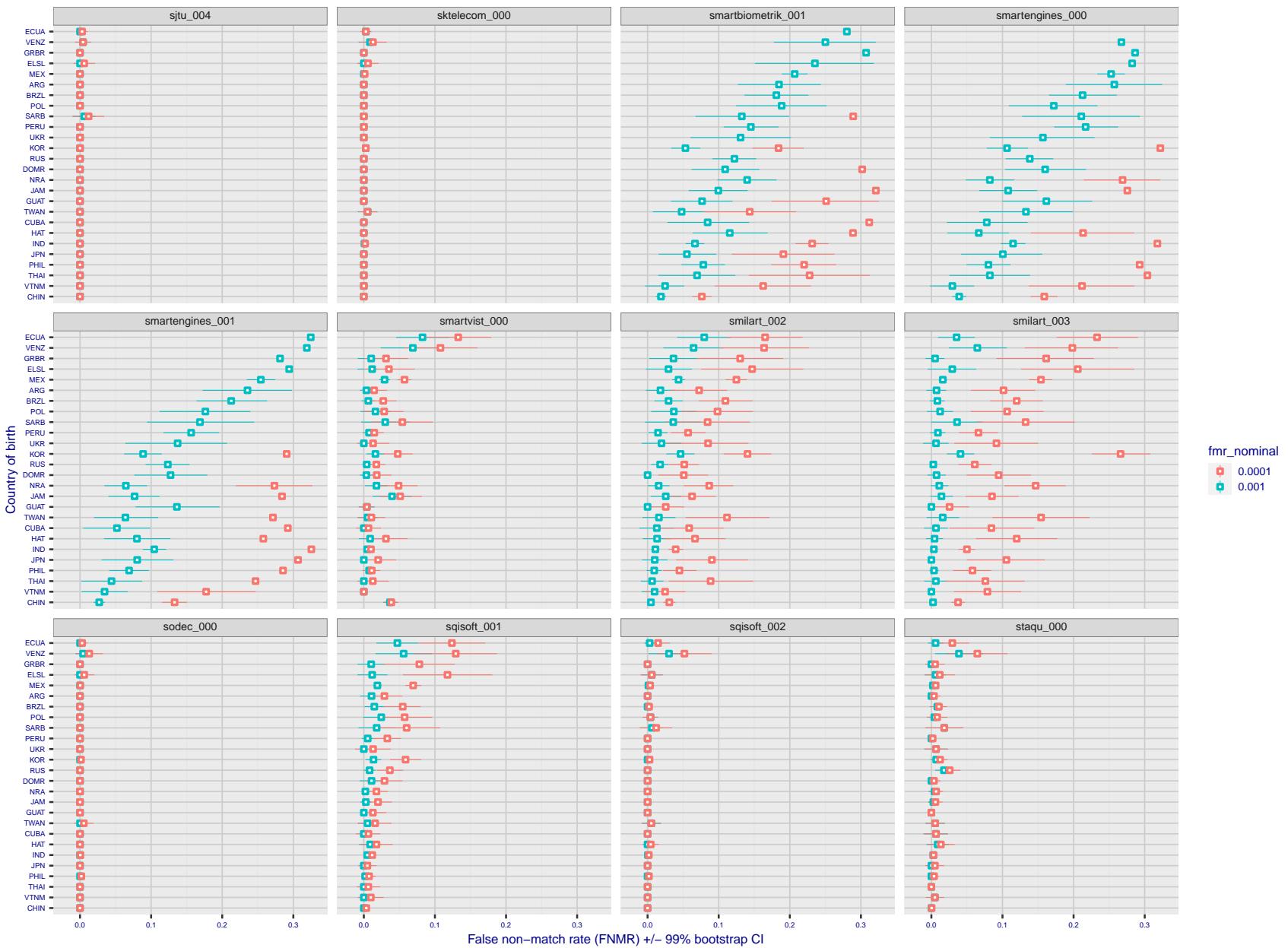


Figure 321: For the visa images, the dots show FNMR by country of birth for two globally set operating thresholds corresponding to $FMR = \{0.001, 0.0001\}$ computed over all on the order of 10^{10} impostor scores. The FMR in each bin will vary also - see subsequent impostor heatmaps in sec. 3.6.1. The figures shows an order of magnitude variation in FNMR across country of birth; these effects are likely due quality variations, then demographics like age and race. The error rates in some cases are zero, and in others the DET is flat so the error rates at the two thresholds are identical. The lines span 1% and 99% of bootstrap replicated FNMR estimates.

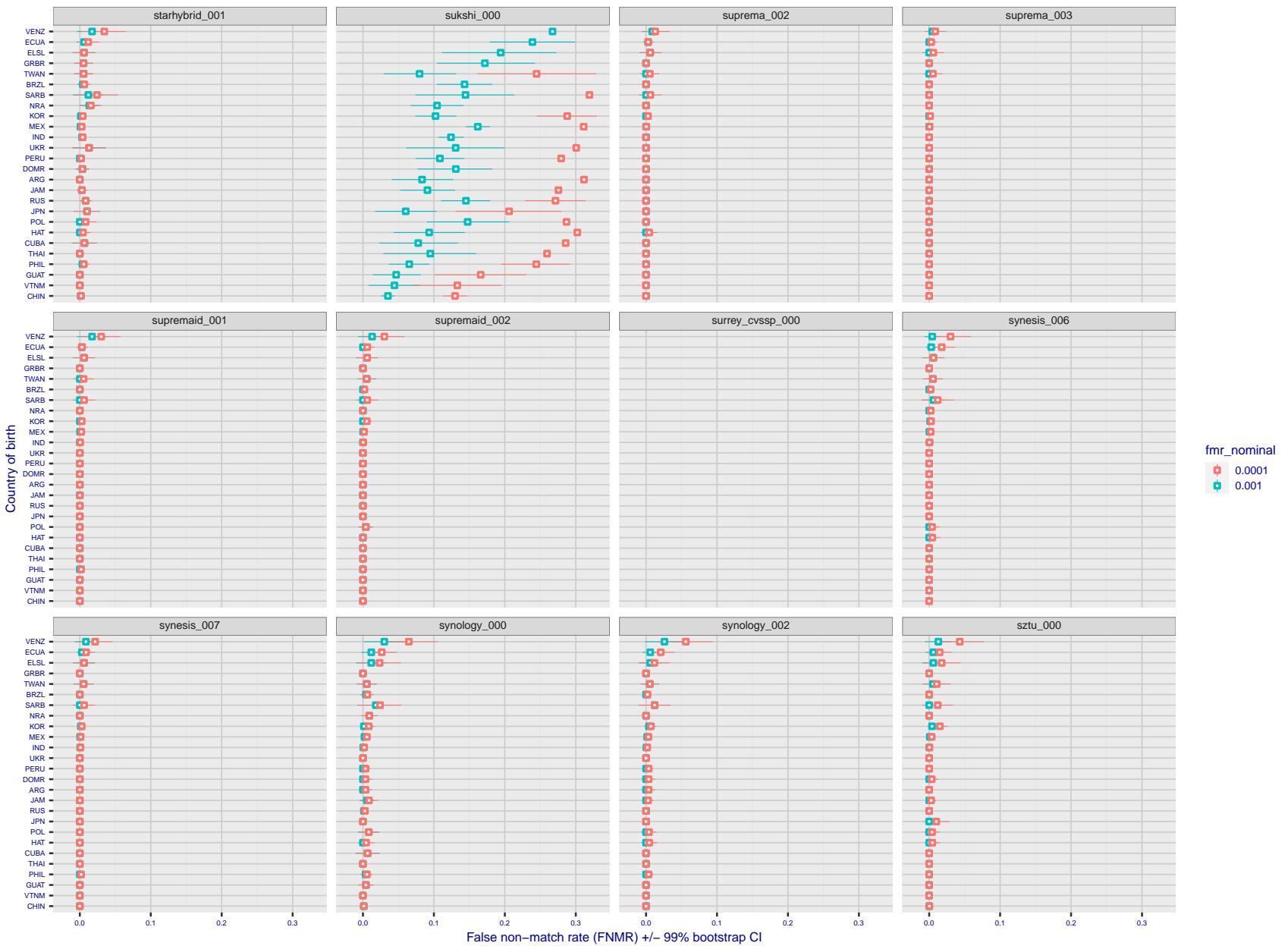


Figure 322: For the visa images, the dots show FNMR by country of birth for two globally set operating thresholds corresponding to $FMR = \{0.001, 0.0001\}$ computed over all on the order of 10^{10} impostor scores. The FMR in each bin will vary also - see subsequent impostor heatmaps in sec. 3.6.1. The figures shows an order of magnitude variation in FNMR across country of birth; these effects are likely due quality variations, then demographics like age and race. The error rates in some cases are zero, and in others the DET is flat so the error rates at the two thresholds are identical. The lines span 1% and 99% of bootstrap replicated FNMR estimates.

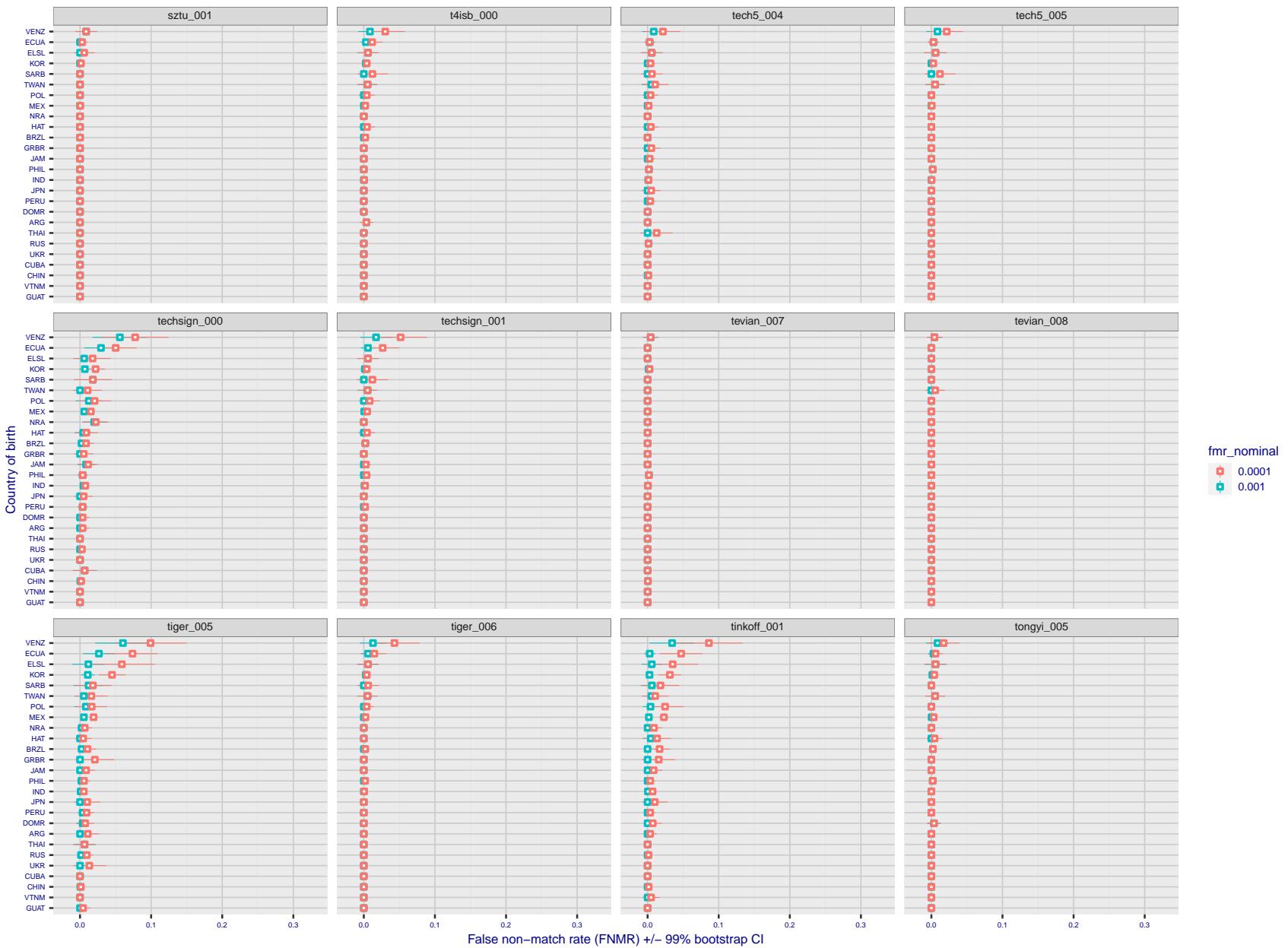


Figure 323: For the visa images, the dots show FNMR by country of birth for two globally set operating thresholds corresponding to $FMR = \{0.001, 0.0001\}$ computed over all on the order of 10^{10} impostor scores. The FMR in each bin will vary also - see subsequent impostor heatmaps in sec. 3.6.1. The figures shows an order of magnitude variation in FNMR across country of birth; these effects are likely due quality variations, then demographics like age and race. The error rates in some cases are zero, and in others the DET is flat so the error rates at the two thresholds are identical. The lines span 1% and 99% of bootstrap replicated FNMR estimates.

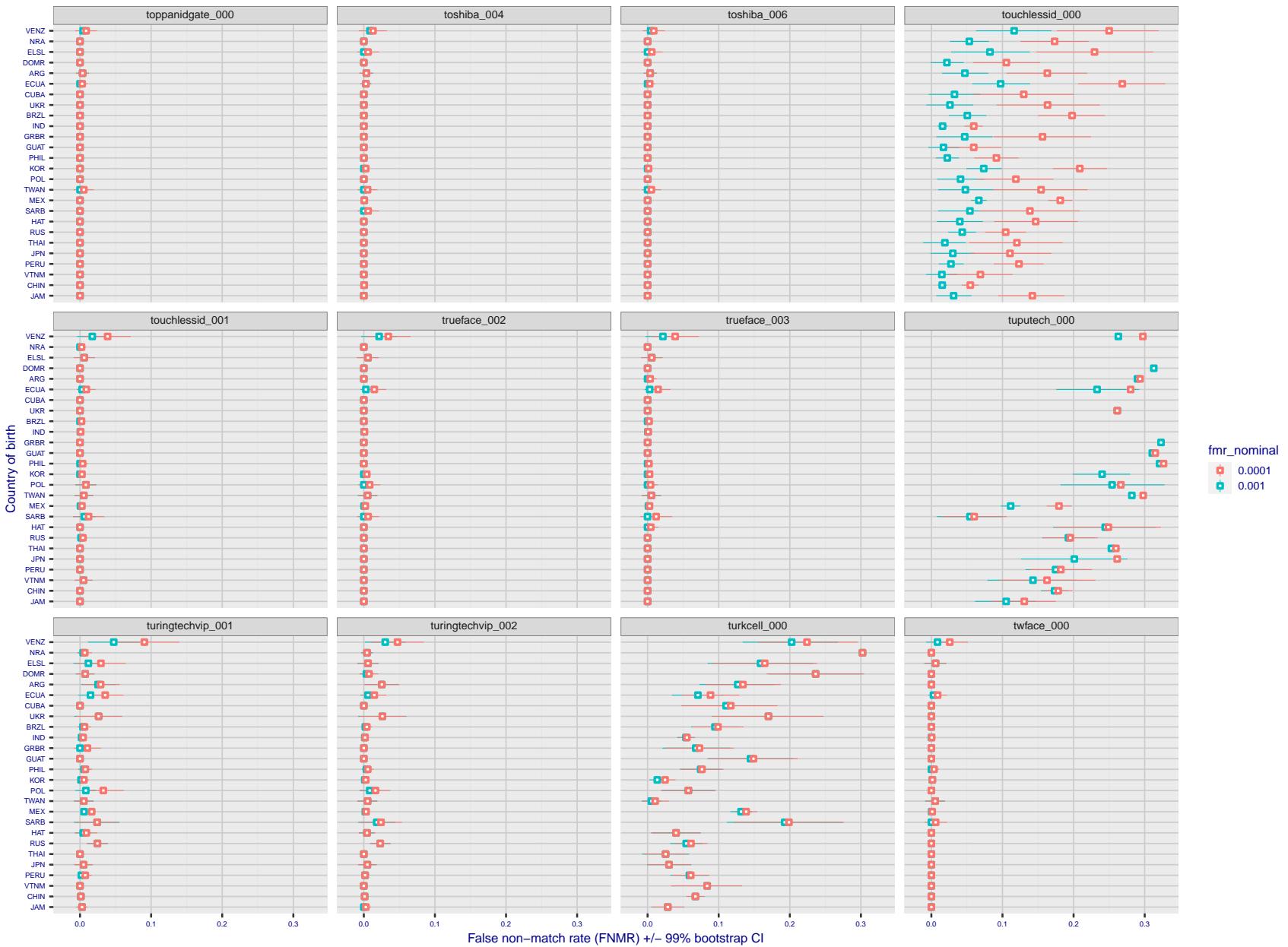


Figure 324: For the visa images, the dots show FNMR by country of birth for two globally set operating thresholds corresponding to $FMR = \{0.001, 0.0001\}$ computed over all on the order of 10^{10} impostor scores. The FMR in each bin will vary also - see subsequent impostor heatmaps in sec. 3.6.1. The figures shows an order of magnitude variation in FNMR across country of birth; these effects are likely due quality variations, then demographics like age and race. The error rates in some cases are zero, and in others the DET is flat so the error rates at the two thresholds are identical. The lines span 1% and 99% of bootstrap replicated FNMR estimates.

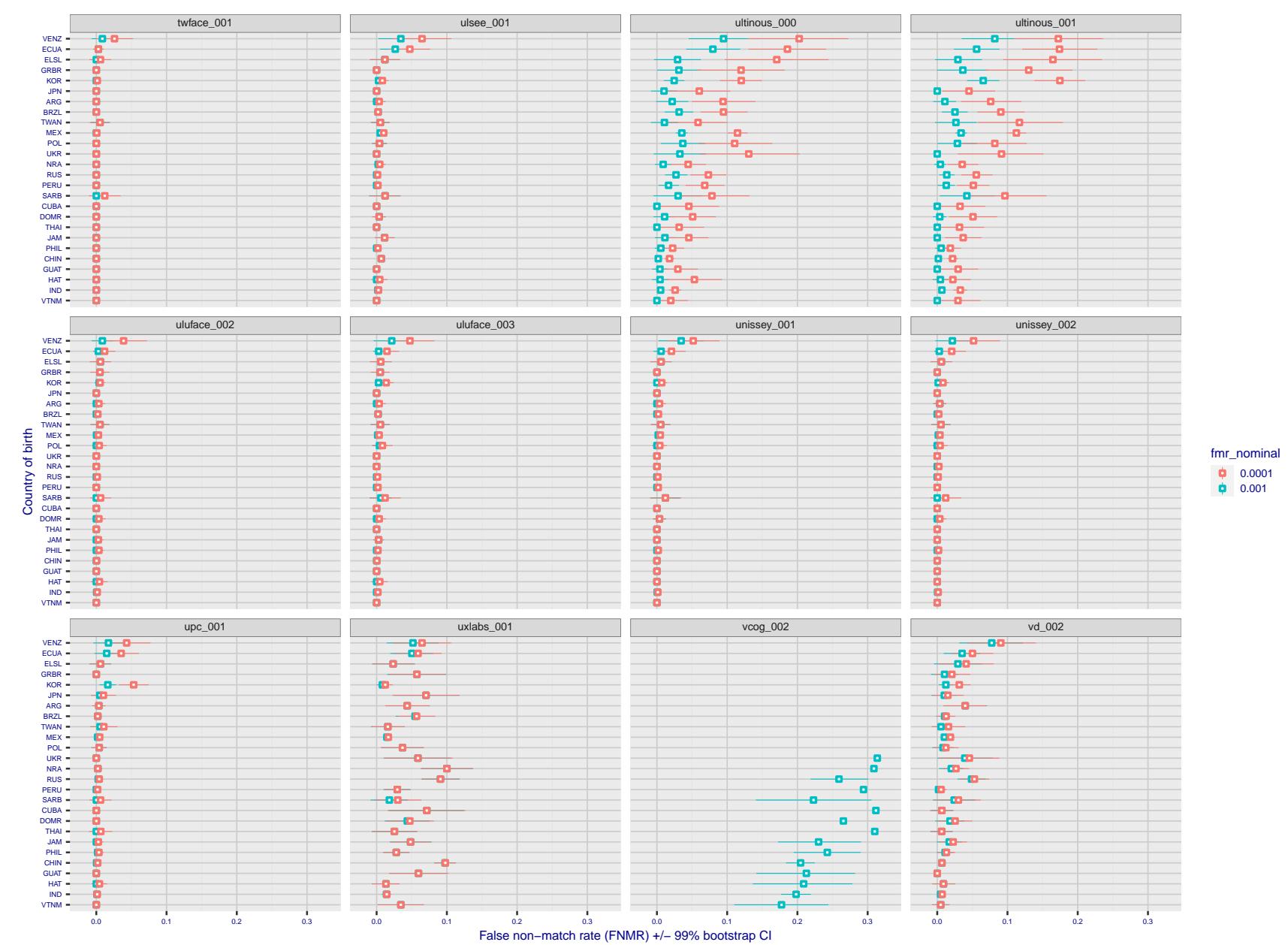


Figure 325: For the visa images, the dots show FNMR by country of birth for two globally set operating thresholds corresponding to $FMR = \{0.001, 0.0001\}$ computed over all on the order of 10^{10} impostor scores. The FMR in each bin will vary also - see subsequent impostor heatmaps in sec. 3.6.1. The figures shows an order of magnitude variation in FNMR across country of birth; these effects are likely due quality variations, then demographics like age and race. The error rates in some cases are zero, and in others the DET is flat so the error rates at the two thresholds are identical. The lines span 1% and 99% of bootstrap replicated FNMR estimates.

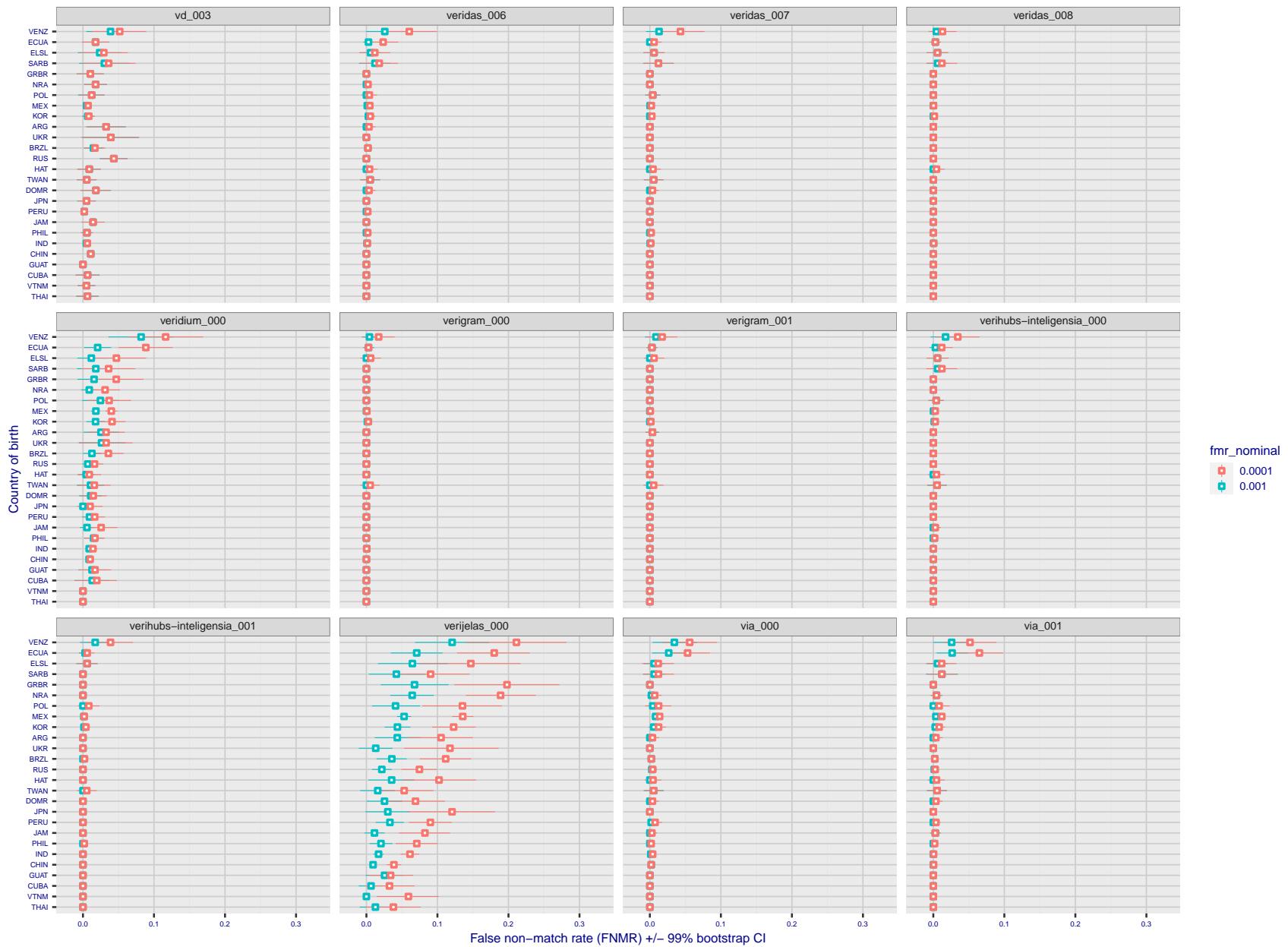


Figure 326: For the visa images, the dots show FNMR by country of birth for two globally set operating thresholds corresponding to $FMR = \{0.001, 0.0001\}$ computed over all on the order of 10^{10} impostor scores. The FMR in each bin will vary also - see subsequent impostor heatmaps in sec. 3.6.1. The figures shows an order of magnitude variation in FNMR across country of birth; these effects are likely due quality variations, then demographics like age and race. The error rates in some cases are zero, and in others the DET is flat so the error rates at the two thresholds are identical. The lines span 1% and 99% of bootstrap replicated FNMR estimates.

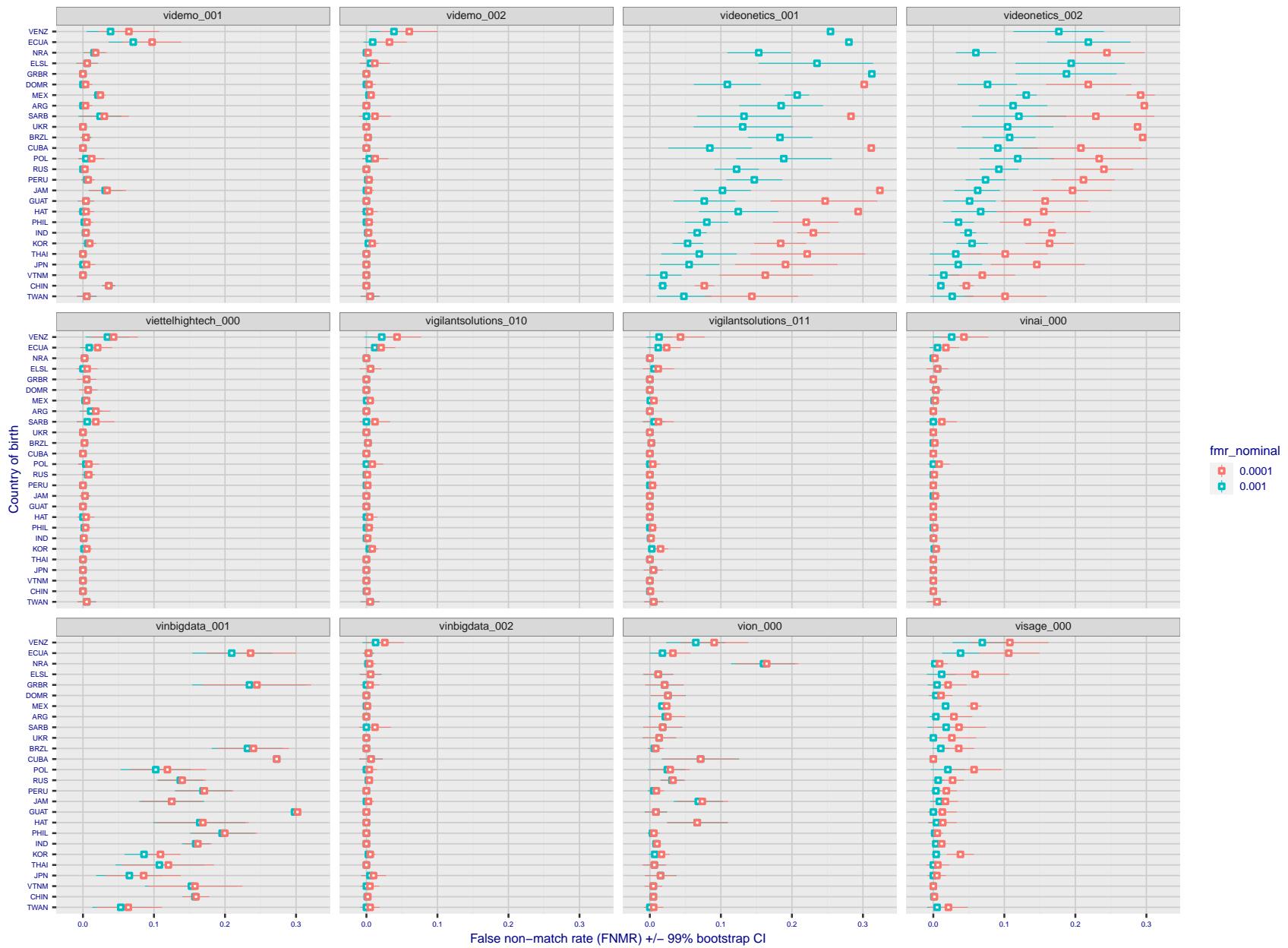


Figure 327: For the visa images, the dots show FNMR by country of birth for two globally set operating thresholds corresponding to $FMR = \{0.001, 0.0001\}$ computed over all on the order of 10^{10} impostor scores. The FMR in each bin will vary also - see subsequent impostor heatmaps in sec. 3.6.1. The figures shows an order of magnitude variation in FNMR across country of birth; these effects are likely due quality variations, then demographics like age and race. The error rates in some cases are zero, and in others the DET is flat so the error rates at the two thresholds are identical. The lines span 1% and 99% of bootstrap replicated FNMR estimates.

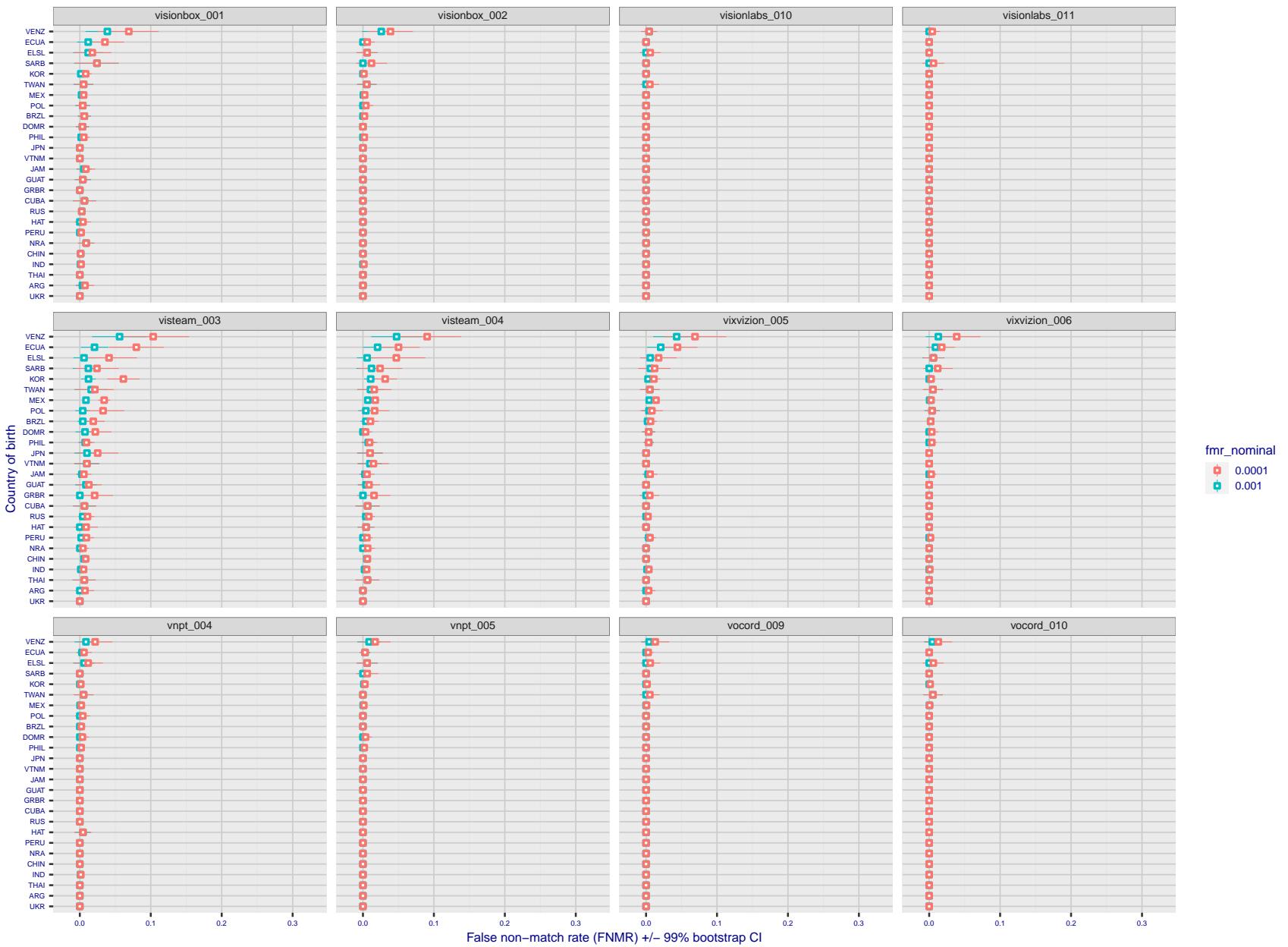


Figure 328: For the visa images, the dots show FNMR by country of birth for two globally set operating thresholds corresponding to $FMR = \{0.001, 0.0001\}$ computed over all on the order of 10^{10} impostor scores. The FMR in each bin will vary also - see subsequent impostor heatmaps in sec. 3.6.1. The figures shows an order of magnitude variation in FNMR across country of birth; these effects are likely due quality variations, then demographics like age and race. The error rates in some cases are zero, and in others the DET is flat so the error rates at the two thresholds are identical. The lines span 1% and 99% of bootstrap replicated FNMR estimates.

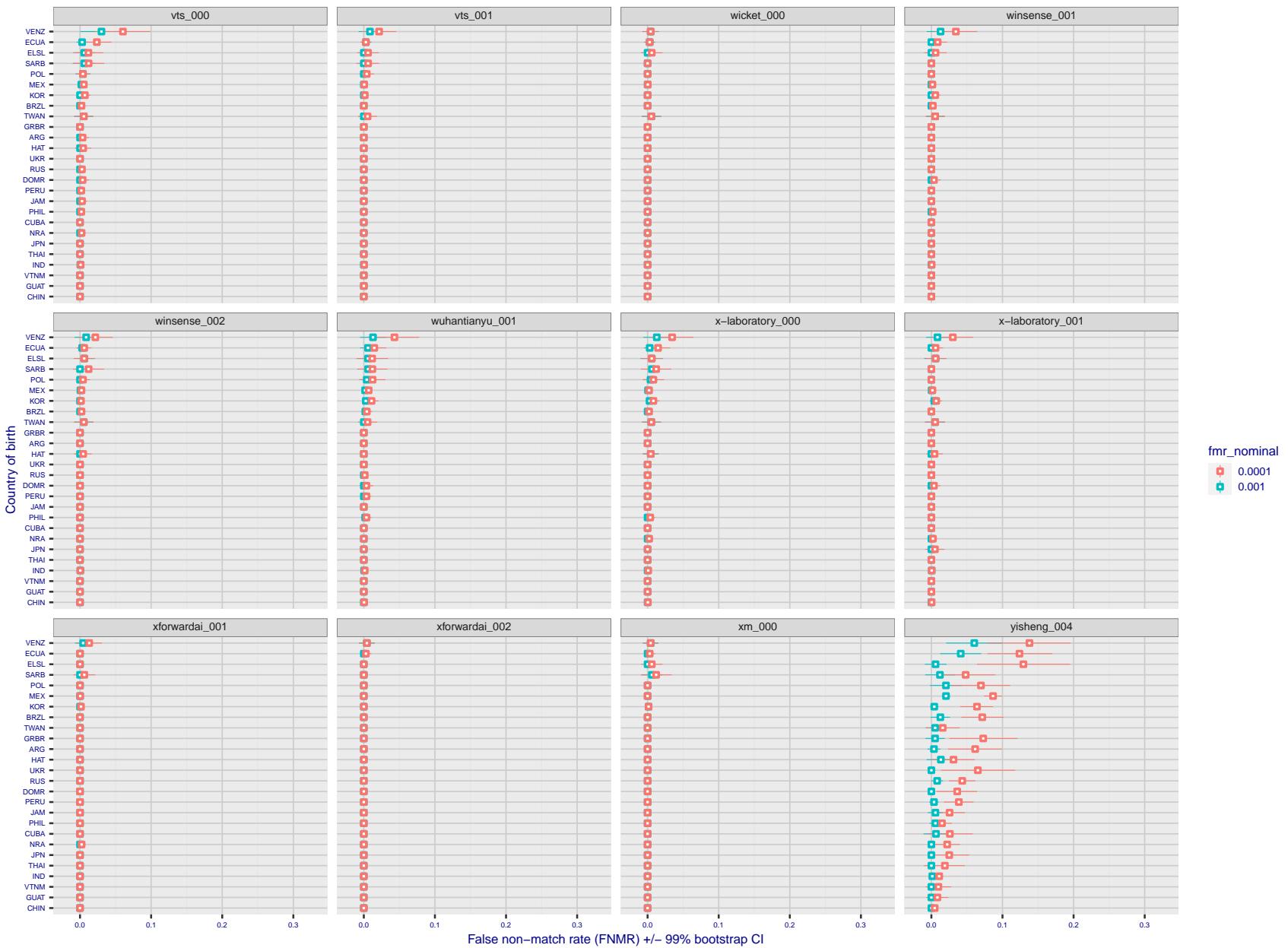


Figure 329: For the visa images, the dots show FNMR by country of birth for two globally set operating thresholds corresponding to $FMR = \{0.001, 0.0001\}$ computed over all on the order of 10^{10} impostor scores. The FMR in each bin will vary also - see subsequent impostor heatmaps in sec. 3.6.1. The figures shows an order of magnitude variation in FNMR across country of birth; these effects are likely due quality variations, then demographics like age and race. The error rates in some cases are zero, and in others the DET is flat so the error rates at the two thresholds are identical. The lines span 1% and 99% of bootstrap replicated FNMR estimates.

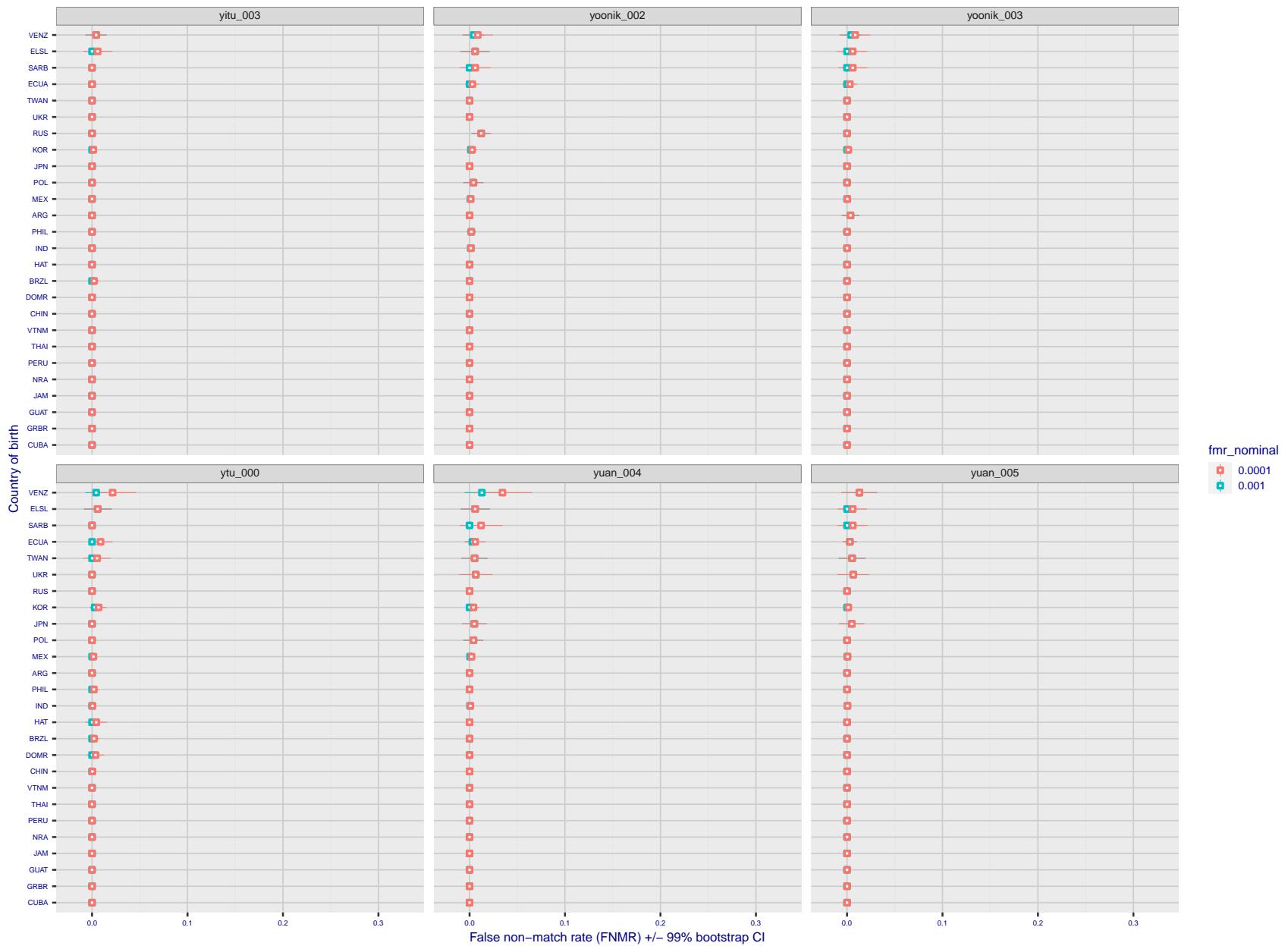


Figure 330: For the visa images, the dots show FNMR by country of birth for two globally set operating thresholds corresponding to $FMR = \{0.001, 0.0001\}$ computed over all on the order of 10^{10} impostor scores. The FMR in each bin will vary also - see subsequent impostor heatmaps in sec. 3.6.1. The figures shows an order of magnitude variation in FNMR across country of birth; these effects are likely due quality variations, then demographics like age and race. The error rates in some cases are zero, and in others the DET is flat so the error rates at the two thresholds are identical. The lines span 1% and 99% of bootstrap replicated FNMR estimates.

Caveats: The results may not relate to subject-specific properties. Instead they could reflect image-specific quality differences, which could occur due to collection protocol or software processing variations.

3.5.2 Effect of ageing

Background: Faces change appearance throughout life. This change gradually reduces similarity of a new image to an earlier image. Face recognition algorithms give reduced similarity scores and more frequent false rejections.

Goal: To quantify false non-match rates (FNMR) as a function of elapsed time in an adult population.

Methods: Using the mugshot images, a threshold is set to give FMR = 0.00001 over the entire impostor set. Then FNMR is measured over 1000 bootstrap replications of the genuine scores.

Results: For the visa images, Figure 359 shows how false non-match rates for genuine users, as a function of age group.

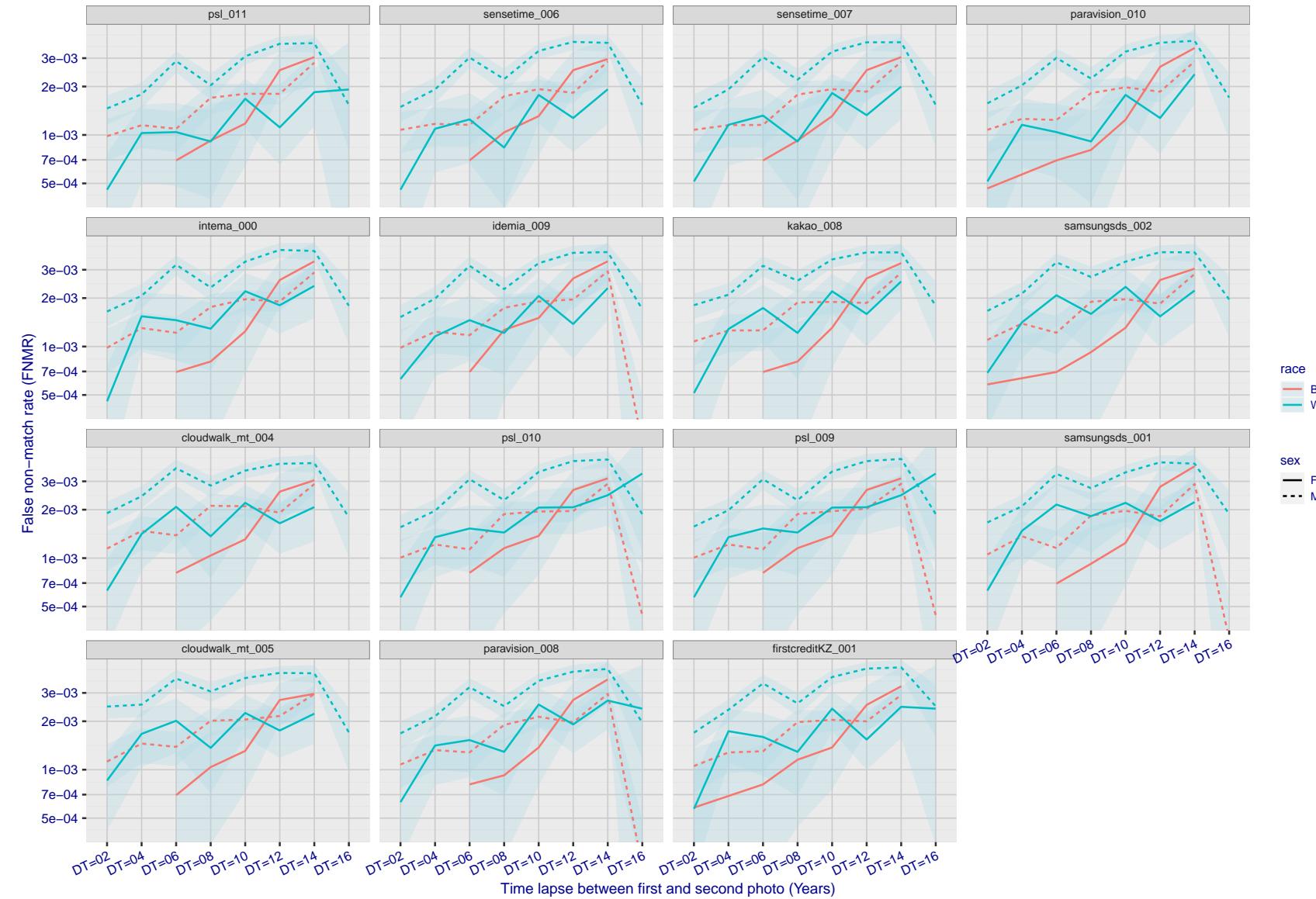


Figure 331: For the mugshot images, FNMR as a function of elapsed time between initial enrollment and second verification images. The panels appear most accurate first, and vertical scale changes on each page. The four traces correspond to images annotated with codes for black female, black male, white female, white male. The threshold is fixed for each algorithm to give $FMR = 0.00001$ over all (10^8) impostor comparisons. For short time-lapses, the most accurate algorithms give very few errors ($FNMR < 0.001$) so that the uncertainty estimates are high.

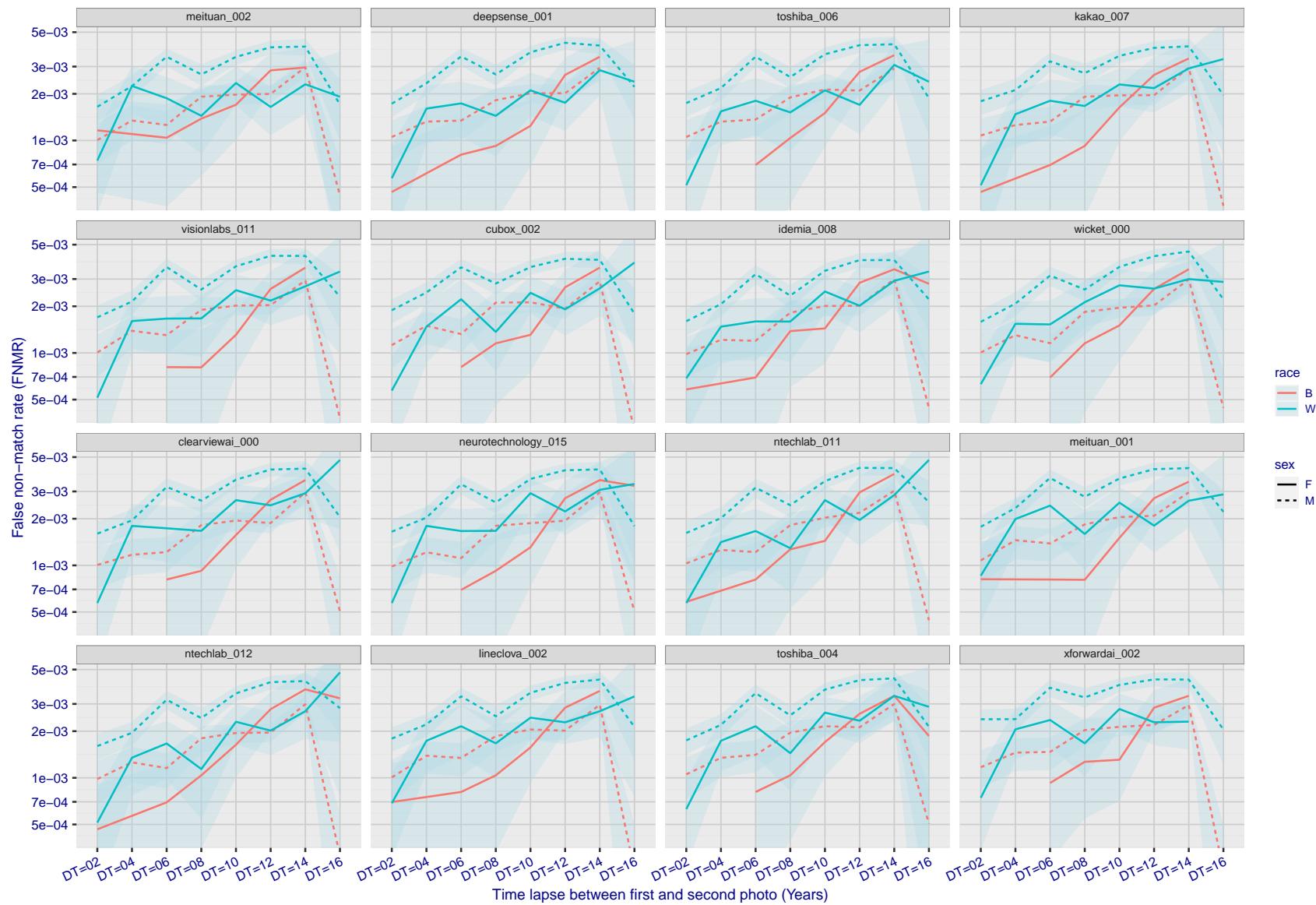


Figure 332: For the mugshot images, FNMR as a function of elapsed time between initial enrollment and second verification images. The panels appear most accurate first, and vertical scale changes on each page. The four traces correspond to images annotated with codes for black female, black male, white female, white male. The threshold is fixed for each algorithm to give FMR = 0.00001 over all (10^8) impostor comparisons. For short time-lapses, the most accurate algorithms give very few errors (FNMR < 0.001) so that the uncertainty estimates are high.

2023/02/09 20:10:38

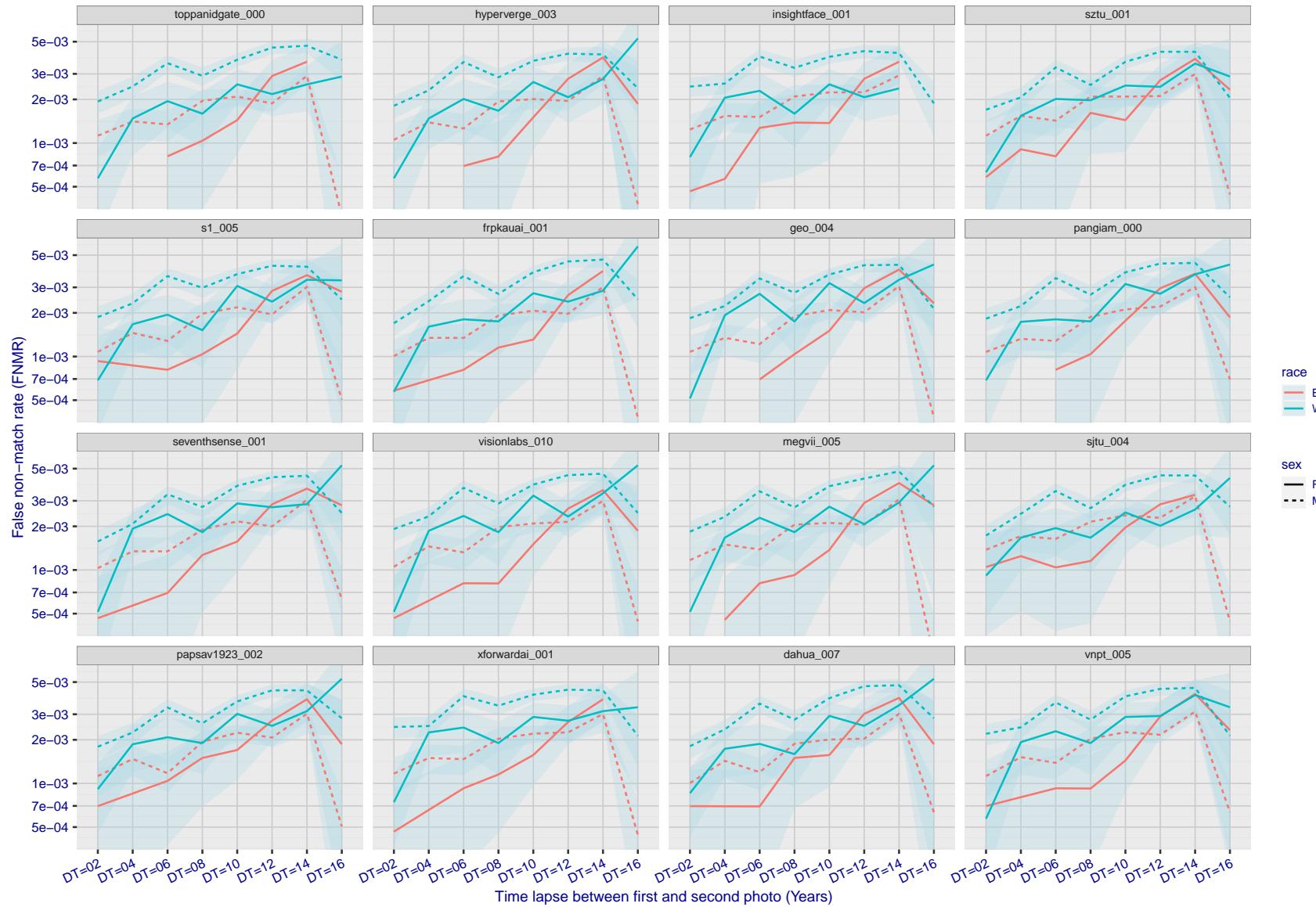


Figure 333: For the mugshot images, FNMR as a function of elapsed time between initial enrollment and second verification images. The panels appear most accurate first, and vertical scale changes on each page. The four traces correspond to images annotated with codes for black female, black male, white female, white male. The threshold is fixed for each algorithm to give $FMR = 0.00001$ over all (10^8) impostor comparisons. For short time-lapses, the most accurate algorithms give very few errors ($FNMR < 0.001$) so that the uncertainty estimates are high.

2023/02/09 20:10:38

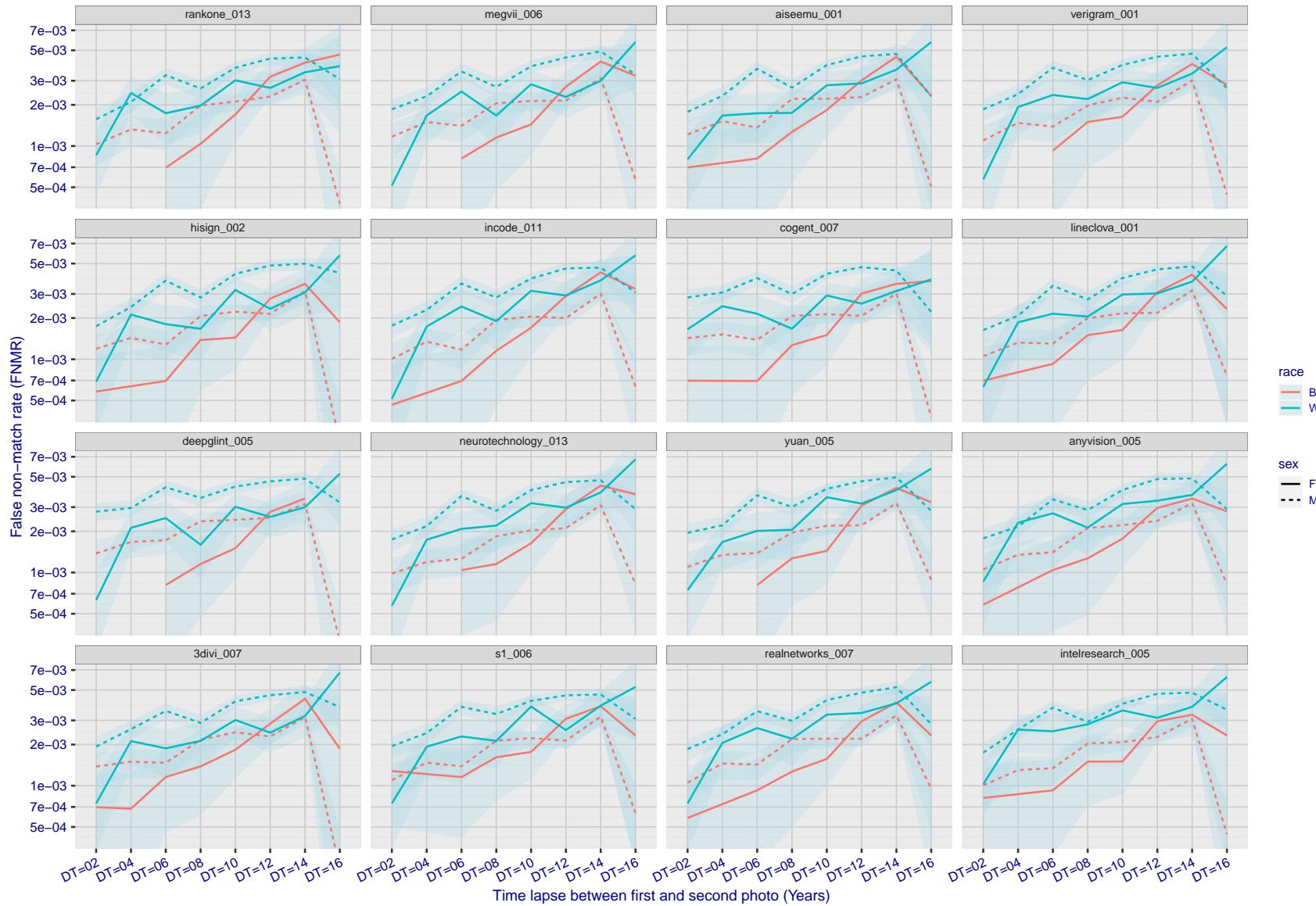


Figure 334: For the mugshot images, FNMR as a function of elapsed time between initial enrollment and second verification images. The panels appear most accurate first, and vertical scale changes on each page. The four traces correspond to images annotated with codes for black female, black male, white female, white male. The threshold is fixed for each algorithm to give FMR = 0.00001 over all (10^8) impostor comparisons. For short time-lapses, the most accurate algorithms give very few errors (FNMR < 0.001) so that the uncertainty estimates are high.

2023/02/09 20:10:38

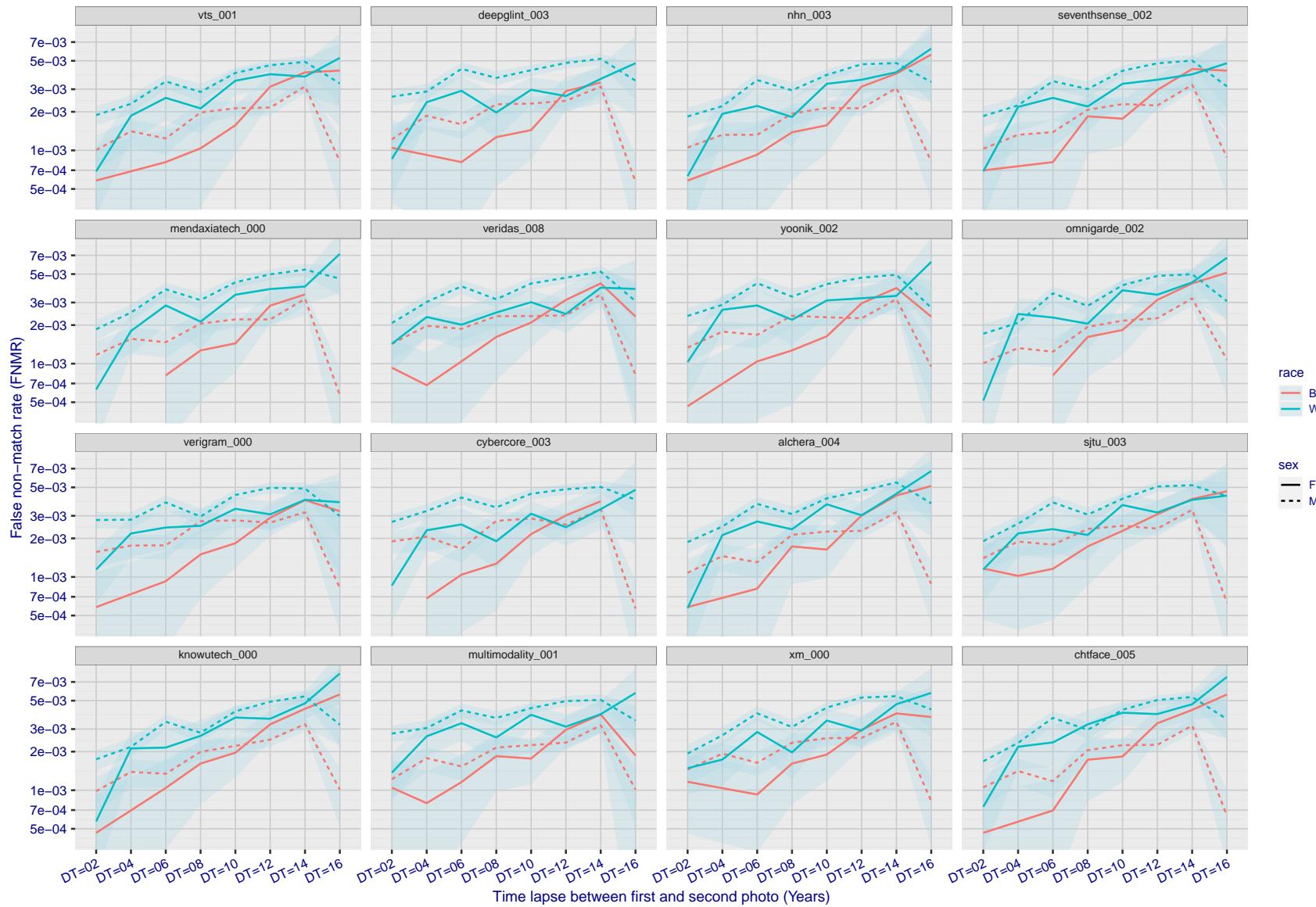


Figure 335: For the mugshot images, FNMR as a function of elapsed time between initial enrollment and second verification images. The panels appear most accurate first, and vertical scale changes on each page. The four traces correspond to images annotated with codes for black female, black male, white female, white male. The threshold is fixed for each algorithm to give FMR = 0.00001 over all (10^8) impostor comparisons. For short time-lapses, the most accurate algorithms give very few errors (FNMR < 0.001) so that the uncertainty estimates are high.

FNMR(T)
FMR(T)
"False non-match rate"
"False match rate"

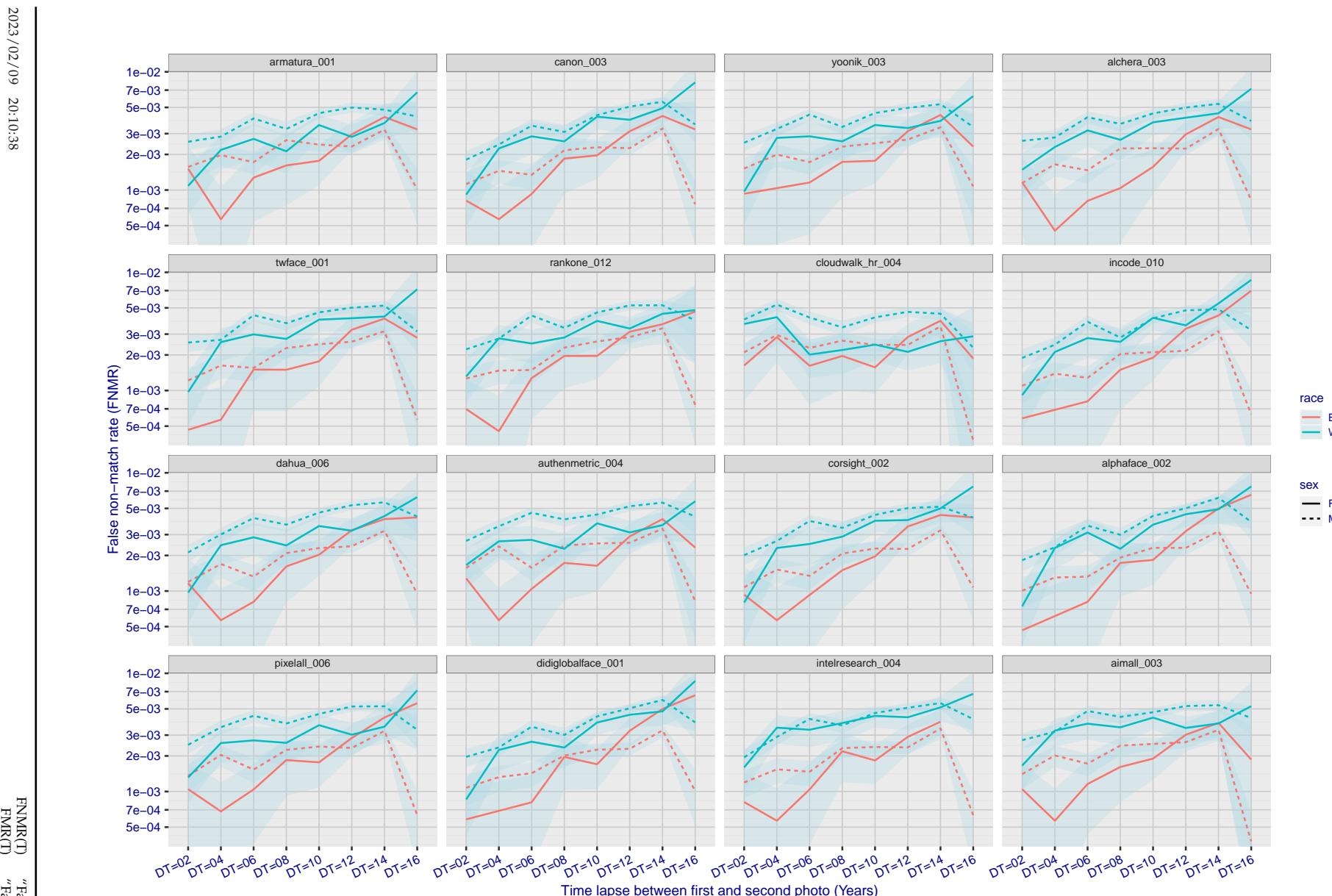


Figure 336: For the mugshot images, FNMR as a function of elapsed time between initial enrollment and second verification images. The panels appear most accurate first, and vertical scale changes on each page. The four traces correspond to images annotated with codes for black female, black male, white female, white male. The threshold is fixed for each algorithm to give $FMR = 0.00001$ over all (10^8) impostor comparisons. For short time-lapses, the most accurate algorithms give very few errors ($FNMR < 0.001$) so that the uncertainty estimates are high.

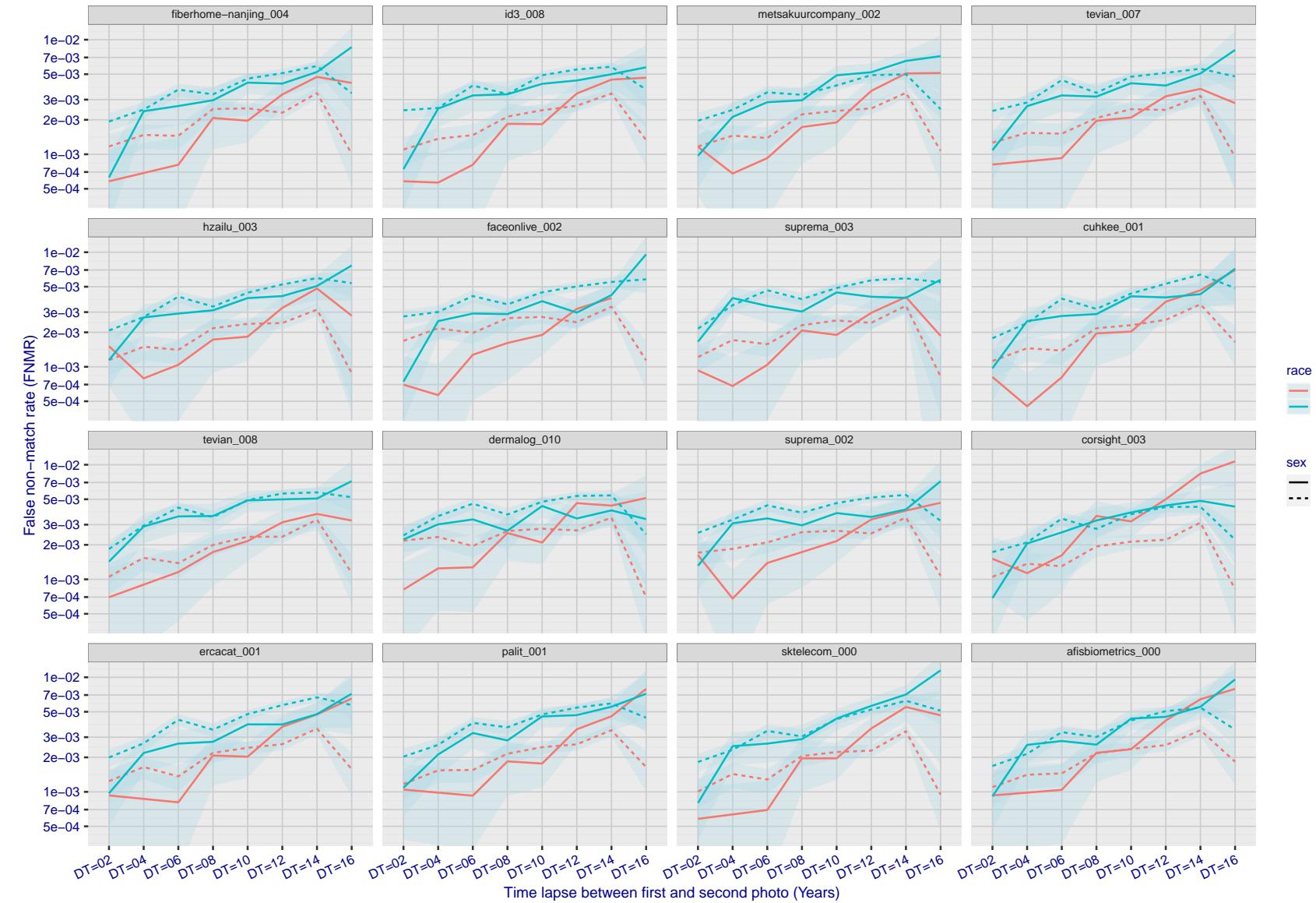


Figure 337: For the mugshot images, FNMR as a function of elapsed time between initial enrollment and second verification images. The panels appear most accurate first, and vertical scale changes on each page. The four traces correspond to images annotated with codes for black female, black male, white female, white male. The threshold is fixed for each algorithm to give $FMR = 0.00001$ over all (10^8) impostor comparisons. For short time-lapses, the most accurate algorithms give very few errors ($FNMR < 0.001$) so that the uncertainty estimates are high.

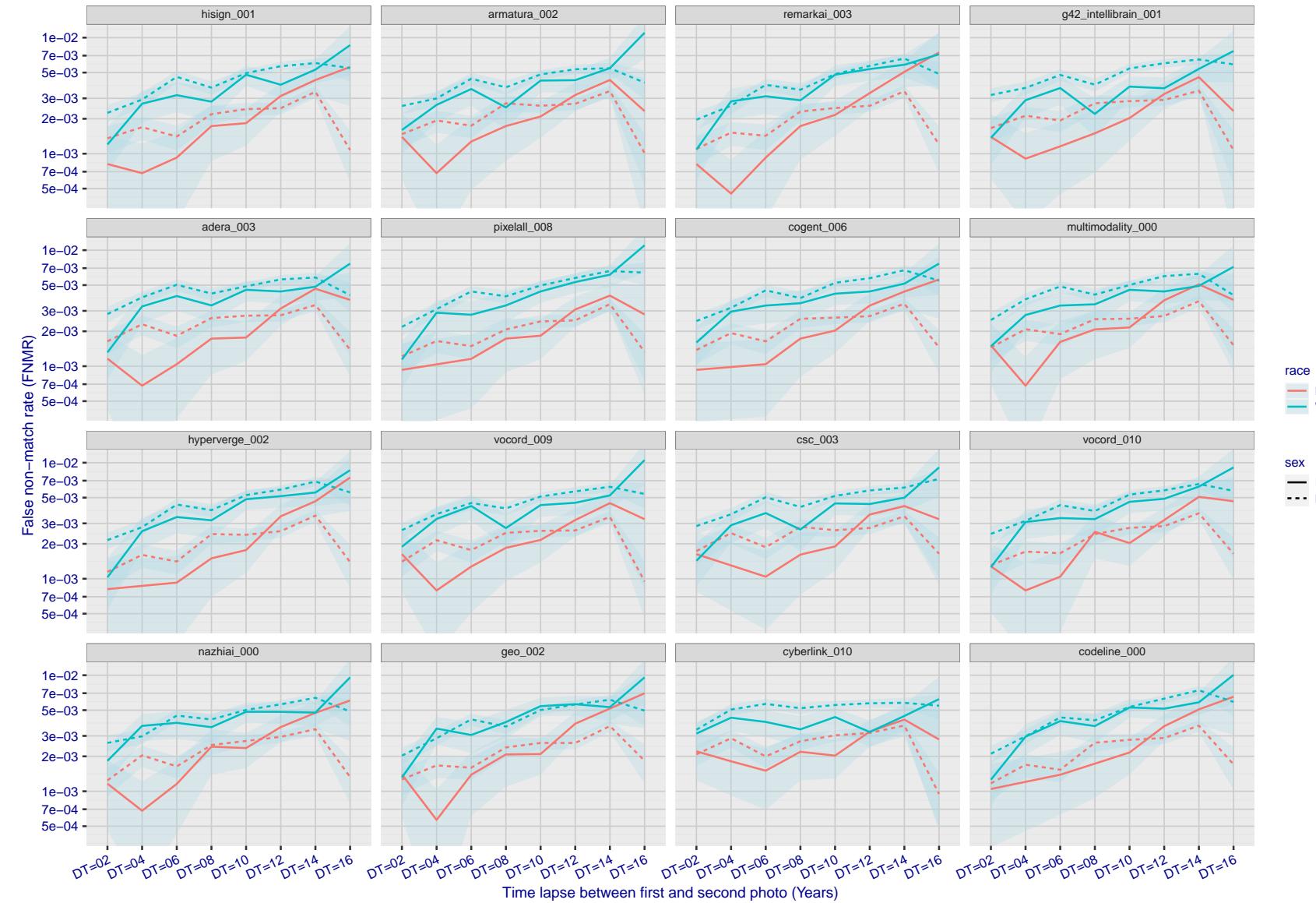


Figure 338: For the mugshot images, FNMR as a function of elapsed time between initial enrollment and second verification images. The panels appear most accurate first, and vertical scale changes on each page. The four traces correspond to images annotated with codes for black female, black male, white female, white male. The threshold is fixed for each algorithm to give FMR = 0.00001 over all (10^8) impostor comparisons. For short time-lapses, the most accurate algorithms give very few errors (FNMR < 0.001) so that the uncertainty estimates are high.

2023/02/09 20:10:38

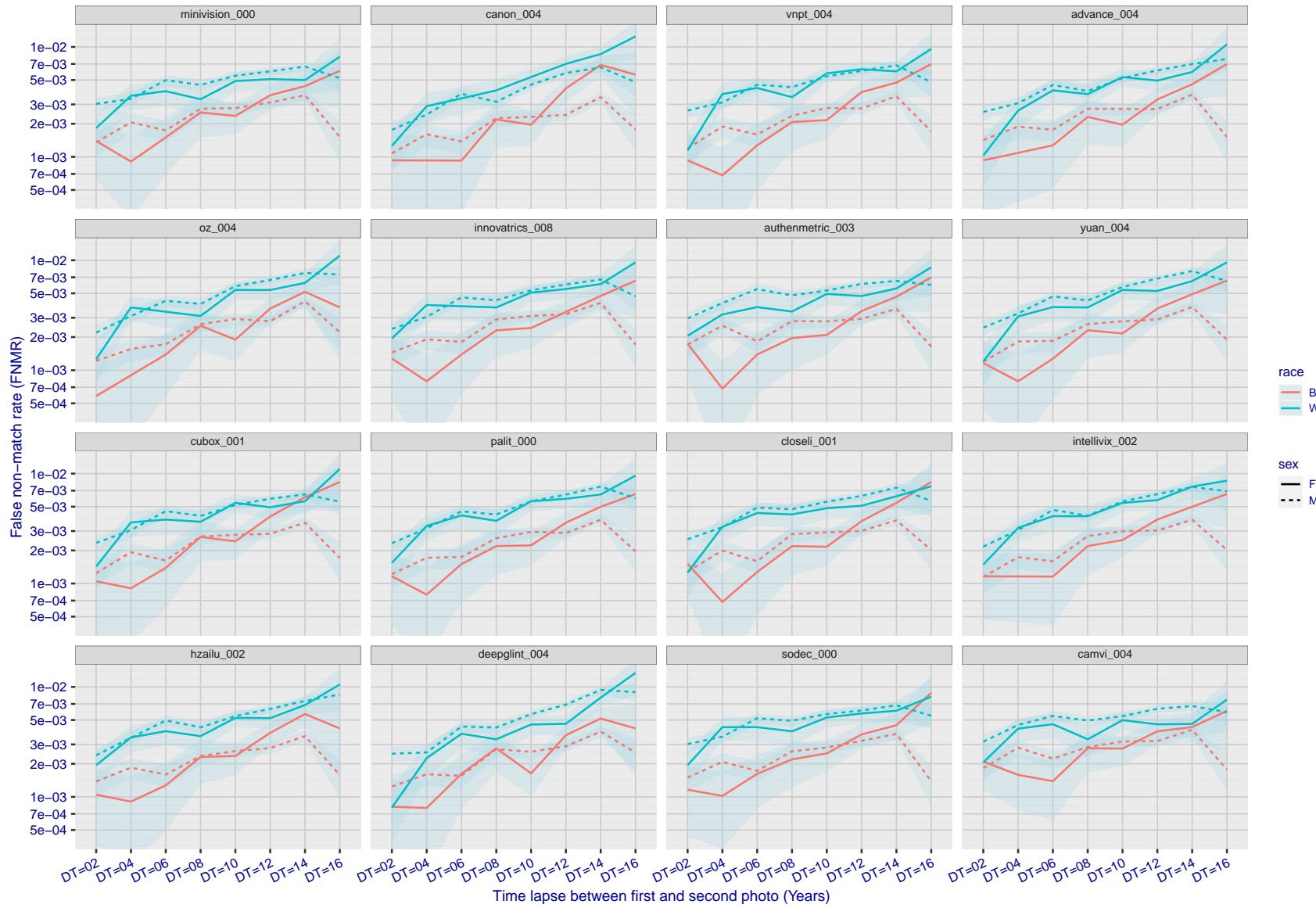


Figure 339: For the mugshot images, FNMR as a function of elapsed time between initial enrollment and second verification images. The panels appear most accurate first, and vertical scale changes on each page. The four traces correspond to images annotated with codes for black female, black male, white female, white male. The threshold is fixed for each algorithm to give FMR = 0.00001 over all (10^8) impostor comparisons. For short time-lapses, the most accurate algorithms give very few errors (FNMR < 0.001) so that the uncertainty estimates are high.

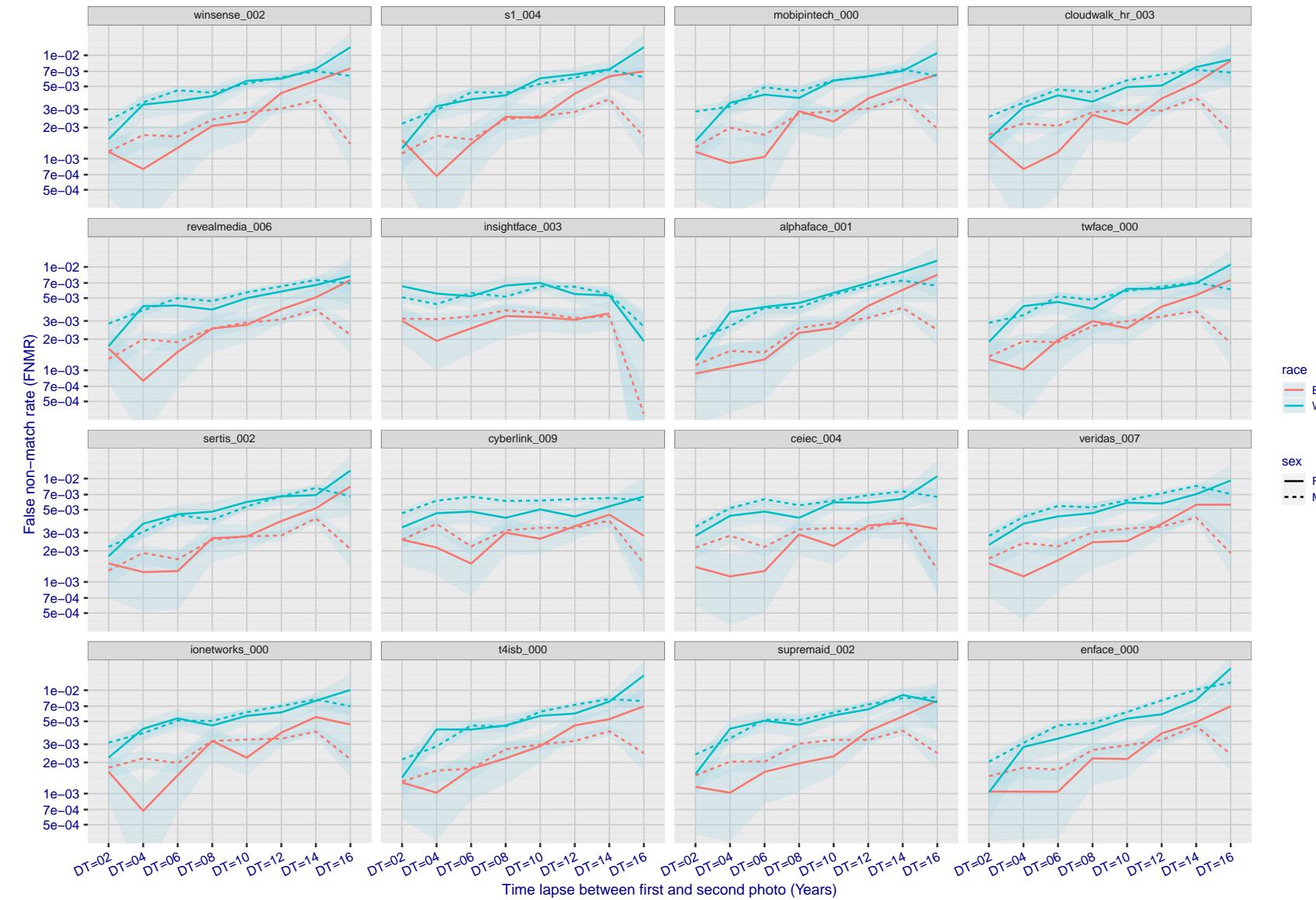


Figure 340: For the mugshot images, FNMR as a function of elapsed time between initial enrollment and second verification images. The panels appear most accurate first, and vertical scale changes on each page. The four traces correspond to images annotated with codes for black female, black male, white female, white male. The threshold is fixed for each algorithm to give FMR = 0.00001 over all (10^8) impostor comparisons. For short time-lapses, the most accurate algorithms give very few errors (FNMR < 0.001) so that the uncertainty estimates are high.

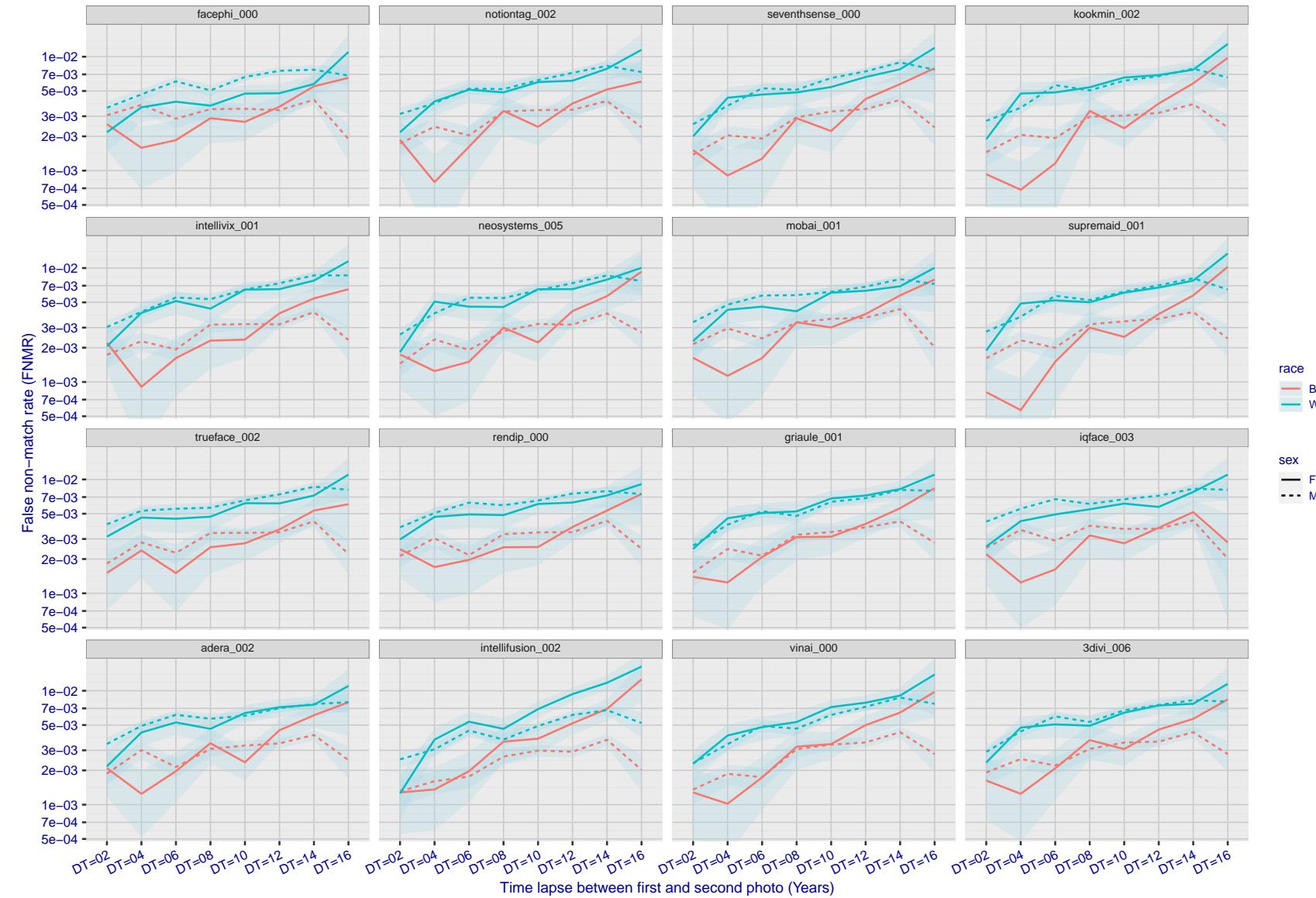


Figure 341: For the mugshot images, FNMR as a function of elapsed time between initial enrollment and second verification images. The panels appear most accurate first, and vertical scale changes on each page. The four traces correspond to images annotated with codes for black female, black male, white female, white male. The threshold is fixed for each algorithm to give $FMR = 0.00001$ over all (10^8) impostor comparisons. For short time-lapses, the most accurate algorithms give very few errors ($FNMR < 0.001$) so that the uncertainty estimates are high.

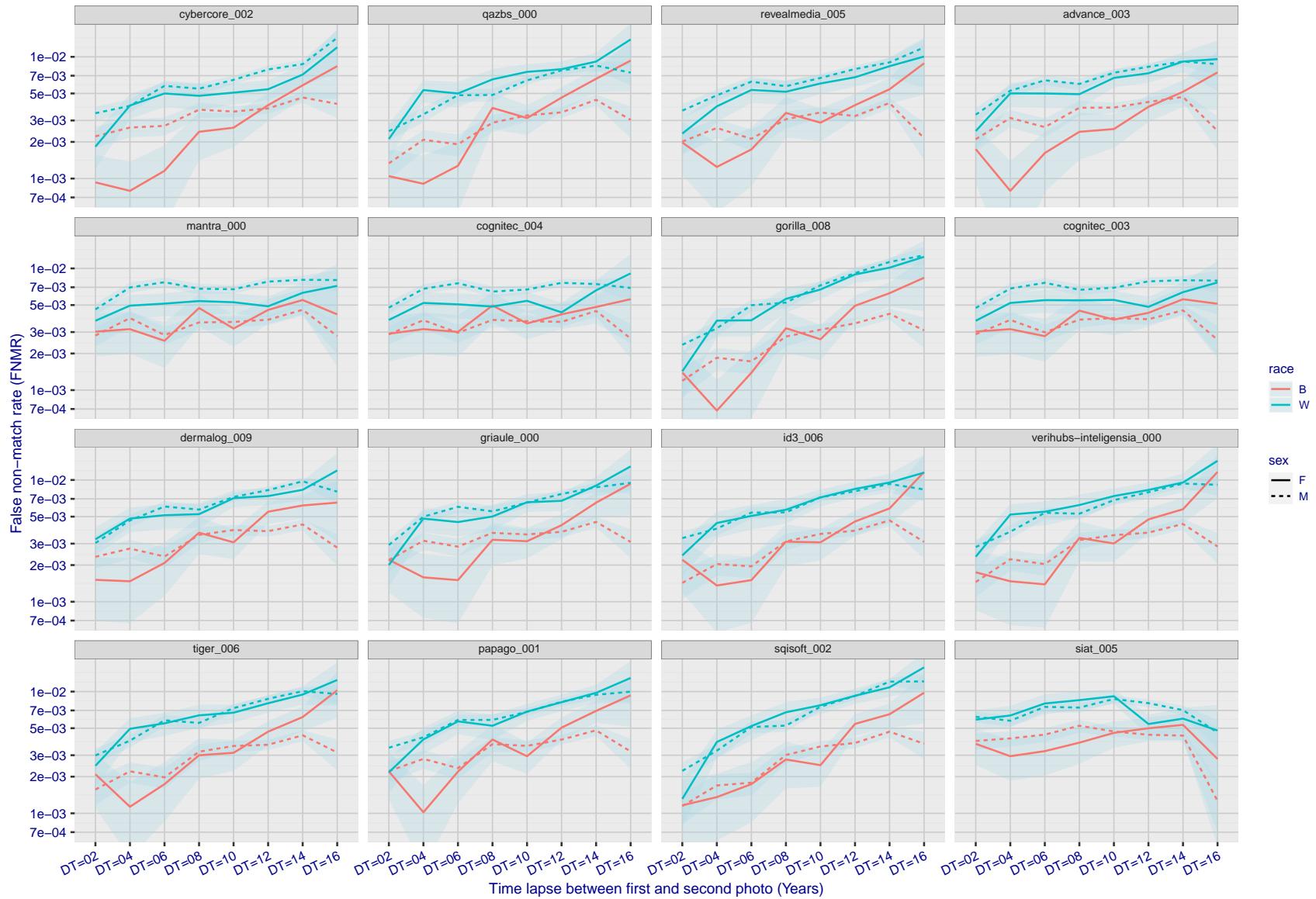


Figure 342: For the mugshot images, FNMR as a function of elapsed time between initial enrollment and second verification images. The panels appear most accurate first, and vertical scale changes on each page. The four traces correspond to images annotated with codes for black female, black male, white female, white male. The threshold is fixed for each algorithm to give $FMR = 0.00001$ over all (10^8) impostor comparisons. For short time-lapses, the most accurate algorithms give very few errors ($FNMR < 0.001$) so that the uncertainty estimates are high.

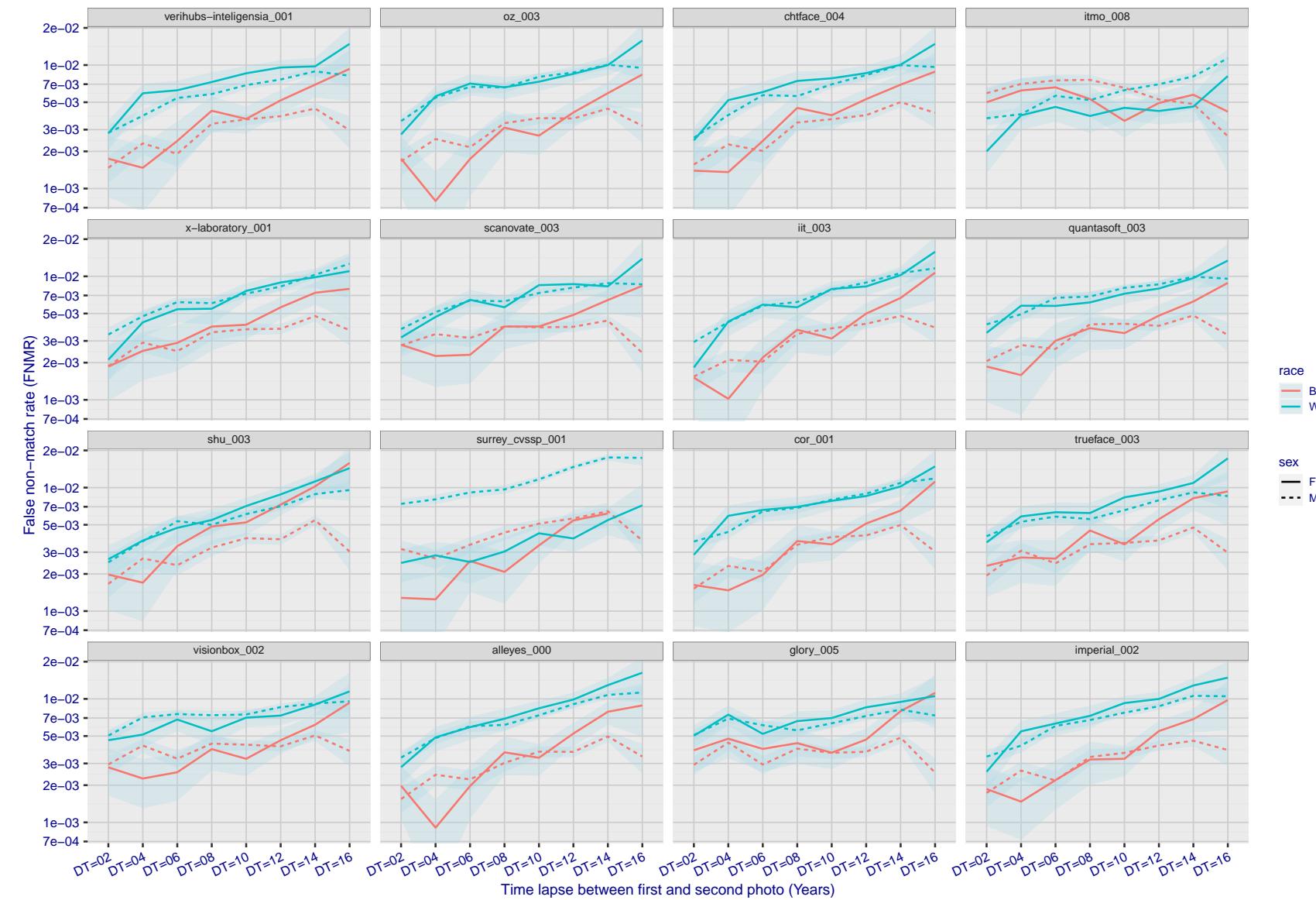


Figure 343: For the mugshot images, FNMR as a function of elapsed time between initial enrollment and second verification images. The panels appear most accurate first, and vertical scale changes on each page. The four traces correspond to images annotated with codes for black female, black male, white female, white male. The threshold is fixed for each algorithm to give $FMR = 0.00001$ over all (10^8) impostor comparisons. For short time-lapses, the most accurate algorithms give very few errors ($FNMR < 0.001$) so that the uncertainty estimates are high.

2023/02/09 20:10:38

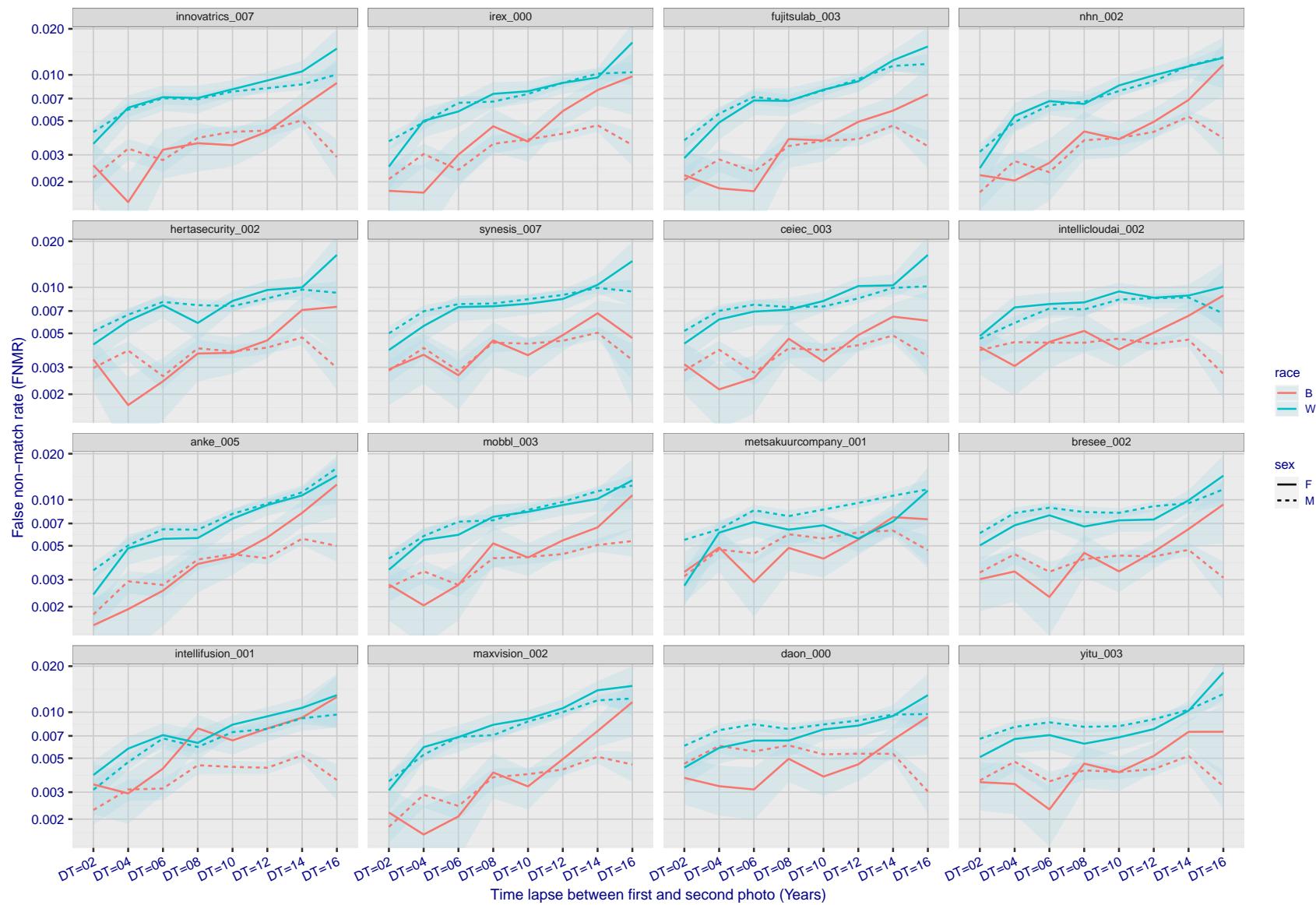
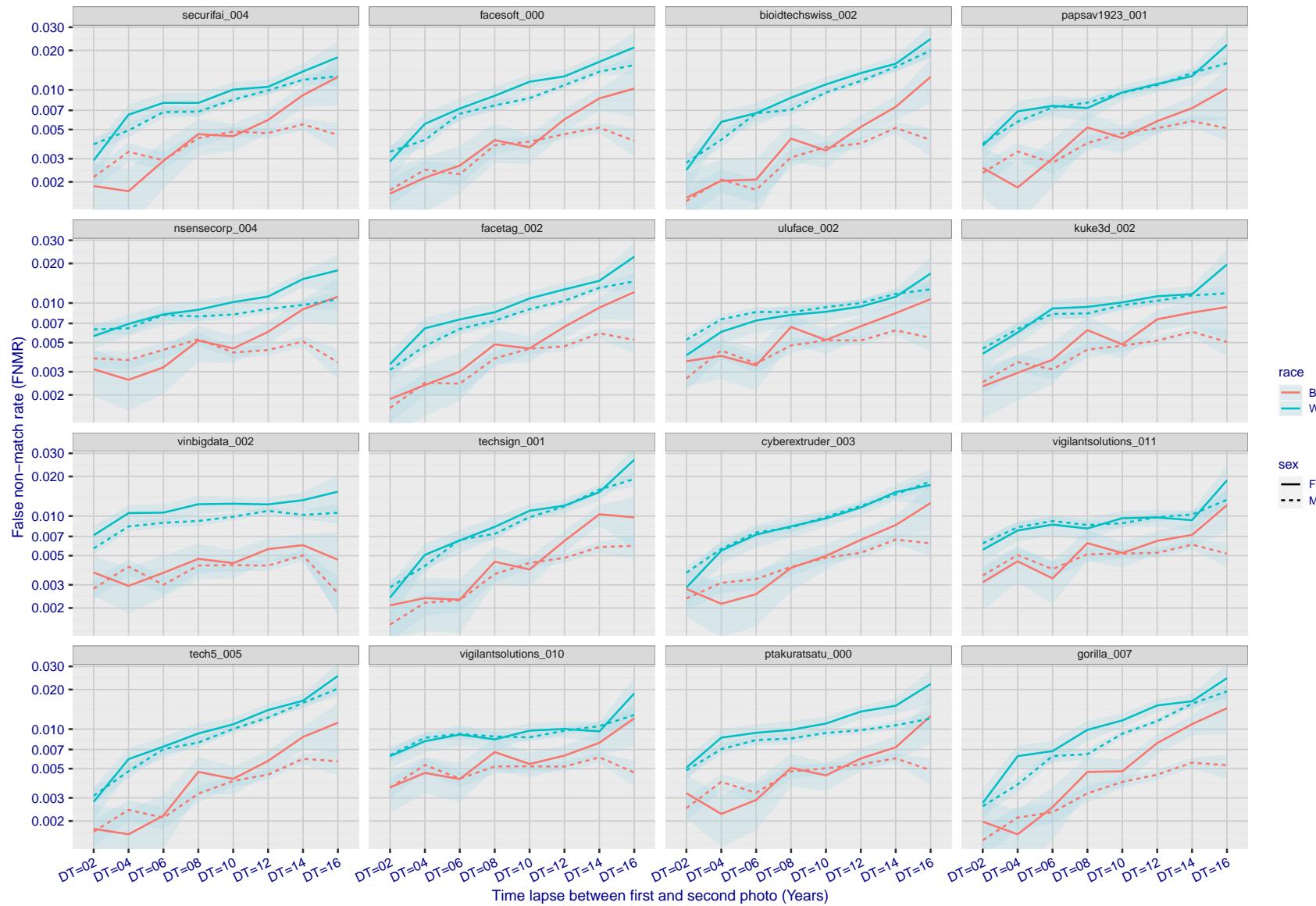


Figure 344: For the mugshot images, FNMR as a function of elapsed time between initial enrollment and second verification images. The panels appear most accurate first, and vertical scale changes on each page. The four traces correspond to images annotated with codes for black female, black male, white female, white male. The threshold is fixed for each algorithm to give FMR = 0.00001 over all (10^8) impostor comparisons. For short time-lapses, the most accurate algorithms give very few errors (FNMR < 0.001) so that the uncertainty estimates are high.

2023/02/09 20:10:38



FNMR(T)
FMR(T)
"False non-match rate"
"False match rate"

Figure 345: For the mugshot images, FNMR as a function of elapsed time between initial enrollment and second verification images. The panels appear most accurate first, and vertical scale changes on each page. The four traces correspond to images annotated with codes for black female, black male, white female, white male. The threshold is fixed for each algorithm to give FMR = 0.00001 over all (10^8) impostor comparisons. For short time-lapses, the most accurate algorithms give very few errors (FNMR < 0.001) so that the uncertainty estimates are high.

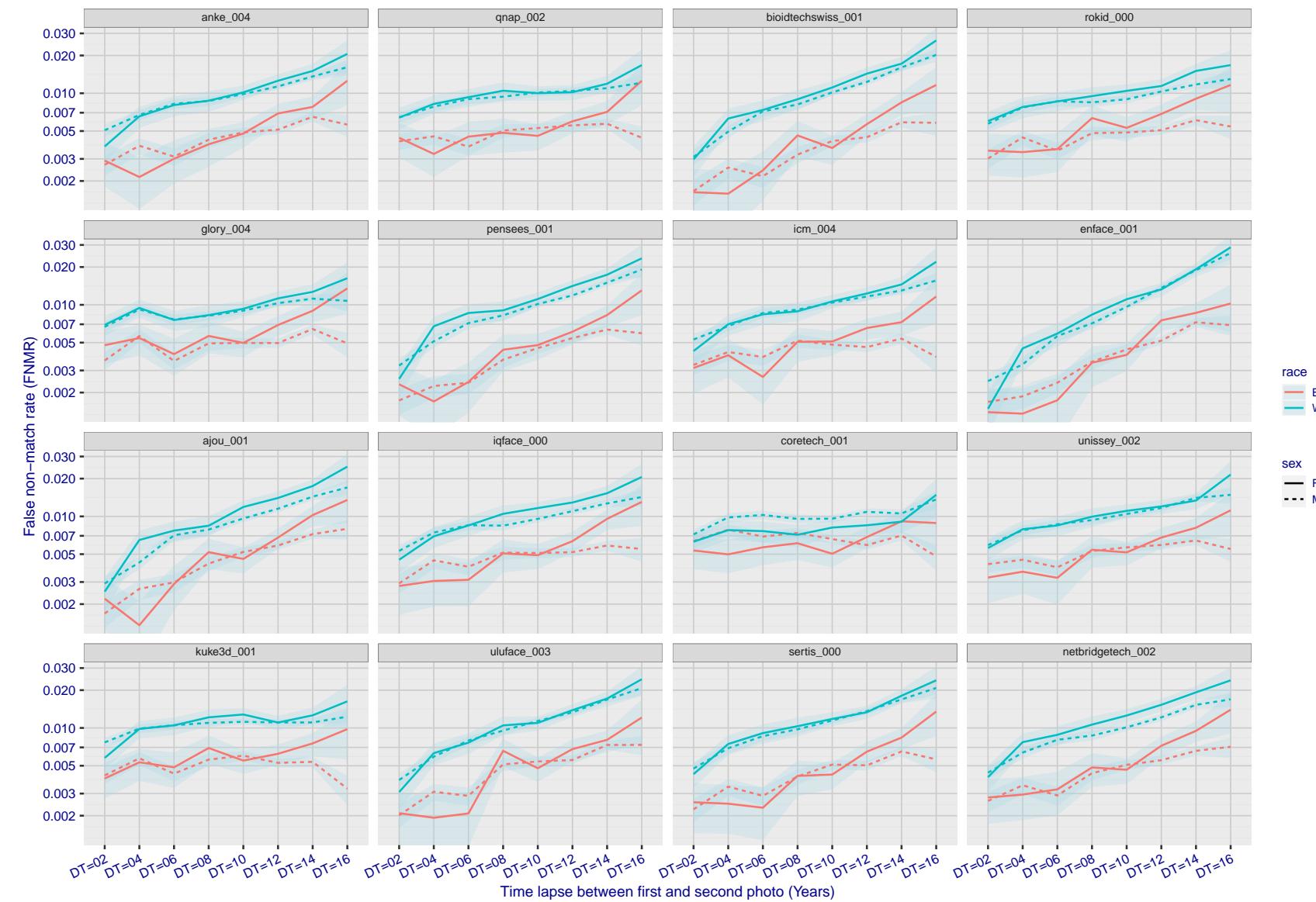


Figure 346: For the mugshot images, FNMR as a function of elapsed time between initial enrollment and second verification images. The panels appear most accurate first, and vertical scale changes on each page. The four traces correspond to images annotated with codes for black female, black male, white female, white male. The threshold is fixed for each algorithm to give FMR = 0.00001 over all (10^8) impostor comparisons. For short time-lapses, the most accurate algorithms give very few errors (FNMR < 0.001) so that the uncertainty estimates are high.

2023/02/09 20:10:38

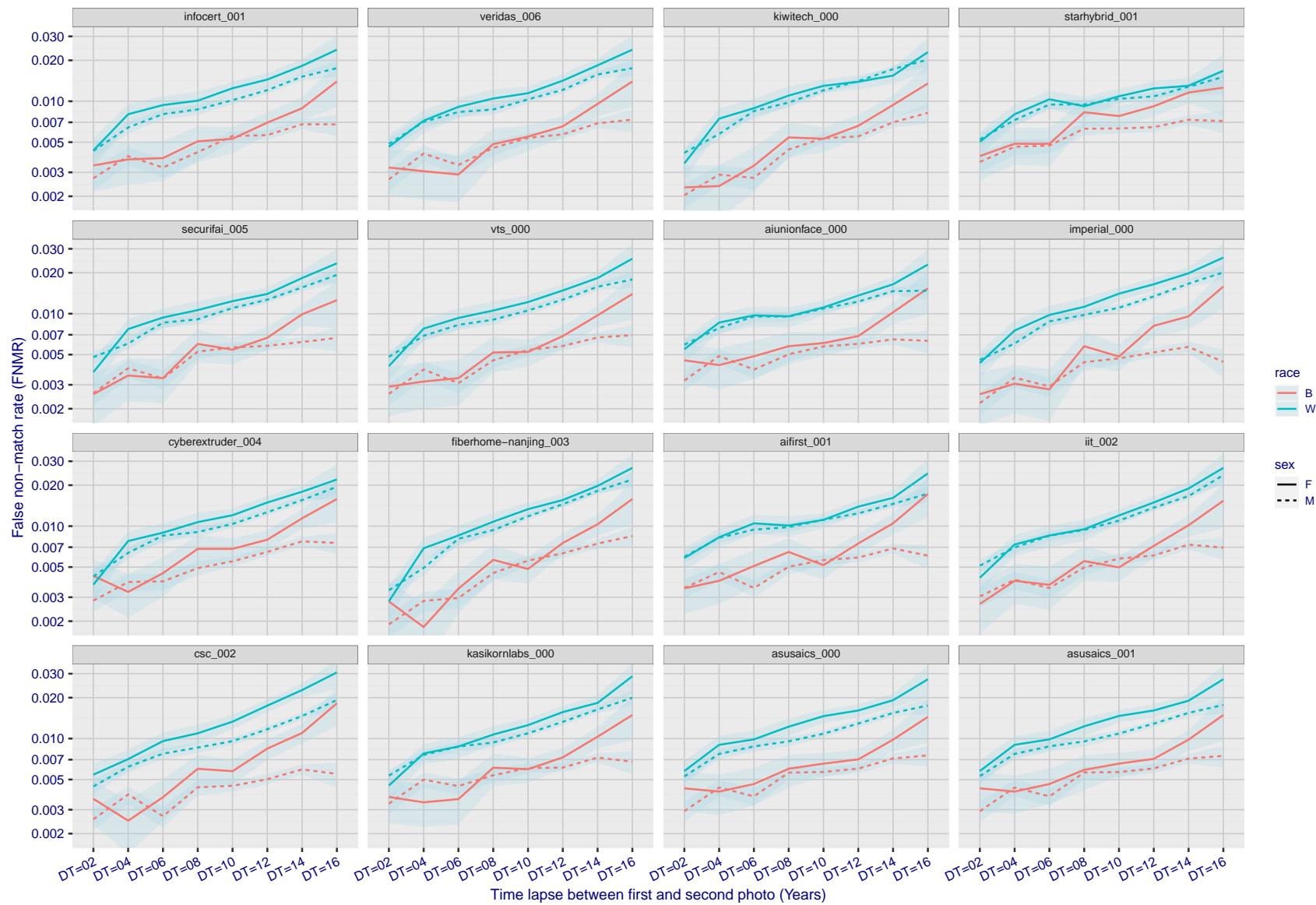


Figure 347: For the mugshot images, FNMR as a function of elapsed time between initial enrollment and second verification images. The panels appear most accurate first, and vertical scale changes on each page. The four traces correspond to images annotated with codes for black female, black male, white female, white male. The threshold is fixed for each algorithm to give $FMR = 0.00001$ over all (10^8) impostor comparisons. For short time-lapses, the most accurate algorithms give very few errors ($FNMR < 0.001$) so that the uncertainty estimates are high.

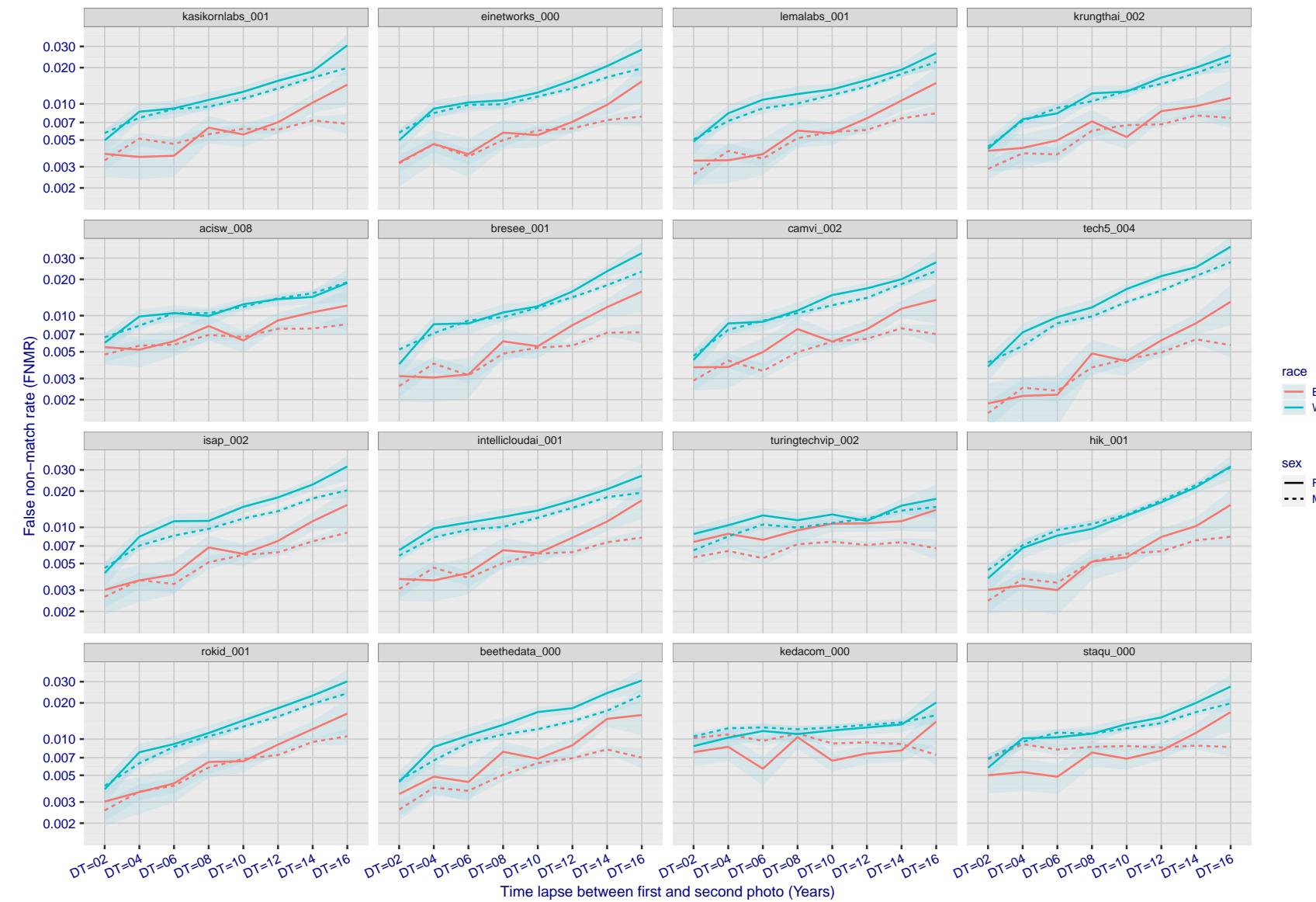


Figure 348: For the mugshot images, FNMR as a function of elapsed time between initial enrollment and second verification images. The panels appear most accurate first, and vertical scale changes on each page. The four traces correspond to images annotated with codes for black female, black male, white female, white male. The threshold is fixed for each algorithm to give FMR = 0.00001 over all (10^8) impostor comparisons. For short time-lapses, the most accurate algorithms give very few errors (FNMR < 0.001) so that the uncertainty estimates are high.

2023/02/09 20:10:38

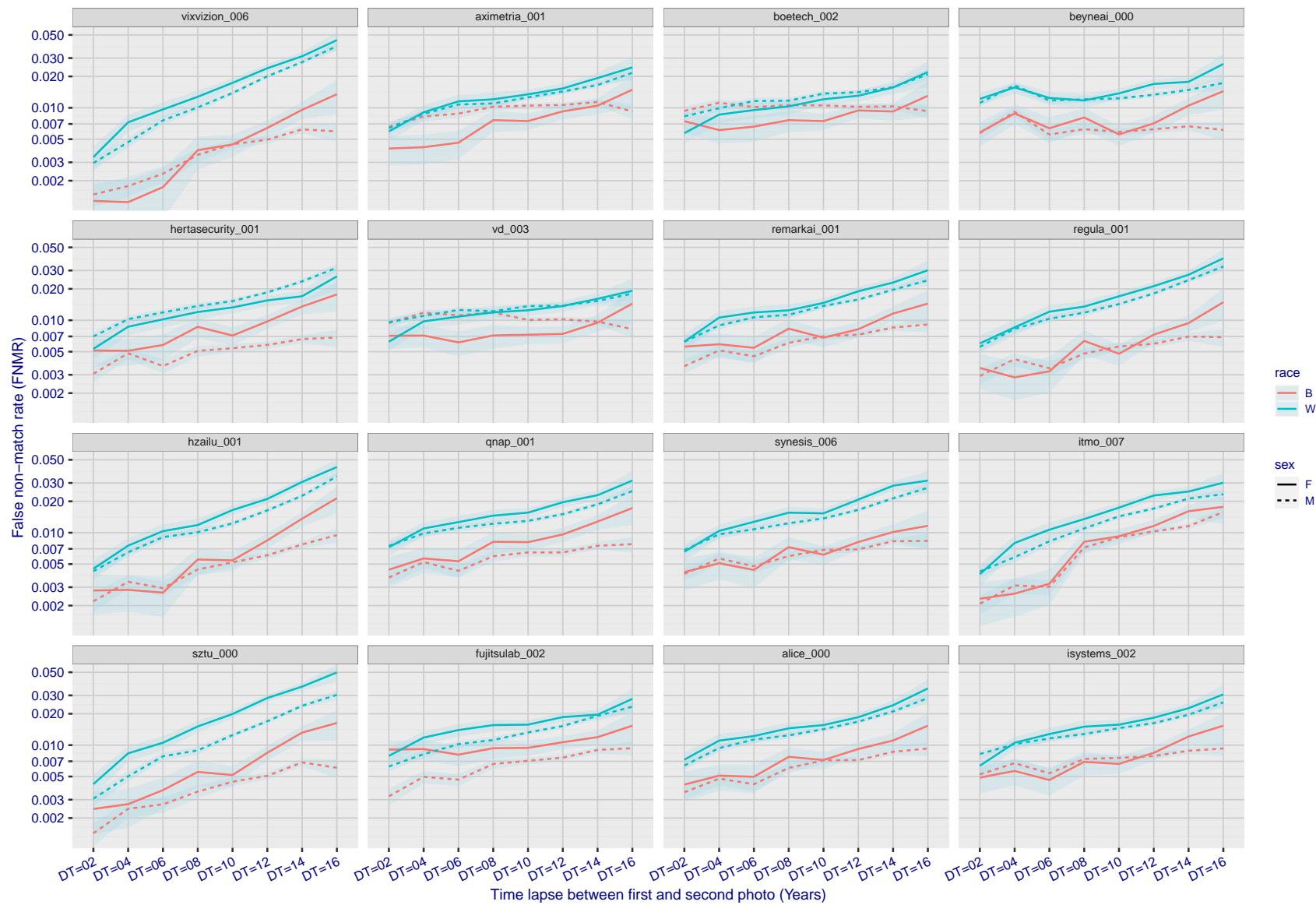


Figure 349: For the mugshot images, FNMR as a function of elapsed time between initial enrollment and second verification images. The panels appear most accurate first, and vertical scale changes on each page. The four traces correspond to images annotated with codes for black female, black male, white female, white male. The threshold is fixed for each algorithm to give FMR = 0.00001 over all (10^8) impostor comparisons. For short time-lapses, the most accurate algorithms give very few errors (FNMR < 0.001) so that the uncertainty estimates are high.

2023/02/09 20:10:38

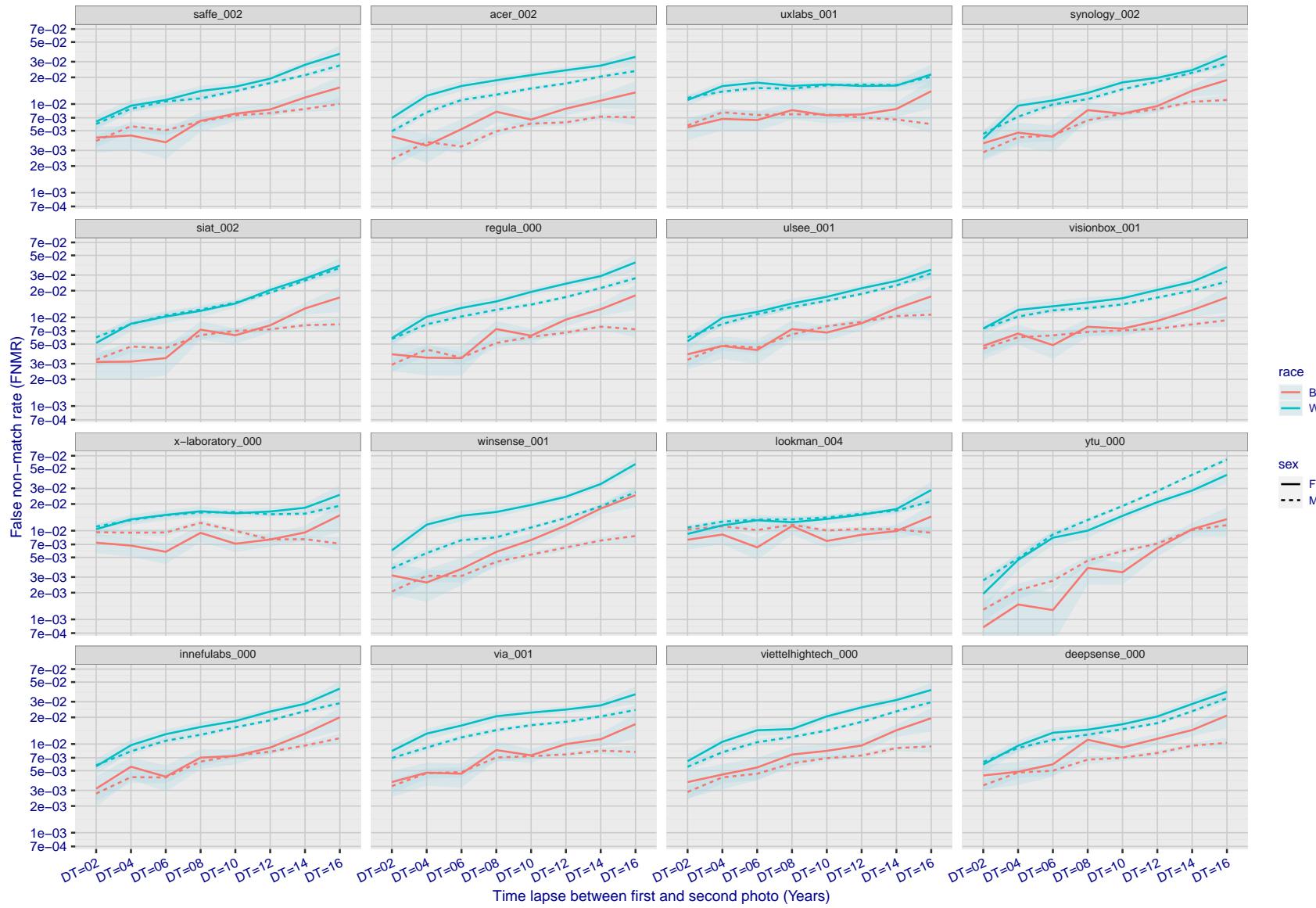


Figure 350: For the mugshot images, FNMR as a function of elapsed time between initial enrollment and second verification images. The panels appear most accurate first, and vertical scale changes on each page. The four traces correspond to images annotated with codes for black female, black male, white female, white male. The threshold is fixed for each algorithm to give $FMR = 0.00001$ over all (10^8) impostor comparisons. For short time-lapses, the most accurate algorithms give very few errors ($FNMR < 0.001$) so that the uncertainty estimates are high.

FNMR(T)
FMR(T)
"False non-match rate"
"False match rate"

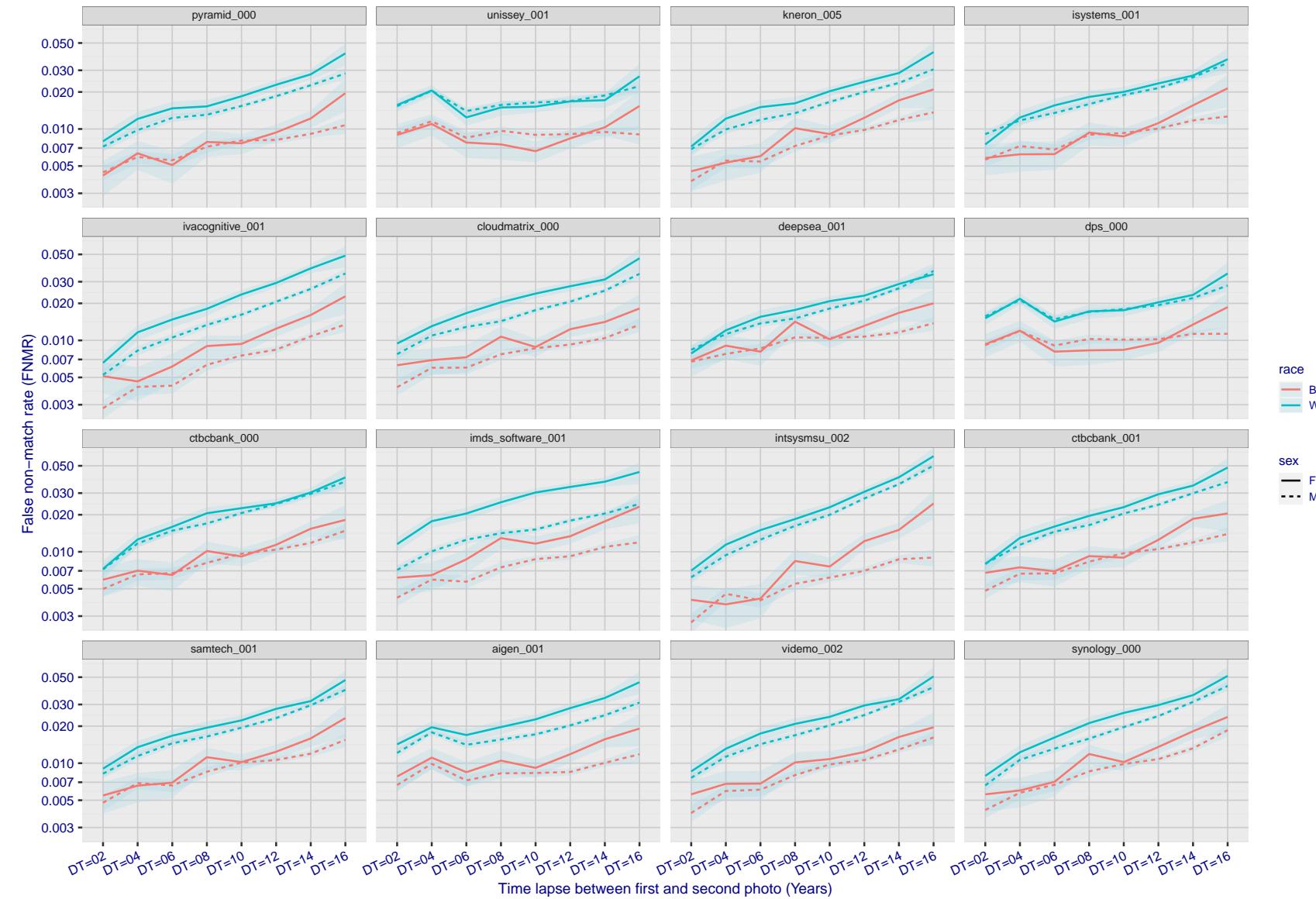


Figure 351: For the mugshot images, FNMR as a function of elapsed time between initial enrollment and second verification images. The panels appear most accurate first, and vertical scale changes on each page. The four traces correspond to images annotated with codes for black female, black male, white female, white male. The threshold is fixed for each algorithm to give FMR = 0.00001 over all (10^8) impostor comparisons. For short time-lapses, the most accurate algorithms give very few errors (FNMR < 0.001) so that the uncertainty estimates are high.

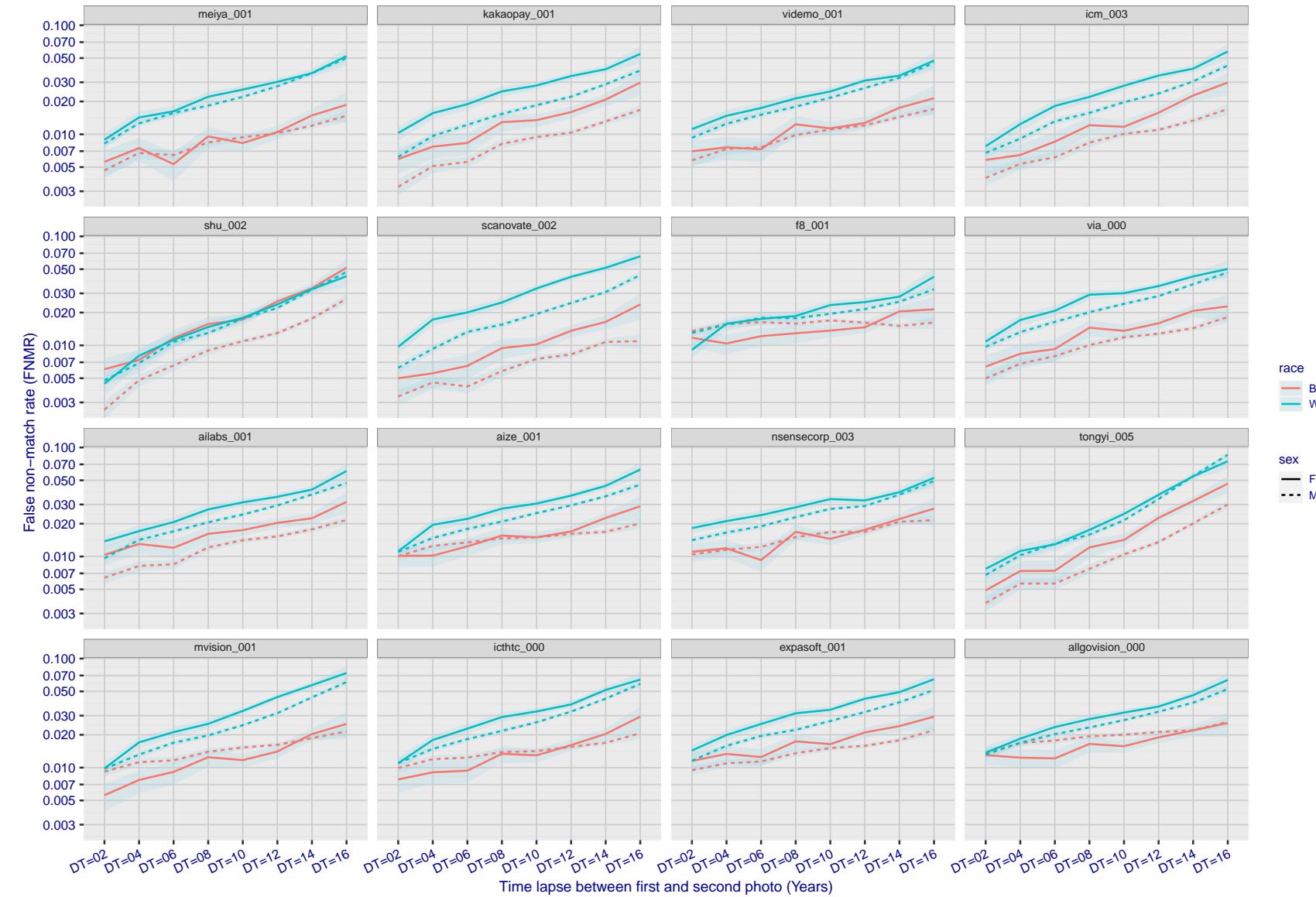


Figure 352: For the mugshot images, FNMR as a function of elapsed time between initial enrollment and second verification images. The panels appear most accurate first, and vertical scale changes on each page. The four traces correspond to images annotated with codes for black female, black male, white female, white male. The threshold is fixed for each algorithm to give FMR = 0.00001 over all (10^8) impostor comparisons. For short time-lapses, the most accurate algorithms give very few errors (FNMR < 0.001) so that the uncertainty estimates are high.

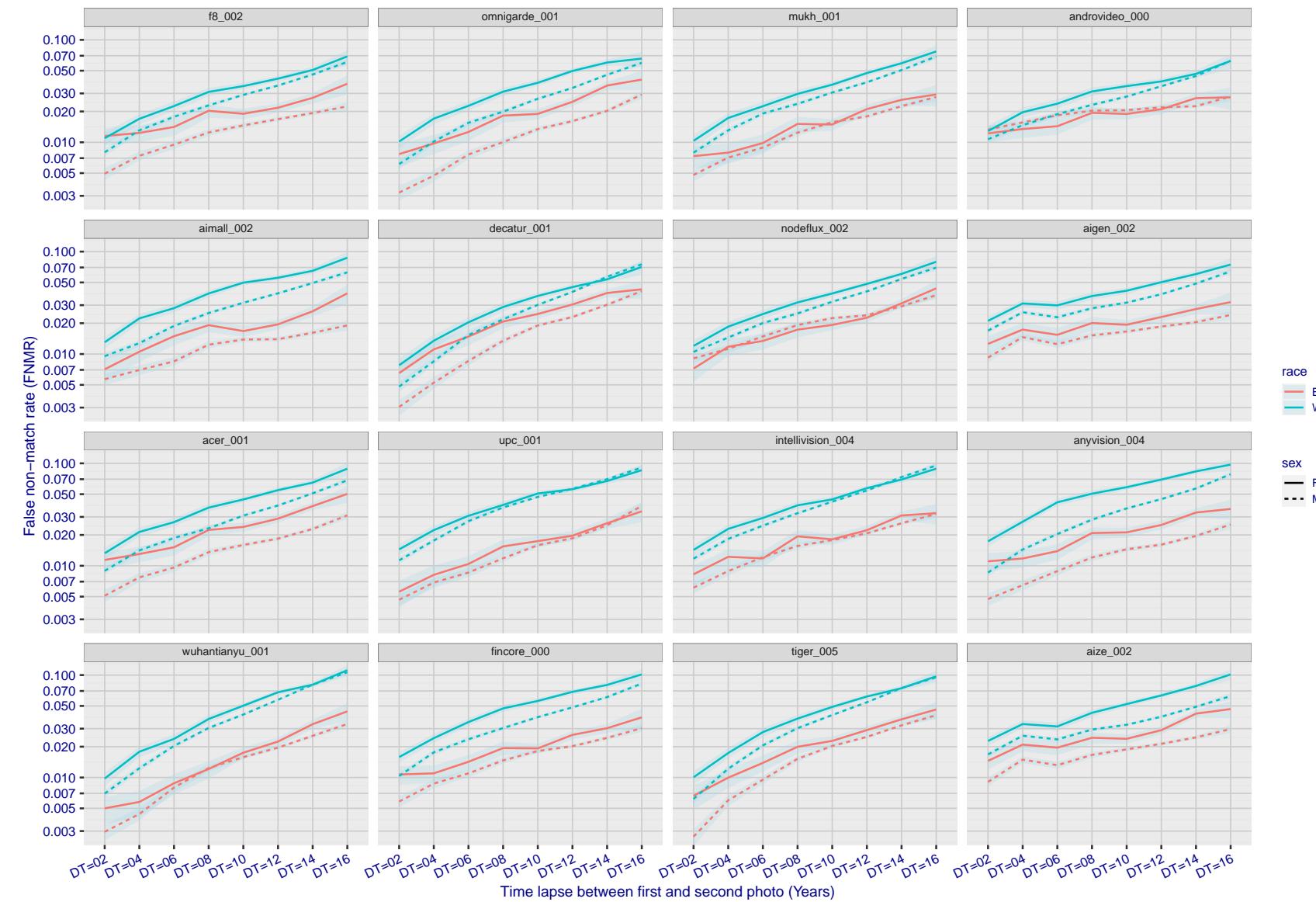


Figure 353: For the mugshot images, FNMR as a function of elapsed time between initial enrollment and second verification images. The panels appear most accurate first, and vertical scale changes on each page. The four traces correspond to images annotated with codes for black female, black male, white female, white male. The threshold is fixed for each algorithm to give $FMR = 0.00001$ over all (10^8) impostor comparisons. For short time-lapses, the most accurate algorithms give very few errors ($FNMR < 0.001$) so that the uncertainty estimates are high.

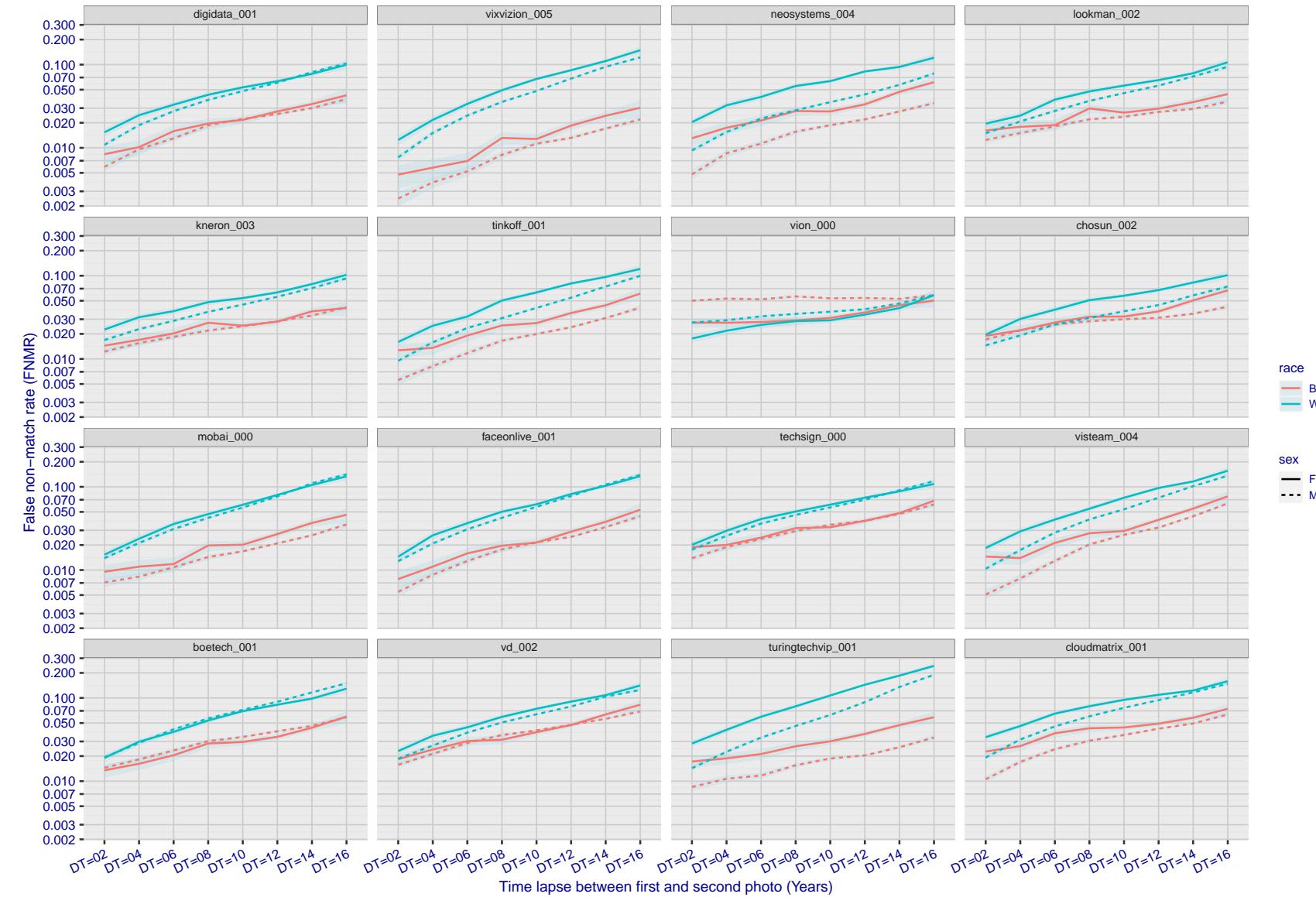


Figure 354: For the mugshot images, FNMR as a function of elapsed time between initial enrollment and second verification images. The panels appear most accurate first, and vertical scale changes on each page. The four traces correspond to images annotated with codes for black female, black male, white female, white male. The threshold is fixed for each algorithm to give FMR = 0.00001 over all (10^8) impostor comparisons. For short time-lapses, the most accurate algorithms give very few errors (FNMR < 0.001) so that the uncertainty estimates are high.

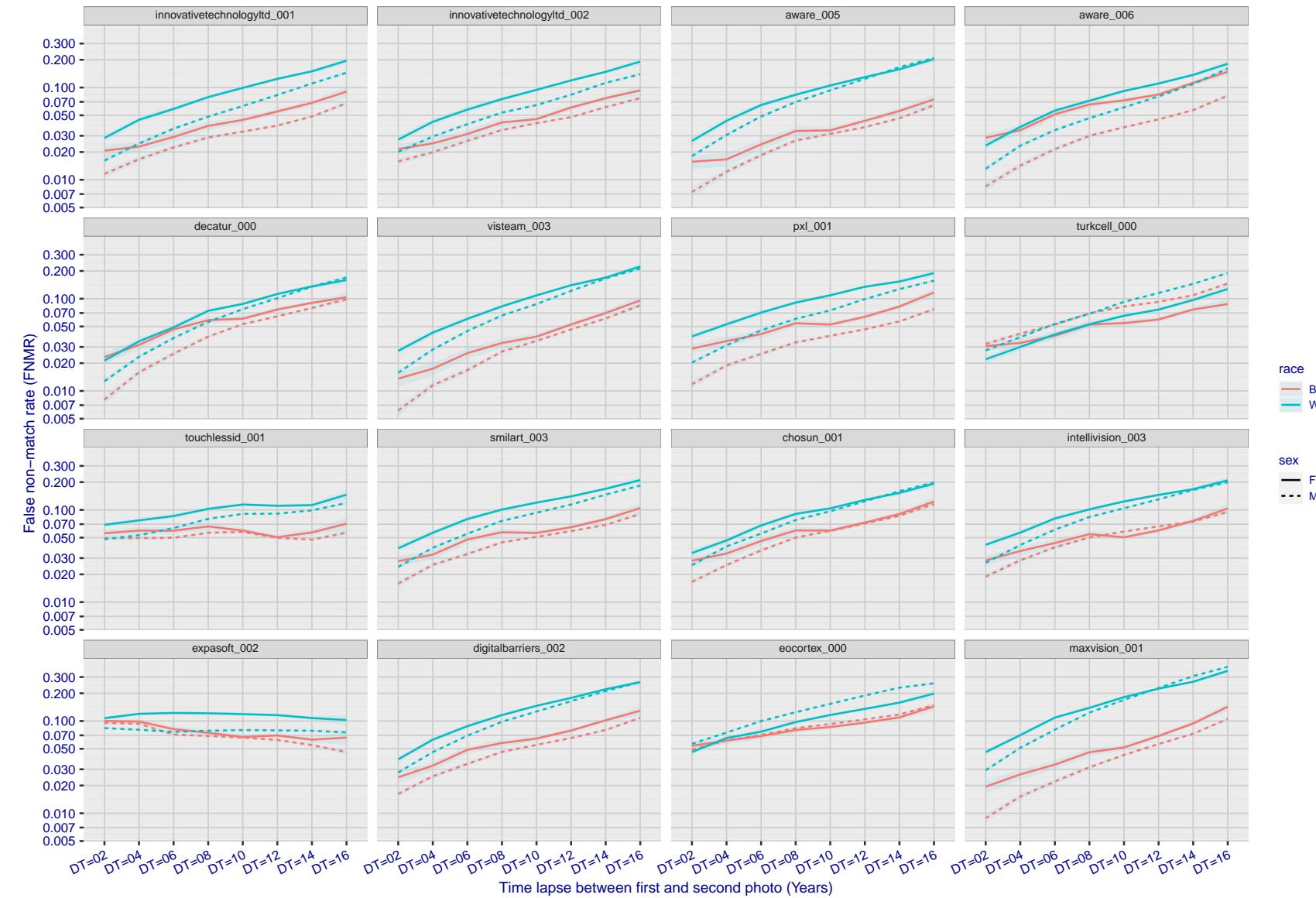


Figure 355: For the mugshot images, FNMR as a function of elapsed time between initial enrollment and second verification images. The panels appear most accurate first, and vertical scale changes on each page. The four traces correspond to images annotated with codes for black female, black male, white female, white male. The threshold is fixed for each algorithm to give FMR = 0.00001 over all (10^8) impostor comparisons. For short time-lapses, the most accurate algorithms give very few errors (FNMR < 0.001) so that the uncertainty estimates are high.

2023/02/09 20:10:38

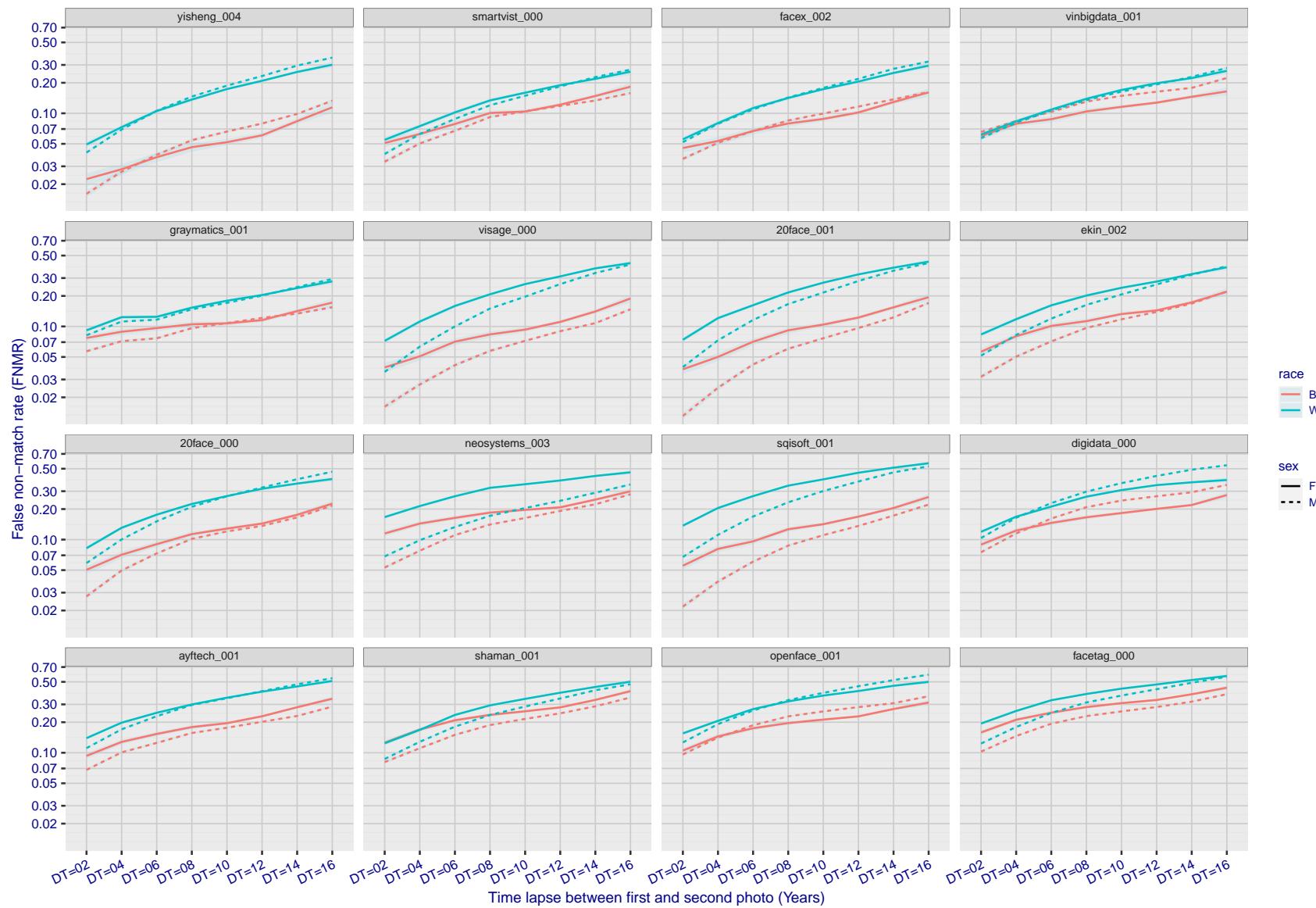


Figure 356: For the mugshot images, FNMR as a function of elapsed time between initial enrollment and second verification images. The panels appear most accurate first, and vertical scale changes on each page. The four traces correspond to images annotated with codes for black female, black male, white female, white male. The threshold is fixed for each algorithm to give FMR = 0.00001 over all (10^8) impostor comparisons. For short time-lapses, the most accurate algorithms give very few errors (FNMR < 0.001) so that the uncertainty estimates are high.

FNMR(T)
"False non-match rate"
"False match rate"

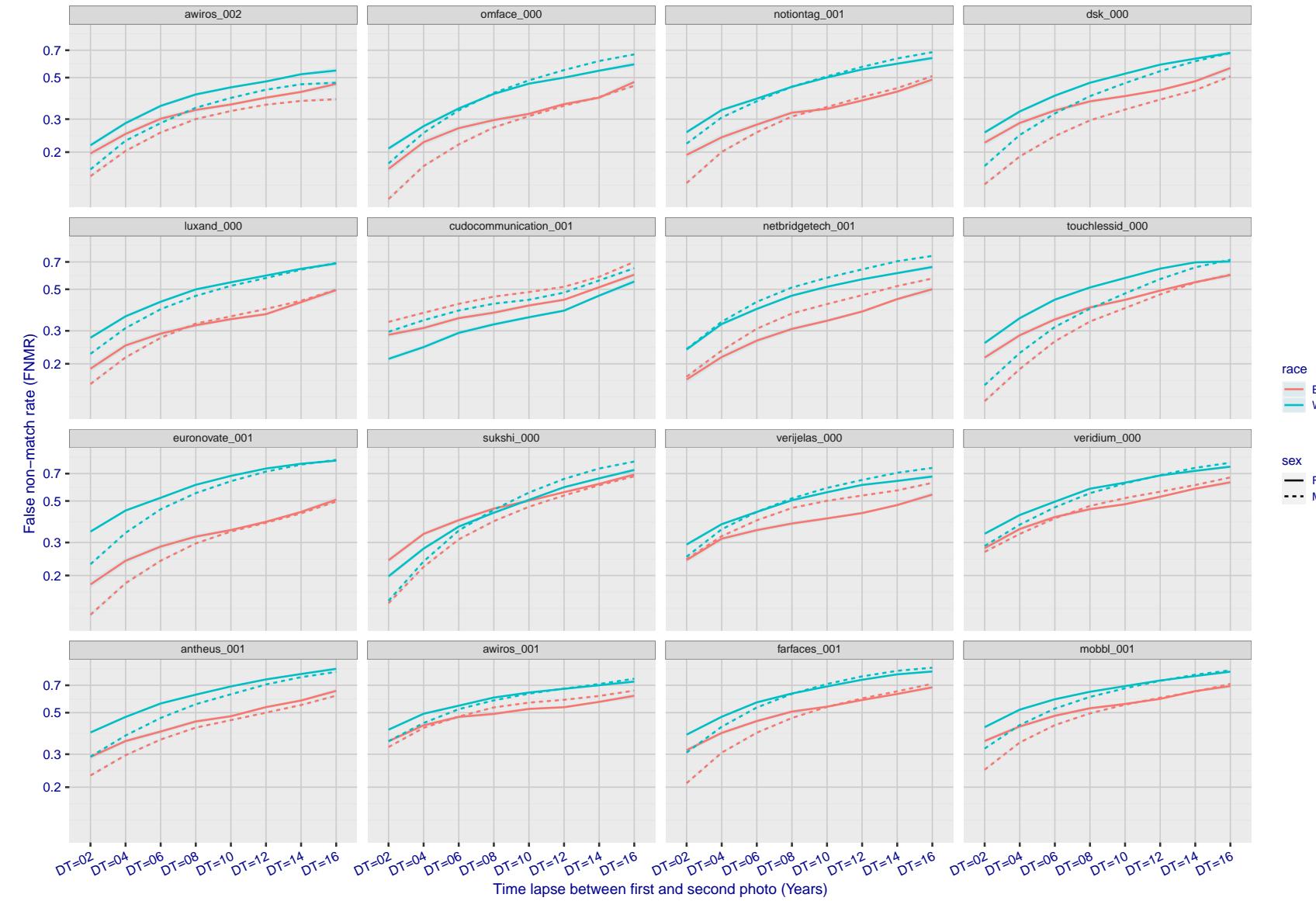


Figure 357: For the mugshot images, FNMR as a function of elapsed time between initial enrollment and second verification images. The panels appear most accurate first, and vertical scale changes on each page. The four traces correspond to images annotated with codes for black female, black male, white female, white male. The threshold is fixed for each algorithm to give $FMR = 0.00001$ over all (10^8) impostor comparisons. For short time-lapses, the most accurate algorithms give very few errors ($FNMR < 0.001$) so that the uncertainty estimates are high.

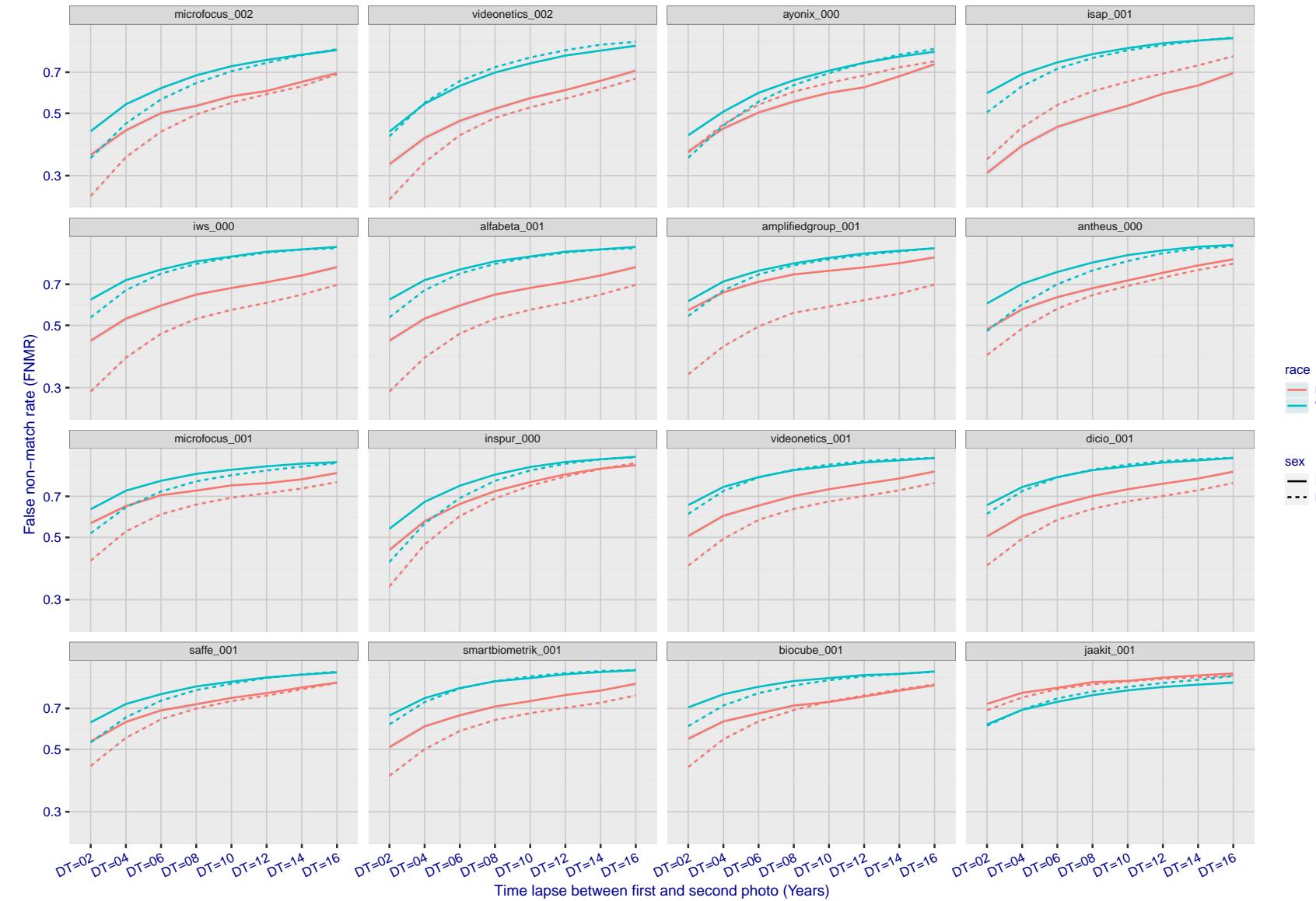


Figure 358: For the mugshot images, FNMR as a function of elapsed time between initial enrollment and second verification images. The panels appear most accurate first, and vertical scale changes on each page. The four traces correspond to images annotated with codes for black female, black male, white female, white male. The threshold is fixed for each algorithm to give FMR = 0.00001 over all (10^8) impostor comparisons. For short time-lapses, the most accurate algorithms give very few errors (FNMR < 0.001) so that the uncertainty estimates are high.

2023/02/09 20:10:38

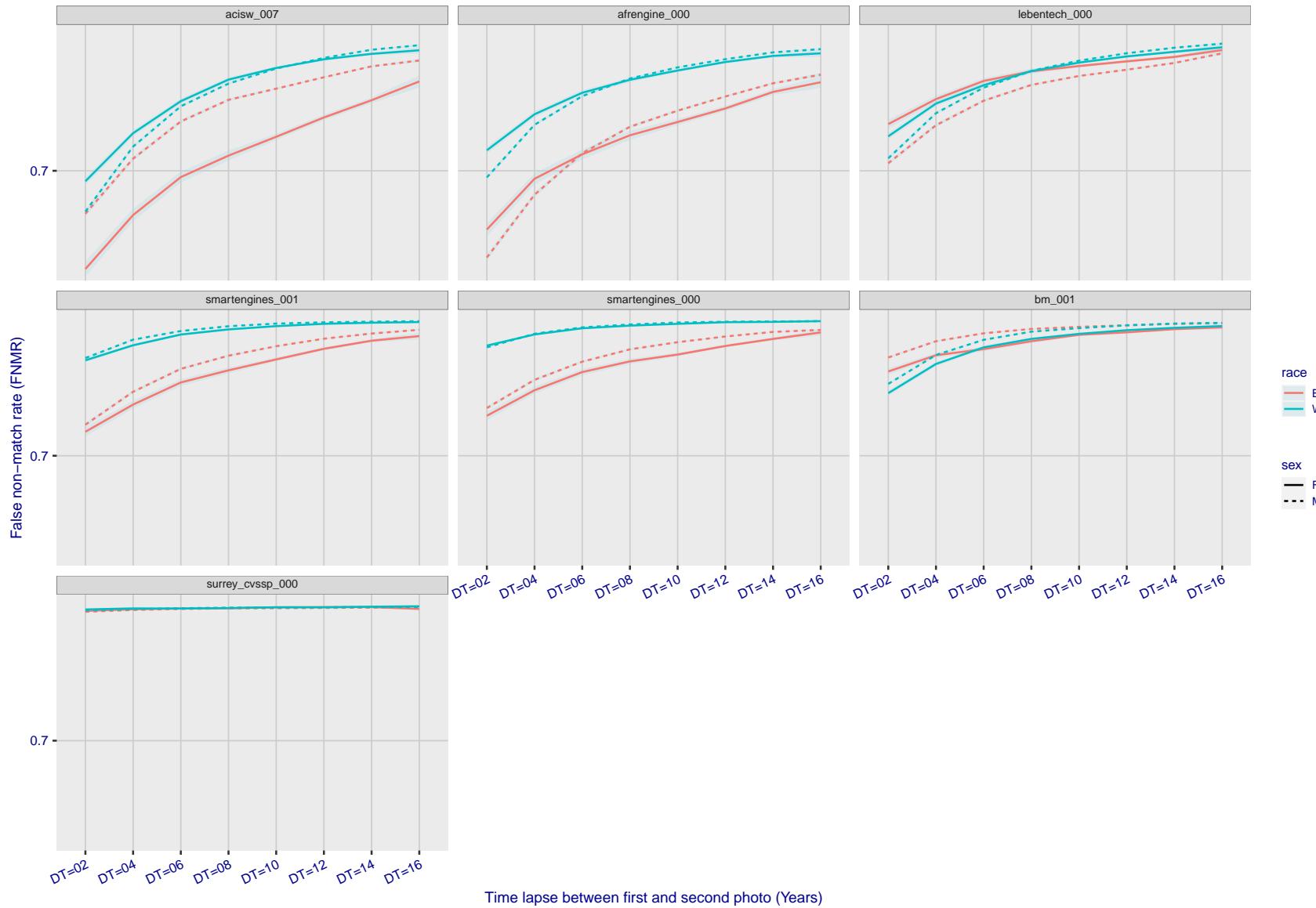


Figure 359: For the mugshot images, FNMR as a function of elapsed time between initial enrollment and second verification images. The panels appear most accurate first, and vertical scale changes on each page. The four traces correspond to images annotated with codes for black female, black male, white female, white male. The threshold is fixed for each algorithm to give FMR = 0.00001 over all (10^8) impostor comparisons. For short time-lapses, the most accurate algorithms give very few errors (FNMR < 0.001) so that the uncertainty estimates are high.

3.5.3 Effect of age on genuine subjects

Background: Faces change appearance throughout life. Face recognition algorithms have previously been reported to give better accuracy on older individuals (See NIST IR 8009).

Goal: To quantify false non-match rates (FNMR) as a function of age, without an ageing component.

Methods: Using the visa images, which span fewer than five years, thresholds are determined that give FMR = 0.001 and 0.0001 over the entire impostor set. Then FNMR is measured over 1000 bootstrap replications of the genuine scores.

Results: For the visa images, Figure 398 shows how false non-match rates for genuine users, as a function of age group.

The notable aspects are:

- ▷ Younger subjects give considerably higher FNMR. This is likely due to rapid growth and change in facial appearance.
- ▷ FNMR trends down throughout life. The last bin, AGE > 72, contains fewer than 140 mated pairs, and may be affected by small sample size.

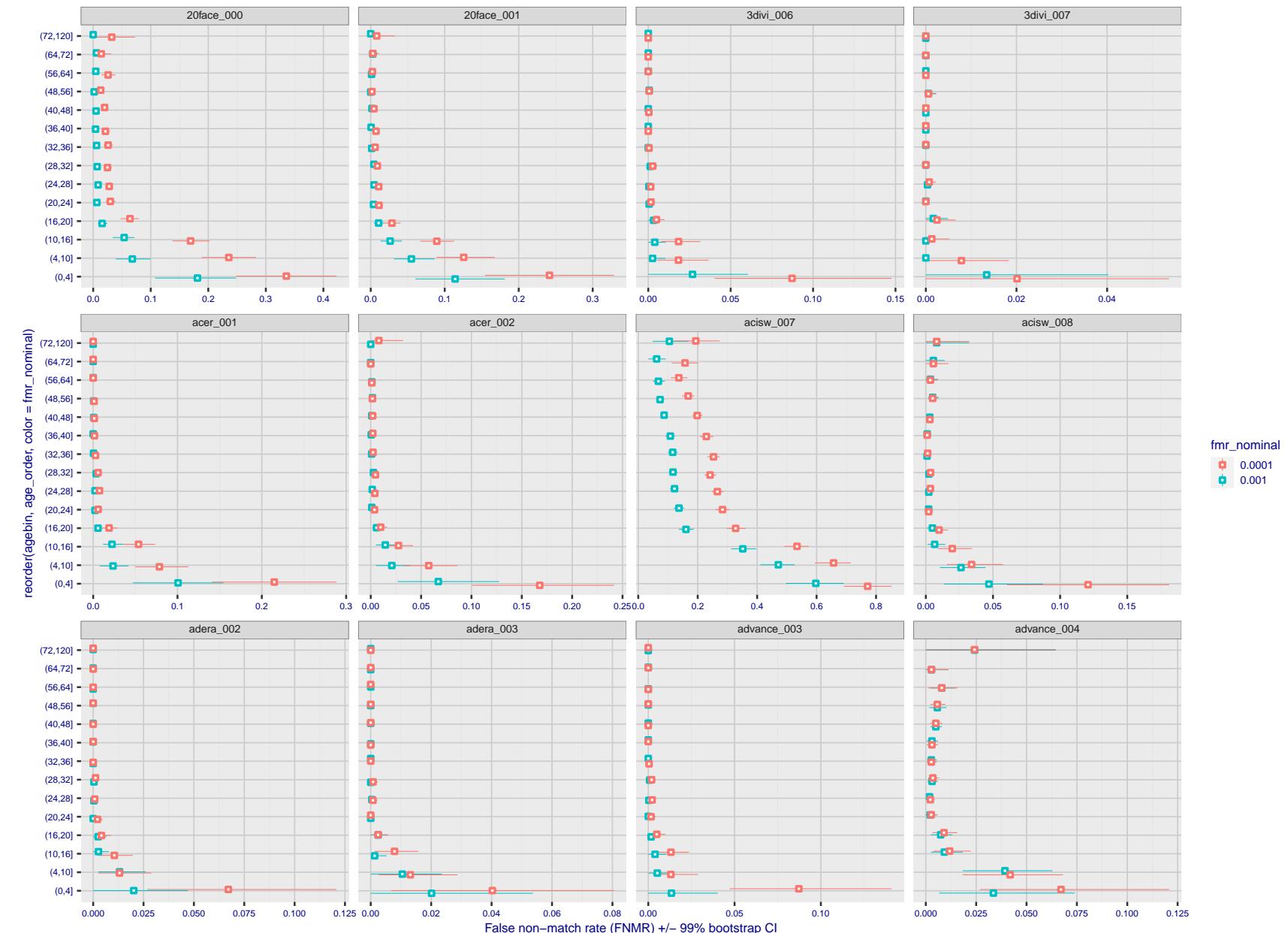


Figure 360: For the visa images, the dots show FNMR by age group for two operating thresholds corresponding to $FMR = \{0.001, 0.0001\}$ computed over all on the order of 10^{10} impostor scores. The FMR in each bin will vary also - see subsequent impostor heatmaps in sec. 3.6.2. Given a pair of face images taken at different times, we assign the comparison to the bin that is the arithmetic average of the subject's ages. This plot shows only the effect of age, not ageing. The number of comparisons in each bin is generally in the thousands, however the first and last bins are computed over 149 and 124 respectively. The error rates in some (adult) cases are zero, and in others the DET is flat so the error rates at the two thresholds are identical. The lines span 1% and 99% of bootstrap replicated FNMR estimates.

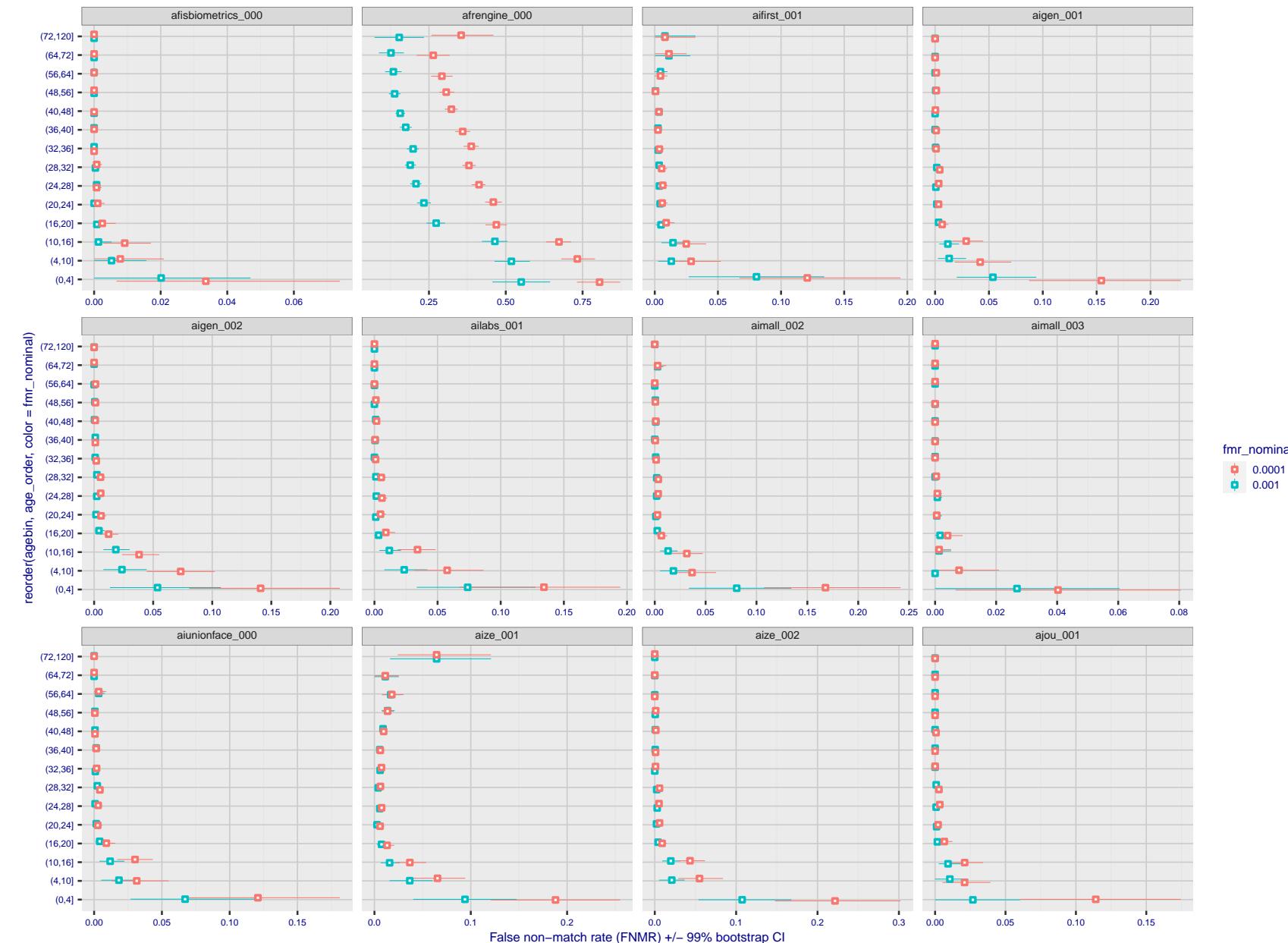


Figure 361: For the visa images, the dots show FNMR by age group for two operating thresholds corresponding to $FMR = \{0.001, 0.0001\}$ computed over all on the order of 10^{10} impostor scores. The FMR in each bin will vary also - see subsequent impostor heatmaps in sec. 3.6.2. Given a pair of face images taken at different times, we assign the comparison to the bin that is the arithmetic average of the subject's ages. This plot shows only the effect of age, not ageing. The number of comparisons in each bin is generally in the thousands, however the first and last bins are computed over 149 and 124 respectively. The error rates in some (adult) cases are zero, and in others the DET is flat so the error rates at the two thresholds are identical. The lines span 1% and 99% of bootstrap replicated FNMR estimates.



Figure 362: For the visa images, the dots show FNMR by age group for two operating thresholds corresponding to $FMR = \{0.001, 0.0001\}$ computed over all on the order of 10^{10} impostor scores. The FMR in each bin will vary also - see subsequent impostor heatmaps in sec. 3.6.2. Given a pair of face images taken at different times, we assign the comparison to the bin that is the arithmetic average of the subject's ages. This plot shows only the effect of age, not ageing. The number of comparisons in each bin is generally in the thousands, however the first and last bins are computed over 149 and 124 respectively. The error rates in some (adult) cases are zero, and in others the DET is flat so the error rates at the two thresholds are identical. The lines span 1% and 99% of bootstrap replicated FNMR estimates.

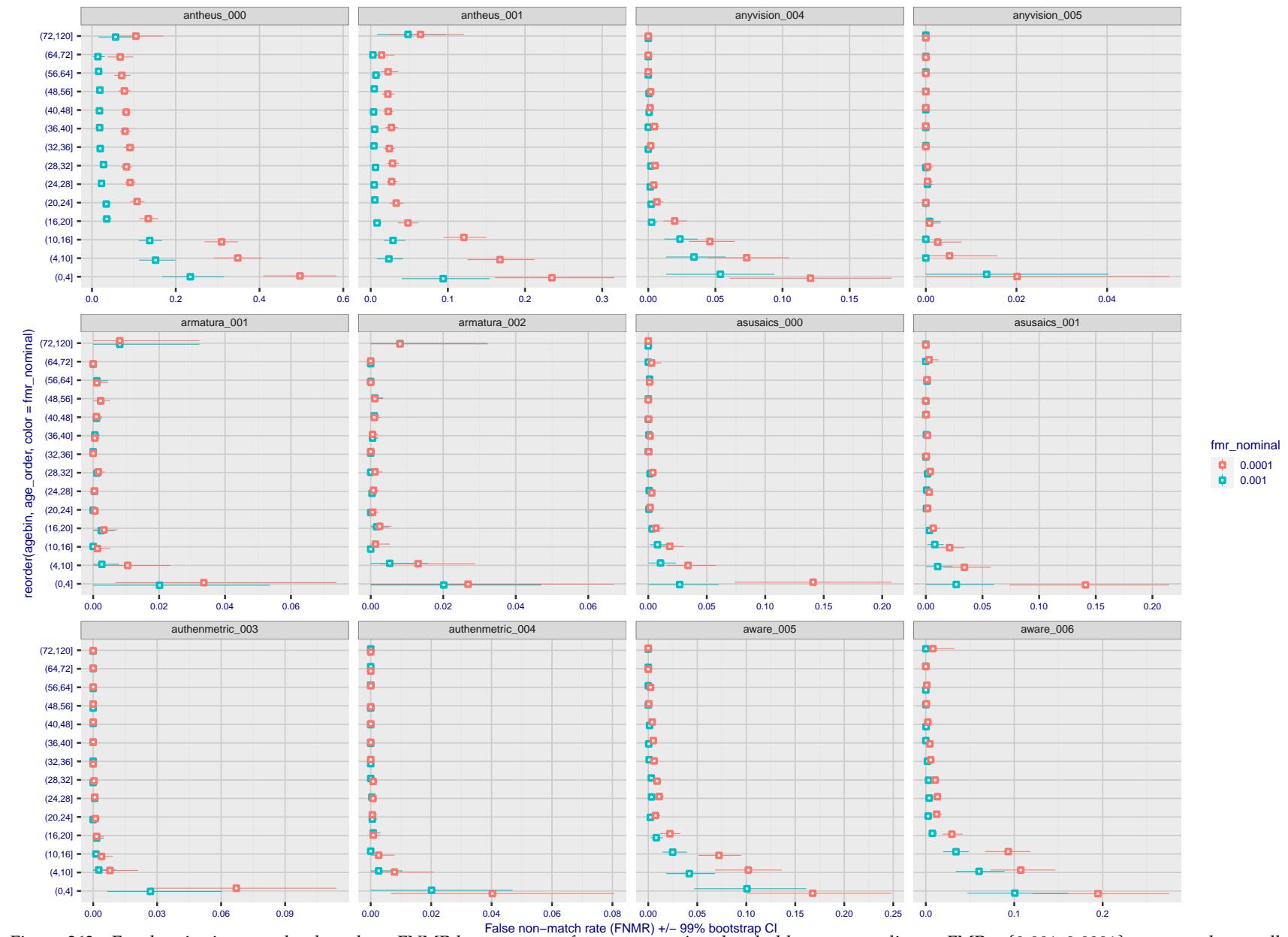


Figure 363: For the visa images, the dots show FNMR by age group for two operating thresholds corresponding to $FMR = \{0.001, 0.0001\}$ computed over all on the order of 10^{10} impostor scores. The FMR in each bin will vary also - see subsequent impostor heatmaps in sec. 3.6.2. Given a pair of face images taken at different times, we assign the comparison to the bin that is the arithmetic average of the subject's ages. This plot shows only the effect of age, not ageing. The number of comparisons in each bin is generally in the thousands, however the first and last bins are computed over 149 and 124 respectively. The error rates in some (adult) cases are zero, and in others the DET is flat so the error rates at the two thresholds are identical. The lines span 1% and 99% of bootstrap replicated FNMR estimates.

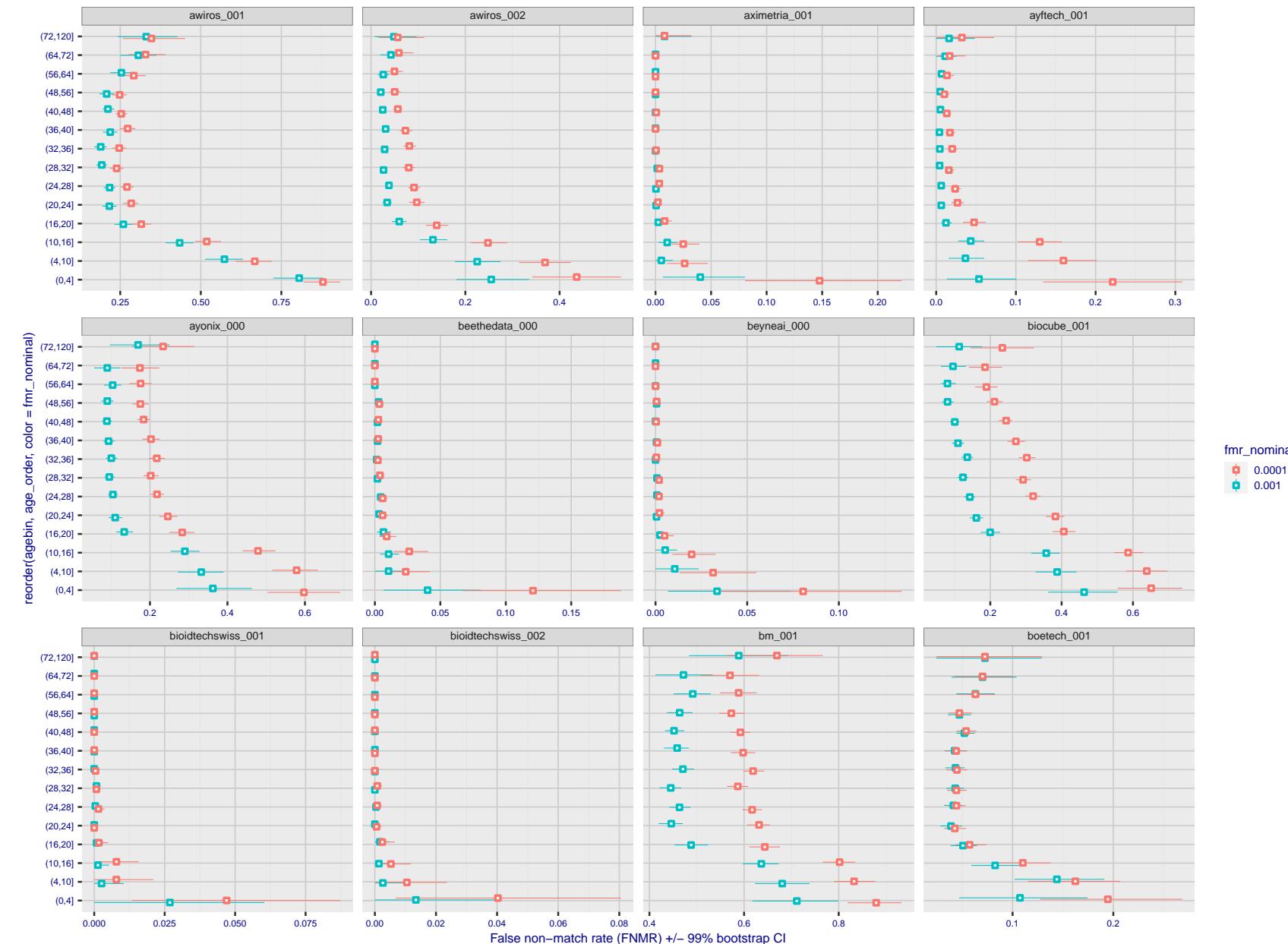
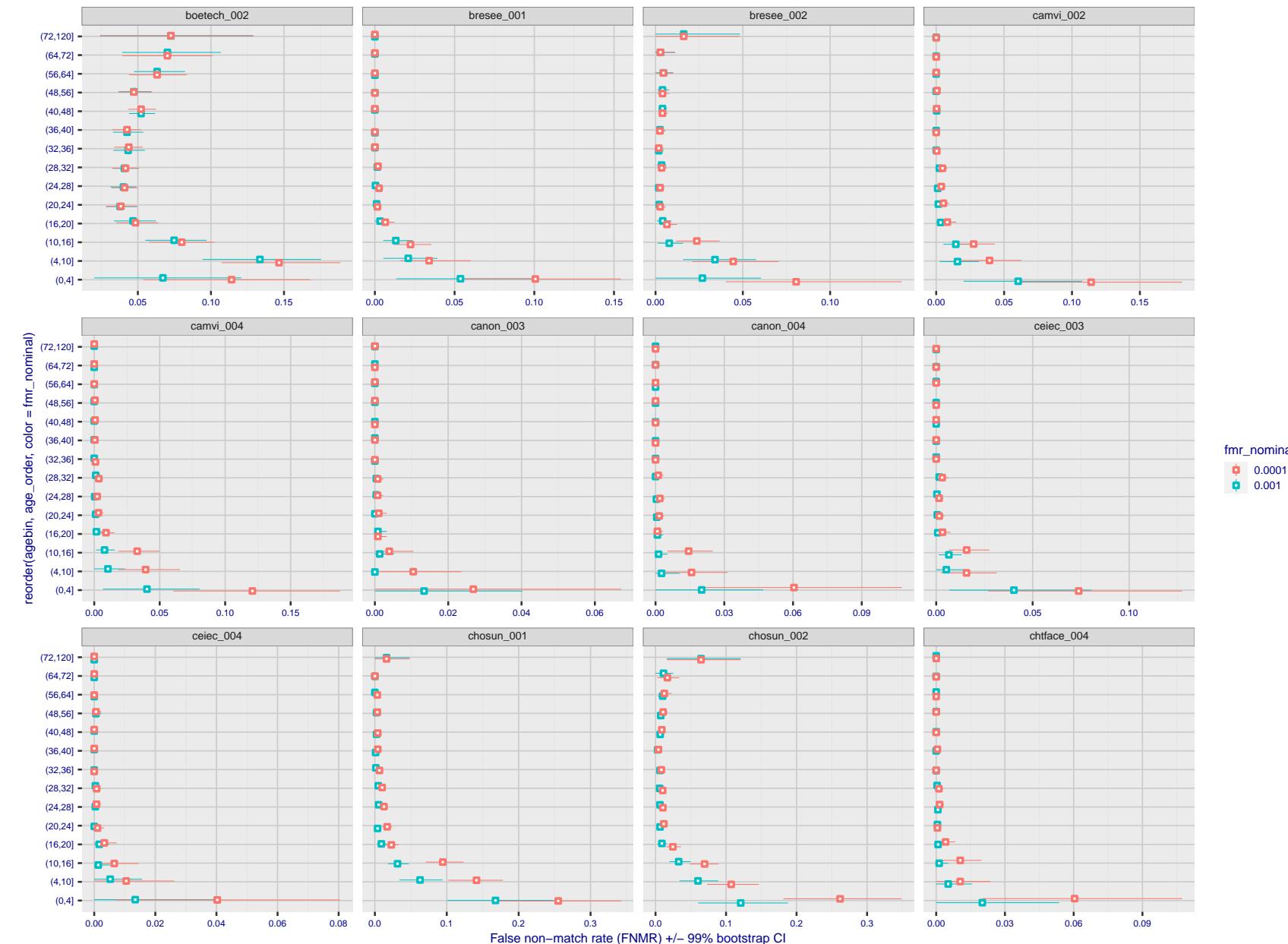


Figure 364: For the visa images, the dots show FNMR by age group for two operating thresholds corresponding to $FMR = \{0.001, 0.0001\}$ computed over all on the order of 10^{10} impostor scores. The FMR in each bin will vary also - see subsequent impostor heatmaps in sec. 3.6.2. Given a pair of face images taken at different times, we assign the comparison to the bin that is the arithmetic average of the subject's ages. This plot shows only the effect of age, not ageing. The number of comparisons in each bin is generally in the thousands, however the first and last bins are computed over 149 and 124 respectively. The error rates in some (adult) cases are zero, and in others the DET is flat so the error rates at the two thresholds are identical. The lines span 1% and 99% of bootstrap replicated FNMR estimates.



FNMR(T)
FMR(T)
"False non-match rate"
"False match rate"

Figure 365: For the visa images, the dots show FNMR by age group for two operating thresholds corresponding to $FMR = \{0.001, 0.0001\}$ computed over all on the order of 10^{10} impostor scores. The FMR in each bin will vary also - see subsequent impostor heatmaps in sec. 3.6.2. Given a pair of face images taken at different times, we assign the comparison to the bin that is the arithmetic average of the subject's ages. This plot shows only the effect of age, not ageing. The number of comparisons in each bin is generally in the thousands, however the first and last bins are computed over 149 and 124 respectively. The error rates in some (adult) cases are zero, and in others the DET is flat so the error rates at the two thresholds are identical. The lines span 1% and 99% of bootstrap replicated FNMR estimates.

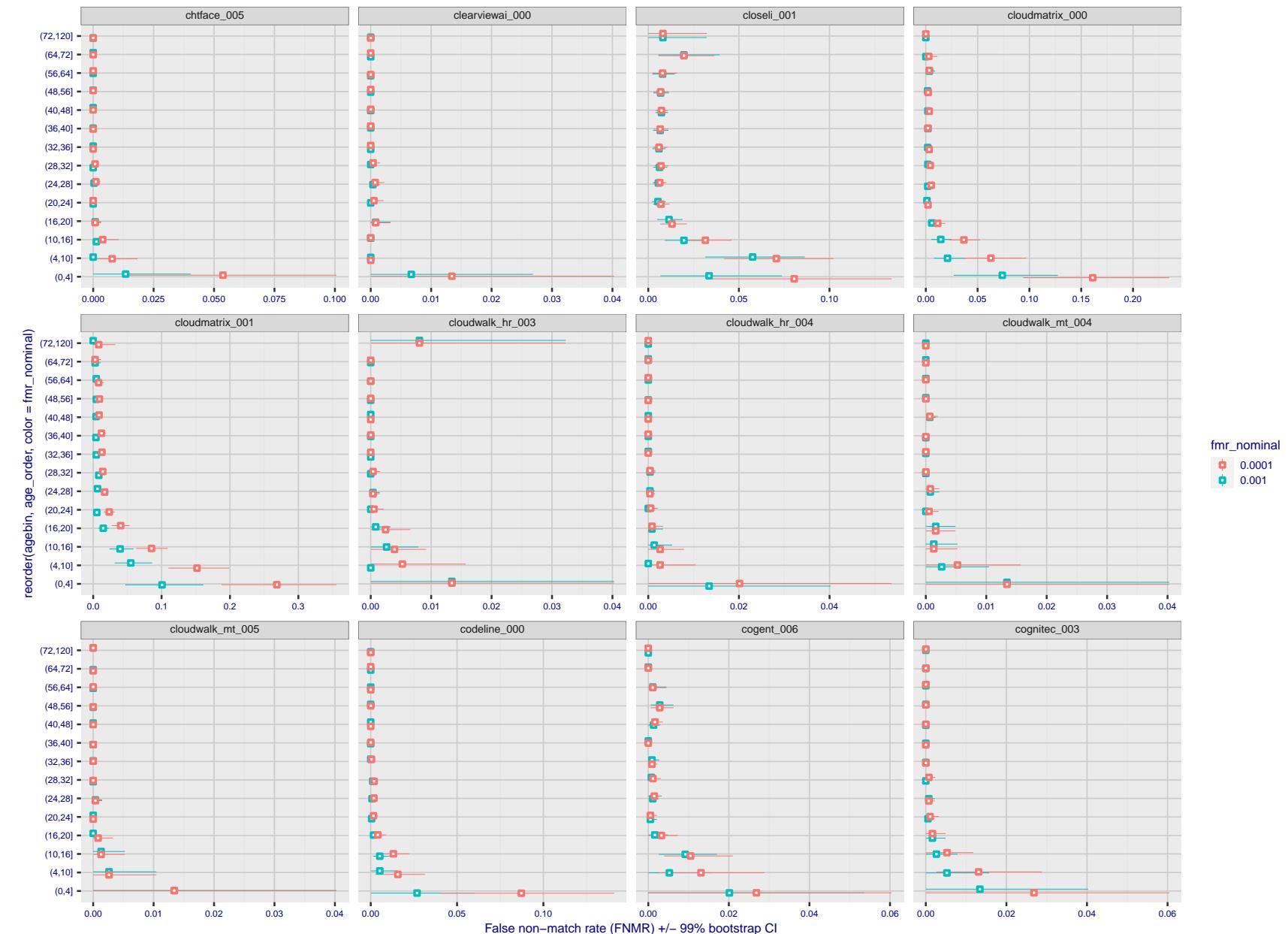


Figure 366: For the visa images, the dots show FNMR by age group for two operating thresholds corresponding to $FMR = \{0.001, 0.0001\}$ computed over all on the order of 10^{10} impostor scores. The FMR in each bin will vary also - see subsequent impostor heatmaps in sec. 3.6.2. Given a pair of face images taken at different times, we assign the comparison to the bin that is the arithmetic average of the subject's ages. This plot shows only the effect of age, not ageing. The number of comparisons in each bin is generally in the thousands, however the first and last bins are computed over 149 and 124 respectively. The error rates in some (adult) cases are zero, and in others the DET is flat so the error rates at the two thresholds are identical. The lines span 1% and 99% of bootstrap replicated FNMR estimates.

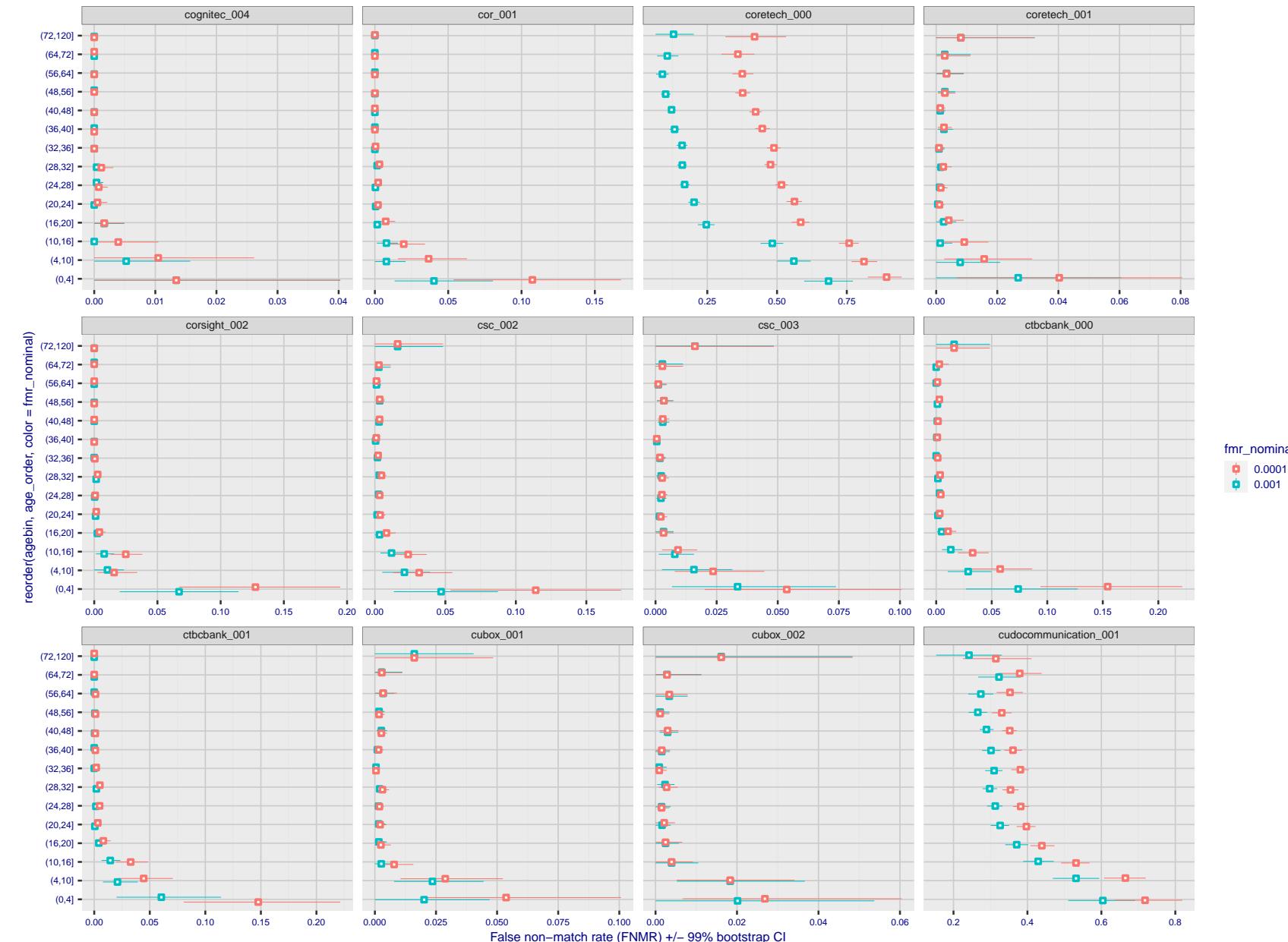


Figure 367: For the visa images, the dots show FNMR by age group for two operating thresholds corresponding to $FMR = \{0.001, 0.0001\}$ computed over all on the order of 10^{10} impostor scores. The FMR in each bin will vary also - see subsequent impostor heatmaps in sec. 3.6.2. Given a pair of face images taken at different times, we assign the comparison to the bin that is the arithmetic average of the subject's ages. This plot shows only the effect of age, not ageing. The number of comparisons in each bin is generally in the thousands, however the first and last bins are computed over 149 and 124 respectively. The error rates in some (adult) cases are zero, and in others the DET is flat so the error rates at the two thresholds are identical. The lines span 1% and 99% of bootstrap replicated FNMR estimates.

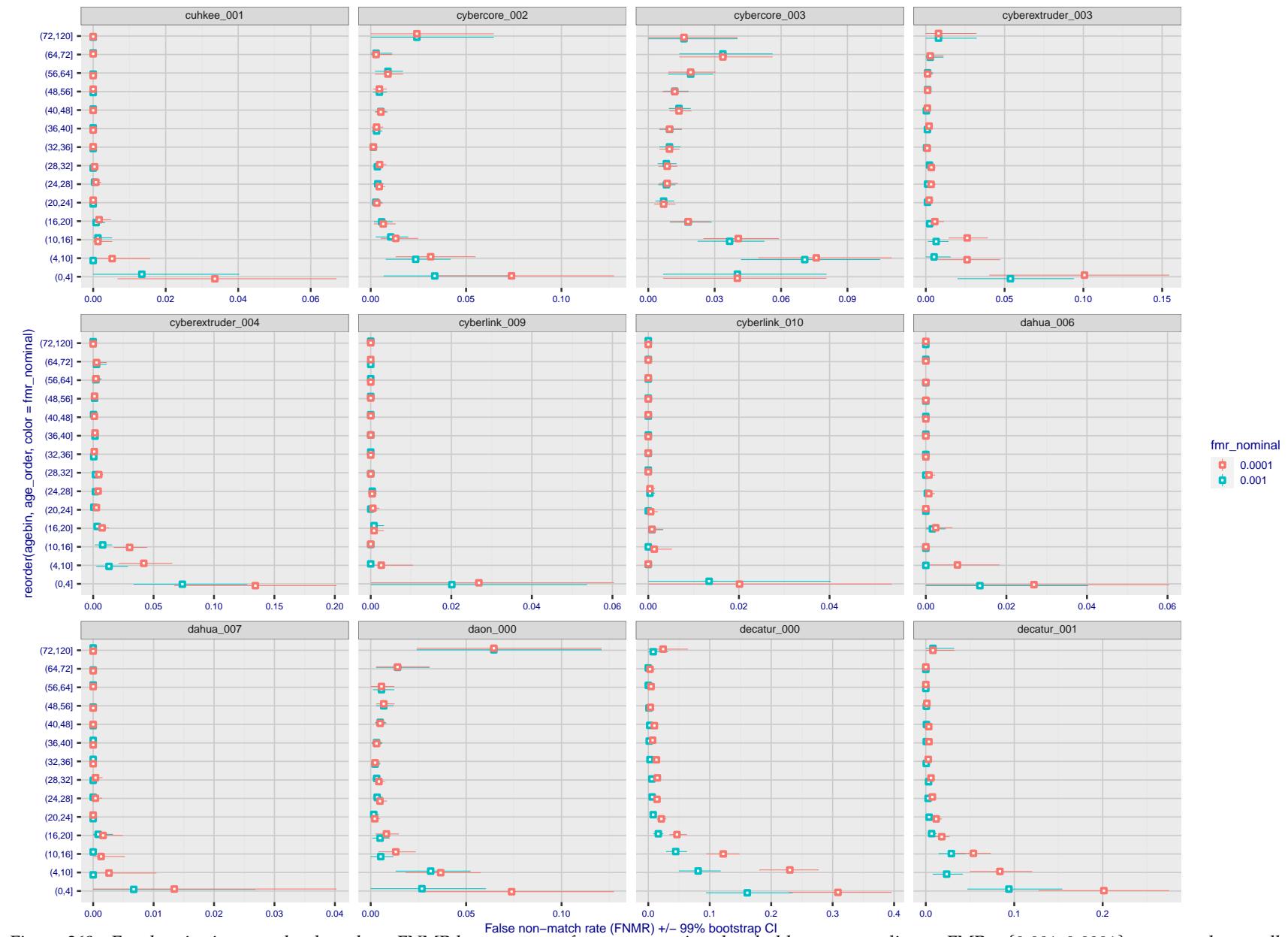


Figure 368: For the visa images, the dots show FNMR by age group for two operating thresholds corresponding to $FMR = \{0.001, 0.0001\}$ computed over all on the order of 10^{10} impostor scores. The FMR in each bin will vary also - see subsequent impostor heatmaps in sec. 3.6.2. Given a pair of face images taken at different times, we assign the comparison to the bin that is the arithmetic average of the subject's ages. This plot shows only the effect of age, not ageing. The number of comparisons in each bin is generally in the thousands, however the first and last bins are computed over 149 and 124 respectively. The error rates in some (adult) cases are zero, and in others the DET is flat so the error rates at the two thresholds are identical. The lines span 1% and 99% of bootstrap replicated FNMR estimates.

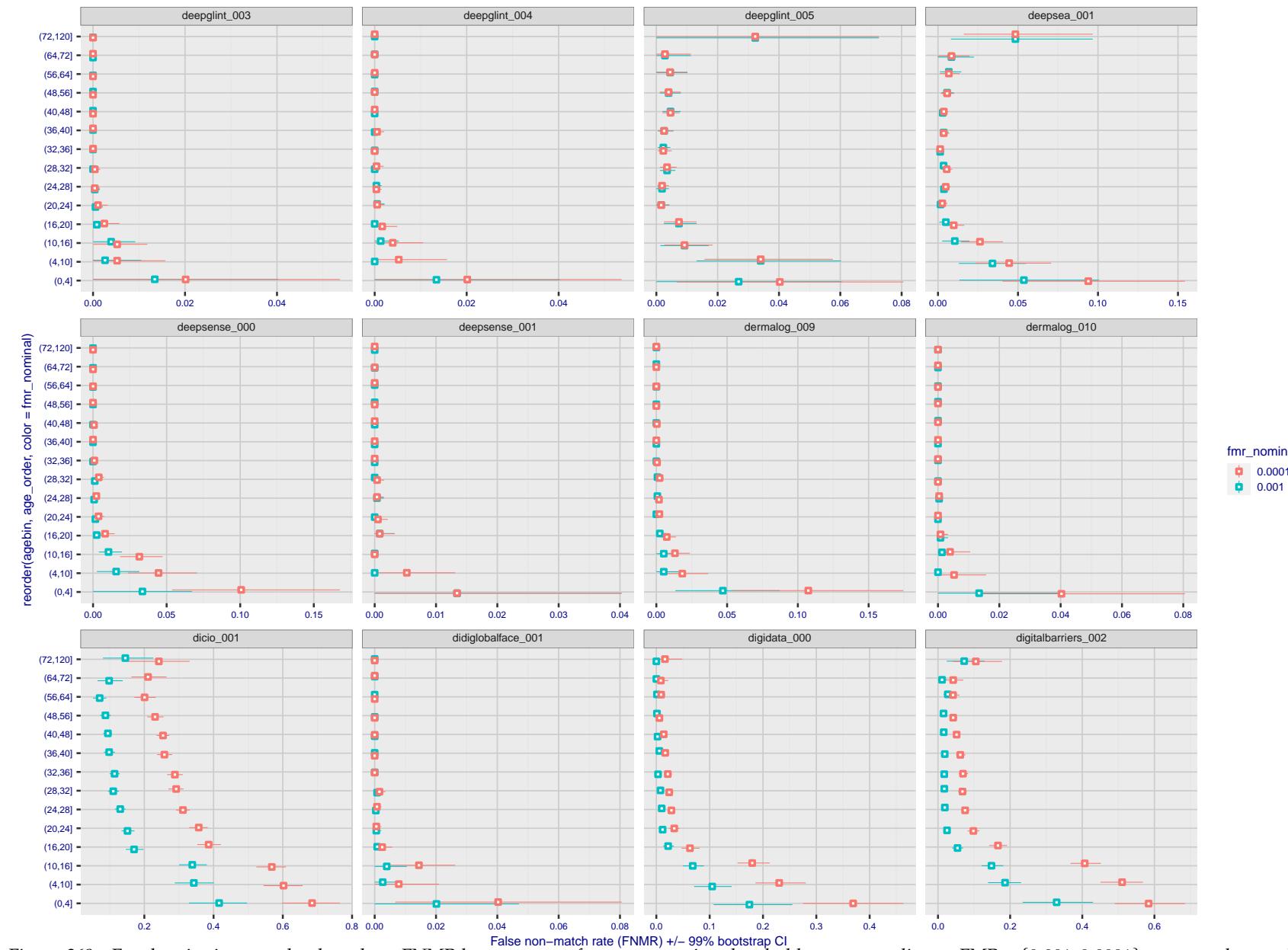


Figure 369: For the visa images, the dots show FNMR by age group for two operating thresholds corresponding to $FMR = \{0.001, 0.0001\}$ computed over all on the order of 10^{10} impostor scores. The FMR in each bin will vary also - see subsequent impostor heatmaps in sec. 3.6.2. Given a pair of face images taken at different times, we assign the comparison to the bin that is the arithmetic average of the subject's ages. This plot shows only the effect of age, not ageing. The number of comparisons in each bin is generally in the thousands, however the first and last bins are computed over 149 and 124 respectively. The error rates in some (adult) cases are zero, and in others the DET is flat so the error rates at the two thresholds are identical. The lines span 1% and 99% of bootstrap replicated FNMR estimates.

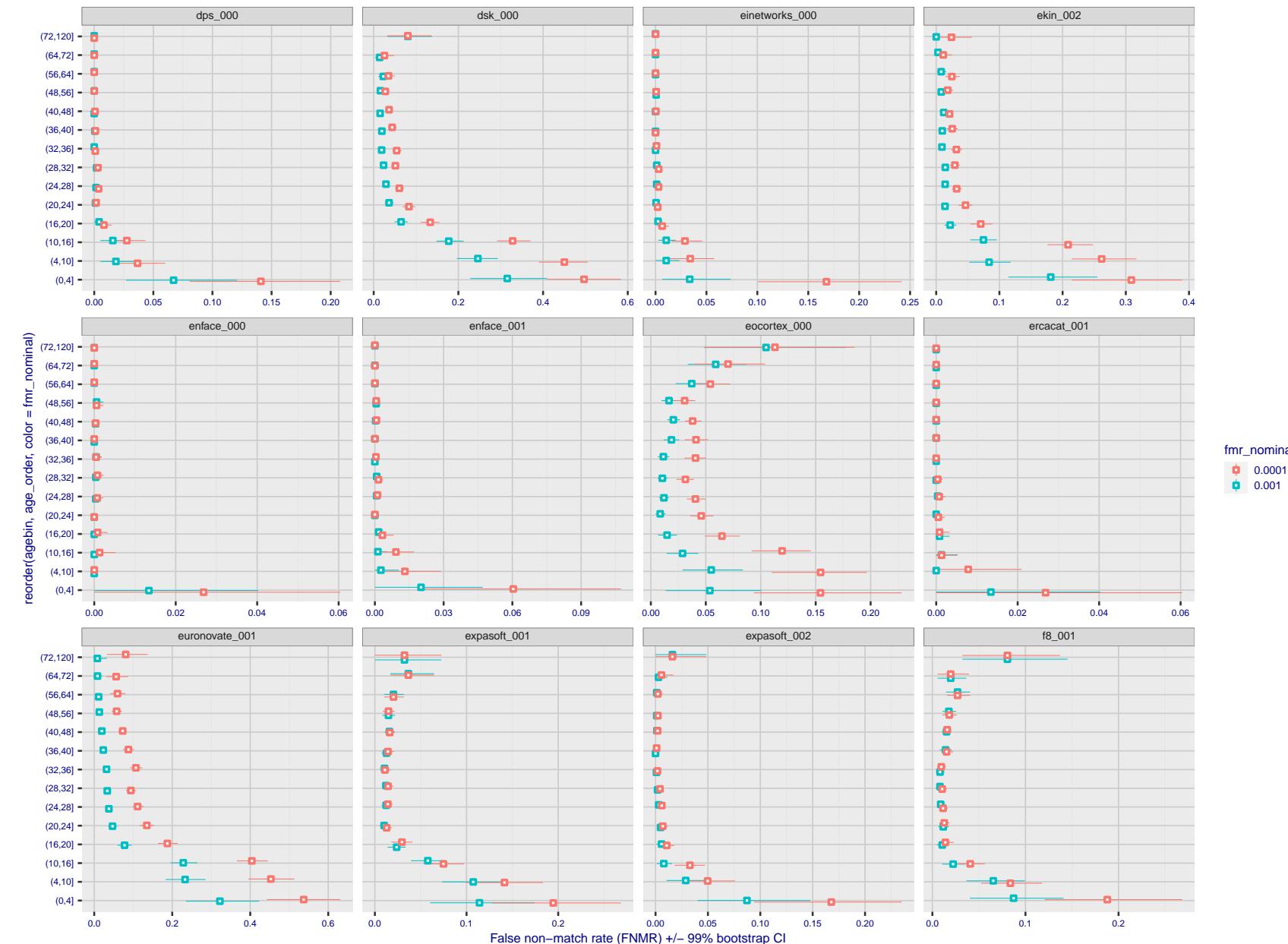


Figure 370: For the visa images, the dots show FNMR by age group for two operating thresholds corresponding to $FMR = \{0.001, 0.0001\}$ computed over all on the order of 10^{10} impostor scores. The FMR in each bin will vary also - see subsequent impostor heatmaps in sec. 3.6.2. Given a pair of face images taken at different times, we assign the comparison to the bin that is the arithmetic average of the subject's ages. This plot shows only the effect of age, not ageing. The number of comparisons in each bin is generally in the thousands, however the first and last bins are computed over 149 and 124 respectively. The error rates in some (adult) cases are zero, and in others the DET is flat so the error rates at the two thresholds are identical. The lines span 1% and 99% of bootstrap replicated FNMR estimates.

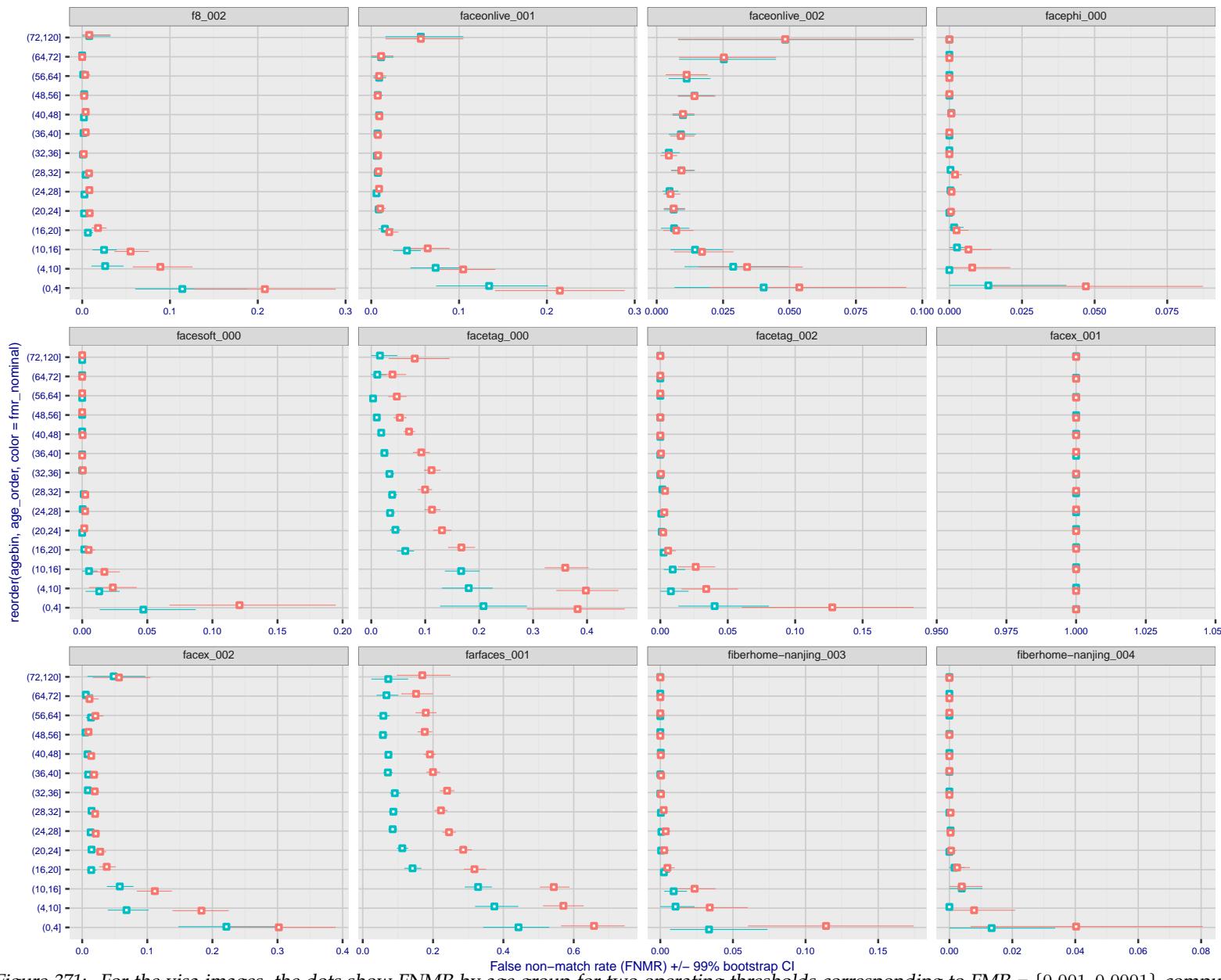


Figure 371: For the visa images, the dots show FNMR by age group for two operating thresholds corresponding to $FMR = \{0.001, 0.0001\}$ computed over all on the order of 10^{10} impostor scores. The FMR in each bin will vary also - see subsequent impostor heatmaps in sec. 3.6.2. Given a pair of face images taken at different times, we assign the comparison to the bin that is the arithmetic average of the subject's ages. This plot shows only the effect of age, not ageing. The number of comparisons in each bin is generally in the thousands, however the first and last bins are computed over 149 and 124 respectively. The error rates in some (adult) cases are zero, and in others the DET is flat so the error rates at the two thresholds are identical. The lines span 1% and 99% of bootstrap replicated FNMR estimates.



Figure 372: For the visa images, the dots show FNMR by age group for two operating thresholds corresponding to $FMR = \{0.001, 0.0001\}$ computed over all on the order of 10^{10} impostor scores. The FMR in each bin will vary also - see subsequent impostor heatmaps in sec. 3.6.2. Given a pair of face images taken at different times, we assign the comparison to the bin that is the arithmetic average of the subject's ages. This plot shows only the effect of age, not ageing. The number of comparisons in each bin is generally in the thousands, however the first and last bins are computed over 149 and 124 respectively. The error rates in some (adult) cases are zero, and in others the DET is flat so the error rates at the two thresholds are identical. The lines span 1% and 99% of bootstrap replicated FNMR estimates.

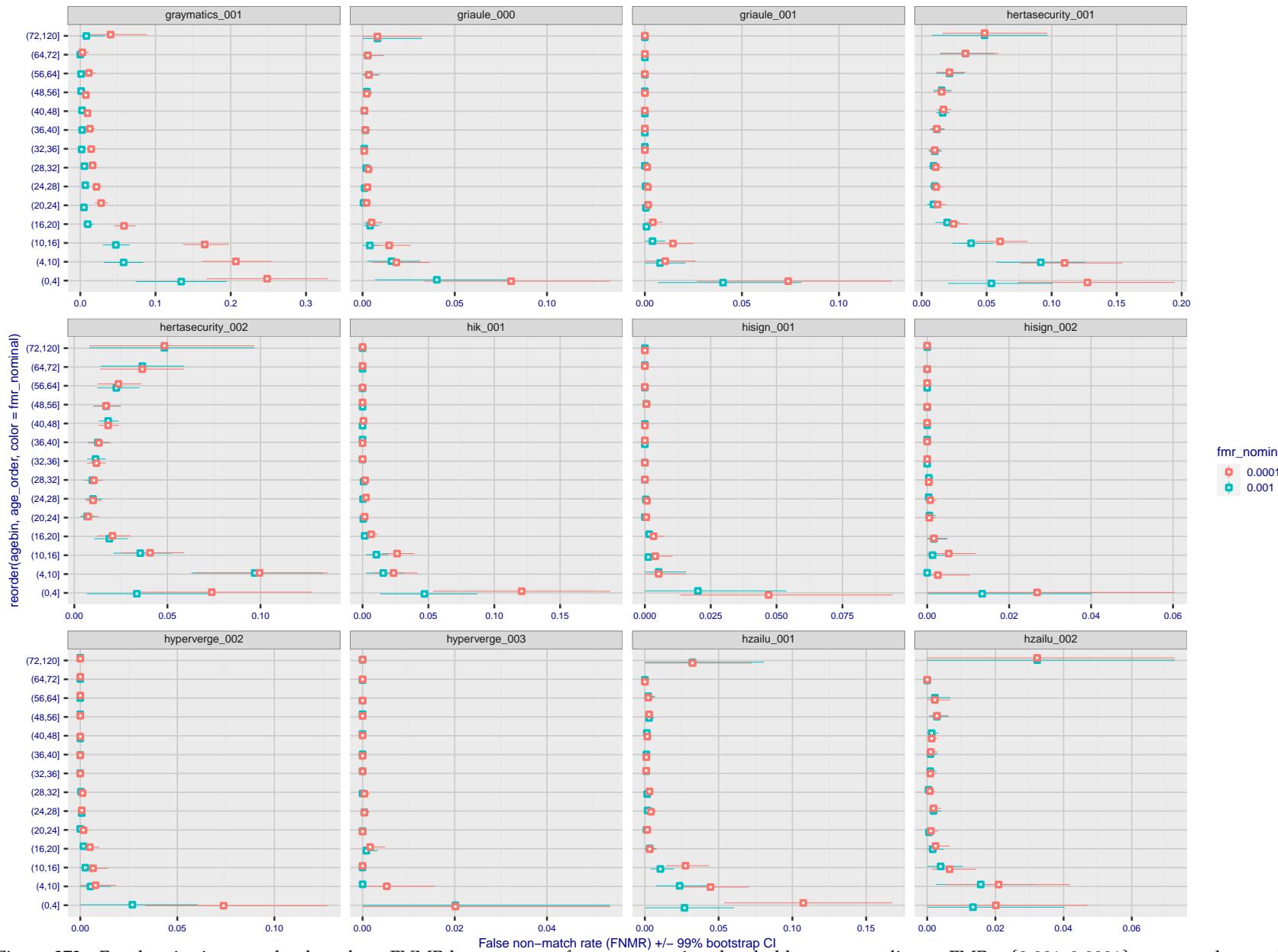


Figure 373: For the visa images, the dots show FNMR by age group for two operating thresholds corresponding to $FMR = \{0.001, 0.0001\}$ computed over all on the order of 10^{10} impostor scores. The FMR in each bin will vary also - see subsequent impostor heatmaps in sec. 3.6.2. Given a pair of face images taken at different times, we assign the comparison to the bin that is the arithmetic average of the subject's ages. This plot shows only the effect of age, not ageing. The number of comparisons in each bin is generally in the thousands, however the first and last bins are computed over 149 and 124 respectively. The error rates in some (adult) cases are zero, and in others the DET is flat so the error rates at the two thresholds are identical. The lines span 1% and 99% of bootstrap replicated FNMR estimates.

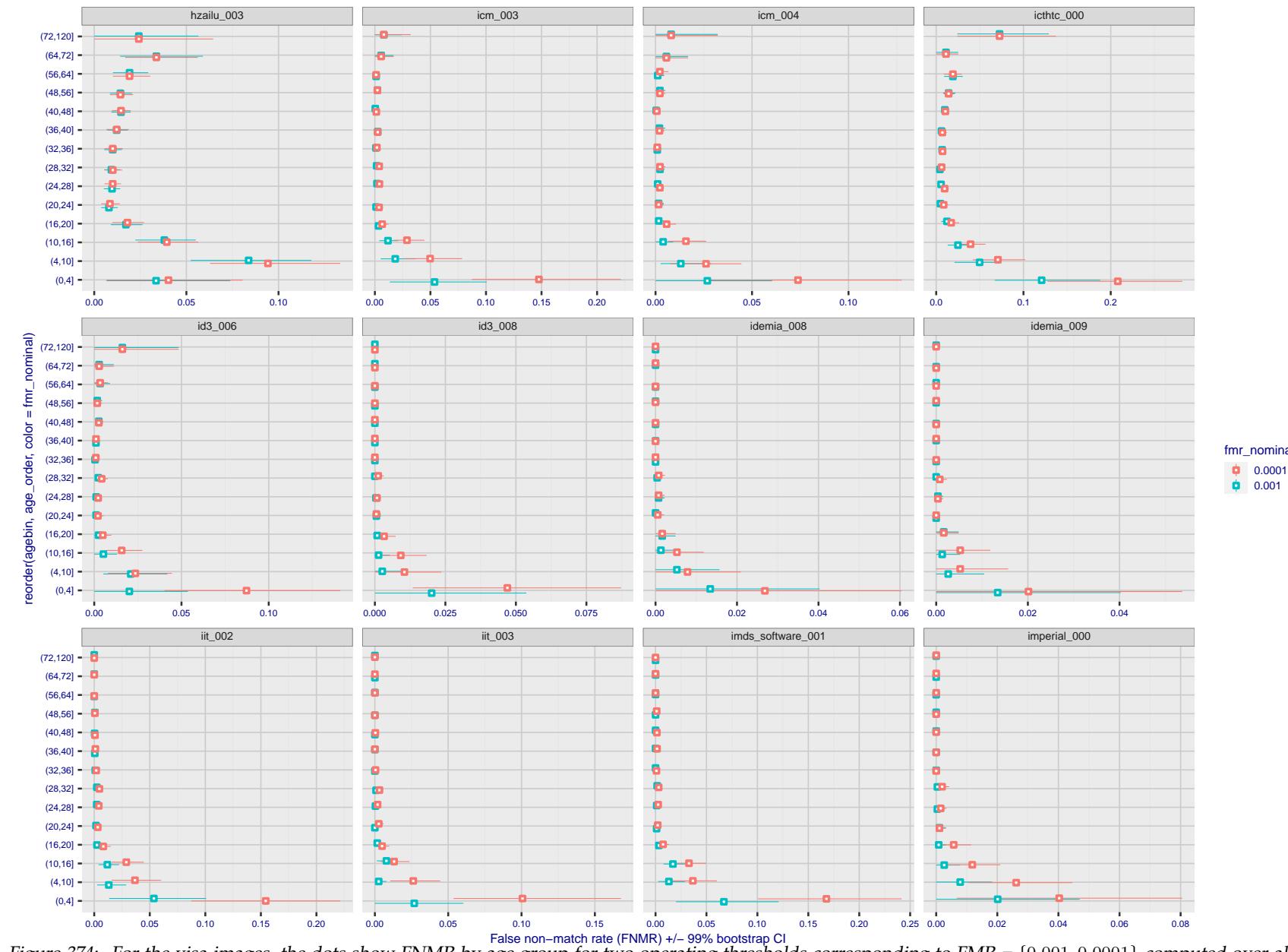


Figure 374: For the visa images, the dots show FNMR by age group for two operating thresholds corresponding to $FMR = \{0.001, 0.0001\}$ computed over all on the order of 10^{10} impostor scores. The FMR in each bin will vary also - see subsequent impostor heatmaps in sec. 3.6.2. Given a pair of face images taken at different times, we assign the comparison to the bin that is the arithmetic average of the subject's ages. This plot shows only the effect of age, not ageing. The number of comparisons in each bin is generally in the thousands, however the first and last bins are computed over 149 and 124 respectively. The error rates in some (adult) cases are zero, and in others the DET is flat so the error rates at the two thresholds are identical. The lines span 1% and 99% of bootstrap replicated FNMR estimates.

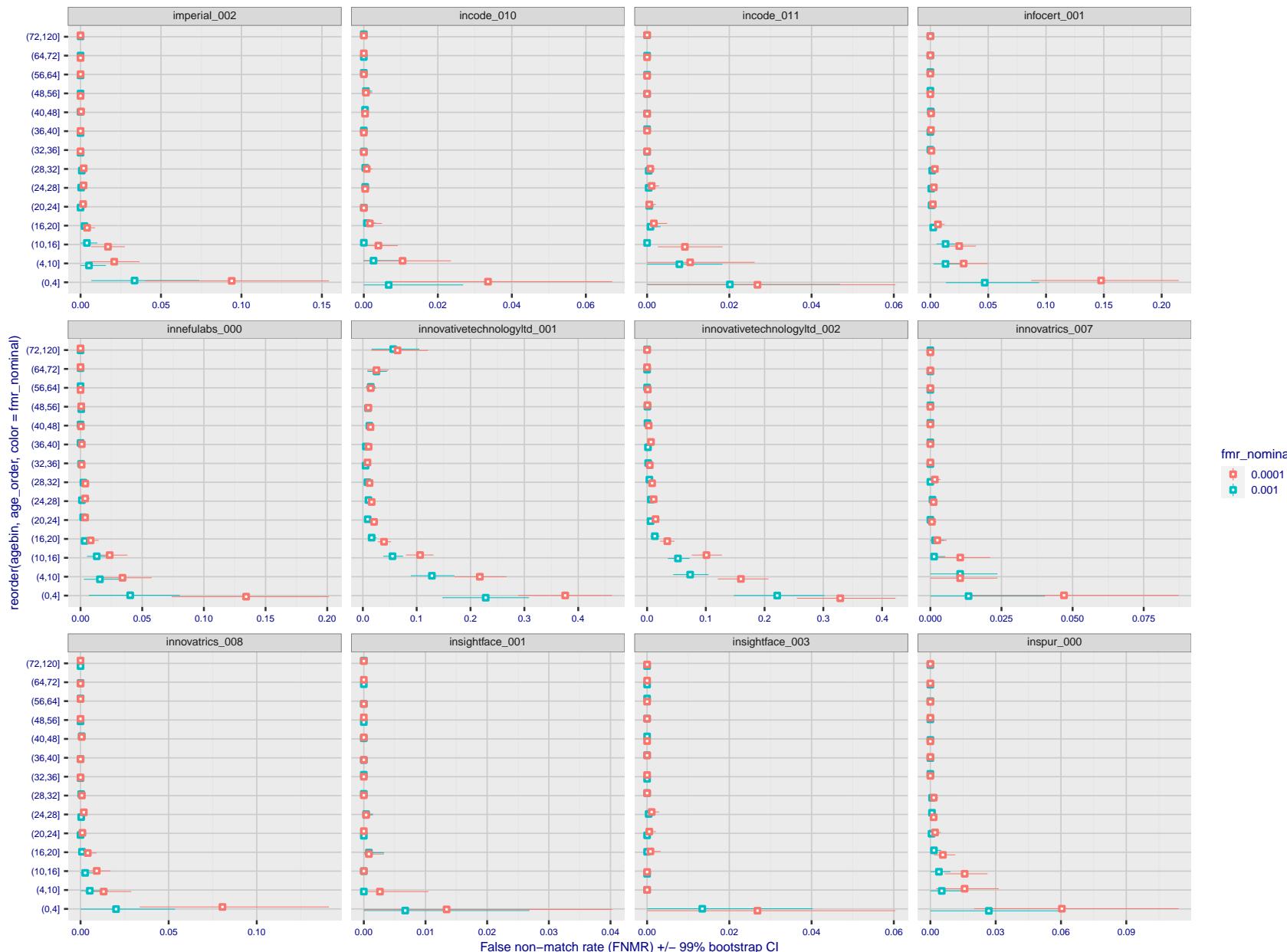


Figure 375: For the visa images, the dots show FNMR by age group for two operating thresholds corresponding to $FMR = \{0.001, 0.0001\}$ computed over all on the order of 10^{10} impostor scores. The FMR in each bin will vary also - see subsequent impostor heatmaps in sec. 3.6.2. Given a pair of face images taken at different times, we assign the comparison to the bin that is the arithmetic average of the subject's ages. This plot shows only the effect of age, not ageing. The number of comparisons in each bin is generally in the thousands, however the first and last bins are computed over 149 and 124 respectively. The error rates in some (adult) cases are zero, and in others the DET is flat so the error rates at the two thresholds are identical. The lines span 1% and 99% of bootstrap replicated FNMR estimates.

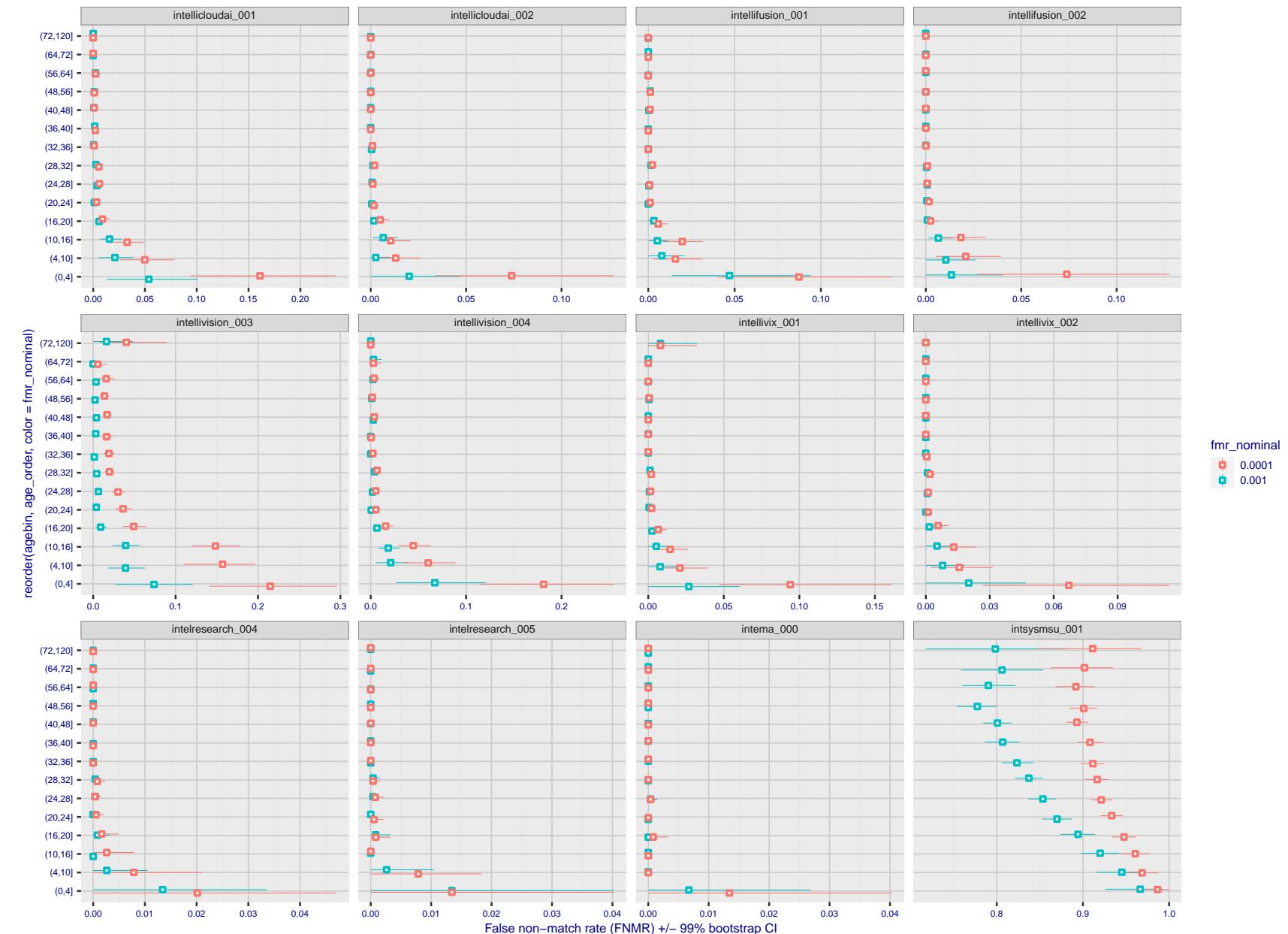


Figure 376: For the visa images, the dots show FNMR by age group for two operating thresholds corresponding to $FMR = \{0.001, 0.0001\}$ computed over all on the order of 10^{10} impostor scores. The FMR in each bin will vary also - see subsequent impostor heatmaps in sec. 3.6.2. Given a pair of face images taken at different times, we assign the comparison to the bin that is the arithmetic average of the subject's ages. This plot shows only the effect of age, not ageing. The number of comparisons in each bin is generally in the thousands, however the first and last bins are computed over 149 and 124 respectively. The error rates in some (adult) cases are zero, and in others the DET is flat so the error rates at the two thresholds are identical. The lines span 1% and 99% of bootstrap replicated FNMR estimates.

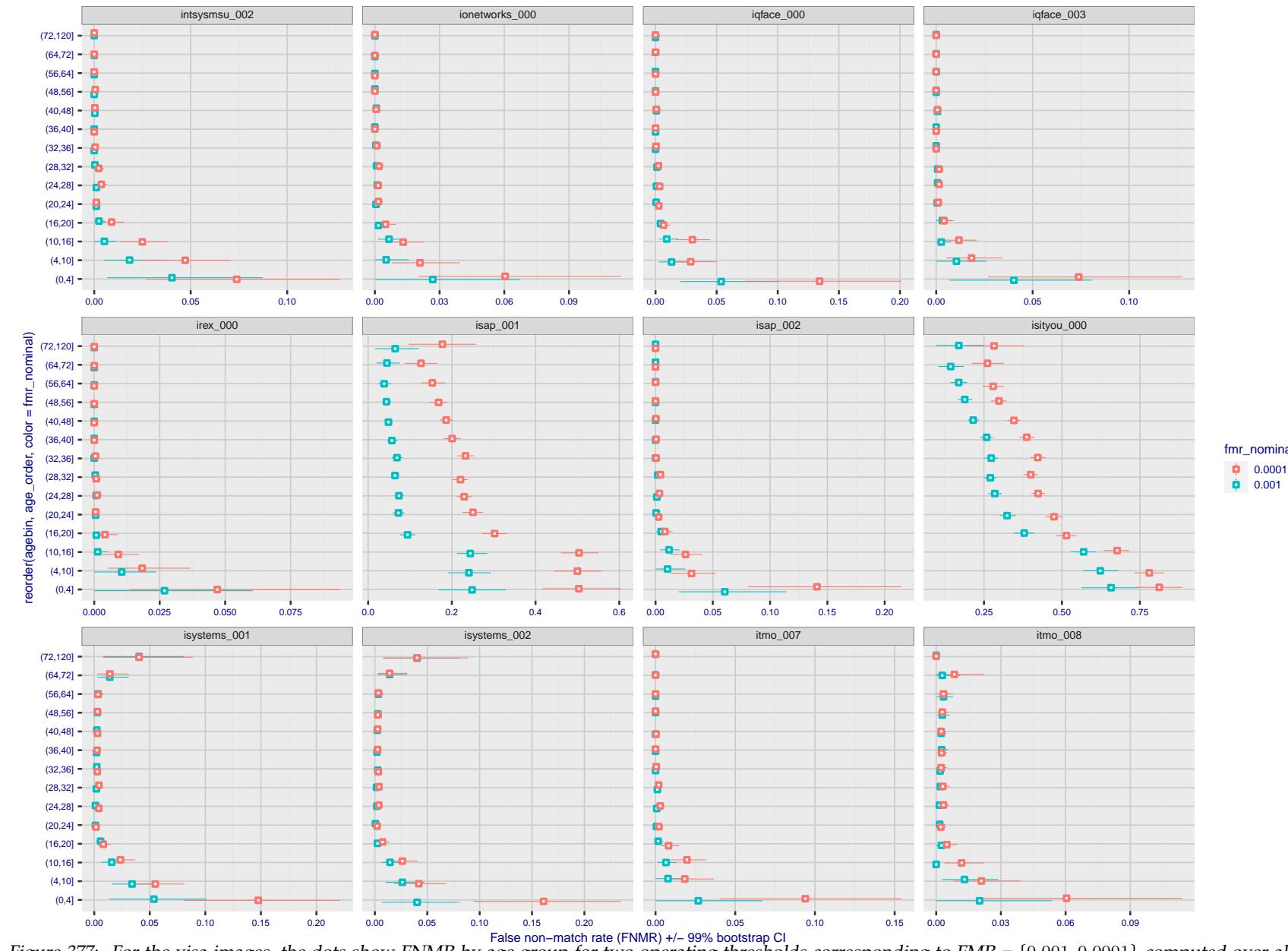


Figure 377: For the visa images, the dots show FNMR by age group for two operating thresholds corresponding to $FMR = \{0.001, 0.0001\}$ computed over all on the order of 10^{10} impostor scores. The FMR in each bin will vary also - see subsequent impostor heatmaps in sec. 3.6.2. Given a pair of face images taken at different times, we assign the comparison to the bin that is the arithmetic average of the subject's ages. This plot shows only the effect of age, not ageing. The number of comparisons in each bin is generally in the thousands, however the first and last bins are computed over 149 and 124 respectively. The error rates in some (adult) cases are zero, and in others the DET is flat so the error rates at the two thresholds are identical. The lines span 1% and 99% of bootstrap replicated FNMR estimates.

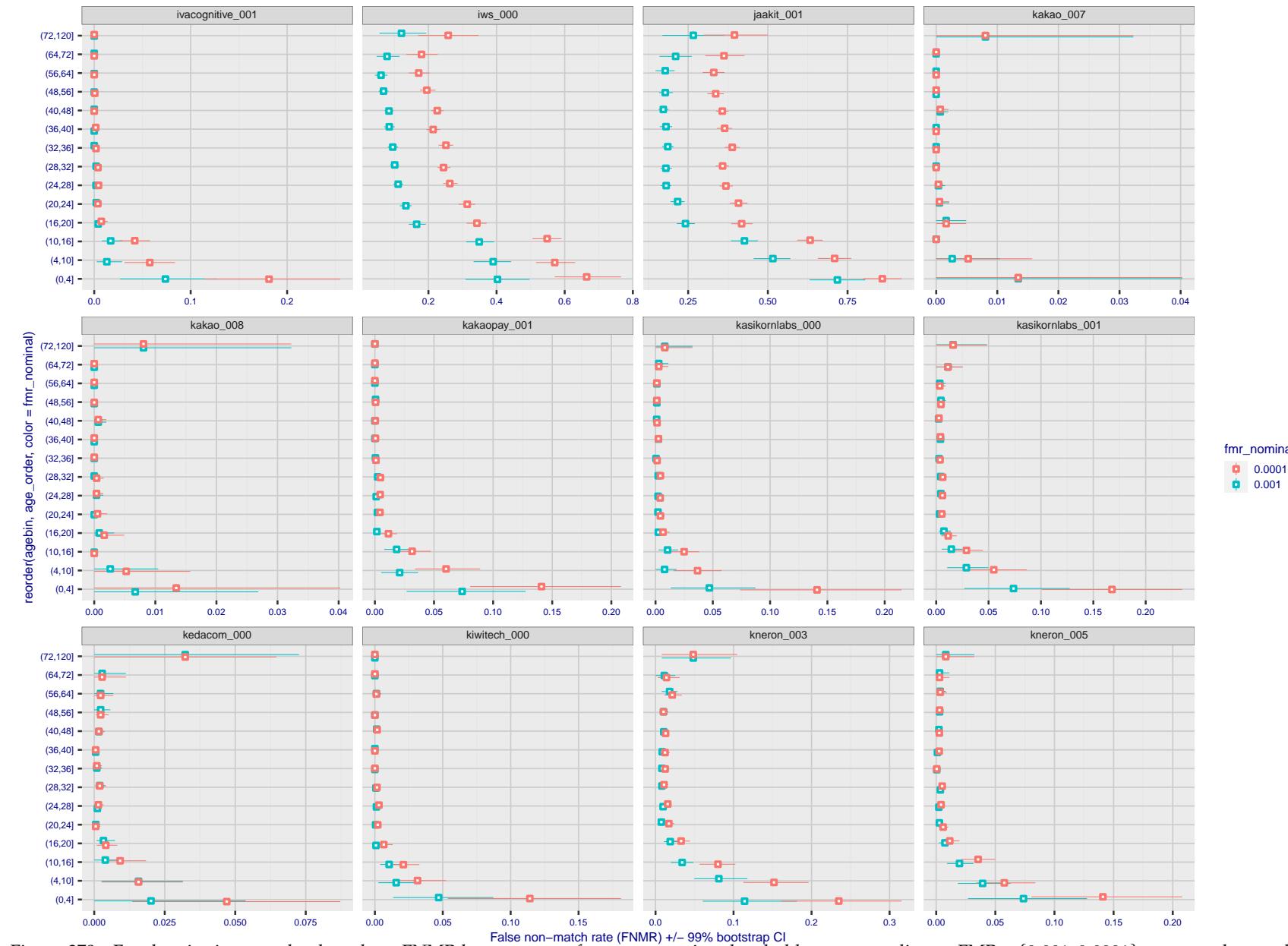
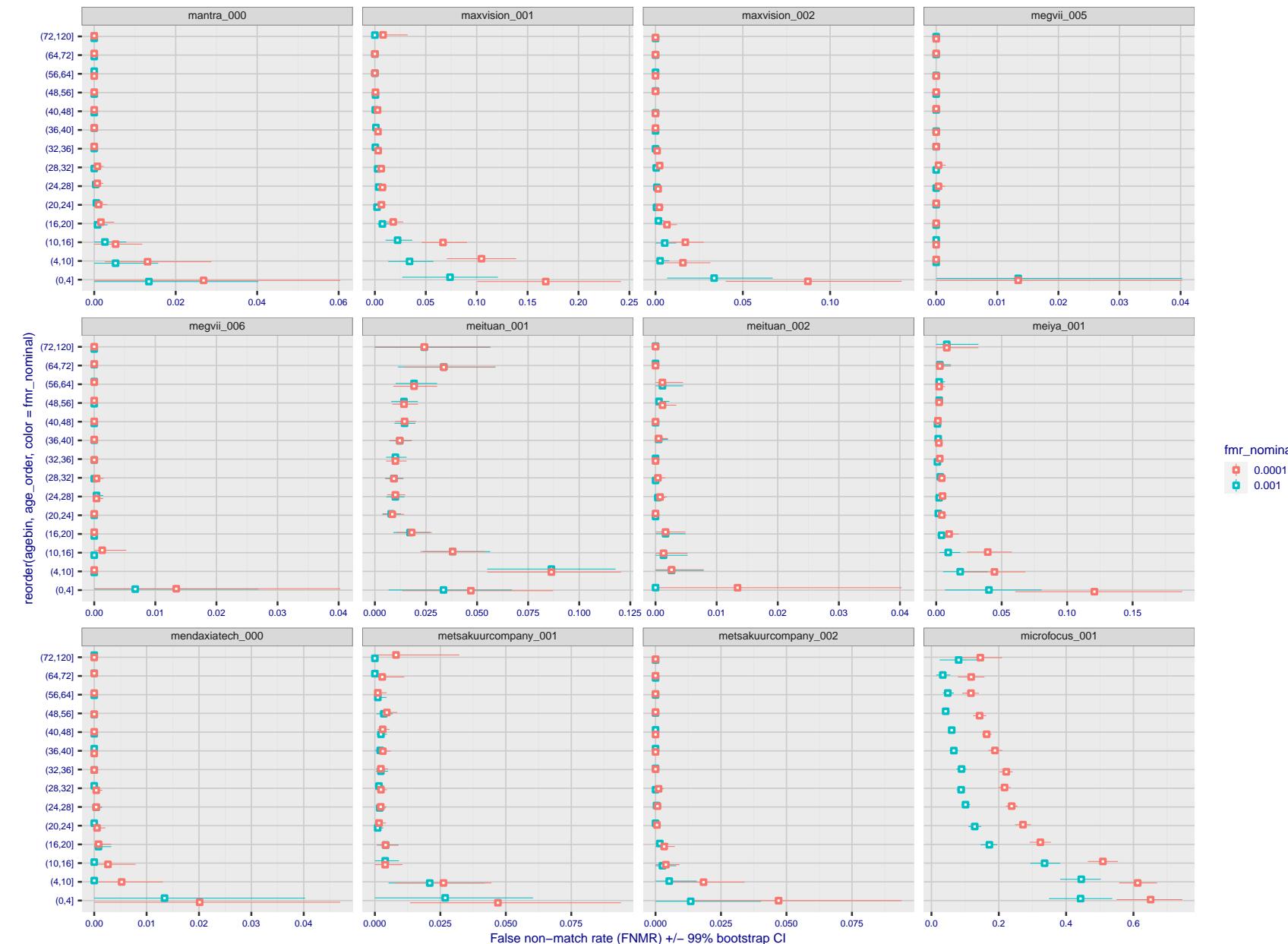


Figure 378: For the visa images, the dots show FNMR by age group for two operating thresholds corresponding to $FMR = \{0.001, 0.0001\}$ computed over all on the order of 10^{10} impostor scores. The FMR in each bin will vary also - see subsequent impostor heatmaps in sec. 3.6.2. Given a pair of face images taken at different times, we assign the comparison to the bin that is the arithmetic average of the subject's ages. This plot shows only the effect of age, not ageing. The number of comparisons in each bin is generally in the thousands, however the first and last bins are computed over 149 and 124 respectively. The error rates in some (adult) cases are zero, and in others the DET is flat so the error rates at the two thresholds are identical. The lines span 1% and 99% of bootstrap replicated FNMR estimates.



Figure 379: For the visa images, the dots show FNMR by age group for two operating thresholds corresponding to $FMR = \{0.001, 0.0001\}$ computed over all on the order of 10^{10} impostor scores. The FMR in each bin will vary also - see subsequent impostor heatmaps in sec. 3.6.2. Given a pair of face images taken at different times, we assign the comparison to the bin that is the arithmetic average of the subject's ages. This plot shows only the effect of age, not ageing. The number of comparisons in each bin is generally in the thousands, however the first and last bins are computed over 149 and 124 respectively. The error rates in some (adult) cases are zero, and in others the DET is flat so the error rates at the two thresholds are identical. The lines span 1% and 99% of bootstrap replicated FNMR estimates.



fmr_nominal
0.0001
0.001

Figure 380: For the visa images, the dots show FNMR by age group for two operating thresholds corresponding to $FMR = \{0.001, 0.0001\}$ computed over all on the order of 10^{10} impostor scores. The FMR in each bin will vary also - see subsequent impostor heatmaps in sec. 3.6.2. Given a pair of face images taken at different times, we assign the comparison to the bin that is the arithmetic average of the subject's ages. This plot shows only the effect of age, not ageing. The number of comparisons in each bin is generally in the thousands, however the first and last bins are computed over 149 and 124 respectively. The error rates in some (adult) cases are zero, and in others the DET is flat so the error rates at the two thresholds are identical. The lines span 1% and 99% of bootstrap replicated FNMR estimates.



Figure 381: For the visa images, the dots show FNMR by age group for two operating thresholds corresponding to $FMR = \{0.001, 0.0001\}$ computed over all on the order of 10^{10} impostor scores. The FMR in each bin will vary also - see subsequent impostor heatmaps in sec. 3.6.2. Given a pair of face images taken at different times, we assign the comparison to the bin that is the arithmetic average of the subject's ages. This plot shows only the effect of age, not ageing. The number of comparisons in each bin is generally in the thousands, however the first and last bins are computed over 149 and 124 respectively. The error rates in some (adult) cases are zero, and in others the DET is flat so the error rates at the two thresholds are identical. The lines span 1% and 99% of bootstrap replicated FNMR estimates.

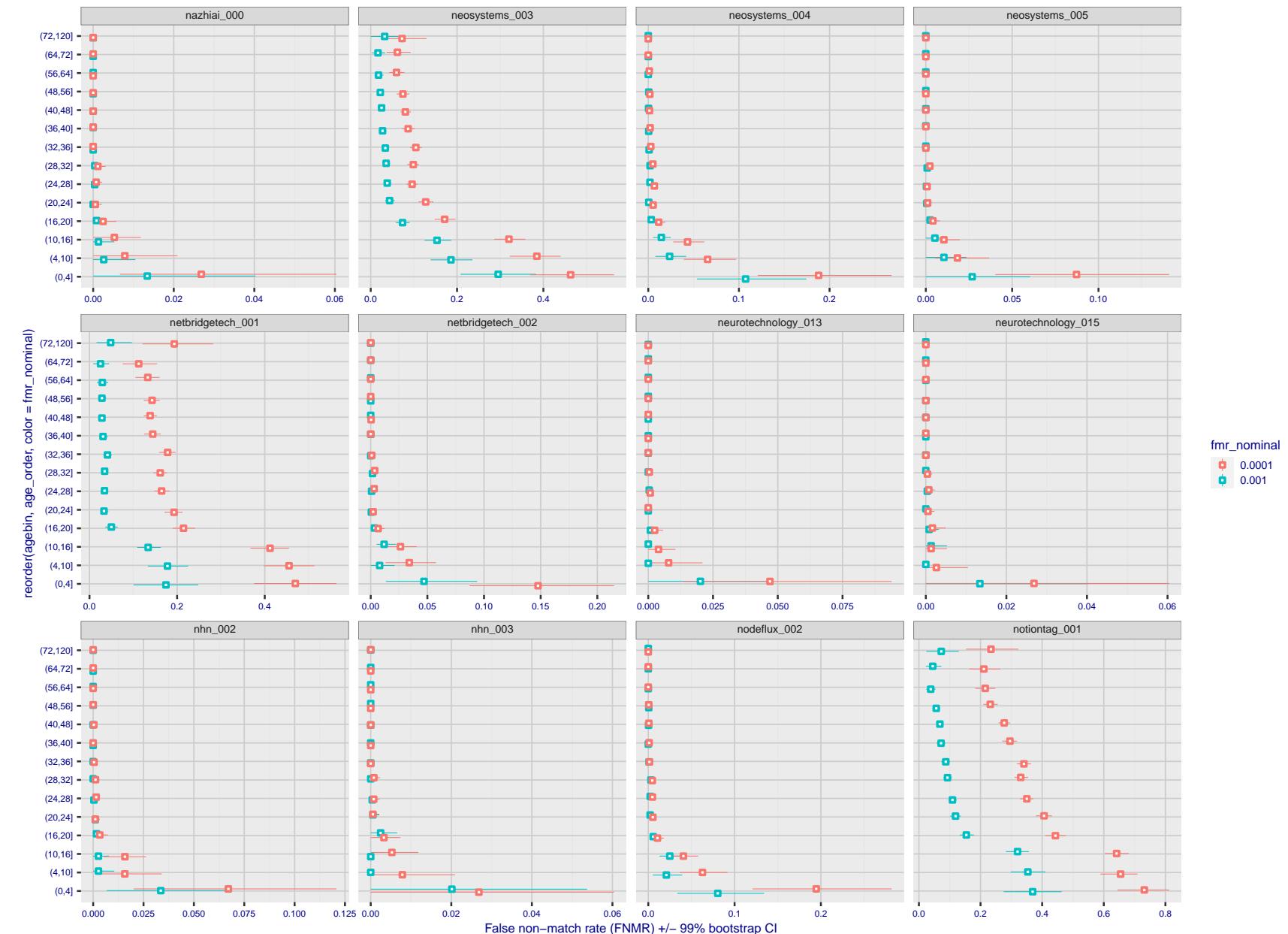


Figure 382: For the visa images, the dots show FNMR by age group for two operating thresholds corresponding to $FMR = \{0.001, 0.0001\}$ computed over all on the order of 10^{10} impostor scores. The FMR in each bin will vary also - see subsequent impostor heatmaps in sec. 3.6.2. Given a pair of face images taken at different times, we assign the comparison to the bin that is the arithmetic average of the subject's ages. This plot shows only the effect of age, not ageing. The number of comparisons in each bin is generally in the thousands, however the first and last bins are computed over 149 and 124 respectively. The error rates in some (adult) cases are zero, and in others the DET is flat so the error rates at the two thresholds are identical. The lines span 1% and 99% of bootstrap replicated FNMR estimates.

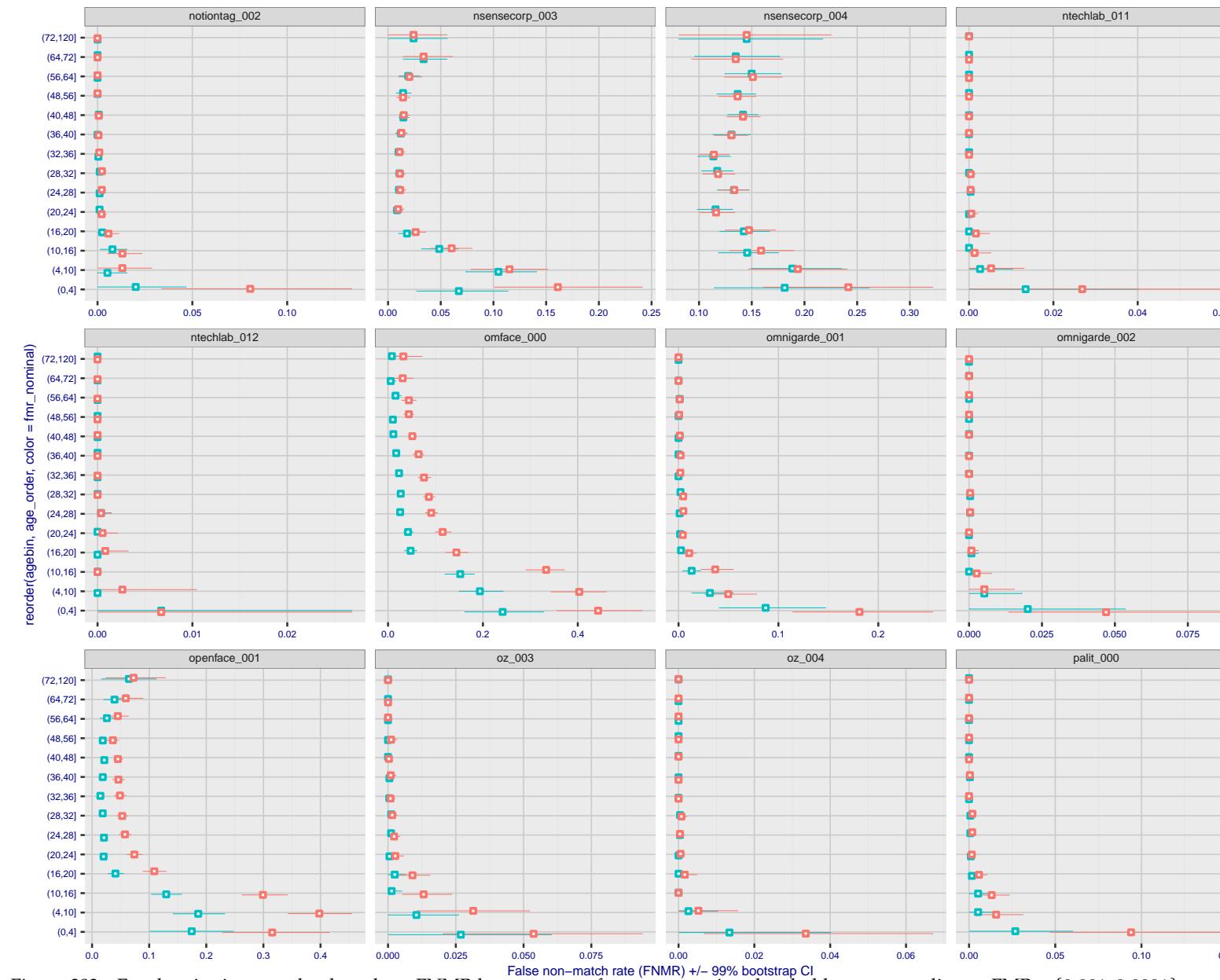


Figure 383: For the visa images, the dots show FNMR by age group for two operating thresholds corresponding to $FMR = \{0.001, 0.0001\}$ computed over all on the order of 10^{10} impostor scores. The FMR in each bin will vary also - see subsequent impostor heatmaps in sec. 3.6.2. Given a pair of face images taken at different times, we assign the comparison to the bin that is the arithmetic average of the subject's ages. This plot shows only the effect of age, not ageing. The number of comparisons in each bin is generally in the thousands, however the first and last bins are computed over 149 and 124 respectively. The error rates in some (adult) cases are zero, and in others the DET is flat so the error rates at the two thresholds are identical. The lines span 1% and 99% of bootstrap replicated FNMR estimates.



Figure 384: For the visa images, the dots show FNMR by age group for two operating thresholds corresponding to $FMR = \{0.001, 0.0001\}$ computed over all on the order of 10^{10} impostor scores. The FMR in each bin will vary also - see subsequent impostor heatmaps in sec. 3.6.2. Given a pair of face images taken at different times, we assign the comparison to the bin that is the arithmetic average of the subject's ages. This plot shows only the effect of age, not ageing. The number of comparisons in each bin is generally in the thousands, however the first and last bins are computed over 149 and 124 respectively. The error rates in some (adult) cases are zero, and in others the DET is flat so the error rates at the two thresholds are identical. The lines span 1% and 99% of bootstrap replicated FNMR estimates.



Figure 385: For the visa images, the dots show FNMR by age group for two operating thresholds corresponding to $FMR = \{0.001, 0.0001\}$ computed over all on the order of 10^{10} impostor scores. The FMR in each bin will vary also - see subsequent impostor heatmaps in sec. 3.6.2. Given a pair of face images taken at different times, we assign the comparison to the bin that is the arithmetic average of the subject's ages. This plot shows only the effect of age, not ageing. The number of comparisons in each bin is generally in the thousands, however the first and last bins are computed over 149 and 124 respectively. The error rates in some (adult) cases are zero, and in others the DET is flat so the error rates at the two thresholds are identical. The lines span 1% and 99% of bootstrap replicated FNMR estimates.



Figure 386: For the visa images, the dots show FNMR by age group for two operating thresholds corresponding to $FMR = \{0.001, 0.0001\}$ computed over all on the order of 10^{10} impostor scores. The FMR in each bin will vary also - see subsequent impostor heatmaps in sec. 3.6.2. Given a pair of face images taken at different times, we assign the comparison to the bin that is the arithmetic average of the subject's ages. This plot shows only the effect of age, not ageing. The number of comparisons in each bin is generally in the thousands, however the first and last bins are computed over 149 and 124 respectively. The error rates in some (adult) cases are zero, and in others the DET is flat so the error rates at the two thresholds are identical. The lines span 1% and 99% of bootstrap replicated FNMR estimates.



Figure 387: For the visa images, the dots show FNMR by age group for two operating thresholds corresponding to $FMR = \{0.001, 0.0001\}$ computed over all on the order of 10^{10} impostor scores. The FMR in each bin will vary also - see subsequent impostor heatmaps in sec. 3.6.2. Given a pair of face images taken at different times, we assign the comparison to the bin that is the arithmetic average of the subject's ages. This plot shows only the effect of age, not ageing. The number of comparisons in each bin is generally in the thousands, however the first and last bins are computed over 149 and 124 respectively. The error rates in some (adult) cases are zero, and in others the DET is flat so the error rates at the two thresholds are identical. The lines span 1% and 99% of bootstrap replicated FNMR estimates.

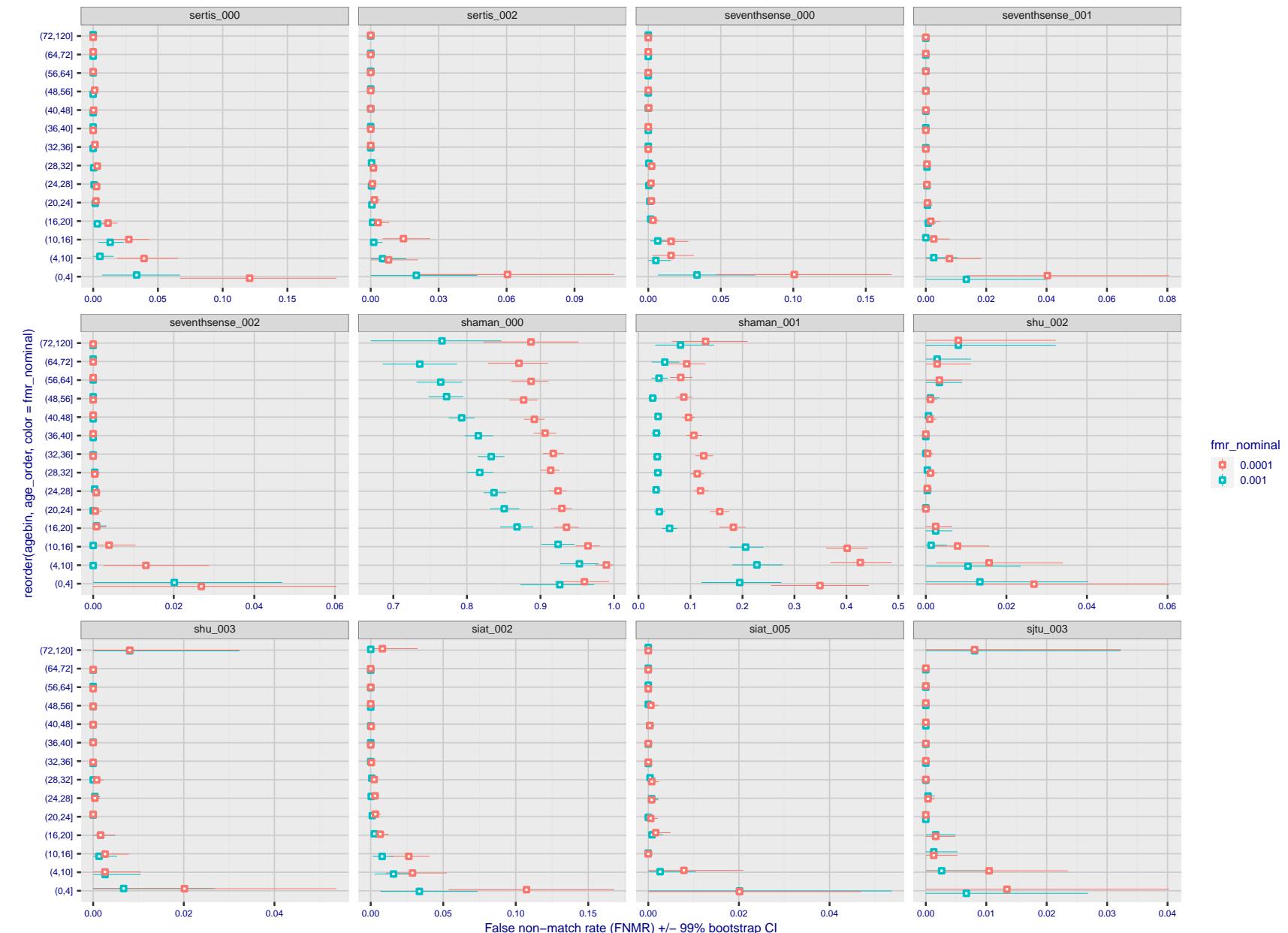


Figure 388: For the visa images, the dots show FNMR by age group for two operating thresholds corresponding to $FMR = \{0.001, 0.0001\}$ computed over all on the order of 10^{10} impostor scores. The FMR in each bin will vary also - see subsequent impostor heatmaps in sec. 3.6.2. Given a pair of face images taken at different times, we assign the comparison to the bin that is the arithmetic average of the subject's ages. This plot shows only the effect of age, not ageing. The number of comparisons in each bin is generally in the thousands, however the first and last bins are computed over 149 and 124 respectively. The error rates in some (adult) cases are zero, and in others the DET is flat so the error rates at the two thresholds are identical. The lines span 1% and 99% of bootstrap replicated FNMR estimates.

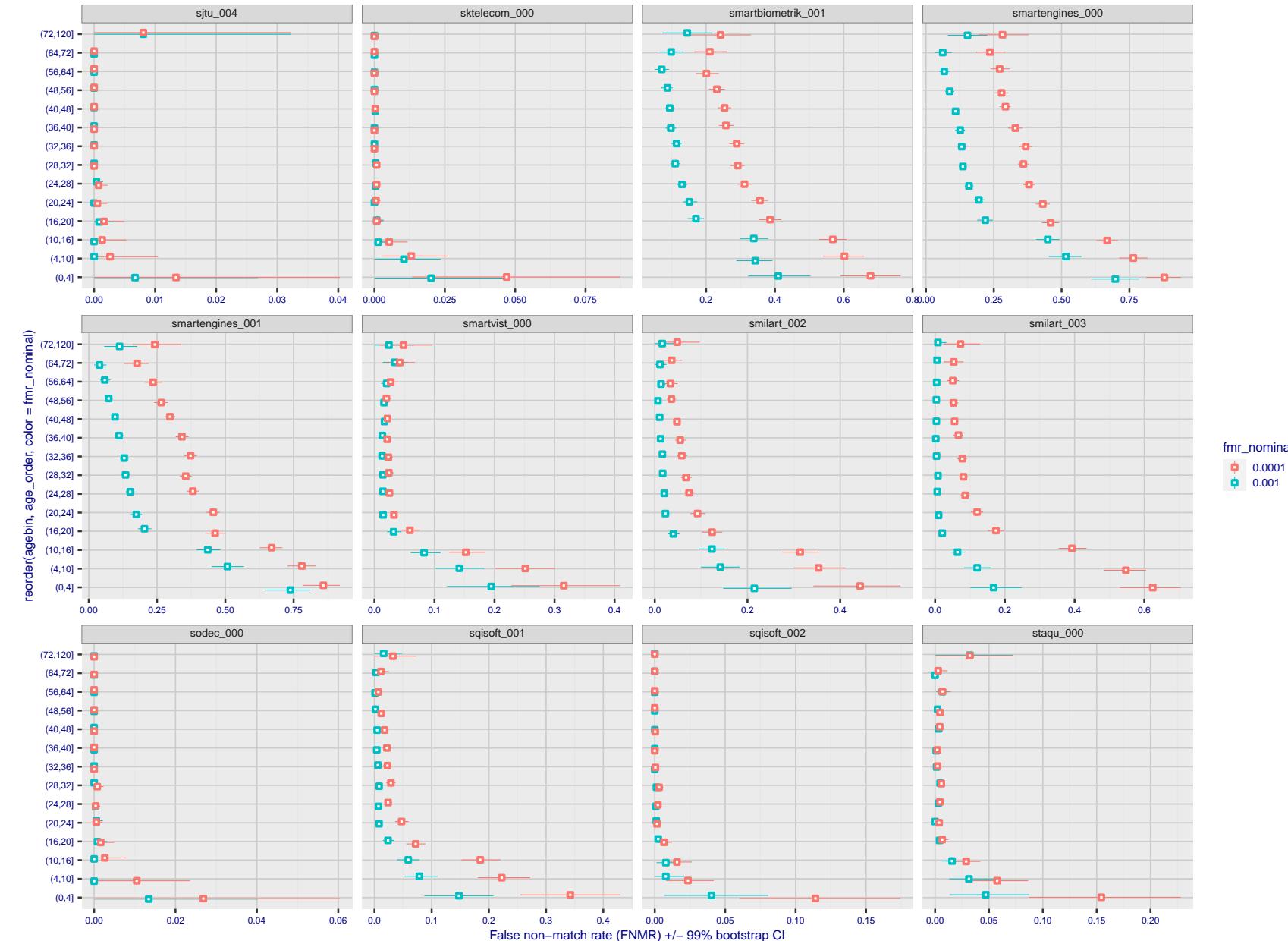


Figure 389: For the visa images, the dots show FNMR by age group for two operating thresholds corresponding to $FMR = \{0.001, 0.0001\}$ computed over all on the order of 10^{10} impostor scores. The FMR in each bin will vary also - see subsequent impostor heatmaps in sec. 3.6.2. Given a pair of face images taken at different times, we assign the comparison to the bin that is the arithmetic average of the subject's ages. This plot shows only the effect of age, not ageing. The number of comparisons in each bin is generally in the thousands, however the first and last bins are computed over 149 and 124 respectively. The error rates in some (adult) cases are zero, and in others the DET is flat so the error rates at the two thresholds are identical. The lines span 1% and 99% of bootstrap replicated FNMR estimates.

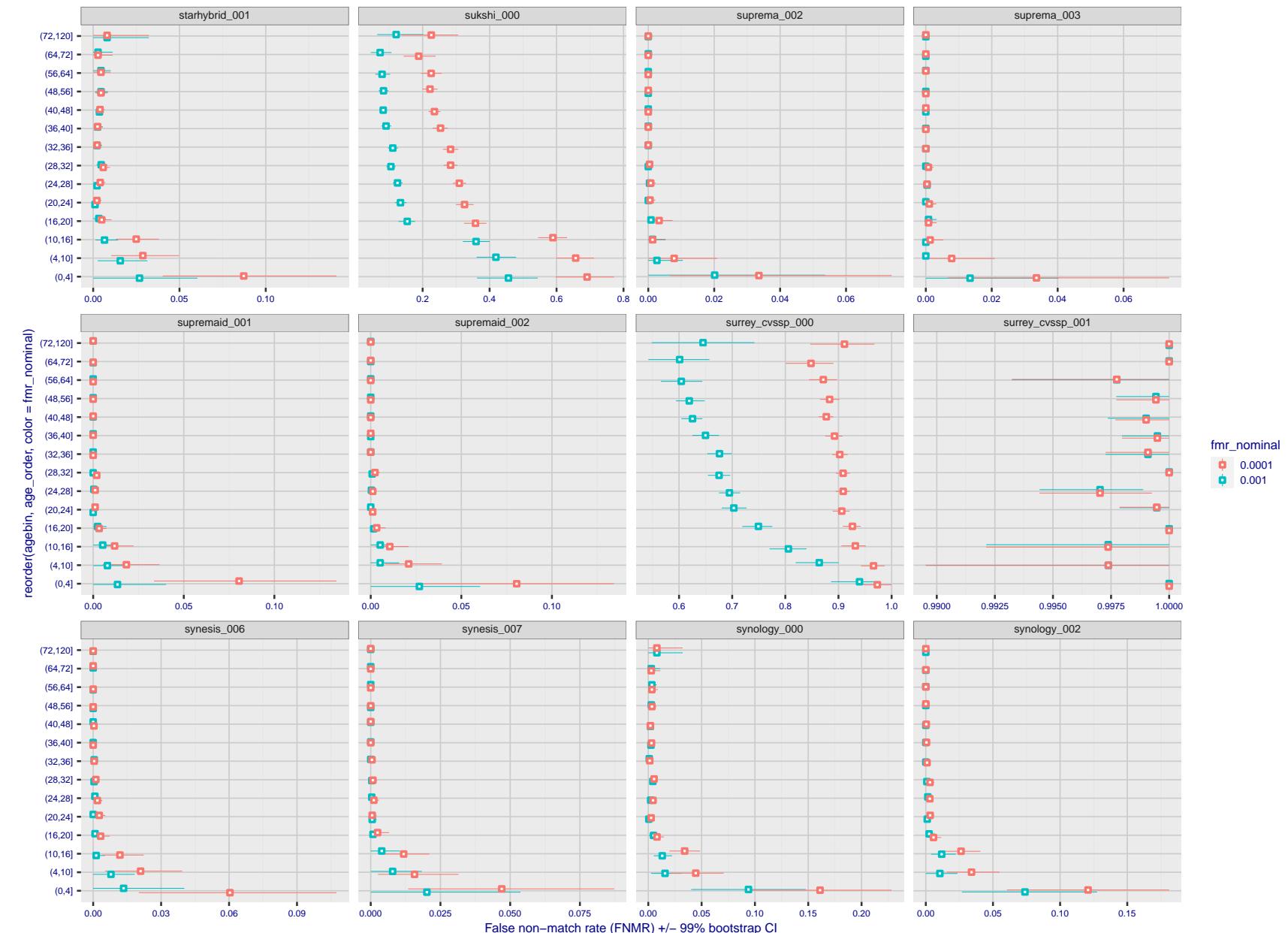


Figure 390: For the visa images, the dots show FNMR by age group for two operating thresholds corresponding to $FMR = \{0.001, 0.0001\}$ computed over all on the order of 10^{10} impostor scores. The FMR in each bin will vary also - see subsequent impostor heatmaps in sec. 3.6.2. Given a pair of face images taken at different times, we assign the comparison to the bin that is the arithmetic average of the subject's ages. This plot shows only the effect of age, not ageing. The number of comparisons in each bin is generally in the thousands, however the first and last bins are computed over 149 and 124 respectively. The error rates in some (adult) cases are zero, and in others the DET is flat so the error rates at the two thresholds are identical. The lines span 1% and 99% of bootstrap replicated FNMR estimates.



Figure 391: For the visa images, the dots show FNMR by age group for two operating thresholds corresponding to $FMR = \{0.001, 0.0001\}$ computed over all on the order of 10^{10} impostor scores. The FMR in each bin will vary also - see subsequent impostor heatmaps in sec. 3.6.2. Given a pair of face images taken at different times, we assign the comparison to the bin that is the arithmetic average of the subject's ages. This plot shows only the effect of age, not ageing. The number of comparisons in each bin is generally in the thousands, however the first and last bins are computed over 149 and 124 respectively. The error rates in some (adult) cases are zero, and in others the DET is flat so the error rates at the two thresholds are identical. The lines span 1% and 99% of bootstrap replicated FNMR estimates.

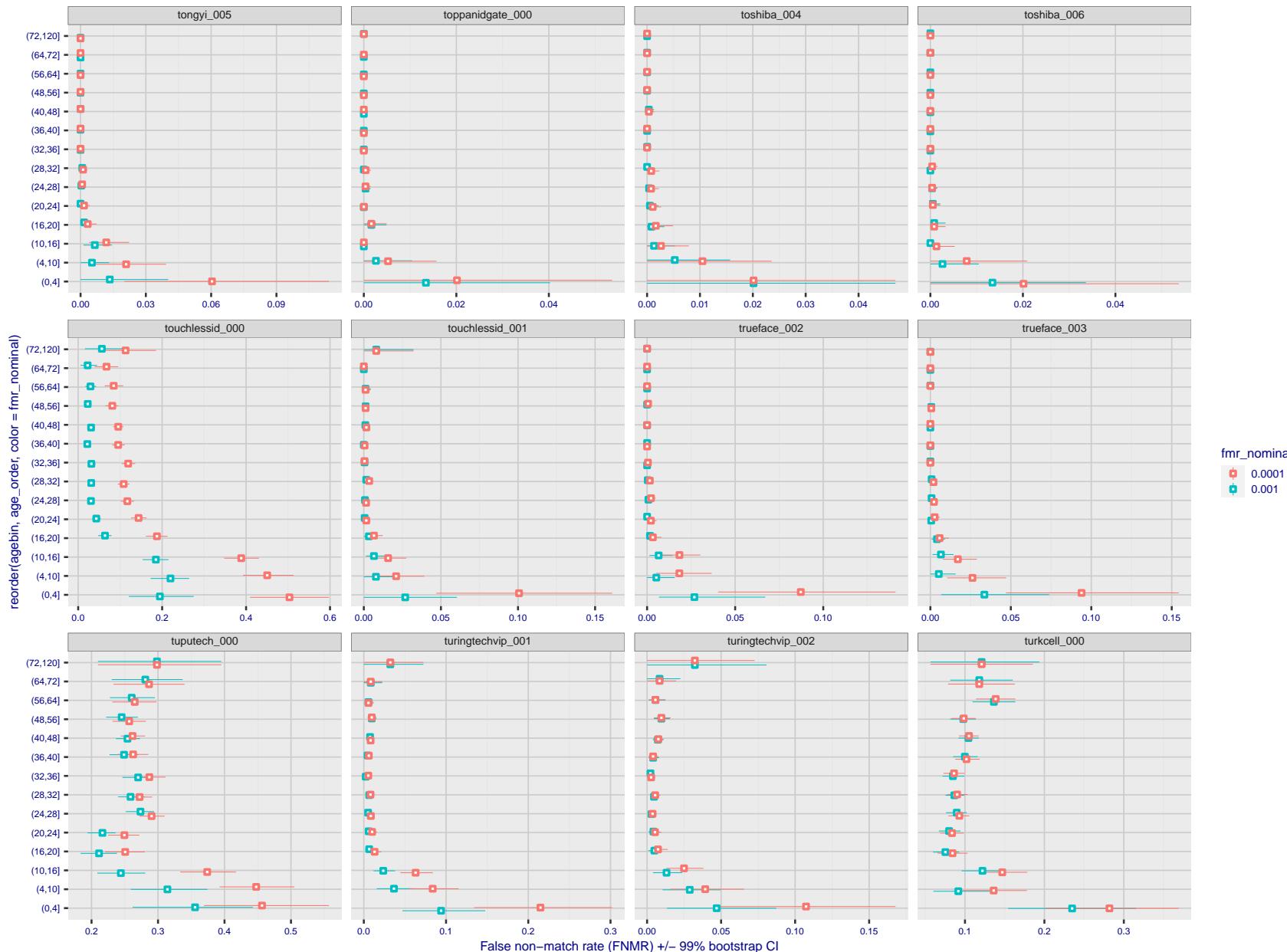


Figure 392: For the visa images, the dots show FNMR by age group for two operating thresholds corresponding to $FMR = \{0.001, 0.0001\}$ computed over all on the order of 10^{10} impostor scores. The FMR in each bin will vary also - see subsequent impostor heatmaps in sec. 3.6.2. Given a pair of face images taken at different times, we assign the comparison to the bin that is the arithmetic average of the subject's ages. This plot shows only the effect of age, not ageing. The number of comparisons in each bin is generally in the thousands, however the first and last bins are computed over 149 and 124 respectively. The error rates in some (adult) cases are zero, and in others the DET is flat so the error rates at the two thresholds are identical. The lines span 1% and 99% of bootstrap replicated FNMR estimates.

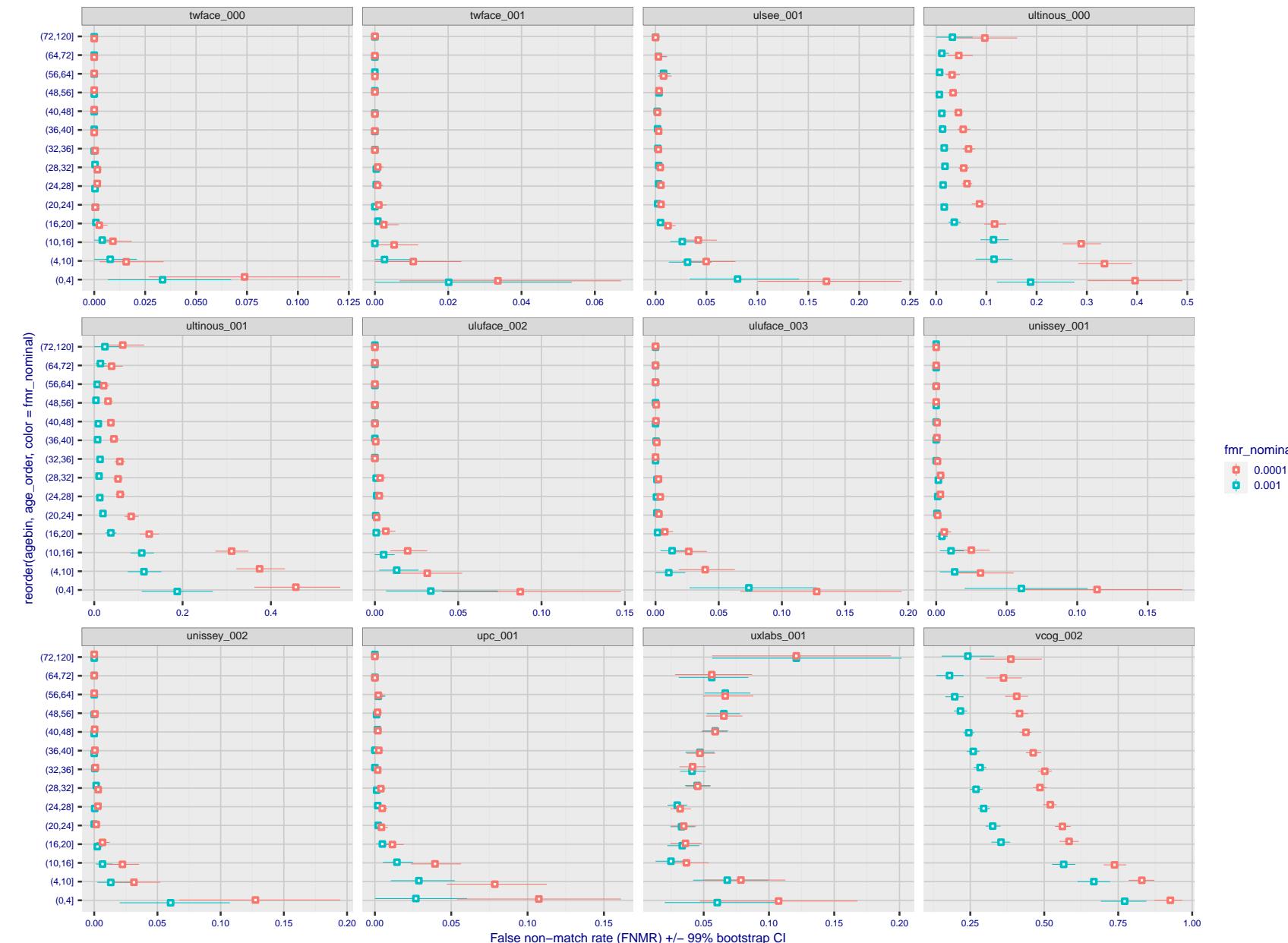


Figure 393: For the visa images, the dots show FNMR by age group for two operating thresholds corresponding to $FMR = \{0.001, 0.0001\}$ computed over all on the order of 10^{10} impostor scores. The FMR in each bin will vary also - see subsequent impostor heatmaps in sec. 3.6.2. Given a pair of face images taken at different times, we assign the comparison to the bin that is the arithmetic average of the subject's ages. This plot shows only the effect of age, not ageing. The number of comparisons in each bin is generally in the thousands, however the first and last bins are computed over 149 and 124 respectively. The error rates in some (adult) cases are zero, and in others the DET is flat so the error rates at the two thresholds are identical. The lines span 1% and 99% of bootstrap replicated FNMR estimates.

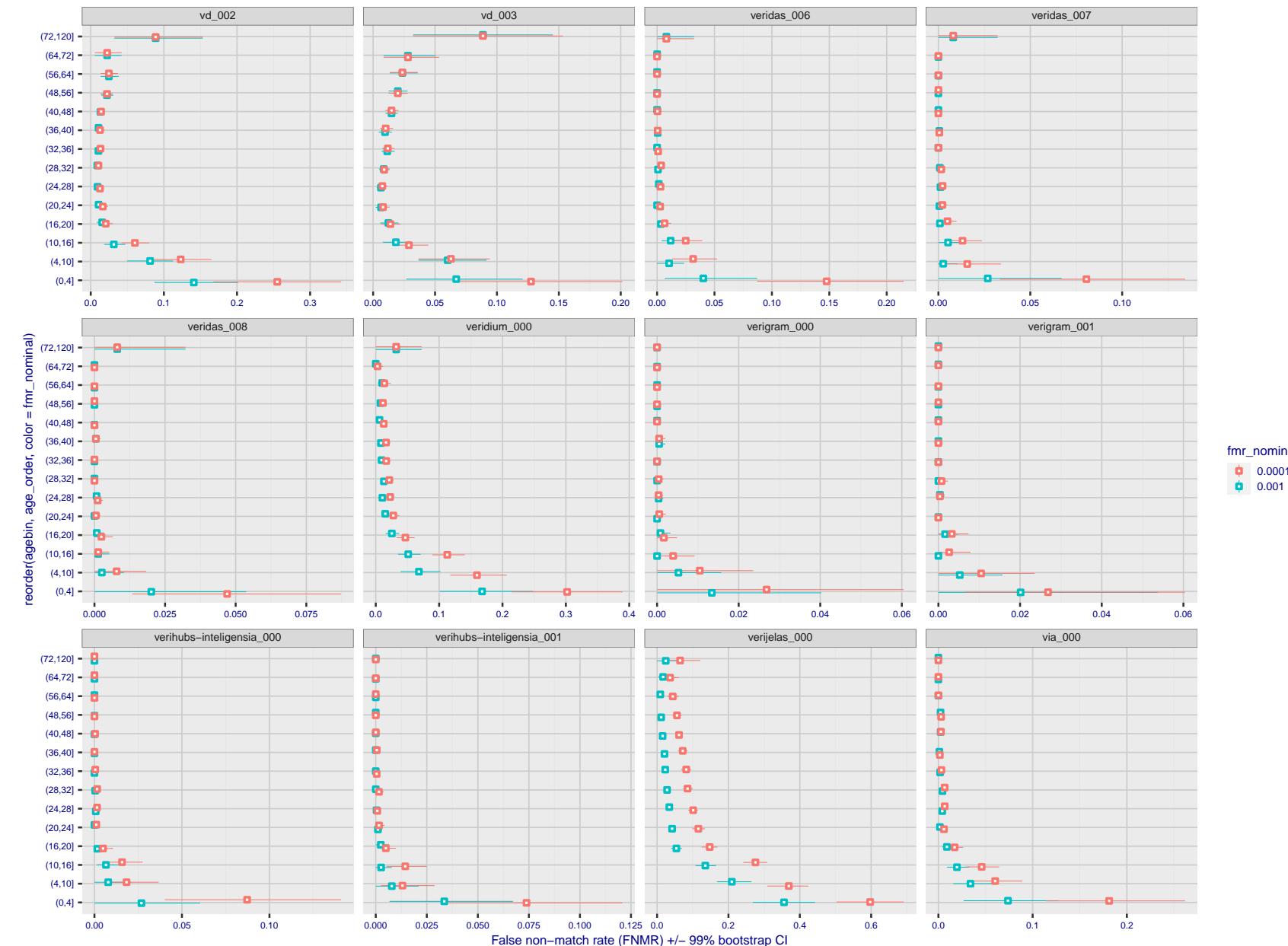


Figure 394: For the visa images, the dots show FNMR by age group for two operating thresholds corresponding to $FMR = \{0.001, 0.0001\}$ computed over all on the order of 10^{10} impostor scores. The FMR in each bin will vary also - see subsequent impostor heatmaps in sec. 3.6.2. Given a pair of face images taken at different times, we assign the comparison to the bin that is the arithmetic average of the subject's ages. This plot shows only the effect of age, not ageing. The number of comparisons in each bin is generally in the thousands, however the first and last bins are computed over 149 and 124 respectively. The error rates in some (adult) cases are zero, and in others the DET is flat so the error rates at the two thresholds are identical. The lines span 1% and 99% of bootstrap replicated FNMR estimates.

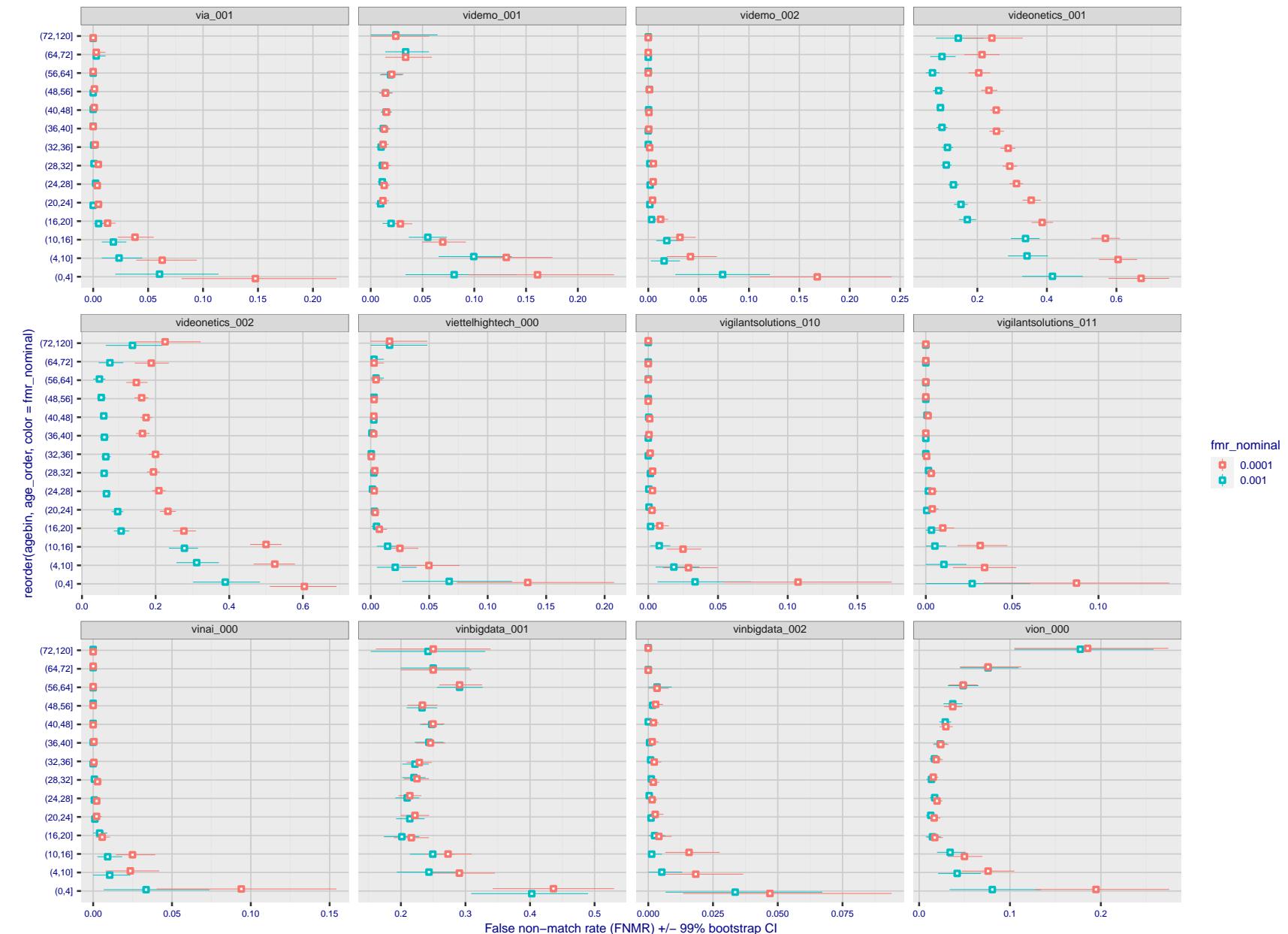


Figure 395: For the visa images, the dots show FNMR by age group for two operating thresholds corresponding to $\text{FMR} = \{0.001, 0.0001\}$ computed over all on the order of 10^{10} impostor scores. The FMR in each bin will vary also - see subsequent impostor heatmaps in sec. 3.6.2. Given a pair of face images taken at different times, we assign the comparison to the bin that is the arithmetic average of the subject's ages. This plot shows only the effect of age, not ageing. The number of comparisons in each bin is generally in the thousands, however the first and last bins are computed over 149 and 124 respectively. The error rates in some (adult) cases are zero, and in others the DET is flat so the error rates at the two thresholds are identical. The lines span 1% and 99% of bootstrap replicated FNMR estimates.



Figure 396: For the visa images, the dots show FNMR by age group for two operating thresholds corresponding to $FMR = \{0.001, 0.0001\}$ computed over all on the order of 10^{10} impostor scores. The FMR in each bin will vary also - see subsequent impostor heatmaps in sec. 3.6.2. Given a pair of face images taken at different times, we assign the comparison to the bin that is the arithmetic average of the subject's ages. This plot shows only the effect of age, not ageing. The number of comparisons in each bin is generally in the thousands, however the first and last bins are computed over 149 and 124 respectively. The error rates in some (adult) cases are zero, and in others the DET is flat so the error rates at the two thresholds are identical. The lines span 1% and 99% of bootstrap replicated FNMR estimates.



Figure 397: For the visa images, the dots show FNMR by age group for two operating thresholds corresponding to $FMR = \{0.001, 0.0001\}$ computed over all on the order of 10^{10} impostor scores. The FMR in each bin will vary also - see subsequent impostor heatmaps in sec. 3.6.2. Given a pair of face images taken at different times, we assign the comparison to the bin that is the arithmetic average of the subject's ages. This plot shows only the effect of age, not ageing. The number of comparisons in each bin is generally in the thousands, however the first and last bins are computed over 149 and 124 respectively. The error rates in some (adult) cases are zero, and in others the DET is flat so the error rates at the two thresholds are identical. The lines span 1% and 99% of bootstrap replicated FNMR estimates.



False non-match rate (FNMR) +/- 99% bootstrap CI

Figure 398: For the visa images, the dots show FNMR by age group for two operating thresholds corresponding to $FMR = \{0.001, 0.0001\}$ computed over all on the order of 10^{10} impostor scores. The FMR in each bin will vary also - see subsequent impostor heatmaps in sec. 3.6.2. Given a pair of face images taken at different times, we assign the comparison to the bin that is the arithmetic average of the subject's ages. This plot shows only the effect of age, not ageing. The number of comparisons in each bin is generally in the thousands, however the first and last bins are computed over 149 and 124 respectively. The error rates in some (adult) cases are zero, and in others the DET is flat so the error rates at the two thresholds are identical. The lines span 1% and 99% of bootstrap replicated FNMR estimates.

Caveats: None.

3.6 Impostor distribution stability

3.6.1 Effect of birth place on the impostor distribution

Background: Facial appearance varies geographically, both in terms of skin tone, cranio-facial structure and size. This section addresses whether false match rates vary intra- and inter-regionally.

Goals:

- ▷ To show the effect of birth region of the impostor and enrollee on false match rates.
- ▷ To determine whether some algorithms give better impostor distribution stability.

Methods:

- ▷ For the visa images, NIST defined 10 regions: Sub-Saharan Africa, South Asia, Polynesia, North Africa, Middle East, Europe, East Asia, Central and South America, Central Asia, and the Caribbean.
- ▷ For the visa images, NIST mapped each country of birth to a region. There is some arbitrariness to this. For example, Egypt could reasonably be assigned to the Middle East instead of North Africa. An alternative methodology could, for example, assign the Philippines to *both* Polynesia and East Asia.
- ▷ FMR is computed for cases where all face images of impostors born in region r_2 are compared with enrolled face images of persons born in region r_1 .

$$\text{FMR}(r_1, r_2, T) = \frac{\sum_{i=1}^{N_{r_1, r_2}} H(s_i - T)}{N_{r_1, r_2}} \quad (5)$$

where the same threshold, T , is used in all cells, and H is the unit step function. The threshold is set to give $\text{FMR}(T) = 0.001$ over the entire set of visa image impostor comparisons.

- ▷ This analysis is then repeated by country-pair, but only for those country pairs where both have at least 1000 images available. The countries¹ appear in the axes of graphs that follow.
- ▷ The mean number of impostor scores in any cross-region bin is 33 million. The smallest number of impostor scores in any bin is 135000, for Central Asia - North Africa. While these counts are large enough to support reasonable significance, the number of individual faces is much smaller, on the order of $N^{0.5}$.
- ▷ The numbers of impostor scores in any cross-country bin is shown in Figure 399.

Results: Subsequent figures show heatmaps that use color to represent the base-10 logarithm of the false match rate. Red colors indicate high (bad) false match rates. Dark colors indicate benign false match rates. There are two series of graphs corresponding to aggregated geographical regions, and to countries. The notable observations are:

- ▷ The on-diagonal elements correspond to within-region impostors. FMR is generally above the nominal value of $\text{FMR} = 0.001$. Particularly there is usually higher FMR in, Sub-Saharan Africa, South Asia, and the Caribbean. Europe and Central Asia, on the other hand, usually give FMR closer to the nominal value.
- ▷ The off-diagonal elements correspond to across-region impostors. The highest FMR is produced between the Caribbean and Sub-Saharan Africa.
- ▷ Algorithms vary.

¹These are Argentina, Australia, Brazil, Chile, China, Costa Rica, Cuba, Czech Republic, Dominican Republic, Ecuador, Egypt, El Salvador, Germany, Ghana, Great Britain, Greece, Guatemala, Haiti, Hong Kong, Honduras, Indonesia, India, Israel, Jamaica, Japan, Kenya, Korea, Lebanon, Mexico, Malaysia, Nepal, Nigeria, Peru, Philippines, Pakistan, Poland, Romania, Russia, South Africa, Saudi Arabia, Thailand, Trinidad, Turkey, Taiwan, Ukraine, Venezuela, and Vietnam.

- ▷ We computed the same quantities for a global FMR = 0.0001. The effects are similar.

Caveats:

- ▷ The effects of variable impostor rates on one-to-many identification systems may well differ from what's implied by these one-to-one verification results. Two reasons for this are a) the enrollment galleries are usually imbalanced across countries of birth, age and sex; b) one-to-many identification algorithms often implement techniques aimed at stabilizing the impostor distribution. Further research is necessary.
- ▷ In principle, the effects seen in this subsection could be due to differences in the image capture process. We consider this unlikely since the effects are maintained across geography - e.g. Caribbean vs. Africa, or Japan vs. China.

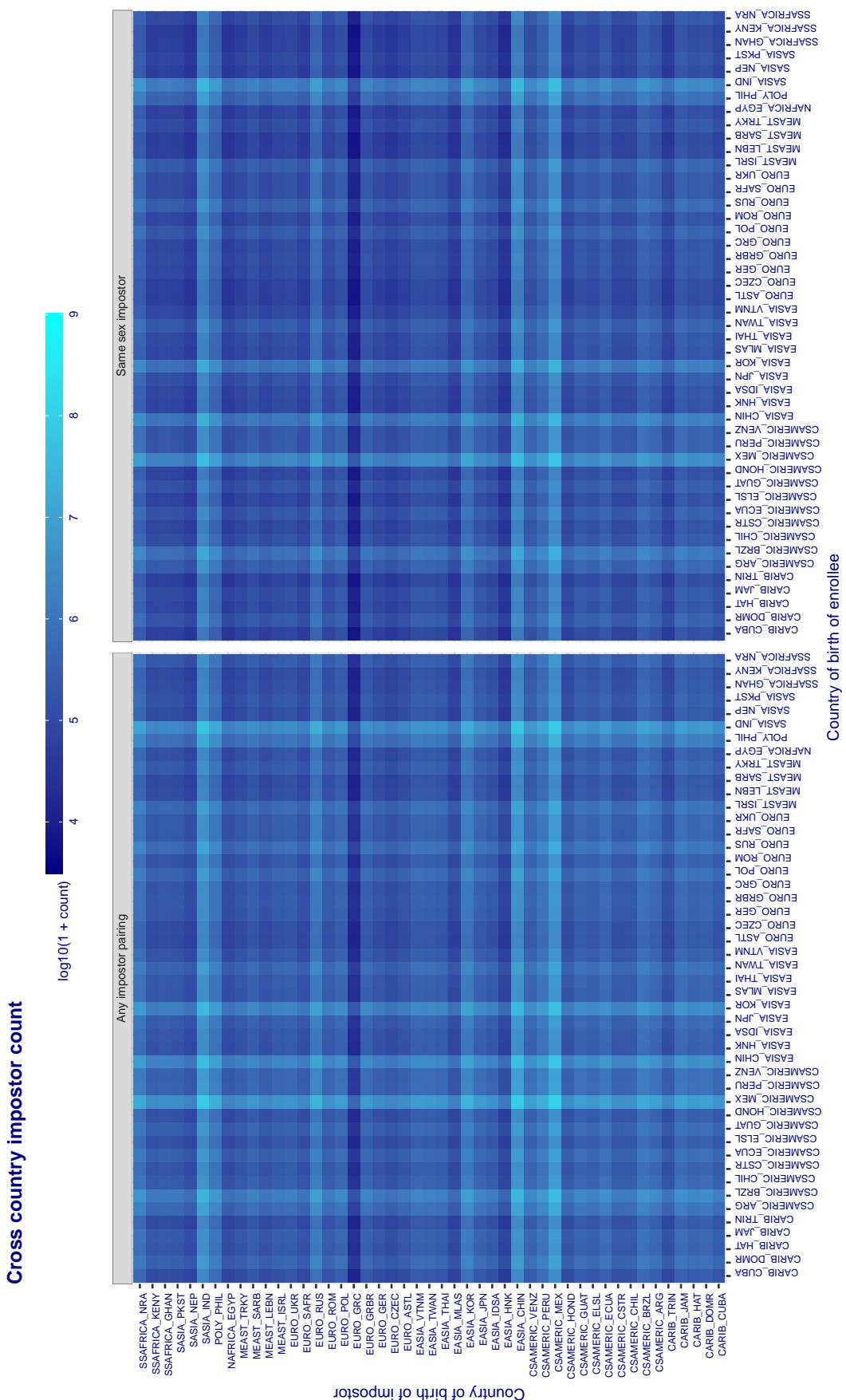


Figure 399: For visa images, the heatmap shows the count of impostor comparisons of faces from different individuals who were born in the given country pair. The FMR heatmaps themselves appear in the 1:1 report cards, for example, [this one](#).

3.6.2 Effect of age on impostors

Background: This section shows the effect of age on the impostor distribution. The ideal behaviour is that the age of the enrollee and the impostor would not affect impostor scores. This would support FMR stability over sub-populations.

Goals:

- ▷ To show the effect of relative ages of the impostor and enrollee on false match rates.
- ▷ To determine whether some algorithms have better impostor distribution stability.

Methods:

- ▷ Define 14 age group bins, spanning 0 to over 100 years old.
- ▷ Compute FMR over all impostor comparisons for which the subjects in the enrollee and impostor images have ages in two bins.
- ▷ Compute FMR over all impostor comparisons for which the subjects are additionally of the same sex, and born in the same geographic region.

Results:

The notable aspects are:

- ▷ Diagonal dominance: Impostors are more likely to be matched against their same age group.
- ▷ Same sex and same region impostors are more successful. On the diagonal, an impostor is more likely to succeed by posing as someone of the same sex. If $\Delta \log_{10} \text{FMR} = 0.2$, then same-sex same-region FMR exceeds the all-pairs FMR by factor of $10^{0.2} = 1.6$.
- ▷ Young children impostors give elevated FMR against young children. Older adult impostor give elevated FMR against older adults. These effects are quite large, for example if $\Delta \log_{10} \text{FMR} = 1.0$ larger than a 32 year old, then these groups have higher FMR by a factor of $10^1 = 10$. This would imply an FMR above 0.01 for a nominal (global) FMR = 0.001.
- ▷ Algorithms vary.
- ▷ We computed the same quantities for a global FMR = 0.0001. The effects are similar.

Note the calculations in this section include impostors paired across all countries of birth.

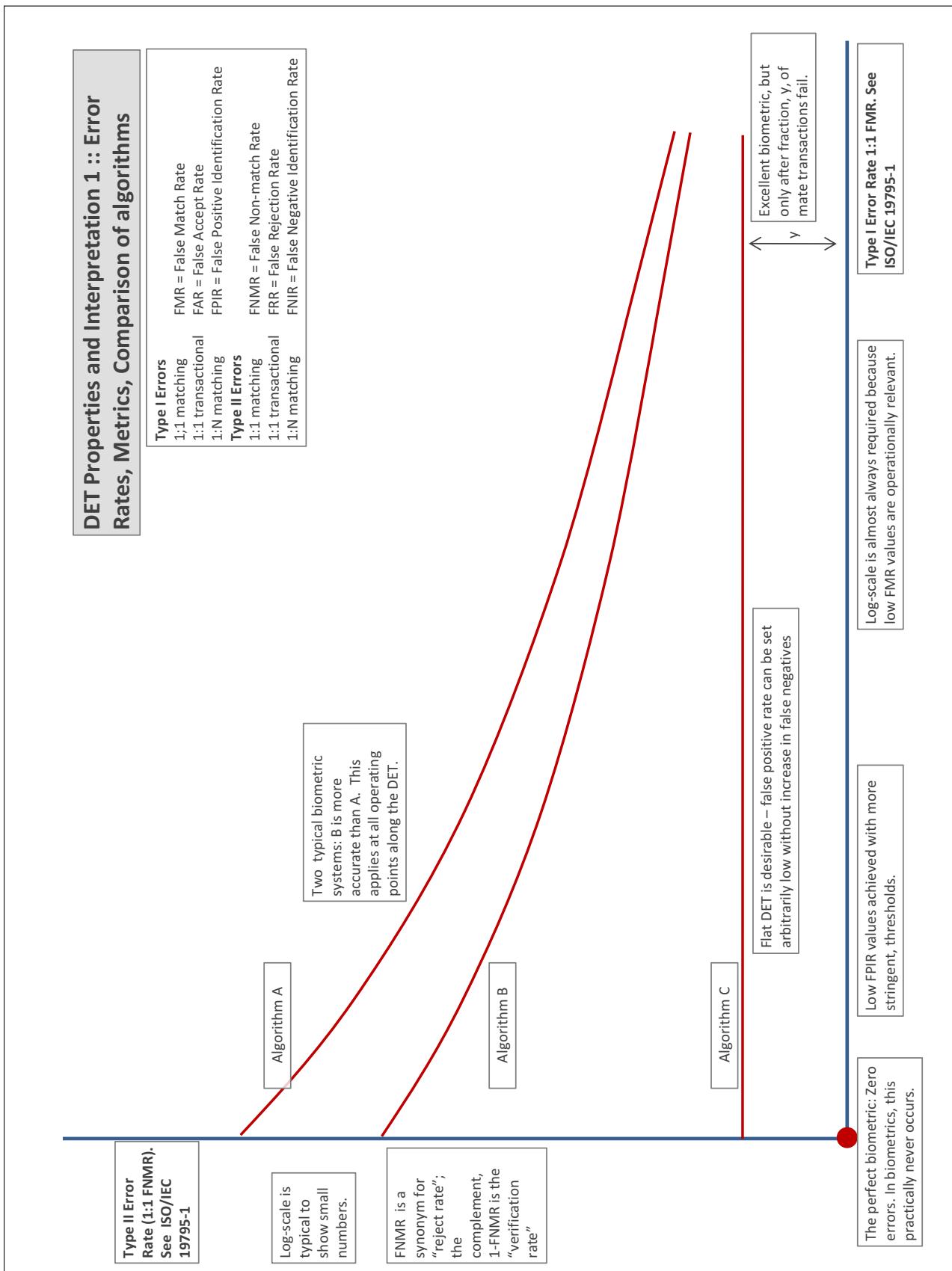
Accuracy Terms + Definitions

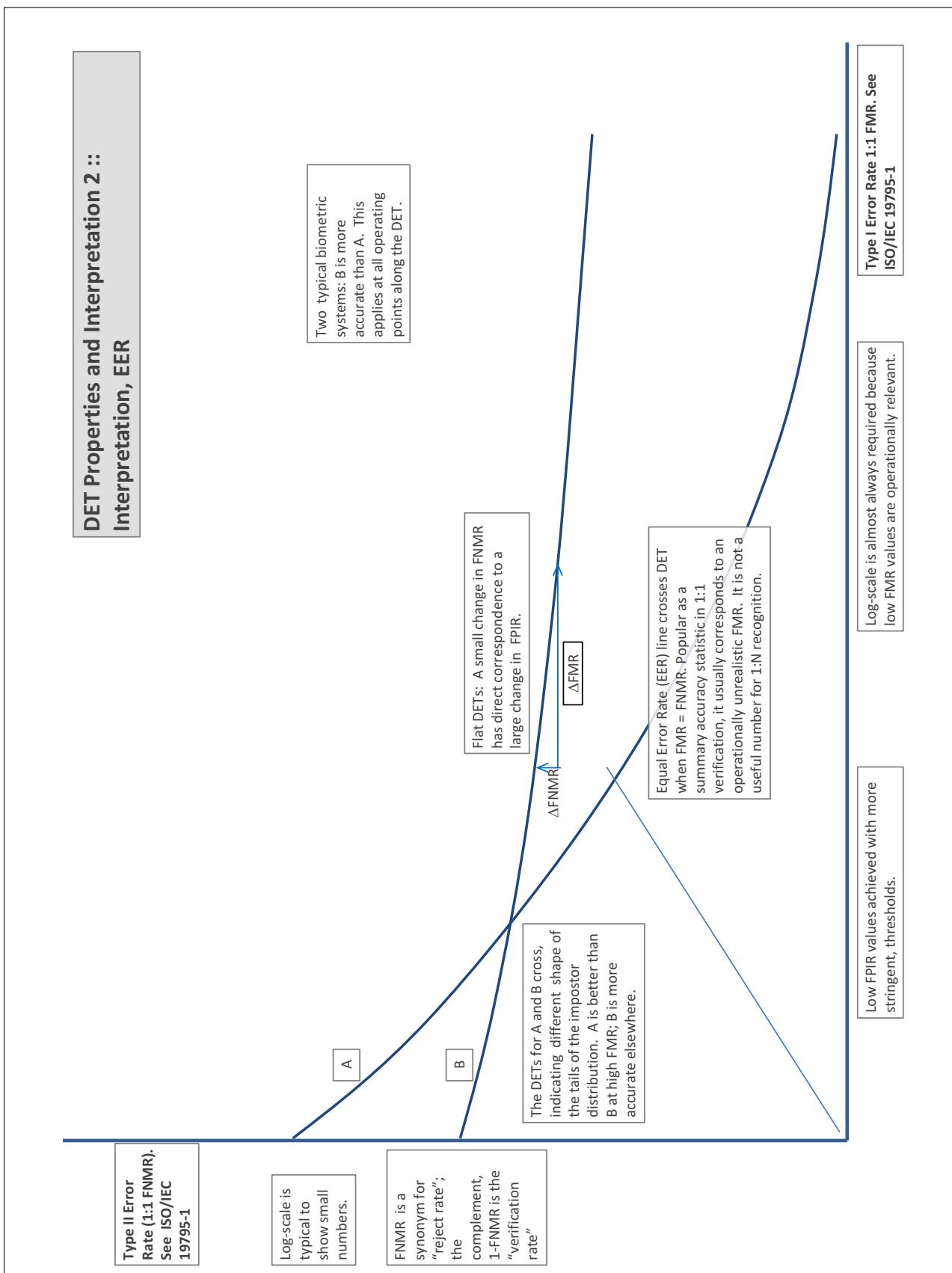
In biometrics, Type II errors occur when two samples of one person do not match – this is called a **false negative**. Correspondingly, Type I errors occur when samples from two persons do match – this is called a **false positive**. Matches are declared by a biometric system when the native comparison score from the recognition algorithm meets some **threshold**. Comparison scores can be either **similarity scores**, in which case higher values indicate that the samples are more likely to come from the same person, or **dissimilarity scores**, in which case higher values indicate different people. Similarity scores are traditionally computed by **fingerprint** and **face** recognition algorithms, while dissimilarities are used in **iris recognition**. In some cases, the dissimilarity score is a distance; this applies only when **metric** properties are obeyed. In any case, scores can be either **mate** scores, coming from a comparison of one person's samples, or **nonmate** scores, coming from comparison of different persons' samples. The words **genuine** or **authentic** are synonyms for mate, and the word **impostor** is used as a synonym for nonmatch. The words mate and nonmatch are traditionally used in identification applications (such as law enforcement search, or background checks) while genuine and impostor are used in verification applications (such as access control).

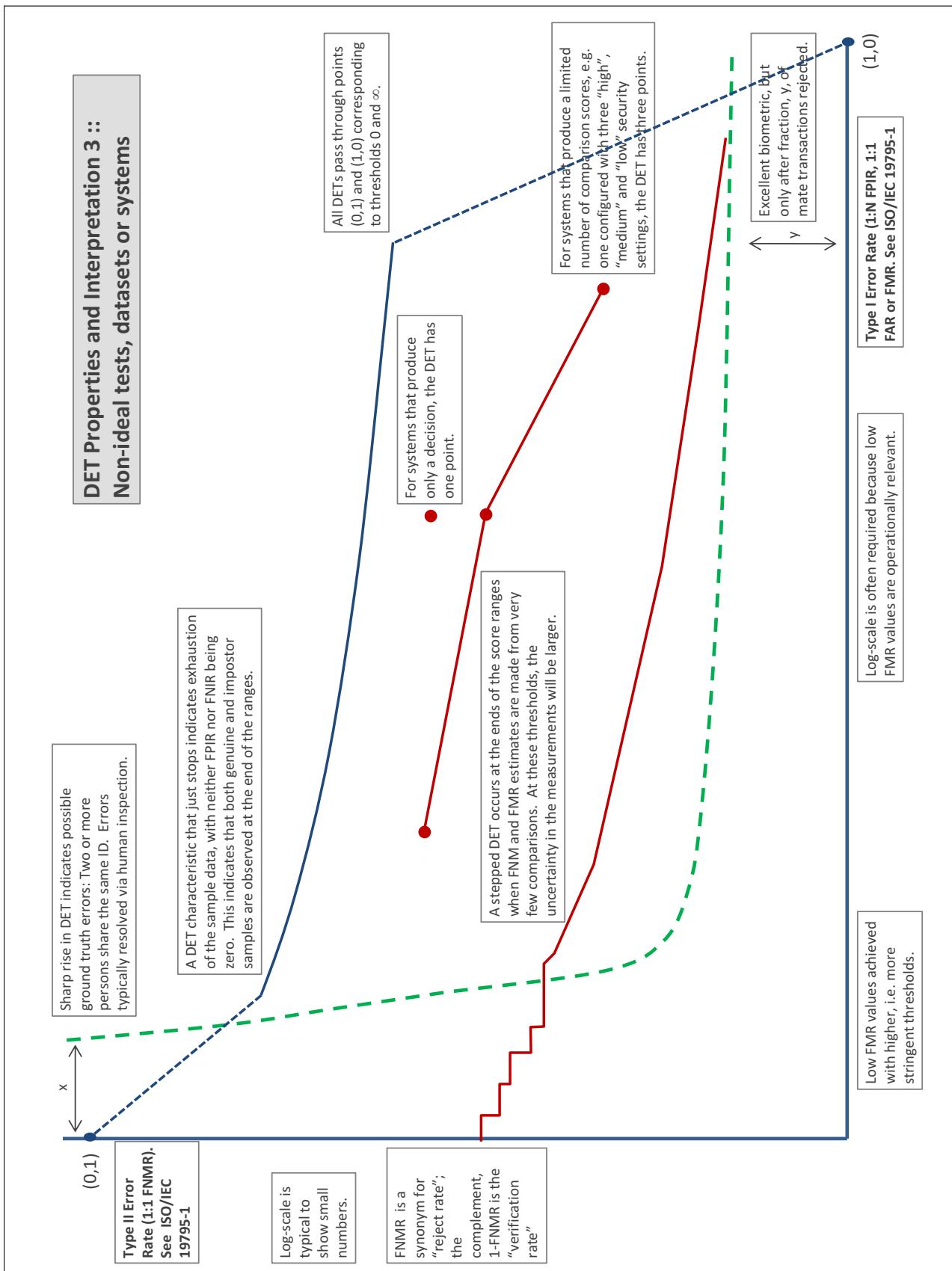
A **error tradeoff** characteristic represents the tradeoff between Type II and Type I classification errors. For verification this plots false non-match rate (FNMR) vs. false match rate (FMR) parametrically with T.

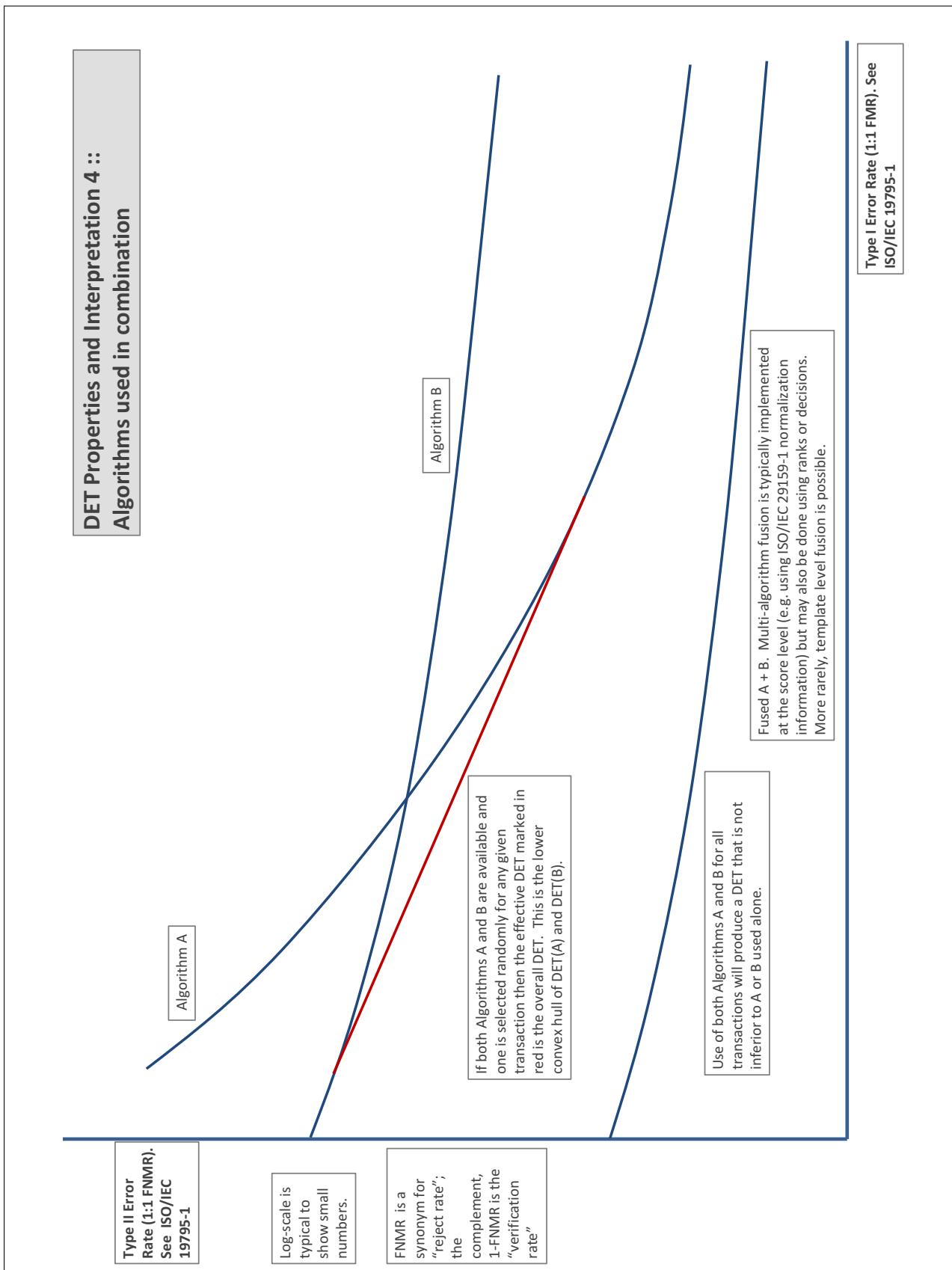
The error tradeoff plots are often called **detection error tradeoff (DET)** characteristics or **receiver operating characteristic (ROC)**. These serve the same function but differ, for example, in plotting the complement of an error rate (e.g., $TMR = 1 - FNMR$) and in transforming the axes most commonly using logarithms, to show multiple decades of FMR. More rarely, the function might be the inverse Gaussian function.

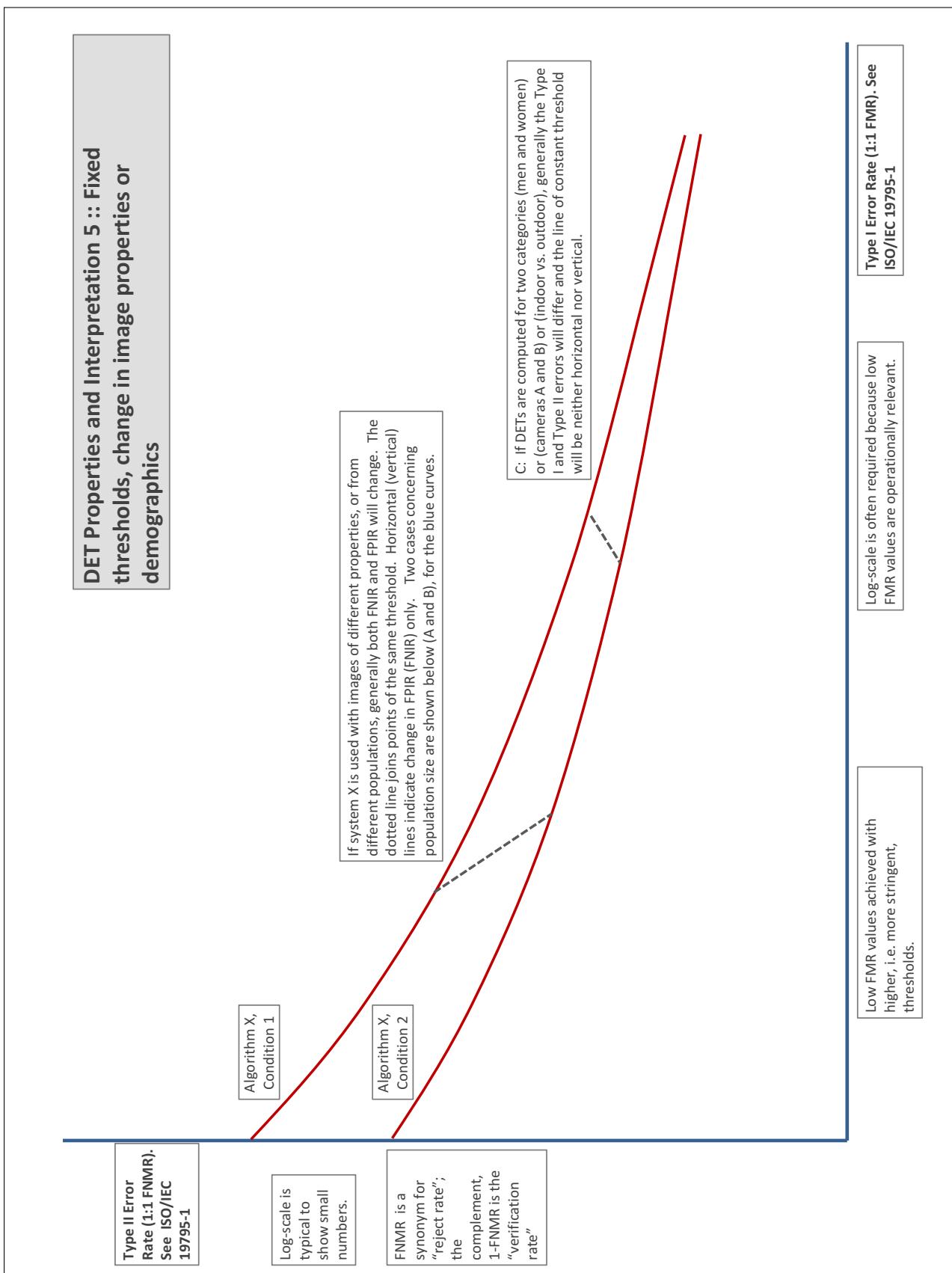
More detail and generality is provided in formal biometrics testing standards, see the various parts of [ISO/IEC 19795 Biometrics Testing and Reporting](#). More terms, including and beyond those to do with accuracy, see [ISO/IEC 2382-37 Information technology -- Vocabulary -- Part 37: Harmonized biometric vocabulary](#)











References

- [1] P. Jonathon Phillips, Amy N. Yates, Ying Hu, Carina A. Hahn, Eilidh Noyes, Kelsey Jackson, Jacqueline G. Cavazos, Géraldine Jeckeln, Rajeev Ranjan, Swami Sankaranarayanan, Jun-Cheng Chen, Carlos D. Castillo, Rama Chellappa, David White, and Alice J. O'Toole. Face recognition accuracy of forensic examiners, superrecognizers, and face recognition algorithms. *Proceedings of the National Academy of Sciences*, 115(24):6171–6176, 2018.